

Copyright is owned by the Author of the thesis. Permission is given for a copy to be downloaded by an individual for the purpose of research and private study only. The thesis may not be reproduced elsewhere without the permission of the Author.

New Routes to Planar Chiral Ligands and their Use in Asymmetric Catalysis

A thesis presented in partial fulfilment of the requirements for the degree of

Doctor of Philosophy in Chemistry

at Massey University, Manawatū, New Zealand

**Maulik Mungalpara
2021**

Dedication

For My Mum, Dad, Sisters, and Friends.

Contents

Acknowledgements	V
Contributions	VII
Abbreviations	VIII
Abstract	X
Chapter 1: Introduction to Asymmetric Catalysis and [2.2]Paracyclophane Chemistry	1
1.0. Introduction	2
1.1. Asymmetric catalysis	2
1.2. [2.2]Paracyclophane	3
1.3. Enantioenriched [2.2]paracyclophane	6
1.4. Recent applications of [2.2]paracyclophane in asymmetric catalysis	9
1.5. References	16
Chapter 2: The Synthesis of a [2.2]Paracyclophane-derived Secondary Phosphine Oxide and a Study of its Reactivity	19
2.0. Secondary phosphine oxides: strategy and objectives	20
2.1. Chiral phosphorus ligands	21
2.2. Results and Discussion	29
2.3. Conclusions	52
2.4. References	53
Chapter 3: Selective Remote β-C(sp^3)-H Activation of Cyclic Amines and Enantioselective γ-C(sp^3)-H Functionalisation of Cyclic Amines	58
3.0. Introduction to C-H Activation	59
3.1. C-H functionalisation	60
3.2. General problems associated with C-H activation	60
3.3. Overview of metal-mediated C-H activation mechanism	61
3.4. A general catalytic cycle for C-H activation	65
3.5. Role of directing group in C-H Functionalisation	65
3.6. Role of ligand in C-H Functionalisation	73
3.7. Role of solvent in C-H functionalisation	77
3.8. Nature of active catalyst in the Pd-catalysed transformations	78
3.9. C-H functionalisation of saturated-N-heterocycles	85
3.10. Results and discussion	89
3.11. Intramolecular C(sp^3)-H activation at enantiotopic carbon - a chiral indoline system	91
3.12. Intramolecular C(sp^3)-H activation at enantiotopic and diastereotopic protons - a 7-azanorbornane system	102
3.13. Intermolecular C(sp^3)-H activation of enantiotopic and diastereotopic methylene protons - a 7-azanorbornane system	106
3.14. Enantioselective γ -C(sp^3)-H of a cyclohexylamine system	126

3.15.	References	136
	Chapter 4: A Facile Single-Step Protocol for the Synthesis of Planar Chiral Oxazolines	142
4.0.	Coupling between [2.2]paracyclophane halides and chiral oxazolines	143
4.1.	Scope of bromo[2.2]paracyclophane for oxazoline coupling	144
4.2.	Scope of dibromo[2.2]paracyclophane derivatives for oxazoline coupling	146
4.3.	Scope of <i>pseudo-gem</i> -[2.2]paracyclophane derivatives for oxazoline coupling	148
4.4.	Scope of <i>pseudo-ortho</i> -[2.2]paracyclophane derivatives for oxazoline coupling	150
4.5.	Scope of <i>ortho</i> -[2.2]paracyclophane derivatives for oxazoline coupling	150
4.6.	Attempts to improve generality of the reaction and resolution of the [2.2]paracyclophane derivatives	151
4.7.	Non-aromatic heterocycle as a coupling partner	156
4.8.	Aromatic heterocycles as coupling partner	157
4.9.	Conclusions	158
4.10.	References	159
	Chapter 5: Regioselective C-H Functionalisation Via Desulfitative Coupling Using Heteroarene Sulfinates	161
5.0.	Introduction to Sulfinates	162
5.1.	Terminologies for extrusion of sulfur from organosulfur compounds	164
5.2.	The ease of desulfination: desulfination vs. decarboxylation	165
5.3.	Sulfinato complexes	165
5.4.	Synthesis of sulfinates	166
5.5.	Role of sulfinates in desulfitative reactions	168
5.6.	Results and Discussion	183
5.7.	Conclusion	196
5.8.	References	199
	Chapter 6: The Synthesis of Pyridyl[2.2]paracyclophanes by Palladium-Catalysed Cross-Coupling of Pyridine Sulfinates	202
6.0	Introduction to six-membered heteroarene sulfinates	203
6.1.	2-Pyridyl boronate as nucleophilic coupling partner	200
6.2.	Investigation of the role of pyridine sulfinates in cross-coupling reaction with bromosubstituted [2.2]paracyclophane derivatives	204
6.3.	Results and discussion	209
6.4.	Conclusions	223
6.5.	References	224

Chapter 7: Future perspective	228
7.0 Future perspective	229
7.1. Hydrazone and hydrazone-based directing groups for the remote C-H functionalisation of cyclic amine system	229
7.2. Planar chiral dicarboxylic acids in Asymmetric catalysis	230
7.3. Expanding the scope of bromo[2.2]paracyclophane derivatives for oxazoline coupling	230
7.4. Optimisation of imidazoline coupling with bromo[2.2]paracyclophanes	231
7.5. Coupling of aromatic/nonaromatic heterocycles with [2.2]paracyclophane derivatives	232
7.6. [2.2]Paracyclophane sulfinate derivatives as potential nucleophilic coupling partners	233
7.7. References	234
Chapter 8: Experimental Section	235
8.0. Experimental Section	236
8.1. General Information	236
8.2. Analytical instruments	237
8.3. Experimental for Chapter 2	238
8.4. Experimental for Chapter 3	256
8.5. Experimental for Chapter 4	271
8.6. Experimental for Chapter 5 and Chapter 6	302
DRC 16 Forms	
Electronic Appendices (Separate Document)	

Acknowledgements

It is my great pleasure to take this opportunity to thank the people who have contributed to my Ph.D. research work and thesis.

Firstly, I would like to thank my supervisor Assoc. Prof. Gareth Rowlands for his sharp-witted guidance and training over the past four years. His support and friendship have been invaluable. I should also thank him for helping me in developing a thorough mechanistic understanding of various organic transformations and for developing an in-depth knowledge of stereochemistry, and molecular conformation in me. Scientific discussions with him throughout my Ph.D. journey have been vital.

I would also like to thank my co-supervisor, Prof. Paul Plieger for his much-valued advice in research projects and sharing his laboratory resources.

I would also like to thank other members of the school, notably Prof. Shane Telfer, Assoc. Prof. Vyacheslav Filichev, and Prof. David Harding for sharing their time and laboratory resources.

I must thank Prof. Martyn Coles of Victoria University of Wellington for X-ray crystal structure studies, Dr. Pat Edwards for assistance with NMR experiments, and David Lun for his technical support as well as providing HRMS data. My special thank also goes to Graham Freeman for helping me in growing crystals and synthesising some starting materials.

I also thank former postdoctoral researchers, Dr. Maxim Kvach and Dr. Tian-You Zhou for scientific discussions and assistance in experiments.

I also thank Leonie Etheridge, Zane Farrow, the late Lily Donnelly, Manuela van Borselen, Tim Engels, Rathika Parthipan, Shashank Tiwari, Suraj Patel, and Aaron Whitehead for scientific discussions and sharing common precursors. I also thank Dr. David Nixon, Becky Severinsen, Jenna Buchanan, Michael Brown, Tyson Dais, Sidney Woodhouse, Hossein Etemadi, Harikrishnan Kurup, Bruce Chilton, Joel Cornelio, Dr. Adil Alkaş, Seok June Lee, Nimisha Mohandas, Dr. Chanjief Chandrakumar, Nikhil Srivastva, and other members of Plieger's group, Telfer's group and Filichev's group.

I also thank the staff of Chemstore, Mechanical workshop, and Electronic workshop.

I would like to acknowledge the financial support from the School of Fundamental Sciences (SFS), Graduate Assistant (GA) Fund, SFS fee remission over four years, SFS travel grant, New Zealand Institute of Chemistry (NZIC) travel grant, and travel assistance from Assoc. Prof. Gareth Rowlands to attend 26th International Symposium: Synthesis in Organic Chemistry, Cambridge University, UK (July 2019).

I also thank SFS administration and technical staff for their assistance during my Ph.D.

Finally, I would like to say a huge thank to my mum and sisters for their love and support. I would also like to thank Vishna Weeraratne for helping me during Ph.D. Also, many thanks to all my friends and family members.

Contributions

All the research work in thesis was completed by Maulik Mungalpara,

Except:

- Prof. Paul Plieger and Prof. Martyn Coles of Victoria University of Wellington obtained crystal structures of SPO-**2.47**, TPO-**2.116**, and phosphine **2.137**.AuCl.
- HASPO-II **3.132** and HASPO-III **3.133** were synthesised by Manuela van Borselen and Tim Engels.
- Graham Freeman helped in growing crystals and synthesising basic precursors for oxazoline (*S*)-**4.10** and C₂-symmetric acid **3.247**.
- All HRMS data were obtained by David Lun.
- Shashank Tiwari, Leonie Etheridge, and Zane Farrow shared [2.2]paracyclophane precursors.

Abbreviations

Ac	Acetyl
COD	1,5-Cyclooctadiene
Cp*	Pentamethylcyclopentadienyl
Cy	Cyclohexyl
dba	Dibenzylideneacetone
DCM	Dichloromethane
<i>de</i>	Diastereomeric excess
DIPEA	<i>N,N</i> -Diisopropylethylamine
DME	Dimethoxyethane
DMF	<i>N,N</i> -Dimethylformamide
DMS	Dimethyl sulfide
dppf	[1,1'-Bis(diphenylphosphino)ferrocene]
<i>dr</i>	Diastereomeric ratio
<i>ee</i>	Enantiomeric excess
eq.	Equivalent
<i>er</i>	Enantiomeric ratio
ESI-MS	Electrospray Ionisation Mass Spectrometry
HASPO	Heteroatom-substituted secondary phosphine oxide
HFIP	Hexafluoroisopropanol
HRMS	High Resolution Mass Spectrometry
hrs	Hours
<i>i</i> -Pr	Isopropyl
min.	Minutes
<i>m/z</i>	Mass to charge ratio
n.d.	Not detected
NMR	Nuclear Magnetic Resonance
Np	Naphthyl
P	Product
SM	Starting material
SPO	Secondary phosphine oxide

rt	Room temperature
^t Bu	tert-Butyl
TDG	Transient directing group
TEA	Triethylamine
THF	Tetrahydrofuran
TLC	Thin layer chromatography
TPO	Tertiary phosphine oxide
TS	Transition state
Ts	(4-Methylphenyl)sulfonyl

New Routes to Planar Chiral Ligands and their Use in Asymmetric Catalysis

Abstract

This thesis contains 8 chapters detailing 3 optimised methods to synthesise [2.2]paracyclophane derivatives and our studies in the C-H activation field, namely selective remote β -C-H activation of cyclic amines, and enantioselective γ -C(sp^3)-H functionalisation of cyclic amines, as well as a future direction.

As the main focus of this thesis is on the development of novel planar chiral [2.2]paracyclophane derivatives, Chapter 1 starts with a brief description of [2.2]paracyclophane chemistry. A short introduction about the synthesis of key enantioenriched [2.2]paracyclophane derivatives is given. Finally, a short introduction of the recent applications of [2.2]paracyclophane-based ligands in asymmetric catalysis is also mentioned.

Chapter 2 describes the synthesis of (RS_p,SR_p)-4-*tert*-butyl[2.2]paracyclophane phosphine oxide (SPO) and attempts to synthesise its asymmetric variant. Further, its synthetic utility is investigated, mainly in Suzuki-Miyaura cross-coupling, Buchwald-Hartwig amination, and Au(I)-catalysed cyclisation reactions. Additionally, a general route to the P-stereogenic [2.2]paracyclophane-derived phosphines *via* the reduction of tertiary phosphine oxides is reported.

Chapter 3 mainly outlines attempts for β -C(sp^3)-H activation of cyclic amine to target the shortest route of epibatidine moiety. A stepwise approach is mentioned. Firstly, a range of heteroatom-substituted secondary phosphine oxides (HASPOs) is evaluated to access (chiral) indolines *via* intramolecular C(sp^3)-H activation. Next, an intramolecular C(sp^3)-H activation of 7-azanorbornane, a core skeleton of epibatidine, is investigated. The third approach is mainly targeted for the directing-group-assisted intermolecular C(sp^3)-H activation of 7-azanorbornane. Lastly, enantioselective γ -C(sp^3)-H activation of *N*-cyclohexylpicolinamide using various chiral Brønsted acids, again targeting the epibatidine moiety by the late-stage cyclisation, is described.

In a search for suitable planar chiral Brønsted acid, an optimised single-step protocol for the synthesis of [2.2]paracyclophanes carboxylic acid derivatives is reported in Chapter 4. This

protocol proceeds *via* C(*sp*²)-H activation of chiral oxazolines and their coupling with bromo[2.2]paracyclophanes.

Chapters 5 & 6 are related to pyridine sulfinates. Chapter 5 describes an attempted regioselective C-H functionalisation of aromatic acids *via* desulfitative coupling with pyridine-2-sulfinate. A detailed study with catalytic Pd(OAc)₂ and pre-formed palladacycle is mentioned. The effect of catalytic Pd(OAc)₂ on homo-coupling of pyridine-2-sulfinates is also investigated.

The potential of sulfinates as nucleophilic coupling partners is investigated in Chapter 6. A novel methodology to synthesise pyridyl[2.2]paracyclophanes is described. The method involves desulfitative cross-coupling reactions between pyridine sulfinates and bromo[2.2]paracyclophanes. One of the interesting results of the desulfitative coupling with the unreactive (±)-4-bromo-5-amino[2.2]paracyclophane is also mentioned.

Chapter 7 explains the future scope of the research work mentioned in this thesis.

Finally, Chapter 8 describes the experimental procedures and characterisation of the synthesised compounds mentioned in Chapters 2 to 6.

Chapter 1

Introduction to Asymmetric Catalysis and [2.2]Paracyclophane Chemistry

1.0. Introduction

At the heart of organic chemistry is the ability to synthesise new molecules with specific properties, be they pharmaceuticals, agrochemicals, or new materials for energy conversion and storage. These novel molecules are crucial to the functioning of modern society. Gone are the days when a chemist's goal was to simply make a compound. Now, the goal is to prepare these molecules in an efficient manner on a large enough scale to feed progress and to perform this without undue impact on the environment. The key to achieving these goals lies in catalysis or the synthesis of replenishable reagents. Catalysts would aim to increase the rate of some reactions and control the selectivity in others. Ultimately, they permit new molecules to be formed with less wasted material or energy.

Chirality or handedness is a prerequisite for life. Without this uniformity in biological molecules, life would not exist. A chiral enantioenriched catalyst can alter the selectivity of a reaction in order to bias a reaction towards the synthesis of a single-handed product. In fact, nature has selected enantioselective catalysis as its means of creating chirality.¹ Despite the significant progress that has been achieved by chemists, asymmetric catalysis remains a fledgling field.² Most catalytic reactions lack generality, working for specific examples only. Chemists are also missing key information about many of the processes involved in asymmetric catalysis, especially how chiral information is communicated from the catalyst to the product. As a result, there is still considerable research that needs to be undertaken in the area of asymmetric catalysis.

1.1. Asymmetric catalysis

The careful selection of a suitable chiral backbone has become a crucial step in the synthesis of any modern chiral ligand for asymmetric catalysis.³ Several natural building blocks have been widely exploited in the development of chiral ligands, although this can lead to limitations if only one enantiomer is naturally available.⁴

Asymmetric catalysts do not solely depend on 'centres' of chirality.⁵ Axial and planar chirality were introduced in the middle of the last century and are found in an increasing number of chiral compounds devoid of a tetrahedral stereocentre.⁶ Some of the commonly used ligands possessing non-traditional chirality are axially chiral binaphthalene derivatives,⁷ planar chiral ferrocene derivatives,^{8,9} and planar chiral arene transition metal complexes.^{10,11} Recently,

planar chiral cyclophanes have also attracted considerable interest due to their unusual structural and electronic properties.^{12,13} Cyclophanes offer a well-defined, three-dimensional structure suited for chiral induction and these characteristics are being harnessed in the formation of planar chiral functional materials.^{14,15}

This thesis covers the chemistry we have developed for the synthesis of planar chiral secondary phosphine oxides (SPO), planar chiral oxazolines, and pyridine derivatives as well as our studies in the field of C-H activation. Each topic is introduced at the beginning of the appropriate chapter. As the whole thesis centres on the planar chiral [2.2]paracyclophane scaffold, the key objective of this general introduction is to provide a brief literature overview on [2.2]paracyclophane chemistry. The following discussion is divided into different sections dealing with the single-crystal structure of [2.2]paracyclophane with fundamental properties (Section 1.2) and the synthesis of key enantioenriched [2.2]paracyclophane derivatives (Section 1.3). Though planar chiral [2.2]paracyclophanes have been largely exploited in catalysis, the biomedical field,^{16,17} and materials science,¹⁸ the applications discussed here are mainly limited to asymmetric catalysis (Section 1.4).

1.2. [2.2]Paracyclophane

[2.2]Paracyclophane¹⁹⁻²⁷ comprises of two eclipsing aryl rings or decks held rigidly in place at the *para* positions by two ethylene groups (Figure 1.1, Structure **1.1**). The discovery of this molecule is considered rather serendipitous. In 1947, Micheal Szwarc of the University of Manchester was conducting pyrolysis-type experiments on *p*-xylene. During this experiment, he observed a di-*p*-xylene impurity in a vapour decomposition product poly(*para*-xylene).²⁸ This impurity is now known as [2.2]paracyclophane. Two years later, the X-ray crystal structure was determined by Brown and Fathering (Figure 1.1).²⁹

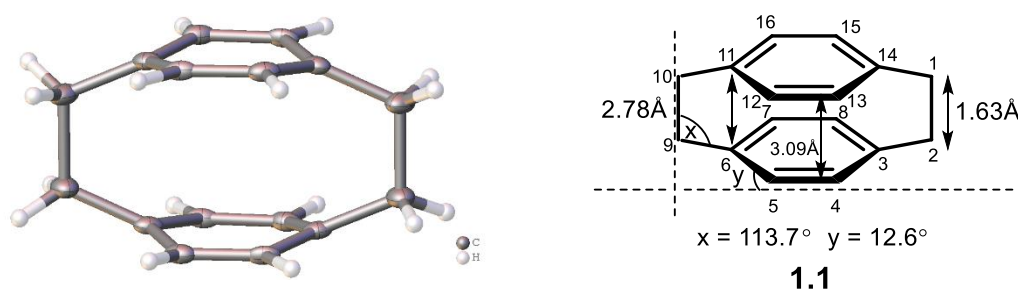


Figure 1.1. Single crystal structure of [2.2]paracyclophane (left) and same at bond lengths and angles (right). (Ellipsoids are drawn at a 50% probability level.)

According to the X-ray crystal structure of [2.2]paracyclophane, the two aromatic rings are distorted out of the plane.²⁹ A strong repulsion between the two decks leads to distortion giving a shallow boat-like conformation. The close proximity of these rings leads to transannular π - π strain in the aromatic rings. The separation of these rings is less than the sum of the van der Waals radii for carbon (3.40 Å) and ranges from 2.78 Å for the bridgehead for carbon (C3-C14) to a maximum of 3.09 Å between C4-C13. This rigid structure results in the bridgehead σ bonds (C1-C2 and C9-C10) being held almost perpendicular to the aryl rings allowing a strong $\sigma_{\text{bridge}}-\pi$ interaction as observed by the lengthening of the C-C bond (1.63 Å *cf.*- 1.54 Å in ethane). The bond angle of C-C_{bridge} to aromatic bond (inner) is 113.7°, which is greater than the normal tetrahedral bond angle of 109.5°. The bond strain energy of [2.2]paracyclophane is 129.8 kJ/mol.

The unusual electronic and distortion of [2.2]paracyclophane rings increase the nucleophilicity of the aromatic ring and it undergoes electrophilic substitution more rapidly than analogous aryl systems. It also has the ability to form π -complexes. [2.2]Paracyclophane derivatives are generally robust, crystalline, stable towards light, mild acids, bases, and thermally stable up to 160-180 °C. The [2.2]paracyclophane framework acts as a bulky shield and planar chirality can be introduced by the addition of single substituents. With the appropriate steric bulk, the chiral environment can be properly modulated on the [2.2]paracyclophane framework for catalysis.^{26,30,31}

1.2.1. π -complexes and transannular effect

A study by Cram and Singer revealed that the transannular effect plays a role in the formation of π -complexes with [2.2]paracyclophane.³² According to the studies, the complexes formed between [2.2]paracyclophane and tetracyanoethylene (TCNE) are more stable than the analogous aryl complexes (Figure 1.2). The substituents on the [2.2]paracyclophane greatly affect the stability of these complexes. Derivatives with electron-donating substituents are found to be more stable than those with electron-withdrawing groups. This is thought to be due to complexes with electron-donating groups on the substituted ring being able to participate in the π - π interaction with TCNE, while in [2.2]paracyclophanes containing an electron-withdrawing group, the unsubstituted ring is more likely to be directly associated with TCNE. Due to the π -cloud system present in [2.2]paracyclophane, reactions taking place on one aromatic ring can be influenced by electronic effects exerted by the substituents on the second aromatic ring. This is defined as the ‘transannular effect’.

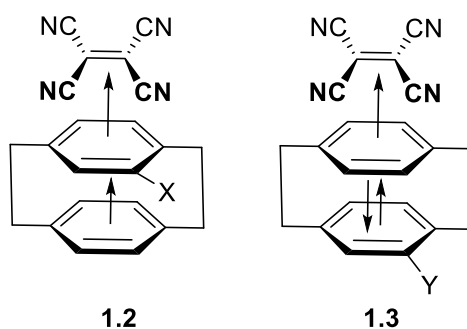


Figure 1.2: π - π Complexes between TCNE and [2.2]paracyclophane with electron-donating group (EDG) X and electron withdrawing group (EWD) Y.

1.2.2. Configuration of [2.2]paracyclophane

The assignment of R_p and S_p for [2.2]paracyclophane is designated by choosing a plane that contains as many of the atoms of the molecule as is possible.³³ As depicted in Figure 1.3, the more substituted benzene ring is considered as the chiral plane. To determine the descriptor, the chiral plane is viewed from the out-of-plane atom closest to the plane. If there are two or more candidates, the one closest to the atom of higher priority is chosen according to the Cahn–Ingold–Prelog (CIP) system^{34,35} of the stereochemical assignment. This pilot atom is assigned as carbon atom number one for cyclophane nomenclature. When viewed from the pilot atom, if atoms a, b, and c are in a clockwise array, the descriptor is R_p and if the array is counterclockwise, the descriptor is S_p , where subscript P ($_p$) denotes planar chirality. For example, the carboxy[2.2]paracyclophane shown in figure 1.3 is S_p .

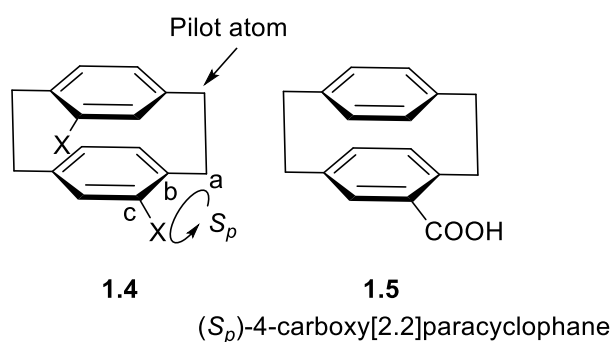


Figure 1.3: Assignment of [2.2]paracyclophane configuration.

1.3. Enantioenriched [2.2]paracyclophanes

For the synthesis of enantiopure compounds, two common methods have been used. The first is the resolution of racemates while the second is the synthesis of a single enantiomer using an asymmetric catalyst. Even though the latter method allows the synthesis of one enantiomer preferentially, thus avoiding the undesired enantiomer, the reports based on this concept are sparse.³⁶ Most of the methodologies that rely on the concept of classical resolution are tedious and costly. The section below summarises some of the methods to resolve commonly employed enantiomerically enriched [2.2]paracyclophane derivatives (Figure 1.4).

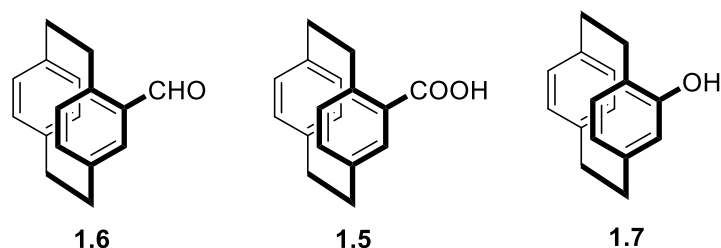
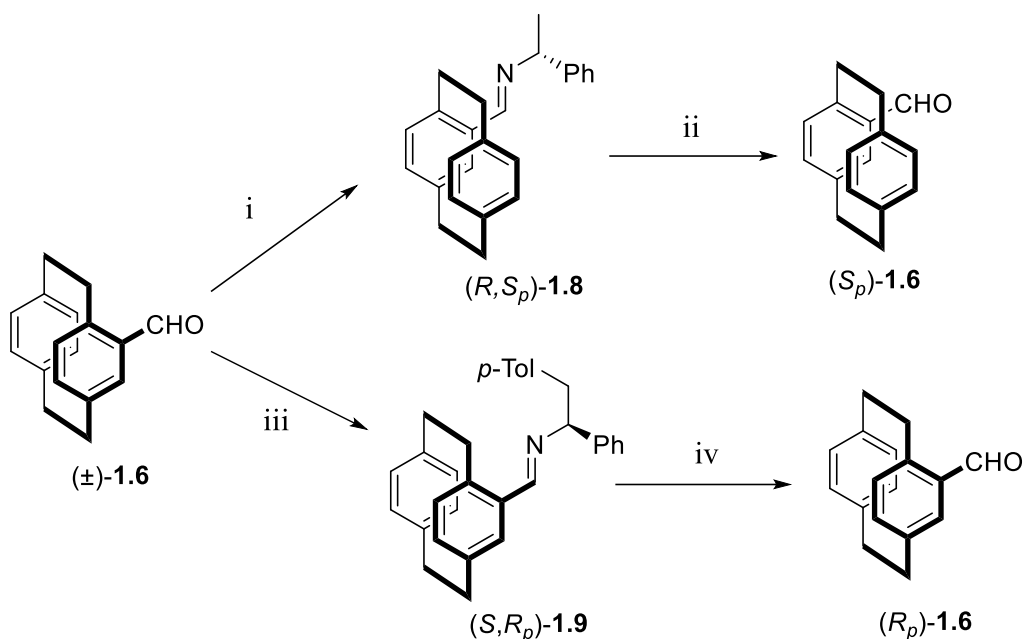


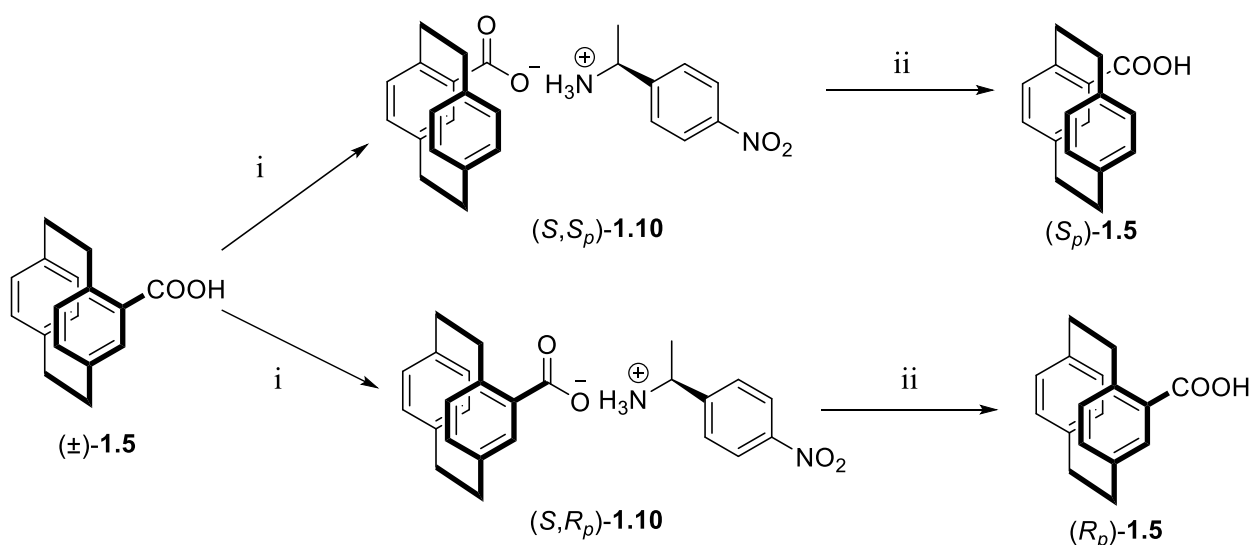
Figure 1.4: Monosubstituted [2.2]paracyclophane derivatives.

Qunici et al. developed a method for the resolution of (\pm)-4-formyl[2.2]paracyclophane **1.6**.³⁷ (*R*)-(+)- α -Methylbenzylamine was reacted with (\pm)-**1.6** to form diastereoisomeric imines (Scheme 1.1). A single crystallisation of the crude product resulted in the crystals being enriched in the (*R*,*S_p*) diastereoisomer **1.8**. The pure (*R*,*S_p*) diastereoisomer was obtained by the second crystallisation in $\geq 98\%$ *de* (diastereomeric excess). Hydrolysis on silica gel during column chromatography gave (*S_p*)-(+)-**1.6** in $\geq 98\%$ *ee* (enantiomeric excess) and 20% isolated yield. However, the enantiomer (*R_p*)-(-)-4-formyl[2.2]paracyclophane **1.6** was not isolated during this procedure. To obtain the *R_p* enantiomer [(*R_p*)-(-)-**1.6**], an alternative method was employed. In this method, (\pm)-4-formyl[2.2]paracyclophane **1.6** was reacted with (*S*)-(+)-1-phenyl-2-(*p*-tolyl)ethylamine and repeated crystallisation of the diastereomeric imine followed by hydrolysis, afforded (*R_p*)-(-)-**1.6** in $\geq 98\%$ *ee* and 26% isolated yield.



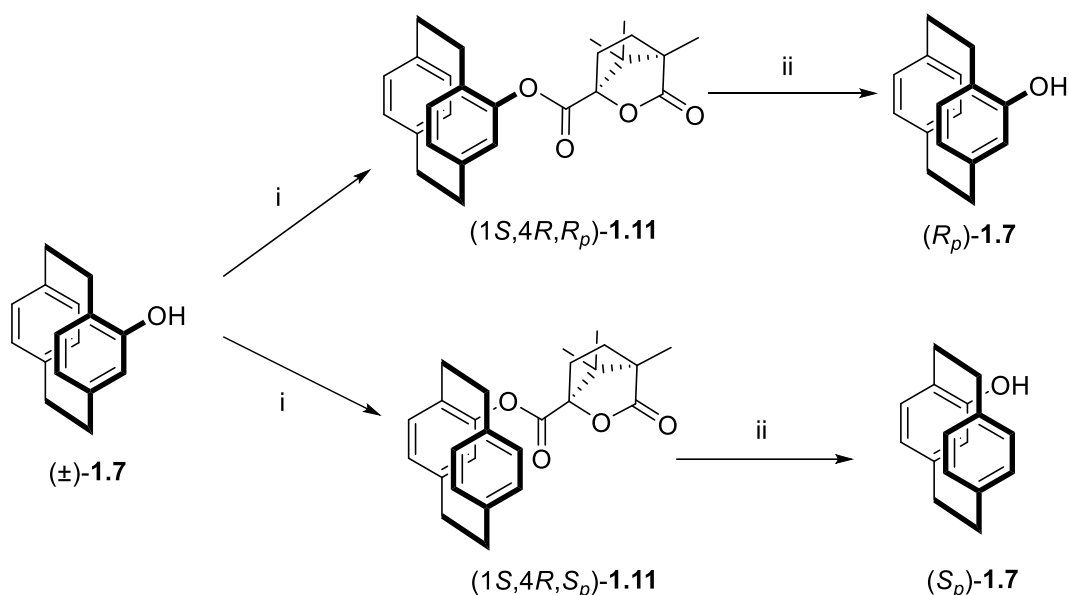
Scheme 1.1: Resolution of (\pm) -4-formyl[2.2]paracyclophane **1.6**. i) (R) - $(+)$ - α -Methylbenzylamine, ii) hydrolysis on silica, iii) (S) - $(+)$ -1-phenyl-2-(*p*-tolyl)ethylamine, iv) Hydrolysis.

The most efficient way to date for the synthesis of an enantiopure carboxylic acid was established by Rozenberg et al. (Scheme 1.2).³⁸ This involves the resolution of (\pm) -**1.5** by diastereomeric salt formation with (S) - $(-)$ - α -(*p*-nitrophenyl)ethylamine. The less soluble (S,S_p) salt **1.10** crystallises from chloroform at $-5\text{ }^\circ\text{C}$ and subsequently by neutralising with hydrochloric acid, gives (S_p) - $(+)$ -4-carboxy[2.2]paracyclophane **1.5** in 32% yield. Concentrating the mother liquor provides (S,R_p) diastereoisomeric salt **1.10** and once hydrolysed, gives (R_p) - $(-)$ -4-carboxy[2.2]paracyclophane **1.5** in 84% *ee* and 24% yield.



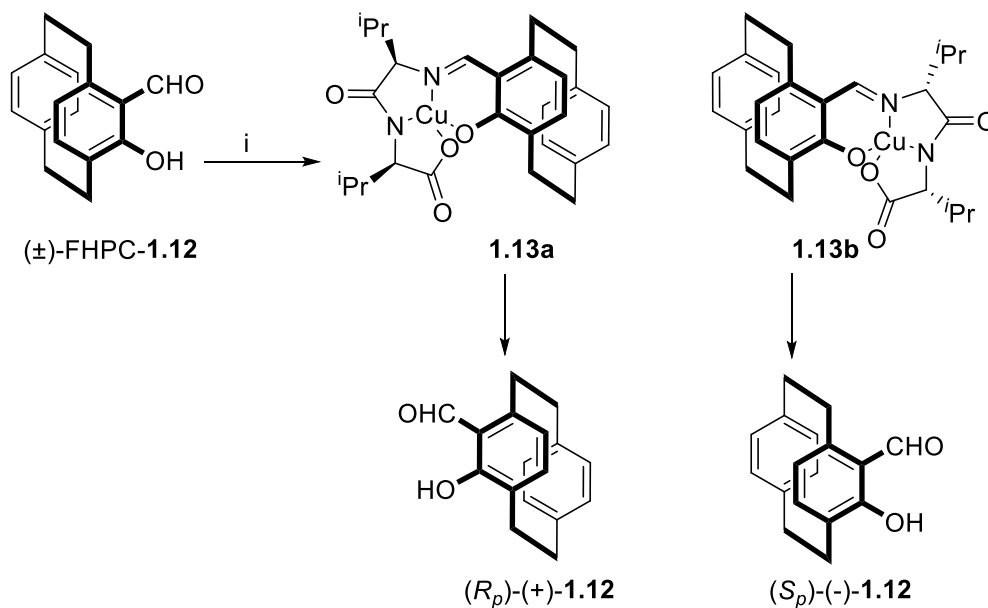
Scheme 1.2: Resolution of (\pm) -4-carboxy[2.2]paracyclophane **1.5** i) (S) - $(-)$ - α -(*p*-nitrophenyl)ethylamine, ii) HCl(aq.).

The resolution of (\pm)-4-hydroxy[2.2]paracyclophane **1.7** was achieved *via* an ester formation with (1*S*,4*R*)-(-)-camphanoyl chloride (Scheme 1.3).³⁹ The first recrystallisation from ethyl acetate produced (1*S*,4*R*,*R_p*) diastereoisomer **1.11** with a *de* >95%. The (1*S*,4*R*,*S_p*) diastereoisomer **1.11** can be obtained after a series of crystallisations from the mother liquor in \geq 99% *de*. The diastereomeric esters can then be reduced separately with lithium aluminium hydride, to afford enantiopure (*R_p*)-(+)-**1.7** and (*S_p*)-(-)-**1.7** (11% isolated yield, >99% *ee*).



Scheme 1.3: Resolution of (\pm)-4-hydroxy[2.2]paracyclophane **1.7** i) (1*S*,4*R*)-(-)-camphanoyl chloride, ii) LiAlH₄.

Disubstituted [2.2]paracyclophane ligands carrying substituents on the same aromatic ring are better ligands than the analogous monodentate ligands. The majority of such bidentate ligands that have two substituents on the same aromatic ring are derived from (*S_p*)- or (*R_p*)-5-formyl-4-hydroxy[2.2]paracyclophane (FHPC) **1.12**. This aldehyde (\pm)-**1.12** can be resolved by complexation with Cu(ClO₄)₂ and the dipeptide, H₂N-Val-Val-OH in presence of sodium isopropoxide to give **1.13a** and **1.13b** (Scheme 1.4).⁴⁰ (*R_p*)-(+)-FHPC **1.12** can be isolated in 86% *ee* and 17% yield after the complex crystallises at a low temperature followed by hydrolysis. Purification of the second diastereomeric complex required flash column chromatography to furnish (*S_p*)-(-)-FHPC **1.12** in 85% *ee* and 17% yield after hydrolysis.



Scheme 1.4: Resolution of (\pm) -FHPC **1.12** i) $\text{Cu}(\text{ClO}_4)_2$, $\text{H}_2\text{N-Val-Val-OH}$, sodium isopropoxide.

1.4. Recent applications of [2.2]paracyclophane in asymmetric catalysis

This section explains different substituents on [2.2]paracyclophane and how they are exploited as chiral ligands in asymmetric catalysis. [2.2]Paracyclophane derivatives are intrinsically planar chiral, and they have been utilised as chiral auxiliaries, reagents and ligands in enantioselective synthesis as outlined in reviews by Gibson,³³ Rozenberg,¹² Rowlands,²⁶ Paradies⁴¹, and Bräse.¹⁸

The majority of [2.2]paracyclophane ligands reported so far are based on one of the four different substitution patterns (*mono* **1.14**, *ortho* **1.15**, *pseudo-ortho* **1.16**, *pseudo-geminal* **1.17**) (Figure 1.5).

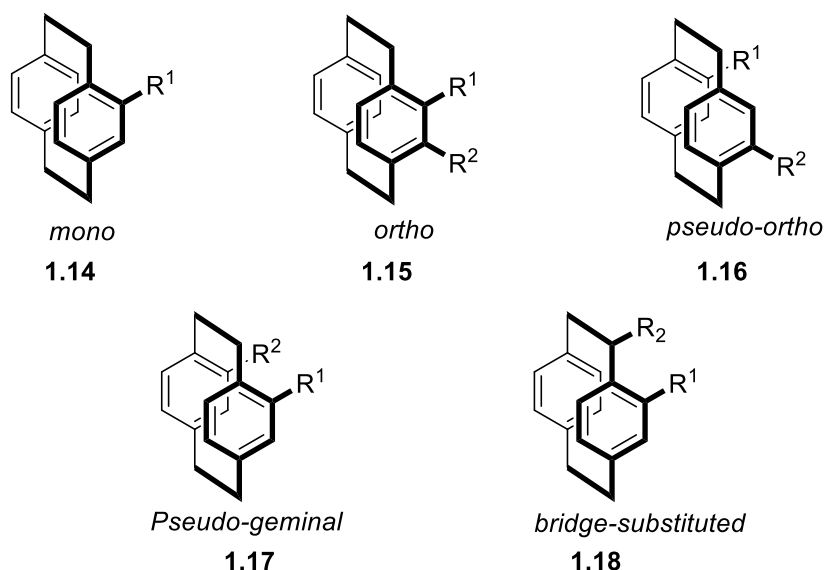
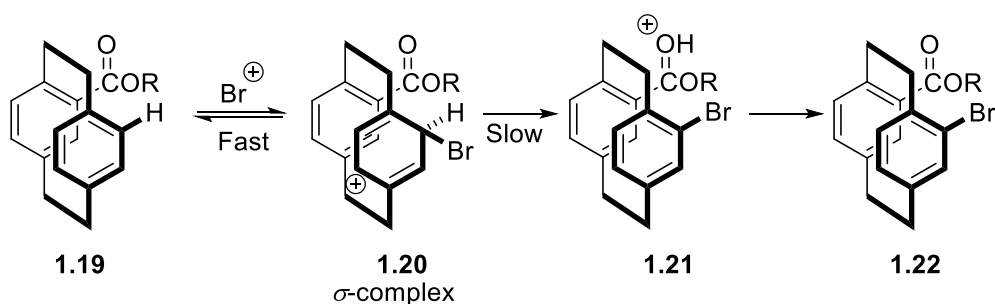


Figure 1.5. [2.2]Paracyclophane substitution patterns.

The *pseudo-ortho* position **1.16** is commonly exploited in asymmetric catalysis due to its characteristic chiral pocket. *Ortho*-[2.2]paracyclophane derivatives **1.15** are also widely explored since they can be easily prepared from the monosubstituted derivatives. The *pseudo-gem*-[2.2]paracyclophane derivatives **1.17** can also be easily synthesised as the transannular effect facilitates regioselective bromination on the monosubstituted derivatives containing O-basic substituents such as nitro, carboxy, and acetyl groups. The oxygen atom of these functionalities acts as an intramolecular base to accept the proton from the *pseudo-gem* position in the σ -complex to facilitate electrophilic aromatic bromination (Scheme 1.5). The first step of dearomatisation-aromatisation is a fast, reversible process. Of note, the mechanism differs from the electrophilic aromatic bromination of benzene, in which the first step involving attack of brominium cation is the rate-determining step. This *pseudo-gem* bromo functionality can be further transformed into a variety of other functional groups.



Scheme 1.5: Mechanism of electrophilic aromatic bromination leading to the *pseudo-gem* product.

1.4.1. Planar chiral [2.2]paracyclophane-derived phosphine ligands

The planar chirality of [2.2]paracyclophane **1.1** has been known since 1955, yet it was not until the 1990s that this chirality was exploited in the field of asymmetric catalysis. The first application was reported by Pye and Rossen in 1997 for [2.2]paracyclophane-based bisphosphine ligand. Amongst the various ligands, (*S_p*)-phanephos **1.23** is the most successful [2.2]paracyclophane-based ligand to date.⁴² It is similar to the axially chiral bisphosphine ligand BINAP **1.24**,⁴³ which has also been extensively employed in asymmetry synthesis as a ligand for many enantioselective transformations (Figure 1.6).

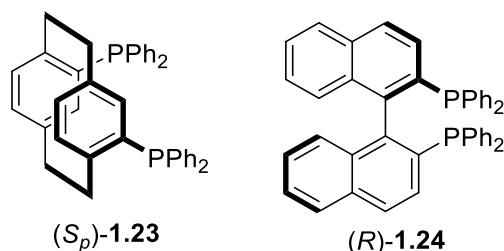
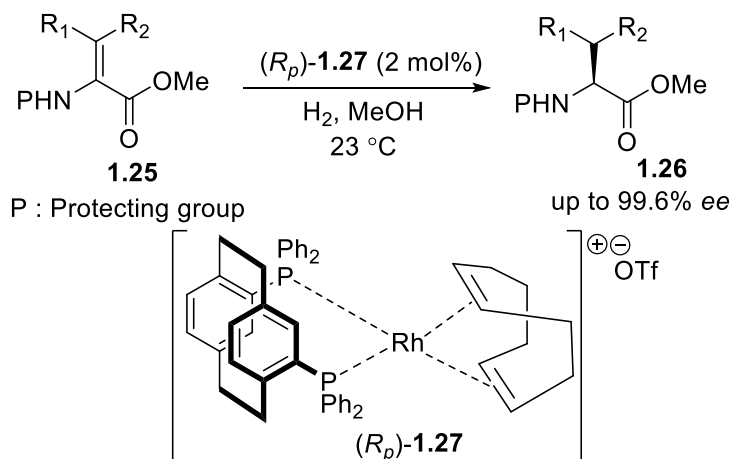


Figure 1.6. (*S_p*)-Phanephos **1.23** and (*R*)-BINAP **1.24**.

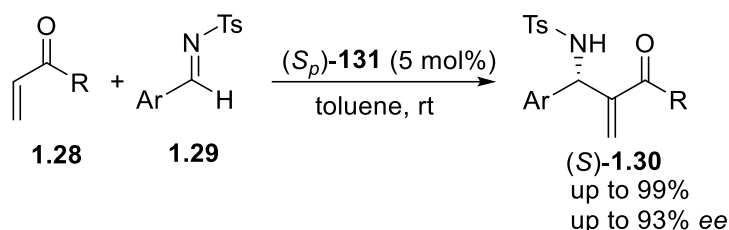
(*S_p*)-Phanephos **1.23** was first applied in the enantioselective hydrogenation of dehydroamino acid methyl ester **1.25** by forming the triflate salt with rhodium(I) (*R_p*)-**1.27** under extremely mild conditions and the product was isolated in 99.6% *ee* (Scheme 1.6).⁴² This planar chiral catalyst has proven efficient under milder conditions compared to many other chiral bisphosphine catalysts. It is worth mentioning that the previous benchmark catalysts require more harsh conditions e.g. (*R*)-BINAP **1.24** required 70 atm, 40 °C for 24 hrs to give the reduction product in 56% *ee*. Dow Chemical Ltd. now uses (*S_p*)-Phanephos **1.23** on an industrial scale for the hydrogenation of ketones, using a catalyst loading as low as 0.001% on a scale of hundreds of kilogrammes.⁴⁴



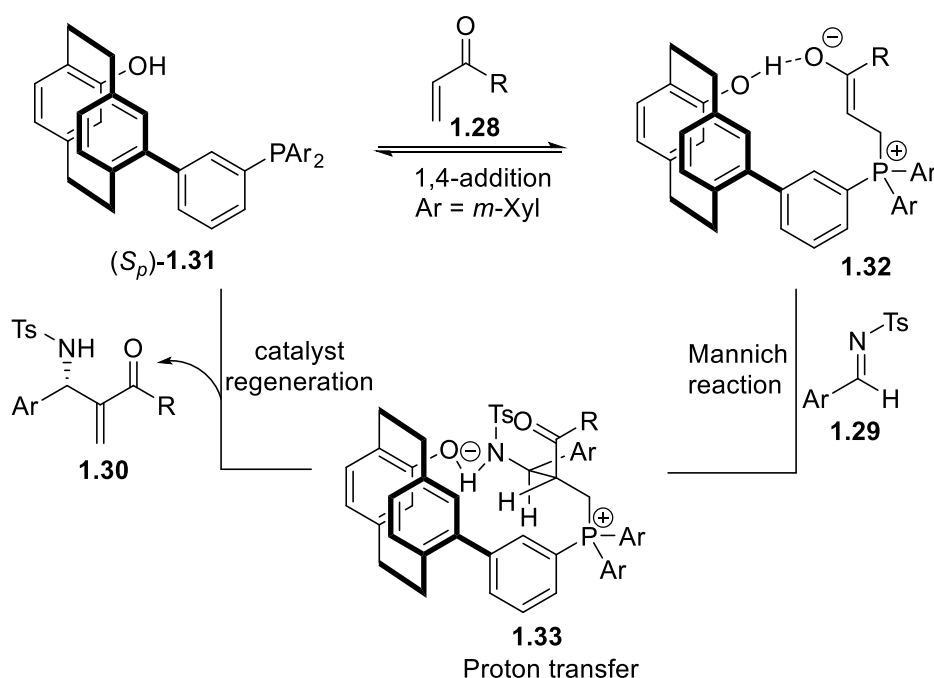
Scheme 1.6: Enantioselective hydrogenation of dehydroamino acid methyl ester **1.25**.

Below are the some examples of recently developed [2.2]paracyclophane-based ligands and their applications in asymmetric catalysis.

A range of planar chiral *pseudo-ortho*-substituted-[2.2]paracyclophane-phosphine-phenol catalysts were synthesised and studied in the aza-Morita-Baylis-Hillman (MBH) reaction of aldimines **1.29** with vinyl ketones **1.28** by Takenaga et al (Scheme 1.7a).⁴⁵ Of these catalysts, the one with the phosphino group in the *meta*-position of the aryl spacer group and hydroxyl functionality at the *pseudo-ortho* position **1.31** was found to be the most efficient. Here, the synergistic interaction of functional groups in the catalyst controls the proton transfer step and hence the enantioselectivity (Scheme 1.7b). The key characteristic of this catalyst is to produce the aza-MBH adducts **1.30** with an unprecedented short reaction time (5-30 min.-) and good enantioselectivity (93% *ee*).

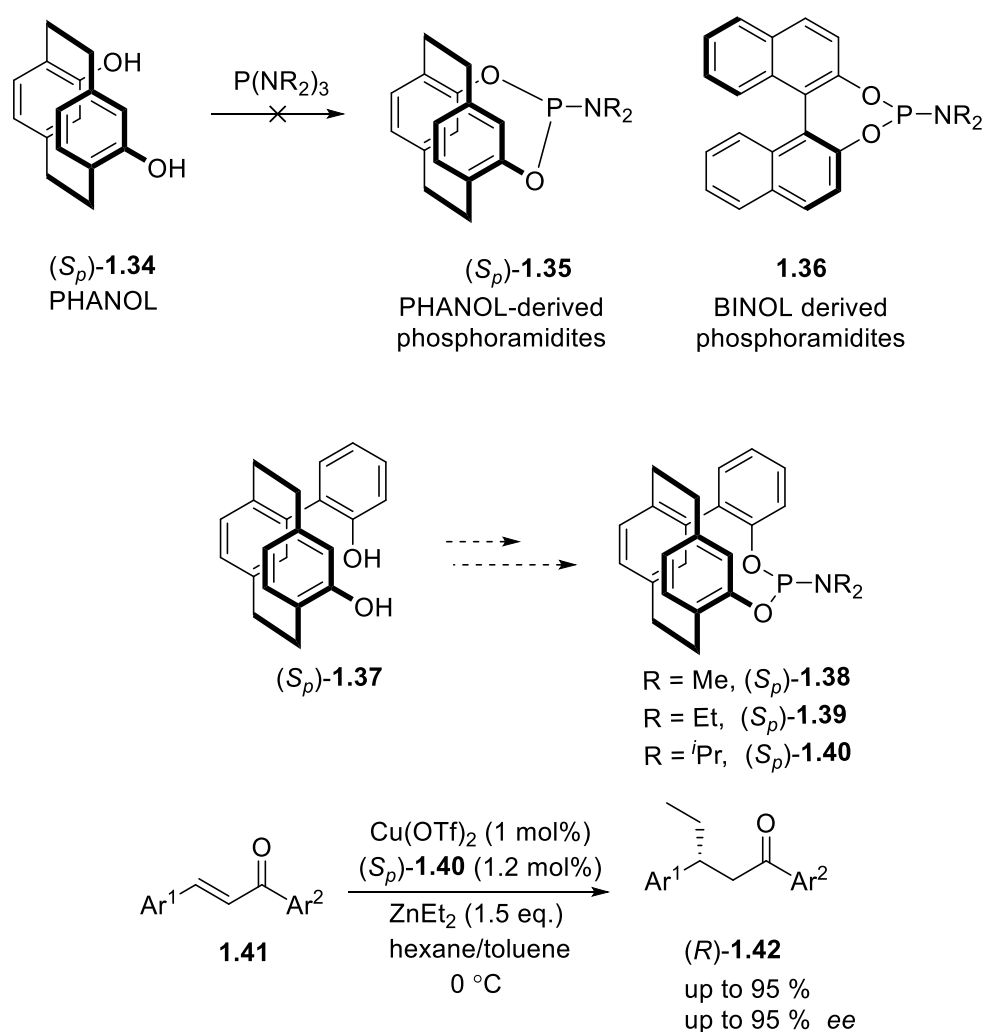


Scheme 1.7a: Aza-MBH reaction catalysed by [2.2]paracyclophane-based phosphine-phenol.



Scheme 1.7b: Influence of catalyst, [2.2]paracyclophane-based phosphine-phenol **1.31** in aza-MBH reaction.

Inspired by the success of axially chiral BINOL ligand and central chiral TADDOL phosphoramidate in asymmetric catalysis, Jiang et al. demonstrated the synthesis of a planar chiral [2.2]paracyclophane phosphoramidite.⁴⁶ In their initial attempt, the PHANOL framework **1.34** (*pseudo-ortho* dihydroxy derivatives) was too rigid to synthesise planar chiral phosphoramidite. Later, the additional phenyl spacer was introduced to impart flexibility and the desired ligands were synthesised. All of the newly synthesised ligands were screened in the copper-catalysed asymmetric conjugate addition of diethylzinc to chalcones **1.41** with a low catalyst loading of 1.0 mol% and the products **1.42** were obtained with high enantioselectivity (up to 95% *ee*, Scheme 1.8).

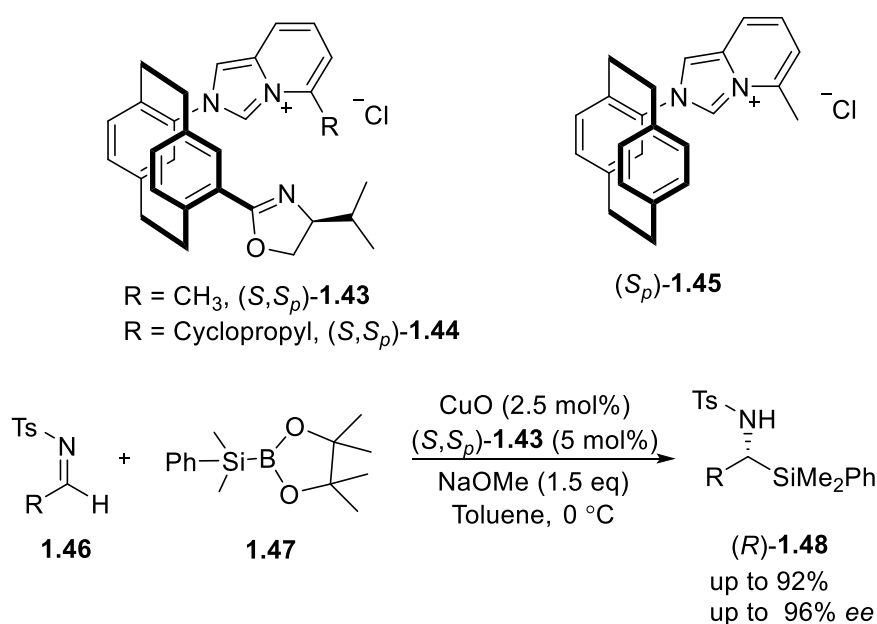


Scheme 1.8: Preparation of chiral phosphoramidite ligands and their application to copper-catalysed asymmetric conjugate addition of diethylzinc to chalcones.

1.4.2. Planar chiral [2.2]paracyclophane-derived *N*-heterocyclic carbene ligands

Bolm et al. reported the first carbene precursors derived from the [2.2]paracyclophane framework.⁴⁷ Since then many other examples have been reported.

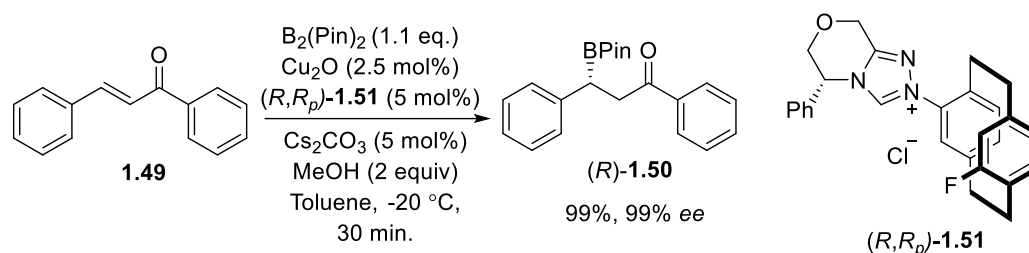
Recently, Wang et al. synthesised new [2.2]paracyclophane oxazoline-NHC ligands **1.43-1.45** derived from L-valinol with planar and central chirality (Scheme 1.9).⁴⁸ The main purpose of this study was to evaluate the effect of various substituents on the catalytic outcome of the different complexes. The oxazoline-carbene copper complex generated *in-situ* by the reaction of the oxazoline-substituted imidazolium (*S,S_p*)-**1.43** and CuO demonstrated an exceptionally high catalytic activity in the asymmetric 1,2-silylation of *N*-tosylaldimines **1.46**, affording chiral α -amino silanes **1.48** with excellent yields and enantioselectivities. The presence of an oxazoline ring had a major influence on the enantioselectivity of the products. Without it, the unsubstituted [2.2]paracyclophane-carbene ligand (*S_p*)-**1.45** catalysed the reaction but failed to induce high selectivity. The authors reasoned that the inhibition of free rotation around the C-N bond led to conformational stability of the copper complex with oxazoline-carbene bidentate ligand (*S,S_p*)-**1.43** over the monodentate carbene ligand **1.45**.



Scheme 1.9: Evaluation of [2.2]paracyclophane oxazoline-carbene ligands in the asymmetric 1,2-silylation of *N*-tosylaldimines.

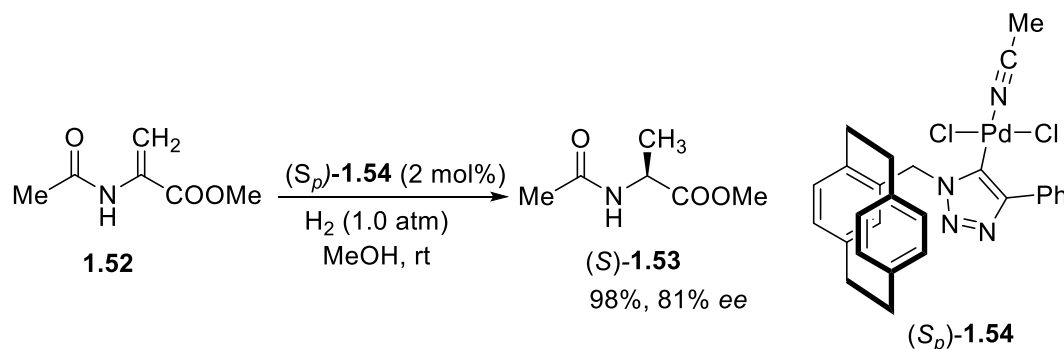
Fluorine-substituted [2.2]paracyclophane-based carbene precursor (*R,R_p*)-**1.51** was reported by Wang et al. (Scheme 1.10).⁴⁹ The main aim of this study was to investigate the effect of a fluorinated [2.2]paracyclophane backbone and the corresponding stereoelectronic effect on

catalytic activity. The copper-catalysed asymmetric β -boration of α,β -unsaturated ketones **1.49** to form chiral β -boryl ketones **1.50** was selected as a model reaction. It was observed that fluorination of the planar chiral carbene has a significant effect on the catalytic performance of the NHC-copper complex. A high conversion rate and good enantioselectivity (up to 99% *ee*) were achieved with the planar chiral imidazolium salts.



Scheme 1.10: Effect of fluorine-substituted [2.2]paracyclophane-based NHC in the asymmetric β -boration of α,β -unsaturated ketones.

Sankararaman and co-workers explored the reactivity of [2.2]paracyclophane-based chiral mesoionic carbene (MIC) metal complex in catalytic asymmetric hydrogenation (Scheme 1.11).⁵⁰ [2.2]Paracyclophane-based 1,2,3-triazole-5-ylidene-Pd complex **1.54** possessing labile acetonitrile (CH_3CN) ligand was synthesised and characterised. This complex **1.54** showed good enantioselectivity in the hydrogenation of prochiral alkene **1.52** at ambient conditions and 1.0 atmosphere of H_2 .

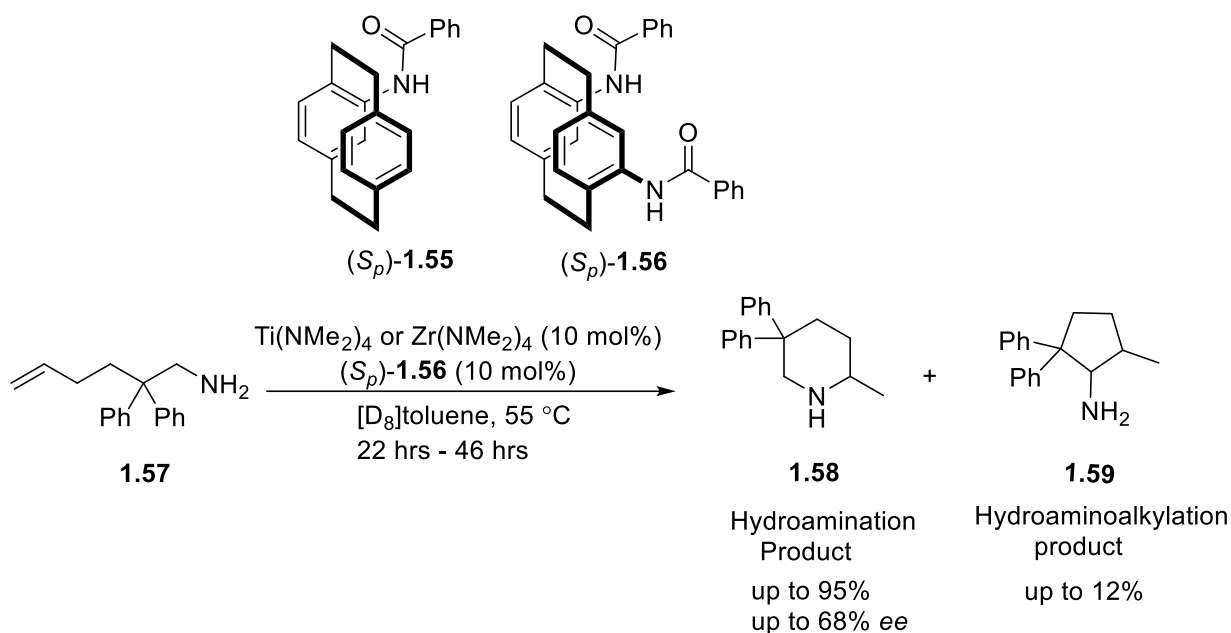


Scheme 1.11: Application of planar chiral NHC complex in catalytic asymmetric hydrogenation.

1.4.3. Planar chiral [2.2]paracyclophane-derived *N,O*-chelating ligands

Bräse and Schafer et al. have recently shown the potential of [2.2]paracyclophane-containing mono- and tethered bis(amide) ligands (S_p) -**1.55** and (S_p) -**1.56** in translating their planar chirality into central chirality of a hydroamination product (Scheme 1.12).⁵¹ These amides act as potent chelating ligands for titanium- and zirconium-catalysed hydroamination of aminoalkenes. The substrate **1.57** produced the hydroamination product **1.58** with

hydroaminoalkylation by-product **1.59** (from C-H activation). The ligand (*S_p*)-**1.56** with Ti(NMe₂)₄ proved superior forenantioselectivity (68% *ee*) and chemoselectivity (**1.58** vs. **1.59**: 36% vs. 6%) albeit in moderate yield and long reaction time. The reactivity of monoamide ligand (*S_p*)-**1.55** was excellent (95%) but failed to induce any enantiocontrol. The authors speculated the lack of enantiocontrol was due to free rotation of [2.2]paracyclophane framework, even though the 1,3-*N,O*-ligand is chelated to the metal center.



Scheme 1.12: Amido[2.2]paracyclophane-catalysed hydroamination reaction.

The general introduction above provides a brief overview of [2.2]paracyclophane derivatives and their potential in the stereoselective synthesis. Despite the recent advancements in [2.2]paracyclophane chemistry, the main limitation is the lack of elegant methods to synthesise the enantiomerically pure planar chiral derivatives. There are still many opportunities to explore before [2.2]paracyclophane derivatives show their full potential in asymmetric catalysis.

1.5. References

- (1) Tanner, M. E. Understanding Nature's Strategies for Enzyme-Catalyzed Racemization and Epimerization. *Acc. Chem. Res.* **2002**, *35*, 237.
- (2) Bolm, C.; Gladysz, J. A. Introduction: Enantioselective Catalysis. *Chem. Rev.* **2003**, *103*, 2761.
- (3) Noyori, R. Asymmetric Catalysis: Science and Opportunities (Nobel Lecture). *Angew. Chem. Int. Ed.* **2002**, *41*, 2008.
- (4) Mohr, J. T.; Krout, M. R.; Stoltz, B. M. Natural products as inspiration for the development of asymmetric catalysis. *Nature* **2008**, *455*, 323.
- (5) Walba, D. M. In *New Developments in Molecular Chirality*; Mezey, P. G., Ed.; Springer Netherlands: Dordrecht, 1991.

- (6) Schlögl, K. Stereochemistry, Berlin, Heidelberg, 1984; p 27.
- (7) Noyori, R.; Ohkuma, T. Asymmetric Catalysis by Architectural and Functional Molecular Engineering: Practical Chemo- and Stereoselective Hydrogenation of Ketones. *Angew. Chem. Int. Ed.* **2001**, *40*, 40.
- (8) Tye, H.; Comina, P. J. Catalytic asymmetric processes. *J. Chem. Soc. Perkin Trans.* **2001**, 1729.
- (9) Farrell, A.; Goddard, R.; Guiry, P. J. Preparation of Ferrocene-Containing Phosphinamine Ligands Possessing Central and Planar Chirality and Their Application in Palladium-Catalyzed Asymmetric Allylic Alkylation. *J. Org. Chem.* **2002**, *67*, 4209.
- (10) Bolm, C.; Muñiz, K. Planar chiral arene chromium(0) complexes: potential ligands for asymmetric catalysis. *Chem. Soc. Rev.* **1999**, *28*, 51.
- (11) Rosillo, M.; Domínguez, G.; Pérez-Castells, J. Chromium arene complexes in organic synthesis. *Chem. Soc. Rev.* **2007**, *36*, 1589.
- (12) Rozenberg, V.; Sergeeva, E.; Hopf, H. *Cyclophanes as Templates in Stereoselective Synthesis*: Wiley-VCH, Weinheim, **2004**, 435.
- (13) Tanaka, K. Catalytic Enantioselective Synthesis of Planar Chiral Cyclophanes. *Bull. Chem. Soc. Jpn.* **2017**, *91*, 187.
- (14) Liu, Z.; Nalluri, S. K. M.; Stoddart, J. F. Surveying macrocyclic chemistry: from flexible crown ethers to rigid cyclophanes. *Chem. Soc. Rev.* **2017**, *46*, 2459.
- (15) Friščić, T.; Macgillivray, L. R. Cyclophanes and Ladderanes: Molecular Targets for Supramolecular Chemists. *Supramol. Chem.* **2005**, *17*, 47.
- (16) Ortner, B.; Waibel, R.; Gmeiner, P. Indoloparacyclophanes: Synthesis and Dopamine Receptor Binding of a Novel Arylbioisostere. *Angew. Chem. Int. Ed.* **2001**, *40*, 1283.
- (17) Schlotter, K.; Boeckler, F.; Hübner, H.; Gmeiner, P. Fancy Bioisosteres: Novel Paracyclophane Derivatives As Super-Affinity Dopamine D3 Receptor Antagonists. *J. Med. Chem.* **2006**, *49*, 3628.
- (18) Hassan, Z.; Spuling, E.; Knoll, D. M.; Lahann, J.; Bräse, S. Planar chiral [2.2]paracyclophanes: from synthetic curiosity to applications in asymmetric synthesis and materials. *Chem. Soc. Rev.* **2018**, *47*, 6947.
- (19) Bodwell, G. J.; Nandaluru, P. R. Olefination Reactions in the Synthesis of Cyclophanes. *Isr. J. Chem.* **2012**, *52*, 105.
- (20) Elacqua, E.; Friščić, T.; MacGillivray, L. R. [2.2]Paracyclophane as a Target of the Organic Solid State: Emergent Properties via Supramolecular Construction. *Isr. J. Chem.* **2012**, *52*, 53.
- (21) Hopf, H. Guest Editorial: [2.2]Paracyclophane - After 60 Years, Stronger Than Ever. *Isr. J. Chem.* **2012**, *52*, 18.
- (22) Marrocchi, A.; Tomasi, I.; Vaccaro, L. Organic Small Molecules for Photonics and Electronics from the [2.2]Paracyclophane Scaffold. *Isr. J. Chem.* **2012**, *52*, 41.
- (23) McGlinchey, M. J.; Milosevic, S. From [10]Paracyclophane to Ferrocenophanones: The Search for Molecular Machines and Bio-Organometallic Anticancer Drugs. *Isr. J. Chem.* **2012**, *52*, 30.
- (24) Mohan, A.; Sankararaman, S. 1,2,3-Triazolophanes-Cyclophanes with an Array of Molecular Structures and Supramolecular Architectures. *Isr. J. Chem.* **2012**, *52*, 92.
- (25) Pochorovski, I.; Diederich, F. Fluorophore-Functionalized and Top-Covered Resorcin[4]arene Cavitands. *Isr. J. Chem.* **2012**, *52*, 20.
- (26) Rowlands, G. J. Planar Chiral Phosphines Derived from [2.2]Paracyclophane. *Isr. J. Chem.* **2012**, *52*, 60.
- (27) Schneider, J. F.; Fröhlich, R.; Paradies, J. [2.2]Paracyclophane-Derived Planar-Chiral Hydrogen-Bond Receptors. *Isr. J. Chem.* **2012**, *52*, 76.
- (28) Szwarc, M. The C–H Bond Energy in Toluene and Xylenes. *J. Chem. Phys.* **1948**, *16*, 128.
- (29) Brown, C. J.; Farthing, A. C. Preparation and Structure of Di-p-Xylylene. *Nature* **1949**, *164*, 915.
- (30) Rozenberg, V.; Sergeeva, E.; Hopf, H. *Cyclophanes as Templates in Stereoselective Synthesis*. *Modern Cyclophane Chemistry* **2004**, 435.
- (31) Paradies, J. [2.2]Paracyclophane Derivatives: Synthesis and Application in Catalysis. *Synthesis* **2011**, *2011*, 3749.

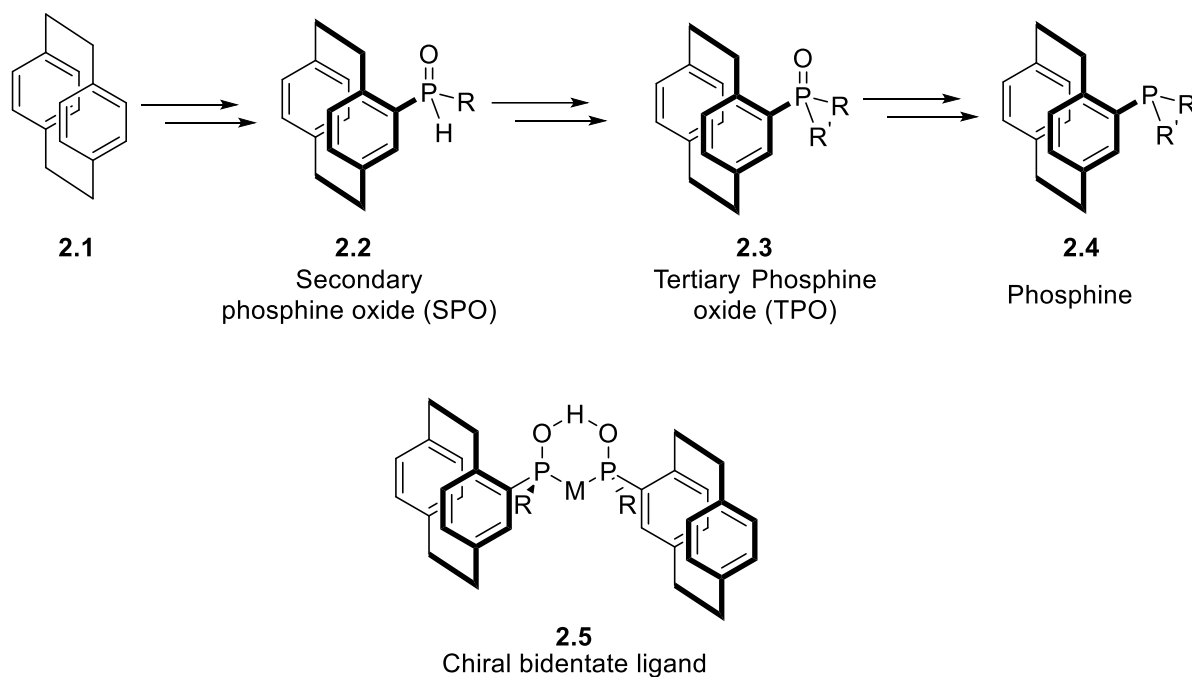
- (32) Singer, L. A.; Cram, D. J. Macro Rings. XXVII. Transannular Substituent Effects in π - π -Complexes of Paracyclophanes. *J. Am. Chem. Soc.* **1963**, *85*, 1080.
- (33) Gibson, S. E.; Knight, J. D. [2.2]Paracyclophane derivatives in asymmetric catalysis. *Org. Biomol. Chem.* **2003**, *1*, 1256.
- (34) Cahn, R. S.; Ingold, C.; Prelog, V. Specification of Molecular Chirality. *Angew. Chem. Int. Ed. Engl.* **1966**, *5*, 385.
- (35) Prelog, V.; Helmchen, G. Basic Principles of the CIP-System and Proposals for a Revision. *Angew. Chem. Int. Ed. Engl.* **1982**, *21*, 567.
- (36) Delcourt, M.-L.; Felder, S.; Benedetti, E.; Micouin, L. Highly Enantioselective Desymmetrization of Centrosymmetric pseudo-para-Diformyl[2.2]paracyclophane via Asymmetric Transfer Hydrogenation. *ACS Catal.* **2018**, *8*, 6612.
- (37) Banfi, S.; Manfredi, A.; Montanari, F.; Pozzi, G.; Quici, S. Synthesis of chiral Mn(III)-meso-tetrakis-[2.2]-p-cyclophanyl-porphyrin: a new catalyst for enantioselective epoxidation. *J. Mol. Catal. A: Chem.* **1996**, *113*, 77.
- (38) Rozenberg, V.; Dubrovina, N.; Sergeeva, E.; Antonov, D.; Belokon, Y. An improved synthesis of (*S*)-(+)- and (*R*)-(-)-[2.2]paracyclophane-4-carboxylic acid. *Tetrahedron: Asymmetry* **1998**, *9*, 653.
- (39) Rozenberg, V.; Danilova, T. y.; Sergeeva, E.; Vorontsov, E.; Starikova, Z.; Korlyukov, A.; Hopf, H. Resolution and Novel Reactions of 4-Hydroxy[2.2]paracyclophane. *Eur. J. Org. Chem.* **2002**, 468.
- (40) Rozenberg, V.; Kharitonov, V.; Antonov, D.; Sergeeva, E.; Aleshkin, A.; Ikonnikov, N.; Orlova, S.; Belokon, Y. Scalemic 2-Formyl-3-hydroxy[2.2]paracyclophane: A New Auxiliary for Asymmetric Synthesis. *Angew. Chem. Int. Ed. Engl.* **1994**, *33*, 91.
- (41) Paradies, J. [2.2]Paracyclophane Derivatives: Synthesis and Application in Catalysis. *Synthesis* **2011**, *23*, 3749.
- (42) Pye, P. J.; Rossen, K.; Reamer, R. A.; Tsou, N. N.; Volante, R. P.; Reider, P. J. A New Planar Chiral Bisphosphine Ligand for Asymmetric Catalysis: Highly Enantioselective Hydrogenations under Mild Conditions. *J. Am. Chem. Soc.* **1997**, *119*, 6207.
- (43) Berthod, M.; Mignani, G.; Woodward, G.; Lemaire, M. Modified BINAP: The How and the Why. *Chem. Rev.* **2005**, *105*, 1801.
- (44) Burk, M. J.; Hems, W.; Herzberg, D.; Malan, C.; Zanotti-Gerosa, A. A Catalyst for Efficient and Highly Enantioselective Hydrogenation of Aromatic, Heteroaromatic, and α,β -Unsaturated Ketones. *Org. Lett.* **2000**, *2*, 4173.
- (45) Takenaga, N.; Adachi, S.; Furusawa, A.; Nakamura, K.; Suzuki, N.; Ohta, Y.; Komizu, M.; Mukai, C.; Kitagaki, S. Planar chiral [2.2]paracyclophane-based phosphine-phenol catalysts: application to the aza-Morita-Baylis-Hillman reaction of *N*-sulfonated imines with various vinyl ketones. *Tetrahedron* **2016**, *72*, 6892.
- (46) Han, L.; Lei, Y.; Xing, P.; Zhao, X.-L.; Jiang, B. [2.2]Paracyclophane-Derived Monodentate Phosphoramidite Ligands for Copper-Catalyzed Asymmetric Conjugate Addition of Diethylzinc to Substituted Chalcones. *J. Org. Chem.* **2015**, *80*, 3752.
- (47) Focken, T.; Raabe, G.; Bolm, C. Synthesis of iridium complexes with new planar chiral chelating phosphinyl-imidazolylidene ligands and their application in asymmetric hydrogenation. *Tetrahedron: Asymmetry* **2004**, *15*, 1693.
- (48) Wang, X.; Chen, Z.; Duan, W.; Song, C.; Ma, Y. Synthesis of [2.2]paracyclophane-based bidentate oxazoline-carbene ligands for the asymmetric 1,2-silylation of *N*-tosylaldimines. *Tetrahedron: Asymmetry* **2017**, *28*, 783.
- (49) Wang, L.; Ye, M.; Wang, L.; Duan, W.; Song, C.; Ma, Y. Synthesis of fluorine-substituted [2.2]paracyclophane-based carbene precursors for copper-catalyzed enantioselective boration of α,β -unsaturated ketones. *Tetrahedron: Asymmetry* **2017**, *28*, 54.
- (50) Dasgupta, A.; Ramkumar, V.; Sankararaman, S. Catalytic asymmetric hydrogenation using a [2.2]paracyclophane based chiral 1,2,3-triazol-5-ylidene-Pd complex under ambient conditions and 1 atmosphere of H₂. *RSC Adv.* **2015**, *5*, 21558.
- (51) Braun, C.; Bräse, S.; Schafer, L. L. Planar-Chiral [2.2]Paracyclophane-Based Amides as Proligands for Titanium- and Zirconium-Catalyzed Hydroamination. *Eur. J. Org. Chem.* **2017**, 1760.

Chapter 2

The Synthesis of a [2.2]Paracyclophane-derived Secondary Phosphine Oxide and a Study of its Reactivity

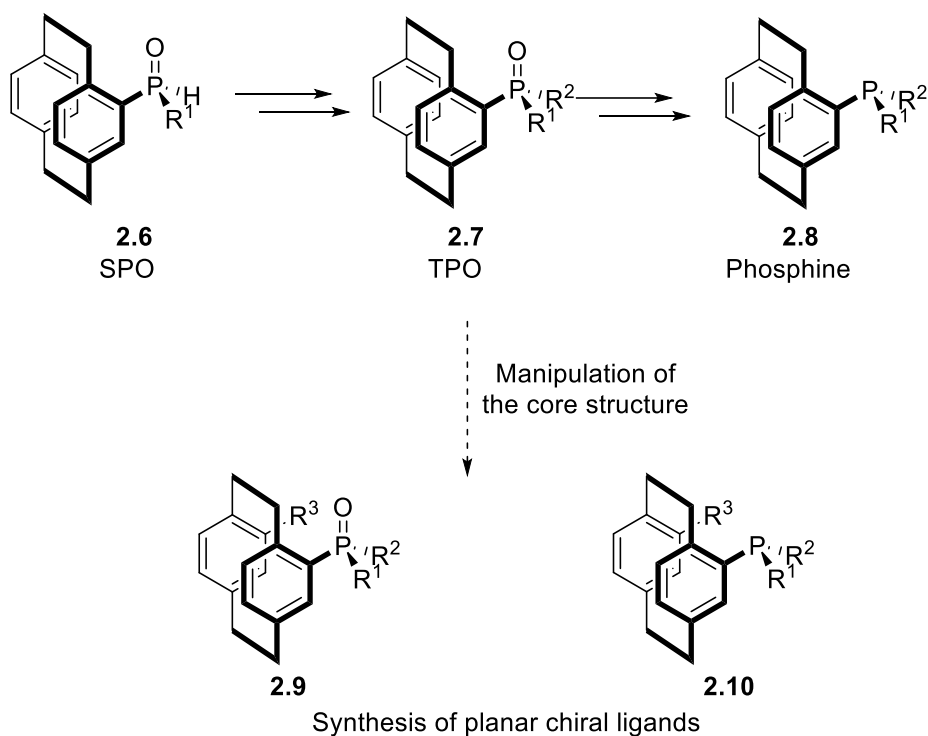
2.0. Secondary phosphine oxides: strategy and objectives

The first objective of this project was to synthesise new planar chiral secondary phosphine oxides (SPOs) based on the [2.2]paracyclophane framework (Scheme 2.1). These SPO ligands will be used to create new palladium and gold catalysts. Further, these new compounds will be screened for a range of key reactions as ligands in transition-metal catalysis.



Scheme 2.1: Synthesis of new planar chiral secondary phosphine oxides and phosphines with [2.2]paracyclophane backbone.

The second objective was the development of new methodologies that would permit enantiospecific synthesis of SPOs and their subsequent conversion into chiral phosphines. The latter will be achieved by derivatisation of both the [2.2]paracyclophane framework and the secondary phosphine functionality. This manipulation of the core structure should allow the modular synthesis of a range of ligands in which the properties of the molecule have been tuned to match a particular reaction (Scheme 2.2). The new SPOs and phosphines will be screened as planar chiral catalysts in metal-mediated transformations.



Scheme 2.2: Modular synthesis of a range of ligands.

Realising both of these objectives will permit the creation of a modular family of ligands in which the steric and electronic characteristics can be systematically varied. This stereochemical information is crucial to the rational design of new catalysts. Before discussing our attempts to achieve these two objectives, it is worth discussing about chiral phosphorus ligands, specifically, SPOs and phosphines.

2.1. Chiral phosphorus ligands

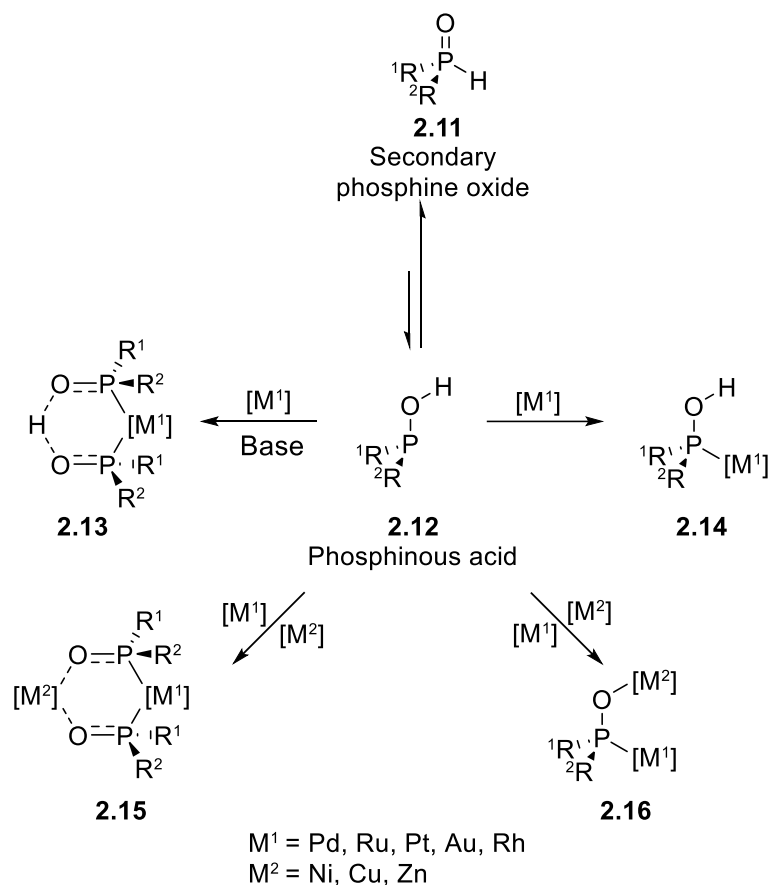
Phosphorus is an abundant element that forms many useful compounds. Organophosphorus molecules normally exist in one of two oxidation states, P(III) and P(V), and these have been used in a diverse range of applications including geochemistry,¹ pharmaceuticals,²⁻⁴ catalysis,⁵ materials,⁶⁻⁸ extracting agents for hydrometallurgy,⁹ and chemical reagents.¹⁰ *P*-Chirogenic compounds have been exploited in the synthesis of ligands for asymmetric catalysis.¹¹

Phosphorus-based ligands and their chiral versions are most commonly employed due to their inherent ability to strongly coordinate to transition metals. Moreover, they are configurationally stable due to the restricted pyramidal inversion at phosphorus. The phosphorus lone pair has greater *s*-character than *p*-character, and inversion must pass through a planar intermediate in which the lone pair is in a *p*-orbital. Interconversion between *s* and *p* orbital is difficult.

2.1.1. Secondary phosphine oxides

Phosphines are the most important type of ligands in transition-metal-catalysed reactions.¹² The number of known transition-metal complexes containing phosphine ligands is truly immense and include monodentate, bidentate, tridentate, and higher chelating phosphines, as well as a great variety of diverse substituents on phosphorus.¹³⁻¹⁵ However, many phosphines are sensitive to aerial oxidation and moisture, which makes them difficult to handle.¹⁶ Secondary phosphine oxides (SPOs) are seen as a potential solution to these issues.¹⁷ They are widely used in homogeneous metal catalysis due to their strong donor properties. They can also be precursors to chiral phosphines *via* cross-coupling,¹⁸ nucleophilic substitution,¹⁹ or alkylation²⁰⁻²² reactions. Organometallic complexes can also be synthesised using SPOs as ligands.²³

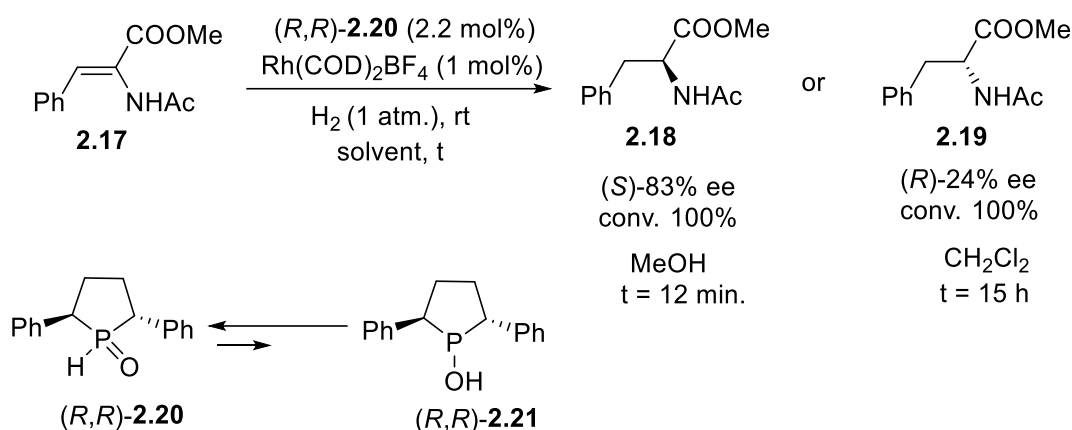
SPOs are air-stable pentavalent phosphorus species **2.11** that exist in equilibrium with the trivalent phosphinous acid **2.12** (Scheme 2.3). The equilibrium strongly favours the P(V) species until a transition metal is added, the equilibrium is then shifted towards the formation of P(III) monodentate ligand **2.14**. SPOs can form bimetallic species **2.15** & **2.16** by coordinating late-transition metals through the ‘soft’ phosphorus atom and early-transition metals through the ‘hard’ oxygen atoms or they can ‘self-assemble’ into a bidentate ligand **2.13** through a hydrogen-bonding or as a bimetallic bidentate complex **2.15**. These complexes have been shown to exhibit interesting reactivity in which the strongly electron-donating OH group may act as a directing group,²⁴⁻²⁶ or an acid.^{27,28}



Scheme 2.3: Tautomeric equilibrium and SPO complexes.

Achiral SPOs have been used as ligands in various transformations such as iridium-catalysed hydrogenation,²⁹ hydrolysis of nitriles,³⁰ amidation of nitriles³¹ and in palladium-catalysed coupling reactions and C-H activation.³² However, the synthetic accessibility of enantiopure SPOs is a fundamental challenge. Only a few examples of asymmetric transformations with enantioenriched SPO have been reported.^{14,33}

Fiaud et al. employed secondary phosphine oxide **2.20** in a Rh-catalysed asymmetric hydrogenation of (*Z*)-methyl-acetamido-cinnamate **2.17** (Scheme 2.4).³⁴ Interestingly, in this study, the solvent used had a profound impact on the stereochemical outcome of hydrogenation. In methanol, a polar protic solvent, full conversion to the *S*-enantiomer **2.18** was observed in 83% *ee*. The same catalyst in dichloromethane gave the opposite *R*-enantiomer **2.19** in 24% *ee*. Though the exact reason is not known, the authors suggested a different equilibrium between (*R,R*)-SPO **2.20** and (*R,R*)-hydroxyphosphine **2.21** for a stereochemical inversion.



Scheme 2.4: Rh-catalysed hydrogenation reaction with (R,R) -2.20 and $\text{Rh}(\text{COD})_2\text{BF}_4$.

Recently, heteroatom-substituted secondary phosphine oxides, (HASPOs) have emerged as useful ligands. Ackermann demonstrated that some N–P–N-type HASPOs **2.22** behave as excellent ligands in various reactions (Figure 2.1).^{35,36}

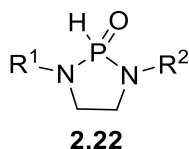
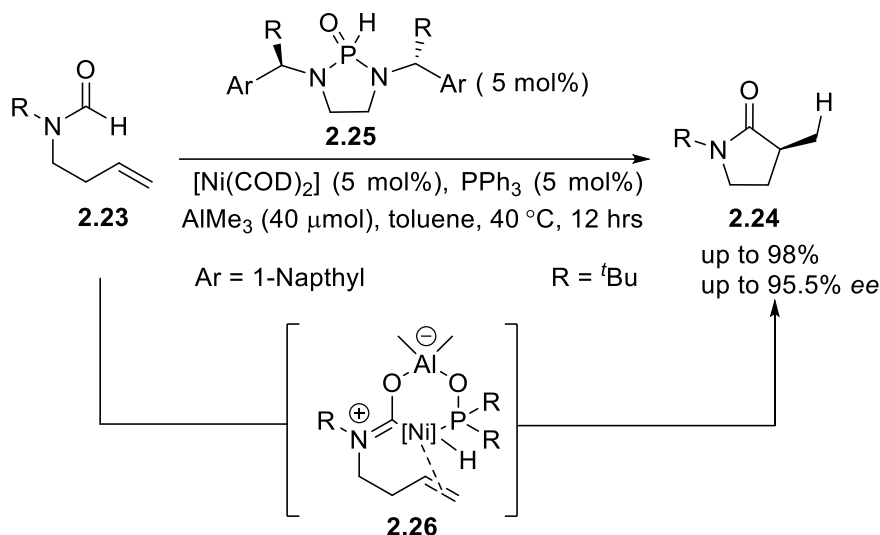


Figure 2.1: Heteroatom-substituted secondary phosphine oxides, (HASPOs).

Cramer and co-workers reported the use of HASPO **2.25** in the hydrocarbamylation of alkenes **2.23** to synthesise chiral γ -lactams **2.24** (Scheme 2.5).³⁷ In this reaction, the HASPO supports two metals, which work in concert to promote the reaction. The key to achieving high enantioselectivity is the chiral N–P–N-type SPO **2.25** possessing large 1-naphthyl and *t*-butyl substituents in a *pseudo* C_2 -symmetric fashion. The authors postulated that AlMe_3 coordinates the oxygen of the phosphinous acid form of the ligand **2.25** and releasing methane gas while retaining its Lewis acidic character. Subsequently, AlMe_3 activates the carbonyl of substrate **2.23** and hence activates the formamide C–H bond. $[\text{Ni}(\text{COD})_2]$ can now oxidatively insert into the activated C–H bond to form a six membered bimetallic heterocycle **2.26**. The resulting intermediate facilitates the hydrocarbamylation of alkenes (88% and 93% *ee*).



Scheme 2.5: Asymmetric Hydrocarbamylation.

2.1.2. Phosphines

Phosphines are extensively employed as ligands,³⁸ reagents,³⁹ and in catalysis³⁸ for preparing various pharmaceuticals, functional materials, and fine chemicals. Trivalent phosphines are used in various classic organic transformations, such as the Mitsunobu reaction,⁴⁰ and the Appel reaction.⁴¹ Such phosphines are also of special interest as ligands for diverse transition-metal catalysed reactions.⁴²

Chiral phosphines are classified into two categories, P-chiral phosphines and backbone chiral ligands. P-Chiral phosphines possess the stereogenic centre on the phosphorus atom (Figure 2.2).⁴² They have limited use due to a lack of efficient synthetic methods to form enantiopure P-chiral phosphines.

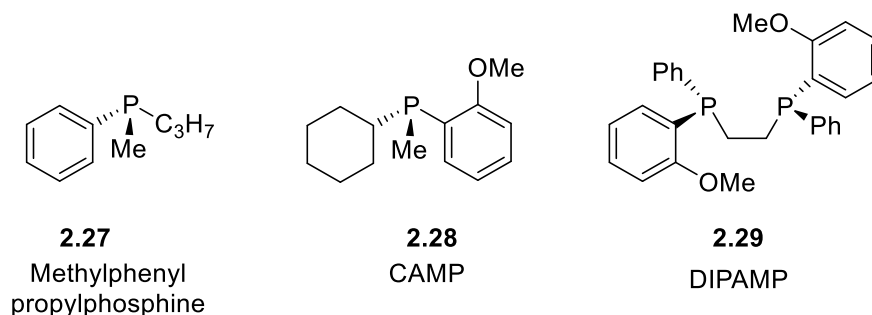


Figure 2.2: Representative examples of P-chiral phosphine ligands.

The majority of phosphines employed in asymmetric transformations have chiral frameworks.⁴³ This chiral backbone possesses either point, planar or axial chirality. In this type of molecules, two substituents on the phosphorus atoms are diastereotopic and are capable of

inducing an asymmetric environment around the reaction centre. Selected examples of ligands with a chiral backbone which have been applied in homogeneous catalysis are shown in Figure 2.3.

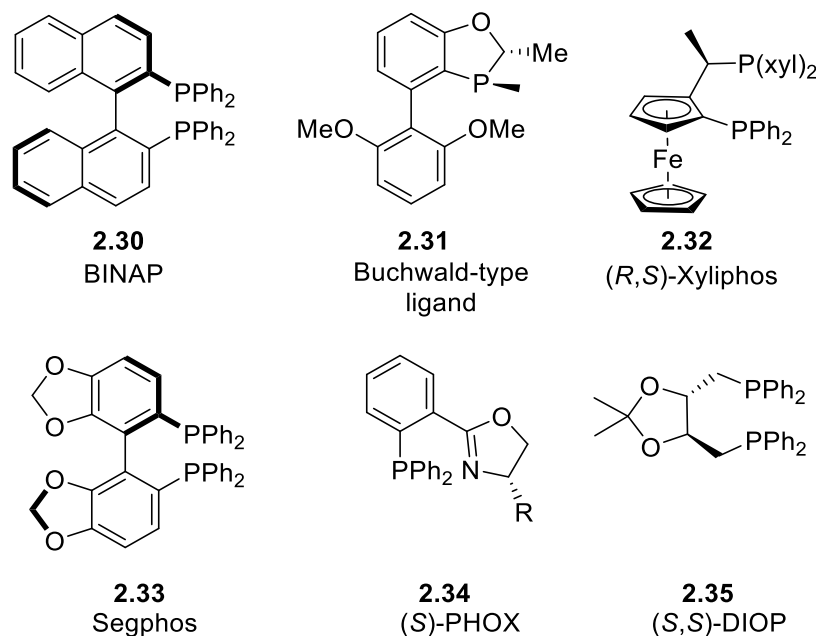
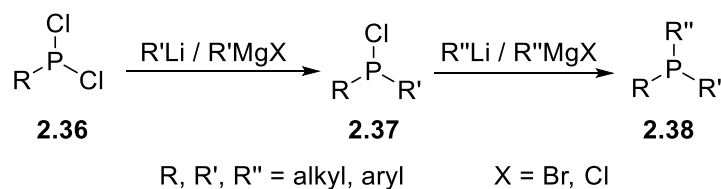


Figure 2.3: Selected phosphine ligands for industrial homogeneous catalysis.

Currently, four major methods are used for the synthesis of phosphines: (1) substitution reactions of P-Cl derivatives with nucleophiles; (2) substitution of electrophiles with alkali metal phosphides; (3) phosphination of alkenes, alkynes, or aromatic halides; and (4) reduction of phosphine oxides.

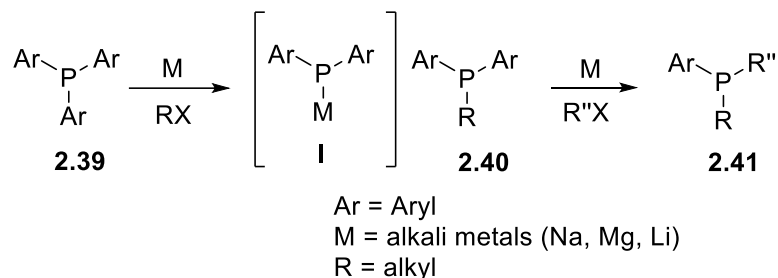
The first approach is mostly limited to the reactions of chlorophosphines **2.36** with Grignard or organolithium reagents (Scheme 2.6).⁴⁴



Scheme 2.6: Substitution reactions of P-Cl derivatives with nucleophiles.

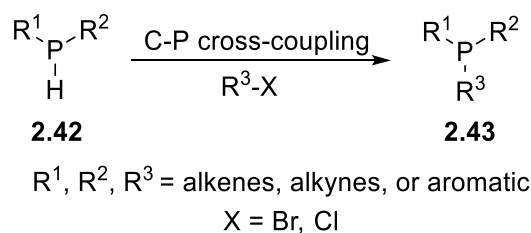
The second approach uses the reaction of an alkali metal with diaryl-, diarylhalo-, or triarylphosphines **2.39** (Scheme 2.7).⁴⁵ This strategy has the advantage that many triarylphosphines are commercially available. Others are readily made following the first approach. The reductive cleavage of triarylphosphines is the commonly used methodology but

is especially difficult to scale up since it requires sodium dispersions in oil. Classic metal ammonia reduction also introduces problems of handling, over-reduction, and operational safety.



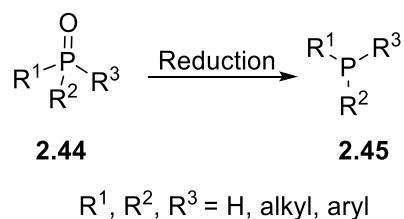
Scheme 2.7: Substitution of electrophiles with alkali metal phosphides.

The third approach involves C-P cross-coupling of alkenes, alkynes, or aromatic halides with phosphine **2.42** or a phosphine-borane (Scheme 2.8).⁴⁶



Scheme 2.8: C-P cross-coupling.

Synthesis of phosphines by the fourth approach - reduction of phosphine oxides is limited by the use of an excess of sensitive and/or highly expensive reducing agents, e.g. LiAlH₄, DIBAL-H or HSiCl₃/Et₃N, and HSiCl₃/PhSiH₃ (Scheme 2.9).⁴⁷ Due to harsh reaction conditions, only poor functional group tolerance is achieved.



Scheme 2.9: Reduction of phosphine oxides.

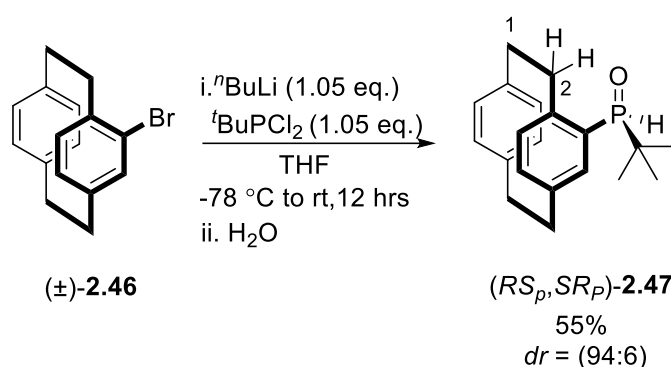
All of the above methods require multistage procedures, sensitive organometallic reagents, anhydrous conditions, and an inert atmosphere. Therefore, the development of metal-free and step-economic routes toward bulky phosphines remains a challenging task in organophosphorus and green chemistry.

Inspired by the success of chiral phosphorus-based ligands in asymmetric transformations,⁴⁸⁻⁵⁰ our first objective of this project was to synthesise new planar chiral secondary phosphine oxides (SPOs) based on the [2.2]paracyclophane framework.

2.2. Results and Discussion

2.2.1. Synthesis of monodentate SPO-based on [2.2]paracyclophane backbone

Our study began with the synthesis of $(RS_p,SR_P)^a$ -4-*tert*-butyl[2.2]paracyclophane phosphine oxide **2.47** to get an electron rich SPO (Scheme 2.10). The synthesis involved generating a highly nucleophilic organolithium species, 4-lithio[2.2]paracyclophane, from 4-bromo[2.2]paracyclophane **2.46** and reacting this with *tert*-butyldichlorophosphine under an inert argon atmosphere. The resulting chlorophosphine was hydrolysed in one-pot to furnish secondary (RS_p,SR_P) -**2.47** in 55% yield with a diastereomeric ratio of 94:6.



Scheme 2.10: Synthesis of (RS_p,SR_P) -4-*tert*-butyl[2.2]paracyclophane phosphine oxide **2.47**.

Several other reaction conditions were attempted in order to improve the reaction conversion such as heating the reaction mixture to reflux (Table 2.1, entry 1) or changing the solvent to dry diethyl ether (entry 2). However, both reactions provided even lower chemical conversions. Further, the formation of organomagnesium intermediate proved ineffective (entry 3).

Table 2.1: Deviation from the reaction conditions of scheme 2.10

Entry	Deviation from scheme 2.10	Yield ^{Isolated}
1	-78 °C to rt to reflux	30%
2	Et ₂ O	18%
3	Mg (1.05 eq.)	-

^a For compounds possessing both a stereogenic plane and a stereogenic centre the following nomenclature is used. S_p (lowercase P) refers to the planar chirality as defined from the C1 pilot atom and S_P (uppercase P) refers to phosphorus stereochemistry. For racemates ($RS, SR = R^*, S^*$) according to Cahn-Ingold-Prelog rules.

The fact that **2.47** formed with a high diastereomeric ratio (94:6, determined from the ^1H NMR spectrum of the crude product)^b indicated that this reaction proceeded with high stereoselectivity and that the *unlike* (RS_p,SR_p) diastereomer was favoured. Moreover, H-2 proton was observed downfield (3.94 ppm) in ^1H NMR spectrum, indicating the anisotropic influence of the proximal oxygen of the SPO (Scheme 2.10). The relative configuration of **2.47** was unambiguously determined as (RS_p,SR_p) by the single crystal X-ray diffraction technique (Figure 2.4).

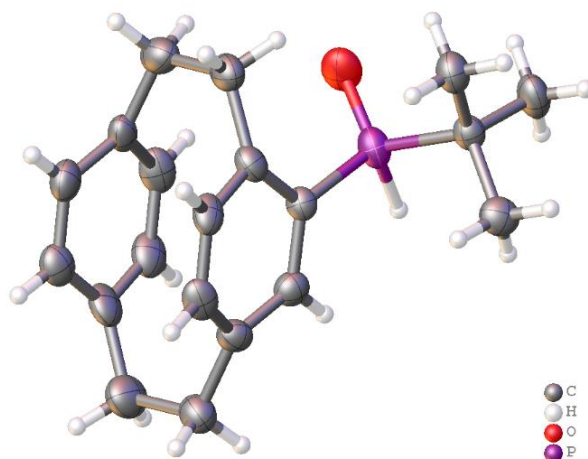
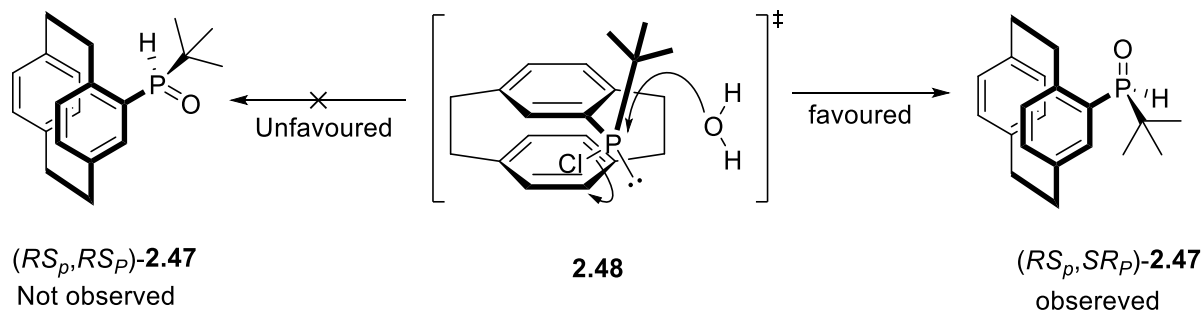


Figure 2.4. Crystal structure of (RS_p,SR_p)-4-*tert*-butyl[2.2]paracyclophane phosphine oxide **2.47**. (Ellipsoids are drawn at a 50% probability level.)

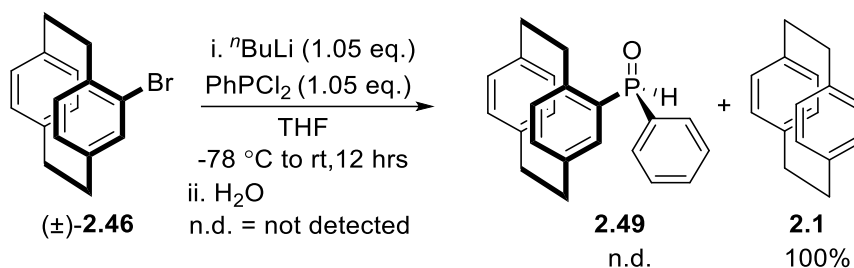
The origin of the diastereoselectivity is not clear. We believe that (RS_p,SR_p)-**2.47** is the more sterically encumbered diastereomer as the oxygen is forced into close proximity to the ethylene bridge. A possible explanation as to its formation might involve addition to the $^t\text{BuPCl}_2$ forming a single diastereomer of chlorophosphine **2.48** with the chlorine atom oriented towards the *ortho* position, in the least sterically demanding position. Hydrolysis then occurs with the inversion of the stereochemistry to give the congested phosphine oxide (Scheme 2.11).



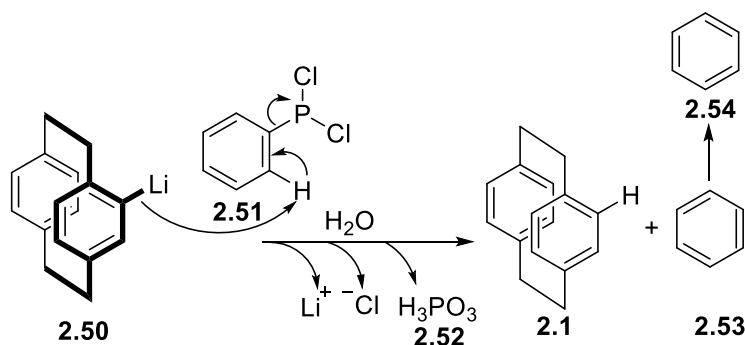
Scheme 2.11: Plausible intermediate to form a favourable diastereomer (RS_p,SR_p)-**2.47**.

^b The diastereomeric ratio of the compound **2.47** was determining from the integration of ^tBu peaks at 1.02 δ and 1.17 δ .

We also attempted to synthesise 4-phenyl[2.2]paracyclophane phosphine oxide **2.49** following the same approach (Scheme 2.12). However, the reaction did not proceed and only [2.2]paracyclophane **2.1** was recovered. This result suggests that the initial metal-halogen exchange is occurring efficiently, but the formation of the corresponding chlorophosphine is a problematic step. Based on 100% recovery of [2.2]paracyclophane, we speculated that the phenyl group of PhPCl₂ might be acting as a proton source *via* benzyne mechanism (Scheme 2.13).



Scheme 2.12: Attempted synthesis of (±)-4-phenyl[2.2]paracyclophane phosphine oxide **2.49**.



Scheme 2.13: Plausible mechanism for formation of **2.1** in scheme 2.12

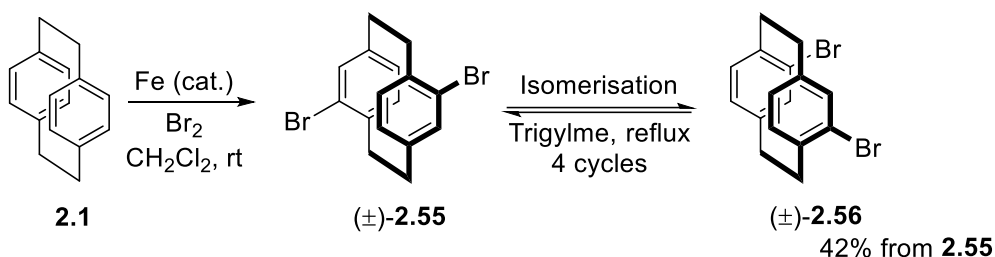
Alternative approaches like, transmetalation (Table 2.2, Li-Mg, entry 1) and the use of PCl₃ (entry 2), were not successful either.

Table 2.2: Deviation from the reaction conditions of scheme 2.12

Entry	Deviation from scheme 2.12	Yield
1	MgBr ₂ .OEt (1.05 eq.), PhPCl ₂ (1.05 eq.)	-
2	PCl ₃ (1.05 eq.), PhMgCl (1.05 eq.)	-

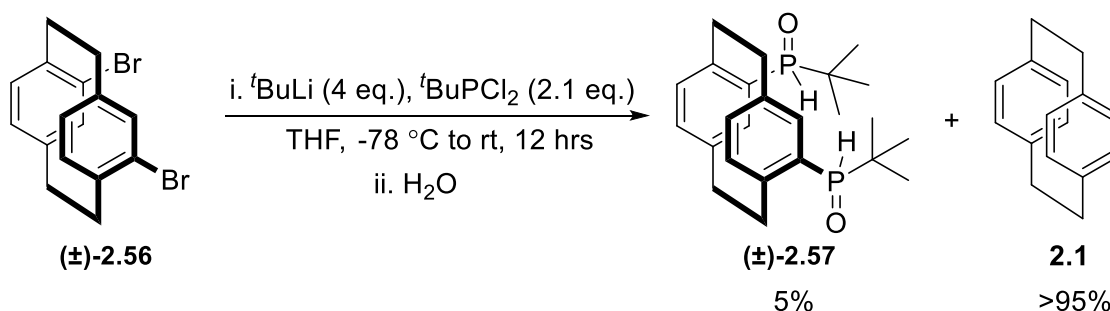
2.2.2. Synthesis of racemic bidentate-SPO based on [2.2]paracyclophane backbone

To synthesise a bidentate SPO, the *pseudo-ortho*-substituted pattern was selected as it is possible to construct a more efficient chiral pocket than the *pseudo-geminal*- or *ortho*-substituted paracyclophanes. First, the bromination was performed with [2.2]paracyclophane **2.1** to obtain *pseudo-para*-dibromo[2.2]paracyclophane **2.55**, which was later isomerised to the *pseudo-ortho*-dibromo[2.2]paracyclophane **2.56** (Scheme 2.14). The aromatic protons were observed downfield in ^1H NMR spectrum of **2.56** *cf.*, giving indication of complete isomerization.



Scheme 2.14: Bromination and isomerisation of *pseudo-para*-dibromo[2.2]paracyclophane **2.55** to *pseudo-ortho*-dibromo[2.2]paracyclophane **2.56**.

The preparation of (\pm) -**2.57** commenced with *rac*-4,12-dibromo[2.2]paracyclophane (\pm) -**2.56**, which after the halogen-metal exchange with $t\text{BuLi}$ was reacted with $t\text{BuPCl}_2$ at $-78\text{ }^\circ\text{C}$ under an inert argon atmosphere (Scheme 2.15). Unfortunately, only 5% of the desired SPO (\pm) -**2.57** was isolated. The major by-product was [2.2]paracyclophane **2.1** formed by protodebromination of (\pm) -**2.56**.

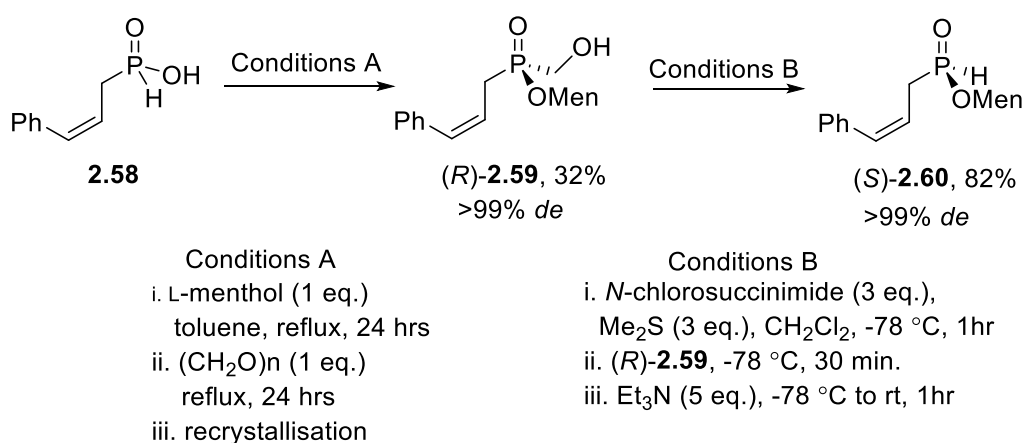


Scheme 2.15: Attempted synthesis of bidentate *pseudo-ortho* SPO (\pm) -**2.57**.

We next planned to resolve the chirality and separate the enantiomers of the major diastereomer of (R_S, S_R) -**2.47**. The section below summarises our attempts to synthesise enantioenriched SPO.

2.2.3. Attempted synthesis of enantioenriched SPO

The synthetic accessibility of enantiopure P-chiral compounds is a fundamental challenge which mainly lies in attaining individual enantiomers with high yields, and through straightforward procedures.⁵¹ Enantiomerically pure SPOs are normally obtained through chemical resolution or chromatographic separation but rarely by asymmetric synthesis.^{52,53} Early asymmetric routes were based on the use of chiral auxiliaries, with a menthol phosphinate being the most common.⁵⁴⁻⁵⁶ For example, Berger et al. synthesised cinnamyl-*H*-phosphonate (*S*)-**2.60** from cinnamyl-*H*-phosphinic acid **2.58** in high yield and diastereoselectivity.⁵⁶ First, **2.58** was esterified and hydroxymethylated in one-pot to give (*R*)-**2.59** (>99% *de*). Next, the Corey-Kim oxidation provided (*S*)-**2.60** in >99% *de* (Scheme 2.16).

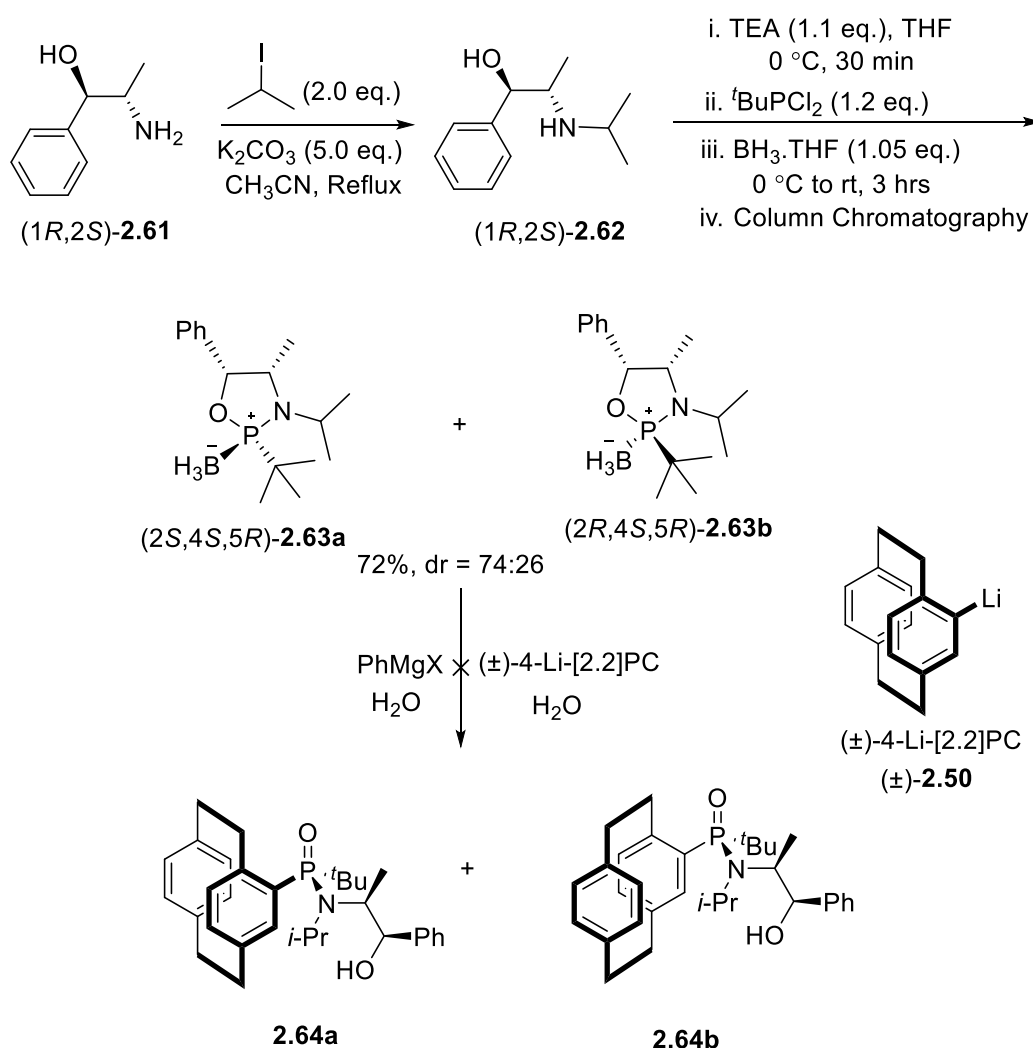


Scheme 2.16: Synthesis of P-stereogenic cinnamyl derivative using a menthol phosphinate.

We wanted to establish a new methodology that would allow efficient and general access to a range of enantioenriched SPOs. Our first approach was based on the norephedrine auxiliary (Scheme 2.17).

First, (1*R*,2*S*)-(-)-phenylpropanolamine **2.61** underwent alkylation to form (1*R*,2*S*)-2-(isopropylamino)-1-phenylpropan-1-ol **2.62**. Further reaction with ^tBuPCl₂ and BH₃.THF complex provided the borane oxazaphospholidine (BOP) as a 74:26 mixture of diastereomers **2.63a** & **2.63b** in 72% yield. After separation of diastereomers, the geometry of each diastereomer was determined using NOESY and COSY techniques. The configuration of major diastereomer **2.63a** was assigned to (2*S*,4*S*,5*R*) while minor **2.63b** to (2*R*,4*S*,5*R*) according to the Cahn–Ingold–Prelog (CIP) sequence rules.⁵⁷ Several attempts were performed on major diastereomer **2.63a** to test the ring-opening with (±)-4-litho[2.2]paracyclophane **2.50** and Grignard reagent (PhMgCl), but to no avail. We reasoned the failure of this reaction to the

steric hindrance of the *tert*-butyl substituent that prevented nucleophilic attack at the phosphorus centre.

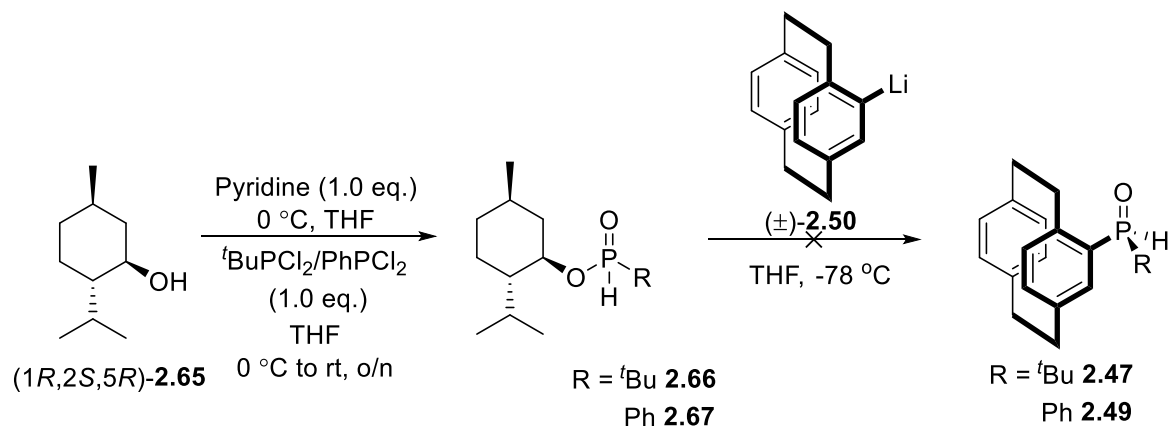


Scheme 2.17: Norephedrine-based approach to chiral SPO.

As the norephedrine-based approach was not looking promising, we decided to investigate a less hindered chiral auxiliary in the hope that addition would occur. (–)-Menthol has been successfully used for the multigramme-scale preparation of diastereomerically pure phosphinates.^{55,56} These diastereomerically enriched menthyl phosphinates are useful precursors in the synthesis of chiral secondary and tertiary phosphines.

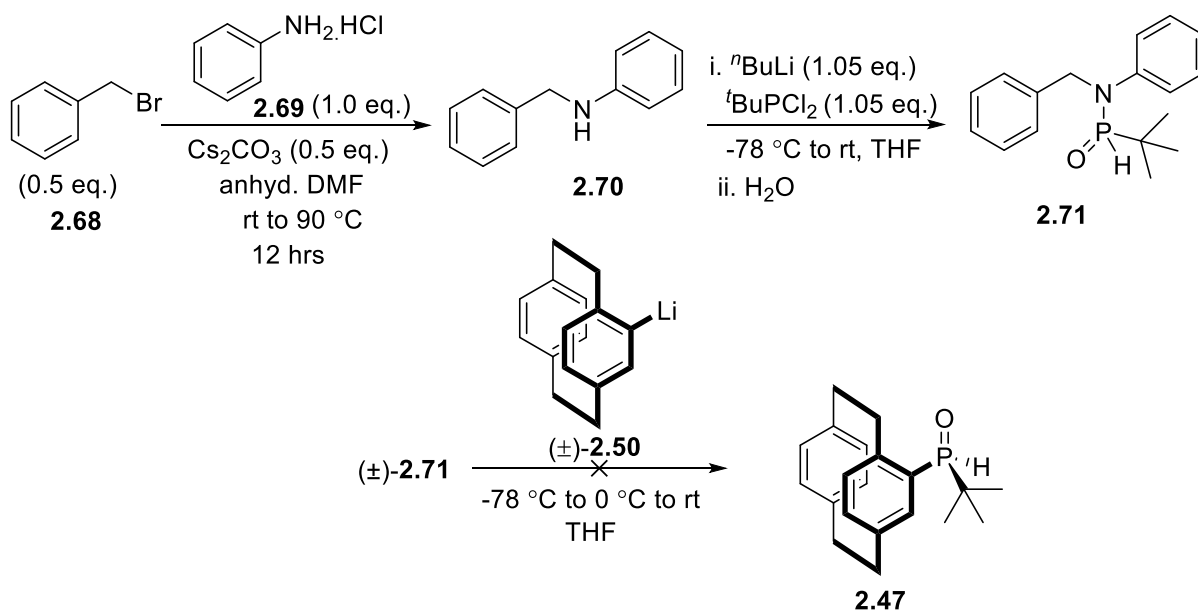
The starting materials for this synthesis, the unsymmetrically substituted menthyl phosphinates (1*R*,2*S*,5*R*)-2.66 & (1*R*,2*S*,5*R*)-2.67, were obtained by the reaction of the corresponding *t*BuPCl₂ or PhPCl₂ with (–)-menthol in the presence of pyridine (Scheme 2.18). Recrystallisation of the menthyl esters (1*R*,2*S*,5*R*)-2.66 & (1*R*,2*S*,5*R*)-2.67 from pentane or

hexane failed to resolve the diastereomers. Further, the reaction of menthyl phosphinates with 4-lithio[2.2]paracyclophane **2.50** did not proceed.



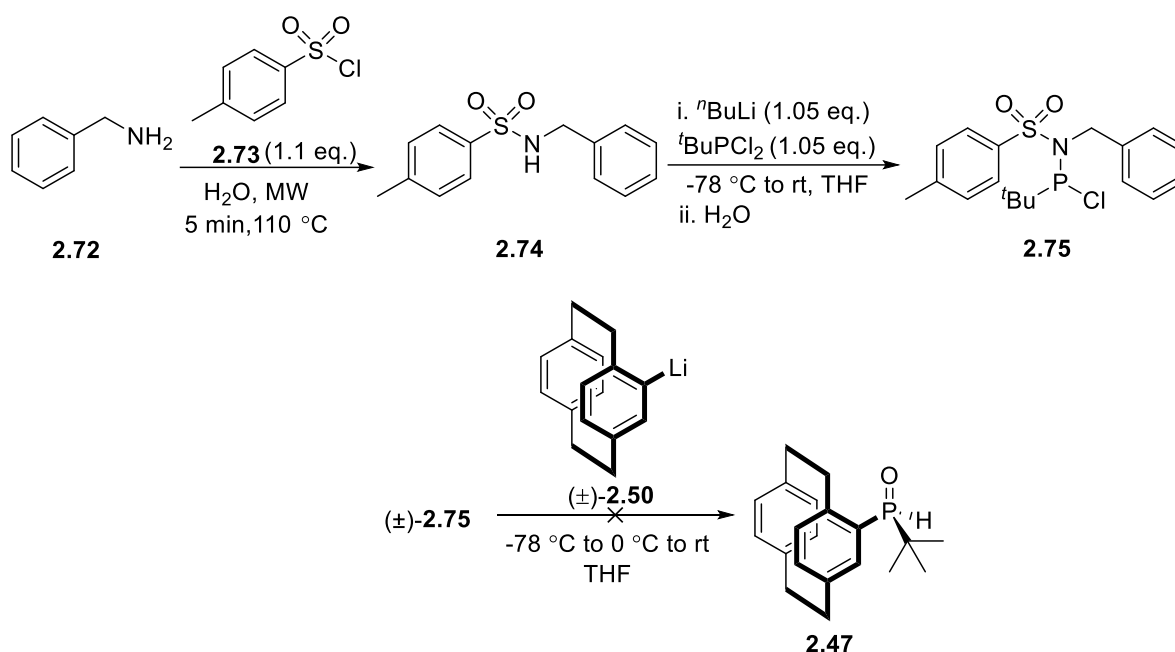
Scheme 2.18: (–)-Menthol-based approach for chiral SPO.

We planned to synthesise aza-SPO so that we could substitute the P-N bond and make our desired SPO. (Scheme 2.19 & 2.20). First, benzyl aniline **2.70** was prepared by reacting benzyl bromide **2.68** with aniline hydrochloride **2.69** in anhydrous DMF using Cs_2CO_3 as a base at 90°C . Subsequently, lithium *N*-benzylanilide was prepared and reacted with $t\text{BuPCl}_2$ at -78°C in dry THF followed by the addition of H_2O to give **2.71**. Unfortunately, the further reaction of **2.71** with 4-lithio-[2.2]paracyclophane **2.50** failed to produce the desired product (Scheme 2.19).



Scheme 2.19: Benzylaniline as an auxiliary-based approach for achiral SPO.

At this stage, the strategy was modified to use the sulfonamide precursor because of its electron-withdrawing nature would make it a better leaving group aiding transfer to 4-lithio[2.2]paracyclophane **2.50**. Benzyl amine **2.72** was converted to sulfonamide under microwave conditions at 110 °C in H₂O as solvent. Attempted synthesis of amino-SPO serendipitously gave an aminophosphine chloride **2.75**. We confirmed the compound **2.75** with different spectroscopy techniques. The HRMS spectra also showed a parent ion peak at 406.0762 m/z with the chlorine isotope pattern. While we anticipated that **2.75** would be a better transfer reagent as the phosphorus would be more electrophilic and chloride a good potential leaving group, the compound remained unreactive and no addition was observed either with aryl lithium or with aryl magnesium chloride (Scheme 2.20).



Scheme 2.20: Tosylbenzylamine as an auxiliary-based approach for achiral SPO.

However, after several attempts, we were not successful in synthesising the enantioenriched SPO. We then decided to move forward to prepare monodentate and bidentate metal complexes with (*RS_p,SR_p*)-**2.47** SPO and explore their reactivities in various organic transformations.

2.2.4. Attempted synthesis of phosphinous acid-coordinated mono- and binuclear palladium (II) & gold(I) complexes

The coordination chemistry of symmetrical ($R^1 = R^2$) and nonsymmetrical ($R^1 \neq R^2 =$ alkyl, aryl) phosphinous acids R^1R^2POH with transition-metal salts is of great interest due to their applications in homogeneous catalysis and asymmetric catalysis using SPOs.⁵⁸⁻⁶² They do exist as monodentate ligands, but more frequently form bidentate ligands with the oxygen functionality acting as a bridge. Generally, bidentate ligands self-assemble through hydrogen bonds.

A number of simple palladium complexes containing phosphinous acid ligands have been studied in the past decade. These complexes are highly efficient catalysts in various cross-coupling reactions e.g. Suzuki, Heck, Kumada, Negishi, and Stille,^{63,64} hydroformylation reactions,⁶⁵ and asymmetric allylic substitution.⁶⁶ Recently, Li reported that Combiphos complexes are efficient catalysts in C-C, C-N, and C-S bond-forming reactions (Figure 2.5).⁶³

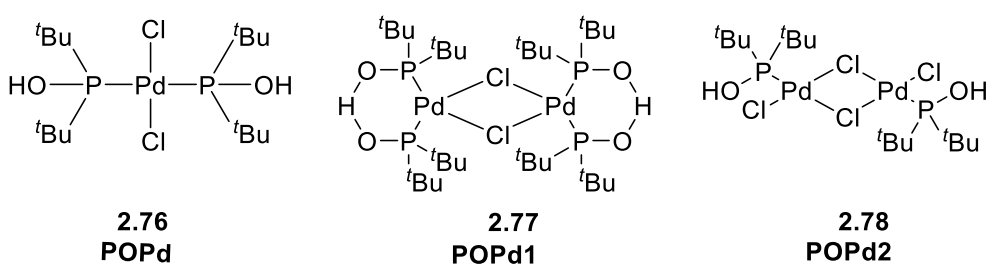
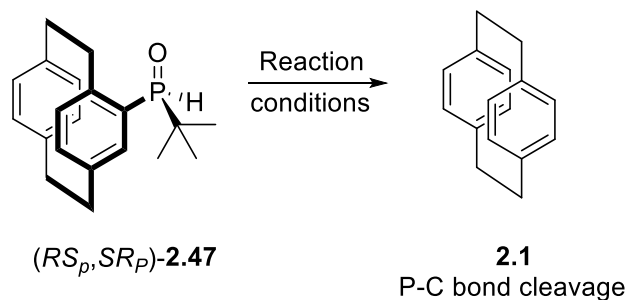


Figure 2.5: Li's Combiphos catalysts.

Considering the impressive success of metal complexes in various organic transformations, we sought to prepare palladium complexes with SPO (RS_p,SR_p)-**2.47** (Scheme 2.21, Table 2.3). Initial attempts with different palladium sources ($[PdCl_2(CH_3CN)_2]$ and $[Pd(COD)Cl_2]$) and changing solvents (dioxane and CH_2Cl_2) did not help to form the desired complex, and only starting material was observed. The failure of forming Pd(II)-SPO-**2.47** complex(es) was reasoned to the presence of a mixture of diastereomers along with potential geometrical isomers. In further attempts, the reaction of (RS_p,SR_p)-**2.47** with 0.5 eq. of $Pd(OAc)_2$ led to its decomposition resulting in the scission of the P-C bond, elimination of the phosphorous-containing fragment, and formation of the [2.2]paracyclophane **2.1** (entry 2 & 3).

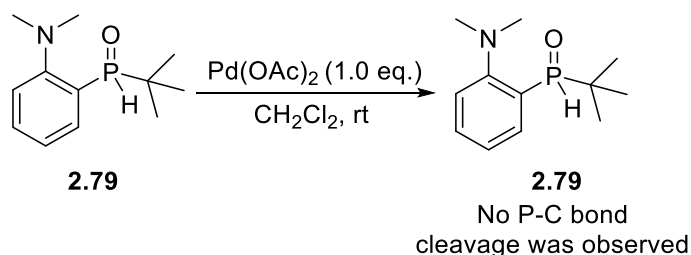


Scheme 2.21: Attempted mono and binuclear palladium complex formation with (RS_p, SR_p) -**2.47**.

Table 2.3: Reaction conditions for palladium complex formation with SPO (RS_p, SR_p) -2.47****

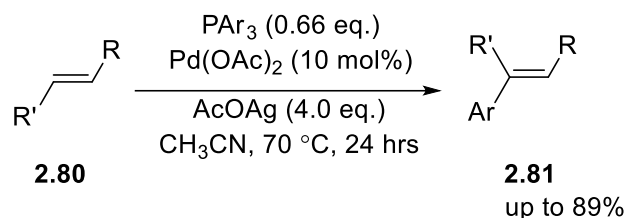
Entry	Reaction conditions	Observation
1	$[PdCl_2(CH_3CN)_2]$ (1.0 eq.) / $Pd(COD)Cl_2$ (1.0 eq.) Toluene / Dioxane / CH_2Cl_2 , rt / reflux	(RS_p, SR_p) - 2.47 recovered
2	$Pd(OAc)_2$ (1.0 eq.), PhMe, 50 °C, 2 hrs	P-C cleavage 2.1
3	$Pd(OAc)_2$ (1.0 eq.), CH_2Cl_2 , rt	P-C cleavage 2.1
4	NaOAc (1.0 eq.), $CDCl_3$, rt	(RS_p, SR_p) - 2.47 recovered

Interested in why C-P cleavage was observed only upon treatment with $Pd(OAc)_2$, we performed two control experiments. The first (entry 4) used NaOAc. Conversely, such C-P bond cleavage was not observed with the different acetate source. The second looked at another electron-rich SPO. We carried out reaction between *tert*-butyl(2-(dimethylamino)phenyl)phosphine oxide **2.79** and a stoichiometric quantity of $Pd(OAc)_2$. However, the C-P bond remained intact in **2.79** (Scheme 2.22). These results suggest that the combination of the *tert*-butyl SPO and [2.2]paracyclophane activates the C-P bond.



Scheme 2.22: Effect of $Pd(OAc)_2$ on *tert*-butyl(2-(dimethylamino)phenyl)phosphine oxide **2.79**.

Generally, Pd-mediated cleavage of C-P bonds is unusual. There have been reports of triarylphosphine (PAr_3) acting as a source of the aryl moiety in cross-coupling reactions when $\text{Pd}(\text{OAc})_2$ was employed in sub-stoichiometric quantity.⁶⁷⁻⁷⁰ For example, Xu and co-workers reported that the aryl group of PAr_3 could be transferred through C-P bond cleavage in the presence of a palladium catalyst (Scheme 2.23).⁷¹

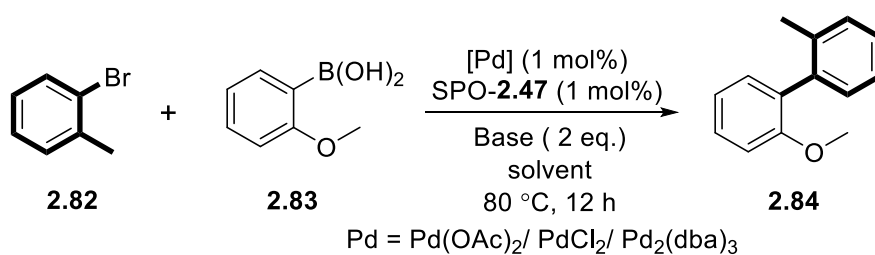


Scheme 2.23: Palladium-catalysed arylation of olefins by PAr_3 .

The formation of palladium complex with SPO-2.47 was not promising, but we could see if they can be formed *in-situ*. We decided to evaluate the role of SPO-2.47 as a potential ligand with an external source of palladium catalyst.

2.2.4.1. Investigation of the role of SPO-2.47 ligand in palladium-catalysed coupling reactions

First, we choose to perform the Suzuki-Miyaura cross-coupling reaction of electronically deactivated coupling partners 2-bromotoluene **2.82** and 2-methoxyboronic acid **2.83** to evaluate the reactivity of SPO-2.47 by using different palladium sources: $\text{Pd}(\text{OAc})_2$, PdCl_2 , $\text{Pd}_2(\text{dba})_3$, bases and solvents (Scheme 2.24, Table 2.4).



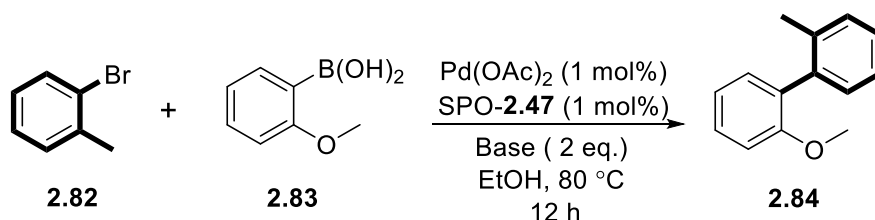
Scheme 2.24: SPO-2.47-catalysed Suzuki-Miyaura cross-coupling.

Table 2.4: Screening conditions for Suzuki-Miyaura Cross Coupling

Entry	Solvent	Base	Yield ^a
1	Toluene	Cs ₂ CO ₃	PdCl ₂ 10%
			Pd ₂ (dba) ₃ 12%
			Pd(OAc) ₂ 19%
2	EtOH	Cs ₂ CO ₃	PdCl ₂ 19%
			Pd ₂ (dba) ₃ 9%
			Pd(OAc) ₂ 23%
3	EtOH	NaO ^t Bu	PdCl ₂ 13%
			Pd ₂ (dba) ₃ 11%
			Pd(OAc) ₂ 24%
4	EtOH	CsF	Pd(OAc) ₂ 5%
5	H ₂ O	K ₃ PO ₄	-

^aIsolated Yield

In the initial reactions conditions by varying different palladium catalysts while keeping Cs₂CO₃ and toluene constant, the reaction with Pd(OAc)₂ gave the best conversion among three (entry 1). The product formation was slightly increased with polar solvent ethanol (entry 2) as well as with NaO^tBu (entry 3). However, the reaction with CsF and K₃PO₄/H₂O did not show much promise (entry 3 & 4). Based on the optimal conversion in Pd(OAc)₂ and ethanol conditions, the next screening was carried out using different bases (Scheme 2.25, Table 2.5).

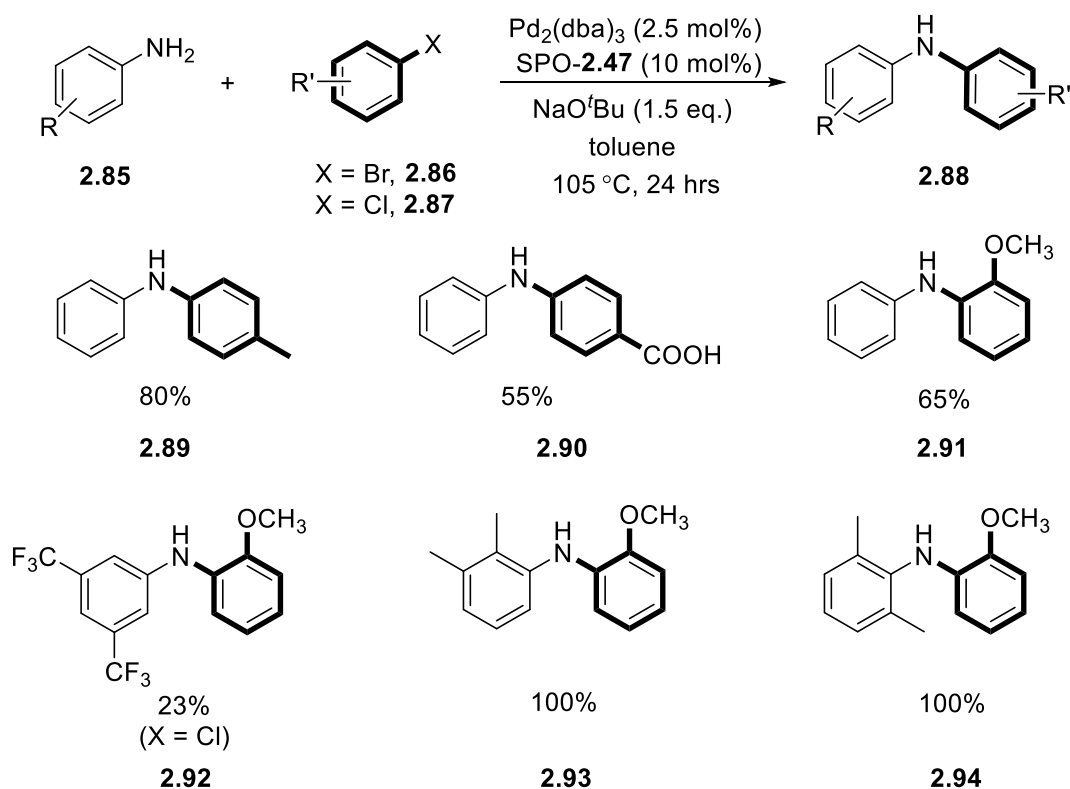
**Scheme 2.25:** SPO-2.47-catalysed Suzuki-Miyaura cross-coupling.**Table 2.5: Screening conditions for Suzuki-Miyaura Cross Coupling**

Entry	Base	% Yield ^a
1	CsF	24
2	KO ^t Bu	11
3	NaOH	24
4	K ₂ CO ₃	20
5	K ₃ PO ₄	45
6	KOH	45
7	KF	46
8	Cs ₂ CO ₃	35
9	NaO ^t Bu	64

^aGC yield is determined using *p*-nitrotoluene as an internal standard.

The reaction conversion was observed in the same range (~20%) as previous conditions with CSF, NaOH, and K₂CO₃ (entry 1, 2, & 3). Surprisingly, the product formation was nearly doubled with K₃PO₄, KOH and KF (entry 5, 6, & 7). Among all of the bases screened, the optimal conversion was obtained with NaO^tBu (entry 9). These results suggest that SPO-**2.47** is a competent ligand to catalyse the Suzuki reaction between unactivated coupling partners at 1 mol% scale.

We next moved to evaluate the catalytic potential of SPO-**2.47** in Buchwald-Hartwig amination reactions (Scheme 2.26). The results were more promising. Both electron-rich and electron-poor aryl bromides can be coupled to various anilines including sterically demanding substrates.



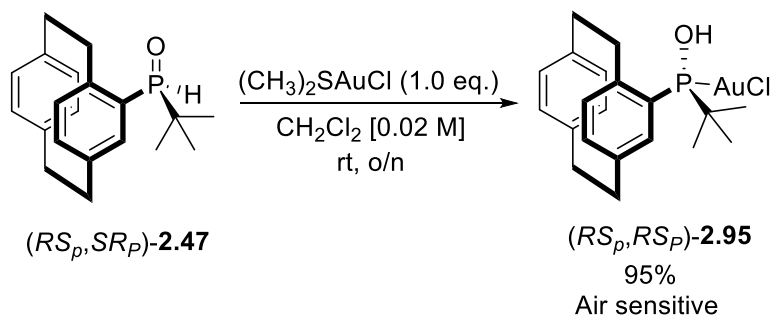
Scheme 2.26: Buchwald-Hartwig coupling of aryl bromides (unless otherwise noted) and anilines.

After evaluating the potential of SPO-**2.47** in palladium-catalysed cross-coupling reactions, we decided to attempt the complex formation with another metal and chose gold. To the best of our knowledge, there has been only a single report of an Au(I)-SPO complex being used in catalysis.⁷²

2.2.4.2. Synthesis of SPO-67-Au(I) complex and investigation of its catalytic potential

Homogeneous gold catalysis has emerged as a highly versatile synthetic tool for the construction of carbon-carbon or carbon-heteroatom bonds.⁷³⁻⁷⁵ Echavarren,⁷⁶ Fürstner,⁷⁷ and Toste⁷⁸ developed enyne cycloisomerisations in the presence of cationic gold(I) complexes. The nature of the ligand coordinated to the gold centre plays a major role in the reactivity and selectivity of gold-catalysed reactions.

The synthesis of the SPO-Au(I) complex **2.95** was readily achieved by following Schmidbaur's procedure (Scheme 2.27).⁷² The complex **2.95** was air-sensitive and had to be stored under an inert atmosphere. Despite this, the formation of the complex **2.95** was confirmed by ¹H and ³¹P NMR spectroscopy. The ³¹P NMR peak was shifted to 125.63 ppm (P^(III) in **2.95**) from the 57.81 ppm P^(V) observed in SPO-**2.47**.

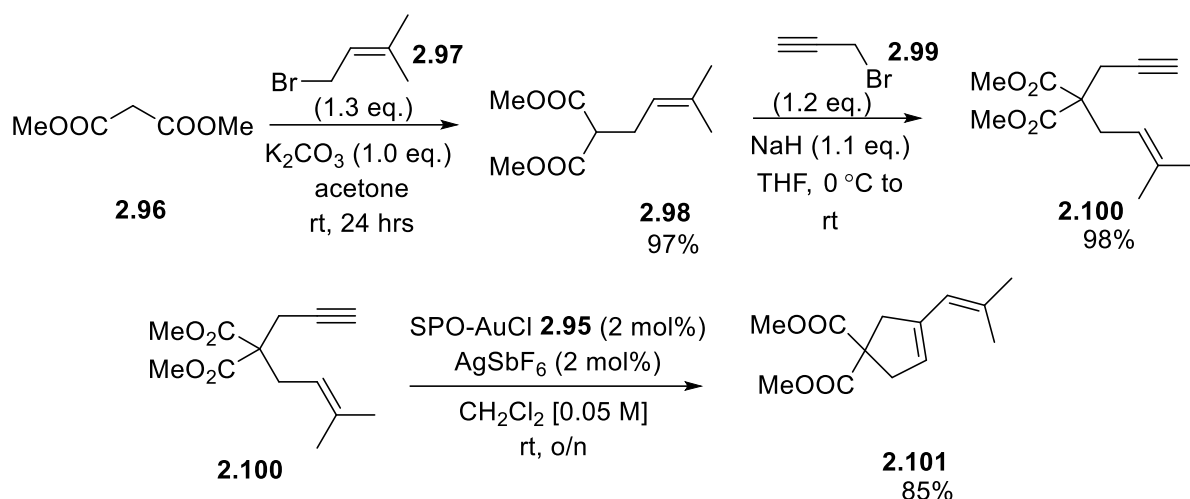


Scheme 2.27: Au(I)-complex formation with SPO-**2.95**.

Having successfully synthesised the desired Au(I)-SPO-**2.95** complex, we proceeded to evaluate its catalytic potential in cycloisomerisation reactions.

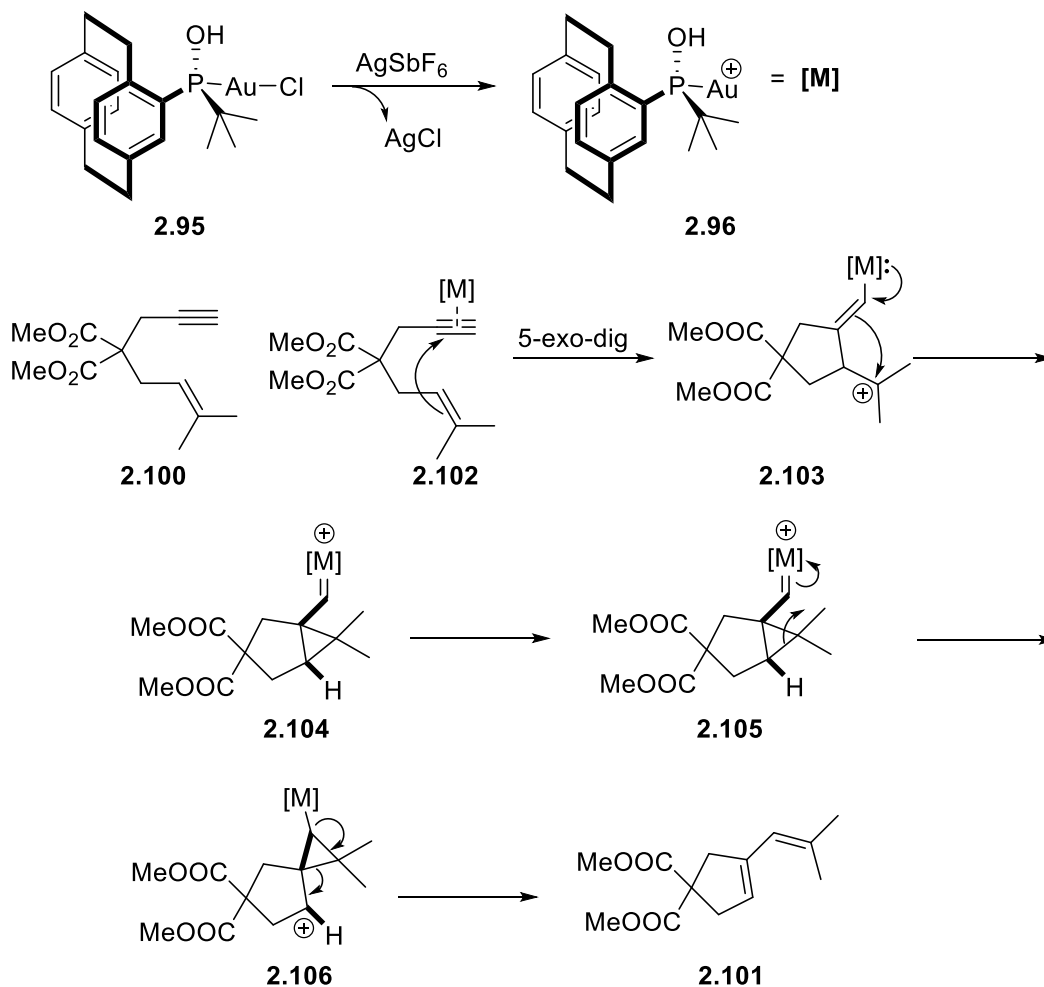
2.2.4.2.1. Enyne cycloisomerisation

To evaluate the activity of complex **2.95**, we investigated two cycloisomerisation reactions and an addition process. One isomerisation and the addition could be performed on enyne **2.100** (Scheme 2.28). This was readily prepared by consecutive alkylations of dimethyl malonate **2.96**. Each step occurred in high yield. The cycloisomerisation was performed in CH₂Cl₂ at room temperature. Mixing the Au(I)-SPO-**2.95** complex with AgSbF₆ leads to a cationic catalyst that activates the alkyne. The cyclopentene **2.101** was isolated in 85% yield.



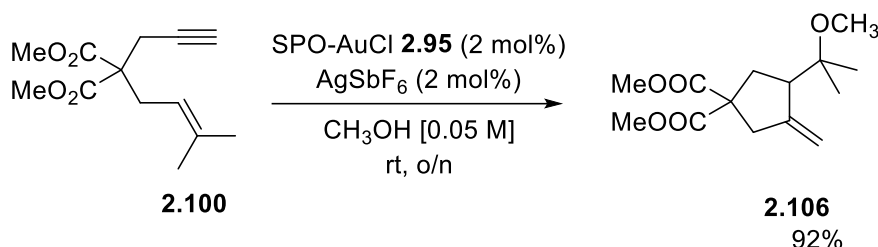
Scheme 2.28: Cycloisomerisation of enyne **2.100**.

The mechanism for this reaction is complex (Scheme 2.29). After activation of the alkyne, the alkene attacks the triple bond to give a vinyl gold species and relatively stable tertiary carbocation **2.103**. This undergoes intramolecular cyclopropanation.



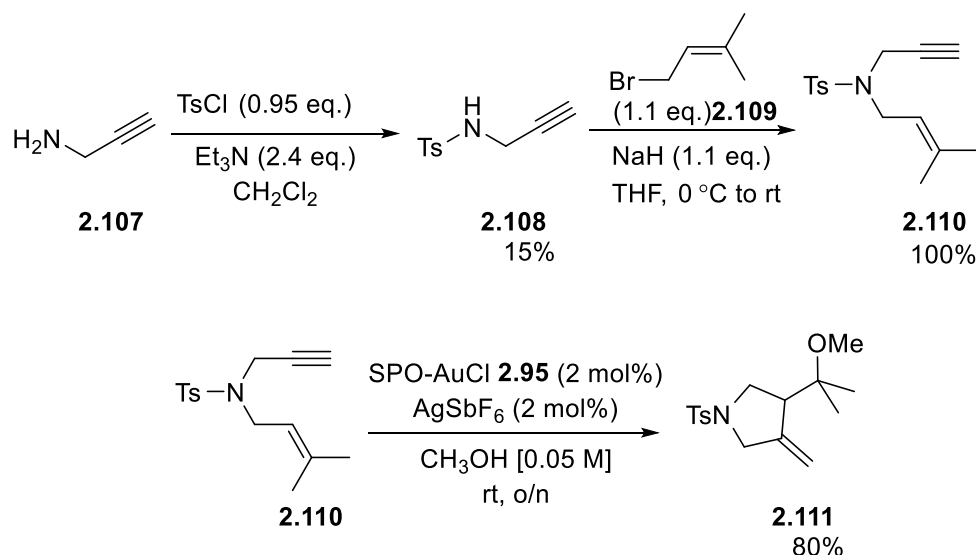
Scheme 2.29: Plausible mechanism of cycloisomerisations enyne **2.100**.

If the reaction is performed in a protic solvent like methanol then the initial intermediate **2.103** can be trapped and methoxycyclisation occurs to give the ether **2.106** (Scheme 2.30). This latter reaction is interesting as the product controls a stereogenic centre and it could be formed in enantiomerically enriched form if the correct ligand was used.



Scheme 2.30: Methoxycyclisation of enyne **2.100**.

This reaction was repeated with a second substrate **2.110** to give pyrrolidine **2.111** (Scheme 2.31).



Scheme 2.31: Methoxycyclisation of enyne **2.110**.

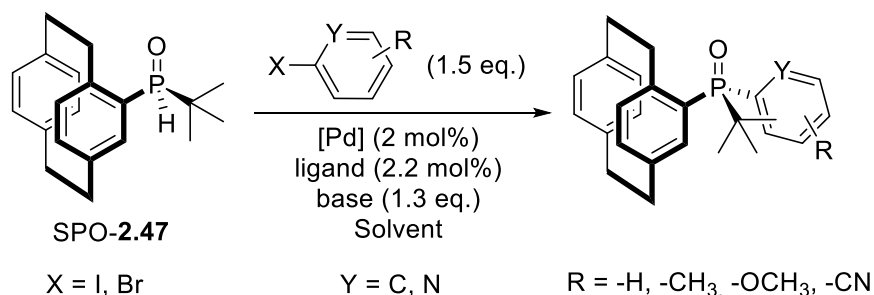
The catalytic reactions of Au(I)-SPO-**2.95** complex were promising and results are similar to those reported for the only other known example of a Au(I)-SPO.⁷² We suggest that if SPO-**2.95** can be synthesised in an enantiomerically pure form, it would be a good catalyst for asymmetric intramolecular cyclisation reactions.

After the initial investigation, we concluded that the synthesis of planar chiral SPO based on a [2.2]paracyclophane framework is limited to the *tert*-butyl substituent. A comprehensive array of reactions had been performed to resolve the planar chirality but all to no avail. Fortunately, the planar chiral SPO has proved to be a competent pre-ligand in different metal-catalysed transformations.

Next, we attempted to synthesise planar chiral phosphines. For this, we chose the reduction of the tertiary phosphine oxide (TPO) route. The section below describes the synthetic route, we have developed to access various planar chiral TPOs from the SPO-2.47.

2.2.5. *P*-Arylation of secondary phosphine oxide (SPO)

The role of *P*-arylation in the formation of tertiary phosphines is significant.²² A direct route to tertiary phosphines involves functionalisation of secondary phosphines. However, secondary phosphines are unstable towards oxidation and require rigorous oxygen-free conditions in their synthesis. An alternative approach that minimises the handling of oxygen-sensitive intermediates, involves the functionalisation of secondary phosphine oxides (SPOs) to form tertiary phosphine oxides (TPOs), which can be reduced to give the desired phosphines.⁷⁹⁻⁸¹ The arylation of SPO-2.47 would provide a general route to *P*-stereogenic [2.2]paracyclophane-phosphine. This is an unstudied area of [2.2]paracyclophane chemistry with only a single example reported in a patent.⁸² We have optimised an efficient method for *P*-arylation of SPO-2.47 in the formation of TPOs (Scheme 2.32, Table 2.6).



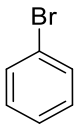
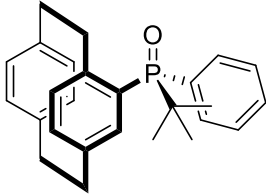
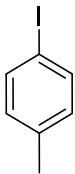
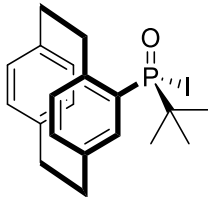
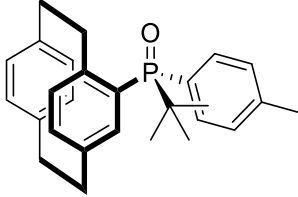
Scheme 2.32: *P*-Arylation of SPO-2.47.

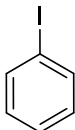
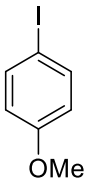
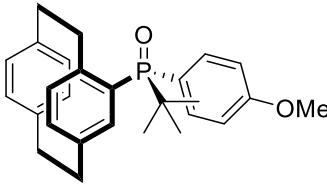
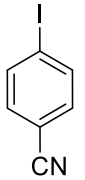
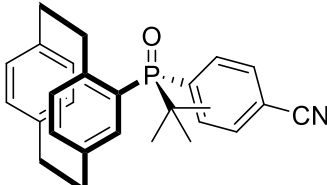
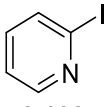
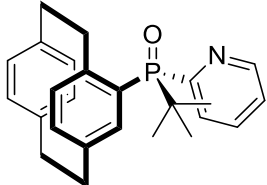
The initial conditions trialed were those of Bloomfield (entry 1),²² but these did not give satisfactory yields so we performed a quick optimisation. Changing the ligand to dppf (entry 2), solvent to toluene (entry 3), and metal to NiCl₂·5H₂O (entry 4) and CuI (entry 5) failed to produce the desired product. Surprisingly, in the latter case, the iodide-adduct **2.115** was formed in 55% yield. It became clear that aryl bromides were not sufficiently reactive so we started coupling aryl iodides.

At this point, the most successful coupling was observed with Pd(OAc)₂, dppf, DIPEA, in dioxane with DCE as a co-solvent (4.5:0.5) (entry 6). In an attempt to improve the reaction conversion, a range of coupling conditions were screened by altering ligands dippf (entry 7), xanthphos (entry 8), solvent dioxane to toluene (entry 9), and palladium source from Pd(OAc)₂

to Pd₂(dba)₃ (entry 10). Unfortunately, product formation was reduced to below 5% in every case. Gratifyingly, changing the base from DIPEA to Cs₂CO₃ increased the reaction yield substantially up to 87% (entry 11). To investigate the scope of this P-arylation protocol, we applied the optimised conditions to a variety of substituted aryl iodides. Neutral (entry 12), electron-rich (entry 13), electron-deficient (entry 14) aryl iodides, and a heteroaromatic iodide (entry 15) were all well-tolerated for the P-arylation with SPO (*RS_p*,*SR_p*)-**2.47** to smoothly produce the corresponding tertiary phosphine oxides (TPOs) in 55-85% yields.

Table 2.6: Optimisation conditions for P-arylation of SPO-2.47

Entry	Ar-X	Reaction conditions*	Product	% Yield ^{a,b}
1	 2.112	Pd(OAc) ₂ , Xantphos, DIPEA, DME, 85 °C, 24 h	 <i>(RS_p</i> , <i>RS_p</i>)- 2.113	23 ^a
2	2.112	Pd(OAc) ₂ , Dppf, DIPEA, DME, 85 °C, 24 h	-	-
3	2.112	Pd(OAc) ₂ , Xantphos, DIPEA, Toluene, 110 °C, 24 h	-	-
4	2.112	NiCl ₂ .5H ₂ O, Zn, 2,2'- bipyridine H ₂ O, 70 °C, 24 h	-	-
5	 2.114	CuI, (<i>S</i>)- α -phenyl ethyl amine, K ₂ CO ₃ , Toluene, 110 °C, 24 h	 <i>(RS_p</i> , <i>RS_p</i>)- 2.115	55 ^a
6	2.114	Pd(OAc) ₂ , dppf, DIPEA, dioxane:DCE (4.5:0.5), 100 °C, 24 h	 <i>(RS_p</i> , <i>RS_p</i>)- 2.116	35 ^a
7	2.114	Pd(OAc) ₂ , dippf, DIPEA, dioxane:DCE (4.5:0.5), 100 °C, 24 h	<i>(RS_p</i> , <i>RS_p</i>)- 2.116	2.37 ^b

8	2.114	Pd(OAc) ₂ , Xantphos, DIPEA, dioxane:DCE (4.5:0.5), 100 °C, 24 h	(<i>RS_p</i> , <i>RS_P</i>)- 2.116	4.13 ^b
9	2.114	Pd(OAc) ₂ , dppf, DIPEA, toluene:DCE (4.5:0.5), 100 °C, 24 h	(<i>RS_p</i> , <i>RS_P</i>)- 2.116	1.13 ^b
10	2.114	Pd ₂ (dba) ₃ , dppf, DIPEA, dioxane:DCE (4.5:0.5), 100 °C, 24 h	(<i>RS_p</i> , <i>RS_P</i>)- 2.116	1.18 ^b
11	2.114	Pd(OAc) ₂ , dppf, Cs ₂ CO ₃ , dioxane:DCE (4.5:0.5), 100 °C, 24 h	(<i>RS_p</i> , <i>RS_P</i>)- 2.116	87 ^a 52.58 ^b
12	 2.117	Pd(OAc) ₂ , dppf, Cs ₂ CO ₃ , dioxane:DCE (4.5:0.5), 100 °C, 24 h	(<i>RS_p</i> , <i>RS_P</i>)- 2.113	85 ^a
13	 2.118	Pd(OAc) ₂ , dppf, Cs ₂ CO ₃ , dioxane:DCE (4.5:0.5), 100 °C, 24 h	 (<i>RS_p</i> , <i>RS_P</i>)- 2.119	80 ^a
14	 2.120	Pd(OAc) ₂ , dppf, Cs ₂ CO ₃ , dioxane:DCE (4.5:0.5), 100 °C, 24 h	 (<i>RS_p</i> , <i>RS_P</i>)- 2.121	55 ^a
15	 2.122	Pd(OAc) ₂ , dppf, Cs ₂ CO ₃ , dioxane:DCE (4.5:0.5), 100 °C, 24 h	 (<i>RS_p</i> , <i>SR_P</i>)- 2.123	71 ^a

*[Pd], [Ni], or [Cu] 2 mol%, ligand 2.2 mol%, base 1.3 eq.

^aIsolated yield

^bNMR yield is determined by using *p*-xylene as an internal standard.

It should be noted that this protocol requires a higher temperature compared to Bloomfield's original couplings, suggesting that the sterically demanding nature of the SPO-**2.47** impedes the reaction. In each case, the new TPO was formed as a single diastereomer as confirmed by

^1H NMR spectroscopy. As we anticipated, the ^1H NMR spectrum indicates the close proximity of one of the H-2 protons (4.48 ppm) to P=O, which suggests the *unlike* diastereomer is favoured. In the case of 2-pyridyl TPO, the *like* diastereomer is formed due to the change in priorities according to the Cahn-Ingold-Prelog guidelines.⁵⁷ This was later confirmed when the structure of the TPO **2.116** was determined by X-ray analysis (Figure 2.6).

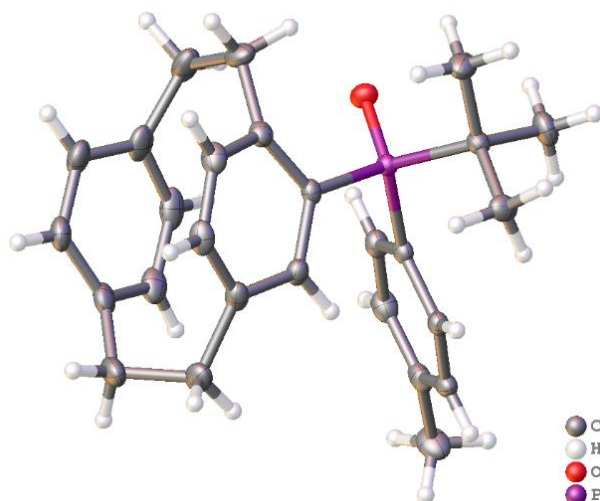
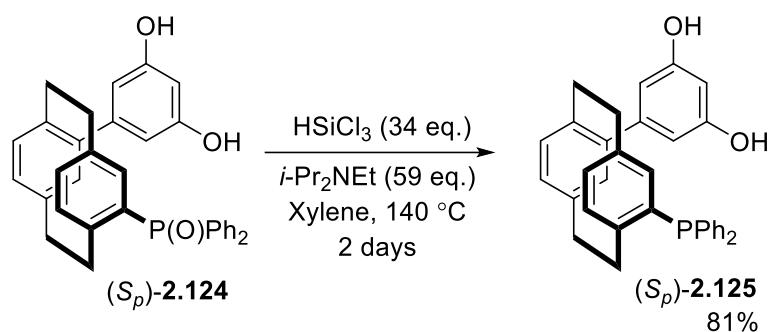


Figure 2.6: X-ray structure of tertiary phosphine oxide (RS_p,SR_P)-**2.116**. (Ellipsoids are drawn at a 50% probability level.)

After synthesising the various TPOs based on [2.2]paracyclophane, our next goal was to reduce them to the corresponding phosphines.

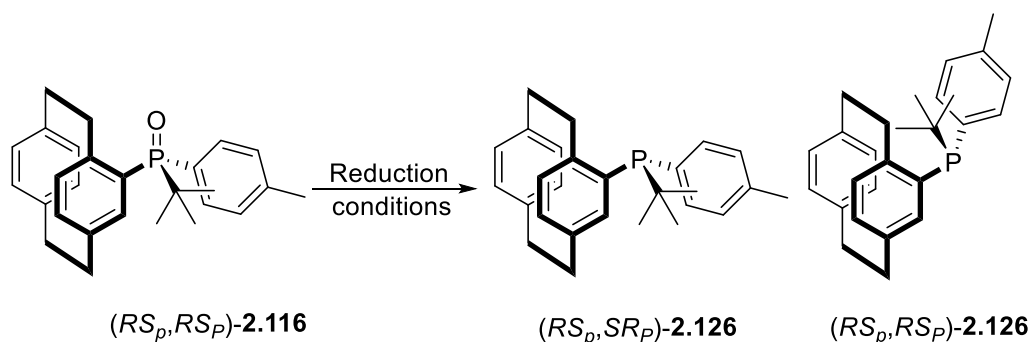
2.2.6. Synthesis of monodentate *P*-ligands

Bulky tertiary phosphines are of special interest as ligands for diverse transition-metal catalysed reactions.⁸³⁻⁸⁵ One of the routes to synthesise phosphines is through the reduction of TPO.^{47,86,87} This is always a challenging reaction, but there are several reported reductions of [2.2]paracyclophane phosphine oxides by trichlorosilane (HSiCl_3).⁸⁸⁻⁹² For example, during the synthesis of planar chiral *pseudo-ortho* aryl[2.2]paracyclophanyl-phosphine **2.125**, Kitagaki et al. used HSiCl_3 to reduce a TPO **2.124** to a phosphine **2.125** (Scheme 2.33).⁹¹ However, the reduction conditions often require an excess of HSiCl_3 with unusually long reaction times. Moreover, silane reagents are toxic and volatile in nature.



Scheme 2.33: Reduction of TPO **2.124** to phosphine **2.125** with HSiCl_3 .

In an attempt to avoid the use of silanes, we initially performed the reduction of TPO-**112** by employing conventional hydride reagents (Scheme 2.34, Table 2.7).



Scheme 2.34: Reduction of tertiary phosphine oxide $(RS_p,RS_P)\text{-2.116}$.

Table 2.7: Optimisation conditions for reduction of $(RS_p,SR_P)\text{-2.116}$

Entry	Reaction conditions	% Yield ^{a,b}
1 ⁹³	MeI, DME, rt, 2 hrs, LAH, 0 °C to reflux	-
2 ⁹⁴	Meerwein's salt, NaBH ₄ , CH ₂ Cl ₂	-
3 ⁹⁴	(COCl) ₂ , LAH, toluene, 0 °C to reflux	-
4 ⁹⁴	(COCl) ₂ , NaBH ₄ in diglyme, toluene, 0 °C to reflux	-
5 ⁹⁵	CeCl ₃ , NaBH ₄ , LAH, THF, 0 °C to reflux	-
6 ⁹⁶	DIBAL, <i>c</i> -hex ₃ P=O, CH ₂ Cl ₂ , 45 °C BH ₃ .THF, 23 °C	-
7 ⁸⁶	HSiCl ₃ , Et ₃ N, toluene, 110 °C, 18 hrs	-

8 ⁸⁶	HSiCl ₃ (35 eq.), <i>p</i> -xylene, 140 °C, 48 hrs	71% ^c dr = 60:40
9 ⁸⁶	HSiCl ₃ (28 eq.), <i>p</i> -xylene, 140 °C, 15 hrs	75% ^c dr = 60:40
10 ⁸⁶	HSiCl ₃ (28 eq.), <i>p</i> -xylene, 110 °C, 15 hrs	68% ^c dr = 60:40

^a Crude yield

^b dr = diastereomeric ratio (determined from crude product by ¹H NMR spectroscopy)

^c reaction was performed in the pressure tube.

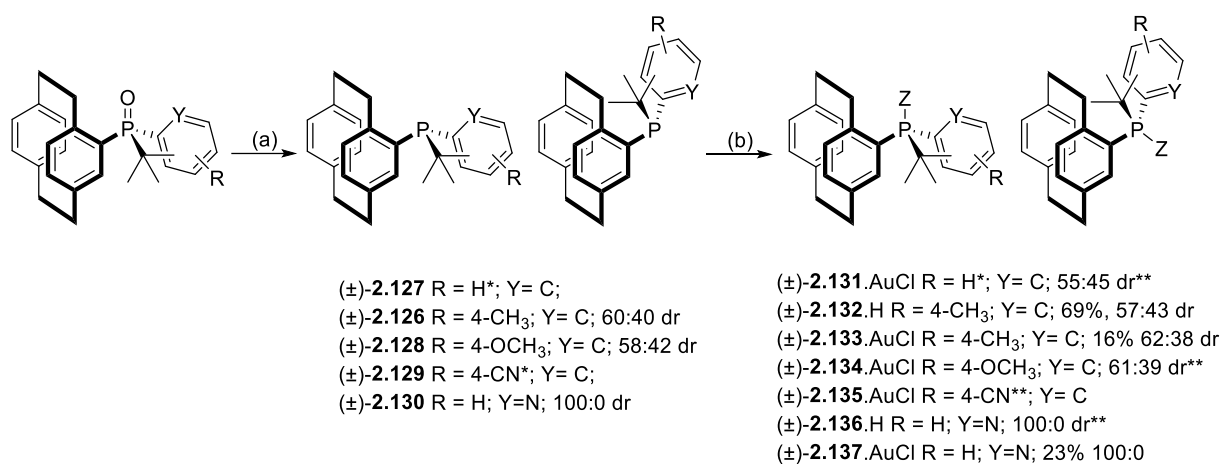
With the hydride reducing agents, strong alkylating agents were first used to form the *phosphonium* species, which was then reduced by the hydride source. Initial attempts to alkylate TPO-**2.116** with MeI and Meerwein's salt [(C₂H₅)₃O(BF₄)] followed by reduction with LiAlH₄ and NaBH₄ (entry 1 & 2) were not promising. Further reactions to form chlorophosphonium ion of TPO-**2.116** by the treatment with oxalyl chloride (COCl)₂ followed by reducing agents LiAlH₄ (entry 3) and NaBH₄ (entry 4) were also not effective. Likewise, other strategies such as activation of phosphine oxide by coordination with trivalent cerium (CeCl₃, entry 5) and employing an ancillary substrate tricyclohexylphosphine oxide (*c*-hex₃P=O, entry 6) also failed.

As the regular reducing agents did not reduce the TPO-**2.116**, we decided to attempt reduction with silane reagents (Table 2.7). The P=O bond in a phosphine oxide can be activated by forming *in-situ* the P-O-Si bond. Heating TPO-**2.116** in toluene (110 °C) with an excess of HSiCl₃ did not produce the desired reduction product (entry 7). Gratifyingly, changing solvent to *p*-xylene and reaction conditions to the pressure tube (140 °C) furnished the desired phosphine **2.126** but with epimerisation (entry 8 & 9). Epimerisation was confirmed by ¹H NMR as a single diastereomer of **2.116** produced two diastereomers of **2.126** (Scheme 2.34).

This reaction left us with a question, whether epimerisation occurred at the phosphorus stereocentre or at the paracyclophane? The paracyclophane ethylene bridge tends to cleave at >150 °C but bulky substituents can lower this. We believed that lowering the temperature would rule out this possibility. The reaction was performed under the same conditions but at lower temperature 110 °C. We observed nearly the same reaction conversion in the same diastereomeric ratio (entry 10). This result ruled out the possibility of epimerisation of planar chirality since it is highly unlikely to cause homolytic scission of the [2.2]paracyclophane

ethylene bridge at this temperature. This evidence suggested that the epimerisation occurred at the phosphorus stereogenic centre (Scheme 2.34).

The optimised reaction conditions of HSiCl_3 in *p*-xylene at 140 °C were used to reduce the rest of the TPOs-**2.113**, **2.119**, **2.121**, and **2.123**. However, in all cases, the reduction of single diastereomer of TPO gave two new compounds as indicated by ^1H NMR spectroscopy of the crude reaction mixture (Scheme 2.35). Moreover, all phosphines appeared to be air-sensitive and it became necessary to protect the putative phosphines. Initially, we attempted to protect them as the borane complex, but this was unsuccessful. It was later found that these phosphines could be protected as the phosphinium salt by reaction with tetrafluoroboric acid or by complexation with chloro(tetrahydrothiophene)gold(I) or chloro(dimethyl sulfide)gold(I) to give, in each case, inseparable diastereomeric compounds (Scheme 2.35). It should be noted that all phosphines were reduced, protected and isolated by these strategies as judged by spectroscopy, however isolation of **2.127**, **2.128**, and **2.129** in pure form was difficult.



Scheme 2.35: Reduction of tertiary phosphine oxides.

(a) HSiCl_3 (28 eq.), xylene, 145 °C, 24 hrs or neat PhSiH_3 , 140 °C, 3-5 days

(b) HBF_4 (15 eq.), H_2O , CH_2Cl_2 or $\text{Au}(\text{dms})\text{Cl}$ (1.0 eq.) CH_2Cl_2 or $\text{Au}(\text{tht})\text{Cl}$ (1.2 eq.), CH_3CN

*Overlapping peaks in the ^1H NMR spectrum prevented the diastereomers ratio of **2.127/2.129** being determined

** **2.127**, **2.128**, **2.129** could be reduced and complexes formed but it proved impossible to remove all impurities

Interestingly, the reduction of pyridine TPO-**2.123** proceeded to give a single diastereomer. Inspection of its gold complex suggests that reduction occurred stereoselectively with the retention of stereochemistry at phosphorus. There were downfield signals that can be assigned to the ethylene bridge by ^1H NMR spectroscopy. This was later confirmed by X-ray crystallography (Figure 2.7).

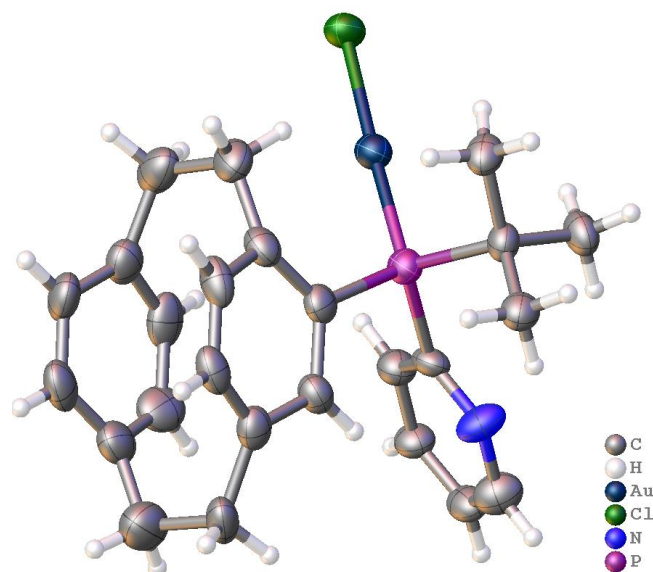
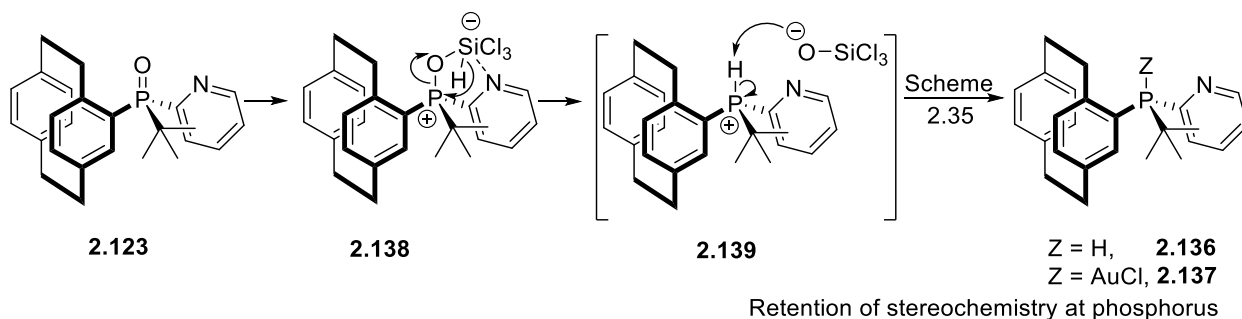


Figure 2.7: X-ray structure of gold complex of phosphine **2.137**.AuCl.
(Ellipsoids are drawn at a 50% probability level.)

It is unclear why pyridine alters the stereochemical course of the reduction. There is speculation that a pyridine-silane adduct **2.138** delivers the hydride in an intramolecular fashion causing the stereoselective reduction (Scheme 2.36).



Scheme 2.36: Plausible mechanism of stereoselective reduction of **2.123**.

2.3. Conclusions

Overall, this project aimed to synthesise planar chiral secondary phosphine oxides based on [2.2]paracyclophane. The *tert*-butyl planar chiral secondary phosphine oxide – SPO-**2.47** proved to be a competent ligand, notably in transition metal-catalysed cross-coupling reactions. The Buchwald-Hartwig aminations were performed with the catalyst derived from SPO-**2.47** in good to excellent yields with both electron-rich and electron-deficient aryl bromide/chlorides as well as sterically hindered anilines. However, this ligand was only moderately efficient in Suzuki-Miyaura cross-coupling reactions. Even more promising was

the complexation of SPO-**2.47** with gold [Au(I)] which facilitated cycloisomerisations and methoxycyclisations. In order to investigate a general route to P-stereogenic [2.2]paracyclophane-derived phosphines, P-arylation of the SPO-**2.47** was first optimised with a variety of substituted aryl iodides. Interestingly, in each case, *tert*-phosphine oxides were obtained as a single diastereomer. After employing an array of reducing agents, these *tert*-phosphine oxides were finally reduced under harsh conditions that caused epimerisation at the phosphorus centre generating two diastereomeric phosphines. Due to the instability of these putative phosphines, they were either protected as the phosphonium salt with tetrafluoroboric acid or directly complexed with chloro(dimethylsulfide)gold(I) or chloro(tetrahydrothiophene)gold(I) to give useful gold complexes. Based on our study, we suggest that if [2.2]paracyclophane SPOs could be synthesised in enantiomerically pure forms, they will have a great potential in asymmetric catalysis.

2.4. References

- (1) Lamberth, C. Amino acid chemistry in crop protection. *Tetrahedron* **2010**, *66*, 7239.
- (2) De Clercq, E. Clinical Potential of The Acyclic Nucleoside Phosphonates Cidofovir, Adefovir, and Tenofovir In Treatment of DNA Virus And Retrovirus Infections. *Clin. Microbiol. Rev.* **2003**, *16*, 569.
- (3) Peterson, L. W.; Sala-Rabanal, M.; Krylov, I. S.; Serpi, M.; Kashemirov, B. A.; McKenna, C. E. Serine Side Chain-Linked Peptidomimetic Conjugates of Cyclic HPMPC and HPMPA: Synthesis and Interaction with hPEPT1. *Mol. Pharm.* **2010**, *7*, 2349.
- (4) Kolodiazhnyi, O. I. In Phosphorus Chemistry I: Asymmetric Synthesis and Bioactive Compounds; Montchamp, J.-L., Ed.; Springer International Publishing: Cham, 2015.
- (5) Martin, R.; Buchwald, S. L. Palladium-Catalyzed Suzuki–Miyaura Cross-Coupling Reactions Employing Dialkylbiaryl Phosphine Ligands. *Acc. Chem. Res.* **2008**, *41*, 1461.
- (6) Abd-El-Aziz, A. S. Organometallic Polymers of the Transition Metals. *Macromol. Rapid Commun.* **2002**, *23*, 995.
- (7) Gleria, M.; De Jaeger, R. In New Aspects in Phosphorus Chemistry V: ; Majoral, J.-P., Ed.; Springer Berlin Heidelberg: Berlin, Heidelberg, 2005.
- (8) Guinó, M.; Hii, K. K. Applications of phosphine-functionalised polymers in organic synthesis. *Chem. Soc. Rev.* **2007**, *36*, 608.
- (9) Flett, D. S. Solvent extraction in hydrometallurgy: the role of organophosphorus extractants. *J. Organomet. Chem.* **2005**, *690*, 2426.
- (10) Rémond, E.; Bayardon, J.; Ondel-Eymin, M.-J.; Jugé, S. Stereoselective Synthesis of Unsaturated and Functionalized 1-NHBoc Amino Acids, Using Wittig Reaction under Mild Phase-Transfer Conditions. *J. Org. Chem.* **2012**, *77*, 7579.
- (11) Gillespie, J. A.; Zuidema, E.; van Leeuwen, P. W. N. M.; Kamer, P. C. J.; Li, W.; Zhang, X.; Gual, A.; Godard, C.; de la Fuente, V.; Castillón, S. et al. Phosphorus Ligand Effects in Homogeneous Catalysis and Rational Catalyst Design. . *Phosphorus(III) Ligands in Homogeneous Catalysis: Design and Synthesis* **2012**, 1.
- (12) Tolman, C. A. Steric effects of phosphorus ligands in organometallic chemistry and homogeneous catalysis. *Chem. Rev.* **1977**, *77*, 313.
- (13) Foye, W. O. Comprehensive organic chemistry. (A series of six volumes.) Edited by Sir D. Barton and W. D. Ollis. Pergamon, Oxford, England. 1979. . *J. Pharm. Sci.* **1980**, *69*, 753.

- (14) Dubrovina, N. V.; Börner, A. Enantioselective Catalysis with Chiral Phosphine Oxide Preligands. *Angew. Chem. Int. Ed.* **2004**, *43*, 5883.
- (15) Nemoto, T.; Hamada, Y. Pd-catalyzed asymmetric allylic substitution reactions using P-chirogenic diaminophosphine oxides: DIAPHOXs. *Chem. Rec.* **2007**, *7*, 150.
- (16) Diver, S. T. *Encyclopedia of Reagents for Organic Synthesis*; Wiley: New York, **1995**, 5014.
- (17) Berlin, K. D.; Butler, G. B. The Preparation and Properties of Tertiary and Secondary Phosphine Oxides. *Chem. Rev.* **1960**, *60*, 243.
- (18) Nemoto, T.; Matsumoto, T.; Masuda, T.; Hitomi, T.; Hatano, K.; Hamada, Y. P-Chirogenic Diaminophosphine Oxide: A New Class of Chiral Phosphorus Ligands for Asymmetric Catalysis. *J. Am. Chem. Soc.* **2004**, *126*, 3690.
- (19) Dai, W.-M.; Yeung, K. K. Y.; Leung, W. H.; Haynes, R. K. Air-stable P-stereogenic secondary phosphine oxides as chiral monodentate ligands for asymmetric catalytic carbon-carbon bond formation. *Tetrahedron: Asymmetry* **2003**, *14*, 2821.
- (20) Hu, G.; Chen, W.; Fu, T.; Peng, Z.; Qiao, H.; Gao, Y.; Zhao, Y. Nickel-Catalyzed C–P Cross-Coupling of Arylboronic Acids with P(O)H Compounds. *Org. Lett.* **2013**, *15*, 5362.
- (21) Xu, J.; Zhang, P.; Gao, Y.; Chen, Y.; Tang, G.; Zhao, Y. Copper-Catalyzed P-Arylation via Direct Coupling of Diaryliodonium Salts with Phosphorus Nucleophiles at Room Temperature. *J. Org. Chem.* **2013**, *78*, 8176.
- (22) Bloomfield, A. J.; Herzon, S. B. Room Temperature, Palladium-Mediated P–Arylation of Secondary Phosphine Oxides. *Org. Lett.* **2012**, *14*, 4370.
- (23) Wang, G.; Shen, R.; Xu, Q.; Goto, M.; Zhao, Y.; Han, L.-B. Stereospecific Coupling of H-Phosphinates and Secondary Phosphine Oxides with Amines and Alcohols: A General Method for the Preparation of Optically Active Organophosphorus Acid Derivatives. *J. Org. Chem.* **2010**, *75*, 3890.
- (24) Hu, D.-F.; Weng, C.-M.; Hong, F.-E. Preparation of New Buchwald-Type Secondary Phosphine Oxide Ligands and Applications in Suzuki–Miyaura Reactions. *Organometallics* **2011**, *30*, 1139.
- (25) Jung, L.-Y.; Tsai, S.-H.; Hong, F.-E. Application of Tautomerism of Ferrocenyl Secondary Phosphine Oxides in Suzuki–Miyaura Cross-Coupling Reactions. *Organometallics* **2009**, *28*, 6044.
- (26) Wei, C.-H.; Wu, C.-E.; Huang, Y.-L.; Kultyshev, R. G.; Hong, F.-E. Experimental and DFT Study of the Tautomeric Behavior of Cobalt-Containing Secondary Phosphine Oxides. *Chem. Eur. J.* **2007**, *13*, 1583.
- (27) Liniger, M.; Gschwend, B.; Neuburger, M.; Schaffner, S.; Pfaltz, A. Unprecedented Reactivity of Iridium(I) Secondary Phosphine Oxide Complexes: Formation of P-Coordinated Phosphinate Complexes by P–Aryl Bond Cleavage. *Organometallics* **2010**, *29*, 5953.
- (28) Helmchen, G.; Pfaltz, A. Phosphinoxazolines A New Class of Versatile, Modular P,N-Ligands for Asymmetric Catalysis. *Acc. Chem. Res.* **2000**, *33*, 336.
- (29) Cano, I.; Martínez-Prieto, L. M.; Vendier, L.; van Leeuwen, P. W. N. M. An iridium–SPO complex as bifunctional catalyst for the highly selective hydrogenation of aldehydes. *Catal. Sci. Technol.* **2018**, *8*, 221.
- (30) Ghaffar, T.; Parkins, A. W. A new homogeneous platinum containing catalyst for the hydrolysis of nitriles. *Tetrahedron Lett.* **1995**, *36*, 8657.
- (31) Copley, C. J.; van den Heuvel, M.; Abbadi, A.; de Vries, J. G. Platinum catalysed hydrolytic amidation of unactivated nitriles. *Tetrahedron Lett.* **2000**, *41*, 2467.
- (32) Lutz, A.; Robert, B.; Julia, H. S.; Andreas, A.; Christian, J. G. Air-stable phosphine oxides as preligands for catalytic activation reactions of C-Cl, C-F, and C-H bonds. *Pure Appl. Chem.* **2006**, *78*, 209.
- (33) Ackermann, L. Air- and Moisture-Stable Secondary Phosphine Oxides as Preligands in Catalysis. *Synthesis* **2006**, 1557.
- (34) Galland, A.; Dobrota, C.; Toffano, M.; Fiaud, J.-C. Enantiopure 1-r-H-2-c,5-t-diphenylphospholane as ligand in Rh-catalyzed asymmetric hydrogenation. *Tetrahedron: Asymmetry* **2006**, *17*, 2354.

- (35) Ackermann, L.; Kapdi, A. R.; Fenner, S.; Kornhaaß, C.; Schulzke, C. Well-Defined Air-Stable Palladium HASPO Complexes for Efficient Kumada–Corriu Cross-Couplings of (Hetero)Aryl or Alkenyl Tosylates. *Chem. Eur. J.* **2011**, *17*, 2965.
- (36) Ackermann, L.; Born, R. Modular Diamino- and Dioxophosphine Oxides and Chlorides as Ligands for Transition-Metal-Catalyzed C-C and C-N Couplings with Aryl Chlorides. *Angew. Chem. Int. Ed.* **2005**, *44*, 2444.
- (37) Donets, P. A.; Cramer, N. Diaminophosphine Oxide Ligand Enabled Asymmetric Nickel-Catalyzed Hydrocarbamoylations of Alkenes. *J. Am. Chem. Soc.* **2013**, *135*, 11772.
- (38) Guo, H.; Fan, Y. C.; Sun, Z.; Wu, Y.; Kwon, O. Phosphine Organocatalysis. *Chem. Rev.* **2018**, *118*, 10049.
- (39) Valentine Jr, D. H.; Hillhouse, J. H. Alkyl Phosphines as Reagents and Catalysts in Organic Synthesis. *Synthesis* **2003**, 0317.
- (40) Sharad Kumar, P. Advances in the Mitsunobu Reaction: An Excellent Organic Protocol with Versatile Applications. *Mini-Rev. Org. Chem.* **2019**, *16*, 127.
- (41) Appel Reaction. *Comprehensive Organic Name Reactions and Reagents* **2010**, 95.
- (42) Imamoto, T. P-Chiral Phosphine Ligands for Transition-Metal-Catalyzed Asymmetric Reactions. *J. Syn. Org. Chem. JPN* **2007**, *65*, 1060.
- (43) Fu, W.; Tang, W. Chiral Monophosphorus Ligands for Asymmetric Catalytic Reactions. *ACS Catalysis* **2016**, *6*, 4814.
- (44) Zapf, A.; Ehrentraut, A.; Beller, M. A New Highly Efficient Catalyst System for the Coupling of Nonactivated and Deactivated Aryl Chlorides with Arylboronic Acids. *Angew. Chem. Int. Ed.* **2000**, *39*, 4153.
- (45) Nandi, P.; Dye, J. L.; Bentley, P.; Jackson, J. E. Preparation of Diphenyl Phosphide and Substituted Phosphines using Alkali Metal in Silica Gel (M–SG). *Org. Lett.* **2009**, *11*, 1689.
- (46) Douglass, M. R.; Stern, C. L.; Marks, T. J. Intramolecular Hydrophosphination/Cyclization of Phosphinoalkenes and Phosphinoalkynes Catalyzed by Organolanthanides: Scope, Selectivity, and Mechanism. *J. Am. Chem. Soc.* **2001**, *123*, 10221.
- (47) Hérault, D.; Nguyen, D. H.; Nuel, D.; Buono, G. Reduction of secondary and tertiary phosphine oxides to phosphines. *Chem. Soc. Rev.* **2015**, *44*, 2508.
- (48) Connon, S. J. Chiral Phosphoric Acids: Powerful Organocatalysts for Asymmetric Addition Reactions to Imines. *Angew. Chem. Int. Ed.* **2006**, *45*, 3909.
- (49) Terada, M. Chiral Phosphoric Acids as Versatile Catalysts for Enantioselective Transformations. *Synthesis* **2010**, 1929.
- (50) Rahman, A.; Lin, X. Development and application of chiral spirocyclic phosphoric acids in asymmetric catalysis. *Org. Biomol. Chem.* **2018**, *16*, 4753.
- (51) Kolodiazhnyi, O. I. Recent developments in the asymmetric synthesis of P-chiral phosphorus compounds. *Tetrahedron: Asymmetry* **2012**, *23*, 1.
- (52) Drabowicz, J.; Łyżwa, P.; Omelańczuk, J.; Pietrusiewicz, K. M.; Mikołajczyk, M. New procedures for the resolution of chiral tert-butylphenylphosphine oxide and some of its reactions. *Tetrahedron: Asymmetry* **1999**, *10*, 2757.
- (53) Jiang, X.-b.; Minnaard, A. J.; Hessen, B.; Feringa, B. L.; Duchateau, A. L. L.; Andrien, J. G. O.; Boogers, J. A. F.; de Vries, J. G. Application of Monodentate Secondary Phosphine Oxides, a New Class of Chiral Ligands, in Ir(I)-Catalyzed Asymmetric Imine Hydrogenation. *Org. Lett.* **2003**, *5*, 1503.
- (54) Yamada, S.; Jahan, I. A new route to 3,4-disubstituted piperidines: formal synthesis of (–)-paroxetine and (+)-femoxetine. *Tetrahedron Lett.* **2005**, *46*, 8673.
- (55) Xu, Q.; Zhao, C.-Q.; Han, L.-B. Stereospecific Nucleophilic Substitution of Optically Pure H-Phosphinates: A General Way for the Preparation of Chiral P-Stereogenic Phosphine Oxides. *J. Am. Chem. Soc.* **2008**, *130*, 12648.
- (56) Berger, O.; Montchamp, J.-L. A General Strategy for the Synthesis of P-Stereogenic Compounds. *Angew. Chem. Int. Ed.* **2013**, *52*, 11377.
- (57) Prelog, V.; Helmchen, G. Basic Principles of the CIP-System and Proposals for a Revision. *Angew. Chem. Int. Ed. Engl.* **1982**, *21*, 567.
- (58) Lühr, S.; Holz, J.; Börner, A. The Synthesis of Chiral Phosphorus Ligands for use in Homogeneous Metal Catalysis. *ChemCatChem* **2011**, *3*, 1708.

- (59) Gatineau, D.; Moraleda, D.; Naubron, J.-V.; Bürgi, T.; Giordano, L.; Buono, G. Enantioselective alkylidenecyclopropanation of norbornenes with terminal alkynes catalyzed by palladium–phosphinous acid complexes. *Tetrahedron: Asymmetry* **2009**, *20*, 1912.
- (60) Chan, E. Y. Y.; Zhang, Q.-F.; Sau, Y.-K.; Lo, S. M. F.; Sung, H. H. Y.; Williams, I. D.; Haynes, R. K.; Leung, W.-H. Chiral Bisphosphinite Metalloligands Derived from a P-Chiral Secondary Phosphine Oxide. *Inorg. Chem.* **2004**, *43*, 4921.
- (61) Nemoto, T.; Jin, L.; Nakamura, H.; Hamada, Y. Pd-catalyzed asymmetric allylic alkylation with nitromethane using a chiral diaminophosphine oxide: (*S,Rp*)-Ph-DIAPHOX. Enantioselective synthesis of (*R*)-preclamol and (*R*)-baclofen. *Tetrahedron Lett.* **2006**, *47*, 6577.
- (62) Jiang, X.-b.; van den Berg, M.; Minnaard, A. J.; Feringa, B. L.; de Vries, J. G. The application of monodentate secondary phosphine oxide ligands in rhodium- and iridium-catalyzed asymmetric hydrogenation. *Tetrahedron: Asymmetry* **2004**, *15*, 2223.
- (63) Li, G. Y.; Zheng, G.; Noonan, A. F. Highly Active, Air-Stable Versatile Palladium Catalysts for the C–C, C–N, and C–S Bond Formations via Cross-Coupling Reactions of Aryl Chlorides. *J. Org. Chem.* **2001**, *66*, 8677.
- (64) Li, G. Y. The First Phosphine Oxide Ligand Precursors for Transition Metal Catalyzed Cross-Coupling Reactions: C–C, C–N, and C–S Bond Formation on Unactivated Aryl Chlorides. *Angew. Chem. Int. Ed.* **2001**, *40*, 1513.
- (65) Hoffmann, A. K.; Tesch, A. G. Reaction Of Aromatic Phosphine Oxides With Alkali Metals. *J. Am. Chem. Soc.* **1959**, *81*, 5519.
- (66) Dahl, O. Alkyl Di-T-Butylphosphinites. Exceptionally Halogenophilic Phosphinites In Arbuzov Reactions. *J. Chem. Soc. Perkin. Trans. I* **1978**, 947.
- (67) Kikukawa, K.; Yamane, T.; Takagi, M.; Matsuda, T. Reaction of co-ordinated phosphines: arylation of olefins by palladium(II) acetate and triarylphosphine. *J. Chem. Soc., Chem. Commun.* **1972**, 695.
- (68) Lu, D.; Xu, Y.; Liu, W.; Guo, L.; Sun, X. Palladium-Catalyzed Arylation of Olefins by Triarylphosphines via C–P Bond Cleavage. *Helv. Chim. Acta* **2015**, *98*, 116.
- (69) Miao, M.; Cao, J.; Huang, X.; Wu, L. Hydroxyphosphinylation Reaction of 3-Cyclopropylideneprop-2-en-1-ones via C–P σ -Bond Cleavage. *J. Org. Chem.* **2013**, *78*, 5999.
- (70) Chaux, F.; Frynas, S.; Laureano, H.; Salomon, C.; Morata, G.; Auclair, M.-L.; Stephan, M.; Merdès, R.; Richard, P.; Ondel-Eymin, M.-J. et al. Enantiodivergent synthesis of P-chirogenic phosphines. *C. R. Chim.* **2010**, *13*, 1213.
- (71) Lu, D.; Xu, Y.; Liu, W.; Guo, L.; Sun, X. Palladium-Catalyzed Arylation of Olefins by Triarylphosphines via C-P Bond Cleavage. *Helv. Chim. Acta* **2015**, *98*, 116.
- (72) Schröder, F.; Tugny, C.; Salanouve, E.; Clavier, H.; Giordano, L.; Moraleda, D.; Gimbert, Y.; Mouriès-Mansuy, V.; Goddard, J.-P.; Fensterbank, L. Secondary Phosphine Oxide–Gold(I) Complexes and Their First Application in Catalysis. *Organometallics* **2014**, *33*, 4051.
- (73) Gorin, D. J.; Toste, F. D. Relativistic effects in homogeneous gold catalysis. *Nature* **2007**, *446*, 395.
- (74) Hashmi, A. S. K.; Hutchings, G. J. Gold Catalysis. *Angew. Chem. Int. Ed.* **2006**, *45*, 7896.
- (75) Zi, W.; Dean Toste, F. Recent advances in enantioselective gold catalysis. *Chem. Soc. Rev.* **2016**, *45*, 4567.
- (76) Nieto-Oberhuber, C.; Muñoz, M. P.; Buñuel, E.; Nevado, C.; Cárdenas, D. J.; Echavarren, A. M. Cationic Gold(I) Complexes: Highly Alkynophilic Catalysts for the exo- and endo-Cyclization of Enynes. *Angew. Chem. Int. Ed.* **2004**, *43*, 2402.
- (77) Mamane, V.; Gress, T.; Krause, H.; Fürstner, A. Platinum- and Gold-Catalyzed Cycloisomerization Reactions of Hydroxylated Enynes. *J. Am. Chem. Soc.* **2004**, *126*, 8654.
- (78) Luzung, M. R.; Markham, J. P.; Toste, F. D. Catalytic Isomerization of 1,5-Enynes to Bicyclo[3.1.0]hexenes. *J. Am. Chem. Soc.* **2004**, *126*, 10858.
- (79) Rémond, E.; Tessier, A.; Leroux, F. R.; Bayardon, J.; Jugé, S. Efficient Synthesis of Quaternary and P-Stereogenic Phosphonium Triflates. *Org. Lett.* **2010**, *12*, 1568.
- (80) Bhunia, A.; Kaicharla, T.; Porwal, D.; Gonnade, R. G.; Biju, A. T. Multicomponent reactions involving phosphines, arynes and aldehydes. *Chem. Commun.* **2014**, *50*, 11389.

- (81) Bayardon, J.; Rousselin, Y.; Jugé, S. Designing P-Chirogenic 1,2-Diphosphinobenzenes at Both P-Centers Using P(III)-Phosphinites. *Org. Lett.* **2016**, *18*, 2930.
- (82) X. Hou, T. Z., L. Dai; Chinese Patent; CN101003549A In *CN101003549A*; Patent, C., Ed. China, 2007.
- (83) Grabulosa, A.; Frew, J. J. R.; Fuentes, J. A.; Slawin, A. M. Z.; Clarke, M. L. Palladium complexes of bulky ortho-trifluoromethylphenyl-substituted phosphines: Unusually regioselective catalysts for the hydroxycarbonylation and alkoxycarbonylation of alkenes. *J. Mol. Catal. A: Chem.* **2010**, *330*, 18.
- (84) Tschan, M. J. L.; García-Suárez, E. J.; Freixa, Z.; Launay, H.; Hagen, H.; Benet-Buchholz, J.; van Leeuwen, P. W. N. M. Efficient Bulky Phosphines for the Selective Telomerization of 1,3-Butadiene with Methanol. *J. Am. Chem. Soc.* **2010**, *132*, 6463.
- (85) Dabbawala, A. A.; Jasra, R. V.; Bajaj, H. C. Selective hydroformylation of 1-hexene to branched aldehydes using rhodium complex of modified bulky phosphine and phosphite ligands. *Catal. Commun.* **2011**, *12*, 403.
- (86) Pye, P. J.; Rossen, K.; Reamer, R. A.; Tsou, N. N.; Volante, R. P.; Reider, P. J. A New Planar Chiral Bisphosphine Ligand for Asymmetric Catalysis: Highly Enantioselective Hydrogenations under Mild Conditions. *J. Am. Chem. Soc.* **1997**, *119*, 6207.
- (87) Falk, F. C.; Fröhlich, R.; Paradies, J. Coupling of ortho-substituted aryl chlorides with bulky amides. *Chem. Commun.* **2011**, *47*, 11095.
- (88) Cheemala, M. N.; Gayral, M.; Brown, J. M.; Rossen, K.; Knochel, P. New Paracyclophane Phosphine for Highly Enantioselective Ruthenium-Catalyzed Hydrogenation of Prochiral Ketones. *Synthesis* **2007**, 3877.
- (89) Driver, T. G.; Harris, J. R.; Woerpel, K. A. Kinetic Resolution of Hydroperoxides with Enantiopure Phosphines: Preparation of Enantioenriched Tertiary Hydroperoxides. *J. Am. Chem. Soc.* **2007**, *129*, 3836.
- (90) Kitagaki, S.; Ohta, Y.; Takahashi, R.; Komizu, M.; Mukai, C. Planar chiral [2.2]paracyclophane-based phosphine-Brønsted acid catalysts bearing exceptionally high reactivity for aza-Morita-Baylis-Hillman reaction. *Tetrahedron Lett.* **2013**, *54*, 384.
- (91) Kitagaki, S.; Ohta, Y.; Tomonaga, S.; Takahashi, R.; Mukai, C. Synthesis of planar chiral pseudo-ortho-substituted aryl[2.2]paracyclophanes by stepwise successive palladium-catalyzed coupling reactions. *Tetrahedron: Asymmetry* **2011**, *22*, 986.
- (92) Zhang, T.-Z.; Dai, L.-X.; Hou, X.-L. Synthesis of planar chiral [2.2]paracyclophane monophosphine ligands and their application in the umpolung allylation of aldehydes. *Tetrahedron: Asymmetry* **2007**, *18*, 251.
- (93) Imamoto, T.; Kusumoto, T.; Suzuki, N.; Sato, K. Phosphine oxides and lithium aluminum hydride-sodium borohydride-cerium(III) chloride: synthesis and reactions of phosphine-boranes. *J. Am. Chem. Soc.* **1985**, *107*, 5301.
- (94) Rajendran, K. V.; Gilheany, D. G. Simple unprecedented conversion of phosphine oxides and sulfides to phosphine boranes using sodium borohydride. *Chem. Commun.* **2012**, *48*, 817.
- (95) Imamoto, T.; Oshiki, T.; Onozawa, T.; Kusumoto, T.; Sato, K. Synthesis and reactions of phosphine-boranes. Synthesis of new bidentate ligands with homochiral phosphine centers via optically pure phosphine-boranes. *J. Am. Chem. Soc.* **1990**, *112*, 5244.
- (96) Busacca, C. A.; Raju, R.; Grinberg, N.; Haddad, N.; James-Jones, P.; Lee, H.; Lorenz, J. C.; Saha, A.; Senanayake, C. H. Reduction of Tertiary Phosphine Oxides with DIBAL-H. *J. Org. Chem.* **2008**, *73*, 1524.

Chapter 3

Selective Remote β -C(sp^3)-H Activation of Cyclic Amines and Enantioselective γ -C(sp^3)-H Functionalisation of Cyclic Amines

3.0. Introduction to C-H activation

It is a possible cliché that organic chemistry is at the heart of modern life. The synthesis of organic molecules supports the global economy through industries such as agriculture, pharmaceuticals, and electronics. It is no exaggeration to say that chemists can synthesise any organic molecule, regardless of its size and complexity. A traditional synthesis undoubtedly requires a multistep sequence that exploits the reactivity of the functional groups embedded in the intermediate compounds. Many of these sequences involve repetitive functional group interconversion into active moieties that facilitate the elaboration of the core structure. Even though this type of chemistry is highly predictable, it demands substantial skill and resources to prepare even a small quantity of any substance. Nonetheless, it generates a vast quantity of waste and is often categorised as inefficient and non-sustainable.

In the late 20th century, transition metal-catalysed cross-coupling reactions have transformed the field of organic chemistry.^{1,2} These classical cross-coupling reactions like Mizoroki-Heck, Suzuki-Miyaura, Stille, and Negishi have enabled convergent synthetic methodologies by pre-functionalisation of the starting materials. Over the past several decades, the development of new families of ligands and metal complexes for these reactions has paved the way for the synthesis of a myriad molecules.³ However, many of the organometallic reactants are highly toxic, air, and moisture sensitive.

In this century, the field of chemistry has been transitioning to a more sustainable approach.⁴⁻⁶ With the direct functionalisation of ‘inert’ C-H bonds, it is offering a direct, atom-economical tool-box. As most organic molecules are built on a hydrocarbon backbone, C-H bonds are ubiquitous, and direct activation of these C-H bonds convert a broader range of simple feedstocks to the complex and valuable building blocks (Figure 3.1).⁷

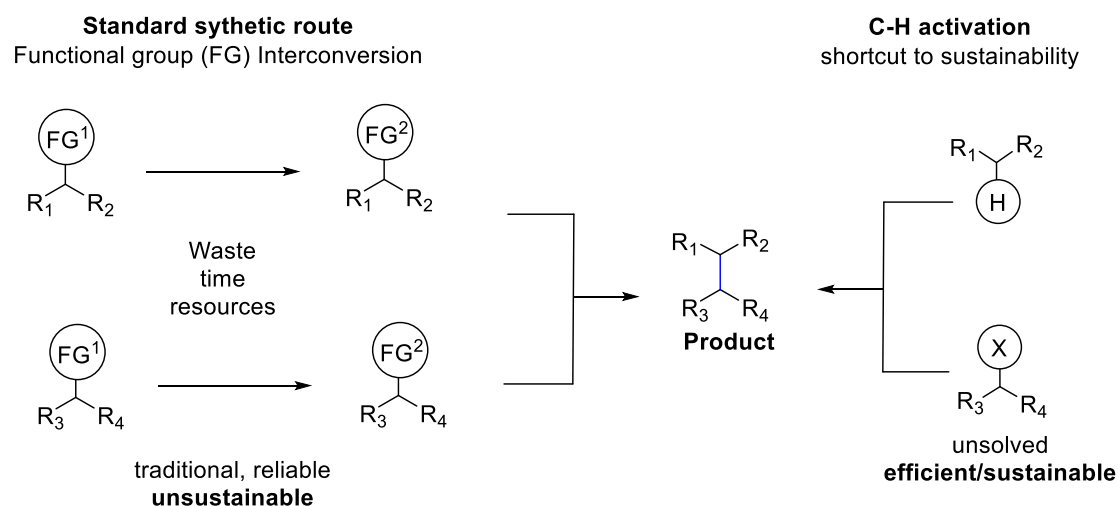


Figure 3.1: Traditional synthetic route vs C-H activation.

3.1. C-H functionalisation

C-H activation is a revolutionising method as it circumvents many of the shortcomings of traditional synthetic methods.⁸ It renders multiple functional group interconversions redundant and directly transforms starting materials into complex molecules. Fundamentally, this technique uses ‘non-activated’ and ‘unarmed’ C-H bonds to couple molecules. C-H functionalisation reactions are mainly based on the noble metals (Pd, Rh, Ru, Ir),^{9,10} while only a few are based on the earth-abundant metals (Fe, Cu, Zn, Ni).¹¹ For this reason, transition-metal catalysed C-H activation is often defined as a ‘Holy Grail’ in organometallic chemistry. Theoretically, the method ‘C-H activation’ looks straightforward, however, it is not easy, and only a specific C-H bond within a molecule must be reacted. In the section below, I will present the principal challenges associated with this field.

3.2. General problems associated with C-H activation

In the C-H activation chemistry, regioselectivity and enantioselectivity are still unsolved problems due to the robust nature of C-H bonds.

C-H bonds are generally unreactive. This is due to their high bond dissociation energies (between 355 and 439 kJ/mol) and similar electronegativities of carbon (2.5) and hydrogen (2.2), leading to a non-polar bond.^{12,13} Although the strength of the bonds follows the increasing trend of $sp^3 < sp^2 < sp$ (bond dissociation enthalpy at 298 K: C(sp^3)-H 406.2, C(sp^2)-H 443.5 and C(sp)-H 548.5, kJ/mol), the activation barrier decreases in the same trend. Studies suggest

that the difference in energy of $\sigma^*_{\text{C-H}}$ LUMO antibonding and $\sigma_{\text{C-H}}$ HOMO bonding orbital and steric hindrance of C-H bonds decide the ease of activation.¹⁴

The second problem is to control the site-selectivity so that only the desired C-H bond can be functionalised in the presence of many C-H bonds with similar reactivity (regioselectivity).¹⁵

An even more challenging problem is distinguishing two prochiral C-H bonds, breaking the symmetry of the molecule, and permitting the synthesis of chiral molecules (enantioselectivity).⁹

The section below will describe the general strategies to address these challenges in C-H functionalisation reactions.

3.3. Overview of metal-mediated C-H activation mechanism

The metal-mediated C-H activation can be *via* either an ‘outer-sphere’ mechanism, which does not involve the direct interaction between the C-H bond and the metal reagents, or an ‘inner-sphere’ mechanism, where the metal reagent is intimately involved in breaking the C-H bond.

3.3.1. Outer-sphere mechanism

The key feature of this type of mechanism is that the substrate does not interact directly with the transition metal but instead reacts with the metal ligand. The mechanism proceeds by two steps, (i) formation of a high oxidation state metal complex containing an activated species such as metal oxo-, imido- or carbene species followed by, (ii) reaction of the activated species with a C-H bond.^{16,17} The latter step proceeds by either direct insertion or H-atom abstraction/radical rebound (Figure 3.2). The selectivity of the reaction is determined either through the intrinsic selectivity of the substrate or through the spatial arrangement of the ligand that controls the substrate approach to the reactive centre.

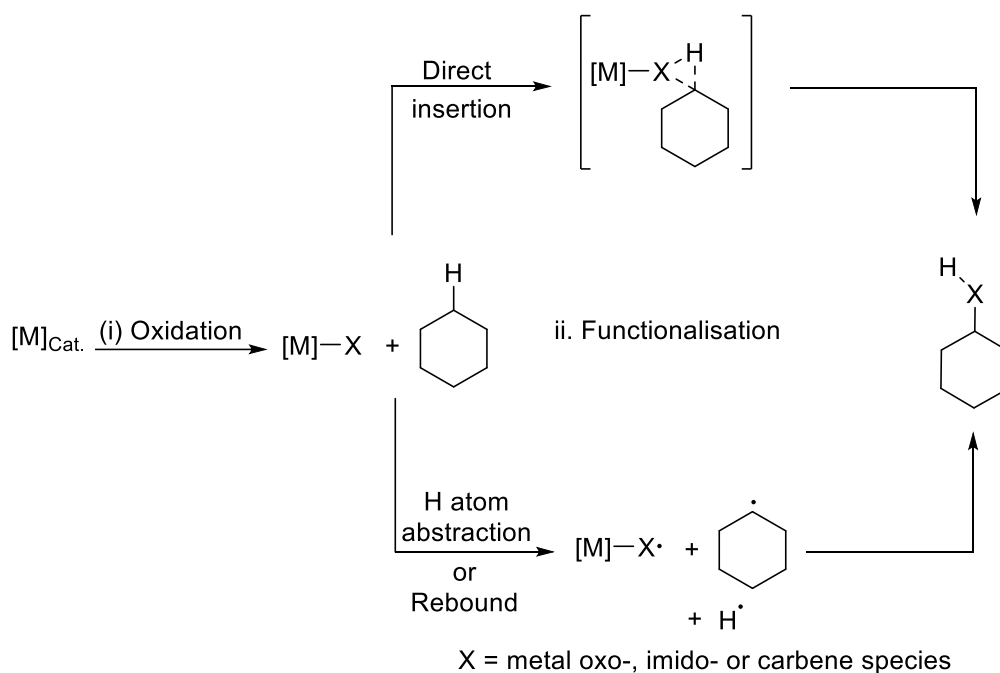


Figure 3.2: Outer-sphere mechanism.

3.3.2. Inner-sphere mechanism

In this mechanism, the substrate directly coordinates to the transition metal that leads to C-H bond cleavage *via* formation of a discrete organometallic intermediate (Figure 3.3). Most inner-sphere reactions utilise a Lewis basic functionality known as a directing group within the substrate to direct the metal to a specific C-H bond.^{18,19}

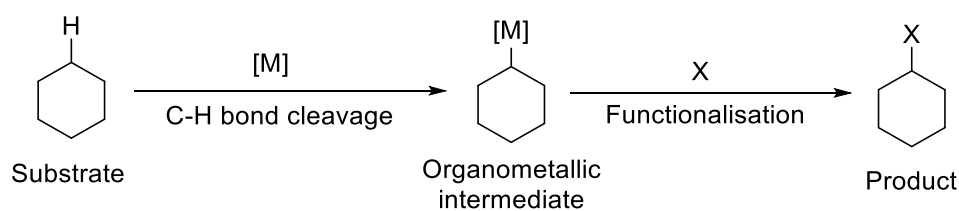


Figure 3.3: Inner-sphere mechanism.

In a large number of C-H activation reactions, insertion into a C-H bond is achieved by the ‘concerted metalation deprotonation’ (CMD) pathway, also named as ambiphilic metal-ligand activation (AMLA) or internal electrophilic substitution (IES). The section below will focus on the palladium-induced CMD.

3.3.4. Concerted metallation deprotonation pathway

In palladium-mediated C-H activation reactions, the first step is a redox neutral insertion of the metal into the C-H bond to give a C-Pd bond, which can be further functionalised. Palladium acetate [Pd(OAc)₂] is generally the best choice for the catalyst since the acetate ligand is believed to play multiple roles in cyclometallation reactions,²⁰ namely;

- It promotes the solvolysis of the reaction intermediates due to its larger effective volume.
- It enhances the electrophilicity of the Pd^(II) centre due to the dual ability of acetate to act as a monodentate or bidentate ligand.
- It also plays the role of an intramolecular base for deprotonation.

Palladium insertion is believed to proceed through concerted metallation deprotonation (CMD). It normally involves a concerted six-membered transition state in which a bound carboxylate, or appropriate conjugate base, transfers the proton while concurrently facilitating the formation of the palladacycle (Figure 3.4). The corresponding palladacycle undergoes a variety of different transformations depending on the reaction partner. Normally, the five-membered palladacycle is kinetically favoured over six- and seven-membered palladacycles, and this preference can be used to control the regioselectivity of the reaction.²¹

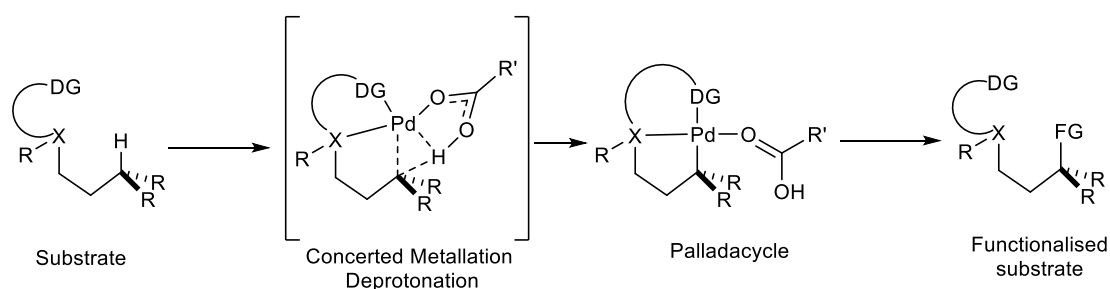


Figure 3.4: Concerted metallation deprotonation.⁷

For most reactions involving the CMD step, the conjugate base removes the hydrogen atom as the carbon-metal bond forms in a concerted process. The base coordinates to the metal giving rise to the cyclic or concerted mechanism. The base can be either external or internal. An internal base could be the part of the ligand and participate in a more organised cyclic mechanism (Figure 3.5).

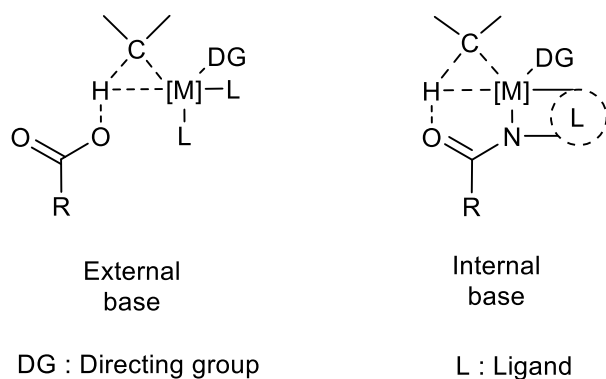


Figure 3.5: Type of base in CMD process.

To give more insight on CMD pathway, Davies et al. performed computational studies on Pd(OAc)₂-promoted cyclometallation of *N,N*-dimethylbenzylamine **3.1**. Studies show the favourable route *via* a palladium and C-H bond interaction followed by an acetate assisted six-membered transition state **3.2** (Figure 3.6).²² In this, the hydrogen bonding between the acetate oxygen and C-H proton orients the base and increases the polarity of the C-H bond. The resulting interaction enhances the acidity of the *ortho*-proton, which can then be readily deprotonated by the acetate base. All the above effects lower the energy barrier to the formation of thermodynamically stable five-membered palladacycle **3.3**. The study further demonstrated that Pd(OAc)₂ was not only the metal that promoted the cyclometallation and other catalysts such as [RuCl₂(*p*-cymene)]₂, [RhCl₂Cp*]₂ and [IrCl₂Cp*]₂, in the presence of acetate reacted similarly with *N,N*-dimethylbenzylamine **3.1** to form the cyclometallated product by the same mechanism.

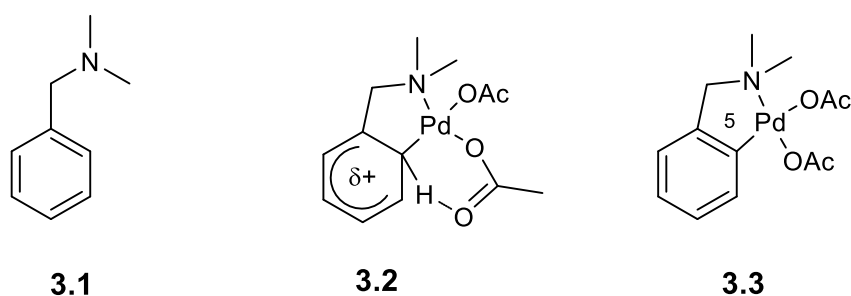


Figure 3.6: Acetate-assisted six-membered transition state & palladacycle.

The discussion below will present the general catalytic cycle for C-H activation reaction and explain the role of each additive or reagent.

3.4. A general catalytic cycle for C-H activation

A typical C-H activation reaction comprises four steps (Figure 3.7).

- The metal insertion process into the C-H bond (C-H activation)
- Functionalisation of the corresponding organometallic intermediate
- Elimination of the functionalised product
- Regeneration of the active catalyst (if required)

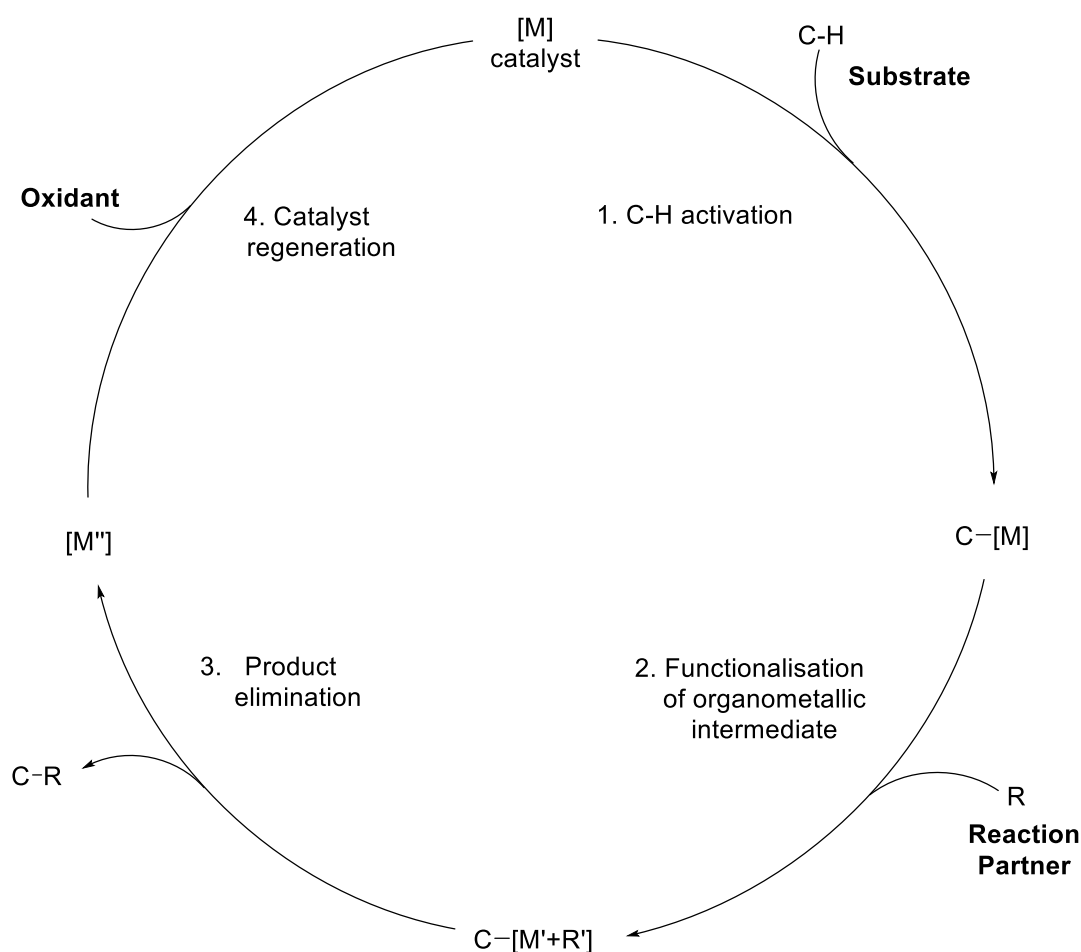


Figure 3.7: General catalytic cycle for C-H functionalisation reactions.

3.5. Role of directing group in C-H Functionalisation

The directing group has a crucial role in controlling the electronics at the metal centre and facilitating the regioselectivity by placing the metal in a close proximity to a single C-H bond in the substrate. In a directing group assisted C-H activation reaction, the directing group first coordinates to the metal which forms a discrete complex (Figure 3.8). In terms of kinetics, this increases the local effective concentration of the metal, accelerating the rate of C-H insertion.

This coordination helps the thermodynamics of the reaction as it stabilises the resulting metallacycle. The stable metallacycle has an important role in facilitating C-H activation. The conformation of the substrate will dictate which C-H bonds are proximal to the metal centre while the size of the metallacycle will determine which complex should be favoured. Ultimately, the structural and electronic requirements of this intermediate control the regio- and stereoselectivity of C-H functionalisation.

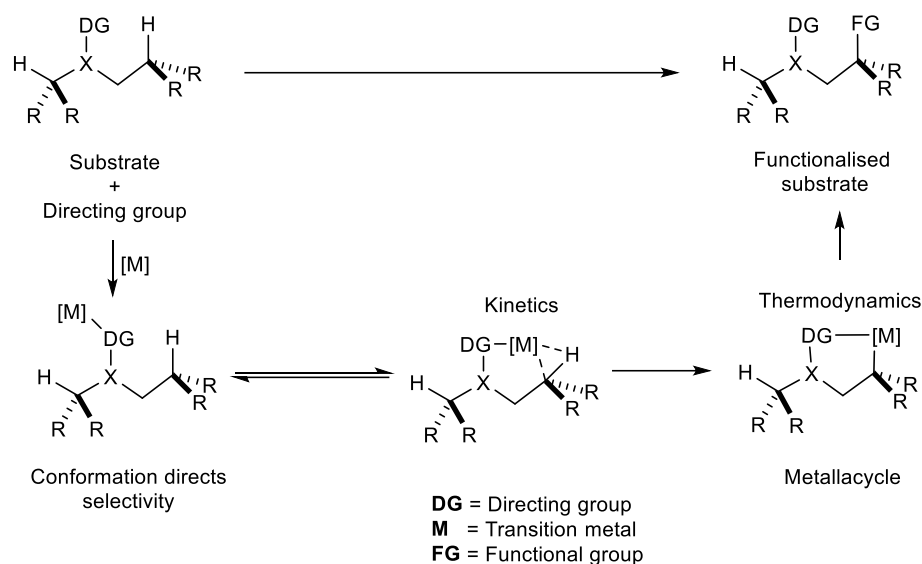
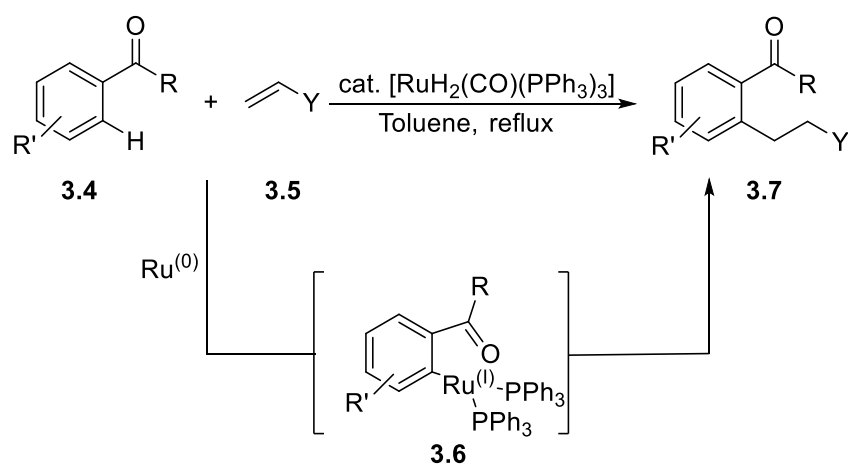


Figure 3.8: Role of directing group in C-H activation.⁷

One of the first examples was in 1993 when a ketone coordinated with the ruthenium catalyst and directed reaction to the *ortho* C-H position (Scheme 3.1).²³ This result showed, for the first time, that the direct C-H activation could be a valuable tool to access the range of small molecule entities.



Scheme 3.1: Ru-catalysed *ortho* alkylation of aromatic ketones.

Since this ground-breaking work, an array of directing groups has been reported for various catalytic C-H transformations. The earliest examples utilised strongly σ -donating or π -accepting directing groups *i.e.* aldehyde, amide, anilide, imine, carboxylic acid, ester, ketone, and hydroxyl groups.²⁴ With the progress in this field, oxazoline, pyridine, and π -chelation-based directing groups have been developed.²⁵ Moreover, directing groups, such as alkene, alkyne, and carbanion have also shown potential applications.²⁶ Recent reviews published in this area cover the whole range of directing groups and their recent advances in different C-H activation reactions with the future scope of expansion.²⁷⁻³⁰

Broadly, the directing groups can be categorised into three types.

- i. Auxiliary directing groups
- ii. Transient directing groups
- iii. Traceless directing groups

3.5.1. Auxiliary-based directing groups

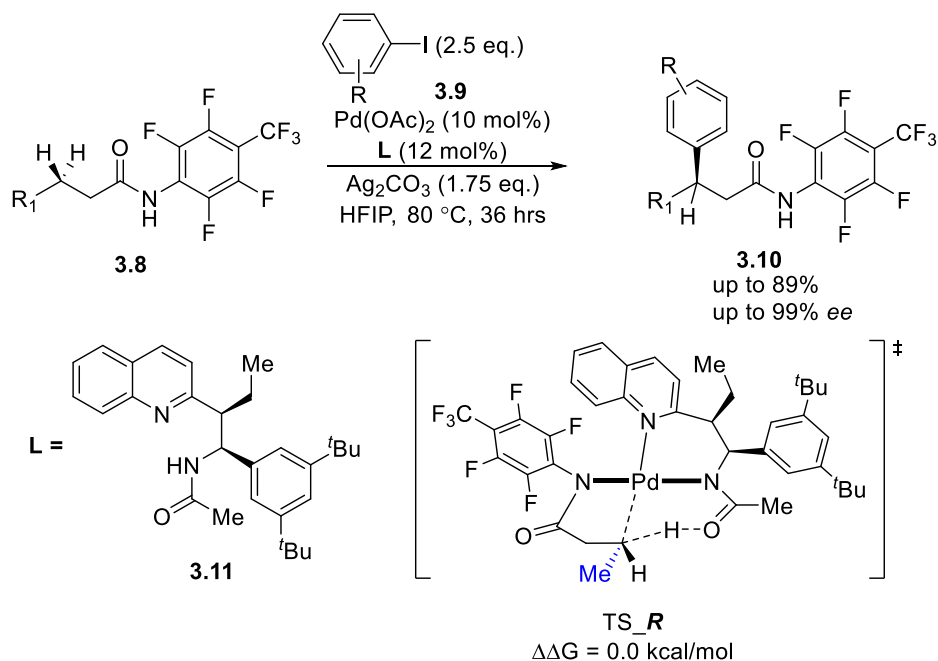
An auxiliary directing group is not an intrinsic part of the substrate. It is appended to the substrate prior to the reaction and removed or converted to the final desired functional group after the reaction. They can be further divided into either monodentate or bidentate.

3.5.1.1. Monodentate directing groups

Monodentate directing groups show more potential, as they can be used to tune the electronics of the metal to exert the reactivity and selectivity. As a monodentate directing group can coordinate to only one valence site on the metal catalyst, an external ligand can influence to the metal, and hence exert better control over reactivity and stereoselectivity compared to bidentate directing group.

Monodentate directing groups are mainly based on nitrogen-containing functionalities such as the Yu-Wasa auxiliary.³¹⁻³⁴ For example, the selective arylation of the methylene β -C-H bond was achieved by employing a monodentate Yu-Wasa auxiliary (Scheme 3.2).³⁵ The combination of a weak directing auxiliary and acetyl protected aminoethyl quinoline (APAQ) ligand proved to impart high enantioselectivity. The authors proposed that the oxygen of an amide of the APAQ ligand **3.11** acts as an intramolecular base to deprotonate the methylene C-H and promote Pd-C bond formation. The transition state (TS) TS_R postulated by DFT calculations was observed to be more favoured than the TS_S by 1.2 kcal/mol. In both transition

states, the six-membered ring and bulky *tert*-butyl substituent orient the amide directing group in a way that the β -C-H bond is activated. The orientation of the terminal methyl group of the substrate controls the *R* or *S* transition state. In the favoured transition state, it is *trans* to the bulky-*tert*-aryl group and the peri-hydrogen of the quinoline.

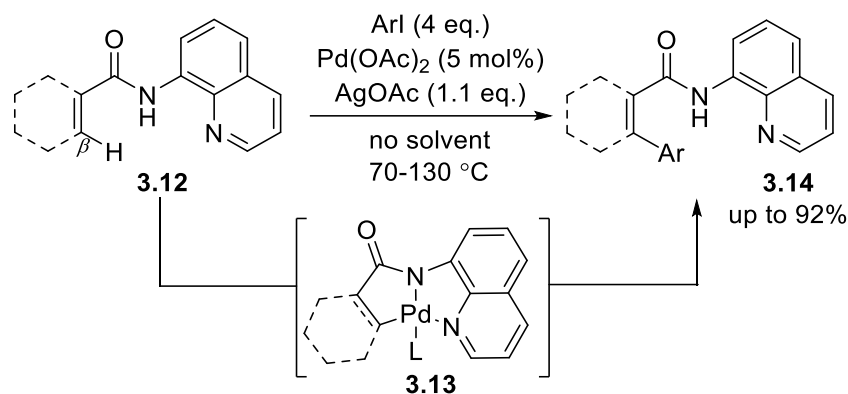


Scheme 3.2: Monodentate Yu-Wasa auxiliary directed enantioselective β -C-H activation.

Monodentate directing groups allow functionalisation of only some primary unactivated $\text{C}(\text{sp}^3)\text{-H}$ bonds. There are only limited examples of activating five- and six-membered rings, and without the addition of the external ligand they struggle to react. Due to this drawback, the reaction generally demands high catalyst loading and harsh reaction conditions to operate which could be detrimental to other sensitive functional groups.

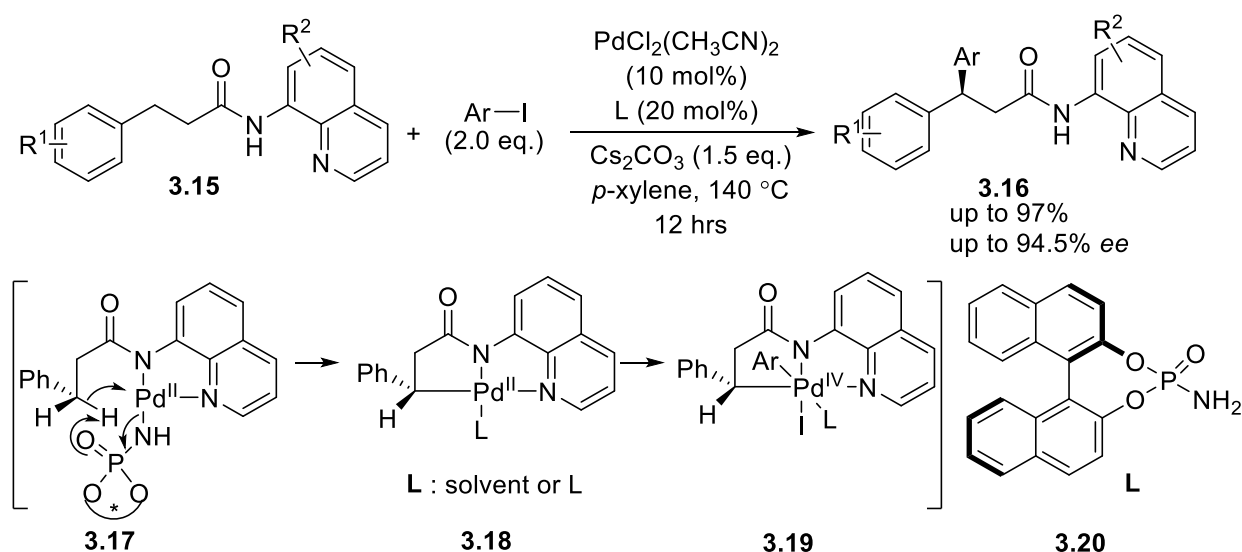
3.5.1.2. Bidentate directing groups

As explained above, most of the directed functionalisation of $\text{C}(\text{sp}^3)\text{-H}$ bonds are not compatible with monodentate ligands and this remains highly challenging. One potential solution would be to install two donating atoms in the directing group to stabilise the resulting metallacycle. For example, Daugulis and coworkers reported the use of 8-aminoquinoline as a bidentate directing group to facilitate the $\beta\text{-C}(\text{sp}^3)\text{-H}$ and $\text{C}(\text{sp}^2)\text{-H}$ functionalisation of various aliphatic and aromatic amides, respectively (Scheme 3.3).³⁶



Scheme 3.3: Bidentate directing group assisted Pd(II)-catalysed arylation.

Bidentate directing groups are mainly known to functionalise primary and secondary unactivated C-H bonds with only a few examples of tertiary C(*sp*³)-H bonds.^{27,37,38} Yan et al. utilised a combination of bidentate 8-aminoquinoline and chiral phosphoramidate **3.20** to achieve the enantioselective methylene β-C(*sp*³)-H arylation (Scheme 3.4).³⁹ A Pd(II)/Pd(IV) catalytic cycle was proposed, based on several kinetic isotope experiments (KIEs). The C-H activation step was thought to be a rate limiting step, resulting in the formation of intermediate **3.17** after deprotonation and complexation of an amide **3.15** with Pd(II) species. Further, the chiral amide **3.20** promotes the selective cleavage of one of the C-H bonds at the β-position to generate an enantioenriched intermediate **3.18**. The oxidative addition of aryl iodide to Pd(II) produces electron-deficient Pd(IV) intermediate **3.19**. Finally, the reductive elimination from the **3.19** delivers the respective product **3.16** and regenerates the Pd(II) catalyst after ligand exchange with the substrate **3.15**.

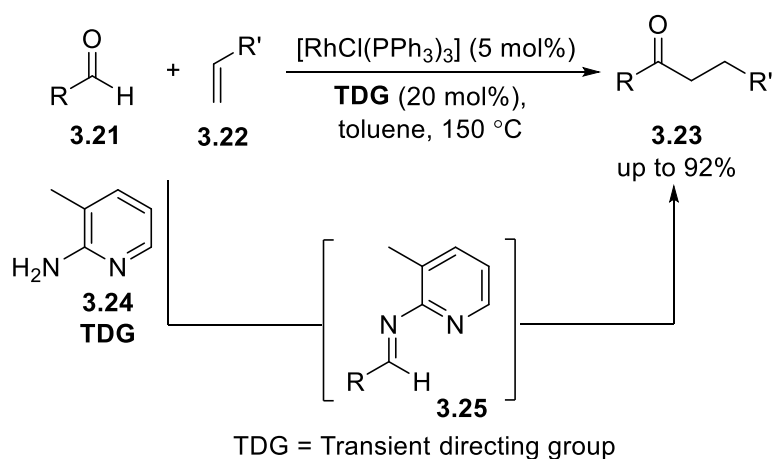


Scheme 3.4: Bidentate 8-aminoquinoline directed benzylic C(*sp*³)-H arylation.

3.5.2. Transient directing group

Transient directing groups are attractive as they can be used in sub-stoichiometric quantity. They can potentially minimise the requirement of structure modification and allow the reaction to proceed under mild reaction conditions. They reversibly react with the existing functionality of the substrate, direct the C-H functionalisation, and undergo cleavage in a one-pot reaction.

Jun and co-workers used the transient existence of an imine to temporarily install a monodentate pyridine directing group for Rh-catalysed hydroacylation of an alkene **3.22** (Scheme 3.5).⁴⁰ The successful transformation used a substoichiometric quantity of 2-amino-3-methyl pyridine **3.24** to temporarily form an imine **3.25** that directed C-H activation to deliver anti-Markovnikov hydroacylated products **3.23**.



Scheme 3.5: Hydroacylation of aldehyde with terminal alkenes by imine transient directing group.

After this seminal report, the C-H activation field has experienced rapid growth in terms of design and utilisation of transient directing groups in myriad C-H functionalisation reactions. A number of reviews cover the use of transient directing groups in C-H transformations.⁴¹⁻⁴³

The catalytic cycle for C-H activation with a transient directing group is slightly different to the standard cycle. (Figure 3.9). Transient directing group will link to an existing functional group on the substrate in a reversible manner (step 1). Further, it will interact selectively with the transition metal catalyst, acting as either a monodentate or bidentate coordination group (step 2). The resulting metallacycle reacts with a coupling partner to form an intermediate **III** (step 3). After selective functionalisation, the intermediate **III** converts into the intermediate **IV** in a way that delivers the desired product, with the regeneration of both the transient directing group and the transition metal catalyst to continue the catalytic cycle (step 4).

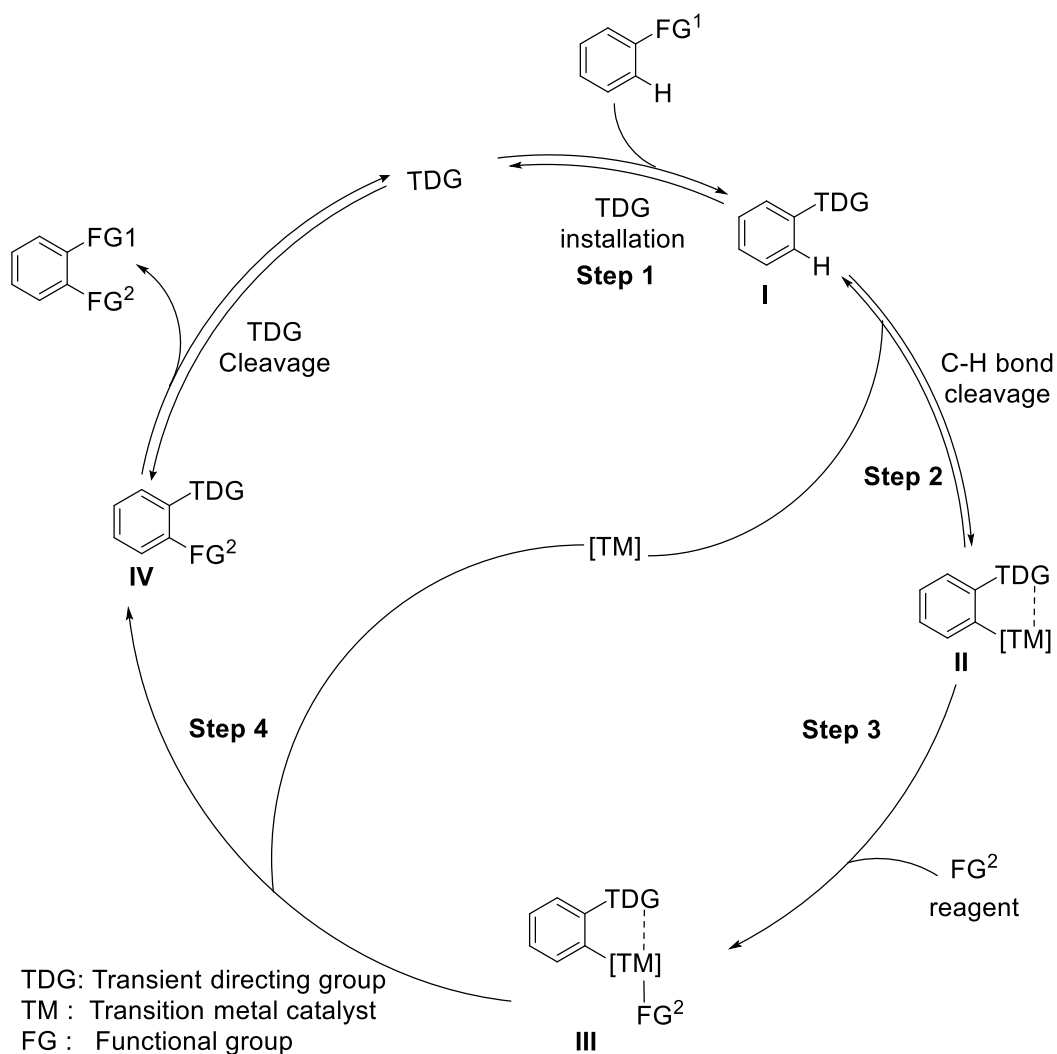
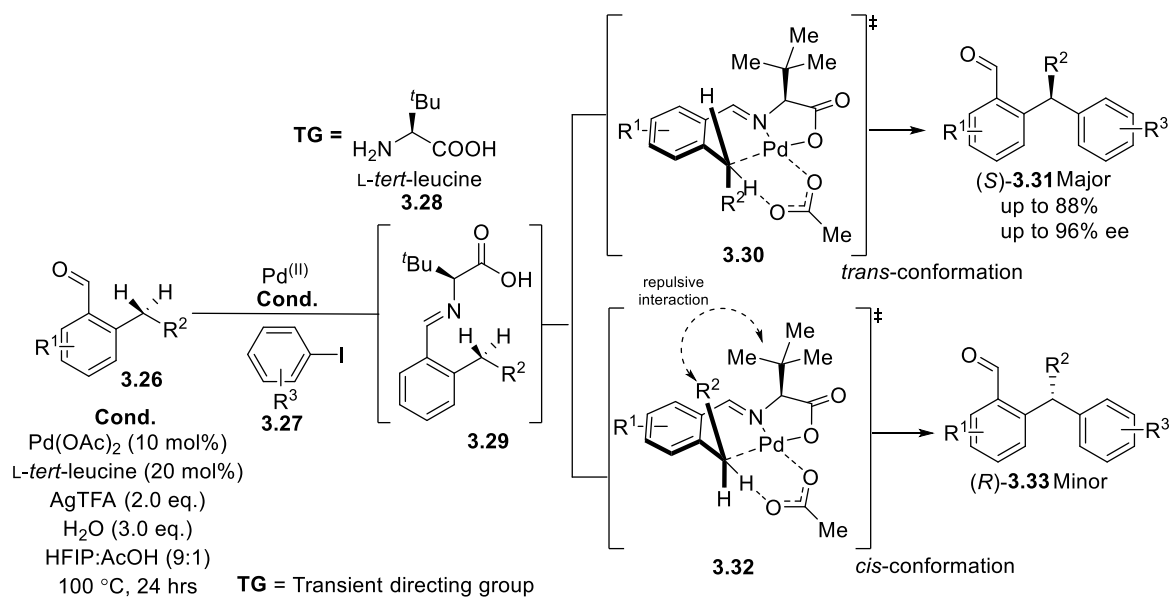


Figure 3.9: Transient directing group mediated C-H functionalisation.

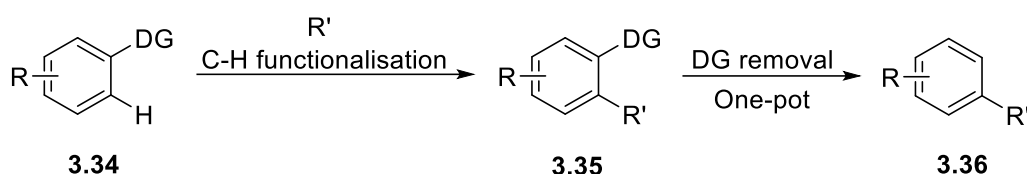
Yu's group achieved a highly enantioselective arylation of 2-alkyl benzaldehyde **3.26** using L-*tert*-leucine **3.28** as the transient directing group.⁴⁴ It was proposed that the geometrical arrangement, resulting from the steric repulsion between the bulky ^tBu group and the R² group of the substrate **3.26** is the deciding factor for enantiocontrol (Scheme 3.6). The *trans*-conformation in the transition state **3.30** is favoured and gives the major product **3.31**. The *cis* transition state **3.32**, which leads to the minor product **3.33**, is disfavoured due to steric interaction between R² and ^tBu.



Scheme 3.6: Transient directing group directed enantioselective benzylic C-H activation of 2-alkyl benzaldehyde.

3.5.3. Traceless directing group

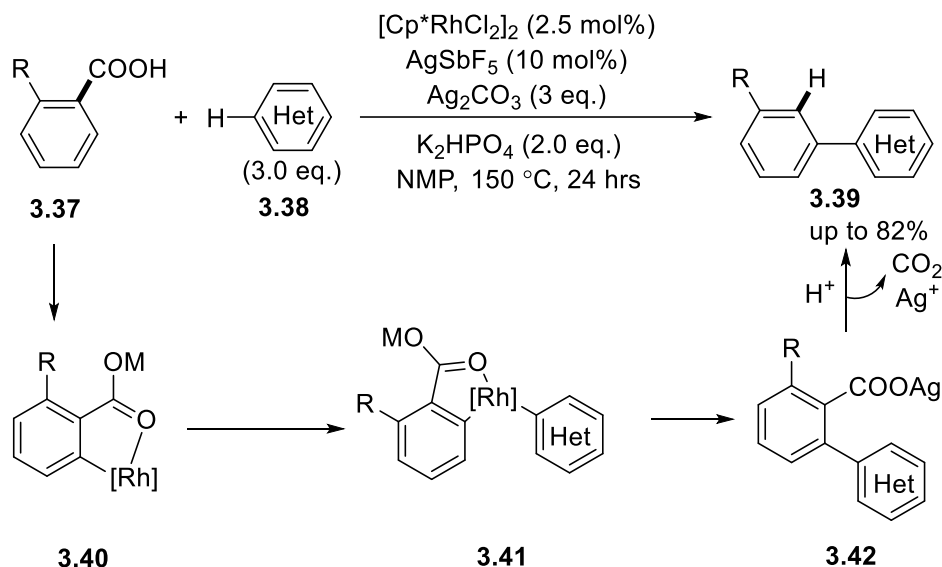
The concept of a traceless directing group involves both C-H functionalisation and removal of directing group in a one-pot reaction (Scheme 3.7). Sometimes, installation of a directing group similar to transient functionality is also possible in one-pot. A review published by Zhang et al. covers a range of examples based on the traceless directing group strategy.⁴⁵



Scheme 3.7: Concept of traceless directing group.

Among different types of functionalities, carboxylic acids are attractive directing groups as they can be tracelessly removed by protodecarboxylation. Both *ortho*- and *para*-substituted moieties can be achieved by a carboxylic *ortho* directing group. Qin et al. utilised carboxylic acids as a traceless directing group to achieve Rh^(III)-catalysed decarboxylative *ortho*-heteroarylation of aromatic carboxylic acids **3.37** (Scheme 3.8). The authors proposed that the decarboxylative step is catalysed by Ag₂CO₃ rather than the Rh-catalyst. The coordination of carboxylic acid functionality to the Rh-catalyst directs the *ortho* C-H activation to form a five-membered rhodacycle **3.40**. Further reaction with heteroarenes forms heteroarene rhodacycle

intermediate **3.41**. Lastly, reductive elimination and protodecarboxylation provide the *ortho*-heteroarylated products **3.39**.



Scheme 3.8: Rh^(III)-catalysed decarboxylative *ortho*-heteroarylation of aromatic carboxylic acids.

3.6. Role of ligand in C-H Functionalisation

The incorporation of the ligand has several beneficial effects in C-H functionalisation reactions. Ligands can stimulate the activity of the metal catalyst to increase the reaction rate, the turn over number (TON: moles of products per mole of the catalyst), the turn over frequency (TOF: moles of products per mole of catalyst per unit time), and yield of the reactions. Ligands can also enhance the selectivity of the reaction (*i.e.* chemo-, regio-, enantioselectivity).^{46,47}

The choice of ligand is mainly dependent on the type of reactions. Generally, phosphines and monoprotected amino acids (MPAA) are used.

3.6.1. Phosphorus-based ligands

Phosphorus-based ligands and their chiral versions are commonly employed in a variety of different C-H functionalisation reactions.⁴⁸ Among this category, chiral phosphoric acids have been extensively studied. They can be employed as a co-catalyst or a ligand in asymmetric transformations due to their ability as strong Brønsted acids ($\text{p}K_a$ 2-4). A recent review published by Engle et al. details the role of chiral phosphoric acids in asymmetric palladium catalysis.⁴⁹ Different mechanisms have been illustrated in the literature for the synergistic co-catalysis performed by the chiral phosphoric acids/amides with palladium transition metal (Figure 3.10).

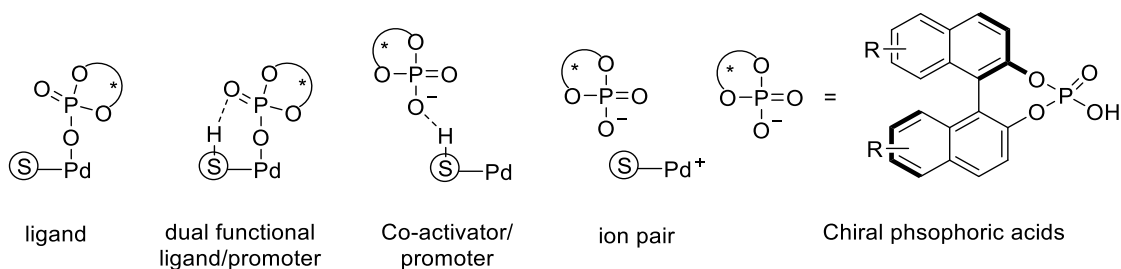
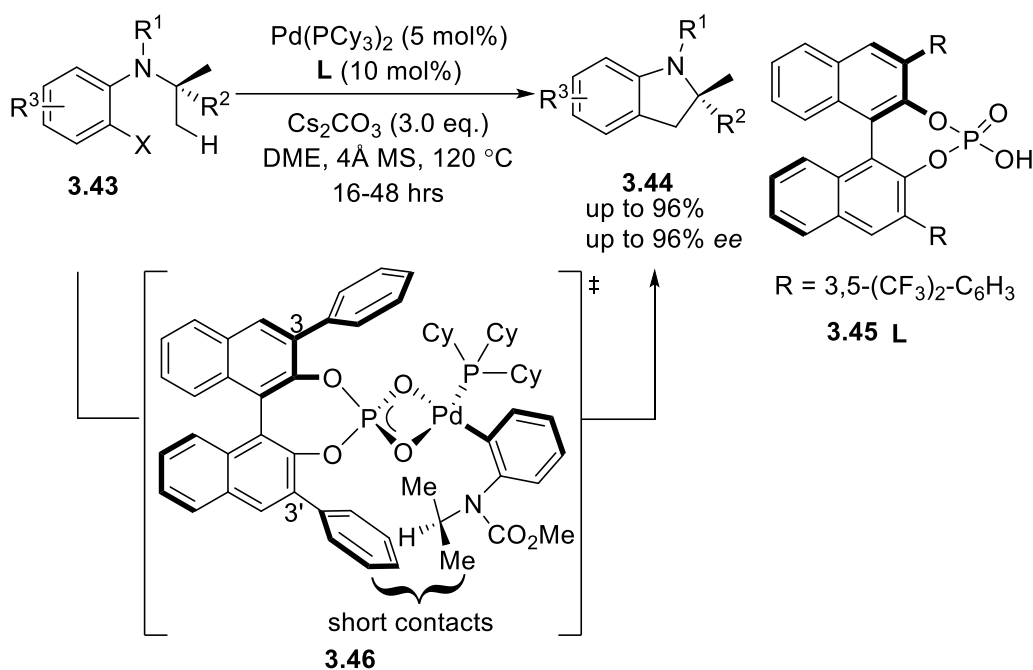


Figure 3.10: Different roles of chiral phosphoric acids with palladium catalysis.

Baudoin and co-workers achieved the Pd(0)-catalysed enantioselective C(*sp*³)-H activation with BINOL-derived phosphoric acid (BPA) **3.45** (Scheme 3.9).⁵⁰ The authors postulated a κ^2 -intermediate **3.46** derived from the 3,3'-disubstituted BPA, which would undergo C-H activation *via* a phosphate induced CMD mechanism. It was observed that tuning of the 3,3'-aryl substituents of chiral phosphoric acids could play a crucial role in controlling the enantioselectivity, allowing the synthesis of a variety of indolines **3.44** up to 96% *ee*.

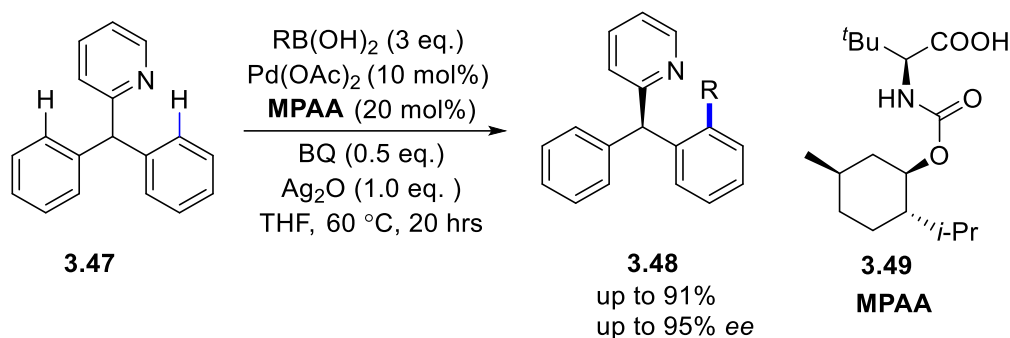


Scheme 3.9: Pd(0)-catalysed enantioselective C(*sp*³)-H activation.

3.6.2. Mono-*N*-protected Amino Acid

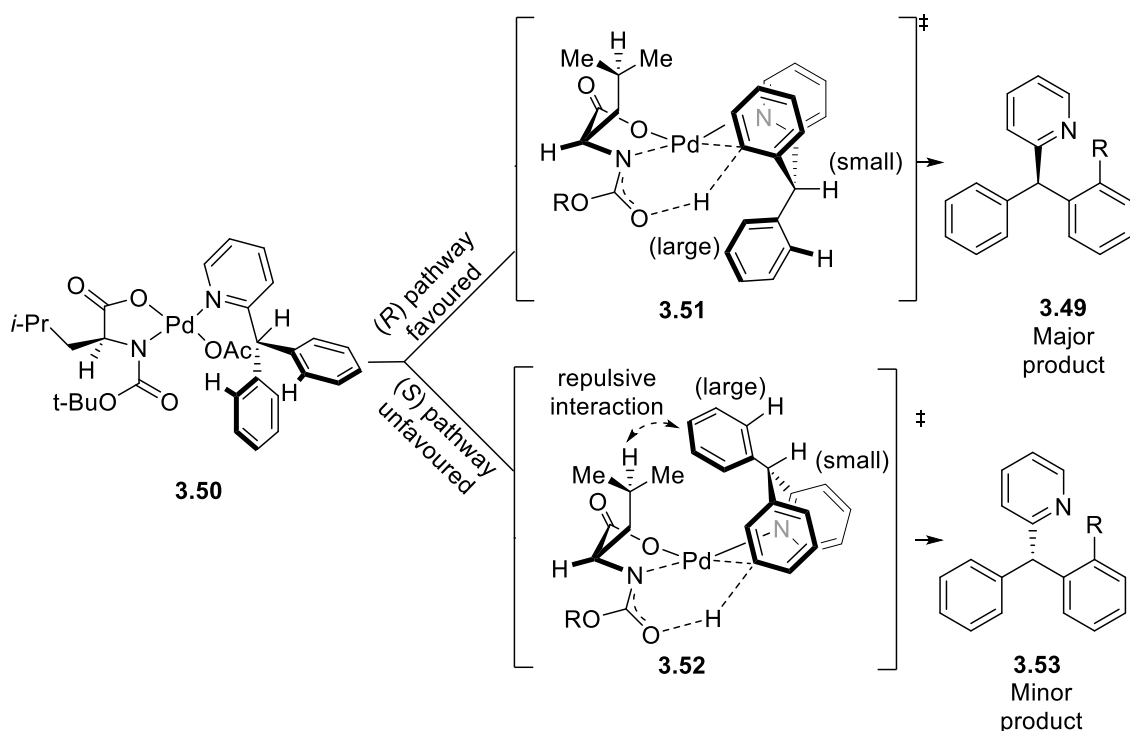
Mono-*N*-protected amino acids (MPAAs) have been thoroughly investigated in Pd(II)-catalysed enantioselective C-H activation.⁵¹ Recently, Yu and coworkers demonstrated the potential of MPAA ligand in Pd(II)-catalysed enantioselective C(*sp*²)-H activation of the 2-benzhydryl pyridine **3.47** (Scheme 3.10).⁵² The prochiral α,α -gem diphenyl substituents

underwent C(*sp*²)-H/R-B(OH)₂ cross-coupling in the presence of Pd(II) and (–)-menthyl substituted amino acid ligand **3.49**.



Scheme 3.10: Enantioselective C(*sp*²)-H activation catalysed by MPAA ligand.

The discovery of the MPPA ligand in the enantioselective C-H activation is intriguing. Initially, the reaction of 2-benzhydryl pyridine **3.47** with stoichiometric Pd(OAc)₂ led to formation of the racemic cyclometallated dimer. This can be converted to a chiral cyclometallated dimer by replacing the bridging acetate of Pd(OAc)₂ with an amino acid ligand. Unprotected amino acids and both *N*-protected amino acids failed to introduce the desired stereoselectivity. Later, MPAA had shown an average enantiocontrol. Further optimisation led to identify the (–)-menthol derivative of leucine **3.49** as an effective MPAA ligand. The proposed transition state is based on the coordination of palladium to both ligand and directing group (Scheme 3.11). The disfavoured transition state **3.52** involves an interaction between the MPAA ligand and the bulky aryl group. The major (*R*)-enantiomer **3.49** is formed when this clash is minimised.



Scheme 3.11: Stereochemical models for MPAA chiral induction.

Initial studies suggested that MPAA reactivity depends on the bidentate coordination ability of both the carboxylate and mono-protected amine to the metal centre. Recently, Musaev and coworkers performed detailed computational studies to gain more insight on the mechanism governed by MPAA.⁵³ The study suggests that a single MPAA-bridged dipalladium complex **3.54** [Pd_2MPAA] – an active catalyst comprised of two Pd centres bridged by a single MPAA ligand, is responsible for stereoinduction (Figure 3.11).⁵⁴

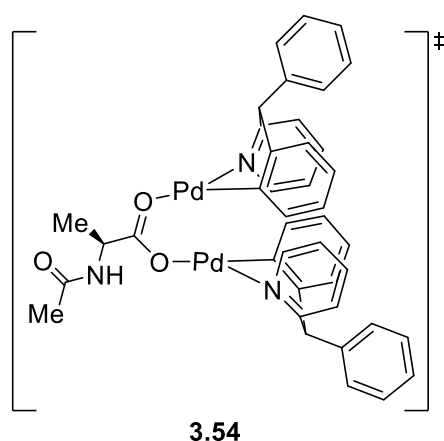


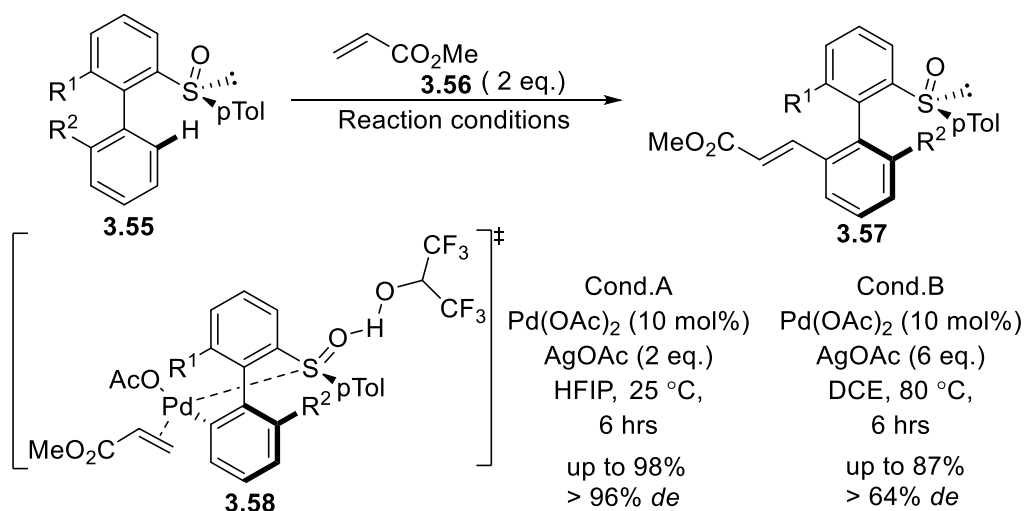
Figure 3.11: MPAA-bridged dipalladium complex **3.54** [Pd_2MPAA].

3.7. Role of solvent in C-H functionalisation

The nature of the reaction medium (polar or non-polar, acidic, or basic) has a significant influence on the outcome of the C-H activation reactions. A wide selection of polar solvents has been employed including polar protic, polar aprotic, acidic, halogenated solvents, and recently biomass-derived green solvents.

One of the more interesting choices is the polyfluorinated alcohol such as 1,1,1,3,3,3-hexafluoroisopropanol (HFIP) and 1,1,1-trifluoroethanol (TFE).⁵⁵⁻⁵⁷ HFIP, which is now considered as a ‘magic’ solvent due to its unique properties. HFIP is a highly polar, protic solvent yet is non-nucleophilic. The inductive effects of six fluorine atoms make it a weakly acidic media with a pK_a of 9.4 (at 25 °C in water). Due to its high dielectric constant, it can be employed as a co-solvent, generally with water, to stabilise the cationic species. All these characteristics allow HFIP to modulate the energy differences between different transition states.

Wencel-Delord and Colobert demonstrated the superior influence of HFIP in chiral sulfoxide-assisted atropo-diastereoselective oxidative olefination (Scheme 3.12).⁵⁸ The reaction was slow in common solvents like DCE, *i*-PrOH, AcOH, and $CHCl_3$, and gave only moderate stereoselectivity. The authors postulated that hydrogen bonding between the sulfoxide directing group and HFIP has two major implications. Firstly, H-bonding modifies the coordination ability of the directing group, which in turn influences the rate of C-H activation. Secondly, H-bonding modulates the geometry of the key palladacycle in a favourable way of stereoinduction.



Scheme 3.12: Chiral sulfoxide-directed atropo-diastereoselective oxidative olefination in HFIP.

C-H functionalisation reactions accomplished so far are mainly based on the platinum group metals such as palladium, rhodium, ruthenium, and iridium.^{8,9} Recently, a new trend of employing the earth-abundant 3*d*-transition metals has also been observed towards the more sustainable C-H activation.¹¹ Among all, palladium is the most employed transition metal. The following discussion will focus on palladium-catalysed C-H activation reactions.

3.8. Nature of active catalyst in Pd-catalysed transformations

Palladium can form complexes at different oxidation states at (0), (I), (II), (III), and (IV). There are different mechanistic cycles in the catalytic activity of palladium involving (a) mononuclear Pd(0)/Pd(II) species, or (b) Pd(II)/Pd(IV) species. Recently, Pd(III)⁵⁹ and Pd(VI)⁶⁰ oxidation states have also been proposed based on spectroscopic evidence, but not yet isolated. Considering the enormous success of palladium in C-H functionalisation reactions, the following discussion will focus on general mechanism of Pd(0)/Pd(II), Pd(II)/Pd(0), and Pd(II)/Pd(IV) catalytic pathways with examples of asymmetric variants.

3.8.1. Pd(0)/Pd(II) catalytic cycle

The Pd(0)/Pd(II) catalytic cycle is normally advanced for the intramolecular cyclisation of aryl halides (Figure 3.12). This strategy involves an initial oxidative addition to carbon-halide or equivalents prior to insertion into C-H bond. The oxidative addition can be accelerated by an electron-rich phosphine. This step requires a monoligated Pd(II) species. The chiral ligand/base has an important role in controlling enantioselectivity. The regeneration of the carboxylate co-catalyst will occur *via* irreversible deprotonation. Finally, the reductive elimination delivers the desired product and regenerates the active Pd(0) catalyst.

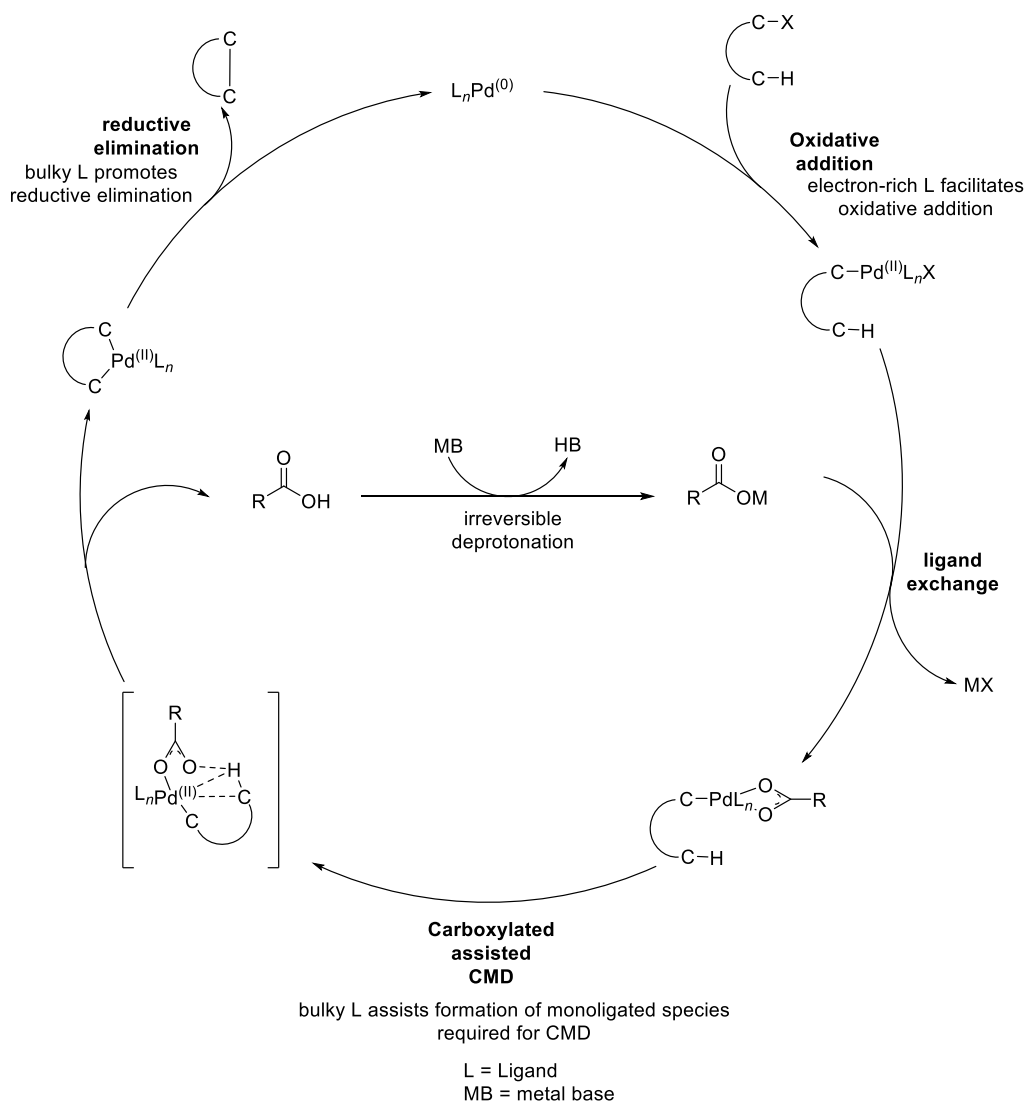
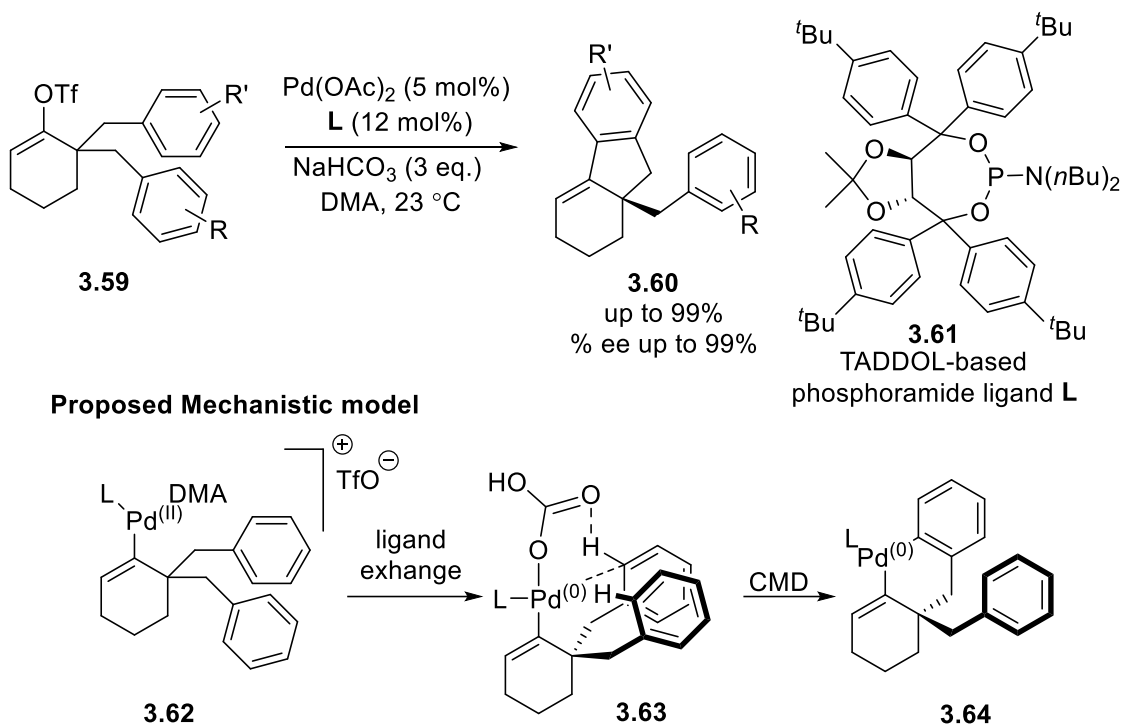


Figure 3.12: General catalytic cycle for Pd(0)-catalysed C-H activation.

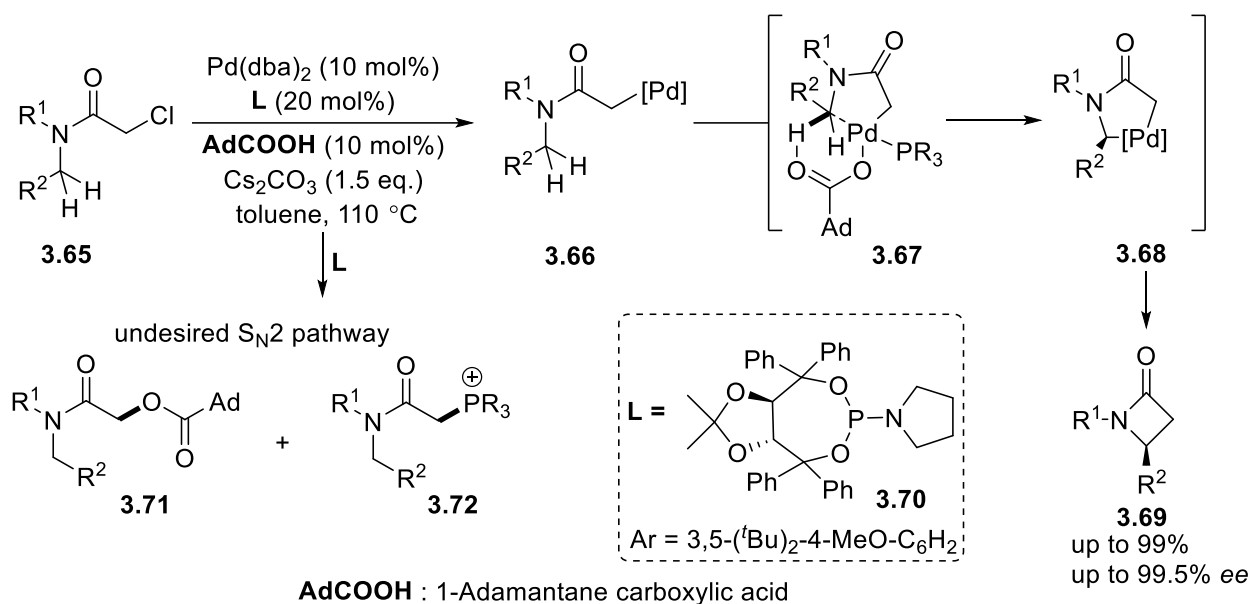
For intramolecular C-H activation reactions, enantioselectivity can be achieved in two different ways. First, by employing a chiral auxiliary ligand in combination with an achiral base and second by utilising a combination of an achiral ligand with a chiral base. These strategies have been successfully employed to synthesise tri- and tetrasubstituted stereocentres in high enantiopurity.

Cramer et al. demonstrated an intramolecular direct arylation of vinyl triflates **3.59** at room temperature to give enantiopure indanes **3.60** bearing an all-carbon quaternary stereocentre (Scheme 3.13).⁶¹ The key to achieving the high enantioselectivity was the tailored TADDOL-based phosphoramidate ligand **3.61** in combination with the highly polar DMA solvent. The authors proposed a mechanistic model in which, sodium carbonate acts as a conjugate base to initiate a CMD of the aryl group to provide a six-membered palladacycle **3.64**.



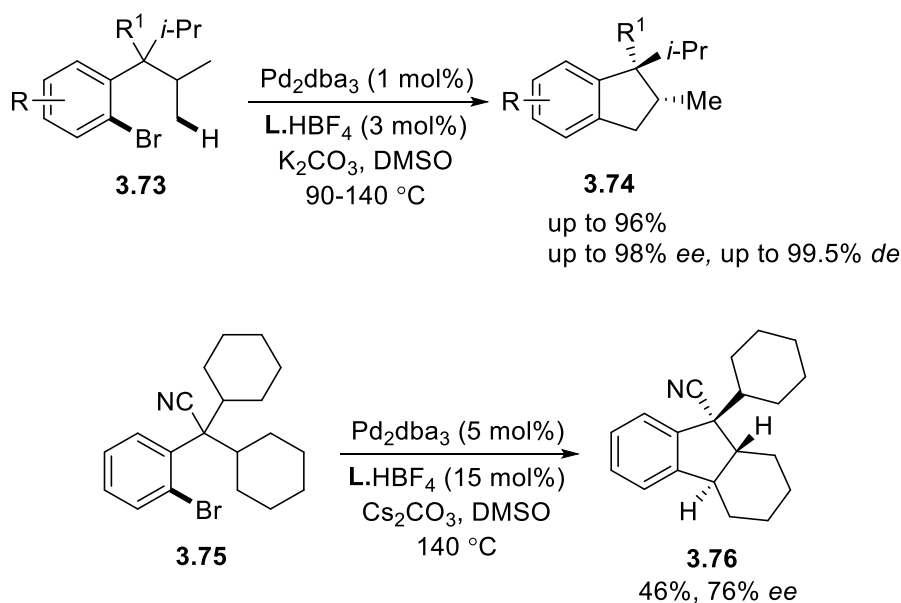
Scheme 3.13: Enantioselective Pd(0)/Pd(II) C(*sp*²)-H activation: synthesis of chiral indanes.

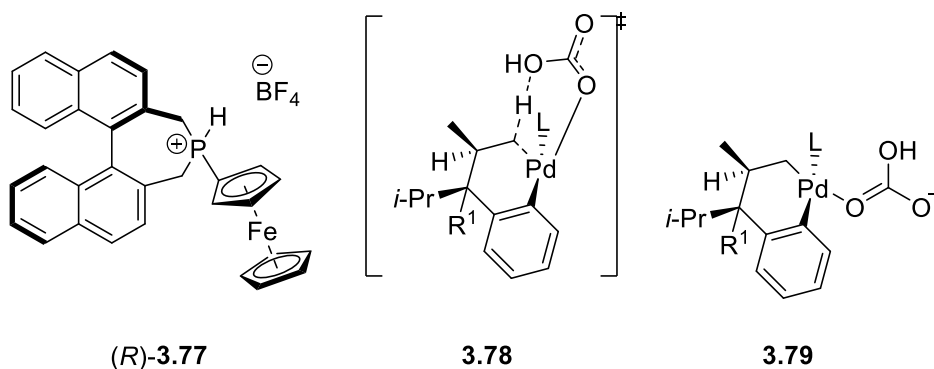
The role of TADDOL-derived phosphoramidites as a chiral ligand was extended for an intramolecular Pd(0)-mediated C(*sp*³)-H activation of chloroacetamide **3.65** for the synthesis of highly functionalised β -lactams **3.69** (Scheme 3.14).³⁷ Under standard conditions, this cyclisation was plagued by unwanted substitution of the chloride with either acid or phosphoramidites. The side products **3.71** & **3.72** were obtained from the undesired nucleophilic substitution at the α -chloro group. This side reaction could be minimised by the collaborative catalyst effect of precisely designed bulky TADDOL ligand **3.70** and 1-adamantane carboxylic acid (AdCOOH).



Scheme 3.14: Enantioselective Pd(0)-catalysed C(sp^3)-H activation approach to β -lactams **3.69**.

Holstein et al. demonstrated diastereoselective and enantioselective intramolecular arylation of primary and secondary C(sp^3)-H bonds of aryl bromides **3.73** & **3.75** to synthesise up to three stereocentres containing fused cyclopentanes **3.74** & **3.76** (Scheme 3.15). Ferrocenylbiphenyl ligand **3.77** proved to be competent to impart high stereoselectivity. Based on computational studies, the authors proposed that the monoligated palladium complex **3.79** is essential for the enantiodetermining step. The selective formation of the (*R,R*)-enantiomer was reasoned to the weak interactions between phosphine ligand, base, and substrate in the favoured transition state **3.78**, in which the O-Pd-C(sp^3) angle is reduced to $\sim 120^\circ$ for proton abstraction by carbonate base.





Scheme 3.15: Enantioselective Pd(0)-catalysed C(*sp*³)-H activation approach to fused cyclopentanes 3.74 & 3.76.

3.8.3. Pd(II)/Pd(0) catalytic cycle

Most of the reported palladium-catalysed C-H activation reactions take place at the Pd(II) centre. The Pd(II)/Pd(0) catalytic cycle is illustrated in Figure 3.13. First, the Pd(II) complex initiates the C-H activation event. This is followed by transmetalation and then reductive elimination to furnish the desired product. The resultant Pd(0) species must be oxidised into Pd(II) with an external oxidant before the completion of the cycle.⁶²

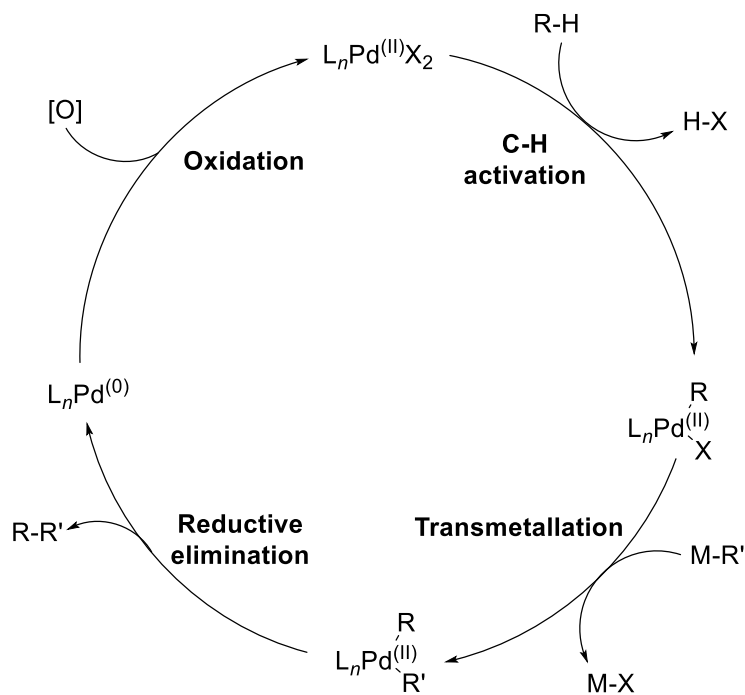
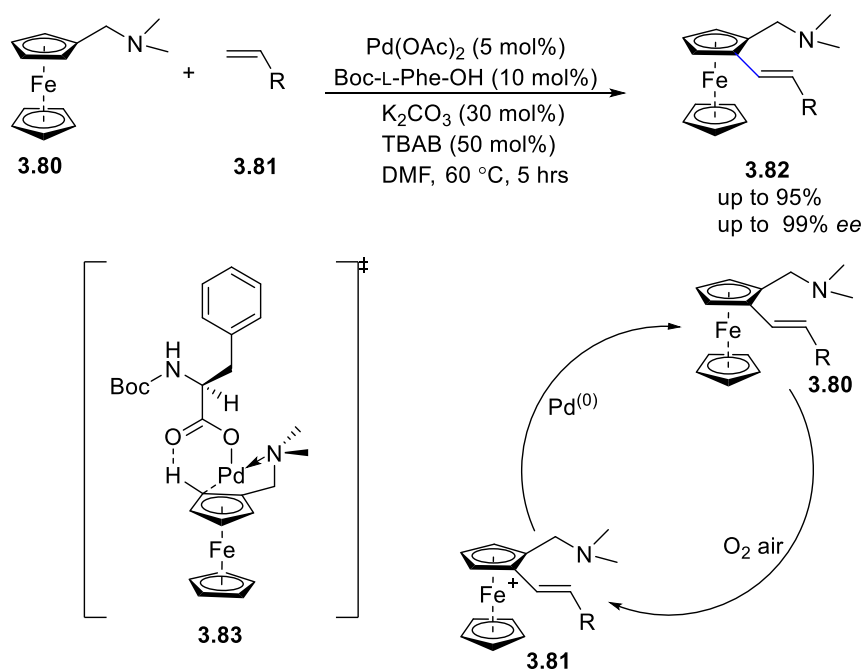


Figure 3.13: General catalytic cycle for Pd(II)-catalysed C-H activation.

Cui and coworkers performed a Pd(II)-mediated desymmetrisation of a ferrocene derivative **3.80** to give the planar chiral product **3.82**.⁶³ In this example the *N,N*-dimethylaminomethyl group was the directing group and the enantioselectivity was achieved by an MPAA ligand, – Boc-L-Phe-OH. Further, the experimental studies suggested that both air, and the ferrocene moiety are crucial. It was proposed that a ferrocenium **3.81** was formed *in situ* by air and this served as a terminal oxidant to regenerate a Pd(II) species from the reduced Pd(0) in the catalytic cycle.



Scheme 3.16: Pd(II)-mediated desymmetrisation of a ferrocene derivative **3.80**.

3.8.4. Pd(II)/Pd(IV) catalytic cycle

The C-H transformation by the Pd(IV) catalytic cycle is an emerging topic, and reactions proceeding through this cycle are generally operationally simple with good functional group compatibility. Moreover, both C-C and C-heteroatom bonds can be constructed. The strong oxidant that converts Pd(II) to Pd(IV) is normally based on electrophilic “F⁺” reagents, hypervalent iodine reagents, or inorganic peroxides. C-H activation reactions that follow the Pd(II)/Pd(IV) catalytic cycle are believed to proceed with the generation of a Pd(II)-C bond prior to the oxidation event.

The general Pd(II)/Pd(IV) catalytic cycle is believed to proceed following the four steps as depicted in Figure 3.14. The first step is similar to the Pd(II)/Pd(0) cycle, C-H activation at Pd(II) centre (step 1). The second step differs, here a stoichiometric external oxidant converts

Pd(II) into an electron deficient Pd(IV) by the loss of two electrons (step 2). In the next step, the organopalladium intermediate **I** can interact with the substrate (R'-H) to form the Pd(IV) complex **III** (step 3). Finally, the reductive elimination closes the catalytic cycle by delivering the desired C-H activation product (step 4).

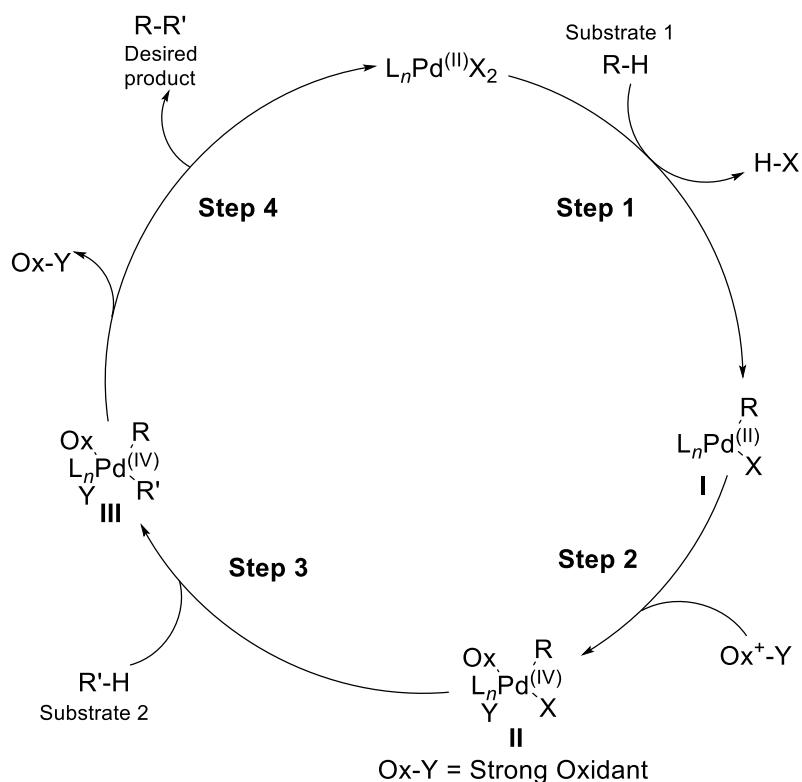
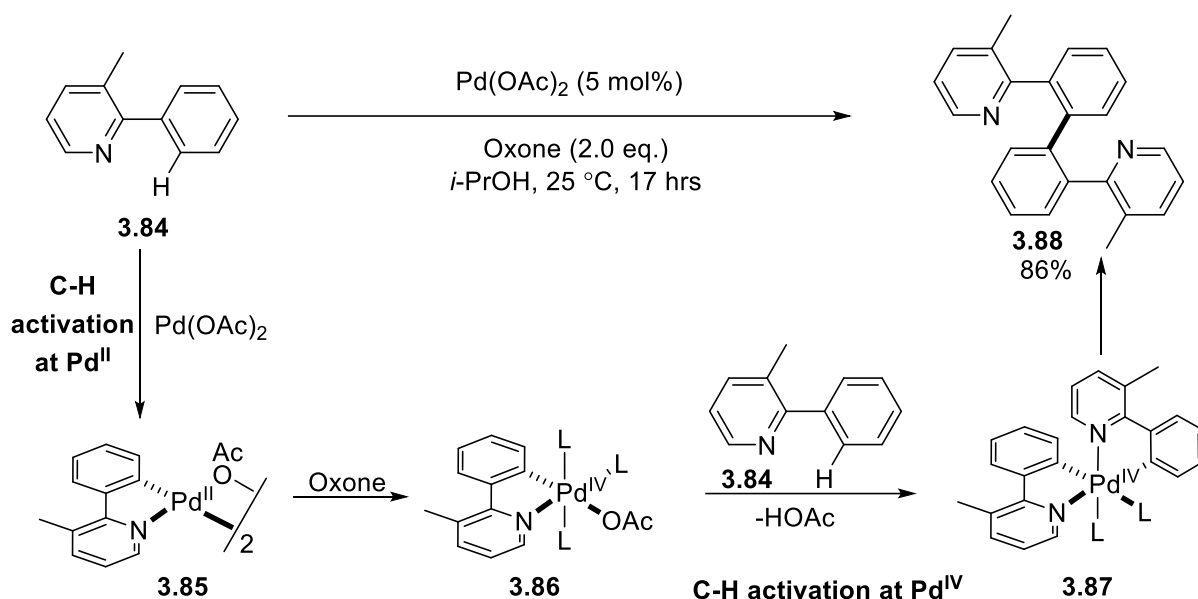


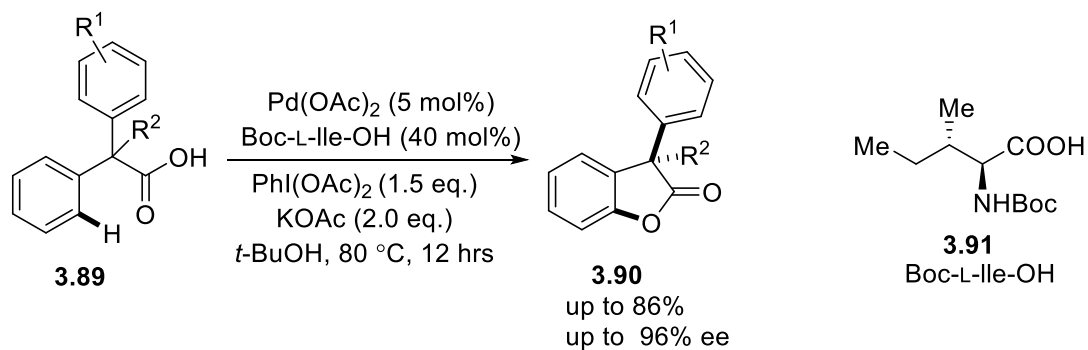
Figure 3.14: General catalytic cycle for Pd(IV)-catalysed C-H activation.

The first report of the Pd(IV) catalytic cycle was disclosed by the Sanford group.⁶⁴ They achieved the intermolecular oxidative coupling of 2-aryl pyridines **3.84** in the presence of oxone as a terminal oxidant (Scheme 3.17). A series of mechanistic investigations proved that the reaction involved two sequential C-H activation steps. The first C-H activation was believed to take place at Pd(II), while the second one at Pd(IV).



Scheme 3.17: Pd(IV)-catalysed dimerization of 2-aryl pyridines **3.84**.

The first enantioselective reaction to proceed through a Pd(II)/Pd(IV) catalytic cycle was reported by Yu and co-workers.⁶⁵ The direct synthesis of α,α -disubstituted chiral benzofuran-2-ones **3.90** was achieved by C-H activation/C-O bond formation from diphenyl acetic acids **3.89**, employing the MPAA ligand, Boc-L-Ile-OH **3.91**, and the oxidant – diacetoxyiodobenzene (Scheme 3.18).



Scheme 3.18: Enantioselective C-H lactonisation of diphenyl acetic acids **3.89**.

3.9. C-H functionalisation of saturated-*N*-heterocycles

Due to the abundance of saturated-*N*-heterocycles in natural products and their prominent biological activities, the efficient synthesis of these scaffolds has always been of great interest to organic chemists.⁶⁶ Among various methods available, C-H functionalisation offers shorter and easier route to access the library of analogues.⁶⁷

For a piperidine system, the proximal position *i.e.* α -position to the nitrogen centre is the easiest to functionalise.^{68,69} However, the research on $C(sp^3)$ -H functionalisation of the remote sites *i.e.* β -position and γ -position is still limited (Figure 3.15).

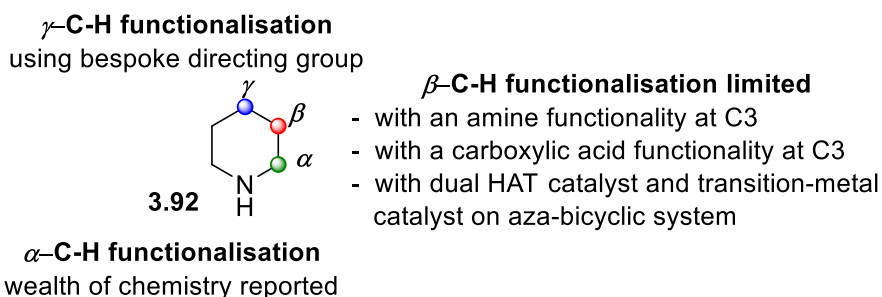
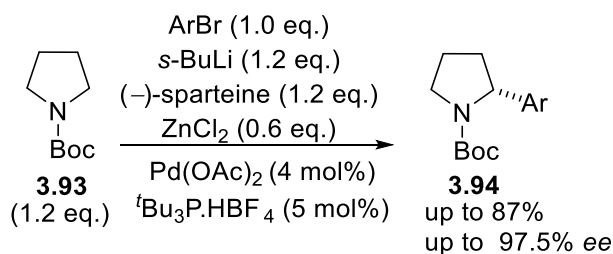


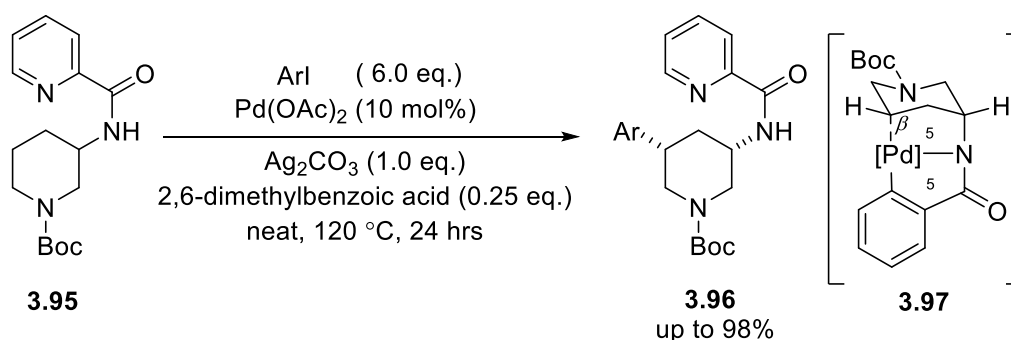
Figure 3.15: $C(sp^3)$ -H functionalisation of saturated cyclic aza-heterocycles.

The $C(sp^3)$ -H functionalisation of saturated aza-heterocycle has been achieved in numerous ways.⁶⁸ Among all, the most common method is deprotonation with strong base. For example, Campos and co-workers reported Pd(II)-catalysed enantioselective α -arylation of *N*-Boc-pyrrolidine **3.93**.⁶⁹ The strategy includes the butyllithium/(-)-sparteine-mediated asymmetric deprotonation from the α -position followed by transmetalation with $ZnCl_2$, and subsequently palladium-catalysed Negishi coupling with aryl bromides (Scheme 3.19).



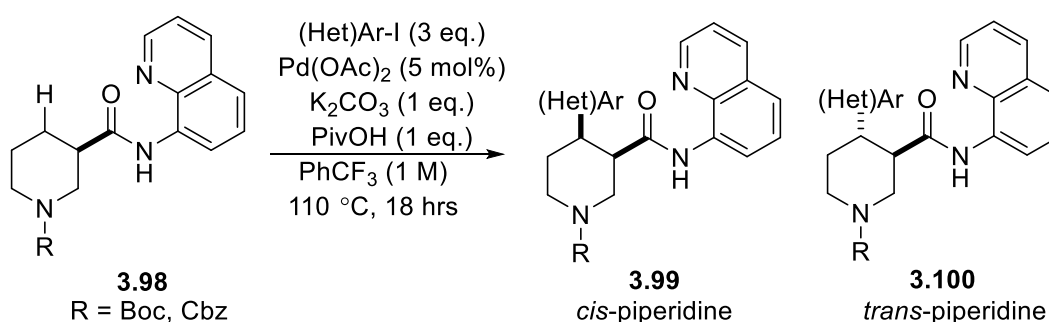
Scheme 3.19: Enantioselective α -arylation of *N*-Boc-pyrrolidine **3.93**.

Reports on the remote β - $C(sp^3)$ -H functionalisation are sparse. Only two methods have been reported to the best of our knowledge.^{70,71} Both of these approaches utilise existing ring substituents to control the regioselectivity. In Maes's approach, a bidentate directing group permits the site-selective arylation of the piperidine ring **3.95**.⁷⁰ The addition of a carboxylic acid additive was crucial to success, suggesting that CMD is an important step. The authors postulated 5,5-fused palladacycle **3.97** for successful transformation.



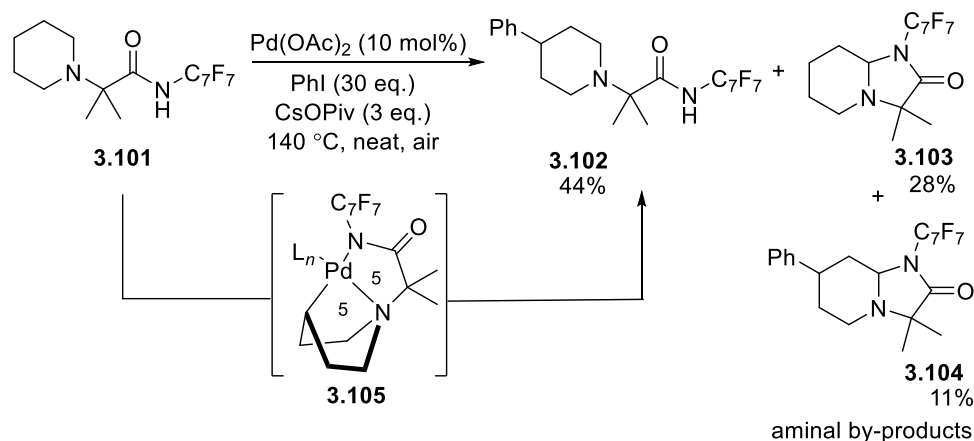
Scheme 3.20: Maes's approach for β -C(sp^3)-H functionalisation.

Bull and co-workers adopted a similar strategy with a carboxylic acid functionality at C3 permitting formation of a bidentate directing group (Scheme 3.21).⁷¹ However, this protocol gave the mixture of both isomers, *cis*- and *trans*-3,4-disubstituted products **3.99** & **3.100**. The authors suggested the formation of *trans*-palladacycle for the minor *trans*-piperidine isomer **3.100**. In both these methods for β -C(sp^3)-H functionalisation, the necessity for an existing functional group on the ring limit the substrate generality.



Scheme 3.21: Bull's approach for β -C(sp^3)-H functionalisation.

Sandford et al. achieved the transannular γ -C(sp^3)-H arylation of cyclic amines with the well-designed fluoroamide directing group.⁷² The authors postulated that the directing group prearranges the cyclic amine system in the presence of the palladium catalyst from the stable chair conformation to the thermodynamically disfavoured boat conformation. However, with the piperidine substrate **3.101**, the desired product **3.102** was obtained only in moderate yield, giving the aminoral by-products **3.103** & **3.104**, both from the starting material **3.101** and the product **3.102** respectively (Scheme 3.22).

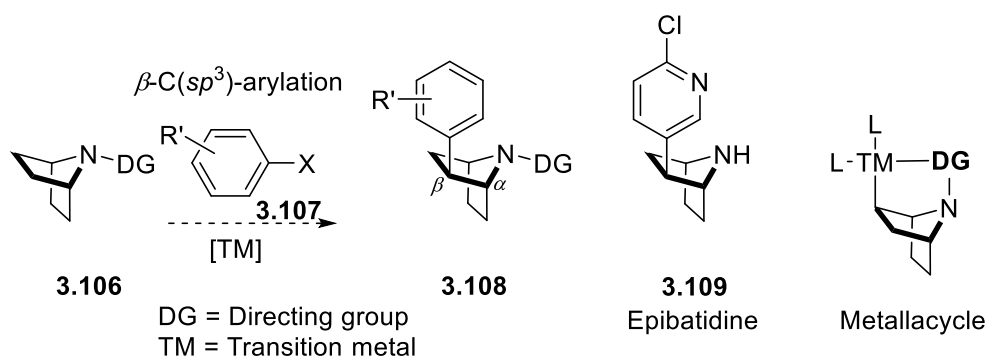


Scheme 3.22: Sandford's approach for γ -C(sp^3)-H functionalisation.

Over the past two decades, the C-H activation field has experienced enormous progress in achieving both chemo- and regioselectivity. Among the different types of C-H activation described in the introductory section, the selective functionalisation of C(sp^3)-H remains the most challenging. The poor reactivity of C(sp^3)-H bond is attributed to its high bond energy (376-416 kJ/mol) and low acidity ($\sim pK_a = 50$). Compared to the C(sp^2)-H system, the C(sp^3)-H holds an added degree of conformational freedom so that metal cannot directly coordinate to the selective C-H bond *via* a π -orbital interaction. Moreover, the methylene C(sp^3)-H functionalisation is more restricted than its methyl counterpart because of more steric hindrance in the key palladacycle formation. Further, the differentiation of enantiotopic methylene C-H bonds is even more challenging.

3.10. Results and discussion

The main aim of this project was to develop the chemistry that would allow the shortest route to synthesise the alkaloid epibatidine **3.109**, a potent analgesic isolated from Ecuadoran poison dart frog in enantiomerically pure form.⁷³ There have been multiple procedures reported in the literature for the total synthesis of epibatidine.⁷⁴ However, the reported multi-steps synthetic procedures restrict the diversity of analogues. We aimed to develop the chemistry by the late-stage β -C(sp^3)-arylation of the 7-azanorbornene (7-azabicyclo[2.2.1]heptane) **3.106**, which is the core skeleton of epibatidine (Scheme 3.23). In this way, a number of analogues can be synthesised simply by altering the aromatic ring. Moreover, this approach would allow us to investigate one of the current limitations in the C-H activation field, namely the β -C(sp^3)-H functionalisation of cyclic amines. The C-H functionalisation of the α -position of cyclic aza-heterocycles is well researched⁶⁸ and the γ -position to some extent,^{72,75} but the chemistry for the β -C(sp^3)-H functionalisation is limited. Here, we aimed to develop the chemistry with a suitable directing group that can lead to form the metallacycle at the β -position.

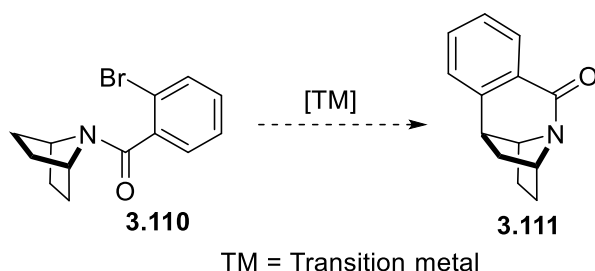


Scheme 3.23: Synthetic plan for the β -C(sp^3)-arylation of the 7-azabicyclo[2.2.1]heptane **3.106** system and the structure of epibatidine **3.109**.

For the asymmetric synthesis of epibatidine, we chose the intermolecular desymmetrisation⁷⁶ of enantiotopic β -C(sp^3)-H bonds. This would be a challenging target. The main problem in this type of C-H activation is that the oxidative insertion into the C-X (X = halide) bond precedes the coordination of the directing group to control regio- and chemoselectivity. This prohibits the coordination of a chiral ligand, making the task of imparting enantioselectivity difficult. It would be nearly unprecedented to achieve the C-H activation without the prior coordination of the substrate.

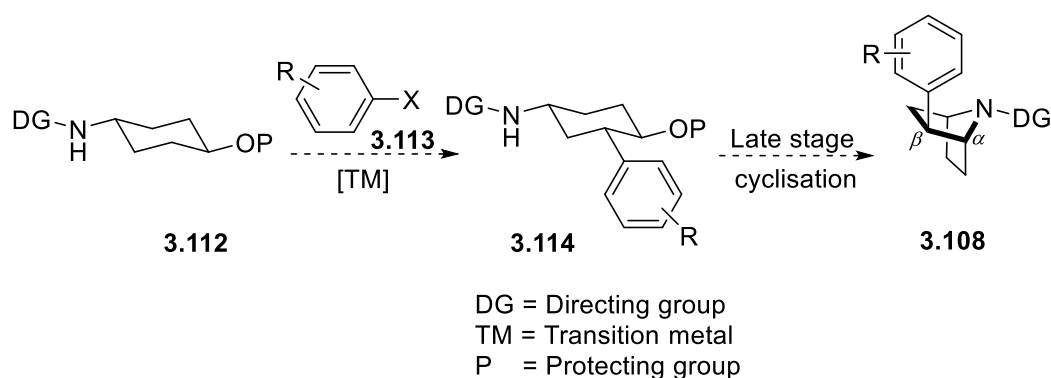
Achieving above goal will be a stepwise process; it is unlikely that we will be able to study this objective straight away. One starting point would be to investigate the intramolecular

functionalisation of the 7-azanorbornene system **3.110** (Scheme 3.24). Intramolecular cyclisation reaction does not require the prior coordination as the coupling partners are in the same molecule, enforcing the proximity into the reacting sites. Additionally, this system would avoid the need for a directing group, so that the main focus will remain the optimisation of the catalytic system while studying the effect of different reaction additives.



Scheme 3.24: Intramolecular β -C(sp^3)-arylation of 7-azanorbornene system **3.110**. (3.110 structure nitrogen in amide looks like Sp^3 - hybridised)

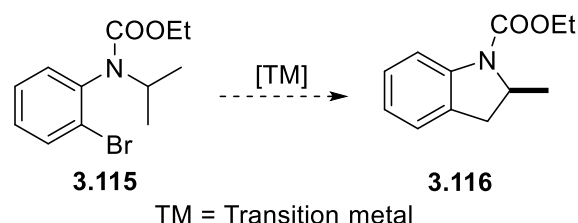
There is always an element of risk in attempting new chemistry. We wanted to minimise this risk by developing a fallback position that would enable us to undertake the challenging task while building upon the past precedent. For this, we planned to achieve the γ -C(sp^3)-H activation on the 1,4-disubstituted cyclohexylamine system **3.112** (Scheme 3.25). The main aim would remain the same. The only difference is formation of azabicyclo[2.2.1]heptane system would be achieved by the late-stage cyclisation. Moreover, the nitrogen would not be a part of the ring system, which will simplify the directing group-assisted C-H activation.



Scheme 3.25: Intramolecular γ -C(sp^3)-arylation of 1,4-disubstituted cyclohexylamine system **3.112**.

It is worth mentioning that the above objective involves the intermolecular desymmetrisation of enantiotopic methylene C-H substituents. Before we study this objective, we first planned to study an intramolecular C(sp^3)-H activation at the enantiotopic carbon. We selected a model reaction based on the construction of (fused) indoline system **3.116** (Scheme 3.26). We wanted

to learn C-H activation chemistry by employing SPO-based ligands. We also planned to synthesise other heteroatom-substituted secondary phosphine oxide (HASPO) ligands and to check if they could be useful ligands. This will help in studying the influence of the chiral ligand and its stereoelectronics on the metal centre. The knowledge gained from this process would be transferred to the former challenging objective.



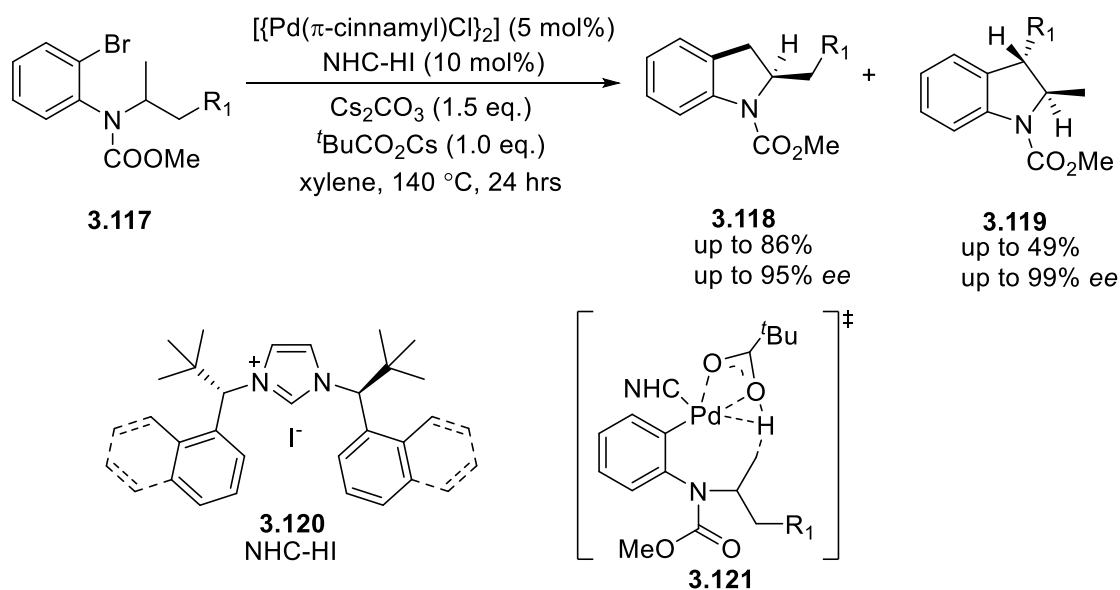
Scheme 3.26: Model reaction to study intramolecular C(sp^3)-H activation at the enantiotopic carbon.

The overall aim of this project was to increase the generality of C-H activation reactions while improving the enantioselectivity. The key to this project would not be exotic ligands but readily available and useful chiral ligands. We wanted to develop efficient chiral catalysts that could be versatile in terms of different substrates. Our focus was also to develop step and atom-economical catalytic processes which could minimise the requirement for specific directing groups.

3.11. Intramolecular C(sp^3)-H activation at enantiotopic carbon - a chiral indoline system

Our study began with accessing chiral indolines by the palladium-mediated functionalisation of unactivated C(sp^3)-H alkyl groups. During the last decade, the research groups of Kundig,⁷⁷ Kagan,⁷⁸ Cramer,^{79,80} and Baudoin,⁵⁰ have all generated indolines by a desymmetrisation strategy. Each group achieved this objective by an intramolecular cyclisation following the Pd(0)/Pd(II) cycle. Notably, the initial step of C-H activation proceeds through proton abstraction by the coordinated base, usually either carbonate or *in situ* generated carboxylate (CMD mechanism).⁸¹ The CMD step is crucial for achieving high enantioselectivity. The method of achieving the CMD step varies based on the type of (chiral) ligand and (chiral) acid in each strategy.

In Kundig's pioneering work, chiral indolines were synthesised by an intramolecular desymmetrisation (Scheme 3.27).⁸² Here, a chiral NHC ligand aided oxidative insertion and induced selectivity during CMD. The key step is CMD promoted by a bulky carboxylate.^{83,84}

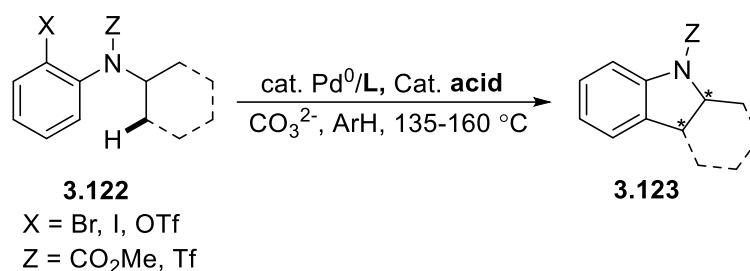


Scheme 3.27: Synthesis of indolines **3.118** & **3.119** via enantioselective C(*sp*³)-H activation.

Subsequently, a combination of other chiral ligands with an achiral conjugated base^c were reported for the same transformation, namely the Sagephos ligand with 9*H*-xanthene-9-carboxylic acid by Saget et al.,⁷⁹ and (*R,R*)-Me-DuPho with pivalic acid by Anas et al.⁷⁸ In all the cases, the bulky substituents on the ligand and resulting interaction with the achiral carboxylic acid were believed to favour the CMD step. Baudoin and co-workers achieved the same transformation with a cooperative effect of an achiral phosphine ligand and BINOL-derived phosphoric acid (BPA) chiral base (Section 3.6.1, Scheme 3.9).⁵⁰

Overall, it was observed that the chiral conjugate base has dominance over ligand in governing the asymmetric induction during C-H functionalisation. For example, Cramer and co-workers observed an 85.5% *ee* with a chiral tetraline carboxylic acid **3.124** and an achiral NHC ligand (Scheme 3.28, Table 3.1, entry 1),⁷⁹ while Kagan and co-workers obtained 82.5% *ee* in the presence of 50 mol% Boc-valine **3.125** in the absence of any ligand (entry 2).⁷⁸

^c Conjugated base of Brønsted acid



Scheme 3.28: Intramolecular desymmetrisation of aryl(*pseudo*)halide to the synthesis of chiral indolines

Table 3.1: Influence of the chiral Brønsted acid on the intramolecular desymmetrisation of aryl(*pseudo*)halide

Entry	Ligand (L)/catalyst	Brønsted acid	Enantiomeric excess
1	[(η^3 -cinnamyl)(^t Pr)PdCl] achiral	 3.124	82.5% <i>ee</i>
2	Ligand free	 3.125 50 mol%	85.5% <i>ee</i>

From the above studies, it is clear that the cooperative effect of a chiral ligand and chiral conjugate base plays a pivotal role in the formation of enantioenriched indolines. We planned to design a bifunctional ligand by combining both functionalities into one molecule (Figure 3.16). In the Pd(0)/(II) mechanism, the C-H insertion occurs through a CMD step with a conjugate base removing the proton. This base can be external or incorporated into the ligand. We prefer the latter approach. Our strategy involves a single molecule that acts as both the chiral ligand and chiral conjugate base. By incorporating both functionalities in a single molecule, we hope the transition state would be more rigid and hence greater control over the environment in which reaction proceeds. Moreover, it will leave the palladium coordinate site free to facilitate the C-H activation step effectively.

Inspired by our previous planar chiral SPO study (Chapter 2), we planned to elaborate on a diverse range of SPOs, such as *P,N*-type SPOs. We surmised that a heteroatom-substituted secondary phosphine oxide (HASPO) ligand could fulfil two roles (Figure 3.16).

- i. The soft phosphorus centre can coordinate to palladium to stabilise the metal catalyst.

- ii. The hard oxygen functionality could act as an internal conjugate base to facilitate the CMD step.²⁰

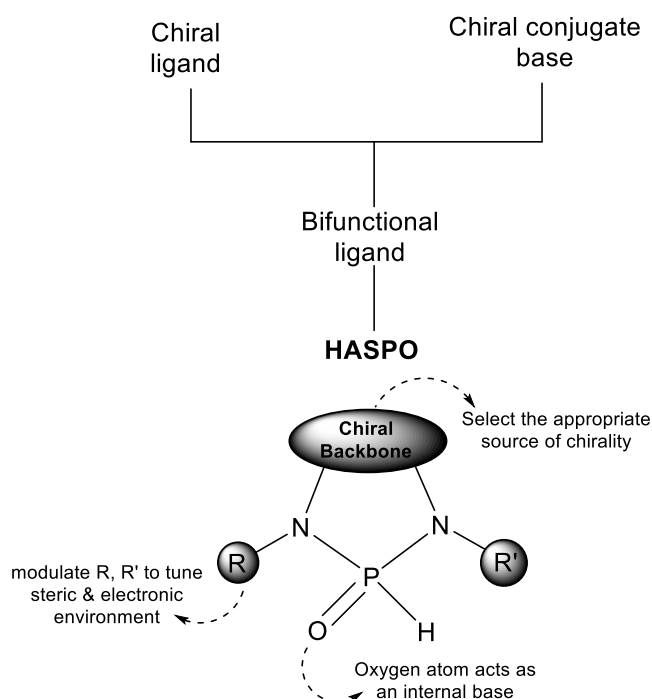
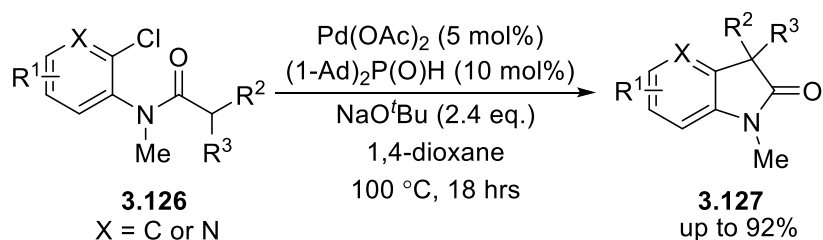


Figure 3.16: Design of bifunctional – HASPO ligands.

HASPO ligands are implemented in the palladium-catalysed coupling of unactivated aryl halides.⁸⁵⁻⁸⁷ The role of HASPO ligands as an internal base is also revealed in the C(*sp*²)-H activation of aromatic rings with palladium^{87,88} or ruthenium.⁸⁹ For example, Ackermann et al. utilised an air-stable sterically hindered adamantyl-substituted phosphine oxide [(1-Ad)₂P(O)H] for the arylation of α -C-H acidic compounds. Various substituted (aza)oxindoles **3.127** were synthesised by intramolecular α -arylation of amides with aryl chlorides **3.126** (Scheme 3.29).

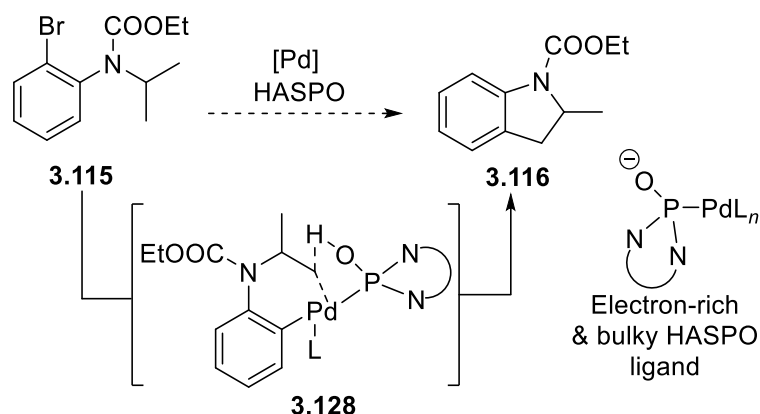


Scheme 3.29: Palladium-catalysed (aza)oxindoles **3.127** synthesis.

The electronic and steric properties of HASPO ligands can be easily modulated by varying both nitrogen substituents and the functional groups on the nitrogen backbone. Several moieties

would be suitable such as amino acids, chiral amines, or chiral diamines. Ideally, this unit should be readily available in an enantiomerically pure form and should be easily modified to synthesise a variety of ligands quickly. This would allow us to acquire more empirical data and help to optimise the ligand design. Ultimately, the main objective is to design modular bifunctional ligands to control the stereoselectivity while improving the versatility of the C-H activation reactions.

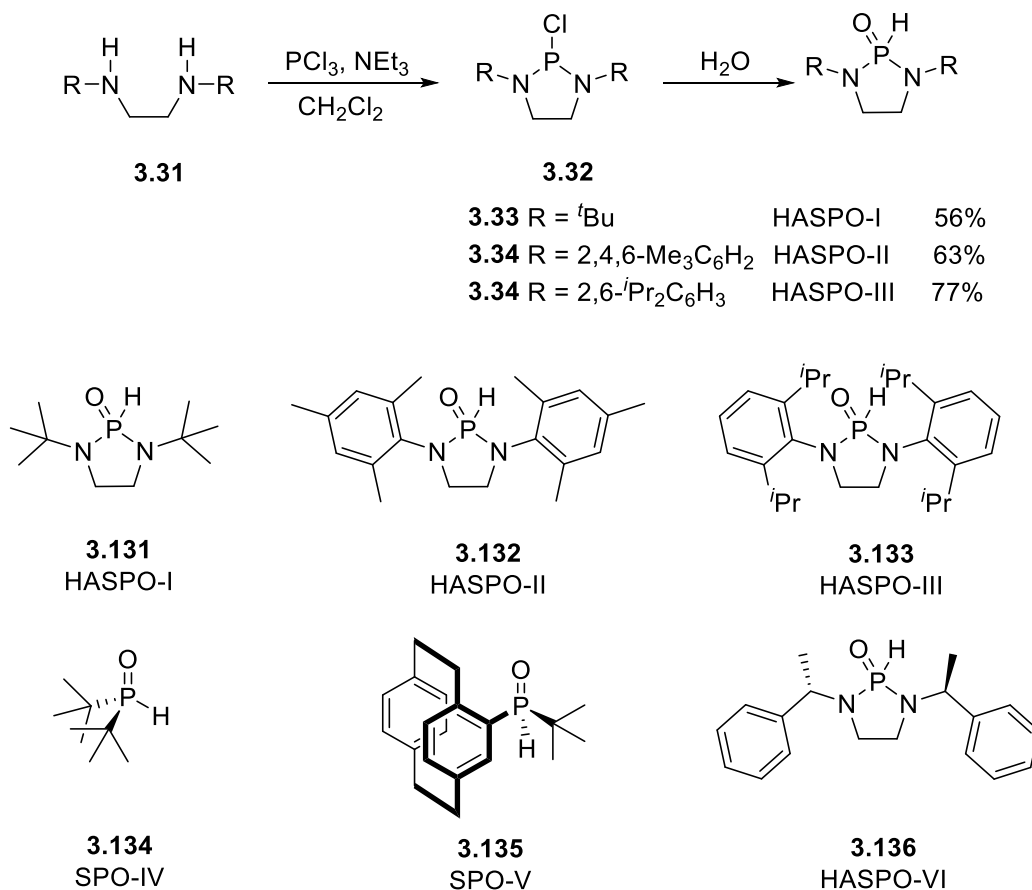
We planned to design an electron-rich and bulky HASPO ligand. Based on the ligand design, the organometallic intermediate **3.128** was predicted (Scheme 3.30). We surmise that the HASPO ligand promotes C-H activation *via* a phosphine oxide – induced CMD mechanism. The model shows the CMD step *via* a five-membered palladacycle, which is usually the kinetically favoured in most of the reported C-H functionalisation reactions.⁹⁰



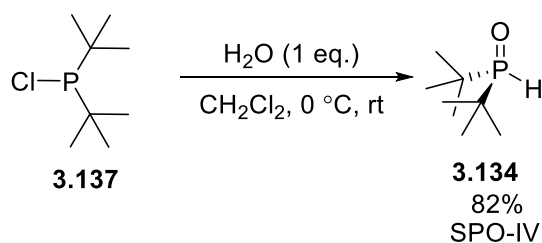
Scheme 3.30: Structural basis for design of HASPO catalyst.

3.11.1. Design and synthesis of HASPO ligands and substrates

Initially, we decided to screen a number of readily available achiral SPO and HASPO ligands. The knowledge obtained from this would be later transferred to study the effect of chiral ligands (Scheme 3.31). As a starting point, we investigated electron-rich HASPO and SPO as Pd(0)-catalysed C-H activation often benefits from the electron-rich phosphine ligands.⁹¹ The first targets were *tert*-butyl (HASPO-I) **3.131**, mesitylene (HASPO-II) **3.132**, and 2,6-diisopropyl phenyl (HASPO-III) **3.133**, and which were synthesised by the reported procedures (Scheme 3.32).⁹² The analogue, SPO-IV, **3.134**, was prepared to compare the activity of an SPO with the HASPO. SPO-IV **3.134** was synthesised from commercially available di-*tert*-butylchlorophosphine **3.137** by the addition of water (Scheme 3.32).⁹³



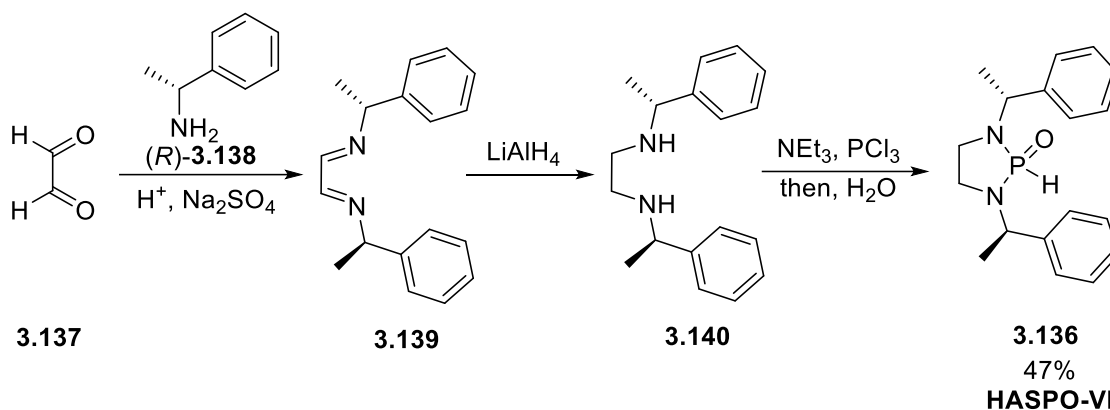
Scheme 3.31: HASPO and SPO ligands for test reaction.^d



Scheme 3.32: Synthesis of SPO-IV **3.134**.

At this stage, we have synthesised only one chiral HAPSO (HASPO-VI) **3.136** to investigate the chiral effect. HASPO-VI **3.136** was readily achieved in three steps from the (*R*)-(-)-1-phenylethylamine **3.138** and glyoxal **3.137** as reported by Cramer and co-workers (Scheme 3.33).⁹⁴

^d HASPO-I, HASPO-II and HASPO-VI were synthesised by the author of this thesis, while HASPO-II and HASPO-III were synthesised by interns during this project.



Scheme 3.33: Synthesis of HASPO-VI **3.136**.

The test precursor, ethyl (2-bromophenyl)(isopropyl)carbamate **3.115** was selected based on the two geminal enantiotopic methyl groups. In Kundig's study, the repulsive interaction between the aryl ring and an ester group was a key factor for determining the enantioselectivity. We also believed that an electron-withdrawing group is required to allow greater rotation of the C_(aryl)-N bond permitting the substrate to adopt the correct conformation.^{77,78}

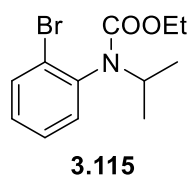
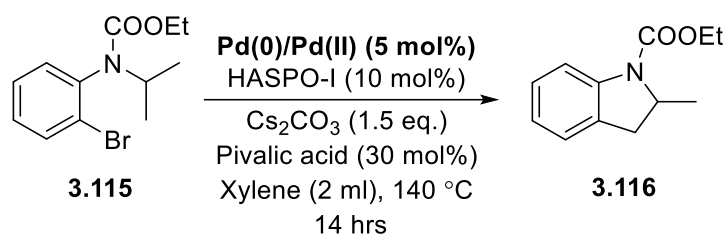


Figure 3.17: Precursor ethyl (2-bromophenyl)(isopropyl)carbamate **3.115**.

Once the initial ligands and substrate were prepared, the screening process commenced. This focused first on HASPO-I and substrate **3.115**.

3.11.2. Optimisation study

A preliminary study was performed with HASPO-I **3.131** ligand to identify a suitable palladium catalyst. As explained different mechanisms in the introductory section, it is clear that the oxidation state of palladium is in Pd(II) state and an acetate ion has an important role in coordinating one of the four sites on Pd(II). We decided to analyse the commercially available Pd(0) and Pd(II) catalysts (Scheme 3.34, Table 3.2). The reaction proceeded with Pd(OAc)₂, giving the product in 22% compared to the starting material (entry 1). However, only minute conversion of the starting material was observed with Pd₂(dba)₃ (entry 2), whereas bis[cinnamyl palladium(II) chloride] and PdCl₂(CH₃CN)₂ failed to give any detectable product at all (entry 3 & 4).



Scheme 3.34: Effect of different palladium catalysts.

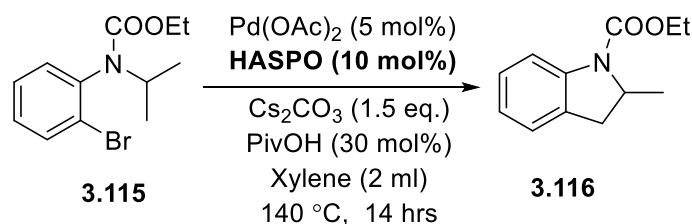
Table 3.2: Effect of different palladium catalysts

Entry	[Pd]	Yield ^a
1	Pd(OAc) ₂	22%
2	Pd ₂ (dba) ₃	2%
3	Bis[cinnamyl palladium(II) chloride]	-
4	PdCl ₂ (CH ₃ CN) ₂	-

^a NMR yield with internal standard: - 1,3,5-trimethoxybenzene

- Reaction did not proceed

Next, we screened different HASPO ligands with Pd(OAc)₂ as the catalyst. Sterically encumbered HASPOs gave unsatisfactory results (Scheme 3.35, Table 3.3). It was observed that the pivalic acid additive had a major influence to promote the reaction (entry 2 & 4). The product formation was observed in an average of 20% yield range except for the case of HASPO-III **3.133** (entry 5). These results were quite contrary to our hypothesis that hard oxygen of HASPO can act as an internal base. These results suggest that pivalic acid promotes the CMD step. However, even a small quantity of product **3.116** formation supported our idea that HASPO may have some potential to catalyse the reaction.



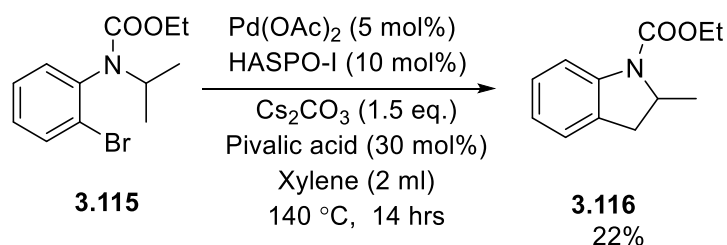
Scheme 3.35: Screening of HASPO ligands and/or achiral acid.

Table 3.3: Optimisation study with different HASPO ligands

Entry	HASPO	Brønsted acid	Yield ^a
1	HASPO-I 3.131	w/o	3%
2	HASPO-I 3.131	Pivalic acid	22%
3	HASPO-II 3.132	w/o	4%
4	HASPO-II 3.132	Pivalic acid	12%
5	HASPO-III 3.133	Pivalic acid	-

^a NMR yield with internal standard: - 1,3,5-trimethoxybenzene
w/o without
- Reaction did not proceed

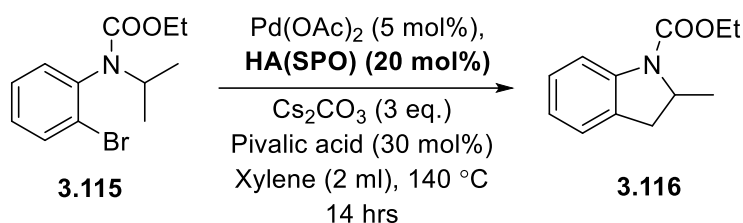
The optimisation was extended to evaluate the influence of base and solvent (Scheme 3.36, Table 3.4). The literature suggests that caesium bases are superior to other metal salts,⁵³ but to confirm this we screened bases such as K₂CO₃, NaO^tBu, and KO^tBu (entry 1, 2 & 3). The reaction conditions involving these bases failed even to initiate the reaction. The enhanced reactivity of caesium may be reasoned to the so-called ‘caesium effect’, better solubility, generation of highly naked anions, the large size of caesium, and its facile polarisability. Changing the solvent from xylene also affected the yield. Compared to xylene, 16% yield was observed when the reaction was conducted in NMP (entry 4), while reactions did not proceed at all in 1,4-dioxane and DCE (entry 5 & 6).

**Scheme 3.36:** Effect of different bases and solvents.**Table 3.4:** Effect of different bases and solvents

Entry	Deviation from scheme 3.36	Yield ^a
1	K ₂ CO ₃	-
2	NaO ^t Bu	-
3	KO ^t Bu	-
4	NMP	16%
5	1,4-dioxane	-
6	DCE	-

- Reaction did not proceed

One common observation in all of the above reactions was that they rapidly turned black, which suggested decomposition of the active palladium species. We decided to increase the amount of ligand and base (Scheme 3.37, Table 3.5). This proved successful with HASPO-I **3.131** but not with HASPO-II **3.132**. Increasing the reaction time led to the highest yield of 38% (entry 6).



Scheme 3.37: Effect of different HASPO ligands.

Table 3.5: Optimisation study with HASPO ligands

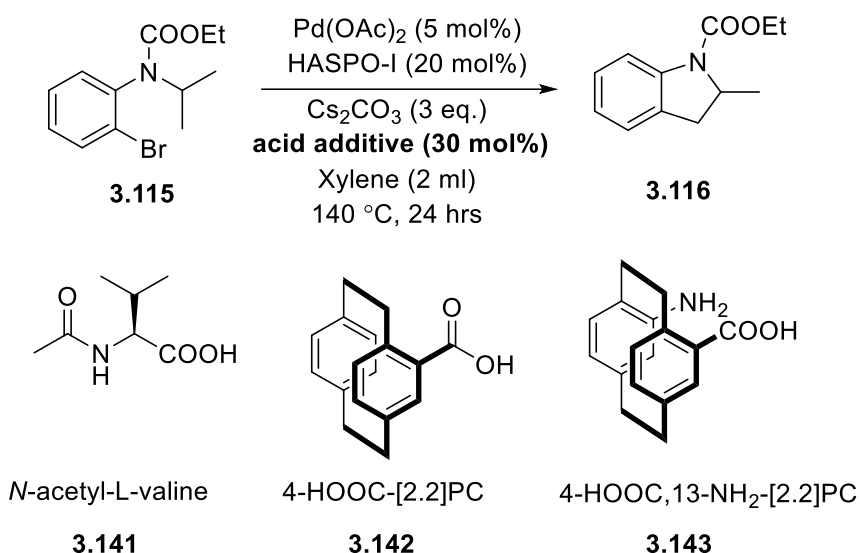
Entry	(HA)SPO	Yield ^a
1	HASPO-I 3.131	27%
2	HASPO-II 3.132	6%
3	HASPO-VI 3.136	-
4	SPO-V 3.135	4%
5	SPO-IV 3.134	1%
6*	HASPO-I 3.131	38% ^b

^a NMR yield with internal standard 1,3,5-trimethoxybenzene

- Reaction did not proceed

* 24 hours, ^b isolated yield

It is clear that our designed HASPO ligands were incapable of the desired proton abstraction to initiate the C-H insertion step. The reactions only proceeded when pivalic acid was incorporated, suggesting it was involved in CMD. It was decided to investigate chiral acid additive. The test reactions were separately performed with *N*-acetyl-L-valine **3.141** and [2.2]paracyclophane acid derivatives **3.142** & **3.143** (Scheme 3.38). In all reactions, only the starting material was returned. We reasoned the failure of these reactions was due to the steric bulk of these acids preventing their participation in the crucial proton abstraction.



Scheme 3.38: Effect of acid additives.

Based on the screening of the reagents for an intramolecular C(*sp*³)-H activation of ethyl (2-bromophenyl)(isopropyl)carbamate **3.115**, it can be concluded that HASPO is capable of stabilising the palladium catalyst through the soft phosphorus centre but does not act as an internal base. It became apparent that reaction progress was observed only when the external acid additive was present. That suggests, the CMD process could be attributed to the external acid additive but not to the HAPSOs.

As per our research objectives, we moved forward from a fused cyclic system to the bridged bicyclic system to study the desymmetrisation of enantiotopic methylene C-H substituents. Here, our focus was to differentiate the enantiotopic protons of the cyclic amine in a remote C-H functionalisation reaction.

3.12. Intramolecular C(*sp*³)-H activation of enantiotopic and diastereotopic protons - a 7-azanorbornane system

Many C-H activation reactions share a common feature with formation of a kinetically favoured five-membered palladacycle. However, other sized metallacycles are possible although they are rarer (Figure 3.18).^{90,7,95}

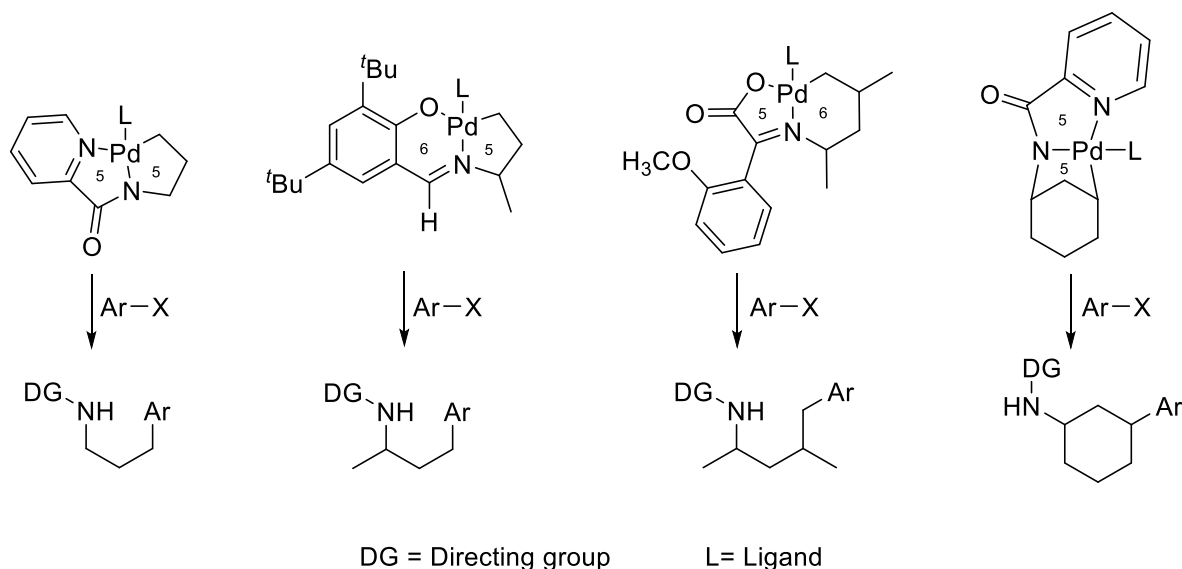


Figure 3.18: Influence of chelate ring on regioselectivity of C-H activation.⁷

Here, we aimed to develop the chemistry with a suitable directing group that can form the metallacycle at the β -position of a saturated cyclic aza-heterocycle. We selected the azabicyclic system - 7-azabicyclo[2.2.1]heptane (7-azanorbornane) system as a test moiety for our study. As shown in Figure 3.19, the six-membered ring in 7-azanorbornane is held by a one-nitrogen bridge to the two bridgehead carbons (C-1 & C-4).

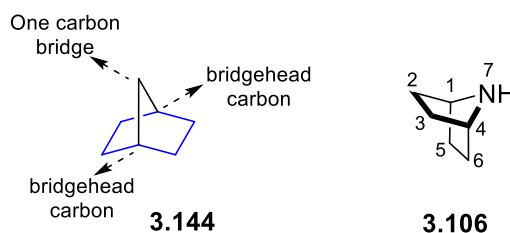
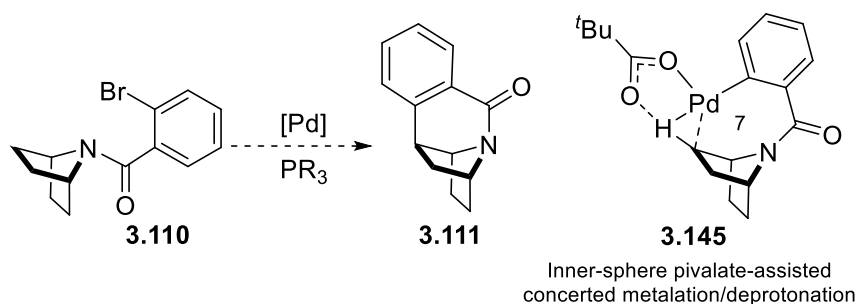


Figure 3.19: Norbornane **3.144** and 7-azanorbornane skeleton **3.106**.

Initially, we planned to study the palladium-catalysed intramolecular β -C(*sp*³)-H activation of 7-azabicyclo[2.2.1]heptane scaffold **3.110** to form a C(*sp*³)-C(*sp*²) bond (Scheme 3.39). This cyclisation does not require the prior coordination since the coupling partners are in the same molecule, enforcing the reacting sites in a closed proximity. The knowledge from this study

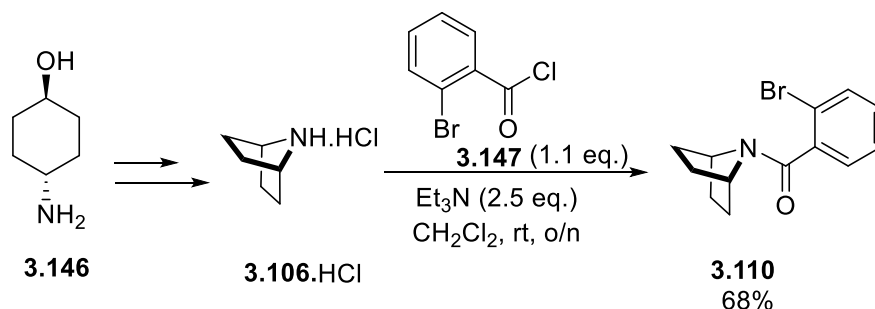
would allow us to gain information required for our next goal of developing an intermolecular variant.

For an intramolecular β -C(sp^3)-H functionalisation, we proposed a seven-membered palladacycle **3.145** based on a pivalate-assisted CMD (Scheme 3.39). As C-H activation through a seven-membered palladacycle is sparse in the literature,^{96,97} we already anticipated the challenges associated with this precursor. If we succeed in an achiral intramolecular cyclisation, the enantioselective version of the reaction will be attempted either by using a chiral ligand or a chiral conjugate base.



Scheme 3.39: Synthetic plan for an intramolecular C-H activation on 7-azabicyclo[2.2.1]heptane.

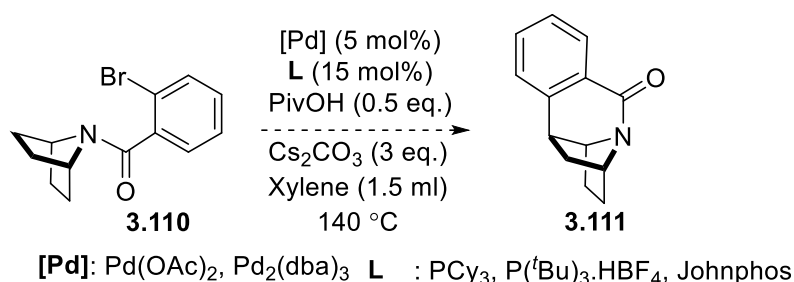
To begin our study, we first synthesised the stable hydrochloride salt of 7-azabicyclo[2.2.1]heptane **3.106** from *trans*-4-aminocyclohexanol **3.146** by following the reported procedure.⁹⁸ Under amide formation conditions, the test precursor **3.110** was formed in 68% by reacting the **3.106**.HCl with 2-bromobenzoyl chloride **3.147** (Scheme 3.40).



Scheme 3.40: Synthesis of 7-(2-bromobenzoyl)-7-azabicyclo[2.2.1]heptane **3.110**.

We assumed that the reaction would proceed through the Pd(0)/Pd(II) cycle with the palladium inserting into the C-Br bond first before C-H activation. As the earlier mechanistic discussion indicates (Figure 3.12, page no. 79), if the reaction proceeds by a CMD mechanism, a conjugate base is required. Therefore, our initial reaction screening varied monodentate phosphines, bases, and Pd sources (Scheme 3.41). We screened different phosphine ligands (PCy₃,

$P(tBu)_3.HBF_4$, JohnPhos) in the presence of $Pd(OAc)_2$. However, in all reactions, only the starting material was recovered, indicating the failure to form the seven-membered palladacycle.



Scheme 3.41: Initial attempts for intramolecular methylene C-H activation.

A possible explanation for the failure could be the amide bond enforcing an unfavourable conformation **3.148** of the molecule. Delocalisation of the nitrogen lone pair results in a trigonal planar nitrogen in the amide. This would place the aromatic ring perpendicular to the ring (Figure 3.20). We wanted to have a desired conformation, in which the amide bond arranges the β -H in the close proximity of the palladium centre. The palladium insertion into the axial β -C-H can only be possible in a favourable conformation **3.149** or **3.150** of the molecule.

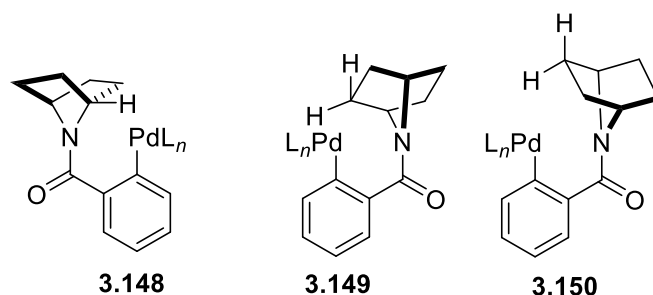
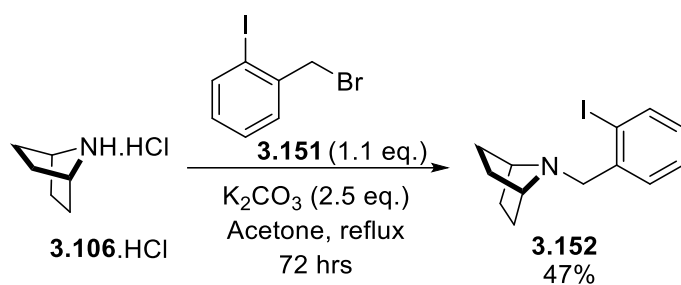


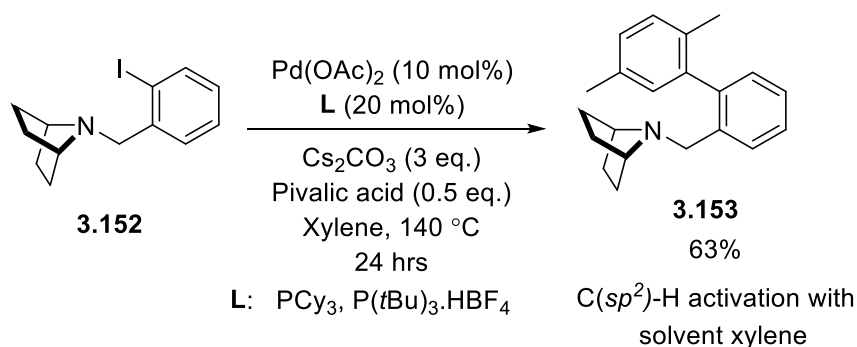
Figure 3.20: Proposed conformation **3.148** and desired conformation **3.149** or **3.150**.

We decided to modify the precursor so that the unfavourable conformational bias was minimised. To allow more freedom in the linker, we removed the carbonyl group. We also selected aryl iodide instead of aryl bromide to rule out the possibility of a slow oxidative insertion. The precursor **3.152** was synthesised by *N*-alkylation of 7-azabicyclo[2.2.1]heptane **3.106.HCl** with 2-iodobenzyl bromide **3.151** in 47% yield.

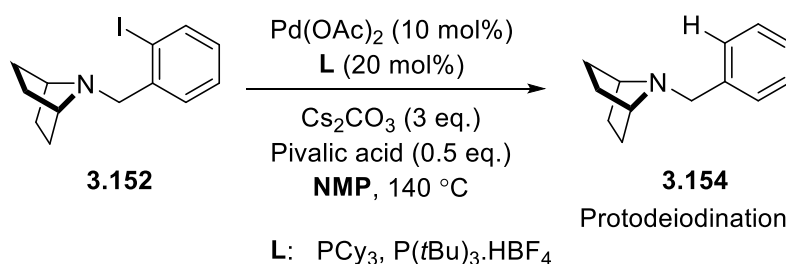


Scheme 3.42: Synthesis of 7-(2-iodobenzyl)-7-azabicyclo[2.2.1]heptane **3.152**.

When the reaction was carried out with the precursor **3.152**, an undesired coupling with the solvent xylene was observed and by-product **3.153** was isolated (Scheme 3.43). The formation of by-product **3.153** was reasoned to the dominance of C(*sp*²)-C(*sp*²) bond formation over C(*sp*²)-C(*sp*³) bond. It became necessary to change the aromatic solvent to an aliphatic solvent. Hence, a polar aprotic solvent, NMP was employed instead of xylene (Scheme 3.44). The substrate **3.152** instead proceeded for a protodeiodination to generate another by-product **3.154**. This result indicates that the palladium inserts into the C-I bond but that C-H activation does not occur.



Scheme 3.43: Initial attempts for an intramolecular methylene C-H activation.



Scheme 3.44: Initial attempts for an intramolecular methylene C-H activation.

It appeared that formation of the atypical seven-membered palladacycle was challenging. Either the size of the ring was disfavoured or the molecule could not adopt the correct conformation to place the palladium close to the C-H bond. Thus, we decided to move to the next goal: an intermolecular desymmetrisation of enantiotopic methylene C-H protons of 7-

azabicyclo[2.2.1]heptane. This protocol can be designed to follow the more usual five- or six-membered palladacycle.

3.13. Intermolecular C(sp³)-H activation of enantiotopic and diastereotopic methylene protons - a 7-azanorbornane system

For this objective, one starting point will be to design an appropriate directing group that can coordinate to the palladium, forcing the metal and C-H bond into close proximity to form a stable metallacycle. At this stage, the insertion of a metal catalyst into the C-H bond would be the key activation step. With the palladium catalyst, we surmise that the catalytic cycle would proceed through either the Pd(II)/Pd(0) or Pd(II)/Pd(IV) pathway (Figure 3.20). Depending on the coupling partner, if a boronic acid was used as the coupling partner, the reaction will most likely follow the Pd(II)/Pd(0) pathway. If an aryl bromide was used the mechanism would be the Pd(II)/Pd(IV) pathway.

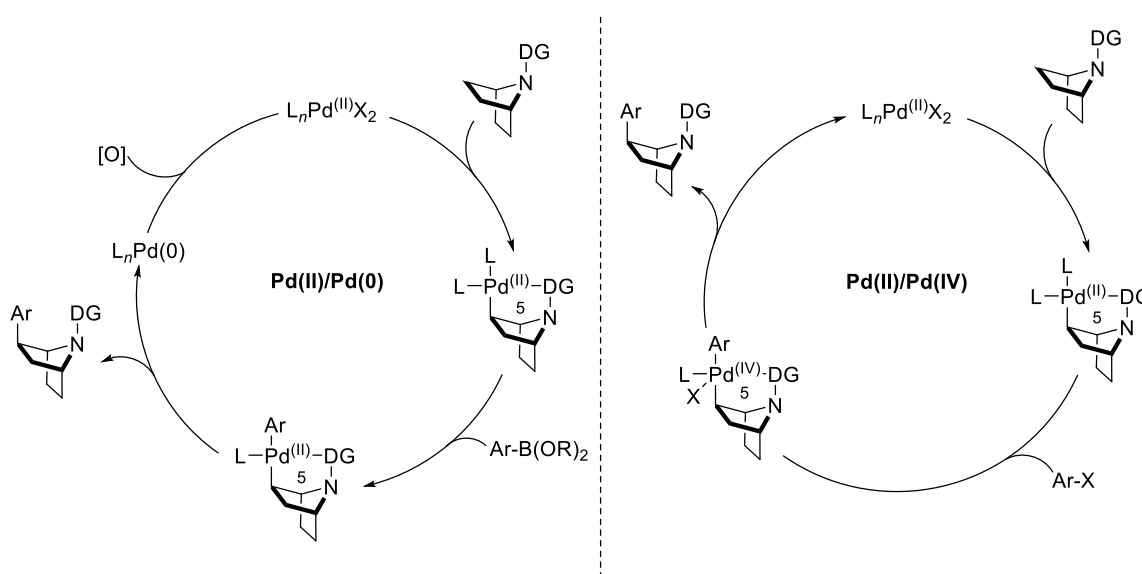
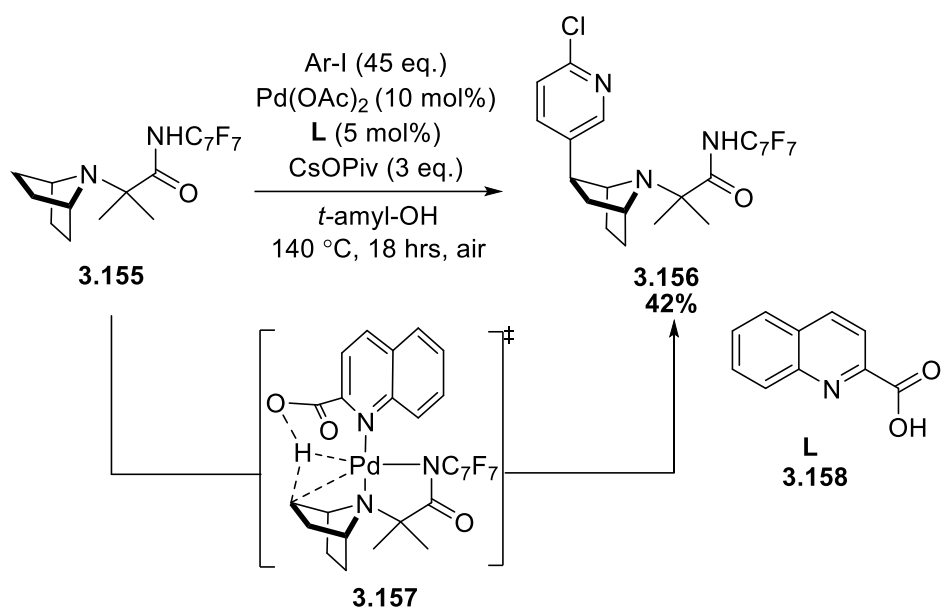


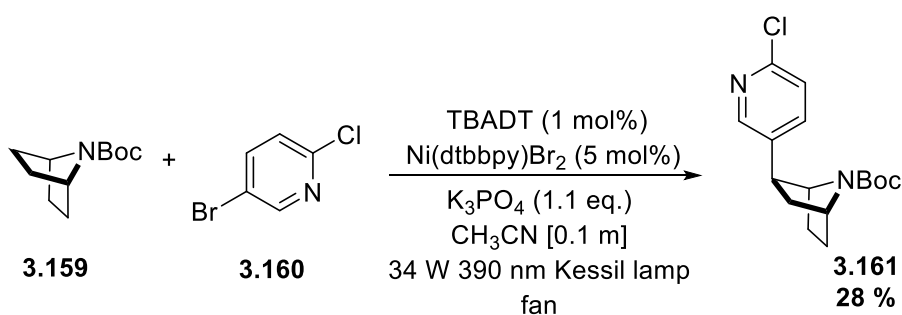
Figure 3.20: Proposed catalytic pathways for intermolecular cyclisation of 7-azanorbornane system.

Sanford et al. revealed the palladium-catalysed transannular C-H arylation of an array of cyclic amines (Scheme 3.45).⁷² The remote C-H functionalisation was achieved through coordination of the amine nitrogen to a tethered directing group and 2-quinaldic acid **3.158** as a bidentate ligand.⁷⁵ They claimed that ligand **3.158** plays a crucial role in recovering the active catalyst during the reaction, and thus, maintaining the high turnover rate.



Scheme 3.45: Sanford's approach for remote C-H functionalisation of cyclic amine.

MacMillan et al. reported a dual catalyst approach that merged hydrogen atom transfer (HAT) catalysis with transition-metal catalysis under photoredox conditions (Scheme 3.46).⁹⁹ A wide range of saturated aliphatic and cyclic scaffolds were functionalised in these site-selective C-H arylation reactions. In this protocol, photoexcited tetrabutylammonium decatungstate (TBADT) abstracts a hydrogen atom from an alkyl/cyclic nucleophile to generate a carbon-centred radical, which is captured by a nickel(0) complex. This nickel(0) complex is generated by HAT and two single-electron reductions from the pre-catalyst, Ni(dtbbpy)Br₂. After oxidative addition of the aryl halide, reductive elimination furnishes the cross-coupled product. With this concept, the synthesis of (\pm)-*N*-Boc-epibatidine **3.161** was accomplished from 7-azabicyclo[2.2.1]heptane in two steps (28% yield).



TBADT: Tetrabutylammonium decatungstate dtbbpy: 4,4'-di-*tert*-butyl-2,2'-bipyridine

Scheme 3.46: MacMillan's approach to (\pm)-*N*-Boc-epibatidine.

Our primary approach was similar to Sanford's approach⁷² *i.e.* to design an appropriate catalytic system based on a directing group. A range of different directing groups was planned that could potentially form a five-, six- or seven-membered metallacycle (Figure 3.21). The design of directing group will have a major influence on directing the transition-metal catalyst to activate the distal β -C-H bond.

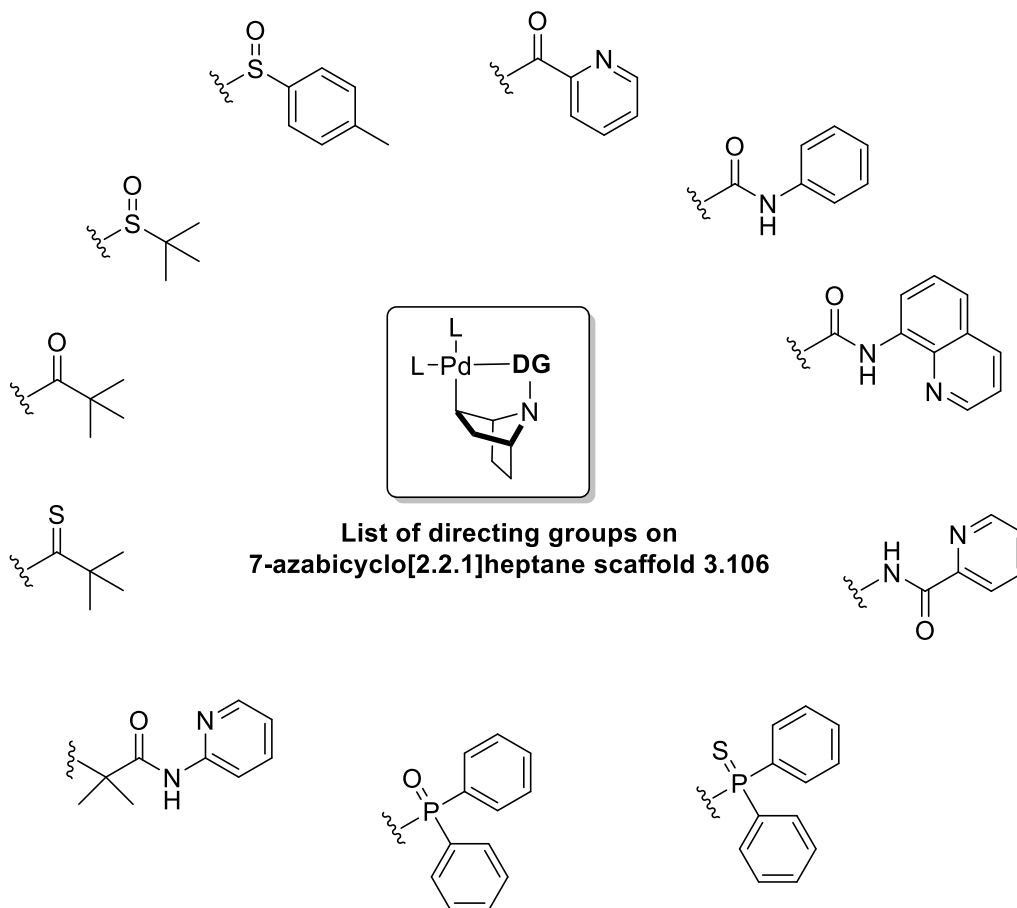


Figure 3.21: List of directing groups to study β -C(sp^3)-H functionalisation of 7-azabicyclo[2.2.1]heptane

3.13.1. Design of nitrogen-containing directing groups

The strong coordinating nitrogen-containing directing groups such as pyridine, quinoline, pyrimidine, and oxazoline have been successfully employed for various C-H transformations.²⁵ They are mainly σ -donating in nature, hence they can bind to the metal reversibly to induce the site-selective C-H functionalisation. Although, the use of strong-coordinating directing groups is not without its limitations (section 3.5.1.),¹⁰⁰ we thought they were more likely to realise the

desired C-H activation. Once we had proved the reaction was possible, we could optimise the directing group.

As shown in Figure 3.22, amide and urea-based directing groups were designed based on the commonly employed auxiliaries.¹⁰¹ At the outset of this research, Sanford's chemistry⁷² had not been reported and we were unsure if the bridge nitrogen would be involved in metallacycle formation.

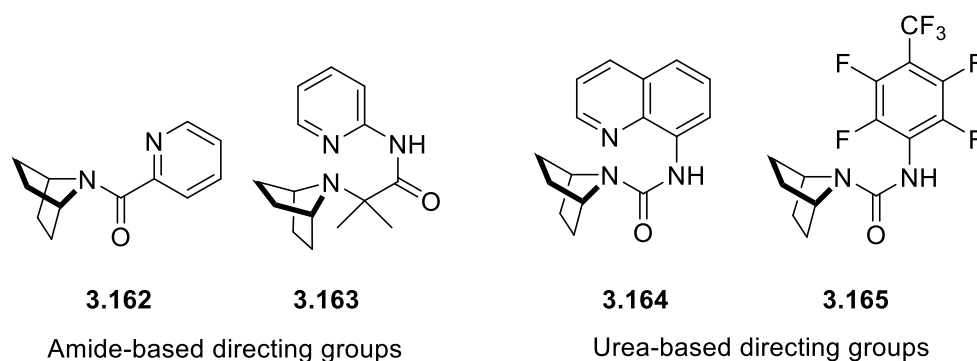
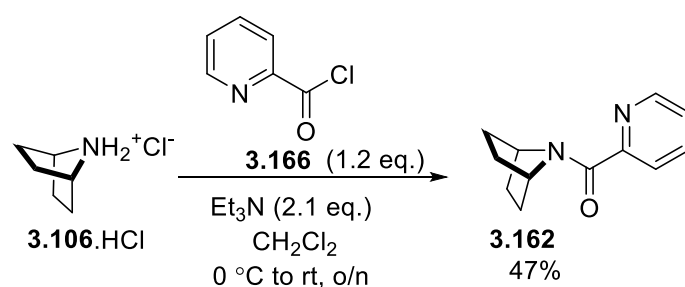


Figure 3.22: Design of amide and urea based directing groups.

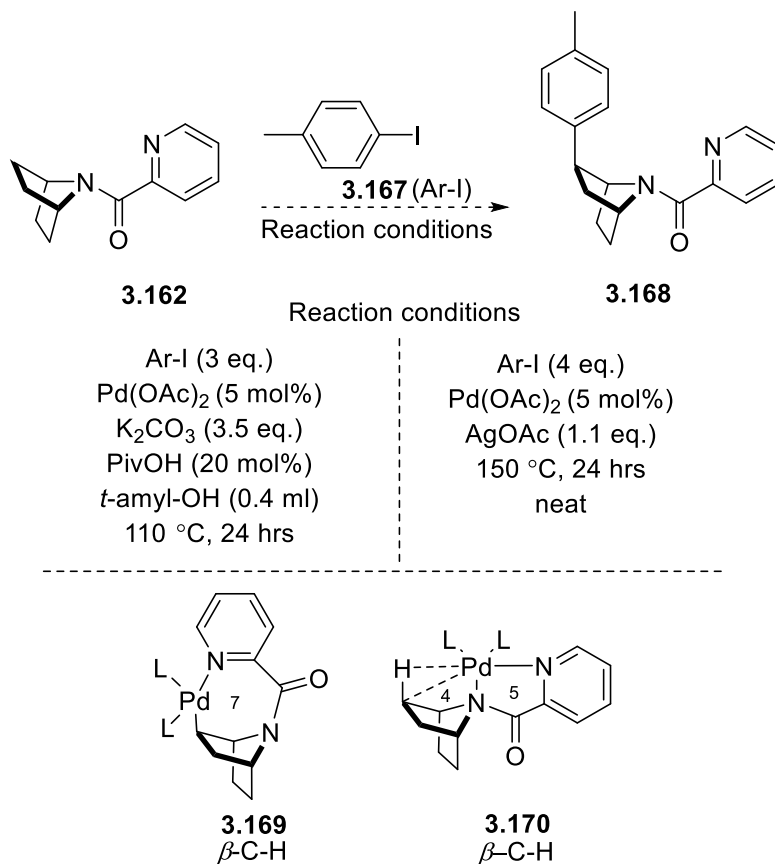
The study began with the pyridine-based auxiliary. The synthesis of the precursor (\pm)-7-(picolinoyl)-7-azabicyclo[2.2.1]heptane **3.162** was achieved by reacting (\pm)-7-azabicyclo[2.2.1]heptane **3.106.HCl** with picolinoyl chloride **3.166** in a moderate yield (Scheme 3.47).



Scheme 3.47: Synthesis of (\pm)-7-(picolinoyl)-7-azabicyclo[2.2.1]heptane **3.162** .

Initially, for the β -arylation of the precursor **3.162**, we decided to follow the procedures reported by Daugulis et al.^{36,102} In these reports, the β -arylation and β -alkylation of (sp^3)- and (sp^2)-C-H bonds of carboxylic acid derivatives were accomplished with pyridine and 8-aminoquinoline-based auxiliaries. However, these conditions proved conformation issues again (Scheme 3.48). With the pyridine auxiliary, β -C-H functionalisation of 7-azabicyclo[2.2.1]heptane would only be possible *via* a 7-membered palladacycle **3.169** unless

the bridgehead nitrogen participated. If this was involved, it would result in a strained 4,5-membered palladacycle **3.170**.



Scheme 3.48: Screening of pyridine auxiliary for intermolecular C-H activation with (±)-7-(picolinoyl)-7-azabicyclo[2.2.1]heptane **3.162** and tentative palladacycles.

Considering the widespread applicability of 8-aminoquinoline¹⁰³ and the Yu-Wasa auxiliary¹⁰⁴ in C-H functionalisation reactions (section 3.5.1), we decided to install these auxiliaries on the 7-azabicyclo[2.2.1]heptane **3.106** skeleton. We envisaged that these auxiliaries would form fused 6,5-membered **3.171** and 6-membered **3.172** palladacycles respectively (Figure 3.23). While the C-H activation with the 6,5-membered metallacycle is unusual, there are several reports based on a 6-membered metallacycle in the literature.^{90,105}

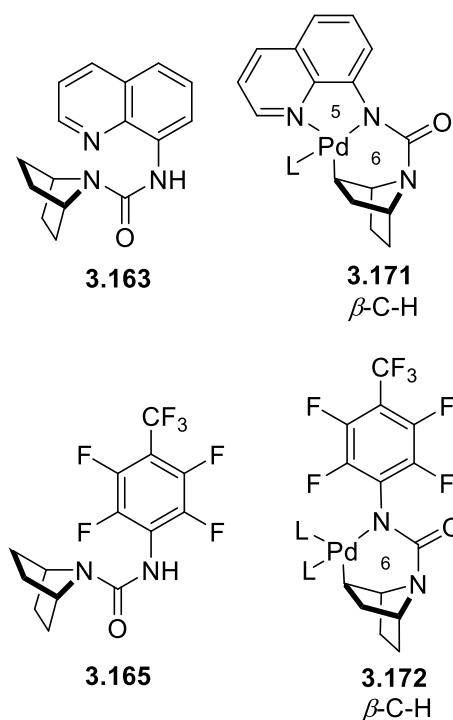
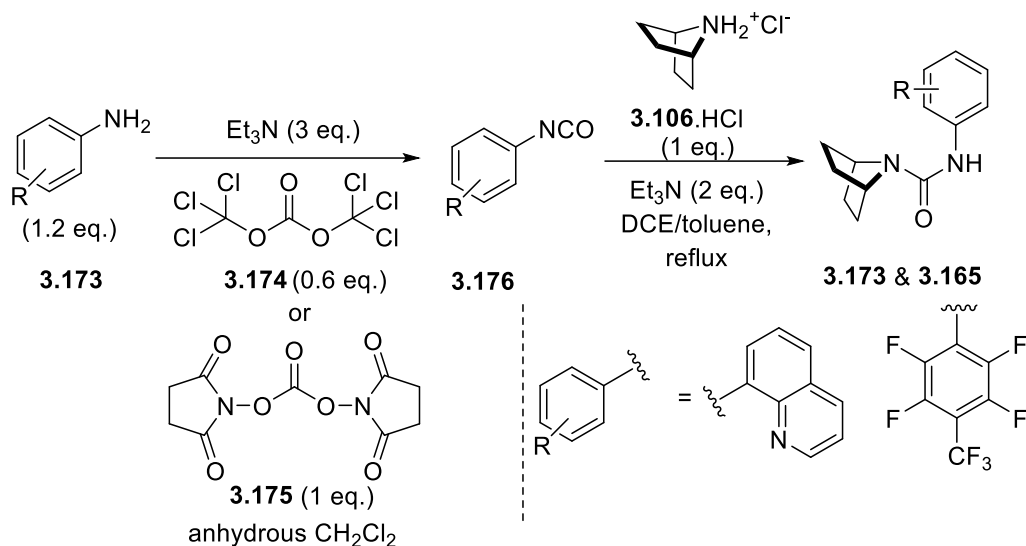


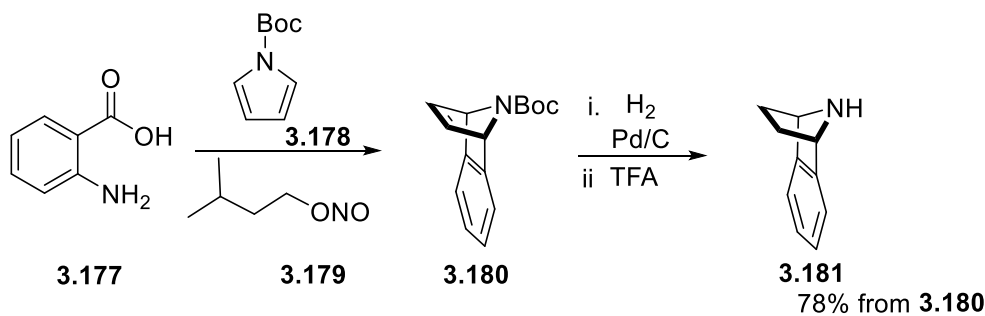
Figure 3.23: Proposed palladacycles with 8-aminoquinoline and Yu-Wasa auxiliaries.

Both 8-aminoquinoline and Yu-Wasa auxiliaries can be installed on the 7-azabicyclo[2.2.1]heptane skeleton **3.106.HCl** from their respective amine moieties by forming urea derivatives. Synthesis of the urea derivative is facile in theory by attack of a nucleophilic amine to an electrophilic isocyanate moiety (ArNCO). Both auxiliaries were converted into their corresponding isocyanate moieties by reacting either with triphosgene or N,N' -disuccinimidyl carbonate (Scheme 3.49). Further reactions were carried out in one-pot with the hydrochloride salt of 7-azabicyclo[2.2.1]heptane **3.106** under reflux, in an appropriate solvent system. However, after several attempts, only minute quantities of the corresponding products were isolated. Due to the difficulties associated with the synthesis of the desired urea precursors, it was decided to abandon the test of C-H functionalisation reactions based on urea directing groups.



Scheme 3.49: Attempted synthesis of urea precursors with 7-azabicyclo[2.2.1]heptane **3.106** based on 8-aminoquinoline and Yu-Wasa auxiliaries.

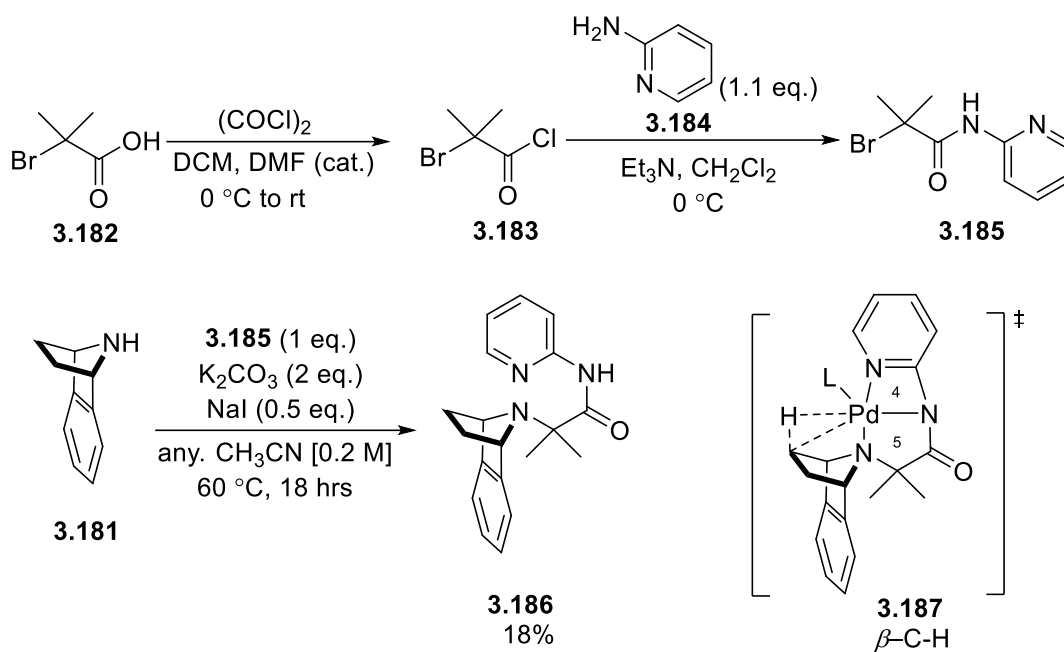
As the synthesis of precursor, 7-azabicyclo[2.2.1]heptane **3.106.HCl**, was itself challenging, a more readily available precursor was proposed, (\pm)-7-azabenzobicyclo[2.2.1]heptane **3.181**. This precursor contains an aromatic ring that makes the precursor less volatile and easier to work with. It can be synthesised in just three steps from the anthranilic acid **3.177** and Boc-*N*-pyrrole **3.178** following the method reported by Ohwada et al. (Scheme 3.50).¹⁰⁶



Scheme 3.50: Synthesis of (\pm)-7-benzoazabicyclo[2.2.1]heptane **3.181**.

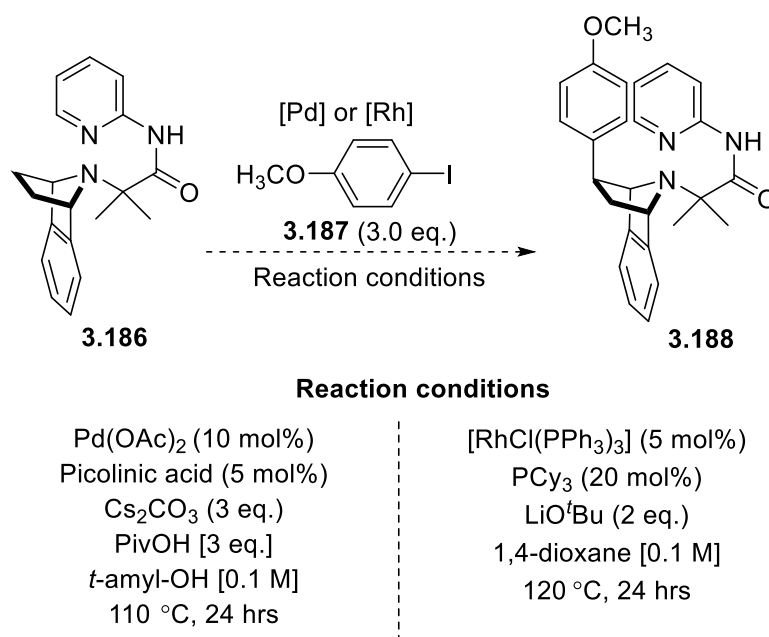
We postulated the failure of pyridine auxiliary was due to the unfavourable conformation of the amide as discussed in Section 3.12 (Figure 3.20). We decided to modify the pyridine auxiliary in such a way that it allows greater rotation around the C-N bond. For this, we proposed an auxiliary **3.185** as shown in Scheme 3.51. For the synthesis of the desired precursor, (\pm)-7-[*N*-(pyridin-2-yl)isobutyramide]-7-benzoazabicyclo[2.2.1]heptane **3.186**, first the alkylating reagent 2-bromo-2-methyl-*N*-phenylpropanamide **3.185** was prepared from 2-bromo-2-methylpropanoic acid **3.182** and 2-aminopyridine **3.184**. Next, the *N*-alkylation of 7-

benzoazabicyclo[2.2.1]heptane **3.181** was performed with **3.185** in the presence of K_2CO_3 to furnish the title precursor **3.186**, albeit in a low yield.



Scheme 3.51: Precursor synthesis, (\pm)-7-[*N*-(pyridin-2-yl)isobutyramide]-7-benzoazabicyclo[2.2.1]heptane **3.186** and tentative palladacycle **3.187**.

With the modified pyridine-based precursor **3.186** in hand, two trial conditions were carried out based on [Pd] and [Rh] catalysts (Scheme 3.52). The former reaction is believed to proceed *via* a Pd(II)/Pd(IV) pathway with the assistance of pivalic acid as a Brønsted acid, whereas the latter reaction is based on Wilkinson's catalyst for a Rh(I)/Rh(III) pathway. Unfortunately, only the starting material was recovered from both reactions, indicating the unfavourable 5,4-membered metallacycle formation for this type of system.



Scheme 3.52: Screening of modified pyridine auxiliary for intermolecular C-H activation with (±)-7-[*N*-(pyridin-2-yl)isobutyr amide]-7-benzoazabicyclo[2.2.1]heptane **3.186**.

3.13.2. Sulfur-containing directing groups

The trend of utilising sulfur-containing directing groups has been rapidly growing in lieu of carbonyl based directing groups (amide, carboxylic acid).¹⁰⁷ Different sulfur-containing directing groups such as thioether, thioamide, sulfoxides, and alkoxythiocarbonyl groups have been employed in a variety of C-H functionalisation reactions.

Considering the influence of sulfur-containing directing groups in successful C-H activation reactions, two electron-rich sulfinamide directing groups **3.189** & **3.190** were planned (Figure 3.24). It was predicted that these directing groups will form either a five-membered (through S atom) or a six-membered (through O atom) palladacycle. Both palladacycles should facilitate the desired product formation. However, one drawback of sulfur-based directing groups is their ability to poison the transition-metal.

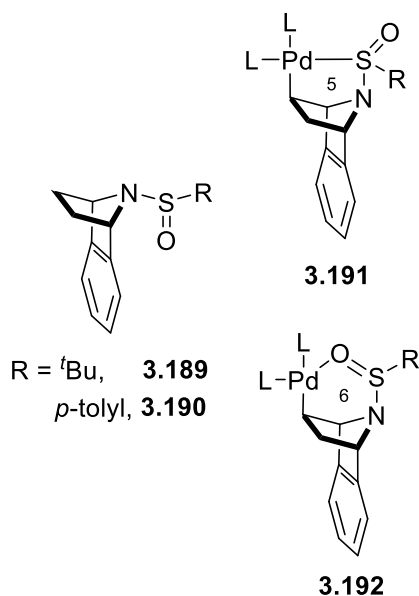
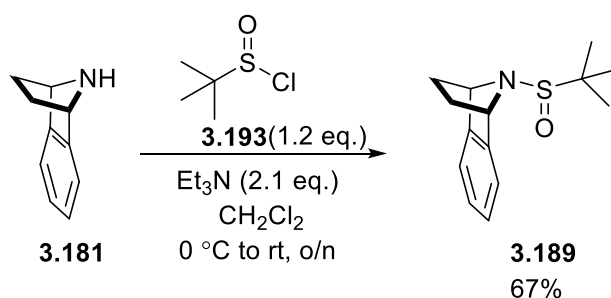


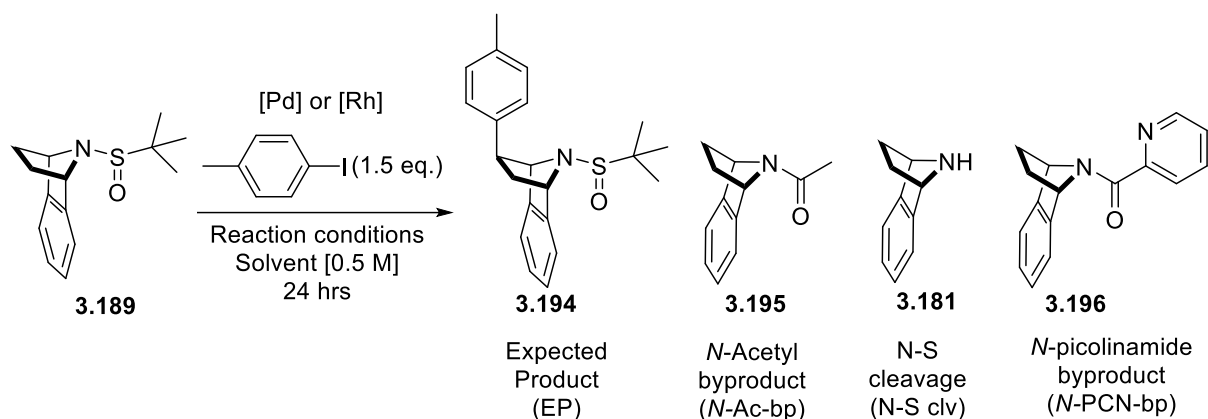
Figure 3.24: Proposed palladacycles **3.191** & **3.192** with sulfur-containing directing groups, **3.189** & **3.190**.

First, we added the sulfinyl directing group to the bicyclic system by reacting (\pm)-7-azabicyclo[2.2.1]heptane **3.181** with *tert*-butylsulfinyl chloride **3.193** with an acceptable yield (Scheme 3.53).



Scheme 3.53: Precursor synthesis, (\pm)-7-(*tert*-butylsulfinyl)-7-benzoazabicyclo[2.2.1]heptane **3.189**

Our biggest concern was the stability of the N-S bond under acidic conditions. We selected reaction parameters accordingly and screened a wide range of reaction conditions (Scheme 3.54, Table 3.6). The Brønsted acid chosen was either organic or inorganic, depending on the compatibility with other additives. In some cases, it was a part of a bidentate ligand such as picolinic acid or MPAA. Mostly, a monodentate ligand was employed. The choice of the base was similar to the cross-coupling reactions such as carbonates/metal *tert*-butoxides. The preference was given to polar solvents, considering their influence in lowering the energy barrier of the transition states of the reactants. All reactions were performed near to the boiling point of the respective solvent, in a sealed Schlenk tube.



Scheme 3.54: Attempted intermolecular C-H activation with (\pm)-7-(*tert*-butylsulfinyl)-7-benzoazabicyclo[2.2.1]heptane **3.189**

Table 3.6: Screening of reaction parameters for intermolecular C-H activation with (\pm)-7-(*tert*-butylsulfinyl)-7-benzoazabicyclo[2.2.1]heptane **3.189**

Entry	Reaction conditions	Observation
1	Pd(OAc) ₂ (10 mol%), Cs ₂ CO ₃ (3 eq.), PivOH (3 eq.), <i>t</i> -BuOH, 130 °C	3.189
2	Pd(OAc) ₂ (10 mol%), K ₂ HPO ₄ (3 eq.), Ag ₂ CO ₃ (1.5 eq.), NaOAc (2 eq.), <i>t</i> -BuOH, 130 °C	3.189 + 3.195 (1:0.5) ^a
3	Pd(OAc) ₂ (10 mol%), PCy ₃ (15 mol%), Ag ₂ CO ₃ (2 eq.), HFIP, 85 °C	3.189 + 3.181
4	Pd(OAc) ₂ (10 mol%), KOAc (2 eq.), DMA, 130 °C	3.195
5	Pd(OAc) ₂ (10 mol%), AgOAc (2.2 eq.), Tol/HFIP (4:1), 110 °C	3.195
6	Pd(OAc) ₂ (10 mol%), KOAc (2 eq.), <i>t</i> -BuOH, 90 °C	3.189
7	Pd(OAc) ₂ (10 mol%), KOAc (2 eq.), DMA, 130 °C	3.195
8	Pd(OAc) ₂ (10 mol%), PhCOOK (2 eq.), DMA, 130 °C	3.195
9	Pd(OAc) ₂ (10 mol%), picolinic acid (2 eq.), Cs ₂ CO ₃ (2 eq.), DMA, 130 °C	3.195 + 3.196 ^a
10	Pd(OAc) ₂ (10 mol%), picolinic acid (2 eq.), K ₂ HPO ₄ (2 eq.), 1,4-dioxane, 150 °C	3.196 ^a
11	Pd(OAc) ₂ (10 mol%), Ag ₂ O, 1,4-dioxane, 100 °C	3.189
12	Pd(OAc) ₂ (10 mol%), K ₂ CO ₃ (2 eq.), PivOH (1 eq.), toluene, 100 °C	3.189
13 ^b	Pd(OAc) ₂ (10 mol%), PivOH (2 eq.), neat, 100 °C	3.189
14	[RhCl(PPh ₃) ₃] (5 mol%), PCy ₃ , NaO ^t Bu (2 eq.), 1,4-dioxane, 120 °C	3.189
15	[RhCl(PPh ₃) ₃] (5 mol%), PCy ₃ , LiO ^t Bu (2 eq.), 1,4-dioxane, 120 °C	3.189

16^c	Pd(OAc) ₂ (10 mol%), KHCO ₃ (3 eq.), BQ (1.2 eq.), ^t BuOH, 130 °C	3.189
17^d	Pd(OAc) ₂ (10 mol%), <i>N</i> -Ac-Leu-OH (20 mol %), BQ (1.5 eq.), NaHCO ₃ (3 eq.), ^t BuOH [0.2 M], 100 °C	3.189

a = Based on crude ¹H NMR

b = 4-Iodotoluene (30 eq.)

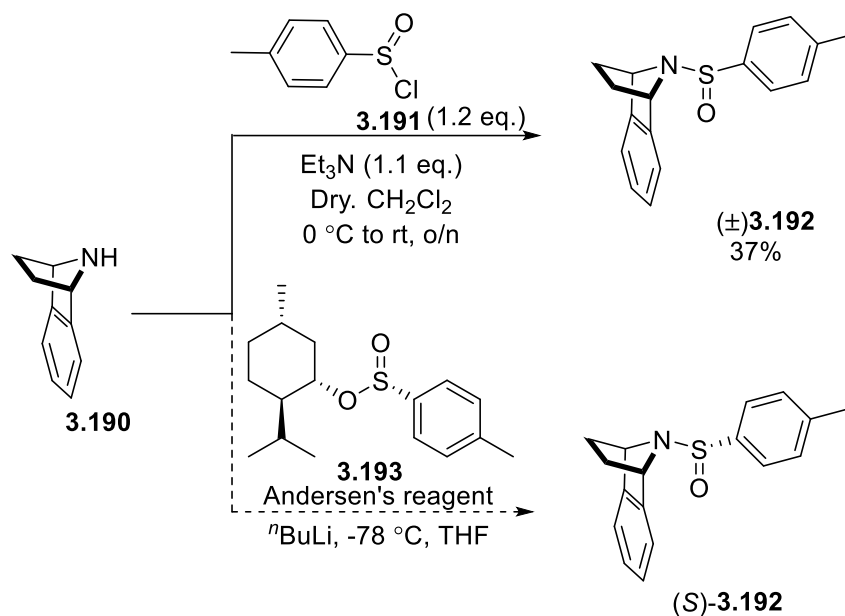
c = Phenyl boronic acid (1.5 eq.) was used instead of 4-iodotoluene.

d = Potassium phenyltrifluoroborate (1.5 eq.) was used instead of 4-iodotoluene.

No product arising from the targeted C-H activation was observed in any reaction. In most of the reactions, the starting material **3.189** was recovered. Moreover, the influence of the polar solvent and/or high temperature were proven to be detrimental in some cases. Cleavage of the weak N-S bond led to the formation of amine **3.181** (N-S clv) (entry 3); which formed an undesired byproduct *N*-Ac-bp **3.195** (entry 2, 4, 5, 7, & 8).^e In all but two reactions we believe that the solvent, DMA, acted as the source of the acetyl group. In the others, the source is less obvious. The same effect was observed when picolinic acid was employed as a bidentate ligand, resulting in an *N*-PCN-bp by-product **3.196** (entry 9 & 10). Surprisingly, the same type of impurity was not found in the presence of pivalic acid (entry 12 & 13) and *N*-Ac-Leu-OH additives (entry 17), presumably due to interference of sterics from the bulky *tert*-butyl or *isobutyl*. Changing the catalyst source to Wilkinson's catalyst (entry 14 & 15) as well as the coupling partner to boronates (entry 16 & 17) did not show any positive effect for C-H functionalisation.

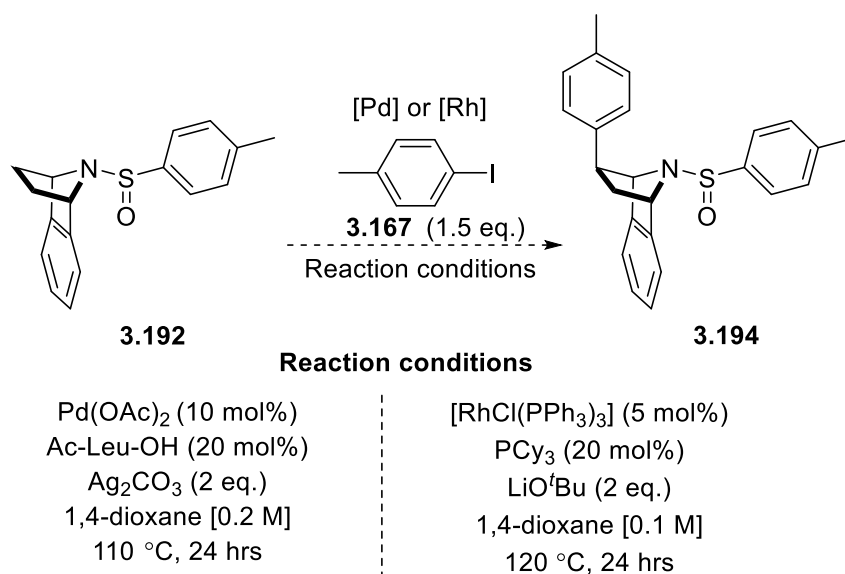
At this stage, we decided to replace the large *tert*-butyl group with the smaller *p*-tolyl group. The synthesis of sulfinamide was achieved albeit in low yield due to the instability of *p*-tolyl sulfinyl chloride **3.191** (Scheme 3.55). We also tried to synthesise this precursor (*S*)-**3.191** by employing (1*R*,2*S*,5*R*)-(-)-menthyl-(*S*)-*p*-tolylsulfinate (Andersen's reagent) **3.192**, *via* lithiation of 7-benzoazabicyclo[2.2.1]heptane **3.190**. However, all attempts were unsuccessful.

^e The protons in the ¹H NMR spectrum are quite distinguishable in both impurities, *N*-Ac-bp **3.195** and *N*-PCN-bp **3.196** due to the restricted rotation of an amide bond, resulting in two rotamers.



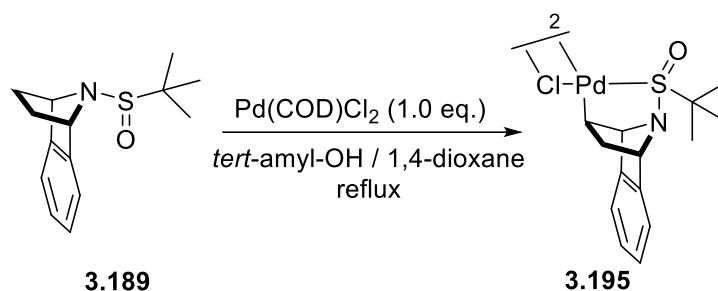
Scheme 3.55: Synthesis of (\pm) -7-(*p*-tolylsulfinyl)-7-benzoazabicyclo[2.2.1]heptane **3.192**.

Sulfinamide **3.192** was screened in two reactions. One used palladium and the other, rhodium. Both reactions failed to produce a product arising from the desired C-H functionalisation (Scheme 3.56).



Scheme 3.56: Attempted for intermolecular C-H activation of (\pm) -7-(*p*-tolylsulfinyl)-7-benzoazabicyclo[2.2.1]heptane **3.192**.

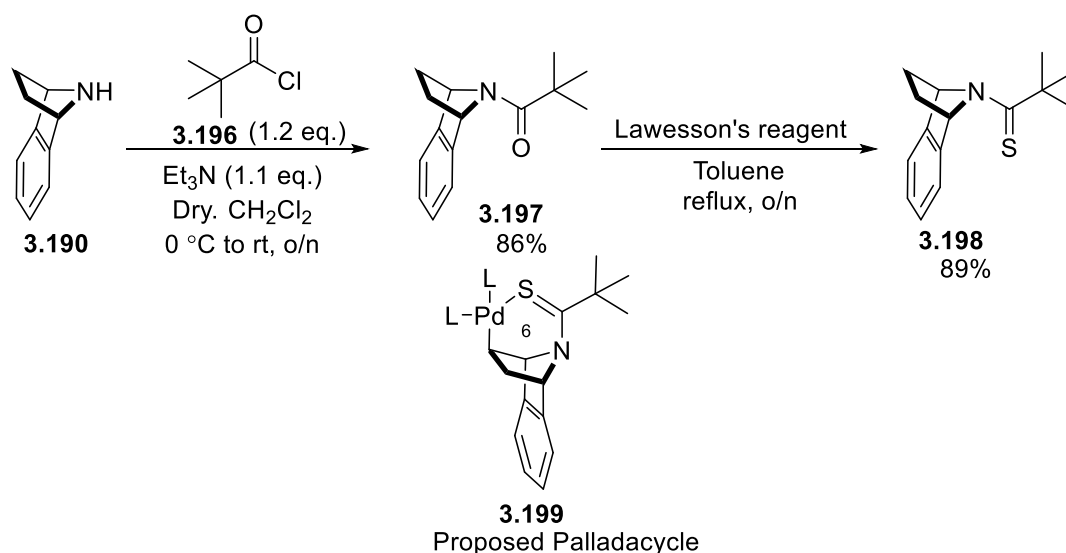
The inactivity of both the ^tBu- and *p*-tolyl sulfinyl directing groups suggests that steric hindrance was not an issue. At this stage, we were curious to see if the sulfinyl directing group would coordinate palladium, and attempted to form a palladium complex with a stoichiometric Pd(COD)Cl₂ but with no success (Scheme 3.57).



Scheme 3.57: Attempted palladium complex **3.195** formation with (\pm)-7-(*tert*-butylsulfinyl)-7-benzoazabicyclo[2.2.1]heptane **3.189**.

3.13.3. Thioamide directing group

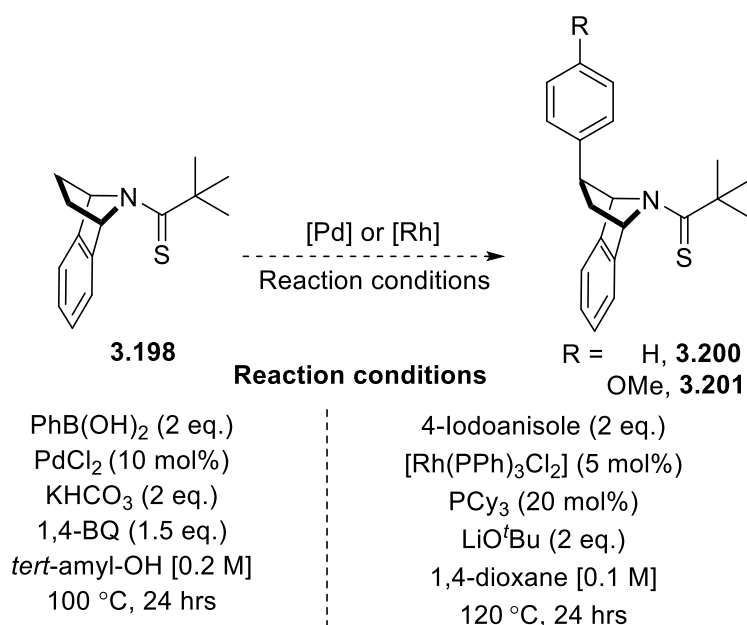
Next, we looked at a thioamide. The reduced electronegativity of sulfur compared to oxygen and its larger size means thioamides are better directing groups than amides. The C=S bond length ($\sim 1.6 \text{ \AA}$) is considerably longer than C=O. Moreover, the C=S π -orbital is higher in energy than the C=O π -orbital. The lone pairs of S can also coordinate to the metal.¹⁰⁷ Considering these properties, the electron-rich *tert*-butyl thioamide directing group was investigated. By reacting 2,2-dimethyl-1-(7-benzoazabicyclo[2.2.1]heptane)-1-propanone **3.197** with Lawesson's reagent, the thioamide precursor 2,2-dimethyl-1-(7-benzoazabicyclo[2.2.1]heptane)-1-propanethione **3.198** was prepared in good yield (Scheme 3.58).



Scheme 3.58: Precursor synthesis, 2,2-dimethyl-1-(7-benzoazabicyclo[2.2.1]heptane)-1-propanethione **3.198** and putative palladacycle **3.199**.

Both Yu and Glorius have used thioamides as directing groups for the α -C(sp^3)-H arylation of saturated azaheterocycles *via* a five-membered metallacycle.^{68,108} We employed their reaction

conditions with our azabicyclic system. Unfortunately, only the starting material was recovered (Scheme 3.59). We believe that the failure of the desired C-H functionalisation may be due to the inability of the thioamide directing group to form a six-membered metallacycle. We speculated that similar to the amide, the larger rotational barrier of the thioamide may arrange the 7-benzoazabicyclo[2.2.1]heptane skeleton in an unfavourable conformation for C-H activation.

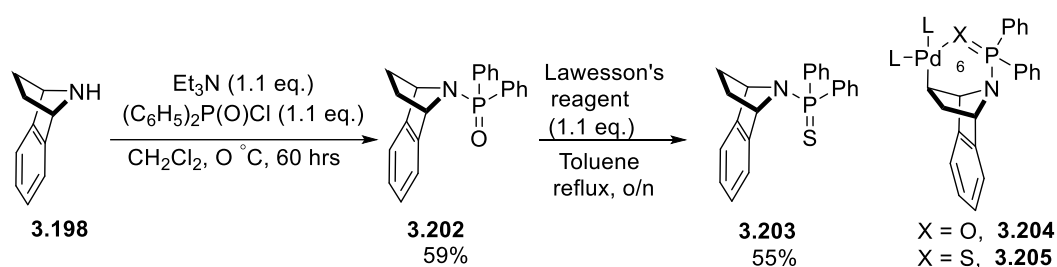


Scheme 3.59: Screening of thioamide directing group for intermolecular C-H activation with (\pm)- 2,2-dimethyl-1-(7-benzoazabicyclo[2.2.1]heptane)-1-propanethione **3.198**.

3.13.4. Phosphine oxide/sulfide directing groups

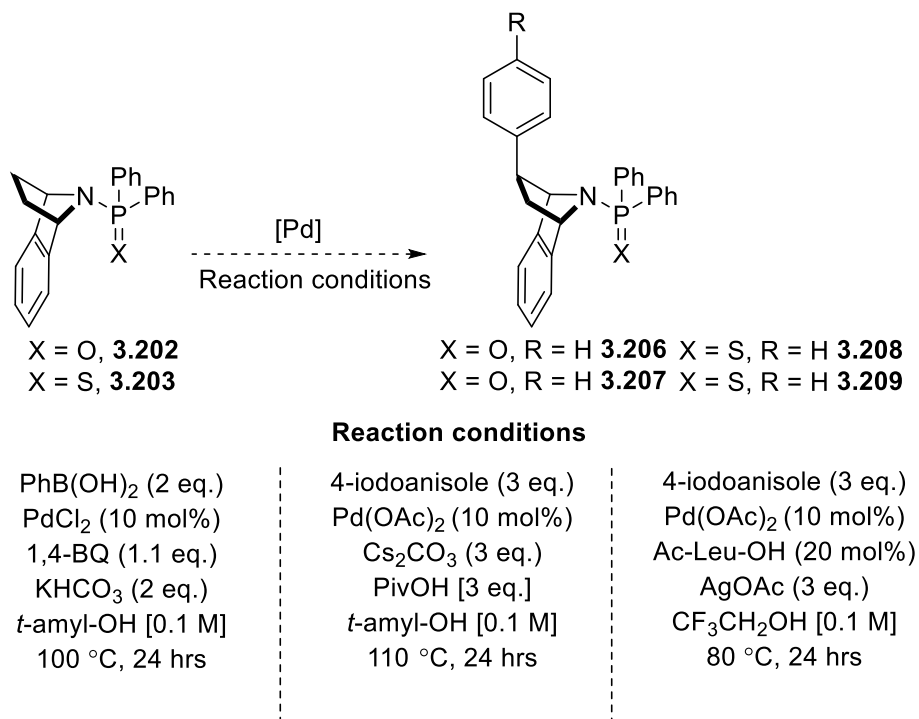
We examined phosphine oxide/sulfides directing groups, which had a single coordination site. Recently, diphenyl phosphine oxide [Ph₂(O)P] directing group has been shown to be competent in various C-H activation reactions.¹⁰⁹⁻¹¹¹

Addition of Ph₂P(O)Cl to the 7-benzoazabicyclo[2.2.1]heptane **3.190** took a surprisingly long reaction time (Scheme 3.60). The resulting phosphinamide **3.202** could be converted to a phosphine sulfide **3.203** by reacting with Lawesson's reagent (Scheme 3.60). We thought that either the Ph₂(O)P/Ph₂(S)P would allow us to form the six-membered metallacycles **3.204** & **3.205** with 7-benzoazabicyclo[2.2.1]heptane skeleton **3.198**.



Scheme 3.60: Synthesis of (\pm)-7-(diphenylphosphine oxide)-7-benzoazabicyclo[2.2.1]heptane **3.202** and (\pm)-7-(diphenylphosphine sulfide)-7-benzoazabicyclo[2.2.1]heptane **3.203**, and proposed palladacycles **3.204** & **3.205**.

As before, a number of different reaction conditions were screened (Scheme 3.61). We believed that the reactions may proceed *via* the Pd(II)/Pd(0) or Pd(II)/Pd(IV) pathway based on the coupling partner. The MPAA was selected as a ligand and pivalic acid was selected as a Brønsted acid in different reactions to promote a CMD. Frustratingly, the starting material was recovered unchanged in all reactions. The only exception was when trifluoroethanol was employed as the solvent. Oddly, the by-product *N*-Ac-bp **3.195** was observed. We speculated that the more acidic character of the solvent led to cleavage of the P-N bond, and the resulting amine **3.198** reacted with the ligand Ac-Leu-OH (yield <20%).



Scheme 3.61: Screening of phosphine oxide/sulfide directing groups for intermolecular C-H.

In all the above studies, monodentate directing groups were used. They would all possibly form a 6-membered metallacycle, except for *tert*-butyl sulfinyl directing group. The latter group could form either a 5- or a 6-membered metallacycle. As stated earlier, monodentate directing groups have shown less success with the activation of methylene positions than have bidentate directing groups. We therefore wanted to investigate a bidentate directing group but we were aware that we could not use the bridge nitrogen as this would lead to a four-membered ring. We needed a donor atom attached directly to the nitrogen. We wondered if hydrazine might work.

3.13.5. Hydrazone/hydrazide directing groups

We envisioned that installing a donor atom next to the ring nitrogen would enable us to form a stable 5-membered metallacycle (Figure 3.24). It was thought that converting the 7-benzoazabicyclo[2.2.1]heptane **3.181** into a hydrazine would allow the formation of hydrazone and hydrazide-based directing groups. Generally, bidentate directing groups are known to facilitate C-H functionalisation through their strong chelation. In a bidentate directing group, it is easier to tune both the steric and electronic environment. This would also, allow us to perfectly position a nitrogen donor to selectively target the β -position *via* the 5,5-chelation system. Moreover, the N-N bond would allow simple removal of the directing group at the end of the sequence to unlock the desired amine product.

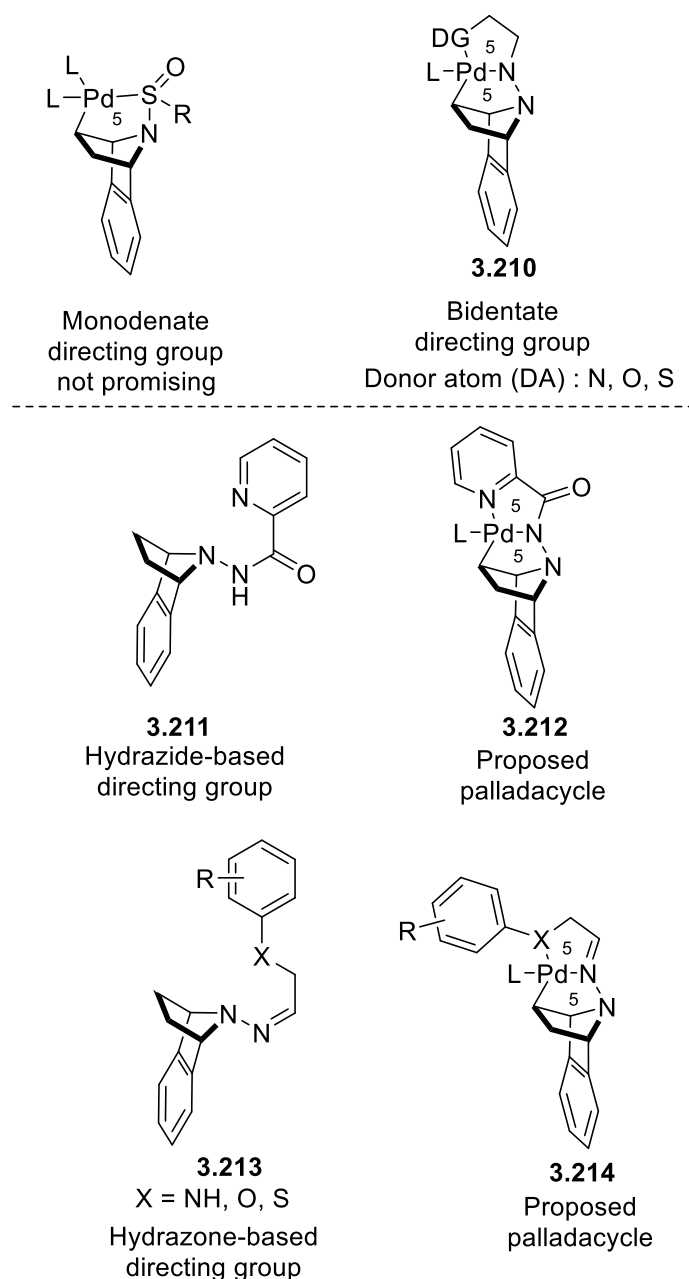
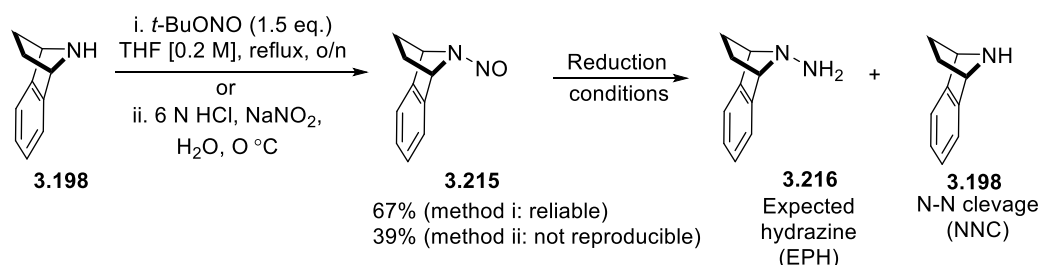


Figure 3.24: Hydrazone- and hydrazide-based directing groups.

Synthesis of the precursor started with the conversion of **3.198** to *N*-nitroso **3.215** by reacting it with *tert*-butyl nitrile in 67% yield (Scheme 3.62). Next, we needed to reduce the N=O bond without cleaving the weak N-N bond. A number of reductants were screened including LAH, DIBAL, and single-electron reducing agents such as Zn/AcOH (Table 3.7). With the former reagents, either the starting material was returned or an uncharacterised side-product was formed. Single-electron reduction conditions showed more promise. It was observed that the reaction time had a major influence on the outcome of the reaction. Longer reaction times led to N-N bond cleavage, returning the amine **3.198**. It is still unclear whether this cleavage is occurring only in the starting material, *N*-nitroso moiety **3.215**, in the expected hydrazine

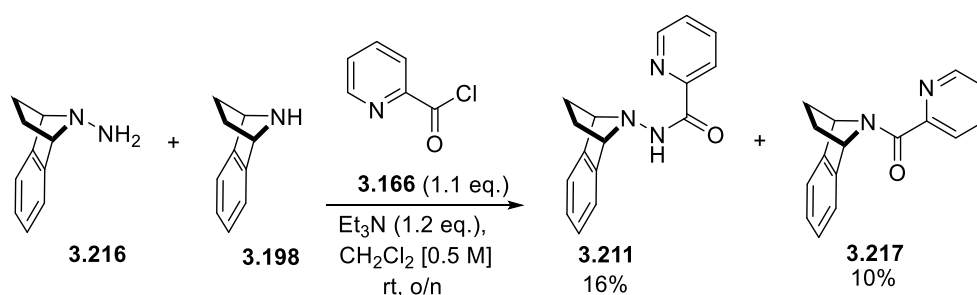
derivative **3.216**, or in both moieties. By reducing the reaction time (4 hrs), the expected hydrazine product **3.216** was obtained as an inseparable mixture with **3.198**. It was, therefore, decided to perform the acetylation on a mixture of **3.216** and **3.198**. Reaction with picolinoyl chloride **3.166**, gave expected hydrazine derivative albeit in 16% yield, with an amide by-product (10%) (Scheme 3.63).



Scheme 3.62: Synthesis of 7-(*N*-nitroso)-7-benzoazabicyclo[2.2.1]heptane **3.215** followed by attempted reduction.

Table 3.7: Attempted reduction conditions of 7-(*N*-nitroso)-benzoazabicyclo[2.2.1]heptane **3.215**

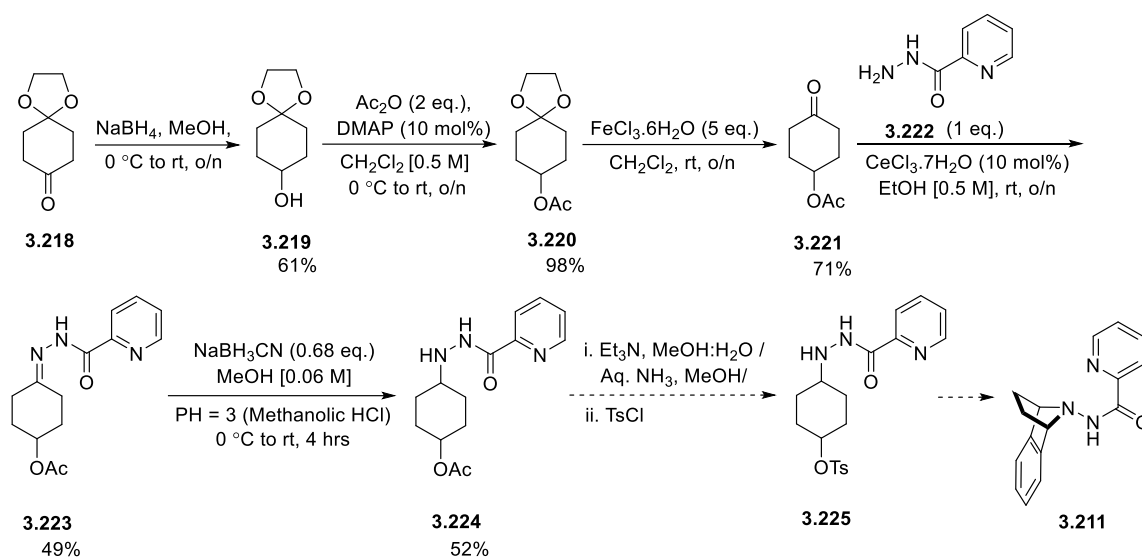
Entry	Reduction conditions	Observations
1	LAH (1.5 eq.), THF, 0 °C to rt to reflux	Starting material 3.125 returned
2	DIBAL (1 M, 2 eq.), CH ₂ Cl ₂ , -78 °C to rt	Uncharacterised by-product
3	Zn (3 eq.), NH ₄ Cl (3 eq.), THF : H ₂ O, 0 °C to rt	Starting material 3.125 returned
4	Zn (4 eq.), AcOH : EtOH : H ₂ O, 0 °C to rt, o/n	N-N cleavage observed
5	Zn (4 eq.), AcOH : H ₂ O (1:1), 0 °C, 4 hrs	Mixture of 3.216 and 3.198



Scheme 3.63: Precursor synthesis, 7-(picolinoylhydrazine)-7-benzoazabicyclo[2.2.1]heptane **3.211**.

Considering the difficulties associated with formation of the hydrazine derivative **3.211**, an alternative strategy was investigated (Scheme 3.64). This involved adding the hydrazine moiety **3.222** before forming the bicyclic molecule. The synthetic scheme proceeded smoothly until the penultimate stage. However, deacetylation of **3.224** did not work. If we would have been able to form the **3.225**, we had anticipated the challenges associated with the cyclisation of cyclohexanol intermediate **3.225**. We expected only the *trans* isomer of **3.225** to cyclise to the

desired bicyclic amine scaffold **3.211** and made the separation feasible from the *cis* isomer of **3.225**.



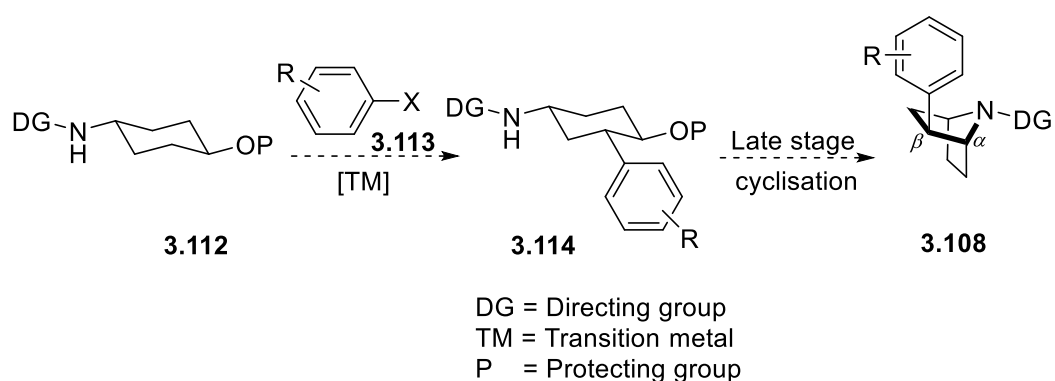
Scheme 3.64: Attempted precursor synthesis, 7-(picolinoylhydrazine)-7-azabicyclo[2.2.1]heptane **3.211**.

After comprehensive screening of a range of directing groups, β -C(sp^3)-H arylation of 7-(benzo)azabicyclo[2.2.1]heptane failed. We believed that all of the directing groups led to an unfavourable conformation of the directing group in the 7-azanorbornane, so that the metal catalyst could access the β -C(sp^3)-H bonds to form a metallacycle. We suggest that it would be advantageous to design an appropriate directing group that could form a thermodynamically more favoured metallacycle such as a 5- or 5,5-membered metallacycle. This suggestion is in agreement of Sanford's γ -C(sp^3)-H arylation of cyclic systems, which was published⁷⁵ when we were evaluating our last designed directing groups. In their study, they proposed the formation of a thermodynamically favoured fused 5,5-membered palladacycle with the tethered directing group, considering the involvement of ring nitrogen.

The β -C(sp^3)-H functionalisation of saturated azaheterocycles would definitely open a new avenue to access substituted azaheterocycles in the shortest way. Considering the timeline of Ph.D., we decided to move to our fallback plan, γ -C(sp^3)-H arylation of 1-cyclohexylamine where the methods to achieve the desired C-H activation have already been reported but its asymmetric version still needs to be addressed.

3.14. Enantioselective γ -C(sp^3)-H of a cyclohexylamine system

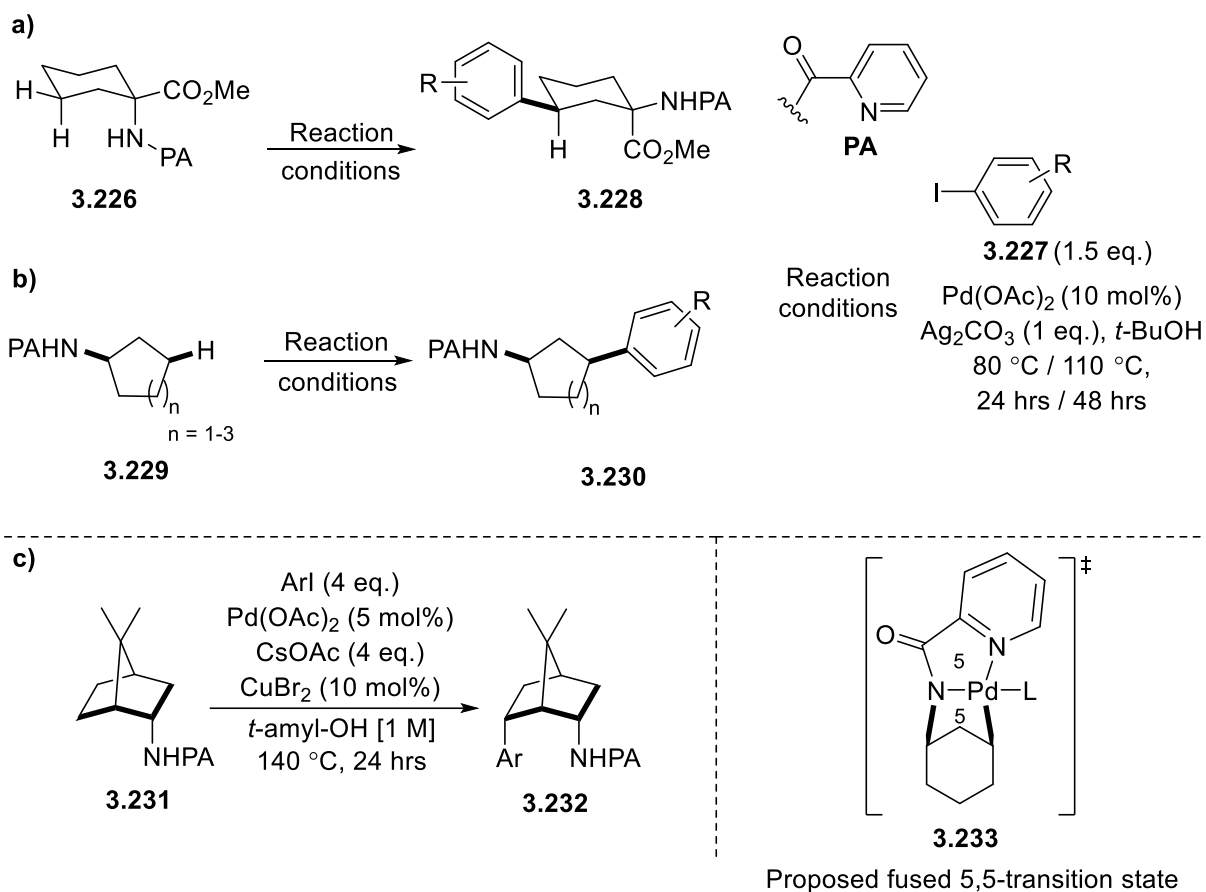
As explained in the objective section of this chapter, we sought to investigate C(sp^3)-H activation on the 1,4-disubstituted cyclohexylamine system **3.112**. We could still achieve the goal of epibatidine synthesis by a late-stage cyclisation approach. With this system, the directing group can be designed based on the external amine functionality.



Scheme 3.65: Intramolecular γ -C(sp^3)-arylation of 1,4-disubstituted cyclohexylamine system **3.112**.

The main goal of this project was to achieve the enantioselective γ -C(sp^3)-H functionalisation of the cyclohexylamine system. The catalytic system leveraging an amide directing group such as picolinamide directing group has been exploited for C(sp^3)-H activation on a wide range of aliphatic and cyclic amine substrates.⁹⁵

Before C(sp^3)-H activation of the 1,4-disubstituted cyclohexylamine system, we thought that the simple 1-aminocyclohexane would be a good test system. The achiral γ -C(sp^3)-H arylation on this system using a picolinamide directing group has been reported (Scheme 3.66a).^{36,112} Seki et al. also achieved C-H activation of unsubstituted cycloalkylamine derivatives using the same conditions (Scheme 3.66b).¹¹³ Very recently, a similar study was published by Sheppard and co-workers with an improved reaction efficiency and diverse substrate scope. Under these silver-free reaction conditions, caesium carboxylate salt and CuBr additive were shown to improve conversions (Scheme 3.66c).¹¹⁴



Scheme 3.66: Different reaction conditions reported for picolinamide-directed γ -C(*sp*³)-H arylation of cycloalkylamine derivatives.

As per the proposed mechanism, the picolinamide directing group coordinates with Pd(OAc)₂ to form a palladium complex **I** (Figure 3.25). The next step would enable the activation of γ -C(*sp*³)-H bond. The bidentate coordination of both the amide and pyridine leads to a thermodynamically favoured 5,5-fused palladacycle **II**. Subsequently, the oxidative addition of aryl iodide generates Pd^(IV) intermediate **III**, which would lead to product formation upon reductive elimination.

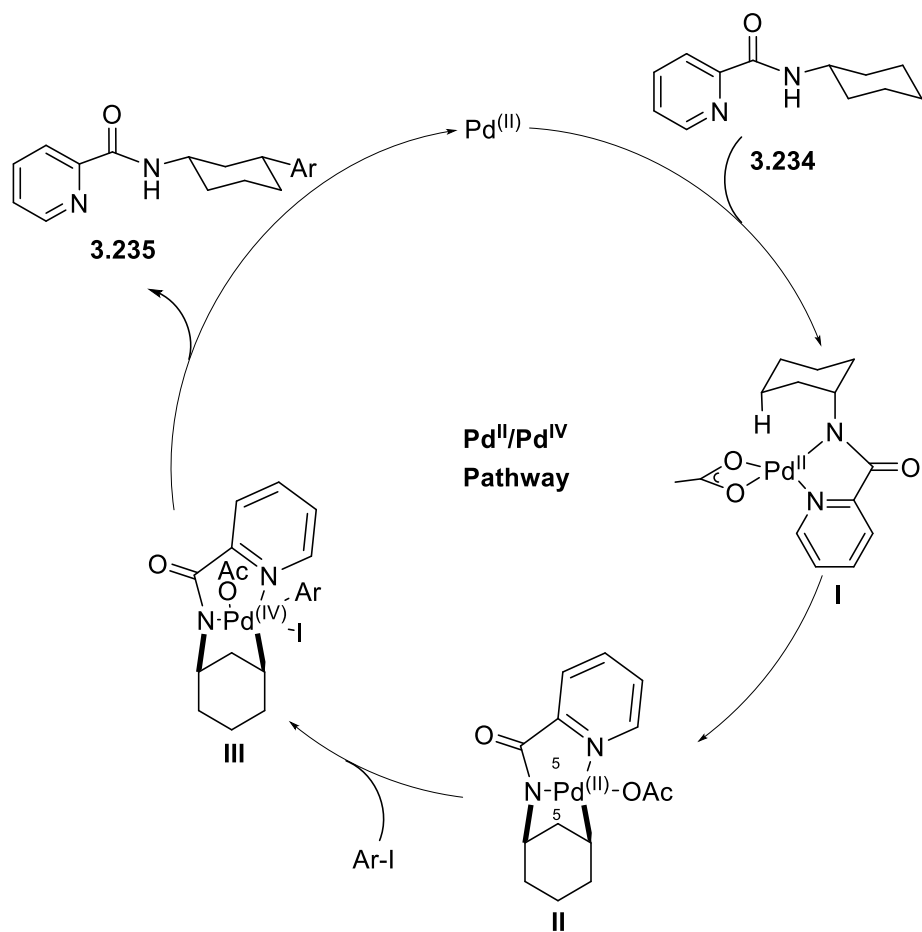


Figure 3.25: Proposed Pd(II)/Pd(IV) pathway for a γ -C(sp^3)-H arylation of *N*-cyclohexylpicolinamide **3.234**.

We sought to achieve an asymmetric version of γ -C(sp^3)-H activation of the *N*-cyclohexylpicolinamide **3.234**. It is noteworthy to mention here that the initial proton abstraction step is enabled by an acetate from the catalyst Pd(OAc)₂. By replacing it with a chiral conjugate base, it may be possible to achieve the enantioselective C-H functionalisation. We envisaged that chirality could be introduced in two possible ways (Figure 3.26).

- i. By introducing a chiral Brønsted acid (chiral conjugate base) (Enantioselective)
- ii. By appending a chiral directing (chiral auxiliary) while maintaining the same fused 5,5-system (Diastereoselective)

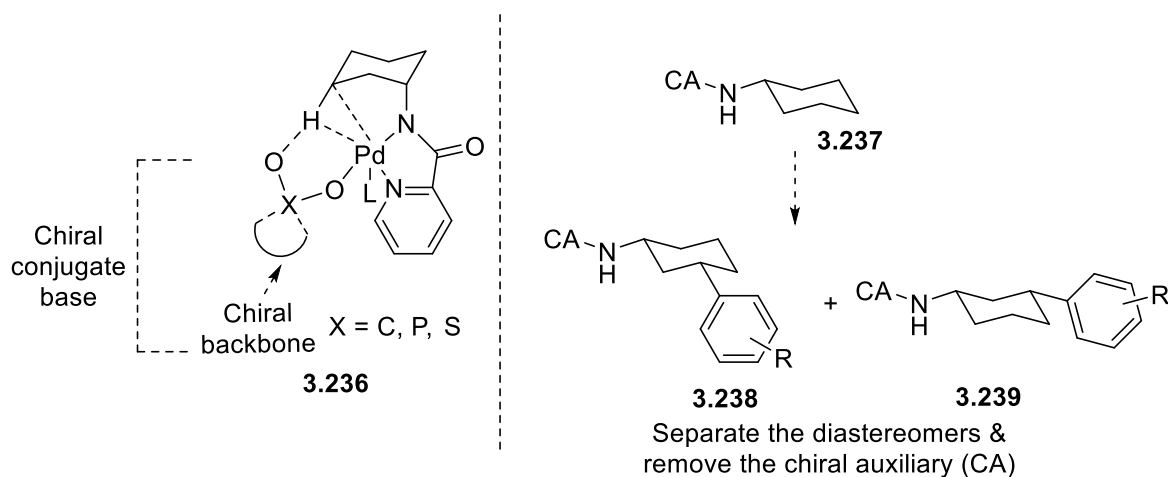
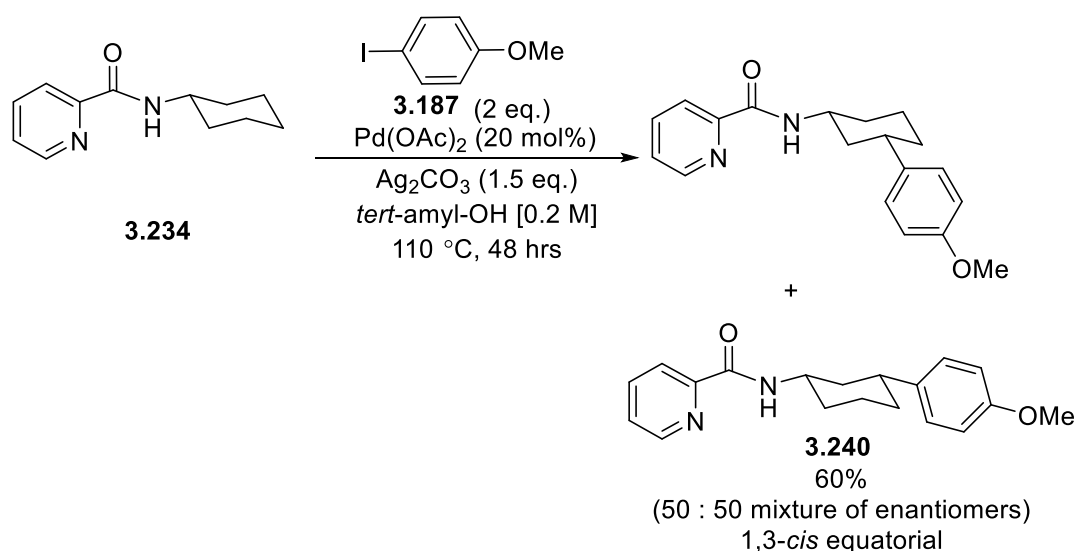


Figure 3.26: Proposed strategies for asymmetric γ -C(sp^3)-H arylation of *N*-cyclohexylpicolinamide **3.234**.

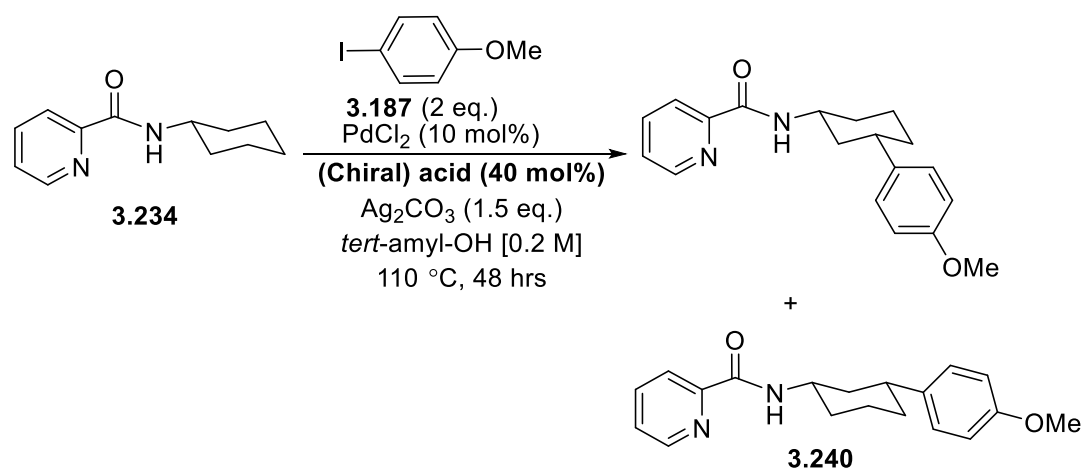
Inducing asymmetry during C-H functionalisation might be possible if the diastereomeric transition states formed by using a chiral conjugate base were sufficiently different. This is particularly challenging in this example where we must also consider about the conformation of the molecule. Our study began by probing various (chiral) Brønsted acids (Scheme 3.68, Table 3.8).

The first experiment was a control to establish that we could functionalise **3.234** (Scheme 3.67).¹¹³ The C-H transformation was accomplished in 60% yield. Using HPLC, Daicel As-H column (normal phase), and Lux Amulose column (reverse phase), it was possible to resolve the two enantiomers distinctly so that the enantiomeric ratio could be accurately determined.



Scheme 3.67: Control reaction for γ -C(sp^3)-H arylation on *N*-cyclohexylpicolinamide **3.234**.

Our screening of different (chiral) Brønsted acids began (Scheme 3.68, Table 3.8). The Pd(OAc)₂ was replaced by PdCl₂ [Pd(II)] as an active catalyst so that we could remove the acetate ion and hopefully avoid a non-selective background reaction. The reaction was set up in the absence of any Brønsted acid (entry 1). Surprisingly, product formation was observed (SM:P 82:18), suggesting that the strong chelating effect of the bidentate directing group was sufficient to initiate the reaction albeit slowly. When pivalic acid was employed as an acid additive, the reaction conversion increased to 88% (entry 2). This clearly shows that a Brønsted acid, presumably, as the carboxylate salt, mediates the concerted metalation deprotonation process. Next, we investigated a range of chiral acid derivatives as shown in Table 3.8.

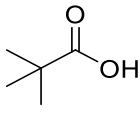
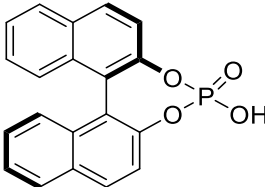
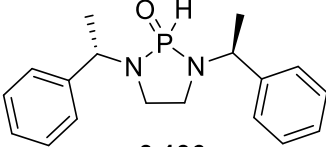
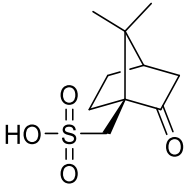
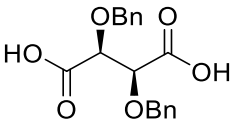
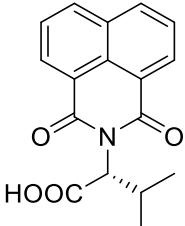


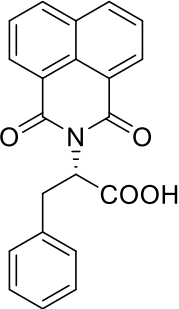
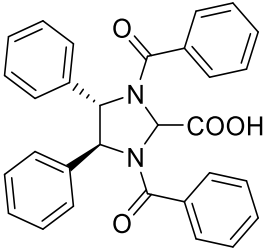
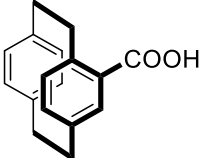
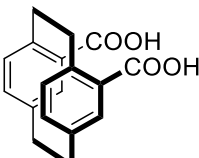
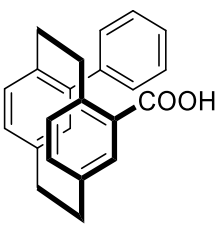
Scheme 3.68: Optimisation study to evaluate the effect of chiral acid on γ -C(*sp*³)-H arylation of *N*-cyclohexylpicolinamide **3.234**.^a

^a = HPLC conditions (Normal Phase) for separation of enantiomers of **3.240**:- stationary phase : Daicel As-H column, mobile phase: 10% *i*Pr-OH: Hexane (1% TFA) for 45 min. Flow rate: 1.0 ml/min, Injection vol. 10 μ l, RT: for enantiomer 1: 18.39 min., for enantiomer 2: 22.99 min.

= HPLC conditions (Reverse Phase) for separation of enantiomers of **3.240**:- stationary phase : Lux Amulose column, mobile phase: 70% CH₃CN: H₂O for 50 min. Flow rate: 0.5 ml/min, Injection vol. 10 μ l, RT: for enantiomer 1: 36.75 min., for enantiomer 2: 42.16 min.

Table 3.8: Effect of various (chiral) Brønsted acid

Entry	(Chiral) Brønsted acid	Observation ^{a, b, c}
1	no Brønsted acid	SM:P = 82:18
2	 3.241	SM:P = 12:88
3 ³⁹	 3.242	SM:P = 78:22*
4	Deviation from the reaction conditions of scheme 3.68^d	SM:P = 95:5*
5 ⁹⁴	 3.136	SM:P = 76:24 er = 49.42:50.58
6	 3.243	SM:P = 81.5:18.5*
7	 3.244	SM:P = 27:73 er = 52.38:47.62
8 ¹¹⁵	 3.245	SM:P = 35:65 er = 51.63:48.37

9 ¹¹⁵	 <p style="text-align: center;">3.246</p>	SM:P = 0:100 er = 47.96: 52.04
10 ¹¹⁶	 <p style="text-align: center;">3.247</p>	SM:P = 25:75 er =49.42:50.58
11 ¹¹⁷	 <p style="text-align: center;">3.142</p>	SM:P = 0:100
12 ¹¹⁸	 <p style="text-align: center;">3.248</p>	SM:P = 0:100
13 ¹¹⁹	 <p style="text-align: center;">3.249</p>	SM:P = 0:100

^a = The ratio of starting material and product (SM:P) was determined based on crude ¹H NMR, comparing the ratio of distinct C1-proton of SM and P.

^b = Enantiomeric ratio (e.r.) was determined based on optimised HPLC conditions on pure product

* e.r. is not determined due to low conversion.

^c = (Chiral) Brønsted acids were synthesised by following the reported procedures of respective references mentioned in the entry column

^d = PdCl₂(CH₃CN)₂ (10 mol%), (*S*)-BINOL-P(O)₂H, (20 mol%), Cs₂CO₃ (1.5 eq.), xylene, 140 °C, 22 hrs.

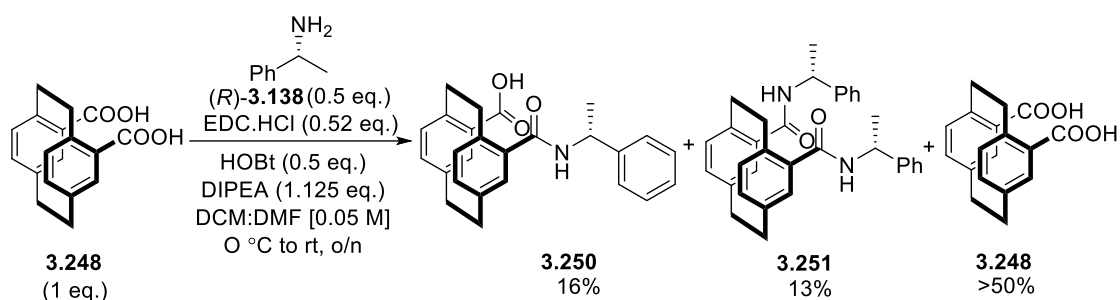
Considering the widespread success of BINOL derivatives in asymmetric catalysis,¹²⁰ we started with the BINOL-based chiral phosphoric acid **3.242**. BINOL possesses an axis of chirality and the high rotational barrier of 1,1'-binaphthyl enables the high configurational stability of the enantiomers. When (*S*)-BINOL-P(O)₂H **3.242** was employed, it had shown a very minimal effect on reaction conversion (entry 3). Product formation was nearly the same as the background reaction (entry 1). Chen et al. reported an enantioselective picolinamide directed benzylic C(*sp*³)-H arylation of phenylpropylamine by employing BINOL phosphate ligand. His team proposed that the cooperative effect of the BINOL with the caesium carbonate, generating caesium phosphate complex may be responsible for the good stereocontrol in the C-H palladation step.¹²¹ When the same reaction conditions were applied for the substrate **3.234**, it proved detrimental to the reaction progress (entry 4). An alternative C2-symmetric additive HASPO-VI **3.136** was also implemented, hoping to act as an internal base but with no success (entry 5).

We then screened a collection of readily accessible chiral acids. With (1*S*)-(+)-10-camphorsulfonic acid **3.243**, the reaction did not show any promise (entry 6) while significant product formation was accomplished with dibenzyl-*L*-tartrate **3.244** (entry 7) but failed to induce good enantiocontrol (er = 52.38:47.62). Due to the bidentate nature of the picolinamide directing group, only one valence site of Pd(II) is available to interact with a chiral acid. Hence, we selected bis-*N*-protected naphthalimide-based amino acids (entry 8 & 9).¹¹⁵ When naphthalimide-*L*-valine **3.245** and naphthalimide-*L*-phenylalanine **3.246** were employed in the reaction, complete product formation was observed in the latter case (entry 9). Unfortunately, neither reaction showed any selectivity (51.63:48.37 and 47.96: 52.04).

In light of the recent success of a novel C2-symmetric carboxylic acid, (4*S*,5*S*)-1,3-dibenzoyl-4,5-diphenylimidazolidine-2-carboxylic acid **3.247** in the enantioselective cobalt(III) catalysed C-H activation,¹¹⁶ it was exciting to explore its potential on the current 1-aminocyclohexyl system (entry 10). The reaction proceeded in 75% yield and 49.42:50.58 er.

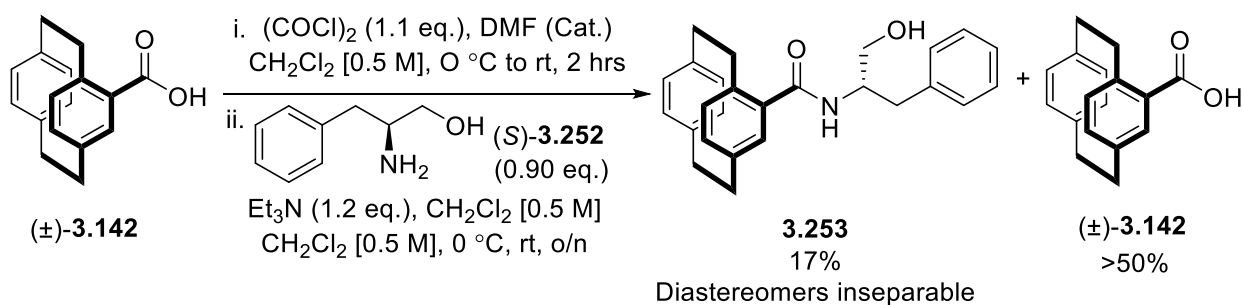
An obvious interest of our group is planar chiral [2.2]paracyclophane derivatives. Generally, the resolution of planar chiral [2.2]paracyclophane carboxylic acid derivatives can be tedious.¹²² Therefore, the efficiency of racemic carboxylic acids was established first. Gratifyingly, all [2.2]paracyclophane carboxylic acid derivatives, including mono- and disubstituted derivatives **3.142**, **3.248**, and **3.249** showed 100% reaction conversion (entry 11, 12 & 13).

With the success of racemic paracyclophane acids, we needed a quick method to resolve them. Initially, we attempted desymmetrisation of the diacid **3.248** by formation of a monoamide. The desymmetrisation of **3.248** was attempted by adding the readily available chiral amine - (*R*)-phenylethylamine **3.138** using standard amide coupling methods (Scheme 3.69).¹²³ Here, our aim was to form only a mono-coupled product with the half equivalent of desired coupling reagents. Unfortunately, the reaction was non-selective, occurring on both carboxylic acid groups to give a chiral monosubstituted product **3.250** in 16% and chiral disubstituted product **3.251** in 13%.



Scheme 3.69: Attempted desymmetrisation of [2.2]paracyclophane-4,13-dicarboxylic acid **3.248**.

Due to the difficulty encountered in desymmetrising the disubstituted derivative, we decided to resolve the monosubstituted derivative (\pm)-[2.2]paracyclophane-4-carboxylic acid **3.142** (Scheme 3.70). The same approach was applied but this time with L-phenyl alaninol **3.252**. Unfortunately, the product formation **3.253** was observed in low yield and the diastereomers were inseparable by column chromatography.



Scheme 3.70: Attempted resolution of (\pm)-[2.2]paracyclophane-4-carboxylic acid **3.142**.

Due to the challenges faced during the synthesis of enantiopure mono- and di-substituted [2.2]paracyclophane carboxylic acid derivatives, we became interested in developing an alternative methodology to access these useful compounds. One of the most intriguing strategies was through the direct synthesis of an oxazoline that would be formed as a

diastereomeric mixture that could be resolved. Once the pure diastereomer was in hand, it could be hydrolysed to obtain the enantiopure [2.2]paracyclophane carboxylic acid (Figure 3.27).

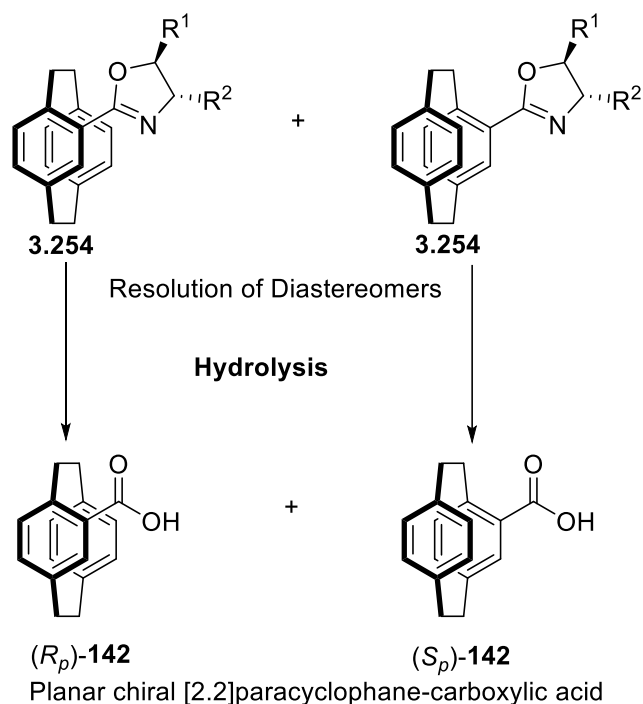


Figure 3.27: Strategy to access enantiopure [2.2]paracyclophane acid derivatives.

At this point, we decided to develop the methodology for the synthesis of [2.2]paracyclophane-oxazoline derivatives. If we succeed to gain access to the planar chiral acid derivatives, the above study of asymmetric γ -C(sp^3)-H of the *N*-cyclohexylpicolinamide would be resumed later.

3.15. References

- (1) Geissler, H. Transition Metal—Catalyzed Cross Coupling Reactions. *Transition Metals for Organic Synthesis* **1998**, 158.
- (2) Suzuki, A. Recent Advances In the Cross-Coupling Reactions of Organoboron Derivatives with Organic Electrophiles, 1995–1998. *J. Organomet. Chem.* **1999**, 576, 147.
- (3) Martin, R.; Buchwald, S. L. Palladium-Catalyzed Suzuki–Miyaura Cross-Coupling Reactions Employing Dialkylbiaryl Phosphine Ligands. *Acc. Chem. Res.* **2008**, 41, 1461.
- (4) Newhouse, T.; Baran, P. S. If C–H Bonds Could Talk: Selective C–H Bond Oxidation. *Angew. Chem. Int. Ed.* **2011**, 50, 3362.
- (5) Wencel-Delord, J.; Glorius, F. C–H bond activation enables the rapid construction and late-stage diversification of functional molecules. *Nat. Chem.* **2013**, 5, 369.
- (6) Cernak, T.; Dykstra, K. D.; Tyagarajan, S.; Vachal, P.; Krska, S. W. The medicinal chemist's toolbox for late stage functionalization of drug-like molecules. *Chem. Soc. Rev.* **2016**, 45, 546.
- (7) Gareth, Hydrazine-Based Directing Groups for The Remote C–H Functionalisation of Cyclic Amines.
- (8) Crabtree, R.; LeiOrcid, A. Introduction: CH Activation. *Chem. Rev.* **2017**, 117, 8481.
- (9) Giri, R.; Shi, B.-F.; Engle, K. M.; Maugel, N.; Yu, J.-Q. Transition metal-catalyzed C–H activation reactions: diastereoselectivity and enantioselectivity. *Chem. Soc. Rev.* **2009**, 38, 3242.
- (10) Jun, C.-H. Transition metal-catalyzed carbon–carbon bond activation. *Chem. Soc. Rev.* **2004**, 33, 610.
- (11) Gandeepan, P.; Müller, T.; Zell, D.; Cera, G.; Warratz, S.; Ackermann, L. 3d Transition Metals for C–H Activation. *Chem. Rev.* **2019**, 119, 2192.
- (12) Blanksby, S. J.; Ellison, G. B. Bond Dissociation Energies of Organic Molecules. *Acc. Chem. Res.* **2003**, 36, 255.
- (13) Afagh, N. A.; Yudin, A. K. Chemoselectivity and the Curious Reactivity Preferences of Functional Groups. *Angew. Chem. Int. Ed.* **2010**, 49, 262.
- (14) Becker, H. G. O. Jan Fleming, Frontier Orbitals and Organic Chemical Reactions. *Journal für Praktische Chemie* **1978**, 320, 879.
- (15) Daugulis, O.; Zaitsev, V. G.; Shabashov, D.; Pham, Q.-N.; Lazareva, A. Regioselective Functionalization of Unreactive Carbon-Hydrogen Bonds. *Synlett* **2006**, 3382.
- (16) Liao, K.; Negretti, S.; Musaev, D. G.; Bacsa, J.; Davies, H. M. L. Site-selective and stereoselective functionalization of unactivated C–H bonds. *Nature* **2016**, 533, 230.
- (17) Davies, H. M. L.; Manning, J. R. Catalytic C–H functionalization by metal carbenoid and nitrenoid insertion. *Nature* **2008**, 451, 417.
- (18) Newton, C. G.; Wang, S.-G.; Oliveira, C. C.; Cramer, N. Catalytic Enantioselective Transformations Involving C–H Bond Cleavage by Transition-Metal Complexes. *Chem. Rev.* **2017**, 117, 8908.
- (19) Chen, Z.; Rong, M.-Y.; Nie, J.; Zhu, X.-F.; Shi, B.-F.; Ma, J.-A. Catalytic alkylation of unactivated C(sp³)–H bonds for C(sp³)–C(sp³) bond formation. *Chem. Soc. Rev.* **2019**, 48, 4921.
- (20) Ryabov, A. D. Mechanisms of intramolecular activation of carbon-hydrogen bonds in transition-metal complexes. *Chem. Rev.* **1990**, 90, 403.
- (21) Chen, Y.-Q.; Wang, Z.; Wu, Y.; Wisniewski, S. R.; Qiao, J. X.; Ewing, W. R.; Eastgate, M. D.; Yu, J.-Q. Overcoming the Limitations of γ - and δ -C–H Arylation of Amines through Ligand Development. *J. Am. Chem. Soc.* **2018**, 140, 17884.
- (22) Davies, D. L.; Donald, S. M. A.; Macgregor, S. A. Computational Study of the Mechanism of Cyclometalation by Palladium Acetate. *J. Am. Chem. Soc.* **2005**, 127, 13754.
- (23) Murai, S.; Kakiuchi, F.; Sekine, S.; Tanaka, Y.; Kamatani, A.; Sonoda, M.; Chatani, N. Efficient catalytic addition of aromatic carbon-hydrogen bonds to olefins. *Nature* **1993**, 366, 529.
- (24) Huang, Z.; Lim, H. N.; Mo, F.; Young, M. C.; Dong, G. Transition metal-catalyzed ketone-directed or mediated C–H functionalization. *Chem. Soc. Rev.* **2015**, 44, 7764.

- (25) Rit, R. K.; Yadav, M. R.; Ghosh, K.; Sahoo, A. K. Reusable directing groups [8-aminoquinoline, picolinamide, sulfoximine] in C(sp^3)-H bond activation: present and future. *Tetrahedron* **2015**, *71*, 4450.
- (26) Dong, Z.; Ren, Z.; Thompson, S. J.; Xu, Y.; Dong, G. Transition-Metal-Catalyzed C-H Alkylation Using Alkenes. *Chem. Rev.* **2017**, *117*, 9333.
- (27) Rouquet, G.; Chatani, N. Catalytic Functionalization of C(sp^2)-H and C(sp^3)-H Bonds by Using Bidentate Directing Groups. *Angew. Chem. Int. Ed.* **2013**, *52*, 11726.
- (28) Chen, Z.; Wang, B.; Zhang, J.; Yu, W.; Liu, Z.; Zhang, Y. Transition metal-catalyzed C-H bond functionalizations by the use of diverse directing groups. *Org. Chem. Front.* **2015**, *2*, 1107.
- (29) Sun, H.; Guimond, N.; Huang, Y. Advances in the development of catalytic tethering directing groups for C-H functionalization reactions. *Org. Biomol. Chem.* **2016**, *14*, 8389.
- (30) Sambiagio, C.; Schönbauer, D.; Blicek, R.; Dao-Huy, T.; Pototschnig, G.; Schaaf, P.; Wiesinger, T.; Zia, M. F.; Wencel-Delord, J.; Besset, T. et al. A comprehensive overview of directing groups applied in metal-catalysed C-H functionalisation chemistry. *Chem. Soc. Rev.* **2018**, *47*, 6603.
- (31) Calleja, J.; Pla, D.; Gorman, T. W.; Domingo, V.; Haffemayer, B.; Gaunt, M. J. A steric tethering approach enables palladium-catalysed C-H activation of primary amino alcohols. *Nat. Chem.* **2015**, *7*, 1009.
- (32) Chen, X.; Goodhue, C. E.; Yu, J.-Q. Palladium-Catalyzed Alkylation of sp^2 and sp^3 C-H Bonds with Methylboroxine and Alkylboronic Acids: Two Distinct C-H Activation Pathways. *J. Am. Chem. Soc.* **2006**, *128*, 12634.
- (33) Desai, L. V.; Hull, K. L.; Sanford, M. S. Palladium-Catalyzed Oxygenation of Unactivated sp^3 C-H Bonds. *J. Am. Chem. Soc.* **2004**, *126*, 9542.
- (34) Giri, R.; Chen, X.; Yu, J.-Q. Palladium-Catalyzed Asymmetric Iodination of Unactivated C-H Bonds under Mild Conditions. *Angew. Chem. Int. Ed.* **2005**, *44*, 2112.
- (35) Chen, G.; Gong, W.; Zhuang, Z.; Andrá, M. S.; Chen, Y.-Q.; Hong, X.; Yang, Y.-F.; Liu, T.; Houk, K. N.; Yu, J.-Q. Ligand-accelerated enantioselective methylene C(sp^3)-H bond activation. *Science* **2016**, *353*, 1023.
- (36) Zaitsev, V. G.; Shabashov, D.; Daugulis, O. Highly Regioselective Arylation of sp^3 C-H Bonds Catalyzed by Palladium Acetate. *J. Am. Chem. Soc.* **2005**, *127*, 13154.
- (37) Stowers, K. J.; Fortner, K. C.; Sanford, M. S. Aerobic Pd-Catalyzed sp^3 C-H Olefination: A Route to Both N-Heterocyclic Scaffolds and Alkenes. *J. Am. Chem. Soc.* **2011**, *133*, 6541.
- (38) Rej, S.; Ano, Y.; Chatani, N. Bidentate Directing Groups: An Efficient Tool in C-H Bond Functionalization Chemistry for the Expedient Construction of C-C Bonds. *Chem. Rev.* **2020**, *120*, 1788.
- (39) Yan, S.-B.; Zhang, S.; Duan, W.-L. Palladium-Catalyzed Asymmetric Arylation of C(sp^3)-H Bonds of Aliphatic Amides: Controlling Enantioselectivity Using Chiral Phosphoric Amides/Acids. *Org. Lett.* **2015**, *17*, 2458.
- (40) Jun, C.-H.; Lee, H.; Hong, J.-B. Chelation-Assisted Intermolecular Hydroacylation: Direct Synthesis of Ketone from Aldehyde and 1-Alkene. *J. Org. Chem.* **1997**, *62*, 1200.
- (41) Gandeepan, P.; Ackermann, L. Transient Directing Groups for Transformative C-H Activation by Synergistic Metal Catalysis. *Chem* **2018**, *4*, 199.
- (42) St John-Campbell, S.; Bull, J. A. Transient imines as 'next generation' directing groups for the catalytic functionalisation of C-H bonds in a single operation. *Org. Biomol. Chem.* **2018**, *16*, 4582.
- (43) Zhao, Q.; Poisson, T.; Pannecoucke, X.; Besset, T. The Transient Directing Group Strategy: A New Trend in Transition-Metal-Catalyzed C-H Bond Functionalization. *Synthesis* **2017**, *49*, 4808.
- (44) Zhang, F.-L.; Hong, K.; Li, T.-J.; Park, H.; Yu, J.-Q. Functionalization of C(sp^3)-H bonds using a transient directing group. *Science* **2016**, *351*, 252.
- (45) Zhang, F.; Spring, D. R. Arene C-H functionalisation using a removable/modifiable or a traceless directing group strategy. *Chem. Soc. Rev.* **2014**, *43*, 6906.
- (46) Fernández-Ibáñez, M. Á. Ligands Control Reactivity and Selectivity in Palladium-Catalyzed Functionalization of Unactivated C(sp^3 -H) Bonds. *ChemCatChem* **2014**, *6*, 2188.

- (47) Shul'pin, G. B. C–H functionalization: thoroughly tuning ligands at a metal ion, a chemist can greatly enhance catalyst's activity and selectivity. *Dalton Transactions* **2013**, 42, 12794.
- (48) Musina, E. I.; Balueva, A. S.; Karasik, A. A. In *Organophosphorus Chemistry: Volume 48*; The Royal Society of Chemistry, 2019; Vol. 48.
- (49) Tran, V. T.; Nimmagadda, S. K.; Liu, M.; Engle, K. M. Recent applications of chiral phosphoric acids in palladium catalysis. *Org. Biomol. Chem.* **2020**, 18, 618.
- (50) Yang, L.; Melot, R.; Neuburger, M.; Baudoin, O. Palladium(0)-catalyzed asymmetric C(*sp*³)–H arylation using a chiral binol-derived phosphate and an achiral ligand. *Chem. Sci.* **2017**, 8, 1344.
- (51) Keary, M. E. The mechanism of palladium(II)-mediated C–H cleavage with mono-*N*-protected amino acid (MPAA) ligands: origins of rate acceleration. *Pure Appl. Chem.* **2016**, 88, 119.
- (52) Shi, B.-F.; Maugel, N.; Zhang, Y.-H.; Yu, J.-Q. Pd^{II}-Catalyzed Enantioselective Activation of C(*sp*²)-H and C(*sp*³)-H Bonds Using Monoprotected Amino Acids as Chiral Ligands. *Angew. Chem. Int. Ed.* **2008**, 47, 4882.
- (53) Musaev, D. G.; Figg, T. M.; Kaledin, A. L. Versatile reactivity of Pd-catalysts: mechanistic features of the mono-*N*-protected amino acid ligand and cesium-halide base in Pd-catalyzed C–H bond functionalization. *Chem. Soc. Rev.* **2014**, 43, 5009.
- (54) Gair, J. J.; Haines, B. E.; Filatov, A. S.; Musaev, D. G.; Lewis, J. C. Di-Palladium Complexes are Active Catalysts for Mono-*N*-Protected Amino Acid-Accelerated Enantioselective C–H Functionalization. *ACS Catal.* **2019**, 9, 11386.
- (55) Wencel-Delord, J.; Colobert, F. A remarkable solvent effect of fluorinated alcohols on transition metal catalysed C–H functionalizations. *Org. Chem. Front.* **2016**, 3, 394.
- (56) Sinha, S. K.; Bhattacharya, T.; Maiti, D. Role of hexafluoroisopropanol in C–H activation. *React. Chem. Eng.* **2019**, 4, 244.
- (57) Yu, C.; Sanjosé-Orduna, J.; Patureau, F. W.; Pérez-Temprano, M. H. Emerging unconventional organic solvents for C–H bond and related functionalization reactions. *Chem. Soc. Rev.* **2020**, 49, 1643.
- (58) Dherbassy, Q.; Schwertz, G.; Chessé, M.; Hazra, C. K.; Wencel-Delord, J.; Colobert, F. 1,1,1,3,3,3-Hexafluoroisopropanol as a Remarkable Medium for Atroposelective Sulfoxide-Directed Fujiwara–Moritani Reaction with Acrylates and Styrenes. *Chem. Eur. J.* **2016**, 22, 1735.
- (59) Mirica, L. M.; Khusnutdinova, J. R. Structure and electronic properties of Pd(III) complexes. *Coord. Chem. Rev.* **2013**, 257, 299.
- (60) Chen, W.; Shimada, S.; Tanaka, M. Synthesis and Structure of Formally Hexavalent Palladium Complexes. *Science* **2002**, 295, 308.
- (61) Albicker, M. R.; Cramer, N. Enantioselective Palladium-Catalyzed Direct Arylations at Ambient Temperature: Access to Indanes with Quaternary Stereocenters. *Angew. Chem. Int. Ed.* **2009**, 48, 9139.
- (62) Li, H.; Li, B.-J.; Shi, Z.-J. Challenge and progress: palladium-catalyzed *sp*³ C–H activation. *Catal. Sci. Technol.* **2011**, 1, 191.
- (63) Pi, C.; Li, Y.; Cui, X.; Zhang, H.; Han, Y.; Wu, Y. Redox of ferrocene controlled asymmetric dehydrogenative Heck reaction via palladium-catalyzed dual C–H bond activation. *Chem. Sci.* **2013**, 4, 2675.
- (64) Hull, K. L.; Lanni, E. L.; Sanford, M. S. Highly Regioselective Catalytic Oxidative Coupling Reactions: Synthetic and Mechanistic Investigations. *J. Am. Chem. Soc.* **2006**, 128, 14047.
- (65) Cheng, X.-F.; Li, Y.; Su, Y.-M.; Yin, F.; Wang, J.-Y.; Sheng, J.; Vora, H. U.; Wang, X.-S.; Yu, J.-Q. Pd(II)-Catalyzed Enantioselective C–H Activation/C–O Bond Formation: Synthesis of Chiral Benzofuranones. *J. Am. Chem. Soc.* **2013**, 135, 1236.
- (66) Vo, C.-V. T.; Bode, J. W. Synthesis of Saturated N-Heterocycles. *J. Org. Chem.* **2014**, 79, 2809.
- (67) Yamaguchi, J.; Yamaguchi, A. D.; Itami, K. C-H Bond Functionalization: Emerging Synthetic Tools for Natural Products and Pharmaceuticals. *Angew. Chem. Int. Ed.* **2012**, 51, 8960.
- (68) Spangler, J. E.; Kobayashi, Y.; Verma, P.; Wang, D.-H.; Yu, J.-Q. α -Arylation of Saturated Azacycles and *N*-Methylamines via Palladium(II)-Catalyzed C(*sp*³)–H Coupling. *J. Am. Chem. Soc.* **2015**, 137, 11876.

- (69) Campos, K. R.; Klapars, A.; Waldman, J. H.; Dormer, P. G.; Chen, C.-y. Enantioselective, Palladium-Catalyzed α -Arylation of *N*-Boc-pyrrolidine. *J. Am. Chem. Soc.* **2006**, *128*, 3538.
- (70) Van Steijvoort, B. F.; Kaval, N.; Kulago, A. A.; Maes, B. U. W. Remote Functionalization: Palladium-Catalyzed C5(sp³)-H Arylation of 1-Boc-3-aminopiperidine through the Use of a Bidentate Directing Group. *ACS Catal.* **2016**, *6*, 4486.
- (71) Antermite, D.; Affron, D. P.; Bull, J. A. Regio- and Stereoselective Palladium-Catalyzed C(sp³)-H Arylation of Pyrrolidines and Piperidines with C(3) Directing Groups. *Org. Lett.* **2018**, *20*, 3948.
- (72) Topczewski, J. J.; Cabrera, P. J.; Saper, N. I.; Sanford, M. S. Palladium-catalysed transannular C-H functionalization of alicyclic amines. *Nature* **2016**, *531*, 220.
- (73) Angerer, K. Frog tales – on poison dart frogs, epibatidine, and the sharing of biodiversity. *Innovation: The European Journal of Social Science Research* **2011**, *24*, 353.
- (74) Oliveira Filho, R. E. d.; Omori, A. T. Recent Syntheses of Frog Alkaloid Epibatidine. *J. Braz. Chem. Soc.* **2015**, *26*, 837.
- (75) Cabrera, P. J.; Lee, M.; Sanford, M. S. Second-Generation Palladium Catalyst System for Transannular C-H Functionalization of Azabicycloalkanes. *J. Am. Chem. Soc.* **2018**, *140*, 5599.
- (76) Saint-Denis, T. G.; Zhu, R.-Y.; Chen, G.; Wu, Q.-F.; Yu, J.-Q. Enantioselective C(sp³)-H bond activation by chiral transition metal catalysts. *Science* **2018**, *359*, eaao4798.
- (77) Nakanishi, M.; Katayev, D.; Besnard, C.; Kündig, E. P. Fused Indolines by Palladium-Catalyzed Asymmetric C-C Coupling Involving an Unactivated Methylene Group. *Angew. Chem. Int. Ed.* **2011**, *50*, 7438.
- (78) Anas, S.; Cordi, A.; Kagan, H. B. Enantioselective synthesis of 2-methyl indolines by palladium catalysed asymmetric C(sp³)-H activation/cyclisation. *Chem. Commun.* **2011**, *47*, 11483.
- (79) Saget, T.; Lemouzy, S. J.; Cramer, N. Chiral Monodentate Phosphines and Bulky Carboxylic Acids: Cooperative Effects in Palladium-Catalyzed Enantioselective C(sp³)-H Functionalization. *Angew. Chem. Int. Ed.* **2012**, *51*, 2238.
- (80) Donets, P. A.; Saget, T.; Cramer, N. Chiral Monodentate Trialkylphosphines Based on the Phospholane Architecture. *Organometallics* **2012**, *31*, 8040.
- (81) García-Cuadrado, D.; Braga, A. A. C.; Maseras, F.; Echavarren, A. M. Proton Abstraction Mechanism for the Palladium-Catalyzed Intramolecular Arylation. *J. Am. Chem. Soc.* **2006**, *128*, 1066.
- (82) Nakanishi, M.; Katayev, D.; Besnard, C.; Kündig, E. P. Fused Indolines by Palladium-Catalyzed Asymmetric C-C Coupling Involving an Unactivated Methylene Group. *Angew. Chem. Int. Ed.* **2011**, *50*, 7438.
- (83) Larionov, E.; Nakanishi, M.; Katayev, D.; Besnard, C.; Kündig, E. P. Scope and mechanism of asymmetric C(sp³)-H/C(Ar)-X coupling reactions: computational and experimental study. *Chem. Sci.* **2013**, *4*, 1995.
- (84) Katayev, D.; Larionov, E.; Nakanishi, M.; Besnard, C.; Kündig, E. P. Palladium-*N*-Heterocyclic Carbene (NHC)-Catalyzed Asymmetric Synthesis of Indolines through Regiodivergent C(sp³)-H Activation: Scope and DFT Study. *Chem. Eur. J.* **2014**, *20*, 14909.
- (85) Ackermann, L. Air- and Moisture-Stable Secondary Phosphine Oxides as Preligands in Catalysis. *Synthesis* **2006**, 1557.
- (86) Ackermann, L. Air- and Moisture-Stable Secondary Phosphine Oxides as Preligands in Catalysis. *Synthesis* **2006**, *2006*, 1557.
- (87) Ackermann, L.; Vicente, R.; Hofmann, N. Air-Stable Secondary Phosphine Oxide as Preligand for Palladium-Catalyzed Intramolecular α -Arylations with Chloroarenes. *Org. Lett.* **2009**, *11*, 4274.
- (88) Ackermann, L.; Barfüsser, S.; Kornhaass, C.; Kapdi, A. R. C-H Bond Arylations and Benzylations on Oxazol(in)es with a Palladium Catalyst of a Secondary Phosphine Oxide. *Org. Lett.* **2011**, *13*, 3082.
- (89) Ackermann, L. Phosphine Oxides as Preligands in Ruthenium-Catalyzed Arylations via C-H Bond Functionalization Using Aryl Chlorides. *Org. Lett.* **2005**, *7*, 3123.
- (90) Dupont, J.; Consorti, C. S.; Spencer, J. The Potential of Palladacycles: More Than Just Precatalysts. *Chem. Rev.* **2005**, *105*, 2527.

- (91) Adrio, L.; Hii, K. Application of phosphine ligands in organic synthesis. *Organometallic Chemistry* **2009**, *35*, 62.
- (92) Ackermann, L.; Born, R. Modular Diamino- and Dioxophosphine Oxides and Chlorides as Ligands for Transition-Metal-Catalyzed C-C and C-N Couplings with Aryl Chlorides. *Angew. Chem. Int. Ed.* **2005**, *44*, 2444.
- (93) Smoll, K. A.; Kaminsky, W.; Goldberg, K. I. Photolysis of Pincer-Ligated PdII–Me Complexes in the Presence of Molecular Oxygen. *Organometallics* **2017**, *36*, 1213.
- (94) Donets, P. A.; Cramer, N. Diaminophosphine Oxide Ligand Enabled Asymmetric Nickel-Catalyzed Hydrocarbonylations of Alkenes. *J. Am. Chem. Soc.* **2013**, *135*, 11772.
- (95) Trowbridge, A.; Walton, S. M.; Gaunt, M. J. New Strategies for the Transition-Metal Catalyzed Synthesis of Aliphatic Amines. *Chem. Rev.* **2020**, *120*, 2613.
- (96) Capapé, A.; Crespo, M.; Granell, J.; Vizcarro, A.; Zafrilla, J.; Font-Bardía, M.; Solans, X. Unprecedented intermolecular C–H bond activation of a solvent toluene molecule leading to a seven-membered platinacycle. *Chem. Commun.* **2006**, 4128.
- (97) Nicasio-Collazo, J.; Álvarez, E.; Alvarado-Monzón, J. C.; Andreu-de-Riquer, G.; Jimenez-Halla, J. O. C.; De León-Rodríguez, L. M.; Merino, G.; Morales, U.; Serrano, O.; López, J. A. New seven membered palladacycles: C–Br bond activation of 2-bromo-pyridine derivative by Pd(II). *Dalton Trans.* **2011**, *40*, 12450.
- (98) Otani, Y.; Nagae, O.; Naruse, Y.; Inagaki, S.; Ohno, M.; Yamaguchi, K.; Yamamoto, G.; Uchiyama, M.; Ohwada, T. An Evaluation of Amide Group Planarity in 7-Azabicyclo[2.2.1]heptane Amides. Low Amide Bond Rotation Barrier in Solution. *J. Am. Chem. Soc.* **2003**, *125*, 15191.
- (99) Perry, I. B.; Brewer, T. F.; Sarver, P. J.; Schultz, D. M.; DiRocco, D. A.; MacMillan, D. W. C. Direct arylation of strong aliphatic C–H bonds. *Nature* **2018**, *560*, 70.
- (100) Gensch, T.; Hopkinson, M. N.; Glorius, F.; Wencel-Delord, J. Mild metal-catalyzed C–H activation: examples and concepts. *Chem. Soc. Rev.* **2016**, *45*, 2900.
- (101) Zhu, R.-Y.; Farmer, M. E.; Chen, Y.-Q.; Yu, J.-Q. A Simple and Versatile Amide Directing Group for C–H Functionalizations. *Angew. Chem. Int. Ed.* **2016**, *55*, 10578.
- (102) Shabashov, D.; Daugulis, O. Auxiliary-Assisted Palladium-Catalyzed Arylation and Alkylation of sp^2 and sp^3 Carbon–Hydrogen Bonds. *J. Am. Chem. Soc.* **2010**, *132*, 3965.
- (103) Corbet, M.; De Campo, F. 8-Aminoquinoline: A Powerful Directing Group in Metal-Catalyzed Direct Functionalization of C–H Bonds. *Angew. Chem. Int. Ed.* **2013**, *52*, 9896.
- (104) Wasa, M.; Chan, K. S. L.; Zhang, X.-G.; He, J.; Miura, M.; Yu, J.-Q. Ligand-Enabled Methylene C(sp^3)–H Bond Activation with a Pd^(II) Catalyst. *J. Am. Chem. Soc.* **2012**, *134*, 18570.
- (105) Xu, J.-W.; Zhang, Z.-Z.; Rao, W.-H.; Shi, B.-F. Site-Selective Alkenylation of δ -C(sp^3)–H Bonds with Alkynes via a Six-Membered Palladacycle. *J. Am. Chem. Soc.* **2016**, *138*, 10750.
- (106) Yanagimoto, T.; Toyota, T.; Matsuki, N.; Makino, Y.; Uchiyama, S.; Ohwada, T. Transnitrosation of Thiols from Aliphatic *N*-Nitrosamines: *S*-Nitrosation and Indirect Generation of Nitric Oxide. *J. Am. Chem. Soc.* **2007**, *129*, 736.
- (107) Tang, K.-X.; Wang, C.-M.; Gao, T.-H.; Chen, L.; Fan, L.; Sun, L.-P. Transition Metal-Catalyzed C–H Bond Functionalizations by Use of Sulfur-Containing Directing Groups. *Adv. Synth. Catal.* **2019**, *361*, 26.
- (108) Greßies, S.; Klauck, F. J. R.; Kim, J. H.; Daniliuc, C. G.; Glorius, F. Ligand-Enabled Enantioselective C–H Activation of Tetrahydroquinolines and Saturated Aza-Heterocycles by RhI. *Angew. Chem. Int. Ed.* **2018**, *57*, 9950.
- (109) Wang, H.-L.; Hu, R.-B.; Zhang, H.; Zhou, A.-X.; Yang, S.-D. Pd^(II)-Catalyzed Ph₂(O)P-Directed C–H Olefination toward Phosphine–Alkene Ligands. *Org. Lett.* **2013**, *15*, 5302.
- (110) Zhang, H.-Y.; Yi, H.-M.; Wang, G.-W.; Yang, B.; Yang, S.-D. Pd^(II)-Catalyzed C(sp^2)–H Hydroxylation with R₂(O)P-Coordinating Group. *Org. Lett.* **2013**, *15*, 6186.
- (111) Hu, R.-B.; Zhang, H.; Zhang, X.-Y.; Yang, S.-D. Palladium-catalyzed P(O)R₂ directed C–H arylation to synthesize electron-rich polyaromatic monophosphorus ligands. *Chem. Commun.* **2014**, *50*, 2193.

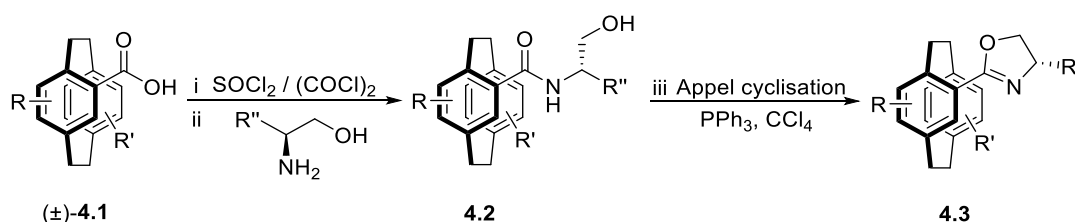
- (112) He, G.; Chen, G. A Practical Strategy for the Structural Diversification of Aliphatic Scaffolds through the Palladium-Catalyzed Picolinamide-Directed Remote Functionalization of Unactivated C(sp³)-H Bonds. *Angew. Chem. Int. Ed.* **2011**, *50*, 5192.
- (113) Seki, A.; Takahashi, Y.; Miyake, T. Synthesis of cis-3-arylated cycloalkylamines through palladium-catalyzed methylene sp³ carbon–hydrogen bond activation. *Tetrahedron Lett.* **2014**, *55*, 2838.
- (114) Coomber, C. E.; Benhamou, L.; Bučar, D.-K.; Smith, P. D.; Porter, M. J.; Sheppard, T. D. Silver-Free Palladium-Catalyzed C(sp³)-H Arylation of Saturated Bicyclic Amine Scaffolds. *J. Org. Chem.* **2018**, *83*, 2495.
- (115) Singha, M.; Roy, S.; Pandey, S. D.; Bag, S. S.; Bhattacharya, P.; Das, M.; Ghosh, A. S.; Ray, D.; Basak, A. Use of azidonaphthalimide carboxylic acids as fluorescent templates with a built-in photoreactive group and a flexible linker simplifies protein labeling studies: applications in selective tagging of HCAII and penicillin binding proteins. *Chem. Commun.* **2017**, *53*, 13015.
- (116) Pesciaioli, F.; Dhawa, U.; Oliveira, J. C. A.; Yin, R.; John, M.; Ackermann, L. Enantioselective Cobalt(III)-Catalyzed C–H Activation Enabled by Chiral Carboxylic Acid Cooperation. *Angew. Chem. Int. Ed.* **2018**, *57*, 15425.
- (117) Truesdale, E. A.; Cram, D. J. Macro rings. 49. Use of transannular reactions to add bridges to [2.2]paracyclophane. *J. Org. Chem.* **1980**, *45*, 3974.
- (118) Meyer-Eppler, G.; Sure, R.; Schneider, A.; Schnakenburg, G.; Grimme, S.; Lützen, A. Synthesis, Chiral Resolution, and Absolute Configuration of Dissymmetric 4,15-Difunctionalized [2.2]Paracyclophanes. *J. Org. Chem.* **2014**, *79*, 6679.
- (119) Roche, A. J.; Canturk, B. An exploration of Suzuki aryl cross coupling chemistry involving [2.2]paracyclophane derivatives. *Org. Biomol. Chem.* **2005**, *3*, 515.
- (120) Brunel, J. M. BINOL: A Versatile Chiral Reagent. *Chem. Rev.* **2005**, *105*, 857.
- (121) Wang, H.; Tong, H.-R.; He, G.; Chen, G. An Enantioselective Bidentate Auxiliary Directed Palladium-Catalyzed Benzylic C–H Arylation of Amines Using a BINOL Phosphate Ligand. *Angew. Chem. Int. Ed.* **2016**, *55*, 15387.
- (122) Gibson, S. E.; Knight, J. D. [2.2]Paracyclophane derivatives in asymmetric catalysis. *Org. Biomol. Chem.* **2003**, *1*, 1256.
- (123) Rozenberg, V.; Dubrovina, N.; Sergeeva, E.; Antonov, D.; Belokon, Y. An improved synthesis of (S)-(+)- and (R)-(-)-[2.2]paracyclophane-4-carboxylic acid. *Tetrahedron: Asymmetry* **1998**, *9*, 653.

Chapter 4

A Facile Single-Step Protocol for the Synthesis of Planar Chiral Oxazolines

4.0. Coupling between [2.2]paracyclophane halides and chiral oxazolines

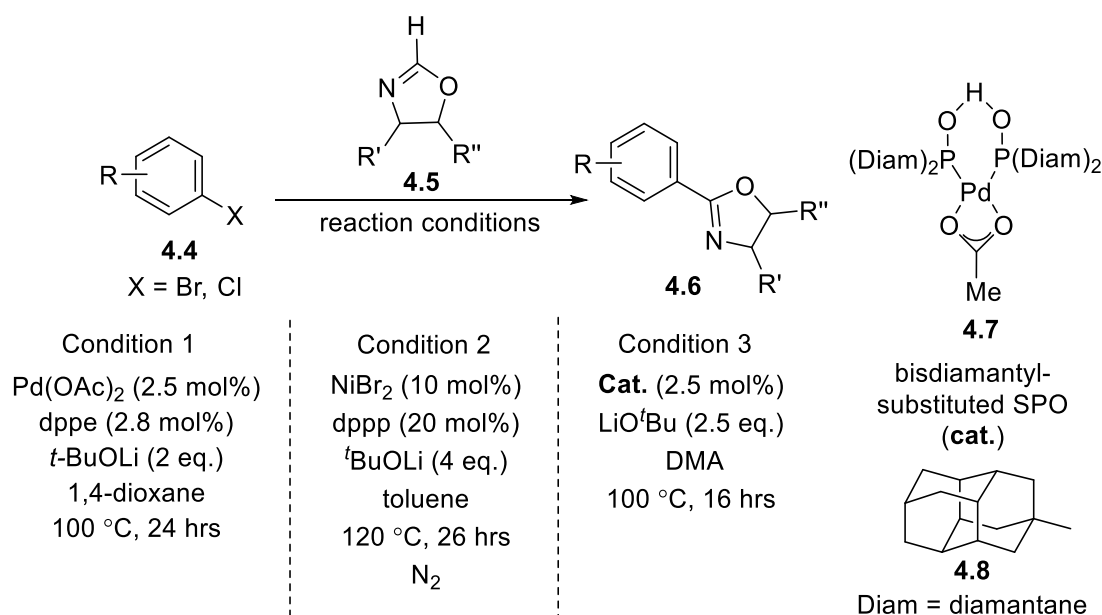
Similar to the success of BOX ligands in asymmetric catalysis,¹⁻⁵ [2.2]paracyclophane-bis-oxazolines could be explored as chiral ligands in various stereoselective transformations. In the literature, [2.2]paracyclophane-oxazoline derivatives are synthesised from the corresponding carboxylic acid derivatives by a traditional route involving three steps (Scheme 4.1).⁶⁻¹⁶ In the first step, carboxylic acid **4.1** is converted into an acyl chloride which subsequently reacts with an amino alcohol to form amide derivative **4.2**. Finally, Appel cyclisation¹⁷ of the amide derivative gives oxazoline derivative **4.3**.



Scheme 4.1: Traditional route to synthesis [2.2]paracyclophane-oxazoline derivatives.

It is worth mentioning that the synthesis of the [2.2]paracyclophane-carboxylic acid derivatives is not always straight forward. The synthesis of the monosubstituted carboxylic acid requires a minimum of two steps from [2.2]paracyclophane. To access disubstituted carboxylic acid derivatives is lengthier. Due to these challenges associated with the synthesis of [2.2]paracyclophane-oxazoline derivatives, there is always a need for practical methodology that can access these valuable compounds.

Recently, Lu et al.^{18,19} and Ackermann et al.²⁰ independently reported the direct C-H (hetero)arylation of oxazolines **4.5** at the 2-position (Scheme 4.2). The former group employed bidentate diphosphine ligands (dppe or dppp) while the latter group used a bulky SPO-based catalyst **4.7**. These protocols are good alternatives to the traditional methods for the synthesis of chiral oxazoline ligands.^{1,2}

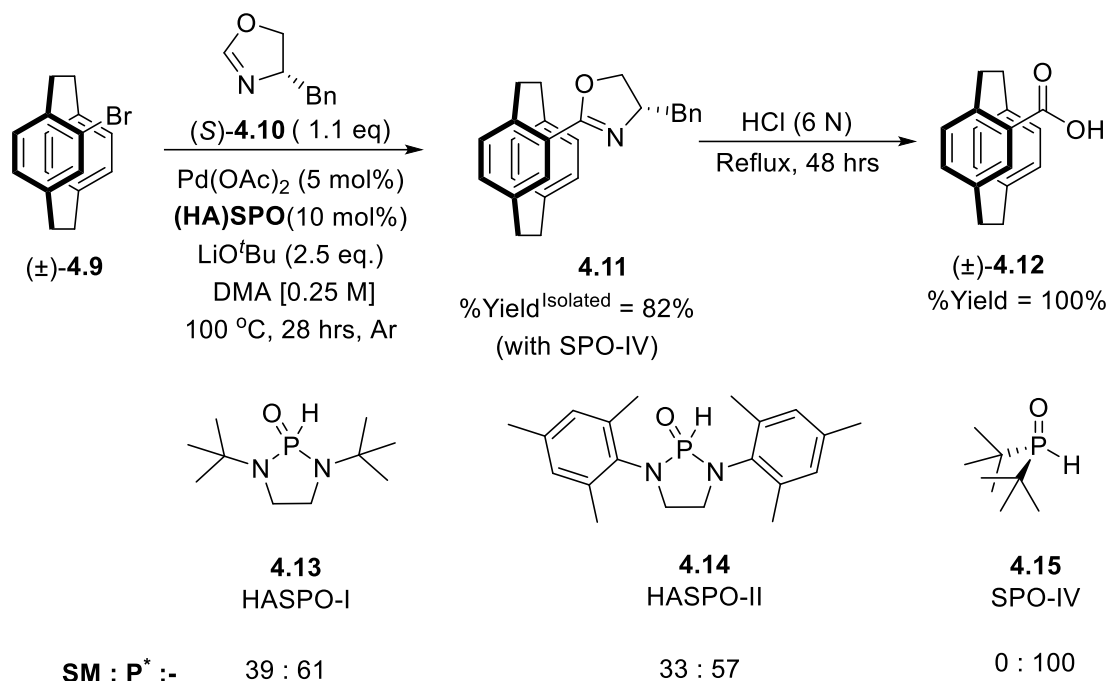


Scheme 4.2: Reported conditions for the C-H (hetero)arylation of oxazolines.

4.1. Scope of bromo[2.2]paracyclophane for oxazoline coupling

The chemistry above served as inspiration for a new synthesis of planar chiral oxazolines. We screened different SPO and HASPO ligands (Scheme 4.3). After a brief optimisation study, we found that a combination of $\text{Pd}(\text{OAc})_2$ and di-*tert*-butyl SPO **4.15** coupled (4*S*)-4-benzyl-oxazoline **4.10** to (±)-4-bromo[2.2]paracyclophane **4.9** in 82% yield. We were unable to separate the diastereomers but it has subsequently become clear that they are separable.^f Further hydrolysis of the coupled product **4.11** proceeded smoothly in an acidic medium to give (±)-[2.2]paracyclophane-4-carboxylic acid **4.12** in 100% yield. While we did not resolve the enantiomers here, it is clear that it can be achieved.

^f A colleague of mine was able to separate two diastereomers of **4.11** by column chromatography.



Scheme 4.3: Synthesis of 4-(4-benzyl-oxazoline-2-yl)[2.2]paracyclophane **4.11** and its hydrolysis.

* SM : P was determined based on the crude ^1H NMR spectroscopy

A plausible mechanism for the coupling is based on the Pd(0) /Pd(II) pathway and is shown in Figure 4.1. The catalytic cycle is initiated by the oxidative addition of the ligated Pd(0) to the [2.2]paracyclophane-halide. The oxazoline **4.5** is deprotonated by the LiO^tBu to generate the lithium oxazoline intermediate, which subsequently undergoes transmetalation with the organopalladium intermediate **I** to give the palladium-oxazoline intermediate **II**. Finally, reductive elimination produces coupled product **4.17**, and simultaneously reducing the Pd(II) back to Pd(0).

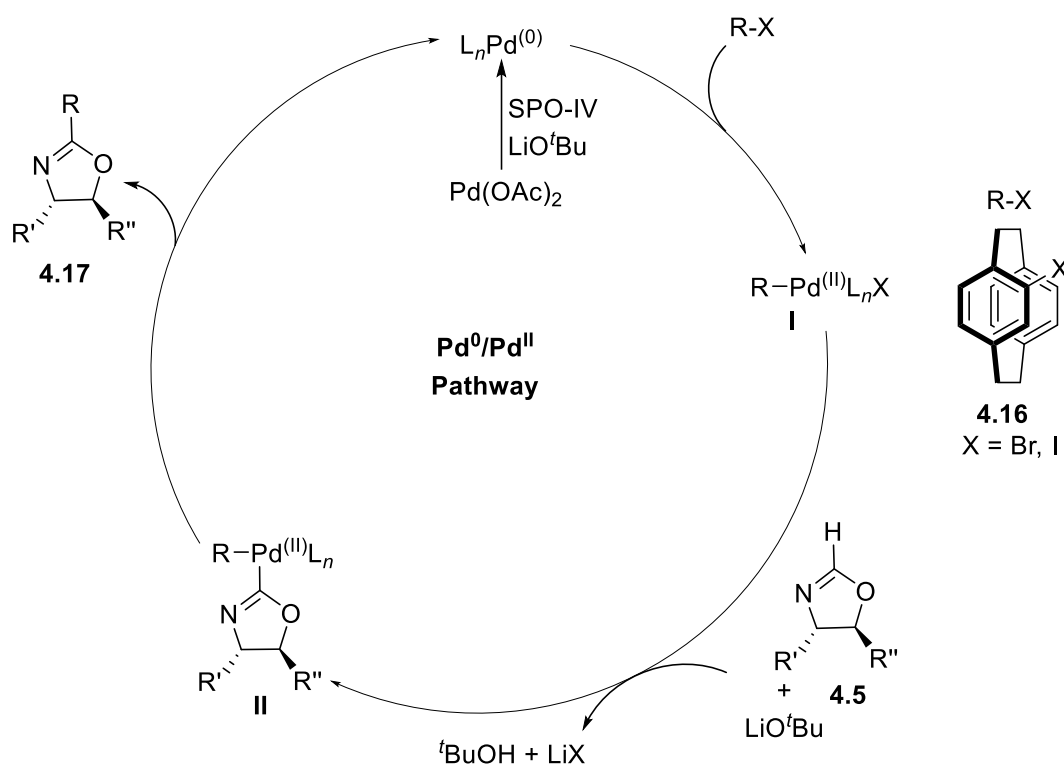


Figure 4.1: Proposed mechanism for [2.2]paracyclophane halide and oxazoline coupling.

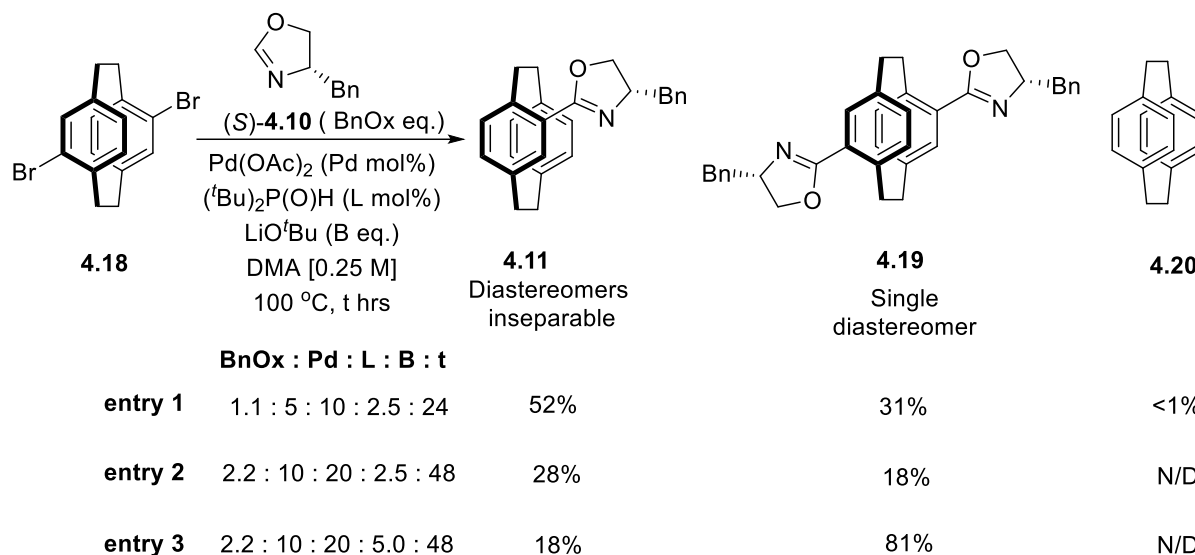
Having optimised the coupling, we decided to delineate the scope of the reaction using various bromo[2.2]paracyclophanes. It would be further exciting to resolve the enantiomers of [2.2]paracyclophane moieties by isolating diastereomers in a pure form. If we succeed, hydrolysis of the pure diastereomers will be carried out to derive an array of planar chiral [2.2]paracyclophane-carboxylic acid derivatives.

4.2. Scope of dibromo[2.2]paracyclophane derivatives for oxazoline coupling

First, we investigated whether the addition of two oxazolines was possible, then whether it was possible to stop the reaction halfway. The latter reaction would retain a bromide for subsequent functionalisation.

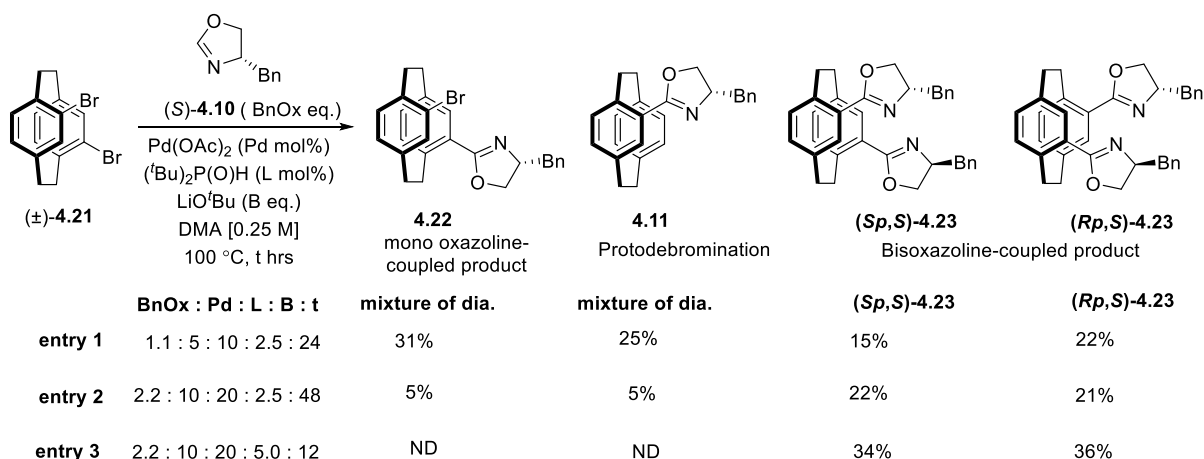
To attempt mono coupling, just one equivalent of (4*S*)-4-benzyl-oxazoline **4.10** was employed with 4,16-dibromo[2.2]paracyclophane (*pseudo-para*) **4.18** under the optimised protocol (Scheme 4.4). Monocoupling was observed but unfortunately also with protodebromination, which resulted in oxazoline **4.11** in 52% yield. A single diastereomer of bis-coupling product **4.19** was also isolated in 31% from the same reaction (entry 1). This result suggests that nothing is stopping the second coupling from occurring. Doubling the catalytic loading, while maintaining the same equivalent of the base was detrimental to the reaction (entry 2). The

reaction conversion dropped by nearly half compared to the previous conditions. It became imperative to double the concentration of base (5 eq.) with other additives to achieve the bis-coupled product **4.19** in maximum yield (81%, entry 3).



Scheme 4.4: Attempted mono- and bis-coupling of 4,16-dibromo[2.2]paracyclophane **4.18** with (4*S*)-4-benzyl-oxazoline **4.10**.

The same strategy was applied to (±)-4,12-dibromo[2.2]paracyclophane (*pseudo-ortho*) substrate **4.21** (Scheme 4.5). Using one equivalent of (4*S*)-4-benzyl-oxazoline **4.10** led to both the mono- and the bis-coupled oxazoline products, **4.22** & **4.23** in 25% and 38% yield, respectively, with **4.11** in 31% (entry 1). It was possible to isolate the bis-oxazolines as single diastereomers by flash chromatography. Again, when performing the double addition, the quantity of base was crucial. Doubling all the reagents except the base (2.5 eq.) had a detrimental effect on the coupling (entry 2). Doubling all the reagents including base (5 eq.) gave bis-oxazolines **4.23** as the exclusive product in 70% yield (entry 3). Moreover, each pure diastereomer of product **4.23** was separated. With that, we achieved the shortest route to access planar chiral [2.2]paracyclophane-based bis-oxazoline ligands in a one-pot reaction.



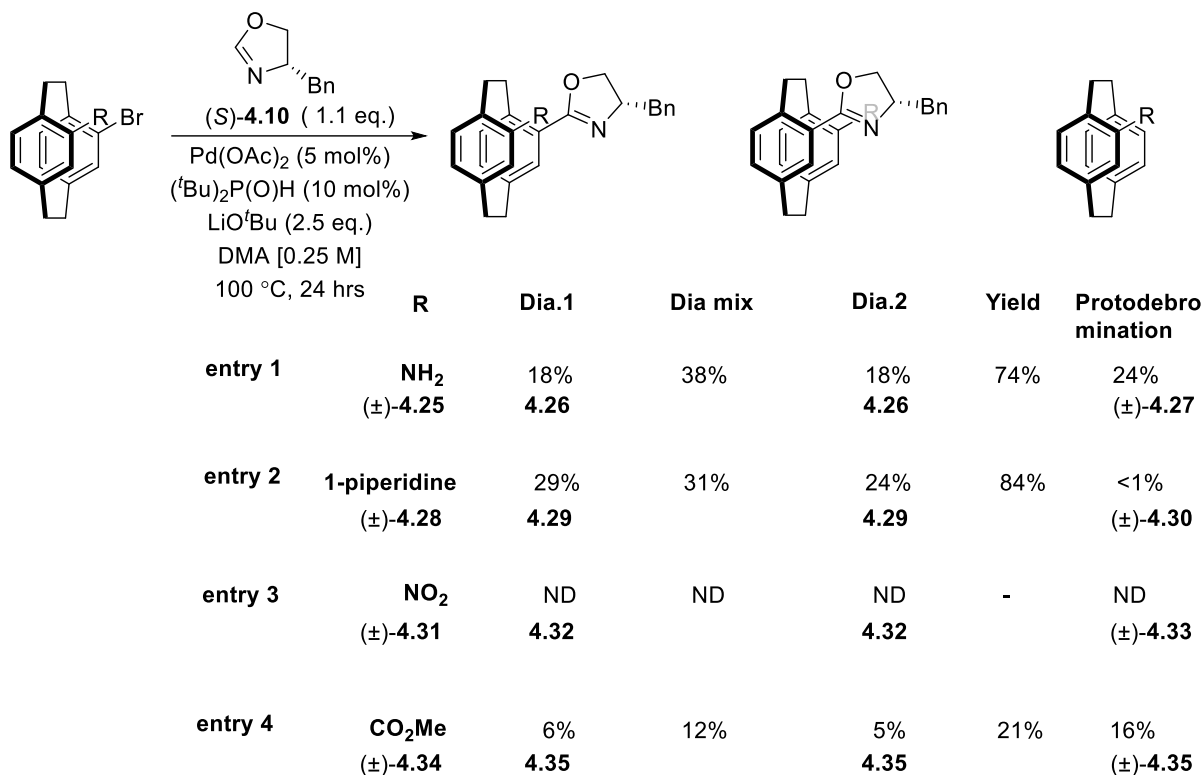
Scheme 4.5: Mono- and bis-coupling of (±)-4,12-dibromo[2.2]paracyclophane **4.21** with (4S)-4-benzyl-oxazoline **4.10**.

Dial: Isolated yield of first diastereomer, Dia 2: Isolated yield of second diastereomer

4.3. Scope of *pseudo-gem*-[2.2]paracyclophane derivatives for oxazoline coupling

The true power of the methodology would be in forming any functionalised oxazoline so we set out to determine the functional group compatibility. We started with the *pseudo-gem* derivatives as we believed they would be the easiest to synthesise but the hardest to react. Surprisingly, the electron-donating groups (NH₂ and 1-piperidine) **4.25** & **4.28** gave good yields (Scheme 4.6, entry 1 & entry 2). Moreover, the separation of diastereomeric products was possible. We were surprised with the results because the same precursor, (±)-4-bromo-13-amino[2.2]paracyclophane **4.25** gave poor yields in the desulfitative reactions (see Section 6.3.1.4).

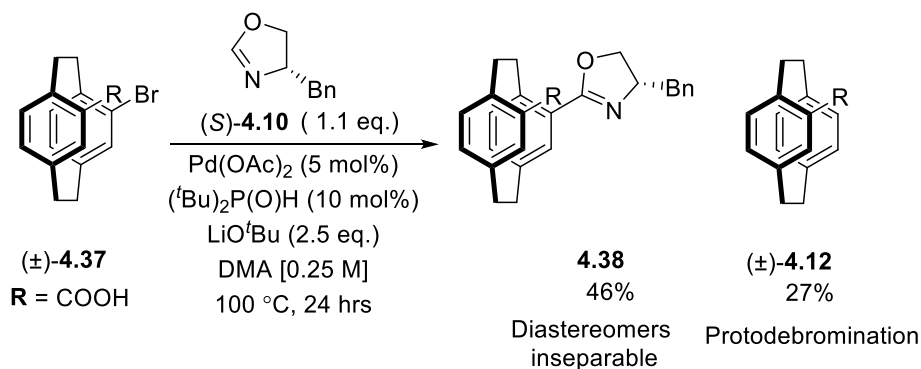
Equally surprising was the lack of success obtained with the electron-deficient nitro and ester derivatives **4.31** & **4.34**. No reaction was obtained with the electron-withdrawing NO₂ group (entry 3). However, the oxazoline coupling was observed in low yield with (±)-4-bromo[2.2]paracyclophane-13-methyl ester **4.34** (entry 4).



Scheme 4.6: Scope of *pseudo-gem*-[2.2]paracyclophane derivatives for oxazoline coupling.

Dia1*: Isolated yield of the first diastereomer, Dia mix: Isolated yield of mixed fraction of first diastereomer and second diastereomer, Dia 2*: Isolated yield of the second diastereomer, Yield: Total isolated yield of the reaction. *The exact configuration of the diastereomer is not determined yet.

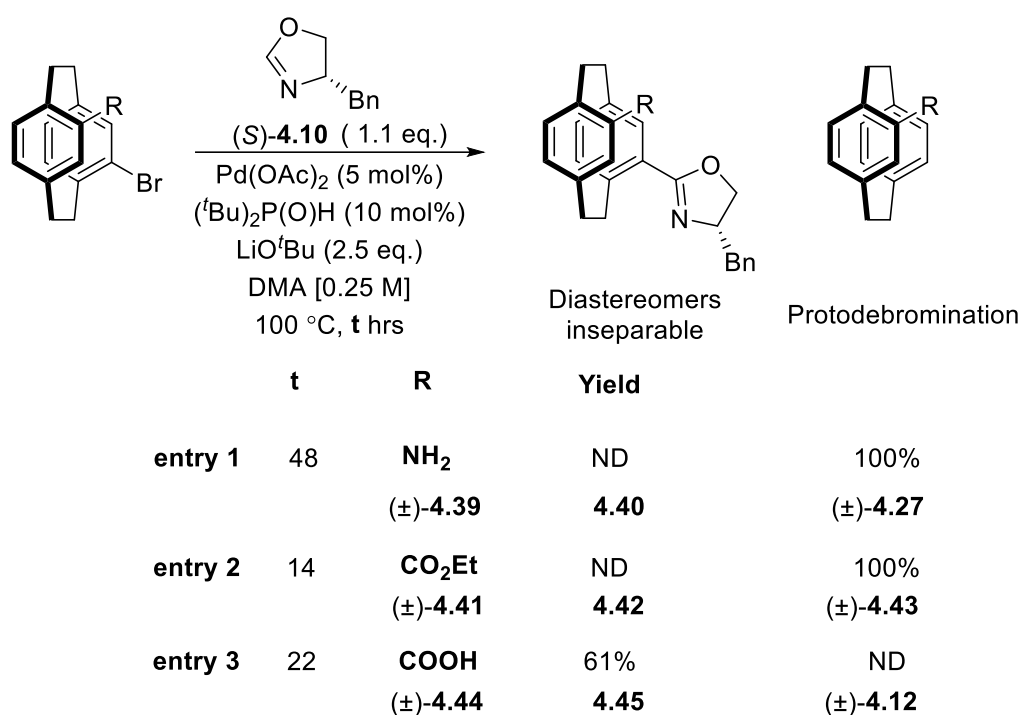
We decided to hydrolyse the ester **4.34** substrate to a carboxylic acid **4.37**. It is also clear that electron-rich systems give better yields, so by making carboxylate, we obtained an electron-rich variant. The reaction was set up with (±)-4-bromo[2.2]paracyclophane-13-carboxylic acid **4.37**. Fortunately, the product formation was nearly doubled. On the down side, the diastereomers of **4.38** were inseparable.



Scheme 4.7: Coupling of (±)-4-bromo[2.2]paracyclophane-13-carboxylic acid **4.37**.

4.4. Scope of *pseudo-ortho*-[2.2]paracyclophane derivatives for oxazoline coupling

Normally, we expect higher yield from *pseudo-ortho* substrates compared to *pseudo-gem* substrates due to a reduction in steric congestion. However, when the oxazoline coupling reaction was performed with (\pm)-4-bromo-13-amino[2.2]paracyclophane **4.39**, we observed the opposite. Only protodebromination coupling was detected (Scheme 4.8, entry 1) The same result was observed with (\pm)-4-bromo[2.2]paracyclophane-13-ethyl ester **4.41** (entry 2). This result suggests that oxidative insertion is occurring but transmetalation is a problematic. When (\pm)-4-bromo[2.2]paracyclophane-13-carboxylic acid **4.41** was employed under the same reaction conditions, the desired coupling was obtained in 61% yield. No protodebromination was observed (entry 3). It is still unclear why the less sterically hindered *pseudo-ortho* pocket isomer is a poor substrate for this reaction. This study suggests that a detailed mechanistic investigation is required to probe the reactivity of these systems.

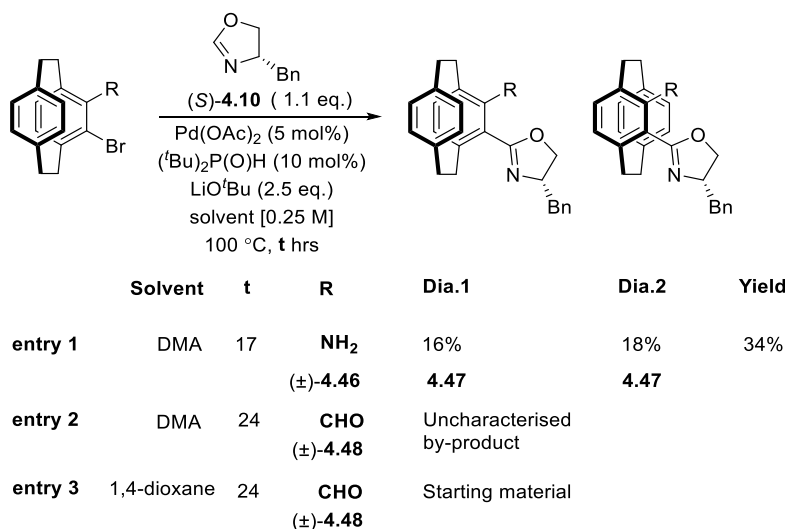


Scheme 4.8: Scope of *pseudo-ortho*-[2.2]paracyclophane derivatives for oxazoline coupling.

4.5. Scope of *ortho*-[2.2]paracyclophane derivatives for oxazoline coupling

Due to steric hindrance, the coupling of *ortho*-substituted bromides is often taxing. The substrate, (\pm)-4-bromo-5-amino[2.2]paracyclophane coupled **4.46** in a moderate yield under the optimised conditions (Scheme 4.9, entry 1). The diastereomers were separable by preparative TLC. The only other *ortho*-substituted derivative we had access to was formyl

derivative **4.48**; however, this failed to react (entry 2). This reaction produced by-products in DMA solvent. By changing the reaction solvent to 1,4-dioxane, only the starting material was recovered (entry 3). These results suggest that further studies are required before this methodology proves its generality.



Scheme 4.9: Scope of *ortho*-[2.2]paracyclophane derivatives for oxazoline coupling.

4.6. Attempts to improve generality of the reaction and resolution of the [2.2]paracyclophane derivatives

The preliminary investigation of the coupling of (4*S*)-4-benzyl-oxazoline **4.10** with various [2.2]paracyclophane derivatives raised several concerns. The coupling was possible and in a number of examples the diastereomers could be separated. But the resolution was challenging and a number of substituents delivered the product of protodebromination. We wondered if a different oxazoline might help the separation of the diastereomers and possibly give more information about the coupling.

Chiral oxazolines can be easily synthesised from chiral 2-amino alcohols and carboxylic acid derivatives such as naturally/specifically designed amino acids and amino alcohols. The oxazoline ring substituents play a major role in tuning the steric property e.g. bulky groups and/or aromatic substituents can exert intra- and intermolecular interactions. Both C-4 and C-5 positions of oxazolines can be modified to regulate the chiral environment.

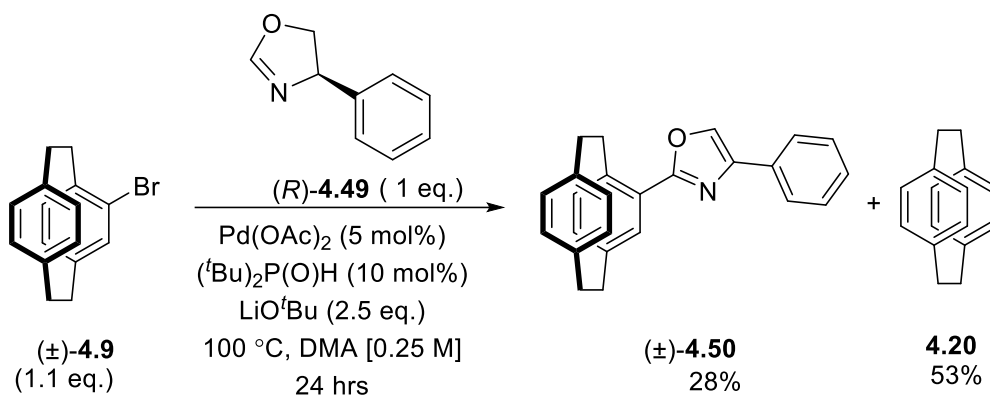
Another problem we encountered was the separation of the resulting diastereomers. Ideally, we wanted to easily separate the diastereomers by column chromatography. By altering the

substituents in the oxazoline ring we hoped to alter the two diastereomers sufficiently that separation would be more facile.

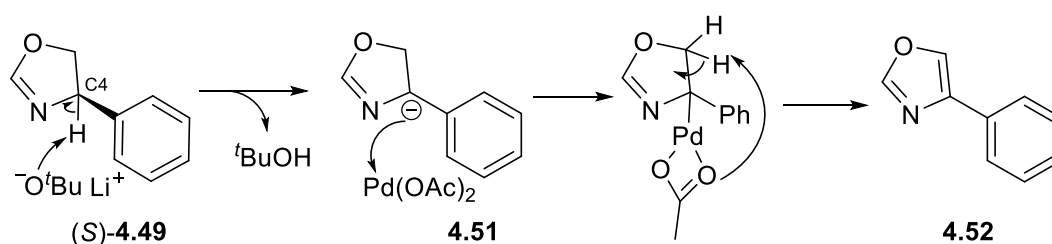
Considering the above factors, we decided to modify the chiral oxazoline substituents at the C4 and C5 positions and evaluate their effects on oxazoline coupling as well as separation of diastereomers.

4.6.1. (4*S*)-4-Phenyl-oxazoline-based coupling partner

Our first attempt brought the aromatic substituent of the oxazoline closer to the [2.2]paracyclophane framework and we investigated (4*R*)-4-phenyl-oxazoline substrate **4.49**. Unexpectedly coupling of (±)-4-bromo[2.2]paracyclophane with **4.49** gave the heteroaromatic compound **4.50** (Scheme 4.10). We speculated that C-4 proton abstraction by a strong base promotes the aromatisation of oxazoline ring to the thermodynamically favourable oxazole (Scheme 4.11). It should be noted that aromatisation only occurred with (4*R*)-4-phenyl-oxazoline substrate **4.49** but not with (4*S*)-4-benzyl-oxazoline **4.10**. We reasoned the conjugated double bonds resulting after proton abstraction leads to a stable heteroaromatic ring. However, it is difficult to predict whether elimination occurred before or after coupling.



Scheme 4.10: Coupling of (±)-4-bromo[2.2]paracyclophane **4.9** with (4*S*)-4-phenyl-oxazoline **4.49**.



Scheme 4.11: Postulated aromatisation of oxazoline ring in presence of strong base.

4.6.2. Modification of C-4 position of oxazoline

Our next oxazoline would increase the steric bulk and add a polar functional group that might interact with silica to facilitate separation. It also avoids the issue of conjugation so should not undergo aromatisation. The synthesis involved addition of Grignard reagent to an ester to form a tertiary amino alcohol, that could rapidly be converted into the family of oxazolines. The ability of the free hydroxy group for hydrogen bonding may induce intermolecular interactions to ease the separation of diastereomers (Figure 4.2).

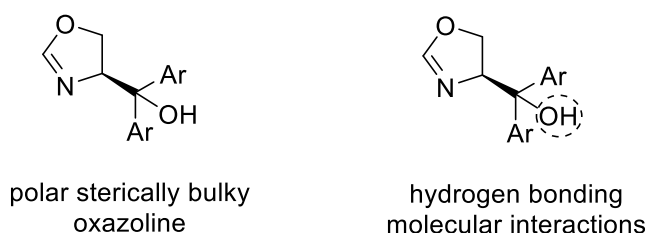
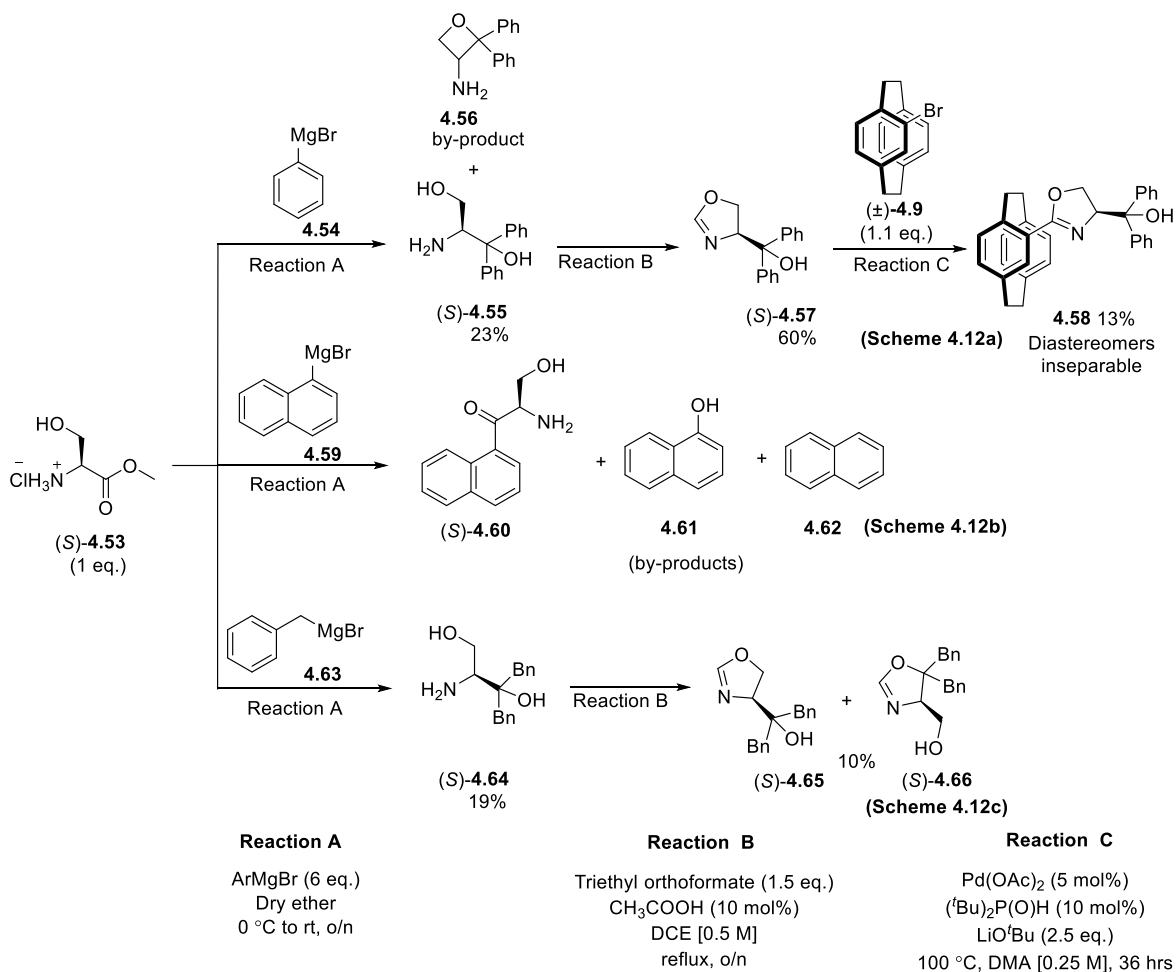


Figure 4.2: Design of polar sterically encumbered oxazoline.

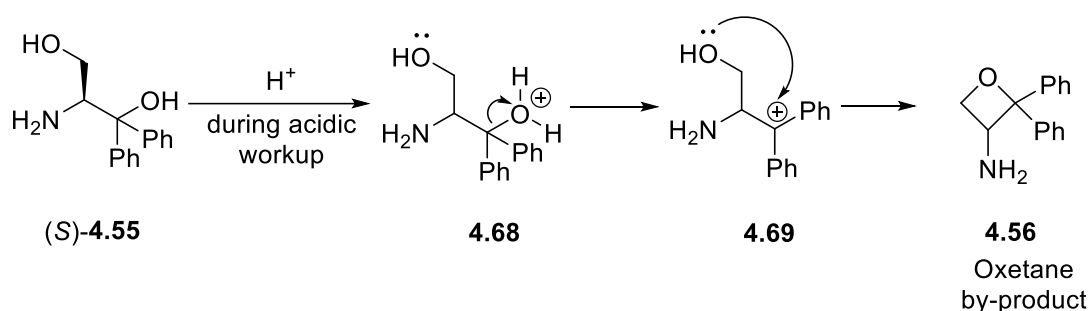
The synthesis of C-4 modified oxazolines and their attempted coupling with (\pm)-4-bromo[2.2]paracyclophane **4.9** is shown in Scheme 4.12.



Scheme 4.12: Coupling of (\pm)-4-bromo[2.2]paracyclophane **4.9** with C-4 modified oxazoline.

As per our plan, the reactions were carried out between L-serine methyl ester hydrochloride **4.53** and Grignard reagents, PhMgBr **4.54**, NaphthMgBr **4.59**, and BnMgBr **4.63** separately to achieve their corresponding diaryl tertiary amino alcohols (Reaction A).

During the synthesis of diphenyl tertiary aminoalcohol **4.55** (Reaction A, Scheme 4.12a), the oxetane-containing by-product **4.56** was detected. We speculated that an S_N1 mechanism accounts for this by-product (Scheme 4.13). Under the strongly acidic workup conditions, the tertiary alcohol **4.55** is protonated. The loss of water from **4.68** creates a tertiary carbocation **4.69**. Next, the attack of primary hydroxyl group to tertiary carbocation forms the oxetane ring.



Scheme 4.13: Proposed S_N1 mechanism for oxetane by-product formation.

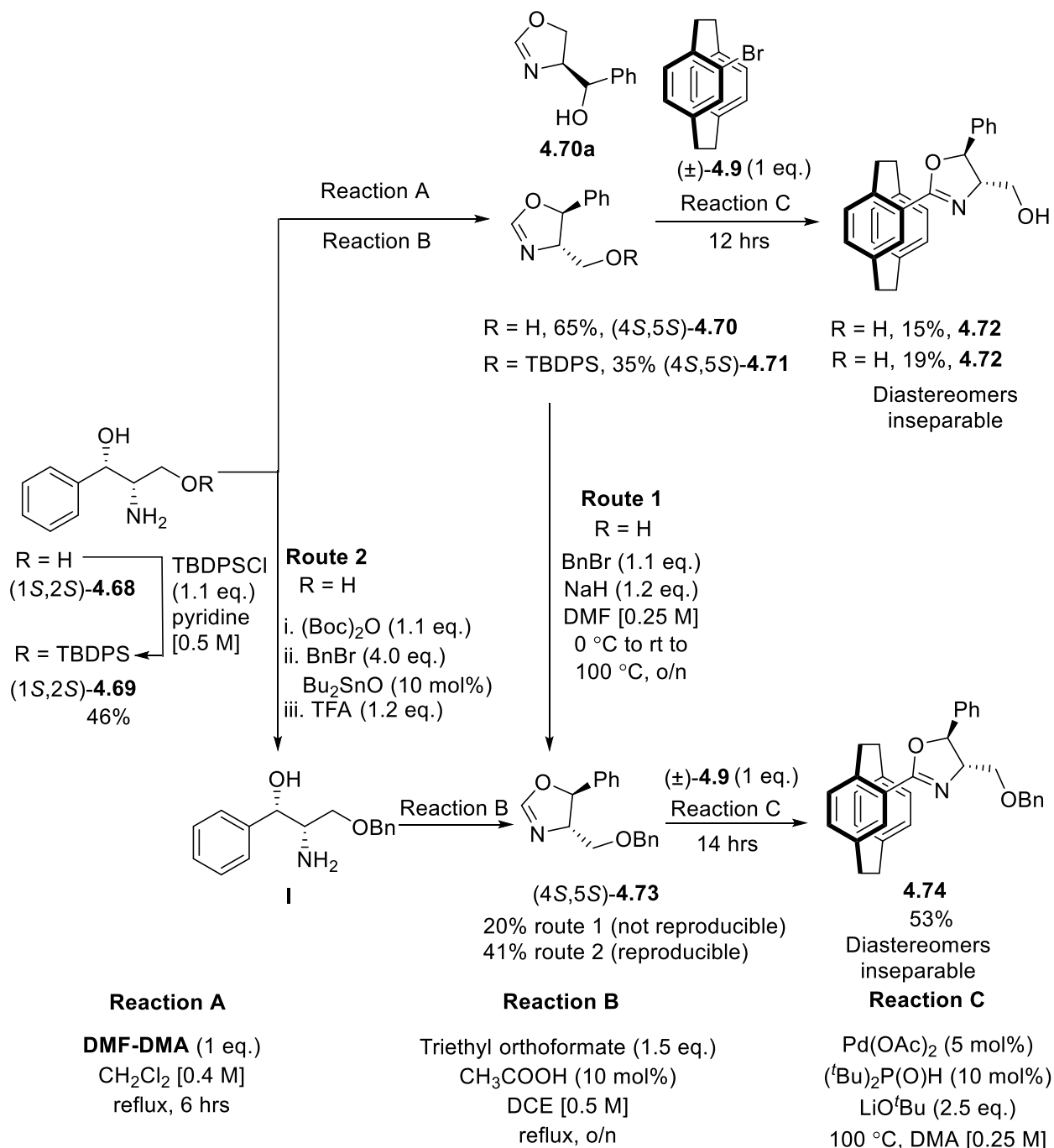
We also decided to introduce bulkier naphthyl groups. However, during the synthesis of dinaphthyl tertiary amino alcohol, only by-products, arising from NaphthMgBr **4.59**, were recovered (Reaction A, Scheme 4.12b). Due to difficulties encountered in the synthesis of dinaphthyl tertiary amino alcohol, we decided to introduce different substituents in the form of the benzyl group. The dibenzyl tertiary aminoalcohol **4.64** was synthesised (Reaction A), which underwent the oxazoline-formation conditions (Reaction B) to furnish two distinct products, (*S*)-4-(*tert*-hydroxyl dibenzyl)oxazoline **4.65** and (*S*)-4-(methan-1-ol)-5,5-dibenzylloxazoline **4.66** (Scheme 4.12c).

Next, we attempted oxazoline coupling. The coupling reaction was set up between (*S*)-4-(*tert*-hydroxyl diphenyl)-oxazoline **4.57** (Scheme 4.12a), and (±)-4-bromo[2.2]paracyclophane **4.9** under optimised conditions (Reaction C). The reaction proceeded in low yield to produce an inseparable diastereomeric mixture **4.58**. Due to the low conversion to the other desired amino alcohols, the next step of coupling was not performed.

Since the results from the modification of C-4 position alone were not encouraging as expected, we then thought to modify both C-4 and C-5 positions on the oxazoline backbone.

4.6.3. Modification of both C-4 and C-5 positions of oxazoline

(1*S*,2*S*)-(+)-2-Amino-1-phenyl-1,3-propanediol **4.68** is a good starting material for the synthesis of 4,5-disubstituted oxazolines (Scheme 4.14). Selective protection of the primary alcohol permits synthesis of the desired compounds.



Scheme 4.14: Coupling of (±)-4-bromo[2.2]paracyclophane **4.9** with C-4 and C-5 modified oxazolines.

(4*S*,5*S*)-4-(Methylalcohol)-5-phenyloxazoline **4.70** was synthesised from **4.68** in 65% yield. (Reaction A). Here, the crude ¹H NMR spectroscopy data revealed **4.70** only product. We speculated that both product **4.70** and **4.70a** had been formed and the kinetic product **4.70a** may rearranged *in situ* to give exclusive **4.70** product. The selective 1° hydroxy group protection of precursor **4.68** was performed with the TBDPS group to increase the steric bulk. However, TBDPS protected substrate **4.69** required different conditions to form the desired oxazoline **4.71** albeit in lower yield (Reaction B). The coupling reaction of oxazoline **4.70** with (±)-4-bromo[2.2]paracyclophane **4.9** produced the desired product **4.72** only in 15% yield while the protodebromination by-product [2.2]paracyclophane was significant (Reaction C). The oxazoline-coupling reaction of TBDPS protected oxazoline **4.71** gave the same product **4.72** in 19% after TBDPS deprotection during the reaction (Reaction C). As satisfactory results were not forthcoming, we considered installing a benzyl group at the primary hydroxyl group (C4 position).

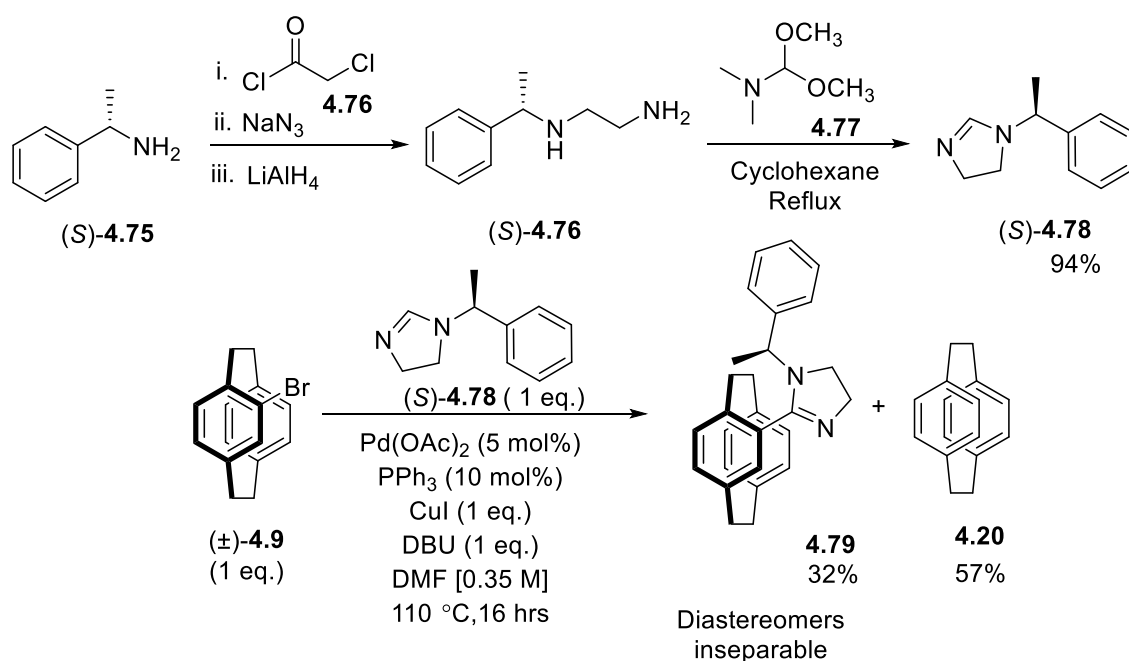
Initially, we attempted the benzylation of oxazoline **4.70** with the typical conditions of NaH and BnBr but the yield was disappointing and could not be reproduced (Route 1). Better results were achieved by the selective protection of Boc carbamate of **4.68** using Bu₂SnO (Route 2).^{21,22} After selective benzylation, the (4*S*,5*S*)-4-((benzyloxy)(methyl))-5-phenyloxazoline **4.73** was synthesised in 41% from **I** (Reaction B). The synthetic route 2 was reproducible. With the desired oxazoline **4.73**, the oxazoline-coupling was carried out with (±)-4-bromo[2.2]paracyclophane **4.9** (Reaction C). The coupling was accomplished in 53% yield. However, the separation of the diastereomers was not possible.

These results show that modified oxazolines can also be coupled with (±)-4-bromo[2.2]paracyclophane **4.9**, albeit in moderate yields. However, separation of the diastereomers was not possible. We proceeded further to evaluate the scope of both aromatic and non-aromatic heterocycles under the coupling conditions.

4.7. Non-aromatic heterocycle as a coupling partner

Inspired by the oxazoline-coupling results, we wondered if the chemistry would work with other heterocycles. We investigated imidazolines first as this would allow the stereocentre to be placed closer to the paracyclophane, which might increase the ease of separation. They can make equally good ligands. The chiral variant of the imidazoline **4.78** was synthesised following the method of Kotschy et al. in good yield (Scheme 4.15).²³ Unfortunately, the

coupling failed under our standard conditions. As we did not recover any imidazoline **4.78** after the reaction, we suspected that the strong LiO^tBu had led to decomposition. Milder conditions were investigated. These were based on Bischoff's methodology and used a copper catalyst to activate the imidazoline and palladium to catalyse the coupling.²⁴ Under these new conditions, the imidazoline substrate **4.78** coupled with (±)-4-bromo[2.2]paracyclophane **4.9** in 32% yield. However, the separation of the diastereomers was not feasible for the resulting product **4.79**.

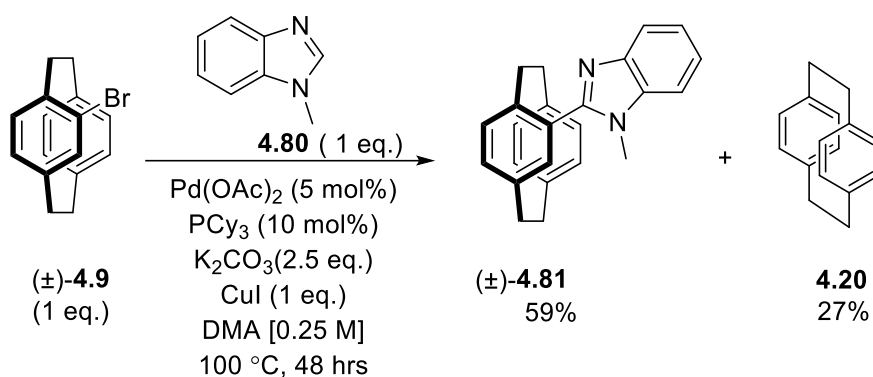


Scheme 4.15: Coupling of (±)-4-bromo[2.2]paracyclophane **4.9** with the imidazoline substrate **4.76**.

As protodebromination product **4.20** was significant, it suggests that oxidative insertion occurred efficiently, while the copper catalyst is only moderately efficient to activate the imidazoline **4.76**. Optimisation with a different catalyst, base, or Brønsted acid may help to improve the above coupling reaction.

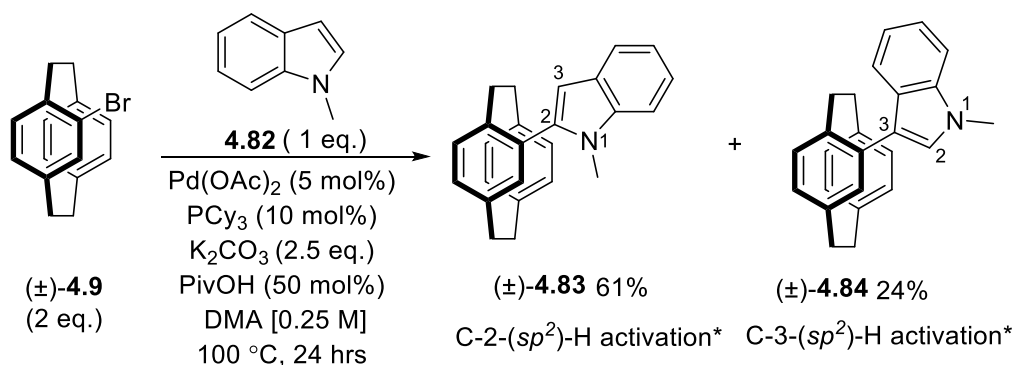
4.8. Aromatic heterocycles as coupling partner

Next, we looked at the coupling of an aromatic heterocycle, 1-methyl benzimidazole **4.80**. Again, the oxazoline coupling conditions failed but modification of the imidazoline conditions were more promising: using a more electron-rich ligand, PCy₃, in conjunction with mild base K₂CO₃, and CuI, gave the coupled product **4.81** in 59% yield (Scheme 4.16).



Scheme 4.16: Coupling of (\pm)-4-bromo[2.2]paracyclophane **4.9** with 1-methyl benzimidazole **4.80**.

We then tried to couple (\pm)-4-bromo[2.2]paracyclophane **4.9** with 1-methylindole **4.82**. Once again, the oxazoline-coupling conditions failed. The above catalytic system (Scheme 4.16) was slightly modified where the CuI was replaced with PivOH (Scheme 4.17). With these modified conditions, the coupling was observed at both C-2 and C-3 positions in the indole system. The C-2 position of indole moiety is most prone to metalation, the major coupling was deduced to occur at the C-2 position. Based on the reported literature, we confirmed that C-H functionalisation at C-2 position delivered the major coupled product **4.83** (61%), while the minor coupled product **4.84** (24%) was as a result of C3-(sp^2)-H activation.²⁵



Scheme 4.17: Coupling of (\pm)-4-bromo[2.2]paracyclophane **4.9** with 1-methylindole **4.82**.

* Data for C2-(sp^2)-H activation product is comparable to that reported in literature.²⁵

4.9. Conclusions

The main goal of this project was to develop a method to access planar chiral [2.2]paracyclophane acid derivatives. For this, we optimised a facile single-step protocol for the synthesis of planar chiral [2.2]paracyclophane-oxazolines, and hence carboxylic acids. Di-*tert*-butyl SPO **4.15** was found to be an adequate ligand for the C(sp^2)-H activation of chiral

oxazolines and for their coupling with bromo[2.2]paracyclophanes. In some cases, such as *pseudo-ortho* and *pseudo-gem* derivatives, the separation of corresponding diastereomers was possible and thus allowed the resolution of the enantiomers. In order to improve the separation of the diastereomers, the C-4 and C-5 positions of chiral oxazolines modified. With these oxazolines, the coupling with (\pm)-4-bromo[2.2]paracyclophane **4.9** was achieved in moderate yield only and separation of corresponding diastereomers was also not successful. Further, the scope of both aromatic and non-aromatic heterocycles was investigated with slightly modified conditions.

Ultimately, our one-pot strategy provides easy access to [2.2]paracyclophane-oxazolines that have great potential as planar chiral ligands in catalysis. These oxazolines could be readily hydrolysed to furnish an array of planar chiral carboxylic acids that could be chiral building blocks. Our initial results of coupling heterocycles to bromo[2.2]paracyclophane were promising. This study can be further elaborated to access a diverse range of planar chiral heterocyclic derivatives.

4.10. References

- (1) Desimoni, G.; Faita, G.; Quadrelli, P. Pyridine-2,6-bis(oxazolines), Helpful Ligands for Asymmetric Catalysts. *Chem. Rev.* **2003**, *103*, 3119.
- (2) Jönsson, C.; Hallman, K.; Andersson, H.; Stemme, G.; Malkoch, M.; Malmström, E.; Hult, A.; Moberg, C. Immobilized oxazoline-containing Ligands in asymmetric catalysis-a review. *Bioorg. Med. Chem. Lett.* **2002**, *12*, 1857.
- (3) Babu, S. A.; Krishnan, K. K.; Ujwaldev, S. M.; Anilkumar, G. Applications of Pybox Complexes in Asymmetric Catalysis. *Asian J. Org. Chem.* **2018**, *7*, 1033.
- (4) Desimoni, G.; Faita, G.; Jørgensen, K. A. C2-Symmetric Chiral Bis(Oxazoline) Ligands in Asymmetric Catalysis. *Chem. Rev.* **2006**, *106*, 3561.
- (5) Ward, B. D.; Gade, L. H. Rare earth metal oxazoline complexes in asymmetric catalysis. *Chem. Commun.* **2012**, *48*, 10587.
- (6) Braun, C.; Nieger, M.; Thiel, W. R.; Bräse, S. [2.2]Paracyclophanes with *N*-Heterocycles as Ligands for Mono- and Dinuclear Ruthenium(II) Complexes. *Chem. Eur. J.* **2017**, *23*, 15474.
- (7) Kitagaki, S.; Sugisaka, K.; Mukai, C. Synthesis of planar chiral [2.2]paracyclophane-based bisoxazoline ligands bearing no central chirality and application to Cu-catalyzed asymmetric O–H insertion reaction. *Org. Biomol. Chem.* **2015**, *13*, 4833.
- (8) Whelligan, D. K.; Bolm, C. Synthesis of *Pseudo-geminal*-, *Pseudo-ortho*-, and *ortho*-Phosphinyl-oxazoliny-[2.2]paracyclophanes for Use as Ligands in Asymmetric Catalysis. *J. Org. Chem.* **2006**, *71*, 4609.
- (9) Hou, X.-L.; Wu, X.-W.; Dai, L.-X.; Cao, B.-X.; Sun, J. Novel - and -planar chiral [2.2]paracyclophane ligands: synthesis and application in Pd-catalyzed allylic alkylation. *Chem. Commun.* **2000**, *13*, 1195.
- (10) Marchand, A.; Maxwell, A.; Mootoo, B.; Pelter, A.; Reid, A. Oxazoline Mediated Routes to a Unique Amino-acid, 4-Amino-13-carboxy[2.2]paracyclophane, of Planar Chirality. *Tetrahedron* **2000**, *56*, 7331.

- (11) Kitagaki, S.; Murata, S.; Asaoka, K.; Sugisaka, K.; Mukai, C.; Takenaga, N.; Yoshida, K. Planar Chiral [2.2]Paracyclophane-Based Bisoxazoline Ligands: Design, Synthesis, and Use in Cu-Catalyzed Inter- and Intramolecular Asymmetric O–H Insertion Reactions. *Chem. Pharm. Bull.* **2018**, *66*, 1006.
- (12) Bolm, C.; Wenz, K.; Raabe, G. Regioselective palladation of 2-oxazolinyll-[2.2]paracyclophanes.: Synthesis of planar-chiral phosphines. *J. Organomet. Chem.* **2002**, *662*, 23.
- (13) Wu, X.-W.; Zhang, T.-Z.; Yuan, K.; Hou, X.-L. Regulation of the flexibility of planar chiral [2.2]paracyclophane ligands and its significant impact on enantioselectivity in asymmetric reactions of diethylzinc with carbonyl compounds. *Tetrahedron: Asymmetry* **2004**, *15*, 2357.
- (14) Wang, X.; Chen, Z.; Duan, W.; Song, C.; Ma, Y. Synthesis of [2.2]paracyclophane-based bidentate oxazoline–carbene ligands for the asymmetric 1,2-silylation of *N*-tosylaldimines. *Tetrahedron: Asymmetry* **2017**, *28*, 783.
- (15) Pelter, A.; Mootoo, B.; Maxwell, A.; Reid, A. The synthesis of homochiral ligands based on [2.2]paracyclophane. *Tetrahedron Lett.* **2001**, *42*, 8391.
- (16) Ackermann, L. Air- and Moisture-Stable Secondary Phosphine Oxides as Preligands in Catalysis. *Synthesis* **2006**, *2006*, 1557.
- (17) Henri, A. v. K.; Floris, L. v. D.; Floris, P. J. T. R. Catalytic Appel reactions. *Pure Appl. Chem.* **2012**, *85*, 817.
- (18) Xi, T.; Mei, Y.; Lu, Z. Palladium-Catalyzed C-2 C–H Heteroarylation of Chiral Oxazolines: Diverse Synthesis of Chiral Oxazoline Ligands. *Org. Lett.* **2015**, *17*, 5939.
- (19) Lu, P.; Ji, C.-L.; Lu, Z. Nickel-Catalyzed C–H Heteroarylation of Chiral Oxazolines. *Asian J. Org. Chem.* **2018**, *7*, 542.
- (20) Ghorai, D.; Müller, V.; Keil, H.; Stalke, D.; Zanoni, G.; Tkachenko, B. A.; Schreiner, P. R.; Ackermann, L. Secondary Phosphine Oxide Preligands for Palladium-Catalyzed C–H (Hetero)Arylations: Efficient Access to Pybox Ligands. *Adv. Synth. Catal.* **2017**, *359*, 3137.
- (21) Giordano, M.; Iadonisi, A. Tin-Mediated Regioselective Benzoylation and Allylation of Polyols: Applicability of a Catalytic Approach Under Solvent-Free Conditions. *J. Org. Chem.* **2014**, *79*, 213.
- (22) Xu, H.; Lu, Y.; Zhou, Y.; Ren, B.; Pei, Y.; Dong, H.; Pei, Z. Regioselective Benzoylation of Diols and Polyols by Catalytic Amounts of an Organotin Reagent. *Adv. Synth. Catal.* **2014**, *356*, 1735.
- (23) Paczal, A.; Bényei, A. C.; Kotschy, A. Modular Synthesis of Heterocyclic Carbene Precursors. *J. Org. Chem.* **2006**, *71*, 5969.
- (24) Muselli, M.; Baudequin, C.; Hoarau, C.; Bischoff, L. Pd-Catalyzed direct C–H functionalization of imidazolones with aryl- and alkenyl halides. *Chem. Commun.* **2015**, *51*, 745.
- (25) Thennakoon, N.; Kaur, G.; Wang, J.; Plieger, P. G.; Rowlands, G. J. Asymmetric Variant of the Bischler–Möhlau Indole Synthesis, *Aust. J. Chem.* **2015**, *68*, 566.

Chapter 5

Regioselective C-H Functionalisation *Via* Desulfitative Coupling Using Heteroarene Sulfinates

5.0. Introduction to Sulfinates

Aryl- or alkyl-(hetero)aryl derivatives are key building blocks for natural products, medicinal drugs, advanced materials, agrochemicals, and fine chemicals.¹ Classical transition metal-mediated cross-coupling reactions, like Mizoroki-Heck,² Suzuki-Miyaura,³ Stille,⁴ or Negishi reactions,⁵ allow rapid and convergent syntheses of these molecules. Palladium is the most commonly utilised transition metal catalyst for such cross-coupling reactions,⁶ although other noble metals, and more recently, earth-abundant metals, such as nickel, copper, and zinc, have all been studied.^{7,8} New methodologies such as C-H activation⁹ and transition metal-free coupling¹⁰ have recently emerged as alternative methods that overcome issue of low efficiency associated with the classical reactions. Each method requires different coupling partners, which can limit their use. As a result, there is ongoing research to find new substrates with greater stability, cheaper access, clean reactions, or alternative functional group tolerances.

Sulfinates are a promising candidate for coupling reactions.^{11,12} They are attractive reagents as they are easy to handle, bench-stable, moisture-resistant, and easily accessible from simple precursors. They can readily be transformed into sulfones and sulfonamides by sulfonylative S-C and S-N bond formation (Figure 5.1). In addition, sulfinates are also employed as electrophilic and nucleophilic partners with the transition metal catalysis in desulfitative cross-coupling reactions like Mizoroki-Heck, Suzuki-Miyaura, Stille couplings, C-H functionalisation for C-C bond formation (Figure 5.2).¹³ Hence, sulfinate chemistry is becoming increasingly popular.

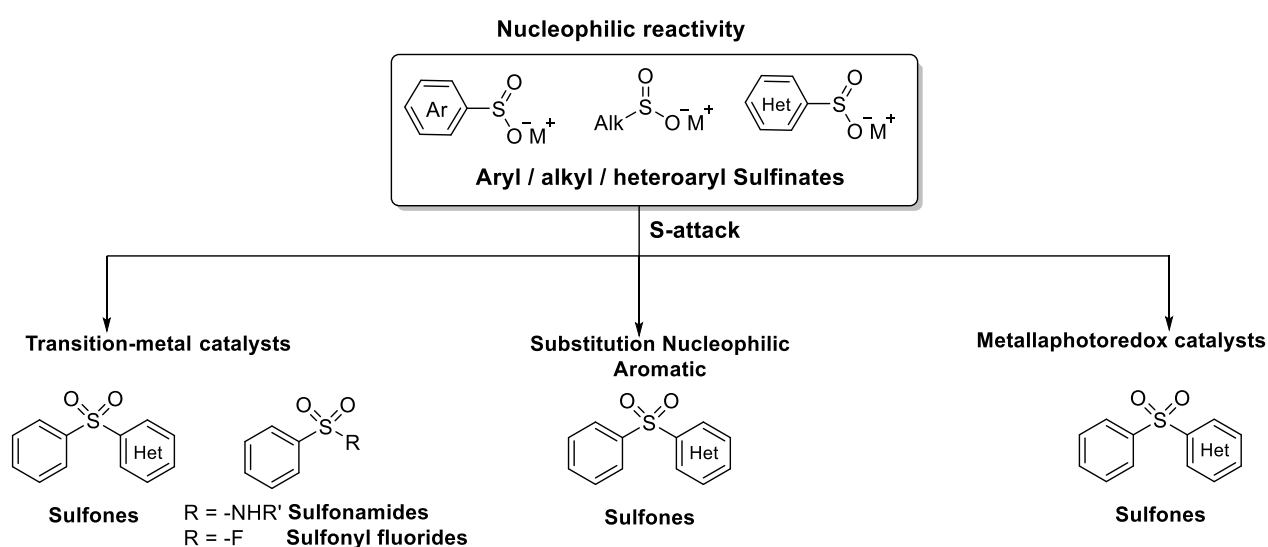


Figure Error! No text of specified style in document..1 : Sulfinates as versatile coupling partners – Nucleophilic reactivity.

Desulfitative Cross-Coupling
C-S cleavage

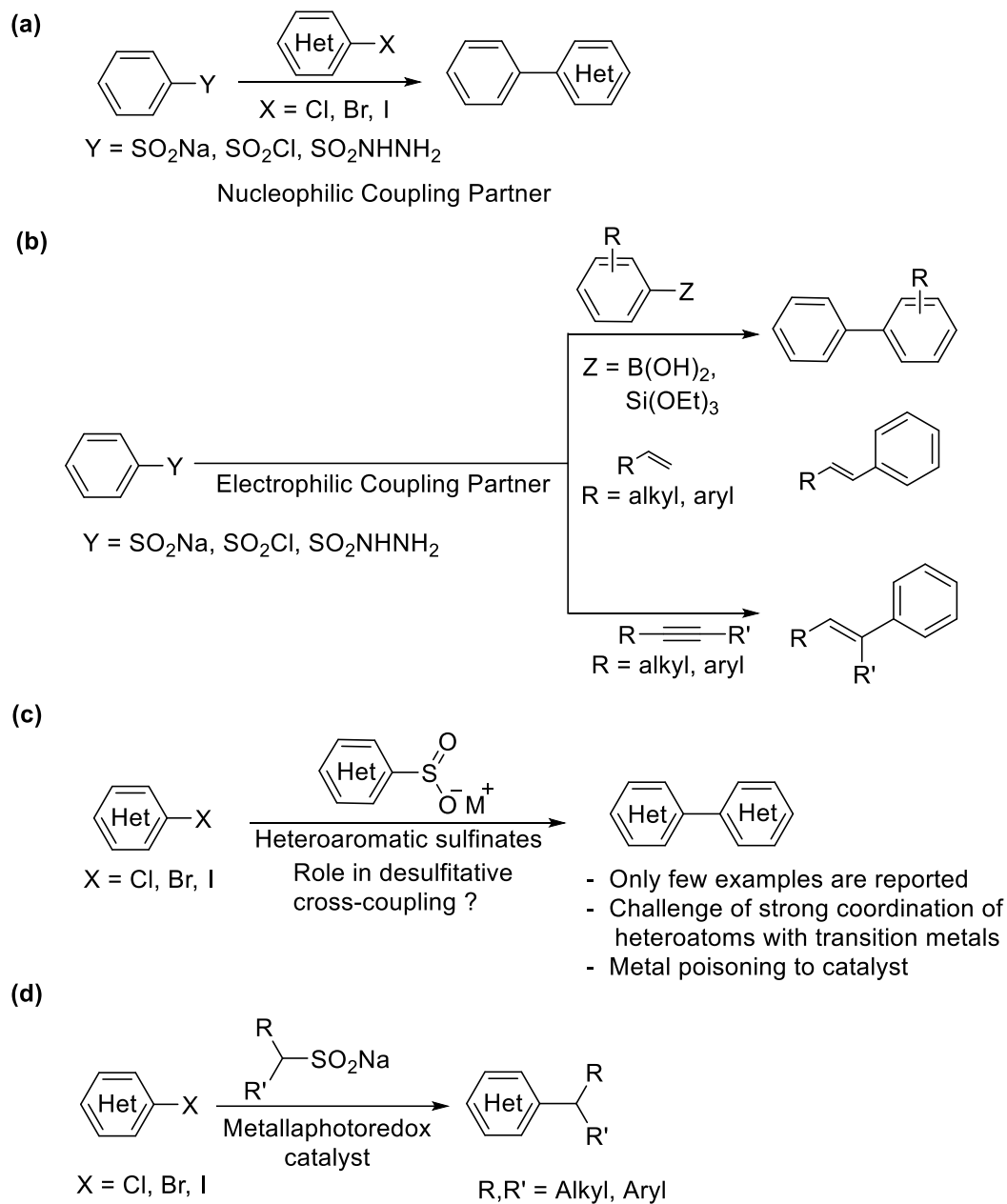


Figure Error! No text of specified style in document..2: Sulfinates as versatile coupling partners (C-S cleavage).

Before explaining the role of sulfinates, it is important to mention the different terminologies used here to describe the loss of the sulfur fragment (SO_2 , SO_3 , SO_3^{2-} or thiolates), compare the ease of this process to decarboxylation, and the nature of sulfinato complexes.

5.1. Terminologies for extrusion of sulfur from organosulfur compounds

Sulfur can exist in a number of oxidation states and this gives rise to a range of organosulfur compounds (Figure 5.3).

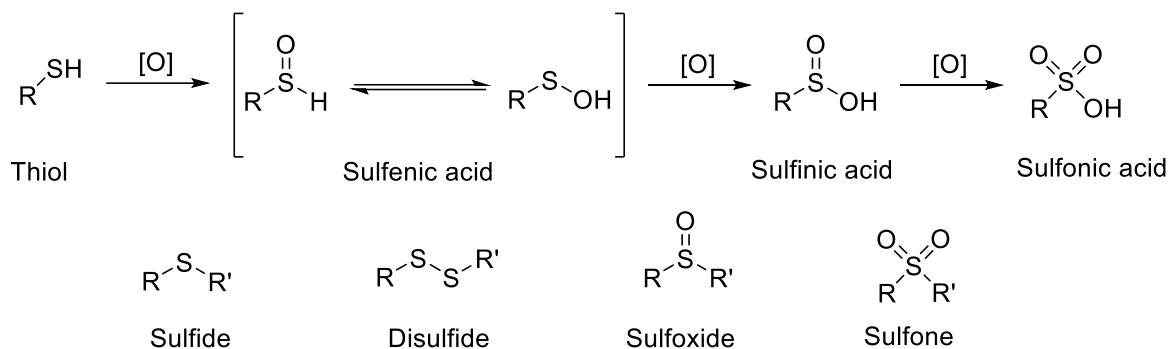
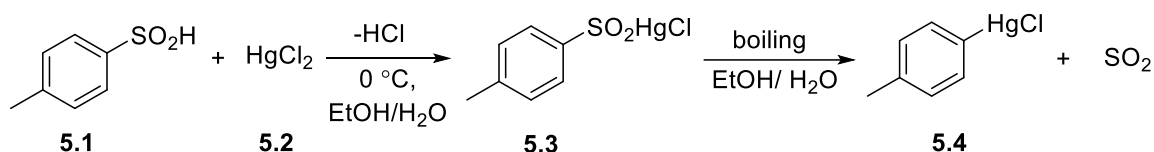


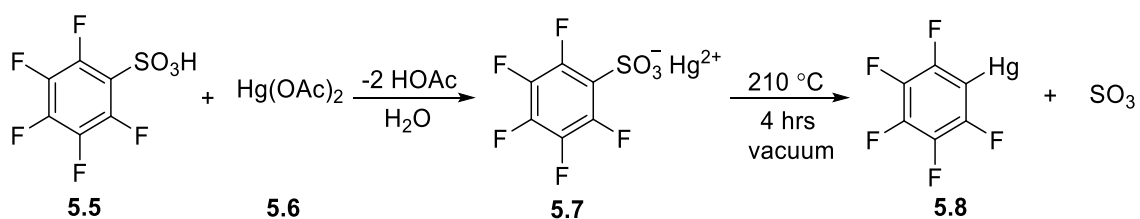
Figure Error! No text of specified style in document..3: Different organosulfur compounds.

Desulfitative means the extrusion of SO₂ gas during a metal-mediated C-S bond cleavage reaction. It is also defined as a desulfination reaction (Scheme 5.1).¹⁴



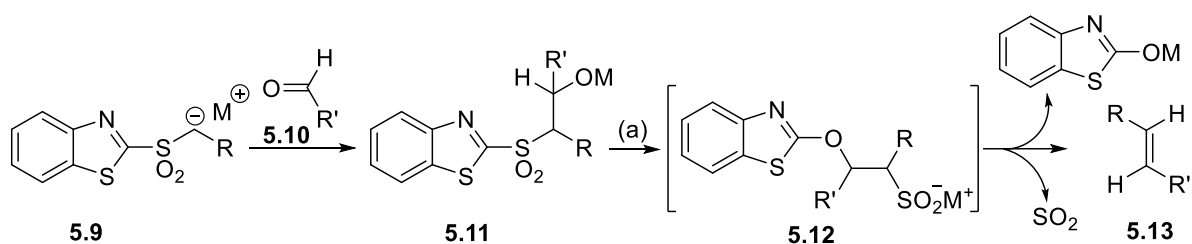
Scheme 5.1: Desulfination reaction, loss of SO₂.

On the other hand, desulfonative means the loss of SO₃ gas during a metal-mediated C-S bond cleavage reaction. It is also called a desulfonation reaction (Scheme 5.2).¹⁵



Scheme 5.2: Desulfonation reaction, loss of SO₃.

A similar terminology, desulfonylation is mainly applicable to demonstrate the loss of RSO₂⁻ from a sulfonyl functional group (RSO₂R'). The classical example, which uses desulfonylation terminology is the Julia-Kocienski olefination reaction (Scheme 5.3).¹⁶



Scheme 5.3: Julia-Kocienski elimination reaction, loss of SO₂, (a) Smiles rearrangement.

In this thesis, both terminologies desulfitative and desulfination are used, meaning the same loss of SO₂ gas in the cleavage of a C-S bond.

5.2. The ease of desulfination: desulfination vs. decarboxylation

It has been shown that extrusion of SO₂ gas from metal complexes is easier than the extrusion of CO₂ and SO₃ from analogues complexes.¹⁷ Sraj et al. compared the intrinsic reactivity orders of three heteroligands, [MeCO₂CuO₂SMe], [MeCO₂CuO₃SMe], and [MeSO₂CuCO₃SMe] for organocuprate formation *via* ligand decomposition in the gas phase. In each case, desulfination (-SO₂) dominates over decarboxylation (-CO₂), while desulfonylation (-SO₃) is least favoured. In addition, DFT calculations were also consistent with an experimental order of organocuprate formation which follows SO₂ loss > CO₂ loss > SO₃ loss.

The above results show that metal-mediated desulfination reactions are relatively easier than metal-assisted decarboxylation reactions, and avoid the need for harsh reaction conditions. The relative ease of desulfination and continued supply of inexpensive organosulfur compounds from the oil industry are the main reasons for the growing interest in the applications of desulfitative reactions in various organic transformations.

5.3. Sulfinato complexes

As transition metal-mediated desulfitative reactions proceed *via* different sulfinato metal complexes, it is first important to understand the types of these complexes. Initial studies of sulfinato metal complexes suggested that there are four possibilities for coordinating the RSO₂⁻ ligands to metals (Figure 5.4). RSO₂⁻ can form a monodentate complex either through lone pair of electrons either on one oxygen atom (sulfinato-*O* complex **5.14**) or sulfur atom (sulfinato-*S* complex **5.15**). The coordination of lone pair of electrons on both oxygen atoms forms an intramolecular (**5.16**) or intermolecular sulfinato-*O,O'* complex **5.17**. The last co-

ordination possibility is by electron donation, by one oxygen and one sulfur to the central metal to produce the intramolecular (**5.18**) or intermolecular sulfinato-*O,S* complex **5.19**.

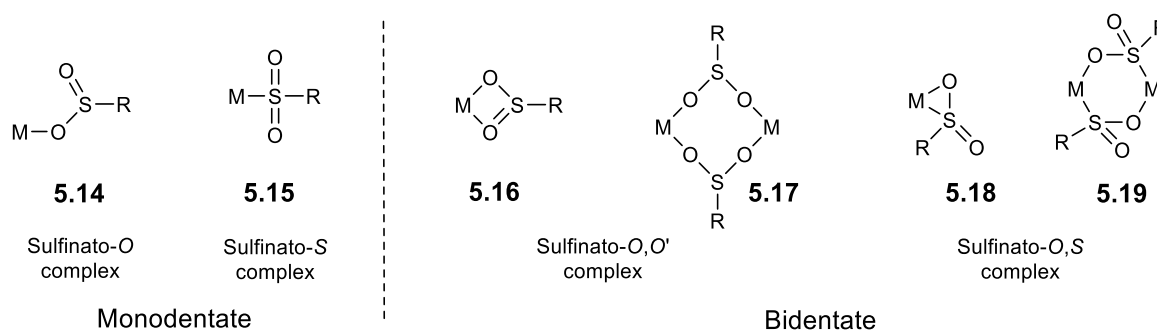


Figure 5.4: Possible sulfinato metal complexes.

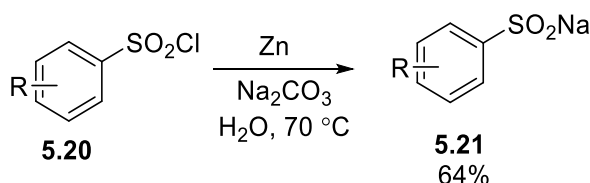
The sulfinate ion, RSO_2^- can act as an electron donor through either the soft *S* atom or the hard *O* atom. The co-ordination of a ligand to a metal follows the HSAB (hard and soft acids and bases) concept. Transition-metals in low oxidation states adopt a soft character and favour the formation of the sulfinato-*S* complex. Based on the Ahrlund-Chatt classification,¹⁸ it was observed that *5d* and *4d* metals tend to form sulfinato-*S*-complexes, while sulfinato-*O*-complexes are formed with *3d* metals.

Before describing the role of sulfinites in desulfitative reactions, I have presented a brief sight on general synthetic methods of sulfinate derivatives.

5.4. Synthesis of sulfinites

Although, there are only a few commercially available substrates, aryl sulfinites ($\text{ArSO}_2^- \text{M}^+$) can easily be synthesised by the following methods.

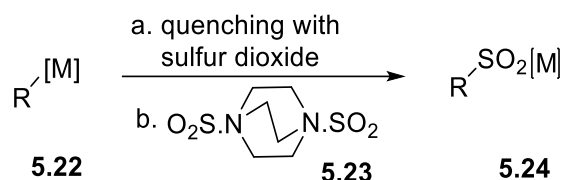
The most common way is by metal-mediated reduction of sulfonyl chlorides **5.20** in water (Scheme 5.4).¹⁹



Scheme 5.4: Reduction of sulfonyl chloride to sulfinites.

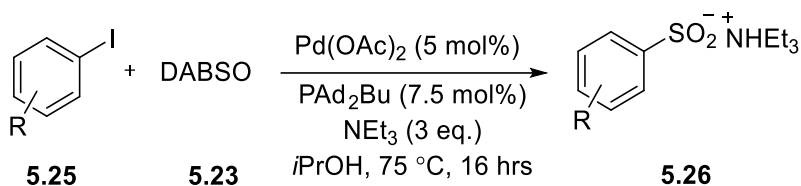
An alternative synthesis involves quenching organometallic compounds **5.22** generated from aryl/alkyl halides with sulfur dioxide (Scheme 5.5). However, use of either gaseous or liquid

SO₂ is problematic. Instead a solid form of SO₂ *i.e.* *in-situ* SO₂ release or DABSO **5.23** (1,4-diazabicyclo[2.2.2]octane bis(sulfur dioxide) permits a well-defined quantity to be added.²⁰ DABSO is an air-stable, white solid, formed by condensing the SO₂ gas over freshly sublimed DABCO (1,4-diazabicyclo[2.2.2]octane).



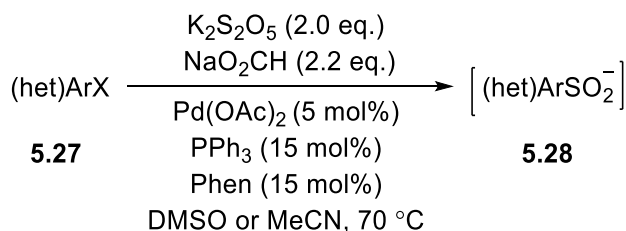
Scheme 5.5: Schematic representation of synthesis of sulfinates from SO₂ or DABSCO.

The organometallic reagent **5.22** can be replaced by an arylhalide **5.25** and a palladium-mediated sulfinite synthesis can be performed. In this Pd(II)-catalysed reaction, the arylhalide **5.25** can be converted into an ammonium sulfinite salt **5.26** by employing a stoichiometric quantity of DABSO **5.23**, and catalytic bulky di(1-adamantyl)-*n*-butylphosphine (PAd₂Bu) ligand (Scheme 5.6).²¹



Scheme 5.6: Pd(II)-catalysed synthesis of ammonium sulfinates.

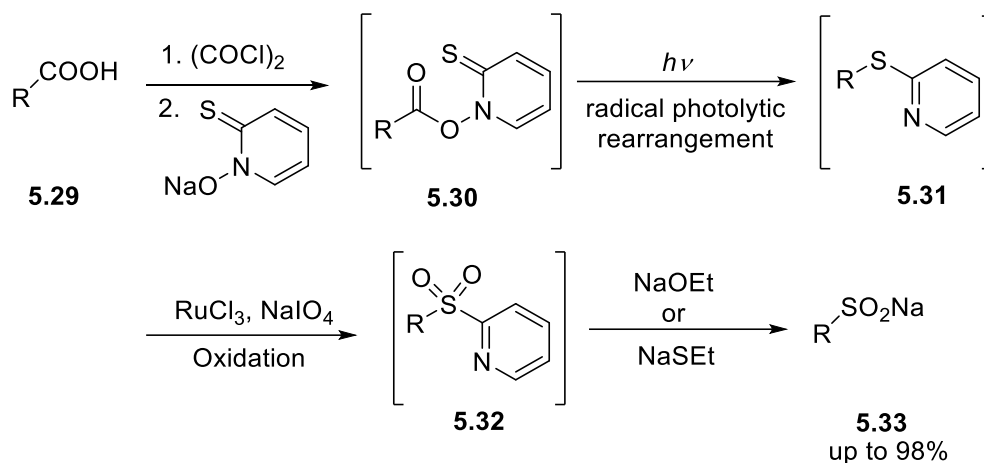
Another palladium-mediated synthesis was reported by the group of Mascitti. In this reaction, potassium metabisulfite was not only the sulfur source but also the buffering agent of the reaction medium, while sodium formate was employed as a hydrogen donor (Scheme 5.7).²²



Scheme 5.7: Pd(II)-catalysed synthesis of aryl/heteroaryl sulfinite.

Recently, it was shown that alkyl sulfinates can be formed from the carboxylic acids.²³ The advantage of this source is the structural diversity of commercially available carboxylic acids. In this method, the carboxylic acid **5.29** is first converted to a thiohydroximate ester **5.30**,

which rearranges to 2-pyridinyl thioether **5.31** under the photolytic Barton-type decarboxylation conditions.²⁴ After oxidation, the resulting pyridine sulfone **5.32** undergoes nucleophilic attack by alkoxide or thiolate to release the sulfinate **5.33** in moderate to excellent yield (Scheme 5.8).



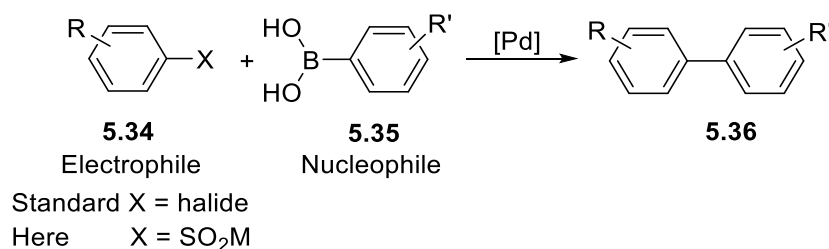
Scheme 5.8: Synthesis of alkyl sulfonates from carboxylic acids *via* a Barton ester.

5.5. Role of sulfonates in desulfurative reactions

Aryl sulfonates have been extensively studied over the last decade. Their most common use is as a replacement for organic halides and boronic acids in arylation reactions. However, alkyl sulfonates (AlkSO_2M^+) and heteroarene sulfonates ($\text{HetArSO}_2\text{M}^+$) have not been thoroughly exploited as organometallic reagents.

5.5.1. Sulfonates as electrophilic coupling partners

In the last few years have, a number of desulfurative $\text{C}(sp^2)\text{-C}(sp^2)$ coupling reactions have been reported. In these reports, the electrophilic properties of sulfonates have been exploited and these reagents have replaced the aryl halide coupling partners (Scheme 5.9).



Scheme 5.9: Sulfonates as electrophilic coupling partners.

As per the bond energy^g for C-I (213), C-S (272), C-Br (285), and C-Cl (327), sulfinates lie somewhere between aryl iodides and aryl bromides in terms of reactivity.²⁵ Due to this reactivity, sulfinates can easily be extended in place of organic halides in metal-catalysed cross-coupling reactions. The most commonly employed aryl sulfinate derivatives for such organic transformations are either ArSO₂Na or ArSO₂NHNH₂. In the last few years, an extensive number of desulfitative cross-coupling catalysed by Pd and Ru have been reported. The section below will highlight the general mechanism and key examples of Mizoroki-Heck, Suzuki-Miyaura, Hiyama, and Sonogashira-type cross-coupling reactions.

5.5.1.1. General mechanism for palladium-catalysed desulfitative reaction: (ArSO₂M⁺) as an electrophile

All the palladium-catalysed reactions described in this section react the aryl sulfinates with nucleophilic coupling reagents. The catalytic cycle differs to the conventional cross-coupling reactions as outlined below.

- In the conventional Heck reaction, an arylpalladium(II) species is generated by the oxidative addition of aryl halides or *pseudohalides* to Pd(0). However, in the Heck-type reaction employing sulfinates, the catalytic cycle is initiated by ligand exchange between Pd(II) and the sulfinate, followed by desulfitative C-S bond cleavage.
- As the first step involves the nucleophilic attack of ArSO₂⁻ anion on the active Pd(II) species, oxidative addition is not a part of the reaction mechanism.

^g Bond energy in kJ mol⁻¹

The plausible general reaction mechanism is illustrated as shown Figure 5.5.

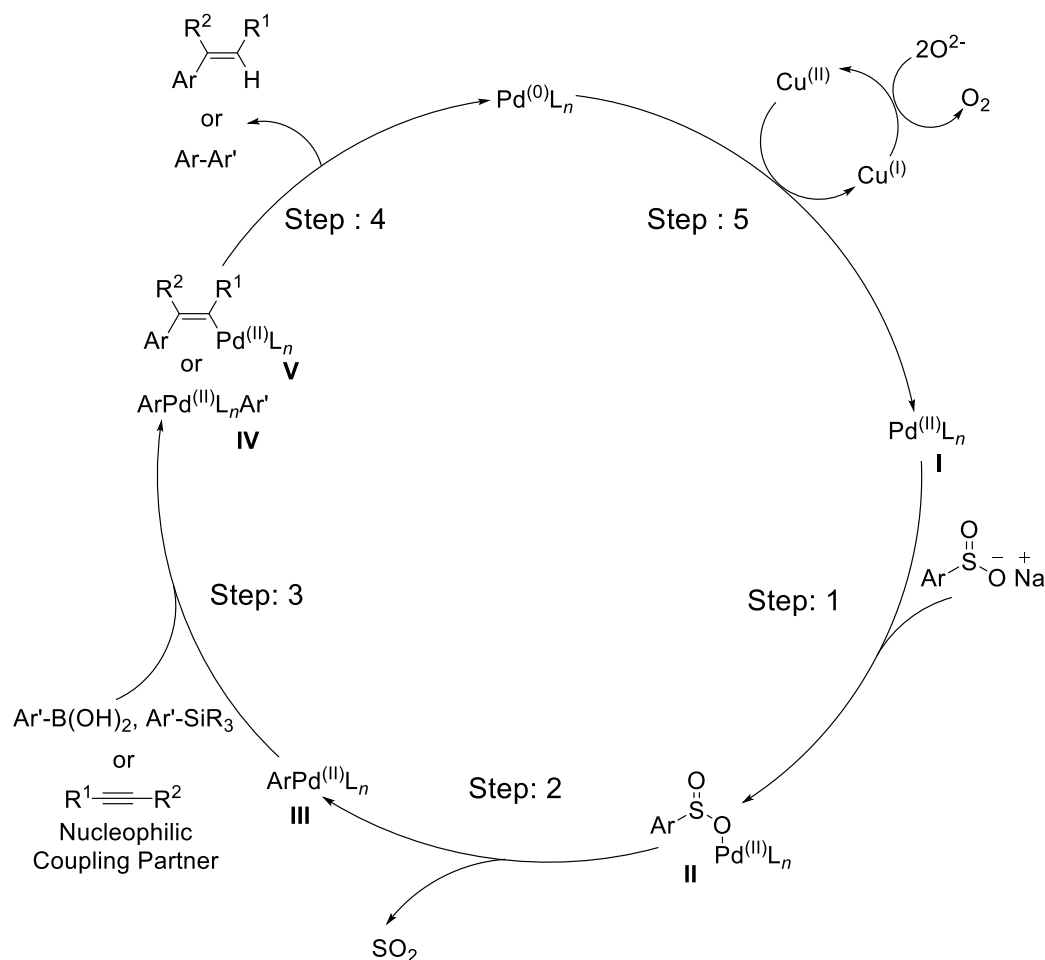


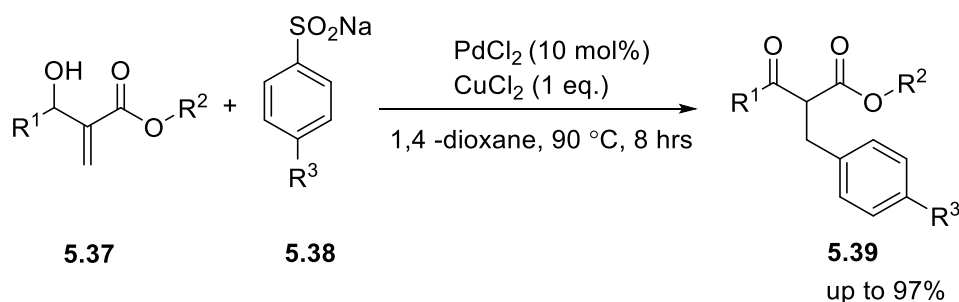
Figure 5.5: General catalytic cycle of aryl sulfonates as electrophile in desulfurative reactions.

Firstly, the co-ordination of Pd(II) species, generated either from Pd(II)-complexes e.g. PdCl₂, Pd(OAc)₂ or by the oxidation of Pd(0) complexes e.g. Pd₂(dba)₃, with ArSO₂⁻ forms ArS(O)OPd(II) O⁻-complex (step: 1). This is followed by the expulsion of SO₂ gas to give an ArPd(II) species (step: 2). The next step (step 3) is transmetalation of the ArPd(II) intermediate with either an organoborane (Suzuki-Miyaura) or organosilane (Hiyama reaction). For the Mizoroki-Heck-type and Sonogashira-type reactions, this step would instead be the insertion of the ArPd(II) intermediate into alkene double bond or alkyne triple bond respectively. Finally, in the first type of the reactions, reductive elimination of the desulfurative coupling product leads to the formation of the reduced Pd(0) species, which is oxidised by the appropriate oxidant (step: 5). In the latter type of reactions, the regeneration of the active Pd(II) catalyst occurs after protonation of the intermediate V by an acid to release the addition product.

5.5.1.2. Mizoroki-Heck-type reaction

The Mizoroki-Heck-type reaction is a powerful technique for the arylation of alkenes.^{2,26} The reaction involves the coupling of an alkene with an aryl halide or equivalent, such as aryl triflates, aryl diazonium salts, and diaryl iodonium salts. Generally, in conventional Heck reactions, a base and a ligand are required for the conversion of the hydropalladium(II)-complex to the active palladium(0)-catalyst. However, Heck type reactions employing sulfonates as coupling partners do not require a base and a ligand.^{11,13}

Raj et al. disclosed a simple and mild Pd(II)-catalysed desulfinitive Heck-type arylation for the synthesis of highly functionalised α -benzyl- β -keto ester **5.39** from sodium arenesulfonates **5.38** and Baylis-Hillman adducts **5.37** in good to excellent yields (Scheme 5.10).²⁷ This reaction tolerates a wider range of functionalities *i.e.* methyl, bromo, and chloro on the sodium arenesulfonate, under these reaction conditions. The authors proposed a plausible catalytic cycle in a sequence of desulfination, oxidative insertion, and β -hydride elimination followed by keto-enol tautomerisation.



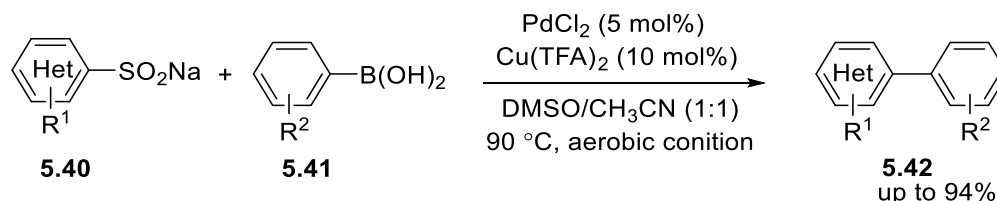
Scheme 5.10: Desulfinitive synthesis of α -benzyl- β -keto ester.

5.5.1.3. Suzuki-Miyaura cross-coupling reaction

The palladium-catalysed cross-coupling of an aromatic halide and organoborane is known as the Suzuki-Miyaura reaction.^{28,29} Recently, C-S bond cleavage by employing aryl sulfinate as the electrophilic coupling partner with organoboronic acid has been shown an attractive approach for Suzuki-Miyaura cross-coupling reactions.^{11,13}

Qi and co-workers used a combination of Pd(II) and Cu(II) to catalyse desulfinitive coupling reactions of sodium arylsulfonates **5.40** with aryl boronic acids **5.41** under aerobic conditions (Scheme 5.11).³⁰ The reaction followed the standard mechanism described in Figure 5.5, with the palladium coupling the substrates and the copper regenerating the active Pd(II) catalyst.

The stoichiometric oxidant is oxygen. The authors found the mixed solvent system was essential to prevent homocoupling of **5.40** but they do not say how it activates it.

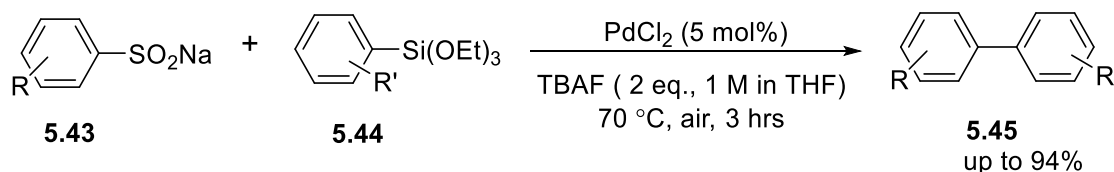


Scheme 5.11: Desulfitative coupling reactions of sodium arylsulfonates with aryl boronic acids.

5.5.1.4. Hiyama-type cross-coupling reaction

Due to inherent drawbacks such as high cost, toxicity, low stability and poor biocompatibility of organotin reagents in cross-coupling reactions, organosilicon reagents have emerged as alternative nucleophilic partners.^{31,32}

Qi et al. described the cross-coupling between aryltrialkoxo silanes **5.44** with arylsulfonates **5.43**.³³ In this protocol, TBAF was employed to activate the silane towards transmetalation. The reaction proceeded in a solution of PdCl₂, TBAF in THF at 70 °C in presence of air as an oxidant in three hours (Scheme 5.12).



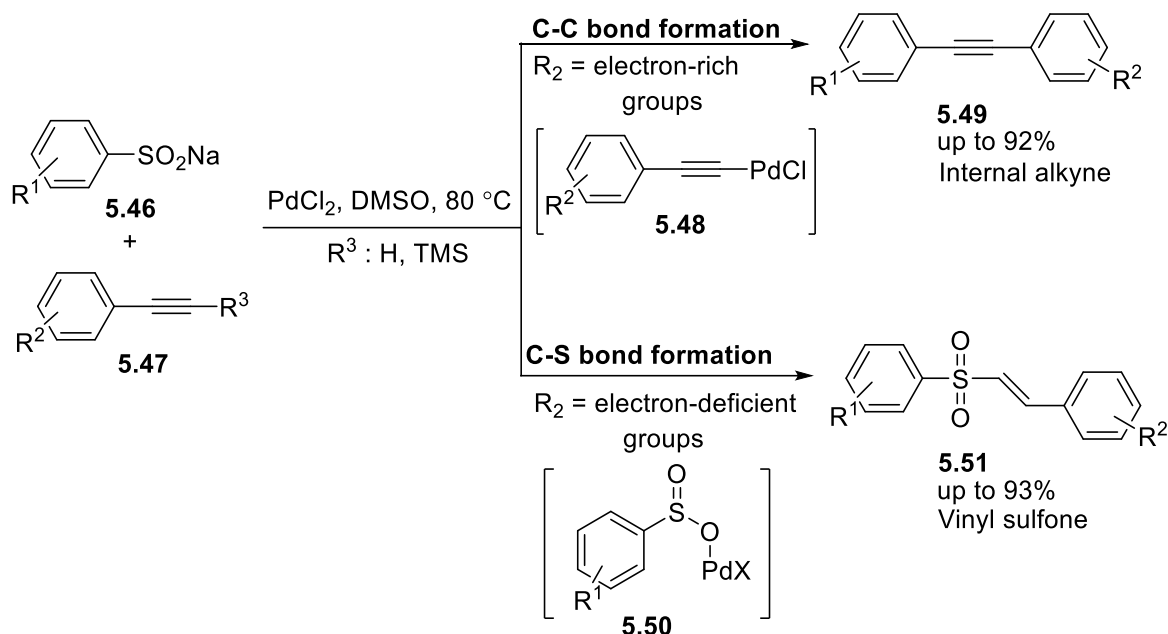
Scheme 5.12: Cross-coupling of trialkoxyaryl-silanes with arylsulfonates.

5.5.1.5. Sonogashira-type cross-coupling reaction

The Sonogashira cross-coupling reaction couples aryl halides and terminal alkynes using palladium and copper catalysts in the presence of a base.^{34,35}

Jiang et al. coupled sodium sulfonates **5.46** and aryl alkynes **5.47** to give unsymmetrical internal alkynes **5.49** and vinyl sulfones **5.51** (Scheme 5.13).³⁶ While evaluating the optimised protocol, the authors noticed that electronic effects on the aromatic ring of the phenylacetylene play a crucial role in the selective formation of either C-C and C-S bond. Electron-rich aryl alkynes (alkoxy, amine and hydroxy substituents) gave the products of C-C bond formation products while strongly electron-withdrawing substituents (-NO₂, -CF₃) led to the sulfone

product. Two different mechanisms were postulated. In the internal alkyne formation, the first step involves coordination of the alkyne with PdCl₂ to give an alkynyl palladium intermediate **5.48**. Formation of the sulfone starts with the oxidative addition of Pd(II) to the sulfinates to afford intermediate **5.50**. Unlike the conventional Sonogashira reaction, this convenient protocol does not employ a copper co-catalyst and base.

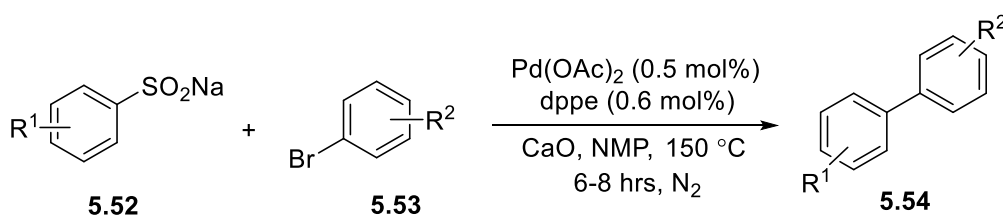


Scheme 5.13: Unsymmetrical alkyne and vinyl sulfones synthesis by coupling of sodium sulfinates and aryl/heteroaryl alkynes.

5.5.2. Aryl/heteroaryl sulfinates as nucleophilic coupling partners

The potential of sulfinates as nucleophilic coupling partners has only been realised recently by the pioneering studies of the Duan and Forgione groups.^{37,38} Their studies demonstrated the desulfurative coupling between aryl triflates or bromides and aryl sulfinates.

Before that, there had only been one report for such a reaction in a 1992 US patent where Sato and Okoshi attempted the reaction of aryl sulfinates with aryl halides under palladium catalysis, in a polar solvent NMP, at high temperature 150 °C (Scheme 5.14).³⁹



Scheme 5.14: Desulfurative cross-coupling between aryl bromide and arylsulfinates.

5.5.2.1. General mechanism for palladium-catalysed desulfinitative reaction: (ArSO₂⁻M⁺) as a nucleophile

When the aryl sulfinate acts as the nucleophilic coupling partner, the catalytic cycle changes (Figure 5.6). The first step is oxidative addition of a Pd(0) species into the aryl halide (step 1). Next, transmetalation gives the tetrahedral sulfinato-*S* complex (step 2). Finally, extrusion of SO₂ gas leads to the formation of the bis-aryl Pd(II) intermediate (step 3); which then undergoes reductive elimination to continue the Pd(0)-Pd(II) catalytic cycle (step 4).

It is important to mention here that most of the reports have employed bidentate phosphine ligands with a wide bite angle. The stereoelectronic property of substituents on the ligand play a major role in controlling the Pd(0)-Pd(II) catalytic cycle as outlined below.

- Electron-rich substituents enhance the rate of oxidative addition. (step 1)
- Large substituents accelerate the reductive elimination step. (step 4)
- Bulky substituents can suppress the homocoupling of the aryl sulfinites.

The plausible general reaction mechanism is illustrated Figure 5.6.

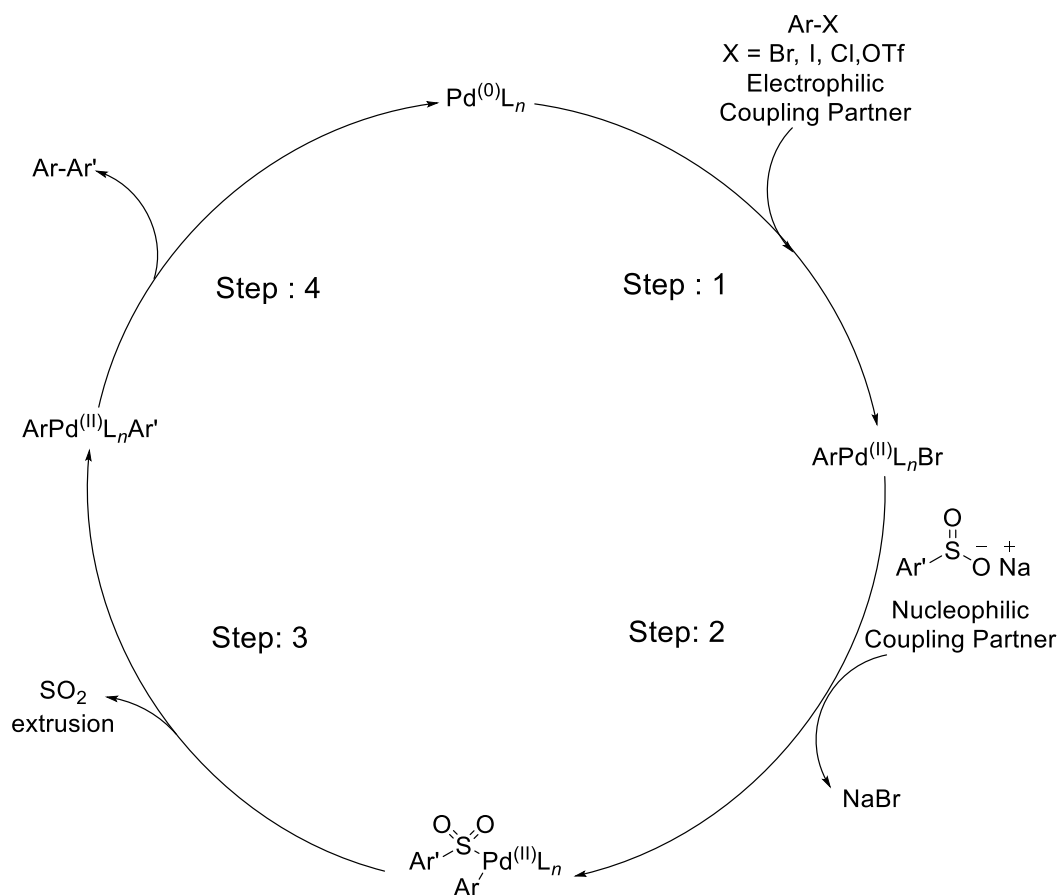
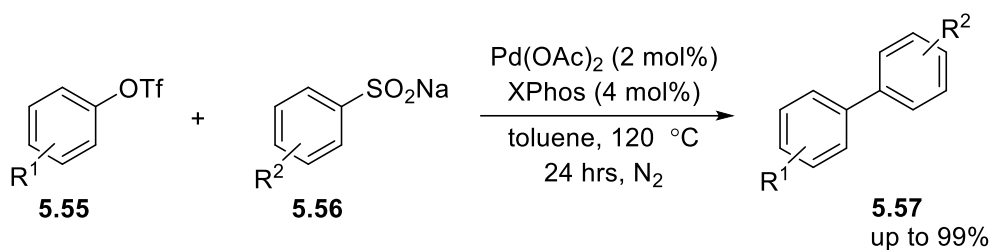


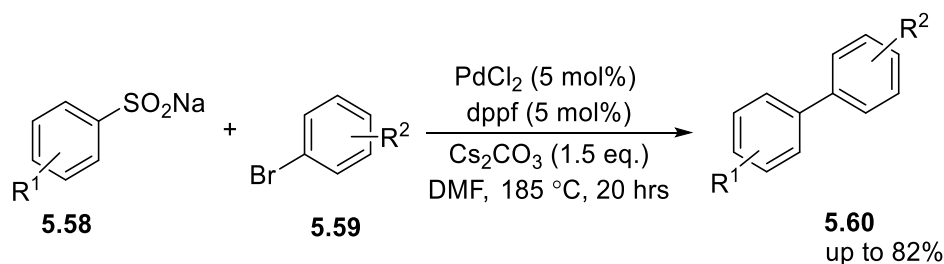
Figure 5.6: A general catalytic cycle of aryl sulfinites as nucleophile in desulfinitative reactions.

Duan et al. have investigated the formation of biaryls **5.57** through the coupling of aryl triflates **5.55** and aryl sulfinates **5.56** (Scheme 5.15).³⁷ This efficient protocol employs only 2 mol% of Pd(OAc)₂ and 4 mol% of the bidentate ligand, Xantphos, at 120 °C in toluene without any additives. Both electron-donating and electron-withdrawing groups are tolerated on either substrate and in any position. The only exception is the nitro-substituted aryl triflate or aryl sulfinate.

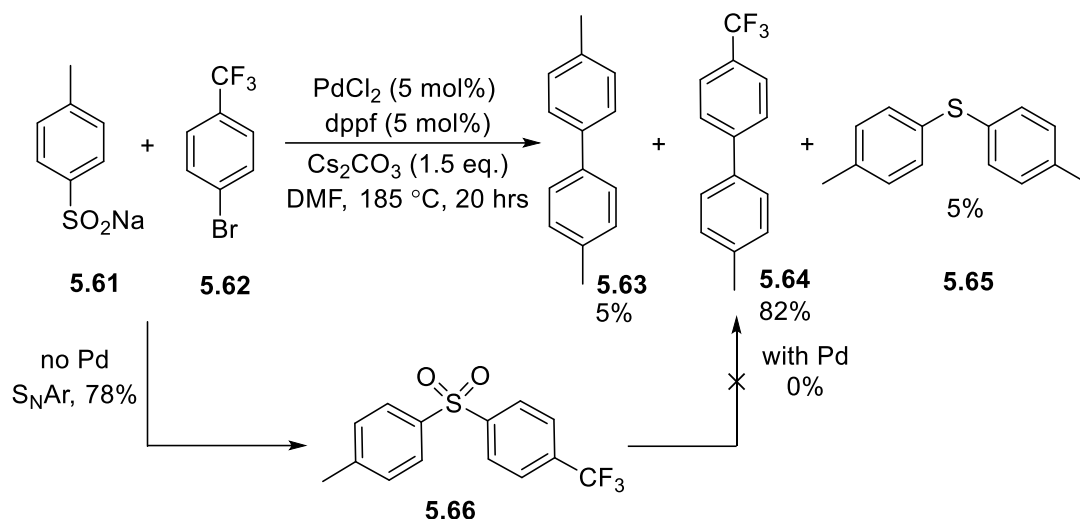


Scheme 5.15: Desulfitative cross-coupling between aryl triflates and arylsulfonates.

Forgione et al. presented a detailed mechanistic study of the desulfitative cross-coupling reaction of aryl sulfinates **5.58** with aryl bromides **5.59**.³⁸ The best results were obtained with PdCl₂ and the bidentate phosphine ligand, dppf (Scheme 5.16). It was observed that increasing the number of equivalents of aryl sulfinate **5.58** led to desulfitative homocoupling. If electron-deficient aryl bromides were used, S_NAr gave sulfones instead. The control experiment between 1-bromo-4-(trifluoromethyl)benzene **5.62** and *p*-tolyl sulfinate **5.61** in the presence or absence of catalyst ruled out the possibility of a palladium-catalysed S_NAr (Scheme 5.17). In addition, thioether **5.65** (C-S bond formation) was also observed and this will be relevant to the discussion in the next chapter (Chapter 6, Section 6.3.1.1, Scheme 6.15).

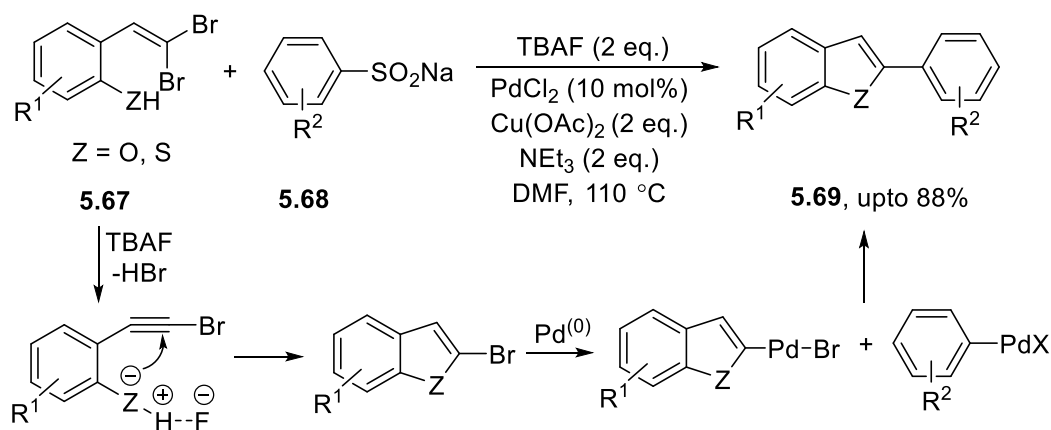


Scheme 5.16: Desulfitative cross-coupling between aryl bromides and arylsulfonates.



Scheme 5.17: Desulfitative cross-coupling between 1-bromo-4-(trifluoromethyl)benzene **5.62** and *p*-tolyl sulfinate **5.61**.

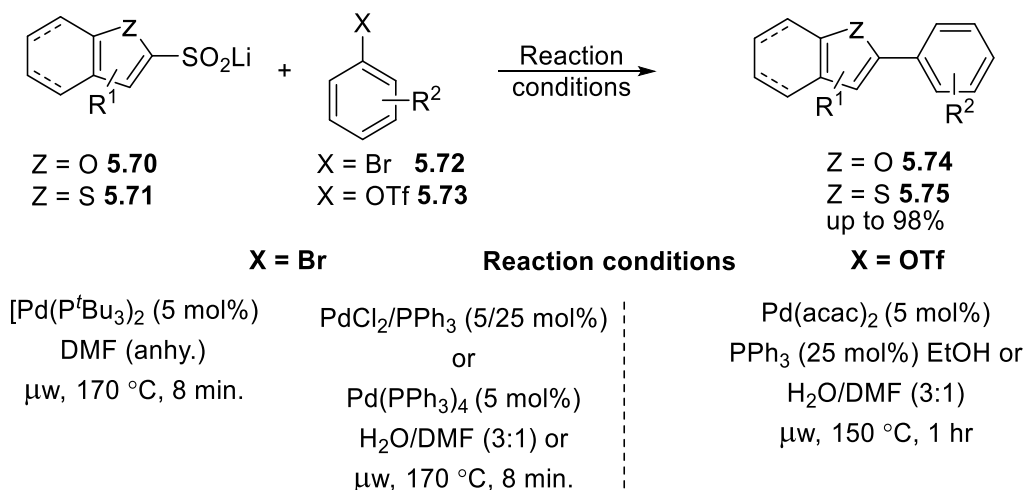
In the same year, Chen's group established a novel one-pot elimination-cyclisation-desulfitative reaction to convert 2-(gem-dibromovinyl)phenols(thiophenols) **5.67** into 2-arylbenzo-furans(thiophene) **5.69** under mild conditions.⁴⁰ In this efficient catalytic protocol, TBAF promotes the *in-situ* elimination of **5.67** followed by the intramolecular nucleophilic addition of aryl sulfinates **5.68** while the Pd(II) system plays a role for the desulfitative coupling reaction. This protocol does not utilise a phosphine ligand, but it incorporates a stoichiometric quantity of Cu(OAc)₂ to maintain the Pd(0) to Pd(II) catalytic cycle.



Scheme 5.18: Tandem elimination-cyclization-desulfitative reaction.

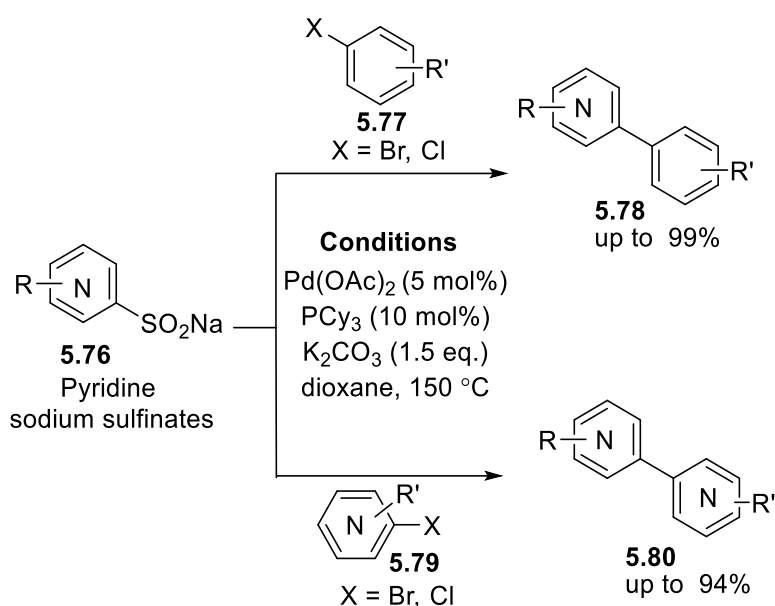
The Forgione and Willis groups have explored the reactivity of heteroaromatic sulfinates in palladium-mediated cross-couplings.^{41,42} The focus of the former group was on five-membered 2-heteroarene sulfinates whereas the latter studied both five- and six-membered heteroarenes.

Initially, Forgiione employed heteroaromatic sulfinates **5.70** & **5.71** to synthesise the C2-arylated heteroaromatics **5.74** & **5.75**. Both palladium pre-catalysts, Pd(P^tBu₃)₂ and Pd(PPh₃)₄ gave nearly similar results under microwave conditions for a short reaction time of 8 min. at 170 °C even when using wet solvents (Scheme 5.19).^{43,44} The presence of water was thought to reduce the rate of sulfinic acid disproportionation. The group has further evaluated the potential of aryl triflates **5.73** instead of aryl bromides **5.72** as electrophilic coupling partners.⁴⁵ Aryl triflates **5.73** have shown similar reactivity albeit with longer reaction times.



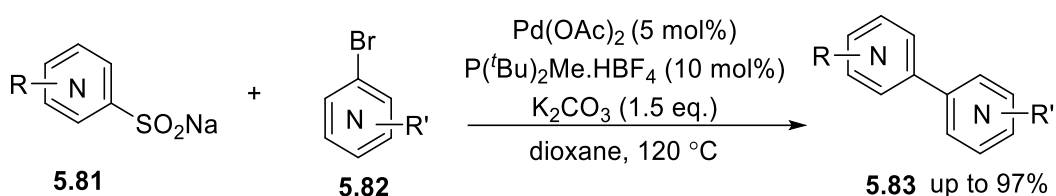
Scheme 5.19: Heteroaromatic desulfinitative cross-coupling with aryl bromides/triflates.

Willis and co-workers have shown that sulfinates are good replacements for azoheteroaryl boronates.⁴⁶ The initial investigation was focused on the reaction of pyridine sulfinates **5.76** (2-, 3- and 4-) as nucleophilic coupling partners with aryl bromide **5.77** (Scheme 5.20). A variety of six-membered heterocycles e.g. pyrazines, pyrimidines, quinolines, iminopyridines, and pyridines **5.79** were efficiently coupled with pyridine sulfinates to provide the corresponding bis-heterocyclic moieties **5.80**.



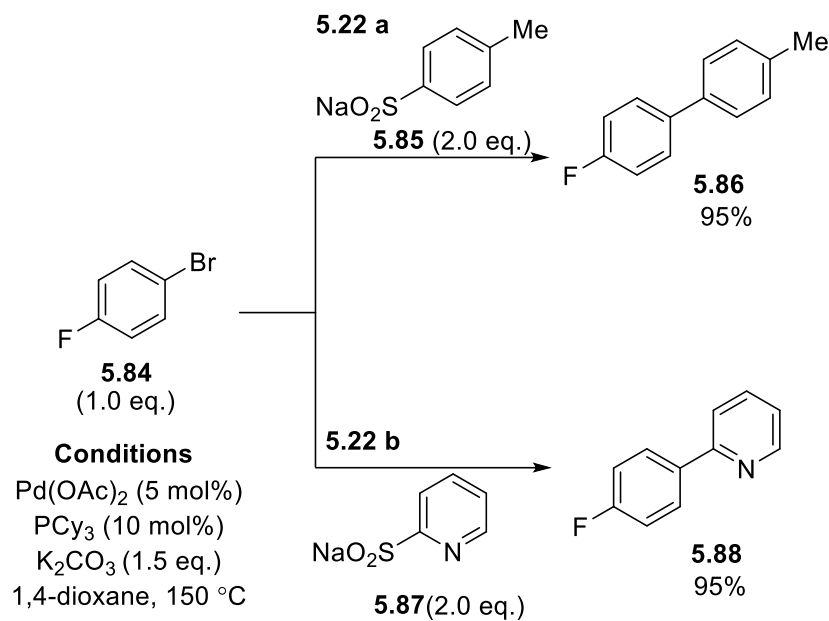
Scheme 5.20: Desulfinitative coupling of pyridine sulfonates **5.76** with aryl/heteroaryl halides **5.77/5.79**.

This methodology was later extended to couple both 5- and 6-membered heteroaryl sulfonates **5.81** (Scheme 5.21).⁴² The reaction protocol used a different ligand di-*tert*-butylmethylphospine [P(*t*-Bu)₂Me] and could be performed at lower temperature (120 °C) with less heteroaryl sulfinate (1.5 eq.). A broad range of heteroaryl sulfonates **5.81**, including pyrazine, pyridazine, pyrimidine, pyrazole, imidazole, and indazole sulfonates were coupled to deliver the bis-heteroaryl and aryl-heteroaryl derivatives **5.83** in an efficient manner.



Scheme 5.21: Desulfinitative coupling of heteroarene sulfonates **5.81** with heteroaryl/aryl halides **5.82**

Willis's group has performed a detail mechanistic investigation of these cross-coupling reactions, which provides better understanding of how the reaction proceeds.⁴⁷ Two model reactions were studied, the coupling of an aryl sulfinate **5.85** and a heteroaryl sulfinate **5.87**. (Scheme 5.22). Based on NMR spectroscopic data and the crystal structure studies of the intermediates, the detailed mechanisms for both reactions are postulated as illustrated in Figure 5.7.



Scheme 5.22: Model reactions to study the mechanism of desulfurative reaction.

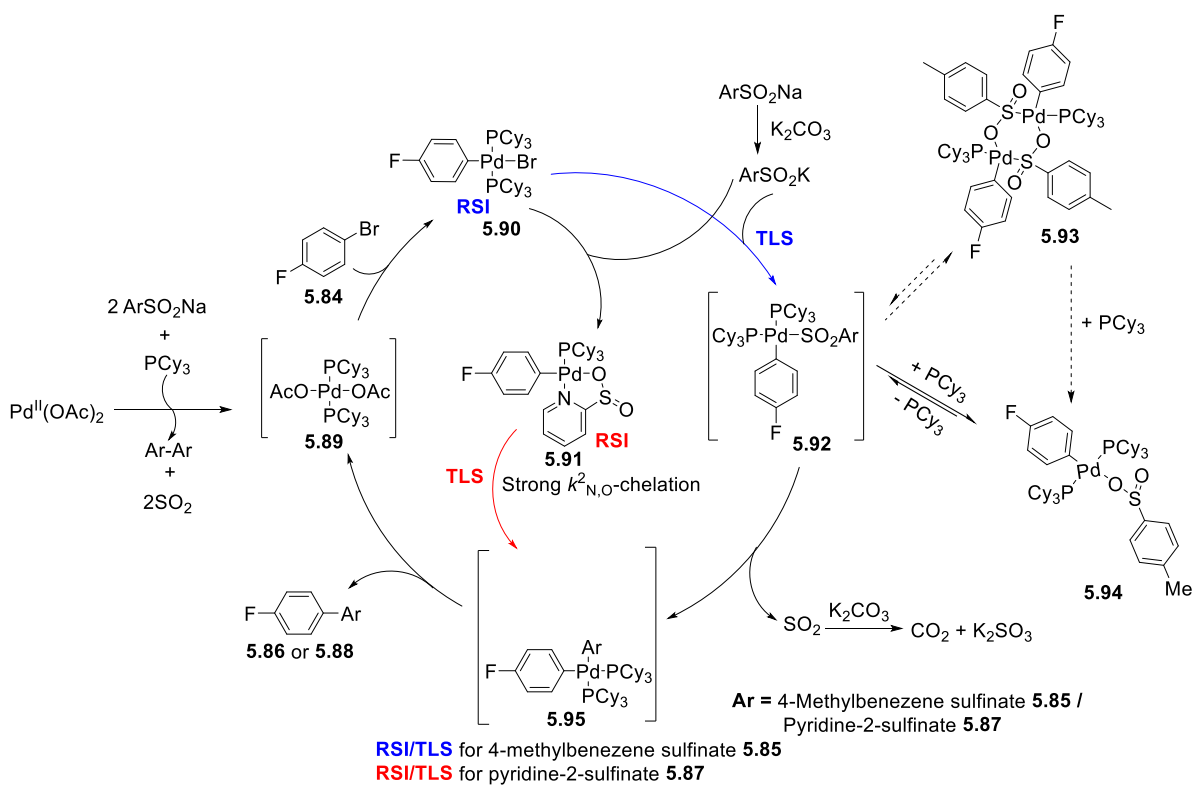


Figure 5.7: Proposed mechanisms of reactions in scheme 5.22.^h

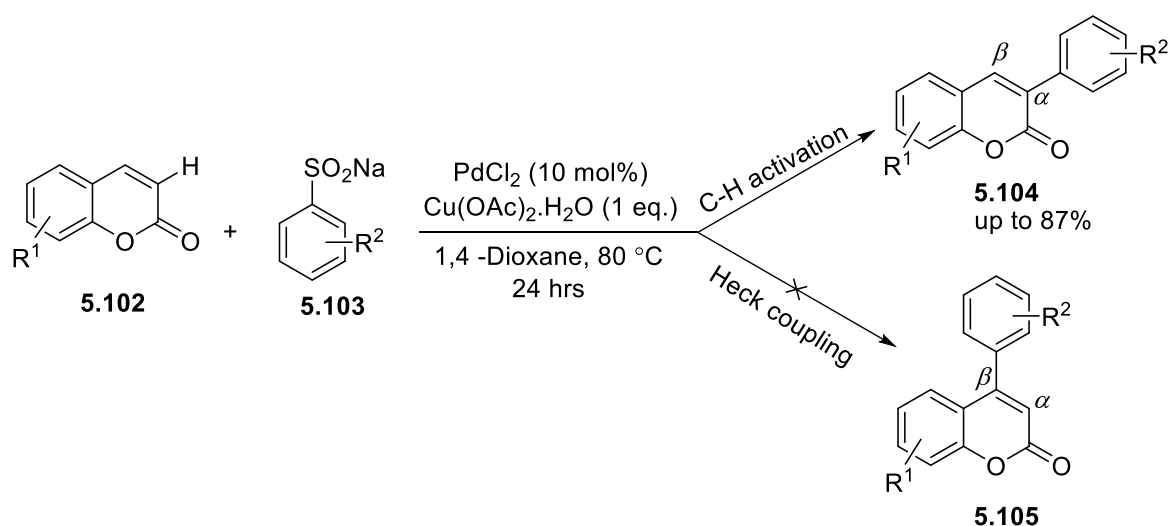
^h Scheme 5.22 to 5.25 and structure 5.95 to 5.101 were removed at the request of examiner.

5.5.3. Role of arylsulfonates in C-H activation reactions

C-H activation offers an efficient method for C-C bond formation and it is no surprise that arene sulfonates have been used as coupling partners. Recently, the arylation or alkylation of (hetero)aromatics *via* metal-catalysed C-H bond activation has revolutionised the field of chemistry. The scope of desulfitative reaction in metal catalysed C-H functionalisation is summarised in the review published by Jean-Francois¹¹ and Henri Doucet.¹² The section below depicts some of the recent advances of desulfitative C-H bond functionalisation using arylsulfonates as coupling partners.

5.5.3.1. Heteroarenes containing one heteroatom

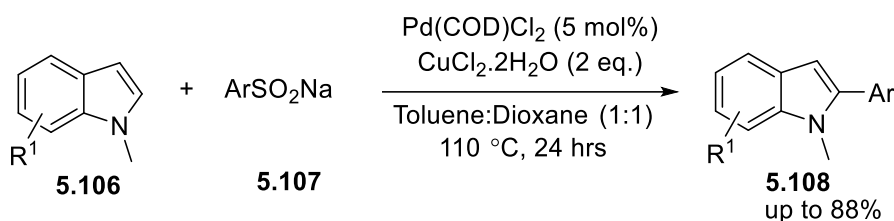
An unexpected and highly regioselective palladium-catalysed desulfitative arylation of coumarin **5.102** was achieved with commercially available arenesulfonates **5.103** by Jafarpour and co-workers (Scheme 5.26).⁴⁸ The authors were surprised to isolate 3-aryl coumarins **5.104** instead of the expected 4-aryl coumarins **5.105** (Heck-type products). The authors did not show the exact reason behind the observed regioselectivity; however, the arylsulfonato-S complex may have changed the course of the reaction. The copper salt was added as an oxidant and it also contributed in the desulfination process to form the aryl metal species.



Scheme 5.26: Regioselective synthesis of 3-aryl coumarin **5.104**.

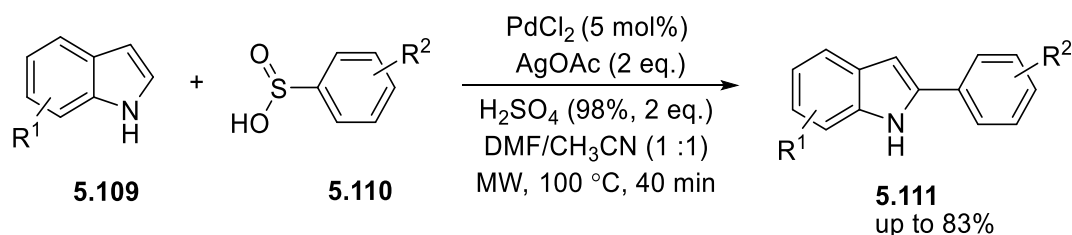
Luo and co-workers demonstrated a palladium-catalysed desulfitative arylation of *N*-methyl indoles **5.106** with sodium sulfonates **5.107** using copper(II) chloride dihydrate as the stoichiometric oxidant.⁴⁹ This methodology permits arylation exclusively in the C-2 position of the *N*-methyl indoles (Scheme 5.27). The coupling tolerates both electron-rich and electron-

poor substituents on *N*-methyl indole. All arylsulfonates reacted in good to excellent yields except those substituted with a nitro group, which was found to be unreactive. One limitation of this chemistry is that the indole had to be *N*-methylated. The free N-H compound failed to react.



Scheme 5.27: Desulfitative arylation of *N*-Methyl indoles **5.106**.

The latter limitation was overcome by performing the reaction under acidic conditions with microwave heating. While this method shared the same broad substrate scope as the previous arylation, it was found that arylsulfonic acids with *ortho*-substituents gave poor yields, presumably due to steric hindrance. The role of H₂SO₄ is still not known, although the authors proposed that it minimises the decomposition of indole and facilitates the regioselective C-2 arylation (Scheme 5.28).³⁷

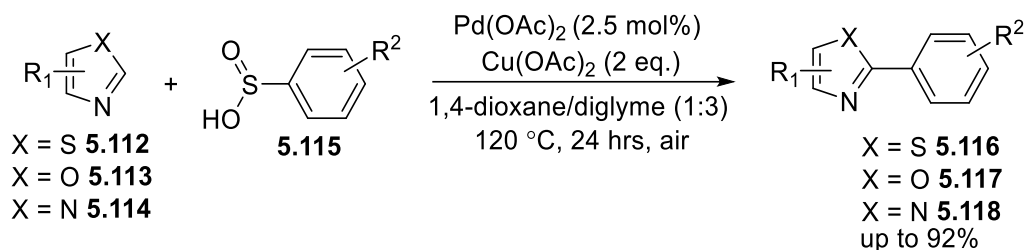


Scheme 5.28: C-2 arylation of free indole **5.109** with arylsulfonic acid **5.110**.

5.5.3.2. Heteroarenes containing more than one heteroatom

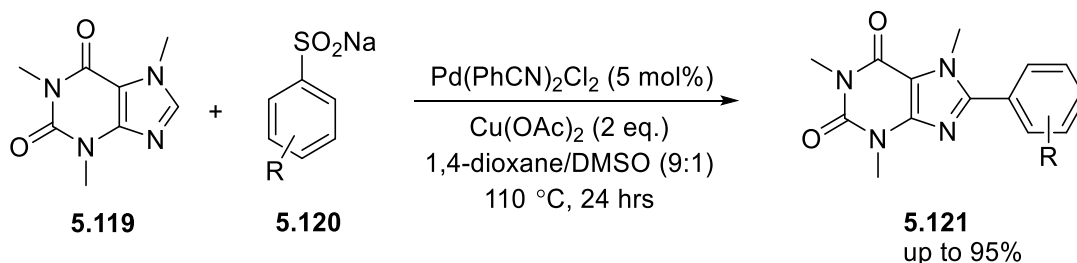
Heteroarenes containing more than one heteroatom, such as benzoxazoles, thiazoles, imidazoles, and purine derivatives, are important building blocks for many drug molecules and catalysts.⁵⁰ These molecules typically react at the most acidic site, which is between the two heteroatoms.

Deng's research group reported a palladium-catalysed direct desulfitative arylation of azoles. The optimised methodology comprises Pd(OAc)₂, Cu(OAc)₂ in 1,4-dioxane/diglyme. A wide range of azoles, such as benzothiazole **5.112**, benzoxazole **5.113**, and imidazoles **5.114** with the diverse substituents tolerated this protocol (Scheme 5.29).⁵¹



Scheme 5.29: Desulfitative C-H arylation of azoles.

Yu et al. revealed the construction of aryl-heteroaryl bonds by the transition-metal catalysed C-H arylation of a wide range of *N*-heteroarenes **5.119** (Scheme 5.30).⁵² The study mainly focused on caffeine derivatives and was subsequently expanded to other xanthines including benzylic theobromine, benzylic theophylline, and *n*-butyl theophylline.



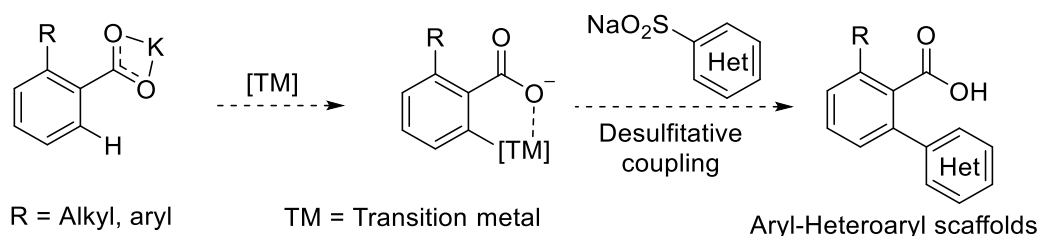
Scheme 5.30: C-H arylation of caffeine with aryl sulfonates.

In general, over the past few years, the role of aryl(heteroaryl) sulfonates as either electrophilic or nucleophilic coupling partners has been expanded from the synthesis of sulfones and sulfonamides to the desulfitative cross-coupling and C-H functionalisation reactions. Despite the substantial improvements in the desulfitative reaction conditions, the application of sulfonate reagents is limited to $\text{C}(sp^2)\text{-C}(sp^2)$ bond formation. However, research in this area is still in its infancy. There are only a few reports of $\text{C}(sp^3)\text{-C}(sp^2)$ bond formation by employing sulfonate derivatives. The scope of sulfonates in C-H functionalisation is also limited. Moreover, the potential of only a few arene/heteroarene sulfonates have been realised in the desired transformations. The nature of heteroarene sulfonates on reactivity and selectivity is yet to be explored. Here, I present our efforts to broaden the scope of sulfonates with emphasis on the heteroarene sulfonates in the desulfitative reactions.

5.6. Results and Discussion

The desulfitative coupling of sulfinates in the direct arylation of (hetero)arenes is becoming increasingly important.¹³ The majority of these coupling reactions are based on the functionalisation of the most acidic proton of a heterocycle.¹² To the best of our knowledge, there have been no reports where heterocyclic sulfinates have been employed in the desulfitative C-H activation reaction. Thus, our research group has decided to answer the following challenge of sulfinate chemistry.

1. Can we develop an efficient system for regioselective C-H functionalisation *via* desulfitative coupling using heteroarene sulfinates? (Scheme 5.31)



Scheme 5.31: Synthetic plan to access aryl-heteroaryl scaffolds *via* desulfitative coupling.

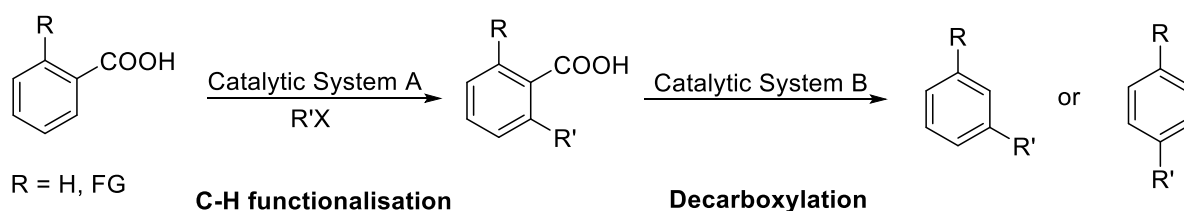
The issue of regioselectivity can be solved by introducing an appropriate directing group for the selective cleavage of the proximal aromatic C-H bond.⁵³⁻⁵⁷ However, there are a few drawbacks,

- Installation and removal of the directing group require additional steps
- Removal of the directing group is often problematic, requiring either harsh or long sequences; leaving the directing group in the molecule limits product utility.
- Directing groups can direct to both *ortho* positions.
- Only a few directing groups allow further *ipso* functionalisation after removal.

Over the last decade, a number of groups have shown that carboxylic acids can act as directing groups, allowing direct C-H activation to form C-C, C-O, C-N, C-S, C-P, and C-halogen bonds.⁵⁸ The main advantage of carboxylic directing groups is their intrinsic weak-coordinating ability and weak σ -donor tendency. They are attractive directing groups in numerous transformations due to their prevalence. These functionalities can be readily synthesised by means of various well-established methods. Furthermore, most of them are air and moisture stable, easy to handle, and have a long-life expectancy.

The majority of the reactions utilise the aromatic acids for the regioselective *ortho*-decarboxylative C-H activation reactions. Recently, the *meta*- and *para*-substituted moieties can also be achieved by a traceless carboxylic *ortho* directing group. In this approach, the products with *meta*- and *para*- substituents can be directly accessed which otherwise require conversion of directing group at *ortho* position into another functional group (Scheme 5.31a). Decarboxylative C-H functionalisation reactions generally follow either of the two mechanistic pathways.

- The redox-neutral decarboxylation to form a nucleophilic organometallic intermediate in which the oxidation state of the metal ion does not change
- Oxidative decarboxylation to form radical intermediates in which the oxidation state of the metal changes as the catalytic cycle progresses.

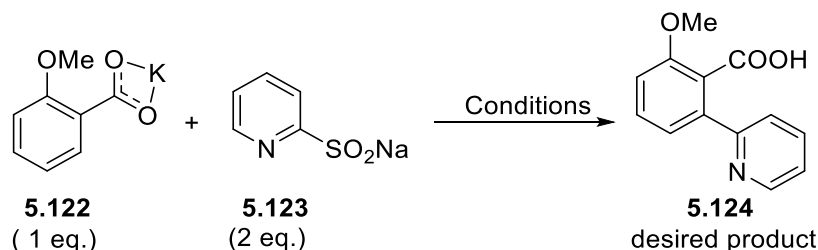


Scheme 5.31a: Traceless/deciduous directing groups.

With such a great potential of carboxylic acid derivatives for an *ortho* C-H functionalisation, we sought to develop a carboxylic acid-directed desulfination to access for aryl-heteroaryl scaffolds in a selective and efficient way (Scheme 5.31). Our main target was to choose an *ortho*-substituted aromatic acid to avoid double functionalisation and use the acid functionality as a directing group to introduce a heteroarene at the *ortho* position in the desulfinitative reaction.

5.6.1. Initial optimisation for desulfinitative coupling

Based on our plan, we selected the potassium salt of 2-methoxybenzoic acid **5.122** and pyridine-2-sulfinate **5.123** as our test substrates (Scheme 5.32).



Scheme 5.32: Initial investigation for desulfinitative coupling.

We postulated the mechanism of this reaction as illustrated in Figure 5.8. The first step would be the carboxylic acid-directed Pd(II) insertion into the *ortho* C-H bond to form the dimeric palladacycle **I** as described by Yu et al. (step 1).⁵⁹ The palladacycle usually adopts dimeric or trinuclear forms in the absence of any external ligand.⁵⁹ For an efficient desulfitative coupling, it is imperative at this stage for the catalytic cycle to proceed through an efficient transmetalation step to give a *trans*-monomeric intermediate **II**. The expulsion of SO₂ gas in the next step will result in the palladium intermediate **III**, which would subsequently deliver the desulfitative coupling product **5.124**.

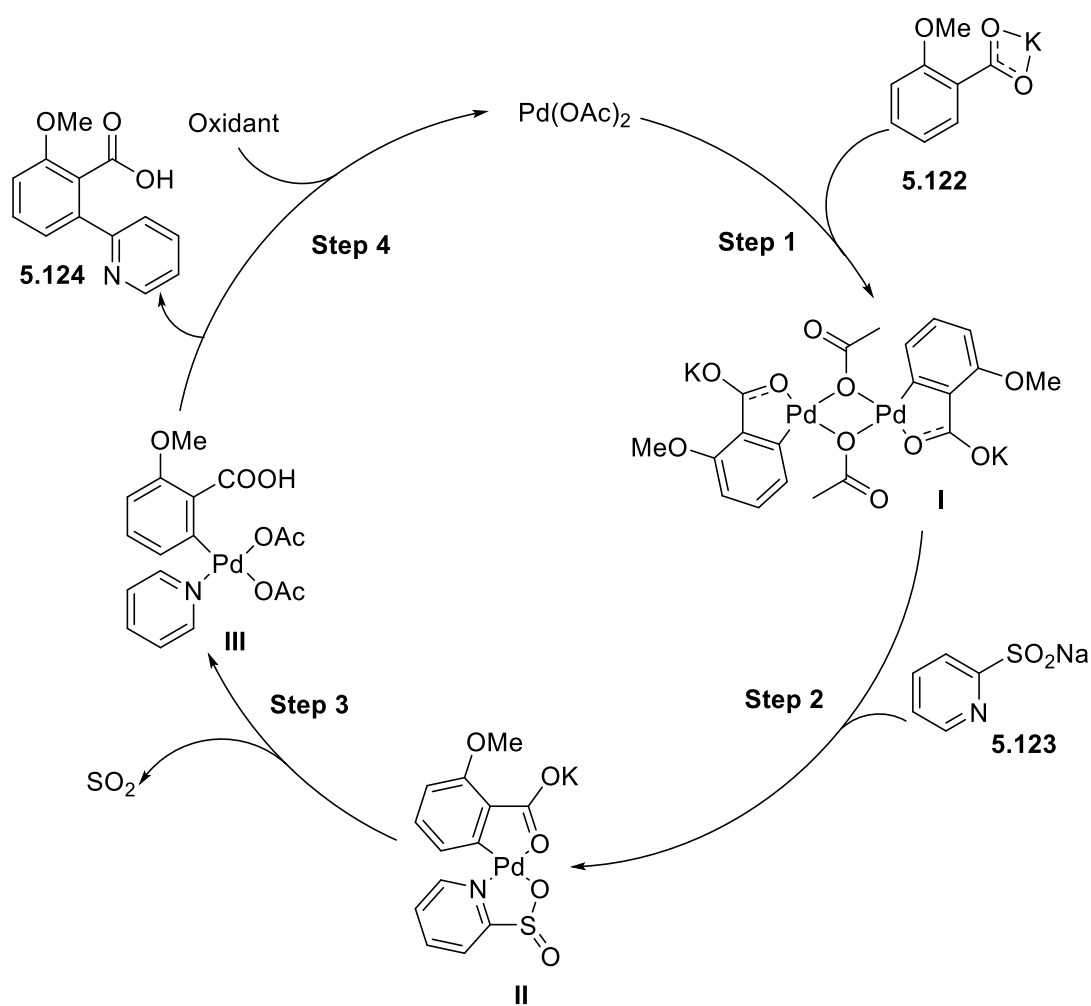
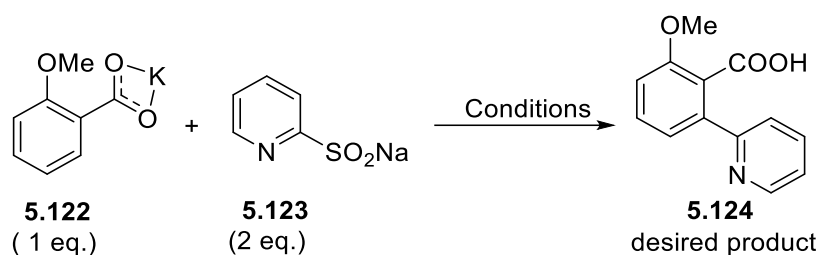


Figure 5.8: Plausible mechanism for desulfitative coupling.

Our initial reaction conditions are shown in Table 5.1.



Scheme 5.33: Initial investigation for desulfative coupling.

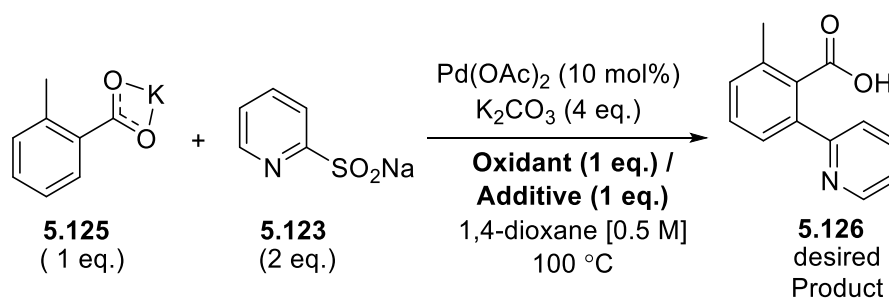
Table 5.1: Test conditions for desulfative coupling between potassium 2-methoxybenzoate and pyridine-2-sulfinate

Entry	[Pd] source	Ligand	Additive	Solvent Temperature	Observation
1 ⁴⁶	Pd(OAc) ₂ (5 mol%)	PCy ₃ (10 mol%)	K ₂ CO ₃ (1.5 eq.)	1,4-dioxane [0.1M], 150 °C	SM
2 ⁶⁰	Pd(OAc) ₂ (10 mol%)	PCy ₃ (20 mol%)	Ag ₂ O (1 eq.), BQ (0.5 eq.)	THF [0.1M], 60 °C	SM
3	Pd(OAc) ₂ (5 mol%)	PCy ₃ (10 mol%)	Ag ₂ O (1.5 eq.), BQ (0.5 eq.)	DMF:THF (1:1), 100 °C	SM
4	Pd(OAc) ₂ (5 mol%)	PCy ₃ (10 mol%)	Ag ₂ O (1.5 eq.), BQ (0.5 eq.)	<i>t</i> BuOH, 100 °C	SM
5 ⁴⁹	Pd(COD)Cl ₂ (5 mol%)	-	CuCl ₂ ·2H ₂ O (2.0 eq.)	toluene:1,4- dioxane (1:1), 110 °C	SM

SM = Starting material 2-methoxybenzoic acid recovered

The initial reaction used the conditions described by Willis for the cross-coupling of 2-pyridyl sulfinate **5.123** and aryl bromides but these conditions failed to deliver any product (entry 1).⁴⁷ Unlike Willis's reactions, directed C-H activation does not involve oxidative insertion into a C-Br bond and is more likely to follow a Pd(II) to Pd(0) pathway. This requires an oxidant to complete the catalytic cycle (Figure 5.8, step 4). We, therefore, decided to check the effects of oxidants like Ag₂O, Ag₂CO₃ and BQ. The reactions were performed with different oxidants in different (co)solvents, THF (entry 2), DMF (entry 3), and *tert*-butyl alcohol (entry 4), but to no avail. In all reactions, the starting material 2-methoxybenzoic acid was recovered without any sign of product formation. We also attempted the established procedure (entry 5) of desulfative direct arylation of indoles with substituted aryl sulfonates in the presence of CuCl₂·2H₂O, which follows the Pd(II) to Pd(0) cycle.⁴⁹ However, the result of this reaction was also disappointing, returning only the starting material.

At this stage, substantial changes were introduced to the reaction parameters. Firstly, the starting material was replaced by the potassium salt of *ortho*-toluic acid **5.125**, as we were concerned that the lone pair of electrons on the ether substituent adversely affected the five-membered palladacycle formation. The next trials were performed in the absence of any ligand. Lastly, we decided to reduce the reaction temperature to 100 °C (Scheme 5.34, Table 5.2).



Scheme 5.34: Screening of different oxidants and their effects on desulfinitative coupling.

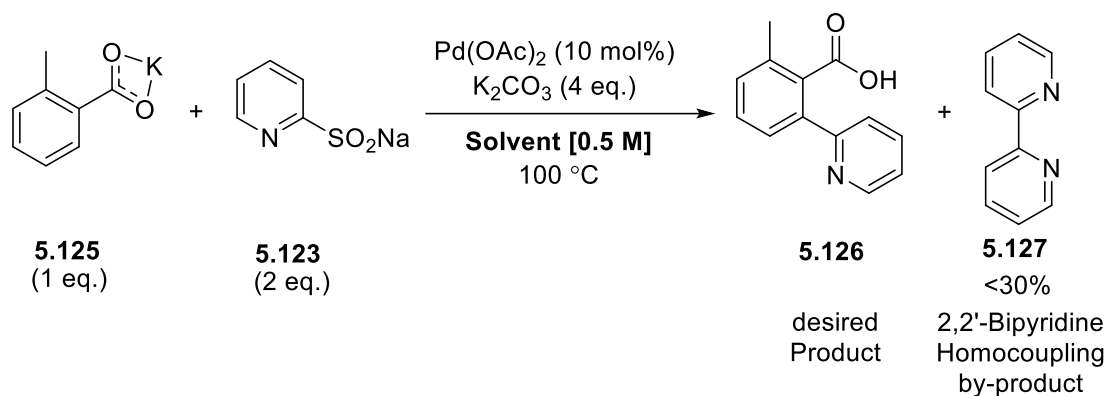
Table 5.2: Effect of different oxidants/additives in desulfinitative coupling between potassium *ortho*-toluic acid **5.125 and sodium pyridine-2-sulfinate **5.123****

Entry	Oxidant/additive	Observation
1	Cu(OAc) ₂ ·H ₂ O	SM
2	CuCl ₂	SM
3	Ag ₂ CO ₃	SM
4	K ₂ S ₂ O ₈	SM
5	CuCl ₂ + Pivalic acid	SM

SM = Starting material *ortho* toluic acid recovered

The next set of trial reactions kept the palladium source, the base, and the solvent constant and varied different oxidants (Scheme 5.34). Employing an excess quantity of carbonate would help to sequester liberated SO₂ gas and thus expedite the transmetalation step. However, only the starting material, *o*-toluic acid was recovered.

After observing no product formation in the above trials, we ruled out the influence of the oxidant. Though 1,4-dioxane has been shown to be an efficient solvent for a desulfinitative coupling,⁴⁶ the poor solubility of the potassium salt of the *ortho* toluic acid **5.125** was a concern. Maintaining the same reaction temperature 100 °C, the effect of polar solvents (THF, DME, *t*-amyl-OH, DMF, HFIP) was evaluated in the absence of the oxidant (Scheme 5.35). Surprisingly, in all cases (Table **5.3**), a significant proportion of homocoupling by-product 2,2'-bipyridine **5.127** was seen without the desired product **5.126** formation.



Scheme 5.35: Screening of different solvents and their effect on desulfitative coupling.

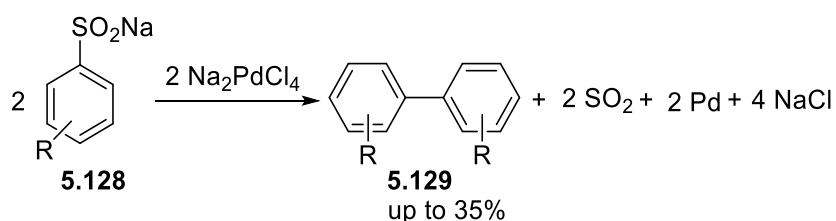
Table 5.3: Effect of different solvents in desulfitative coupling between potassium *ortho*-toluic acid and sodium pyridine-2-sulfinate

Entry	Solvent/oxidant	Observation*
1	THF	SM + 5.127
2	DME	SM + 5.127
3	<i>t</i> -amyl-OH	SM + 5.127
4	DMF	SM + 5.127
5	HFIP	SM + 5.127
6	1,4-dioxane	SM + 5.127
7	1,4-dioxane + Ag ₂ CO ₃	SM

SM = Starting material *ortho* toluic acid recovered

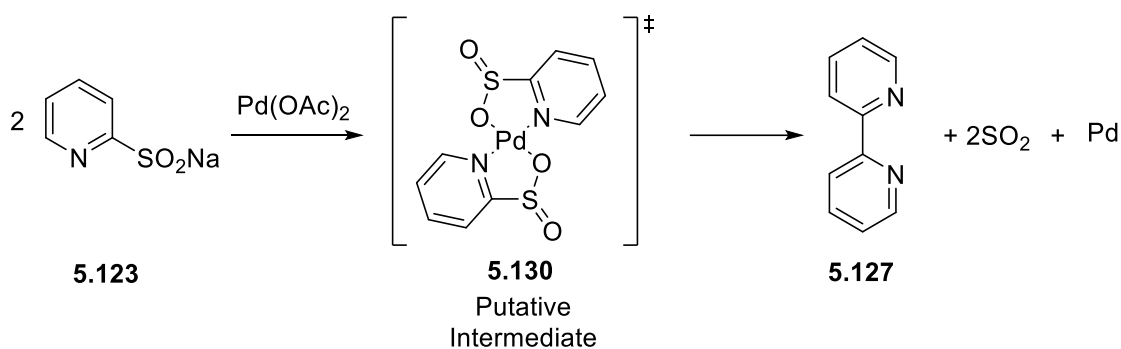
* 2,2'-bipyridine **5.127** was detected on the average <30%

The homocoupling of two arylsulfonates using a stoichiometric quantity of Pd(II) was reported by Garves.⁶¹ The author observed the evolution of SO₂ gas during the addition of a palladium salt to aromatic sulfonates **5.128** in a heated solution (Scheme 5.36). The aryl groups coupled to form biaryls **5.129** and Pd(II) was reduced to metallic palladium. The author proposed an electrophilic aromatic substitution process for this reaction.



Scheme 5.36: Homocoupling of arylsulfonates using a stoichiometric quantity of Pd(II).

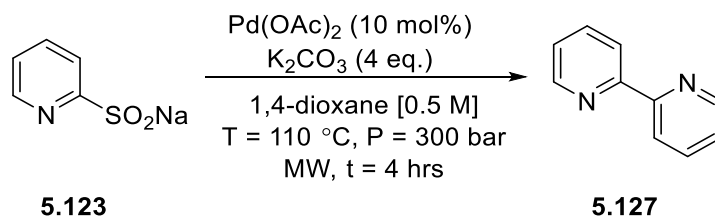
Based on this report, we speculated a similar palladium-mediated homocoupling with pyridyl-2-sulfonates **5.123**. We believed that the strong chelation of the Pd(II) catalyst in a $\kappa^2_{\text{N,O}}$ -mode of 2-pyridyl sulfinate leads to a five-membered palladacycle **5.130**, which ultimately forms the homocoupled by-product **5.127** (Scheme 5.37). However, the same homocoupling was not observed in the presence of oxidant Ag_2CO_3 . We surmise that silver replaces the palladium in the complex **5.130**.



Scheme 5.37: Plausible pathway of homocoupling of 2-pyridine sulfinate.

5.6.2. Investigation of the effect of catalytic Pd(OAc)_2 on the desulfitative homocoupling

We were curious to know whether the above homocoupling by stoichiometric Pd(OAc)_2 (Scheme 5.36) could be converted into a catalytic process. Initially, we screened the standard parameters such as solvent, base, temperature, and time under microwave irradiation as depicted in Table 5.4 (Scheme 5.38).



Scheme 5.38: Palladium-catalysed desulfitative homocoupling

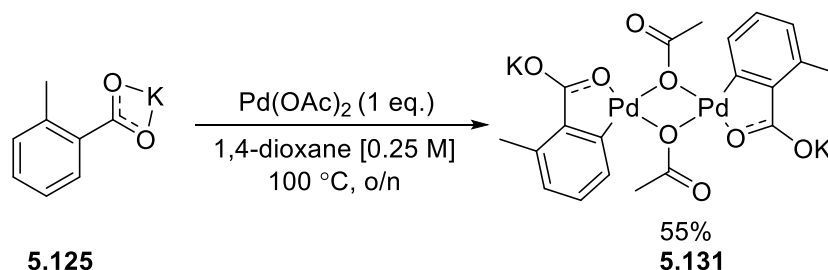
Table 5.4: Effect of catalytic palladium on the desulfitative homocoupling

Entry	Deviation from standard conditions	Yield ^a
1	No deviation	0%
2	Without K ₂ CO ₃	0%
3	NMP	25%
4	DMF	45%
5	DMF, t = 12 hrs	43%
6	DMF, without K ₂ CO ₃ , t = 12 hrs	46%
7	K-Me-palladacycle (10 mol%)	0%
8	K-Me-palladacycle (10 mol%), DMF, t = 12 hrs	42%

a: % Yield^{HPLC}, HPLC condition:- stationary phase: reverse phase C¹⁸ column, mobile phase: 5% H₂O: CH₃CN for 5 min., 100% CH₃CN for 25 min. RT for SM: 0.899 min., P: 2.790 min.

No self-coupling of pyridine-2-sulfinate **5.123** was observed with the sub-stoichiometric quantity of Pd(OAc)₂ (entry 1) or without K₂CO₃ in 1,4-dioxane at 110 °C (entry 2). It was reasoned that the poor solubility of pyridine-2-sulfinate **5.123** could be the problem, and hence more polar solvents *i.e.* DMF and NMP were investigated. The desulfitative self-coupled product **5.127** was observed in 25% (NMP, entry 3) and 45% (DMF, entry 4) yield. Proceeding further with the DMF solvent system, the experiment was set up for a long time 12 hrs, under the same reaction conditions. However, no significant change was seen in homocoupling product formation compared to the previous reaction (entry 5 & 6).

We also trialled a different palladium catalyst – pre-formed palladacycle of substrate **5.125**. The K-Me-palladacycle (K-Me-Palla.) **5.131** was easily synthesised by reacting equimolar amounts of potassium *o*-toluic acid **5.125** and Pd(OAc)₂ in dry 1,4-dioxane at 100 °C overnight (Scheme 5.39).^{59,62}

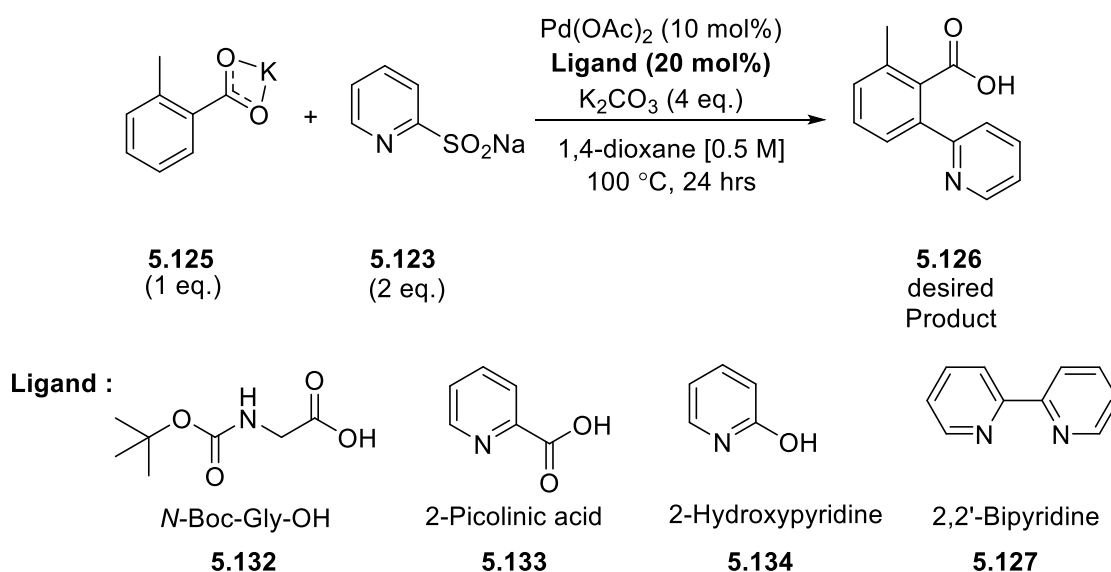
**Scheme 5.39:** Formation of K-Me-palladacycle **5.131**.

We thought that the metal metathesis (K/Na) between both substrates may alleviate the solubility problem. However, homocoupling was not observed with the catalytic palladacycle **5.131** (entry 7). When the reaction was performed with a pre-formed palladacycle **5.131** (10 mol%, 20 mol% Pd) in DMF (entry 8), the homocoupled product formed in the same range as in entry 4 & 5. This result suggests that increasing catalyst loading (10 mol% to 20 mol%) does not have any influence on homocoupling.

Based on this study, it became apparent that strong chelation of the palladium in a $\kappa^2_{\text{N,O}}$ -mode of pyridine-2-sulfinate **5.123** and resulting homocoupling by-product **5.127** hindered the desired cross-coupling. Even catalytic palladium can initiate the homocoupling between sulfonates in nearly 45% yield. It became necessary to prevent such chelation so that the palladium catalyst can actively participate in the desired desulfitative reaction. For this purpose, we decided to introduce an alternative ligand that would coordinate the palladium in the reaction parameters.

5.6.3. Investigation of effect of nitrogen-containing ligands

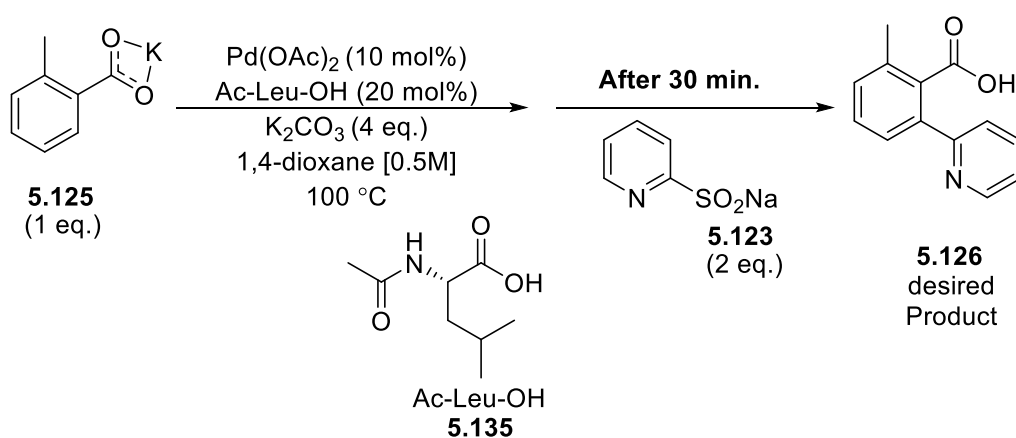
We postulated that the ligand may coordinate to the palladium catalyst and restrict the self-coupling of pyridine-2-sulfonates **5.123**. Particularly, nitrogen-based bidentate ligands possessing $\kappa^2_{\text{N,O}}$ -mode were selected which resembled pyridine-2-sulfinate **5.123** (Scheme 5.40).



Scheme 5.40: Screening of nitrogen-containing ligands and their effects on desulfitative coupling.

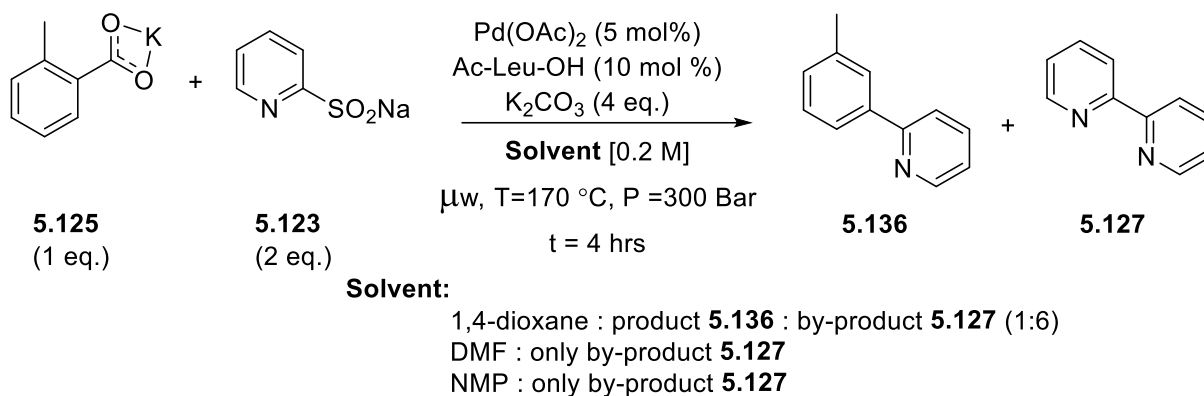
N-Boc-Gly-OH **5.132** and pyridine-based ligands, namely 2-picolinic acid **5.133**, 2-hydroxypyridine **5.134**, 2,2'-bipyridine **5.127** were screened in desulfitative reaction. To our surprise, only the starting material *o*-toluic acid was recovered. We were correct, the ligands prevent homocoupling. Unfortunately, they did not promote the desired coupling either.

We decided to change the order of addition of reactants. We thought if pyridine-2-sulfinate **5.123** is introduced at a later stage, in the reaction mixture, once the stable palladacycle had formed between *o*-toluic acid and Pd(OAc)₂, this time period may avoid any interference of chelate formation between Pd(OAc)₂ and 2-pyridinesulfinic acid. Unfortunately, the results were still not promising and only starting material was returned (Scheme 5.41).



Scheme 5.41: Reaction of changing the order of addition of pyridine-2-sulfinate **5.97**.

Next we also decided to reduce the number of equivalents of pyridine-2-substrate **5.123**, as well as the catalytic loading, while maintaining the 1:2 ratio of Pd(II) and Ac-Leu-OH **5.135** (MPAA) ligand. Reactions were set up separately in three different solvents, 1,4-dioxane, DMF, and NMP in microwave irradiation conditions (T = 170 °C, P = 300 Bar) with nearly half the concentration of solvent [0.5 M to 0.2 M] (Scheme 5.35). Gratifyingly, the desulfitative coupled product **5.136** was observed for the first time in 1,4-dioxane reaction conditions. We did not expect decarboxylation but the high reaction temperature caused it. The ratio of product **5.136** : 2,2'-bipyridine **5.127** was only 1:6 based on crude ¹H NMR spectroscopy. This result served as an inspiration for further optimisation.



Scheme 5.42: Pd(II)-catalysed desulfinitative coupling under microwave irradiation.

We thought that it made sense to study the reaction using a stoichiometric amount of palladium as this may allow to isolate intermediates and remove the need to regenerate the catalyst. If we succeed, then, this knowledge could be applied to developing a catalytic version.

5.6.4. Study with stoichiometric quantity of Pd(OAc)₂

The next experiment was set up to minimise the formation of complex **5.130** (Figure 5.9) so that the palladium catalyst could participate in C-H activation.

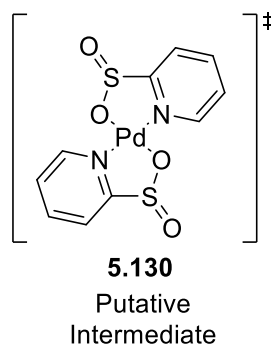
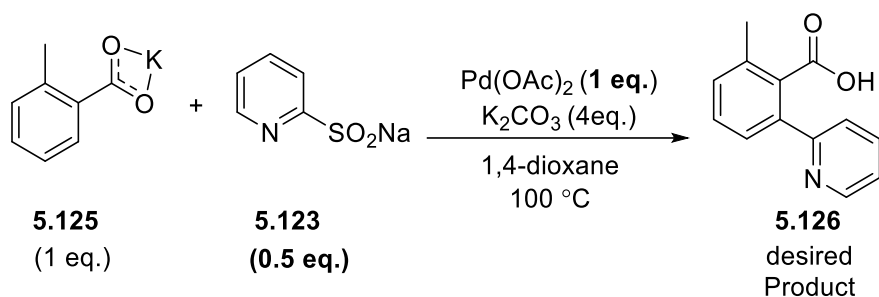


Figure 5.9: Putative complex of pyridine-2-sulfinate **5.123** with Pd(OAc)₂.

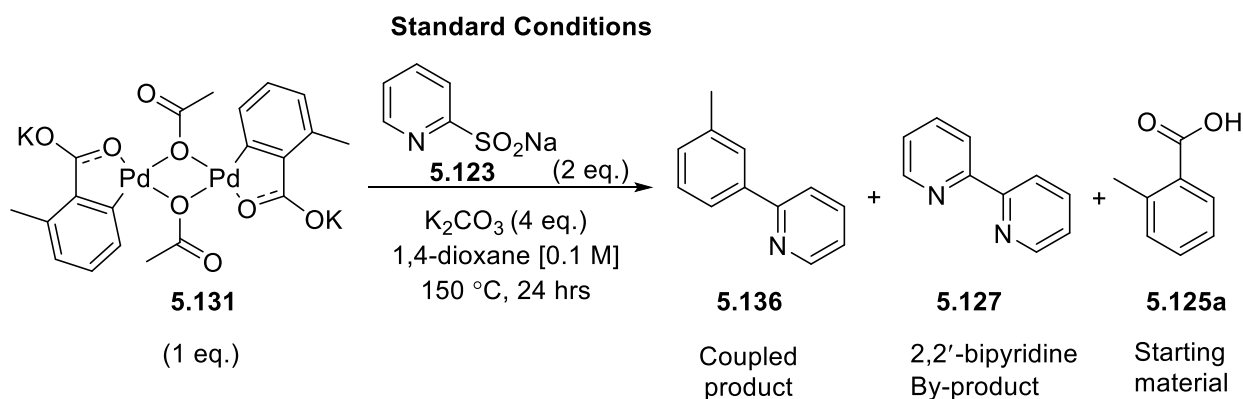
The reaction was set up by taking the same equivalent of Pd(OAc)₂ as the starting material, the potassium salt of *o*-toluic acid **5.125**, but reducing the amount (0.5 equivalent) of pyridine-2-sulfinate **5.123** (Scheme 5.43). To our surprise, neither homocoupling nor desulfinitative coupling was observed and only the starting material returned. The conclusion made from this reaction was that reducing the equivalent of pyridine substrate helps to repress both homocoupling and desulfinitative coupling.



Scheme 5.43: Attempted desulfitative coupling with 0.5 eq. of 2-pyridine sulfinate.

In order to simplify the reaction still further, we decided to attempt the reaction with K-Me-palladacycle **5.131**. This would mean directed C-H activation had already occurred and that all we would study was whether this could react with sulfinate. If this one step was impossible, we felt the entire methodology would be impossible.

As mentioned before, the K-Me-palladacycle **5.131** was easily synthesised by reacting equimolar quantities of potassium *o*-toluic acid and Pd(OAc)₂ in dry 1,4-dioxane at 100 °C overnight.^{59,62} The resulting dimeric palladacycle **5.131** was subsequently utilised for an optimisation study (Scheme 5.44, Table 5.5). Based on the previous study, the first reaction used a stoichiometric quantity of pyridine-2-sulfinate **5.123** compared to the palladacycle **5.131** with two equivalents of base, K₂CO₃ in 1,4-dioxane at 150 °C in a Schlenk tube. Pleasingly, the desulfitative coupling was observed and the product **5.136** was isolated in 27% isolated yield. Here also decarboxylation was observed. The homocoupling by-product **5.127** and the starting material **5.125a** were observed but could not be recovered from the reaction. Three repetitions were performed to prove the consistency and in all of them, the desired product was isolated in nearly the same yield (entry 1).



Scheme 5.44: Attempted desulfitative coupling with K-Me-palladacycle.

Table 5.5: Optimisation study: deviation from the standard conditions

Entry	Deviation from the standard conditions	Yield ^a		
		5.136	5.127	5.125a
1	Standard conditions (three repetitions)	27%	n.d.	n.d.
2	Oxidant: Benzoquinone B.Q. (2 eq.)	32%	n.d.	n.d.
3	Without base (K ₂ CO ₃)	33%	n.d.	n.d.
4	Pyridine-2-sulfinate 5.123 (4 eq.) without K ₂ CO ₃ , 165 °C	26%	n.d.	34%
5	Low temperature (100 °C)	20%	n.d.	n.d.
6	Solvent: NMP, at 165 °C	37%	33%	n.d.
7	Solvent: ^t BuOH, at 165 °C	n.d.	42%	n.d.
8	Solvent: DMF, at 165 °C	n.d.	46%	33%
9	MW: DMF, T = 170 °C, P = 300 bar, t = 4 hrs	17%	n.d.	n.d.

^a Isolated yield

n.d. = not detected

Encouraged by the initial result, we attempted to optimise the reaction conditions (Table 5.5). The inclusion of an oxidant, B.Q. was seen to improve product formation with a slightly higher yield (32%, entry 2). Removing the base also gave the product in nearly the same yield (33%, entry 3). We decided to double the loading of pyridine substrate **5.123** (2 eq.) and increase temperature to 166 °C, the reaction proceeded, albeit in lower yield (26%) with 34% *o*-toluic acid recovery (entry 4), once again showing an excess of pyridine-2-sulfinate **5.123** was detrimental to the reaction.

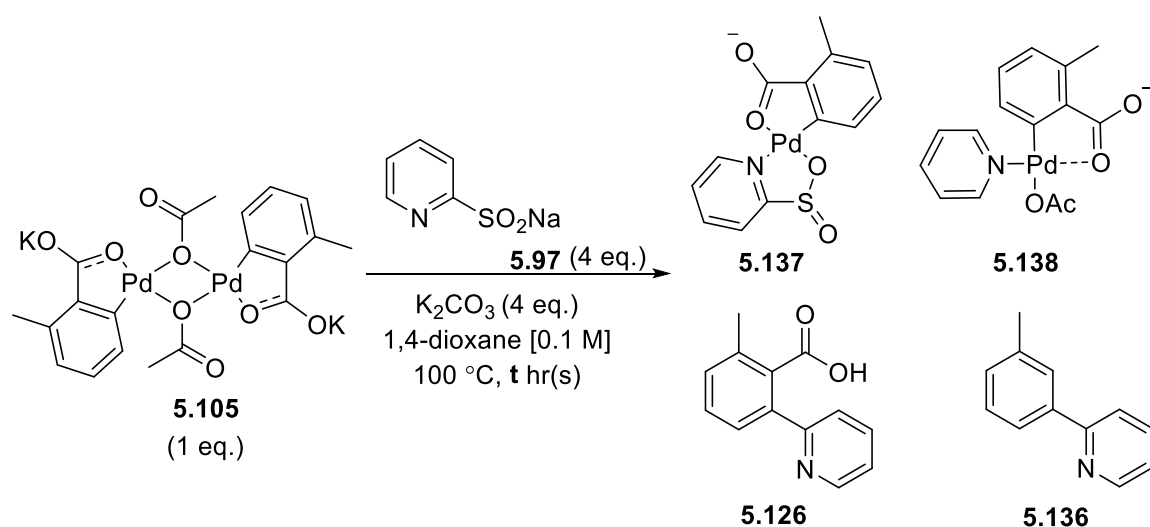
In a further optimisation attempt, the reaction was performed at 100 °C (entry 5), however, the yield dropped to 20%. The effect of different solvents was also evaluated. Using a more polar solvent was beneficial only for NMP. In this case, the conversion was seen in 37% with the recovery of 33% homocoupled by-product **5.127** (entry 6). On the contrary, the reaction in both ^tBuOH and DMF failed to produce desulfitative coupling, giving either the by-product **5.127** or the starting material **5.125a** only (entry 7 & 8). Further, the effect of microwave irradiation was also studied in order to reduce reaction time. The reaction conversion was affected and the product was isolated only in 17% yield.

Results from the attempted desulfitative coupling of pre-formed palladacycle **5.131** with pyridine-2-sulfinate **5.123** showed that the maximum yield could be achieved in a range of 27% to 37%. Changing the reaction parameters did not improve the product **5.136** formation.

We thought that the transmetallation might be the problematic step, which hindered the reaction progress. In order to gain more insight into the reaction mechanism, we planned to isolate products or intermediates at different time intervals.

5.6.5. Time-based study with a stoichiometric quantity of Pd(OAc)₂

In this study, a total six reactions were set up with the same reaction conditions for 1 h, 2 hrs, 4 hrs, 8 hrs, 12 hrs, and 24 hrs to check the reaction progress (Scheme 5.45, Table 5.6). All reactions were purposefully carried out at 100 °C to allow isolation of the all-possible stable intermediates and subsequently their characterisation.



Scheme 5.45: Time-based study for desulfurative coupling with dimeric K-Me-palladacycle.

Table 5.6: Time-based study

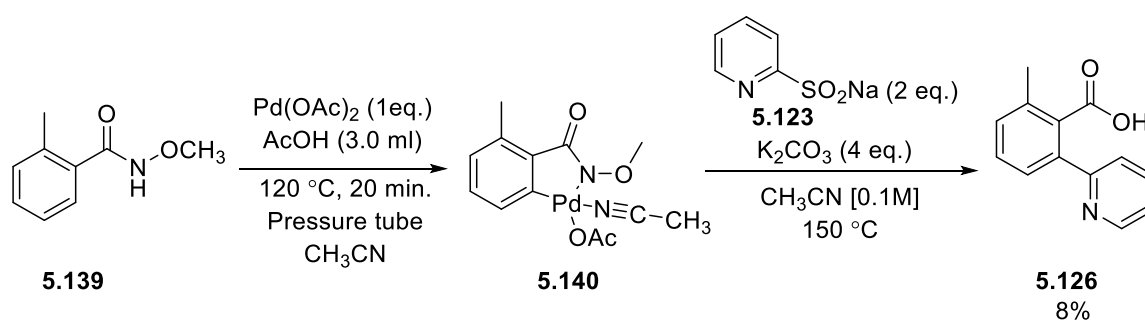
Entry	Time hr(s)	Observation
1	1 hr	5.137 + 5.138
2	2 hrs	5.137 + 5.138
3	4 hrs	5.137 + 5.138
4	8 hrs	5.126
5	12 hrs	5.126
6	24 hrs	5.136

After 1 hour, the data implies that complex **5.137** was formed although we did not isolate it. The ¹H NMR spectroscopy was showing a shift of the resonance for the proton adjacent to the pyridine nitrogen at 9.1 ppm which was at 8.6 in pyridine-2-sulfinate **5.123**. The isotope pattern in mass spectrometry (m/z = 381) and fragmentation peak at m/z = 318 also indicated the formation of plausible complex **5.137** and intermediate **5.138** after SO₂ extrusion (entry 1). However, the intermediate **5.137** was not isolated in enough quantity for ¹³C NMR and

attempted crystallisation also failed to give a single crystal for X-ray crystallography. The reaction gave the same results after 2 hours (entry 2). Based on these results, we speculated that the tendency of pyridine-2-sulfinate **5.123** towards the strong co-ordination to the palladium *via* $\kappa^2_{\text{N,O}}$ is a driving force for the transmetallation step. Once the intermediate **5.137** is formed, it might possess lower energy, making the expulsion of SO₂ slower as seen from the outcome of the reaction after 4 hrs.

The reaction data after 8 hrs indicated the formation of the coupled product **5.126** (with an acid functionality). The analysis of the reaction after 12 hrs produced similar characterisation data. These results suggest a chelated Pd(II)-sulfinate intermediate **5.138** formed post-transmetallation is the resting-state intermediate, while the extrusion of the SO₂ is the turnover-limiting step. This suggestion is in agreement with Willis's study published later in 2020.⁴⁷ The loss of CO₂ is most likely to be a slower rate, delivering the decarboxylative product **5.136** in between 12 hrs to 24 hrs.

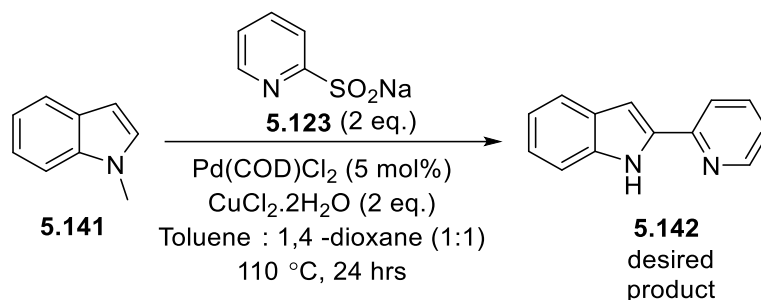
In an extension of our study, we thought to check the desulfitative reaction on palladacycle **5.140**. The *N*-methylbenzamide **5.139** was reacted with a stoichiometric quantity of Pd(OAc)₂ in AcOH at 120 °C as reported by Masilamani et al. (Scheme 5.46).⁶³ The reaction was carried out with the resultant palladacycle **5.140** and pyridine-2-sulfinate **5.123** in dry CH₃CN at 150 °C. The reaction proceeded to furnish the desulfitative coupled product **5.126** without corresponding decarboxylation as suggested by the crude ¹H NMR spectroscopy and mass spectrometry techniques.



Scheme 5.46: Study of desulfitative coupling with palladacycle **5.140**.

Due to the problem of coupling of pyridine-2-sulfinate **5.123**, we sought to simplify the experiment. Lao and co-workers have shown that aryl sulfonates can be coupled to *N*-methyl indole **5.141** in good yield.⁴⁹ We attempted to replicate this experiment but replacing the aryl sulfonate with the pyridine-2-sulfinate **5.123** (Scheme 5.47). A large number of conditions were attempted but all to no avail. This study suggests that the presence of strong chelation in

a $\kappa^2_{\text{N,O}}$ -mode of pyridine-2-sulfinate **5.123** by the Pd(II)-catalyst and resulting five-membered palladacycle **5.130** is impeding the desulfitative coupling.



Scheme 5.47: Attempted desulfitative coupling of *N*-methyl indole with pyridine-2-sulfinate.

5.7. Conclusions

This project was aimed at the site-selective carboxylic acid-directed C-H functionalisation *via* desulfitative coupling with pyridine-2-sulfinate **5.123**. Initial optimisation with a Pd(OAc)₂ catalyst failed to deliver any desired product. Moreover, significant homocoupling between the 2-pyridyl substrate was observed to form 2,2'-bipyridine **5.127**. Hence, we evaluated the efficiency of catalytic Pd(OAc)₂ to probe such homocoupling. Surprisingly, it can initiate this side-reaction up to 45%. We sought to suppress homocoupling by introducing nitrogen-based bidentate ligands. Fortunately, we were able to solve this problem with *N*-Ac-Leu ligand **5.135**, but the desired desulfitative coupling was obtained in a minute yield. Further, in our study with pre-formed palladacycle **5.131**, where directed C-H activation had already been achieved, the desulfitative coupling was obtained in a moderate yield. Our time-based study allowed us to investigate the course of this reaction with analysis of possible intermediates.

Our designed method involves two progressive steps: directed C-H activation and desulfination. It became clear that the last step of desulfitative coupling is a problematic step. We reasoned this owing to the slow SO₂ expulsion from the intermediate **5.137** and reductive elimination thereafter. Based on our study, we surmised that extrusion of SO₂ is a problematic step. In general, the kinetics of reductive elimination is difficult to predict but a detailed kinetic analysis will provide insight into the reaction mechanism. We also suggest that further optimisation can be performed in order to improve the reductive elimination step e.g. by varying transition metals, improving bidentate ligand design with the wide bite angle, and increasing the steric hindrance to the metal centre.

5.8. References

- (1) Pitt, W. R.; Parry, D. M.; Perry, B. G.; Groom, C. R. Heteroaromatic Rings of the Future. *J. Med. Chem.* **2009**, *52*, 2952.
- (2) Knowles, J. P.; Whiting, A. The Heck–Mizoroki cross-coupling reaction: a mechanistic perspective. *Org. Biomol. Chem.* **2007**, *5*, 31.
- (3) Han, F.-S. Transition-metal-catalyzed Suzuki–Miyaura cross-coupling reactions: a remarkable advance from palladium to nickel catalysts. *Chem. Soc. Rev.* **2013**, *42*, 5270.
- (4) Cordovilla, C.; Bartolomé, C.; Martínez-Ilarduya, J. M.; Espinet, P. The Stille Reaction, 38 Years Later. *ACS Catal.* **2015**, *5*, 3040.
- (5) Phapale, V. B.; Cárdenas, D. J. Nickel-catalysed Negishi cross-coupling reactions: scope and mechanisms. *Chem. Soc. Rev.* **2009**, *38*, 1598.
- (6) Nicolaou, K. C.; Bulger, P. G.; Sarlah, D. Palladium-Catalyzed Cross-Coupling Reactions in Total Synthesis. *Angew. Chem. Int. Ed.* **2005**, *44*, 4442.
- (7) Schafer, L. L.; Mountford, P.; Piers, W. E. Earth abundant element compounds in homogeneous catalysis. *Dalton Trans.* **2015**, *44*, 12027.
- (8) Larsen, C. B.; Wenger, O. S. Photoredox Catalysis with Metal Complexes Made from Earth-Abundant Elements. *Chem. Eur. J.* **2018**, *24*, 2039.
- (9) Introduction: CH Activation. *Chem. Rev.* **2017**, *117*, 8481.
- (10) Sun, C.-L.; Shi, Z.-J. Transition-Metal-Free Coupling Reactions. *Chem. Rev.* **2014**, *114*, 9219.
- (11) Ortgies, D. H.; Hassanpour, A.; Chen, F.; Woo, S.; Forgione, P. Desulfination as an Emerging Strategy in Palladium-Catalyzed C–C Coupling Reactions. *Eur. J. Org. Chem.* **2016**, *2016*, 408.
- (12) Yuan, K.; Soulé, J.-F.; Doucet, H. Functionalization of C–H Bonds via Metal-Catalyzed Desulfinitative Coupling: An Alternative Tool for Access to Aryl- or Alkyl-Substituted (Hetero)arenes. *ACS Catal.* **2015**, *5*, 978.
- (13) Aziz, J.; Messaoudi, S.; Alami, M.; Hamze, A. Sulfinatate derivatives: dual and versatile partners in organic synthesis. *Org. Biomol. Chem.* **2014**, *12*, 9743.
- (14) W. Peters. *Ber. Dtsch. Chem. Ges.* **1905**, *38*, 2567.
- (15) Cookson, P. G.; Deacon, G. B. The formation of mercury-carbon bonds by sulphur trioxide elimination. *J. Organomet. Chem.* **1971**, *27*, C9.
- (16) Blakemore, P. R.; Sephton, S. M.; Ciganek, E. The Julia–Kocienski Olefination. *Org. React.* **2018**, *1*.
- (17) Sraj, L. O. C.; Khairallah, G. N.; da Silva, G.; O’Hair, R. A. J. Who Wins: Pesci, Peters, or Deacon? Intrinsic Reactivity Orders for Organocuprate Formation via Ligand Decomposition. *Organometallics* **2012**, *31*, 1801.
- (18) Ahrland, S.; Chatt, J.; Davies, N. R. The relative affinities of ligand atoms for acceptor molecules and ions. *Q. Rev. Chem. Soc.* **1958**, *12*, 265.
- (19) F. C. Whitmore, F. H. H. *Org. Synth.* **1922**, *2*, 89.
- (20) Deeming, A. S.; Russell, C. J.; Hennessy, A. J.; Willis, M. C. DABSO-Based, Three-Component, One-Pot Sulfone Synthesis. *Org. Lett.* **2014**, *16*, 150.
- (21) Zapf, A.; Beller, M. The development of efficient catalysts for palladium-catalyzed coupling reactions of aryl halides. *Chem. Commun.* **2005**, 431.
- (22) Shavnya, A.; Coffey, S. B.; Smith, A. C.; Mascitti, V. Palladium-Catalyzed Sulfinatation of Aryl and Heteroaryl Halides: Direct Access to Sulfones and Sulfonamides. *Org. Lett.* **2013**, *15*, 6226.
- (23) Gianatassio, R.; Kawamura, S.; Eprile, C. L.; Foo, K.; Ge, J.; Burns, A. C.; Collins, M. R.; Baran, P. S. Simple sulfinatate synthesis enables C-H trifluoromethylcyclopropanation. *Angew. Chem. Int. Ed. Engl.* **2014**, *53*, 9851.
- (24) Saraiva, M. F.; Couri, M. R. C.; Le Hyaric, M.; de Almeida, M. V. The Barton ester free-radical reaction: a brief review of applications. *Tetrahedron* **2009**, *65*, 3563.
- (25) Cottrell, T. L. *The Strengths of Chemical Bonds*; Butterworths Publications Ltd., London, **1958**.

- (26) Christoffel, F.; Ward, T. R. Palladium-Catalyzed Heck Cross-Coupling Reactions in Water: A Comprehensive Review. *Catal. Lett.* **2018**, *148*, 489.
- (27) Bal Raju, K.; Mari, V.; Nagaiah, K. Regioselective Palladium(II)-Catalyzed Desulfinitive Heck-Type Reaction: Access to α -Benzyl- β -keto Esters from Baylis–Hillman Adducts and Sodium Sulfinates. *Synthesis* **2013**, *45*, 2867.
- (28) Zhang, D.; Wang, Q. Palladium catalyzed asymmetric Suzuki–Miyaura coupling reactions to axially chiral biaryl compounds: Chiral ligands and recent advances. *Coord. Chem. Rev.* **2015**, *286*, 1.
- (29) Lennox, A. J. J.; Lloyd-Jones, G. C. Selection of boron reagents for Suzuki–Miyaura coupling. *Chem. Soc. Rev.* **2014**, *43*, 412.
- (30) Cheng, K.; Yu, H.-Z.; Zhao, B.; Hu, S.; Zhang, X.-M.; Qi, C. Palladium-catalyzed desulfinitive cross-coupling of arylsulfinates with arylboronic acids. *RSC Adv.* **2014**, *4*, 57923.
- (31) Nakao, Y.; Hiyama, T. Silicon-based cross-coupling reaction: an environmentally benign version. *Chem. Soc. Rev.* **2011**, *40*, 4893.
- (32) Hiyama, T. How I came across the silicon-based cross-coupling reaction. *J. Organomet. Chem.* **2002**, *653*, 58.
- (33) Cheng, K.; Hu, S.; Zhao, B.; Zhang, X.-M.; Qi, C. Palladium-Catalyzed Hiyama-Type Cross-Coupling Reactions of Arenesulfinates with Organosilanes. *J. Org. Chem.* **2013**, *78*, 5022.
- (34) Chinchilla, R.; Nájera, C. Recent advances in Sonogashira reactions. *Chem. Soc. Rev.* **2011**, *40*, 5084.
- (35) Wang, X.; Song, Y.; Qu, J.; Luo, Y. Mechanistic Insights into the Copper-Cocatalyzed Sonogashira Cross-Coupling Reaction: Key Role of an Anion. *Organometallics* **2017**, *36*, 1042.
- (36) Xu, Y.; Zhao, J.; Tang, X.; Wu, W.; Jiang, H. Chemoselective Synthesis of Unsymmetrical Internal Alkynes or Vinyl Sulfones via Palladium-Catalyzed Cross-Coupling Reaction of Sodium Sulfinates with Alkynes. *Adv. Synth. Catal.* **2014**, *356*, 2029.
- (37) Zhou, C.; Liu, Q.; Li, Y.; Zhang, R.; Fu, X.; Duan, C. Palladium-Catalyzed Desulfinitive Arylation by C–O Bond Cleavage of Aryl Triflates with Sodium Arylsulfinates. *J. Org. Chem.* **2012**, *77*, 10468.
- (38) Ortgies, D. H.; Barthelme, A.; Aly, S.; Desharnais, B.; Rioux, S.; Forgione, P. Scope of the Desulfinylative Palladium-Catalyzed Cross-Coupling of Aryl Sulfinates with Aryl Bromides. *Synthesis* **2013**, *45*, 694.
- (39) K. Sato, T. O. In *Process for producing aromatic compounds US 5159282 A*, 1992.
- (40) Chen, W.; Li, P.; Miao, T.; Meng, L.-G.; Wang, L. An efficient tandem elimination–cyclization–desulfinitive arylation of 2-(gem-dibromovinyl)phenols(thiophenols) with sodium arylsulfinates. *Org. Biomol. Chem.* **2013**, *11*, 420.
- (41) Ortgies, D. H.; Hassanpour, A.; Chen, F.; Woo, S.; Forgione, P. Desulfination as an Emerging Strategy in Palladium-Catalyzed C–C Coupling Reactions. *Eur. J. Org. Chem.* **2016**, DOI:10.1002/ejoc.201501231 10.1002/ejoc.201501231, 408.
- (42) Markovic, T.; Rocke, B. N.; Blakemore, D. C.; Mascitti, V.; Willis, M. C. Catalyst Selection Facilitates the Use of Heterocyclic Sulfinates as General Nucleophilic Coupling Partners in Palladium-Catalyzed Coupling Reactions. *Org. Lett.* **2017**, *19*, 6033.
- (43) Sévigny, S.; Forgione, P. Palladium-Catalyzed Intermolecular Desulfinylative Cross-Coupling of Heteroaromatic Sulfinates. *Chem. Eur. J.* **2013**, *19*, 2256.
- (44) Sévigny, S.; Forgione, P. Efficient desulfinylative cross-coupling of thiophene and furan sulfinates with aryl bromides in aqueous media. *New J. Chem.* **2013**, *37*, 589.
- (45) Forgione, P.; Mangel, D.; Buonomano, C.; Sevigny, S.; Di Censo, G.; Thevendran, G. ChemInform Abstract: Efficient Desulfinitive Cross-Coupling of Heteroaromatic Sulfinates with Aryl Triflates in Environmentally Friendly Protic Solvents. *ChemInform* **2015**, *46*.
- (46) Markovic, T.; Rocke, B. N.; Blakemore, D. C.; Mascitti, V.; Willis, M. C. Pyridine sulfinates as general nucleophilic coupling partners in palladium-catalyzed cross-coupling reactions with aryl halides. *Chem. Sci.* **2017**, *8*, 4437.
- (47) de Gombert, A.; McKay, A. I.; Davis, C. J.; Wheelhouse, K. M.; Willis, M. C. Mechanistic Studies of the Palladium-Catalyzed Desulfinitive Cross-Coupling of Aryl Bromides and (Hetero)Aryl Sulfinates. *J. Am. Chem. Soc.* **2020**, *142*, 3564.

- (48) Jafarpour, F.; Ollia, M. B. A.; Hazrati, H. Highly Regioselective α -Arylation of Coumarins via Palladium-Catalyzed C-H Activation/Desulfitative Coupling. *Adv. Synth. Catal.* **2013**, *355*, 3407.
- (49) Wu, M.; Luo, J.; Xiao, F.; Zhang, S.; Deng, G.-J.; Luo, H.-A. Palladium-Catalyzed Direct and Site-Selective Desulfitative Arylation of Indoles with Sodium Sulfinates. *Adv. Synth. Catal.* **2012**, *354*, 335.
- (50) Zhao, D.; You, J.; Hu, C. Recent Progress in Coupling of Two Heteroarenes. *Chem. Eur. J.* **2011**, *17*, 5466.
- (51) Chen, R.; Liu, S.; Liu, X.; Yang, L.; Deng, G.-J. Palladium-catalyzed desulfitative C-H arylation of azoles with sodium sulfinates. *Org. Biomol. Chem.* **2011**, *9*, 7675.
- (52) Liu, B.; Guo, Q.; Cheng, Y.; Lan, J.; You, J. Palladium-Catalyzed Desulfitative C-H Arylation of Heteroarenes with Sodium Sulfinates. *Chem. Eur. J.* **2011**, *17*, 13415.
- (53) Zhang, M.; Zhang, Y.; Jie, X.; Zhao, H.; Li, G.; Su, W. Recent advances in directed C-H functionalizations using monodentate nitrogen-based directing groups. *Org. Chem. Front.* **2014**, *1*, 843.
- (54) Zhu, R.-Y.; Farmer, M. E.; Chen, Y.-Q.; Yu, J.-Q. A Simple and Versatile Amide Directing Group for C-H Functionalizations. *Angew. Chem. Int. Ed.* **2016**, *55*, 10578.
- (55) Rouquet, G.; Chatani, N. Catalytic Functionalization of C(sp²)-H and C(sp³)-H Bonds by Using Bidentate Directing Groups. *Angew. Chem. Int. Ed.* **2013**, *52*, 11726.
- (56) Chen, Z.; Wang, B.; Zhang, J.; Yu, W.; Liu, Z.; Zhang, Y. Transition metal-catalyzed C-H bond functionalizations by the use of diverse directing groups. *Org. Chem. Front.* **2015**, *2*, 1107.
- (57) Sun, H.; Guimond, N.; Huang, Y. Advances in the development of catalytic tethering directing groups for C-H functionalization reactions. *Org. Biomol. Chem.* **2016**, *14*, 8389.
- (58) Font, M.; Quibell, J. M.; Perry, G. J. P.; Larrosa, I. The use of carboxylic acids as traceless directing groups for regioselective C-H bond functionalisation. *Chem. Commun.* **2017**, *53*, 5584.
- (59) Giri, R.; Yu, J.-Q. Synthesis of 1,2- and 1,3-Dicarboxylic Acids via Pd(II)-Catalyzed Carboxylation of Aryl and Vinyl C-H Bonds. *J. Am. Chem. Soc.* **2008**, *130*, 14082.
- (60) Shi, B.-F.; Maugel, N.; Zhang, Y.-H.; Yu, J.-Q. Pd(II)-Catalyzed Enantioselective Activation of C(sp²)-H and C(sp³)-H Bonds Using Monoprotected Amino Acids as Chiral Ligands. *Angew. Chem. Int. Ed.* **2008**, *47*, 4882.
- (61) Garves, K. Coupling, carbonylation, and vinylation reactions of aromatic sulfinic acids via organopalladium intermediates. *J. Org. Chem.* **1970**, *35*, 3273.
- (62) Giri, R.; Liang, J.; Lei, J.-G.; Li, J.-J.; Wang, D.-H.; Chen, X.; Naggar, I. C.; Guo, C.; Foxman, B. M.; Yu, J.-Q. Pd-Catalyzed Stereoselective Oxidation of Methyl Groups by Inexpensive Oxidants under Mild Conditions: A Dual Role for Carboxylic Anhydrides in Catalytic C-H Bond Oxidation. *Angew. Chem. Int. Ed.* **2005**, *44*, 7420.
- (63) Pimparkar, S.; Jeganmohan, M. Palladium-catalyzed cyclization of benzamides with arynes: application to the synthesis of phenaglydon and *N*-methylcrinasiadine. *Chem. Commun.* **2014**, *50*, 12116.

Chapter 6

The Synthesis of Pyridyl[2.2]paracyclophanes by Palladium-Catalysed Cross-Coupling of Pyridine Sulfinates

6.0. Introduction to Six-membered heteroarene sulfinates

In heteroarene organometallic reagents, heteroarene boronates are a common choice of coupling partner.^{1,2} They are the main reagents for Suzuki-Miyaura,^{3,4} Chan-Evans-Lam,^{5,6} Liebeskind-Srogl,⁷ and oxidative Heck coupling reactions.⁸ Apart from being nucleophilic coupling partners, they have also been utilised in much wider fields e.g. as radical precursors,⁹ Lewis acid catalysts,^{10,11} traceless-directing groups,¹² in materials science,¹³ and in drug design.¹⁴ However, reactions employing heteroarene boronates have several limitations due to their poor functional group tolerance and low reactivity.¹⁵ In particular, the coupling of 2-substituted nitrogen-containing heteroarene boronates e.g. 2-pyridyl boronate is notoriously challenging.^{16,17}

The following discussion focuses on the limitations of 2-pyridyl boronates in cross-coupling reactions. In the ensuing discussion, the main emphasis will be given to the ‘pyridyl sulfinates’ – an emerging coupling partner to replace the pyridyl boronates.^{18,19}

6.1. 2-Pyridyl boronate as nucleophilic coupling partnerⁱ

The 2-pyridyl motif is an important building block in many natural products,^{20,21} medicinal compounds,²²⁻²⁴ unnatural nucleotides,^{25,26} metal-complexing ligands,^{27,28} and materials.^{29,30} Extensive efforts have been made to develop 2-pyridyl organometallic reagents that can be employed efficiently in cross-coupling reactions.^{31,32} However, they are not suitable substrates for coupling to aryl halides.^{16,17}

In comparison to 3- and 4-pyridyl boronates,^{33,34} 2-pyridyl boronates readily undergo hydrolysis in Suzuki-Miyaura coupling reactions.^{35,36} This hydrolytic instability is attributed to two main factors.³⁷ First, the transmetallation from boron to palladium of electron-deficient 2-heteroarene boronates is a slow process, and second, 2-pyridyl boronates rapidly undergo protodeboronation.^{38,37}

Due to the ease of protodeboration of 2-pyridyl boronates, different techniques have been investigated to overcome this problem including the use of additives (Cu, Zn, and Ag salts),³⁹⁻⁴¹ high catalyst loading,⁴² improvement in ligand design,⁴³ masked reagents,⁴⁴ and slow-release

ⁱ Scheme 6.1 to 6.4, structure 6.1 to 6.8, and figure 6.1 to 6.3 were removed at the request of examiner.

from 2-pyridyl-*N*-methyl-iminodiacetic acid (MIDA) boronates **6.12**.^{39,45,46} The most common approach is to increase the stability of the 2-pyridyl boronate **6.4** by modifying its structure (Figure 6.4).⁴⁷

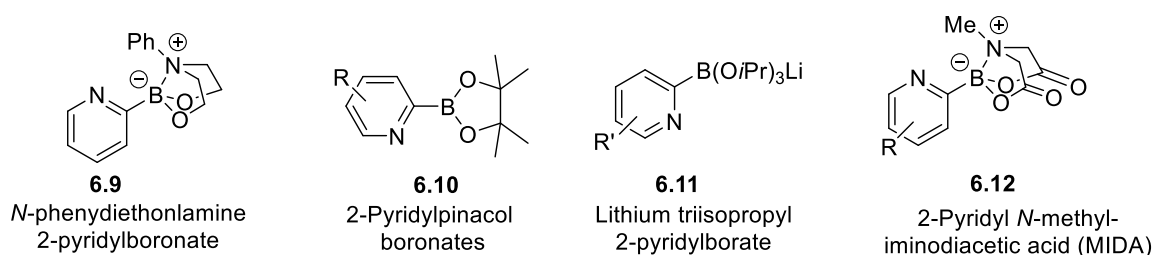


Figure 6.4: 2-Pyridyl boronates exhibiting enhanced stability.

Significant efforts have been carried out to improve the generality of the 2-pyridyl coupling partner in cross-coupling reactions. However, they are not as competent as other heteroarene coupling partners. There are still unsolved challenges associated with the coupling of 2-pyridyl derivatives in the Suzuki-Miyaura reactions. Due to the abundance of *N*-heterocycles and related pyridine-heteroaryl moieties in natural products and drug molecules, the chemistry community still needs new heteroaryl coupling partners. In recent years, ‘heteroarene sulfinates’ have emerged as alternative coupling reagents.^{18,19}

6.2. Investigation of the role of pyridine sulfinates in cross-coupling reaction with bromo-substituted [2.2]paracyclophane derivatives

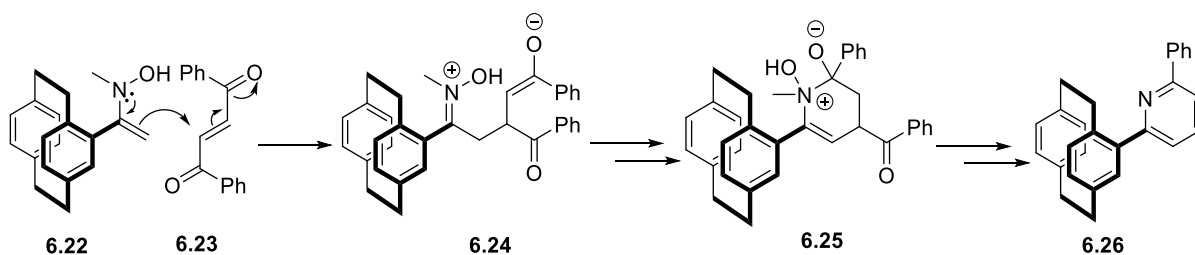
[2.2]Paracyclophane-*N*-heterocycles are promising scaffolds for catalysis. They can coordinate to transition metals through the lone pair on the sp^2 -nitrogen and form planar chiral catalysts.^{48,49} However, the synthesis of these derivatives is problematic. Most of the transition metal-mediated cross-coupling reactions reported in [2.2]paracyclophane chemistry involve aryl nucleophiles.⁵⁰⁻⁵² The corresponding reactions with heteroarene coupling partners have not been thoroughly investigated. Inspired by the potential of hetero(arene)sulfinates as nucleophilic coupling partners, we sought to investigate their cross-coupling with bromo[2.2]paracyclophanes. If successful, this approach would provide a new avenue to access planar chiral heteroarenes based on the [2.2]paracyclophane framework.

Our initial focus was on [2.2]paracyclophane-based pyridine derivatives since planar chiral pyridines are prospective ligands for catalysis,^{53,54} in the formation of supramolecular structures,^{55,56} and even as organocatalysts.^{57,49} Most planar chiral pyridines that have been

reported are based on the ferrocene moiety⁵⁸⁻⁶⁰ but the [2.2]paracyclophane skeleton also offers a potential platform. The reported procedures for the synthesis of [2.2]paracyclophane-pyridine derivatives are mainly based on cross-coupling reactions.⁶¹⁻⁶⁶ However, these methodologies have several problems as discussed in the section below.

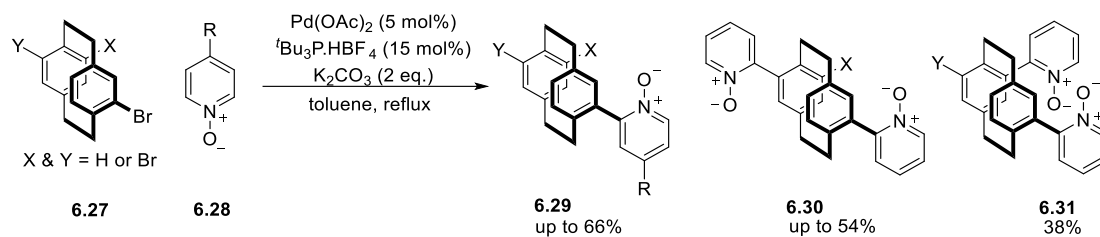
6.2.1. [2.2]Paracyclophane-pyridine derivatives

Hopf et al. reported the preparation of a pyridinyl[2.2]paracyclophane by a nitronc cycloaddition (Scheme 6.5).⁶⁷ In this approach, **6.22** synthesised from 4-acetyl[2.2]paracyclophane and *N*-methylhydroxylamine.hydrochloride undergoes Michael-type addition with an activated double bond of the dipolarophile **6.23** to furnish the intermediate enolate **6.24**. This intermediate **6.24** further proceeds for a sequence of steps to finally give [2.2]paracyclophane-6-phenyl pyridine **6.26**. However, this approach has not proven versatile and does not work if there are other substituents on [2.2]paracyclophane.



Scheme 6.5: Hopf's approach for [2.2]paracyclophane-pyridine derivative.

Rowlands et al. developed a convenient regioselective cross-coupling method⁶⁶ between bromo[2.2]paracyclophanes **6.27** and pyridine *N*-oxides **6.28** based on the direct arylation chemistry of Fagnou et al. (Scheme 6.6).⁶⁸ The author proposed a $S_{E}Ar$ mechanism of pyridine *N*-oxides arylation. Even though this two-steps strategy opened a new route to access pyridinyl[2.2]paracyclophanes, there are several limitations. Firstly, this protocol is limited to 2-pyridine substrates only. Moreover, all the products and by-products have limited solubility, making the purification tedious by chromatography technique. Lastly, the conversion of pyridine *N*-oxides to the corresponding pyridine derivatives involves reduction with the highly volatile and hazardous trichlorosilane, which limits the potential of the pyridine substrate for further investigation with more challenging [2.2]paracyclophane derivatives.

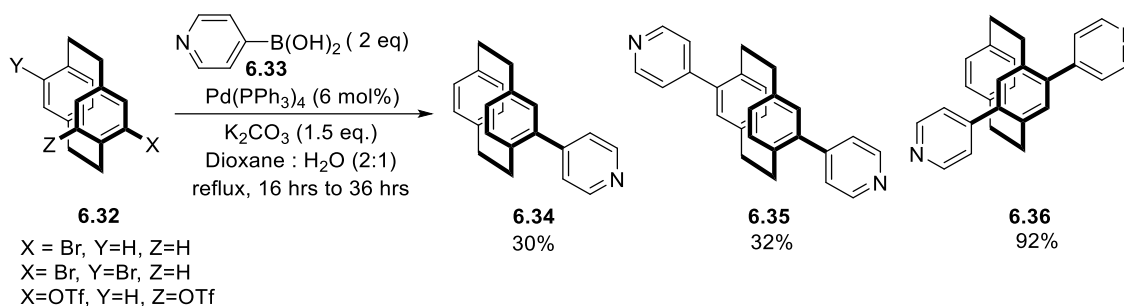


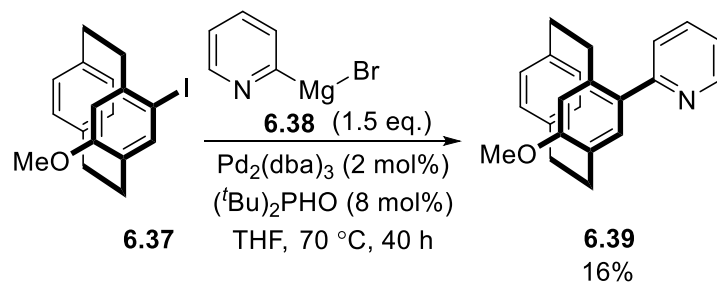
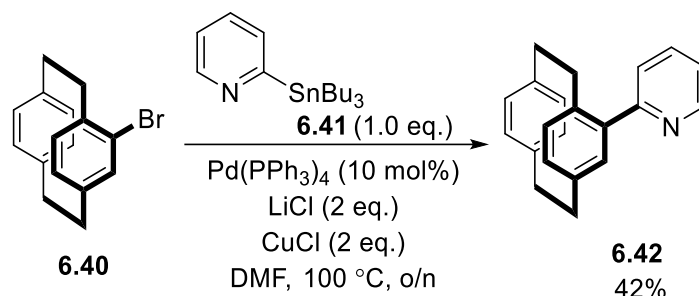
Scheme 6.6: Rowlands's approach for the synthesis of [2.2]paracyclophane-mono- and bis(pyridine *N*-oxides).

Over the last decade, Bräse and co-workers have investigated the scope of various cross-coupling reactions for the synthesis of (hetero)arene substituted [2.2]paracyclophanes. The scope of Suzuki, Stille, Kumada and Negishi cross-coupling reactions have been extended by utilising [2.2]paracyclophane derivatives as either the electrophilic or nucleophilic coupling partner.

Their initial approach employed readily accessible [2.2]paracyclophane substrates (Br, I or, OTf) as the electrophilic coupling partners under Suzuki conditions (Scheme 6.7a) with pyridyl organometallic reagents as nucleophilic coupling partners.⁶¹ With pyridyl boronic acids, only 4-pyridyl[2.2]paracyclophane **6.33** was obtained albeit in a moderate yield. Kumada cross-coupling by *in-situ* magnesiation of 2-bromopyridine (Scheme 6.7b) and the Stille approach with stannylated 2-pyridine **6.41** (Scheme 6.7c) were not proven effective to provide the coupled products in high yields.

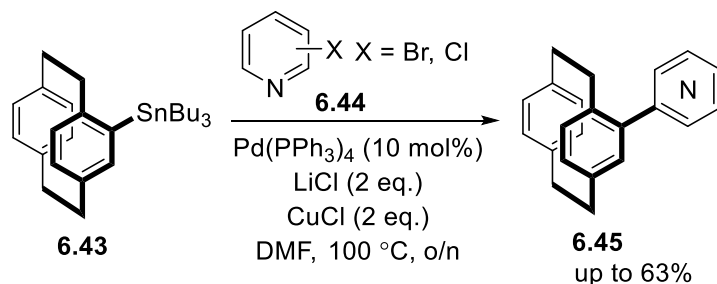
a



b**c**

Scheme 6.7: Bräse's approaches for (a) Suzuki coupling, (b) Kumada, and (c) Stille coupling.

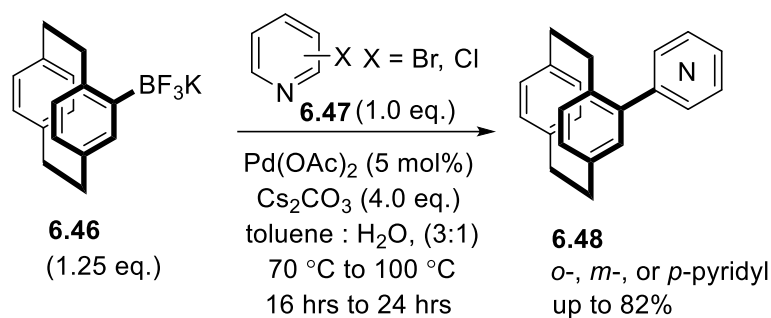
The alternative is to make [2.2]paracyclophane the nucleophilic coupling partner. As mentioned, boronic acids cannot be used⁵¹ so Bräse investigated 4-(tributylstannyl)[2.2]paracyclophane **6.43**.^{62,63} The Stille coupling reaction with bromopyridines **6.44** proceeded with poor to average yields (Scheme 6.8). Moreover, the synthesis of bis-pyridyl[2.2]paracyclophane gave a low yield (27%). The problems appear to be the synthesis of precursor. It requires the lithiation approach ($t\text{BuLi}$), which limits the functional group tolerance of sensitive groups. Moreover, stannylated [2.2]paracyclophanes are unstable and difficult to purify, often leading to low yields.



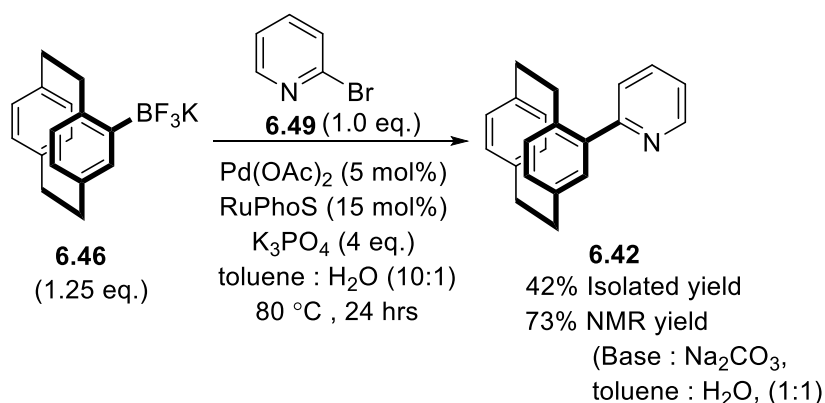
Scheme 6.8: Bräse's approach for Stille coupling.

The authors circumvented the problem of instability of paracyclophane boronic acids and unreactivity of esters⁵¹ by using 4-trifluoroborate[2.2]paracyclophane **6.46**.^{64,65} The potassium trifluoroborate BF_3^-K^+ salt was selected because [2.2]paracyclophane boronic acids are prone to rapid decomposition. Moreover, boronic esters are proven inactive under catalytic reaction

conditions.⁵¹ Pyridyl- and pyrimidyl-substituted [2.2]paracyclophanes were obtained in comparable yields compared to the previous methods (Scheme 6.9). The above strategy was extended to different aryl halides (Scheme 6.10).⁶⁵ With modified conditions (replacing base K_3PO_4 with Na_2CO_3 and solvent system to toluene : H_2O 1:1), improvement was observed in the synthesis of 2-pyridyl[2.2]paracyclophane **6.42** (73%). However, both these methods are limited to only the monosubstituted [2.2]paracyclophane derivative. Of note, these strategies were published when we had already started our study to synthesise pyridyl[2.2]paracyclophanes.



Scheme 6.9: Bräse's approach for Suzuki coupling.



Scheme 6.10: Bräse's modified approach for Suzuki coupling.

The above examples clearly show that the synthesis of paracyclophane-substituted pyridines is an unsolved challenge. Most common cross-couplings have been studied and yet none have been proven general or high yielding. Furthermore, the synthesis of [2.2]paracyclophane-based organoboranes and stannanes requires a minimum of two-steps with low functional group tolerance. In addition, the modular synthesis with bis-substituted derivatives and diverse functional group tolerance on [2.2]paracyclophane is still not proven.

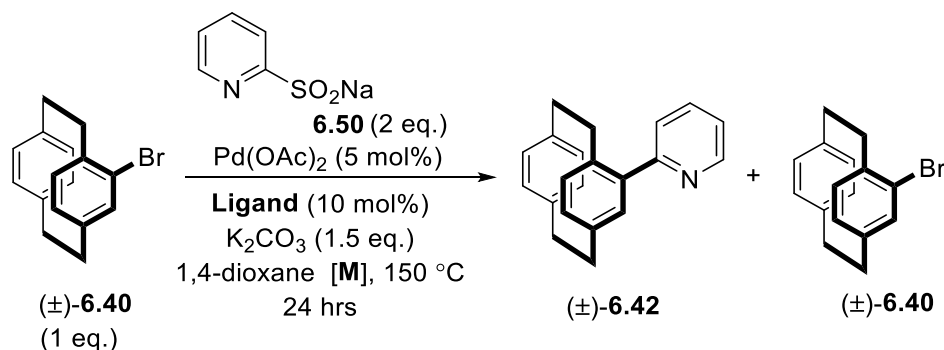
6.3. Results and discussion

We were inspired by the recently reported nucleophilic characteristic of pyridylsulfonates in cross-coupling reactions.^{18,19} We sought to address the above challenges associated with the synthesis of pyridyl[2.2]paracyclophanes by employing pyridyl sulfonates. We thought this would give a more general route with a greater functional group tolerance than those previously reported.

6.3.1. Role of pyridine sulfonates as a nucleophilic coupling partner in cross-coupling with bromo [2.2]paracyclophane derivatives

The obvious starting point was the coupling of pyridinylsulfonates to (\pm)-4-bromo[2.2]paracyclophane **6.40** using Willis's methodology (Scheme 6.11, Table 6.1, entry 1).¹⁹ The desired coupling was achieved in 27% isolated yield. However, this methodology suffered a problem of reproducibility (entry 2 & 3). It was, therefore, decided to evaluate the reaction parameters to achieve the optimal conversion.

A number of different ligands, including, SPhos and Johnphos were screened (entry 4 to 9). None improved the yield compared to PCy₃.



Scheme 6.11: Optimisation study for synthesis of (\pm)-4-(2-pyridyl)[2.2]paracyclophane **6.42**.

Table 6.1: Optimisation study for the synthesis of **6.42**

Entry	Ligand	[M]	Yield
1	PCy ₃	[0.1]	27% ^a
2	PCy ₃	[0.1]	SM: 6.42 ^b = 90:10
3	PCy ₃	[0.1]	SM: 6.42 ^b = 86:14
4	SPhos	[0.1]	SM
5	Johnphos	[0.1]	SM
6	P(<i>o</i> -tolyl) ₃	[0.1]	SM
7	Dppf	[0.2]	10% ^c

8	Xanthphos	[0.2]	5% ^c
9	PCy ₃	[0.2]	19% ^c

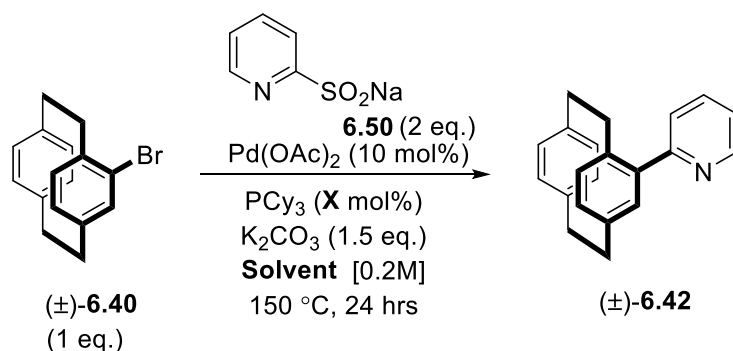
SM = Starting material recovered

^a = Isolated yield

^b = NMR yield

^c = HPLC yield, conditions:- stationary phase : reverse phase C¹⁸ column, mobile phase : 5-100% H₂O : CH₃CN over 20 min., flow rate = 0.3 ml/min., RT for 4-bromo[2.2]paracyclophane **6.40**: 24.50 min., Sodium pyridine-2-sulfinate **6.50** : 0.899 min., 4-(2-pyridyl)[2.2]paracyclophane **6.42**: 10.103 min., bipyridine: 2.790 min.

Early results suggested that the best combination of reagents was Pd(OAc)₂, PCy₃, and K₂CO₃. As a result, we decided to optimise the ratio of these reagents and the solvents. We increased the Pd(OAc)₂ loading from 5 mol% to 10 mol% in the hope to improve the catalytic turnover. We also thought that increasing ligand would minimise the dissociation of the 2-pyridine sulfinate **6.50**. This may reduce the formation of thermodynamically stable chelated Pd(II)-sulfinate complex through $\kappa^2_{N,O}$ -chelation. The solvent concentration was also changed from [0.1 M] to [0.2 M]. Gratifyingly, the reaction conversion improved with increasing ratio of Pd(OAc)₂ to PCy₃ from 1:1 to 1:4 (Scheme 6.12, Table 6.2).



Scheme 6.12: Optimisation study with increasing ligand loading and different solvents.

Table 6.2: Effect of altering the catalyst: ligand ratio and solvents

Entry	Pd(OAc) ₂ : PCy ₃	Solvent	Yield
1	1:1	1,4-dioxane	16% ^a
2	1:2	1,4-dioxane	26% ^a
3	1:2	DMF	27% ^b
4	1:4	1,4-dioxane	33% ^a
5	1:4	DMF	38% ^a
6	1:4	DMA	100% ^a (63%) ^b

^aHPLC yield

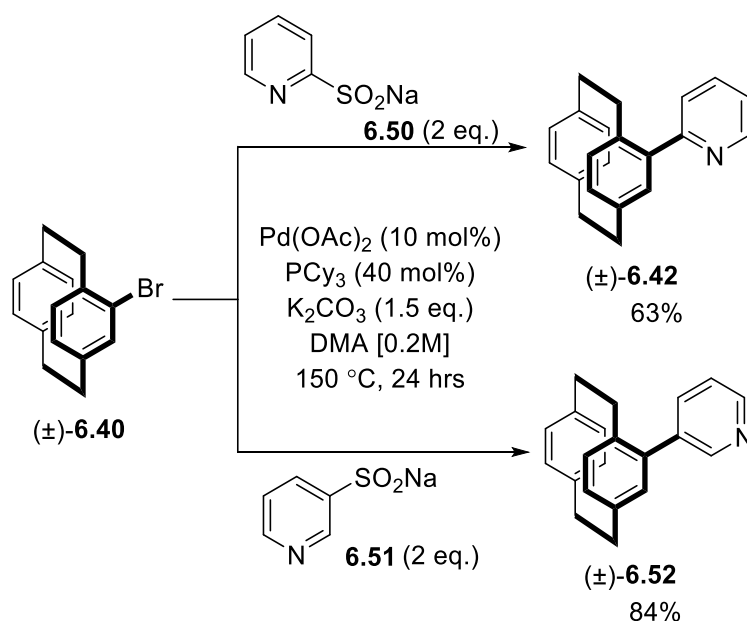
^bIsolated yield

At this stage, we also considered evaluating the solvent, particularly the use of more polar aprotic solvent in hope to increase the solubility of 2-pyridine sulfinate **6.50**. A slightly increased conversion was detected with DMF solvent, both in Pd(OAc)₂ : PCy₃, 1:2 and 1:4 (entry 3 & 5, Table 1). To our delight, 100% conversion was observed under HPLC conditions using DMA. Further purification of this reaction mixture allowed us to isolate the coupled product **6.42** in 63% (entry 2). At this time, this was the highest yield for (±)-4-(2-pyridyl)[2.2]paracyclophane **6.42** in our studies and in the literature.

With the optimised reaction conditions in hand, we decided to expand the scope of desulfitative coupling to both substituted [2.2]paracyclophane derivatives and pyridine sulfinates.

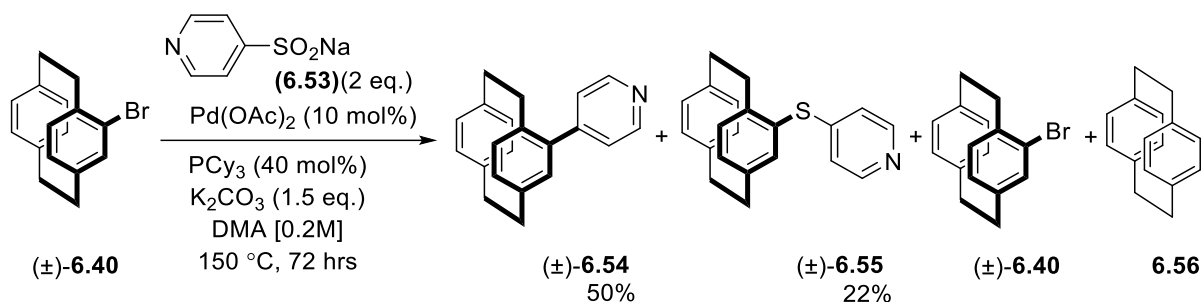
6.3.1.1. Scope of desulfitative coupling with bromo[2.2]paracyclophane

Next, we looked at different sulfinates. Both 2- and 3-pyridine sulfinate **6.50** & **6.51** gave the desired product in good yields under the optimised reaction conditions (Scheme 6.13).



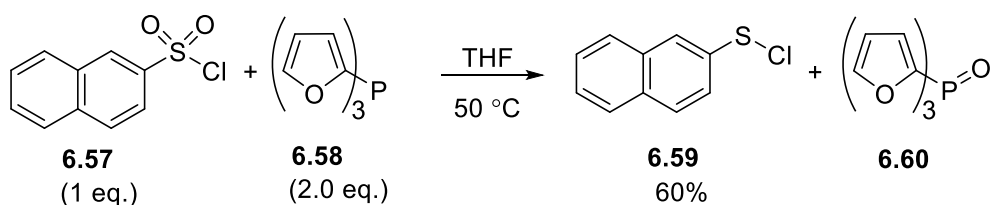
Scheme 6.13: Desulfitative coupling between (±)-4-bromo[2.2]paracyclophane **6.40** and sodium 2- & 3-pyridine sulfinates **6.50** & **6.51**.

The coupling with 4-pyridine sulfinate **6.53** was problematic and proceeded in only 50% isolated yield. The purification of the crude reaction mixture led to the isolation of the desired product **6.54**, unreacted starting material **6.40**, protodebrominated by-product **6.56**, and surprisingly the thioether **6.55**.



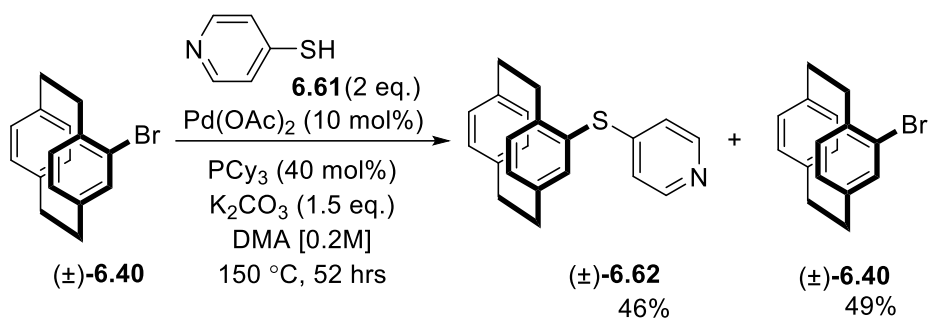
Scheme 6.14: Desulfitative coupling between monosubstituted (\pm)-4-bromo[2.2]paracyclophane **6.40** and 4-pyridine sulfinate **6.53**.

It is unclear how the thioether formed but a similar product was identified by Vogel et al. during their study of palladium-catalysed Stille cross-coupling of sulfonyl chlorides and organostannanes.⁶⁹ They reasoned that the thioether was formed first by the reduction of the sulfonyl chloride to the sulfenyl chloride by the phosphine, then a palladium catalysed coupling. The reduction was confirmed by the synthesis of 1-naphthalenesulfenyl chloride **6.59** from 1-naphthalenesulfonyl chloride **6.57** (Scheme 6.15).⁷⁰ We assumed that the same process is occurring here. The 4-pyridine sulfinate **6.53** might be less reactive than the 2- and 3-pyridine sulfinate **6.50** & **6.51** due to delocalisation of the lone pair electrons on pyridine nitrogen. The slower coupling allows the phosphine time to reduce the sulfinate.

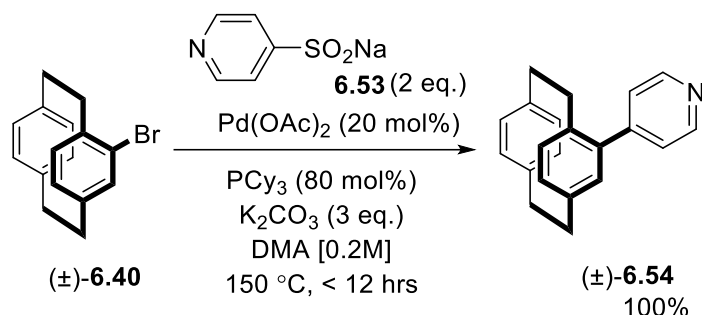


Scheme 6.15: Vogel's explanation of thioether formation.

A separate reaction was carried out between (\pm)-4-bromo[2.2]paracyclophane **6.40** and 4-pyridine thiol **6.61** under the standard reaction conditions. The thioether was formed in 46% yield with the rest of the material being unreacted **6.40**. (Scheme 6.16). It was later observed that the competitive thioether formation could be suppressed by increasing the concentration of catalyst/ligand. Presumably, this increases the rate of the desired reaction so that reduction cannot compete. Based on our hypothesis, when we carried out the reaction with 4-pyridine sulfinate **6.53** as the reaction conditions shown in the scheme 6.17, the desired conversion was achieved in 100% isolated yield of **6.54**.



Scheme 6.16: Coupling between (\pm)-4-bromo[2.2]paracyclophane **6.40** and 4-pyridine thiol **6.61**.

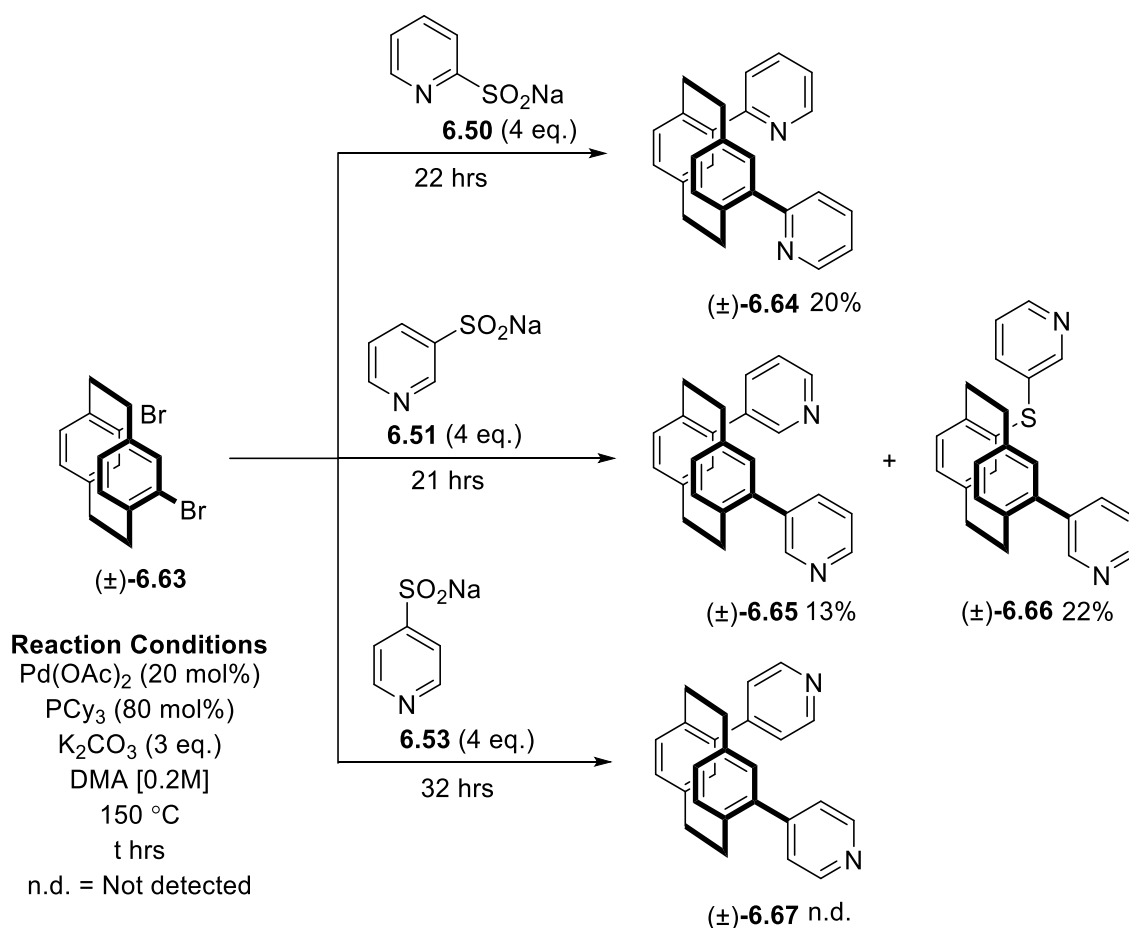


Scheme 6.17: Desulfitative coupling between monosubstituted (\pm)-4-bromo[2.2]paracyclophane **6.40** and 4-pyridine sulfinate **6.53** with double concentration of catalyst/ligand.

6.3.1.2. Scope of bis-desulfitative coupling with dibromo[2.2]paracyclophane

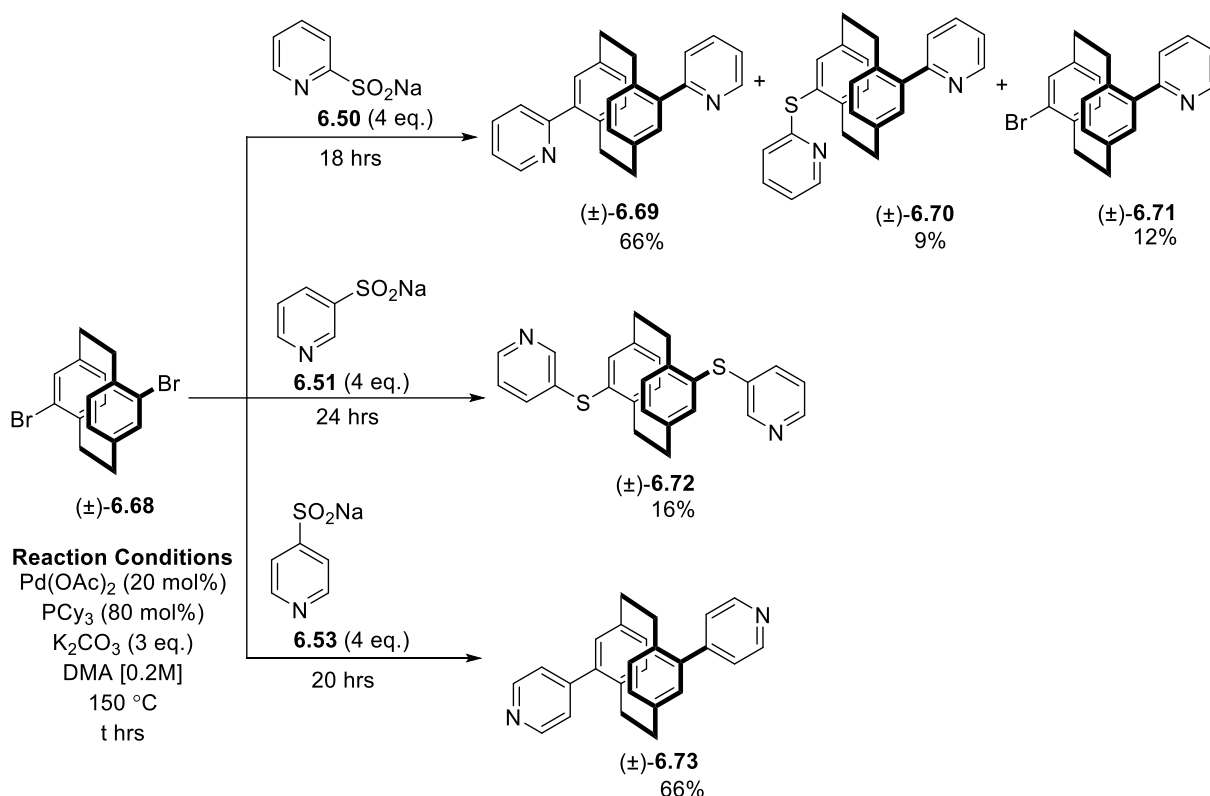
After successful results with mono desulfitative coupling, the scope of the reaction was further broadened to dibromo[2.2]paracyclophanes.

We first decided to perform a bis-coupling with the *pseudo-ortho*-dibromo substrate **6.63**. It was crucial that the number of equivalents of palladium and ligands were doubled. The results were not promising. The 2- and 3-pyridine sulfinates **6.50** & **6.51** gave a low yield of bis-coupled product while the 4-pyridine sulfinate **6.53** did not react at all. (Scheme 6.18). For the reaction of 3-pyridine sulfinate **6.51**, the thioether by-product **6.66** was the predominant product. This result suggests that the rate of oxidative addition is slower in this dibromo derivative than in the monobromo compound.



Scheme 6.18: Bis-desulfinitative coupling with *pseudo-ortho*-dibromo[2.2]paracyclophane **6.63**.

Unsurprisingly, the *pseudo-para*-dibromo derivative is generally a good substrate in the bis-coupling. In terms of the steric environment, it is identical to the 4-bromo substrate **6.40**. Electronically, it is potentially activated. The desired products isolated in good yield for the 2- and 4-pyridine sulfinate **6.50** & **6.53**. However, 3-pyridine sulfinate **6.51** only produced the thioether by-product **6.72** in 19% yield (Scheme 6.19). During 2-pyridine bis-coupling the minor thioether by-product **6.70** was also observed.

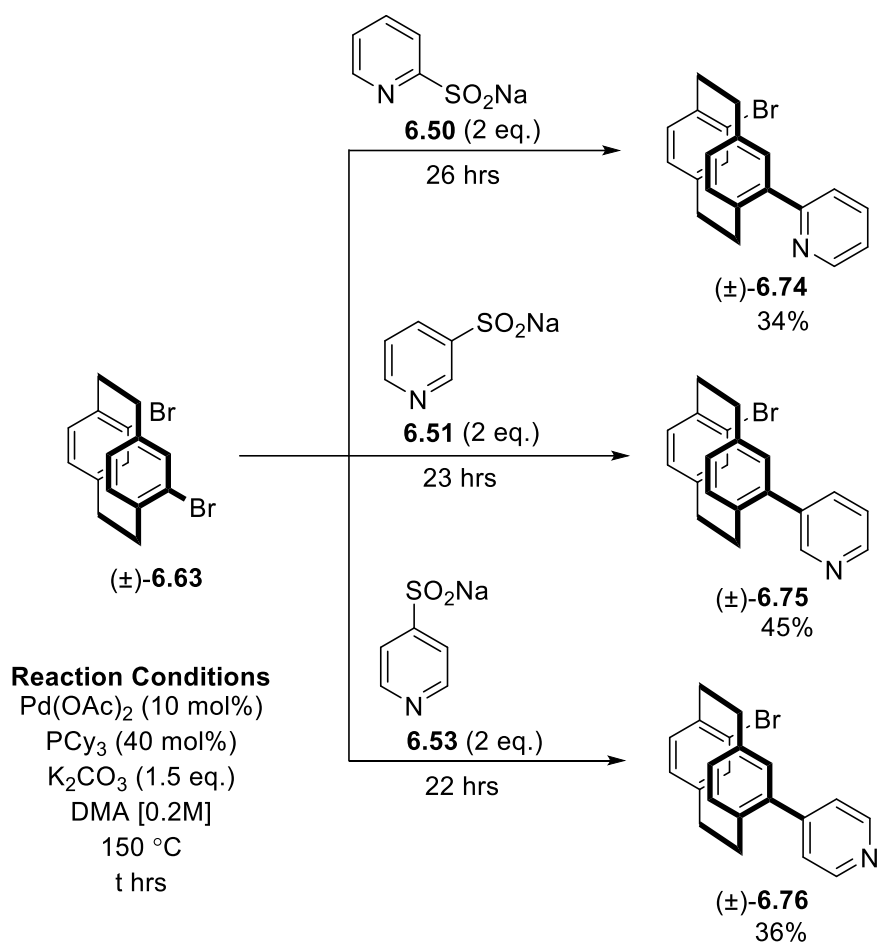


Scheme 6.19: Bis-desulfitative coupling with *pseudo-ortho*-dibromo[2.2]paracyclophane **6.68**.

6.3.1.3. Scope of mono-desulfitative coupling with dibromo[2.2]paracyclophane

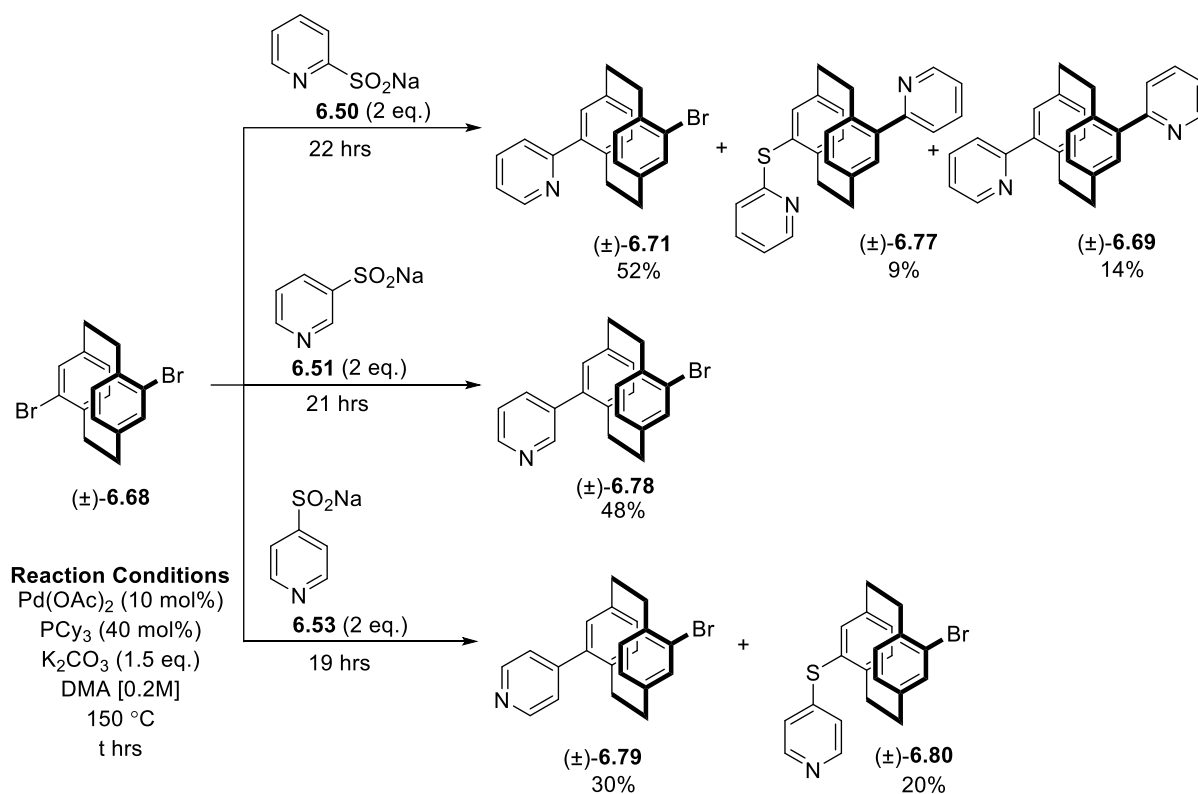
We wondered if we could selectively add a single pyridine to a dibromo derivative as this would leave a bromide group suitable for further functionalisation. If we succeeded in the desired transformation, it will open a new route to synthesise bulky *N*-heteroarene-[2.2]paracyclophane derivatives that could be of great potential in catalysis.

Under the optimised conditions, the individual reaction was carried out between *pseudo-ortho*-dibromo[2.2]paracyclophane and 2-, 3-, and 4-pyridine sulfonates **6.50**, **6.51**, & **6.53**. These reactions were maintained by taking all reagents equivalent to mono-coupling. All three reactions were carefully monitored for consumption of the starting material, in an effort to avoid bis-coupling. The desired products were isolated albeit in moderate yield (34% to 45%) and bis-coupling was not observed in any case (Scheme 6.20).



Scheme 6.20: Mono-desulfinitative coupling of *pseudo-ortho*-dibromo[2.2]paracyclophane **6.63**.

Similarly, reactions were also performed with *pseudo-para*-dibromo[2.2]paracyclophane **6.68** under the same conditions. In each case, the reaction conversion was slightly higher compared to the corresponding *pseudo-ortho* derivative presumably due to less steric hindrance. However, this time the unusual by-products, the monothioether product and bis-coupling product were isolated as shown in the Scheme 6.21. It is worth mentioning that all reactions were repeated three times and no consistency was found in the formation of by-products. It is still not clear which factors are attributed to such inconsistency.



Scheme 6.21: Mono-desulfitative coupling with *pseudo-para*-dibromo[2.2]paracyclophane **6.68**.

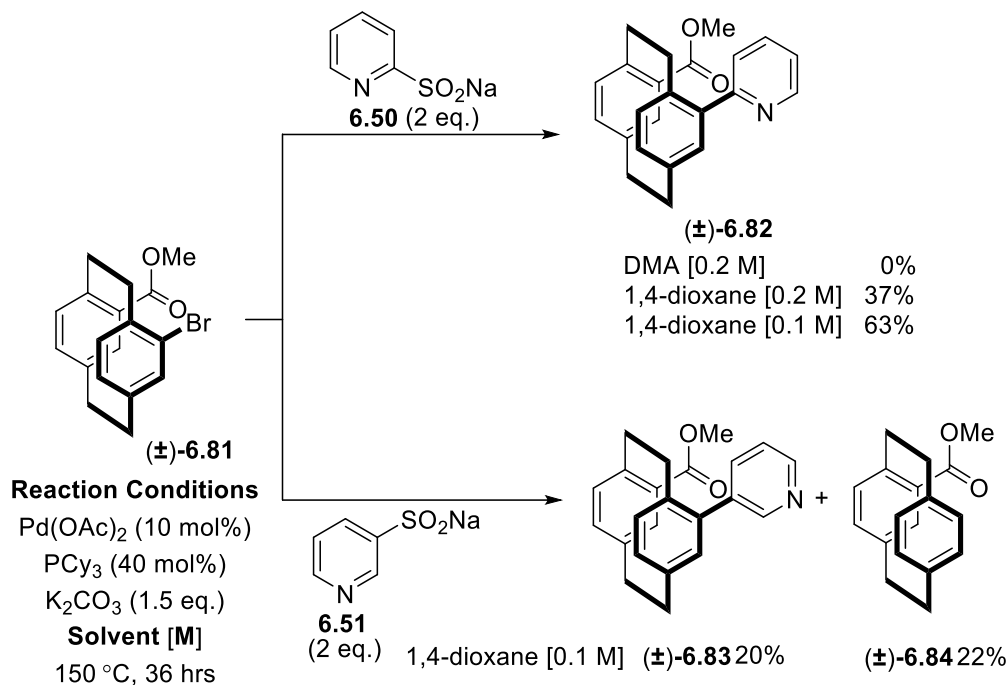
This inconsistency in desulfitative coupling with dibromo[2.2]paracyclophane suggests that a detailed mechanistic investigation is required. More understanding will allow us to reduce the by-product formation and subsequently to achieve better yields.

The scope of the methodology was extended to evaluate the functional group tolerance at different positions on the [2.2]paracyclophane. The challenging *pseudo-gem* position was selected first for the study to assess the influence of steric hindrance on desulfitative coupling.

6.3.1.4. Scope of *pseudo-gem*-[2.2]paracyclophane for desulfitative coupling

First, we decided to check the compatibility of electron-withdrawing functionalities such as an ester and a nitro group. The synthesis of precursor, methyl (±)-4-bromo[2.2]paracyclophane-13-carboxylate **6.81** was achieved in four steps from [2.2]paracyclophane **6.56** following the literature.⁷¹ Unfortunately, the coupling of **6.81** with 2-pyridine sulfinate **6.50** did not proceed under our standard reaction conditions. We then chose a non-nucleophilic solvent 1,4-dioxane as per Willis's reaction conditions.¹⁹ The coupling product using 2-pyridine sulfinate **6.50** was isolated in 37% yield at the concentration [0.2 M] of 1,4-dioxane. We observed that the yield could be increased to 62% by reducing the reaction concentration to [0.1 M], probably due to

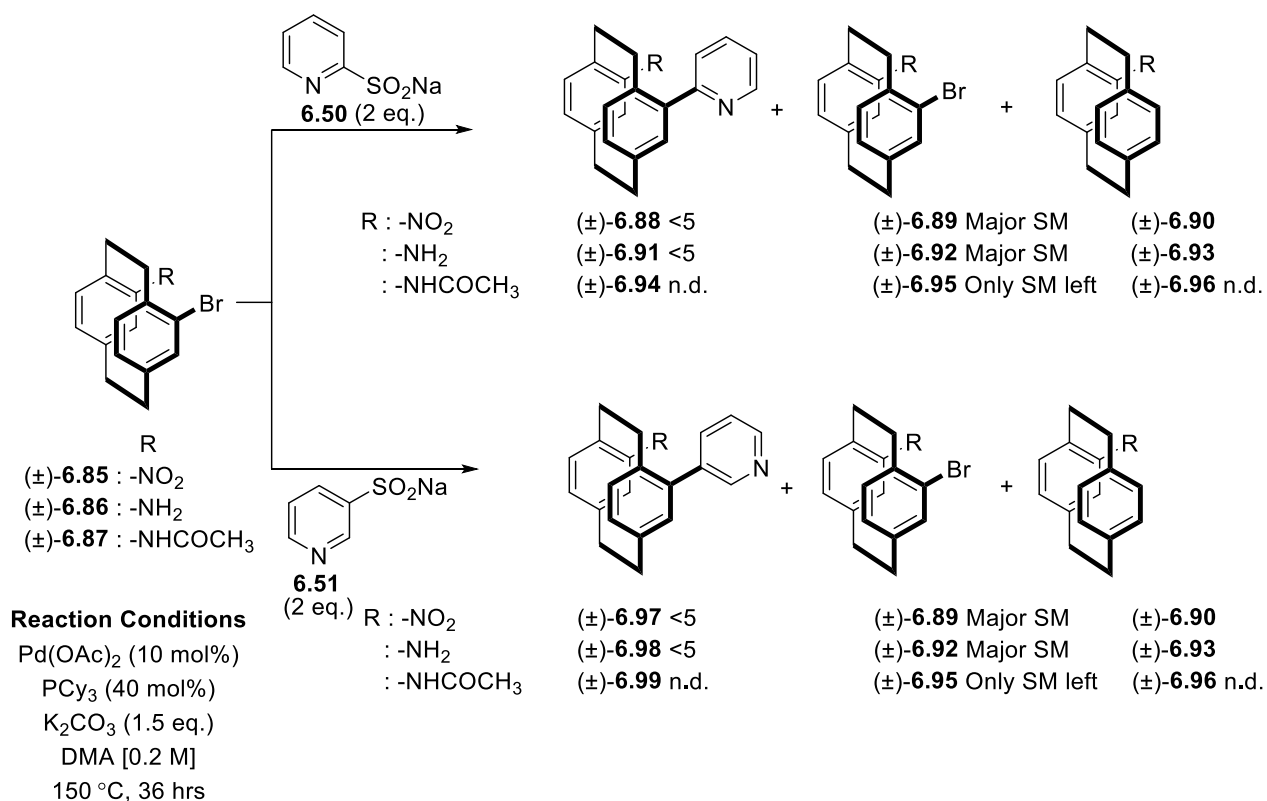
the more solubility of reagents. The coupling of 3-pyridine sulfinate **6.51** was, however, not promising as the reaction gave the coupled product **6.83** only in 20% yield with the protodebromination by-product **6.84** in 22%.



Scheme 6.22: Desulfitative coupling with methyl (±)-4-bromo[2.2]paracyclophane-13-carboxylate **6.81**.

We also checked the desulfitative coupling with the *pseudo-gem* nitro functionality (Scheme 6.23). The precursor, (±)-4-bromo-13-nitro[2.2]paracyclophane **6.85** was synthesised by following Rowlands's report.⁷² The precursor was found to be less reactive towards desulfitative coupling, furnishing the main starting material back **6.85** with minor protodebrominated by-product **6.90**.

We reduced the nitro group and investigated the reaction of (±)-4-bromo-13-amino[2.2]paracyclophane **6.86**. However, this bromide **6.86** was largely unreactive. Traces of the desulfitative coupling were observed with both 2- and 3-pyridine sulfinate **6.50** & **6.51** but mostly unreacted starting material was returned. Protecting the primary amino group as an acetamide did not help to improve the coupling reaction.

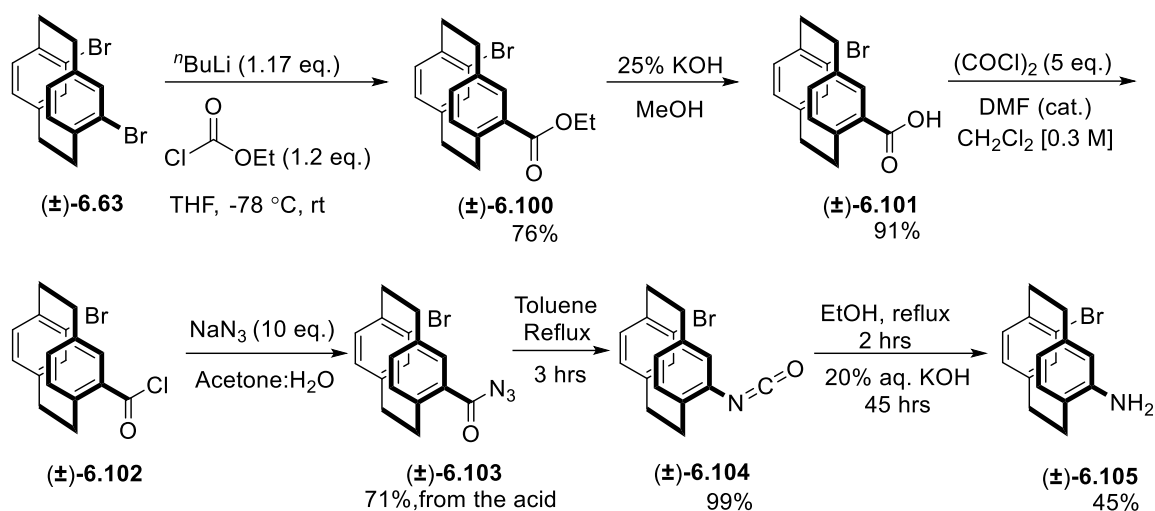


n.d. = not detected

Scheme 6.23: Desulfitative coupling with (±)-4-bromo-13-nitro/amino/*N*-acetyl amino[2.2]paracyclophane **6.85/6.86/6.87**.

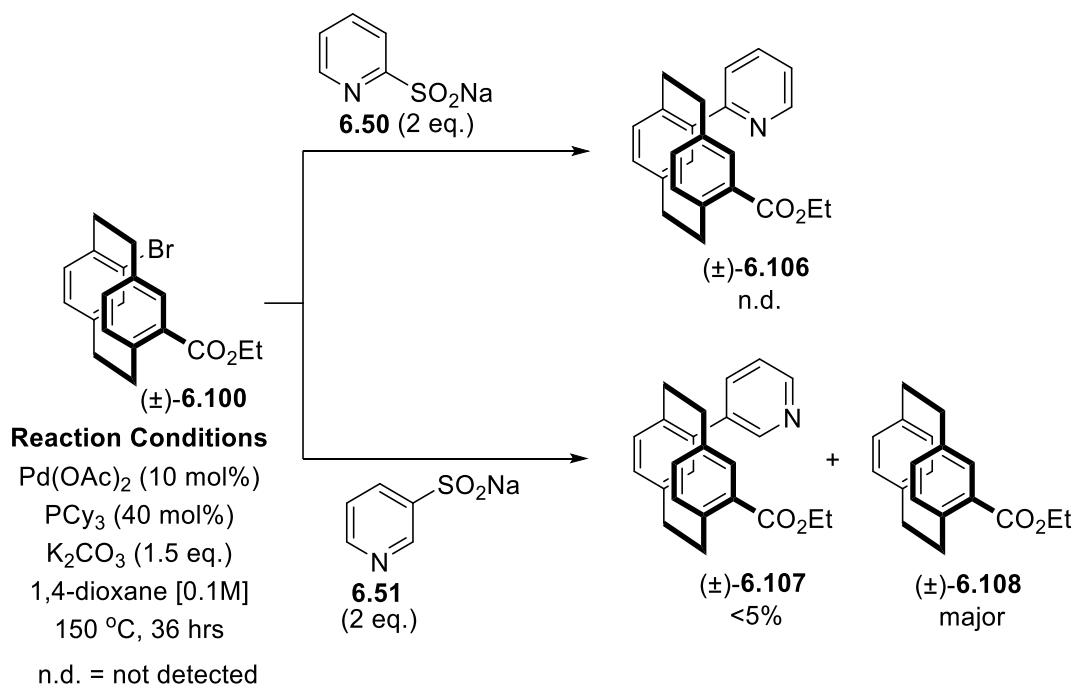
6.3.1.5. Scope of *pseudo-ortho*-[2.2]paracyclophane for desulfitative coupling

Next, we checked *pseudo-ortho*-[2.2]paracyclophane derivatives. The synthesis of *pseudo-ortho*-substituted derivatives requires multistep sequences and can be low-yielding. The routes to ethyl (±)-4-bromo-[2.2]paracyclophane-12-carboxylate **6.100** and (±)-4-bromo-12-amino-[2.2]paracyclophane **6.105** are given in Scheme 6.24. Ester **6.100** was synthesised from (±)-4,12-dibromo[2.2]paracyclophane **6.63** by a lithium-halogen exchange followed by nucleophilic attack of the resulting organolithium intermediate on ethyl chloroformate. After hydrolysis, the resulting product **6.101** was first converted to an acyl chloride **6.102** and later to an acyl azide **6.103**, which subsequently underwent a Curtius rearrangement to furnish the desired amine **6.105** in a moderate yield.



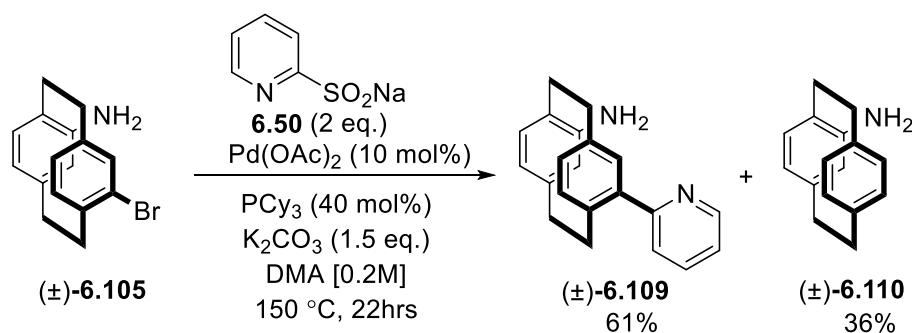
Scheme 6.24: Synthesis of ethyl (±)-4-bromo-[2.2]paracyclophane-12-carboxylate **6.100** and 4-bromo-12-amino-[2.2]paracyclophane **6.105**.

First, we investigated the reactions of ethyl (±)-4-bromo-[2.2]paracyclophane-12-carboxylate **6.100** with 2- and 3-pyridine sulfinates **6.50** & **6.51** under the optimised reaction conditions found for the *pseudo-gem* isomer (Scheme 6.25). However, this time, the results were not promising. The 2-pyridine sulfinate **6.50** failed to couple whereas only a trace of desulfitative coupling was observed with 3-pyridine sulfinate **6.51**.



Scheme 6.25: Desulfitative coupling with ethyl (±)-4-bromo-[2.2]paracyclophane-12-carboxylate **6.100**.

The desulfitative coupling of 2-pyridine sulfinate **6.50** and (\pm)-4-bromo-12-amino-[2.2]paracyclophane **6.105** gave the desulfitative product **6.109** in 61% yield along with the 36% of protodebrominated amine **6.110**. Based on our previous assumption about the *pseudo-gem* substrate, it is evident that steric hindrance has a crucial role in deciding the course of the reaction.

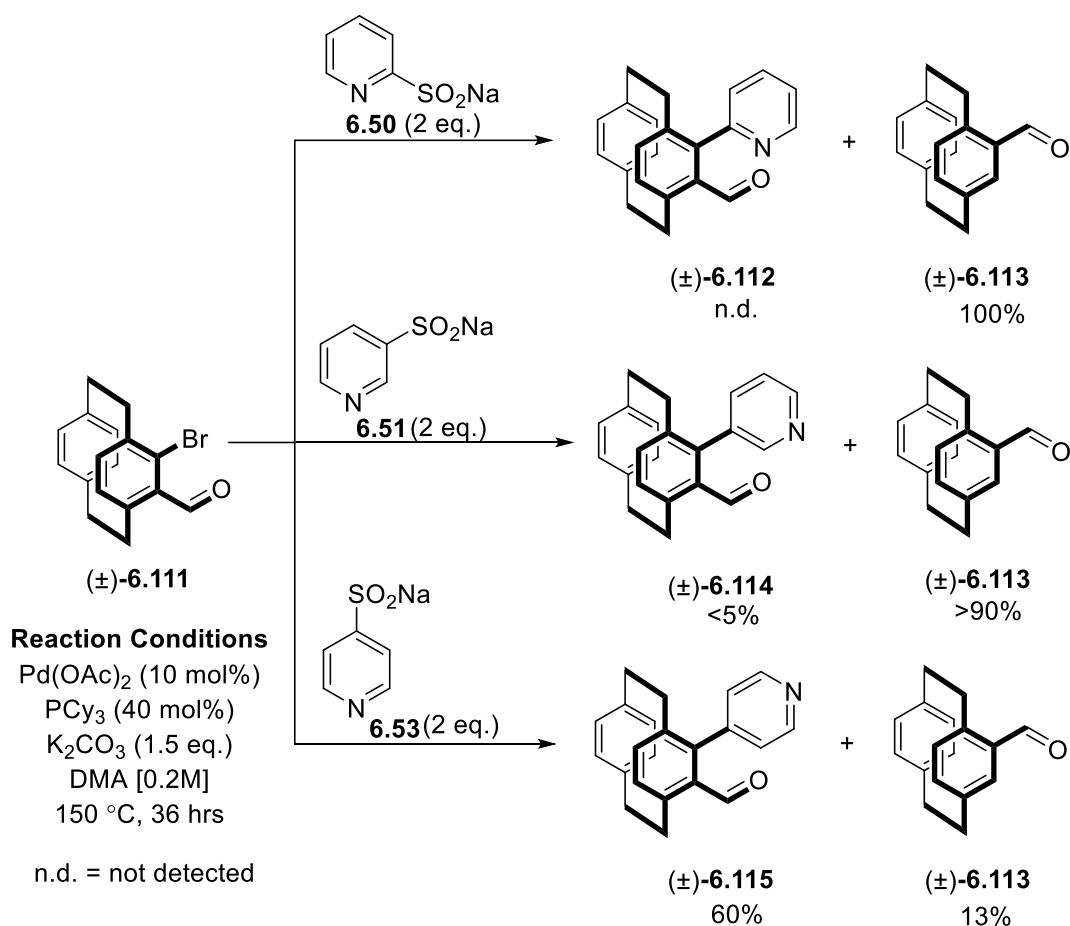


Scheme 6.26: Desulfitative coupling with (\pm)-4-bromo-12-amino-[2.2]paracyclophane **6.105**.

6.3.1.6. Scope of *ortho*-[2.2]paracyclophane for desulfitative coupling

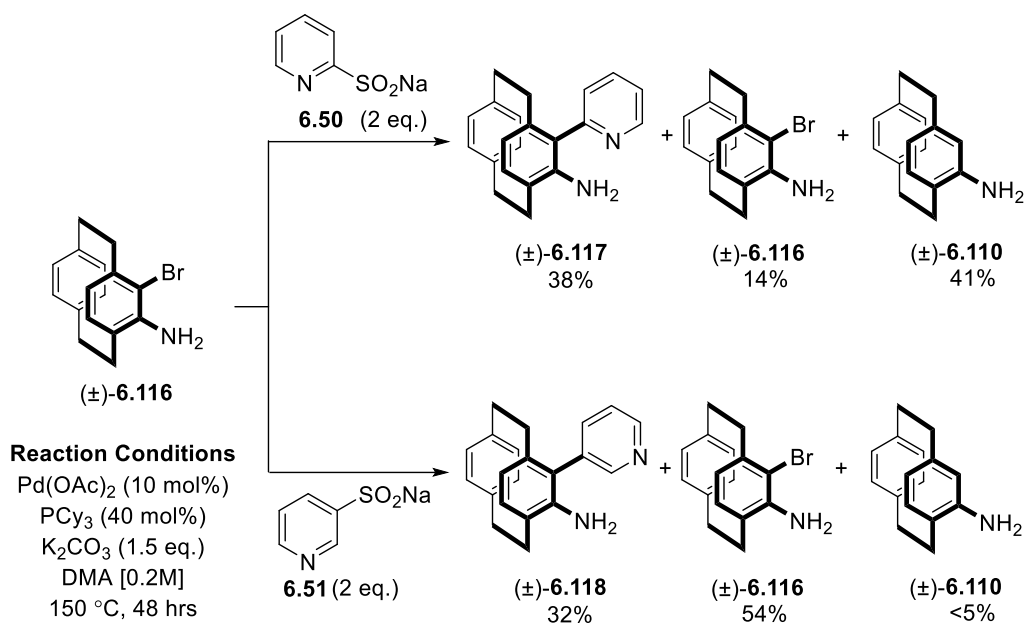
After evaluating the versatility of pyridine sulfinates to *pseudo-gem* and *pseudo-ortho* positions, we looked at the *ortho*-substituted-bromo[2.2]paracyclophane derivatives. *Ortho*-substituted [2.2]paracyclophane derivatives are highly desirable but their synthesis is taxing as one cannot apply many standard aromatic transformations.

The synthesis of (\pm)-4-bromo-5-formyl[2.2]paracyclophane **6.111** was achieved by Bräse's methodology,⁷³ where Pd(II)-catalysed *ortho*-bromination was performed on oxime derivative of (\pm)-4-formyl[2.2]paracyclophane. Disappointingly, the protodebromination was the major product of the attempted coupling. Unexpectedly, only 4-pyridine sulfinate **6.53** gave the coupled product **6.115** (60% yield, Scheme 6.27). This is unusual as the 4-pyridyl derivative **6.53** more frequently gave the thioether product. Increased steric congestion and the electron-withdrawing effect resulting from the formyl substituent could be the possible reasons for the low reactivity of 2- & 3-pyridine sulfinates **6.51** & **6.52**.



Scheme 6.27: Desulfinitative coupling with (±)-4-bromo-5-formyl-[2.2]paracyclophane **6.111**.

Next, we considered performing coupling with (±)-4-bromo-5-amino[2.2]paracyclophane **6.116**. The desired precursor was obtained by treating 4-bromo-5-formyl[2.2]paracyclophane **6.111** with Koser's reagent followed by Lossen-type rearrangement.⁷¹ Desulfinitative coupling of **6.116** with 2- & 3-pyridine sulfonates **6.50** & **6.51** was accomplished in a moderate yield with the remainder of the reaction mixture containing unreacted starting material (Scheme 6.28). We assumed that steric bulk arising from proximal *ortho* groups might have impeded further reaction. These results were exciting that the precursor **6.116** reacted at all as we have found this material to be surprisingly unreactive in other reactions.



Scheme 6.28: Desulfitative coupling with (±)-4-bromo-5-amino[2.2]paracyclophane **6.116**.

6.4. Conclusions

Over all, the goal of this project was to overcome the shortcomings in the synthesis of pyridyl[2.2]paracyclophanes. We have shown that pyridyl sulfonates can be employed as nucleophilic coupling partners successfully in desulfitative cross-coupling with the bromo[2.2]paracyclophane derivatives. Under the optimised reaction conditions, bromo- and dibromo[2.2]paracyclophane derivatives allow access to pyridines that can be problematic to synthesise via other routes. For example, the reported maximum isolated yield of 2-pyridyl[2.2]paracyclophane **6.42** is 42%, while the same compound can be synthesised in a relatively higher yield of 62% with our optimised method. In some cases, thioether by-products were observed, suggesting an in-depth study is required to improve the desired coupling reactions. A wide range of pyridyl[2.2]paracyclophane derivatives with diverse functionalities were also synthesised. One of the intriguing results was the desulfitative coupling with the stubborn scaffold (±)-4-bromo-5-amino[2.2]paracyclophane **6.116**, which, so far, has not reacted in any other reaction. Should these derivatives be synthesised in enantiomerically pure form, they should show great potential in asymmetric catalysis.

The initial results of desulfitative couplings are promising. Nevertheless, some challenges still remain. We suggest that studies in this direction will create a new avenue to synthesise various

heteroarene[2.2]paracyclophanes. Further, there will be a great opportunity to create a modular family of planar chiral ligands based on heteroarene[2.2]paracyclophane framework.

6.5. References

- (1) Hall, D., Ed. *Boronic Acids: Preparation and Applications in Organic Synthesis, Medicine and Materials*; 2nd ed.; Wiley VCH: Weinheim: Germany, **2011**, 1.
- (2) Tyrrell, E.; Brookes, P. The Synthesis and Applications of Heterocyclic Boronic Acids. *Synthesis* **2003**, *2003*, 0469.
- (3) Miyaura, N.; Suzuki, A. Palladium-Catalyzed Cross-Coupling Reactions of Organoboron Compounds. *Chem. Rev.* **1995**, *95*, 2457.
- (4) Lennox, A. J. J.; Lloyd-Jones, G. C. Selection of Boron Reagents for Suzuki–Miyaura Coupling. *Chem. Soc. Rev.* **2014**, *43*, 412.
- (5) Chan, D. M. T.; Monaco, K. L.; Wang, R.-P.; Winters, M. P. New *N*- and *O*-arylations with phenylboronic acids and cupric acetate. *Tetrahedron Lett.* **1998**, *39*, 2933.
- (6) Lam, P. Y. S.; Clark, C. G.; Saubern, S.; Adams, J.; Winters, M. P.; Chan, D. M. T.; Combs, A. New aryl/heteroaryl C–N bond cross-coupling reactions via arylboronic acid/cupric acetate arylation. *Tetrahedron Lett.* **1998**, *39*, 2941.
- (7) Liebeskind, L. S.; Srogl, J. Thiol Ester-Boronic Acid Coupling. A Mechanistically Unprecedented and General Ketone Synthesis. *J. Am. Chem. Soc.* **2000**, *122*, 11260.
- (8) Cho, C. S.; Uemura, S. Palladium-catalyzed cross-coupling of aryl and alkenyl boronic acids with alkenes via oxidative addition of a carbon-boron bond to palladium(0). *J. Organomet. Chem.* **1994**, *465*, 85.
- (9) Seiple, I. B.; Su, S.; Rodriguez, R. A.; Gianatassio, R.; Fujiwara, Y.; Sobel, A. L.; Baran, P. S. Direct C–H Arylation of Electron-Deficient Heterocycles with Arylboronic Acids. *J. Am. Chem. Soc.* **2010**, *132*, 13194.
- (10) Dimitrijević, E.; Taylor, M. S. Organoboron Acids and Their Derivatives as Catalysts for Organic Synthesis. *ACS Catal.* **2013**, *3*, 945.
- (11) Ishihara, K.; Ohara, S.; Yamamoto, H. Direct Polycondensation of Carboxylic Acids and Amines Catalyzed by 3,4,5-Trifluorophenylboronic Acid. *Macromolecules* **2000**, *33*, 3511.
- (12) Ihara, H.; Suginome, M. Easily Attachable and Detachable ortho-Directing Agent for Arylboronic Acids in Ruthenium-Catalyzed Aromatic C–H Silylation. *J. Am. Chem. Soc.* **2009**, *131*, 7502.
- (13) Vancoillie, G.; Hoogenboom, R. Synthesis and polymerization of boronic acid containing monomers. *Polymer Chemistry* **2016**, *7*, 5484.
- (14) Wang, J.; Sánchez-Roselló, M.; Aceña, J. L.; del Pozo, C.; Sorochinsky, A. E.; Fustero, S.; Soloshonok, V. A.; Liu, H. Fluorine in Pharmaceutical Industry: Fluorine-Containing Drugs Introduced to the Market in the Last Decade (2001–2011). *Chem. Rev.* **2014**, *114*, 2432.
- (15) Lennox, A. J. J.; Lloyd-Jones, G. C. The Slow-Release Strategy in Suzuki–Miyaura Coupling. *Isr. J. Chem.* **2010**, *50*, 664.
- (16) Campeau, L.-C.; Fagnou, K. Applications of and alternatives to π -electron-deficient azine organometallics in metal catalyzed cross-coupling reactions. *Chem. Soc. Rev.* **2007**, *36*, 1058.
- (17) Billingsley, K.; Buchwald, S. L. Highly Efficient Monophosphine-Based Catalyst for the Palladium-Catalyzed Suzuki–Miyaura Reaction of Heteroaryl Halides and Heteroaryl Boronic Acids and Esters. *J. Am. Chem. Soc.* **2007**, *129*, 3358.
- (18) Markovic, T.; Rocke, B. N.; Blakemore, D. C.; Mascitti, V.; Willis, M. C. Catalyst Selection Facilitates the Use of Heterocyclic Sulfinates as General Nucleophilic Coupling Partners in Palladium-Catalyzed Coupling Reactions. *Org. Lett.* **2017**, *19*, 6033.
- (19) Markovic, T.; Rocke, B. N.; Blakemore, D. C.; Mascitti, V.; Willis, M. C. Pyridine sulfinates as general nucleophilic coupling partners in palladium-catalyzed cross-coupling reactions with aryl halides. *Chem. Sci.* **2017**, *8*, 4437.

- (20) Aida, W.; Ohtsuki, T.; Li, X.; Ishibashi, M. Isolation of new carbamate- or pyridine-containing natural products, fuzanins A, B, C, and D from *Kitasatospora* sp. IFM10917. *Tetrahedron* **2009**, *65*, 369.
- (21) Nicolaou, K. C.; Scarpelli, R.; Bollbuck, B.; Werschkun, B.; Pereira, M. M. A.; Wartmann, M.; Altmann, K. H.; Zaharevitz, D.; Gussio, R.; Giannakakou, P. Chemical synthesis and biological properties of pyridine epothilones *Chem. Biol.* **2000**, *7*, 593.
- (22) Richardson, C. M.; Gillespie, R. J.; Williamson, D. S.; Jordan, A. M.; Fink, A.; Knight, A. R.; Sellwood, D. M.; Misra, A. Identification of Non-Furan Containing A2A Antagonists Using Database Mining and Molecular Similarity Approaches. *Bioorg. Med. Chem. Lett.* **2006**, *16*, 5993.
- (23) Gellibert, F.; de Gouville, A.-C.; Woolven, J.; Mathews, N.; Nguyen, V.-L.; Bertho-Ruault, C.; Patikis, A.; Grygielko, E. T.; Laping, N. J.; Huet, S. Discovery of 4-[4-[3-(Pyridin-2-yl)-1H-pyrazol-4-yl]pyridin-2-yl]-N-(tetrahydro-2H-pyran-4-yl)benzamide (GW788388): A Potent, Selective, and Orally Active Transforming Growth Factor- β Type I Receptor Inhibitor. *J. Med. Chem.* **2006**, *49*, 2210.
- (24) Anderson, D. R.; Meyers, M. J.; Vernier, W. F.; Mahoney, M. W.; Kurumbail, R. G.; Caspers, N.; Poda, G. I.; Schindler, J. F.; Reitz, D. B.; Mourey, R. J. Pyrrolopyridine Inhibitors of Mitogen-Activated Protein Kinase-Activated Protein Kinase 2 (MK-2). *J. Med. Chem.* **2007**, *50*, 2647.
- (25) Hwang, G. T.; Hari, Y.; Romesberg, F. E. The effects of unnatural base pairs and mismatches on DNA duplex stability and solvation. *Nucleic Acids Res.* **2009**, *37*, 4757.
- (26) Gutierrez, A. J.; Terhorst, T. J.; Matteucci, M. D.; Froehler, B. C. 5-Heteroaryl-2'-deoxyuridine Analogs. Synthesis and Incorporation into High-Affinity Oligonucleotides. *J. Am. Chem. Soc.* **1994**, *116*, 5540.
- (27) Chi, C.-C.; Chiang, C.-L.; Liu, S.-W.; Yueh, H.; Chen, C.-T.; Chen, C.-T. Achieving high-efficiency non-doped blue organic light-emitting diodes: charge-balance control of bipolar blue fluorescent materials with reduced hole-mobility. *J. Mater. Chem.* **2009**, *19*, 5561.
- (28) Yamaguchi, Y.; Kobayashi, S.; Miyamura, S.; Okamoto, Y.; Wakamiya, T.; Matsubara, Y.; Yoshida, Z.-i. Synthesis and Light-Emitting Characteristics of Doughnut-Shaped π -Electron Systems. *Angew. Chem. Int. Ed.* **2004**, *43*, 366.
- (29) Schubert, U. S.; Eschbaumer, C. New Synthetic Strategy toward Pyridine-Based Ligands for Supramolecular Chemistry Utilizing 2,6-Bis(trimethyltin)pyridine as the Central Building Block. *Org. Lett.* **1999**, *1*, 1027.
- (30) Havas, F.; Leygue, N.; Danel, M.; Mestre, B.; Galaup, C.; Picard, C. 6,6'-Dimethyl-2,2'-bipyridine-4-ester: A pivotal synthon for building tethered bipyridine ligands. *Tetrahedron* **2009**, *65*, 7673.
- (31) Littke, A. F.; Schwarz, L.; Fu, G. C. Pd/P(*t*-Bu)₃: A Mild and General Catalyst for Stille Reactions of Aryl Chlorides and Aryl Bromides. *J. Am. Chem. Soc.* **2002**, *124*, 6343.
- (32) Denmark, S. E.; Smith, R. C.; Chang, W.-T. T.; Muhuhi, J. M. Cross-Coupling Reactions of Aromatic and Heteroaromatic Silanolates with Aromatic and Heteroaromatic Halides. *J. Am. Chem. Soc.* **2009**, *131*, 3104.
- (33) Li, W.; Nelson, D. P.; Jensen, M. S.; Hoerner, R. S.; Cai, D.; Larsen, R. D.; Reider, P. J. An Improved Protocol for the Preparation of 3-Pyridyl- and Some Arylboronic Acids. *J. Org. Chem.* **2002**, *67*, 5394.
- (34) Mitchell, M. B.; Wallbank, P. J. Coupling of heteroaryl chlorides with arylboronic acids in the presence of [1,4-bis-(diphenylphosphine)butane]palladium(II) dichloride. *Tetrahedron Lett.* **1991**, *32*, 2273.
- (35) Molander, G. A.; Biolatto, B. Palladium-Catalyzed Suzuki-Miyaura Cross-Coupling Reactions of Potassium Aryl- and Heteroaryltrifluoroborates. *J. Org. Chem.* **2003**, *68*, 4302.
- (36) Stefani, H. A.; Cella, R.; Vieira, A. S. Recent advances in organotrifluoroborates chemistry. *Tetrahedron* **2007**, *63*, 3623.
- (37) Cox, P. A.; Leach, A. G.; Campbell, A. D.; Lloyd-Jones, G. C. Protodeboronation of Heteroaromatic, Vinyl, and Cyclopropyl Boronic Acids: pH-Rate Profiles, Autocatalysis, and Disproportionation. *J. Am. Chem. Soc.* **2016**, *138*, 9145.

- (38) Kuivila, H. G.; Reuwer Jr, J. F.; Mangravite, J. A. Electrophilic Displacement Reactions: XV. Kinetics and Mechanism of the Base-Catalyzed Protodeboronation of Areneboronic Acids. *Can. J. Chem.* **1963**, *41*, 3081.
- (39) Deng, J. Z.; Paone, D. V.; Ginnetti, A. T.; Kurihara, H.; Dreher, S. D.; Weissman, S. A.; Stauffer, S. R.; Burgey, C. S. Copper-Facilitated Suzuki Reactions: Application to 2-Heterocyclic Boronates. *Org. Lett.* **2009**, *11*, 345.
- (40) Chen, J.; Cammers-Goodwin, A. 2-(Fluorophenyl)pyridines by the Suzuki–Miyaura method: Ag₂O accelerates coupling over undesired ipso substitution (S_NAr) of fluorine. *Tetrahedron Lett.* **2003**, *44*, 1503.
- (41) Chen, K.; Peterson, R.; Math, S. K.; LaMunyon, J. B.; Testa, C. A.; Cefalo, D. R. Lithium trihydroxy/triisopropoxy-2-pyridylborate salts (LTBS): synthesis, isolation, and use in modified Suzuki–Miyaura cross-coupling reactions. *Tetrahedron Lett.* **2012**, *53*, 4873.
- (42) Kinzel, T.; Zhang, Y.; Buchwald, S. L. A New Palladium Precatalyst Allows for the Fast Suzuki–Miyaura Coupling Reactions of Unstable Polyfluorophenyl and 2-Heteroaryl Boronic Acids. *J. Am. Chem. Soc.* **2010**, *132*, 14073.
- (43) Wolf, C.; Lerebours, R. Efficient Stille Cross-Coupling Reaction Using Aryl Chlorides or Bromides in Water. *J. Org. Chem.* **2003**, *68*, 7551.
- (44) Robbins, D. W.; Hartwig, J. F. A C–H Borylation Approach to Suzuki–Miyaura Coupling of Typically Unstable 2-Heteroaryl and Polyfluorophenyl Boronates. *Org. Lett.* **2012**, *14*, 4266.
- (45) Dick, G. R.; Woerly, E. M.; Burke, M. D. A General Solution for the 2-Pyridyl Problem. *Angew. Chem. Int. Ed.* **2012**, *51*, 2667.
- (46) Billingsley, K. L.; Buchwald, S. L. A General and Efficient Method for the Suzuki–Miyaura Coupling of 2-Pyridyl Nucleophiles. *Angew. Chem. Int. Ed.* **2008**, *120*, 4773.
- (47) Hodgson, P. B.; Salingue, F. H. The preparation of a stable 2-pyridylboronate and its reactivity in the Suzuki–Miyaura cross-coupling reaction. *Tetrahedron Lett.* **2004**, *45*, 685.
- (48) Busch, M.; Cayir, M.; Nieger, M.; Thiel, W. R.; Bräse, S. Roadmap towards *N*-Heterocyclic [2.2]Paracyclophanes and Their Application in Asymmetric Catalysis. *Eur. J. Org. Chem.* **2013**, 6108.
- (49) Hassan, Z.; Spuling, E.; Knoll, D. M.; Lahann, J.; Bräse, S. Planar chiral [2.2]paracyclophanes: from synthetic curiosity to applications in asymmetric synthesis and materials. *Chem. Soc. Rev.* **2018**, *47*, 6947.
- (50) Ruan, J.; Shearer, L.; Mo, J.; Bacsá, J.; Zanotti-Gerosa, A.; Hancock, F.; Wu, X.; Xiao, J. [2.2]Paracyclophane-based monophosphine ligand for palladium-catalyzed cross-coupling reactions of aryl chlorides. *Org. Biomol. Chem.* **2009**, *7*, 3236.
- (51) Roche, A. J.; Canturk, B. An exploration of Suzuki aryl cross coupling chemistry involving [2.2]paracyclophane derivatives. *Org. Biomol. Chem.* **2005**, *3*, 515.
- (52) Rozenberg, V. I.; Antonov, D. Y.; Zhuravsky, R. P.; Vorontsov, E. V.; Starikova, Z. A. A novel class of bidentate ligands with a conformationally flexible biphenyl unit built into a planar chiral [2.2]paracyclophane backbone. *Tetrahedron Lett.* **2003**, *44*, 3801.
- (53) Fu, G. C. Asymmetric Catalysis with “Planar-Chiral” Derivatives of 4-(Dimethylamino)pyridine. *Acc. Chem. Res.* **2004**, *37*, 542.
- (54) Fu, G. C. Enantioselective Nucleophilic Catalysis with “Planar-Chiral” Heterocycles. *Acc. Chem. Res.* **2000**, *33*, 412.
- (55) Di Salvo, F.; Teixidor, F.; Viñas, C.; Planas, J. G.; Light, M. E.; Hursthouse, M. B.; Aliaga-Alcalde, N. Metallo-supramolecular Chemistry of Novel Chiral closo-*o*-Carboranylalcohol Pyridine and Quinoline Ligands: Syntheses, Characterization, and Properties of Cobalt Complexes. *Cryst. Growth Des.* **2012**, *12*, 5720.
- (56) He, W.; Pan, G.; Yang, Z.; Zhao, D.; Niu, G.; Huang, W.; Yuan, X.; Guo, J.; Cao, H.; Yang, H. Wide Blue Phase Range in a Hydrogen-Bonded Self-Assembled Complex of Chiral Fluoro-Substituted Benzoic Acid and Pyridine Derivative. *Adv. Mater.* **2009**, *21*, 2050.
- (57) Rowlands, G. J. Planar Chiral Phosphines Derived from [2.2]Paracyclophane. *Isr. J. Chem.* **2012**, *52*, 60.
- (58) Seitzberg, J. G.; Dissing, C.; Sjøtofte, I.; Norrby, P.-O.; Johannsen, M. Design and Synthesis of a New Type of Ferrocene-Based Planar Chiral DMAP Analogues. A New Catalyst System for Asymmetric Nucleophilic Catalysis. *J. Org. Chem.* **2005**, *70*, 8332.

- (59) Ogasawara, M.; Wada, S.; Isshiki, E.; Kamimura, T.; Yanagisawa, A.; Takahashi, T.; Yoshida, K. Enantioselective Synthesis of Planar-Chiral Ferrocene-Fused 4-Pyridones and Their Application in Construction of Pyridine-Based Organocatalyst Library. *Org. Lett.* **2015**, *17*, 2286.
- (60) Yoshida, K.; Yasue, R. Planar-Chiral Ferrocene-Based *N*-Heterocyclic Carbene Ligands. *Chem. Eur. J.* **2018**, *24*, 18575.
- (61) Braun, C.; Spuling, E.; Heine, N. B.; Cakici, M.; Nieger, M.; Bräse, S. Efficient Modular Synthesis of Isomeric Mono- and Bispyridyl[2.2]paracyclophanes by Palladium-Catalyzed Cross-Coupling Reactions. *Adv. Synth. Catal.* **2016**, *358*, 1664.
- (62) Braun, C.; Nieger, M.; Bräse, S. Unprecedented One-Pot Reaction towards Chiral, Non-Racemic Copper(I) Complexes of [2.2]Paracyclophane-Based *P,N*-Ligands. *Chem. Eur. J.* **2017**, *23*, 16452.
- (63) Braun, C.; Nieger, M.; Thiel, W. R.; Bräse, S. [2.2]Paracyclophanes with *N*-Heterocycles as Ligands for Mono- and Dinuclear Ruthenium(II) Complexes. *Chem. Eur. J.* **2017**, *23*, 15474.
- (64) Knoll, D. M.; Bräse, S. Suzuki Cross-Coupling of [2.2]Paracyclophane Trifluoroborates with Pyridyl and Pyrimidyl Building Blocks. *ACS Omega* **2018**, *3*, 12158.
- (65) Knoll, D. M.; Šimek, H.; Hassan, Z.; Bräse, S. Preparation and Synthetic Applications of [2.2]Paracyclophane Trifluoroborates: An Efficient and Convenient Route to Nucleophilic [2.2]Paracyclophane Cross-Coupling Building Blocks. *Eur. J. Org. Chem.* **2019**, *2019*, 6198.
- (66) Fulton, J. R.; Glover, J. E.; Kamara, L.; Rowlands, G. J. Facile synthesis of planar chiral *N*-oxides and their use in Lewis base catalysis. *Chem. Commun.* **2011**, *47*, 433.
- (67) Hopf, H.; Aly, Ashraf A.; Swaminathan, Vijay N.; Ernst, L.; Dix, I.; Jones, Peter G. A Simple Route to a Pyridinyl[2.2]paracyclophane. *Eur. J. Org. Chem.* **2005**, 68.
- (68) Campeau, L.-C.; Rousseaux, S.; Fagnou, K. A Solution to the 2-Pyridyl Organometallic Cross-Coupling Problem: Regioselective Catalytic Direct Arylation of Pyridine *N*-Oxides. *J. Am. Chem. Soc.* **2005**, *127*, 18020.
- (69) Dubbaka, S. R.; Vogel, P. Palladium-Catalyzed Suzuki–Miyaura Cross-Couplings of Sulfonyl Chlorides and Boronic Acids. *Org. Lett.* **2004**, *6*, 95.
- (70) Dubbaka, S. R.; Vogel, P. Palladium-Catalyzed Stille Cross-Couplings of Sulfonyl Chlorides and Organostannanes. *J. Am. Chem. Soc.* **2003**, *125*, 15292.
- (71) Jayasundera, K. P.; Kusmus, D. N. M.; Deuilhé, L.; Etheridge, L.; Farrow, Z.; Lun, D. J.; Kaur, G.; Rowlands, G. J. The synthesis of substituted amino[2.2]paracyclophanes. *Org. Biomol. Chem.* **2016**, *14*, 10848.
- (72) Jayasundera, K. P.; Engels, T. G. W.; Lun, D. J.; Mungalpara, M. N.; Plieger, P. G.; Rowlands, G. J. The synthesis of planar chiral pseudo-gem aminophosphine pre-ligands based on [2.2]paracyclophane. *Org. Biomol. Chem.* **2017**, *15*, 8975.
- (73) Kramer, J. J. P.; Yildiz, C.; Nieger, M.; Bräse, S. Direct Access to 4,5-Disubstituted [2.2]Paracyclophanes by Selective ortho-Halogenation with Pd-Catalyzed C-H Activation. *Eur. J. Org. Chem.* **2014**, 1287.

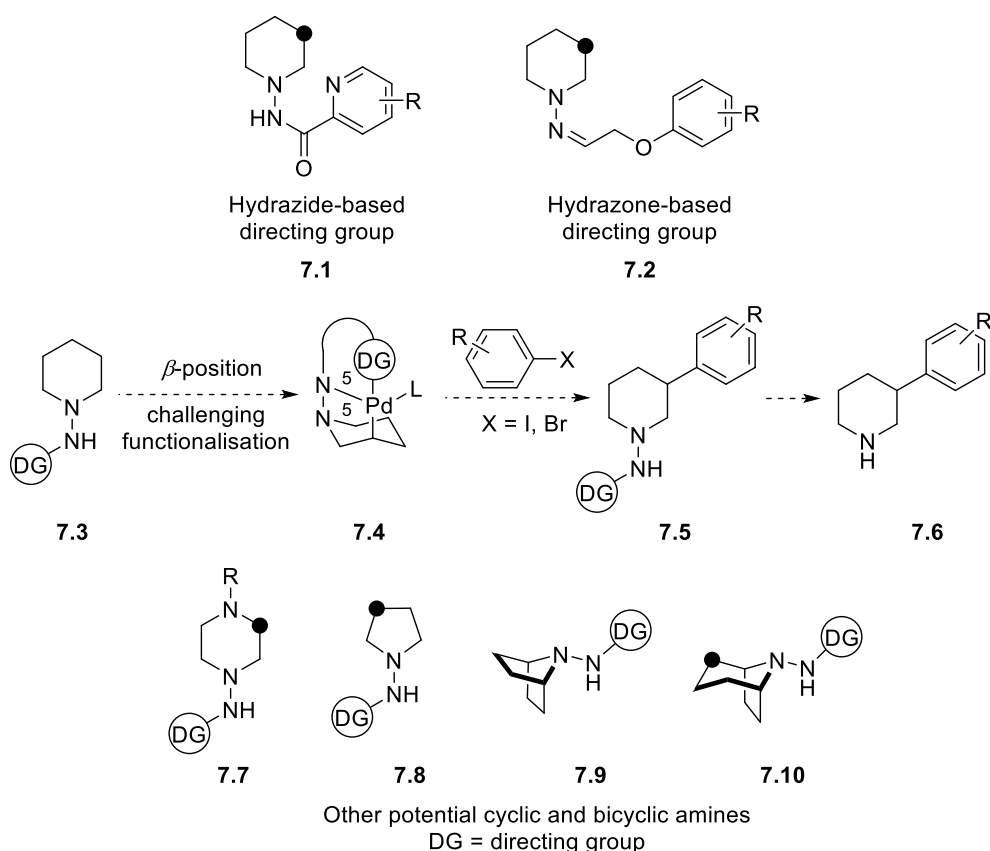
Chapter 7

Future Perspective

7.0. Future perspective

7.1. Hydrazone and hydrazone-based directing groups for the remote C-H functionalisation of cyclic amines

We have screened various directing groups in order to investigate the β -C(sp^3)-H arylation of 7-(benzo)azabicyclo[2.2.1]heptane (Chapter 3). Based on this study, we surmise that the thermodynamically favoured fused 5,5-metallacycle may facilitate the desired C-H functionalisation (Scheme 7.1). We also proposed hydrazone and hydrazone-based directing groups.¹ The next strategy would be to study β -C(sp^3)-H arylation on the piperidine system **7.3**.

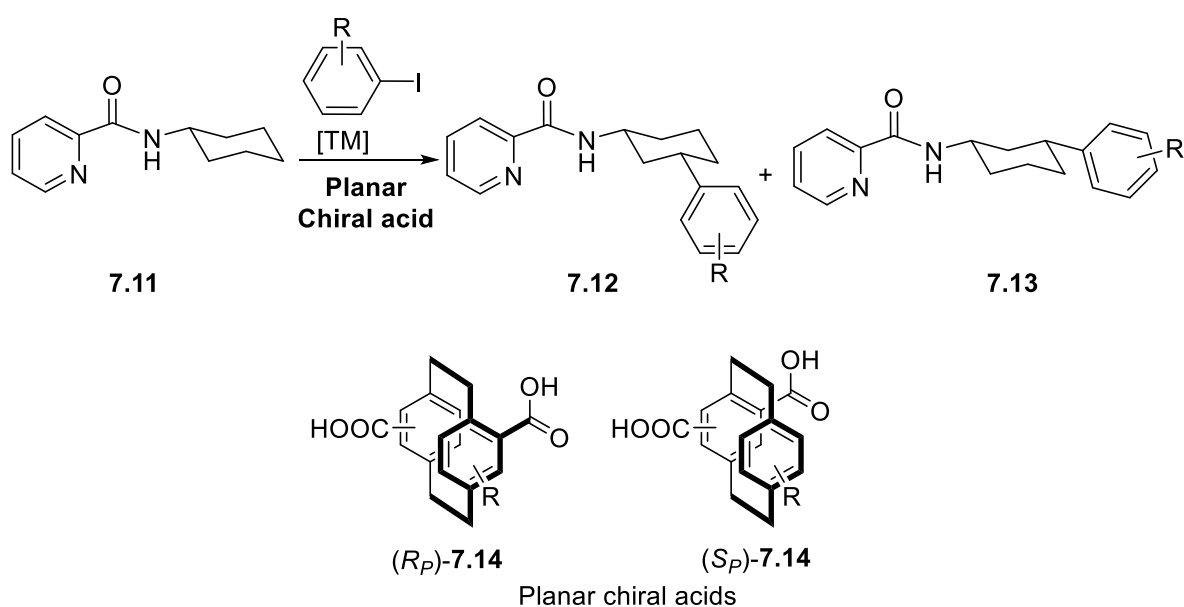


Scheme 7.1: Hydrazone and hydrazone-based directing groups for the remote C-H functionalisation of cyclic and bicyclic amines.

Once we have obtained ‘proof-of-concept’, this chemistry can be elaborated to investigate different heterocyclic derivatives. The ultimate goal will be to develop an asymmetric variant of this methodology. A number of directing groups can accommodate a stereogenic element, permitting diastereoselective functionalisation and the creation of a chiral auxiliary. Another approach could be to employ an enantioselective catalyst for an asymmetric C-H functionalisation.

7.2. Planar chiral dicarboxylic acids in Asymmetric catalysis

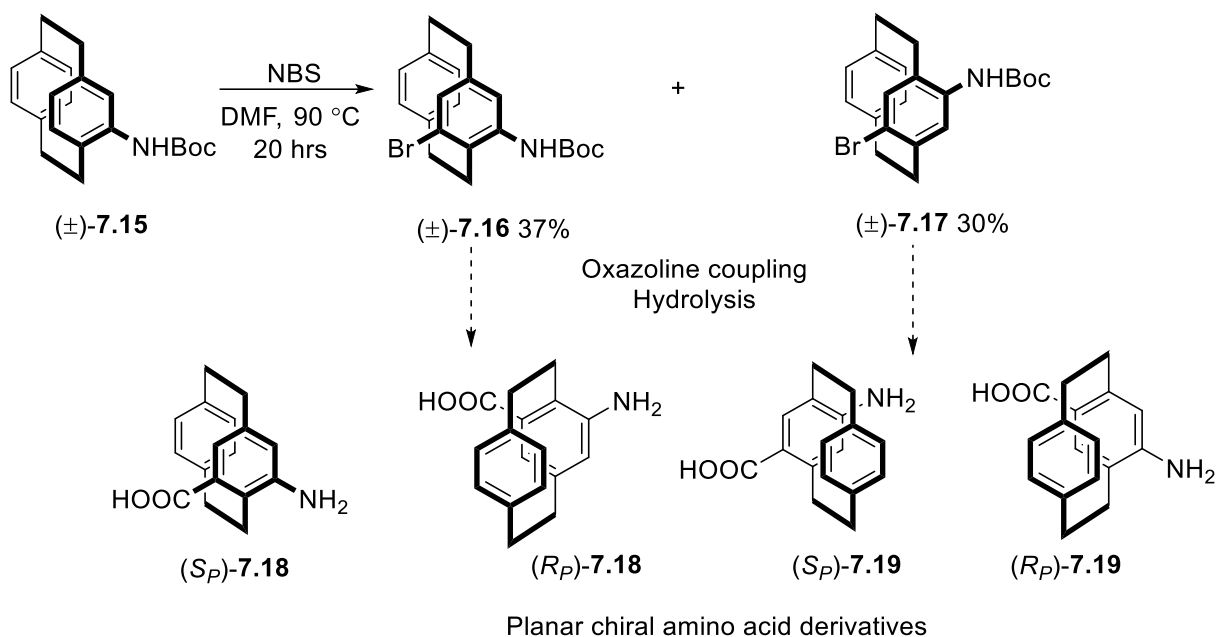
In Chapter 3, we have shown that planar chiral [2.2]paracyclophane carboxylic acid derivatives can catalyse the γ -C(sp^3)-H functionalisation of the *N*-cyclohexylpicolinamide **7.11**. We did not have access to the enantiomerically enriched versions, however, once we obtain enantiopure planar chiral acids *via* the oxazoline coupling protocol (Chapter 4), it would be intriguing to investigate their potential in enantioselective C-H activation (Scheme 7.2). Further, taking inspiration from the success of chiral phosphoric acids in asymmetric catalysis,²⁻⁴ exploiting the scope of these planar chiral acids would be instrumental.



Scheme 7.2: Exploiting planar chiral acids in asymmetric C-H functionalisation.

7.3. Expanding the scope of bromo[2.2]paracyclophane derivatives for oxazoline coupling

We have developed a protocol to couple chiral oxazolines with bromo[2.2]paracyclophane derivatives (Chapter 4). This methodology has provided exciting results. In some cases, the resolution of diastereomers was possible. It would be intriguing to elaborate the scope of bromo[2.2]paracyclophane derivatives. For example, we have synthesised two new bromo[2.2]paracyclophane precursors, (\pm)-4-(*tert*-butylamino)-7-bromo[2.2]paracyclophane carbamate **7.16** and (\pm)-4-(*tert*-butylamino)-8-bromo[2.2]paracyclophane carbamate **7.17** (Scheme 7.3). With the oxazoline coupling, different amino[2.2]paracyclophane-oxazoline derivatives can be synthesised, which could be hydrolysed to provide planar chiral amino acids.

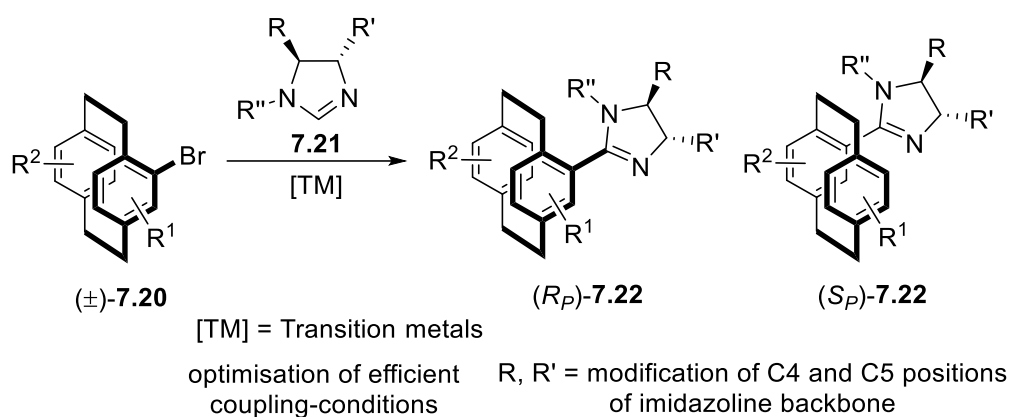


Scheme 7.3: Synthesis of 4-(*tert*-butylamino)-8-bromo[2.2]paracyclophane carbamate **7.16** & 4-(*tert*-butylamino)-7-bromo[2.2]paracyclophane carbamate **7.17**, and access to planar chiral amino acids.

Planar chiral [2.2]paracyclophane amino acids (*pseudo* amino acids) provide a unique opportunity to prepare planar chiral *pseudo*peptides. They can be promising supramolecular organic frameworks. With these fascinating properties, planar chiral *pseudo*peptides can be applied in asymmetric catalysis, the biomedical field, and the development of new materials.

7.4. Optimisation of imidazoline coupling with bromo[2.2]paracyclophanes

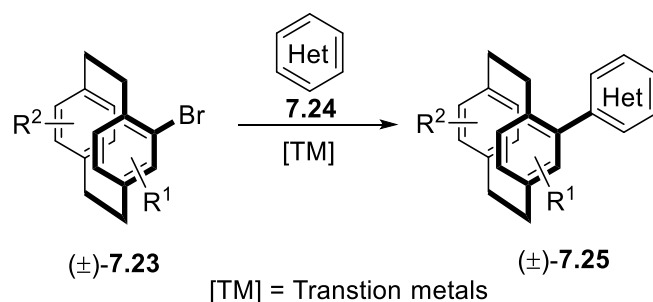
Similar to oxazoline coupling, it would be interesting to broaden the scope of imidazolines **7.21** in coupling reactions with bromo[2.2]paracyclophane derivatives **7.20** (Scheme 7.4). Imidazolines can be readily synthesised from basic precursors such as 1,2-diamines and β -hydroxy amides.⁵ We have shown that (*S*)-1-(1-phenylethyl)-4,5-dihydro-1*H*-imidazole can be coupled with (±)-4-bromo[2.2]paracyclophane (Chapter 4). It would be interesting to optimise the coupling conditions of imidazolines. Introducing bulky substituents and polar/apolar functionalities at C4 and/or C5 position of the imidazoline framework may help in the resolution of [2.2]paracyclophane-imidazoline derivatives **7.22**. These planar chiral imidazolines can be exploited as ligands in homogenous catalysis.⁵



Scheme 7.4: Optimisation of imidazoline coupling with bromo[2.2]paracyclophanes and expand the scope of imidazolines.

7.5. Coupling of aromatic/nonaromatic heterocycles with [2.2]paracyclophane derivatives

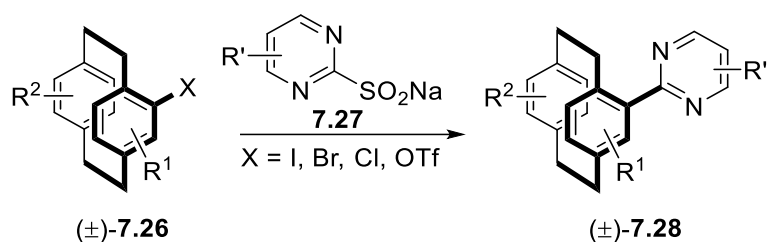
In [2.2]paracyclophane chemistry, the direct coupling of heteroarene derivatives *via* C-H functionalisation is uncommon. Most methodologies rely on traditional cross-coupling reactions, where heterocyclic compounds possess either halides (electrophilic partner) or organometallic intermediates (nucleophilic partner). These cross-coupling methodologies are not versatile and are limited due to poor functional group tolerance. Moreover, preparing appropriate [2.2]paracyclophane organometallic precursors requires multiple steps, and some of them are even unstable such as boronates. In Chapter 4, our initial study demonstrated the potential of the C-H functionalisation of both aromatic (benzimidazole and indole system) and non-aromatic (imidazoline system) heterocycles followed by coupling with (±)-4-bromo[2.2]paracyclophane. It would be interesting to expand this study to various heterocyclic compounds **7.24** and bromo[2.2]paracyclophane derivatives **7.23** with diverse functionalities (Scheme 7.5). With this methodology, it will be a new paradigm in paracyclophane chemistry, allowing access to a wide range of planar chiral [2.2]paracyclophane-heterocyclic compounds **7.25**.



Scheme 7.5: New strategy to synthesise the [2.2]paracyclophane-heterocyclic compounds.

7.6. [2.2]Paracyclophane sulfinate derivatives as potential nucleophilic coupling partners

In Chapter 6, we explored pyridine sulfonates as nucleophilic coupling partners in the desulfitative cross-coupling reactions with the various bromo[2.2]paracyclophanes. This approach could be further extended to couple other heteroarene sulfonates **7.27** (Scheme 7.6). This will provide a new route to heteroarene[2.2]paracyclophane derivatives **7.28**. These could be valuable moieties in the synthesis of bioactive molecules,⁶ materials,⁷ and ligands for catalysis.⁸



Scheme 7.6: Scope of heteroarene sulfonates in desulfitative coupling with [2.2]paracyclophane halides/triflates.

Recently, heterocyclic allyl sulfones **7.29** have emerged as latent heteroaryl nucleophiles. They are easy to synthesise and soluble in standard reaction solvents (Figure 7.1).⁹

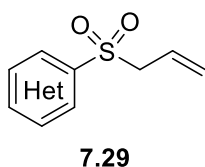
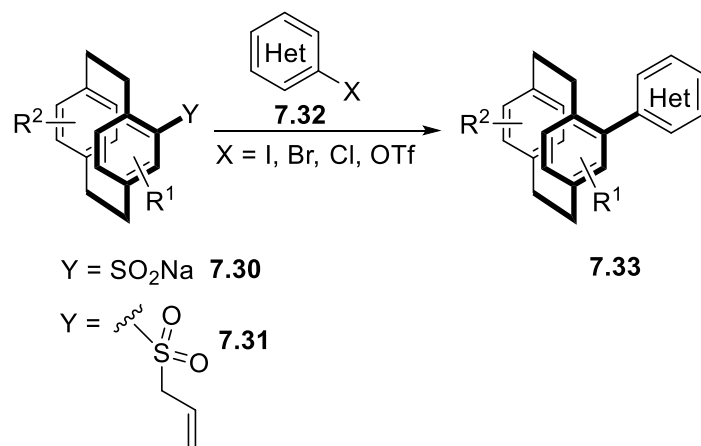


Figure 7.1: Heterocyclic allyl sulfone as latent nucleophile.

In the reverse approach, it would be intriguing to evaluate the potential of [2.2]paracyclophane sulfinate/allyl sulfone derivatives **7.30** & **7.31** as potential nucleophilic coupling partners with aryl- and heteroaryl halides **7.32** (Scheme 7.7). Since [2.2]paracyclophane boronic acids and derivatives are not stable or user friendly, finding an alternative nucleophilic coupling partner would be very useful. This reverse strategy will have more advantages since heterocyclic halides are commercially available and relatively easy to synthesis. Research work in this direction has already been initiated in our laboratory. We have synthesised both [2.2]paracyclophane sulfinate **7.30** and [2.2]paracyclophane allyl sulfone **7.31** derivatives. We are at the stage of investigating their potential in desulfitative reactions. If successful, this method will provide a new route to a myriad of [2.2]paracyclophane-(hetero)aryl derivatives

from simple precursors. Even more intriguing would be combining this with our original sulfoxide chemistry method to synthesise enantiomerically enriched compounds.¹⁰



Scheme 7.7: [2.2]Paracyclophane sulfinate/allyl sulfone derivatives as potential nucleophilic coupling partners.

7.7. References

- (1) Rowlands, G. J. Hydrazine-Based Directing Groups for the Remote C-H Functionalisation of Cyclic Amines. *ACS Petroleum Research Fund.*, 2018.
- (2) Connon, S. J. Chiral Phosphoric Acids: Powerful Organocatalysts for Asymmetric Addition Reactions to Imines. *Angew. Chem. Int. Ed.* **2006**, *45*, 3909.
- (3) Terada, M. Chiral Phosphoric Acids as Versatile Catalysts for Enantioselective Transformations. *Synthesis* **2010**, *12*, 1929.
- (4) Rahman, A.; Lin, X. Development and Application of Chiral Spirocyclic Phosphoric Acids In Asymmetric Catalysis. *Org. Biomol. Chem.* **2018**, *16*, 4753.
- (5) Liu, H.; Du, D.-M. Recent Advances in the Synthesis of 2-Imidazolines and Their Applications in Homogeneous Catalysis. *Adv. Synth. Catal.* **2009**, *351*, 489.
- (6) Ortner, B.; Waibel, R.; Gmeiner, P. Indoloparacyclophanes: Synthesis and Dopamine Receptor Binding of a Novel Arylbioisostere. *Angew. Chem. Int. Ed.* **2001**, *40*, 1283.
- (7) Hassan, Z.; Spuling, E.; Knoll, D. M.; Lahann, J.; Bräse, S. Planar Chiral [2.2]Paracyclophanes: From Synthetic Curiosity to Applications in Asymmetric Synthesis and Materials. *Chem. Soc. Rev.* **2018**, *47*, 6947.
- (8) Rowlands, G. J. Planar Chiral Phosphines Derived from [2.2]Paracyclophane. *Isr. J. Chem.* **2012**, *52*, 60.
- (9) Markovic, T.; Murray, P. R. D.; Rocke, B. N.; Shavnya, A.; Blakemore, D. C.; Willis, M. C. Heterocyclic Allylsulfones as Latent Heteroaryl Nucleophiles in Palladium-Catalyzed Cross-Coupling Reactions. *J. Am. Chem. Soc.* **2018**, *140*, 15916.
- (10) Rowlands, G. J. The synthesis of Enantiomerically Pure [2.2]Paracyclophane Derivatives. *Org. Biomol. Chem.* **2008**, *6*, 1527.

Chapter 8

Experimental Section

8.0. Experimental Section

8.1. General Information

All reactions were performed in oven- and/or flame-dried glassware under an atmosphere of dry argon or nitrogen unless otherwise noted. Schlenk tubes, pressure tubes, and scintillation vials were used as mentioned in the respective procedures. Moisture-sensitive reactions were carried out using standard syringe septum techniques and under an inert atmosphere of argon or nitrogen. All solvents and reagents were purified by standard techniques unless otherwise noted. Reaction solvent tetrahydrofuran (Fisher, HPLC grade) was dried by distillation from sodium-benzophenone radical ketyl. Dichloroethane (Fisher) was freshly dried by distillation over phosphorus pentoxide. Dichloromethane (Fisher) and acetonitrile (Fisher) were freshly dried by distillation over calcium hydride. DMA (Sigma-Aldrich) was stored under microwave-activated 4 Å molecular sieves. Toluene (Fisher, HPLC grade) was dried by percolation through two columns packed with neutral alumina under a positive pressure of argon. Solvents for filtration, transfers, and chromatography were certified ACS grade. NMR solvent, CDCl₃ was stored under activated neutral alumina and dried over phosphorus pentoxide when applicable. Evaporation of solvents was carried out under reduced pressure on a rotary evaporator with the water bath below 42 °C. “Brine” refers to a saturated solution of sodium chloride in water. Palladium catalysts and phosphine ligands were purchased from Sigma-Aldrich, Sterm, and Apollo Scientific. Other reagents were purchased from Sigma-Aldrich, Alfa Aesar or Acros.

Purification of crude reaction mixtures was performed by column chromatography, Bruker Flash chromatography or preparative TLC. The stationary phase for column chromatography was silica gel 40-63 UM 60A, 230-400 mesh or neutral alumina Brockmann-I. Preparative TLC was performed on MERCK precoated silica gel 60- F254 (0.5-mm) aluminium plates. Solvents for purification were purchased from LabServe. TLC visualisation was carried out using ultraviolet light (254 nm) and different staining reagents such as potassium permanganate, 2,4-dinitropyridine, ethanolic phosphomolybdic acid, or ninhydrin when applicable. The structures of compounds were drawn using ChemDraw Professional 18.0.

8.2. Analytical instruments

Optical rotation was recorded on a Perkin Elmer 241 polarimeter using the sodium emitting at 589 nm. All samples were measured in chloroform unless otherwise noted ($c=1$) in a 10 cm cell and an average taken of 3 readings.

Infrared spectroscopy was carried out on ThermoScientific Nicolet iS5 iD7 ATR using solid, semisolid, or solution of the sample in CH_2Cl_2 .

NMR spectroscopy was carried out on a Bruker 400 MHz, Bruker 500 MHz or Bruker 700 MHz. Chemical shifts are reported in parts per million (ppm) downfield from tetramethylsilane. All spectra were run in CDCl_3 unless otherwise stated. Spin multiplicities are described as s (singlet), bs (broad singlet), d (doublet), dd (doublet of doublets), ddd (doublet of doublet of doublets), dddd (doublet of doublet of doublet of doublets), t (triplet), td (triplet of doublets), q (quartet), m (multiplet), dt (doublet of triplet), ddt (doublet of doublet of doublets), dtd (doublet of triplet of doublets), dq (doublet of quartets). Coupling constants are reported in Hertz (Hz).

HRMS data were recorded by David Lun using a ThermoScientific Q Exactive Focus Hybrid Quadrupole-orbitrap Mass Spectrometer. Sample(s) were injected *via* Dionex Ultimate 3000 HPLC system running at 0.1 mL/min CH_3OH .

Gas chromatography was carried out on Shimadzu GC2010. The injector temperature was set to 200 °C and flame ionisation detector set to 300 °C with a temperature ramp 15 °C/min.

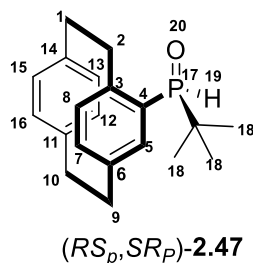
HPLC was carried out on Dionex Ultimate 3000, both normal phase and reverse phase using optimised conditions, as described in Results and Discussion section.

Single crystal X-ray analyses were performed by Prof. Paul Plieger and Prof. Martyn Coles of Victoria University of Wellington using a RigakuSpider X-ray diffractometer.

Melting points were recorded on a Gallenkamp melting point apparatus and are uncorrected.

8.3. Experimental for Chapter 2

(*RS_p*,*SR_p*)-4-*tert*-butyl[2.2]paracyclophane phosphine oxide **2.47**



A solution of *n*-BuLi (1.2 M in hexanes; 18.3 ml, 21.9 mmol, 1.05 eq.) was added dropwise over 30 min. to a solution of (\pm)-4-bromo[2.2]paracyclophane **2.46** (6.0 g, 20.9 mmol, 1.0 eq.) in THF (60 ml), at -78 °C. The resulting yellow solution was stirred at -78 °C for 40 min. *tert*-Butyldichlorophosphine (1M in Et₂O; 21.9 ml, 21.9 mmol, 1.05 eq.) was added dropwise over 20 min. The solution was warmed to room temperature overnight. H₂O (75 ml) was added to the reaction mixture and the resulting organic phases were separated. The aqueous phase was extracted with EtOAc (3 \times 50 ml), the combined organic fractions dried (MgSO₄) and concentrated under reduced pressure to yield a yellow residue, which was purified by column chromatography on silica gel (EtOAc : Hexanes 6 :4) followed by recrystallisation (CH₂Cl₂ : pentane 2 : 8) to give white crystals of **2.47** (3.3 g, 1.05 mmol, 55 %).

R_f (4 : 6 Hex : EtOAc) 0.40.

mp: 142 °C - 144 °C

IR ν_{max} (Solid) 2959, 2930, 2865, 1700, 1594, 1499, 1473, 1431, 1410, 1392, 1358, 1263, 1129, 1094, 1069, 1022, 994, 925, 900 cm⁻¹.

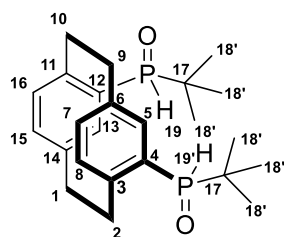
¹H NMR (CDCl₃, 500 MHz): δ 7.42 (d, $J_{\text{P-H}} = 398.1$ Hz, 1H, P-H), 6.92 (d, $J = 7.7$ Hz, 1H, H-5), 6.67 (d, $J = 8.1$ Hz, 1H, H-13), 6.61-6.58 (m, 2H, H-7, H-8), 6.53-6.52 (m, 2H, H-15, H-16), 6.45 (d, $J = 8.1$ Hz, 1H, H-12), 3.94 (t, $J = 11.5$ Hz, 1H, H-2b), 3.45 (td, $J = 12.0, 4.5$ Hz, 1H, H-2a), 3.22-3.18 (m, H-1a, 2H, H-10a), 3.13-2.99 (m, 4H, H-1b, H-10b, H-9a, H-9b), 1.00 (d, $J = 16.2$ Hz, 9H, ^tBu).

^{13}C NMR (CDCl_3 , 125 MHz) δ 173.7, 145.3, 140.02, 139.6 (d, $J_{\text{P-C}} = 54.1$ Hz), 135.5 (d, $J_{\text{P-C}} = 71.3$ Hz), 134.2 (d, $J_{\text{P-C}} = 133.8$ Hz), 133.2 (d, $J_{\text{P-C}} = 105.2$ Hz), 132.2, 126.3 (d, $J_{\text{P-C}} = 375.7$ Hz) 39.53, 36.2, 35.2, 32.6 (d, $J_{\text{P-C}} = 273.0$ Hz), 23.5.

^{31}P NMR (CDCl_3 , 200 MHz) δ 57.81.

HRMS-EI: m/z found: [M], 312.1747. $\text{C}_{25}\text{H}_{25}\text{OP}$ requires [M] 312.1643.

(\pm)-4,13-ditert-butyl-[2.2]paracyclophane phosphine oxide **2.57**

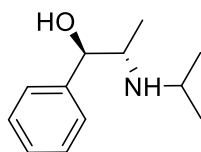


(\pm)-**2.57**

$^t\text{BuLi}$ (1.6 M solution in hexane, 1.37 ml, 2.16 mmol) was added dropwise over 15 min. to a solution of (\pm)-4,12-dibromo-[2.2]paracyclophane **2.56** (200 mg, 0.54 mmol) in dry THF (7 ml), at -78 °C under an inert argon atmosphere. The resulting yellow solution was stirred for 40 min. at -78 °C. After that *tert*-butyldichlorophosphine ($^t\text{BuPCl}_2$) (1 M solution in Et_2O , 1.15 ml, 1.15 mmol) was added dropwise over 10 min., through a steady stream, *via* syringe. The solution was allowed to warm at room temperature overnight. H_2O (75 ml) was then added to the reaction mixture. The resulting organic phase was separated and the aqueous phase was further extracted with EtOAc (3×10 ml), the combined organics dried (MgSO_4) and concentrated under reduced pressure to yield a yellow residue, which was purified by column chromatography on silica gel using methanol : DCM (1:9) give yellow solid. Analysis by ^1H -NMR spectroscopy indicated the compound isolated to be bis-phosphine oxide (\pm)-**2.57** (10 mg, 0.024 mmol, 5% yield).

^1H NMR ($\text{MeOD}-d^4$, 500 MHz): δ 7.52 (d, $J_{\text{P-H}} = 116.6$ Hz, 2H, H-19, H-19'), 7.10 (d, $J = 18.1$ Hz, 2H, H-5, H-13), 6.72 (d, $J = 7.9$ Hz, 2H, H-7, H-8), 6.62 - 6.60 (m, 2H, H-15, H-16), 3.91 (t, $J = 11.0, 11.4$ Hz, 2H, H-2a, H-2b), 3.48 - 3.45 (m, 2H, H-9a, H-9b), 3.09 (t, $J = 10.0$ Hz, H-1a, H-1b), 3.00 (td, $J = 12.4, 4.5$ Hz, 2H, H-10a, H-10b), 0.96 (d, $J = 16.5$ Hz, 18H, H-18, H-20).

(1*R*,2*S*)-(isopropylamino)-1-phenylpropan-1-ol **2.61**

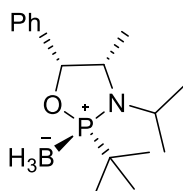


2.61

To a solution of (1*R*,2*S*)-phenylpropanolamine (2.0 g, 13.2 mmol, 1.0 eq.) in CH₃CN (20 ml) was added K₂CO₃ (9.14 g, 66 mmol, 5.0 Eq.) followed by isopropyl iodide (2.64 ml, 26.4 mmol, 2.0 eq.). The reaction mixture was heated to reflux overnight. After cooling, the resulting slurry was filtered to remove salts. The filtrate was then concentrated under reduced pressure to yield a yellow residue. The residue was further purified by column chromatography [SiO₂, EtOAc : hexane (4:6)] to give (1*R*,2*S*)-2-(isopropylamino)-1-phenylpropan-1-ol **2.61** (1.86 g, 9.73 mmol, 93% yield); ¹H NMR (CDCl₃, 500 MHz): δ 7.37 - 7.32 (m, 4H), 7.25 (m, 1H), 4.71 (d, *J* = 3.9 Hz, 1H), 3.09 - 3.05 (m, 1H), 2.99 (heptet, 1H), 1.12 (dd, *J* = 8.2, 6.3 Hz, 6H), 0.82 (d, *J* = 6.6 Hz, 3H).

Data comparable to that reported in literature.¹

(2*S*,4*S*,5*R*)-Borane-2-*tert*-butyl-oxazaphospholidine **2.63a**



(2*S*,4*S*,5*R*)-**2.63a**

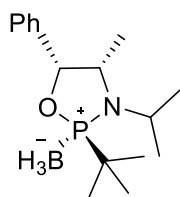
Et₃N (1.78 mL, 6.8 mmol) was added to a stirred solution of (1*R*,2*S*)-2-(isopropylamino)-1-phenylpropan-1-ol (1.0 g, 6.7 mmol, 1.0 eq.) in THF (10 mL) at 0 °C under nitrogen. The reaction mixture was then allowed to stir for 30 min. ^tBuPCl₂ (1 M solution in Et₂O, 7.45 ml, 8.04 mmol, 1.2 eq) was then added drop wise over 10 min.- and reaction mixture was allowed to stir overnight at room temperature. The reaction was again cooled to 0 °C and BH₃.THF (0.67 mL, 7.0 mmol) was added dropwise. The reaction was allowed to reach room temperature and after 3 hrs the solvent was removed under vacuum. The residue was solved in CH₂Cl₂ and washed with distilled water. The organic phase was then washed with a brine solution, dried with MgSO₄ and the solvent removed under vacuum. Purification by column chromatography [SiO₂, EtOAc : hexane (3:7)] furnished the product (72% yield, d.r. 74:26) as a white

crystalline solid. This solid was further separated by column chromatography [SiO_2 , EtOAc : hexane (2:8)] to provide pure diastereomer **2.63a** and **2.63b** respectively.

2.63a

^1H NMR (CDCl_3 , 500 MHz): δ 7.43 - 7.37 (m, 4H), 7.34 - 7.31 (m, 1H), 5.38 - 5.36 (m, 1H), 3.88 (sept, 1H), 3.70 (quint, 1H), 1.34 (d, $J = 16.3$ Hz, 9H), 1.33 (d, $J = 6.7$ Hz, 3H), 0.90 (d, $J = 6.5$ Hz, 3H).

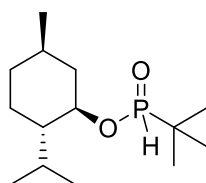
(2R,4S,5R)-Borane-2-tert-butyl-oxazaphospholidine 2.63b



(2R,4S,5R)-2.63b

^1H NMR (CDCl_3 , 500 MHz): δ 7.40 - 7.37 (m, 2H), 7.33 - 7.29 (m, 3H), 5.63 (d, $J = 5.9$ Hz, 1H), 3.91 (sept, 1H), 3.73 (quint, 1H), 1.40 (d, $J = 5.2$ Hz, 3H), 1.35 (d, $J = 16.6$ Hz, 9H), 1.27 (d, $J = 5.2$ Hz, 3H), 0.76 (d, $J = 6.7$ Hz, 3H); ^{13}C NMR (CDCl_3 , 125 MHz) δ 136.50 (d, $J_{\text{P-C}} = 43.7$ Hz), 128.35, 127.84, 125.59, 80.38 (d, $J_{\text{P-C}} = 91.8$ Hz), 53.54 (d, $J_{\text{P-C}} = 6.52$ Hz), 47.80 (d, $J_{\text{P-C}} = 124.7$ Hz), 32.90 (d, $J_{\text{P-C}} = 127.87$), 26.36 (d, $J_{\text{P-C}} = 44.6$ Hz), 21.80 (d, $J_{\text{P-C}} = 46.3$ Hz), 18.51; ^{31}P NMR (CDCl_3 , 200 MHz) δ 53.88

(1R,2S,5R)-2-isopropyl-5-methylcyclohexyl-tert-butylphosphinate 2.66²



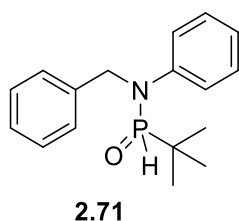
2.66

To an oven dried 100 ml RBF, pyridine (0.51 ml, 6.3 mmol) was added to a solution of menthol **2.65** (1.0 g, 6.39 mmol, 1.0 eq.) in dry THF at 0 °C. The reaction mixture was stirred for 30 min.- at 0 °C. $^t\text{BuPCl}_2$ (1 M solution in Et_2O , 6.39 ml, 6.3 mmol, 1.0 eq.) was then added dropwise over 10 min. and reaction mixture was allowed to stir overnight at room temperature. The reaction was allowed to reach room temperature overnight and the solvent was removed under vacuum. The residue was dissolved in CH_2Cl_2 and washed with distilled water. The

organic phase was then washed with a brine solution, dried with MgSO₄ and the solvent removed under vacuum. Purification was performed by column chromatography [SiO₂, EtOAc : hexane (6:4)]. Analysis by ¹H-NMR spectroscopy indicated the compound isolated to be **2.66** (860 mg, 0.99 mmol, 86% yield) as oily product. ¹H NMR (CDCl₃, 500 MHz): δ 7.23 (d, *J*_{P-H} = 491.8 Hz, 1H), 4.17-4.07 (m, 2H), 2.20-1.99 (m, 2H), 1.63 (d, *J* = 5.9 Hz, 2H), 1.42-1.32 (m, 2H), 1.07 (dd, *J* = 17.8, 1.6 Hz, 9H), 0.86 (d, *J* = 4.9 Hz, 6H), 0.76 (d, *J* = 7.3 Hz, 3H).

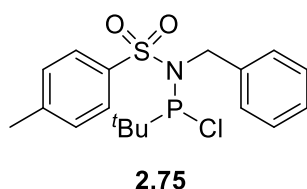
Data comparable to that reported in literature.²

***N*-benzylaniline phosphine oxide 2.71**



N-Benzylaniline phosphine oxide **2.71** was prepared by the procedure mentioned for **2.47** (page no. **236**) by taking *N*-benzylaniline **2.70** (1.1 g, 6.26 mmol, 1.0 eq.), *n*-BuLi (2.2M solution in hexane, 3.1 ml, 6.57 mmol, 1.05 eq.) and ^tBuPCl₂ (1M solution in Et₂O, 6.58 ml, 6.57 mmol). Residues were purified by column chromatography [SiO₂, (EtOAc : hexane) (8:2)]. Analysis by ¹H-NMR spectroscopy indicated the compound isolated to be white solid of **2.71** (113 mg, 0.40 mmol, 18% yield,); ¹H NMR (CDCl₃, 500 MHz): δ 7.41 (d, *J*_{P-H} = 498.4 Hz, 1H), 7.31 (d, *J* = 6.8 Hz, 2H), 7.27-7.26 (m, 1H), 7.26 - 7.24 (m, 5H), 7.21 - 7.19 (m, 1H), 7.08 (quintet, *J* = 8.6, 4.4 Hz, 1H), 4.90 (dd, 15.4, 9.2 Hz, 1H), 4.63 (dd, *J* = 15.4, 8.5 Hz, 1H), 1.14 (d, 13.6 Hz, 9H).

***N*-benzyl-*N*-(*tert*-butylchlorophosphanyl)-4-methylbenzenesulfonamide 2.75**

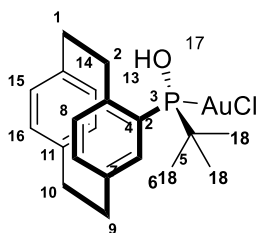


N-Benzyl-*N*-(*tert*-butylchlorophosphanyl)-4-methylbenzenesulfonamide **2.75** was obtained by the following procedure **2.47** (page no. **236**) using *N*-benzyl-4-methylbenzenesulfonamide **2.74** (1.0 g, 3.82 mmol, 1.0 eq.), *n*-BuLi (1.2M solution in hexane, 3.34 ml, 4.01 mmol, 1.05 eq.)

and $t\text{BuPCl}_2$ (1M solution in Et_2O , 4.01 ml, 4.01 mmol). Analysis by $^1\text{H-NMR}$ spectroscopy of crude product indicated the compound isolated to be **2.75** (980 mg, 2.55 mmol, 98% yield). $^1\text{H NMR}$ (CDCl_3 , 500 MHz): δ 7.50 (d, $J = 8.3$ Hz, 2H), 7.27 (d, $J = 3.4$ Hz, 1H), 7.21 - 7.18 (m, 3H), 7.15 (d, $J = 15$ Hz, 1H), 7.11 (d, $J = 8.1$ Hz, 1H), 4.73 (d, $J = 16.1$ Hz, 1H), 4.59 (d, $J = 15.9$ Hz, 9H), 2.40 (s, 3H), 1.18 (d, $J = 15.8$ Hz, 9H).

HRMS calcd for $\text{C}_{18}\text{H}_{23}\text{ONNaO}_2\text{PS}$ 406.0773; found 406.0762.

(*RS_p*,*RS_p*)-chloro(*tert*-butyl([2.2]paracyclophan-4-yl)phosphinous acid)gold (I) **2.95**



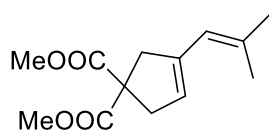
(*RS_p*,*RS_p*)-2.95

To a solution of secondary phosphine oxide **2.47** (30 mg, 0.01 mmol, 1.0 eq.) in CH_2Cl_2 (5 mL) was added chloro(dimethyl sulfide)gold(I) (28 mg, 0.01 mmol, 1.0 eq.). The mixture was stirred at room temperature overnight in the absence of light. The crude mixture was concentrated under reduced pressure to give a greyish solid of **2.95**.

$^1\text{H NMR}$ (CDCl_3 , 500 MHz): δ 7.33 (dd, $J = 20.1$, 1H, 1.7 Hz, H-5), 6.96 (d, $J = 7.7$ Hz, 2H, H-8, H-7), 6.65 (d, $J = 8.0$ Hz, 2H, H-15, H-16), 6.55 (dd, $J = 7.7$, 3.2 Hz, 2H, H-12, H-13), 6.52 (dd, $J = 7.8$, 1.7 Hz, 1H, H-5), 4.01 (t, 11.2 Hz, 1H, H-2a), 3.29-3.21 (m, H-9a, H-9b, 2H), 3.22-3.16 (m, 2H, H-1a, H-1b), 3.15-3.11 (m, 1H, H-9b), 3.10-3.02 (m, 2H, H-10a, H-10b), 1.00 (d, $J = 17.3$ Hz, 9H, $t\text{Bu}$);

$^{31}\text{P NMR}$ (CDCl_3 , 200 MHz) δ 125.63.

(Dimethyl 3-(2-methylprop-1-en-1-yl)cyclopent-3-ene-1,1-dicarboxylate **2.101**

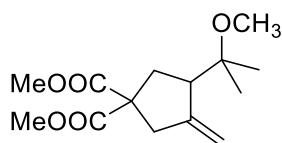


2.101

To a solution of **2.95** (3 mg, 0.0074 mmol, 0.02 eq.) in CH₂Cl₂ (5 ml) was added AgSbF₆ (4 mg, 0.0074 mmol, 0.02 eq.) and suspension stirred for 10 min. During this time AgCl precipitates as a white solid. A solution of 1,6 enyne **2.100** (90 mg, 0.37 mmol, 1 eq.) in CH₂Cl₂ (5.5 ml) was to make a final concentration 0.05 M. The mixture was stirred at room temperature and was monitored by TLC. When reaction was completed (10 hrs), the mixture was filtered through a short pad of silica (CH₂Cl₂, 10 ml) and concentrated under reduced pressure. Subsequent purification by column chromatography on silica gel (EtOAc : hexanes 0.2 : 9.8) afforded product **2.101** as colourless oil (66 mg, 0.25 mmol, 76 %); ¹H NMR (CDCl₃, 500 MHz): δ 5.75 (1H, s), 5.41 (1H, s), 3.76 (6H, s), 3.22 (2H, s), 3.07 (2H, s), 1.84 (3H, s), 1.80 (3H, s).

Data comparable to that reported in literature.³

Dimethyl 3-(2-methoxypropan-2-yl)-4-methylenecyclopentane-1,1-dicarboxylate **2.106**⁴

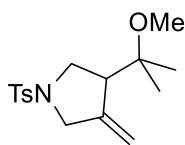


2.106

To a solution of **2.95** (3 mg, 0.0074 mmol, 0.02 eq.) in CH₃OH (2 ml) was added AgSbF₆ (5 mg, 0.0074 mmol, 0.02 eq.) and suspension stirred for 10 min.- During this time AgCl precipitates as a white solid. A solution of 1,6 enyne **2.100** (100 mg, 0.41 mmol, 1.0 eq.) in CH₃OH (6.3 ml) was added to make a final concentration 0.05 M. The mixture was stirred at room temperature and was monitored by TLC. When reaction was completed (12 hrs), the mixture was filtered through a short pad of silica (CH₂Cl₂, 10 ml) and concentrated under reduced pressure. Subsequent purification by column chromatography on silica gel (EtOAc : hexanes 0.2 : 9.8) afforded product **2.95** as colorless oil (81 mg, 0.34 mmol, 92 %); ¹H NMR (CDCl₃, 500 MHz): δ 5.04 (1H, bs), 4.98 (1H, bs), 3.73 (3H, s), 3.72 (3H, s), 3.19 (3H, s), 2.94-2.83 (3H, m), 2.55 (1H, ddd, *J* = 13.5, 9.4, 1.7 Hz), 2.00 (2H, dd, *J* = 13.5, 9.4 Hz), 1.18 (3H, s), 1.12 (3H, s).

Data comparable to that reported in literature.⁴

3-(2-methoxypropan-2-yl)-4-methylene-1-tosylpyrrolidine **2.111**³



2.111

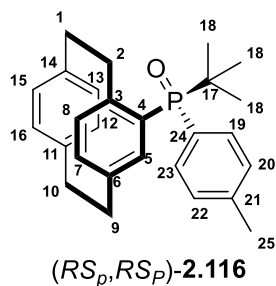
To a solution of **2.95** (3 mg, 0.0054 mmol, 0.02 eq.) in CH₂Cl₂ (2 ml) was added AgSbF₆ (2 mg, 0.0054 mmol, 0.02 eq.) and suspension stirred for 10 min. During this time AgCl precipitates as a white solid. A solution of 1,6 enyne **2.110** (75 mg, 0.27 mmol, 1.0 eq.) in CH₃OH (3.4 ml) was added to make a final concentration: 0.05 M. The mixture was stirred at room temperature and was monitored by TLC. When reaction was completed (12 hrs), the mixture was filtered through a short pad of silica (CH₂Cl₂, 10 ml) and concentrated under reduced pressure. Subsequent purification by column chromatography on silica gel (EtOAc : hexanes 0.1 : 9.9) afforded product **2.111** as a white solid (67 mg, 0.21 mmol, 80%); ¹H NMR (CDCl₃, 500 MHz): δ 7.74 (2H, d, *J* = 6.1 Hz), 7.35 (2H, d, *J* = 7.9 Hz), 5.04 (2H, m), 3.80 (2H, m), 3.43 (1H, dd, *J* = 9.9, 4.2 Hz), 3.32-3.29 (1H, m), 2.74 (3H, s), 2.45 (3H, s), 1.14 (3H, s), 1.14 (3H, s), 1.03 (3H, s).

Data comparable to that reported in literature.³

General procedure for *P*-arylation of secondary phosphine oxide (SPO)

To a flame-dried 25 ml RBF was added Pd(OAc)₂ (2 mol%), dppf (2.2 mol%), and Cs₂CO₃ (1.3 eq.). The reaction vessel was degassed and dioxane (2 ml) was added. The resulting suspension was stirred under a flow of argon for 10 min. SPO (*RSp,SR*)-**2.47** (1.0 eq., 0.19 mmol) and the respective electrophile (1.5 eq., 0.29 mmol) were dissolved separately in dioxane : DCE (9 : 1) and resulting solution was added *via* syringe. The reaction mixture was heated at 100 °C until the starting material had been completely consumed as judged by TLC (24 h). The mixture was cooled to room temperature, passed through a celite pad, washed the celite pad with EtOAc, and purified by column chromatography on silica gel (EtOAc: hexanes 4 : 6) to obtain the desired cross-coupled products.

(*RS_p*,*RS_p*)-*tert*-butyl([2.2]paracyclophan-4-yl)(*p*-tolyl)phosphine oxide **2.116**



Pd(OAc)₂ (1 mg, 0.0038 mmol, 0.02 eq.), dppf (2 mg, 0.0042 mmol, 0.02 eq.), Cs₂CO₃ (81 mg, 0.25 mmol, 1.3 eq.), **SPO-2.47** (60 mg, 0.191 mmol, 1.0 eq.), 4-iodotoulene **2.114** (49.24 mg, 0.287 mmol, 1.5 eq.), white solid of (*RS_p*,*RS_p*)-**2.116** (52 mg, 0.086 mmol, 68 %).

R_f (7 : 3 Hex : EtOAc) 0.50.

mp: 216 °C - 218 °C

IR ν_{\max} (Solid) 2925, 2851, 1725, 1598, 1500, 1466, 1433, 1394, 1365, 1293, 1259, 1205, 1162, 1150, 1111, 1066, 1013, 942, 919, 906, 906, 813, 799, 720 cm⁻¹.

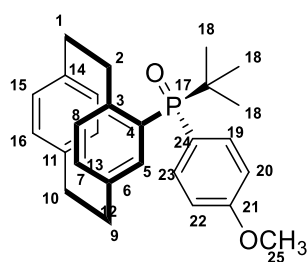
¹H NMR (CDCl₃, 500 MHz): δ 8.05 (t, *J* = 8.5 Hz, 2H, H-22, H-20), 7.46 (d, *J* = 8.0 Hz, 2H, H-23, H-19), 6.68 (d, *J* = 5.7 Hz, 1H, H-5), 6.59 (m, 3H, H-7, H-8, H-13), 6.56 (dd, *J* = 7.8, 1.7 Hz, 1H, H-15), 6.46 (dd, *J* = 7.7, 1.8 Hz, 1H, H-16), 5.79 (dd, *J* = 7.7, 1.8 Hz, 1H, H-12), 4.48 (t, *J* = 10.8 Hz, 1H, H-2a), 3.50 (td, *J* = 10.7, 5.4 Hz, 1H, H-9a), 3.12-3.07 (m, 2H, H-1a, H-1b), 3.01- 2.91 (m, 3H, H-2b, H-9b, H-10a), 2.85-2.78 (m, 1H, H-10b), 2.54 (s, 3H, Me), 1.04 (d, *J* = 16.9 Hz, 9H, ^tBu).

¹³C NMR (CDCl₃, 125 MHz) δ 138.6 (d, *J_{P-C}* = 47.9 Hz), 136.7 (d, *J_{P-C}* = 47.5 Hz), 136.2 (d, *J_{P-C}* = 48.8 Hz), 135.9 (d, *J_{P-C}* = 12.7 Hz), 135.9, 134.0, 133.0 (d, *J_{P-C}* = 29.4 Hz), 132.2 (t, *J_{P-C}* = 37.60 Hz), 129.0 (d, *J_{P-C}* = 42.05 Hz), 128.6, 127.5, 126.7, 36.8, 36.2, 35.2, 35.0, 25.1, 21.6.

³¹P NMR (CDCl₃, 200 MHz) δ 42.19.

HRMS-EI: *m/z* found: [M + H]⁺, 403.2178. C₂₇H₃₂OP requires 403.2191; [M + Na]⁺ 425.2003. C₂₇H₃₁NaOP requires 425.2010.

(*RS_p*,*RS_p*)-*tert*-butyl(4-methoxyphenyl)([2.2]paracyclophan-4-yl)phosphine oxide **2.119**



(*RS_p*,*RS_p*)-2.119

Pd(OAc)₂ (1 mg, 0.0038 mmol, 0.02 eq.), dppf (2 mg, 0.0042 mmol, 0.022 eq.), Cs₂CO₃ (81 mg, 0.25 mmol, 1.3 eq.), **SPO-2.47** (60 mg, 0.19 mmol, 1.0 eq.), 4-iodoanisole **2.118** (67 mg, 0.29 mmol, 1.5 eq.), yellow solid of (*RS_p*,*RS_p*)-**2.119** (48 mg, 0.114, 60 %).

R_f (7 : 3 Hex : EtOAc) 0.50.

mp: 137 °C - 139 °C

IR ν_{\max} (Solid) 2925, 2851, 1725, 1598, 1500, 1466, 1433, 1394, 1365, 1293, 1259, 1205, 1162, 1150, 1111, 1066, 1013, 942, 919, 906, 906, 813, 799, 720 cm⁻¹.

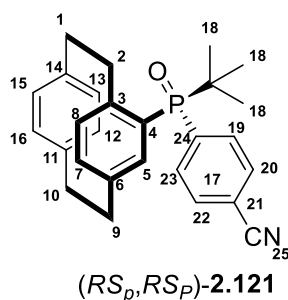
¹H NMR (CDCl₃, 500 MHz): δ 8.09 (t, *J* = 8.7 Hz, 2H, H-22, H-20), 7.18 (d, *J* = 7.2 Hz, 2H, H-23, H-19), 6.66 (d, *J* = 13.2 Hz, 1H, H-5), 6.60-6.54 (m, 4H, H-7, H-8, H-15, H-16), 6.47 (d, *J* = 7.5 Hz, 1H, H-13), 5.81 (d, *J* = 7.4 Hz, 1H, H-12), 4.45 (d, *J* = 11.4 Hz, 1H, H-2a), 3.98 (s, 3H, OCH₃), 3.50 (dd, *J* = 11.8, 5.3 Hz, 1H, H-9a), 3.10 (t, *J* = 4.4 Hz, 2H, H-1a, H-1b), 3.01-2.89 (m, 3H, H-9b, H-10a, H-10b), 2.84-2.78 (m, 1H, H-2b), 1.04 (d, *J* = 14.8 Hz, 9H, ^tBu).

¹³C NMR (CDCl₃, 125 MHz) δ 162.0 (d, *J_{P-C}* = 10.3 Hz), 146.4 (d, *J_{P-C}* = 28.8 Hz), 140.5, 138.7, 138.6 (d, *J_{P-C}* = 48.1 Hz), 136.7 (d, *J_{P-C}* = 47.7 Hz), 136.3 (d, *J_{P-C}* = 48.6 Hz), 135.9, 134.7 (d, *J_{P-C}* = 32.9 Hz), 134.0, 132.2 (d, *J_{P-C}* = 40.1 Hz), 132.1, 127.5, 126.8, 122.5, 121.7, 113.9 (d, *J_{P-C}* = 44.9 Hz), 64.1, 55.3, 36.8, 36.2, 35.2 (d, *J_{P-C}* = 27.5 Hz), 35.2, 35.0, 25.1.

³¹P NMR (CDCl₃, 200 MHz) δ 42.37.

HRMS-EI: *m/z* found: [M + H]⁺, 419.2132. C₂₇H₃₁O₂P requires 419.2140; [M + Na]⁺ 441.1952 C₂₇H₃₁NaO₂P requires 441.1959.

(*RS_p*,*RS_P*)-*tert*-butyl(4-cyanophenyl)([2.2]paracyclophan-4-yl)phosphine oxide **2.121**



Pd(OAc)₂ (1 mg, 0.0038 mmol, 0.02 eq.), dppf (2 mg, 0.0042 mmol, 0.022 eq.), Cs₂CO₃ (81 mg, 0.25 mmol, 1.3 eq.), **SPO-2.47** (60 mg, 0.19 mmol, 1.0 eq.), 4-iodobenzonitrile **2.120** (66 mg, 0.29 mmol, 1.5 eq.), white solid of (*RS_p*,*RS_P*)-**2.121** (50 mg, 0.12 mmol, 64 %).

mp: 118 °C -120 °C

IR ν_{\max} (Solid) 3430, 2960, 2926, 2855, 2230, 1669, 1500, 1476, 1465, 1394, 1367, 1263, 1200, 1156, 1130, 1091, 1065, 1017, 942, 915 cm⁻¹.

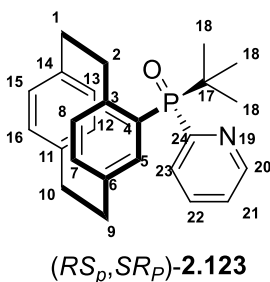
¹H NMR (CDCl₃, 500 MHz): δ 8.31 (t, *J* = 5.7 Hz, 2H, H-22, H-20), 7.95 (d, *J* = 8.2 Hz, 2H, H-23, H-19), 6.62 (s, 2H, H-8, H-7), 6.56 (dd, *J* = 7.7, 1.6 Hz, 1H, H-5), 6.53-6.47 (m, 3H, H-15, H-16, H-13), 5.74 (dd, *J* = 1.8, 7.8 Hz, 1H, H-12), 4.40 (t, *J* = 11.2 Hz, 1H, H-2a), 3.46 (td, *J* = 10.9, 5.4 Hz, 1H, H-9a), 3.13-3.05 (m, 2H, H-1a, H-1b), 3.00-2.96 (m, 1H, H-2b), 2.98-2.90 (m, 2H, H-10a, H-10b), 2.81-2.75 (m, 1H, H-9b), 1.05 (d, *J* = 15.2 Hz, 9H, ^tBu).

¹³C NMR (CDCl₃, 125 MHz) δ 146.7 (d, *J_{P-C}* = 26.7 Hz), 140.3, 139.0 (d, *J_{P-C}* = 48.1 Hz), 138.6, 137.1 (d, *J_{P-C}* = 47.2 Hz), 136.5, 135.9 (d, *J_{P-C}* = 47.9 Hz), 133.7, 133.6 (d, *J_{P-C}* = 25.4 Hz), 132.3 (d, *J_{P-C}* = 58.1 Hz), 132.0, 131.7 (d, *J_{P-C}* = 38.1 Hz), 118.1, 115.2, 36.7, 36.2, 35.0, 25.0.

³¹P NMR (CDCl₃, 200 MHz) δ 41.75.

HRMS-EI: *m/z* found: [M + H]⁺ 414.1979 C₂₇H₂₉NOP requires 414.1987; [M + Na]⁺, 436.1800. C₂₇H₂₈NNaOP requires [M + Na]⁺ 436.1806.

(*RS_p*,*SR_p*)-*tert*-butyl(pyridine-2-yl)([2.2]paracyclophan-4-yl)phosphine oxide **2.123**



Pd(OAc)₂ (1 mg, 0.0038 mmol, 0.02 eq.), dppf (2 mg, 0.0042 mmol, 0.022 eq.), Cs₂CO₃ (81 mg, 0.25 mmol, 1.3 eq.), **SPO-2.47** (60 mg, 0.19 mmol, 1.0 eq.), 2-iodopyridine **117** (59 mg, 0.29 mmol, 1.5 eq.), brownish solid of (*RS_p*,*SR_p*)-**2.123** (43 mg, 0.11 mmol, 58 %).

mp: 136 °C - 137 °C

IR ν_{\max} (Solid) 3042, 2953, 2928, 2852, 1726, 1573, 1564, 1500, 1473, 1450, 1431, 1420, 1391, 1364, 1262, 1177, 1152, 1134, 1081, 1064, 1045, 1021, 991, 945, 918, 882 cm⁻¹.

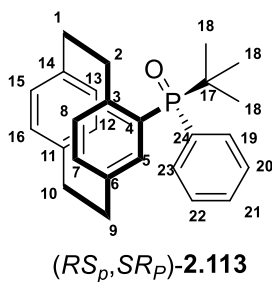
¹H NMR (CDCl₃, 500 MHz): δ 8.93 (d, $J = 3.9$ Hz, H-20, 1H), 8.64 (t, $J = 6.5$ Hz, H-23, 1H), 8.03 (tq, $J = 7.7, 3.1, 1.7$ Hz, 1H, H-22), 7.53-7.50 (m, 1H, H-22), 7.34 (d, $J = 12.4$ Hz, 1H, H-5), 6.60-6.54 (m, 3H, H-8, H-7, H-15), 6.45 (d, $J = 7.8$ Hz, 1H, H-13), 6.37 (d, $J = 7.8$ Hz, 1H, H-12), 4.52 (t, $J = 10.8$ Hz, 1H, H-2a), 3.44 (td, $J = 10.5, 5.9$ Hz, 1H, H-9a), 3.16-3.08 (m, 2H, H-1a, H-1b), 2.96-2.85 (m, 4H, H-10a, H-10b, H-2b, H-9b), 1.06 (d, 9H, $J = 15.1$ Hz, 'Bu).

¹³C NMR (CDCl₃, 125 MHz) δ 149.0 (d, $J_{\text{P-C}} = 65.5$ Hz), 146.4 (d, $J_{\text{P-C}} = 24.9$ Hz), 140.5, 138.9, 138.3 (d, $J_{\text{P-C}} = 47.2$ Hz), 136.7 (d, $J_{\text{P-C}} = 41.8$ Hz), 136.4 (d, $J_{\text{P-C}} = 47.2$ Hz), 138.3 (d, $J_{\text{P-C}} = 41.8$ Hz), 136.2 (d, $J_{\text{P-C}} = 47.9$ Hz), 135.8 (d, $J_{\text{P-C}} = 13.2$ Hz), 133.4, 132.6, 132.3, 131.9, 130.0 (d, $J_{\text{P-C}} = 65.8$ Hz), 124.7 (d, $J_{\text{P-C}} = 12.1$ Hz), 35.2 (d, $J_{\text{P-C}} = 48.1$ Hz), 34.9, 34.4, 24.4.

³¹P NMR (CDCl₃, 200 MHz) δ 36.12.

HRMS-EI: m/z found: [M + H]⁺, 390.1978. C₂₅H₂₉NOP requires 390.1987; [M + Na]⁺ 412.1798
C₂₅H₂₈NaOP requires 412.1806.

(*RS_p,RS_p*)-*tert*-butyl(phenyl)([2.2]paracyclophan-4-yl)phosphine oxide 2.113



Pd(OAc)₂ (1 mg, 0.0038 mmol, 0.02 eq.), dppf (2 mg, 0.0042 mmol, 0.022 eq.), Cs₂CO₃ (81 mg, 0.25 mmol, 1.3 eq.), **SPO-47** (60 mg, 0.19 mmol, 1 eq.), Phenylbromide **2.112** (0.03 ml, 47.53 mg, 0.30 mmol, 1.5 eq.); yellow solid of (*RS_p,RS_s*)-**2.113** (45 mg, 61%).

mp: 166 °C - 168 °C

IR ν_{\max} (Soild) 2924, 2856, 1586, 1497, 1474, 1433, 1409, 1393, 1365, 1263, 1209, 1165, 1153, 1129, 1100, 1074, 1066, 1020, 996, 941, 916, 902 cm⁻¹.

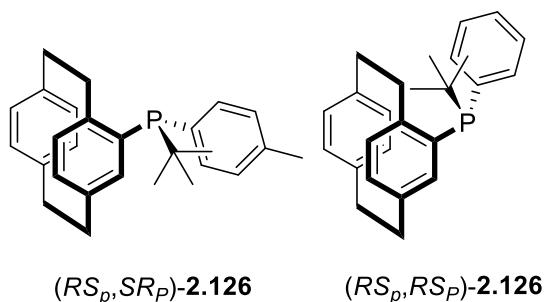
¹H NMR (CDCl₃, 500 MHz): δ 8.20-8.16 (m, 2H, H-22, H-20), 7.69-7.61 (m, 3H, H-23, H-21, H-19), 6.68 (dd, $J = 7.8, 1.7$ Hz, 1H, H-5), 6.60-6.58 (m, 3H, H-7, H-8, H-15), 6.56 (dd, $J = 7.8, 1.5$ Hz, 1H, H-13), 6.47 (dd, $J = 7.8, 1.8$ Hz, 1H, H-16), 5.76 (dd, $J = 7.8, 1.8$ Hz, 1H, H-12), 4.49 (t, $J = 10.9$ Hz, 1H, H-2b), 3.50 (td, $J = 8.3, 5.6$ Hz, 1H, H-1a), 3.13-3.06 (m, 2H, H-9a, H-9b), 3.02-2.96 (m, 2H, H-10a, H-10b), 2.94- 2.90 (m, 1H, H-2a), 2.82-2.76 (m, 1H, H-1b), 1.07 (d, $J = 16.1$ Hz, 9H, ^tBu).

¹³C NMR (CDCl₃, 125 MHz) δ 146.6 (d, $J_{\text{P-C}} = 27.4$ Hz), 140.4, 138.7, 138.6 (d, $J_{\text{P-C}} = 47.7$ Hz), 136.7 (d, $J_{\text{P-C}} = 47.8$ Hz), 136.2 (d, $J_{\text{P-C}} = 47.7$ Hz), 135.9 (d, $J_{\text{P-C}} = 11.5$ Hz), 134.0, 133.0 (d, $J_{\text{P-C}} = 27.9$ Hz), 132.2 (d, $J_{\text{P-C}} = 40.5$ Hz), 131.8, 131.3 (d, $J_{\text{P-C}} = 10.1$ Hz), 131.1, 128.3, 127.3, 126.6, 36.8, 36.2, 35.2 (d, $J_{\text{P-C}} = 25.5$ Hz), 35.0, 34.6, 25.1.

³¹P NMR (CDCl₃, 200 MHz) δ 41.93.

HRMS-EI: m/z found: [M + H]⁺, 389.2024. C₂₆H₃₀OP requires 389.2034; [M + Na]⁺ 411.1846 C₂₆H₂₉NaOP requires 411.1854.

(RS_p,SR_p)-tert-butyl*([2.2]paracyclophan-4-yl)*(p-tolyl)phosphine 2.126* & *(RS_p,RS_p)-tert-butyl*([2.2]paracyclophan-4-yl)*(p-tolyl)phosphine 2.126

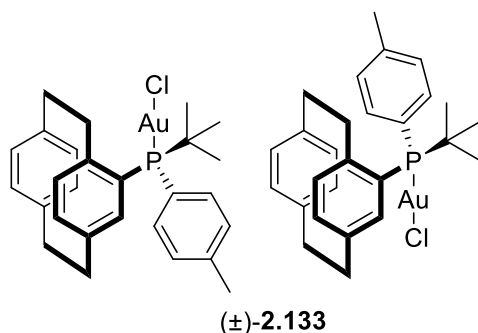


Trichlorosilane (0.73 ml, 7.30 mmol, 28 eq.) was added to a stirred suspension of *(RS_p,RS_p)-tert-butyl*([2.2]paracyclophan-4-yl)*(p-tolyl)phosphine oxide 2.116* (105 mg, 0.261 mmol, 1.0 eq.) in *p*-xylene (2 mL) and slowly heated to 140 °C in a pressure tube for 20 h. The reaction mixture was cooled to 0 °C and quenched by the addition of 30% aqueous sodium hydroxide (10 mL) (Exothermic). The aqueous layer was extracted with ethyl acetate (3 x 15 mL), dried (MgSO₄) and the solvent was removed *in vacuo*. The crude product was obtained as a yellowish solid. (80 mg, 80% yield)

¹H NMR (CDCl₃, 500 MHz): δ 7.76 (t, *J* = 7.9 Hz, 2H), 7.21 (d, *J* = 7.6 Hz, 2H), 7.10 (d, *J* = 7.7 Hz, 1H), 7.03-6.99 (m, 3H), 6.93 (d, *J* = 7.8 Hz, 1H), 6.73 (d, *J* = 6.4 Hz, 1H), 6.51 (d, *J* = 7.7 Hz, 1H), 6.46-6.43 (3H, m), 6.39-6.33 (m, 5H), 6.23-6.20 (m, 1H), 5.67 (d, *J* = 7.8 Hz, 1H), 4.12-4.07 (m, 1H), 3.35-3.30 (m, 2H), 3.19-3.14 (m, 1H), 3.11-3.05 (m, 2H), 3.00-2.91 (m, 3H), 2.90-2.84 (m, 3H), 2.82-2.77 (m, 2H), 2.76 (m, 2H), 2.39 (s, 3H, Me), 2.21 (s, 2H, Me), 1.15 (d, *J* = 12.2 Hz, 6H, ^tBu), 0.90 (d, 9H *J* = 12.5 Hz, ^tBu).

³¹P NMR (CDCl₃, 200 MHz) δ 16.21, 8.40.

(±)-Chloro[*tert*-butyl([2.2]paracyclophan-4-yl)(*p*-tolyl)phosphine]gold(I) 2.133



To a flame dried two necked 25 ml RBF was added racemic *tert*-butyl([2.2]paracyclophan-4-yl)(*p*-tolyl)phosphine **2.126** (80 mg, 0.20 mmol, 1.0 eq.) and Chloro(tetrahydrothiophene)gold(I) (66.3 mg, 0.20 mmol, 1.0 eq.) in dry CH₃CN (5 ml). The mixture was refluxed under an argon atmosphere for 2 h. The crude mixture was concentrated under vacuum. The resulting yellow solid was dissolved in CH₂Cl₂ (1 mL) and pentane (10 mL) was added to precipitate the desired complex as a yellow solid, which was isolated by decantation to obtain desired complex (20 mg, 0.032 mmol, 16 % yield).

mp: 98 °C - 99 °C

IR ν_{\max} (Soild) 2961, 2920, 1710, 1600, 1498, 1460, 1394, 1261, 1090, 805, 713 cm⁻¹.

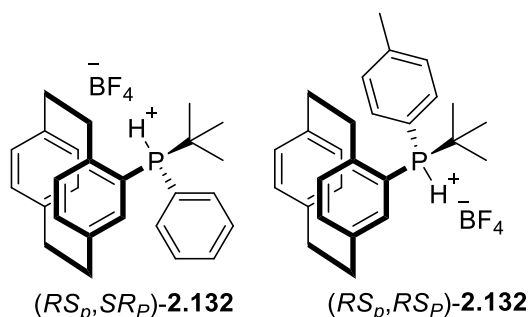
¹H NMR (CDCl₃, 500 MHz): δ 8.05-8.01 (m, 2H), 7.66 (d, $J = 7.7$ Hz, 1H), 7.44 (d, $J = 6.4$ Hz, 2H), 7.38-7.34 (m, 1H), 7.16-7.15 (m, 1H), 7.10-7.09 (m, 1H), 7.04-6.98 (m, 2H), 6.65-6.60 (m, 3H), 6.58-6.54 (m, 3H), 6.42-6.37 (m, 1H), 6.34 (d, $J = 12.8$ Hz, 1H), 5.91 (dd, $J = 7.8, 1.5$ Hz, 1H), 4.81-4.76 (m, 1H), 4.28-4.17 (m, 1H), 3.86-3.71 (m, 2H), 3.23-3.09 (m, 5H), 3.14-3.03 (m, 6H), 2.98-2.95 (m, 3H), 2.89 (d, $J = 7.2$ Hz, 1H), 2.78-2.73 (m, 2H), 2.54 (s, 3H), 2.38 (s, 2H), 1.36 (d, $J = 16.4$ Hz, 6H), 1.17 (d, $J = 16.8$ Hz, 9H).

¹³C NMR (CDCl₃, 125 MHz) δ 144.1 (d, $J_{P-C} = 48.2$ Hz), 142.9, 139.2 (d, $J_{P-C} = 33.3$ Hz), 139.0, 136.9 (d, $J_{P-C} = 36.8$ Hz), 136.7, 136.6, 136.4, 136.1, 135.6 (d, $J_{P-C} = 50.9$ Hz), 133.0 (d, $J_{P-C} = 35.1$ Hz), 132.6, 132.3 (d, $J_{P-C} = 40.5$ Hz), 132.0, 129.9 (d, $J_{P-C} = 46.4$ Hz), 129.0 (d, $J_{P-C} = 47.3$ Hz), 42.1, 36.6, 36.5 (d, $J_{P-C} = 22.8$ Hz), 36.2, 35.6, 35.1, 30.0, 34.9, 30.1, 28.3 (d, $J_{P-C} = 23.6$ Hz), 21.5 (d, $J_{P-C} = 79.7$ Hz), 1.0.

³¹P NMR (CDCl₃, 200 MHz) δ 47.8, 46.7

HRMS-EI: m/z found: [M + Na]⁺ 641.1402 C₂₇H₃₁ClNaP requires 641.1415.

(*RS_p,SR_p*)-*tert*-butyl([2.2]paracyclophan-4-yl)(*p*-tolyl)phosphonium tetrafluoroborate 2.132 & (*RS_p,RS_p*)-*tert*-butyl([2.2]paracyclophan-4-yl)(*p*-tolyl)phosphonium tetrafluoroborate 2.132



Racemic *tert*-butyl([2.2]paracyclophan-4-yl)(*p*-tolyl)phosphine **2.126** (80 mg, 0.214 mmol, 1.0 eq.), HBF₄·OEt₂ (0.52 ml, 3.22 mmol, 15.0 eq., 54% solution in Et₂O) and CH₂Cl₂ (7 ml) were combined at 0 °C. After 2 hrs, the reaction mixture was warmed to 22 °C and aqueous tetrafluoroboric acid (5 ml) was added. The reaction mixture was allowed to stir for more 2 hrs. The aqueous phase was separated with EtOAc (3 x 15 ml), dried (MgSO₄) and the solvent was removed *in vacuo*. The crude product **2.132** was obtained as fluffy white powder (55 mg, 0.12 mmol, 69 % yield).

mp: 123 °C - 125 °C

IR ν_{\max} (Soild) 2956, 2851, 1598, 1467, 1407, 1317, 1180, 1031, 919, 857, 809, 719 cm⁻¹.

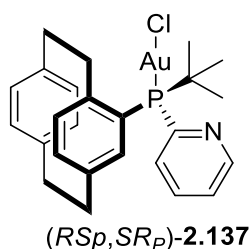
¹H NMR (CDCl₃, 500 MHz): δ 8.68 (s, 1H), 8.55 (s, 1H), 8.22-8.18 (m, 2H), 7.78-7.74 (m, 1H), 7.68 (s, 2H), 7.45-7.44 (m, 1H), 7.40 (d, $J = 14.8$ Hz, 1H), 7.00 (d, $J = 12.8$ Hz, 1H), 6.87-6.79 (m, 3H), 6.68-6.65 (m, 1H), 6.62-6.60 (m, 2H), 6.55-6.47 (m, 2H), 5.96 (d, $J = 7.6$ Hz, 1H), 5.78 (d, $J = 7.3$ Hz, 1H), 3.92 (t, $J = 11.4$ Hz, 1H), 3.53-3.49 (m, 1H), 3.41-3.37 (m, 1H), 3.30-3.25 (m, 3H), 3.22 (d, $J = 10.2$ Hz, 2H), 3.17 (d, $J = 9.2$ Hz, 2H), 3.06-3.00 (m, 4H), 2.59 (s, 3H), 2.48 (s, 2H), 1.59 (d, $J = 18.0$ Hz, 6H), 1.31 (d, $J = 16.1$ Hz, 9H).

¹³C NMR (CDCl₃, 125 MHz) δ 146.7, 146.5 (d, $J = 30.6$ Hz), 146.2, 145.6, 141.9, 141.5 (d, $J = 46.1$ Hz), 140.0, 139.6, 139.5, 139.1 (d, $J = 60.0$ Hz), 138.8, 137.9 (d, $J = 45.5$ Hz), 137.3 (d, $J = 47.0$ Hz), 136.0 (d, $J = 32.5$ Hz), 134.6 (d, $J = 37.0$ Hz), 134.4 (d, $J = 41.2$ Hz), 133.0 (d, $J = 34.1$ Hz), 132.8, 132.6 (d, $J = 42.7$ Hz), 132.2, 131.9, 131.7 (d, $J = 50.2$ Hz), 131.05 (d, $J = 51.1$ Hz), 35.51, 35.2 (d, $J = 21.2$ Hz), 35.1, 34.6, 33.5, 33.1, 29.7, 26.1, 25.2, 22.01 (d, $J = 65.5$ Hz).

³¹P NMR (CDCl₃, 200 MHz) δ 18.5, 11.6.

(*RS_P*,*SR_P*)-Chloro[(*tert*-butyl(pyridine-2-yl)([2.2]paracyclophan-4-yl)phosphine)gold(I)

2.137



To a solution of racemic *tert*-butyl([2.2]paracyclophan-4-yl)(*p*-tolyl)phosphine **2.126** (40 mg, 0.10 mmol, 1.0 eq.) in dry CH₂Cl₂ (3 ml) was added chloro(dimethyl sulfide)gold(I) (31.57 mg, 0.10 mmol, 1.0 eq.). The mixture was stirred at room temperature in the absence of light under an argon atmosphere. The crude mixture was concentrated after 2 hrs under vacuum. The resulting grey solid was dissolved in CH₂Cl₂ (1 ml) and pentane (10 ml) was added to precipitate the desired complex as a white solid, which was isolated by decantation. The solid was dissolved in CH₂Cl₂ (1 ml) and pentane was slowly added to get a biphasic solution. Slow crystallisation furnished crystals of the desired complex **2.137** (15 mg, 0.024 mmol, 23% yield).

mp: 223 °C - 224 °C

IR ν_{\max} (Solid) 2958, 2920, 1568, 1446, 1413, 1359, 1258, 1134, 1093, 805, 716 cm⁻¹.

¹H NMR (CDCl₃, 500 MHz): δ 8.90 (d, $J = 4.1$ Hz, 1H), 8.69-8.65 (m, 1H), 8.00-7.99 (m, 1H), 7.57-7.53 (m, 1H), 6.82 (d, $J = 7.8$ Hz, 1H), 6.62 (dd, $J = 7.8, 1.9$ Hz, 1H), 6.59-6.58 (m, 1H), 6.54 (dd, $J = 7.8, 1.8$ Hz, 1H), 6.49 (d, $J = 12.1$ Hz, 1H), 5.80 (dd, $J = 7.8, 1.8$ Hz, 1H), 4.89-4.82 (m, 1H), 3.84-3.75 (m, 1H), 3.22-3.16 (m, 2H), 3.11-3.03 (m, 1H), 2.99-2.90 (m, 2H), 2.76-2.71 (m, 1H), 1.21 (d, $J = 17.4$ Hz, 9H).

¹³C NMR (CDCl₃, 125 MHz) δ 150.3 (d, $J = 50.6$ Hz), 144.2 (d, $J = 49.5$ Hz), 139.8 (d, $J = 34.8$ Hz), 139.3, 139.1, 137.2 (d, $J = 11.3$ Hz), 136.8, 136.7 (d, $J = 16.7$ Hz), 136.58, 136.51 (d, $J = 11.7$ Hz), 134.8, 134.6, 133.0, 132.7, 132.4, 132.0, 125.4 (d, $J = 8.9$ Hz), 124.0, 36.6, 36.5 (d, $J = 31.2$ Hz), 36.3, 35.7, 35.0 (d, $J = 21.7$ Hz), 34.1, 27.4 (d, $J = 21.6$ Hz), 22.3, 14.0.

³¹P NMR (CDCl₃, 200 MHz) δ 40.6.

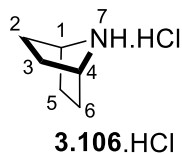
HRMS-EI: m/z found: [M + Na]⁺ 628.1193 C₂₅H₂₈AuClNNaP requires 628.1211.

8.3.1. References

- (1) Parrott, R. W.; Hitchcock, S. R., β -Amino alcohols derived from (1*R*,2*S*)-norephedrine and (1*S*,2*S*)-pseudonorephedrine as catalysts in the asymmetric addition of diethylzinc to aldehydes *Tetrahedron: Asymmetry* **2008**, *19*, 19.
- (2) Wang, X.-B.; Goto, M.; Han, L.-B. Efficient Asymmetric Hydrogenation of α -Acetamidocinnamates through a Simple, Readily Available Monodentate Chiral H-Phosphinate. *Chem. Eur. J.* **2014**, *20*, 3631.
- (3) Nieto-Oberhuber, C.; Muñoz, M. P.; López, S.; Jiménez-Núñez, E.; Nevado, C.; Herrero-Gómez, E.; Raducan, M.; Echavarren, A. M. Gold(I)-Catalyzed Cyclizations of 1,6-Enynes: Alkoxy cyclizations and exo/endo Skeletal Rearrangements. *Chem. Eur. J.* **2006**, *12*, 1677.
- (4) Méndez, M.; Muñoz, M. P.; Nevado, C.; Cárdenas, D. J.; Echavarren, A. M. Cyclizations of Enynes Catalyzed by PtCl₂ or Other Transition Metal Chlorides: Divergent Reaction Pathways. *J. Am. Chem. Soc.* **2001**, *123*, 10511.

8.4. Experimental for Chapter 3

7-Azabicyclo[2.2.1]heptane.hydrochloride salt **3.106**¹

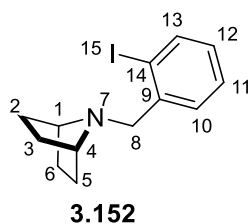


Trans-4-(tosyloxy)cyclohexylamine hydrobromide (7.78 g, 22.3 mmol, 1.0 eq.) was dissolved in EtOH-H₂O (65:35, 277 ml : 71.15 ml) and treated with NaOH (2.40 g, 22.3 mmol, 1.0 eq.). The resulting solution was allowed to stir for 24 hours. To the solution, 32% aqueous HCl (15 ml) was added and solvent was evaporated under reduced pressure. The solid residues were treated with 10% NaOH (125 ml) and extracted with Et₂O (3 × 120 ml). The combined organic layers were dried over MgSO₄ and HCl gas (generated from H₂SO₄ and NaCl) was bubbled through the solution. The solvent was evaporated under reduced pressure to get pale yellow solid of 7-azabicyclo[2.2.1]heptane.hydrochloride salt **3.106** (2.0 g, 15.0 mmol, 72%).

¹H NMR (DMSO, 500 MHz): δ 8.30 (bs, 1H, NH), 4.75 (t, $J = 3.2$ Hz, 1H, H-4), 3.11-3.06 (m, 1H, H-1), 2.02-1.90 (m, 4H, H-6a, H-6b, H-5a, H-5b), 1.89-1.73 (m, 4H, H-3a, H-3b, H-2a, H-2b).

Data comparable to that reported in literature.¹

7-(2-Iodobenzyl)-7-azabicyclo[2.2.1]heptane **3.152**.

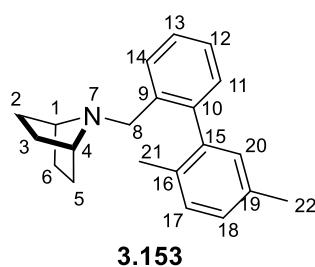


A 25ml RBF charged with 7-azabicyclo[2.2.1]heptane.hydrochloride salt (300 mg, 2.25 mmol, 1eq.), K₂CO₃ (736 mg, 2.47 mmol, 1.1eq.), and magnetic stirrer in acetone. To the reaction mixture, 2-iodobenzyl bromide (778 mg, 5.6 mmol, 2.5 eq.) was added dropwise. The reaction mixture was allowed to stir under reflux for 16 h. The reaction mixture was cooled and filtered through a pad of silica gel, washing with acetone. The filtrate was concentrated under reduced

pressure. Purification of the residues was performed by column chromatography on silica gel (EtOAc : hexanes 10:90) to give a colourless oil of **3.186** (496 mg, 1.58 mmol, 47%).

^1H NMR (CDCl_3 , 500 MHz): δ 7.83-7.81 (d, $J = 7.8$ Hz, 1H, H-13), 7.63 (d, $J = 7.6$ Hz, 1H, H-11), 7.37 (t, $J = 7.5$ Hz, 2H, H-12), 6.97 (t, $J = 7.6$ Hz, 1H, H-11), 3.56 (s, 2H, H-8), 3.32 (s, 2H, H-1, H-4), 1.87 (d, $J = 6.9$ Hz, 4H, H-6a, H-6b, H-5a, H-5b), 1.37 (d, $J = 7.1$ Hz, 4H, H-2a, H-2b, H-3a, H-3b).

7-((2',5'-Dimethyl-[1,1'-biphenyl]-2-yl)methyl)-7-azabicyclo[2.2.1]heptane **3.153**



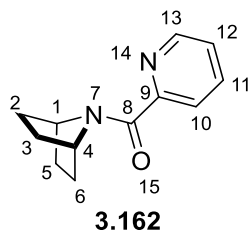
In a 5 ml Schlenk tube, 7-(2-iodobenzyl)-7-azabicyclo[2.2.1]heptane (30 mg, 0.09 mmol, 1 eq.), pivalic acid (0.5 mg, 0.019 mmol, 0.5 eq.), caesium carbonate (94 mg, 0.28 mmol, 3 eq.), tricyclohexyl phosphine (PCy_3) (5.3 mg, 0.01 mmol, 0.2 eq.) and $\text{Pd}(\text{OAc})_2$ (2.1 mg, 0.009 mmol, 0.1 eq.) were loaded accurately with a magnetic stirrer. The vial was purged and degassed with argon for three times. The solvent xylene (1 ml, 0.1 M) was transferred in a vial via syringe and the screw capped vial was heated at 140 °C for 24 h. The reaction mixture was allowed to cooled down at room temperature and diluted with CH_2Cl_2 and MeOH before passing through a pad of Celite. The resulting filtrate was removed under reduced pressure and crude product was purified by column chromatography on silica gel (EtOAc : hexanes 10:90) to give a pale yellow oil of **3.153** (18 mg, 0.06 mmol, 63%).

^1H NMR (CDCl_3 , 500 MHz): δ 7.74 (d, $J = 7.1$ Hz, 1H, H-20), 7.38 (td, $J = 7.5, 1.4$ Hz, 1H, H-11), 7.29-7.26 (m, 1H, H-14), 7.15 (d, $J = 7.7$ Hz, 1H, H-13), 7.11 (d, $J = 7.5$ Hz, 1H, H-12), 7.08 (d, $J = 7.7$ Hz, 1H, H-18), 6.99 (s, 1H, H-17), 3.31 (dd, $J = 14.3, 11.8$ Hz, 2H, H-7, H-4), 3.16 (s, 2H, H-8a, H-8b), 2.34 (s, 3H, -Me), 2.02 (s, 3H, -Me), 1.65-1.55 (m, 4H, H-6a, H-6b, H-5a, H-5b), 1.23-1.17 (m, 4H, H-3a, H-3b, H-2a, H-2b).

^{13}C NMR (CDCl_3 , 125 MHz): δ 134.57 (C-19, C-9), 132.77 (C-15, C-10), 130.23 (C-17), 129.54 (C-17), 129.24 (C-12), 128.58 (C-13), 127.82 (C-18), 127.13 (C-20), 126.07 (C-20),

59.40 (C-4, C-1), 48.62 (C-8), 30.50 (C-6), 29.98 (C-5), 23.85 (C-3, C-2), 29.92 (C-21), 19.53 (C-22).

7-(Picolinoyl)-7-azabicyclo[2.2.1]heptane **3.162**



To a solution of 7-azabicyclo[2.2.1]heptane.hydrochloride salt (800 mg, 6.6 mmol, 1 eq.) and Et₃N (1.69 ml, 13.22 mmol, 2.2 eq.) in CH₂Cl₂ was picolinoyl chloride* (932.38 mg, 6.6 mmol, 1.2 eq.) under argon at 0 °C. The mixture was allowed to reach at room temperature and stirred overnight. The crude mixture was concentrated under reduced pressure and purified with column chromatography on silica gel (EtOAc : hexanes 30:70) to give a brownish semisolid of **3.162** (656 mg, 3.24 mmol, 54%).

*Picolinoyl chloride was freshly prepared by adding a few drops of DMF in a solution of 2-picolinic acid and oxalyl chloride in CH₂Cl₂.

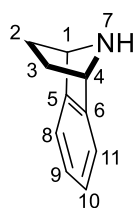
mp: 75 °C - 76 °C

IR: ν_{\max} 3288, 2937, 1646, 1512, 1467, 1261, 1096 cm⁻¹

¹H NMR (CDCl₃, 500 MHz): δ 8.58 (d, $J = 4.5$ Hz, 1H, H-13), 8.21 (d, $J = 7.8$ Hz, 1H, H-10), 8.10 (bs, 1H, NH), 7.86 (td, $J = 7.6, 1.6$ Hz, H-11), 7.45 - 7.42 (m, 1H, H-12), 4.59 - 4.57 (m, 1H, H-4), 4.11 - 4.04 (m, 1H, H-1), 2.18 - 2.14 (m, 2H, H-6a, H-6b), 2.06 - 2.00 (m, 2H, H-5a, H-5b), 1.95 - 1.91 (m, 4H, H-3b, H-3a, H-2b, H-2a).

¹³C NMR (CDCl₃, 125 MHz): δ 163.4 (C-8), 149.9 (C-9), 148.0 (C-13), 137.3 (C-11), 126.1 (C-12), 122.2 (C-10), 53.4 (C-1), 52.4 (C-4), 46.7 (C-5), 33.6 (C-3, C-2), 27.3 (C-6).

7-Benzoazabicyclo[2.2.1]heptane **3.181**^{1,2}



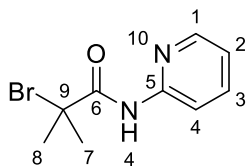
3.181

The compound **3.181** was synthesised from the starting materials, anthranilic acid, *N*-Boc pyrrole and isoamyl nitrile following a literature procedure.

¹H NMR (CDCl₃, 400 MHz): δ 7.22 (d, $J = 5.2, 3.0$ Hz, 2H, H-11, H-8), 7.11 (dd, $J = 5.2, 3.0$ Hz, 2H, H-10, H-9), 4.56-4.53 (m, 2H, H-4, H-1), 2.61 (bs, 1H, -NH), 2.07-2.04 (m, 2H, H-3a, H-3b), 1.29 (m, 2H, H-2a, H-2b).

Data comparable to that reported in literature.^{1,2}

2-Bromo-2-methyl-*N*-(pyridin-2-yl)propanamide **3.185**



3.185

The compound **3.185** was synthesised from 2-bromo-2-methylpropanoyl chloride and 2-amino pyridine following a literature procedure of amide formation.³

mp: 67 °C - 69 °C

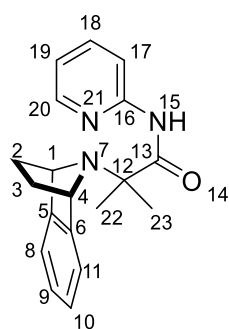
IR ν_{max} (Solid) 3172, 2978, 1682, 1597, 1574, 1434, 1303, 1260, 1166, 1003 cm⁻¹.

¹H NMR (CDCl₃, 500 MHz): δ 8.9 (bs, 1H, NH), 8.32 (d, $J = 6.1$ Hz, 1H, ArH-1), 8.19 (d, $J = 9.5$ Hz, 1H, ArH-1), 7.74 (td, $J = 9.8, 2.2$ Hz, 1H, ArH-3), 7.10 (dd, $J = 6.1, 1.2$ Hz, 1H, ArH-4), 2.06 (s, 6H, -CH₃).

¹³C NMR (CDCl₃, 125 MHz) δ 170.4 (C-6), 150.9 (C-5), 148.0 (C-7), 138.3 (C-1), 120.2 (C-2), 113.6 (C-4), 61.1 (C-9), 32.1 (C-7, C-8).

HRMS (ESI-TOF) m/z : [M + H]⁺ Calcd for C₉H₁₁Br⁷⁹N₂NaO 243.0133; Found 243.1040; [M + Na]⁺ Calcd for C₉H₁₁Br⁷⁹N₂O 264.9952; Found 264.9943.

7-[N-(Pyridin-2-yl)isobutyramide]-7-benzoazabicyclo[2.2.1]heptane 3.186



3.186

In an oven dried pressure tube was charged with 7-benzoazabicyclo[2.2.1]heptane **3.181** (200 mg, 1.37 mmol, 1.0 eq.), 2-bromo-2-methyl-*N*-(pyridin-2-yl)propenamide **3.185** (333 mg, 1.37 mmol, 1.0 eq.), K_2CO_3 (381 mg, 2.74 mmol, 2.0 eq.), and NaI (103 mg, 0.68 mmol, 0.5 eq.). Anhydrous acetonitrile (7 ml, 0.2 M) was added. The tube was equipped with a stir bar, sealed with a Teflon-lined screw cap, and heated at 60 °C. The reaction was cooled after 18 h, diluted with EtOAc, and filtered through a pad of silica gel, washing with EtOAc. The filtrate was concentrated under reduced pressure. Purified of the residues by column chromatography on silica gel (AcOH : Et₂O : toluene 10 : 20 : 70) to give an orange powder of **3.186** (78 mg, 0.25 mmol, 18%).

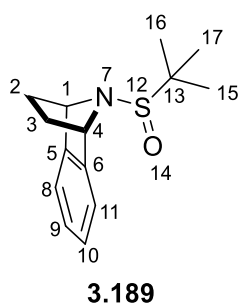
¹H NMR (CDCl₃, 500 MHz): δ 10.1 (bs, 1H, -NH), 8.34 (d, J = 3.3 Hz, 1H, H-20), 8.28 (d, J = 8 Hz, 1H, H-17), 7.72 (t, J = 14.4, 7.1 Hz, 1H, H-18), 7.21 -7.11 (m, 4H, H-11, H-10, H-9, H-8), 7.05 (t, J = 11.9, 5.5 Hz, 1H, H-19), 4.47 (s, 2H, H-4, H-1), 2.30 (d, J = 6.2 Hz, 2H, H-3a, H-3b), 1.31 (d, J = 6.6 Hz, 2H, H-2a, H-2b), 1.00 (s, 6H, CH₃-23, CH₃-22).

¹³C NMR (CDCl₃, 125 MHz) δ 176.2 (C-13), 151.6 (C-16), 147.9 (C-20), 145.8 (C-6), 138.21 (C-5), 126.5 (C-19, C-18), 119.4 (C-11, C-10, C-9, C-8), 61.6 (C-4, C-1), 61.8 (C-12), 27.9 (C-3, C-2), 24.2 (C-23, C-22).

General procedure for synthesis of 7-benzoazabicyclo[2.2.1]heptane-directing group

To a solution of 7-benzoazabicyclo[2.2.1]heptane **3.181** and Et₃N in CH₂Cl₂ was added acetyl/sulfinyl/phosphinic chloride under argon at 0 °C. The mixture was allowed to reach at room temperature and stirred overnight unless mentioned. The crude mixture was concentrated under reduced pressure and purified with column chromatography with a solvent system described in the respective compound section.

(±)-7-(*Tert*-butylsulfinyl)-7-benzoazabicyclo[2.2.1]heptane **3.189**



General procedure was followed using 7-benzoazabicyclo[2.2.1]heptane **3.181** (800 mg, 5.51 mmol, 1eq.), Et₃N (0.85 ml, 6.06 mmol, 1.1 eq.), *tert*-butylsulfinyl chloride (140 mg, 6.06 mmol, 1.1eq.). The crude mixture was obtained as a pure dark brown solid of **3.189** (870 mg, 3.59 mmol, 67%).

mp: 64 °C - 65 °C

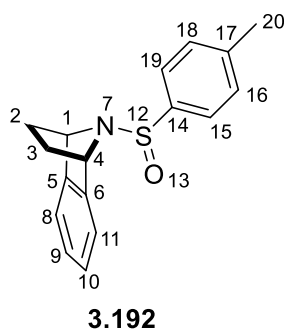
IR (Solid) ν_{\max} 2956, 1717, 1476, 1361, 1189, 1013 cm⁻¹.

¹H NMR (CDCl₃, 500 MHz): δ 7.25 - 7.20 (m, 2H, H-11, H-10), 7.15 (dt, J = 8.4, 4.6 Hz, 2H, H-9, H-8), 4.83 (t, J = 9.6, 4.8 Hz, 2H, H-4, H-1), 2.33 - 2.28 (m, 1H, H-3a), 2.22 - 2.16 (m, 1H, H-3b), 1.44 - 1.39 (m, 1H, H-2a), 1.33 - 1.28 (m, 1H, H-2b), 1.19 (s, 9H, ^tBu).

¹³C NMR (CDCl₃, 125 MHz): δ 145.89 (C-6), 144.2 (C-5), 126.4 (C-10), 126.3 (C-9), 119.1 (C-11), 118.9 (C-8), 64.3 (C-13), 64.0 (C-3), 57.6 (C-2), 27.7 (C-17), 26.4 (C-16), 22.5 (C-15).

HRMS (ESI-TOF) m/z : [M + H]⁺ Calcd for C₅H₂₀NOS 250.1266; Found 250.1256; [M + Na]⁺ Calcd for C₁₄H₁₉NNaOS 272.1085; Found 272.1075.

(±)-7-(*p*-Tolylsulfinyl)-7-benzoazabicyclo[2.2.1]heptane **3.192**



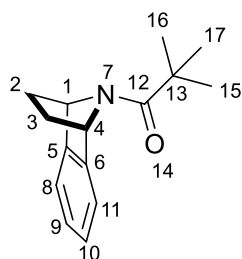
General procedure was followed using 7-benzoazabicyclo[2.2.1]heptane **3.181** (200 mg, 1.37 mmol, 1eq.), Et₃N (0.21 ml, 1.50 mmol, 1.1 eq.) *p*-tolylsulfinyl chloride (287 mg, 1.64 mmol, 1.2 eq.). The crude mixture was obtained as a pure brown solid of **3.192** (145 mg, 0.51 mmol, 37%).

¹H NMR (CDCl₃, 500 MHz): δ 7.57 (d, *J* = 8.1 Hz, 2H, H-19, H-15), 7.31 (d, *J* = 9.5 Hz, 2H, H-18, H-16), 7.25 (d, *J* = 6.7 Hz, 1H, H-8), 7.18 - 7.12 (m, 3H, H-11, H-10, H-9), 4.92 (d, *J* = 3.8 Hz, 1H, H-4), 4.71 (d, *J* = 3.8 Hz, 1H, H-1), 2.44 (s, 3H, -CH₃), 2.37 - 2.28 (m, 2H, H-3a, H-3b), 1.42 - 1.38 (m, 1H, H-2a), 1.30 - 1.27 (m, 1H, H-2b).

¹³C NMR (CDCl₃, 125 MHz) δ 145.57 (C-14), 144.84 (C-6), 141.61 (C-5), 141.02 (C-17), 129.47 (C-19, C-15), 126.40 (d, *J* = 43.2 Hz, C-18, C-16), 126.08 (C-10, C-9), 118.74 (d, *J* = 35.05 Hz, C-11, C-8), 63.60 (C-4), 63.00 (C-1), 28.06 (d, *J* = 19.25 Hz, C-3, C-2), 21.36 (C-20).

HRMS *m/z*: [M + H]⁺ Calcd for C₁₇H₁₈NOS 284.1109; Found 284.1099; [M + Na]⁺ Calcd for C₁₇H₁₇NNaOS 306.0929; Found 309.0916.

2,2-Dimethyl-1-(7-benzoazabicyclo[2.2.1]heptane)-1-propanone **3.197**



3.197

General procedure was followed using 7-benzoazabicyclo[2.2.1]heptane **3.181** (500 mg, 3.44 mmol, 1eq.), Et₃N (0.53 ml, 3.79 mmol, 1.1 eq.), pivaloyl chloride (498 mg, 4.95 mmol, 1.2 eq.). The crude mixture was obtained as a pure brown solid of **3.197** (678 mg, 2.95 mmol, 87%).

mp: 125 °C - 128 °C

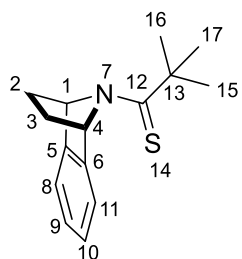
IR(Solid) ν_{\max} 2977, 2954, 1621, 1588, 1404, 1375, 1258, 1166 cm⁻¹.

¹H NMR (CDCl₃, 500 MHz): δ 7.27 - 7.25 (m, 2H, H-11, H-8), 7.17 -7.16 (dd, J = 5.3, 3.0 Hz, 2H, H-10, H-9), 5.55 (s, 2H, H-4, H-1), 2.16 (d, J = 7.3 Hz, 2H, H-3a, H-3b), 1.38 (d, J = 6.1 Hz, 2H, H-2a, H-2b), 1.22 (s, 9H, ^tBu).

¹³C NMR (CDCl₃, 125 MHz) δ 174.29 (C-12), 144.81 (C-6), 126.51 (C-11, C-10, C-9, C-8), 119.2 (C-5), 60.2 (C-13), 38.9 (C-4, C-3, C-2, C-1), 27.6 (C-17, C-16, C-15).

HRMS (ESI-TOF) m/z : [M + H]⁺ Calcd for C₁₅H₂₀NO 230.1545; Found 230.1537; [M + Na]⁺ Calcd for C₁₅H₁₉NNaO 252.1364; Found 252.1356.

2,2-Dimethyl-1-(7-benzoazabicyclo[2.2.1]heptane)-1-propanethione **3.198**



3.198

In a 25ml RBF, 7-benzoazabicyclo[2.2.1]heptane **3.181** (200 mg, 0.87 mmol, 1eq.), Lawesson's reagent (404 mg, 0.95 mmol, 1.1eq.) were loaded accurately with a magnetic stirrer

in toluene. The reaction was set up under reflux overnight. The crude mixture was concentrated under reduced pressure and purified with flash chromatography [SiO₂, EtOAc: hexanes (4:6)] to obtain the title compound **3.198** as greyish powder (190 mg, 0.77 mmol, 89%).

mp: 122 °C - 124 °C

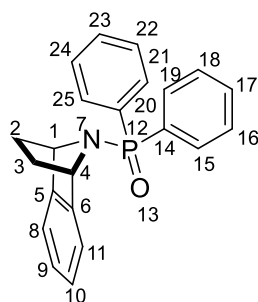
IR(Solid) ν_{\max} 2960, 2924, 1723, 1593, 1458, 1396, 1260, 1111, 1020 cm⁻¹.

¹H NMR (CDCl₃, 500 MHz): δ 7.36-7.34 (m, 1H, H-11), 7.27 (d, J = 2.1 Hz, 1H, H-8), 7.25-7.22 (m, 2H, H-10, H-9), 6.52 (d, J = 3.5 Hz, 1H, H-4), 5.80 (d, J = 3.2 Hz, 1H, H-1), 2.30 (m, 2H, H-3a, H-3b), 1.52 (d, J = 7.7 Hz, 1H, H-2a), 1.44 (d, J = 8.2 Hz, 1H, H-2b), 1.37 (s, 9H, ^tBu).

¹³C NMR (CDCl₃, 125 MHz) δ 203.4 (C-12), 143.2 (C-6), 142.3 (C-5), 127.3 (C-10), 126.9 (C-8), 120.3 (C-11), 118.7 (C-9), 66.1 (C-4), 64.6 (C-1), 43.2 (C-13), 30.3 (C-17, C-16, C-15), 27.9 (C-3), 23.8 (C-2).

HRMS (ESI-TOF) m/z : [M + H]⁺ Calcd for C₁₅H₂₀NS 246.1316; Found 246.1309.

7-(Diphenylphosphine oxide)-7-benzoazabicyclo[2.2.1]heptane **3.200**



3.200

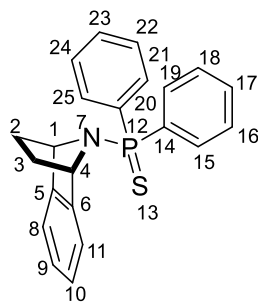
General procedure was followed using 7-benzoazabicyclo[2.2.1]heptane **3.181** (400 mg, 2.75 mmol, 1.0 eq.), Et₃N (0.10 ml, 0.42 mmol, 1.1 eq.), diphenylphosphinic chloride (465 mg, 3.30 mmol, 1.2 eq.). The reaction was allowed to stir for 60 h. The crude mixture was obtained as a pure brown solid of **3.200** (68 mg, 0.19 mmol, 59%).

¹H NMR (CDCl₃, 500 MHz): δ 7.88-7.84 (m, 4H, H-25, H-21, H-19, H-15), 7.52 - 7.49 (m, 2H, H-23, H-7), 7.45-7.42 (m, 4H, H-24, H-22, H-18, H-16), 7.19 - 7.14 (m, 4H, H-11, H-10, H-9, H-8), 4.77 (bs, 2H, H-4, H-1), 2.37 (d, J = 7.6 Hz, 2H, H-3a, H-3b), 1.36 (d, J = 7.2 Hz, 2H, H-2a, H-2b).

^{13}C NMR (CDCl_3 , 125 MHz) δ 145.88 (d, $J = 7.2$ Hz, C-6, C-5), 132.35 (d, $J = 36.7$ Hz, C-25, C-21, C-19, C-15), 131.71 (d, $J = 9.7$ Hz, C-23, C-17), 128.47 (d, $J = 48.7$ Hz, C-24, C-22, C-18, C-16); 126.21 (C-11, C-8), 118.76 (C-10, C-9), 61.6 (C-4, C-1), 28.48 (C-3, C-2).

^{31}P NMR (CDCl_3 , 200 MHz) δ 20.07.

7-(Diphenylphosphine sulfide)-7-benzoazabicyclo[2.2.1]heptane **3.201**



3.201

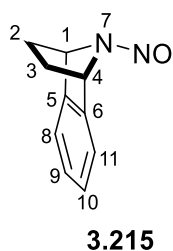
In a 25ml RBF, 7-benzoazabicyclo[2.2.1]heptane **3.181** (230 mg, 0.67 mmol, 1.0 eq.), Lawesson's reagent (404 mg, 0.73 mmol, 1.1 eq.) were loaded accurately with a magnetic stirrer in toluene. The reaction was set up under reflux overnight. The crude mixture was concentrated under reduced pressure and purified with flash chromatography [SiO_2 , EtOAc: hexanes (4:6)] to obtain the title compound **3.201** as greyish powder (133 mg, 0.36 mmol, 55%).

^1H NMR (CDCl_3 , 500 MHz): δ 7.99 - 7.95 (m, 4H, H-25, H-21, H-19, H-15), 7.50 - 7.47 (m, 2H, H-23, H-7), 7.44 - 7.40 (m, 4H, H-24, H-22, H-18, H-16), 7.13 (br, 4H, H-11, H-10, H-9, H-8), 4.73 (m, 2H, H-4, H-1), 2.47 (d, $J = 5.15$ Hz, 2H, H-3a, H-3b), 1.35 (m, 2H, H-2a, H-2b).

^{13}C NMR (CDCl_3 , 125 MHz) δ 145.84 (d, $J = 29.1$ Hz, C-6, C-5), 134.91 (C-20), 133.32 (C-14), 131.81 (d, $J = 43.4$ Hz, C-25, C-21, C-19, C-15), 131.52 (C-23, C-7), 128.37 (d, $J = 51.2$ Hz, C-24, C-22, C-18, C-16), 126.18 (C-11, C-8), 118.81 (C-10, C-9), 62.83 (C-4, C-1), 27.89 (d, $J = 20.3$ Hz, C-3, C-2).

^{31}P NMR (CDCl_3 , 200 MHz) δ 54.32.

7-(*N*-Nitroso)-7-benzoazabicyclo[2.2.1]heptane **3.215**²

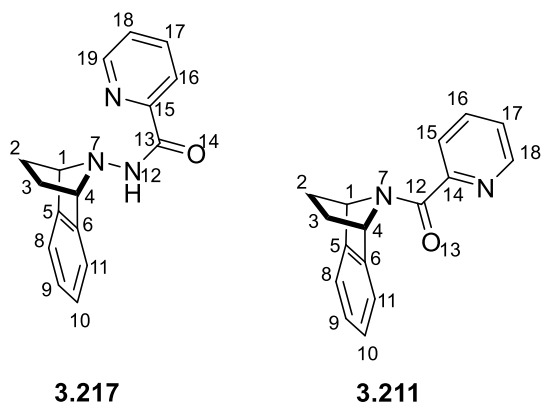


To a solution of 7-benzoazabicyclo[2.2.1]heptane **3.181** (250 mg, 1.72 mmol, 1.0 eq.) in THF (8.6 ml, 0.2 M) was added *tert*-butyl nitrile (0.37 ml, 2.58 mmol, 1.5 eq.) under argon. The reaction mixture was heated under reflux overnight. The excess of the *tert*-butyl nitrile and solvent were removed under reduced pressure. The title compound 7-(*N*-nitroso)-7-benzoazabicyclo[2.2.1]heptane **3.215** was obtained as a residual yellowish oil. (200 mg, 1.15 mmol, 67%) (The compound **3.215** is volatile under reduce pressure)

¹H NMR (CDCl₃, 400 MHz): δ 7.37 (d, J = 6.2 Hz, 1H, H-11), 7.29-7.27 (m, 1H, H-10), 7.25-7.22 (m, 2H, H-9, H-8), 5.94 (t, J = 6.3 Hz, 2H, H-4, H-1), 2.29-2.21 (m, 1H, H-3a), 2.09-2.01 (m, 1H, H-3b), 1.61 (td, J = 9.2, 3.8 Hz, 1H, H-2a), 1.39-1.35 (m, 1H, H-2b).

Data comparable to that reported in literature.²

7-(Picolinoylhydrazine)-7-benzoazabicyclo[2.2.1]heptane **3.217** & 7-(Picolinoylhydrazine)-7-benzoazabicyclo[2.2.1]heptane **3.211**



General procedure was followed using a mixture of 7-benzoazabicyclo[2.2.1]heptane **3.198** and 7-(amino)-7-benzoazabicyclo[2.2.1]heptane **3.216** (90 mg, 0.55 mmol, 1eq.)*, Et₃N (0.093 ml, 0.66 mmol, 1.2 eq.), and picolinoyl chloride** (75.65 mg, 0.60 mmol, 1.1 eq.). The crude mixture was purified with flash chromatography [SiO₂, EtOAc: hexanes + Et₃N (4:6)] to obtain

the brownish semisolid of **3.217** (23 mg, 0.08 mmol, 16%) and yellow semisolid of **3.211** (16 mg, 0.06 mmol, 10%).

* Calculated according to 1.0 eq. of 7-(amino)-7-benzoazabicyclo[2.2.1]heptane **3.216**

** Picolinoyl chloride was freshly prepared by adding a few drops of DMF in a solution of 2-picolinic acid and oxalyl chloride in CH₂Cl₂.

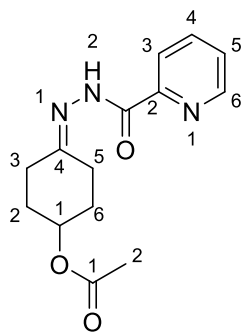
3.217

¹H NMR (CDCl₃, 400 MHz): δ 8.30 (d, $J = 4.4$ Hz, 1H, H-16) 8.16 (d, $J = 7.8$ Hz, 1H, H-8), 7.78 (td, $J = 7.6, 1.5$ Hz, 1H, H-17), 7.39-7.36 (m, 2H, H-11, H-8), 7.32-7.28 (m, 3H, H-10, H-9, NH), 4.51 (s, 2H, H-4, H-1), 2.50-2.38 (m, 2H, H-3a, H-3b), 1.28 (q, $J = 4.1$ Hz, 2H, H-1a, H-1b).

3.211

¹H NMR (CDCl₃, 400 MHz): δ 7.37 (d, $J = 4.1$ Hz, 1H, H-18), 7.90 (d, $J = 7.8$ Hz, 1H, H-15), 7.80 (td, $J = 7.6, 1.7$ Hz, 1H, H-17), 7.40 (m, 1H, H-16), 7.34 (d, $J = 7.2$ Hz, 1H, H-11), 7.23-7.15 (m, 3H, H-10, H-9, H-8), 6.17 (d, $J = 3.9$ Hz, 1H, H-4), 5.79 (d, $J = 4.0$ Hz, 1H, H-1), 2.35-2.19 (m, 2H, H-3a, H-3b), 1.45 (d, $J = 10.7$ Hz, 2H, H-2a, H-2b).

4-(2-Picolinoylhydrazineylidene)cyclohexyl acetate **3.223**

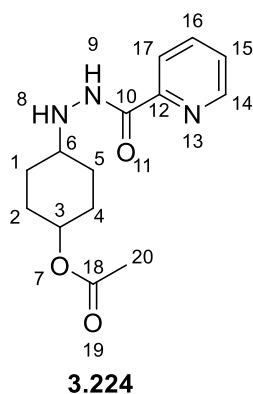


3.223

A 25 ml RBF was charged with 4-oxocyclohexyl acetate **3.221** (1000 mg, 6.40 mmol, 1.0 eq.), picolinohydrazide **3.222** (878 mg, 6.40 mmol, 1.0 eq.), CeCl₃·7H₂O (238 mg, 0.64 mmol, 0.1 eq.) and ethanol (12.81 ml, 0.5 M) and a stir bar. The reaction mixture was stirred overnight. The reaction mixture was filtered through a pad of silica gel, washing with EtAOc. The filtrate was concentrated under reduced pressure. Purification of the residue was performed by flash chromatography on neutral alumina (MeOH:CH₂Cl₂ 10:90) to give a greyish powder of 4-(2-picolinoylhydrazineylidene)cyclohexyl acetate **3.223** (862 mg, 3.13 mmol, 49%).

^1H NMR (CDCl_3 , 400 MHz): δ 8.54 (d, $J = 4.6$ Hz, 1H, H-17), 8.28 (d, $J = 7.8$ Hz, 1H, H-14), 7.89 (td, $J = 7.6, 2.0$ Hz, 1H, H-16), 7.47 (dd, $J = 7.51, 6.7$ Hz, 1H, H-15), 5.09 - 5.04 (m, 1H, H-3), 2.75 (ddt, $J = 14.0, 8.3, 5.2$ Hz, 2H, H-5a, H-5b), 2.56 (ddt, $J = 13.2, 8.0, 5.1$ Hz, 2H, H-1a, H-1b), 2.07 (s, 3H, $-\text{CH}_3$), 2.03-1.84 (m, 4H, H-4a, H-4b, H-2a, H-2b).

4-(2-Picolinoylhydrazineyl)cyclohexyl acetate **3.224**



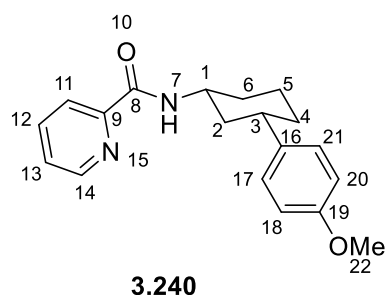
A 50 ml RBF was charged with 4-(2-picolinoylhydrazineylidene)cyclohexyl acetate **3.223** (458 mg, 1.66 mmol, 1.0 eq.), sodium cyanoborohydride (878 mg, 1.12 mmol, 0.68 eq.) and a stir bar under argon. Methanolic HCl (5M, pH = 3) (27.5, 0.06M) was added dropwise over 15 min.- The reaction mixture carefully quenched with saturated solution of NaHCO_3 at 0 °C. Methanol evaporated under reduced pressure. The aqueous was extracted with EtOAc (3 \times 20 ml), washed with brine and dried over MgSO_4 . The filtrate was concentrated under reduced pressure. Purification of the residue was performed by flash chromatography on silica gel (EtOAc : hexanes 50:50, Et_3N few drops) to give a brownish powder of 4-(2-picolinoylhydrazineyl)cyclohexyl acetate **3.224** (241 mg, 0.87 mmol, 52%).

^1H NMR (CDCl_3 , 500 MHz): δ 9.22 (bs, 1H, $-\text{NH}$ -9), 8.57 (d, $J = 3.7$ Hz, 1H, H-17), 8.18 (d, $J = 7.7$ Hz, 1H, H-14), 7.89 (t, $J = 7.7$ Hz, 1H, H-16), 7.47 (t, $J = 6.0$ Hz, 1H, H-15), 4.9 (bs, 1H, $-\text{NH}$ 8), 4.75 - 4.74 (m, 1H, H-3), 3.06-2.97 (m, 1H, H-6), 2.07 (s, 3H, $-\text{CH}_3$), 1.97 - 1.77 (m, 3H, H-5a, H-5b, H-1a), 1.69 - 1.55 (m, 3H, H-4a, H-4b), 1.47 - 1.35 (m, 2H, H-2a, H-2b).

*Repetition of the same numbers in the below ^{13}C NMR is indicating *cis* and *trans* isomers of **3.224**

^{13}C NMR (CDCl_3 , 125 MHz)* δ 170.60 (C-18), 163.58 (C-10), 163.52 (C-10), 149.16 (C-12), 149.11 (C-12), 148.33 (C-17), 148.32 (C-17), 137.37 (C-14, C-14), 126.46 (C-16), 126.43 (C-16), 122.24 (C-15, C-15), 72.40 (C-3), 69.64 (C-3), 57.83 (C-6), 57.26 (C-6), 29.30 (C-4, C-4), 28.69 (C-2, C-2), 27.83 (C-5, C-5), 26.09 (C-1, C-1), 24.40 (-CH₃), 21.63 (-CH₃).

***N*-3-(4-Methoxyphenyl)cyclohexylpicolinamide 3.240**



A Schlenk tube was charged with *N*-picolinoylcyclohexylamine **3.234** (40 mg, 0.2 mmol, 1.0 eq.), 4-iodoanisole **3.187** (94 mg, 0.4 mmol, 1.0 eq.), Ag_2CO_3 (83 mg, 0.3 mmol, 1.5 eq.), and $\text{Pd}(\text{OAc})_2$ (9 mg, 0.04 mmol, 0.2 eq.). The tube was covered with aluminium foil, then purged, and degassed with argon for three times. The solvent *tert*-amyl-OH (1 ml, 0.2M) was transferred in a tube *via* syringe and the screw capped tube was heated at 110 °C for 48 h under dark. The reaction mixture was diluted with CH_2Cl_2 and filtered through a pad of silica gel, washing with CH_2Cl_2 and MeOH. The filtrate was concentrated under reduced pressure. Purification of the residue was performed by flash chromatography on silica gel (EtOAc : hexanes 30 : 70) to give a pale brown solid of *N*-3-(4-methoxyphenyl)cyclohexylpicolinamide **3.240** (37 mg, 0.12 mmol, 60%).

^1H NMR (CDCl_3 , 400 MHz): δ 8.54 (d, $J = 4.6$ Hz, 1H, H-14), 8.22 (d, $J = 7.8$ Hz, 1H, H-11), 7.98 (bs, 1H, -NH), 7.86 (td, $J = 7.6, 1.5$ Hz, 1H, H-13), 7.43 (dd, $J = 7.5, 4.7$ Hz, 1H, H-12), 7.15 (d, $J = 8.7$ Hz, 2H, H-21, H-17), 6.85 (d, $J = 10.8$ Hz, 2H, H-20, H-18), 4.17 (dtt, $J = 19.6, 6.8, 3.9$ Hz, 1H, H-1ax), 3.79 (s, 3H, -OMe), 2.74 (ddt, $J = 15.4, 4.0$ Hz, 1H, H-1ax), 2.28 (d, $J = 12.2$ Hz, 1H, H-2eq), 2.17 (d, $J = 12.3$ Hz, 1H, H-5eq), 1.98-1.89 (m, 2H, H-5eq, H-4eq), 1.65 (qt, $J = 16.6, 3.4$ Hz, 1H, H-5ax), 1.48-1.26 (m, 3H, H-2ax, H-4ax, H-6ax).

^{13}C NMR (CDCl_3 , 125 MHz) δ 163.28 (C-8), 157.89 (C-19), 150.11 (C-9), 147.89 (C-14), 138.48 (C-16), 137.40 (C-12), 127.61 (C-21, C-17), 126.04 (C-13), 122.28 (C-11), 113.76 (C-

20, C-18), 55.25 (C-22 -OMe), 48.79 (C-1), 42.30 (C-2), 41.50 (C-3), 33.50 (C-4), 32.82 (C-6), 25.21 (C-5).

8.4.1. References

- (1) Otani, Y.; Nagae, O.; Naruse, Y.; Inagaki, S.; Ohno, M.; Yamaguchi, K.; Yamamoto, G.; Uchiyama, M.; Ohwada, T. An Evaluation of Amide Group Planarity in 7-Azabicyclo[2.2.1]heptane Amides. Low Amide Bond Rotation Barrier in Solution. *J. Am. Chem. Soc.* **2003**, *125*, 15191.
- (2) Yanagimoto, T.; Toyota, T.; Matsuki, N.; Makino, Y.; Uchiyama, S.; Ohwada, T. Transnitrosation of Thiols from Aliphatic *N*-Nitrosamines: *S*-Nitrosation and Indirect Generation of Nitric Oxide. *J. Am. Chem. Soc.* **2007**, *129*, 736.
- (3) Montalbetti, C. A. G. N.; Falque, V. Amide bond formation and peptide coupling. *Tetrahedron* **2005**, *61*, 10827.

8.5. Experimental for Chapter 4

General procedures for the synthesis of oxazoline

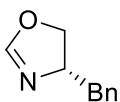
Method I

A solution of amino alcohol (1.0 eq.), triethyl orthoformate (1.5 eq.), and catalytic glacial acetic acid (10 mol%) in dry. DCE (dried over P₂O₅) was heated to reflux overnight under argon. The solution was allowed to cool down and volatiles were removed under reduced pressure. The residues were purified either Kugelrohr distillation or flash chromatography as specified in the respective compound procedure.

Method II

A solution of amino alcohol (1.0 eq.), DMF-DMA (1.0 eq.), in dry. CH₂Cl₂ (dried over CaH) was heated to reflux for 6 hrs under argon. The residues were purified either Kugelrohr distillation or flash chromatography as specified in the respective compound procedure.

(4*S*)-4-benzyl-oxazoline **4.10**¹



(*S*)-**4.10**

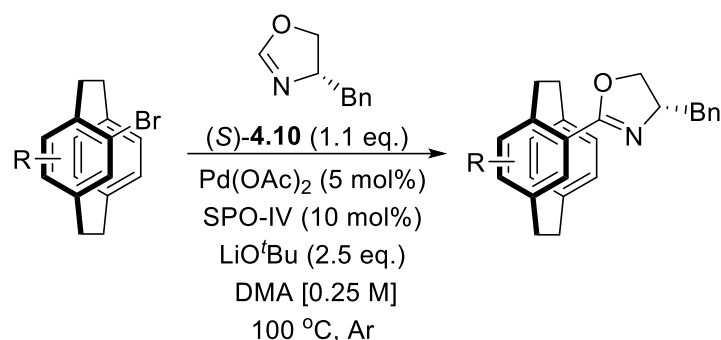
General method A was used to synthesise (*4S*)-**4.10** by taking (*S*)-phenylalaninol (3.0 g, 29.09 mmol, 1.0 eq.), triethyl orthoformate (6.4 g, 43.64 mmol, 1.0 eq.), and glacial acetic acid (0.17 ml, 2.90 mmol, 0.1 eq.).

Purification: Kugelrohr distillation at 55 °C, 5 mTorr to obtain a colourless liquid of **4.10** (1.8 g, 11.18 mmol, 56% yield).

¹H NMR (CDCl₃, 400 MHz): δ 7.33-7.21 (5H, m), 6.83 (1H, d, $J = 1.8$ Hz), 4.43 (1H, ddd, $J = 15.5, 7.8, 1.8$ Hz), 4.19 (1H, t, $J = 9.2, 8.5$ Hz), 3.95 (1H, dd, $J = 8.3, 7.5$ Hz), 3.12 (1H, dd, $J = 13.8, 5.8$ Hz), 2.71 (1H, dd, $J = 13.9, 8.3$ Hz).

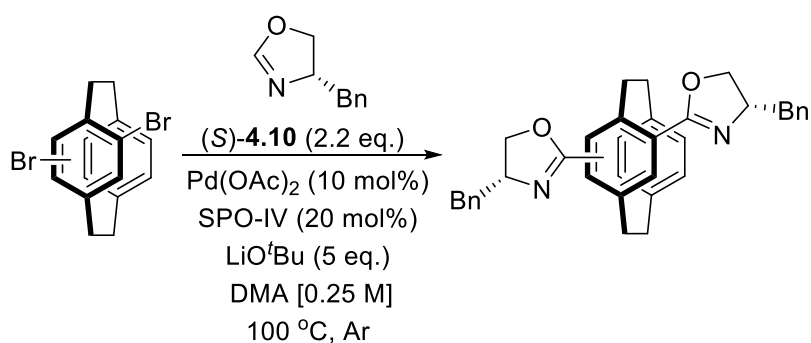
Data comparable to that reported in literature.¹

General procedure A: Coupling of (4*S*)-4-benzyl-oxazoline with bromo[2.2]paracyclophane



A 4 ml scintillation vial was charged with bromo[2.2]paracyclophane (1.0 eq.), (4*S*)-4-benzyl-oxazoline **4.10** (1.1 eq.), LiO^tBu (2.5 eq.), di-*tert*-butyl SPO [(^tBu)₂P(O)H] **4.15** (0.1 eq.), and Pd(OAc)₂ (0.05 eq.). The vial was purged and degassed with argon three times. The degassed DMA (0.25 M) was transferred by syringe and the screw-capped vial was heated at 100 °C until the time indicated in the respective compound section. The reaction mixture was cooled down at room temperature and diluted with CH₂Cl₂ and MeOH before passing through a pad of Celite[®]. The resulting filtrate was removed under reduced pressure and the crude product was purified by flash chromatography with a solvent system described in respective compound section.

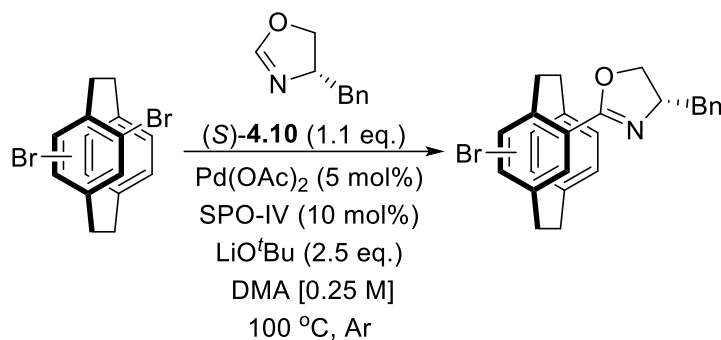
General procedure B: Bis-coupling of (4*S*)-4-benzyl-oxazoline with dibromo[2.2]paracyclophane



A 4 ml scintillation vial was charged with dibromo[2.2]paracyclophane (1.0 eq.), (4*S*)-4-benzyl-oxazoline **4.10** (2.2 eq.), LiO^tBu (5 eq.), di-*tert*-butyl SPO [(^tBu)₂P(O)H] **4.15** (0.2 eq.), and Pd(OAc)₂ (0.1 eq.). The vial was purged and degassed with argon three times. The degassed DMA (0.25 M) was transferred by syringe and the screw-capped vial was heated at 100 °C until the time indicated in the respective compound section. The reaction mixture was cooled down at room temperature and diluted with CH₂Cl₂ and MeOH before passing through

a pad of Celite[®]. The resulting filtrate was removed under reduced pressure and the crude product was purified by flash chromatography with a solvent system described in the respective compound section.

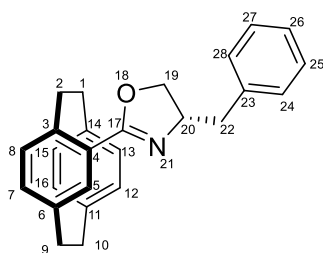
General procedure C: Mono-coupling of (4S)-4-benzyl-oxazoline with dibromo[2.2]paracyclophane



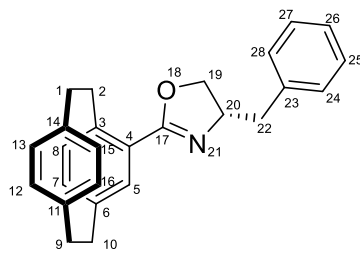
A 4 ml scintillation vial was charged with dibromo[2.2]paracyclophane (1.0 eq.), (4S)-4-benzyl-oxazoline **4.10** (1.1 eq.), LiO^tBu (2.5 eq.), di-*tert*-butyl SPO [(^tBu)₂P(O)H] **4.15** (0.1 eq.), and Pd(OAc)₂ (0.05 eq.). The vial was purged and degassed with argon three times. The degassed DMA (0.25 M) was transferred by syringe and the screw-capped vial was heated at 100 °C until the time indicated in the respective compound section. The reaction mixture was cooled down at room temperature and diluted with CH₂Cl₂ and MeOH before passing through a pad of Celite[®]. The resulting filtrate was removed under reduced pressure and the crude product was purified by flash chromatography with a solvent system described in the respective compound section.

Repetitions of the same numbers in the section below is assigning ¹H/¹³C NMR peaks of a mixture of diastereomers.

4-((4*S*)-Benzyl-oxazoline-2-yl)[2.2]paracyclophane **4.11**



4.11 Dia. 1



4.11 Dia.2

General procedure **A** was followed using 4-bromo[2.2]paracyclophane **4.9** (70 mg, 0.24 mmol, 1.0 eq.), (4*S*)-4-benzyl-oxazoline **4.10** (43 mg, 0.27 mmol, 1.1 eq.), LiO^tBu (49 mg, 0.61 mmol, 2.5 eq.), (^tBu)₂P(O)H (4 mg, 0.025 mmol, 0.1 eq.), Pd(OAc)₂ (4 mg, 0.012 mmol, 0.05 eq.), DMA (0.98 ml) for 28 h.

Purification: Flash chromatography [SiO₂, EtOAc : hexanes (30:70)] to obtain the title compound **4.11** as pinkish semisolid (74 mg, 0.20 mmol, 82% yield).

R_f: 0.6

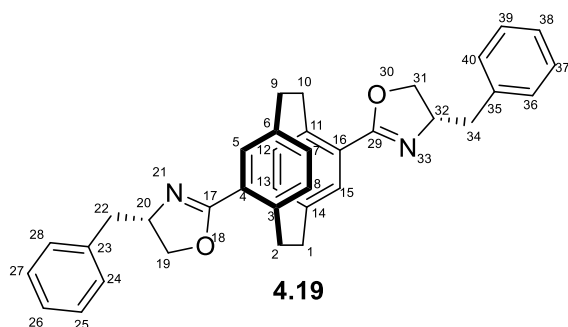
IR: ν_{max} 2925, 2852, 2121, 1896, 1712, 1634, 1497 cm⁻¹.

¹H NMR (MeOD₄, 500 MHz): δ 7.35-7.34 (m, 8H, H-28, H-28, H-27, H-27, H-25, H-25, H-24, H-24), 7.27-7.24 (m, 2H, H-26, H-26), 7.01 (d, *J* = 19.4 Hz, 2H, H-5, H-5), 6.65-6.63 (m, 1H, H-8, H-8), 6.57-6.50 (m, 3H, H-7, H-7, H-13, H-13, H-12, H-12), 6.48-6.46 (m, 1H, H-16, H-16), 6.42 (s, 1H, H-15, H-15), 4.66-4.58 (m, 1H, H-20, H-20), 4.45 (q, *J* = 17.7, 8.7 Hz, 2H, H-19a, H-19a), 4.28-4.22 (m, 2H, H-19b, H-19b), 4.04-3.89 (m, 2H, H-22a, H-22a), 3.19-2.82 (m, 18H, H-22b, H-22b, H-2a, H-2a, H-2b, H-2b, H-9a, H-9a, H-9b, H-9b, H-1a, H-1a, H-1b, H-1b, H-10a, H-10a, H-10b, H-10b).

¹³C NMR (MeOD₄, 125 MHz): δ 165.93 (C-17), 165.51 (C-17), 140.87 (C-14), 140.68 (C-14), 139.75 (C-11, C-11), 139.48 (C-3, C-3), 139.27 (C-23, C-23), 137.99 (C-4), 137.59 (C-4), 135.81 (C-6, C-6), 135.23 (C-7, C-7), 133.91 (C-15, C-15), 132.73 (C-16, C-16), 132.50 (C-13, C-13), 132.06 (C-5, C-5), 131.18 (C-27, C-27), 129.34 (C-25, C-25), 129.19 (C-28, C-28), 128.20 (C-8, C-8, C-7, C-7), 127.80 (C-24, C-24), 126.24 (C-26, C-26), 71.2 (C-20, C-20), 61.17 (C-19), 66.85 (C-19), 41.30 (C-22), 40.84 (C-22), 35.27 (C-2, C-2), 35.12 (C-9, C-9), 34.80 (C-1, C-1), 34.57 (C-10, C-10).

HRMS (ESI-TOF) *m/z*: [M + H]⁺ Calcd C₂₆H₂₆NO for 368.2009; Found 368.2003.

4,16-Bis-((4*S*)-benzyl-oxazoline-2-yl)[2.2]paracyclophane **4.19**



General procedure B was followed using 4,16-dibromo[2.2]paracyclophane **4.18** (50 mg, 0.13 mmol, 1.0 eq.), (4*S*)-4-benzyl-oxazoline **4.10** (49 mg, 0.30 mmol, 2.2 eq.), LiO^tBu (55 mg, 0.68 mmol, 5 eq.), (^tBu)₂P(O)H (4 mg, 0.027 mmol, 0.2 eq.), Pd(OAc)₂ (4 mg, 0.013 mmol, 0.1 eq.), DMA (0.55 ml) for 48 h.

Purification: Flash chromatography [SiO₂, EtOAc: hexanes (30:70)] to obtain the title compound **4.19** as a pale yellowish semisolid (58 mg, 0.11 mmol, 81% yield).

R_f: 0.6

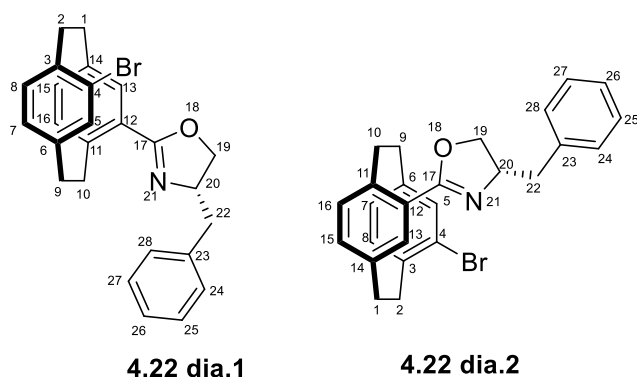
IR: ν_{max} 3018, 2988, 2900, 1393 cm⁻¹.

¹H NMR (CDCl₃, 500 MHz): δ 7.40-7.27 (m, 8H, H-40, H-39, H-36, H-37, H-28, H-27, H-24, H-25), 7.30-7.27 (m, 2H, H-38, H-26), 7.11 (d, *J* = 11.6 Hz, 2H, H-15, H-5), 6.66-6.63 (m, 2H, H-12, H-8), 6.56 (t, *J* = 7.6 Hz, 2H, H-13, H-7), 4.72-4.63 (m, 2H, H-32, H-20), 4.44 (dt, *J* = 22.7, 8.7 Hz, 2H, H-10a, H-2a), 4.26-4.09 (m, 4H, H-31a, H-31b, H-19a, H-19b), 3.35 (quint, *J* = 13.5, 5.5 Hz, 2H, H-34a, H-22a), 3.13-3.03 (m, 4H, H-9a, H-9b, H-1a, H-1b), 2.96-2.90 (m, 2H, H-10b, H-2b), 2.87 (m, 2H, H-34b, H-22b).

¹³C NMR (CDCl₃, 125 MHz): δ 164.40 (C-20), 164.12 (C-16), 140.92 (C-11), 140.66 (C-3), 139.81 (C-35), 139.68 (C-23), 138.18 (C-16), 138.14 (C-4), 135.14 (C-14), 135.06 (C-6), 134.21 (C-8), 134.14 (C-5), 135.14 (C-14), 135.06 (C-6), 134.21 (C-8), 134.14 (C-5), 133.37 (C-12), 133.25 (C-15), 129.40 (C-37, C-25), 129.36 (C-39, C-27), 128.63 (C-36, C-24), 128.58 (C-40, C-28), 128.50 (C-13), 128.31 (C-7), 126.55 (C-38, C-26), 71.85 (C-32), 70.92 (C-20), 68.20 (C-31), 66.16 (C-19), 42.05 (C-34), 41.92 (C-22), 34.94 (C-9, C-1), 34.42 (C-2), 34.32 (C-10).

HRMS (ESI-TOF) *m/z*: [M + H]⁺ Calcd C₃₆H₃₄N₂O₂ 527.2693 for; Found 527.2689.

4-Bromo-12-((4*S*)-benzyl-oxazoline-2-yl)[2.2]paracyclophane **4.22**



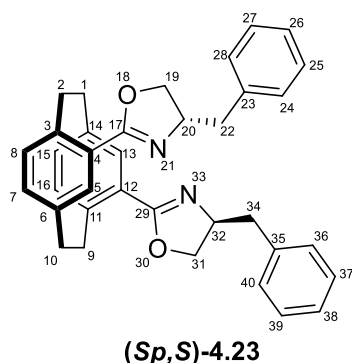
General procedure C was followed using (\pm)-4,12-dibromo-[2.2]paracyclophane **4.21** (50 mg, 0.14 mmol, 1.0 eq.), (4*S*)-4-benzyl-oxazoline **4.10** (24 mg, 0.15 mmol, 1.1 eq.), LiO^tBu (27 mg, 0.34 mmol, 2.5 eq.), (^tBu)₂P(O)H (2 mg, 0.013 mmol, 0.1 eq.), Pd(OAc)₂ (2 mg, 0.006 mmol, 0.05 eq.), DMA (0.55 ml) for 24 h. Purification: Flash chromatography [SiO₂, EtOAc : hexanes (30:70)] to obtain the title compound **4.22** as a white semisolid (19 mg, 0.042 mmol, 31% yield). R_f : 0.5, IR: ν_{\max} 3675, 2989, 2900, 1405, 1393 cm⁻¹.

¹H NMR (CDCl₃, 500 MHz): δ 7.70 (d, J = 8.5 Hz, 2H, H-13, H-13), 7.40-7.35 (m, 8H, H-28, H-28, H-24, H-24, H-27, H-27, H-25, H-25), 7.31-7.26 (m, 2H, H-26, H-26), 6.66-6.58 (m, 8H, H-16, H-16, H-15, H-15, H-8, H-8, H-7, H-7), 6.52 (d, J = 7.7 Hz, 2H, H-5, H-5), 4.70-4.60 (m, 2H, H-20, H-20), 4.40 (t, J = 8.6 Hz, 1H, H-22a), 4.34 (t, J = 8.6 Hz, 1H, H-22b), 4.28-4.12 (m, 4H, H-19a, H-19a, H-19b, H-19b), 3.51 (t, J = 10.2 Hz, 2H, H-22a, H-22b), 3.37 (dd, J = 13.8, 5.6 Hz, 1H, H-10a), 3.30 (dd, J = 13.7, 5.4 Hz, 1H, H-10b), 3.24-3.19 (m, 2H, H-10a, H-10b), 3.12-2.78 (m, 12H, 9a, 9b, 1a, 1b, 2a, 2b).

¹³C NMR (CDCl₃, 125 MHz): δ 163.92 (C-17), 163.63 (C-17), 142.16 (C-6), 142.03 (C-6), 140.73 (C-11), 140.57 (C-11), 139.25 (C-23), 139.20 (C-23), 138.86 (C-3), 138.82 (C-3), 138.39 (C-12), 138.32 (C-12), 135.67 (C-16, C-16, C-15, C-15), 135.16 (C-14), 135.11 (C-14), 134.97 (C-5), 134.90 (C-5), 131.36 (C-27), 131.25 (C-25), 130.44 (C-25), 130.19 (C-25), 129.40 (C-28, C-28), 129.30 (C-24, C-24), 128.61 (C-8, C-8), 128.54 (C-7, C-7), 128.06 (C-26), 127.97 (C-26), 126.68 (C-13), 126.63 (C-13), 126.49 (C-4), 126.45 (C-4), 71.05 (C-20), 70.90 (C-20), 65.51 (C-19), 68.29 (C-19), 42.22 (C-22), 42.03 (C-22), 36.06 (C-10), 35.85 (C-10), 35.79 (C-9), 35.69 (C-9), 33.93 (C-1), 33.68 (C-1), 32.66 (C-2), 32.60 (C-2).

HRMS (ESI-TOF) m/z : [M + H]⁺ Calcd for C₂₆H₂₅Br⁷⁹NO 446.1114; Found 446.1111; C₂₆H₂₅Br⁸¹NO 448.1114; Found 448.1089.

(*Sp,S*)-4,16-Bis-(4-benzyl-oxazoline-2-yl)[2.2]paracyclophane 4.23



General procedure B was followed using (\pm)-4,16-dibromo-[2.2]paracyclophane **4.21** (60 mg, 0.16 mmol, 1.0 eq.), (4*S*)-4-benzyl-oxazoline **4.10** (58 mg, 0.36 mmol, 2.2 eq.), LiO^tBu (66 mg, 0.82 mmol, 5 eq.), (^tBu)₂P(O)H (5 mg, 0.032 mmol, 0.2 eq.), Pd(OAc)₂ (4 mg, 0.016 mmol, 0.1 eq.), DMA (0.66 ml) for 12 hrs. Purification: Flash chromatography [SiO₂, EtOAc:hexanes (0-5 to 5:20, gradient elution)] to obtain the title compound **4.23** (70% yield) as separate diastereomer, (*Sp,S*)-**4.23**, pale yellowish semisolid (30 mg, 0.057 mmol, 34% yield) and (*Rp,S*)-**4.23**, pale yellowish semisolid (31 mg, 0.068 mmol, 36% yield).

R_f: 0.6

[α]_D²²: -61.70 (*c*=0.47, CHCl₃)

IR: ν_{\max} 3627, 2955, 2919, 1639, 1601, 1590, 1452 cm⁻¹.

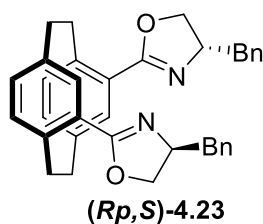
¹H NMR (CDCl₃, 500 MHz): δ 7.36-7.30 (m, 8H, H-24, H-25, H-28, H-27, H-36, H-37, H-40, H-39), 7.28-7.25 (m, 2H, H-26, H-38), 7.17 (s, 2H, H-5, H-13), 6.69 (d, *J* = 7.6 Hz, 2H, H-8, H-15), 6.60 (d, *J* = 7.7 Hz, 2H, H-7, H-16), 4.71-4.65 (m, 2H, H-20, H-32), 4.33-4.26 (m, 4H, H-19a, H-19b, H-31a, H-31b), 4.08-4.05 (t, *J* = 7.5 Hz, 2H, H-2a, H-9a), 3.29 (dd, *J* = 13.7, 4.8 Hz, 2H, H-1a, H-10a), 3.18-3.15 (m, 4H, H-22a, H-22b, H-34a, H-34b), 2.88-2.82 (m, 2H, H-2b, H-9b), 2.73-2.68 (dd, *J* = 13.4, 9.4 Hz, 2H, H-1b, H-10b).

¹³C NMR (CDCl₃, 125 MHz): δ 163.69 (C-29, C-17), 141.02 (C-35, C-23), 140.10 (C-11, C-3), 138.44 (C-12, C-4), 135.75 (C-14, C-6), 134.87 (C-27, C-25), 132.57 (C-39, C-37), 129.25 (C-40, C-36, C-28, C-24), 128.55 (C-16, C-13, C-8, C-5), 127.98 (C-15, C-7), 126.43 (C-38, C-26), 70.73 (C-32, C-20), 68.43 (C-31, C-19), 41.97 (C-34, C-22), 36.04 (C-9, C-1), 34.02 (C-11, C-2).

HRMS (ESI-TOF) *m/z*: [M + H]⁺ Calcd C₃₆H₃₄N₂O₂ 527.2693 for; Found 527.2690.

Data comparable to that reported in literature.²

(Rp,S)-4,16-Bis-(4-benzyl-oxazoline-2-yl)[2.2]paracyclophane 4.23



R_f : 0.5

$[\alpha]_D^{24}$: +23.61 ($c=0.72$, CHCl_3)

IR: ν_{max} 3674, 2925, 1634, 1590, 1495, 1352 cm^{-1} .

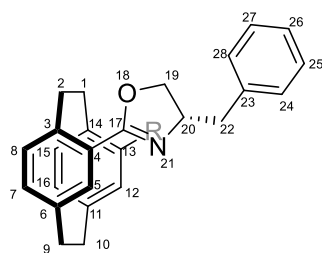
^1H NMR (CDCl_3 , 500 MHz): δ 7.39-7.38 (m, 8H, H-24, H-25, H-28, H-27, H-36, H-37, H-40, H-39), 7.32-7.29 (m, 2H, H-26, H-38), 7.20 (s, 2H, H-5, H-13), 6.68 (d, $J = 7.7$ Hz, 2H, H-8, H-15), 6.59 (d, $J = 7.8$ Hz, 2H, H-7, H-16), 4.67-4.61 (m, 2H, H-20, H-32), 4.35-4.30 (m, 4H, H-19a, H-19b, H-31a, H-31b), 4.11 (t, $J = 7.7$ Hz, 2H, H-2a, H-9a), 3.41 (dd, $J = 13.8, 5.9$ Hz, 2H, H-1a, H-10a), 3.26-3.20 (m, 2H, H-22a, H-34a), 3.16 (t, $J = 10.5$ Hz, 2H, H-2b, H-9b), 2.93 (dd, $J = 13.8, 8.5$ Hz, 2H, H-1b, H-10b), 2.87-2.83 (m, 2H, H-22b, H-34b)

^{13}C NMR (CDCl_3 , 125 MHz): δ 163.51 (C-29, C-17), 141.10 (C-35, C-23), 140.14 (C-11, C-3), 138.64 (C-12, C-4), 135.95 (C-14, C-6), 135.00 (C-27, C-25), 132.11 (C-39, C-37), 129.28 (C-40, C-36, C-28, C-24), 128.65 (C-16, C-13, C-8, C-5), 128.00 (C-15, C-7), 126.50 (C-38, C-26), 70.71 (C-32, C-20), 68.74 (C-31, C-19), 42.27 (C-34, C-22), 35.66 (C-9, C-1), 33.72 (C-11, C-2).

HRMS (ESI-TOF) m/z : $[\text{M} + \text{H}]^+$ Calcd $\text{C}_{36}\text{H}_{34}\text{N}_2\text{O}_2$ 527.2693 for; Found 527.2690.

Data comparable to that reported in literature.²

4-((4*S*)-Benzyl-oxazoline-2-yl)-13-amino[2.2]paracyclophane **4.26dia1***



4.26 Dia. 1

R = NH₂

General procedure A was followed using (\pm)-4-bromo-13-amino[2.2]paracyclophane **4.25** (58 mg, 0.19 mmol, 1.0 eq.), (4*S*)-4-benzyl-oxazoline **4.10** (34 mg, 0.21 mmol, 1.1 eq.), LiO^tBu (39 mg, 0.48 mmol, 2.5 eq.), (^tBu)₂P(O)H (3 mg, 0.019 mmol, 0.1 eq.), Pd(OAc)₂ (2 mg, 0.009 mmol, 0.05 eq.), DMA (0.77 ml) for 24 h.

Purification: Flash chromatography [SiO₂, Et₃N:EtOAc:hexanes (2:14:86)] to obtain the title compound **4.26** (74% yield) as a separate diastereomer, **4.26dia1**, brownish semisolid (13 mg, 0.033 mmol, 18% yield), mixture of diastereomers (28 mg, 0.073 mmol, 38% yield), and a separate diastereomer **4.23dia2**, brownish semisolid (13 mg, 0.033 mmol, 18% yield).

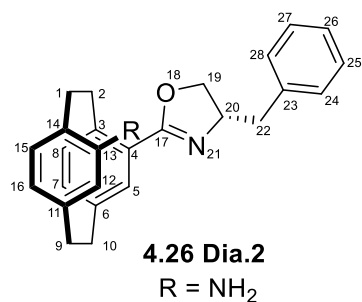
R_f: 0.4 (dia.1)

¹H NMR (CDCl₃, 500 MHz): δ 7.37-7.34 (m, 2H, H-28, H-27), 7.31-7.26 (m, 3H, H-26, H-25, H-24), 7.16 (s, 1H, H-5), 6.64-6.62 (d, *J* = 10.0 Hz, 1H, H-8), 6.44 (d, *J* = 7.7 Hz, 1H, H-7), 6.38 (d, *J* = 7.6 Hz, 1H, H-16), 6.20 (d, *J* = 8.1 Hz, 1H, H-15), 5.49 (s, 1H, H-16), 4.63-4.57 (m, 1H, H-20), 4.33-4.27 (m, 2H, H-22a, H-22b), 4.13 (t, *J* = 8.1 Hz, 1H, H-19a), 3.34 (dd, *J* = 13.7, 4.4 Hz, 1H, H-19b), 3.21-3.09 (m, 2H, H-9a, H-9b), 3.07-3.00 (m, 2H, H-10a, H-10b), 2.94-2.91 (m, 2H, H-2a, H-2b), 2.79-2.72 (m, 2H, H-1a, H-1b).

HRMS (ESI-TOF) *m/z*: [M + H]⁺ Calcd C₂₆H₂₆N₂O 383.2118 for; Found 383.2114.

*The exact configuration of the diastereomer is not determined yet.

4-((4*S*)-Benzyl-oxazoline-2-yl)-13-amino[2.2]paracyclophane **4.26dia2***



General procedure A was followed using (\pm)-4-bromo-(piperidin-1-yl)-[2.2]paracyclophane **4.29** (36 mg, 0.097 mmol, 1.0 eq.), (4*S*)-4-benzyl-oxazoline **4.10** (17 mg, 0.017 mmol, 1.1 eq.), LiO^tBu (20 mg, 0.24 mmol, 2.5 eq.), (^tBu)₂P(O)H (2 mg, 0.009 mmol, 0.1 eq.), Pd(OAc)₂ (1 mg, 0.004 mmol, 0.05 eq.), DMA (0.39 ml) for 24 h.

Purification: Preparative TLC [SiO₂, Et₃N:EtOAc:hexanes (2:09:89)] to obtain the title compound **4.29** (83% yield) as a separate diastereomer, **4.29dia1**, brownish semisolid (17 mg, 0.037 mmol, 29% yield), mixture of diastereomers (14 mg, 0.031 mmol, 31% yield), and a separate diastereomer **4.23dia2**, brownish semisolid (11 mg, 0.024 mmol, 24% yield).

R_f: 0.3 (dia.2)

[α]_D²⁰: -77.78 (*c*=0.90, CHCl₃)

IR: ν_{\max} 3745, 3020, 2938, 2400, 1312 cm⁻¹.

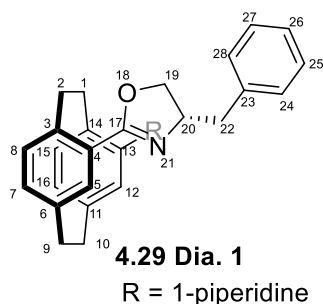
¹H NMR (CDCl₃, 500 MHz): δ 7.41-7.28 (m, 5H, H-28, H-27, H-26, H-25, H-24), 7.10 (s, 1H, H-5), 6.62 (d, *J* = 7.7 Hz, 1H, H-8), 6.42 (d, *J* = 7.7 Hz, 1H, H-7), 6.35 (d, *J* = 7.6 Hz, 1H, H-16), 6.17 (d, *J* = 7.7 Hz, 1H, H-15), 5.42 (s, 1H, H-12), 4.67 (m, 1H, H-20a), 4.40 (t, *J* = 8.6 Hz, 1H, H-22a), 4.34-4.29 (m, 1H, H-20b), 4.20 (t, *J* = 7.8 Hz, 1H, H-22b), 3.18 (dd, *J* = 13.8, 4.5 Hz, 1H, H-20), 3.11-2.88 (m, 6H, H-9a, H-9b, H-10a, H-10b, H-2a, H-2b), 3.04-2.96 (bs, 2H, -NH₂), 2.75-2.69 (m, 2H, H-1a, H-1b).

¹³C NMR (CDCl₃, 125 MHz): δ 165.22 (C-17), 146.36 (C-13), 140.55 (C-3), 140.13 (C-23), 138.33 (C-11), 137.90 (C-4), 136.00 (C-6), 134.84 (C-26), 134.28 (C-7), 132.17 (C-8), 129.95 (C-25), 128.62 (C-27), 126.66 (C-24), 125.09 (C-28), 123.99 (C-14), 122.15 (C-16), 121.15 (C-12), 70.25 (C-20), 67.64 (C-19), 40.84 (C-22), 34.80 (C-10), 32.34 (CC-2), 30.72 (C-1).

HRMS (ESI-TOF) *m/z*: [M + H]⁺ Calcd C₂₆H₂₆N₂O 383.2118 for; Found 383.2114.

*The exact configuration of the diastereomer is not determined yet.

4-((4*S*)-Benzyl-oxazoline-2-yl)-13-(piperidin-1-yl)-[2.2]paracyclophane **4.29dia1***



General procedure A was followed using (\pm)-4-bromo-(piperidin-1-yl)-[2.2]paracyclophane **4.28** (36 mg, 0.097 mmol, 1.0 eq.), (4*S*)-4-benzyl-oxazoline **4.10** (17 mg, 0.017 mmol, 1.1 eq.), LiO*t*Bu (20 mg, 0.24 mmol, 2.5 eq.), (*t*Bu)₂P(O)H (2 mg, 0.009 mmol, 0.1 eq.), Pd(OAc)₂ (1 mg, 0.004 mmol, 0.05 eq.), DMA (0.39 ml) for 24 h.

Purification: Preparative TLC [SiO₂, Et₃N:EtOAc:hexanes (2:09:89)] to obtain the title compound **4.29** (83% yield) as a separate diastereomer, **4.29dia1**, brownish semisolid (17 mg, 0.037 mmol, 29% yield), mixture of diastereomers (14 mg, 0.031 mmol, 31% yield), and a separate diastereomer **4.23dia2**, brownish semisolid (11 mg, 0.024 mmol, 24% yield).

R_f: 0.5 (dia.1)

[α]_D²⁰: +50.91 (*c*=1.1, CHCl₃)

IR: ν_{\max} 3681, 3019, 2931, 2400, 2183, 1517 cm⁻¹.

¹H NMR (CDCl₃, 500 MHz): δ 7.36-7.31 (m, 2H, H-31, H-33), 7.29-7.25 (m, 3H, H-30, H-34, H-32), 7.04 (s, 1H, H-5), 6.66 (d, *J* = 7.6 Hz, 1H, H-8), 6.61 (d, *J* = 5.6 Hz, 1H, H-7), 6.56 (d, *J* = 7.5 Hz, 1H, H-15), 6.33 (d, *J* = 7.5 Hz, 1H, H-16), 5.75 (s, 1H, H-12), 4.68 (m, 1H, H-26), 4.48 (tt, *J* = 13.6, 5.3 Hz, 1H, H-25a), 4.31 (t, *J* = 8.8 Hz, 1H, H-28a), 3.95 (t, *J* = 8.6 Hz, 1H, H-28b), 3.55 (tt, *J* = 13.5, 4.5 Hz, 1H, H-25b), 3.42 (dd, *J* = 13.7, 4.5 Hz, 1H, H-22a), 3.13-3.08 (m, 1H, H-18a), 3.07-3.02 (m, 1H, H-18b), 3.01-2.92 (m, 3H, H-2a, H-2b, H-9a), 2.85-2.74 (m, 5H, H-9b, H-1a, H-10a, H-10b), 2.66 (dd, *J* = 13.5, 9.8 Hz, 1H, H-22b), 1.74-1.72 (m, 2H, H-21a, H-21b), 1.58-1.56 (m, 2H, H-19a, H-19b), 1.51-1.48 (m, 2H, H-2a, H-20b)

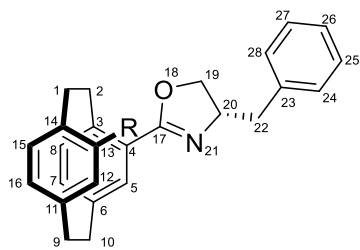
¹³C NMR (CDCl₃, 125 MHz): δ 152.60 (C-23), 142.03 (C-13), 140.05 (C-3), 138.51 (C-29), 137.99 (C-11), 135.81 (C-5), 135.74 (C-7, C-8), 134.75 (C-4), 132.29 (C-6), 131.58 (C-14), 129.14 (C-15, C-31, C-33), 128.59 (C-30, C-34), 126.43 (C-16), 126.30 (C-12), 119.01 (C-32), 70.91 (C-26), 68.67 (C-25), 53.40 (C-22, C-18), 42.50 (C-28), 35.04 (C-9), 34.80 (C-10), 34.21

(C-2), 34.19 (C-1), 26.60 (C-21, C-19), 24.53 (C-20). HRMS (ESI-TOF) m/z: [M + H]⁺ Calcd for; Found

HRMS (ESI-TOF) m/z: [M + H]⁺ Calcd C₃₁H₃₄N₂O 451.2744 for; Found 454.2741.

*The exact configuration of the diastereomer is not determined yet.

4-((4S)-Benzyl-oxazoline-2-yl)-13-(piperidin-1-yl)-[2.2]paracyclophane 4.29dia2*



4.29 Dia.2

R = 1-piperidine

R_f: 0.4 (dia.1)

IR: ν_{max} 3680, 3019, 2929, 2165, 2087 cm⁻¹.

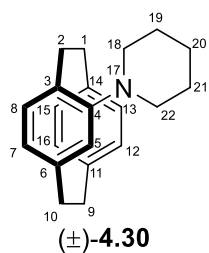
¹H NMR (CDCl₃, 500 MHz): δ 7.36-7.33 (m, 2H, H-31, H-33), 7.29-7.25 (m, 3H, H-30, H-34, H-32), 7.19 (s, 1H, H-5), 6.69 (d, *J* = 7.5 Hz, 1H, H-8), 6.59 (d, *J* = 7.7 Hz, 1H, H-8), 6.54 (d, *J* = 9.0 Hz, 1H, H-15), 6.31 (d, *J* = 7.4 Hz, 1H, H-16), 5.86 (s, 1H, H-12), 4.54 (m, 1H, H-26), 4.34 (t, *J* = 8.7 Hz, 1H, H-25a), 4.22-4.19 (m, 2H, H-28a, H-28b), 3.53-3.48 (m, 1H, H-25b), 3.30 (dd, *J* = 13.6, 4.9 Hz, 1H, H-22a), 3.17-3.11 (m, 1H, H-18a), 3.08-3.02 (m, 1H, H-18b), 2.97-2.82 (m, 8H, H-2a, H-2b, H-9a, H-9b, H-1a, H-1b, H-10a, H-10b), 2.74 (dd, *J* = 13.6, 9.4 Hz, 1H, H-22b), 1.78-1.72 (m, 2H, H-21a, H-21b), 1.63-1.57 (m, 2H, H-19a, H-19b), 1.54-1.51 (m, 2H, H-20a, H-20b)

¹³C NMR (CDCl₃, 125 MHz): δ 152.76 (C-23), 141.47 (C-13), 140.06 (C-3), 138.45 (C-29), 138.38 (C-11), 135.85 (C-5), 135.38 (C-7, C-8), 134.65 (C-4), 132.49 (C-6), 131.87 (C-14), 129.22 (C-15, C-31, C-33), 128.59 (C-30, C-34), 126.63 (C-16), 126.45 (C-12), 118.84 (C-32), 71.24 (C-26), 67.74 (C-25), 53.31 (C-22, C-18), 41.91 (C-28), 35.28 (C-9), 35.07 (C-10), 34.76 (C-2), 33.40 (C-1), 26.46 (C-21, C-19), 24.46 (C-20).

HRMS (ESI-TOF) m/z: [M + H]⁺ Calcd C₃₁H₃₄N₂O 451.2744 for; Found 454.2741

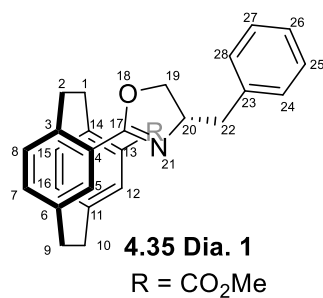
*The exact configuration of the diastereomer is not determined yet.

(±)-4-(Piperidin-1-yl)-[2.2]paracyclophane 4.30



^1H NMR (CDCl_3 , 500 MHz): δ 6.74 (d, $J = 7.6$ Hz, 1H, H-8), 6.55 (d, $J = 7.7$ Hz, 1H, H-15), 6.47 (d, $J = 7.7$ Hz, 1H, H-16), 6.42-6.41 (m, 2H, H-12, H-13), 6.27 (d, $J = 7.5$ Hz, 1H, H-7), 5.73 (s, 1H, H-5), 3.44-3.39 (m, 1H, H-2a), 3.31-3.25 (m, 1H, H-18a), 3.07-3.01 (m, 3H, H-12b, H-9a, H-9b), 3.01-2.97 (m, 1H, H-22), 2.96-2.89 (m, 4H, H-1a, H-1b, H-10a, H-10b), 2.73-2.67 (m, 1H, H-18b), 1.88-1.73 (m, 4H, H-19a, H-19b, H-21a, H-21b), 1.62-1.59 (m, 3H, H-22b, H-22a, H-20b).

4-((4S)-Benzyl-oxazoline-2-yl)-[2.2]paracyclophane-13-methyl ester 4.35dia1*



General procedure A was followed using (\pm)-4-bromo[2.2]paracyclophane-13-methyl ester **4.34** (75 mg, 0.22 mmol, 1.0 eq.), (4S)-4-benzyl-oxazoline **4.10** (39 mg, 0.24 mmol, 1.1 eq.), LiO^tBu (44 mg, 0.54 mmol, 2.5 eq.), (^tBu)₂P(O)H (4 mg, 0.022 mmol, 0.1 eq.), Pd(OAc)₂ (2 mg, 0.010 mmol, 0.05 eq.), DMA (0.87 ml) for 24 h.

Purification: Flash chromatography [SiO₂, EtOAc : hexanes (0-10 to 30:70, gradient elution)] to obtain the title compound **4.35** (21% yield) as a separate diastereomer, **4.35dia1**, white semisolid (6 mg, 0.037 mmol, 6% yield), mixture of diastereomers (11 mg, 0.031 mmol, 12% yield), and a separate diastereomer **4.23dia2**, brownish semisolid (5 mg, 0.024 mmol, 5% yield).

R_f: 0.7 (dia.1)

IR: ν_{\max} 3676, 3019, 2970, 2399, 1523, 1394 cm⁻¹.

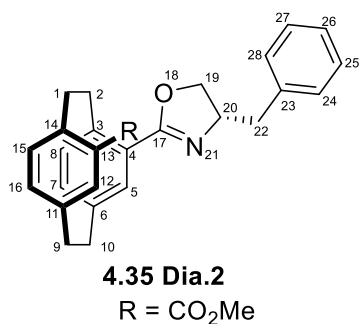
¹H NMR (CDCl₃, 500 MHz): δ 7.35-7.32 (m, 2H, H-24, H-28), 7.29-7.24 (m, 3H, H-24, H-25, H-26), 7.19 (s, 1H, H-12), 7.02 (s, 1H, H-5), 6.71-6.61 (m, 4H, H-8, H-7, H-16, H-15), 4.63-4.57 (m, 1H, H-20), 4.42 (td, J = 14.1, 3.9 Hz, 1H, H-19a), 4.31 (t, J = 8.7 Hz, 1H, H-22a), 4.20 (td, J = 10.6, 3.4 Hz, 1H, H-19b), 4.02 (t, J = 8.05 Hz, 1H, H-22b), 3.80 (s, 3H, -OMe), 3.31 (dd, J = 13.7, 4.9 Hz, 1H, H-2a), 3.18-3.00 (m, 6H, H-1a, H-1b, H-9a, H-9b, H-10a, H-10b), 2.70 (dd, J = 14.0, 9.4 Hz, 1H, H-2b).

¹³C NMR (CDCl₃, 125 MHz): δ 167.28 (C-29), 163.30 (C-17), 142.76 (C-14), 141.31 (C-3), 139.35 (C-23), 139.08 (C-4), 138.48 (C-6), 136.40 (C-11), 135.99 (C-13), 135.63 (C-25), 134.89 (C-27), 134.01 (C-16), 132.84 (C-12), 129.78 (C-5), 129.18 (C-28, C-24), 128.56 (C-8, C-15), 128.03 (C-7), 126.42 (C-25), 70.98 (C-20), 68.66 (C-19), 51.47 (C-31, -OMe), 41.86 (C-22), 34.70 (C-9, C-10), 34.57 (C-2), 34.48 (C-1).

HRMS (ESI-TOF) m/z : [M + H]⁺ Calcd C₂₈H₂₇NO₃ 426.2064 for; Found 426.2060.

*The exact configuration of the diastereomer is not determined yet.

4-((4S)-Benzyl-oxazoline-2-yl)-[2.2]paracyclophane-13-methyl ester 4.35dia2*



R_f: 0.6 (dia.2)

IR: ν_{\max} 3680, 2971, 2325, 2167, 1707, 1522 1410 cm⁻¹.

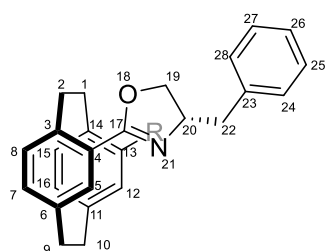
¹H NMR (CDCl₃, 500 MHz): δ 7.36-7.30 (m, 4H, H-28, H-27, H-25, H-24), 7.27-7.24 (m, 1H, H-26), 7.13 (s, 1H, H-12), 6.71-6.67 (m, 1H, H-5), 6.67-6.60 (m, 4H, H-15, H-16, H-8, H-7), 4.55-4.49 (m, 1H, H-20), 4.35 (t, $J = 8.6$ Hz, 1H, H-19a), 4.28 (tt, $J = 22.9, 10.6, 4.1$ Hz, 2H, H-2a, H-2b), 4.14 (t, $J = 7.3$ Hz, 1H, H-19b), 3.87 (s, 3H, -OMe), 3.33 (dd, $J = 13.7, 5.1$ Hz, 1H, H-22a), 3.20-2.97 (m, 6H, H-9a, H-9b, H-10a, H-10b, H-1a, H-1b), 2.83 (dd, $J = 13.6, 9.3$ Hz, 1H, H-22b).

¹³C NMR (CDCl₃, 125 MHz): δ 166.94 (C-29), 164.26 (C-17), 143.19 (C-14), 141.14 (C-3), 139.53 (C-23), 139.06 (C-4), 138.45 (C-6), 136.37 (C-11), 135.99 (C-13), 135.68 (C-25), 135.21 (C-27), 134.14 (C-16), 132.91 (C-12), 129.34 (C-5), 129.24 (C-28, C-24), 128.59 (C-8, C-15), 128.09 (C-7), 126.42 (C-25), 71.47 (C-20), 67.95 (C-19), 51.53 (C-31, -OMe), 41.39 (C-22), 34.85 (C-2), 34.70 (C-9, C-10), 34.16 (C-1).

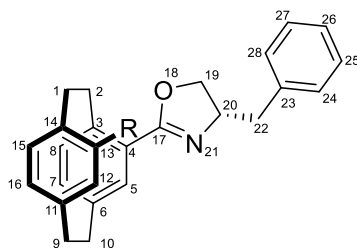
HRMS (ESI-TOF) m/z : [M + H]⁺ Calcd C₂₈H₂₇NO₃ 426.2064 for; Found 426.2060.

*The exact configuration of the diastereomer is not determined yet.

4-((4S)-Benzyl-oxazoline-2-yl)-[2.2]paracyclophane-13-carboxylic acid **4.38**



4.38 Dia. 1
R = COOH



4.38 Dia.2
R = COOH

General procedure A was followed using (\pm)-4-bromo[2.2]paracyclophane-13-carboxylic acid **4.37** (50 mg, 0.15 mmol, 1.0 eq.), (4S)-4-benzyl-oxazoline **4.10** (27 mg, 0.16 mmol, 1.1 eq.), LiO^tBu (30 mg, 0.38 mmol, 2.5 eq.), (^tBu)₂P(O)H (2 mg, 0.015 mmol, 0.1 eq.), Pd(OAc)₂ (2 mg, 0.0075 mmol, 0.05 eq.), DMA (0.6 ml) for 24 h.

Purification: Flash chromatography [SiO₂, EtOAc : hexanes 40:60] to obtain the title compound as a mixture of diastereomers **4.38**, white semisolid (27 mg, 0.065 mmol, 44% yield).

R_f: 0.3

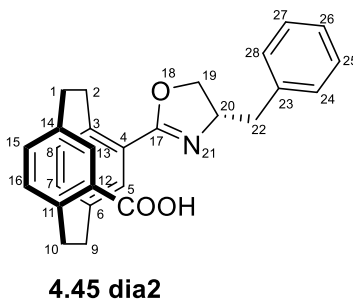
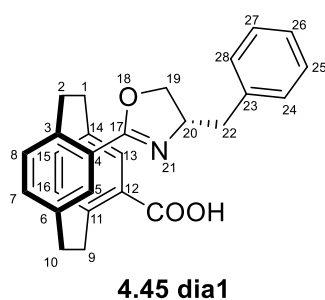
IR: ν_{\max} 3650, 2973, 2196, 2007, 1683, 1419 cm⁻¹.

¹H NMR (CDCl₃, 500 MHz): δ 7.50 (s, 1H, H-12), 7.30 (s, 1H, H-12), 7.23 (d, J = 6.8 Hz, 2H, H-5, H-5), 7.19-7.15 (m, 4H, H-24, H-24, H-28, H-28), 7.10-1.05 (m, 6H, H-27, H-27, H-26, H-26, H-25, H-25), 6.79 (dd, J = 15.6, 6.2 Hz, 2H, H-15, H-15), 6.71-6.65 (m, 6H, H-16, H-16, H-7, H-7, H-8, H-8), 4.69-4.55 (m, 2H, H-20, H-20), 4.38-4.34 (m, 2H, H-19a, H-19a), 4.28-4.21 (m, 3H, H-2a, H-2a, H-22a), 4.17-4.12 (m, 2H, H-19b, H-19b), 3.90 (t, J = 8.3 Hz, 1H, H-22a), 3.34-3.27 (m, 2H, H-2b, H-2b), 3.20-3.08 (m, 12H, H-9a, H-9ad₂, H-9b, H-9b, H-10a, H-10b, H-10b), 3.00-2.95 (m, 1H, H-22b), 2.63-2.56 (m, 2H, H-1b, H-1b).

¹³C NMR (CDCl₃, 125 MHz): δ 172.07 (C-29), 170.72 (C-29), 165.77 (C-17), 163.36 (C-17), 143.92 (C-14), 143.11 (C-14), 141.53 (C-3), 141.29 (C-3), 139.75 (C-23), 139.51 (C-23), 139.32 (C-4), 139.18 (C-4), 138.21 (C-6), 137.25 (C-6), 136.33 (C-11), 136.22 (C-11), 129.26 (C-28, C-28), 128.89 (C-24, C-24), 128.43 (C-27, C-27), 128.35 (C-25, C-25), 129.81 (C-8), 128.78 (C-8), 126.29 (C-7), 126.13 (C-7), 71.81 (C-19), 71.07 (C-19), 68.12 (C-20), 66.45 (C-20), 41.54 (C-22), 41.18 (C-22), 34.94 (C-2), 34.61 (C-2), 34.74 (C-9, C-9), 34.68 (C-1), 34.61 (C-1), 34.49 (C-10), 34.11 (C-10).

HRMS (ESI-TOF) m/z: [M + H]⁺ Calcd C₂₇H₂₅NO₃ 412.1907 for; Found 412.1904.

4-((4*S*)-Benzyl-oxazoline-2-yl)-[2.2]paracyclophane-12-carboxylic acid **4.45**



General procedure A was followed using (\pm)-4-bromo[2.2]paracyclophane-12-carboxylic acid **4.44** (50 mg, 0.15 mmol, 1.0 eq.), (4*S*)-4-benzyl-oxazoline **4.10** (27 mg, 0.16 mmol, 1.1 eq.), LiO^tBu (30 mg, 0.38 mmol, 2.5 eq.), (^tBu)₂P(O)H (2 mg, 0.015 mmol, 10 mol%), Pd(OAc)₂ (2 mg, 0.0075 mmol, 5 mol%), DMA (0.6 ml) for 22 h.

Purification: Flash chromatography [SiO₂, EtOAc:hexanes 40:60] to obtain the title compound as a mixture of diastereomers **4.45**, white semisolid (41 mg, 0.093 mmol, 61% yield). R_f : 0.3

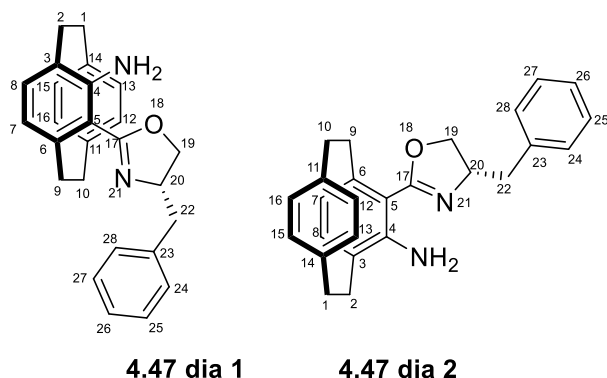
IR: ν_{\max} 3647, 2980, 2906, 2240, 2043, 1713, 1523 cm⁻¹.

¹H NMR (CDCl₃, 500 MHz): δ 7.41-7.25 (m, 10H, H-28, H-28, H-24, H-24, H-27, H-27, H-25, H-25, H-26, H-26), 7.16 (s, 2H, H-13, H-13), 6.94 (d, J = 9.0 Hz, 2H, H-5, H-5), 6.81 (d, J = 7.7 Hz, 2H, H-16, H-16), 6.65-6.59 (m, 6H, H-15, H-15, H-8, H-8, H-7, H-7), 4.83-4.70 (m, 2H, H-20, H-20), 4.54-4.49 (m, 2H, H-19a, H-19a), 4.37 (t, J = 17.0 Hz, 2H, H-10a, H-10a), 4.02-3.95 (m, 2H, H-10b, H-10b), 3.74-3.66 (m, 2H, H-22a, H-22a), 3.59 (dd, J = 13.8, 4.3 Hz, 1H, H-19b), 3.31 (dd, J = 13.7, 4.4 Hz, 1H, H-19b), 3.21-2.84 (m, 14H, H-10b, H-10b, H-2ad₁, H-2a, H-2b, H-2b, H-1a, H-1a, H-1b, H-1b, H-9a, H-9a, H-9b, H-9b), 2.83-2.73 (m, 2H, H-22b, H-22b).

¹³C NMR (CDCl₃, 125 MHz): δ 169.48 (C-29), 169.30 (C-29), 168.81 (C-17), 168.58 (C-17), 140.93 (C-23), 140.83 (C-23), 140.02 (C-11), 139.73 (C-11), 139.02 (C-3), 138.93 (C-3), 136.84 (C-5), 136.57 (C-5), 135.97 (C-6, C-14), 135.92 (C-6, C-14), 135.56 (C-8, C-7), 135.51 (C-8, C-7), 134.99 (C-12), 134.97 (C-12), 129.49 (C-27, C-27), 129.26 (C-25, C-25), 129.06 (C-16), 129.03 (C-16), 128.94 (C-28, C-28), 128.71 (C-24, C-24), 127.87 (C-4), 127.85 (C-4), 127.04 (C-26), 126.90 (C-26), 73.91 (C-20), 72.64 (C-20), 66.48 (C-19), 65.67 (C-19), 41.06 (C-22, C-22), 34.76 (C-10), 34.72 (C-10), 34.48 (C-9), 34.44 (C-9), 34.29 (C-1, C1), 33.95 (C-2), 33.93 (C-2).

HRMS (ESI-TOF) m/z : [M + H]⁺ Calcd C₂₇H₂₅NO₃ 412.1907 for; Found 412.1901.

4-((4S)-Benzyl-oxazoline-2-yl)-5-amino[2.2]paracyclophane 4.47dia1* & 4-((4S)-benzyl-oxazoline-2-yl)-5-amino[2.2]paracyclophane 4.47dia2*



General procedure was followed using (\pm)-4-Bromo-5-amino[2.2]paracyclophane **4.48** (48 mg, 0.16 mmol, 1.0 eq.), (4S)-4-benzyl-oxazoline **4.10** (28 mg, 0.17 mmol, 1.1 eq.), LiO^tBu (32 mg, 0.39 mmol, 2.5 eq.), (^tBu)₂P(O)H (3 mg, 0.015 mmol, 10 mol%), Pd(OAc)₂ (2 mg, 0.0079 mmol, 5 mol%), DMA (0.64 ml) for 24 h.

Purification: Preparative TLC [SiO₂, EtOAc:hexanes 15:85] to obtain the separate diastereomers of **4.47**, yellowish semisolid (21 mg, 0.054 mmol, 34% yield).

R_f: 0.6 & 0.5

Dia 1

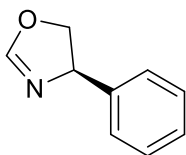
¹H NMR (CDCl₃, 500 MHz): δ 7.34-7.31 (m, 4H, H-28, H-27, H-24, H-23), 7.25-7.24 (m, 1H, H-26), 7.08 (d, J = 9.6 Hz, 1H, H-16), 6.63 (d, J = 9.7 Hz, 1H, 1H, H-15), 6.43 (d, J = 9.7 Hz, 1H, H-8), 6.38-6.35 (m, 2H, H-13, H-12), 6.14 (d, J = 9.4 Hz, 1H, H-7), 4.65-4.58 (m, 1H, H-20), 4.27-4.18 (m, 2H, H-19a, H-19b), 4.04 (t, J = 7.9 Hz, 1H, H-10a), 3.85-3.76 (m, 1H, H-10b), 3.11-3.03 (m, 4H, H-22a, H-22b, H-9a, H-9b), 2.75-2.65 (m, 4H, H-2a, H-2b, H-9a, H-9b).

Dia 2

¹H NMR (CDCl₃, 500 MHz): δ 7.40-7.37 (m, 4H, H-28, H-27, H-24, H-23), 7.30-7.28 (m, 1H, H-26), 7.10 (d, J = 9.6 Hz, 1H, H-16), 6.63 (d, J = 9.8 Hz, 1H, H-15), 6.43 (d, J = 9.7 Hz, 1H, H-8), 6.38 (d, J = 9.5 Hz, 2H, H-13, H-12), 6.12 (d, J = 9.4 Hz, 1H, H-7), 4.62-4.54 (m, 1H, H-20), 4.27 (t, J = 10.5 Hz, 1H, H-19a), 4.05 (t, J = 10.1 Hz, 1H, H-19b), 3.82-3.75 (m, 1H, H-10a), 3.25 (dd, J = 17.04, 7.4 Hz, 1H, H-22a), 3.13-3.05 (m, 4H, H-9a, H-9b, H-2a, H-2b), 2.96 (dd, J = 17.0, 9.5 Hz, 1H, H-22b), 2.75-2.64 (m, 3H, H-10b, H-1a, H-1b).

*The exact configuration of the diastereomer is not determined yet.

(R)-4-Phenyl-oxazoline



(R)-4.49

General method I was followed to synthesise (4*R*)-**4.49** by taking (*R*)-(-)-2-phenyl glycinol (2.5 g, 18.22 mmol, 1.0 eq.), triethyl orthoformate (4.54 ml, 27.33 mmol, 1.0 eq.), and glacial acetic acid (0.10 ml, 1.82 mmol, 0.1 eq.).

Purification: Kugelrohr distillation at 45 °C, 60 mTorr to obtain a colourless liquid of **4.49** (1.4 g, 9.51 mmol, 52% yield).

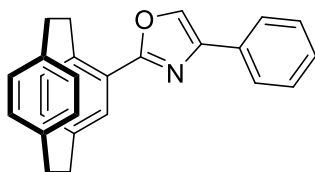
IR: ν_{max} 3020, 2973, 2399, 2166, 2009, 1917, 1684, 1517, 1215 cm^{-1} .

^1H NMR (CDCl_3 , 400 MHz): δ 7.38-7.24 (5H, m), 7.05 (1H, d, $J = 1.8$ Hz), 5.23 (1H, ddd, $J = 10.2, 8.5, 1.9$ Hz), 4.62 (1H, ddd, $J = 10.5, 8.6$ Hz), 4.09 (1H, d, $J = 8.3$ Hz).

^{13}C NMR (CDCl_3 , 125 MHz): δ 161.68, 138.34, 128.92, 128.02, 126.66, 66.02, 54.75.

HRMS (ESI-TOF) m/z : $[\text{M}+\text{H}]^+$ Calcd $\text{C}_9\text{H}_{10}\text{NO}$ 148.0757 for; Found 148.0755.

(±)-4-(4-Phenyloxazole)[2.2]paracyclophane 4.50



(±)-4.50

General procedure A was followed using (±)-4-bromo[2.2]paracyclophane **4.9** (40 mg, 0.27 mmol, 1.0 eq.), (*R*)-4-Phenyl-oxazoline **4.49** (86 mg, 0.29 mmol, 1.1 eq.), LiO^tBu (54 mg, 0.68 mmol, 2.5 eq.), (^tBu)₂P(O)H (4 mg, 0.027 mmol, 0.1 eq.), Pd(OAc)₂ (3 mg, 0.013 mmol, 0.05 eq.), DMA (1.09 ml) for 24 h.

Purification: Flash chromatography [SiO₂, EtOAc:hexanes 05:95] gave the by-product **4.50**, white semisolid (27 mg, 0.076 mmol, 28% yield).

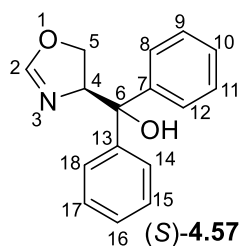
R_f: 0.7

IR: ν_{max} 3019, 2972, 2401, 2254, 2008, 1968, 1394, 1215 cm⁻¹.

¹H NMR (CDCl₃, 400 MHz): δ 7.73-7.62 (2H, m), 7.53-7.42 (1H, m), 7.34-7.29 (1H, m), 7.26-7.18 (1H, m), 6.94 (1H, d, *J* = 7.9 Hz), 6.79 (1H, d, *J* = 1.3 Hz), 6.76 (1H, d, *J* = 7.9 Hz), 6.62 (1H, d, *J* = 7.9 Hz), 6.55 (2H, s), 6.53 (1H, d, *J* = 7.9 Hz), 3.57 (1H, ddd, *J* = 13.4, 10.5, 2.3 Hz), 3.35 (1H, ddd, *J* = 13.2, 10.8, 4.6 Hz), 3.20-3.04 (6H, m).

¹³C NMR (CDCl₃, 125 MHz): δ 144.26, 140.94, 139.54, 139.19, 137.13, 136.80, 134.53, 133.52, 132.90, 132.71, 130.98, 129.93, 129.58, 129.03, 128.96, 128.29, 128.09, 127.30, 118.94, 114.92, 35.33, 35.09, 34.47, 34.24.

(S)-4-(*Tert*-hydroxyl diphenyl)-oxazoline 4.57



General method I was used to synthesise (4*S*)-**4.57** by taking (*R*)-2-amino-1,1-diphenylpropane-1,3-diol **4.55** (350 mg, 1.43 mmol, 1.0 eq.), triethyl orthoformate (320 mg, 2.15 mmol, 1.0 eq.), and glacial acetic acid (8 mg, 0.14 mmol, 0.1 eq.).

Purification: Kugelrohr distillation at 45 °C, 60 mTorr to obtain a colourless liquid of **4.57** (462 mg, 1.83 mmol, 60% yield).

$[\alpha]_D^{20}$: -70.00 ($c=1.7$, CHCl₃)

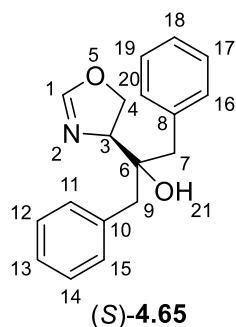
IR: ν_{\max} 2989, 2158, 2013, 1652, 1449, 1394 cm⁻¹.

¹H NMR (CD₃OD, 700 MHz): δ 7.60 (2H, d, $J = 8.4, 1.5$ Hz), 7.52 (2H, dd, $J = 8.4, 1.7$ Hz), 7.32-7.29 (4H, m), 7.21 (2H, t, $J = 7.3$ Hz), 7.05 (1H, d, $J = 1.6$ Hz), 5.44 (1H, td, $J = 10.0, 1.5$ Hz), 4.22 (2H, dd, $J = 9.9, 1.7$ Hz).

¹³C NMR (CD₃OD, 176 MHz): δ 159.59, 147.23, 147.05, 129.53, 129.21, 128.19, 128.06, 128.00, 127.52, 79.51, 73.17, 69.56.

HRMS (ESI-TOF) m/z : $[M+H]^+$ Calcd C₁₆H₁₆NO₂ 254.1176 for; Found 254.1170.

(S)-4-(*Tert*-hydroxyl dibenzyl)oxazoline 4.65



General method I was used to synthesise (4*S*)-**4.65** and (4*S*)-**4.66** by taking dibenzyl tertiary aminoalcohol **4.64** (150 mg, 0.55 mmol, 1.0 eq.), triethyl orthoformate (123 mg, 0.82 mmol, 1.5 eq.), and glacial acetic acid (3 mg, 0.05 mmol, 0.1 eq.).

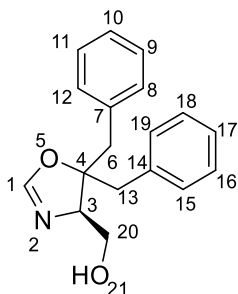
Purification: Flash chromatography [SiO₂, EtOAc:hexanes 30:70] to obtain the title compounds, (4*S*)-**4.65** and (4*S*)-**4.66** yellowish liquid (15 mg, 0.05 mmol, 10% yield).

¹H NMR (CDCl₃, 500 MHz): δ 7.36-7.24 (m, 10H, H-20, H-16, H-15, H-11, H-19, H-17, H-14, H-12, H-18, H-13), 6.93 (s, 1H, H-2), 4.23-4.19 (t, $J = 9.6$ Hz, 1H, H-5a), 4.12-4.09 (m, 1H, H-4), 4.06 (t, $J = 10.2$ Hz, 1H, H-5b), 2.96 (d, $J = 17.3$ Hz, 1H, H-9a), 2.87 (q, $J = 12.5$ Hz, 2H, H-7a, H-7b), 2.68 (d, $J = 17.3$ Hz, 1H, H-9b).

¹³C NMR (CDCl₃, 125 MHz): δ 156.62 (C-2), 136.62 (C-10), 136.51 (C-8), 130.89 (C-20, C-16), 130.84 (C-15, C-11), 128.32 (C-19, C-17, C-14, C-12), 126.69 (C-18, C-13), 75.19 (C-6), 70.60 (C-4), 67.28 (C-5), 42.18 (C-9), 41.84 (C-7).

HRMS (ESI-TOF) m/z : [M + Na]⁺ Calcd C₁₈H₁₉NNaO₂ 304.1313 for; Found 304.0514.

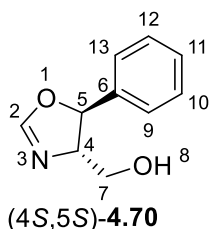
(*S*)-4-(Methan-1-ol)-5,5-dibenzylloxazoline **4.66**



¹H NMR (CDCl₃, 500 MHz): δ 7.37-7.33 (m, 5H, H-19, H-15, H-12, H-8, H-18), 7.23-7.19 (m, 3H, H-16, H-11, H-9), 7.12-7.10 (m, 2H, H-17, H-10), 6.72 (s, 1H, H-1), 5.23 (s, 1H, -OH), 4.16 (td, $J = 10.1, 2.7$ Hz, 1H, H-3), 3.88 (dd, $J = 12.9, 6.5$ Hz, 1H, H-20a), 3.78 (d, $J = 10.9$ Hz, 1H, H-20b), 3.27 (d, $J = 17.7$ Hz, 1H, H-9a), 3.06 (q, $J = 17.7$ Hz, 2H, H-13a, H-13b), 2.74 (d, $J = 17.7$ Hz, 1H, H-9b).

(4*S*,5*S*)-4-(Methylalcohol)-5-phenyloxazoline **4.70**

General method II was used to synthesise (4*S*,5*S*)-**4.70** by taking (1*S*,2*S*)-(+)-2-amino-1-phenyl-1,3-propanediol **4.68** (700 mg, 4.18 mmol, 1.0 eq.), DMF-DMA (499 mg, 4.18 mmol, 1.0 eq.). Purification: Kugelrohr distillation at 135 °C, 30 mTorr to obtain a white liquid of **4.10** (482 mg, 2.72 mmol, 65% yield).



$[\alpha]_D^{20}$: -66.30 ($c=0.92$, MeOH)

IR: ν_{\max} 3390, 3266, 2994, 2900, 1679, 1637, 1559, 1394, 1280 1084 cm^{-1} .

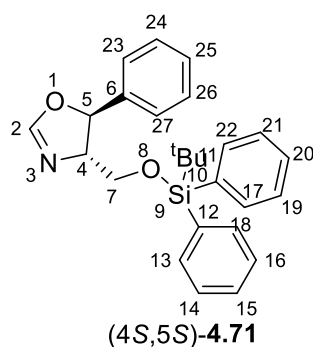
^1H NMR (CDCl_3 , 500 MHz): δ 7.47-7.31 (m, 5H, H-13, H-12, H-11, H-10, H-11, H-9), 7.08 (s, 1H, H-2), 5.33 (d, $J = 7.8$ Hz, 1H, H-5), 4.10-4.07 (m, 1H, H-4), 3.99-3.95 (m, 1H, H-7a), 3.74 (dd, $J = 11.7, 3.6$ Hz, 1H, H-7b), 3.37 (bs, 1H, -OH).

^{13}C NMR (CDCl_3 , 125 MHz): δ 155.76 (C-2), 1339.87 (C-6), 128.31 (C-12, C-10), 128.54 (C-13, C-9), 128.54 (C-11), 82.22 (C-5), 74.75 (C-4), 62.23 (C-7).

HRMS (ESI-TOF) m/z : $[\text{M}+\text{H}]^+$ Calcd $\text{C}_{10}\text{H}_{12}\text{NO}_2$ 178.0863 for; Found 178.0861.

Data comparable to that reported in literature.³

(4*S*,5*S*)-4-(*Tert*-butyldiphenylsilyl-methylalcohol)-5-phenyloxazoline 4.71



General method I was used to synthesise (4*S*,5*S*)-**4.71** by taking (1*S*,2*S*)-(+)-2-amino-1-phenyl-1,3-propanediol **4.68** (350 mg, 0.86 mmol, 1.0 eq.), triethyl orthoformate (192 mg, 0.21 mmol, 1.5 eq.), and glacial acetic acid (5 mg, 0.05 mmol, 0.1 eq.).

Purification: Flash chromatography [SiO_2 , EtOAc:hexanes 20:80] to obtain the title compound, (4*S*,5*S*)-**4.68** as a white solid (378 mg, 0.91 mmol, 35% yield).

R_f : 0.7

$[\alpha]_D^{20}$: +33.68 ($c=0.95$, CHCl_3)

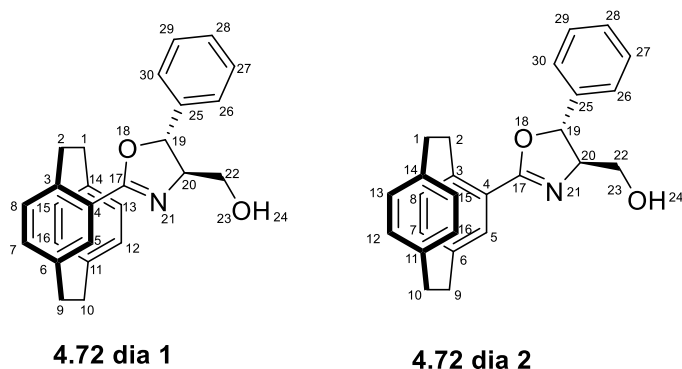
IR: ν_{max} 3308, 3070, 2930, 2865, 1699, 1659, 1427, 1114, 1039 cm^{-1} .

^1H NMR (CDCl_3 , 500 MHz): δ 7.72 (t, $J = 7.5$ Hz, 4H, H-18, H-13, H-22, H-17), 7.48-7.28 (m, 11H, H-27, H-26, H-25, H-24, H-23, H-21, H-20, H-19, H-16, H-15, H-14), 7.06 (s, 1H, H-2), 5.46 (d, $J = 6.7$ Hz, 1H, H-5), 4.15-4.12 (m, 1H, H-4), 3.96 (dd, $J = 10.7, 3.7$ Hz, 1H, H-7a), 3.86 (dd, $J = 9.4, 6.0$ Hz, 1H, H-7b), 1.1 (s, 9H, ^tBu).

^{13}C NMR (CDCl_3 , 125 MHz): δ 154.90, 140.64, 136.25, 135.70, 135.63, 133.28, 133.12, 133.03, 129.84, 129.81, 128.75, 128.58, 128.46, 128.34, 128.21, 127.80, 125.81, 81.25, 75.36, 65.17, 26.87, 19.06.

HRMS (ESI-TOF) m/z : $[\text{M}+\text{H}]^+$ Calcd $\text{C}_{26}\text{H}_{30}\text{NOSi}$ 416.2040 for; Found 416.2031.

(4-(4S)-(Methylalcohol)-(5S)-phenyloxazoline-2-yl)[2.2]paracyclophane 4.72



General procedure A was followed using (\pm)-4-bromo[2.2]paracyclophane **4.9** (70 mg, 0.24 mmol, 1.0 eq.), (4*S*,5*S*)-4-(methylalcohol)-5-phenyloxazoline **4.70** (45 mg, 0.26 mmol, 1.05 eq.), LiO^tBu (49 mg, 0.61 mmol, 2.5 eq.), (^tBu)₂P(O)H (4 mg, 0.024 mmol, 0.1 eq.), Pd(OAc)₂ (3 mg, 0.012 mmol, 0.05 eq.), DMA (0.98 ml) for 12h. Purification: Flash chromatography [SiO₂, EtOAc:hexanes 50:50] to obtain the title compound as a mixture of diastereomers **4.72**, white semisolid (14 mg, 0.039 mmol, 15% yield). *R_f*: 0.4

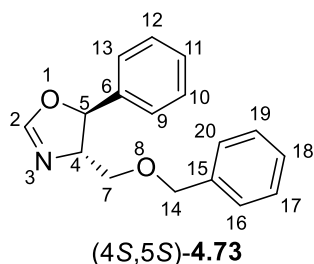
IR: ν_{\max} 3020, 2996, 2908, 2398, 2170, 1521cm⁻¹.

¹H NMR (CDCl₃, 500 MHz): δ 7.48-7.44 (m, 8H, H-30, H-30, H-26, H-26, H-29, H-29, H-27, H-27), 7.41-7.37 (m, 2H, H-28, H-28), 7.20-7.16 (d, *J* = 17.8 Hz, 2H, H-5, H-5), 6.66-6.63 (m, 4H, H-8, H-8, H-7, H-7), 6.60-6.50 (m, 8H, H-16, H-16d, H-15, H-15, H-13, H-13, H-12, H-12), 5.51 (d, *J* = 7.7 Hz, 2H, H-19, H-19), 4.40 (s, 2H, OH-24, OH-24), 4.27-4.21 (q, *J* = 11.5 Hz, 2H, H-22a, H-22a), 4.12 (dd, *J* = 11.4, 3.9 Hz, 2H, H-22a, H-22b), 3.91 (dd, *J* = 11.2, 4.4 Hz, 1H, H-20), 3.85 (dd, *J* = 9.7, 4.0 Hz, 1H, H-20), 3.22-2.76 (m, 16H, H-1a, H-1a, H-1b, H-1b, H-9a, H-9a, H-9b, H-9b, H-10a, H-10a, H-10b, H-10b, H-2a, H-2a, H-2b, H-2b).

¹³C NMR (CDCl₃, 125 MHz): δ 165.21 (C-17, C-17), 141.39 (C-14), 141.27 (C-14), 140.77 (C-11), 140.64 (C-14), 139.87 (C-25), 139.78 (C-25), 139.47 (C-3), 139.42 (C-3), 136.11 (C-4), 136.05 (C-4), 134.66 (C-16), 134.51 (C-16), 133.09 (C-15), 133.05 (C-15), 132.89 (C-13), 132.80 (C-13), 132.42 (C-12), 132.22 (C-12), 131.42 (C-5), 131.33 (C-5), 128.97 (C-29, C-27), 128.95 (C-29, C-27), 128.48 (C-8), 128.41 (C-8), 125.99 (C-30, C-26, C-30, C-26), 125.78 (C-7, C-28, C-7, C-28), 82.42 (C-19), 82.19 (C-19), 76.94 (C-20), 76.55 (C-20), 64.43 (C-22), 64.03 (C-22), 35.97 (C-1, C-1), 35.32 (C-9, C-9), 35.08 (C-10, C-10), 34.98 (C-2, C-2).

HRMS (ESI-TOF) *m/z*: [M + H]⁺ Calcd C₂₆H₂₆NO₂ 384.1964 for; Found 384.1955.

(4*S*,5*S*)-4-((Benzyloxy)(methyl))-5-phenyloxazoline 4.73



General method I was used to synthesise (4*S*,5*S*)-**4.71** by taking (1*S*,2*S*)-2-amino-3-(benzyloxy)-1-phenylpropan-1-ol (400 mg, 1.5 mmol, 1.0 eq.), triethyl orthoformate (346 mg, 1.5 mmol, 1.5 eq.), and glacial acetic acid (9 mg, 0.15 mmol, 0.1 eq.).

Purification: Flash chromatography [SiO₂, EtOAc:hexanes 20:80] to obtain the title compound, (4*S*,5*S*)-**4.73** as a yellow semisolid (170 mg, 0.63 mmol, 41% yield).

R_f: 0.4

[α]_D²⁰: +20.19 (*c*=5.10, CHCl₃)

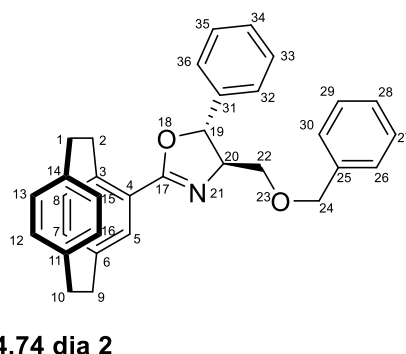
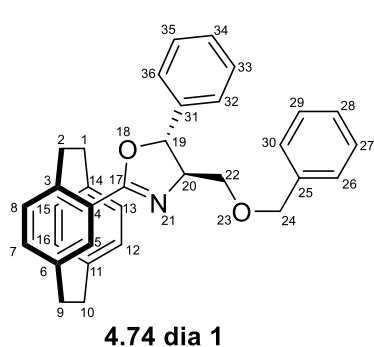
IR: ν_{max} 3019, 2986, 2897, 2400, 2044, 1685 cm⁻¹.

¹H NMR (CDCl₃, 500 MHz): δ 7.40-7.28 (m, 10H, H-20, H-19, H-18, H-17, H-16, H-13, H-12, H-11, H-10, H-9), 7.05 (s, 1H, H-2), 5.36 (d, *J* = 7.0 Hz, 2H, 1H, H-5), 4.67 (q, *J* = 12.1 Hz, 2H, H-14a, H-14b), 4.20-4.18 (m, 1H, H-4), 3.80 (dd, *J* = 9.7, 4.0 Hz, 1H, H-7a), 3.66 (dd, *J* = 9.6, 6.4 Hz, 1H, H-7b).

¹³C NMR (CDCl₃, 125 MHz): δ 155.04 (C-2), 140.35 (C-6), 137.98 (C-5), 128.77 (C-19, C-17), 128.44 (C-12, C-10), 128.26 (C-18), 127.75 (C-11), 127.69 (C-13, C-9), 125.58 (C-20, C-16), 82.58 (C-5), 74.01 (C-4), 73.40 (C-14), 71.34 (C-7).

HRMS (ESI-TOF) *m/z*: [M+H]⁺ Calcd C₁₇H₁₈NO₂ 268.1330 for; Found 268.1332.

4-((4S)-((Benzyloxy)(methyl))-5-phenyloxazoline-2-yl)[2.2]paracyclophane **4.74**



General procedure was followed using (\pm)-4-bromo[2.2]paracyclophane **4.9** (70 mg, 0.24 mmol, 1.0 eq.), (4*S*,5*S*)-4-((benzyloxy)(methyl))-5-phenyloxazoline **4.73** (69 mg, 0.25 mmol, 1.05 eq.), LiO^tBu (49 mg, 0.61 mmol, 2.5 eq.), (^tBu)₂P(O)H (4 mg, 0.024 mmol, 0.1 eq.), Pd(OAc)₂ (3 mg, 0.012 mmol, 0.05 eq.), DMA (0.98 ml) for 14 h.

Purification: Flash chromatography [SiO₂, EtOAc:hexanes 20:80] to obtain the title compound as a mixture of diastereomers **4.74**, white semisolid (62 mg, 0.13 mmol, 53% yield).

R_f: 0.6

IR: ν_{\max} 2997, 2880, 2398, 2209, 2171, 1989, 1635, 1516 cm⁻¹.

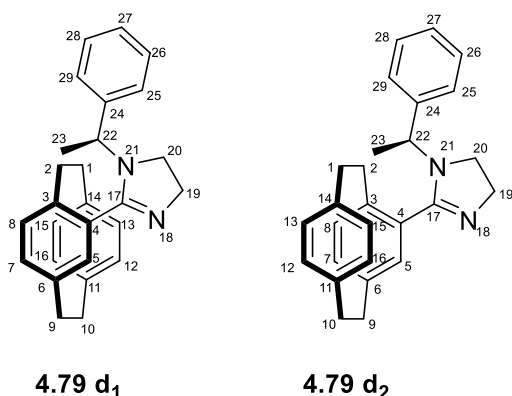
¹H NMR (CDCl₃, 500 MHz): δ 7.47-7.30 (m, 20H, H-30, H-30, H-26, H-26, H-29, H-29, H-27, H-27, H-28, H-28, H-36, H-36, H-32, H-32, H-35, H-35, H-33, H-33, H-34, H-34), 7.21 (d, $J = 7.1$ Hz, 2H, H-5, H-5), 6.73-6.72 (d, $J = 6.7$ Hz, 1H, H-8), 6.67-6.64 (m, 3H, H-8, H-7, H-7), 6.60-6.52 (m, 8H, H-16, H-16, H-15, H-15, H-13, H-13, H-12, H-12), 5.59 (d, $J = 6.3$ Hz, 2H, H-19, H-19), 4.77 (dt, $J = 21.6, 9.8$ Hz, 4H, H-24a, H-24a, H-24b, H-24b), 4.48 (dddd, $J = 13.4, 10.4, 6.5, 4.1$ Hz, 2H, H-20, H-20), 4.39-4.31 (m, 1H, H-10a), 4.25 (t, $J = 9.4$ Hz, 1H, H-10a), 3.95 (tt, $J = 5.8, 4.0$ Hz, 2H, H-22a, H-22a), 3.88 (dd, $J = 9.5, 6.1$ Hz, 1H, H-22b), 3.82 (dd, $J = 9.6, 6.4$ Hz, 1H, H-22b), 3.22-3.02 (m, 12H, H-10b, H-10b, H-9a, H-9a, H-9b, H-9b, H-1a, H-1a, H-1b, H-1b, H-2a, H-2a), 2.92-2.85 (m, 2H, H-2b, H-2b).

¹³C NMR (CDCl₃, 125 MHz): δ 164.61 (C-17), 164.05 (C-17d), 141.55 (C-14d), 141.44 (C-14d), 141.36 (C-11), 141.33 (C-11), 140.10 (C-3), 140.01 (C-3), 139.68 (C-31), 139.62 (C-31), 139.37 (C-25), 139.31 (C-25), 138.15 (C-4, C-4), 135.99 (C-5), 135.95 (C-5), 135.11 (C-6, C-6), 134.61 (C-16), 134.53 (C-16), 133.03 (C-15), 132.92 (C-15), 132.85 (C-8, C-8), 132.42 (C-13), 132.24 (C-13), 131.51 (C-12), 131.32 (C-12), 128.80 (C-29, C-29, C-27, C-27, C-35, C-35), 128.47 (C-36, C-36), 128.45 (C-32, C-32), 128.16 (C-30, C-30), 128.09 (C-26, C-26),

127.87 (C-33, C-33), 127.77 (C-8, C-8), 127.75 (C-7, C-7), 125.76 (C-34, C-34), 125.58 (C-28, C-28), 82.96 (C-19), 82.52 (C-19), 75.28 (C-20, C-20), 73.50 (C-24), 73.48 (C-24), 72.00 (C-22), 71.97 (C-22), 36.08 (C-10), 35.97 (C-10), 35.35 (C-9, C-9), 35.10(C-1, C-1), 34.87 (C-2), 34.52 (C-2).

HRMS (ESI-TOF) m/z : $[M + H]^+$ Calcd $C_{33}H_{32}NO_2$ 474.2428 for; Found 474.2424.

4-([2.2]Paracyclophane-12-yl)-1-(2*S*)-phenylethyl)-19,20-dihydro-21*H*-imidazole **4.79**



A 4 ml scintillation vial was charged with, (\pm)-4-bromo[2.2]paracyclophane **4.9** (50 mg, 0.28 mmol, 1.0 eq.), (*S*)-1-(1-phenylethyl)-4,5-dihydro-1*H*-imidazole **4.78** (82 mg, 0.28 mmol, 1.0 eq.), DBU (44 mg, 0.28 mmol, 1.0 eq.), CuI (55 mg, 0.28 mmol, 1.0 eq.), PPh₃ (8 mg, 0.028 mmol, 10 mol%), Pd(OAc)₂ (3 mg, 0.014 mmol, 5 mol%). The vial was purged and degassed with argon for three times. The degassed DMF (0.82 ml, 0.35 M) was transferred in a vial *via* syringe and the screw capped vial was heated at 110 °C for 16 hrs. The reaction mixture was allowed to cooled down at room temperature and diluted with CH₂Cl₂ and MeOH before passing through a pad of Celite[®]. The resulting filtrate was removed under reduced pressure and crude product was purified.

Purification: Flash chromatography [Neutral Alumina, CH₂Cl₂ : hexanes 40:60] to obtain the title compound as a mixture of diastereomers **4.79**, brownish semisolid (36 mg, 0.094 mmol, 33% yield).

R_f : 0.5

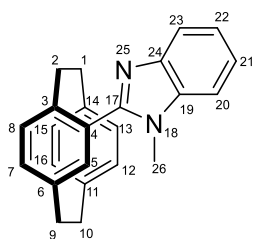
¹H NMR (CDCl₃, 500 MHz): δ 7.37-7.26 (m, 5H, H-29, H-29, H-28, H-28, H-27d₁), 7.19-7.13 (m, 3H, H-27, H-26, H-26), 7.05 (dd, $J = 18.9, 7.8$ Hz, 2H, H-8, H-8), 6.88-6.81 (m, 4H, H-5, H-5, H-7, H-7), 6.63-6.47 (m, 10H, H-27, H-27, H-16, H-16, H-15, H-15, H-13, H-13, H-12,

H-12), 4.71 (q, $J = 7.0$ Hz, 1H, H-22), 4.57 (q, $J = 5.8$ Hz, 1H, H-22), 4.07 (qd, $J = 8.1, 5.3$ Hz, 1H, H-20a), 3.98-3.86 (dddd, $J = 20.6, 11.3, 3.0$ Hz, 3H, H-20a, H-20b), 3.55-3.40 (m, 3H, H-19a, H-19a, H-19b), 3.31-3.28 (m, 1H, H-19b), 3.24-3.12 (m, 7H, H-10a, H-10a, H-10b, H-10b, H-9a, H-9a, H-9b), 3.08-2.96 (m, 9H, H-9b, H-2a, H-2a, H-2b, H-2b, H-1a, H-1a, H-1b, H-1b), 1.55 (d, $J = 7.0$ Hz, 3H, -CH₃), 1.55 (d, $J = 6.8$ Hz, 3H, -CH₃).

¹³C NMR (CDCl₃, 125 MHz): δ 166.86 (C-17), 166.22 (C-17), 141.68 (C-24, C-24), 140.40 (C-14), 140.24 (C-14), 140.06 (C-11, C-11), 139.37 (C-6), 139.28 (C-6), 139.25 (C-3), 139.07 (C-3), 138.44 (C-4), 138.35 (C-4), 135.04 (C-16), 134.96 (C-16), 134.51 (C-15), 134.41 (C-15), 133.52 (C-13), 133.41 (C-15), 133.52 (C-13), 133.43 (C-13), 132.84 (C-12, C-12), 132.39 (C-29, C-1), 132.39 (C-29), 132.35 (C-29), 132.30 (C-25), 132.24 (C-25), 131.71 (C-5, C-5), 128.37 (C-28, C-28), 128.15 (C-26, C-26), 127.10 (C-27, C-27), 127.03 (C-8), 126.99 (C-8), 126.78 (C-7, (C-7)), 53.37 (C-22), 52.73 (C-22), 44.08 (C-20, C-20), 43.44 (C-19, C-19), 35.38 (C-10, C-10), 35.32 (C-9, C-9), 35.22 (C-2), 35.18 (C-2), 33.80 (C-1), 33.60 (C-1), 18.08 (C-23, -CH₃), 14.91 (C-23, -CH₃).

HRMS (ESI-TOF) m/z : [M + H]⁺ Calcd C₂₇H₂₉N₂ 381.2331 for; Found 381.2317.

(±)-4-([2.2]Paracyclophane-1-yl)-18-methyl-18*H*-benzo[d]imidazole **4.81**



(±)-**4.81**

The compound **4.81** was synthesised following the same procedure (Page no. **296**) as the synthesis of **4.79** by taking reagents, (±)-4-bromo[2.2]paracyclophane (87 mg, 0.30 mmol, 1.0 eq.), 1-methyl-benzimidazole **4.80** (40 mg, 0.30 mmol, 1.0 eq.), K₂CO₃ (105 mg, 0.75 mmol, 2.5 eq.), CuI (58 mg, 0.30 mmol, 1.0 eq.), PCy₃ (9 mg, 0.030 mmol, 0.1 eq.), Pd(OAc)₂ (3 mg, 0.015 mmol, 0.05 eq.), DMA (1.21 ml, 0.25 M), for 48 h.

Purification: Flash chromatography [SiO₂, EtOAc : hexanes 30:70] to obtain the title compound (±)-**4.81**, brownish solid (60 mg, 0.18 mmol, 59% yield).

R_f : 0.5

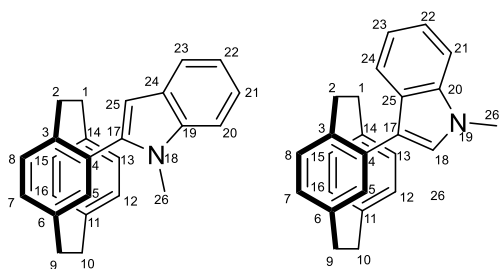
$^1\text{H NMR}$ (CDCl_3 , 400 MHz): δ 8.01 (m, 1H, H-20), 7.42-7.35 (m, 3H, H-23, H-22, H-21), 7.00 (s, 1H, H-5), 7.00 (d, $J = 9.8$ Hz, 1H, H-8), 6.78 (d, $J = 9.8$ Hz, 1H, H-7), 6.67-6.59 (m, 4H, H-16, H-15, H-13, H-12), 3.62 (s, 3H, $-\text{CH}_3$), 3.32-3.05 (m, 5H, H-10a, H-10b, H-9a, H-9b, H-2a), 2.97-2.89 (m, 3H, H-2b, H-1a, H-1b).

$^{13}\text{C NMR}$ (CDCl_3 , 125 MHz): δ 140.69 (C-17), 139.49 (C-24), 139.35 (C-14, C-11), 138.98 (C-19), 135.10 (C-6, C-4), 134.17 (C-23, C-20), 133.77 (C-3), 132.59 (C-22, C-21), 132.18 (C-16, C-15), 131.70 (C-13, C-12), 122.68 (C-8), 119.89 (C-5), 109.67 (C-7), 35.34 (C-10), 35.24 (C-9), 35.15 (C-1), 34.02 ($-\text{CH}_3$), 30.81 (C-2).

HRMS (ESI-TOF) m/z : $[\text{M} + \text{H}]^+$ Calcd $\text{C}_{24}\text{H}_{23}\text{N}_2$ 339.1856 for; Found 339.1852.

(\pm)-3-(4-([2.2]Paracyclophane-1-yl))-1-methyl-1*H*-indolezole **4.83** &

(\pm)-2-(4-([2.2]paracyclophane-1-yl))-1-methyl-1*H*-indolezole **4.84**



(\pm)-**4.83**

(\pm)-**4.84**

The compound **4.83** & **4.84** were synthesised following the same procedure (Page no. **296**) as the synthesis of **4.79** by taking reagents, 1-methyl-indole **4.82** (20 mg, 0.30 mmol, 1.0 eq.), (\pm)-4-bromo[2.2]paracyclophane **4.9** (87 mg, 0.30 mmol, 2.0 eq.), K_2CO_3 (53 mg, 0.75 mmol, 2.5 eq.), PivOH (8 mg, 0.076 mmol, 0.5 eq.) PCy_3 (4 mg, 0.015 mmol, 0.1 eq.), $\text{Pd}(\text{OAc})_2$ (2 mg, 0.0076 mmol, 0.05 eq.), DMA (0.61 ml, 0.25 M) for 24 h.

Purification: Flash chromatography [SiO_2 , EtOAc:hexanes 5:95] to obtain the title compounds (\pm)-**4.83**, brownish semisolid (31 mg, 0.09 mmol, 61% yield) and (\pm)-**4.84**, brownish semisolid (12 mg, 0.038 mmol, 24% yield).

R_f : 0.6 for (\pm)-**4.83** and 0.5 for (\pm)-**4.84**.

(±)-4.83

¹H NMR (CDCl₃, 500 MHz): δ 7.78 (d, *J* = 7.8 Hz, 1H, H-24), 7.43 (d, *J* = 8.1 Hz, 1H, H-23), 7.30 (d, *J* = 7.0 Hz, 1H, H-21), 7.23 (t, *J* = 9.8 Hz, 1H, H-22), 6.88 (d, *J* = 7.8 Hz, 1H, H-8), 6.77 (s, 1H, H-5), 6.70 (d, *J* = 7.8 Hz, 1H, H-8), 6.77 (s, 1H, H-5), 6.70-6.68 (m, 2H, H-16, H-15), 6.62-6.65 (m, 3H, H-7, H-13, H-12), 6.60 (s, 1H, H-18), 3.55 (s, 3H, -CH₃), 3.21-2.79 (m, 8H, H-10a, H-10b, H-9a, H-9b, H-2a, H-2b, H-1a, H-1b).

Data comparable to that reported in literature.⁴

(±)-4.84

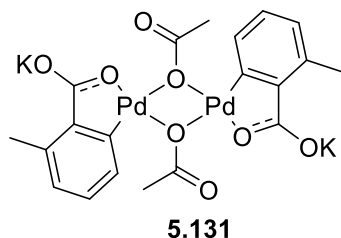
¹H NMR (CDCl₃, 500 MHz): δ 7.65 (d, *J* = 7.9 Hz, 1H, H-23), 7.41 (d, *J* = 8.2 Hz, 1H, H-22), 7.31 (d, *J* = 7.4 Hz, 1H, H-20), 7.25 (s, 1H, H-5), 7.18 (t, *J* = 7.7 Hz, 1H, H-21), 6.77 (d, *J* = 8.0 Hz, 1H, H-8), 6.68 (d, *J* = 6.3 Hz, 1H, H-7), 6.62-6.50 (m, 4H, H-16, H-15, H-13, H-12), 6.60 (s, 1H, H-25), 3.95 (s, 3H, -CH₃), 3.41 (td, *J* = 13.4 Hz, 1H, H-10a), 3.21-2.65 (m, 7H, H-10b, H-9a, H-9b, H-2a, H-2b, H-1a, H-1b).

8.5.1. Reference

- (1) Leonard, W. R.; Romine, J. L.; Meyers, A. I. A rapid and efficient synthesis of chiral 2-hydro-2-oxazolines. *J. Org. Chem.* **1991**, *56*, 1961.
- (2) Kitagaki, S.; Murata, S.; Asaoka, K.; Sugisaka, K.; Mukai, C.; Takenaga, N.; Yoshida, K., *Chem. Pharm. Bull.* **2018**, *66*, 1006.
- (3) Poelert, M. A.; Kellogg, R. M.; Hulshof, L. A., *Recl. Trav. Chim. Pays-Bas* **1994**, *113*, 355.
- (4) Thennakoon, N.; Kaur, G.; Wang, J.; Plieger, P. G.; Rowlands, G. J. Asymmetric Variant of the Bischler–Möhlau Indole Synthesis, *Aust. J. Chem.* **2015**, *68*, 566.

8.6. Experimental for Chapter 5 and Chapter 6

Preparation of Palladacycle **5.131**^{1,2}

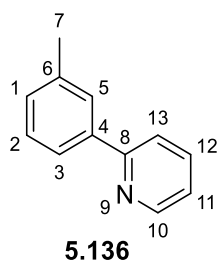


Ortho-toluic acid (2.0 g, 14.68 mmol, 1.0 eq.) was treated with KOH (0.659 g, 11.74 mmol, 0.8 eq.) in water (15 ml) at room temperature. Water was removed in a rotary evaporator, the white solid was washed with CH₂Cl₂ (20 ml × 3) to remove excess of *ortho*-toluic acid and dried under vacuum at 100 °C to give potassium *ortho*-toluate (1.8 g, 10.3 mmol, 73% yield).

Pd(OAc)₂ (516 mg, 2.29 mmol, 1.0 eq.) was added to a suspension of potassium *ortho*-toluate (400 mg, 2.29 mmol, 1.0 eq.) in 1,4-dioxane (9 ml) and heated to 100 °C for overnight. The reaction mixture was filtered and washed with CH₂Cl₂ (5 ml) and dried under vacuum to get the palladacycle **5.131** (880 mg, 1.19 mmol, 55% yield).

Data comparable to that reported in the literature.^{1,2}

2-(*m*-tolyl)pyridine **5.136**³



A flame dried Schlenk tube was charged with palladacycle (100 mg, 0.13 mmol, 1.0 eq.), pyridine-2-sulfinate (44.83 mg, 0.27 mmol, 2.0 eq.), potassium carbonate (75 mg, 0.54 mmol, 4.0 eq.). The Schlenk tube was degassed and back filled with argon three time. The dry 1,4-dioxane (1.3 ml, 0.1 M) was transferred into tube under constant argon flow. The Hi-Vac valve was closed and the reaction allowed to stir at 150 °C. After 24 h, the reaction mixture was passed through a pad of celite and washed CH₂Cl₂ (5 ml × 2) and MeOH (5 ml). The combined

solvent fractions were removed in a rotary evaporator. The resulting crude was purified by column chromatography [SiO₂, Et₂O : Pentane (3:7)] to obtain title compound as pale brownish powder (7 mg, 0.088 mmol, 15% yield).

R_f: 0.7

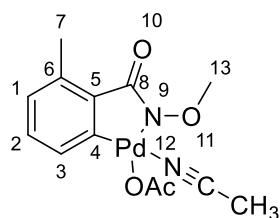
¹H NMR (CDCl₃, 500 MHz): δ 8.73 (d, *J* = 4.7 Hz, 1H, H-12), 7.86 (s, 1H, H-5), 7.80-7.44 (m, 3H, H-11, H-10, H-9), 7.41 (t, *J* = 7.62 Hz, 1H, H-2), 7.27-7.24 (m, 2H, H-3, H-1), 2.47 (s, 3H, -CH₃).

¹³C NMR (CDCl₃, 125 MHz): δ 149.47 (C-8), 139.18 (C-12), 136.89 (C-6), 129.82 (C-4), 128.67 (C-10, C-5), 127.67 (C-2, C-1), 124.04 (C-3), 122.06 (C-11), 120.73 (C-9), 21.52 (C-7, -Me).

MS (ESI-TOF) *m/z*: [M + H]⁺ Calcd for C₁₂H₁₂N 170.09; Found 170.03.

Data comparable to that reported in the literature.³

Palladacycle **5.140**⁴



5.140

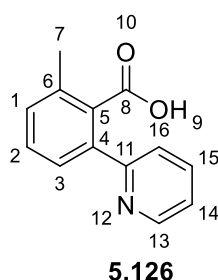
N-Methoxy-2-methylbenzamide (100 mg, 0.60 mmol, 1.0 eq.), and Pd(OAc)₂ (135 mg, 0.60 mmol, 1.0 eq.), were suspended in 15 ml pressure tube. accurately. Then glacial AcOH (6.0 ml) was added *via* cannula and the tube was evacuated and back filled with argon gas three times. The septum was removed under an optimal flow of argon and the tube was closed with a screw cap. The reaction was allowed to stir at 120 °C for 15 min. the reaction was cooled down to room temperature and diluted with CH₂Cl₂ (5 ml) and MeOH (5 ml), filtered through a pad of Celite[®], and filtrate was concentrated under vacuum. The crude residue (107 mg, 0.397 mmol, 66%) was used directly for the next reaction without purification.

^1H NMR (CD_3CN , 500 MHz): δ 7.03 (d, $J = 7.2$ Hz, 1H, H-2), 6.84 - 6.78 (m, 2H, H-1, H-3), 3.58 (s, 3H, -OMe), 2.52 (s, 3H, -Me).

^{13}C NMR (CDCl_3 , 125 MHz): δ 177.5 (C-8), 144.04 (C-6), 137.9 (C-5), 133.5 (C-2), 129.9 (C-1), 128.4 (C-13), 126.6 (C-7).

Data comparable to that reported in the literature.⁴

2-methyl-6-(pyridin-2-yl)benzoic acid **5.126**⁵



The compound **5.126** was synthesised by following the same procedure as mentioned in for **5.136** (page no. 237) by taking palladacycle **5.140** (65 mg, 0.24 mmol, 1.0 eq.), pyridine-2-sulfinate (79.74 mg, 0.48 mmol, 2.0 eq.), potassium carbonate (133.56 mg, 0.96 mmol, 4.0 eq.), solvent CH_3CN ([0.1M], 2.4 ml), The crude was purified using a preparative TLC [SiO_2 , EtOAc : hexanes (7:3)] to obtain the title compound **5.126** as white powder (4 mg, 0.018 mmol, 8% yield).

R_f : 0.3

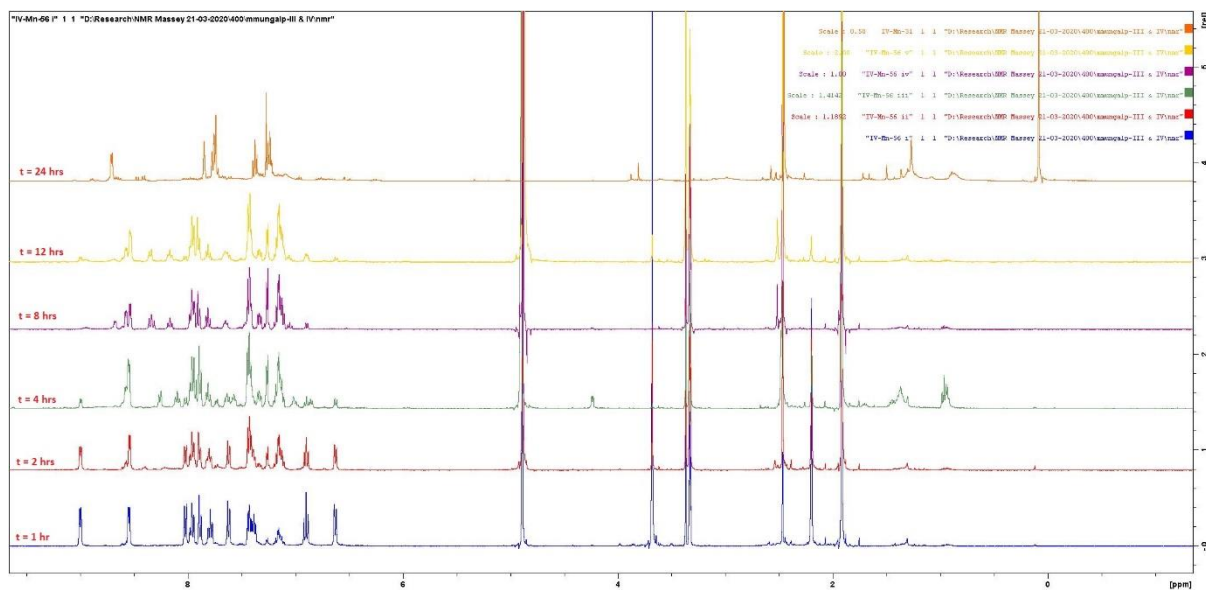
^1H NMR (CDCl_3 , 500 MHz): δ 8.57 - 8.52 (m, 1H, H-13), 7.84 - 7.74 (m, 3H, H-16, H-15), 7.63 - 7.62 (m, 1H, H-14), 7.39 - 7.36 (m, 2H, H-3, H-2), 7.29 - 7.27 (m, 1H, H-1), 2.47 (s, 3H, - CH_3).

MS (ESI-TOF) m/z : $[\text{M} + \text{H}]^+$ Calcd for $\text{C}_{13}\text{H}_{10}\text{NNaO}_2$ 235.06; Found 235.21.

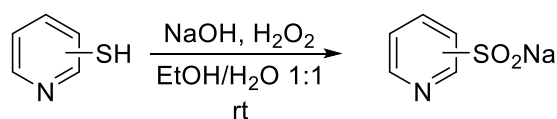
Data comparable to that reported in the literature.⁵

Time-based study with stoichiometric quantity of Pd(OAc)₂

¹H NMR data comparison as described in section 5.6.5.

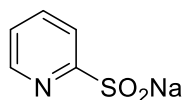


Procedure for pyridine thiol oxidation:



Pyridine thiol (1 g, 9 mmol, 1.0 eq.) was dissolved in a mixture of 40 ml of water containing sodium hydroxide (468 mg, 11.7 mmol, 1.3 eq.) and 40 ml of ethanol. An aqueous solution of hydrogen peroxide (1 ml, 9.9 mmol, 1.1 eq., 30% (w/w) in H₂O) was added dropwise at room temperature. The reaction was stirred until completion (TLC monitoring). The solvent was removed under vacuum and the remaining residue was washed with ethyl acetate (40 ml × 3). The aqueous phase was evaporated to obtain wet sulfinate salt which was dried under freeze dryer overnight to afford dry sulfinate salts.

Sodium pyridine-2-sulfinate 5.123 & 6.51⁶



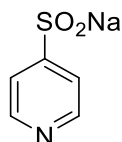
5.123 & 6.50

The above procedure was followed using pyridine-2-thiol (1000 mg, 9 mmol, 1.0 eq.). The product was obtained as a white solid (985 mg, 6.00 mmol, 58 %).

Data comparable to that reported in literature.⁶

¹H NMR (CD₃OD, 400 MHz): δ 8.54 (1H, dt, $J = 5.0, 1.0$ Hz), 7.99 (1H, td, $J = 7.6, 1.8$ Hz), 7.91 (1H, dt, $J = 7.8, 2.0$ Hz), 7.44 (1H, ddd, $J = 7.3, 4.8, 1.2$ Hz).

Sodium pyridine-4-sulfinate 6.53⁶



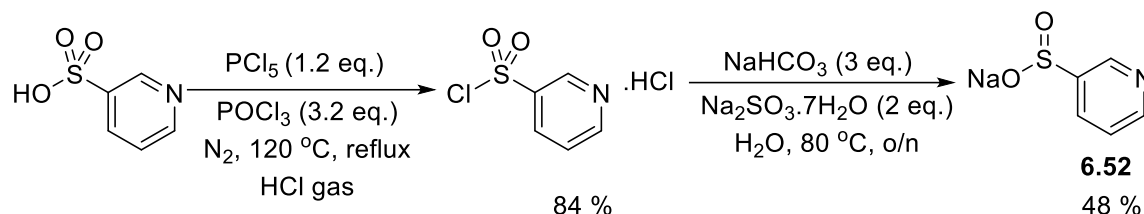
6.53

The above procedure was followed using pyridine-2-thiol (1000 mg, 9 mmol, 1.0 eq.). The product was obtained as a white solid (710 mg, 4.32 mmol, 42 %).

¹H NMR (CD₃OD, 400 MHz): δ 8.78 (2H, d, $J = 6.2$ Hz), 7.69 (2H, d, $J = 6.2$ Hz).

Data comparable to that reported in literature.⁶

Sodium pyridine-3-sulfinate **6.52**⁷



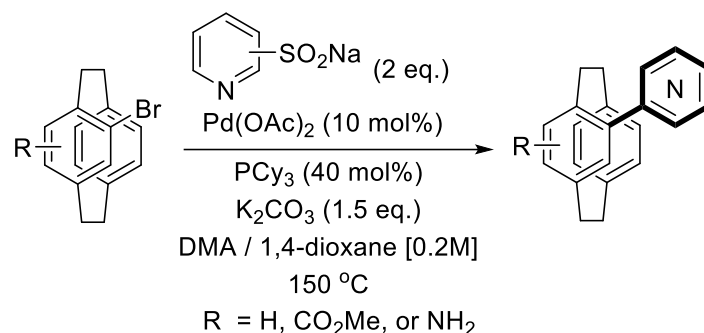
Phosphorus pentachloride (16.25 g, 78.0 mmol, 1.2 eq.) and phosphorus oxychloride (20.0 ml, 213.9 mmol, 3.2 eq.) were added to 3-pyridinesulfonic acid (10.40 g, 65.0 mmol, 1 eq.) at $0\text{ }^\circ\text{C}$. The reaction mixture was brought to reflux and stirred overnight at $120\text{ }^\circ\text{C}$. Next morning, the reaction mixture was cooled to room temperature and diluted with dry CH_2Cl_2 (30 ml). The reaction mixture was further cooled to $5\text{ }^\circ\text{C}$ and saturated with HCl gas. The white precipitate was collected by filtration, washed with dry CH_2Cl_2 (50 ml) and dried under reduced pressure. 3-Pyridinesulfonyl chloride was obtained as a white powder and used immediately for the next reaction (11.73 g, 55.3 mmol, 84%).

3-Pyridinesulfonyl chloride (11.73 g, 55.08 mmol, 1 eq.) was added to a solution of NaHCO_3 (13.88 g, 165.24 mmol, 3 eq.) and $\text{Na}_2\text{SO}_3 \cdot 7\text{H}_2\text{O}$ (110.16 g, 27.76 mmol, 2 eq.) and H_2O (75 ml). The reaction mixture was heated at $80\text{ }^\circ\text{C}$ for 3 hrs. The resulting crude was filtered and filtrate was concentrated under reduced pressure to give 3-pyridylsulfonic acid sodium salt as pale yellow solid. (4.32 g, 26.3 mmol, 48%) (ASC 2004 925, PCT. INT.Appl. 2008014199 31 Jan 2008)

^1H NMR (CD_3OD , 400 MHz): δ 8.78 (1H, d, $J = 1.4\text{ Hz}$), 8.57 (1H, dd, $J = 5.0, 1.7\text{ Hz}$), 8.09 (1H, dt, $J = 7.8, 2.0\text{ Hz}$), 7.54 (1H, dd, $J = 7.2, 4.4\text{ Hz}$).

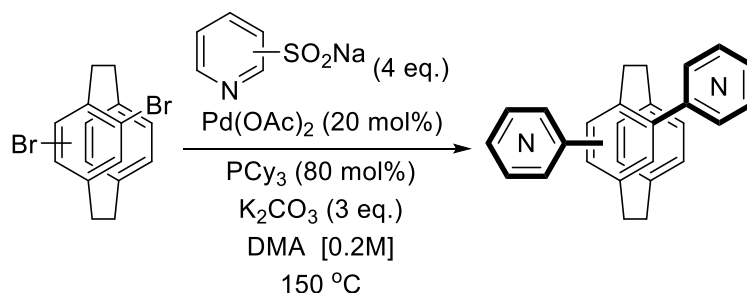
Data comparable to that reported in literature.⁷

General procedure A: Desulfitative coupling with bromo[2.2]paracyclophane



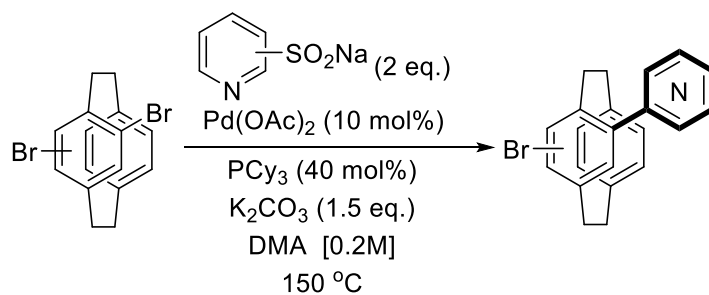
A 4 ml scintillation vial was charged with bromo[2.2]paracyclophane (1.0 eq.), pyridine sulfinate (2.0 eq.), K_2CO_3 (1.5 eq.), PCy_3 (0.4 eq.), and $\text{Pd}(\text{OAc})_2$ (0.1 eq.). The vial was purged and degassed with argon for three times. Degassed DMA or 1,4-dioxane (0.2 M) was transferred by syringe and the screw-capped vial was heated at 150 °C until completion. The reaction mixture was cooled to room temperature and diluted with CH_2Cl_2 and MeOH before passing through a pad of Celite[®]. The resulting filtrate was removed under reduced pressure and the crude product was purified by flash chromatography.

General procedure B: Bis-desulfitative coupling with dibromo[2.2]paracyclophane



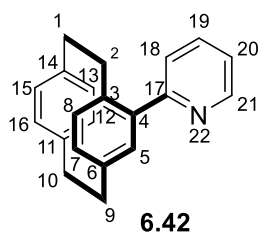
A 4 ml scintillation vial was charged with dibromo[2.2]paracyclophane (1.0 eq.), pyridine sulfinate (4.0 eq.), K_2CO_3 (3 eq.), PCy_3 (0.8 eq.), and $\text{Pd}(\text{OAc})_2$ (0.2 eq.). The vial was purged and degassed with argon for three times. Degassed DMA (0.2 M) was transferred by syringe and the screw-capped vial was heated at 150 °C until completion. The reaction mixture was cooled to room temperature and diluted with CH_2Cl_2 and MeOH before passing through a pad of Celite[®]. The resulting filtrate was removed under reduced pressure and the crude product was purified by flash chromatography.

General procedure C: Mono-desulfinitative coupling with dibromo[2.2]paracyclophane



A 4 ml scintillation vial was charged with dibromo[2.2]paracyclophane (1.0 eq.), pyridine sulfinate (2.0 eq.), K₂CO₃ (1.5 eq.), PCy₃ (0.4 eq.), and Pd(OAc)₂ (0.1 eq.). The vial was purged and degassed with argon for three times. Degassed DMA (0.2 M) was transferred by syringe and the screw-capped vial was heated at 150 °C until completion. The reaction mixture was cooled to room temperature and diluted with CH₂Cl₂ and MeOH before passing through a pad of Celite[®]. The resulting filtrate was removed under reduced pressure and the crude product was purified by flash chromatography.

4-(Pyridin-2-yl)[2.2]paracyclophane **6.42**^{8,9}



General procedure **A** was followed using (\pm)-4-bromo[2.2]paracyclophane **6.40** (50 mg, 0.17 mmol, 1.0 eq.), pyridine-2-sulfinate **6.50** (58 mg, 0.35 mmol, 2 eq.), K_2CO_3 (36 mg, 0.26 mmol, 1.5 eq.), PCy_3 (20 mg, 0.069 mmol, 40 mol%), $Pd(OAc)_2$ (4 mg, 0.017 mmol, 10 mol%), DMA (0.87 ml) for 24 hrs.

Purification: Flash chromatography [SiO_2 , EtOAc: hexanes (30 : 70)] to obtain the title compound **6.42** as pinkish white powder (31mg, 0.10 mmol, 63% yield).

R_f : 0.5

IR: ν_{max} 3418, 2927, 2849, 1892, 1651, 1584, 1511, 1446, 1261, 1178, 1035 cm^{-1}

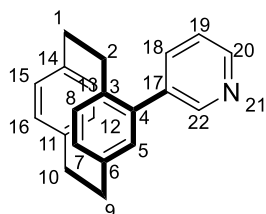
1H NMR ($CDCl_3$, 500 MHz): δ 8.79 (d, $J = 4.7$ Hz, 1H, H-21), 7.82 (t, $J = 7.7, 1.4$ Hz, H-19), 7.55 (d, $J = 7.8$ Hz, 1H, H-18), 7.28-7.25 (m, 1H, H-20), 6.88 (s, 1H, H-5), 6.65-6.57 (m, 6H, H-7, H-8, H-12, H-13, H-15, H-16), 3.74-3.68 (m, 1H, H-2a), 3.25-3.17 (m, 2H, H-1a, H-1b), 3.14-3.05 (m, 2H, H-9a, H-9b), 3.01-2.94 (m, 2H, H-10a, H-10b), 2.72-2.65 (m, 1H, H-2b).

^{13}C NMR ($CDCl_3$, 125 MHz): δ 159.21 (C-17), 149.64 (C-21), 140.62 (C-14), 139.79 (C-11), 139.61 (C-6), 139.39 (C-4), 138.17 (C-3), 136.25 (C-12), 136.18 (C-13), 133.16 (C-19), 132.88 (C-5), 132.65 (C-15), 132.57 (C-16), 132.38 (C-7), 130.67 (C-20), 124.17 (C-18), 35.49 (C-2), 35.26 (C-9), 35.12 (C-10), 34.50 (C-1).

HRMS (ESI-TOF) m/z : $[M + H]^+$ Calcd for $C_{21}H_{20}N$ 286.1590; Found 286.1588.

Data comparable to that reported in literature.^{8,9}

4-(Pyridin-3-yl)[2.2]paracyclophane **6.52**¹⁰



(±)-**6.52**

General procedure **A** was followed using (±)-4-bromo[2.2]paracyclophane **6.40** (50 mg, 0.17 mmol, 1.0 eq.), pyridine-3-sulfinate **6.51** (58 mg, 0.35 mmol, 2 eq.), K₂CO₃ (36 mg, 0.26 mmol, 1.5 eq.), PCy₃ (20 mg, 0.069 mmol, 40 mol%), Pd(OAc)₂ (4 mg, 0.017 mmol, 10 mol%), DMA (0.87 ml) for 24 hrs.

Purification: Flash chromatography [SiO₂, EtOAc: hexanes (30 : 70)] to obtain the title compound **6.52** as a white powder (41mg, 0.14 mmol, 84% yield).

R_f: 0.5

IR: ν_{max} 3850, 3742, 3673, 2975, 2252, 2199, 2155, 2029, 1975, 1469, 1384, 1089 cm⁻¹

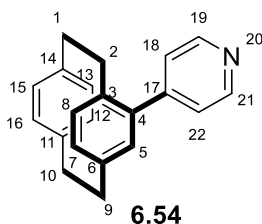
¹H NMR (CDCl₃, 500 MHz): δ 8.78 (s, 1H, H-22), 8.64 (d, *J* = 4.1 Hz, 1H, H-20), 7.82 (dt, *J* = 6.3, 1.4 Hz, 1H, H-18), 7.44 (dd, *J* = 7.8, 4.8 Hz, 1H, H-19), 6.68-6.65 (m, 2H, H-5, H-7), 6.60-6.58 (m, 5H, H-8, H-13, H-12, H-15, H-16), 3.41 (td, *J* = 10.4, 3.3 Hz, 1H, H-2a), 3.23-3.06 (m, 4H, H-1a, H-1b, H-9a, H-9b), 3.03-2.89 (m, 2H, H-10a, H-10b), 2.69-2.64 (m, 1H, H-2b).

¹³C NMR (CDCl₃, 125 MHz): δ 150.57 (C-22), 148.00 (C-21), 140.16 (C-14), 139.58 (C-11), 139.52 (C-17), 138.19 (C-6), 137.18 (C-4), 136.86 (C-13), 136.57 (C-3), 136.09 (C-12), 133.27 (C-15), 133.04 (C-16), 132.76 (C-18), 132.10 (C-5), 131.99 (C-7), 129.59 (C-19), 123.42 (C-8), 35.50 (C-2), 35.22 (C-9), 34.87 (C-10), 33.91 (C-1).

HRMS (ESI-TOF) m/z: [M + H]⁺ Calcd for C₂₁H₂₀N 286.1590; Found 286.1587.

Data comparable to that reported in literature.¹⁰

4-(Pyridin-4-yl)[2.2]paracyclophane **6.54**^{10,11}



General procedure **A** was followed using (\pm)-4-bromo[2.2]paracyclophane **6.40** (50 mg, 0.17 mmol, 1.0 eq.), pyridine-4-sulfinate **6.53** (57 mg, 0.35 mmol, 2 eq.), K_2CO_3 (72 mg, 0.26 mmol, 3 eq.), PCy₃ (39 mg, 0.14 mmol, 80 mol%), Pd(OAc)₂ (8 mg, 0.035 mmol, 20 mol%), DMA (0.87 ml) for 72 hrs.

Purification: Flash chromatography [SiO₂, Et₃N:CH₂Cl₂:hexanes (2:19:79)] to obtain the title compound **6.54** as a white powder (50 mg, 0.17 mmol, 100% yield).

R_f: 0.5

IR: ν_{max} 3070, 3022, 2953, 2925, 2897, 2853, 1922, 1896, 1617, 1595, 1496, 1399, 1259, 1091 cm⁻¹

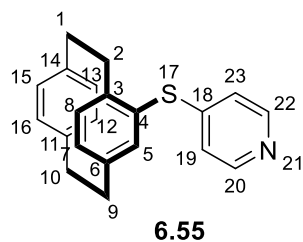
¹H NMR (CDCl₃, 500 MHz): δ 8.73 (d, J = 3.7 Hz, 2H, H-22, H-21), 7.45 (d, J = 5.6 Hz, 2H, H-18, H-19), 6.67-6.64 (m, 2H, H-5, H-7), 6.61-6.54 (m, 5H, H-8, H-12, H-13, H-15, H-16), 3.44 (td, J = 10.6 Hz, 1H, H-2a), 3.22-3.05 (m, 4H, H-1a, H-1b, H-9a, H-9b), 3.03-2.90 (m, 2H, H-10a, H-10b), 2.71-2.65 (m, 1H, H-2b).

¹³C NMR (CDCl₃, 125 MHz): δ 150.06 (C-21, C-19, C-22, C-18), 148.59 (C-17), 140.19 (C-6), 139.54 (C-11, C-14), 139.18 (C-4), 137.24 (C-3), 136.20 (C-12, C-13), 133.51 (C-5), 133.03 (C-15, C-16), 132.73 (C-5), 132.02 (C-7), 131.99 (C-8), 129.76 (C-18), 124.47 (C-22), 35.49 (C-1), 35.21 (C-10), 34.92 (C-9), 33.91 (C-2).

HRMS (ESI-TOF) m/z : [M + H]⁺ Calcd for C₂₁H₂₀N 286.1590; Found 286.1588.

Data comparable to that reported in literature.^{10,11}

4-(Pyridin-4-ylthio)[2.2]paracyclophane **6.55**



A 4 ml scintillation vial was charged with 4-bromo[2.2]paracyclophane **6.40** (40 mg, 0.14 mmol, 1.0 eq.), pyridine-4-thiol **6.61** (57 mg, 0.35 mmol, 2 eq.), K_2CO_3 (29 mg, 0.21 mmol, 1.5 eq.), PCy_3 (16 mg, 0.055 mmol, 0.4 eq.), and $Pd(OAc)_2$ (3 mg, 0.014 mmol, 0.1 eq.). The vial was purged and degassed with argon for three times. Degassed DMA (0.7 ml, 0.2 M) was transferred by syringe and the screw-capped vial was heated at 150 °C for 52 hrs. The reaction mixture was cooled to room temperature and diluted with CH_2Cl_2 and MeOH before passing through a pad of Celite[®]. The resulting filtrate was removed under reduced pressure and the crude product was purified by flash chromatography.

Purification: Flash chromatography [SiO_2 , EtOAc: Hexane (30:70)] to obtain the title compound **6.55** as a white powder (20 mg, 0.15 mmol, 46%).

R_f : 0.6

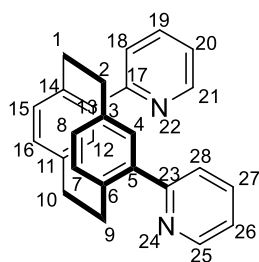
IR: ν_{max} 3850, 3742, 3673, 2975, 2292, 2199, 2155, 2029, 1975, 1469, 1384, 1089 cm^{-1}

1H NMR ($CDCl_3$, 500 MHz): δ 8.30 (d, $J = 5.05$ Hz, 2H, H-20, H-22), 6.92 (d, $J = 5.25$ Hz, 2H, H-19, H-23), 6.88 (d, $J = 4.1$ Hz, 1H, H-5), 6.70-6.65 (m, 3H, H-12, H-13, H-15), 6.58 (q, $J = 13.7, 7.8$ Hz, 2H, H-7, H-8), 6.49 (d, $J = 7.8$ Hz, 1H, H-16), 3.40-3.35 (m, 1H, H-2a), 3.25 (td, $J = 13.1, 5.7$ Hz, 1H, H-2b), 3.18-3.10 (m, 4H, H-1a, H-1b, H-10a, H-10b), 3.07-3.00 (m, 1H, H-9a), 2.86-2.80 (m, 1H, H-9b).

^{13}C NMR ($CDCl_3$, 125 MHz): δ 150.34 (C-18), 148.98 (C-22, C-20), 144.20 (C-14), 141.47 (C-11), 140.10 (C-6), 139.57 (C-4), 139.38 (C-3), 135.54 (C-15), 134.85 (C-13), 133.37 (C-12), 133.31 (C-16), 132.30 (C-8), 129.96 (C-5), 129.80 (C-7), 120.35 (C-23, C-19), 35.32 (C-10), 34.84 (C-9), 34.71 (C-1), 34.35 (C-2).

HRMS (ESI-TOF) m/z : $[M+H]^+$ Calcd for $C_{21}H_{20}NS$ 318.1311; Found 318.1308.

4,12-Bis(pyridin-2,2'-yl)[2.2]paracyclophane **6.64**



6.64

General procedure **B** was followed using 4,12-dibromo-[2.2]paracyclophane **6.63** (60 mg, 0.16 mmol, 1.0 eq.), pyridine-2-sulfinate **6.50** (109 mg, 0.66 mmol, 4 eq.), K_2CO_3 (68 mg, 0.49 mmol, 3.0 eq.), PCy_3 (37 mg, 0.131 mmol, 80 mol%), $Pd(OAc)_2$ (7 mg, 0.017 mmol, 20 mol%), DMA (0.82 ml) for 22 hrs.

Purification: Flash chromatography [SiO_2 , $Et_3N:CH_2Cl_2:hexanes$ (2:39:59)] to obtain the title compound **6.64** as yellowish semisolid (12 mg, 0.05 mmol, 20% yield).

R_f : 0.3

IR: ν_{max} 37.86, 3693, 3532, 2252, 2197, 2183, 2166, 2002, 1957 cm^{-1}

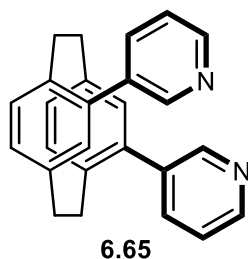
1H NMR ($CDCl_3$, 500 MHz): δ 8.97 (bs, 2H, H-25, H-21), 7.97 (d, $J = 7.8$ Hz, 2H, H-28, H-18), 7.87-7.85 (m, 2H, H-27, H-20), 7.38-7.27 (m, 2H, H-26, H-21), 6.90 (s, 2H, H-4, H-12), 6.79 (d, $J = 7.7$ Hz, H-18, H-15), 6.70 (d, $J = 7.3$ Hz, H-7, H-16), 3.87 (m, 2H, H-9a, H-2a), 3.07-3.03 (m, 2H, H-9b, H-2b), 2.94-2.87 (m, 2H, H-1a, H-10a), 2.50-2.42 (m, 2H, H-1b, H-10b)

^{13}C NMR ($CDCl_3$, 125 MHz): δ 148.96 (C-17, C-23, C-21, C-25), 139.98 (C-11, C-3), 138.10 (C-27, C-19, C-6, C-5), 136.22 (C-13, C-14, C-12, C-4), 133.02 (C-16, C-8, C-26, C-20), 130.78 (C-7, C-15, C-28, C-18), 35.67 (C-2), 35.13 (C-10), 34.24 (C-10, C-9).

HRMS (ESI-TOF) m/z : $[M + H]^+$ Calcd for $C_{26}H_{23}N_2$ 363.1856; Found 363.1849.

Data comparable to that reported in literature.¹²

4,12-Bis(pyridin-3,3'-yl)[2.2]paracyclophane 6.65 and 4-(Pyridin-3-ylthio)-12-(pyridin-3-yl)[2.2]paracyclophane 6.66



General procedure **B** was followed using 4,12-dibromo[2.2]paracyclophane **6.63** (60 mg, 0.16 mmol, 1.0 eq.), pyridine-3-sulfinate **6.51** (109 mg, 0.66 mmol, 4 eq.), K_2CO_3 (68 mg, 0.49 mmol, 3.0 eq.), PCy_3 (37 mg, 0.131 mmol, 0.8 eq.), $Pd(OAc)_2$ (7 mg, 0.017 mmol, 0.2 eq.), DMA (0.82 ml) for 21 hrs.

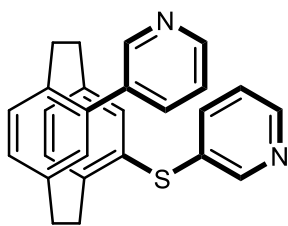
Purification: Flash chromatography [SiO_2 , $Et_3N:CH_2Cl_2:hexanes$ (2:39:59)] gave the title compound **6.65** as yellowish semisolid (7 mg, 0.01 mmol, 13%) and by-product **6.66** yellowish semisolid (14 mg, 0.03 mmol, 22%).

R_f : 0.3

1H NMR ($CDCl_3$, 500 MHz): δ 8.61(2H, dd, $J = 5.1, 1.8$ Hz), 8.59 (2H, d, $J = 1.5$ Hz), 7.62 (2H, ddd, $J = 7.9, 3.8, 1.8$ Hz), 7.36 (2H, dd, $J = 7.9, 5.2$ Hz), 6.80 (2H, d, $J = 7.7$ Hz), 6.73 (2H, dd, $J = 7.9, 1.8$ Hz), 6.62 (2H, d, $J = 1.5$ Hz), 3.51 (2H, ddd, $J = 13.2, 10.1, 1.8$ Hz), 3.21 (2H, ddd, $J = 12.3, 10.1, 2.0$ Hz), 3.05 (2H, ddd, $J = 13.7, 10.4, 6.6$ Hz), 2.79 (2H, ddd, $J = 13.3, 10.2, 6.6$ Hz).

MS (ESI-TOF) m/z : $[M+H]^+$ Calcd for $C_{26}H_{23}N_2$ 363.18; Found 363.07.

4-(Pyridin-3-ylthio)-12-(pyridin-3-yl)[2.2]paracyclophane 28



6.66

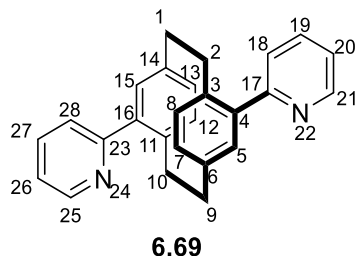
R_f : 0.5

^1H NMR (CDCl_3 , 500 MHz): δ 8.83 (1H, d, $J = 1.6$ Hz), 8.62 (1H, dd, $J = 4.8, 1.5$ Hz), 8.47 (1H, d, $J = 1.8$ Hz), 8.37 (1H, dd, $J = 4.7, 1.4$ Hz), 8.00 (1H, ddd, $J = 7.9, 4.2, 2.1$ Hz), 7.45 (1H, dd, $J = 7.2, 4.2$ Hz), 7.42 (1H, ddd, $J = 8.0, 3.9, 1.6$ Hz), 7.13 (1H, ddd, $J = 7.9, 4.7, 0.4$ Hz), 6.95 (1H, d, $J = 1.7$ Hz), 6.74-6.68 (3H, m), 6.62 (2H, dd, $J = 7.3, 1.7$ Hz), 3.51-3.43 (2H, m), 3.29-3.20 (2H, m), 2.93-2.82 (3H, m), 2.46-2.36 (1H, m).

MS (ESI-TOF) m/z : $[\text{M}+\text{H}]^+$ Calcd for $\text{C}_{26}\text{H}_{23}\text{N}_2\text{S}$ 395.15; Found 395.05.

4,16-Bis(pyridin-2,2'-yl)[2.2]paracyclophane
yl)[2.2]paracyclophane 6.71, and
[2.2]paracyclophane 6.70

6.69¹³, 4-Bromo-16-(pyridin-2-
4-(Pyridin-2-ylthio)-16-(pyridin-2-yl)



General procedure **B** was followed using 4,16-dibromo-[2.2]paracyclophane **6.63** (60 mg, 0.16 mmol, 1.0 eq.), pyridine-2-sulfinate **6.50** (109 mg, 0.66 mmol, 4 eq.), K₂CO₃ (68 mg, 0.49 mmol, 3.0 eq.), PCy₃ (37 mg, 0.131 mmol, 0.8 eq.), Pd(OAc)₂ (7 mg, 0.017 mmol, 0.2 eq.), DMA (0.82 ml) for 18 hrs.

Purification: Flash chromatography [SiO₂, Et₃N:CH₂Cl₂:hexanes (2:39:59)] gave the title compound **6.69** as a yellowish semisolid (38 mg, 0.10 mmol, 66%), by-product **6.71** as yellowish semisolid (7 mg, 0.01 mmol, 12%), and by-product **6.70** as white semisolid (6 mg, 0.01 mmol, 9%).

R_f: 0.3

IR: ν_{max} 3743, 3674, 2988, 2899, 2253, 2143, 2106, 1998, 1393, 1240, 1240, 1062, 1057 cm⁻¹

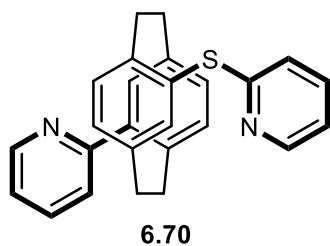
¹H NMR (CDCl₃, 500 MHz): δ 8.80 (d, *J* = 5.2 Hz, 2H, H-21, H-25), 7.82 (td, *J* = 2.1, 9.6 Hz, 2H, H-19, H-26), 7.56 (d, *J* = 9.8 Hz, H-18, H-28), 7.28-7.26 (m, 2H, H-20, H-27), 6.96 (s, 2H, H-5, H-15), 6.74 (d, *J* = 9.7 Hz, 2H, H-8 H-7), 6.63 (d, *J* = 9.6 Hz, H-13, H-12), 3.67 (td, *J* = 12.6, 4.9 Hz, H-2a, H-2b), 3.15 (td, *J* = 12.7, 6.0 Hz, H-10a, H-10b), 2.99 (td, *J* = 12.7, 4.9 Hz, H-1a, H-b), 2.86 (td, *J* = 12.5, 5.9 Hz, H-9a, H-9b).

¹³C NMR (CDCl₃, 125 MHz): δ 159.21 (C-17, C-23), 149.68 (C-21, C-25), 140.82 (C-14, C-3), 139.78 (C-11, C-6), 137.82 (C-4, C-16), 136.26 (C-12, C-13), 135.47 (C-19, C-27), 132.55 (C-5, C-15), 131.19 (C-20, C-26), 124.44 (C-7, C-8), 121.41 (C-18, C-28), 34.95 (C-2, C-10), 33.87 (C-1), 29.70 (C-9).

HRMS (ESI-TOF) *m/z*: [M + H]⁺ Calcd for C₂₆H₂₃N₂ 363.1856; Found 363.1852.

Data comparable to that reported in literature.¹³

4-(Pyridin-2-ylthio)-16-(pyridin-2-yl) [2.2]paracyclophane 6.70



R_f : 0.4

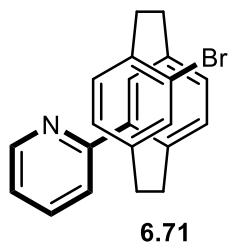
IR: ν_{\max} 3675, 2989, 2900, 2253, 1393, 1241, 1066 cm^{-1} .

^1H NMR (CDCl_3 , 500 MHz): δ 8.81 (1H, d, $J = 4.2$ Hz), 8.44 (1H, d, $J = 4.6$ Hz), 7.81 (1H, td, $J = 7.6, 1.6$ Hz), 7.51 (1H, d, $J = 7.8$ Hz), 7.39 (1H, td, $J = 7.8, 1.7$ Hz), 7.28-7.26 (1H, m), 6.99-6.95 (2H, m), 6.92 (1H, d, $J = 1.4$ Hz), 6.84 (1H, d, $J = 1.0$ Hz), 6.79 (1H, d, $J = 8.1$ Hz), 6.76-6.74 (1H, m), 6.71 (1H, d, $J = 7.8$ Hz), 6.62 (1H, d, $J = 7.9$ Hz), 3.70 (1H, ddd, $J = 13.5, 10.1, 3.5$ Hz), 3.57 (1H, ddd, $J = 13.1, 10.4, 2.7$ Hz), 3.36 (1H, ddd, $J = 13.0, 10.5, 4.9$ Hz), 3.13-3.00 (2H, m), 2.95 (2H, ddd, $J = 13.1, 10.5, 5.6$ Hz), 2.80 (1H, ddd, $J = 14.5, 10.0, 4.8$ Hz).

Due to small quantity, a satisfactory ^{13}C NMR was not obtained.

HRMS (ESI-TOF) m/z : $[\text{M} + \text{H}]^+$ Calcd for $\text{C}_{26}\text{H}_{23}\text{N}_2\text{S}$ 395.1576; Found 395.1572.

4-Bromo-16-(pyridin-2-yl)[2.2]paracyclophane 6.71



R_f : 0.5

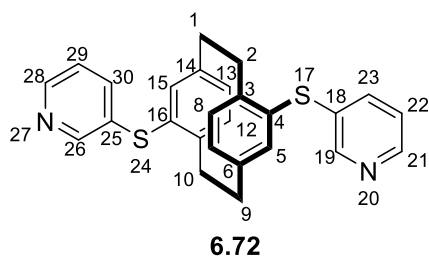
IR: ν_{\max} 3674, 2988, 2899, 2253, 2154, 2000, 1967, 1471, 1393, 1204 cm^{-1} .

^1H NMR (CDCl_3 , 500 MHz): δ 8.82 (1H, d, $J = 4.2$ Hz), 7.84 (1H, t, $J = 7.2$ Hz), 7.52 (1H, d, $J = 7.8$ Hz), 7.32 (1H, t, $J = 6.1$ Hz), 7.22 (1H, d, $J = 7.7$ Hz), 6.94 (1H, s), 6.65-6.61 (3H, m), 6.54 (1H, d, $J = 7.7$ Hz), 3.66 (1H, ddd, $J = 13.8, 10.1, 4.0$ Hz), 3.56 (1H, ddd, $J = 12.8, 10.2, 2.2$ Hz), 3.30-3.25 (1H, ddd, $J = 13.0, 10.3, 5.2$ Hz), 3.13-2.95 (3H, m), 2.87 (1H, ddd, $J = 13.8, 10.2, 3.9$ Hz), 2.78 (1H, ddd, $J = 14.4, 10.2, 4.8$ Hz).

^{13}C NMR (CDCl_3 , 125 MHz): δ 158.96, 149.67, 141.79, 139.37, 138.76, 137.62, 136.22, 137.01, 135.29, 134.51, 132.87, 129.92, 129.38, 129.08, 126.46, 124.43, 121.46, 35.38, 34.54, 33.93, 33.34.

HRMS (ESI-TOF) m/z : $[\text{M}+\text{H}]^+$ Calcd for $\text{C}_{21}\text{H}_{19}\text{Br}^{79}\text{N}$ 364.0695; Found 364.0693; $\text{C}_{21}\text{H}_{29}\text{Br}^{81}\text{N}$ 366.0670; Found 366.0670.

4,16-Bis(pyridin-3,3'-ylthio)[2.2]paracyclophane **6.72**



General procedure **B** was followed using (\pm)-4,16-dibromo-[2.2]paracyclophane **6.68** (70 mg, 0.19 mmol, 1.0 eq.), pyridine-3-sulfinate **6.51** (127 mg, 0.77 mmol, 4 eq.), K_2CO_3 (80 mg, 0.57 mmol, 3.0 eq.), PCy_3 (43 mg, 0.15 mmol, 80 mol%), $Pd(OAc)_2$ (9mg, 0.039 mmol, 20 mol%), DMA (0.96 ml) for 24 hrs.

Purification: Flash chromatography [SiO_2 , EtOAc: hexanes (40:60)] to obtain the by-product compound **6.72** as yellowish semisolid (13 mg, 0.03 mmol, 16% yield).

R_f : 0.3

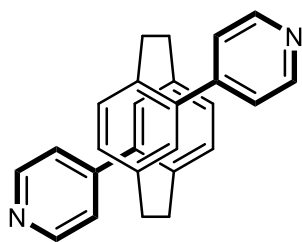
IR: ν_{max} 3683, 3674, 3666, 2988, 2971, 2899, 2245, 2155, 2029, 1406, 1393, 1249, 1075 cm^{-1}

1H NMR ($CDCl_3$, 500 MHz): δ 8.47 (s, 2H, H-19, H-26), 8.39 (d, $J = 4.2$ Hz, 2H, H-21, H-28), 7.40 (d, $J = 8.05$ Hz, 1H, H-23, H-30), 7.15 (dd, $J = 8.05, 4.75$ Hz, 1H, H-22, H-29), 7.08 (d, $J = 7.7$ Hz, 2H, H-5, H-15), 6.52-6.49 (m, 4H, H-7, H-8, H-12, H-13), 3.44-3.39 (m, 2H, H-2a, H-2b), 3.27 (ddd, $J = 13.1, 10.5, 5.0$ Hz, 1H, H-9a, H-9b), 3.03-2.98 (m, 2H, H-10a, H-10b), 2.83 (ddd, $J = 13.3, 10.8, 5.1$ Hz, 2H, H-1a, H-1b).

^{13}C NMR ($CDCl_3$, 125 MHz): δ 148.99 (C-25,C-18), 147.01 (C-26, C-19), 142.05 (C-28,C-21), 140.89 (C-14, C-6), 138.59 (C-29, C-22, C-23,C-30), 135.78 (C-8,C-12), 134.54 (C-5, C-15), 133.36 (C-4, C-16), 130.26 (C-7, C-15), 123.82 (C-3,C-11), 34.03 (C-1,C-9), 33.33 (C-2, C-10).

HRMS (ESI-TOF) m/z : $[M + H]^+$ Calcd for $C_{26}H_{23}N_2S_2$ 427.1303; Found 427.1295.

4,16-Bis(pyridin-4,4'-yl)[2.2]paracyclophane **6.73**



6.73

General procedure **B** was followed using 4,16-dibromo[2.2]paracyclophane **6.68** (50 mg, 0.14 mmol, 1.0 eq.), pyridine-4-sulfinate **6.53** (91 mg, 0.55 mmol, 4 eq.), K_2CO_3 (57 mg, 0.41 mmol, 3.0 eq.), PCy_3 (34 mg, 0.11 mmol, 0.8 eq.), $Pd(OAc)_2$ (6 mg, 0.013 mmol, 0.2 eq.), DMA (0.69 ml) for 20 hrs.

Purification: Flash chromatography [EtOAc:hexanes (0 – 100 to 100:0, gradient elution)] to obtain the title compound **6.73** as a white solid powder (33 mg, 0.10 mmol, 66%).

R_f : 0.2 [EtOAc:hexanes (80:20)]

IR: ν_{max} 3683, 3675, 2989, 2900, 2197, 1405, 1393, 1241, 1076, 1057 cm^{-1} .

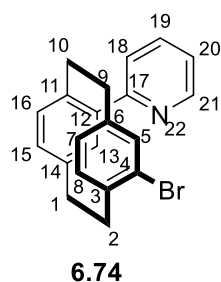
1H NMR ($CDCl_3$, 500 MHz): δ 8.76 (4H, bs), 7.48 (4H, d, $J = 5.3$ Hz), 6.70-6.71 (4H, m), 6.63 (2H, dd, $J = 8.0, 1.7$ Hz), 3.49 (2H, ddd, $J = 13.9, 9.8, 4.0$ Hz), 3.14 (2H, ddd, $J = 14.3, 10.2, 4.5$ Hz), 2.97 (2H, ddd, $J = 13.4, 10.3, 4.0$ Hz), 2.85 (2H, ddd, $J = 14.2, 10.1, 4.4$ Hz).

^{13}C NMR ($CDCl_3$, 175 MHz): δ 150.02, 148.56, 140.16, 139.56, 137.17, 135.10, 132.28, 130.41, 124.51, 34.69, 33.56.

HRMS (ESI-TOF) m/z : $[M+H]^+$ $C_{26}H_{23}N_2$ 363.1856; Found 363.1854.

Data comparable to that reported in literature.⁴

4-Bromo-12-(pyridin-2-yl)[2.2]paracyclophane **6.74**



General procedure **C** was followed using (\pm)-4,12-dibromo-[2.2]paracyclophane **6.63** (50 mg, 0.14 mmol, 1.0 eq.), pyridine-2-sulfinate **6.50** (45 mg, 0.27 mmol, 2 eq.), K_2CO_3 (28 mg, 0.26 mmol, 1.5 eq.), PCy_3 (15 mg, 0.069 mmol, 40 mol%), $Pd(OAc)_2$ (3 mg, 0.017 mmol, 10 mol%), DMA (0.69 ml) for 26 hrs.

Purification: Flash chromatography [SiO_2 , EtOAc: hexanes (30:70)] to obtain the title compound **6.74** as yellowish semisolid (17 mg, 0.046 mmol, 34% yield).

R_f : 0.6

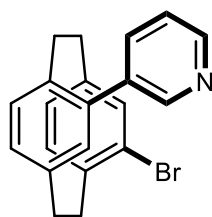
IR: ν_{max} 3616.06, 2973.20, 2252.56, 2189.84, 2007.88, 1793.65, 1587.10 cm^{-1}

1H NMR ($CDCl_3$, 500 MHz): δ 8.74 (d, $J = 4.7$ Hz, 1H, H-21), 7.90-7.86 (m, 2H, H-18, H-19), 7.27 (d, $J = 3.4$ Hz, 1H, H-20), 7.25 (s, 1H, H-13), 6.74 (d, $J = 7.7$ Hz, 1H, H-16), 6.69 (s, 1H, H-5), 6.62 (s, 2H, H-8, H-7), 6.61 (dd, $J = 7.8, 1.7$ Hz, 1H, H-15), 3.97 (dd, $J = 12.4, 10.3$ Hz, 1H, H-9a), 3.57 (ddd, $J = 1.8, 9.3, 13.2$ Hz, 1H, H-10a), 3.25-3.18 (m, 2H, H-9a, H-10b), 2.98-2.93 (m, 1H, H-2a), 2.92-2.85 (m, 2H, H-1a, H-1b), 2.42-2.36 (m, 1H, H-2b).

^{13}C NMR ($CDCl_3$, 125 MHz): δ 159.40 (C-17), 149.40 (C-21), 142.12 (C-6), 140.28 (C-14), 139.15 (C-3), 138.85 (C-5), 138.42 (C-12), 136.81 (C-11), 136.38 (C-8), 135.07 (C-13), 133.62 (C-7), 133.04 (C-15), 131.61 (C-16), 129.00 (C-20), 125.97 (C-19), 122.91 (C-4), 121.52 (C-18), 36.06 (C-9), 34.92 (C-2), 33.92 (C-10), 32.54 (C-1).

HRMS (ESI-TOF) m/z : $[M + H]^+$ Calcd for $C_{21}H_{18}Br^{79}N$ 364.0701; Found 364.0690; $C_{21}H_{29}Br^{81}N$ 366.0680; Found 366.0668.

4-Bromo-12-(pyridin-3-yl)[2.2]paracyclophane **6.75**



6.75

General procedure **C** was followed using 4,12-dibromo[2.2]paracyclophane **6.63** (60 mg, 0.14 mmol, 1.0 eq.), pyridine-3-sulfinate **6.51** (54 mg, 0.27 mmol, 2 eq.), K_2CO_3 (34 mg, 0.26 mmol, 1.5 eq.), PCy_3 (20 mg, 0.065 mmol, 0.4 eq.), $Pd(OAc)_2$ (4 mg, 0.017 mmol, 0.1 eq.), DMA (0.82 ml) for 23 hrs.

Purification: Flash chromatography [SiO_2 , $Et_3N:CH_2Cl_2:hexanes$ (2:39:59)] to obtain the title compound **6.75** as brownish semisolid (27 mg, 0.074 mmol, 45%).

R_f : 0.4

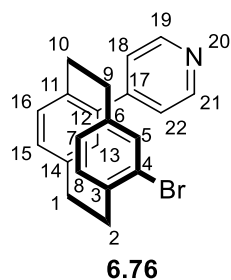
IR: ν_{max} 3673, 2925, 2888, 2850, 1906, 1584, 1537, 1274, 1186, 1036 cm^{-1} .

1H NMR ($CDCl_3$, 500 MHz): δ 8.44 (2H, d, $J = 10.1$ Hz), 7.65 (1H, d, $J = 8.0$ Hz), 7.30-7.28 (1H, m), 7.14 (1H, d, $J = 1.6$ Hz), 7.01 (1H, s), 6.68 (1H, d, $J = 7.8$ Hz), 6.66-6.58 (1H, m), 6.57-6.54 (2H, m), 3.49 (1H, ddd, $J = 12.0, 9.8, 2.0$ Hz), 3.36 (1H, ddd, $J = 12.2, 9.6, 2.4$ Hz), 3.16-3.02 (4H, m), 2.87-2.79 (2H, m).

^{13}C NMR ($CDCl_3$, 125 MHz): δ 141.73, 141.39, 141.23, 138.87, 137.95, 135.58, 135.08, 133.93, 133.70, 133.60, 131.69, 126.63, 124.30, 35.61, 34.45, 33.14, 32.48.

HRMS (ESI-TOF) m/z : $[M+H]^+$ Calcd for $C_{21}H_{18}Br^{79}N$ 364.0695; Found 364.0691; $C_{21}H_{29}Br^{81}N$ 366.0691; Found 366.0668.

4-Bromo-12-(pyridin-4-yl)[2.2]paracyclophane **6.76**



General procedure **C** was followed using (\pm)-4,12-dibromo-[2.2]paracyclophane **6.63** (50 mg, 0.14 mmol, 1.0 eq.), pyridine-4-sulfinate **6.53** (45 mg, 0.27 mmol, 2 eq.), K_2CO_3 (28 mg, 0.21 mmol, 1.5 eq.), PCy_3 (15 mg, 0.069 mmol, 40 mol%), $Pd(OAc)_2$ (3 mg, 0.017 mmol, 10 mol%), DMA (0.69 ml) for 22 hrs.

Purification: Flash chromatography [SiO_2 , EtOAc : hexanes (20:80)] to obtain the title compound **6.76** as yellowish semisolid (18 mg, 0.049 mmol, 36%).

R_f : 0.6

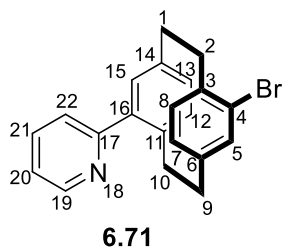
IR: ν_{max} 3742, 3682, 3673, 3649, 3626, 2977, 2966, 2904, 2225, 2166, 1990, 1574, 1399, 1248, 1065 cm^{-1}

1H NMR ($CDCl_3$, 500 MHz): δ 8.74 (d, $J = 5.7$ Hz, 2H, H-21, H-19), 7.60 (d, $J = 4.5$ Hz, 2H, H-22, H-18), 7.15 (s, 1H, H-4), 6.75 (d, $J = 7.4$ Hz, 1H, H-12), 6.66-6.59 (m, 4H, H-8, H-7, H-15, H-16), 3.59-3.52 (m, 2H, H-9a, H-9b), 3.24-3.18 (m, 2H, H-1a, H-1b), 2.95-2.83 (m, 3H, H-2a, H-10a, H-10b), 2.41-2.36 (m, 1H, H-2b)

^{13}C NMR ($CDCl_3$, 125 MHz): δ 149.22 (C-21, C-19), 141.42 (C-17), 139.95 (C-11), 139.06 (C-14), 138.51 (C-3), 136.89 (C-5), 136.33 (C-12), 135.04 (C-15), 133.71 (C-6), 133.45 (C-4, C-8), 131.71 (C-16, C-7), 128.75 (C-18), 125.98 (C-13), 124.50 (C-22), 36.01 (C-2), 34.35 (C-10), 33.69 (C-9), 32.42 (C-1).

HRMS (ESI-TOF) m/z : $[M+H]^+$ Calcd for $C_{21}H_{19}Br^{79}N$ 364.0695; Found 364.0693; $C_{21}H_{19}Br^{81}N$ 366.0675; Found 366.0670.

4-Bromo-16-(pyridin-2-yl)[2.2]paracyclophane **6.71**



General procedure **C** was followed using (\pm)-4,16-dibromo-[2.2]paracyclophane **6.68** (50 mg, 0.14 mmol, 1.0 eq.), pyridine-2-sulfinic acid **6.50** (45 mg, 0.27 mmol, 2 eq.), K_2CO_3 (28 mg, 0.21 mmol, 1.5 eq.), PCy_3 (15 mg, 0.069 mmol, 40 mol%), $Pd(OAc)_2$ (3 mg, 0.014 mmol, 10 mol%), DMA (0.69 ml).

Purification: Flash chromatography [SiO_2 , EtOAc : hexanes (30:70)] to obtain the title compound **6.71** as yellowish semisolid (18 mg, 0.04 mmol, 36% yield).

R_f : 0.5

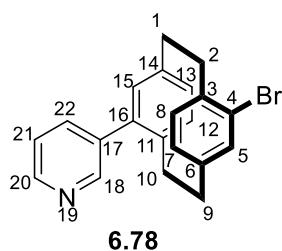
IR: ν_{max} 3674, 2988, 2899, 2253, 2154, 2000, 1967, 1471, 1393, 1204 cm^{-1}

1H NMR ($CDCl_3$, 500 MHz): δ 8.82 (d, $J = 4.2$ Hz, 1H, H-19), 7.84 (d, $J = 7.3$ Hz, 1H, H-22), 7.52 (d, $J = 7.8$ Hz, 1H, H-21), 7.32 (t, $J = 6.1$ Hz, H-20), 7.22 (d, $J = 7.7$ Hz, 1H, H-12), 6.94 (s, 1H, H-15), 6.65-6.61 (m, 3H, H-13, H-8, H-7), 3.66 (td, $J = 10.2, 4.0$ Hz, 1H, H-10a), 3.56 (td, $J = 12.8, 2.2$ Hz, 1H, H-10b), 3.30-3.25 (m, 1H, H-9a) 3.13-2.95 (m, 3H, H-9a, H-2a, H-2b), 2.87 (m, 1H, H-1a), 2.78 (m, 1H, H-1b).

^{13}C NMR ($CDCl_3$, 125 MHz): δ 158.96 (C-17), 149.67 (C-19), 141.79 (C-6), 139.37 (C-14), 138.76 (C-3), 137.62 (C-5), 136.22 (C-11), 137.01 (C-16), 135.29 (C-8), 134.51 (C-15), 132.87 (C-7), 129.92 (C-13), 129.38 (C-20), 129.08 (C-12), 126.46 (C-4), 124.43 (C-22), 121.46 (C-21), 35.38 (C-1), 34.54 (C-9), 33.93 (C-10), 33.34 (C-2)

HRMS (ESI-TOF) m/z : $[M+H]^+$ Calcd for $C_{21}H_{19}Br^{79}N$ 364.0695; Found 364.0693; $C_{21}H_{29}Br^{81}N$ 366.0670; Found 366.0670.

4-Bromo-16-(pyridin-3-yl)[2.2]paracyclophane **6.78**



General procedure **C** was followed using (\pm)-4,16-dibromo-[2.2]paracyclophane **6.63** (60 mg, 0.16 mmol, 1.0 eq.), pyridine-3-sulfinate **6.51** (54 mg, 0.33 mmol, 2 eq.), K_2CO_3 (34 mg, 0.25 mmol, 1.5 eq.), PCy_3 (18 mg, 0.066 mmol, 40 mol%), $Pd(OAc)_2$ (4 mg, 0.016 mmol, 10 mol%), DMA (0.82 ml) for 21 hrs.

Purification: Flash chromatography [SiO_2 , $Et_3N:CH_2Cl_2:hexanes$ (2:39:59)] to obtain the title compound **6.78** as yellowish semisolid (29 mg, 0.07 mmol, 48% yield).

R_f : 0.4

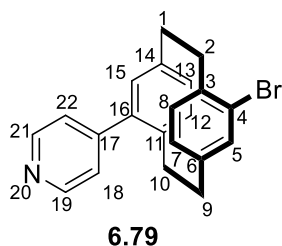
IR: ν_{max} 3852, 3743, 3674, 2976, 2252, 2177, 20004, 1975, 1472, 1380, 1078.01 cm^{-1}

1H NMR ($CDCl_3$, 500 MHz): δ 8.77 (d, $J = 1.7$ Hz, 1H, H-18), 8.65 (d, $J = 4.7$ Hz, 1H, H-20), 7.80 (dt, $J = 6.1, 1.7$ Hz, 1H, H-22), 7.44 (dd, $J = 7.8, 4.9$ Hz, 1H, H-15), 7.25 (dd, $J = 7.7, 1.6$ Hz, 1H, H-21), 6.65-6.61 (m, 3H, H-5, H-7, H-8), 6.57-6.54 (m, 2H, H-12, H-13), 3.60-3.55 (m, 1H, H-10a), 3.37 (ddt, $J = 29.0, 10.4, 5.9$ Hz, 2H, H-9a, H-9b), 3.12-3.02 (m, 2H, H-2a, H-2b), 2.97-2.91 (m, 1H, H-10b), 2.83-2.77 (m, 1H, H-1a), 2.75-2.68 (m, 1H, H-1b).

^{13}C NMR ($CDCl_3$, 125 MHz): δ 150.47 (C-18), 148.10 (C-20), 141.59 (C-9), 139.91 (C-6), 138.98 (C-17), 138.63 (C-3), 137.48 (C-14), 136.96 (C-5), 136.74 (C-16), 136.52 (C-11), 135.29 (C-22), 133.93 (C-8), 132.13 (C-15), 129.20 (C-13), 128.70 (C-7), 126.65 (C-21), 123.46 (C-4), 35.63 (C-9), 34.34 (C-1), 33.87 (C-10), 33.20 (C-2).

HRMS (ESI-TOF) m/z : $[M+H]^+$ Calcd for $C_{21}H_{19}Br^{79}N$ 364.0695; Found 364.0693; $C_{21}H_{19}Br^{81}N$ 366.0675; Found 366.0669.

4-Bromo-16-(pyridin-4-yl)[2.2]paracyclophane 6.79 and 4-Bromo-16-(pyridin-4-ylthio)[2.2]paracyclophane 6.80



General procedure **C** was followed using (\pm)-4,16-dibromo-[2.2]paracyclophane **6.68** (60 mg, 0.16 mmol, 1.0 eq.), pyridine-4-sulfinate **6.53** (54 mg, 0.33 mmol, 2 eq.), K_2CO_3 (34 mg, 0.25 mmol, 1.5 eq.), PCy_3 (18 mg, 0.066 mmol, 40 mol%), $Pd(OAc)_2$ (4 mg, 0.016 mmol, 10 mol%), DMA (0.82 ml) for 19 hrs.

Purification: Flash chromatography [SiO_2 , $Et_3N:CH_2Cl_2:hexanes$ (2:39:59)] gave the title compound **6.79** as yellowish semisolid (15 mg, 0.04 mmol, 30%) and the by-product **6.80** as yellowish semisolid (10 mg, 0.04 mmol, 20%).

R_f : 0.5

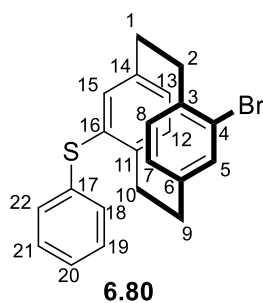
IR: ν_{max} 3674, 2980, 2968, 2905, 2252, 2023, 1966, 1596, 1472, 1383 cm^{-1}

1H NMR ($CDCl_3$, 500 MHz): δ 8.73 (d, $J = 5.3$ Hz, 2H, H-19, H-21), 7.41 (d, $J = 5.9$ Hz, 2H, H-18, H-22), 7.26 (dd, $J = 7.7, 1.6$ Hz, 1H, H-15), 6.65-6.63 (m, 3H, H-13, H-12, H-5), 6.56-6.51 (m, 2H, H-8, H-7), 3.61 (td, $J = 12.8, 2.1$ Hz, 1H, H-10a), 3.41 (td, $J = 14.1, 4.6$ Hz, 1H, H-10b), 3.33 (dq, $J = 7.5, 5.6$ Hz, 1H, H-2a), 3.12-3.02 (m, 2H, H-9a, H-9b), 2.97 (dq, $J = 7.8, 5.5$ Hz, 1H, H-2b), 2.83 (dddd, $J = 28.1, 17.9, 10.2, 4.5$ Hz, 2H, H-1a, H-1b).

^{13}C NMR ($CDCl_3$, 125 MHz): δ 150.02 (C-21, C-19), 148.56 (C-17), 141.55 (C-6), 139.95 (C-14), 139.63 (C-3), 139.00 (C-16), 137.51 (C-11, C-5), 136.80 (C-8), 135.41 (C-15), 133.91 (C-13), 132.09 (C-7), 129.64 (C-22), 128.84 (C-18), 126.65 (C-12), 124.54 (C-4), 35.62 (C-1), 34.37 (C-9), 33.39 (C-10), 33.18 (C-2)

HRMS (ESI-TOF) m/z : $[M + H]^+$ Calcd for $C_{21}H_{18}Br^{79}N$ 364.0701; Found 364.0691; $C_{21}H_{29}Br^{81}N$ 366.0680; Found 366.0668.

4-Bromo-16-(pyridin-4-ylthio)[2.2]paracyclophane **6.80**



R_f : 0.6

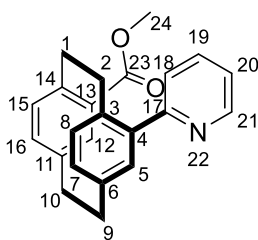
IR: ν_{\max} 2971, 2935, 2252, 2160, 2017, 2010, 1992, 1575, 1478, 1393, 1066 cm^{-1} .

^1H NMR (CDCl_3 , 500 MHz): δ 8.46 (s, 1H, H-18), 8.38 (d, $J = 3.5$ Hz, 1H, H-20), 7.40-7.37 (m, 1H, H-22), 7.13-7.11 (m, 1H, H-21), 7.01 (d, $J = 7.7$ Hz, 1H, H-15), 6.61-6.51 (m, 4H, H-13, H-12, H-8, H-7), 6.46-6.43 (m, 1H, H-5), 3.44-3.37 (m, 1H, H-1a), 3.30-2.92 (m, 6H, H-1b, H-10a, H-10b, H-9a, H-9b, H-2a), 2.84-2.77 (m, 1H, H-2b).

^{13}C NMR (CDCl_3 , 125 MHz): δ 142.39 (C-17), 141.14 (C-20), 139.31 (C-18), 139.31 (C-6), 138.69 (C-3), 138.31 (C-21), 137.41 (C-14), 135.68 (C-4), 135.48 (C-22), 134.62 (C-11), 134.07 (C-5), 133.45 (C-16), 133.04 (C-8), 132.19 (C-12), 129.92 (C-17), 129.45 (C-15), 128.64 (C-13), 35.23 (C-1), 34.86 (C-9), 34.61 (C-2), 34.08 (C-10)

HRMS (ESI-TOF) m/z : $[\text{M}+\text{H}]^+$ Calcd for $\text{C}_{21}\text{H}_{19}\text{Br}^{79}\text{NS}$ 396.0416; Found 396.0415; $\text{C}_{21}\text{H}_{19}\text{Br}^{81}\text{NS}$ 398.0396; Found 398.0391.

Methyl 13-(pyridin-3-yl)[2.2]paracyclophane-4-carboxylate **6.82**



6.82

General procedure was followed using 4-bromo[2.2]paracyclophane-13-carboxylate **6.81** (60 mg, 0.17 mmol, 1.0 eq.), pyridine-2-sulfinate **6.50** (58 mg, 0.35 mmol, 2 eq.), K_2CO_3 (36 mg, 0.21 mmol, 1.5 eq.), PCy_3 (20 mg, 0.069 mmol, 40 mol%), $Pd(OAc)_2$ (4 mg, 0.017 mmol, 10 mol%), 1,4-dioxane (0.87 ml) for 36 hrs.

Purification: Flash chromatography [SiO_2 , EtOAc: hexanes (30:70)] to obtain the title compound **6.82** as a white solid (41 mg, 0.12 mmol, 68% yield).*

R_f : 0.4

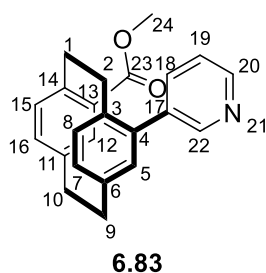
IR: ν_{max} 3866, 3813, 3746, 3673, 2988, 2927, 1712, 1582.83, 1556.83, 1457, 1449, 1266 cm^{-1}

1H NMR ($CDCl_3$, 500 MHz): δ 8.73 (d, $J = 4.7$ Hz, 1H, H-21), 7.73 (td, $J = 7.7, 1.7$ Hz, 1H, H-19), 7.44 (d, $J = 7.9$ Hz, 1H, H-18), 7.22 (m, 1H, H-20), 7.07 (s, 1H, H-5), 6.82 (d, $J = 7.7$ Hz, 1H, H-8), 6.77 (d, $J = 7.7$ Hz, H-7), 6.70 (d, $J = 7.7$ Hz, H-5), 6.59 (d, $J = 6.2$ Hz, 1H, H-16), 6.53 (s, 1H, H-12), 3.98 (t, $J = 10.3$ Hz, H-1a), 3.79 (ddd, $J = 13.5, 9.45, 7.05$ Hz, 2H, H-1a, H-2a), 3.51 (s, 3H, OMe), 3.29-3.13 (m, 4H, H-1b, H-2b, H-9a, H-9b), 2.90-2.84 (m, 2H, H-10a, H-10b).

HRMS (ESI-TOF) m/z : $[M + H]^+$ Calcd for $C_{23}H_{22}NO_2$ 344.1645; Found 344.1637.

* Compound **6.82** has pyridine-based impurities.

Methyl 13-(pyridin-3-yl)[2.2]paracyclophane-4-carboxylate **6.82**



General procedure was followed using 4-bromo[2.2]paracyclophane-13-carboxylate **6.81** (60 mg, 0.17 mmol, 1.0 eq.), pyridine-3-sulfinate **6.51** (58 mg, 0.35 mmol, 2 eq.), K_2CO_3 (36 mg, 0.21 mmol, 1.5 eq.), PCy_3 (20 mg, 0.069 mmol, 40 mol%), $Pd(OAc)_2$ (4 mg, 0.017 mmol, 10 mol%), 1,4-dioxane (0.87 ml).

Purification: Flash chromatography [SiO_2 , EtOAc: hexanes (30:70)] to obtain the title compound **6.82** as a white solid (12 mg, 0.034 mmol, 20% yield).

R_f : 0.5

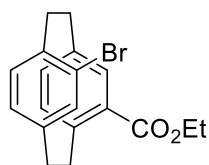
IR: ν_{max} 3793, 3682, 3674, 3491, 2988, 2970, 2899, 2252, 2202, 2157, 1711.57, 1449, 1406, 1393, 1382, 1075, 1065, 1057 cm^{-1}

1H NMR ($CDCl_3$, 500 MHz): δ 8.63 (d, $J = 1.85$ Hz, 1H, H-18), 8.57 (d, $J = 4.7$ Hz, 1H, H-20), 7.73 (dt, $J = 7.8, 1.7$ Hz, 1H, H-22), 7.37-7.33 (m, 2H, H-5, H-12), 6.86 (d, $J = 7.7, 1.65$ Hz, 1H, H-21), 6.80 (d, $J = 7.7$ Hz, 1H, H-8), 6.72-6.70 (m, 2H, H-15, H-16), 6.60 (dd, $J = 7.7, 1.5$ Hz, 1H, H-7), 4.01 (dd, $J = 12.5, 8.9$ Hz, 1H, H-1a), 3.55 (s, 3H, -OMe), 3.46-3.40 (m, 1H, H-1b), 3.33-3.20 (m, 3H, H-2a, H-2b, H-9a), 3.13-3.06 (m, 2H, H-10a, H-10b), 2.87-2.81 (m, 1H, H-9b).

^{13}C NMR ($CDCl_3$, 125 MHz): δ 166.30 (-C=O), 150.34 (C-18), 147.88 (C-19), 143.38 (C-14), 139.75 (C-17), 139.45 (C-6), 138.74 (C-3), 137.77 (C-11), 136.69 (C-4), 136.51 (C-2), 136.29 (C-13), 135.65 (C-7), 134.58 (C-15), 133.54 (C-16), 130.24 (C-12), 128.12 (C-21), 123.07 (C-8), 51.47 (-Me, C-24), 37.25 (C-1), 35.03 (C-2), 34.96 (C-9), 32.68 (C-10).

HRMS (ESI-TOF) m/z : $[M + H]^+$ Calcd for $C_{23}H_{22}NO_2$ 344.1645; Found 344.1639.

Ethyl 4-bromo[2.2]paracyclophane-12-carboxylate **6.101**



6.101

A solution of *n*-BuLi (1.2 M in hexanes; 0.80 ml, 1.60 mmol, 1.17 eq.) was added dropwise over 15 min. to a solution of 4,12-dibromo[2.2]paracyclophane **6.63** (500 mg, 1.37 mmol, 1.0 eq.) in THF (11 ml, 0.1M), at -78 °C. The resulting yellow solution was stirred at -78 °C for 40 min. Ethyl chloroformate (0.16 ml in 1 ml dry THF, 1.64 mmol, 1.2 eq.) was added dropwise over 10 min. The solution was warmed to room temperature overnight. Saturated NH₄Cl (10 ml) was added to the reaction mixture at 0 °C and the resulting organic phases were separated. The aqueous phase was extracted with EtOAc (3 × 15 ml), the combined organics dried (MgSO₄) and concentrated under reduced pressure to give a yellow residue.

Purification: Flash chromatography [SiO₂, EtOAc:hexanes (3:97)] to obtain the title compound **6.101** as a white semisolid (357 mg, 0.99 mmol, 73%).

R_f: 0.7

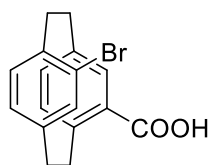
IR: ν_{max} 3683, 3675, 2989, 2900, 2304, 1976, 1696, 1407, 1265, 1076 cm⁻¹.

¹H NMR (CDCl₃, 400 MHz): δ 7.79 (1H, d, *J* = 1.6 Hz), 6.69 (1H, d, *J* = 7.8, 1.6 Hz), 6.65 (1H, d, *J* = 1.7 Hz), 6.61-6.59 (2H, m), 6.51 (1H, d, *J* = 7.5 Hz), 4.51 (1H, dq, *J* = 10.7, 7.1 Hz), 4.38 (1H, dq, *J* = 10.7, 7.1 Hz), 4.13 (1H, dd, *J* = 12.2, 10.6 Hz), 3.52 (1H, ddd, *J* = 11.9, 10.0, 1.5 Hz), 3.28 (1H, ddd, *J* = 13.1, 10.1, 1.6 Hz), 3.16 (2H, q, *J* = 11.4 Hz), 3.07 (1H, ddd, *J* = 13.1, 10.1, 7.5 Hz), 2.88-2.79 (2H, m), 1.49 (3H, t, *J* = 7.1 Hz).

¹³C NMR (CDCl₃, 125 MHz): δ 166.93, 142.01, 142.05, 139.50, 138.87, 136.61, 135.90, 135.46, 135.01, 131.25, 131.04, 130.74, 126.68, 60.56, 36.01, 35.68, 34.04, 32.60, 14.53.

HRMS (ESI-TOF) *m/z*: [M+H]⁺ Calcd for C₁₉H₂₀Br⁷⁹O₂ 359.0641; Found 359.0647; C₁₉H₂₀Br⁸¹O₂ 361.0621; Found 361.0625.

4-Bromo[2.2]paracyclophane-12-carboxylic acid **6.102**



6.102

A solution of ethyl 4-bromo[2.2]paracyclophane-12-carboxylate **6.101** (357 mg, 0.99 mmol, 1.0 eq.) in 25% methanolic KOH (10 ml) was heated to reflux overnight. The reaction mixture cooled to room temperature and diluted with 10 ml H₂O. The reaction mixture was acidified cautiously with concentrated HCl till pH 3 and extracted with CH₂Cl₂ (3 × 10 ml). The combined organics dried (MgSO₄) and concentrated under reduced pressure to yield a white residue of 4-bromo[2.2]paracyclophane-12-carboxylic acid **6.101** (300 mg, 0.91 mmol, 91% yield). The crude was used in the next reaction without purification.

R_f: 0.3 [EtOAc: hexanes (30:70)]

IR: ν_{max} 3046, 2930, 2852, 1679, 1587, 1479, 1319, 1268, 1197, 1035 cm⁻¹.

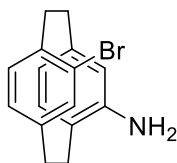
¹H NMR (CDCl₃, 400 MHz): δ 7.96 (1H, s), 6.74 (1H, dd, *J* = 7.8, 1.4 Hz), 6.69-6.67 (2H, m), 6.64 (1H, dd, *J* = 8.1, 1.6 Hz), 6.53 (1H, d, *J* = 7.7 Hz), 4.24 (1H, dd, *J* = 12.1, 10.4 Hz), 3.55 (1H, d, *J* = 12.2, 10.2 Hz), 3.32-3.23 (1H, m), 3.22-3.02 (3H, m), 2.96-2.79 (2H, m).

¹³C NMR (CDCl₃, 125 MHz): δ 171.77, 143.09, 142.09, 139.72, 138.98, 137.71, 136.19, 135.81, 135.00, 131.87, 131.17, 129.31, 126.80, 36.24, 35.78, 34.09, 32.51.

HRMS (ESI-TOF) *m/z*: [M+H]⁺ Calcd for C₁₆H₁₄Br⁷⁹O₂ 329.0172; Found 329.0175; C₁₇H₁₄Br⁸¹O₂ 331.0151; Found 331.0155.

Data comparable to that reported in literature.⁷

4-Bromo-12-amino[2.2]paracyclophane **6.105**



6.105

To 4-bromo[2.2]paracyclophane-12-carboxylic acid **6.101** (300 mg, 0.91 mmol, 1.0 eq.) in an anhydrous CH_2Cl_2 (9 ml, 0.1 M) was added oxalyl chloride (0.39 ml, 4.54 mmol, 5 eq.) and DMF (3 drops) under argon at 0 °C. The reaction mixture was stirred for 3 hrs at room temperature and concentrated under reduced pressure to afford the crude 4-bromo[2.2]paracyclophane-12-carbonyl chloride **6.102** (300 mg, 0.90 mmol). The crude was used in the next reaction without purification.

To a suspension of the crude 4-bromo[2.2]paracyclophane-12-carbonyl chloride **6.102** (300 mg, 0.86 mmol, 1.0 eq.) in acetone (20 ml) was added dropwise an aqueous solution of NaN_3 (65 mg, 0.90 mmol, 10.0 eq.) in water (10 ml) at 0 °C. The reaction mixture was stirred for 2 hrs. An ice-cold water (30 ml) was added and the precipitate was filtered off. The precipitates were further washed three times with an ice-cold water and dried to obtain the an off white powder of 4-bromo[2.2]paracyclophane-12-carbonyl azide **6.103** (229 mg, 0.64 mmol). The crude was used further without purification.

The crude 4-bromo[2.2]paracyclophane-12-carbonyl azide **6.103** (229 mg, 0.64 mmol, 1.0 eq.) was refluxed in dry toluene (10 ml) under argon for 3 hrs. The solvent was evaporated under reduced pressure to afford a white solid of 4-bromo-12-(isocyanato)[2.2]paracyclophane **6.104** (209 mg, 0.63 mmol). The crude was used in the next reaction without purification.

The crude 4-bromo-12-(isocyanato)[2.2]paracyclophane **6.104** (209 mg, 0.63 mmol, 1.0 eq) was dissolved in ethanol (20 ml) and refluxed for 2 hrs. After cooling down, 20% aqueous KOH solution (10 ml) was added, and the resulting reaction mixture was refluxed for 45 hrs. To the cooled reaction mixture was added 20% aqueous KOH (20 ml), and mixture was stirred for 5 minutes. The precipitates were removed by filtration and purified.

Purification: Flash chromatography [SiO_2 , EtOAc:Hexane (30:70)] to obtain the title compound **6.105** as a pale brown solid (95 mg, 0.31 mmol, 49 %).

R_f : 0.4

IR: ν_{\max} 3472, 3381, 2998, 2925, 2855, 1615, 1497, 1288, 1034 cm^{-1} .

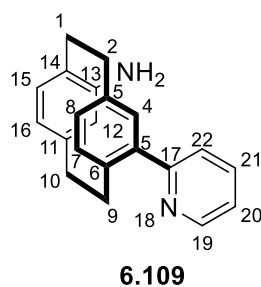
^1H NMR (CDCl_3 , 500 MHz): δ 7.30 (1H, d, $J = 1.6$ Hz), 6.60 (1H, d, $J = 7.7$ Hz), 6.45 (1H, d, $J = 7.7$ Hz), 6.38 (1H, d, $J = 7.6$ Hz), 6.16 (1H, d, $J = 7.7$ Hz), 6.11 (1H, s), 3.52 (2H, bs), 3.42 (1H, ddd, $J = 12.1, 9.9, 1.7$ Hz), 3.15 (1H, d, $J = 10.8, 7.4, 3.4$ Hz), 3.06-3.03 (2H, m), 3.01-2.91 (2H, m), 2.84-2.79 (1H, m), 2.71-2.65 (1H, m).

^{13}C NMR (CDCl_3 , 125 MHz): δ 144.92, 141.25, 141.51, 138.28, 135.32, 134.41, 131.92, 130.96, 125.93, 124.33, 122.71, 117.59, 35.55, 32.91, 32.31, 32.11.

HRMS (ESI-TOF) m/z : $[\text{M}+\text{H}]^+$ Calcd for $\text{C}_{16}\text{H}_{17}\text{Br}^{79}\text{N}$ 302.0539; Found 302.0536; $\text{C}_{16}\text{H}_{17}\text{Br}^{81}\text{N}$ 304.0518; Found 304.0514.

Data comparable to that reported in literature.⁸

4-Amino-12-(pyridin-2-yl)[2.2]paracyclophane **6.109**



General procedure **A** was followed using (\pm)-4-bromo-12-amino[2.2]paracyclophane **6.105** (40 mg, 0.11 mmol, 1.0 eq.), pyridine-2-sulfinate **6.50** (36 mg, 0.22 mmol, 2 eq.), K_2CO_3 (23 mg, 0.21 mmol, 1.5 eq.), PCy_3 (12 mg, 0.043 mmol, 40 mol%), $Pd(OAc)_2$ (2 mg, 0.011 mmol, 10 mol%), DMA (0.55 ml) for 22 hrs.

Purification: Flash chromatography [SiO_2 , CH_2Cl_2 :hexanes (40:60)] to obtain the title compound **6.109** as a brownish semisolid (20 mg, 0.06 mmol, 61% yield).

R_f : 0.4

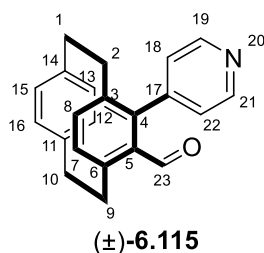
IR: ν_{max} 3912, 3845, 3769, 3741, 3683, 3658, 3612, 3403, 2988, 2968, 2929, 2849, 2251, 2197, 2189, 1586, 1462, 1425, 1065 cm^{-1}

1H NMR ($CDCl_3$, 500 MHz): δ 8.80 (d, $J = 4.7$ Hz, 1H, H-19), 7.75 (td, $J = 7.6, 1.7$ Hz, 1H, H-21), 7.52 (d, $J = 1.7$ Hz, 1H, H-22), 7.44 (d, $J = 7.8$ Hz, 1H, H-20), 7.27 (tdd, $J = 7.2, 4.8, 0.9$ Hz, 1H, H-4), 6.70 (d, $J = 7.7$ Hz, 1H, H-7), 6.45 (dd, $J = 7.7, 1.5$ Hz, 1H, H-8), 6.41 (d, $J = 7.6$ Hz, 1H, H-15), 6.23 (dd, $J = 7.7, 1.5$ Hz, 1H, H-16), 5.57 (d, $J = 1.2$ Hz, 1H, H-9a), 4.14 (bs, 2H, -NH₂), 3.43 (td, $J = 13.8, 3.8$ Hz, 1H, H-9a), 3.27-3.22 (m, 1H, H-9b), 3.20-3.14 (m, 2H, H-2a, H-2b), 3.00 (td, $J = 14.6$ Hz, 1H, H-1a), 2.80-2.73 (m, 2H, H-10a, H-10b), 2.58 (d, $J = 14.7, 4.6$ Hz, 1H, H-1b).

^{13}C NMR ($CDCl_3$, 125 MHz): δ 159.18 (C-17), 149.95 (C-19), 146.42 (C-13), 140.96 (C-21), 140.30 (C-3), 138.77 (C-11), 137.01 (C-6), 135.95 (C-5), 134.47 (C-4), 133.76 (C-15), 127.55 (C-8), 125.12 (C-20), 124.64 (C-16), 123.17 (C-8), 121.42 (C-16), 120.15 (C-12), 34.48 (C-2), 33.37 (C-10), 32.60 (C-9), 31.84 (C-1).

HRMS (ESI-TOF) m/z : $[M + H]^+$ Calcd for $C_{21}H_{21}N_2$ 301.1705; Found 301.1696.

4-Formyl-5-(pyridin-4-yl)[2.2]paracyclophane **6.115**



General procedure was followed using (±)-4-bromo-5-formyl[2.2]paracyclophane **6.111** (50 mg, 0.16 mmol, 1.0 eq.), pyridine-4-sulfinate **6.53** (53 mg, 0.32 mmol, 2 eq.), K₂CO₃ (33 mg, 0.24 mmol, 1.5 eq.), PCy₃ (18 mg, 0.064 mmol, 40 mol%), Pd(OAc)₂ (4 mg, 0.016 mmol, 10 mol%), DMA (0.8 ml) for 36 hrs.

Purification: Flash chromatography [SiO₂, EtOAc: hexanes (3:7) + Et₃N] to obtain the title compound **6.115** as white solid (30 mg, 0.09 mmol, 60% yield).

R_f: 0.4

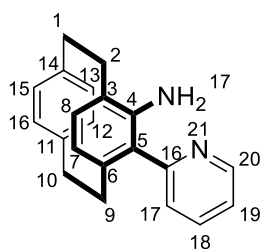
IR: ν_{max} 3835, 3746, 3685, 2951, 2923, 2850, 2749, 1907, 1759, 1673, 1589, 1553, 1497, 1446, 1409, 1158 cm⁻¹

¹H NMR (CDCl₃, 500 MHz): δ 9.50 (s, 1H, -CHO), 8.76 (d, *J* = 5.3 Hz, 2H, H-19, H-22), 7.39 (bs, 1H, H-22), 7.14 (s, 1H, H-18), 6.84 (d, *J* = 9.75 Hz, 1H, H-8), 6.76 (dd, *J* = 9.7, 2.1 Hz, 2H, H-7), 6.66-6.62 (m, 2H, H-12, H-13), 6.55 (dd, *J* = 9.9, 2.2 Hz, 1H, H-15), 3.97-3.87 (m, 1H, H-20), 3.35-3.26 (m, 2H, H-9a, H-9b), 3.06-2.99 (m, 1H, H-2b), 2.97-2.80 (m, 4H, H-1a, H-1b, H-10a, H-10b)

¹³C NMR (CDCl₃, 125 MHz): δ 192.17 (C-23), 149.65 (C-21), 144.41 (C-19), 142.63 (C-17), 142.09 (C-4), 140.57 (C-6), 139.15 (C-3), 138.95 (C-11, C-14), 138.36 (C-5), 135.93 (C-12, C-13), 133.37 (C-15, C-16), 132.15 (C-8), 131.24 (C-7), 129.61 (C-18), 126.65 (C-22), 35.39 (C-1), 35.20 (C-10), 34.91 (C-2), 32.40 (C-9).

HRMS (ESI-TOF) *m/z*: [M+H]⁺ Calcd C₂₂H₂₀NO 314.1539 for; Found 314.1536.

4-Amino-5-(pyridin-2-yl)[2.2]paracyclophane **6.117**



6.117

General procedure **A** was followed using (\pm)-4-bromo-5-amino[2.2]paracyclophane **6.116** (50 mg, 0.16 mmol, 1.0 eq.), pyridine-2-sulfinate **6.50** (55 mg, 0.33 mmol, 2 eq.), K_2CO_3 (34 mg, 0.25 mmol, 1.5 eq.), PCy_3 (19 mg, 0.066 mmol, 40 mol%), $Pd(OAc)_2$ (4 mg, 0.017 mmol, 10 mol%), DMA (0.83 ml) for 48 hrs.

Purification: Flash chromatography [SiO_2 , CH_2Cl_2 :hexanes (40:60)] to obtain the title compound **6.117** as a brownish semisolid (19 mg, 0.06 mmol, 38% yield).

R_f : 0.3

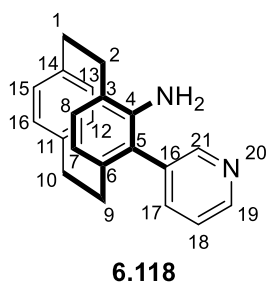
IR: ν_{max} 3799, 3743, 3674, 3156, 2988, 2899, 2252, 2199, 2148, 2031, 1793, 1647, 1467, 1393, 1066 cm^{-1}

1H NMR ($CDCl_3$, 500 MHz): δ 8.76 (d, $J = 4.8$ Hz, 1H, H-20), 7.71 (td, $J = 7.7, 1.7$ Hz, 1H, H-18), 7.27 (d, $J = 7.8$ Hz, 2H, H-19, H-17), 7.20 (t, $J = 5.2$ Hz, 1H, H-7), 6.68 (d, $J = 7.8$ Hz, 1H, H-8), 6.63 (d, $J = 7.7$ Hz, 1H, H-11), 6.58 (d, $J = 7.7$ Hz, 1H, H-12), 6.36 (d, $J = 7.6$ Hz, 1H, H-15), 6.27 (d, $J = 7.6$ Hz, 1H, H-16), 5.14 (bs, 2H, -NH₂), 3.25-3.08 (m, 4H, H-9a, H-9b, H-10a, H-10b), 2.80 (m, 2H, H-2a, H-2b), 2.76-2.70 (m, 1H, H-1a), 2.59-2.53 (m, 1H, H-1b).

^{13}C NMR ($CDCl_3$, 125 MHz): δ 158.23 (C-16), 148.44 (C-20), 139.43 (C-14), 138.93 (C-11), 138.75 (C-18), 135.98 (C-6), 135.51 (C-12), 132.57 (C-13), 132.15 (C-15), 131.08 (C-16), 128.02 (C-3), 127.23 (C-19), 125.89 (C-5), 125.30 (C-7), 124.93 (C-4), 120.74 (C-8), 34.96 (C-9), 34.50 (C-2), 33.33 (C-10), 32.07 (C-1).

HRMS (ESI-TOF) m/z : $[M + H]^+$ Calcd for $C_{21}H_{21}N_2$ 301.1705; Found 301.1695.

4-Amino-5-(pyridin-3-yl)[2.2]paracyclophane **6.118**



General procedure **A** was followed using (\pm)-4-bromo-5-amino[2.2]paracyclophane **6.116** (50 mg, 0.16 mmol, 1.0 eq.), pyridine-3-sulfinate **6.51** (55 mg, 0.33 mmol, 2 eq.), K_2CO_3 (34 mg, 0.25 mmol, 1.5 eq.), PCy_3 (19 mg, 0.066 mmol, 40 mol%), $Pd(OAc)_2$ (4 mg, 0.017 mmol, 10 mol%), DMA (0.83 ml) for 48 hrs.

Purification: Flash chromatography [SiO_2 , CH_2Cl_2 : hexanes (40:60)] to obtain the title compound **6.118** as a brownish semisolid (16 mg, 0.05 mmol, 32% yield).

R_f : 0.3

IR: ν_{max} 3912, 3877, 3742, 3520, 2977, 2252, 2058, 2016, 1644, 1467, 1382, 1102 cm^{-1}

1H NMR ($CDCl_3$, 500 MHz): δ 8.34 (s, 1H, H-21), 8.28 (d, $J = 4.5$ Hz, 1H, H-19), 7.18 (d, $J = 8.3$ Hz, 1H, H-7), 7.06-7.03 (m, 2H, H-17, H-18), 6.64-6.62 (m, 2H, H-13, H-12), 6.47-6.45 (m, 2H, H-15, H-16), 6.31 (d, $J = 7.6$ Hz, 1H, H-8), 4.32 (bs, 2H, $-NH_2$), 3.44-3.39 (m, 1H, H-9a), 3.17-3.04 (m, 6H, H-2a, H-2b, H-1a, H-1b, H-10a, H-10b), 2.80-2.73 (m, 1H, H-9b).

^{13}C NMR ($CDCl_3$, 125 MHz): δ 147.94 (C-21), 147.23 (C-19), 145.83 (C-4), 138.76 (C-14), 138.41 (C-11), 136.48 (C-17), 134.97 (C-3), 133.72 (C-16), 133.52 (C-15), 132.40 (C-13), 128.94 (C-12), 126.48 (C-8), 125.41 (C-6), 123.92 (C-18), 123.60 (C-5), 115.00 (C-7), 34.57 (C-1), 34.80 (C-10), 32.78 (C-9), 32.30 (C-2).

8.6.1. References

- (1) Giri, R.; Yu, J.-Q. Synthesis of 1,2- and 1,3-Dicarboxylic Acids via Pd(II)-Catalyzed Carboxylation of Aryl and Vinyl C-H Bonds. *J. Am. Chem. Soc.* **2008**, *130*, 14082.
- (2) Giri, R.; Liang, J.; Lei, J.-G.; Li, J.-J.; Wang, D.-H.; Chen, X.; Naggar, I. C.; Guo, C.; Foxman, B. M.; Yu, J.-Q. Pd-Catalyzed Stereoselective Oxidation of Methyl Groups by Inexpensive Oxidants under Mild Conditions: A Dual Role for Carboxylic Anhydrides in Catalytic C-H Bond Oxidation. *Angew. Chem. Int. Ed.* **2005**, *44*, 7420.
- (3) Ouyang, J.-S.; Li, Y.-F.; Huang, F.-D.; Lu, D.-D.; Liu, F.-S. The Highly Efficient Suzuki–Miyaura Cross-Coupling of (Hetero)aryl Chlorides and (Hetero)arylboronic Acids Catalyzed by “Bulky-yet-Flexible” Palladium–PEPPSI Complexes in Air. *ChemCatChem* **2018**, *10*, 371.
- (4) Pimparkar, S.; Jeganmohan, M. Palladium-Catalyzed Cyclization of Benzamides with Arynes: Application to the Synthesis of Phenaglydon and *N*-methylcrinasiadine. *Chem. Commun.* **2014**, *50*, 12116.
- (5) Weber, P.; Rank, C. K.; Yalcinkaya, E.; Dyga, M.; van Lingen, T.; Schmid, R.; Patureau, F. W.; Gooßen, L. J. Rhodium-Catalyzed *ortho*-Arylation of (Hetero)aromatic Acids. *Adv. Synth. Catal.* **2019**, *361*, 3925.
- (6) Markovic, T.; Rocke, B. N.; Blakemore, D. C.; Mascitti, V.; Willis, M. C. Pyridine Sulfinates as General Nucleophilic Coupling Partners in Palladium-Catalyzed Cross-Coupling Reactions with Aryl Halides. *Chem. Sci.* **2017**, *8*, 4437.
- (7) Panchaud, P.; Renaud, P. 3-Pyridinesulfonyl Azide: A Useful Reagent for Radical Azidation. *Adv. Synth. Catal.* **2004**, *346*, 925.
- (8) Wasylenko, D. J.; Ganesamoorthy, C.; Borau-Garcia, J.; Berlinguette, C. P. Electrochemical Evidence for Catalyticwater Oxidation Mediated By a High-Valent Cobalt Complex. *Chem. Commun.* **2011**, *47*, 4249.
- (9) Glover, J. E.; Plieger, P. G.; Rowlands, G. J. An Enantiomerically Pure Pyridine *NC*-Palladacycle Derived from [2.2]Paracyclophane. *Aust. J. Chem.* **2014**, *67*, 374.
- (10) Knoll, D. M.; Bräse, S. Suzuki Cross-Coupling of [2.2]Paracyclophane Trifluoroborates with Pyridyl and Pyrimidyl Building Blocks. *ACS Omega* **2018**, *3*, 12158.
- (11) Braun, C.; Spuling, E.; Heine, N. B.; Cakici, M.; Nieger, M.; Bräse, S. Efficient Modular Synthesis of Isomeric Mono- and Bispyridyl[2.2]paracyclophanes by Palladium-Catalyzed Cross-Coupling Reactions. *Adv. Synth. Catal.* **2016**, *358*, 1664.
- (12) Braun, C.; Nieger, M.; Bräse, S. Unprecedented One-Pot Reaction towards Chiral, Non-Racemic Copper(I) Complexes of [2.2]Paracyclophane-Based *P,N*-Ligands. *Chem. Eur. J.* **2017**, *23*, 16452.
- (13) Fulton, J. R.; Glover, J. E.; Kamara, L.; Rowlands, G. J. Facile synthesis of planar chiral *N*-oxides and their use in Lewis base catalysis. *Chem. Commun.* **2011**, *47*, 433.



STATEMENT OF CONTRIBUTION DOCTORATE WITH PUBLICATIONS/MANUSCRIPTS

We, the candidate and the candidate's Primary Supervisor, certify that all co-authors have consented to their work being included in the thesis and they have accepted the candidate's contribution as indicated below in the *Statement of Originality*.

Name of candidate:	Maulik Mungalpara	
Name/title of Primary Supervisor:	Assoc. Prof. Gareth Rowland	
Name of Research Output and full reference:		
1. Mungalpara, M N; Wang, J; Cole, M P; Pledger, P G; Rowlands, G J. The synthesis of a β -glycosyl phosphate-derived secondary phosphate ester and its catalytic activity. <i>Tetrahedron</i> 2019, 75 (36), 6619-6627		
In which Chapter is the Manuscript /Published work:	Chapter 2	
Please indicate:		
• The percentage of the manuscript/Published Work that was contributed by the candidate:	60%	
and		
• Describe the contribution that the candidate has made to the Manuscript/Published Work:		
The candidate carried out all the experimental work, wrote the experimental section, and put the electronic supporting information.		
For manuscripts intended for publication please indicate target journal:		
Chapter 4:- Chemical Communications, Chapter 6:-Organic and Biomolecular Chem		
Candidate's Signature:	Maulik Mungalpara	<small>Digitally signed by Maulik Mungalpara Date: 2020.09.05 09:06:55 +1200'</small>
Date:	05/09/2020	
Primary Supervisor's Signature:	Gareth Rowlands	<small>Digitally signed by Gareth Rowlands Date: 2020.09.05 21:06:04 +1200'</small>
Date:	05/09/2020	

(This form should appear at the end of each thesis chapter/section/appendix submitted as a manuscript/ publication or collected as an appendix at the end of the thesis)



MASSEY UNIVERSITY
GRADUATE RESEARCH SCHOOL

STATEMENT OF CONTRIBUTION DOCTORATE WITH PUBLICATIONS/MANUSCRIPTS

We, the candidate and the candidate's Primary Supervisor, certify that all co-authors have consented to their work being included in the thesis and they have accepted the candidate's contribution as indicated below in the *Statement of Originality*.

Name of candidate:	Maulik Mungalpara	
Name/title of Primary Supervisor:	Assoc. Prof. Gareth Rowlands	
Name of Research Output and full reference:		
Mungalpara, M. N.; Plieger, P. G.; Rowlands, G. J., The Synthesis of pyridyl[2,2]paracyclophanes by palladium-catalysed cross-coupling of pyridine sulfonates. <i>Adv. Synth. Catal.</i> 2021, 363, 1069-1080.		
In which Chapter is the Manuscript /Published work:	Chapter 6	
Please indicate:		
<ul style="list-style-type: none"> The percentage of the manuscript/Published Work that was contributed by the candidate: 	75%	
and		
<ul style="list-style-type: none"> Describe the contribution that the candidate has made to the Manuscript/Published Work: 	The candidate has carried out all the experimental work, wrote the experimental section, and prepared the electronic supporting information.	
For manuscripts intended for publication please indicate target journal:		
Chapter 4:- Chemical Communications		
Candidate's Signature:	Maulik Mungalpara	Digitally signed by Maulik Mungalpara Date: 2021.03.03 19:50:27 +13'00'
Date:	03/03/2021	
Primary Supervisor's Signature:	Gareth Rowlands	Digitally signed by Gareth Rowlands Date: 2021.03.04 09:42:29 +13'00'
Date:	04/03/2021	

(This form should appear at the end of each thesis chapter/section/appendix submitted as a manuscript/ publication or collected as an appendix at the end of the thesis)



MASSEY UNIVERSITY
GRADUATE RESEARCH SCHOOL

STATEMENT OF CONTRIBUTION DOCTORATE WITH PUBLICATIONS/MANUSCRIPTS

We, the candidate and the candidate's Primary Supervisor, certify that all co-authors have consented to their work being included in the thesis and they have accepted the candidate's contribution as indicated below in the *Statement of Originality*.

Name of candidate:	Maulik Mungalpara	
Name/title of Primary Supervisor:	Assoc. Prof. Gareth Rowlands	
Name of Research Output and full reference:		
Mungalpara, M. N.; Tewari, S. D.; Plieger, P. G.; Rowlands, G. J., A rapid route to planar chiral oxazolines based on [2.2]paracyclophane		
In which Chapter is the Manuscript /Published work:	Chapter 4	
Please indicate:		
<ul style="list-style-type: none"> The percentage of the manuscript/Published Work that was contributed by the candidate: 	50%	
and		
<ul style="list-style-type: none"> Describe the contribution that the candidate has made to the Manuscript/Published Work: 		
The candidate has performed an initial optimisation study, synthesised analogues and wrote the experimental section of the respective compounds.		
For manuscripts intended for publication please indicate target journal:		
Chemical Communications		
Candidate's Signature:	Maulik Mungalpara	<small>Digitally signed by Maulik Mungalpara Date: 2021.03.03 19:56:32 +13'00'</small>
Date:	03/03/2021	
Primary Supervisor's Signature:	Gareth Rowlands	<small>Digitally signed by Gareth Rowlands Date: 2021.03.04 09:43:56 +13'00'</small>
Date:	04/03/2021	

(This form should appear at the end of each thesis chapter/section/appendix submitted as a manuscript/ publication or collected as an appendix at the end of the thesis)

New Routes to Planar Chiral Ligands and their Use in Asymmetric Catalysis

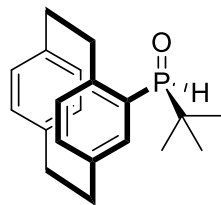
This document contains electronic appendices for the Ph.D. thesis of Maulik Mungalpara

Table of Contents

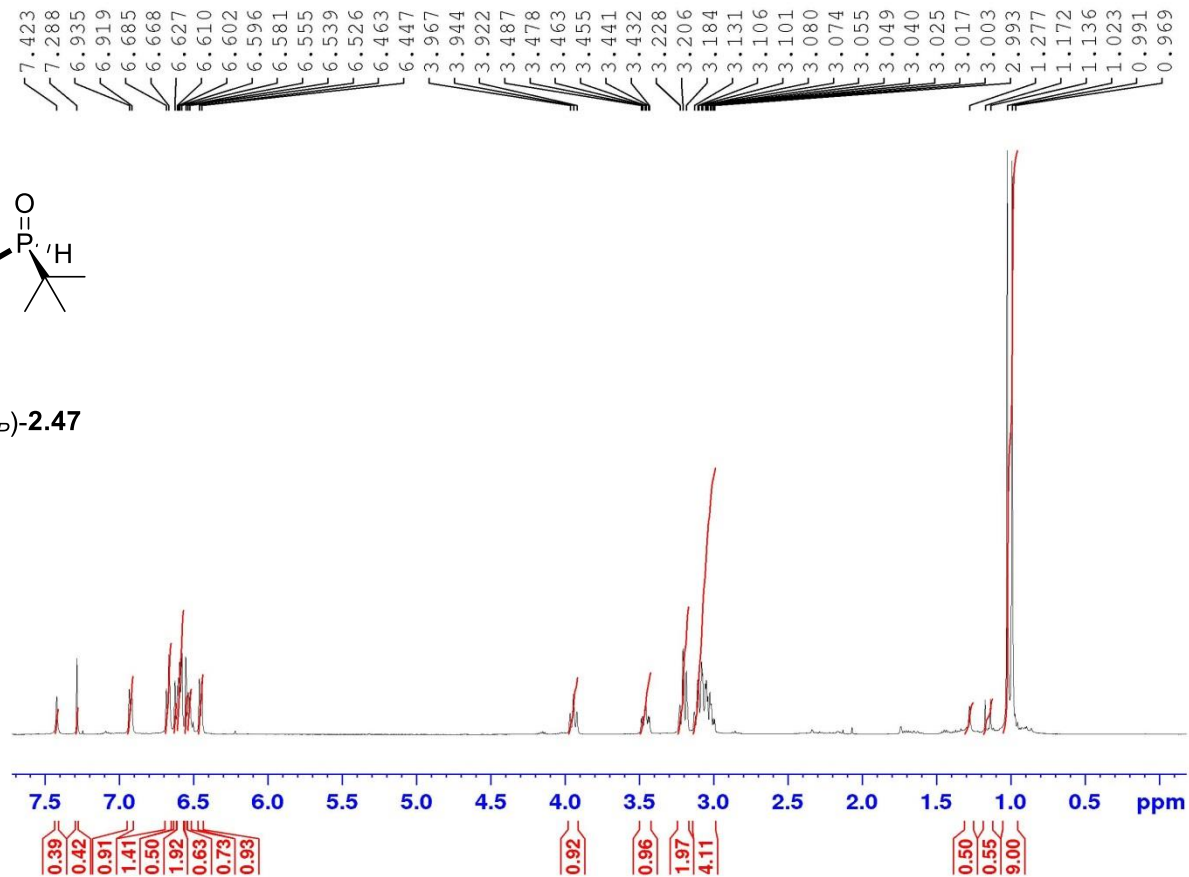
Electronic Appendix for Chapter 2	S2
Electronic Appendix for Chapter 3	S81
Electronic Appendix for Chapter 4	S113
Electronic Appendix for Chapter 5 and Chapter 6	S166

Electronic Appendix for Chapter 2

Formation of SOP with 22PC



(RS_p, SR_p)-2.47



Current Data Parameters
 NAME I-Mn-06
 EXPNO 1
 PROCNO 1

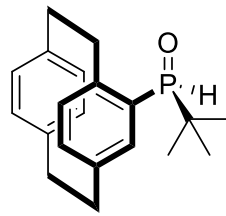
F2 - Acquisition Parameters
 Date_ 20160805
 Time_ 15.17
 INSTRUM spect
 PROBHD 5 mm PAQXI 1H/
 PULPROG zg30
 TD 65536
 SOLVENT CDCl3
 NS 16
 DS 0
 SWH 10330.578 Hz
 FIDRES 0.157632 Hz
 AQ 3.1719425 sec
 RG 90.5
 DW 48.400 usec
 DE 6.50 usec
 TE 294.5 K
 D1 2.0000000 sec
 TD0 1

----- CHANNEL f1 -----
 NUC1 1H
 P1 8.60 usec
 PL1 4.00 dB
 PL1W 12.1000038 W
 SFO1 500.1330885 MHz

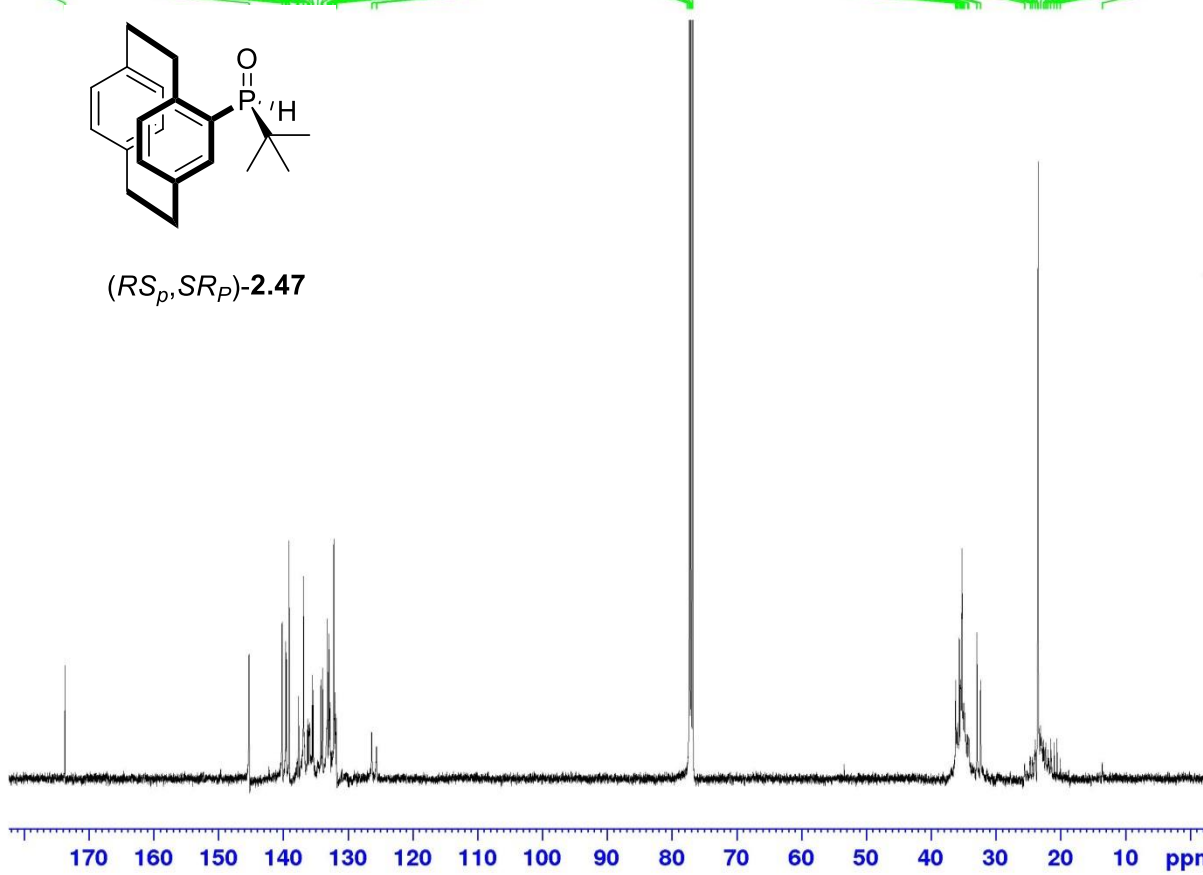
F2 - Processing parameters
 SI 32768
 SF 500.1300000 MHz
 WDW EM
 SSB 0
 LB 0.30 Hz
 GB 0
 PC 1.00

Mono, SPO, 13C

173.71, 148.54, 140.22, 138.60, 138.60, 139.50, 139.50, 139.10, 139.11, 137.891, 137.64, 136.94, 136.22, 136.16, 136.02, 135.96, 135.53, 135.39, 134.72, 134.21, 133.95, 133.23, 133.19, 132.98, 132.84, 132.77, 132.65, 132.56, 132.22, 132.20, 132.13, 132.05, 132.02, 131.82, 126.38, 125.63, 77.68, 77.33, 77.21, 77.08, 76.82, 36.21, 36.06, 35.92, 35.66, 35.47, 35.28, 35.23, 35.10, 34.88, 34.40, 34.23, 32.94, 32.39, 25.57, 24.71, 24.40, 23.94, 23.58, 23.54, 23.51, 23.13, 22.68, 22.58, 22.30, 22.01, 21.55, 21.05, 20.60, 20.09, 13.61



(RS,SR)-2.47



```

Current
NAME      I-Mn-146 13C
EXPNO     2
PROCNO    1

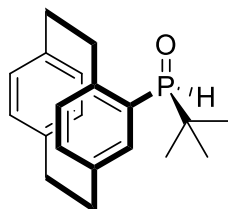
F2 - Acquisition Parameters
Date_     20170322
Time      8.45
INSTRUM   spect
PROBHD    5 mm PAQXI 1H/
PULPROG   zgpg30
TD         65536
SOLVENT   CDCl3
NS         14954
DS         4
SWH        30030.029 Hz
FIDRES     0.458222 Hz
AQ         1.0911744 sec
RG         181
DW         16.650 usec
DE         6.50 usec
TE         299.9 K
D1         2.00000000 sec
D11        0.03000000 sec
TD0        1

===== CHANNEL f1 =====
NUC1       13C
P1         12.00 usec
PL1        -3.50 dB
PL1W       154.08152771 W
SFO1       125.7703643 MHz

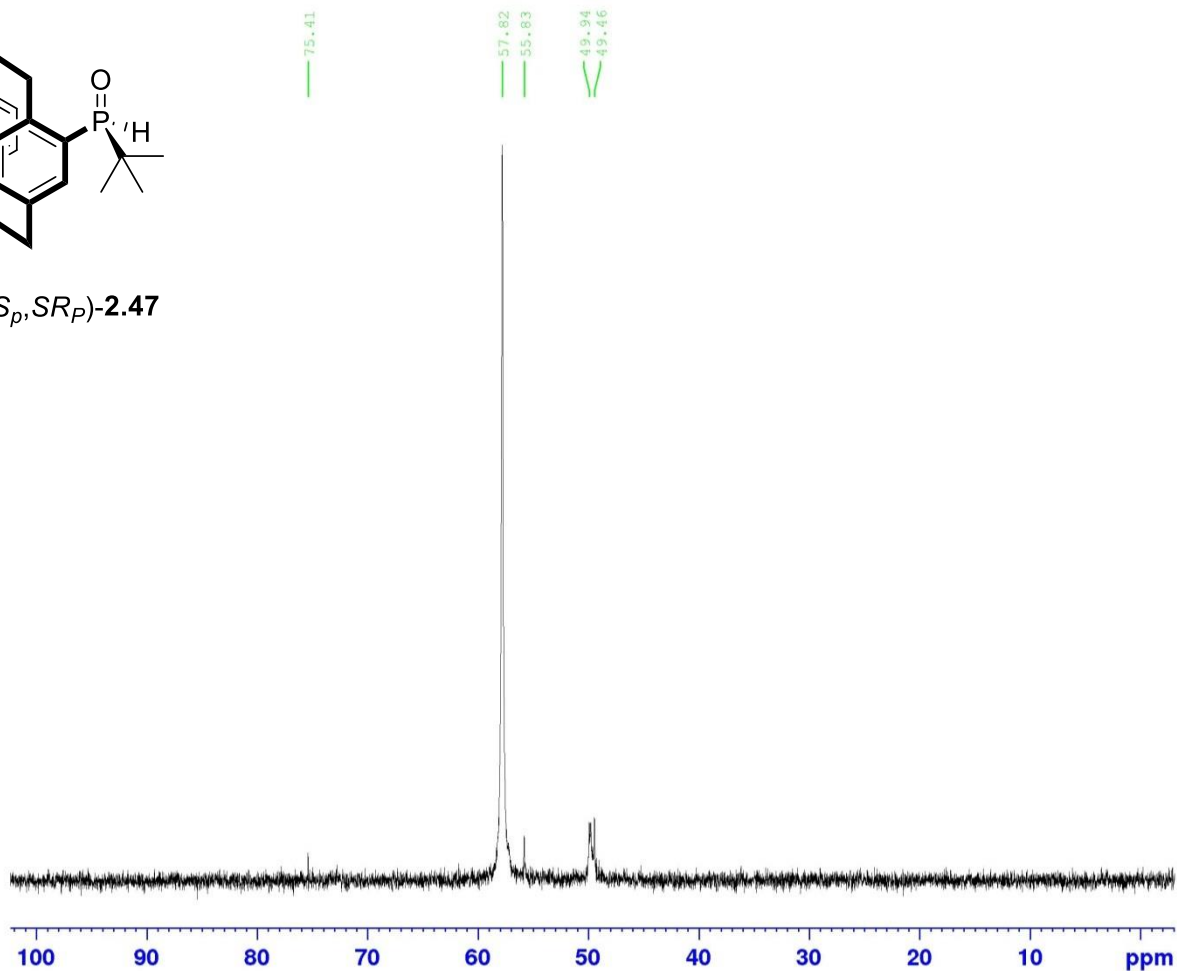
===== CHANNEL f2 =====
CPDPRG[2] waltz16
NUC2       1H
PCPD2      80.00 usec
PL2        4.00 dB
PL12       23.37 dB
PL13       25.00 dB
PL2W       12.10000038 W
PL12W      0.13988955 W
PL13W      0.09611372 W
SFO2       500.1320005 MHz

F2 - Processing parameters
SI         32768
SF         125.7577890 MHz
WDW        EM
SSB        0
LB         1.00 Hz
GB         0
PC         1.40
  
```

Phos NMR SOP formation with PC



(*RS_P*, *SR_P*)-2.47



```

Current Data Parameters
NAME          I-Mn-06
EXPNO         4
PROCNO        1

F2 - Acquisition Parameters
Date_         20160826
Time          15.44
INSTRUM       spect
PROBHD        5 mm PAQXI 1H/
PULPROG       zgpg30
TD            65536
SOLVENT       CDC13
NS            64
DS            4
SWH           80645.164 Hz
FIDRES        1.230548 Hz
AQ            0.4063232 sec
RG            20642.5
DW            6.200 usec
DE            6.50 usec
TE            298.2 K
D1            2.0000000 sec
D11           0.0300000 sec
TD0           1

===== CHANNEL f1 =====
NUC1          31P
P1            20.00 usec
PL1           -2.40 dB
PL1W          131.39126587 W
SFO1          202.4462122 MHz

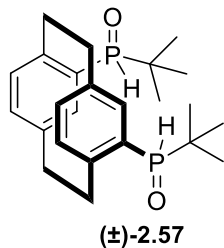
===== CHANNEL f2 =====
CPDPRG[2]    waltz16
NUC2          1H
PCPD2         80.00 usec
PL2           4.00 dB
PL12          23.37 dB
PL13          25.00 dB
PL2W          12.10000038 W
PL12W         0.13988955 W
PL13W         0.09611372 W
SFO2          500.1320005 MHz

F2 - Processing parameters
SI            32768
SF            202.4563350 MHz
WDW           EM
SSB           0
LB            1.00 Hz
GB            0
PC            1.40
    
```

Attempted SPO formation with bibromo {2.2} PC



7.520
7.287
6.728
6.712
6.623
6.615
6.610
6.600
3.742
3.737
3.734
3.729
3.724
3.721
3.716
3.469
3.455
3.367
3.364
2.066
1.848
1.842
1.839
1.835
1.831
1.828
1.822
1.269
1.262
1.239
1.204
1.190
1.176
1.145
1.142
1.109
1.107
1.044
1.031
1.021
1.006
0.991
0.977
0.958
0.945
0.929
0.912
0.865

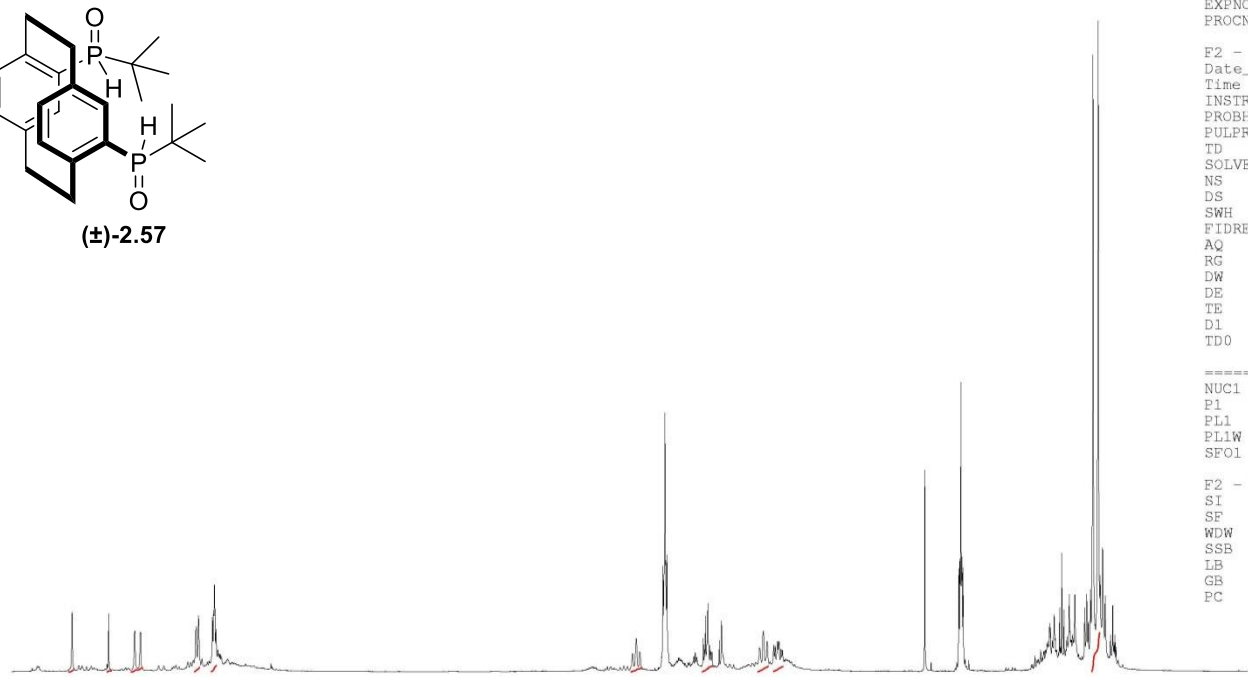


Current Data Parameters
NAME I-Mn-47 1 after drying
EXPNO 1
PROCNO 2

F2 - Acquisition Parameters
Date_ 20161019
Time 9.39
INSTRUM spect
PROBHD 5 mm PAQXI 1H/
PULPROG zg30
TD 65536
SOLVENT CDCl3
NS 16
DS 2
SWH 10330.578 Hz
FIDRES 0.157632 Hz
AQ 3.1719425 sec
RG 32
DW 48.400 usec
DE 6.50 usec
TE 298.2 K
D1 1.00000000 sec
TD0 1

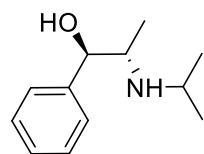
===== CHANNEL f1 =====
NUC1 1H
P1 8.60 usec
PL1 4.00 dB
PL1W 12.10000038 W
SFO1 500.1330885 MHz

F2 - Processing parameters
SI 32768
SF 500.1300000 MHz
WDW EM
SSB 0
LB 0.30 Hz
GB 0
PC 1.00

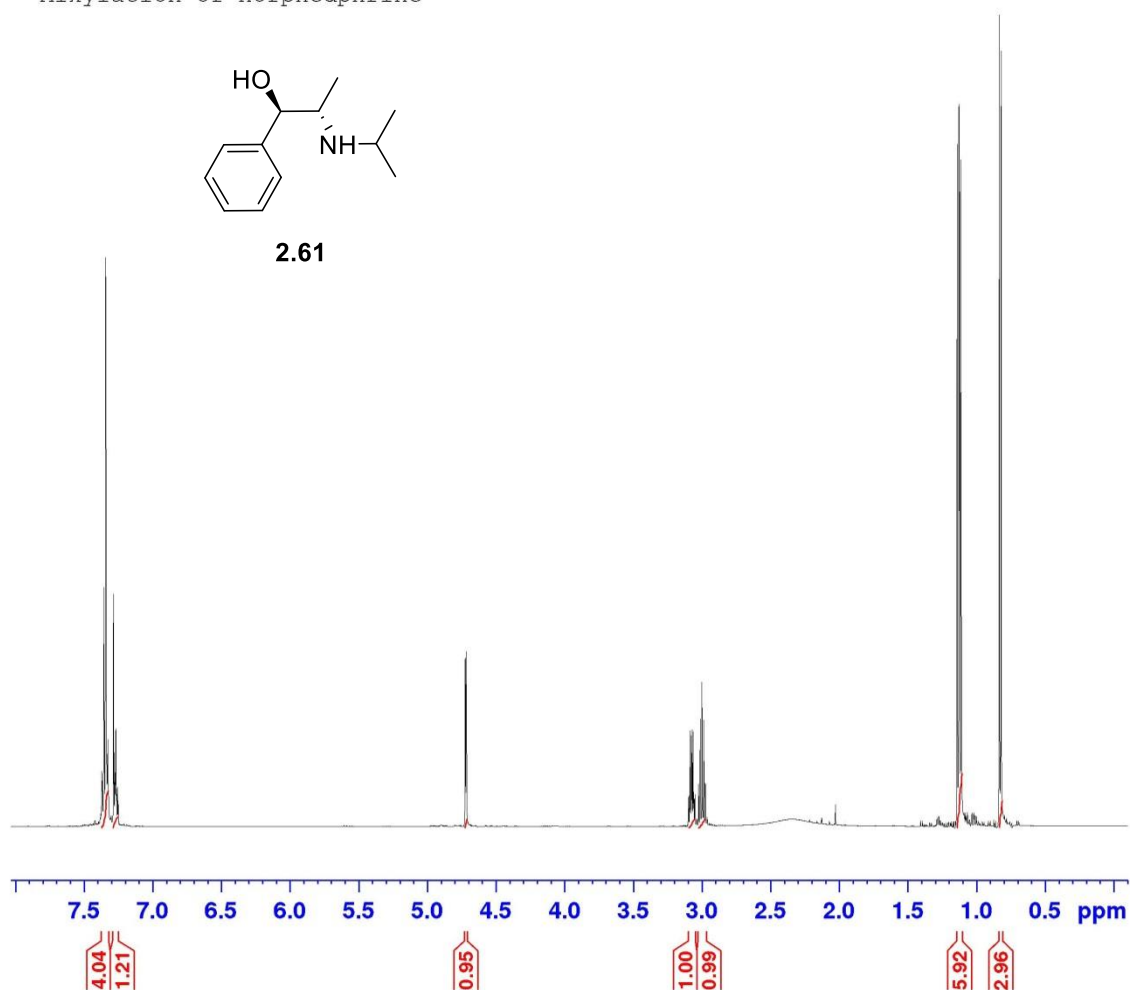


0.84
0.47
1.70
2.08
2.99
1.73
2.76
2.60
2.49
18.00

Alkylation of norphedrine



2.61



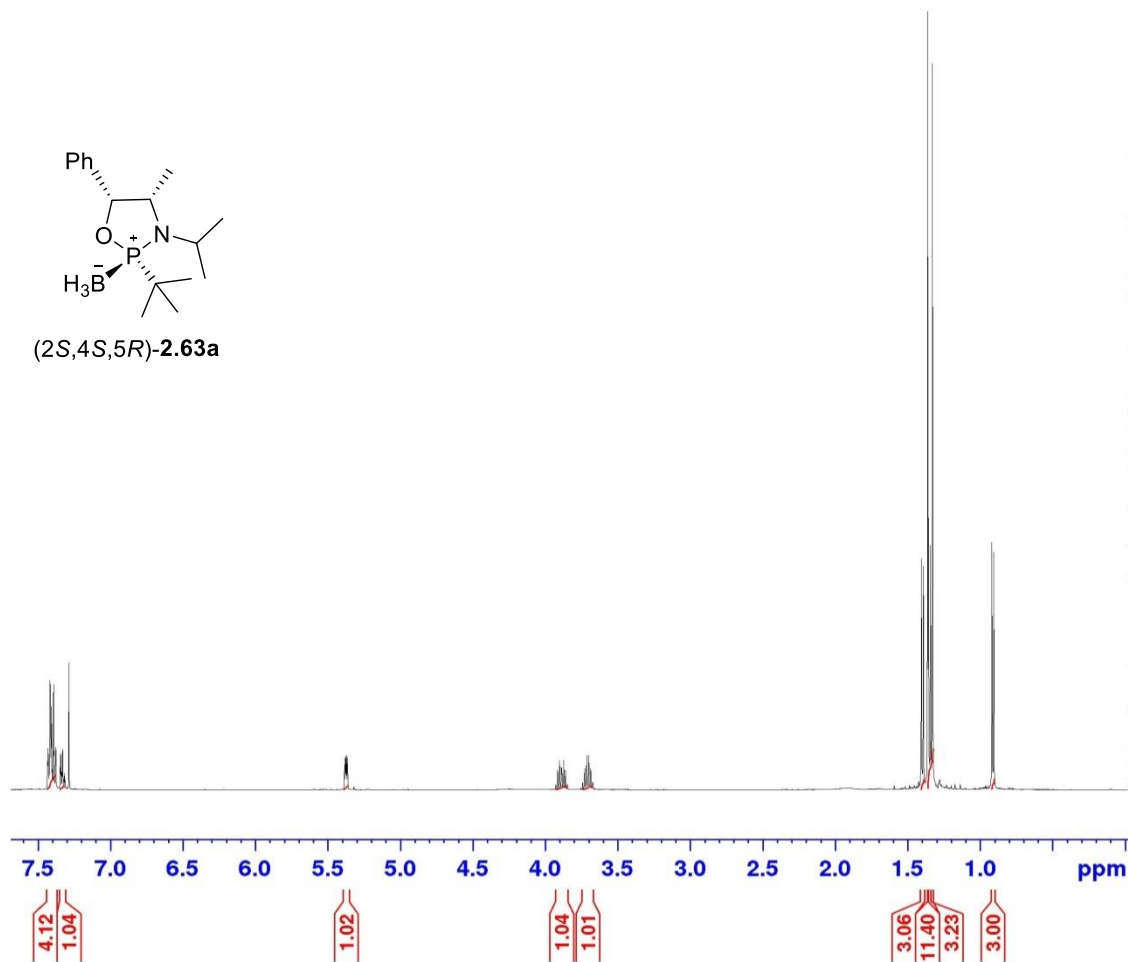
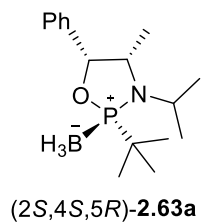
Current Data Parameters
NAME I-Mn-16
EXPNO 1
PROCNO 1

F2 - Acquisition Parameters
Date_ 20160826
Time 12.56
INSTRUM spect
PROBHD 5 mm PAQXI 1H/
PULPROG zg30
TD 65536
SOLVENT CDCl3
NS 16
DS 2
SWH 10330.578 Hz
FIDRES 0.157632 Hz
AQ 3.1719425 sec
RG 71.8
DW 48.400 usec
DE 6.50 usec
TE 298.2 K
D1 1.00000000 sec
TD0 1

===== CHANNEL f1 =====
NUC1 1H
P1 8.60 usec
PL1 4.00 dB
PL1W 12.10000038 W
SFO1 500.1330885 MHz

F2 - Processing parameters
SI 32768
SF 500.1300000 MHz
WDW EM
SSB 0
LB 0.30 Hz
GB 0
PC 1.00

Boran complex formation first spot from column



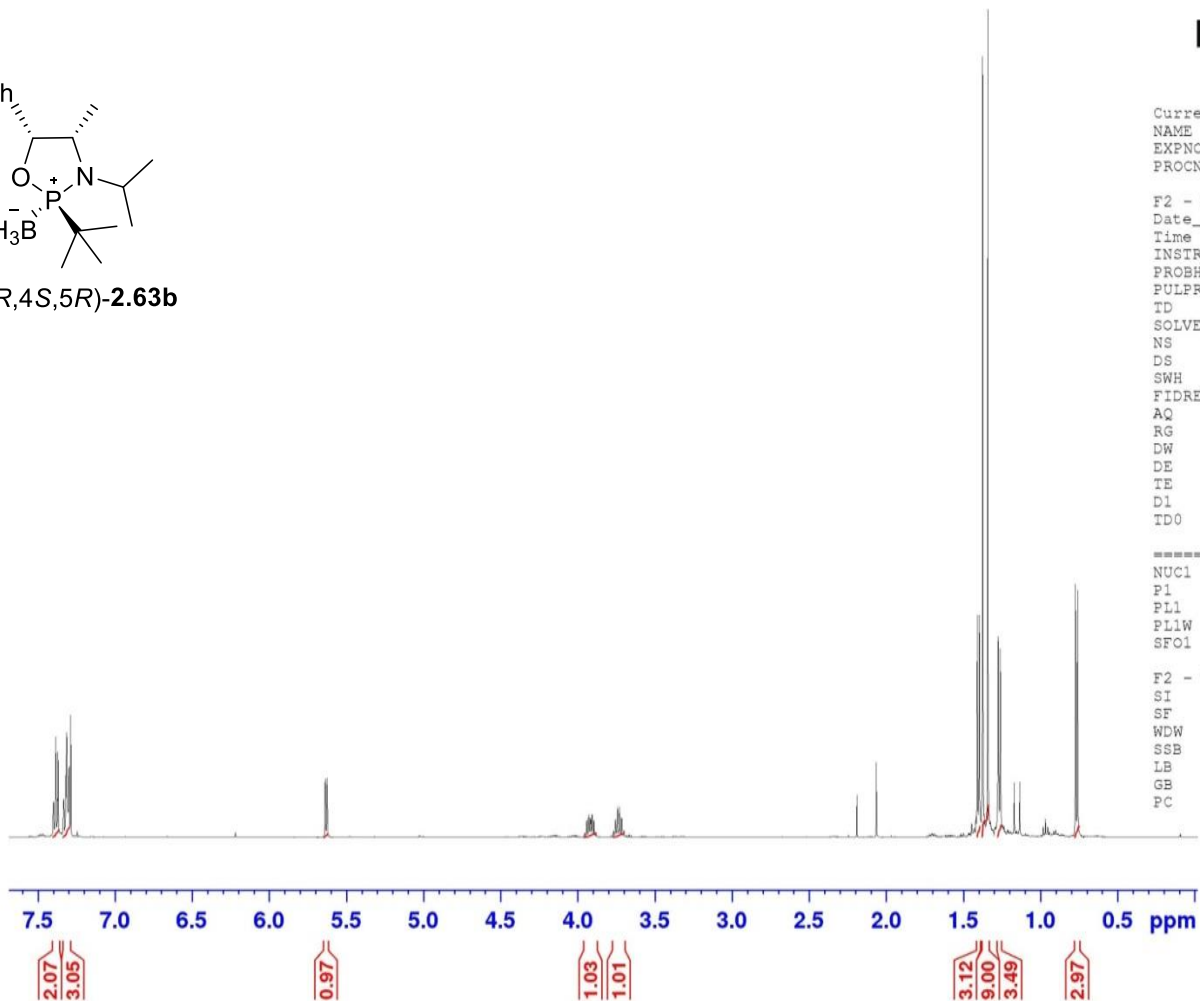
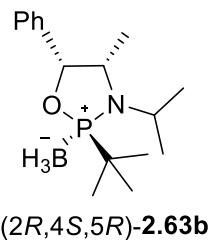
Current Data Parameters
NAME I-Mn-32 1
EXPNO 1
PROCNO 1

F2 - Acquisition Parameters
Date_ 20160919
Time_ 18.30
INSTRUM spect
PROBHD 5 mm PAQXI 1H/
PULPROG zg30
TD 65536
SOLVENT CDCl3
NS 16
DS 2
SWH 10330.578 Hz
FIDRES 0.157632 Hz
AQ 3.1719425 sec
RG 114
DW 48.400 usec
DE 6.50 usec
TE 298.3 K
D1 1.00000000 sec
TD0 1

----- CHANNEL f1 -----
NUC1 1H
P1 8.60 usec
PL1 4.00 dB
PL1W 12.10000038 W
SFO1 500.1330885 MHz

F2 - Processing parameters
SI 32768
SF 500.1300000 MHz
WDW EM
SSB 0
LB 0.30 Hz
GB 0
PC 1.00

Boran complex formation 3rd spot from column



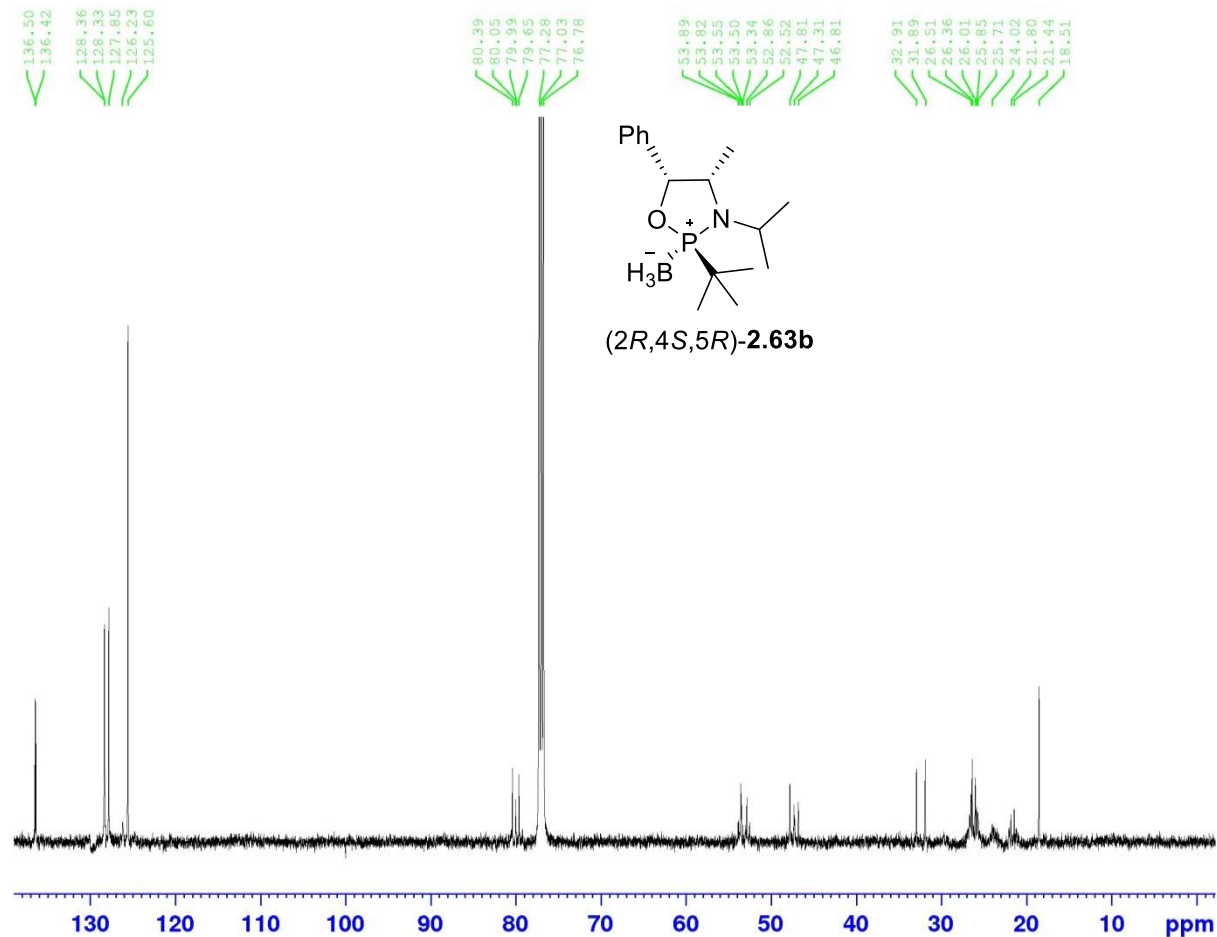
Current Data Parameters
NAME I-Mn-32 3
EXPNO 1
PROCNO 1

F2 - Acquisition Parameters
Date_ 20160919
Time 18.53
INSTRUM spect
PROBHD 5 mm PAQXI 1H/
PULPROG zg30
TD 65536
SOLVENT cdcl3
NS 16
DS 2
SWH 10330.578 Hz
FIDRES 0.157632 Hz
AQ 3.1719425 sec
RG 90.5
DW 48.400 usec
DE 6.50 usec
TE 298.1 K
D1 1.00000000 sec
TD0 1

===== CHANNEL f1 =====
NUC1 1H
P1 8.60 usec
PL1 4.00 dB
PL1W 12.10000038 W
SFO1 500.1330885 MHz

F2 - Processing parameters
SI 32768
SF 500.1300000 MHz
WDW EM
SSB 0
LB 0.30 Hz
GB 0
PC 1.00

Boran complex - 13C



Current Data Parameters
 NAME I-Mn-32 3 13C
 EXPNO 1
 PROCNO 1

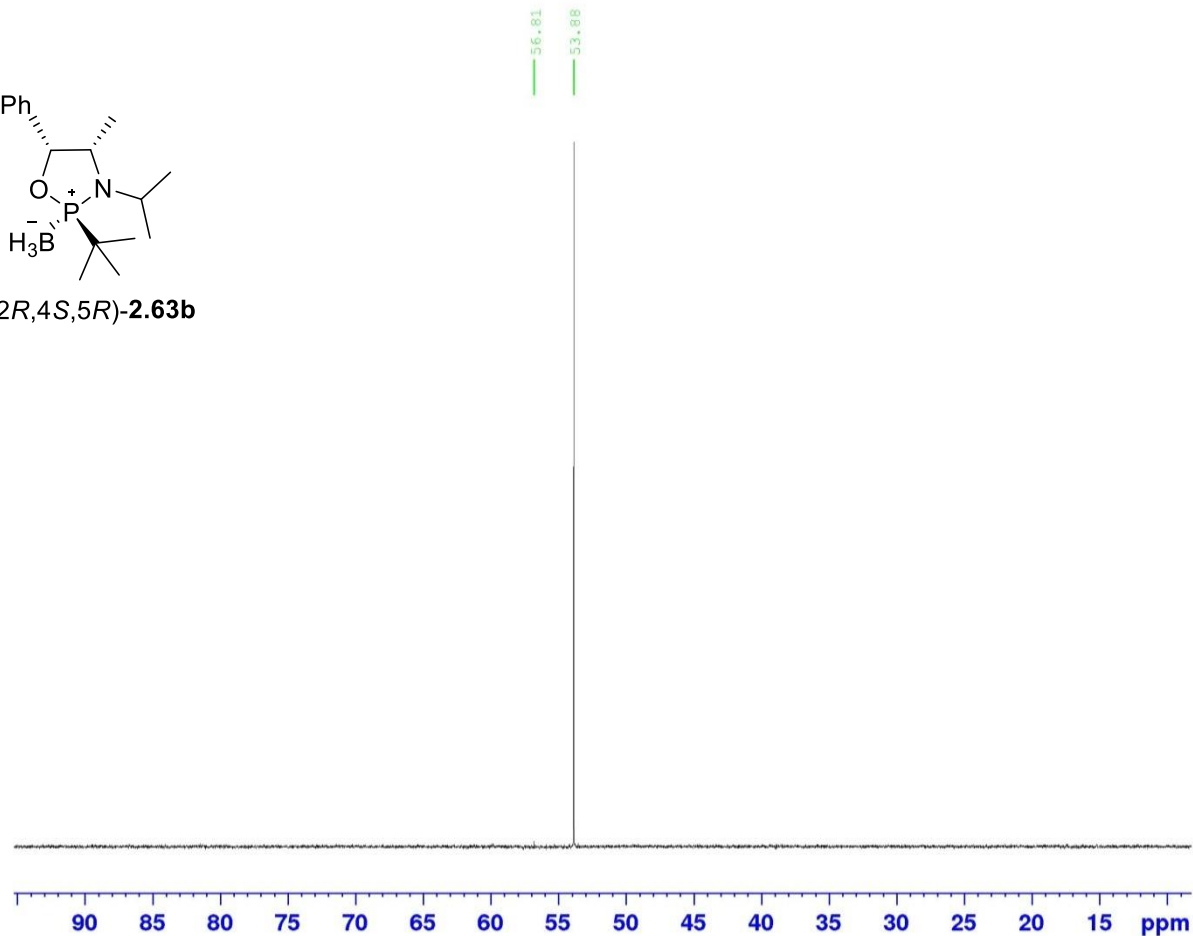
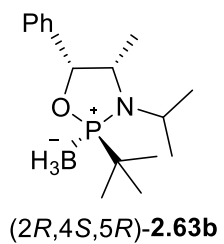
F2 - Acquisition Parameters
 Date_ 20161117
 Time 8.22
 INSTRUM spect
 PROBHD 5 mm PAQXI 1H/
 PULPROG zgpg30
 TD 65536
 SOLVENT CDCl3
 NS 15536
 DS 4
 SWH 30030.029 Hz
 FIDRES 0.458222 Hz
 AQ 1.0911744 sec
 RG 228.1
 DW 16.650 usec
 DE 6.50 usec
 TE 298.2 K
 D1 2.00000000 sec
 D11 0.03000000 sec
 TD0 1

===== CHANNEL f1 =====
 NUC1 13C
 P1 12.00 usec
 PL1 -3.50 dB
 PL1W 154.08152771 W
 SFO1 125.7703643 MHz

===== CHANNEL f2 =====
 CPDPRG[2] waltz16
 NUC2 1H
 PCPD2 80.00 usec
 PL2 4.00 dB
 PL12 23.37 dB
 PL13 25.00 dB
 PL2W 12.10000038 W
 PL12W 0.13988955 W
 PL13W 0.09611372 W
 SFO2 500.1320005 MHz

F2 - Processing parameters
 SI 32768
 SF 125.7577890 MHz
 WDW EM
 SSB 0
 LB 1.00 Hz
 GB 0
 PC 1.40

Boran complex 2nd diastereomer - 31P



Current Data Parameters
NAME I-Mn-32 3 31P
EXPNO 1
PROCNO 1

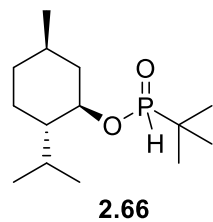
F2 - Acquisition Parameters
Date_ 20161118
Time 8.57
INSTRUM spect
PROBHD 5 mm PAQXI 1H/
PULPROG zgpg30
TD 65536
SOLVENT CDCl3
NS 80
DS 4
SWH 80645.164 Hz
FIDRES 1.230548 Hz
AQ 0.4063232 sec
RG 20642.5
DW 6.200 usec
DE 6.50 usec
TE 298.2 K
D1 2.0000000 sec
D11 0.0300000 sec
TD0 1

===== CHANNEL f1 =====
NUC1 31P
P1 20.00 usec
PL1 -2.40 dB
PL1W 131.39126587 W
SFO1 202.4462122 MHz

===== CHANNEL f2 =====
CPDPRG[2] waltz16
NUC2 1H
PCPD2 80.00 usec
PL2 4.00 dB
PL12 23.37 dB
PL13 25.00 dB
PL2W 12.10000038 W
PL12W 0.13988955 W
PL13W 0.09611372 W
SFO2 500.1320005 MHz

F2 - Processing parameters
SI 32768
SF 202.4563350 MHz
WDW EM
SSB 0
LB 1.00 Hz
GB 0
PC 1.40

Reaction of menthol with tBuPCl2 - first spot from column

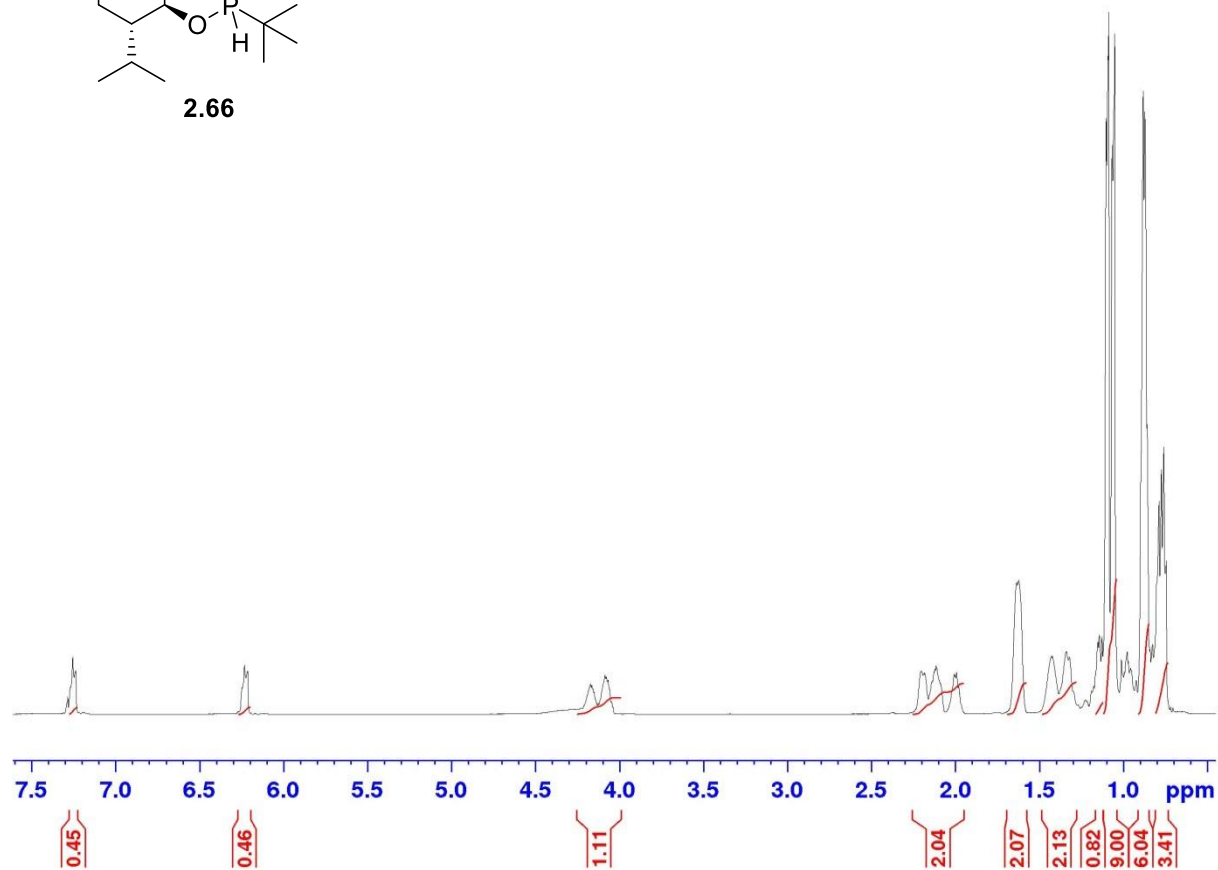


Current Data Parameters
NAME I-Mn-102 1
EXPNO 1
PROCNO 1

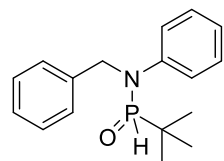
F2 - Acquisition Parameters
Date_ 20170110
Time 16.42
INSTRUM spect
PROBHD 5 mm PAQXI 1H/
PULPROG zg30
TD 65536
SOLVENT CDCl3
NS 16
DS 2
SWH 10330.578 Hz
FIDRES 0.157632 Hz
AQ 3.1719425 sec
RG 18
DW 48.400 usec
DE 6.50 usec
TE 298.2 K
D1 1.0000000 sec
TD0 1

----- CHANNEL f1 -----
NUC1 1H
P1 8.60 usec
PL1 4.00 dB
PL1W 12.10000038 W
SFO1 500.1330885 MHz

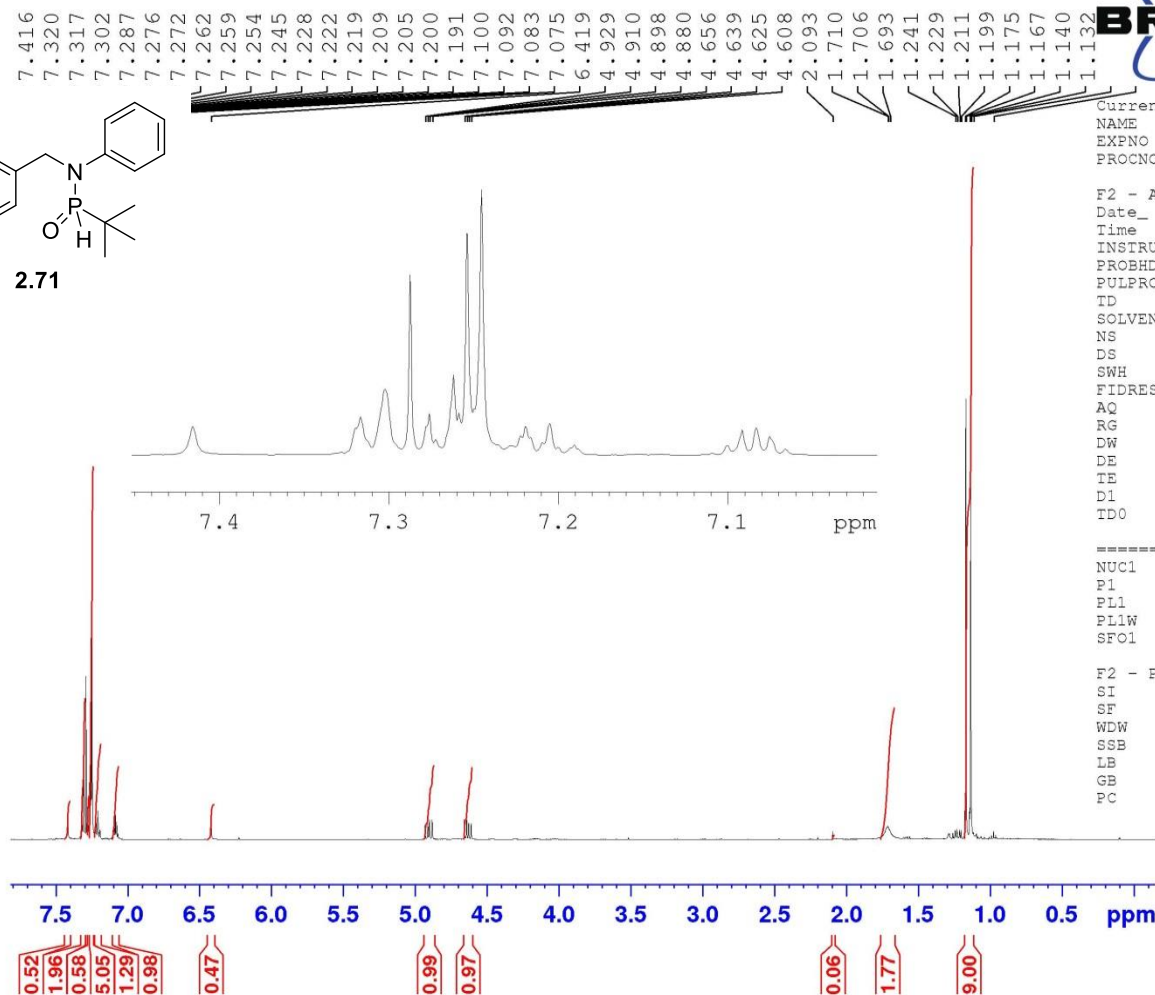
F2 - Processing parameters
SI 32768
SF 500.1300000 MHz
WDW EM
SSB 0
LB 0.30 Hz
GB 0
PC 1.00



benzyl aniline SPO formation



2.71



Current Data Parameters
 NAME I-Mn-101 1
 EXPNO 1
 PROCNO 1

F2 - Acquisition Parameters
 Date_ 20170110
 Time_ 17.42
 INSTRUM spect
 PROBHD 5 mm PAQXI 1H/
 PULPROG zg30
 TD 65536
 SOLVENT CDCl3
 NS 16
 DS 2
 SWH 10330.578 Hz
 FIDRES 0.157632 Hz
 AQ 3.1719425 sec
 RG 181
 DW 48.400 usec
 DE 6.50 usec
 TE 298.2 K
 D1 1.00000000 sec
 TDO 1

===== CHANNEL f1 =====
 NUC1 1H
 P1 8.60 usec
 PL1 4.00 dB
 PL1W 12.10000038 W
 SFO1 500.1330885 MHz

F2 - Processing parameters
 SI 32768
 SF 500.1300000 MHz
 WDW EM
 SSB 0
 LB 0.30 Hz
 GB 0
 PC 1.00

Attempted SPO formation with tosylated benzyl amine



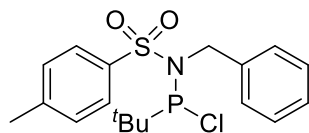
Current Data Parameters
 NAME I-Mn-110 crude
 EXPNO 1
 PROCNO 1

F2 - Acquisition Parameters
 Date_ 20170118
 Time 14.09
 INSTRUM spect
 PROBHD 5 mm PAQXI 1H/
 PULPROG zg30
 TD 65536
 SOLVENT CDCl3
 NS 16
 DS 2
 SWH 10330.578 Hz
 FIDRES 0.157632 Hz
 AQ 3.1719425 sec
 RG 90.5
 DW 48.400 usec
 DE 6.50 usec
 TE 298.3 K
 D1 1.00000000 sec
 TD0 1

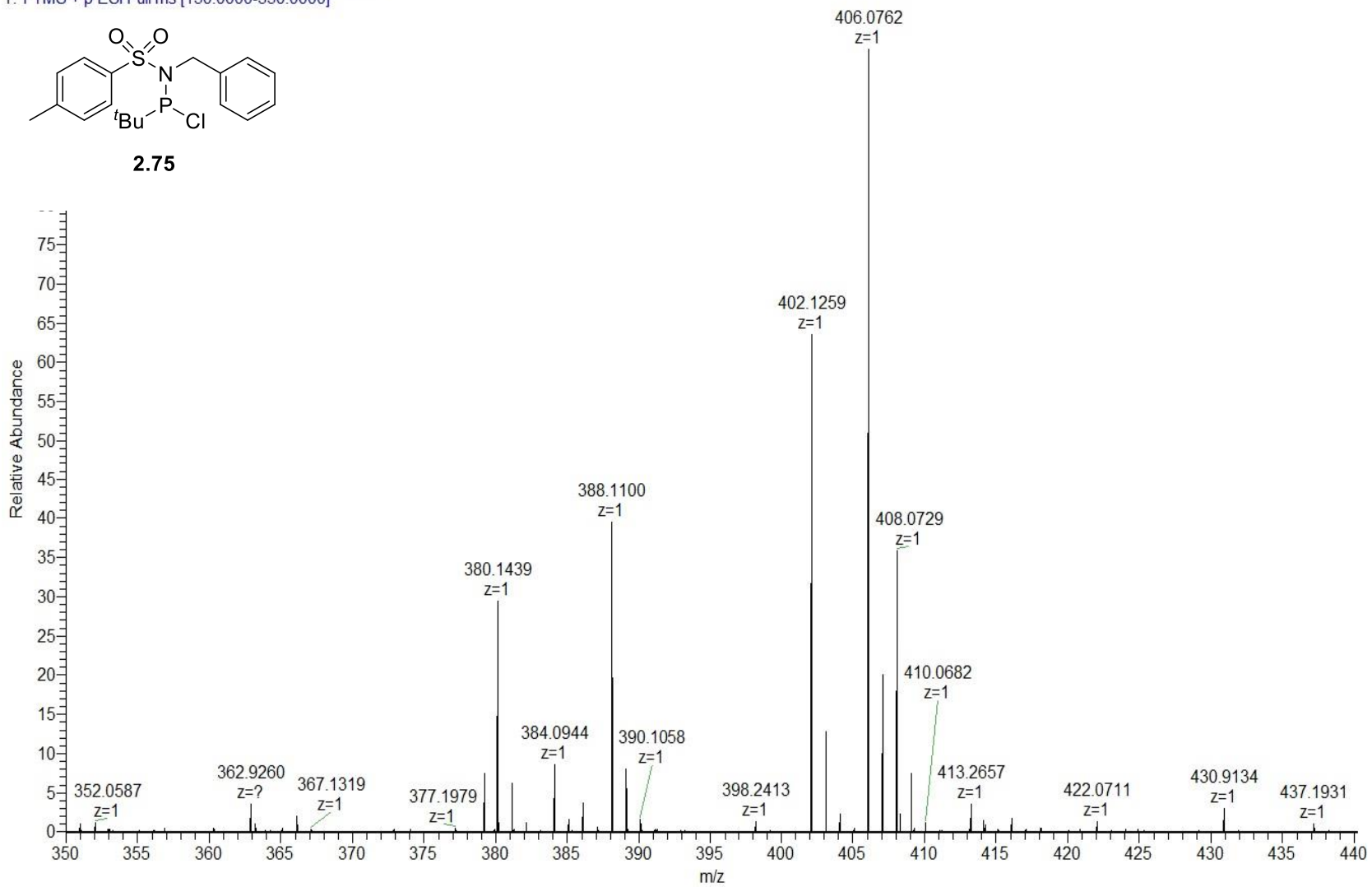
----- CHANNEL f1 -----
 NUC1 1H
 P1 8.60 usec
 PL1 4.00 dB
 PL1W 12.10000038 W
 SFO1 500.1330885 MHz

F2 - Processing parameters
 SI 32768
 SF 500.1300000 MHz
 WDW EM
 SSB 0
 LB 0.30 Hz
 GB 0
 PC 1.00

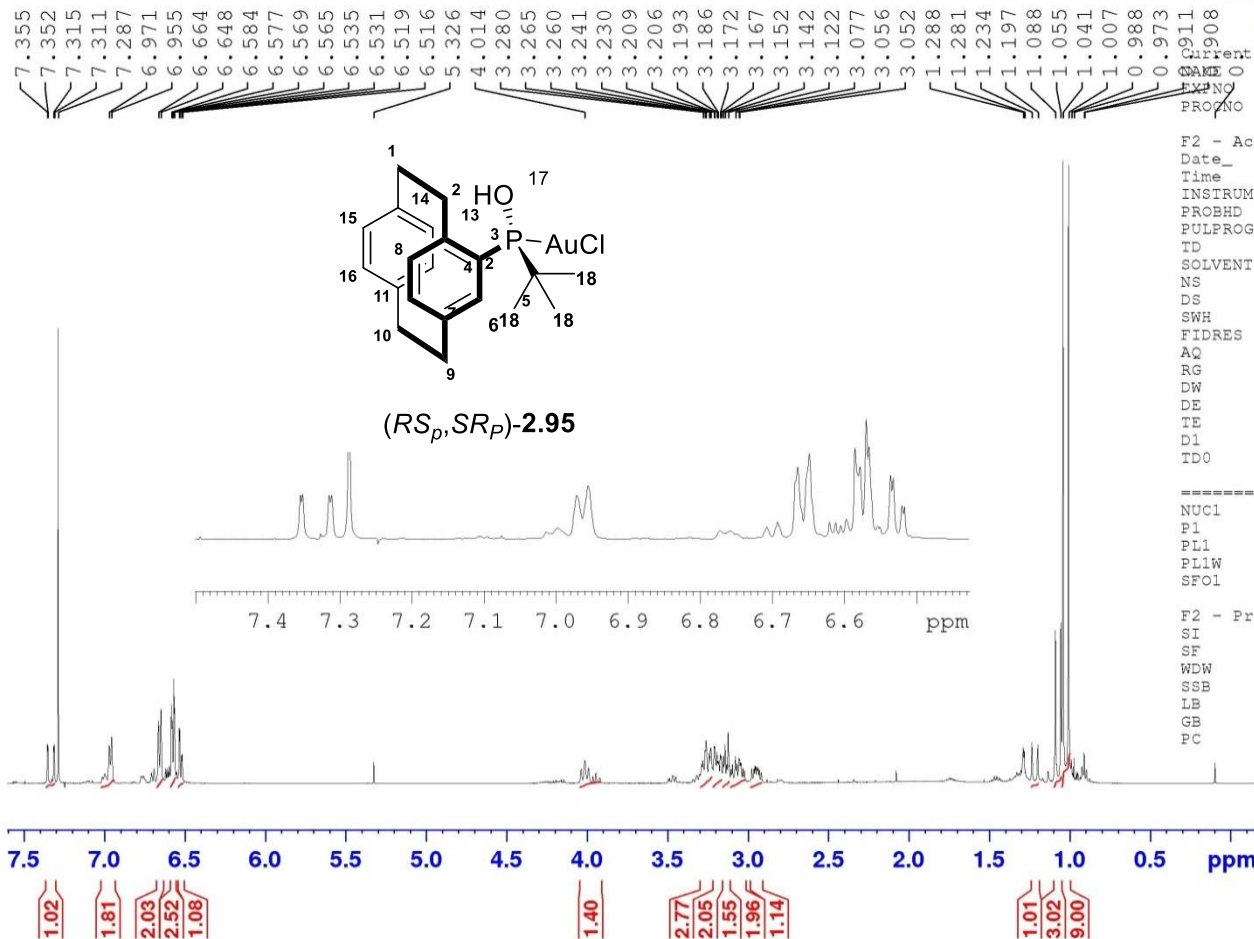
HMN-106 #38-87 RT: 0.17-0.39 AV: 50 NL: 8.03E7
T: FTMS + p ESI Full ms [150.0000-550.0000]



2.75



Gold complex formation - Filtrate



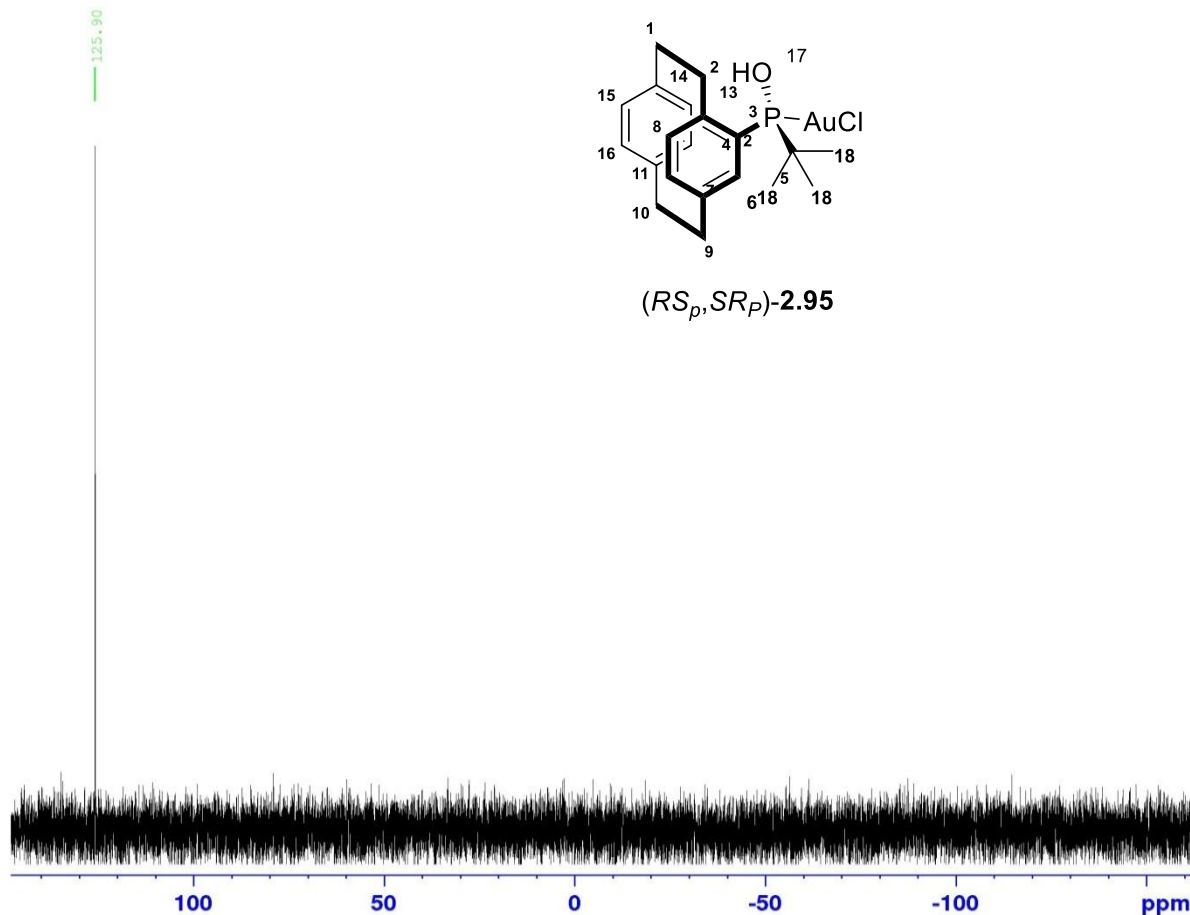
Data Parameters
 I-Mn-122 Filtrate
 F2NO 1
 PROXNO 1

F2 - Acquisition Parameters
 Date_ 20170203
 Time 9.22
 INSTRUM spect
 PROBHD 5 mm PAQXI 1H/
 PULPROG zg30
 TD 65536
 SOLVENT CDCl3
 NS 16
 DS 2
 SWH 10330.578 Hz
 FIDRES 0.157632 Hz
 AQ 3.1719425 sec
 RG 228.1
 DW 48.400 usec
 DE 6.50 usec
 TE 298.2 K
 D1 1.00000000 sec
 TDO 1

===== CHANNEL f1 =====
 NUC1 1H
 P1 8.60 usec
 PL1 4.00 dB
 PL1W 12.10000038 W
 SFO1 500.1330885 MHz

F2 - Processing parameters
 SI 32768
 SF 500.1300000 MHz
 WDW EM
 SSB 0
 LB 0.30 Hz
 GB 0
 PC 1.00

Au complex 31P after a week in CDCl3 solvent



Current Data Parameters
NAME Au complex 31P
EXPNO 2
PROCNO 1

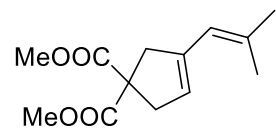
F2 - Acquisition Parameters
Date_ 20170427
Time 18.13
INSTRUM spect
PROBHD 5 mm PAQXI 1H/
PULPROG zgpg30
TD 65536
SOLVENT CDCl3
NS 32
DS 4
SWH 80645.164 Hz
FIDRES 1.230548 Hz
AQ 0.4063232 sec
RG 20642.5
DW 6.200 usec
DE 6.50 usec
TE 300.0 K
D1 2.0000000 sec
D11 0.0300000 sec
TDO 1

===== CHANNEL f1 =====
NUC1 31P
P1 20.00 usec
PL1 -2.40 dB
PL1W 131.39126587 W
SFO1 202.4462122 MHz

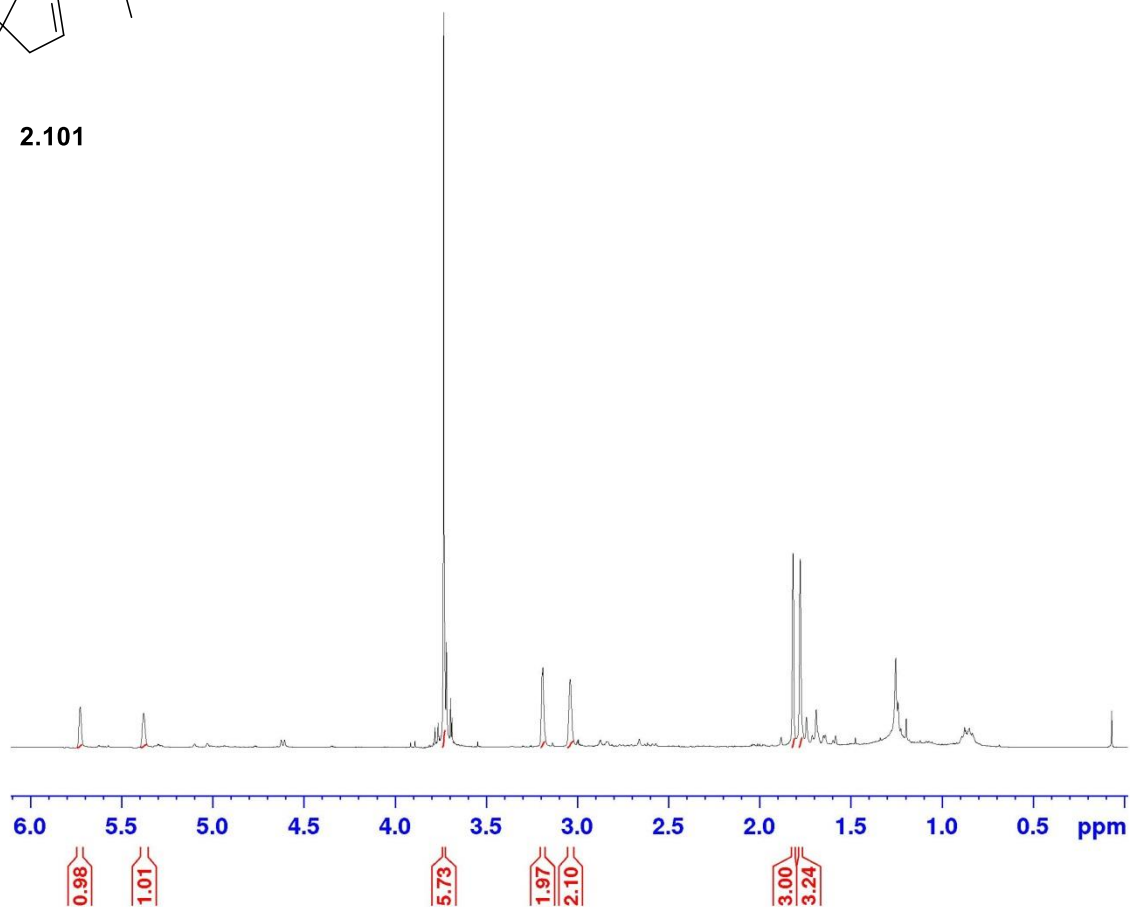
===== CHANNEL f2 =====
CPDPRG[2] waltz16
NUC2 1H
PCPD2 80.00 usec
PL2 4.00 dB
PL12 23.37 dB
PL13 25.00 dB
PL2W 12.10000038 W
PL12W 0.13988955 W
PL13W 0.09611372 W
SFO2 500.1320005 MHz

F2 - Processing parameters
SI 32768
SF 202.4563350 MHz
WDW EM
SSB 0
LB 1.00 Hz
GB 0
PC 1.40

P-Au catalysed cyclization in DCM



2.101



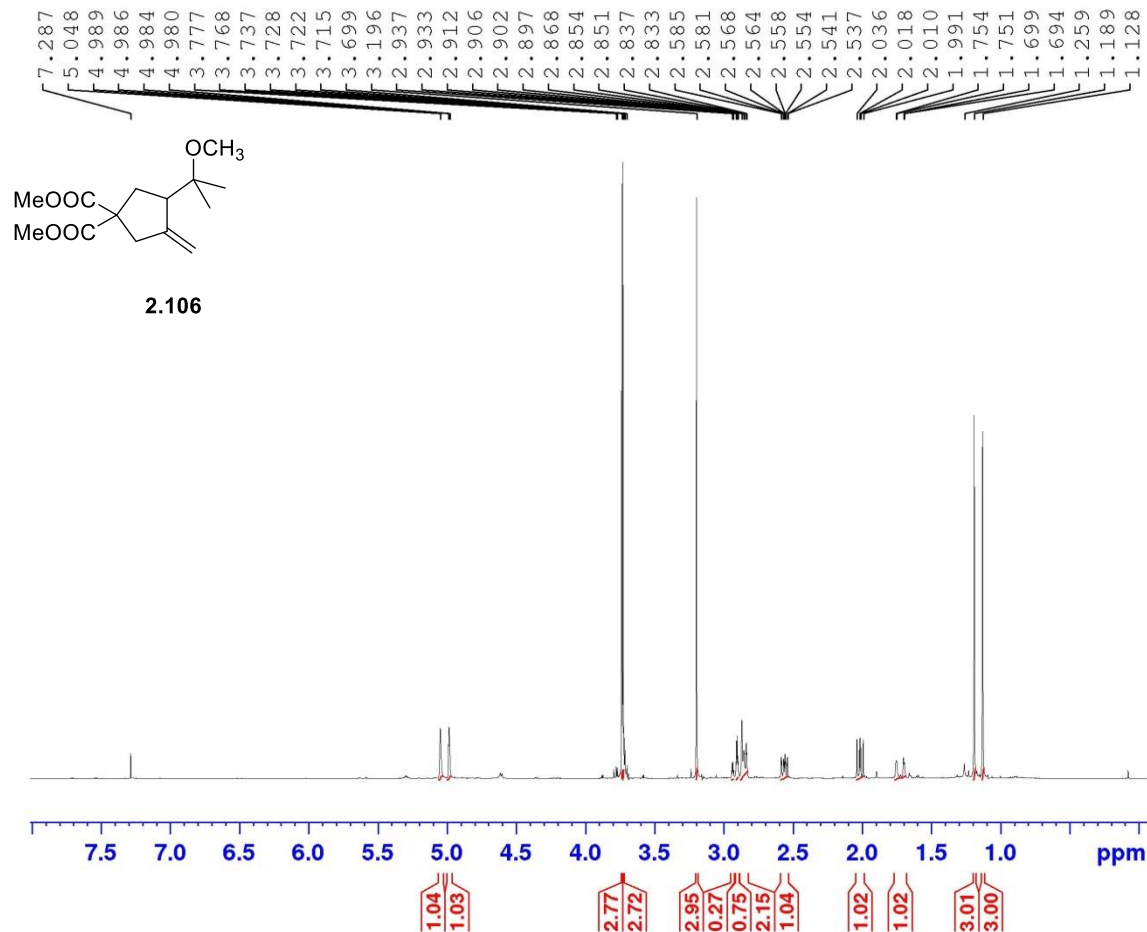
Current Data Parameters
NAME II-Mn-32 crude
EXPNO 1
PROCNO 1

F2 - Acquisition Parameters
Date_ 20170801
Time 14.12
INSTRUM spect
PROBHD 5 mm Multinucl
PULPROG zg30
TD 65536
SOLVENT CDCl3
NS 16
DS 2
SWH 8278.146 Hz
FIDRES 0.126314 Hz
AQ 3.9583745 sec
RG 20.2
DW 60.400 usec
DE 6.00 usec
TE 300.0 K
D1 1.00000000 sec
TD0 1

----- CHANNEL f1 -----
NUC1 1H
P1 10.00 usec
PL1 2.70 dB
SFO1 400.1324710 MHz

F2 - Processing parameters
SI 32768
SF 400.1300000 MHz
WDW EM
SSB 0
LB 0.30 Hz
GB 0
PC 1.00

Au catalysed methoxy cyclization



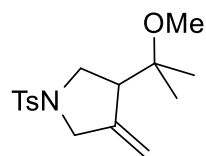
Current
NAME I-Mn-177 1 crude
EXPNO 1
PROCNO 1

F2 - Acquisition Parameters
Date_ 20170508
Time 11.56
INSTRUM spect
PROBHD 5 mm PAQXI 1H/
PULPROG zg30
TD 65536
SOLVENT CDCl3
NS 16
DS 2
SWH 10330.578 Hz
FIDRES 0.157632 Hz
AQ 3.1719425 sec
RG 35.9
DW 48.400 usec
DE 6.50 usec
TE 296.3 K
D1 1.00000000 sec
TD0 1

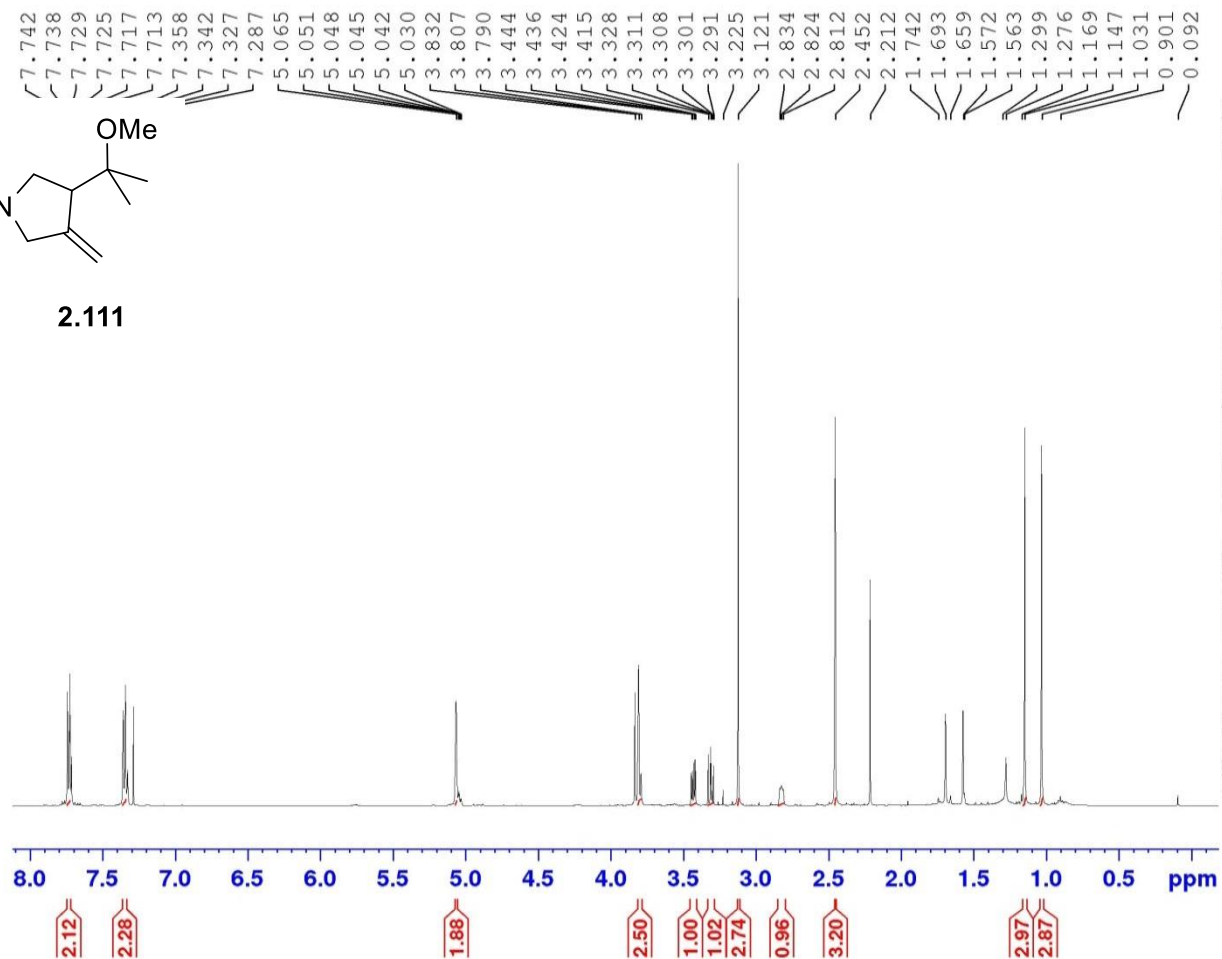
==== CHANNEL f1 =====
NUC1 1H
P1 8.60 usec
PL1 4.00 dB
PLLW 12.10000038 W
SFO1 500.1330885 MHz

F2 - Processing parameters
SI 32768
SF 500.1300000 MHz
WDW EM
SSB 0
LB 0.30 Hz
GB 0
PC 1.00

Au cyclization : tosyl



2.111



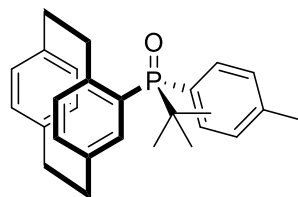
Current Data Parameters
NAME I-Mn-186 1
EXPNO 1
PROCNO 1

F2 - Acquisition Parameters
Date_ 20170506
Time 15.48
INSTRUM spect
PROBHD 5 mm PAQXI 1H/
PULPROG zg30
TD 65536
SOLVENT CDCl3
NS 16
DS 2
SWH 10330.578 Hz
FIDRES 0.157632 Hz
AQ 3.1719425 sec
RG 90.5
DW 48.400 usec
DE 6.50 usec
TE 297.9 K
D1 1.00000000 sec
TDO 1

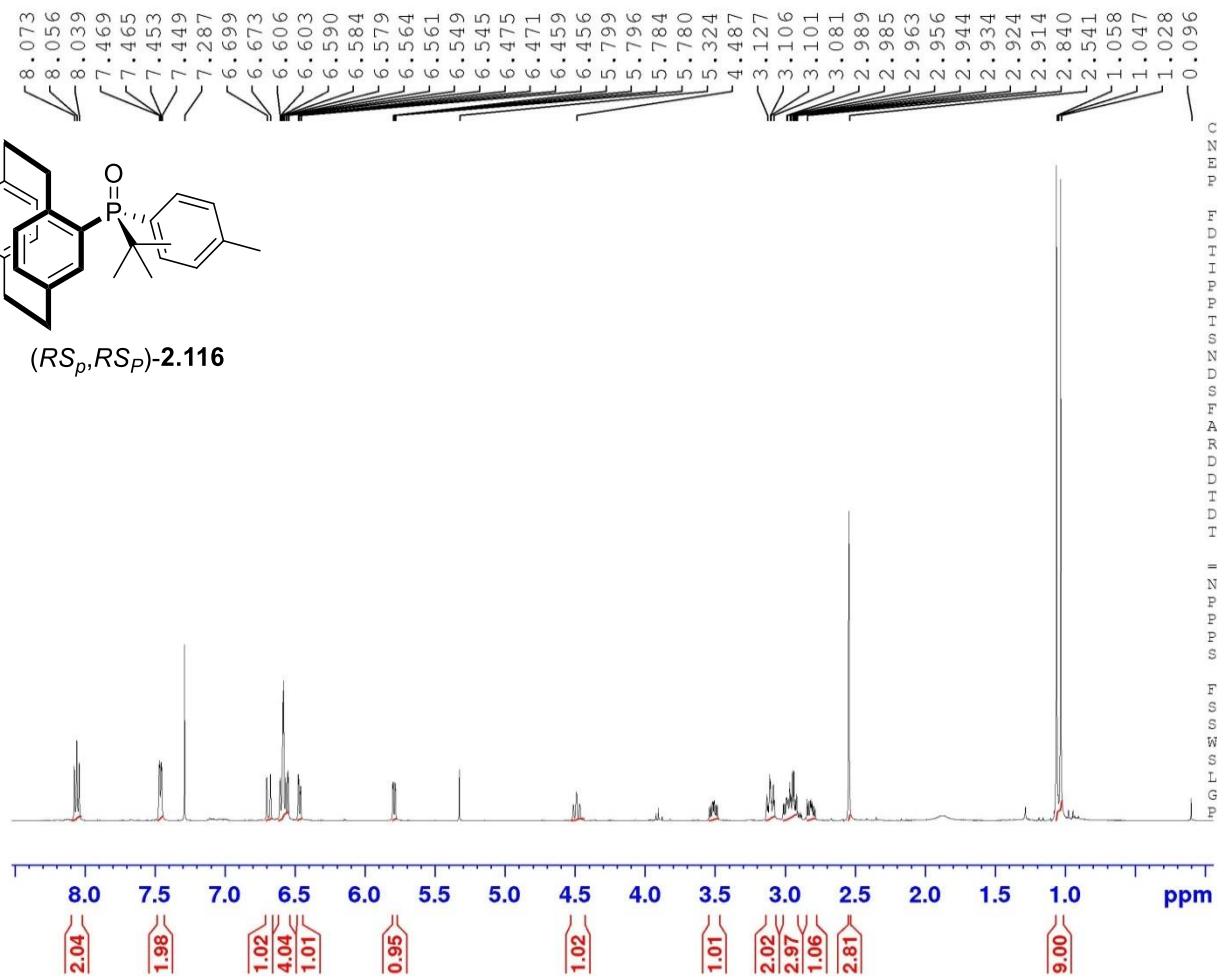
----- CHANNEL f1 -----
NUC1 1H
P1 8.60 usec
PL1 4.00 dB
PL1W 12.10000038 W
SFO1 500.1330885 MHz

F2 - Processing parameters
SI 32768
SF 500.1300000 MHz
WDW EM
SSB 0
LB 0.30 Hz
GB 0
PC 1.00

P-Arylation : 4-iodo toluene



(*RS_p*, *RS_p*)-2.116



Current Data Parameters
 NAME I-Mn-193 2
 EXPNO 1
 PROCNO 1

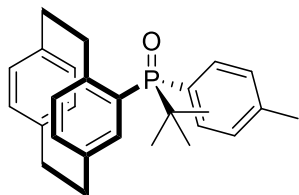
F2 - Acquisition Parameters
 Date_ 20170513
 Time 17.57
 INSTRUM spect
 PROBHD 5 mm PAQXI 1H/
 PULPROG zg30
 TD 65536
 SOLVENT CDCl3
 NS 16
 DS 2
 SWH 10330.578 Hz
 FIDRES 0.157632 Hz
 AQ 3.1719425 sec
 RG 128
 DW 48.400 usec
 DE 6.50 usec
 TE 296.0 K
 D1 1.00000000 sec
 TD0 1

==== CHANNEL f1 =====
 NUC1 1H
 P1 8.60 usec
 PL1 4.00 dB
 PL1W 12.10000038 W
 SF01 500.1330885 MHz

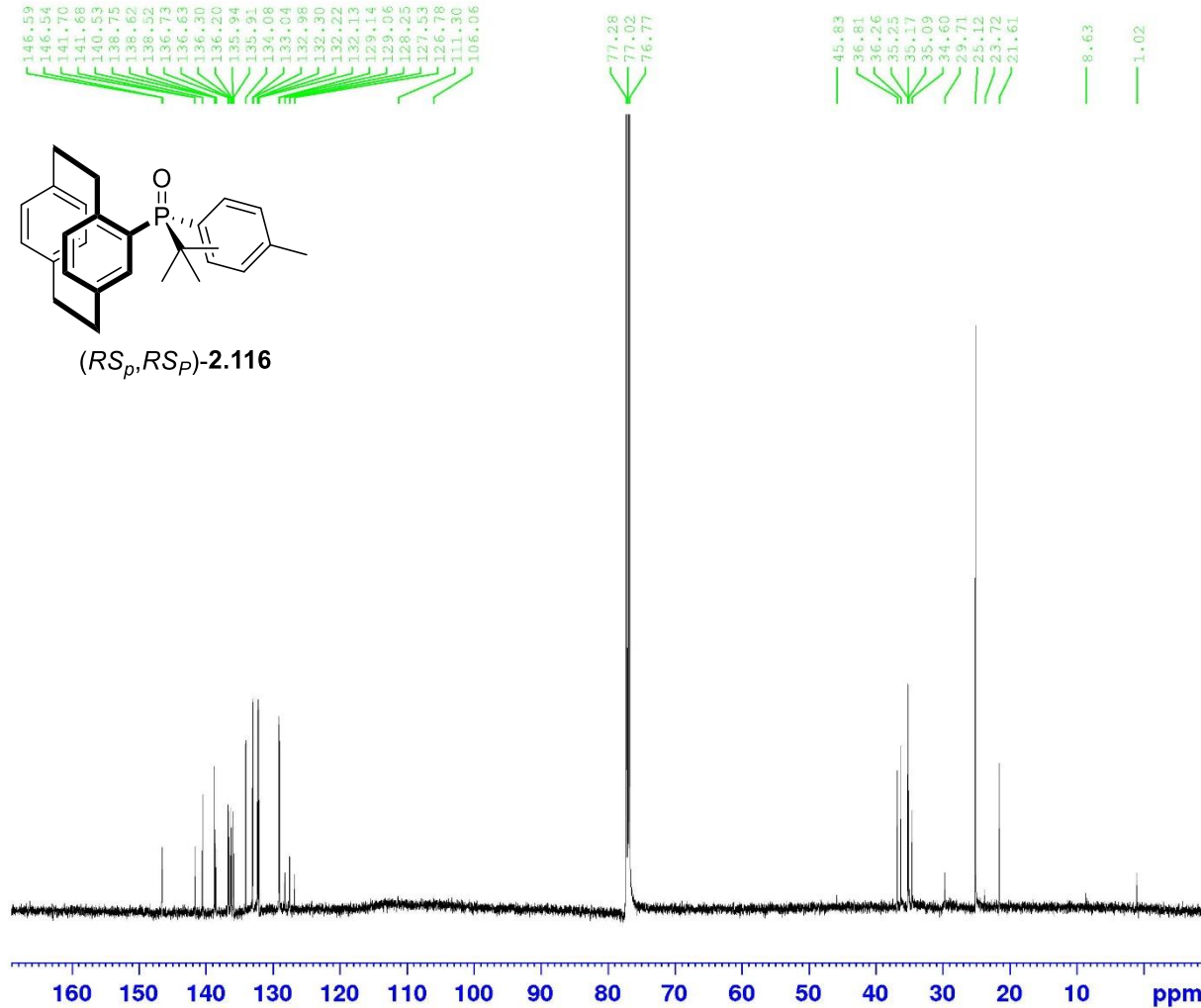
F2 - Processing parameters
 SI 32768
 SF 500.1300000 MHz
 WDW EM
 SSB 0
 LB 0.30 Hz
 GB 0
 PC 1.00

13C : SPO & p-tolyl

146.59
146.54
141.70
141.68
140.53
138.75
138.62
138.52
136.73
136.63
136.30
136.20
135.94
135.91
134.08
133.04
132.98
132.30
132.22
132.13
129.14
129.06
128.25
127.53
126.78
111.30
106.06



(*RS_p*,*RS_p*)-2.116



Current Data Parameters
NAME TPO-1 13C
EXPNO 1
PROCNO 1

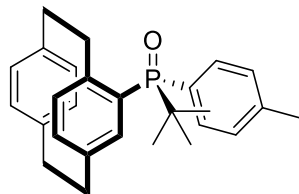
F2 - Acquisition Parameters
Date_ 20171004
Time 8.39
INSTRUM spect
PROBHD 5 mm PAQXI 1H/
PULPROG zgpg30
TD 65536
SOLVENT CDCl3
NS 15567
DS 4
SWH 30030.029 Hz
FIDRES 0.458222 Hz
AQ 1.0911744 sec
RG 32768
DW 16.650 usec
DE 6.50 usec
TE 298.2 K
D1 2.00000000 sec
D11 0.03000000 sec
TD0 1

----- CHANNEL f1 -----
NUC1 13C
P1 12.00 usec
PL1 -3.50 dB
PL1W 154.08152771 W
SFO1 125.7703643 MHz

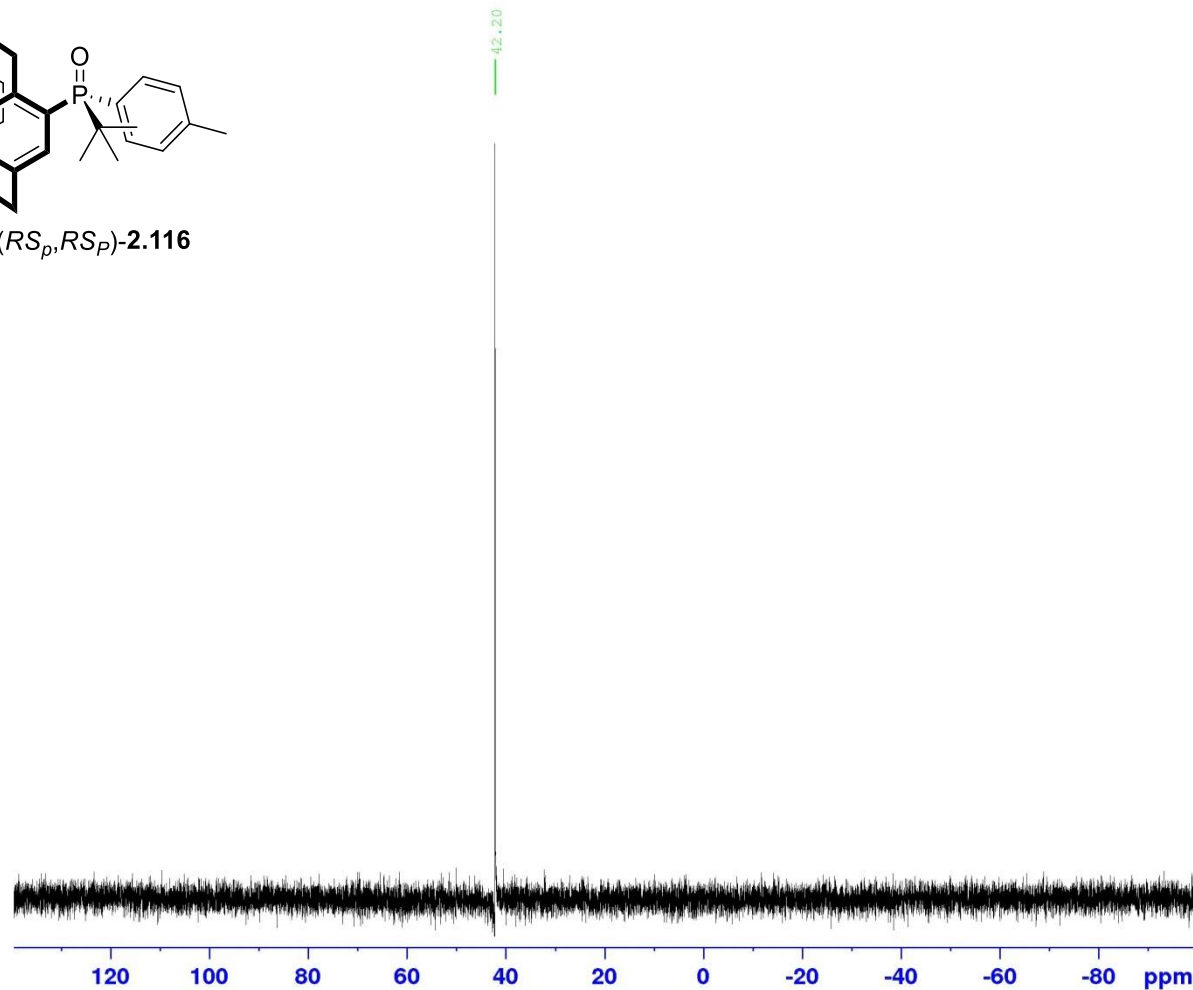
----- CHANNEL f2 -----
CPDPRG2 waltz16
NUC2 1H
PCPD2 80.00 usec
PL2 4.00 dB
PL12 23.37 dB
PL13 25.00 dB
PL2W 12.10000036 W
PL12W 0.13988955 W
PL13W 0.09612372 W
SFO2 500.1320005 MHz

F2 - Processing parameters
SI 32768
SF 125.7577890 MHz
WDW EM
SSB 0
LB 1.00 Hz
GB 0
FC 1.40

P-Arylation



(*RS_p*, *RS_p*)-2.116



Current Data Parameters
NAME I-Mn-155 1 P31
EXPNO 1
PROCNO 1

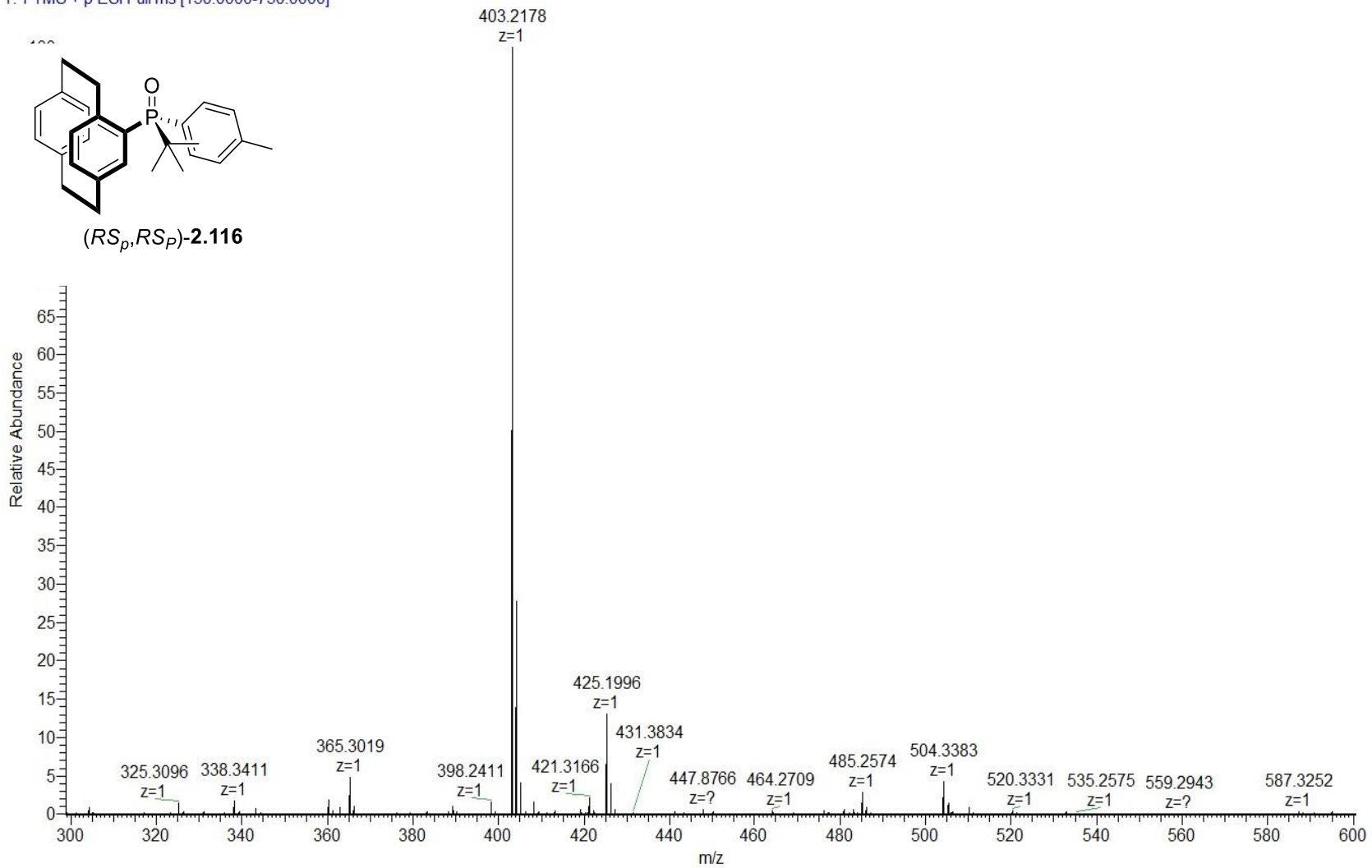
F2 - Acquisition Parameters
Date_ 20170405
Time 10.16
INSTRUM spect
PROBHD 5 mm PAQXI 1H/
PULPROG zgpg30
TD 65536
SOLVENT CDCl3
NS 64
DS 4
SWH 80645.164 Hz
FIDRES 1.230548 Hz
AQ 0.4063232 sec
RG 20642.5
DW 6.200 usec
DE 6.50 usec
TE 296.5 K
D1 2.0000000 sec
D11 0.0300000 sec
TD0 1

===== CHANNEL f1 =====
NUC1 31P
P1 20.00 usec
PL1 -2.40 dB
PL1W 131.39126587 W
SFO1 202.4462122 MHz

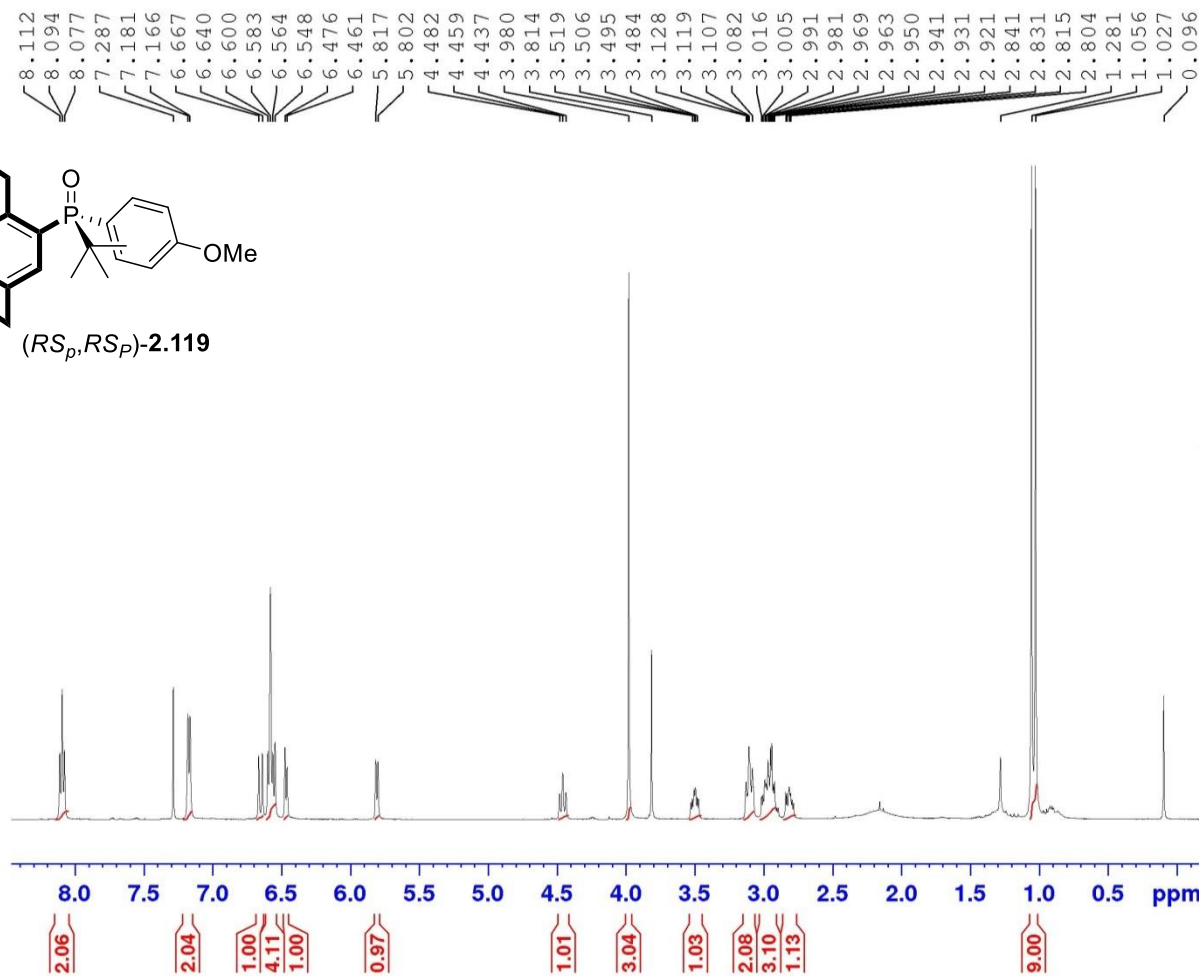
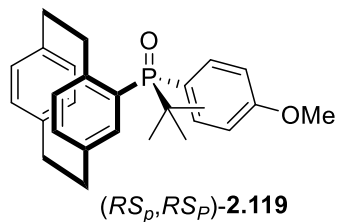
===== CHANNEL f2 =====
CPDPRG[2] waltz16
NUC2 1H
PCPD2 80.00 usec
PL2 4.00 dB
PL12 23.37 dB
PL13 25.00 dB
PL2W 12.10000038 W
PL12W 0.13988955 W
PL13W 0.09611372 W
SFO2 500.1320005 MHz

F2 - Processing parameters
SI 32768
SF 202.4563350 MHz
WDW EM
SSB 0
LB 1.00 Hz
GB 0
PC 1.40

HMN-175 #36-96 RT: 0.17-0.43 AV: 61 NL: 2.13E8
T: FTMS + p ESI Full ms [150.0000-750.0000]



P-arylation : 4-iodo anisole



```

Current Data Parameters
NAME      I-Mn-165 ii 0807
EXPNO     1
PROCNO    1

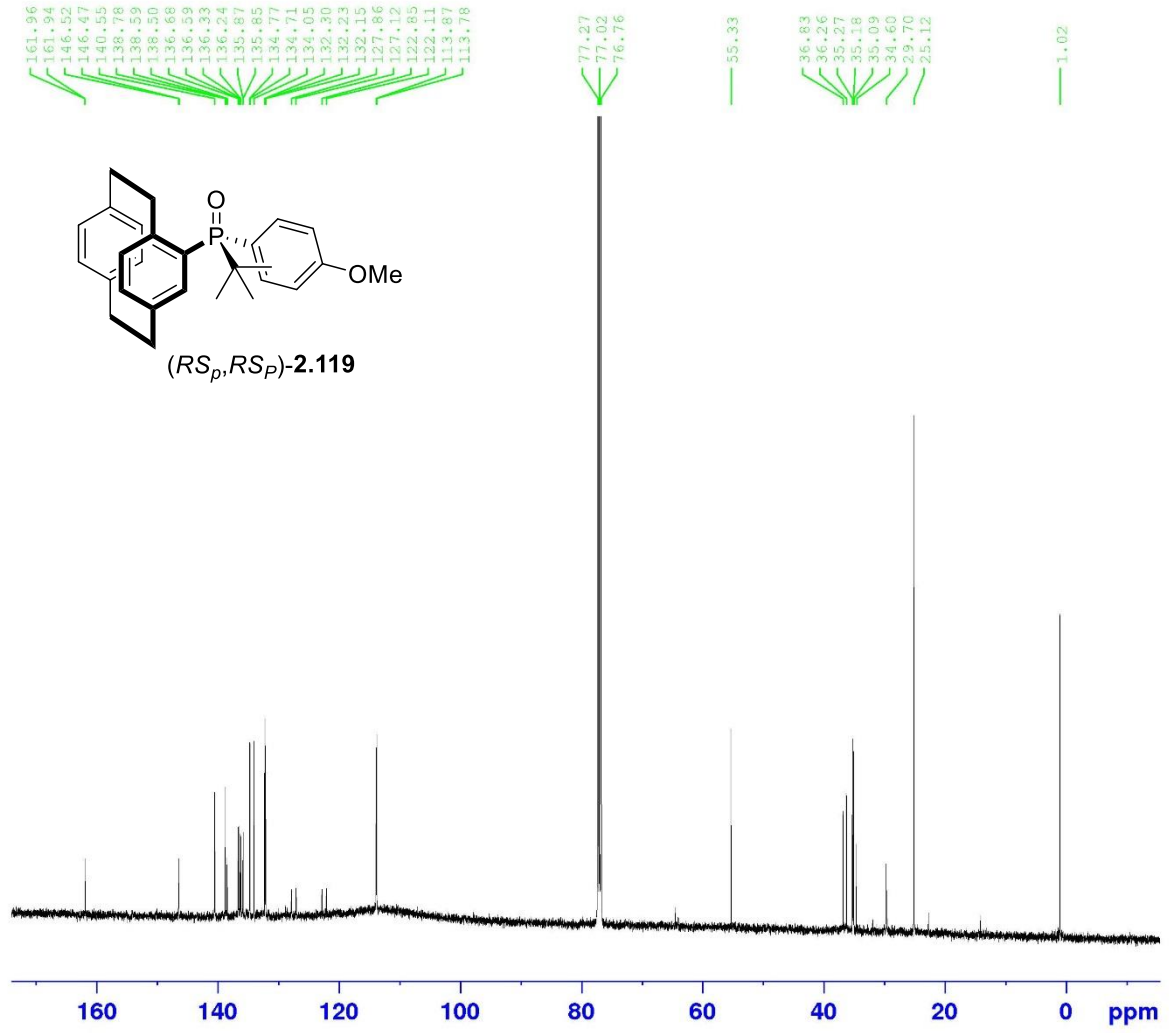
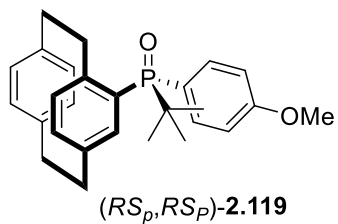
F2 - Acquisition Parameters
Date_     20170708
Time      14.12
INSTRUM   spect
PROBHD    5 mm PAQXI 1H/
PULPROG   zg30
ID        65536
SOLVENT   CDCl3
NS        16
DS        2
SWH       10330.578 Hz
FIDRES    0.157632 Hz
AQ        3.1719425 sec
RG        114
DW        48.400 usec
DE        6.50 usec
TE        298.2 K
D1        1.00000000 sec
TD0       1

----- CHANNEL f1 -----
NUC1      1H
P1        8.60 usec
PL1       4.00 dB
PL1W      12.10000038 W
SFO1      500.1330885 MHz

F2 - Processing parameters
SI        32768
SF        500.1300000 MHz
WDW       EM
SSB       0
LB        0.30 Hz
GB        0
PC        1.00
    
```

13C - TPO-2 210118

161.96
161.94
146.52
146.47
140.55
138.78
138.59
138.50
136.68
136.59
136.33
136.24
135.87
135.85
134.77
134.71
134.05
132.30
132.23
132.15
127.86
127.12
122.85
122.11
113.87
113.78



Current Data Parameters
NAME TPO-2 210118 13C
EXPNO 1
PROCNO 1

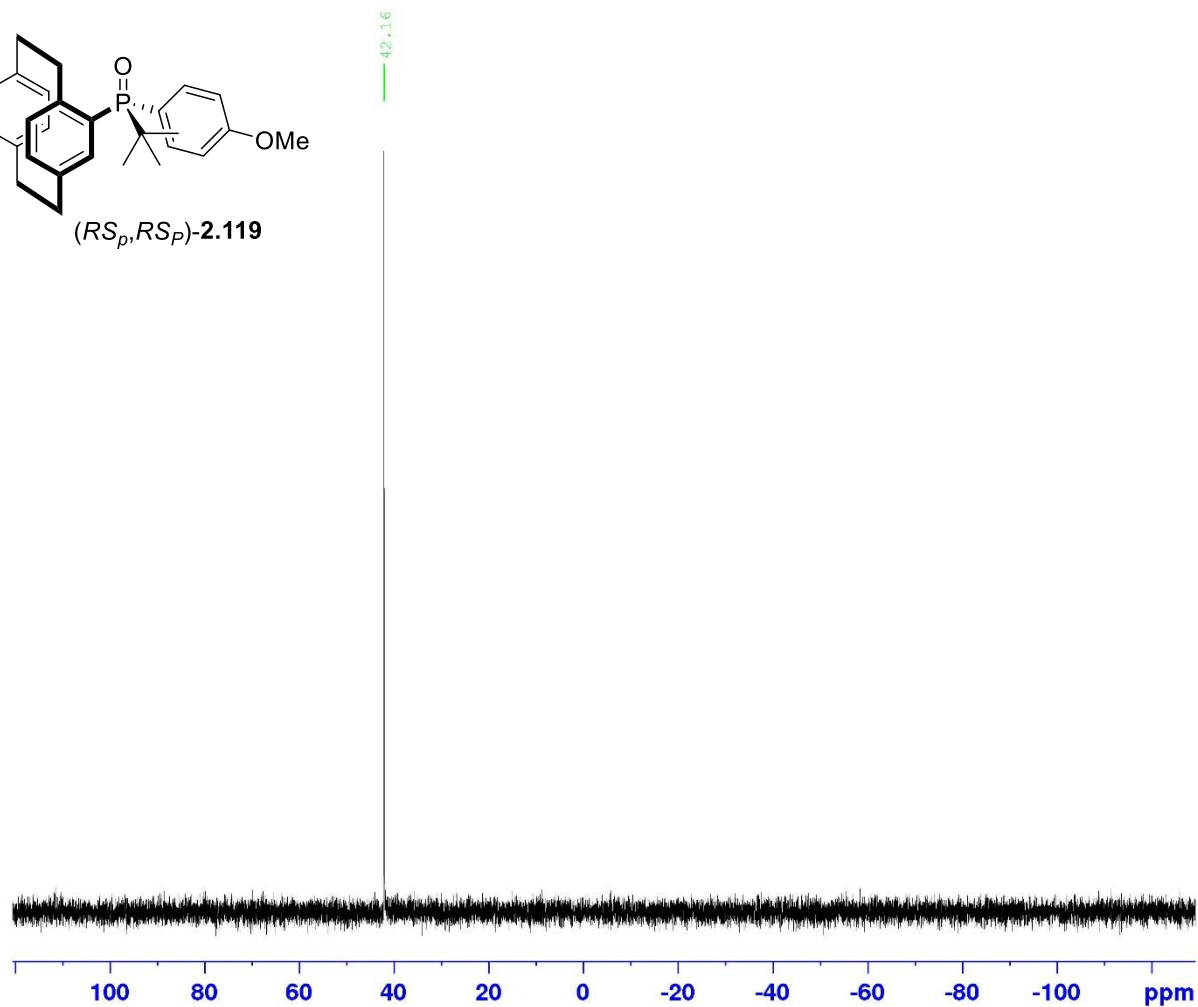
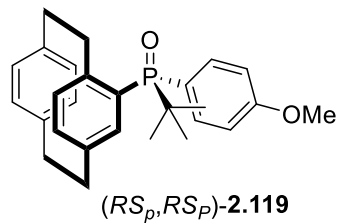
F2 - Acquisition Parameters
Date_ 20180125
Time 7.40
INSTRUM spect
PROBHD 5 mm PAQXI 1H/
PULPROG zgpg30
TD 65536
SOLVENT CDCl3
NS 11350
DS 4
SWH 30030.029 Hz
FIDRES 0.458222 Hz
AQ 1.0911744 sec
RG 32768
DW 16.650 usec
DE 6.50 usec
TE 299.1 K
D1 2.0000000 sec
D11 0.0300000 sec
TD0 1

===== CHANNEL f1 =====
NUC1 13C
P1 12.00 usec
PL1 -3.50 dB
PL1W 154.08152771 W
SFO1 125.7703643 MHz

===== CHANNEL f2 =====
CPDPRG[2] waltz16
NUC2 1H
PCPD2 80.00 usec
PL2 4.00 dB
PL12 23.37 dB
PL13 25.00 dB
PL12W 12.10000038 W
PL12W 0.13988955 W
PL13W 0.09611372 W
SFO2 500.1320005 MHz

F2 - Processing parameters
SI 32768
SF 125.7577890 MHz
WDW EM
SSB 0
LB 1.00 Hz
GB 0
PC 1.40

31P - TPO-2 210118



Current Data Parameters
NAME TPO-2 210118 13P
EXPNO 1
PROCNO 1

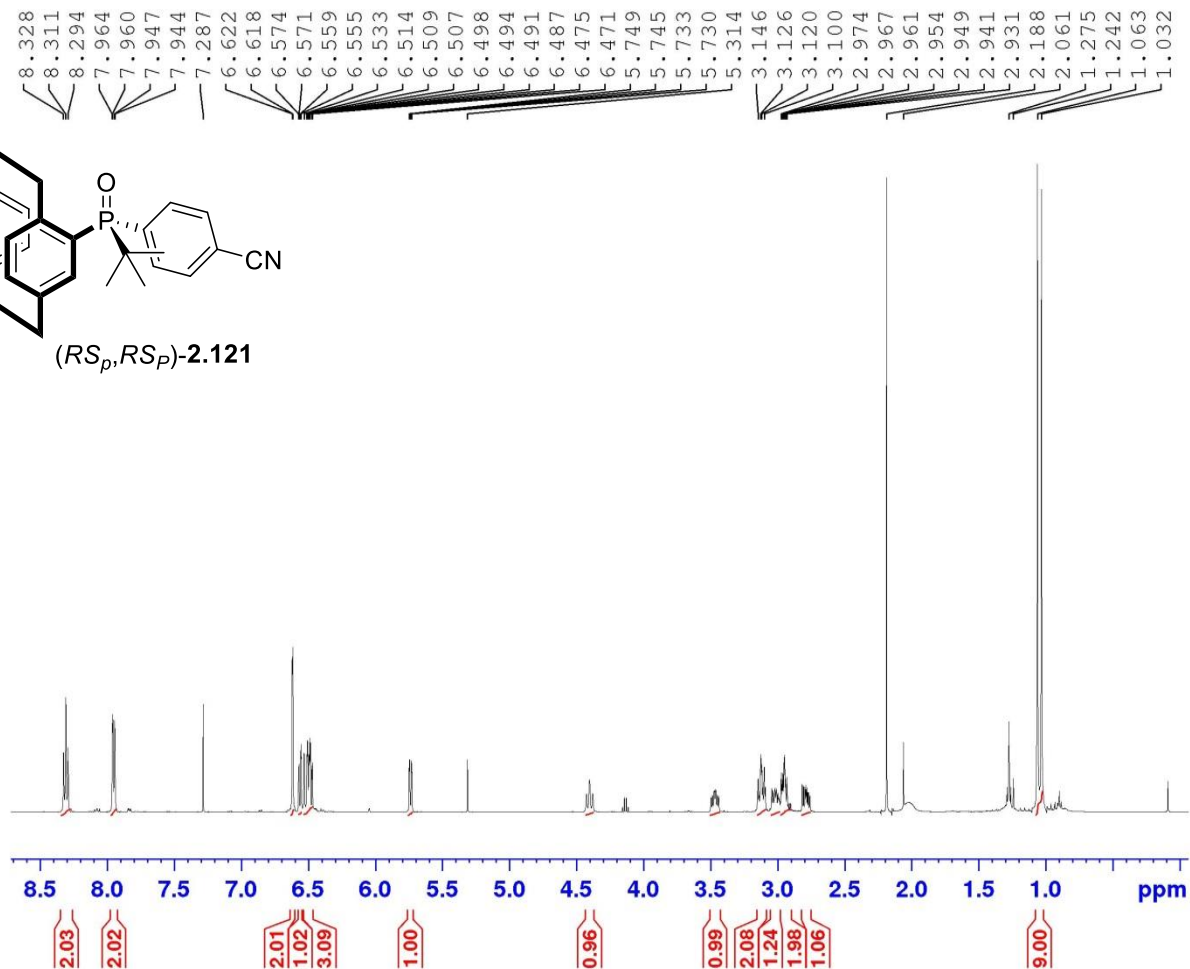
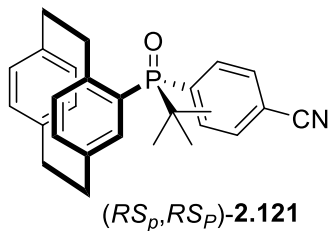
F2 - Acquisition Parameters
Date_ 20180125
Time 7.56
INSTRUM spect
PROBHD 5 mm PAQXI 1H/
PULPROG zgpg30
TD 65536
SOLVENT CDCl3
NS 64
DS 4
SWH 80645.164 Hz
FIDRES 1.230548 Hz
AQ 0.4063232 sec
RG 20642.5
DW 6.200 usec
DE 6.50 usec
TE 298.9 K
D1 2.0000000 sec
D11 0.0300000 sec
TDC 1

===== CHANNEL f1 =====
NUC1 31P
P1 20.00 usec
PL1 -2.40 dB
PL1W 131.39126587 W
SFO1 202.4462122 MHz

===== CHANNEL f2 =====
CPDPRG[2] waltz16
NUC2 1H
PCPD2 80.00 usec
PL2 4.00 dB
PL12 23.37 dB
PL13 25.00 dB
PL2W 12.10000038 W
PL12W 0.13988955 W
PL13W 0.09611372 W
SFO2 500.1320005 MHz

F2 - Processing parameters
SI 32768
SF 202.4563350 MHz
WDW EM
SSB 0
LB 1.00 Hz
GB 0
PC 1.40

P-Arylation : 4-iodo-benzonitrile



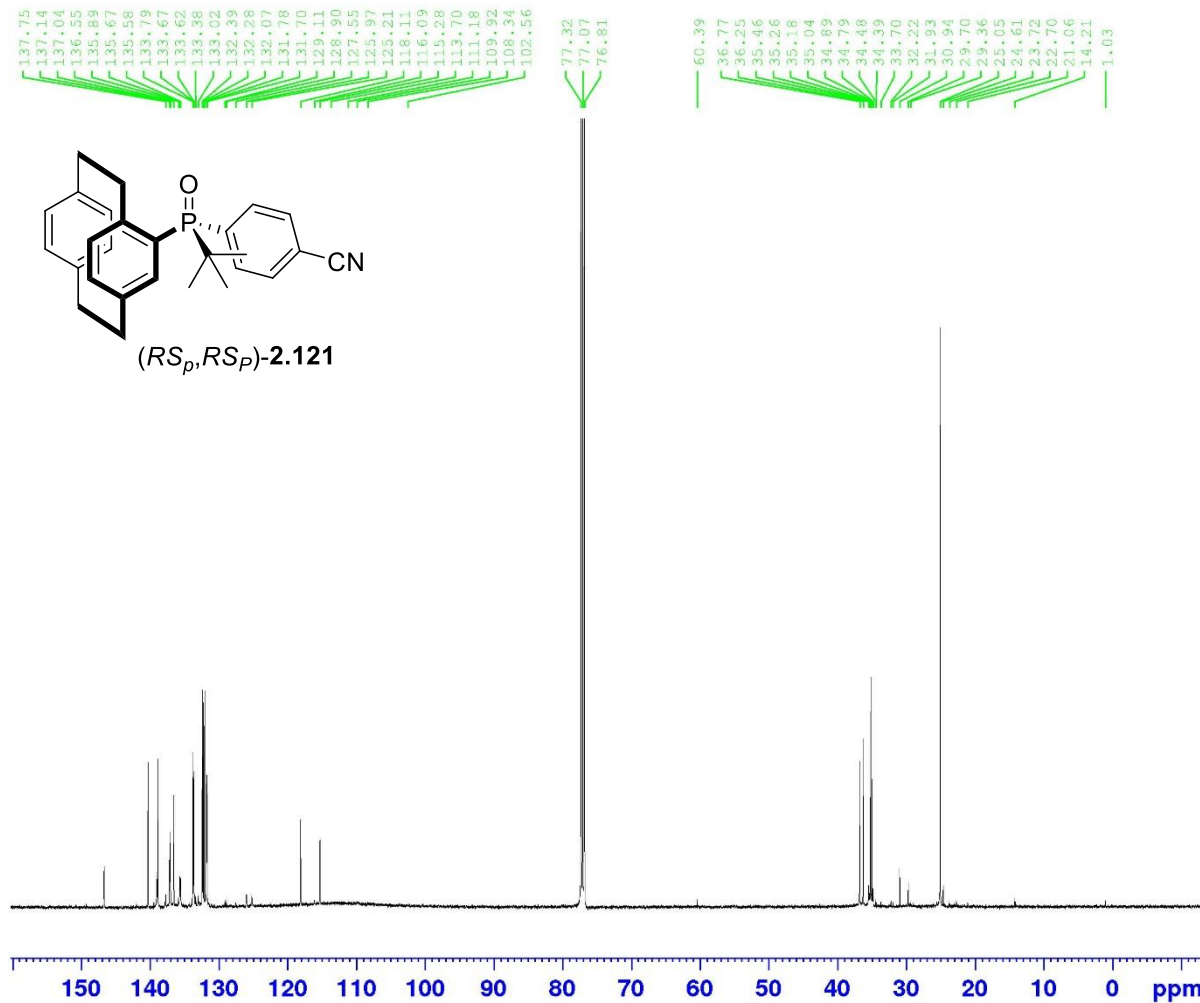
Current Data Parameters
 NAME I-Mn-165 iii
 EXPNO 1
 PROCNO 1

F2 - Acquisition Parameters
 Date_ 20170513
 Time 11.14
 INSTRUM spect
 PROBHD 5 mm PAQXI 1H/
 PULPROG zg30
 TD 65536
 SOLVENT CDCl3
 NS 16
 DS 2
 SWH 10330.578 Hz
 FIDRES 0.157632 Hz
 AQ 3.1719425 sec
 RG 64
 DW 48.400 usec
 DE 6.50 usec
 TE 295.4 K
 D1 1.00000000 sec
 TD0 1

===== CHANNEL f1 =====
 NUC1 1H
 P1 8.60 usec
 PL1 4.00 dB
 PL1W 12.10000038 W
 SFO1 500.1330885 MHz

F2 - Processing parameters
 SI 32768
 SF 500.1300000 MHz
 WDW EM
 SSB 0
 LB 0.30 Hz
 GE 0
 PC 1.00

13C : SPO & 4-iodobezonitrile



Current Data Parameters
 NAME TPO-iii 13C
 EXPNO 1
 PROCNO 1

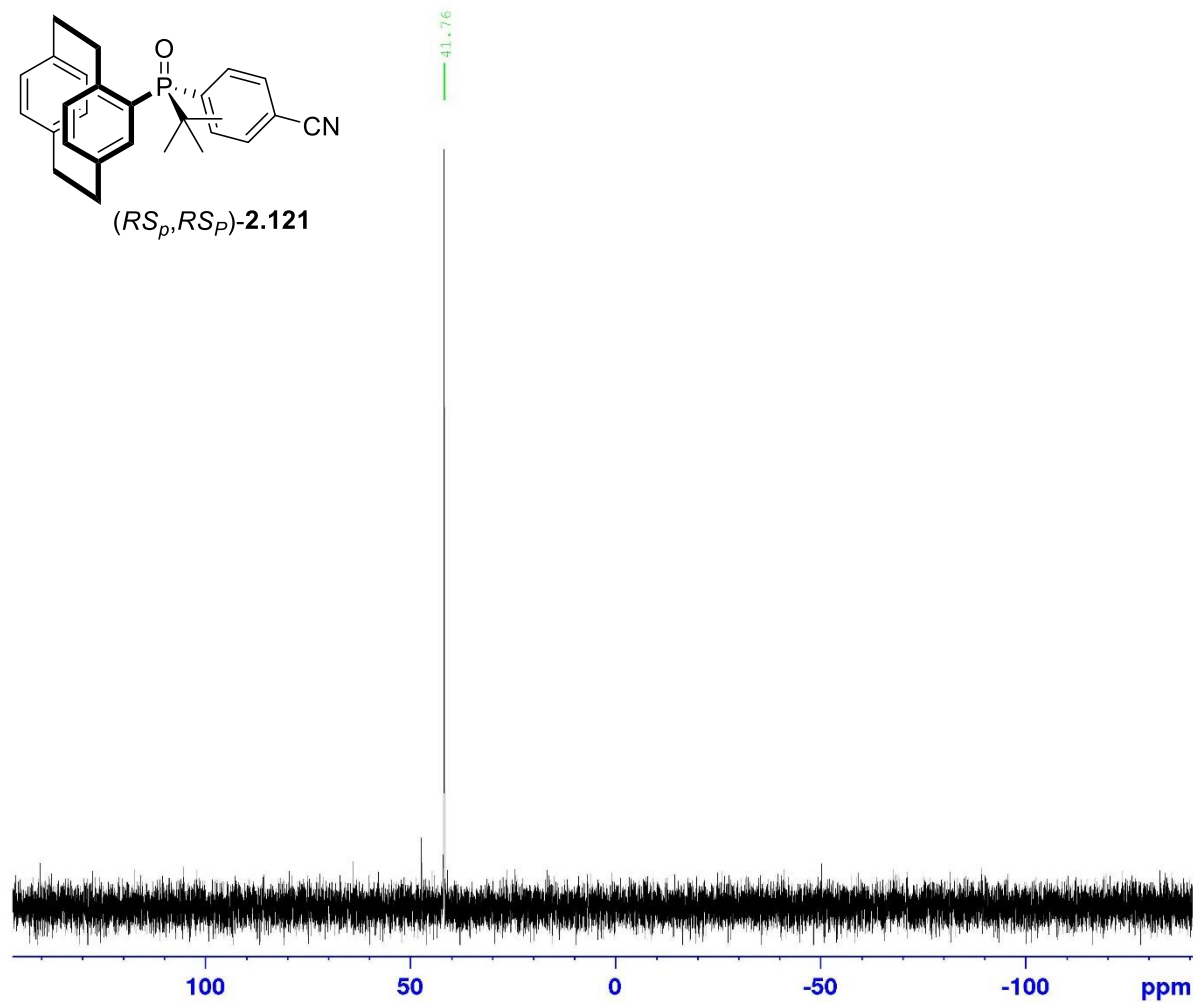
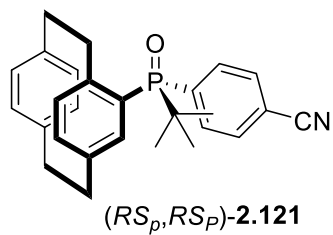
F2 - Acquisition Parameters
 Date_ 20170928
 Time 8.26
 INSTRUM spect
 PROBHD 5 mm PAQXI 1H/
 PULPROG zgpg30
 TD 65336
 SOLVENT CDCl3
 NS 15435
 DS 4
 SWH 30030.029 Hz
 FIDRES 0.458222 Hz
 AQ 1.0911744 sec
 RG 32768
 DW 16.650 usec
 DE 6.50 usec
 TE 298.2 K
 D1 2.0000000 sec
 D11 0.0300000 sec
 TD0 1

===== CHANNEL f1 =====
 NUC1 13C
 P1 12.00 usec
 PL1 -3.50 dB
 PL1W 154.08152771 W
 SFO1 125.7703643 MHz

===== CHANNEL f2 =====
 CPDPRG[2] waltz16
 NUC2 1H
 PCPD2 80.00 usec
 PL2 4.00 dB
 PL12 23.37 dB
 PL13 25.00 dB
 PL2W 12.10000038 W
 PL12W 0.13988955 W
 PL13W 0.09611372 W
 SFO2 500.1320005 MHz

F2 - Processing parameters
 SI 32768
 SF 125.7577890 MHz
 WDW EM
 SSB 0
 LB 1.00 Hz
 GB 0
 PC 1.40

TPO-3, p-benzonitrile



Current Data Parameters
NAME TPO-3 31P
EXPNO 1
PROCNO 1

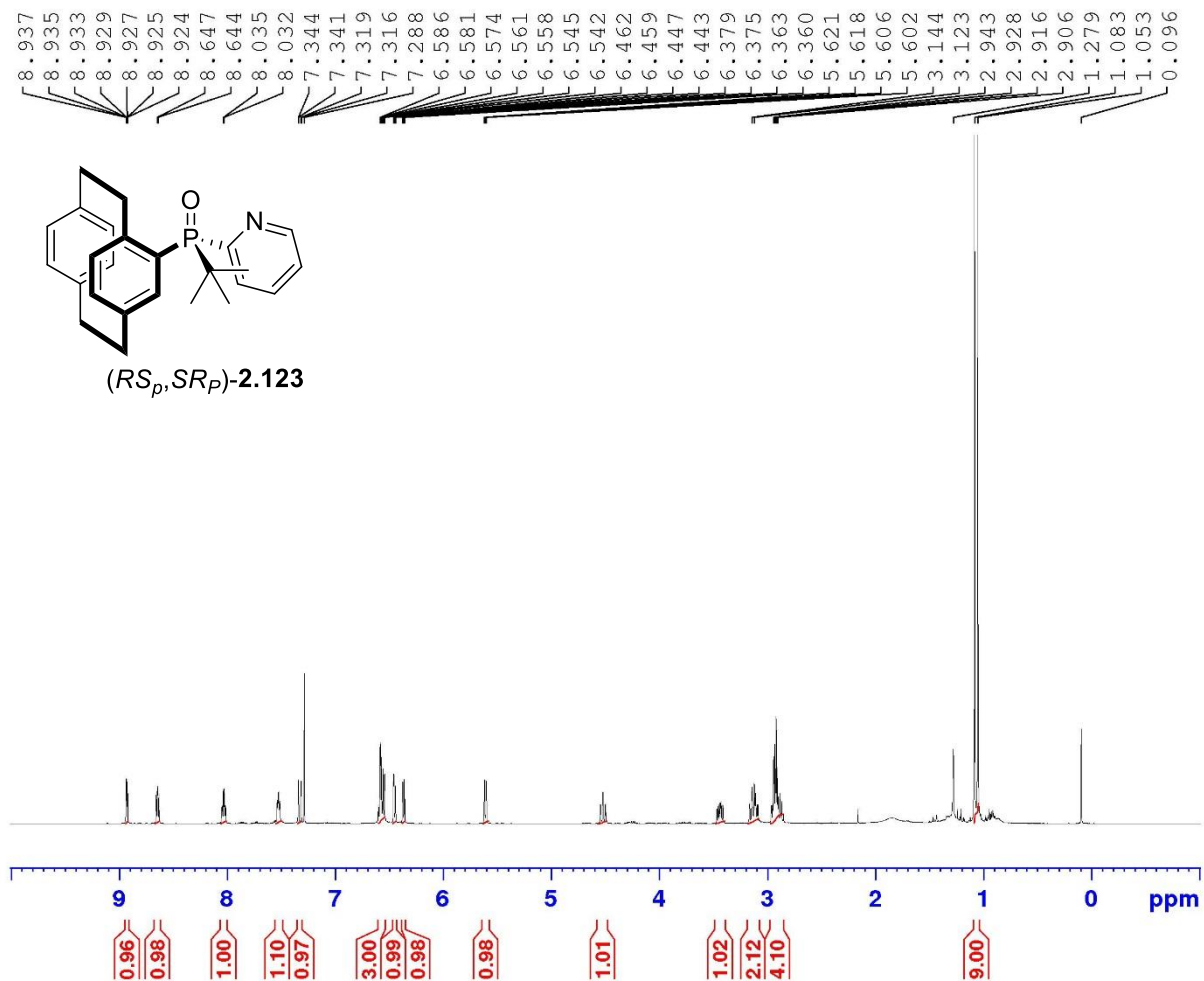
F2 - Acquisition Parameters
Date_ 20171012
Time 18.42
INSTRUM spect
PROBHD 5 mm PAQXI 1H/
PULPROG zgpg30
TD 65536
SOLVENT CDC13
NS 16
DS 4
SWH 80645.164 Hz
FIDRES 1.230548 Hz
AQ 0.4063232 sec
RG 20642.5
DW 6.200 usec
DE 6.50 usec
TE 298.3 K
D1 2.0000000 sec
D11 0.0300000 sec
TDC 1

===== CHANNEL f1 =====
NUC1 31P
P1 20.00 usec
PL1 -2.40 dB
PL1W 131.39126587 W
SFO1 202.4462122 MHz

===== CHANNEL f2 =====
CPDPRG[2] waltz16
NUC2 1H
PCPD2 80.00 usec
PL2 4.00 dB
PL12 23.37 dB
PL13 25.00 dB
PL2W 12.10000038 W
PL12W 0.13988955 W
PL13W 0.09611372 W
SFO2 500.1320005 MHz

F2 - Processing parameters
SI 32768
SF 202.4563350 MHz
WDW EM
SSB 0
LB 1.00 Hz
GB 0
PC 1.40

P-Arylation SPO & 2-Br pyridine



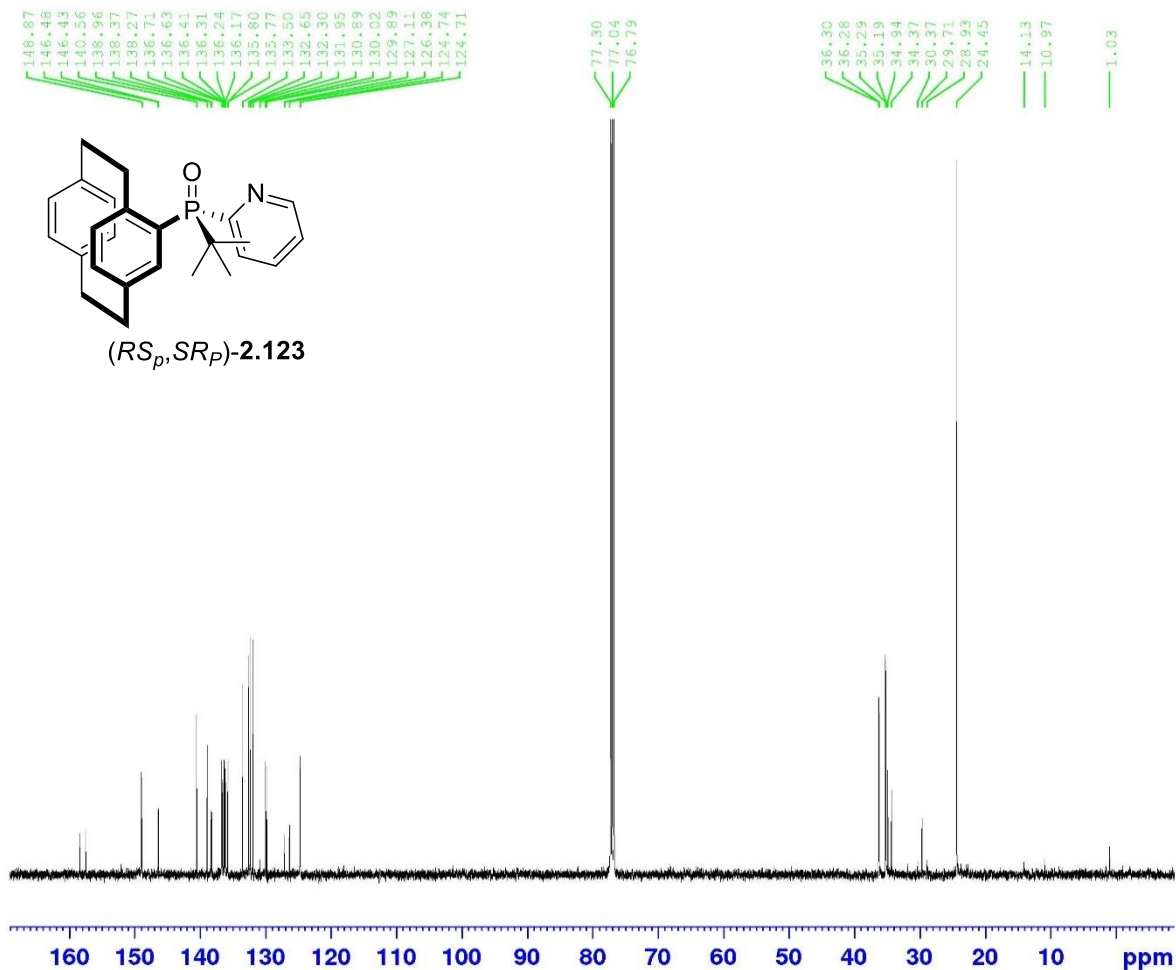
Current Data Parameters
 NAME I-Mn-165 iv 2
 EXPNO 1
 PROCNO 1

F2 - Acquisition Parameters
 Date_ 20170603
 Time 15.00
 INSTRUM spect
 PROBHD 5 mm PAQXI 1H/
 PULPROG zg30
 TD 65536
 SOLVENT CDCl3
 NS 16
 DS 2
 SWH 10330.578 Hz
 FIDRES 0.157632 Hz
 AQ 3.1719425 sec
 RG 114
 DW 48.400 usec
 DE 6.50 usec
 TE 295.8 K
 D1 1.00000000 sec
 TD0 1

===== CHANNEL f1 =====
 NUC1 1H
 P1 8.60 usec
 PL1 4.00 dB
 PLLW 12.10000038 W
 SFO1 500.1330885 MHz

F2 - Processing parameters
 SI 32768
 SF 500.1300000 MHz
 WDW EM
 SSB 0
 LB 0.30 Hz
 GB 0
 PC 1.00

13C : P-arylation : SPO & 2-Br pyridine



```

Current Data Parameters
NAME      11-Mn-163 iv 09092017 13C
EXPNO    1
PROCNO   1

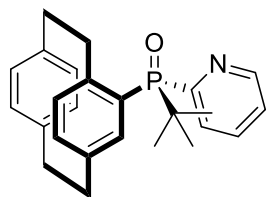
F2 - Acquisition Parameters
Date_    20170909
Time     14.03
INSTRUM  spect
PROBHD   5 mm PAQXI 1H/
PULPROG  zgpg30
TD       65536
SOLVENT  CDCl3
NS       1852
DS       4
SWH      30030.029 Hz
FIDRES   0.458222 Hz
AQ       1.0911744 sec
RG       32768
DW       16.650 usec
DE       6.50 usec
TE       298.2 K
D1       2.0000000 sec
D11      0.9300000 sec
TD0      1

----- CHANNEL f1 -----
NUC1     13C
P1       12.00 usec
PL1      -3.50 dB
PL1W     154.08152771 W
SFO1     125.7703643 MHz

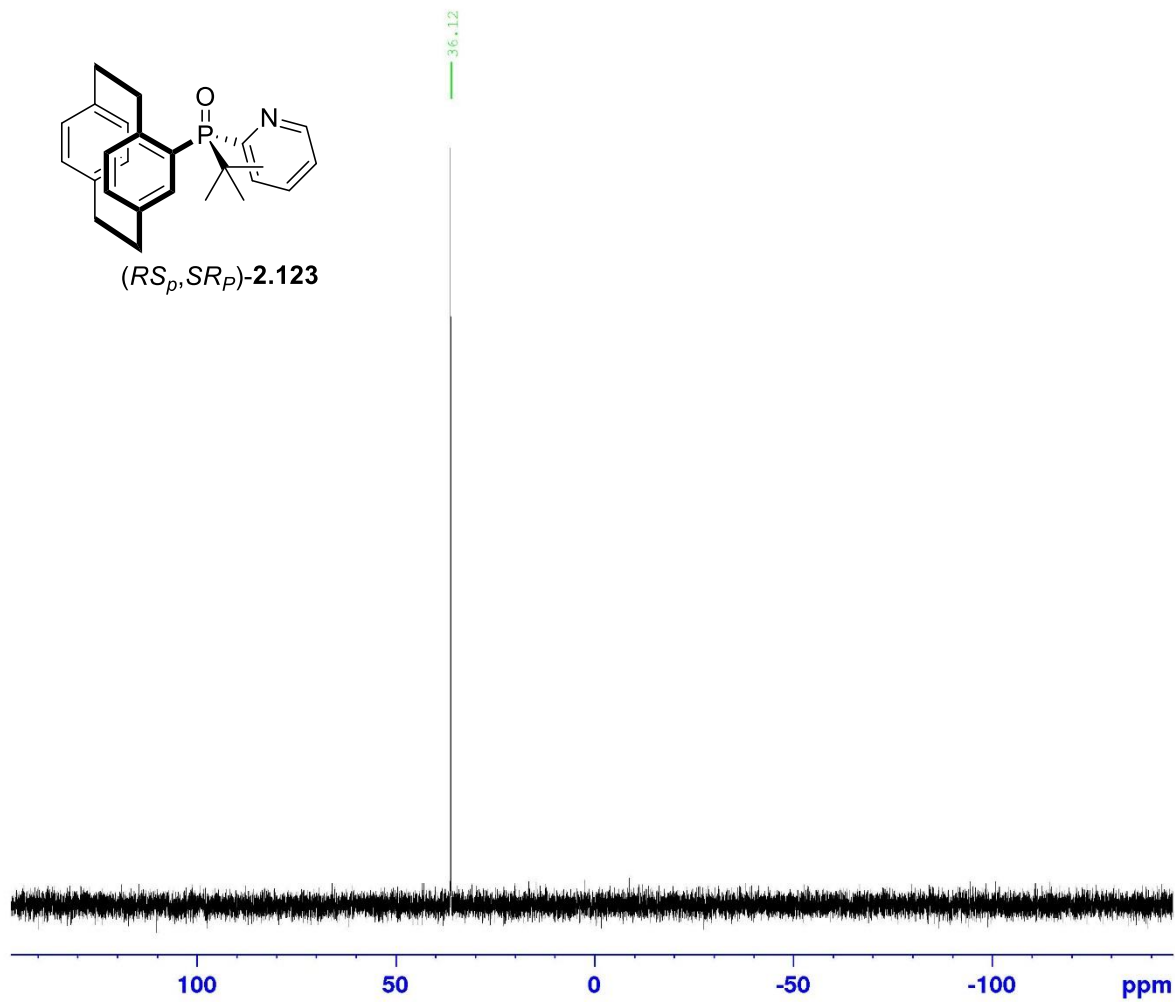
----- CHANNEL f2 -----
CPDPRG[2] waltz16
NUC2     1H
PCPD2    80.00 usec
PL2      4.00 dB
PL12     23.37 dB
PL13     25.00 dB
PL2W     12.10000038 W
PL12W    0.13988955 W
PL13W    0.09611372 W
SFO2     500.1320005 MHz

F2 - Processing parameters
SI       32768
SF       125.7577890 MHz
WDW      EM
SSB      0
LB       1.00 Hz
GB       0
PC       1.40
    
```

2-pyridyl



(*RS_P*, *SR_P*)-2.123



```
Current Data Parameters
NAME          IPC-4 31P
EXPNO         1
PROCNO        1

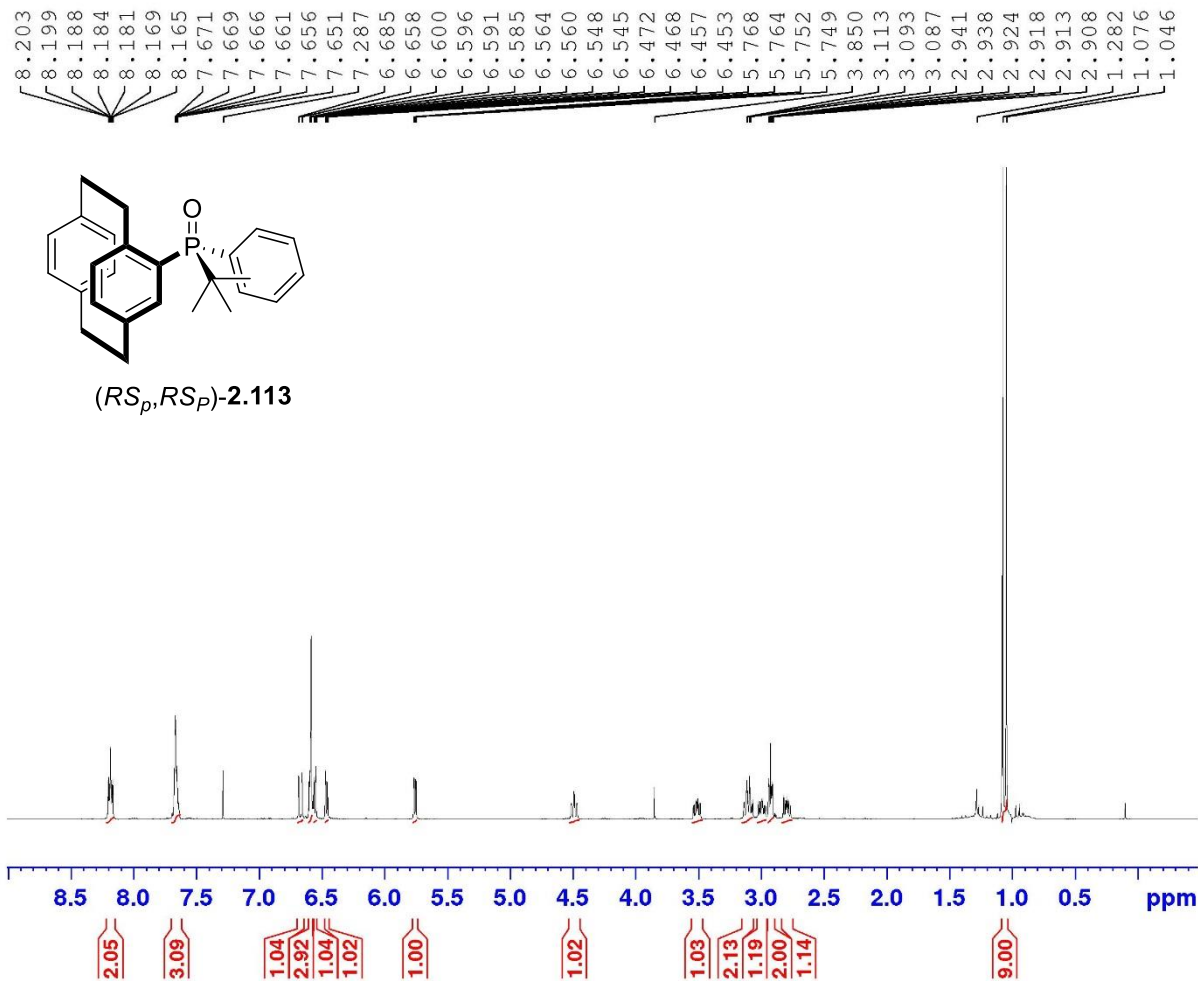
F2 - Acquisition Parameters
Date_         20171012
Time          18.49
INSTRUM       spect
PROBHD        5 mm FAQXI 1H/
PULPROG       zgpg30
TD            65536
SOLVENT       CDCl3
NS            16
DS            4
SWH           80645.164 Hz
FIDRES        1.230548 Hz
AQ            0.4063232 sec
RG            20642.5
DW            6.200 usec
DE            6.50 usec
TE            298.3 K
D1            2.0000000 sec
D11           0.0300000 sec
TD0           1

===== CHANNEL #1 =====
NUC1           31P
P1             20.00 usec
PL1            -2.40 dB
PL1W           131.39126387 W
SFO1           202.4462122 MHz

===== CHANNEL #2 =====
CPDPRG[2]     waltz16
NUC2           1H
PCPD2          80.00 usec
PL2            4.00 dB
PL12           23.37 dB
PL13           25.00 dB
PL2W           12.10000038 W
PL12W          0.13988955 W
PL13W          0.09611372 W
SFO2           500.1320005 MHz

F2 - Processing parameters
SI             32768
SF            202.4563350 MHz
WDW            EM
SSB            0
LB             1.00 Hz
GB            0
PC             1.40
```

SPO & Phenyl iodide



Current Data Parameters
 NAME I-Mn-165 I 26092017
 EXPNO 1
 PROCNO 1

F2 - Acquisition Parameters
 Date_ 20170926
 Time 19.24
 INSTRUM spect
 PROBHD 5 mm PAQXI 1H/
 PULPROG zg30
 TD 65536
 SOLVENT CDCl3
 NS 16
 DS 2
 SWH 10330.578 Hz
 FIDRES 0.157632 Hz
 AQ 3.1719425 sec
 RG 45.3
 DW 48.400 usec
 DE 6.50 usec
 TE 298.2 K
 D1 1.00000000 sec
 TDO 1

==== CHANNEL f1 =====
 NUC1 1H
 P1 8.60 usec
 PL1 4.00 dB
 PLLW 12.10000038 W
 SFO1 500.1330885 MHz

F2 - Processing parameters
 SI 32768
 SF 500.1300000 MHz
 WDW EM
 SSB 0
 LB 0.30 Hz
 GB 0
 PC 1.00

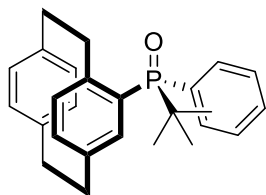
13C : SPO & Phenyl iodide

146.57
140.48
138.77
138.66
138.56
136.77
136.67
136.25
136.15
135.99
135.97
134.02
133.82
133.05
132.99
132.65
132.25
132.17
131.83
131.39
131.37
131.13
130.89
128.32
128.24
127.36
126.62

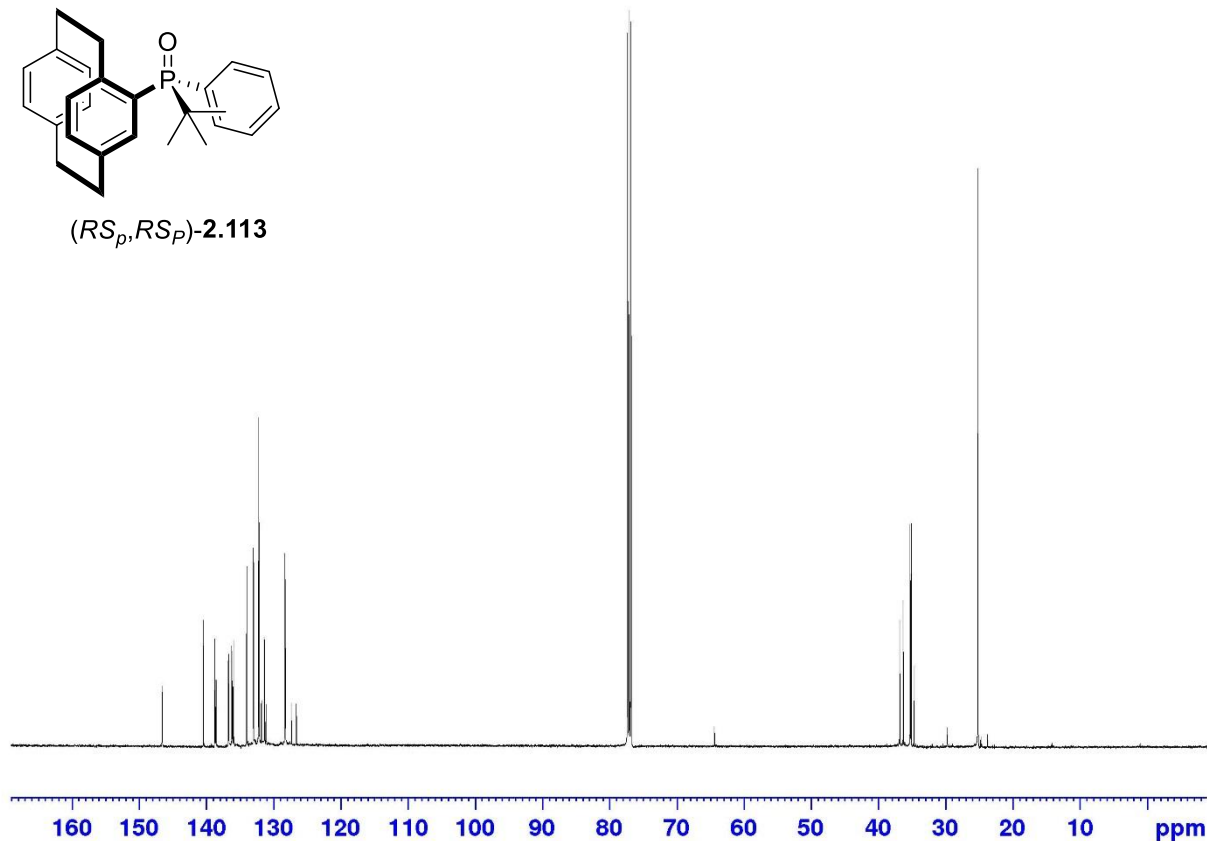
77.51
77.06
76.80

64.38

36.80
36.28
35.26
35.21
35.09
34.63
33.71
33.16
32.74
23.73



(*RS_p*,*RS_p*)-2.113



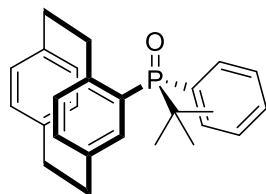
Current Data Parameters
NAME I-Mn-165 I 13C 26092017
EXPNO 1
PROCNO 1

F2 - Acquisition Parameters
Date_ 20170927
Time 8.31
INSTRUM spect
PROBHD 5 mm PAQXI 1H/
PULPROG zgpg30
TD 65536
SOLVENT CDCl3
NS 14901
DS 4
SWH 30030.029 Hz
FIDRES 0.458222 Hz
AQ 1.0911744 sec
RG 32768
DW 16.650 usec
DE 6.50 usec
TE 298.2 K
D1 2.0000000 sec
D11 0.0300000 sec
TD0 1

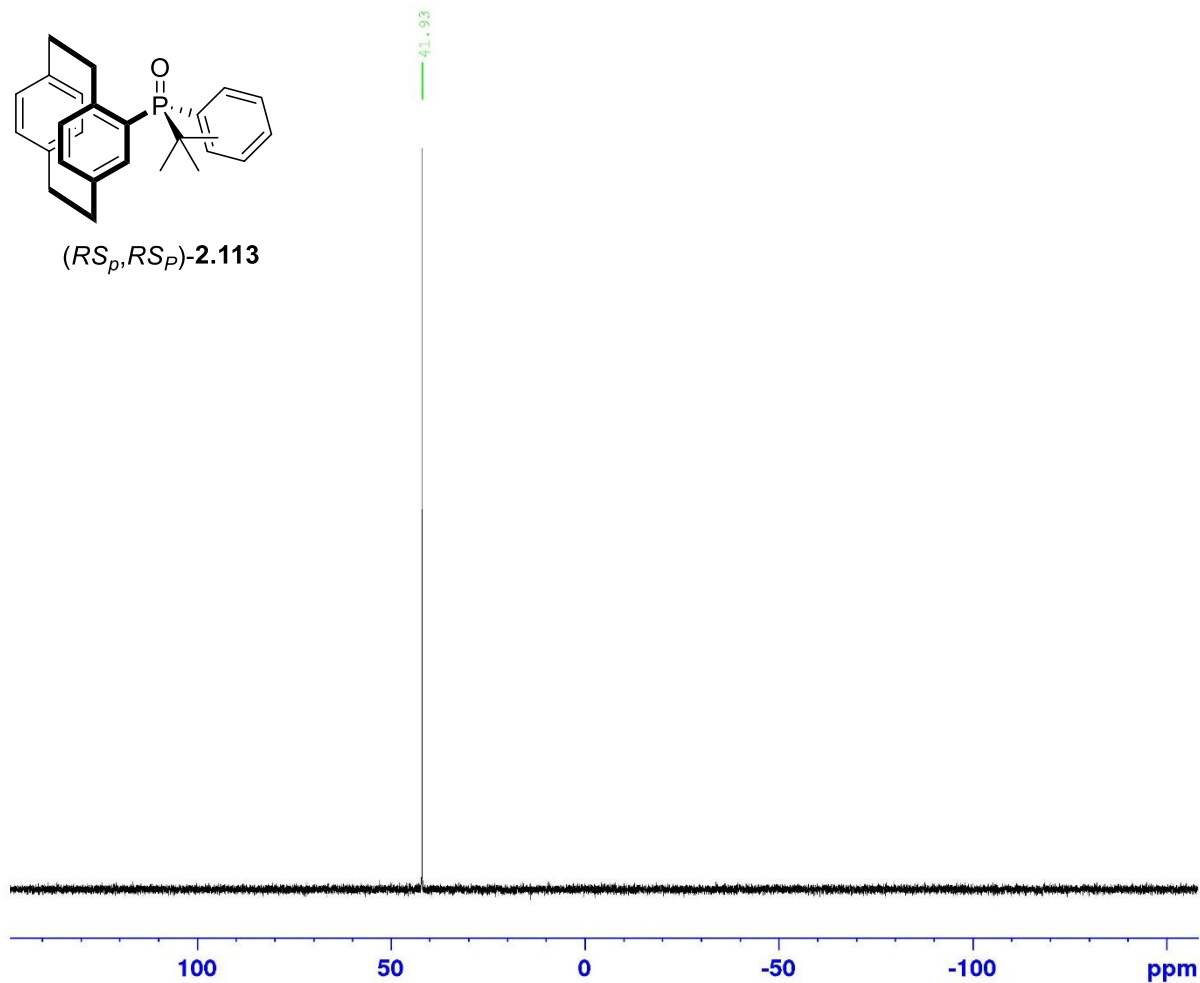
===== CHANNEL f1 =====
NUC1 13C
P1 12.00 usec
PL1 -3.50 dB
PL1W 154.08152771 W
SFO1 125.7703643 MHz

===== CHANNEL f2 =====
CPDPRG[2] waltz16
NUC2 1H
PCPD2 80.00 usec
PL2 4.00 dB
PL12 23.37 dB
PL13 25.00 dB
PL2W 12.10000038 W
PL12W 0.13988955 W
PL13W 0.09611372 W
SFO2 500.1320005 MHz

F2 - Processing parameters
SI 32768
SF 125.7577890 MHz
WDW EM
SSB 0
LB 1.00 Hz
GB 0
PC 1.40



(RS_p, RS_p)-2.113



Current Data Parameters
 NAME TPO-5 31P
 EXPNO 1
 PROCNO 1

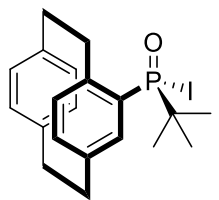
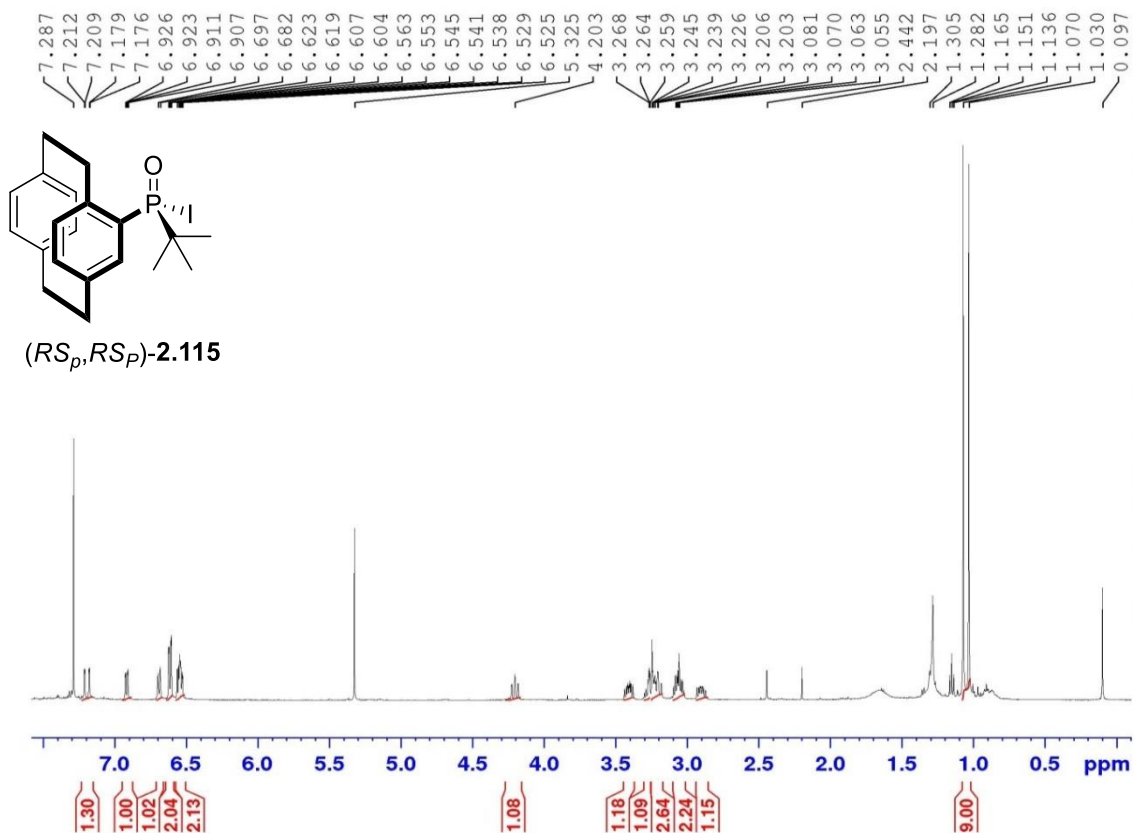
F2 - Acquisition Parameters
 Date_ 20171012
 Time 18.54
 INSTRUM spect
 PROBHD 5 mm PAQXI 1H/
 PULPROG zgpg30
 TD 65536
 SOLVENT CDCl3
 NS 16
 DS 4
 SWH 80645.164 Hz
 FIDRES 1.230548 Hz
 AQ 0.4063232 sec
 RG 20642.5
 DW 6.200 usec
 DE 6.50 usec
 TE 298.3 K
 D1 2.0000000 sec
 D11 0.0300000 sec
 TD0 1

===== CHANNEL f1 =====
 NUC1 31P
 P1 20.00 usec
 PL1 -2.40 dB
 PL1W 131.39126587 W
 SFO1 202.4462122 MHz

===== CHANNEL f2 =====
 CPDPRG2 waltz16
 NUC2 1H
 PCPD2 80.00 usec
 PL2 4.00 dB
 PL12 23.37 dB
 PL13 25.00 dB
 PL2W 12.10000038 W
 PL12W 0.13988955 W
 PL13W 0.09611372 W
 SFO2 500.1320005 MHz

F2 - Processing parameters
 SI 32768
 SF 202.4563350 MHz
 WDW EM
 SSB 0
 LB 1.00 Hz
 GB 0
 PC 1.40

P-Arylation : CuI



(RS_p,RS_p)-2.115

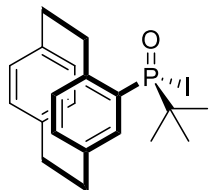
Current Data Parameters
NAME I-Mn-159 1
EXPNO 1
PROCNO 1

F2 - Acquisition Parameters
Date_ 20170427
Time 11.43
INSTRUM spect
PROBHD 5 mm PAQXI 1H/
PULPROG zg30
TD 65536
SOLVENT CDCl3
NS 16
DS 2
SWH 10330.578 Hz
FIDRES 0.157632 Hz
AQ 3.1719425 sec
RG 181
DW 48.400 usec
DE 6.50 usec
TE 299.2 K
D1 1.00000000 sec
TD0 1

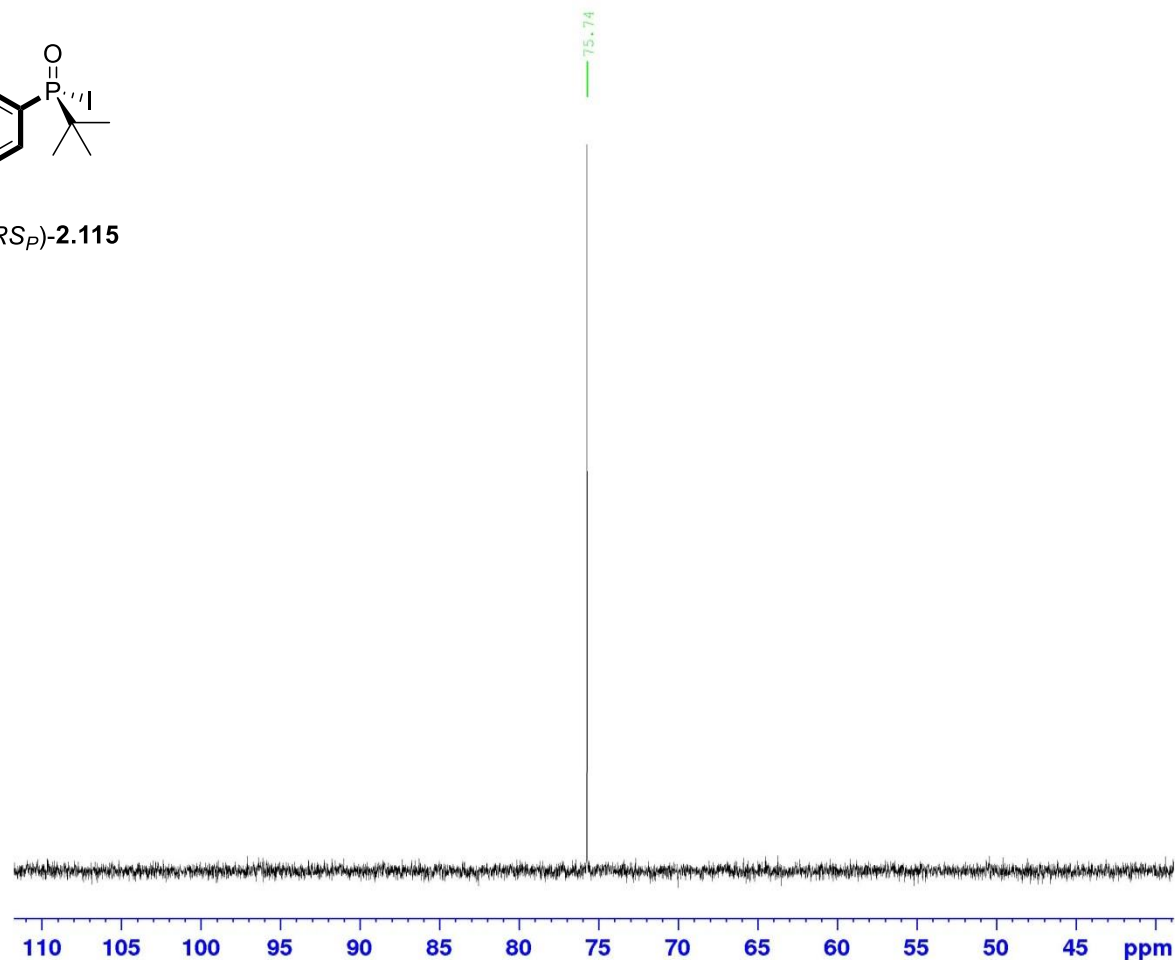
----- CHANNEL f1 -----
NUC1 1H
P1 8.60 usec
PL1 4.00 dB
PL1W 12.10000038 W
SFO1 500.1330885 MHz

F2 - Processing parameters
SI 32768
SF 500.1300000 MHz
WDW EM
SSB 0
LB 0.30 Hz
GB 0
PC 1.00

P31 - P-Arylation on Mono SPO with 4-iodo toluene (CuI)



(RS_p,RS_p) -2.115



Current Data Parameters
 NAME I-Mn-151 crude P31
 EXPNO 1
 PROCNO 1

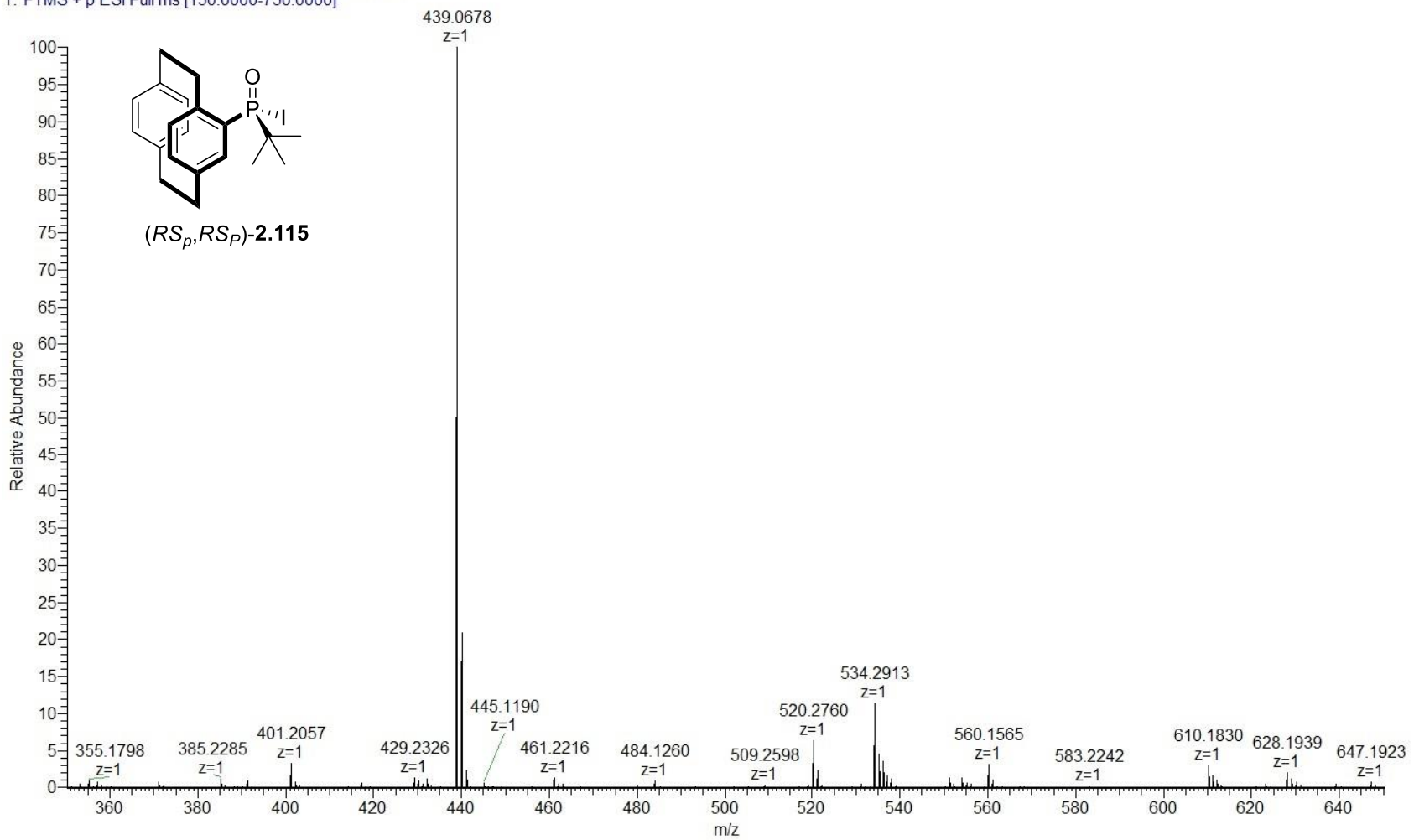
F2 - Acquisition Parameters
 Date_ 20170313
 Time 9.49
 INSTRUM spect
 PROBHD 5 mm PAQXI 1H/
 PULPROG zgpg30
 TD 65536
 SOLVENT CDC13
 NS 64
 DS 4
 SWH 80645.164 Hz
 FIDRES 1.230548 Hz
 AQ 0.4063232 sec
 RG 20642.5
 DW 6.200 usec
 DE 6.50 usec
 TE 298.6 K
 D1 2.0000000 sec
 D11 0.0300000 sec
 TD0 1

===== CHANNEL f1 =====
 NUC1 31P
 P1 20.00 usec
 PL1 -2.40 dB
 PL1W 131.39126587 W
 SFO1 202.4462122 MHz

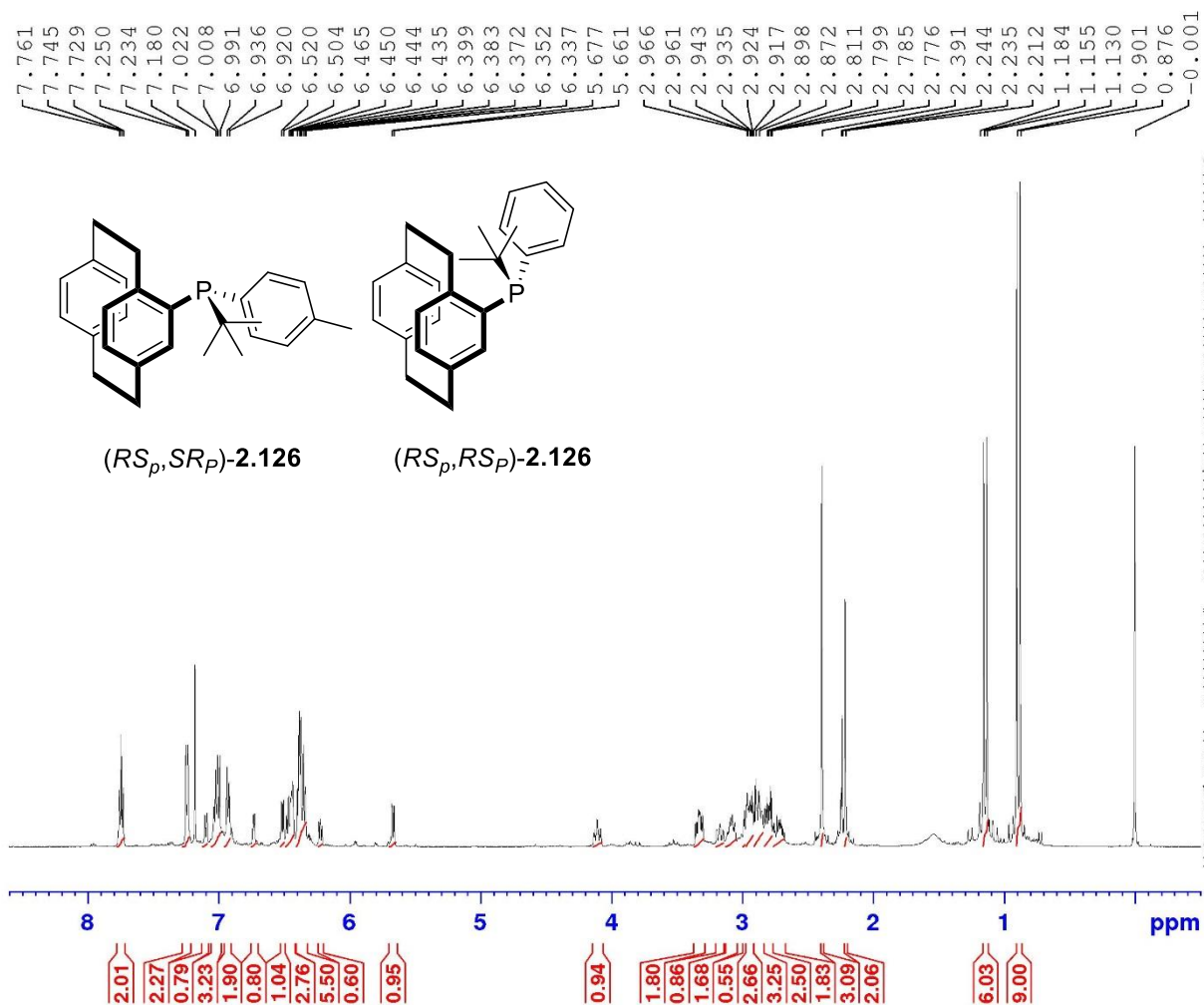
===== CHANNEL f2 =====
 CPDPRG[2] waltz16
 NUC2 1H
 PCPD2 80.00 usec
 PL2 4.00 dB
 PL12 23.37 dB
 PL13 25.00 dB
 PL2W 12.10000038 W
 PL12W 0.13988955 W
 PL13W 0.09611372 W
 SFO2 500.1320005 MHz

F2 - Processing parameters
 SI 32768
 SF 202.4563350 MHz
 WDW EM
 SSB 0
 LB 1.00 Hz
 GB 0
 PC 1.40

LMN-151_(2) #40-91 RT: 0.19-0.42 AV: 52 NL: 2.72E7
T: FTMS + p ESI Full ms [150.0000-750.0000]



Reduction



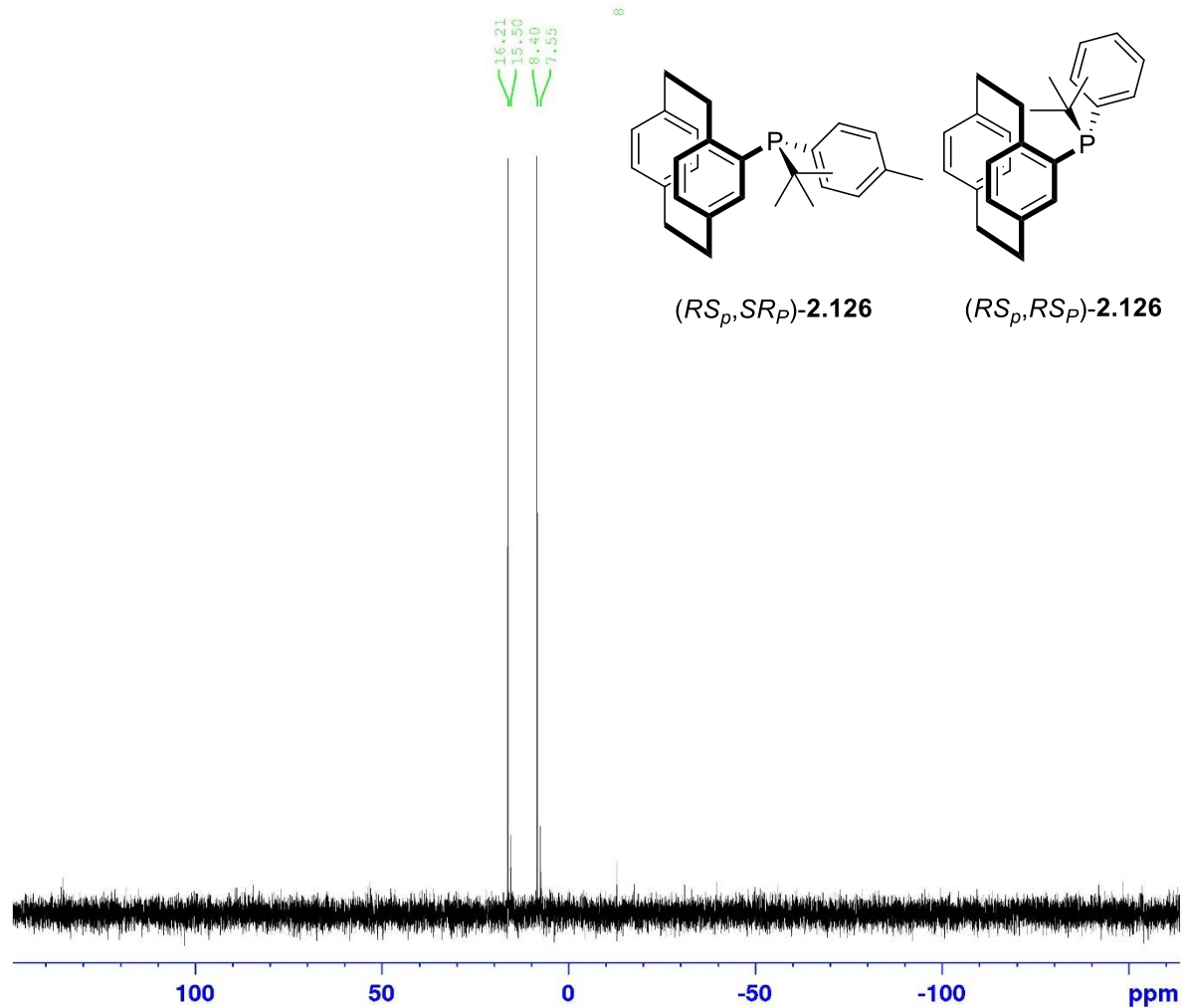
Current Data Parameters
 NAME II-Mn-53 28082017
 EXPNO 1
 PROCNO 1

F2 - Acquisition Parameters
 Date_ 20170828
 Time 8.42
 INSTRUM spect
 PROBHD 5 mm PAQXI 1H/
 PULPROG zg30
 TD 65536
 SOLVENT CDCl3
 NS 16
 DS 2
 SWH 10330.578 Hz
 FIDRES 0.157632 Hz
 AQ 3.1719425 sec
 RG 90.5
 DW 48.400 usec
 DE 6.50 usec
 TE 298.2 K
 D1 1.0000000 sec
 TD0 1

===== CHANNEL f1 =====
 NUC1 1H
 P1 8.60 usec
 PL1 4.00 dB
 PL1W 12.10000038 W
 SFO1 500.1330865 MHz

F2 - Processing parameters
 SI 32768
 SF 500.1300534 MHz
 WDW EM
 SSB 0
 LB 0.30 Hz
 GB 0
 PC 1.00

31P - Reduction



Current Data Parameters
 NAME II-Mn-53 crude 31P
 EXPNO 1
 PROCNO 1

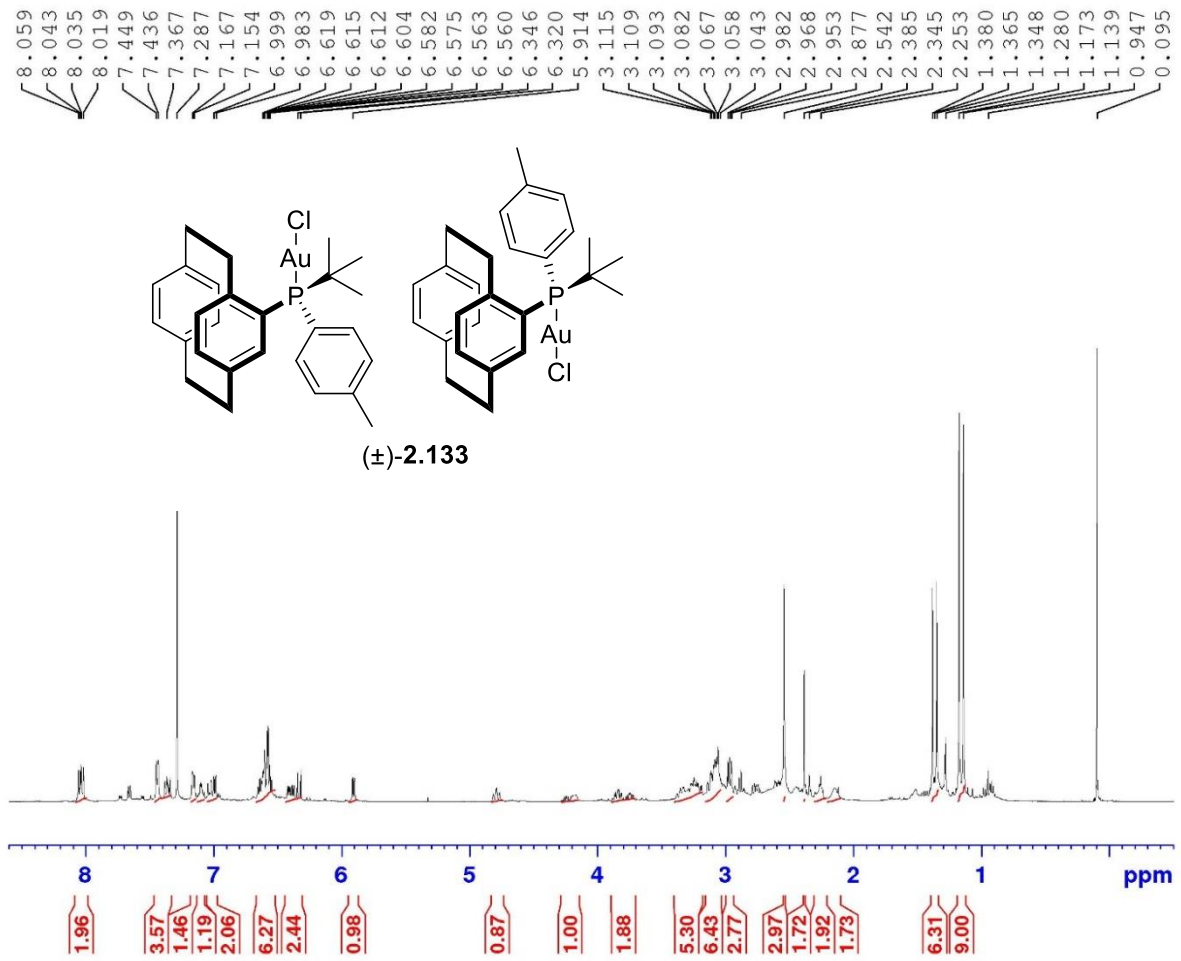
F2 - Acquisition Parameters
 Date_ 20170827
 Time 16.45
 INSTRUM spect
 PROBHD 5 mm PAQXI 1H/
 PULPROG zgpg30
 TD 65536
 SOLVENT CDCl3
 NS 16
 DS 4
 SWH 80645.164 Hz
 FIDRES 1.230548 Hz
 AQ 0.4063232 sec
 RG 20642.5
 DW 6.200 usec
 DE 6.50 usec
 TE 298.2 K
 D1 2.00000000 sec
 D11 0.03000000 sec
 TD0 1

===== CHANNEL f1 =====
 NUC1 31P
 P1 20.00 usec
 PL1 -2.40 dB
 PL1W 131.39126587 W
 SF01 202.4462122 MHz

===== CHANNEL f2 =====
 CPDPRG2 waltz16
 NUC2 1H
 PCPD2 80.00 usec
 PL2 4.00 dB
 PL12 23.37 dB
 PL13 25.00 dB
 PL2W 12.10000038 W
 PL12W 0.13988955 W
 PL13W 0.09611372 W
 SF02 500.1320005 MHz

F2 - Processing parameters
 SI 32768
 SF 202.4563350 MHz
 WDW EM
 SSB 0
 LB 1.00 Hz
 GB 0
 PC 1.40

P1-Au 180218



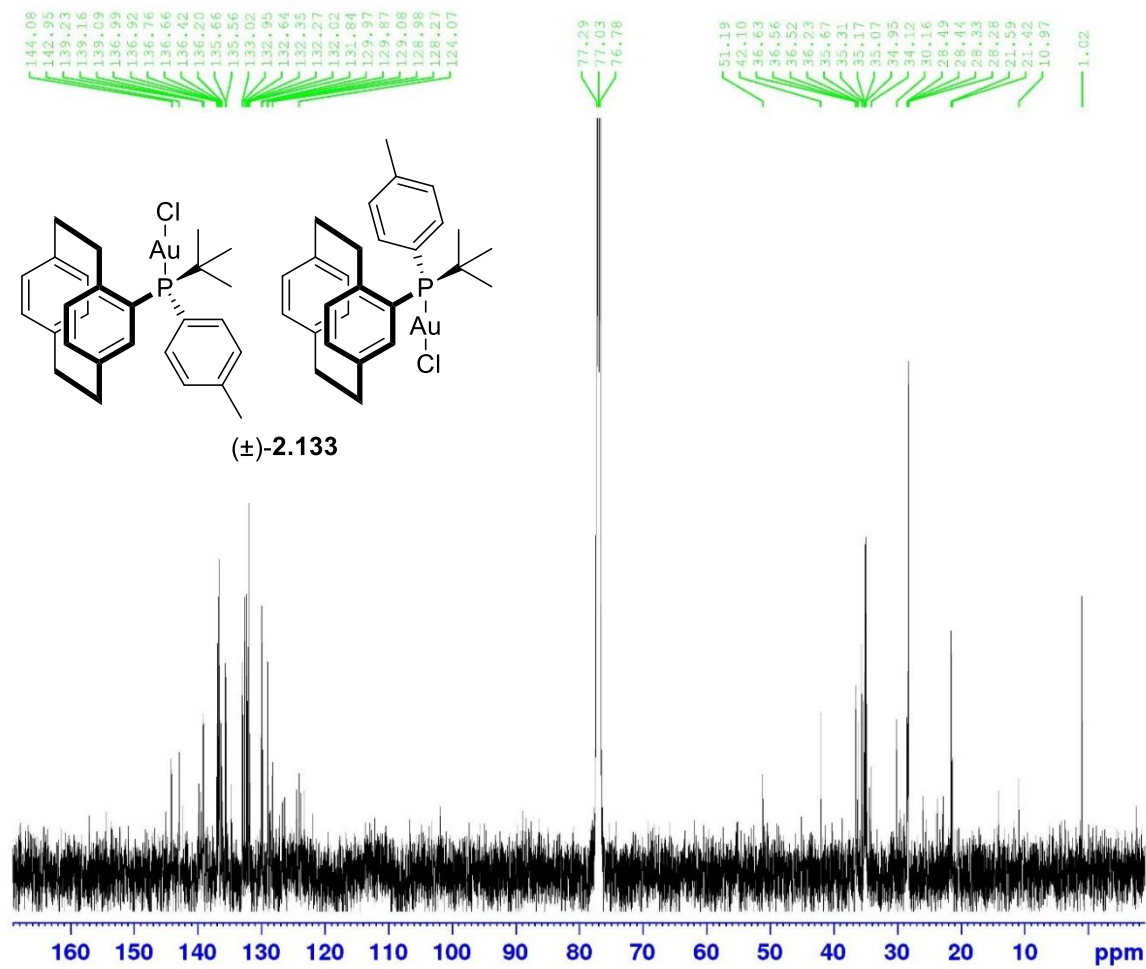
Current Data Parameters
NAME P1-Au 180218
EXPNO 1
PROCNO 1

F2 - Acquisition Parameters
Date_ 20180218
Time 11.52
INSTRUM spect
PROBHD 5 mm PAQXI 1H/
PULPROG zg30
TD 65536
SOLVENT CDCl3
NS 64
DS 2
SWH 10330.578 Hz
FIDRES 0.157632 Hz
AQ 3.1719425 sec
RG 256
DW 48.400 usec
DE 6.50 usec
TE 298.2 K
D1 1.00000000 sec
TD0 1

----- CHANNEL f1 -----
NUC1 1H
P1 9.50 usec
PL1 4.00 dB
PL1W 12.10000038 W
SFO1 500.1330885 MHz

F2 - Processing parameters
SI 32768
SF 500.1300000 MHz
WDW EM
SSB 0
LB 0.30 Hz
GB 0
PC 1.00

13C : P1-Au 180218



```

Current Data Parameters
NAME      P1-Au 180218
EXPNO     2
PROCNO    1

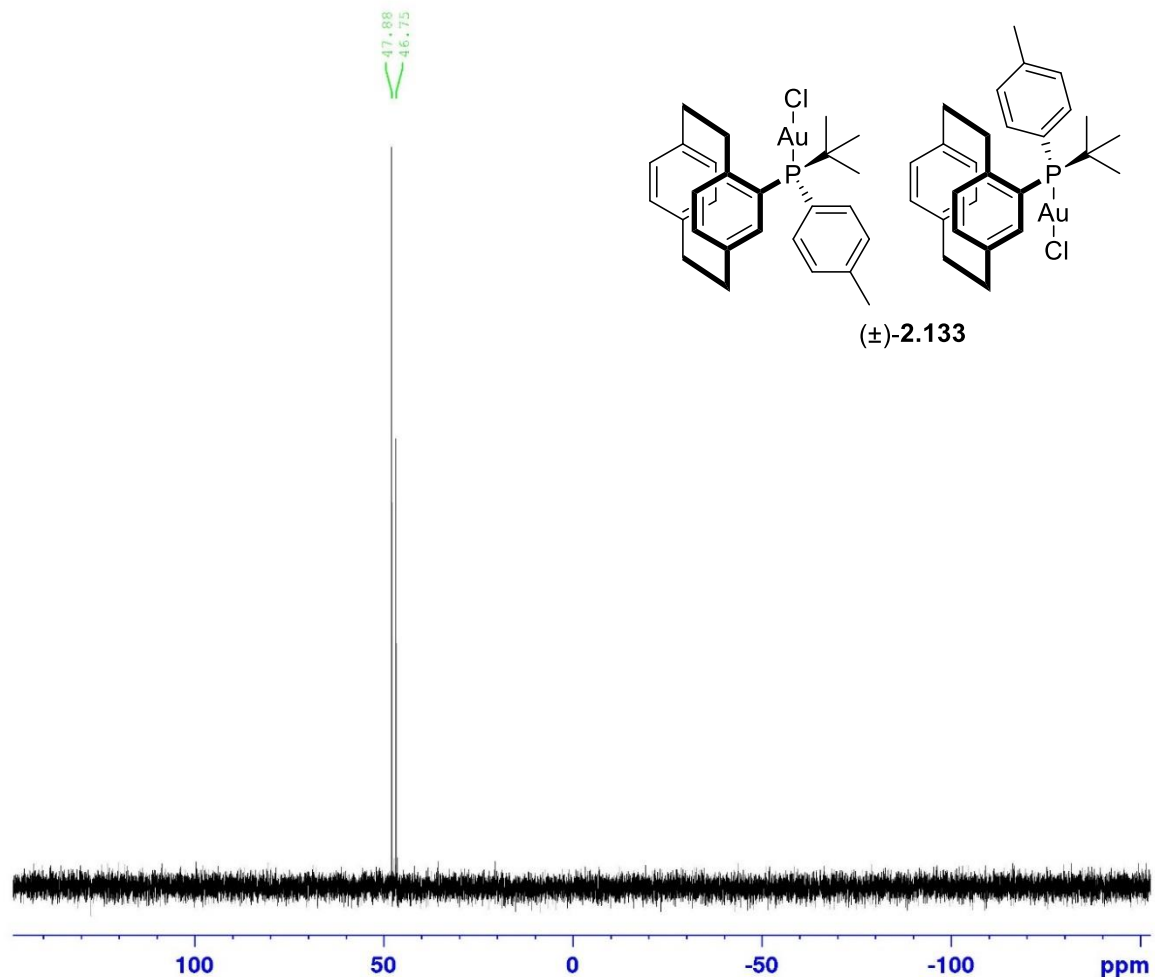
F2 - Acquisition Parameters
Date_     20180219
Time      2.21
INSTRUM   spect
PROBHD    5 mm PAQXI 1H/
PULPROG   zgpg30
TD         65536
SOLVENT   CDCl3
NS         16384
DS         4
SWH        30030.029 Hz
FIDRES     0.458222 Hz
AQ         1.0911744 sec
RG         32768
DW         16.650 usec
DE         6.50 usec
TE         298.2 K
D1         2.00000000 sec
D11        0.03000000 sec
TD0        1

===== CHANNEL f1 =====
NUC1       13C
P1         12.00 usec
PL1        -4.00 dB
PL1W       172.88230896 W
SFO1       125.7703643 MHz

===== CHANNEL f2 =====
CPDPRG[2] waltz16
NUC2       1H
PCPD2      80.00 usec
PL2         4.00 dB
PL12       22.51 dB
PL13       25.00 dB
PL2W       12.10000038 W
PL12W      0.17052394 W
PL13W      0.39611372 W
SFO2       500.1320005 MHz

F2 - Processing parameters
SI         32768
SF         125.7577890 MHz
WDW        EM
SSB        0
LB         1.00 Hz
GB         0
PC         1.40
    
```

31p - P1-Au 170218



Current Data Parameters
NAME P1-Au 170218 31P
EXPNO 1
PROCNO 1

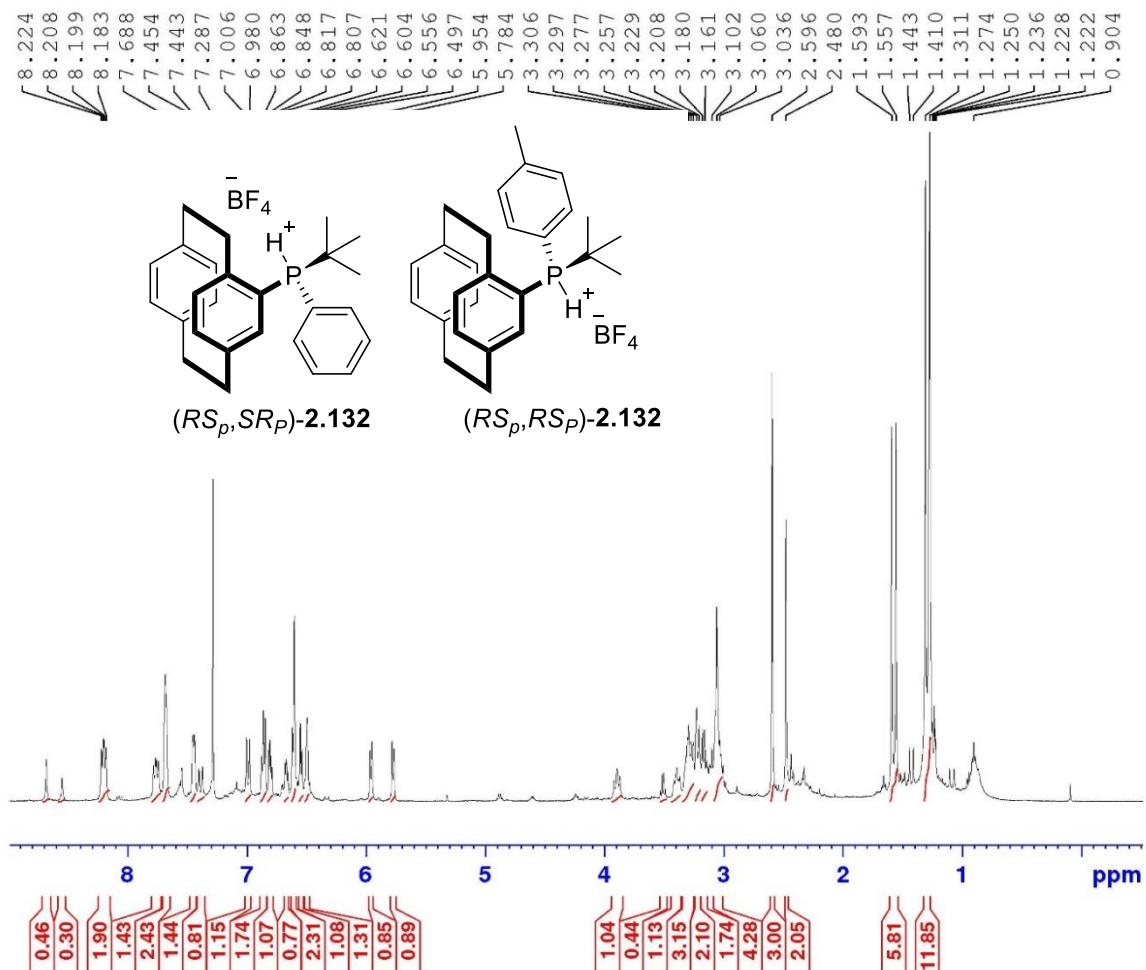
F2 - Acquisition Parameters
Date_ 20180217
Time 17.19
INSTRUM spect
PROBHD 5 mm PAQXI 1H/
PULPROG zgpg30
TD 65536
SOLVENT CD3CN
NS 64
DS 4
SWH 80645.164 Hz
FIDRES 1.230548 Hz
AQ 0.4063232 sec
RG 20642.5
DW 6.200 usec
DE 6.50 usec
TE 298.4 K
D1 2.0000000 sec
D11 0.0300000 sec
TD0 1

----- CHANNEL f1 -----
NUC1 31P
P1 20.00 usec
PL1 -2.40 dB
PL1W 131.39126587 W
SFO1 202.4462122 MHz

----- CHANNEL f2 -----
CPDPRG[2] waltz16
NUC2 1H
PCPD2 80.00 usec
PL2 4.00 dB
PL12 22.51 dB
PL13 25.00 dB
PL2W 12.10000038 W
PL12W 0.17052394 W
PL13W 0.09611372 W
SFO2 500.1320005 MHz

F2 - Processing parameters
SI 32768
SF 202.4563350 MHz
WDW EM
SSB 0
LB 1.00 Hz
GB 0
PC 1.40

HBF₄



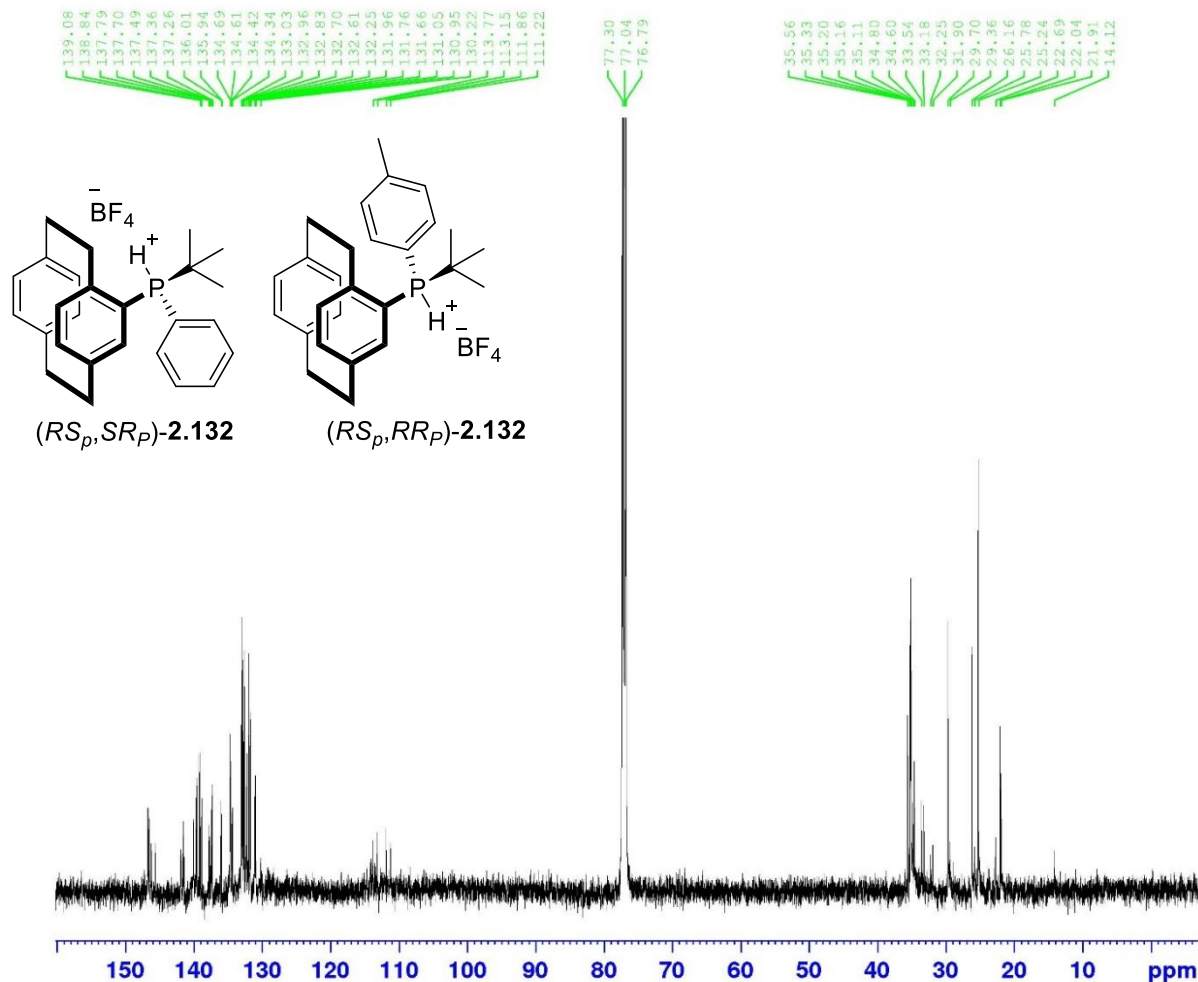
Current Data Parameters
NAME II-Mn-28 Crude
EXPNO 1
PROCNO 1

F2 - Acquisition Parameters
Date_ 20170727
Time 8.47
INSTRUM spect
PROBHD 5 mm PAQXI 1H/
PULPROG zg30
TD 65536
SOLVENT CDCl3
NS 16
DS 2
SWH 10330.578 Hz
FIDRES 0.157632 Hz
AQ 3.1719425 sec
RG 128
DW 48.400 usec
DE 6.50 usec
TE 298.2 K
D1 1.00000000 sec
TDD 1

----- CHANNEL f1 -----
NUC1 1H
P1 8.60 usec
PL1 4.00 dB
PL1W 12.10000038 W
SFO1 500.1330885 MHz

F2 - Processing parameters
SI 32768
SF 500.1300000 MHz
WDW EM
SSB 0
LB 0.30 Hz
GB 0
PC 1.00

13C - P1-HBF4



Current Data Parameters
 NAME P1-HBF4 040218 13C
 EXPNO 1
 PROCNO 1

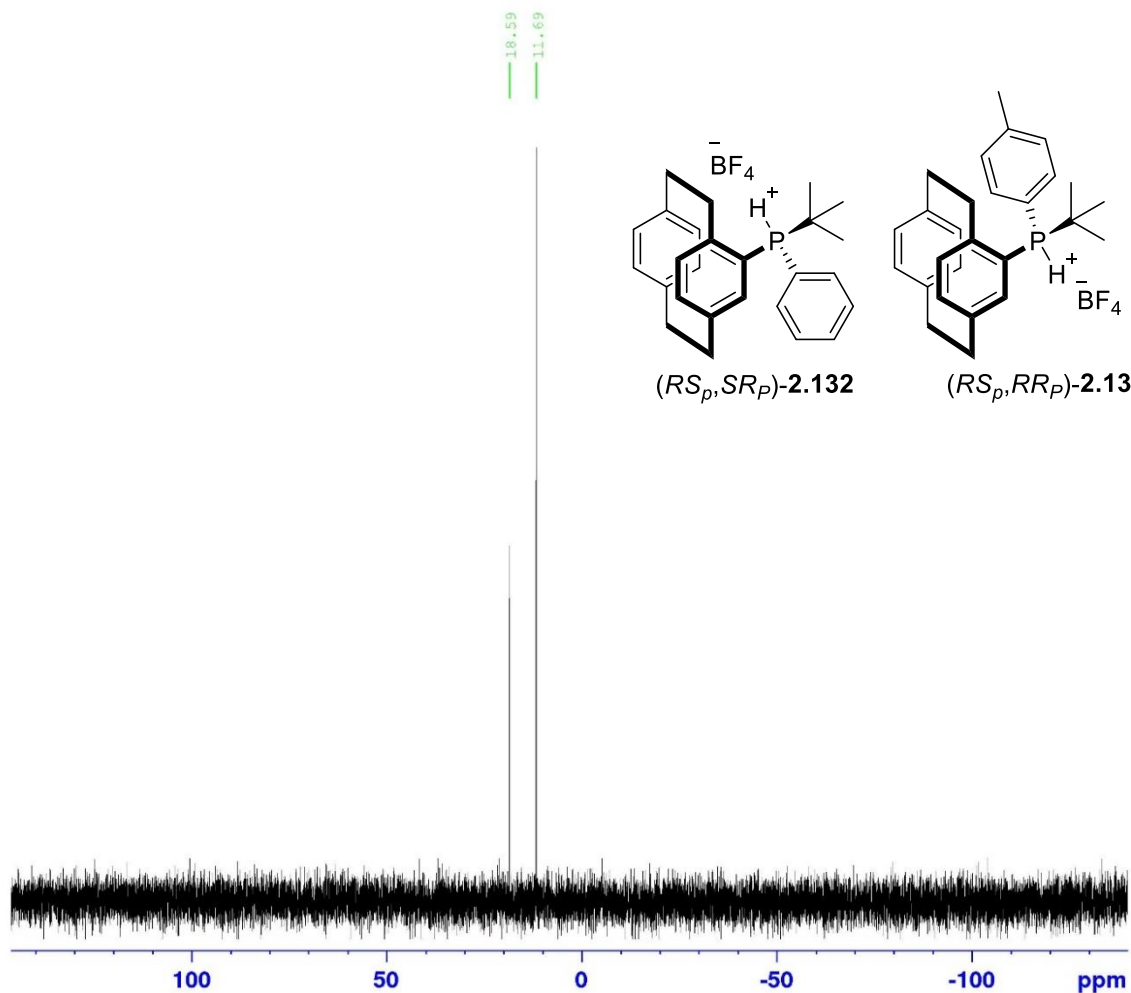
F2 - Acquisition Parameters
 Date_ 20180205
 Time 7.33
 INSTRUM spect
 PROBED 5 mm PAQXI 1H/
 PULPROG zgpg30
 TD 65536
 SOLVENT CDC13
 NS 14384
 DS 4
 SWH 30030.029 Hz
 FIDRES 0.458222 Hz
 AQ 1.0911744 sec
 RG 32768
 DW 16.650 usec
 DE 6.50 usec
 TE 298.2 K
 D1 2.0000000 sec
 D11 0.0300000 sec
 TD0 1

===== CHANNEL f1 =====
 NUC1 13C
 P1 12.00 usec
 PL1 -3.50 dB
 PL1W 154.08152771 W
 SFO1 125.7703643 MHz

===== CHANNEL f2 =====
 CPDPRG[2] waltz16
 NUC2 1H
 PCPD2 80.00 usec
 PL2 4.00 dB
 PL12 23.37 dB
 PL13 25.00 dB
 PL2W 12.10000038 W
 PL12W 0.13988955 W
 PL13W 0.09611372 W
 SFO2 500.1320005 MHz

F2 - Processing parameters
 SI 32768
 SF 125.7577890 MHz
 WDW EM
 SSB 0
 LB 1.00 Hz
 GB 0
 PC 1.40

31P : HBF4 complex formation



Current Data Parameters
NAME II-Mn-10 crude 31P
EXPNO 1
PROCNO 1

F2 - Acquisition Parameters
Date_ 20170621
Time 18.32
INSTRUM spect
PROBHD 5 mm PAQXI 1H/
PULPROG zgpg30
TD 65536
SOLVENT CDCl3
NS 64
DS 4
SWH 80645.164 Hz
FIDRES 1.230548 Hz
AQ 0.4063232 sec
RG 20642.5
DW 6.200 usec
DE 6.50 usec
TE 297.2 K
D1 2.0000000 sec
D11 0.0300000 sec
TDC 1

===== CHANNEL f1 =====
NUC1 31P
P1 20.00 usec
PL1 -2.40 dB
PL1W 131.39126387 W
SFO1 202.4462122 MHz

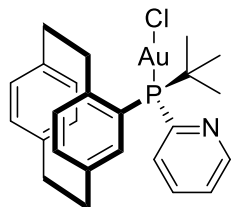
===== CHANNEL f2 =====
CPDPRG[2] waltz16
NUC2 1H
PCPD2 80.00 usec
PL2 4.00 dB
PL12 23.37 dB
PL13 25.00 dB
PL2W 12.10000038 W
PL12W 0.13988955 W
PL13W 0.09611372 W
SFO2 500.1320005 MHz

F2 - Processing parameters
SI 32768
SF 202.4563350 MHz
WDW EM
SSB 0
LB 1.00 Hz
GB 0
PC 1.40

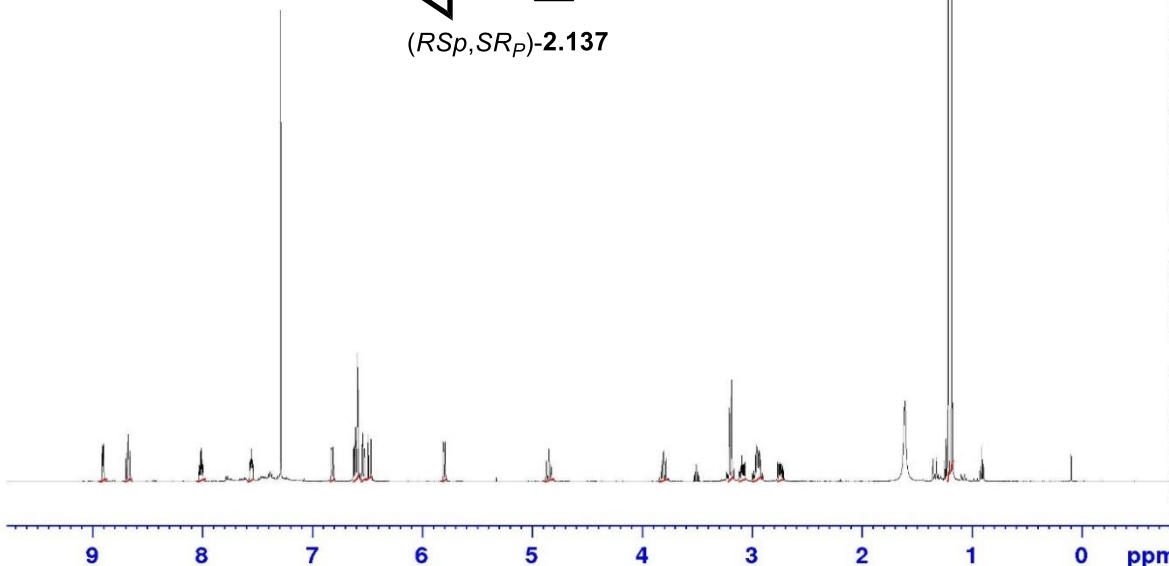
P4-Au 190118



8.910
8.901
8.677
8.675
8.660
8.013
8.010
8.006
7.556
7.554
7.287
6.828
6.825
6.813
6.810
6.623
6.619
6.607
6.604
6.591
6.589
6.583
6.544
6.540
6.528
6.525
6.491
6.467
5.809
5.805
5.793
5.790
4.846
3.209
3.206
3.202
3.186
2.959
2.956
2.952
2.936
1.609
1.234
1.216
1.181
0.909



(R_{sp},S_{Rp})-2.137



0.96
1.00
0.99
1.11
0.99
3.01
2.14
0.99
1.00
1.00
1.93
1.07
2.11
1.01
9.00

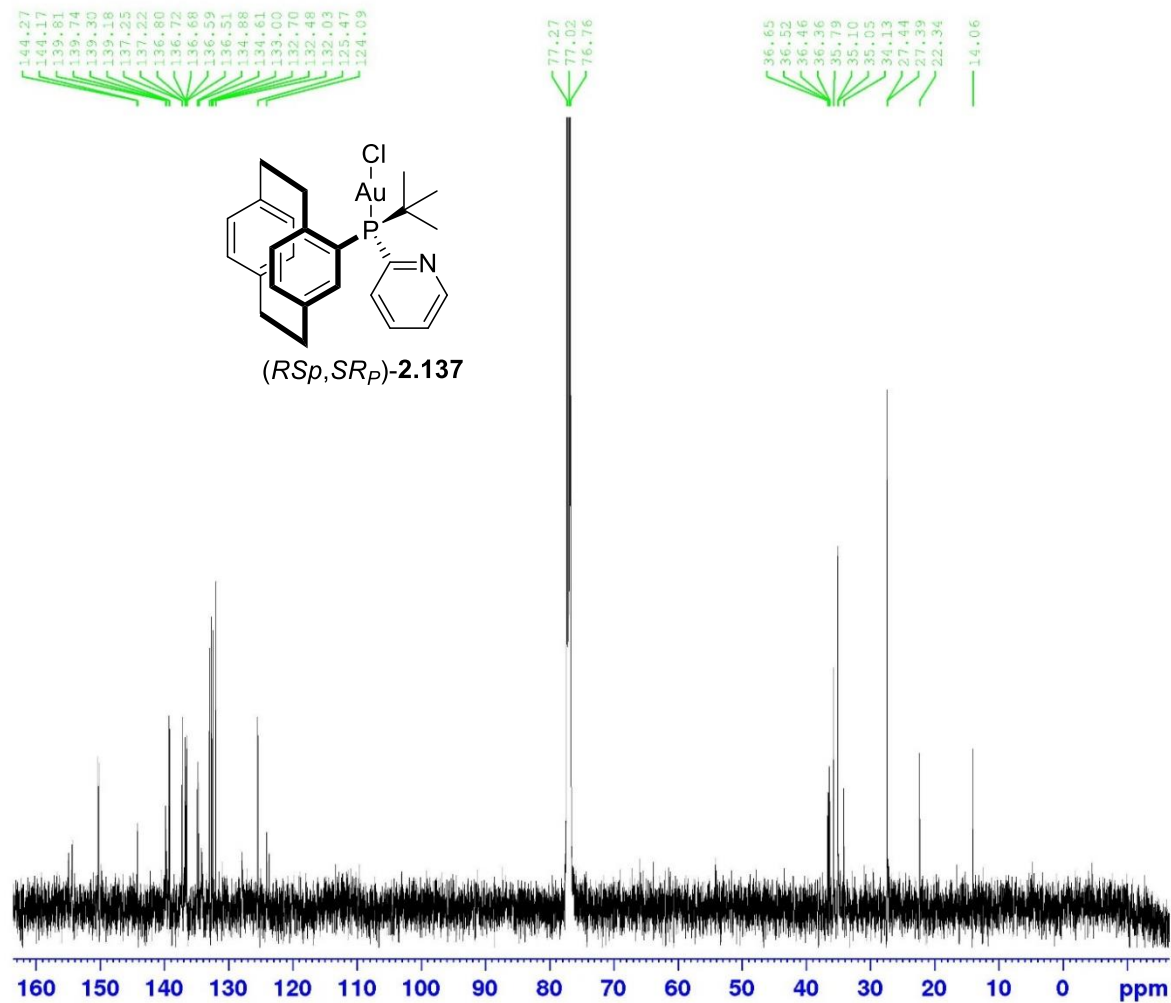
Current Data Parameters
NAME P4-Au 190118
EXPNO 1
PROCNO 1

F2 - Acquisition Parameters
Date_ 20180119
Time 11.22
INSTRUM spect
PROBHD 5 mm PAQXI 1H/
PULPROG zg30
TD 65536
SOLVENT CDCl3
NS 16
DS 2
SWH 10330.578 Hz
FIDRES 0.157632 Hz
AQ 3.1719425 sec
RG 322.5
DW 48.400 usec
DE 6.50 usec
TE 298.2 K
D1 1.00000000 sec
TDC 1

----- CHANNEL f1 -----
NUC1 1H
P1 8.60 usec
PL1 4.00 dB
PL1W 12.10000038 W
SFO1 500.1330885 MHz

F2 - Processing parameters
SI 32768
SF 500.1300000 MHz
WDW EM
SSB 0
LB 0.30 Hz
GB 0
PC 1.00

13C - P4Au



```

Current Data Parameters
NAME      P4Au 020218 13C
EXPNO    1
PROCNO    1

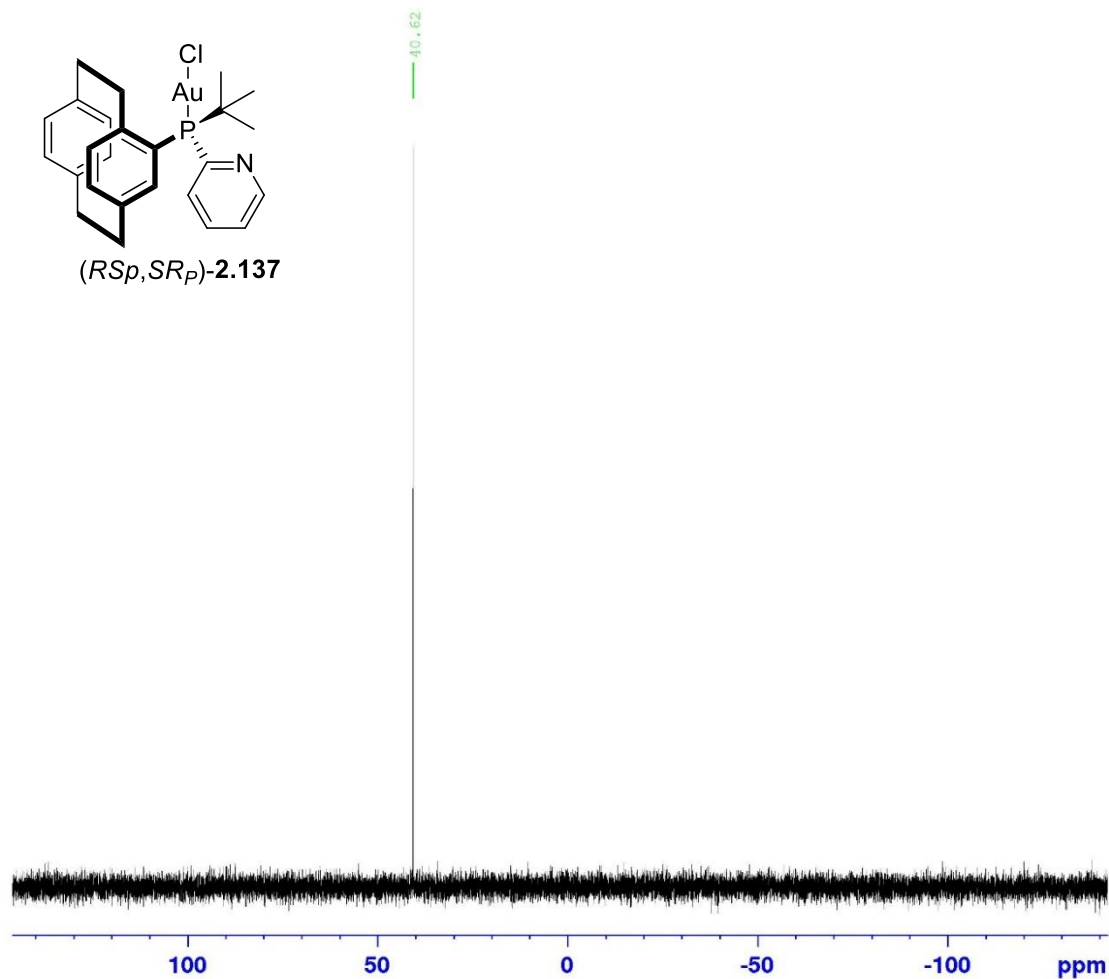
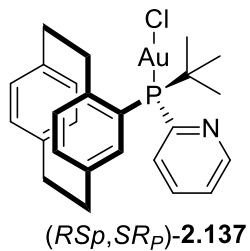
F2 - Acquisition Parameters
Date_     20180203
Time      10.46
INSTRUM   spect
PROBHD    5 mm PAQXI 1H/
PULPROG   zgpg30
TD         65536
SOLVENT   CDCl3
NS         16384
DS         4
SWH        30030.029 Hz
FIDRES     0.458222 Hz
AQ         1.0911744 sec
RG         32768
DW         16.650 usec
DE         6.50 usec
TE         298.2 K
D1         2.0000000 sec
D11        0.0300000 sec
TD0        1

===== CHANNEL f1 =====
NUC1       13C
P1         12.00 usec
PL1        -3.50 dB
PL1W       154.08152771 W
SFO1       125.7703643 MHz

===== CHANNEL f2 =====
CPDPRG[2] waltz16
NUC2       1H
PCPD2      80.00 usec
PL2        4.00 dB
PL12       23.37 dB
PL13       25.00 dB
PL2W       12.10000038 W
PL12W      0.13988955 W
PL13W      0.09611372 W
SFO2       500.1320005 MHz

F2 - Processing parameters
SI         32768
SF         125.7577890 MHz
WDW        EM
SSB        0
LB         1.00 Hz
GB         0
PC         1.40
    
```

31P - P4-Au 190118



Current Data Parameters
NAME P4-Au 190118 31P
EXPNO 1
PROCNO 1

F2 - Acquisition Parameters
Date_ 20180119
Time 11.33
INSTRUM spect
PROBHD 5 mm PAQXI 1H/
PULPROG zgpg30
TD 65536
SOLVENT CDC13
NS 64
DS 4
SWH 80645.164 Hz
FIDRES 1.230548 Hz
AQ 0.4063232 sec
RG 20642.5
DW 6.200 usec
DE 6.50 usec
TE 298.5 K
D1 2.0000000 sec
D11 0.0300000 sec
TD0 1

----- CHANNEL f1 -----
NUC1 31P
P1 20.00 usec
PL1 -2.40 dB
PL1W 131.39126587 W
SFO1 202.4462122 MHz

===== CHANNEL f2 =====
CPDPRG[2] waltz16
NUC2 1H
PCPD2 80.00 usec
PL2 4.00 dB
PL12 23.37 dB
PL13 25.00 dB
PL2W 12.10000038 W
PL12W 0.13988955 W
PL13W 0.09611372 W
SFO2 500.1320005 MHz

F2 - Processing parameters
SI 32768
SF 202.4563350 MHz
WDW EM
SSE 0
LB 1.00 Hz
GB 0
PC 1.40

Bond distance and angle of crystal structures

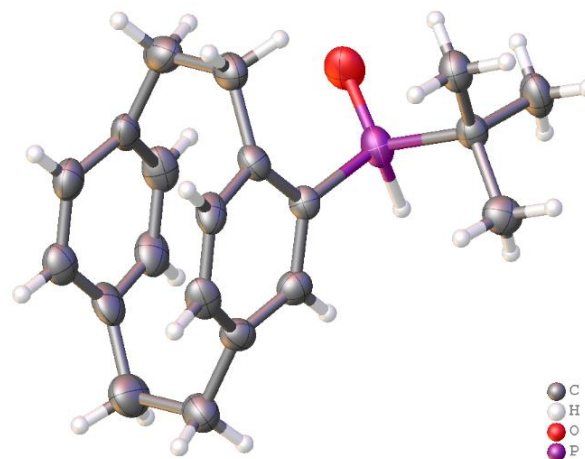


Figure 2.4. Crystal structure of (*RS_p*,*SR_p*)-4-*tert*-butyl[2.2]paracyclophane phosphine oxide **2.47**.
(Ellipsoids are drawn at a 50% probability level.)

bond_distance

P1 O1 1.504(4)

P1 C4 1.817(5)

P1 C17 1.819(5)

P1 H1 1.52(4)

C3 C4 1.397(6)

C3 C8 1.391(6)

C3 C2 1.519(7)

C11 C12 1.385(7)

C11 C16 1.383(7)

C11 C10 1.520(7)

C4 C5 1.396(6)

C8 H8 0.9300

C8 C7 1.397(6)

C17 C18 1.529(6)

C17 C19 1.532(6)

C17 C20 1.531(6)

C18 H18A 0.9600

C18 H18B 0.9600

C18 H18C 0.9600

C7 H7 0.9300

C7 C6 1.388(6)

C14 C15 1.391(7)

C14 C13 1.393(7)

C14 C1 1.504(7)

C19 H19A 0.9600

C19 H19B 0.9600

C19 H19C 0.9600

C5 H5 0.9300
C5 C6 1.377(6)
C15 H15 0.9300
C15 C16 1.386(7)
C6 C9 1.518(6)
C20 H20A 0.9600
C20 H20B 0.9600
C20 H20C 0.9600
C12 H12 0.9300
C12 C13 1.384(7)
C13 H13 0.9300
C2 H2A 0.9700
C2 H2B 0.9700
C2 C1 1.590(6)
C1 H1A 0.9700
C1 H1B 0.9700
C16 H16 0.9300
C10 H10A 0.9700
C10 H10B 0.9700
C10 C9 1.574(6)

C9 H9A 0.9700

C9 H9B 0.9700

angle

O1 P1 C4 115.7(2) .

O1 P1 C17 113.5(2) .

O1 P1 H1 110.7(15) .

C4 P1 C17 107.9(2) .

C4 P1 H1 104.3(15) .

C17 P1 H1 103.8(15) .

C4 C3 C2 123.7(5) .

C8 C3 C4 116.4(5) .

C8 C3 C2 118.6(5) .

C12 C11 C10 120.9(6) .

C16 C11 C12 116.3(6) .

C16 C11 C10 121.0(6) .

C3 C4 P1 122.0(4) .

C5 C4 P1 117.8(4) .

C5 C4 C3 119.9(5) .

C3 C8 H8 119.4 .

C3 C8 C7 121.2(5) .

C7 C8 H8 119.4 .

C18 C17 P1 109.6(4) .

C18 C17 C19 110.1(5) .

C18 C17 C20 110.6(5) .

C19 C17 P1 107.3(4) .

C20 C17 P1 109.4(4) .

C20 C17 C19 109.8(5) .

C17 C18 H18A 109.5 .

C17 C18 H18B 109.5 .

C17 C18 H18C 109.5 .

H18A C18 H18B 109.5 .

H18A C18 H18C 109.5 .

H18B C18 H18C 109.5 .

C8 C7 H7 119.7 .

C6 C7 C8 120.6(5) .

C6 C7 H7 119.7 .

C15 C14 C13 116.6(6) .

C15 C14 C1 121.8(6) .

C13 C14 C1 120.2(5) .

C17 C19 H19A 109.5 .

C17 C19 H19B 109.5 .

C17 C19 H19C 109.5 .

H19A C19 H19B 109.5 .

H19A C19 H19C 109.5 .

H19B C19 H19C 109.5 .

C4 C5 H5 118.9 .

C6 C5 C4 122.1(6) .

C6 C5 H5 118.9 .

C14 C15 H15 119.4 .

C16 C15 C14 121.2(6) .

C16 C15 H15 119.4 .

C7 C6 C9 120.8(5) .

C5 C6 C7 116.5(5) .

C5 C6 C9 121.4(5) .

C17 C20 H20A 109.5 .

C17 C20 H20B 109.5 .

C17 C20 H20C 109.5 .

H20A C20 H20B 109.5 .

H20A C20 H20C 109.5 .

H20B C20 H20C 109.5 .
C11 C12 H12 118.9 .
C13 C12 C11 122.3(6) .
C13 C12 H12 118.9 .
C14 C13 H13 120.0 .
C12 C13 C14 120.0(6) .
C12 C13 H13 120.0 .
C3 C2 H2A 109.1 .
C3 C2 H2B 109.1 .
C3 C2 C1 112.4(4) .
H2A C2 H2B 107.9 .
C1 C2 H2A 109.1 .
C1 C2 H2B 109.1 .
C14 C1 C2 113.5(4) .
C14 C1 H1A 108.9 .
C14 C1 H1B 108.9 .
C2 C1 H1A 108.9 .
C2 C1 H1B 108.9 .
H1A C1 H1B 107.7 .
C11 C16 C15 121.0(6) .

C11 C16 H16 119.5 .
C15 C16 H16 119.5 .
C11 C10 H10A 108.9 .
C11 C10 H10B 108.9 .
C11 C10 C9 113.4(4) .
H10A C10 H10B 107.7 .
C9 C10 H10A 108.9 .
C9 C10 H10B 108.9 .
C6 C9 C10 113.4(4) .
C6 C9 H9A 108.9 .
C6 C9 H9B 108.9 .
C10 C9 H9A 108.9 .
C10 C9 H9B 108.9 .
H9A C9 H9B 107.7 .

loop_

_geom_torsion_atom_site_label_1

_geom_torsion_atom_site_label_2

_geom_torsion_atom_site_label_3

_geom_torsion_atom_site_label_4

_geom_torsion
_geom_torsion_site_symmetry_1
_geom_torsion_site_symmetry_2
_geom_torsion_site_symmetry_3
_geom_torsion_site_symmetry_4
_geom_torsion_publ_flag
P1 C4 C5 C6 -176.3(4) . . .
O1 P1 C4 C3 -44.4(5) . . .
O1 P1 C4 C5 129.9(4) . . .
O1 P1 C17 C18 61.4(4) . . .
O1 P1 C17 C19 -58.1(4) . . .
O1 P1 C17 C20 -177.1(4) . . .
C3 C4 C5 C6 -1.8(7) . . .
C3 C8 C7 C6 -0.7(8) . . .
C3 C2 C1 C14 10.1(7) . . .
C11 C12 C13 C14 1.2(8) . . .
C11 C10 C9 C6 -3.1(7) . . .
C4 P1 C17 C18 -68.2(5) . . .
C4 P1 C17 C19 172.3(4) . . .
C4 P1 C17 C20 53.3(5) . . .

C4 C3 C8 C7 -14.4(7) . . .
C4 C3 C2 C1 74.5(6) . . .
C4 C5 C6 C7 -13.4(8) . . .
C4 C5 C6 C9 153.8(5) . . .
C8 C3 C4 P1 -170.1(4) . . .
C8 C3 C4 C5 15.6(7) . . .
C8 C3 C2 C1 -91.9(6) . . .
C8 C7 C6 C5 14.6(8) . . .
C8 C7 C6 C9 -152.7(5) . . .
C17 P1 C4 C3 83.9(5) . . .
C17 P1 C4 C5 -101.7(4) . . .
C7 C6 C9 C10 87.3(7) . . .
C14 C15 C16 C11 -0.4(8) . . .
C5 C6 C9 C10 -79.3(7) . . .
C15 C14 C13 C12 -14.0(8) . . .
C15 C14 C1 C2 74.2(7) . . .
C12 C11 C16 C15 -12.3(8) . . .
C12 C11 C10 C9 85.8(7) . . .
C13 C14 C15 C16 13.6(8) . . .
C13 C14 C1 C2 -91.6(6) . . .

C2 C3 C4 P1 23.2(7) . . .

C2 C3 C4 C5 -151.0(5) . . .

C2 C3 C8 C7 152.9(5) . . .

C1 C14 C15 C16 -152.7(5) . . .

C1 C14 C13 C12 152.6(5) . . .

C16 C11 C12 C13 12.0(8) . . .

C16 C11 C10 C9 -78.3(7) . . .

C10 C11 C12 C13 -152.9(5) . . .

C10 C11 C16 C15 152.5(5) . . .

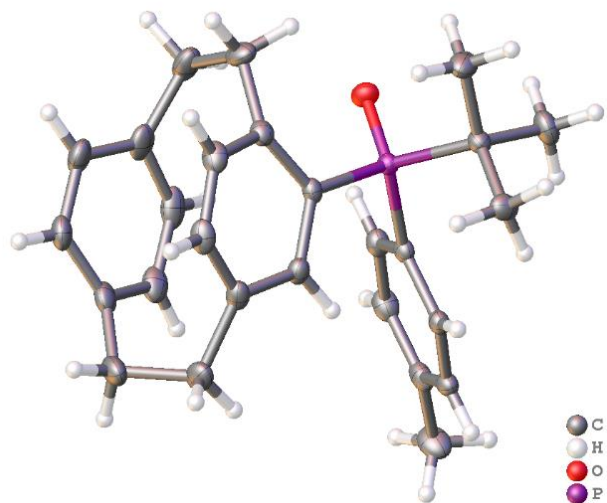


Figure 2.6: X-ray structure of tertiary phosphine oxide (RS_{ρ},SR_{ρ})-**2.116**.
(Ellipsoids are drawn at a 50% probability level.)

bond_distance

P O 1.4902(13)

P C17 1.8153(19)

P C4 1.8246(18)

P C24 1.845(2)

C1 C14 1.513(3)

C1 C2 1.579(3)

C1 H1A 0.99

C1 H1B 0.99

C2 C3 1.515(3)

C2 H2A 0.99

C2 H2B 0.99

C3 C8 1.398(3)

C3 C4 1.412(2)

C4 C5 1.403(2)

C5 C6 1.394(3)

C5 H5 0.95

C6 C7 1.392(3)

C6 C9 1.515(3)

C7 C8 1.383(3)

C7 H7 0.95

C8 H8 0.95

C9 C10 1.571(3)

C9 H9A 0.99

C9 H9B 0.99

C10 C11 1.512(3)

C10 H10A 0.99

C10 H10B 0.99

C11 C16 1.392(3)

C11 C12 1.397(3)

C12 C13 1.388(3)

C12 H12 0.95

C13 C14 1.393(3)

C13 H13 0.95

C14 C15 1.396(3)

C15 C16 1.387(3)

C15 H15 0.95

C16 H16 0.95

C17 C22 1.402(3)

C17 C18 1.404(3)

C18 C19 1.386(3)

C18 H18 0.95

C19 C20 1.393(3)

C19 H19 0.95

C20 C21 1.394(3)

C20 C23 1.505(3)

C21 C22 1.388(2)

C21 H21 0.95

C22 H22 0.95

C23 H23A 0.98

C23 H23B 0.98

C23 H23C 0.98

C24 C27 1.530(3)

C24 C25 1.534(3)

C24 C26 1.535(3)

C25 H25A 0.98

C25 H25B 0.98

C25 H25C 0.98

C26 H26A 0.98

C26 H26B 0.98

C26 H26C 0.98

C27 H27A 0.98

C27 H27B 0.98

C27 H27C 0.98

angle

O P C17 109.44(8) .

O P C4 113.44(8) .
C17 P C4 107.21(8) .
O P C24 110.53(8) .
C17 P C24 109.72(8) .
C4 P C24 106.38(8) .
C14 C1 C2 112.28(17) .
C14 C1 H1A 109.1 .
C2 C1 H1A 109.1 .
C14 C1 H1B 109.1 .
C2 C1 H1B 109.1 .
H1A C1 H1B 107.9 .
C3 C2 C1 112.58(16) .
C3 C2 H2A 109.1 .
C1 C2 H2A 109.1 .
C3 C2 H2B 109.1 .
C1 C2 H2B 109.1 .
H2A C2 H2B 107.8 .
C8 C3 C4 116.84(18) .
C8 C3 C2 116.87(17) .
C4 C3 C2 124.80(16) .

C5 C4 C3 118.32(16) .

C5 C4 P 119.88(13) .

C3 C4 P 121.53(14) .

C6 C5 C4 122.41(17) .

C6 C5 H5 118.8 .

C4 C5 H5 118.8 .

C7 C6 C5 116.73(18) .

C7 C6 C9 121.29(18) .

C5 C6 C9 120.54(18) .

C8 C7 C6 119.99(17) .

C8 C7 H7 120 .

C6 C7 H7 120 .

C7 C8 C3 122.03(17) .

C7 C8 H8 119 .

C3 C8 H8 119 .

C6 C9 C10 112.09(17) .

C6 C9 H9A 109.2 .

C10 C9 H9A 109.2 .

C6 C9 H9B 109.2 .

C10 C9 H9B 109.2 .

H9A C9 H9B 107.9 .
C11 C10 C9 111.97(17) .
C11 C10 H10A 109.2 .
C9 C10 H10A 109.2 .
C11 C10 H10B 109.2 .
C9 C10 H10B 109.2 .
H10A C10 H10B 107.9 .
C16 C11 C12 117.0(2) .
C16 C11 C10 119.9(2) .
C12 C11 C10 121.1(2) .
C13 C12 C11 120.5(2) .
C13 C12 H12 119.7 .
C11 C12 H12 119.7 .
C12 C13 C14 120.83(19) .
C12 C13 H13 119.6 .
C14 C13 H13 119.6 .
C13 C14 C15 117.2(2) .
C13 C14 C1 120.1(2) .
C15 C14 C1 121.2(2) .
C16 C15 C14 120.5(2) .

C16 C15 H15 119.8 .
C14 C15 H15 119.8 .
C15 C16 C11 121.0(2) .
C15 C16 H16 119.5 .
C11 C16 H16 119.5 .
C22 C17 C18 117.94(17) .
C22 C17 P 126.64(14) .
C18 C17 P 115.41(14) .
C19 C18 C17 121.06(18) .
C19 C18 H18 119.5 .
C17 C18 H18 119.5 .
C18 C19 C20 121.10(18) .
C18 C19 H19 119.4 .
C20 C19 H19 119.4 .
C19 C20 C21 117.84(18) .
C19 C20 C23 121.4(2) .
C21 C20 C23 120.7(2) .
C22 C21 C20 121.77(18) .
C22 C21 H21 119.1 .
C20 C21 H21 119.1 .

C21 C22 C17 120.28(18) .

C21 C22 H22 119.9 .

C17 C22 H22 119.9 .

C20 C23 H23A 109.5 .

C20 C23 H23B 109.5 .

H23A C23 H23B 109.5 .

C20 C23 H23C 109.5 .

H23A C23 H23C 109.5 .

H23B C23 H23C 109.5 .

C27 C24 C25 109.27(16) .

C27 C24 C26 109.57(16) .

C25 C24 C26 109.37(17) .

C27 C24 P 114.18(13) .

C25 C24 P 106.61(13) .

C26 C24 P 107.73(13) .

C24 C25 H25A 109.5 .

C24 C25 H25B 109.5 .

H25A C25 H25B 109.5 .

C24 C25 H25C 109.5 .

H25A C25 H25C 109.5 .

H25B C25 H25C 109.5 .

C24 C26 H26A 109.5 .

C24 C26 H26B 109.5 .

H26A C26 H26B 109.5 .

C24 C26 H26C 109.5 .

H26A C26 H26C 109.5 .

H26B C26 H26C 109.5 .

C24 C27 H27A 109.5 .

C24 C27 H27B 109.5 .

H27A C27 H27B 109.5 .

C24 C27 H27C 109.5 .

H27A C27 H27C 109.5 .

H27B C27 H27C 109.5 .

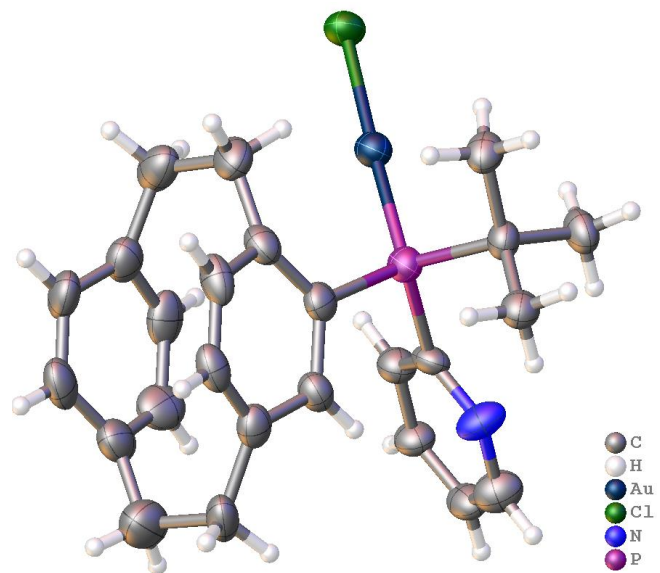


Figure 2.7: X-ray structure of gold complex of phosphine **2.137**.AuCl.
(Ellipsoids are drawn at a 50% probability level.)

bond_distance

P O 1.4902(13)

P C17 1.8153(19)

P C4 1.8246(18)

P C24 1.845(2)

C1 C14 1.513(3)

C1 C2 1.579(3)

C1 H1A 0.99

C1 H1B 0.99

C2 C3 1.515(3)

C2 H2A 0.99

C2 H2B 0.99

C3 C8 1.398(3)

C3 C4 1.412(2)

C4 C5 1.403(2)

C5 C6 1.394(3)

C5 H5 0.95

C6 C7 1.392(3)

C6 C9 1.515(3)

C7 C8 1.383(3)

C7 H7 0.95

C8 H8 0.95

C9 C10 1.571(3)

C9 H9A 0.99

C9 H9B 0.99

C10 C11 1.512(3)

C10 H10A 0.99

C10 H10B 0.99

C11 C16 1.392(3)

C11 C12 1.397(3)

C12 C13 1.388(3)

C12 H12 0.95

C13 C14 1.393(3)

C13 H13 0.95

C14 C15 1.396(3)

C15 C16 1.387(3)

C15 H15 0.95

C16 H16 0.95

C17 C22 1.402(3)

C17 C18 1.404(3)

C18 C19 1.386(3)

C18 H18 0.95

C19 C20 1.393(3)

C19 H19 0.95

C20 C21 1.394(3)

C20 C23 1.505(3)

C21 C22 1.388(2)

C21 H21 0.95

C22 H22 0.95

C23 H23A 0.98

C23 H23B 0.98

C23 H23C 0.98

C24 C27 1.530(3)

C24 C25 1.534(3)

C24 C26 1.535(3)

C25 H25A 0.98

C25 H25B 0.98

C25 H25C 0.98

C26 H26A 0.98

C26 H26B 0.98

C26 H26C 0.98

C27 H27A 0.98

C27 H27B 0.98

C27 H27C 0.98

angle

O P C17 109.44(8) .

O P C4 113.44(8) .

C17 P C4 107.21(8) .

O P C24 110.53(8) .

C17 P C24 109.72(8) .

C4 P C24 106.38(8) .

C14 C1 C2 112.28(17) .

C14 C1 H1A 109.1 .

C2 C1 H1A 109.1 .

C14 C1 H1B 109.1 .

C2 C1 H1B 109.1 .

H1A C1 H1B 107.9 .

C3 C2 C1 112.58(16) .
C3 C2 H2A 109.1 .
C1 C2 H2A 109.1 .
C3 C2 H2B 109.1 .
C1 C2 H2B 109.1 .
H2A C2 H2B 107.8 .
C8 C3 C4 116.84(18) .
C8 C3 C2 116.87(17) .
C4 C3 C2 124.80(16) .
C5 C4 C3 118.32(16) .
C5 C4 P 119.88(13) .
C3 C4 P 121.53(14) .
C6 C5 C4 122.41(17) .
C6 C5 H5 118.8 .
C4 C5 H5 118.8 .
C7 C6 C5 116.73(18) .
C7 C6 C9 121.29(18) .
C5 C6 C9 120.54(18) .
C8 C7 C6 119.99(17) .
C8 C7 H7 120 .

C6 C7 H7 120 .
C7 C8 C3 122.03(17) .
C7 C8 H8 119 .
C3 C8 H8 119 .
C6 C9 C10 112.09(17) .
C6 C9 H9A 109.2 .
C10 C9 H9A 109.2 .
C6 C9 H9B 109.2 .
C10 C9 H9B 109.2 .
H9A C9 H9B 107.9 .
C11 C10 C9 111.97(17) .
C11 C10 H10A 109.2 .
C9 C10 H10A 109.2 .
C11 C10 H10B 109.2 .
C9 C10 H10B 109.2 .
H10A C10 H10B 107.9 .
C16 C11 C12 117.0(2) .
C16 C11 C10 119.9(2) .
C12 C11 C10 121.1(2) .
C13 C12 C11 120.5(2) .

C13 C12 H12 119.7 .
C11 C12 H12 119.7 .
C12 C13 C14 120.83(19) .
C12 C13 H13 119.6 .
C14 C13 H13 119.6 .
C13 C14 C15 117.2(2) .
C13 C14 C1 120.1(2) .
C15 C14 C1 121.2(2) .
C16 C15 C14 120.5(2) .
C16 C15 H15 119.8 .
C14 C15 H15 119.8 .
C15 C16 C11 121.0(2) .
C15 C16 H16 119.5 .
C11 C16 H16 119.5 .
C22 C17 C18 117.94(17) .
C22 C17 P 126.64(14) .
C18 C17 P 115.41(14) .
C19 C18 C17 121.06(18) .
C19 C18 H18 119.5 .
C17 C18 H18 119.5 .

C18 C19 C20 121.10(18) .

C18 C19 H19 119.4 .

C20 C19 H19 119.4 .

C19 C20 C21 117.84(18) .

C19 C20 C23 121.4(2) .

C21 C20 C23 120.7(2) .

C22 C21 C20 121.77(18) .

C22 C21 H21 119.1 .

C20 C21 H21 119.1 .

C21 C22 C17 120.28(18) .

C21 C22 H22 119.9 .

C17 C22 H22 119.9 .

C20 C23 H23A 109.5 .

C20 C23 H23B 109.5 .

H23A C23 H23B 109.5 .

C20 C23 H23C 109.5 .

H23A C23 H23C 109.5 .

H23B C23 H23C 109.5 .

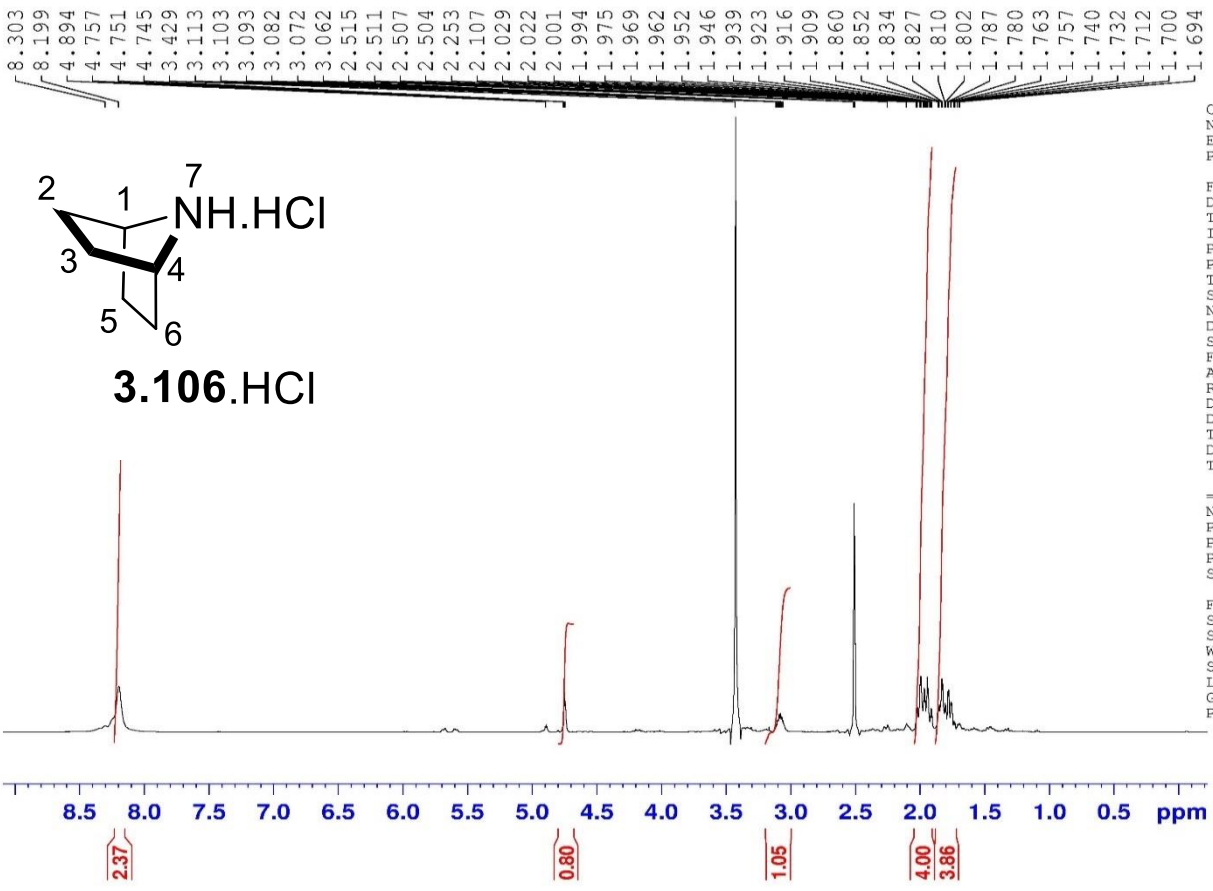
C27 C24 C25 109.27(16) .

C27 C24 C26 109.57(16) .

C25 C24 C26 109.37(17) .
C27 C24 P 114.18(13) .
C25 C24 P 106.61(13) .
C26 C24 P 107.73(13) .
C24 C25 H25A 109.5 .
C24 C25 H25B 109.5 .
H25A C25 H25B 109.5 .
C24 C25 H25C 109.5 .
H25A C25 H25C 109.5 .
H25B C25 H25C 109.5 .
C24 C26 H26A 109.5 .
C24 C26 H26B 109.5 .
H26A C26 H26B 109.5 .
C24 C26 H26C 109.5 .
H26A C26 H26C 109.5 .
H26B C26 H26C 109.5 .
C24 C27 H27A 109.5 .
C24 C27 H27B 109.5 .
H27A C27 H27B 109.5 .
C24 C27 H27C 109.5 .

Electronic Appendix for Chapter 3

Cyclic amine



Current Data Parameters
 NAME III-Mn-76 crude
 EXPNO 1
 PROCNO 1

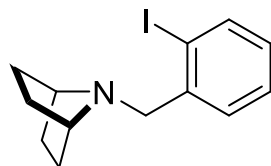
F2 - Acquisition Parameters
 Date_ 20180310
 Time 14.15
 INSTRUM spect
 PROBHD 5 mm PAQXI 1H/
 PULPROG zg30
 TD 65536
 SOLVENT DMSO
 NS 16
 DS 2
 SWH 10330.578 Hz
 FIDRES 0.157632 Hz
 AQ 3.1719425 sec
 RG 90.5
 DW 48.400 usec
 DE 6.50 usec
 TE 298.2 K
 D1 1.00000000 sec
 TD0 1

===== CHANNEL f1 =====
 NUC1 1H
 P1 9.50 usec
 PL1 4.00 dB
 PL1W 12.10000038 W
 SFO1 500.1330885 MHz

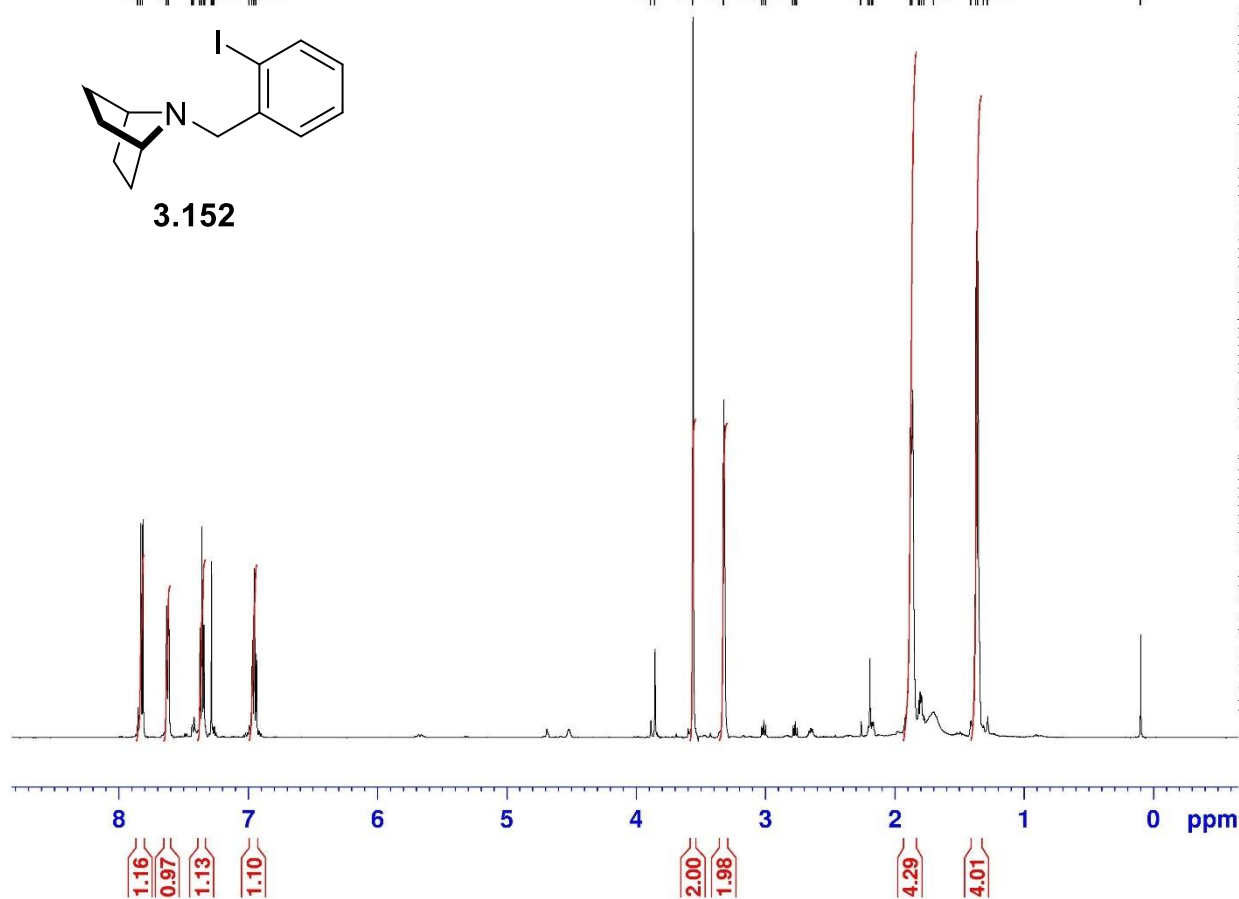
F2 - Processing parameters
 SI 32768
 SF 500.1300000 MHz
 WDW EM
 SSB 0
 LB 0.30 Hz
 GB 0
 PC 1.00

N-alkylation

7.856
7.834
7.818
7.634
7.619
7.436
7.423
7.376
7.361
7.346
7.335
7.287
7.278
7.267
7.263
6.994
6.971
6.956
6.941
3.889
3.857
3.563
3.324
3.032
3.017
3.001
2.788
2.772
2.757
2.262
2.206
2.194
2.178
2.169
1.879
1.865
1.817
1.807
1.796
1.775
1.700
1.414
1.373
1.359
1.316
1.284
0.100



3.152



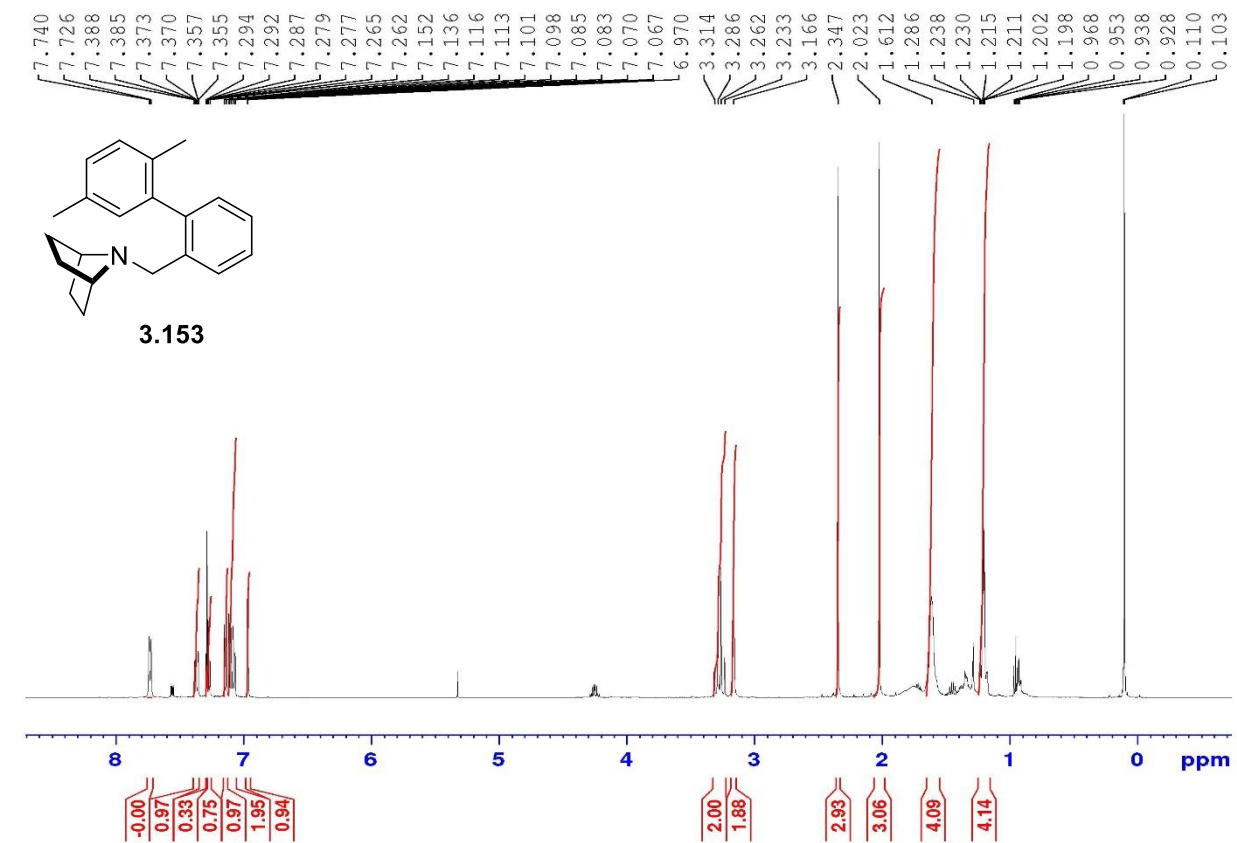
Current Data Parameters
NAME III-Mn-58 i
EXPNO 1
PROCNO 1

F2 - Acquisition Parameters
Date_ 20180222
Time 8.26
INSTRUM spect
PROBHD 5 mm PAQXI 1H/
PULPROG zg30
TD 65536
SOLVENT CDCl3
NS 16
DS 2
SWH 10330.578 Hz
FIDRES 0.157632 Hz
AQ 3.1719425 sec
RG 71.8
DW 48.400 usec
DE 6.50 usec
TE 298.2 K
D1 1.00000000 sec
TD0 1

==== CHANNEL f1 =====
NUC1 1H
P1 9.50 usec
PL1 4.00 dB
PL1W 12.10000038 W
SFO1 500.1330885 MHz

F2 - Processing parameters
SI 32768
SF 500.1300000 MHz
WDW EM
SSB 0
LB 0.30 Hz
GB 0
PC 1.00

Sp3-H



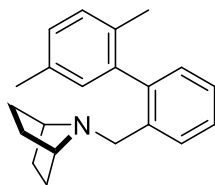
Current Data Parameters
NAME III-Mn-50 i
EXPNO 1
PROCNO 1

F2 - Acquisition Parameters
Date_ 20180218
Time 14.58
INSTRUM spect
PROBHD 5 mm PAQXI 1H/
PULPROG zg30
TD 65536
SOLVENT CDCl3
NS 16
DS 2
SWH 10330.578 Hz
FIDRES 0.157632 Hz
AQ 3.1719425 sec
RG 71.8
DW 48.400 usec
DE 6.50 usec
TE 298.2 K
D1 1.0000000 sec
TD0 1

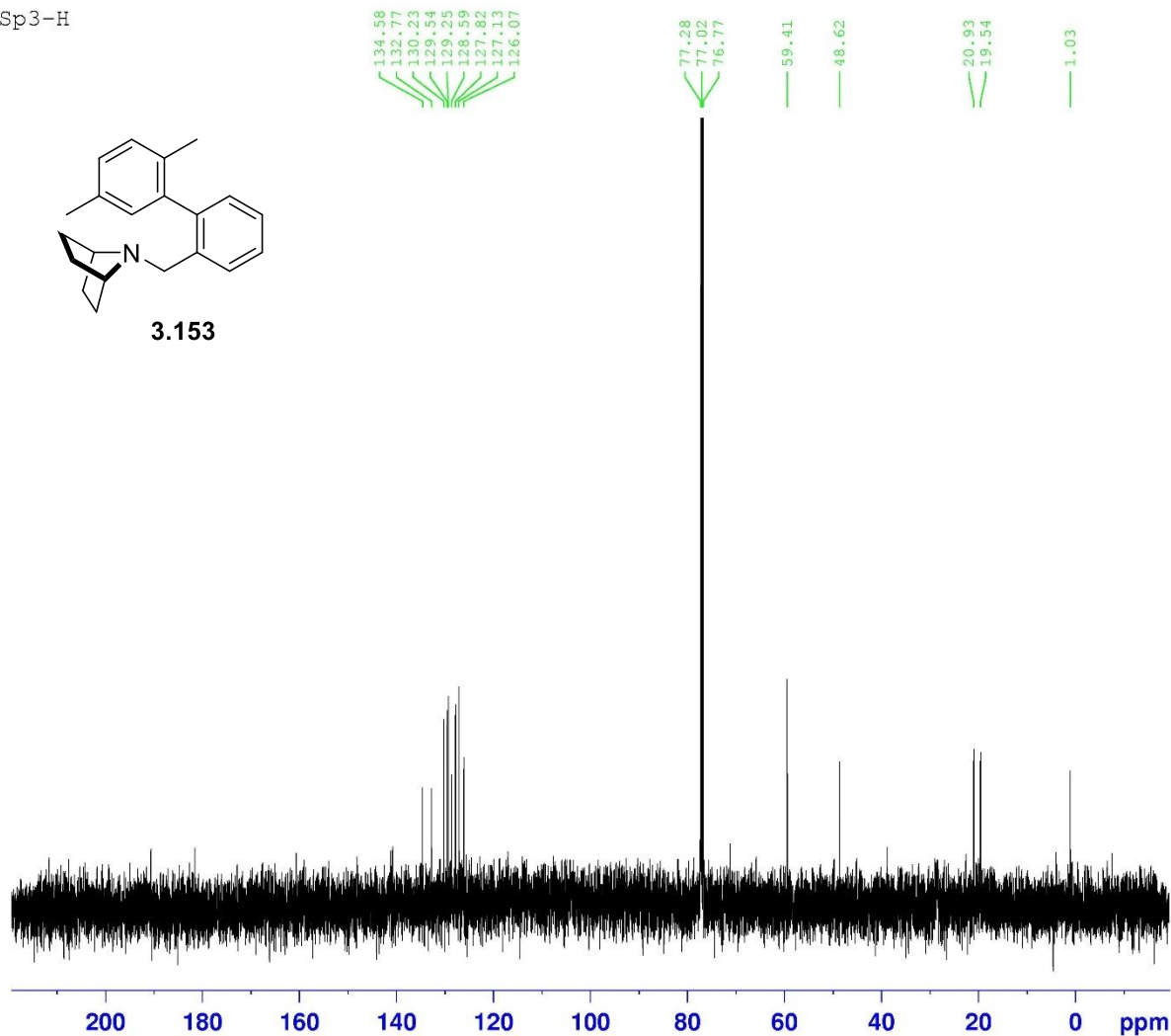
----- CHANNEL f1 -----
NUC1 1H
P1 9.50 usec
PL1 4.00 dB
PL1W 12.10000038 W
SFO1 500.1330885 MHz

F2 - Processing parameters
SI 32768
SF 500.1300000 MHz
WDW EM
SSB 0
LB 0.30 Hz
GB 0
PC 1.00

Sp3-H



3.153



Current Data Parameters
NAME III-Mn-50 i
EXPNO 2
PROCNO 1

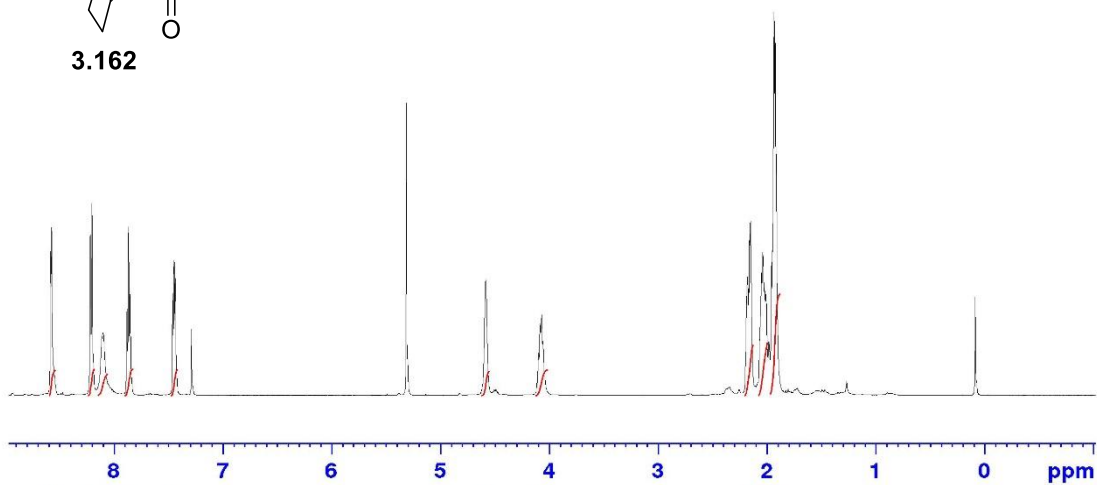
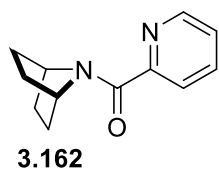
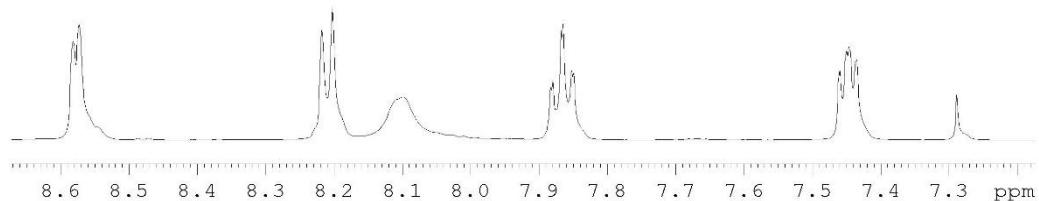
F2 - Acquisition Parameters
Date_ 20180216
Time 15.09
INSTRUM spect
PROBHD 5 mm PAQXI 1H/
PULPROG zgpg30
TD 65536
SOLVENT CDCl3
NS 64
DS 4
SWH 30030.029 Hz
FIDRES 0.458222 Hz
AQ 1.0911744 sec
RG 32768
DW 16.650 usec
DE 6.50 usec
TE 298.2 K
D1 2.0000000 sec
D11 0.0300000 sec
TDO 1

===== CHANNEL f1 =====
NUC1 13C
P1 12.00 usec
PL1 -4.00 dB
PL1W 172.88230896 W
SFO1 125.7703643 MHz

===== CHANNEL f2 =====
CPDPRG[2] waltz16
NUC2 1H
PCPD2 80.00 usec
PL2 4.00 dB
PL12 22.51 dB
PL13 25.00 dB
PL2W 12.10000038 W
PL12W 0.17052394 W
PL13W 0.09611372 W
SFO2 500.1320005 MHz

F2 - Processing parameters
SI 32768
SF 125.7577890 MHz
WDW EM
SSB 0
LB 1.00 Hz
GB 0
PC 1.40

Cyclic amine and 2-picolinic acid



1.00
1.03
0.86
1.04
1.03

0.96
1.01

1.99
2.10
4.00



Current Data Parameters
NAME III-Xn-81
EXPNO 4
PROCNO 1

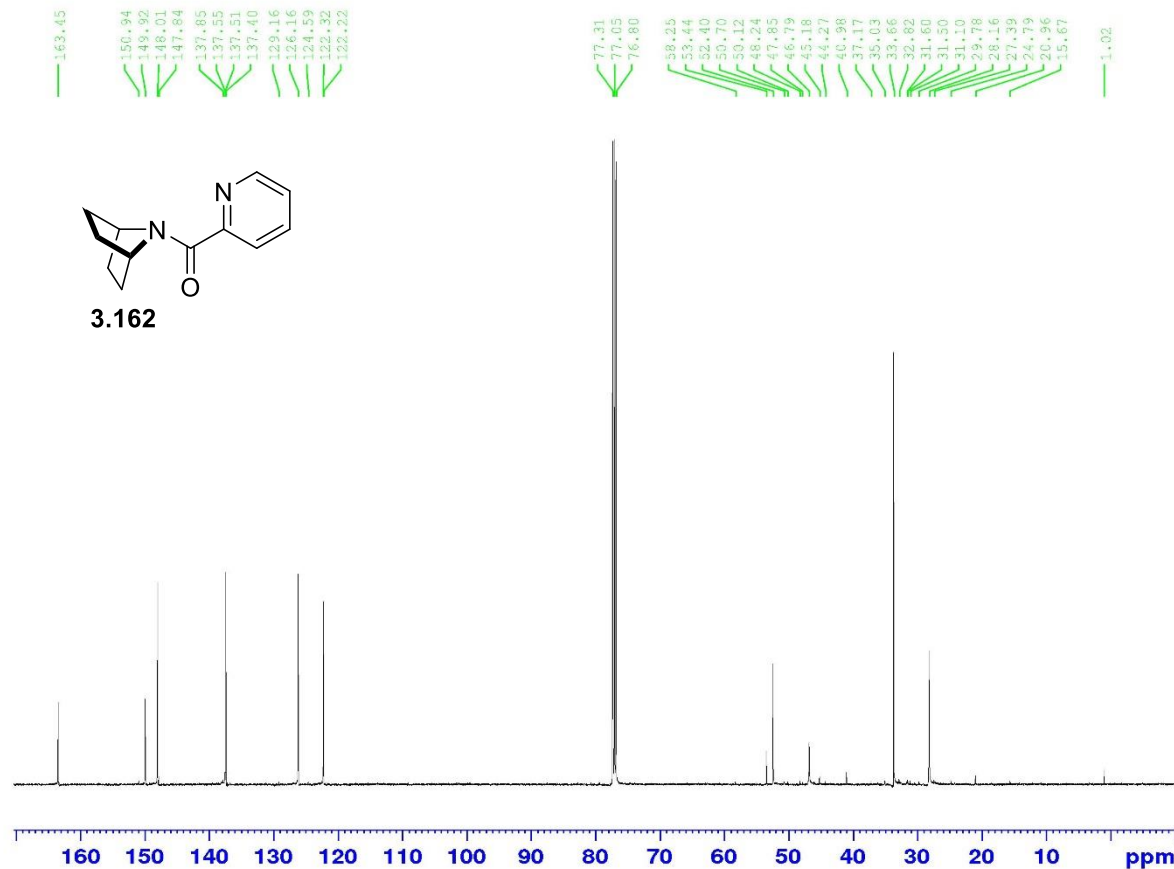
F2 - Acquisition Parameters
Date_ 20181007
Time 20.00
INSTRUM spect
PROBHD 5 mm PAQXI 1H/
PULPROG zg30
TD 65536
SOLVENT CDCl3
NS 16
DS 2
SWH 10330.578 Hz
FIDRES 0.157632 Hz
AQ 3.1719425 sec
RG 64
DW 48.400 usec
DE 6.50 usec
TE 298.2 K
D1 1.00000000 sec
TDO 1

----- CHANNEL f1 -----
NUC1 1H
P1 9.50 usec
PL1 4.00 dB
PL1W 12.10000038 W
SFO1 500.1330885 MHz

F2 - Processing parameters
SI 32768
SF 500.1300000 MHz
WDW EM
SSB 0
LB 0.30 Hz
GB 0
PC 1.00

SSB 0
LB 1.00 Hz
GB 0

Cyclic amine and 2-picolic acid



Current Data Parameters
 NAME_1 111-Mn-81 4
 EXPNO 5
 PROCNO 1

F2 - Acquisition Parameters
 Date_ 20181008
 Time 8.10
 INSTRUM spect
 PROBP1 5 mm PAQXT 1H/
 PULPROG zgpg30
 TD 65536
 SOLVENT CDCl3
 NS 13848
 DS 4
 SWE 30030.029 Hz
 FIDRES 0.458222 Hz
 AQ 1.0911744 sec
 RG 32768
 DW 16.650 usec
 DE 6.50 usec
 TE 298.2 K
 D1 2.00000000 sec
 D11 0.03000000 sec
 TD0 1

----- CHANNEL f1 -----
 NUC1 13C
 P1 12.00 usec
 PL1 -4.00 dB
 PL1W 172.88230896 W
 SFO1 125.7703643 MHz

----- CHANNEL f2 -----
 CPDPRG2 waltz16
 NUC2 1H
 PCPD2 80.00 usec
 PL2 4.00 dB
 PL12 22.51 dB
 PL13 25.00 dB
 PL2W 12.10000038 W
 PL12W 0.17052394 W
 PL13W 0.09611372 W
 SFO2 500.1320005 MHz

F2 - Processing parameters
 SI 32768
 SF 125.7577890 MHz
 WDW EM
 SSB 0
 LB 1.00 Hz
 GB 0
 PC 1.40

Boc deprotection

7.302
7.272
7.221
7.213
7.208
7.200
7.190
7.182
7.152
7.123
7.113
7.105
7.100
7.092
7.083
4.566
4.561
4.555
3.694
3.677
3.660
2.618
2.078
2.072
2.067
2.059
2.055
2.049
2.014
2.006
1.642
1.484
1.467
1.355
1.328
1.293
1.281
1.263
1.251
1.217
0.976
0.960
0.938
0.925
0.922
0.914
0.863



Current Data Parameters
NAME III-Mn-196 crude
EXPNO 1
PROCNO 1

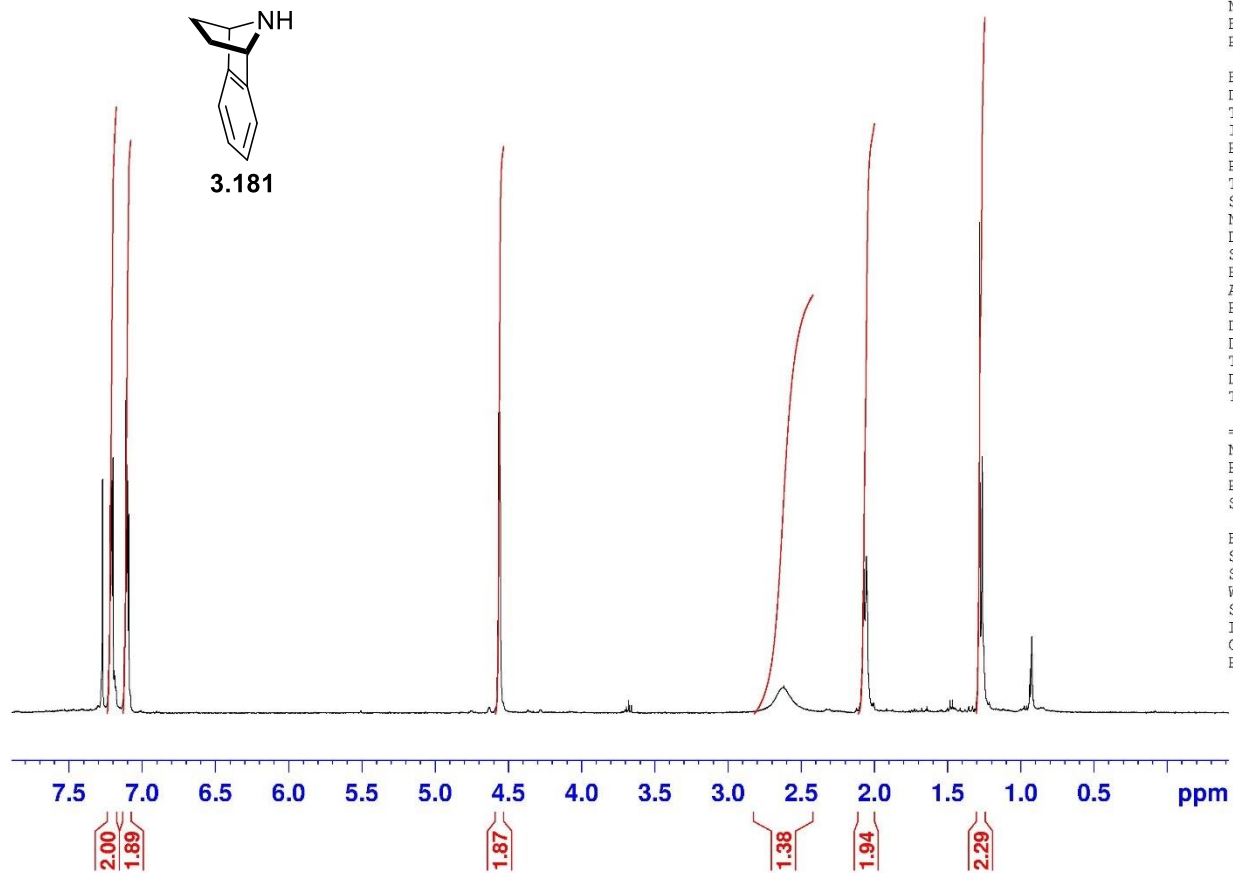
F2 - Acquisition Parameters
Date_ 20180613
Time 10.04
INSTRUM spect
PROBHD 5 mm Multinucl
PULPROG zg30
TD 65536
SOLVENT CDC13
NS 16
DS 2
SWH 8278.146 Hz
FIDRES 0.126314 Hz
AQ 3.9583745 sec
RG 912.3
DW 60.400 usec
DE 6.00 usec
TE 300.0 K
D1 1.00000000 sec
TD0 1

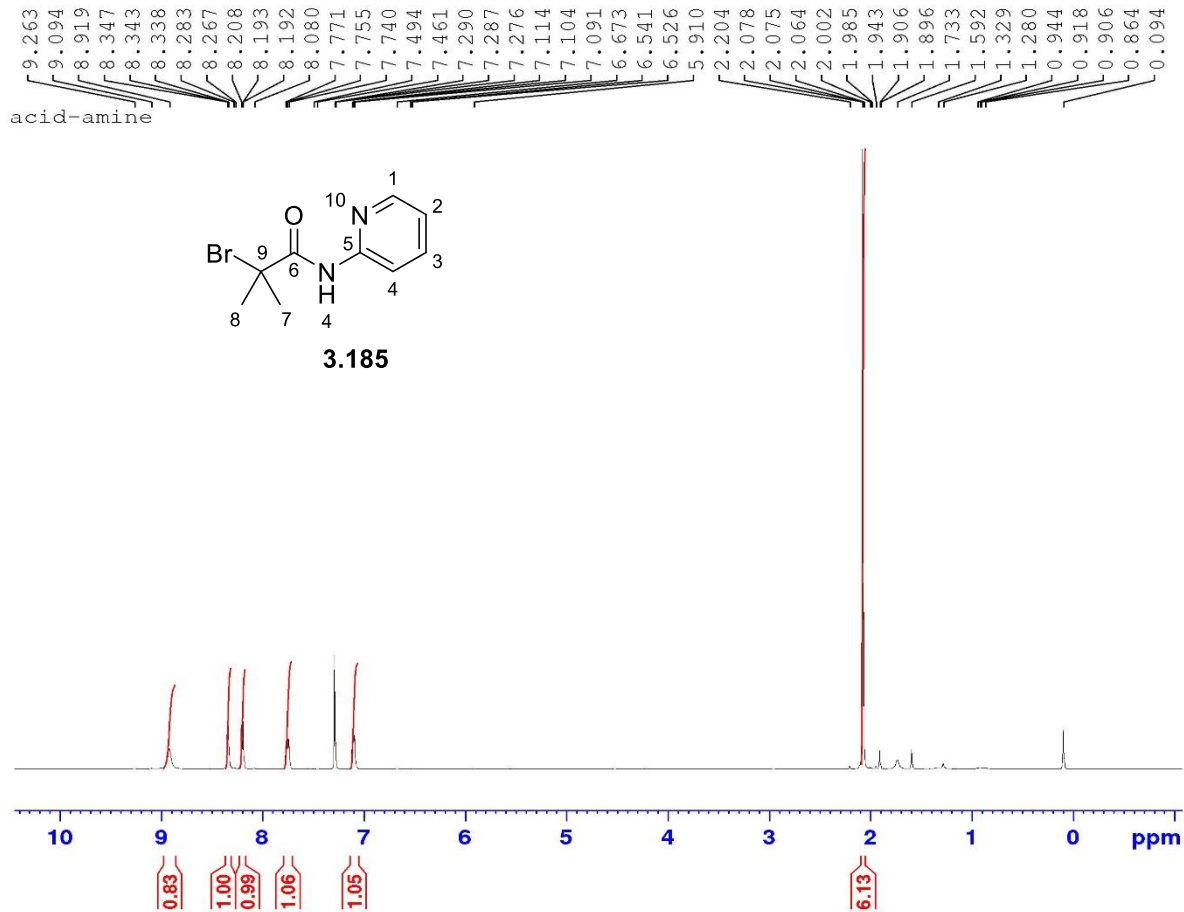
===== CHANNEL f1 =====
NUC1 1H
P1 10.00 usec
PL1 3.80 dB
SFO1 400.1324710 MHz

F2 - Processing parameters
SI 32768
SF 400.1300000 MHz
WDW EM
SSB 0
LB 0.30 Hz
GB 0
PC 1.00



3.181





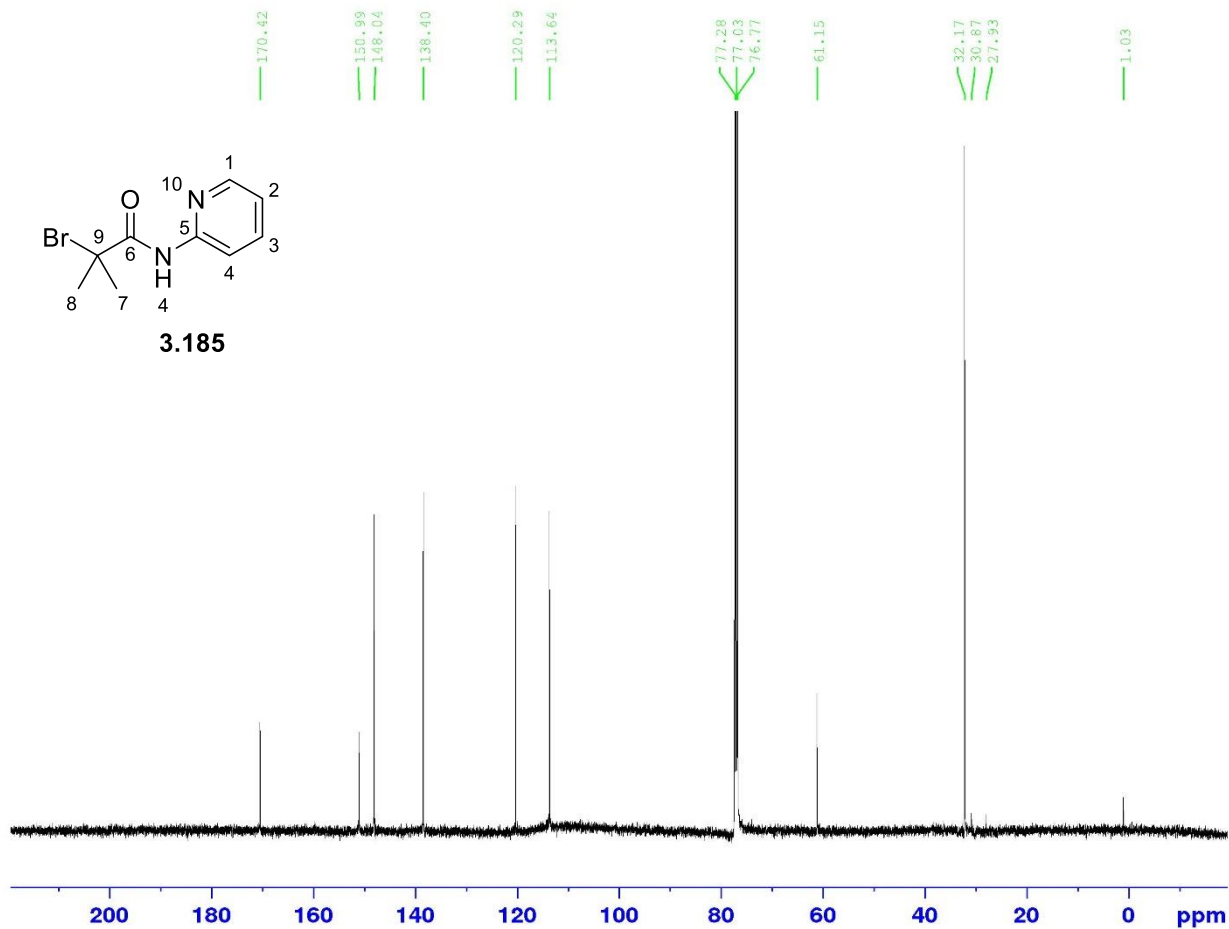
Current Data Parameters
 NAME IV-Mn-110 i
 EXPNO 3
 PROCNO 1

F2 - Acquisition Parameters
 Date_ 20180920
 Time 8.17
 INSTRUM spect
 PROBHD 5 mm PAQXI 1H/
 PULPROG zg30
 TD 65536
 SOLVENT CDCl3
 NS 16
 DS 2
 SWH 10330.578 Hz
 FIDRES 0.157632 Hz
 AQ 3.1719425 sec
 RG 128
 DW 48.400 usec
 DE 6.50 usec
 TE 298.2 K
 D1 1.00000000 sec
 TD0 1

===== CHANNEL f1 =====
 NUC1 1H
 P1 9.50 usec
 PL1 4.00 dB
 PL1W 12.10000038 W
 SFO1 500.1330885 MHz

F2 - Processing parameters
 SI 32768
 SF 500.1300000 MHz
 WDW EM
 SSB 0
 LB 0.30 Hz
 GB 0
 FC 1.00

acid-amine



Current Data Parameters
NAME 1V-MN-110 i
EXPNO 2
PROCNO 1

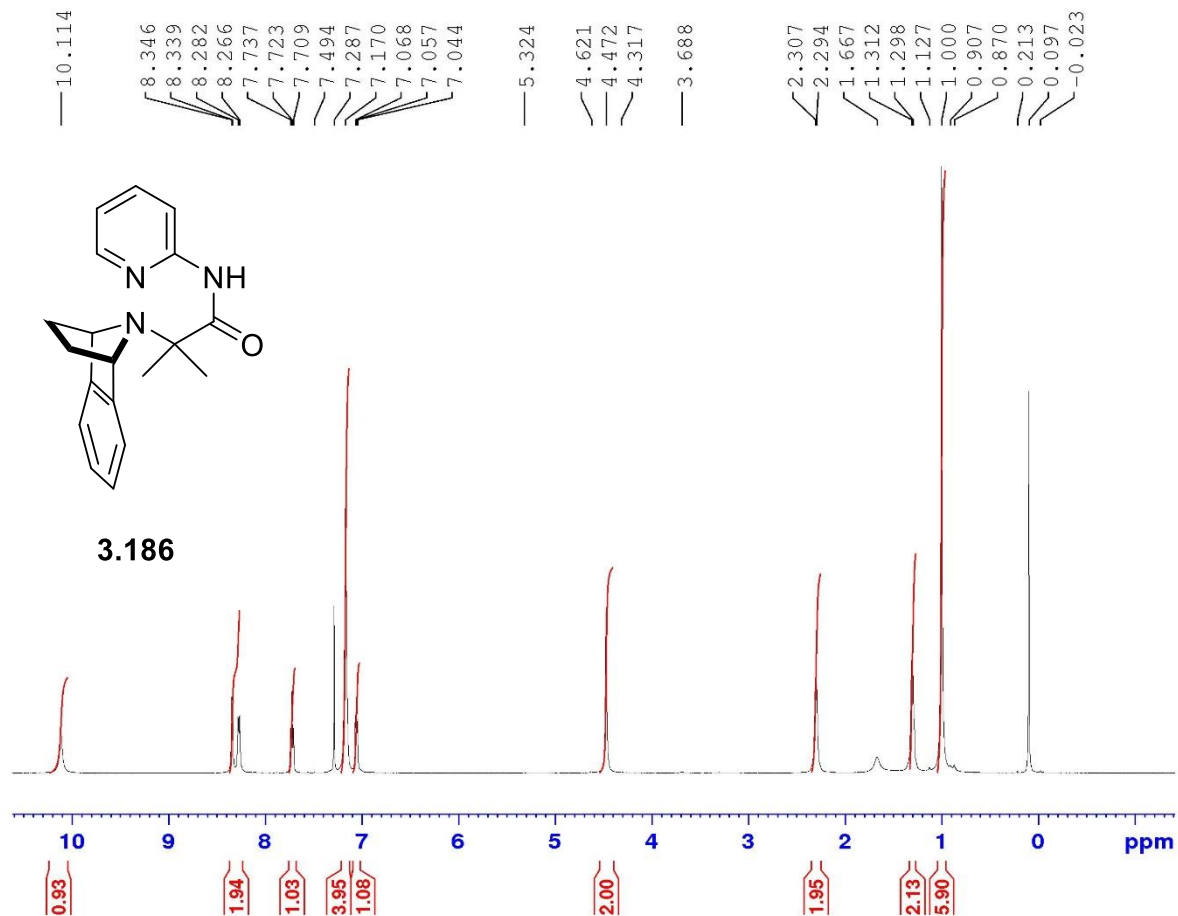
F2 - Acquisition Parameters
Date_ 20180920
Time 7.54
INSTRUM spect
PROBHD 5 mm PAQXI 1H/
PULPROG zgpg30
TD 65536
SOLVENT CDCl3
NS 11978
DS 4
SWH 30030.029 Hz
FIDRES 0.458222 Hz
AQ 1.0911744 sec
RG 32768
DW 16.650 usec
DE 6.50 usec
TE 298.2 K
D1 2.0000000 sec
D11 0.0300000 sec
TDC 1

----- CHANNEL f1 -----
NUC1 13C
P1 12.00 usec
PL1 -4.00 dB
PL1W 172.88230896 W
SFO1 125.7703643 MHz

===== CHANNEL f2 =====
CPDPRG[2] waltz16
NUC2 1H
PCPD2 80.00 usec
PL2 4.00 dB
PL12 22.51 dB
PL13 25.00 dB
PL2W 12.10000038 W
PL12W 0.17052394 W
PL13W 0.09611372 W
SFO2 500.1320005 MHz

F2 - Processing parameters
SI 32768
SF 125.7577890 MHz
WDW EM
SSB 0
LB 1.00 Hz
GB 0
PC 1.40

Precursor



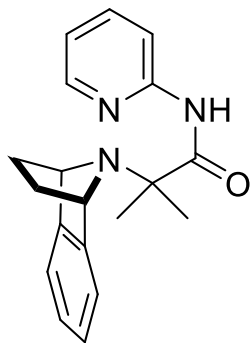
Current Data Parameters
NAME IV-Mn-122 I 0510
EXPNO 1
PROCNO 1

F2 - Acquisition Parameters
Date_ 20181005
Time 18.26
INSTRUM spect
PROBHD 5 mm PAQXI 1H/
PULPROG zg30
TD 65536
SOLVENT CDCl3
NS 16
DS 2
SWH 10330.578 Hz
FIDRES 0.157632 Hz
AQ 3.1719425 sec
RG 128
DW 48.400 usec
DE 6.50 usec
TE 298.2 K
D1 1.0000000 sec
TD0 1

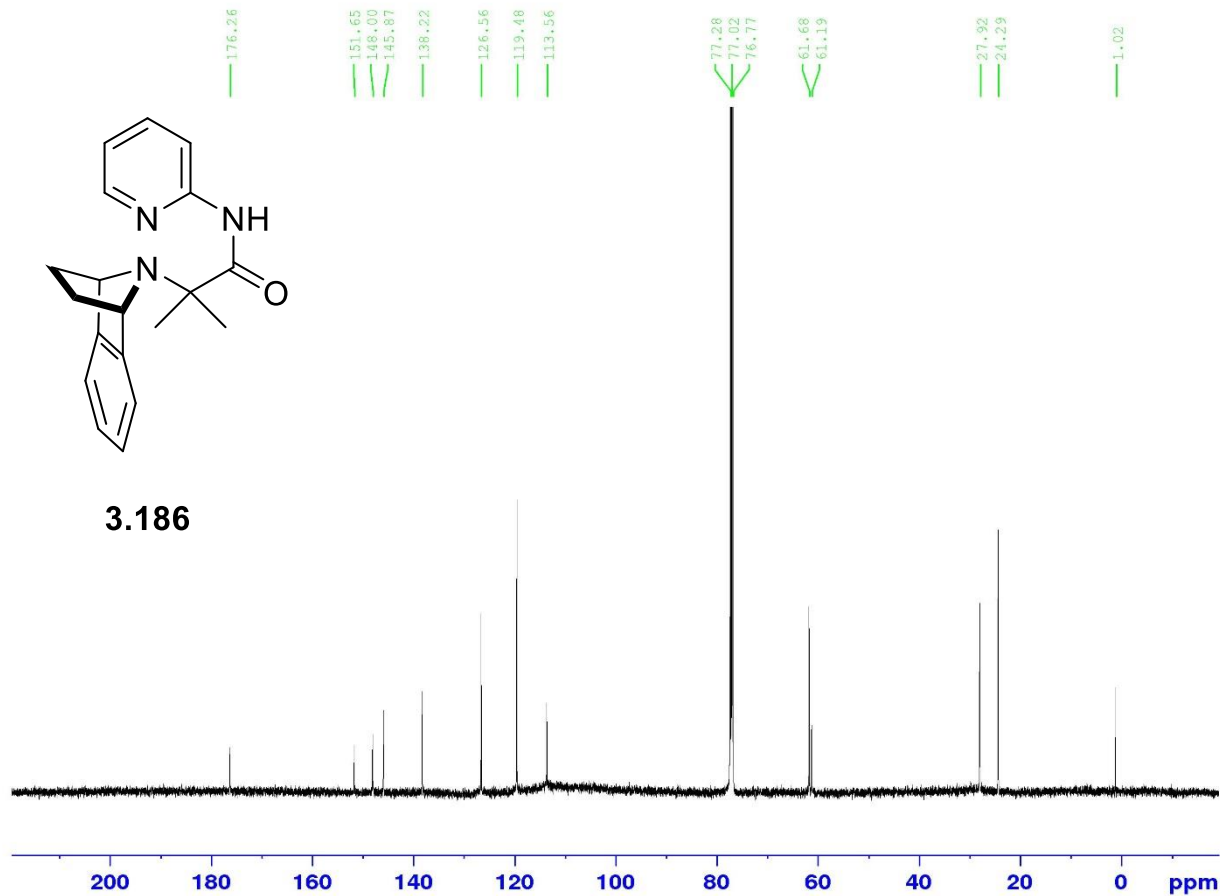
===== CHANNEL f1 =====
NUC1 1H
P1 9.50 usec
PL1 4.00 dB
PLLW 12.10000038 W
SFO1 500.1330885 MHz

F2 - Processing parameters
SI 32768
SF 500.1300000 MHz
WDW EM
SSB 0
LB 0.30 Hz
GB 0
PC 1.00

Precursor



3.186



Current Data Parameters
NAME IV-Mn-122 I 0510
EXPNO 2
PROCNO 1

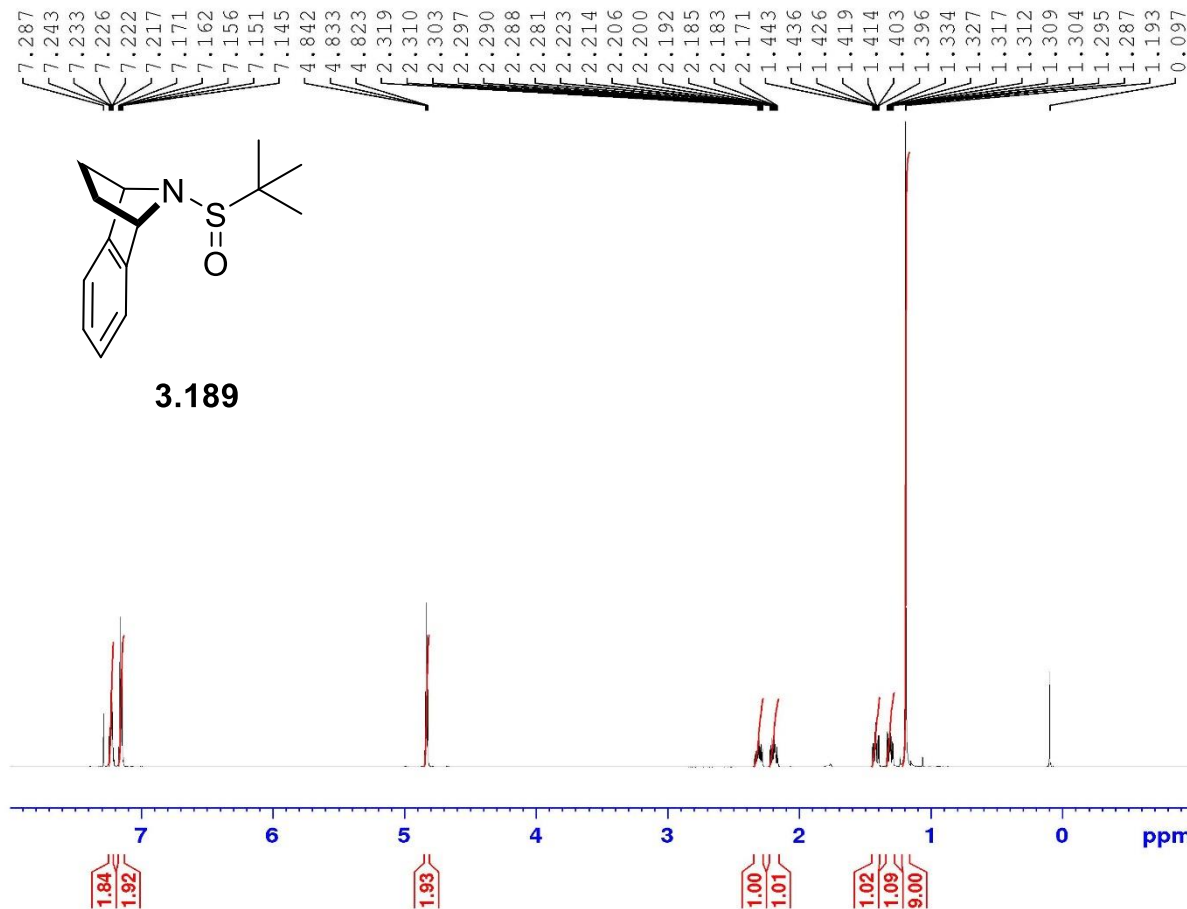
F2 - Acquisition Parameters
Date_ 2018-006
Time 8:49
INSTRUM spect
PROBHD 5 mm PAQXI 1H/
PULPROG zgpg30
TD 65536
SOLVENT CDCl3
NS 16384
DS 4
SWH 30030.029 Hz
FIDRES 0.458222 Hz
AQ 1.0911744 sec
RG 32768
DW 16.650 usec
DE 6.50 usec
TE 298.2 K
D1 2.0000000 sec
D11 0.0300000 sec
TD0 1

===== CHANNEL f1 =====
NUC1 13C
P1 12.00 usec
PL1 -4.00 dB
PL1W 172.88230896 W
SFO1 125.7703643 MHz

===== CHANNEL f2 =====
CPDPRG[2] waltz16
NUC2 1H
PCPD2 80.00 usec
PL2 4.00 dB
PL12 22.51 dB
PL13 25.00 dB
PL2W 12.10000038 W
PL12W 0.17052394 W
PL13W 0.09611372 W
SFO2 500.1320005 MHz

F2 - Processing parameters
SI 32768
SF 125.7577890 MHz
WDW EM
SSB 0
LB 1.00 Hz
GB 0
PC 1.40

Sulfinamide



```

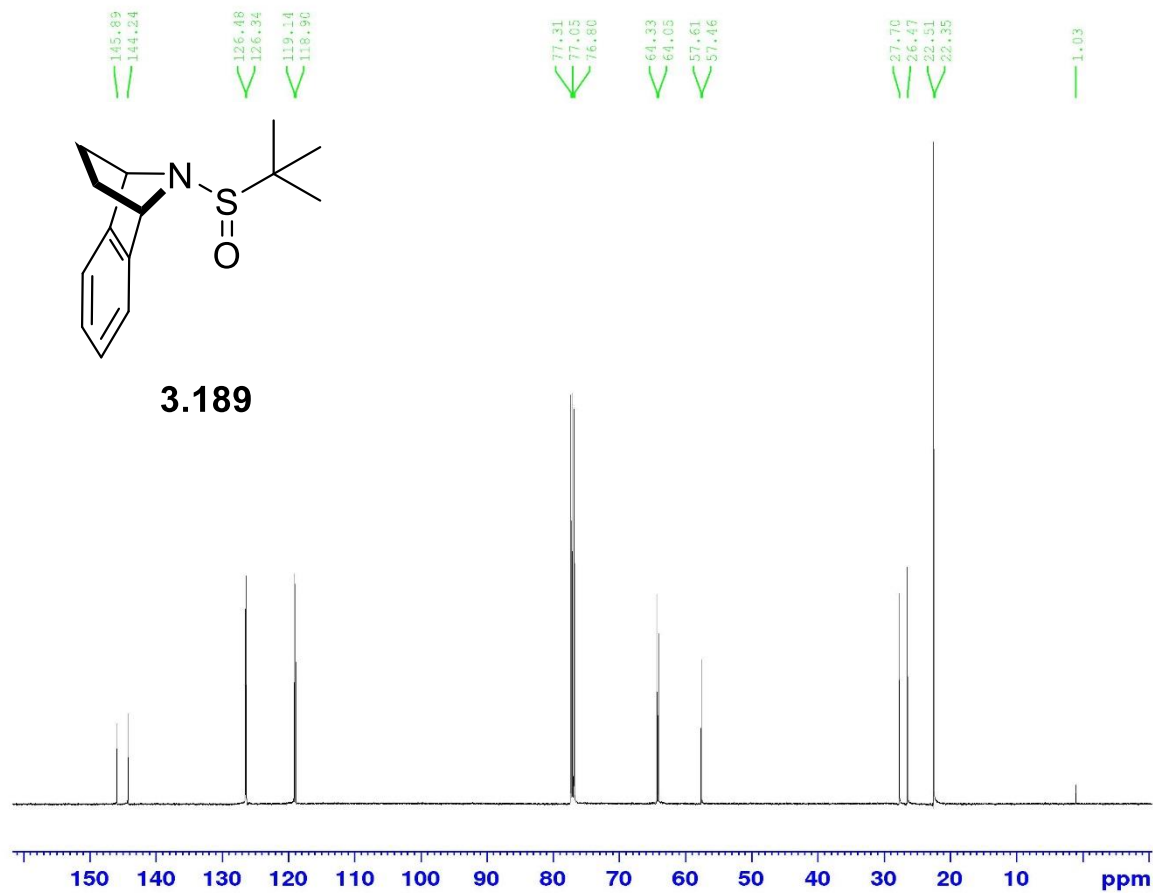
Current Data Parameters
NAME          IV-Mn-02 i
EXPNO         1
PROCNO        1

F2 - Acquisition Parameters
Date_         20180615
Time          18.55
INSTRUM       spect
PROBHD        5 mm PAQXI 1H/
PULPROG       zg30
TD            65536
SOLVENT       CDCl3
NS            16
DS            2
SWH           10330.578 Hz
FIDRES        0.157632 Hz
AQ            3.1719425 sec
RG            57
DW            48.400 usec
DE            6.50 usec
TE            298.2 K
D1            1.00000000 sec
TD0           1

----- CHANNEL f1 -----
NUC1          1H
P1            9.50 usec
PL1           4.00 dB
PL1W          12.10000038 W
SFO1          500.1330885 MHz

F2 - Processing parameters
SI            32768
SF            500.1300000 MHz
WDW           EM
SSB           0
LB            0.30 Hz
GB            0
PC            1.00
    
```

13 C - Sulfinamide



```

Current Data Parameters
NAME      IV-Mn-02  1
EXPNO    2
PROCNO   1

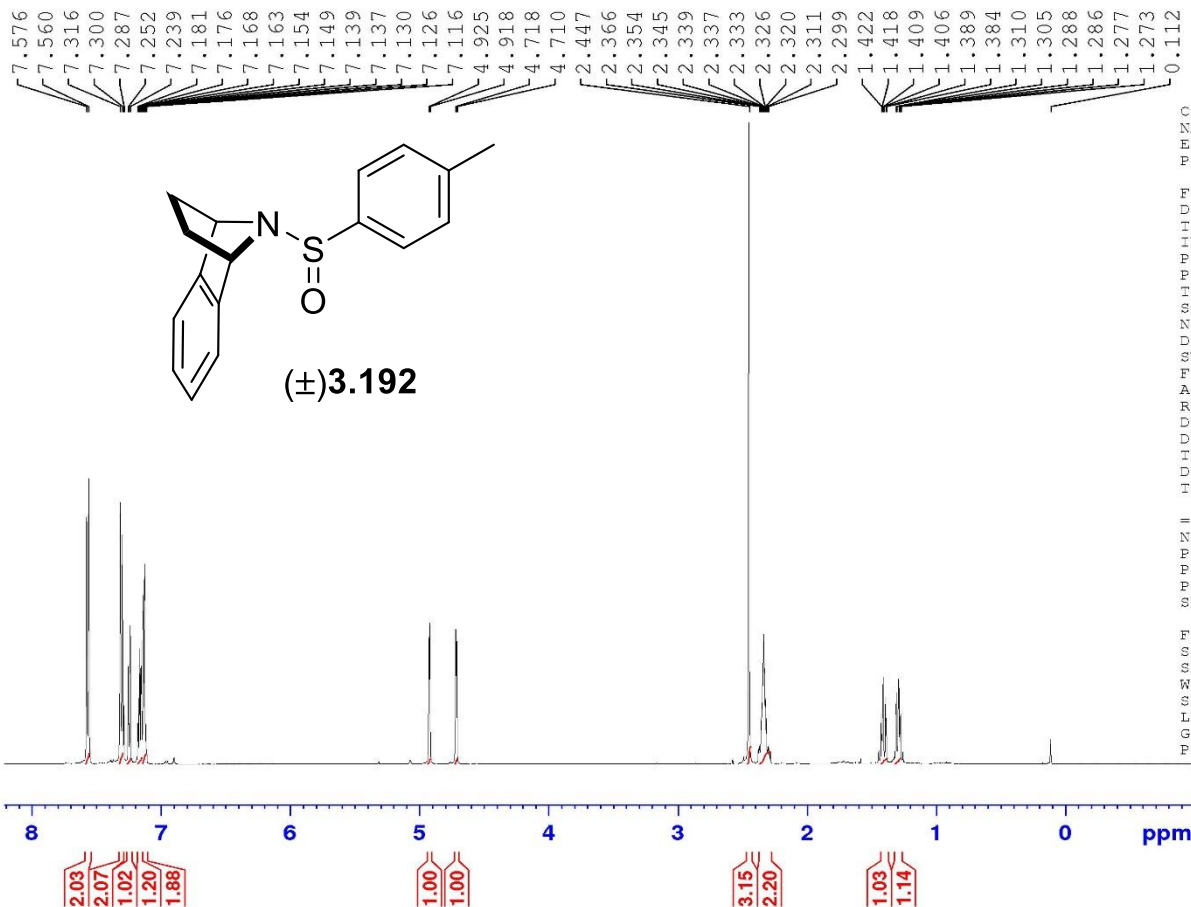
F2 - Acquisition Parameters
Date_    20180616
Time     3.57
INSTRUM  spect
PROBHD   5 mm FAQXI 1H/
PULPROG  zgpg30
TD       65536
SOLVENT  CDCl3
NS       10240
DS       4
SWE      30030.029 Hz
FIDRES   0.458222 Hz
AQ       1.0911744 sec
RG       32768
DW       16.650 usec
DE       6.50 usec
TE       298.2 K
D1       2.00000000 sec
D11      0.03000000 sec
TD0      1

----- CHANNEL f1 -----
NUC1     13C
P1       12.00 usec
PI1      -4.00 dB
PL1W    172.88230896 W
SF01     125.7703643 MHz

----- CHANNEL f2 -----
CPDPRG[2] waltz16
NUC2     1H
PCPD2    80.00 usec
PI2       4.00 dB
PI12     22.51 dB
PI13     25.00 dB
PL2W    12.10000038 W
PL12W   0.77052394 W
PL13W   0.09611372 W
SF02     500.1320005 MHz

F2 - Processing parameters
SI       32768
SF       125.7577890 MHz
WDW      RM
SSB      0
LB       1.00 Hz
GB       0
PC       1.40
    
```

p-tolylsulfinate (Ph cyclicamine)



```

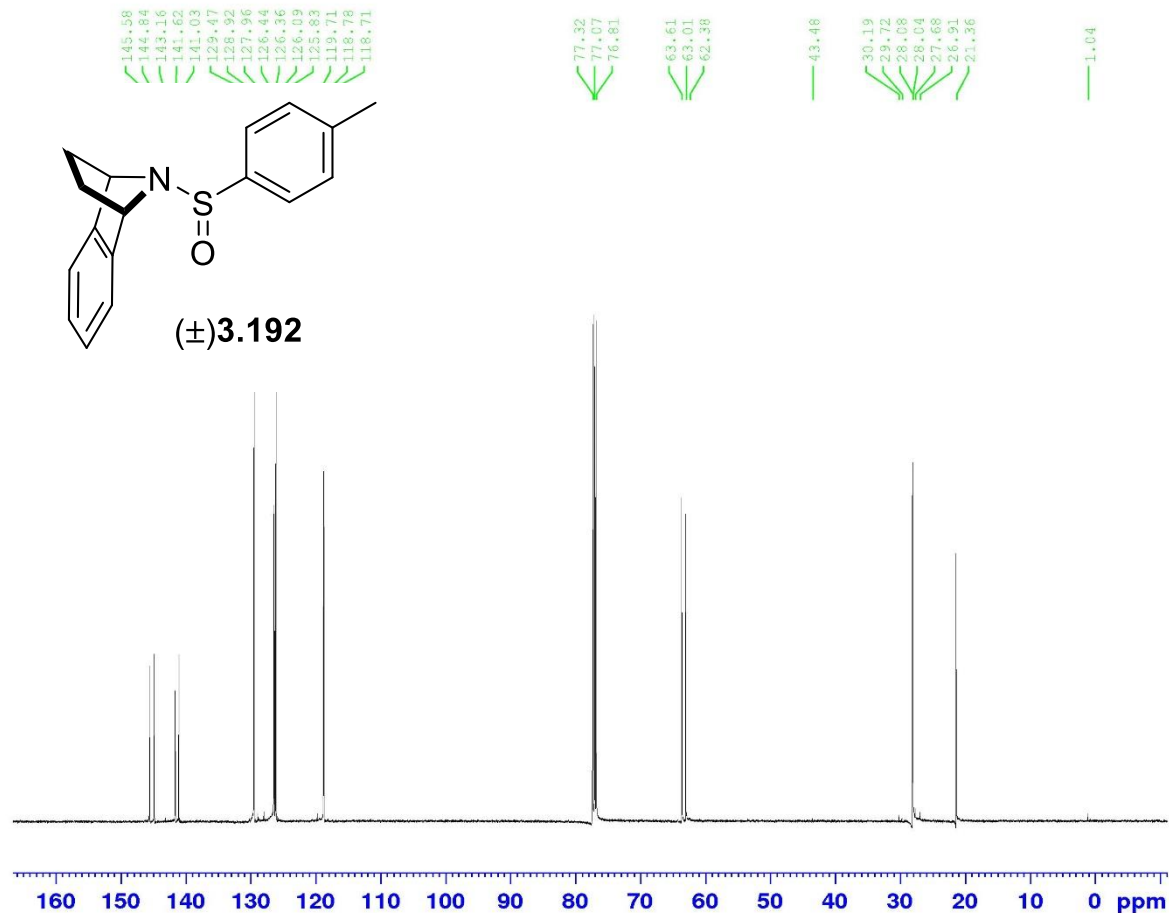
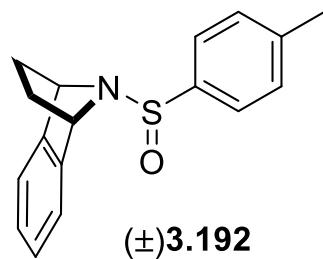
Current Data Parameters
NAME          IV-Mn-36 i
EXPNO         1
PROCNO        1

F2 - Acquisition Parameters
Date_         20180718
Time          19.02
INSTRUM       spect
PROBHD        5 mm PAQXI 1H/
PULPROG       zg30
TD            65536
SOLVENT       CDCl3
NS            16
DS            2
SWH           10330.578 Hz
FIDRES        0.157632 Hz
AQ            3.1719425 sec
RG            57
DW            48.400 usec
DE            6.50 usec
TE            298.2 K
D1            1.00000000 sec
TDC           1

===== CHANNEL f1 =====
NUC1          1H
P1            9.50 usec
PL1           4.00 dB
PL1W          12.10000038 W
SFO1          500.1330885 MHz

F2 - Processing parameters
SI            32768
SF            500.1300000 MHz
WDW           EM
SSB           0
LB            0.30 Hz
GB            0
PC            1.00
    
```

13C - p-tolylsulfinate (Ph cyclicamine)



Current Data Parameters
 NAME IV Mn 36 1
 EXPNO 2
 PROCNO 1

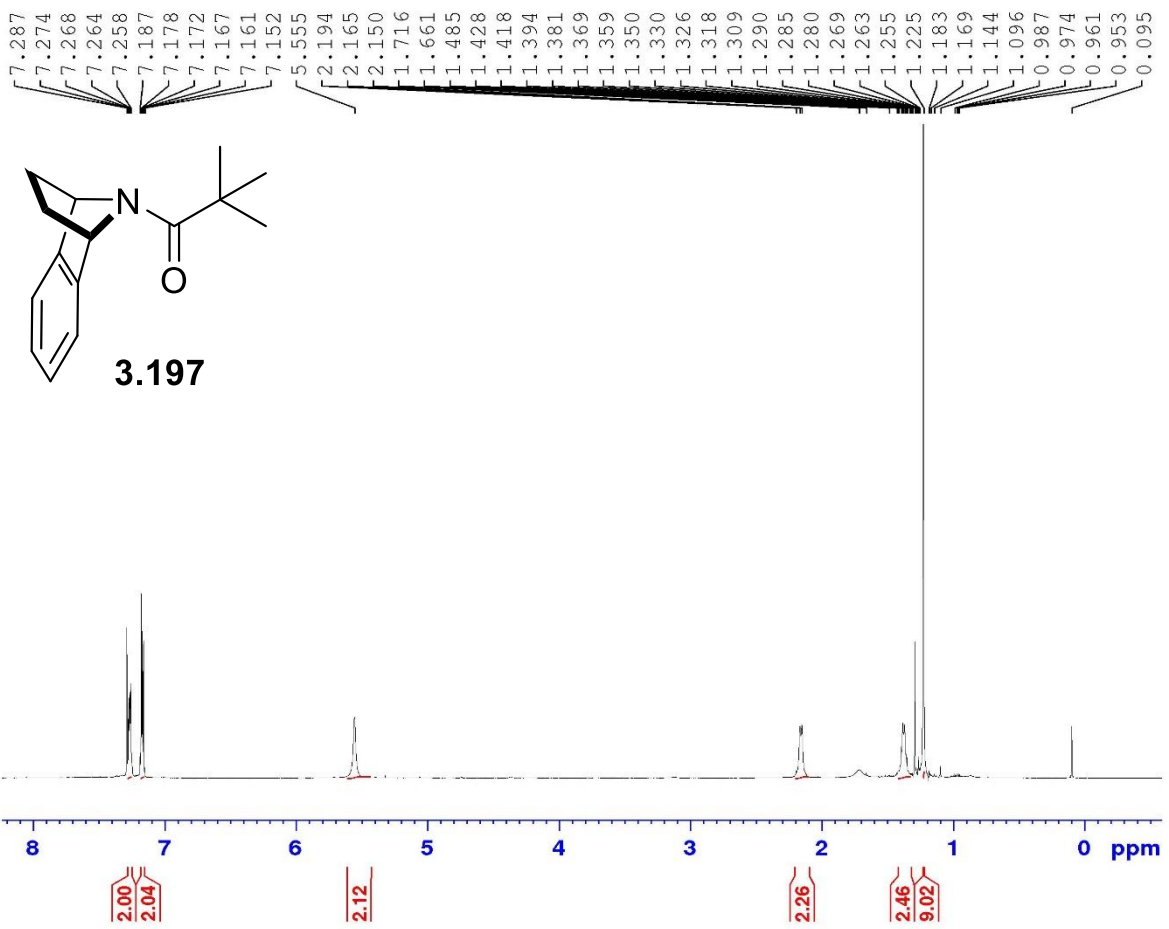
F2 - Acquisition Parameters
 Date_ 20180719
 Time 8.18
 INSTRUM spect
 PROBHD 5 mm PAQXI 1H/
 PULPROG zgpg30
 TD 63536
 SOLVENT CDCl3
 NS 15108
 DS 4
 SWH 30030.029 Hz
 FIDRES 0.458222 Hz
 AQ 1.0911744 sec
 RG 32768
 DW 16.650 usec
 DE 6.50 usec
 TE 298.2 K
 D1 2.0000000 sec
 D11 0.0300000 sec
 TD0 1

----- CHANNEL f1 -----
 NUC1 13C
 P1 12.00 usec
 PL1 -4.00 dB
 PL1W 172.88230896 W
 SFO1 125.7703643 MHz

----- CHANNEL f2 -----
 CPDPRG2 waltz16
 NUC2 1H
 PCPD2 80.00 usec
 PL2 4.00 dB
 PL12 22.51 dB
 PL13 25.00 dB
 PL2W 12.10000038 W
 PL12W 0.17052394 W
 PL13W 0.09611372 W
 SFO2 500.1320005 MHz

F2 - Processing parameters
 SI 32768
 SF 125.7577890 MHz
 WDW EM
 SSB 0
 LB 1.00 Hz
 GB 0
 PC 1.40

PhCyamine and pivaloyl chloride



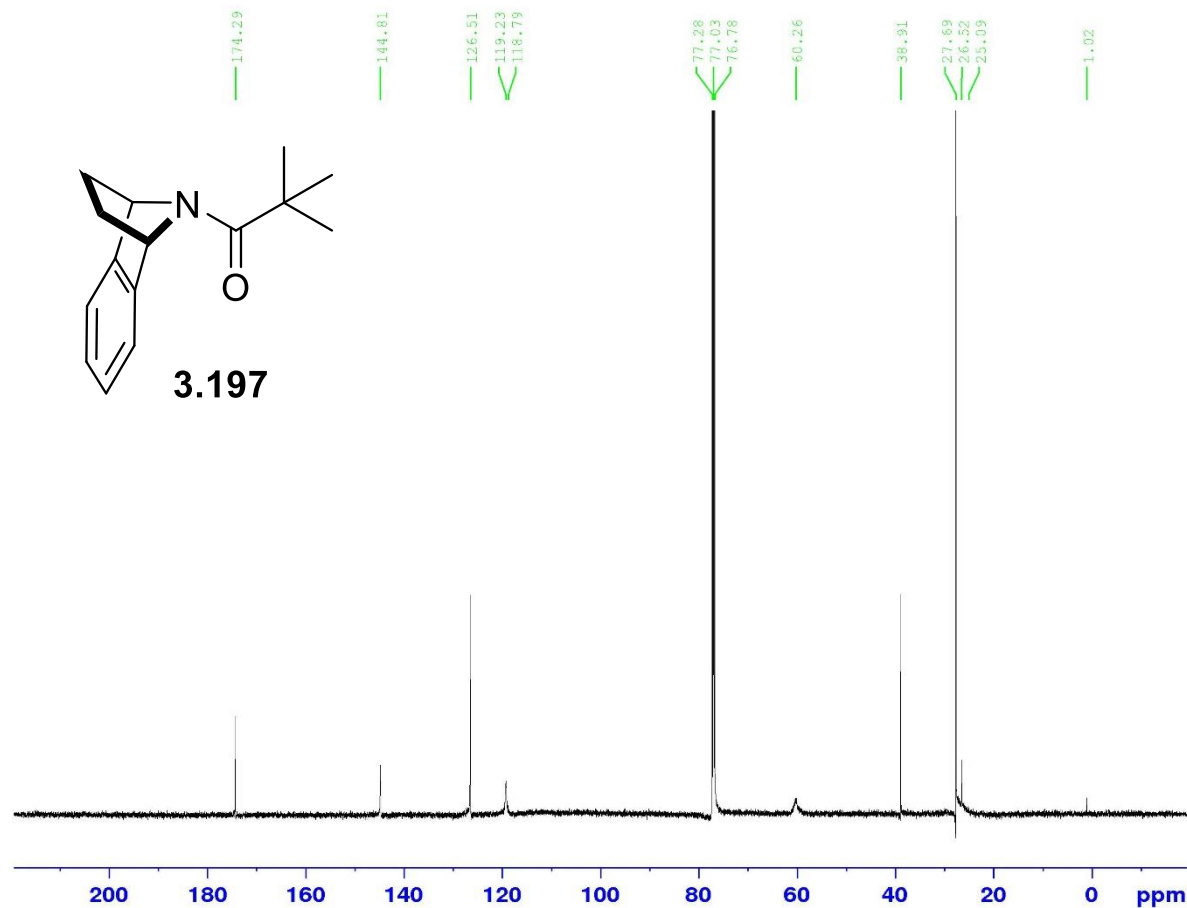
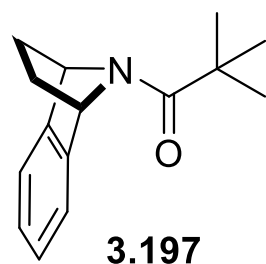
Current Data Parameters
 NAME IV-Mn-60
 EXPNO 1
 PROCNO 1

F2 - Acquisition Parameters
 Date_ 20180805
 Time 20.16
 INSTRUM spect
 PROBHD 5 mm PAQXI 1H/
 PULPROG zg30
 TD 65536
 SOLVENT CDCl3
 NS 16
 DS 2
 SWH 10330.578 Hz
 FIDRES 0.157632 Hz
 AQ 3.1719425 sec
 RG 90.5
 DW 48.400 usec
 DE 6.50 usec
 TE 298.2 K
 D1 1.0000000 sec
 TDC 1

----- CHANNEL f1 -----
 NUC1 1H
 P1 9.50 usec
 PL1 4.00 dB
 PLIw 12.10000038 W
 SF01 500.1330885 MHz

F2 - Processing parameters
 SI 32768
 SF 500.1300000 MHz
 WDW EM
 SSB 0
 LB 0.30 Hz
 GB 0
 PC 1.00

13C : PhCyamine and pivaloyl chloride



```

Current Data Parameters
NAME          TV-Mn-60
EXPNO         2
PROCNO        1

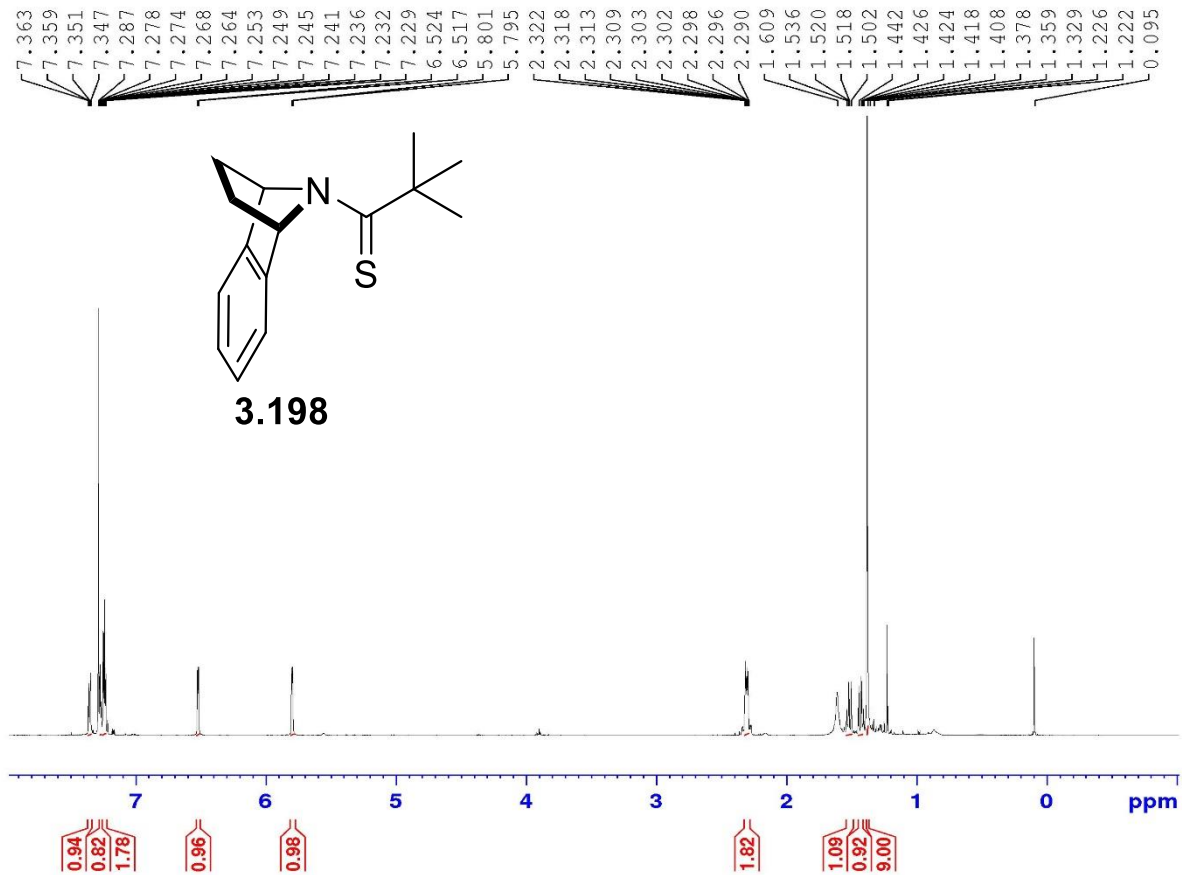
F2 - Acquisition Parameters
Date_         20180806
Time          7.49
INSTRUM       spect
PROBHD        5 mm PAQXI 1H/
PULPROG       zgpg30
TD            65536
SOLVENT       CDCl3
NS            13168
DS            4
SWH           30030.029 Hz
FIDRES        0.458222 Hz
AQ            1.0911744 sec
RG            32768
DW            16.650 usec
DE            6.50 usec
TE            298.2 K
D1            2.0000000 sec
D11           0.0300000 sec
TD0           1

===== CHANNEL f1 =====
NUC1           13C
P1             12.00 usec
PL1            -4.00 dB
PL1W           172.88230896 W
SFO1           125.7703643 MHz

===== CHANNEL f2 =====
CPDPRG12      waltz16
NUC2           1H
PCPD2          80.00 usec
PL2            4.00 dB
PL12           22.51 dB
PL13           25.00 dB
PL2W           12.10000038 W
PL12W          0.17052394 W
PL13W          0.09611372 W
SFO2           500.1320005 MHz

F2 - Processing parameters
SI             32768
SF            125.7577890 MHz
WDW            EM
SSB            0
LB             1.00 Hz
GB             0
PC             1.40
    
```

thioester



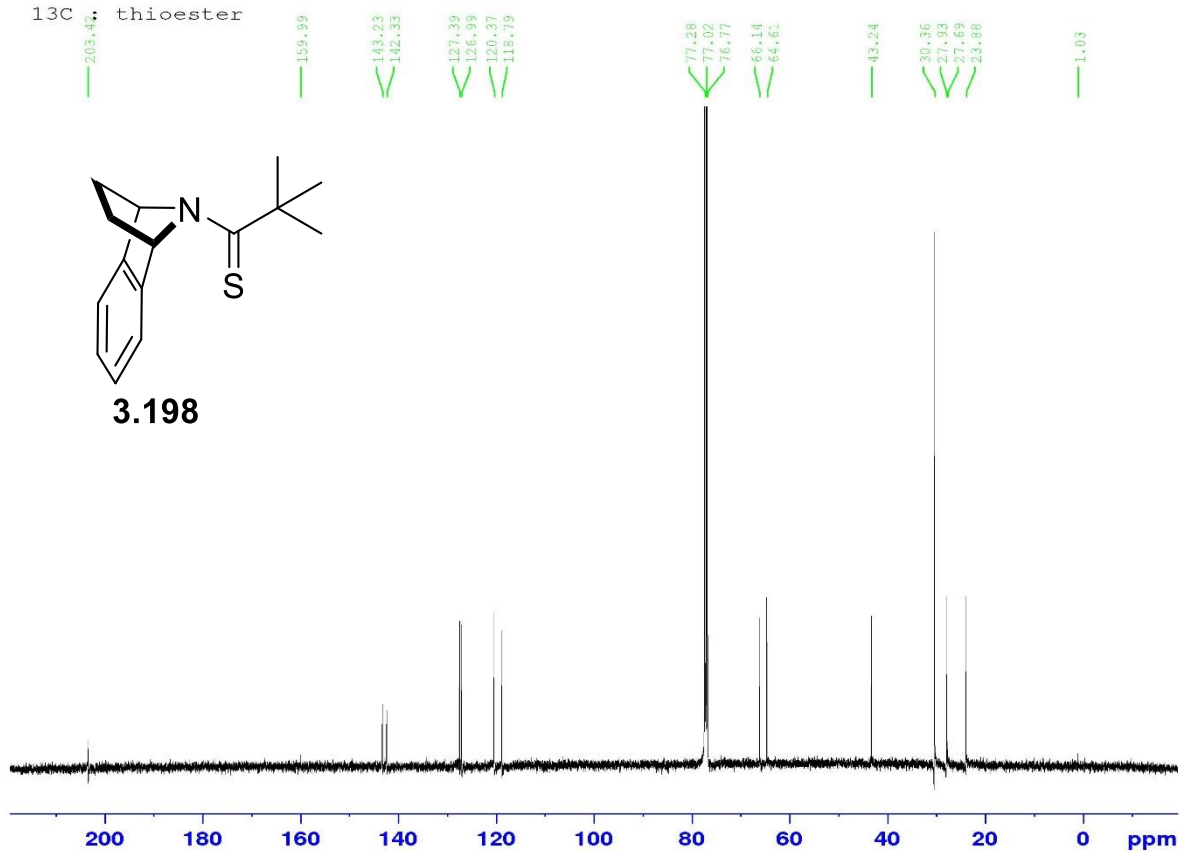
Current Data Parameters
NAME IV-Mn-61 i
EXPNO 1
PROCNO 1

F2 - Acquisition Parameters
Date_ 20180801
Time_ 21.17
INSTRUM spect
PROBHD 5 mm FAQXI 1H/
PULPROG zg30
TD 65536
SOLVENT CDCl3
NS 16
DS 2
SWH 10330.578 Hz
FIDRES 0.157632 Hz
AQ 3.1719425 sec
RG 181
DW 48.400 usec
DE 6.50 usec
TE 296.3 K
D1 1.00000000 sec
TDO 1

===== CHANNEL f1 =====
NUC1 1H
P1 9.50 usec
PL1 4.00 dB
PL1W 12.10000038 W
SF01 500.1330885 MHz

F2 - Processing parameters
SI 32768
SF 500.1300000 MHz
WDW EM
SSB 0
LB 0.30 Hz
GB 0
PC 1.00

¹³C: thioester



Current Data Parameters
NAME IV-Mn-61
EXPNO 2
PROCNO 1

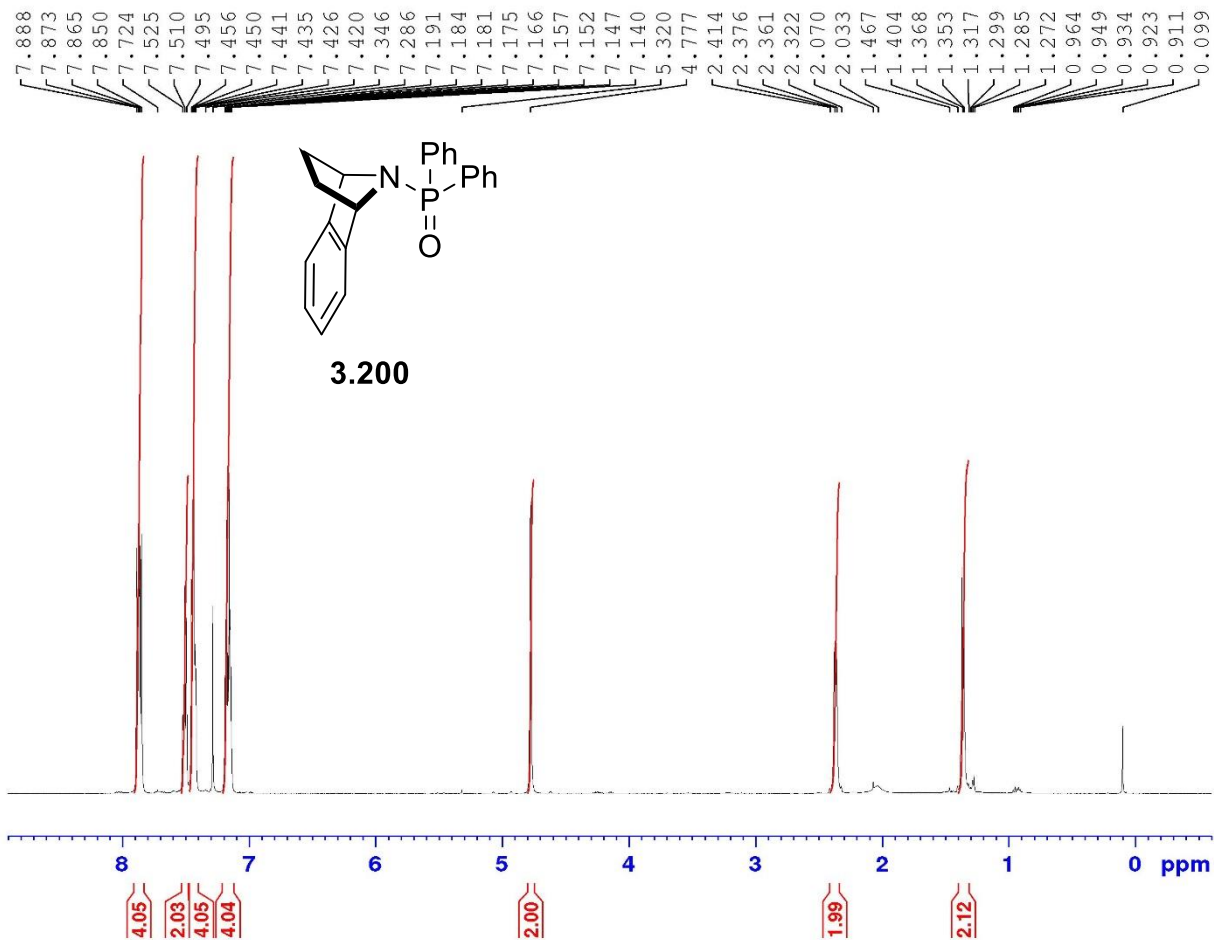
F2 - Acquisition Parameters
Date_ 20180802
Time 7.41
INSTRUM spect
PROBHD 5 mm PAQX1 1H/
PULPROG zgpg30
TD 65536
SOLVENT CDCl3
NS 11835
DS 4
SWE 30030.029 Hz
FIDRES 0.458222 Hz
AQ 1.0911744 sec
RG 32768
DW 16.650 usec
DE 6.50 usec
TE 294.6 K
D1 2.0000000 sec
D11 0.0300000 sec
TD0 1

----- CHANNEL f1 -----
NUC1 ¹³C
P1 12.00 usec
PL1 -4.00 dB
PT1W 172.88230896 W
SFO1 125.7703643 MHz

----- CHANNEL f2 -----
CPDPRG12 waltz16
NUC2 ¹H
PCPD2 80.00 usec
PL2 4.00 dB
PL12 22.51 dB
PL13 25.00 dB
PL2W 12.10000038 W
PL12W 0.17052394 W
PL13W 0.09611372 W
SFO2 500.1320005 MHz

F2 Processing parameters
SI 32768
SF 125.7577890 MHz
WDW EM
SSB 0
LB 1.00 Hz
GB 0
PC 1.40

cyclic amine and Ph2POCl



```

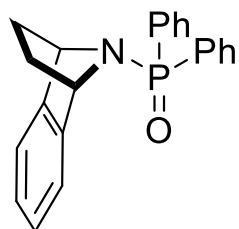
Current Data Parameters
NAME          IV-Mn-138 i
EXPNO         1
PROCNO        1

F2 - Acquisition Parameters
Date_         20181024
Time_         19.59
INSTRUM       spect
PROBHD        5 mm PAQXI 1H/
PULPROG       zg30
TD            65536
SOLVENT       CDCl3
NS            16
DS            2
SWH           10330.578 Hz
FIDRES        0.157632 Hz
AQ            3.1719425 sec
RG            128
DW            48.400 usec
DE            6.50 usec
TE            298.2 K
D1            1.0000000 sec
TDO           1

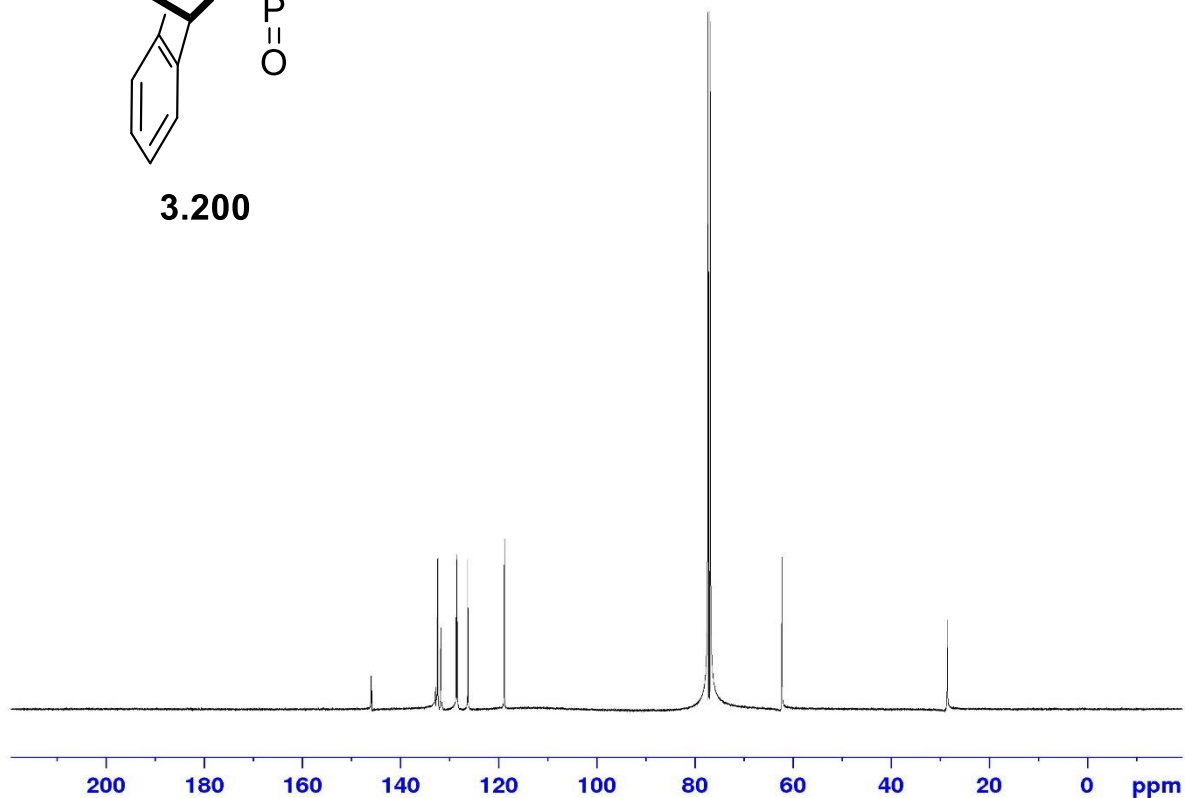
----- CHANNEL f1 -----
NUC1           1H
P1             9.50 usec
PL1            4.00 dB
PL1W           12.10000038 W
SF01           500.1330885 MHz

F2 - Processing parameters
SI             32768
SF            500.1300000 MHz
WDW            EM
SSB            0
LB             0.30 Hz
GB            0
PC             1.00
    
```

Cyclic amine and Ph₂POCl



3.200



Current Data Parameters
NAME IV-Mn-158 i
EXPNO 2
PROCNO 1

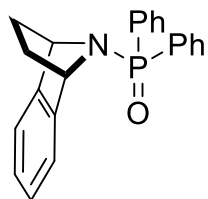
F2 - Acquisition Parameters
Date_ 20181025
Time 7.48
INSTRUM spect
PROBHD 5 mm PAQXI 1H/
PULPROG zgpg30
TD 65536
SOLVENT CDC13
NS 13421
DS 4
SWH 30030.029 Hz
FIDRES 0.458222 Hz
AQ 1.0911744 sec
RG 32768
DW 16.650 usec
DE 6.50 usec
TE 298.2 K
D1 2.0000000 sec
D11 0.0300000 sec
TD0 1

===== CHANNEL f1 =====
NUC1 13C
P1 12.00 usec
PL1 -4.00 dB
PL1W 172.88230896 W
SFO1 125.7703643 MHz

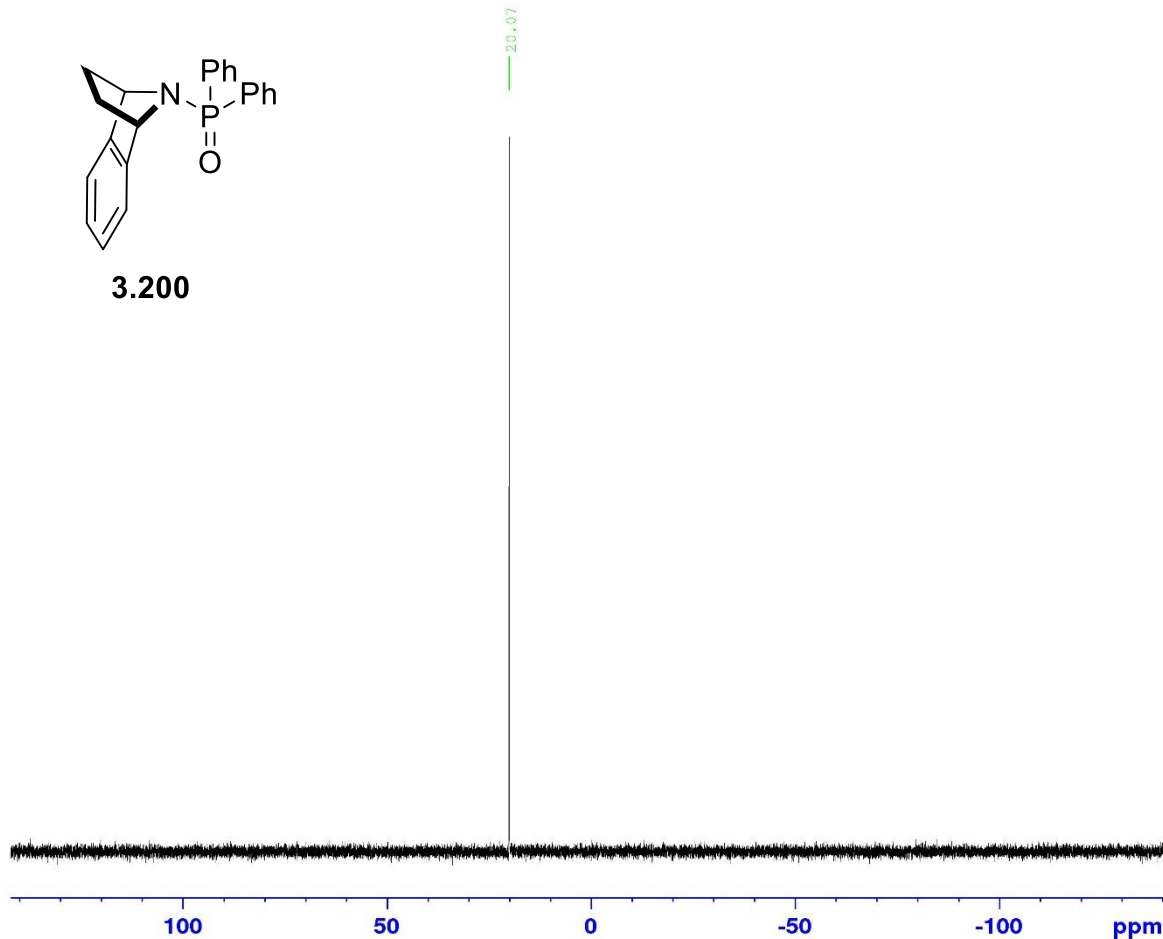
===== CHANNEL f2 =====
CPDPRG[2] waltz16
NUC2 1H
PCPD2 80.00 usec
PL2 4.00 dB
PL12 22.51 dB
PL13 25.00 dB
PL2W 12.10000038 W
PL12W 0.17052394 W
PL13W 0.09611372 W
SFO2 500.1320005 MHz

F2 - Processing parameters
SI 32768
SF 125.7577890 MHz
WDW EM
SSB 0
LB 1.00 Hz
GB 0
PC 1.40

31P - Cyclic amine and Ph2POCl



3.200



Current Data Parameters
 NAME IV-Mn-158 1
 EXPNO 3
 PROCNO 1

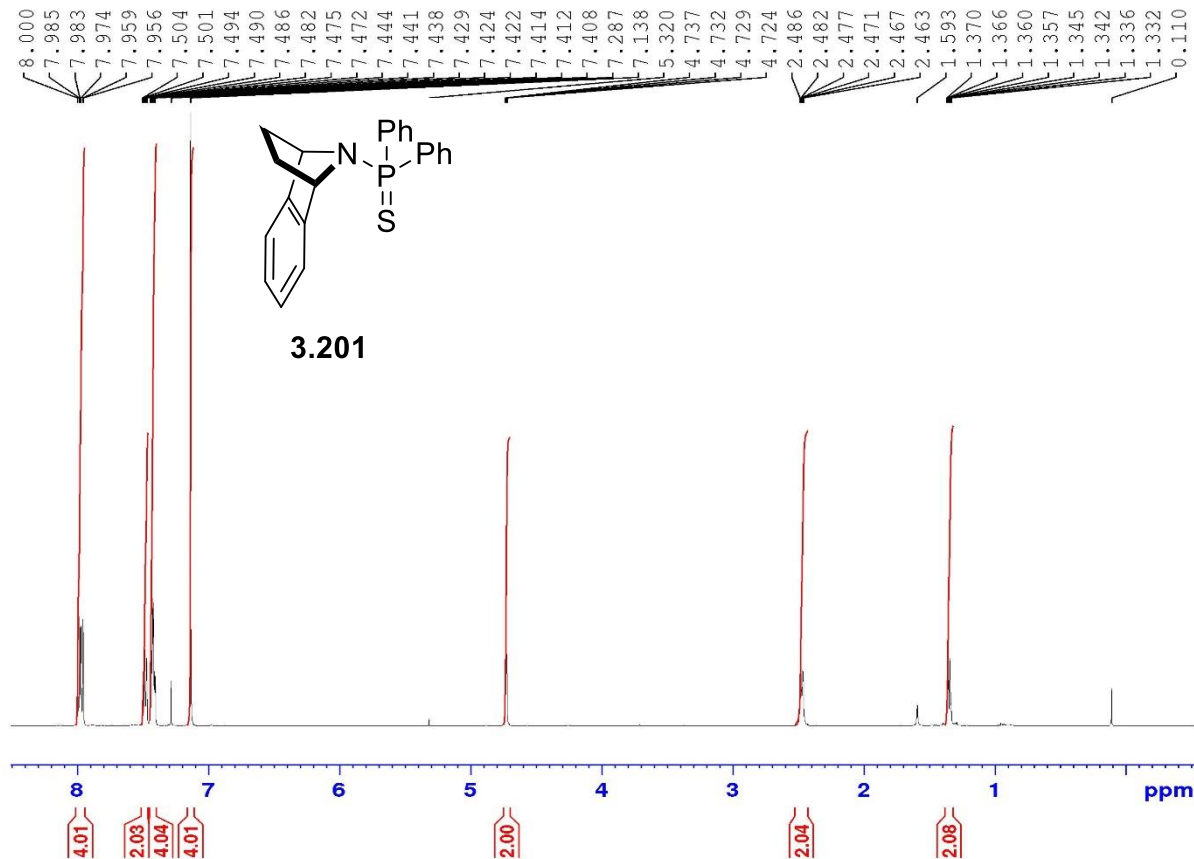
F2 - Acquisition Parameters
 Date_ 20181025
 Time 7.57
 INSTRUM spect
 PROBHD 5 mm PAQXI 1H/
 PULPROG zgpg30
 TD 65536
 SOLVENT CDCl3
 NS 4
 DS 4
 SWH 80645.164 Hz
 FIDRES 1.230548 Hz
 AQ 0.4063232 sec
 RG 20642.5
 DW 6.200 usec
 DE 6.50 usec
 TE 298.2 K
 D1 2.0000000 sec
 D11 0.0300000 sec
 TD0 1

----- CHANNEL f1 -----
 NUC1 31P
 P1 20.00 usec
 PL1 -2.40 dB
 PL1W 131.39126587 W
 SF01 202.4462122 MHz

----- CHANNEL f2 -----
 CPDPRG12 waltz16
 NUC2 1H
 PCPD2 80.00 usec
 PL2 4.00 dB
 PL12 22.51 dB
 PL13 25.00 dB
 PL2W 12.10000038 W
 PL12W 0.17052394 W
 PL13W 0.09611372 W
 SF02 500.1320005 MHz

F2 - Processing parameters
 S1 32768
 SF 202.4563350 MHz
 WDW EM
 SSB 0
 LB 1.00 Hz
 GB 0
 PC 1.40

cyclic amine P=S



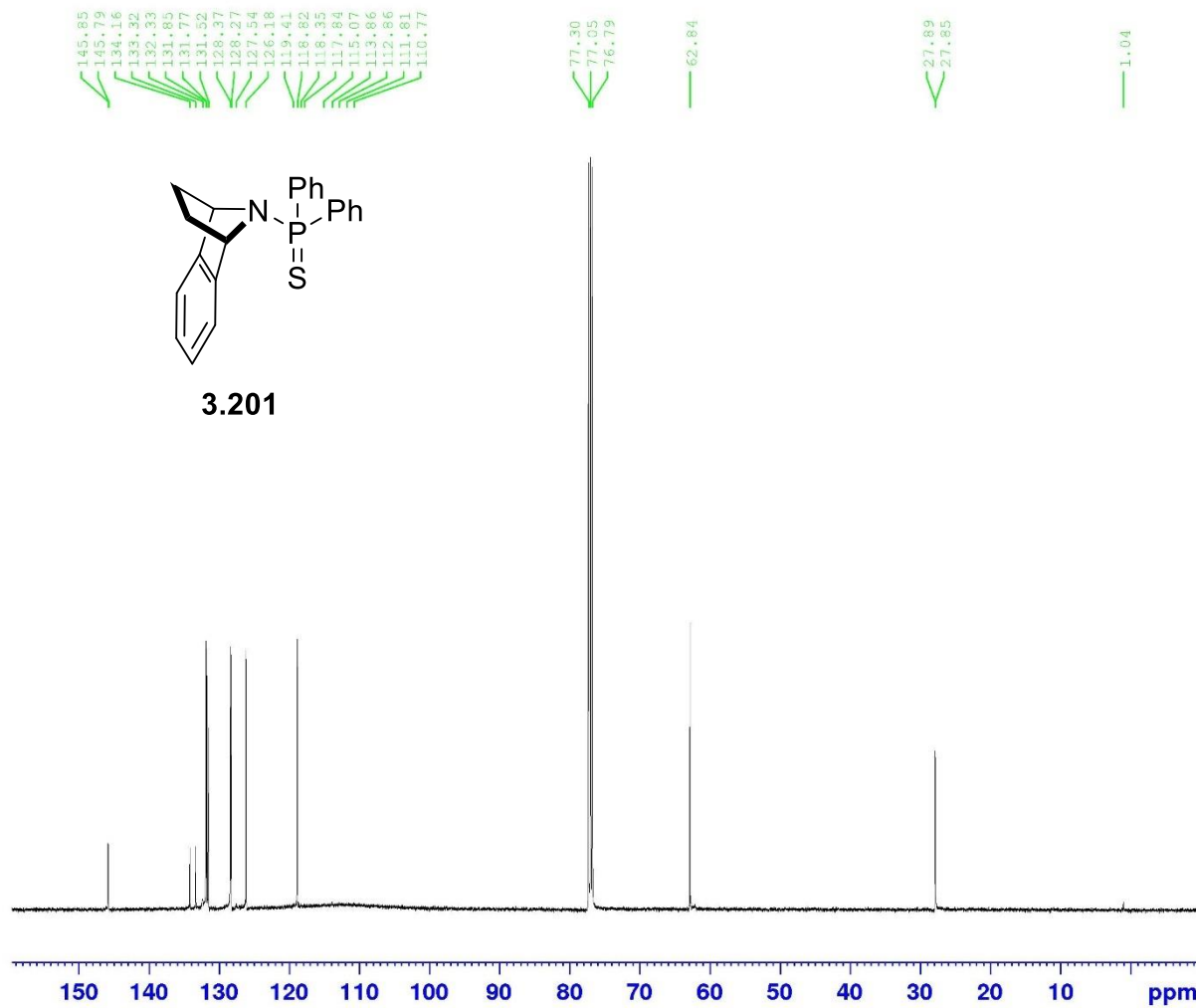
Current Data Parameters
NAME IV-Mn-166 i
EXPNO 6
PROCNO 1

F2 - Acquisition Parameters
Date_ 20181101
Time 11.09
INSTRUM spect
PROBHD 5 mm PAQXI 1H/
PULPROG zg30
TD 65536
SOLVENT CDCl3
NS 16
DS 2
SWH 10330.578 Hz
FIDRES 0.157632 Hz
AQ 3.1719425 sec
RG 71.8
DW 48.400 usec
DE 6.50 usec
TE 298.2 K
D1 1.00000000 sec
TDO 1

===== CHANNEL f1 =====
NUC1 1H
P1 9.50 usec
PL1 4.00 dB
PL1W 12.1000038 W
SFO1 500.1330885 MHz

F2 - Processing parameters
SI 32768
SF 500.1300000 MHz
WDW EM
SSB 0
LB 0.30 Hz
GB 0
PC 1.00

Cyclic amine P=S



Current Data Parameters
 NAME IV-Mn-166 i
 EXPNO 2
 PROCNO 1

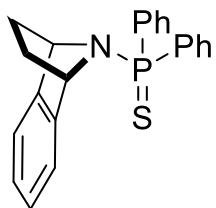
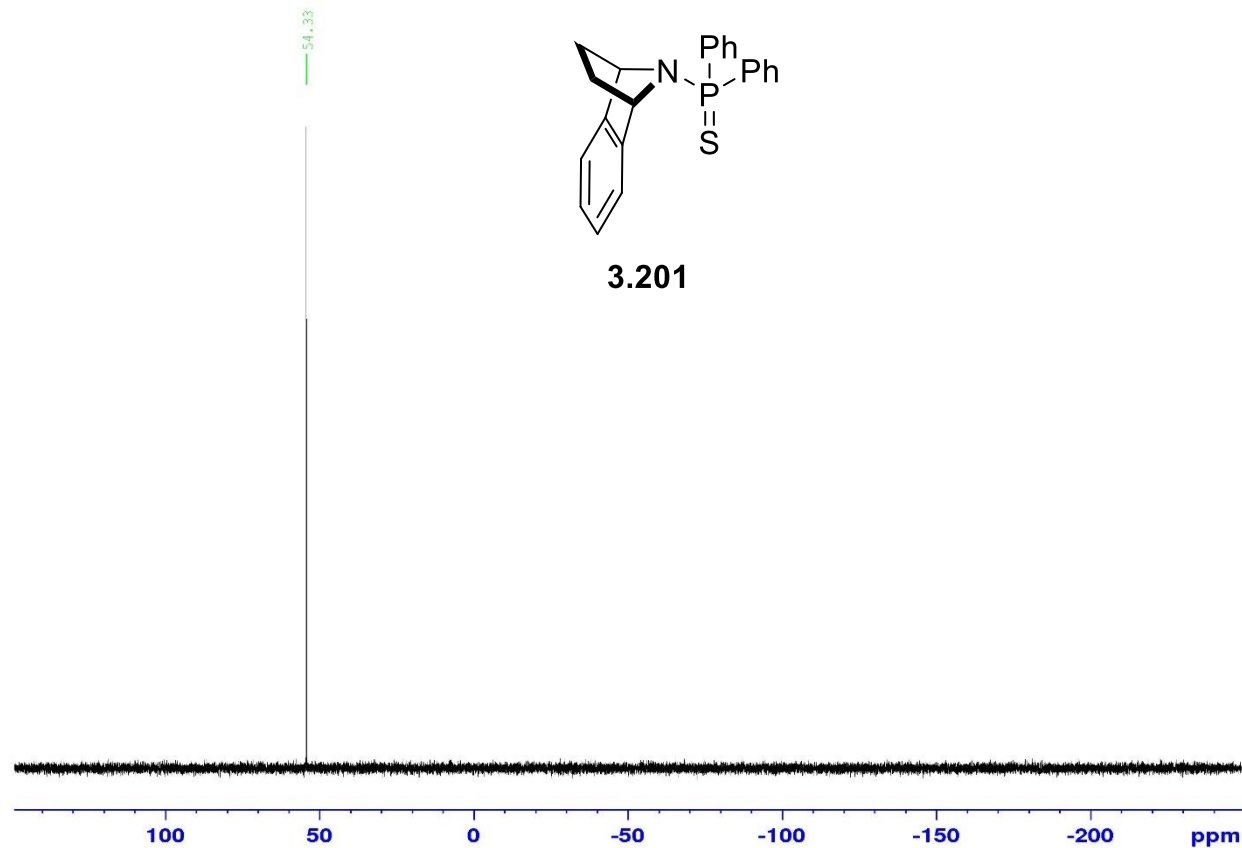
F2 - Acquisition Parameters
 Date_ 20181029
 Time 7.49
 INSTRUM spect
 PROBD 5 mm PAQXI 1H/
 PULPROG zgpg30
 TD 65536
 SOLVENT CDCl3
 NS 12832
 DS 4
 SWH 30030.029 Hz
 FIDRES 0.456222 Hz
 AQ 1.0911744 sec
 RG 32768
 DW 16.650 usec
 DE 6.50 usec
 TE 298.2 K
 D1 2.0000000 sec
 D11 0.0300000 sec
 TDC 1

===== CHANNEL f1 =====
 NUC1 13C
 P1 12.00 usec
 PL1 -4.00 dB
 PL1W 172.88230896 W
 SFO1 125.7703643 MHz

===== CHANNEL f2 =====
 CPDPRG[2] waltz16
 NUC2 1H
 PCPD2 80.00 usec
 PL2 4.00 dB
 PL12 22.51 dB
 PL13 25.00 dB
 PL2W 12.10000038 W
 PL12W 0.17052394 W
 PL13W 0.09611372 W
 SFO2 500.1320005 MHz

F2 - Processing parameters
 SI 32768
 SF 125.7577890 MHz
 WDW EM
 SSB 0
 LB 1.00 Hz
 GB 0
 PC 1.40

31 P - Cyclic amine P=S



```

Current Data Parameters
NAME      IV-Mn-166 i
EXPNO     5
PROCNO    1

F2 - Acquisition Parameters
Date_     20181029
Time      8.31
INSTRUM   spect
PROBHD    5 mm PAQXI 1H/
PULPROG   zgpg30
TD        65536
SOLVENT   CDC13
NS         16
DS         4
SWH        80645.164 Hz
FIDRES     1.230548 Hz
AQ         0.4063232 sec
RG         20642.5
DW         6.200 usec
DE         6.50 usec
TE         298.2 K
D1         2.0000000 sec
D11        0.0300000 sec
TDC        1

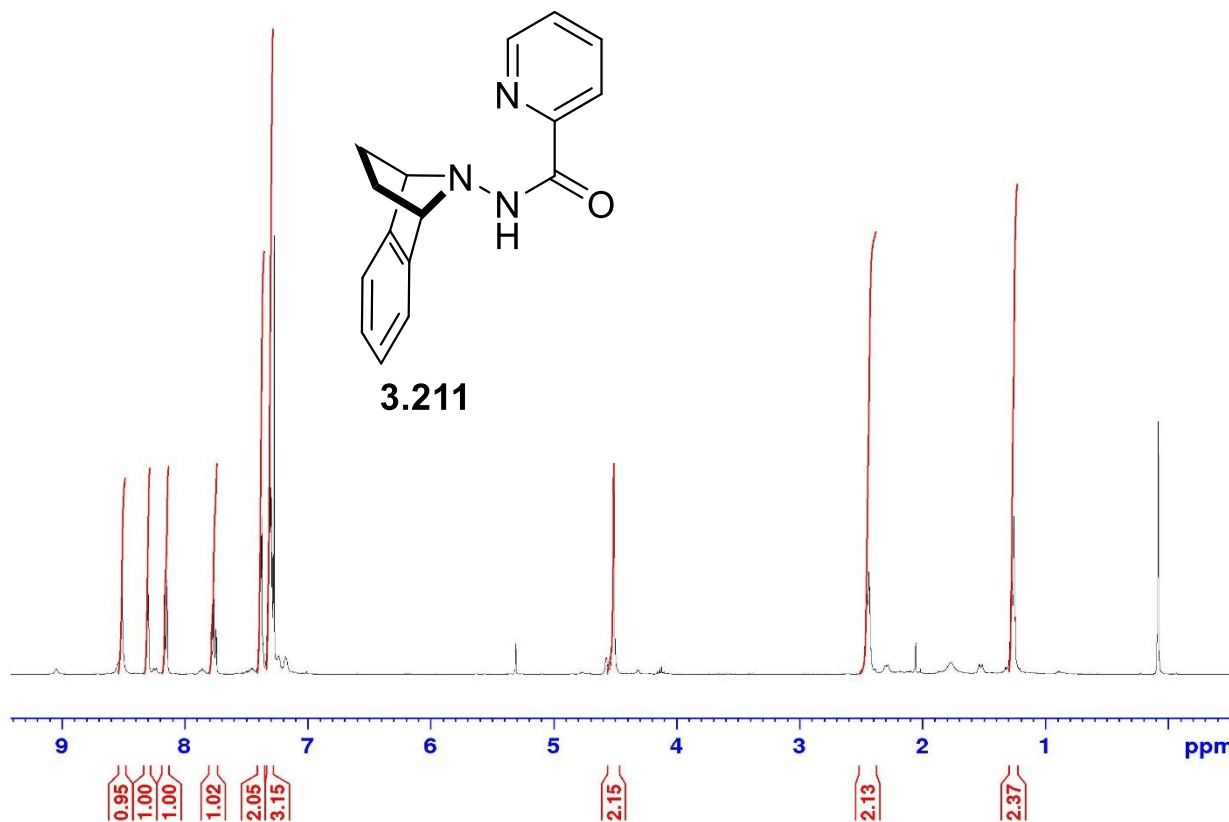
===== CHANNEL f1 =====
NUC1       31P
P1         20.00 usec
PL1        -2.40 dB
PL1W       131.39126587 W
SFO1       202.4462122 MHz

===== CHANNEL f2 =====
CPDPRG2    waltz16
NUC2        1H
PCPD2       80.00 usec
PL2         4.00 dB
PL12        22.51 dB
PL13        25.00 dB
PL12W       12.10000038 W
PL13W       0.17052394 W
PL13W       0.09611372 W
SFO2        500.1320005 MHz

F2 - Processing parameters
SI          32768
SF          202.4563350 MHz
WDW         EM
SSB         0
LB          1.00 Hz
GB          0
PC          1.40
    
```

Amide formation

8.511
8.308
8.297
8.164
8.144
7.785
7.781
7.766
7.762
7.747
7.743
7.393
7.385
7.380
7.372
7.363
7.328
7.326
7.310
7.302
7.297
7.289
7.284
7.272
7.237
7.177
5.306
4.570
4.514
4.510
4.119
2.455
2.450
2.445
2.432
2.417
2.299
2.277
2.052
1.767
1.533
1.512
1.281
1.271
1.253
1.242
0.078



Current Data Parameters
NAME V-Mn-117 ii
EXPNO 1
PROCNO 1

F2 - Acquisition Parameters
Date_ 20190426
Time 12.00
INSTRUM spect
PROBHD 5 mm Multinucl
PULPROG zg30
TD 65536
SOLVENT CDCl3
NS 16
DS 2
SWH 8278.146 Hz
FIDRES 0.126314 Hz
AQ 3.9583745 sec
RG 181
DW 60.400 usec
DE 6.00 usec
TE 300.0 K
D1 1.00000000 sec
TDO 1

===== CHANNEL f1 =====
NUC1 1H
P1 10.00 usec
PL1 3.80 dB
SFO1 400.1324710 MHz

F2 - Processing parameters
SI 32768
SF 400.1300000 MHz
WDW EM
SSB 0
LB 0.30 Hz
GB 0
PC 1.00

Amide formation

8.661
8.659
8.651
8.649
7.904
7.886
7.884
7.790
7.786
7.403
7.400
7.391
7.388
7.384
7.372
7.349
7.346
7.331
7.273
7.228
7.221
7.212
7.208
7.182
7.178
7.171
7.166
7.161
7.157
7.154
7.150
6.173
6.163
5.794
5.784
2.310
2.302
2.298
2.286
2.278
2.000
1.438
1.434
1.419
1.271
1.266
0.082

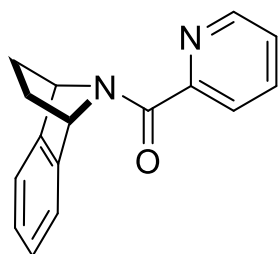


Current Data Parameters
NAME V-Mn-117 1
EXPNO 1
PROCNO 1

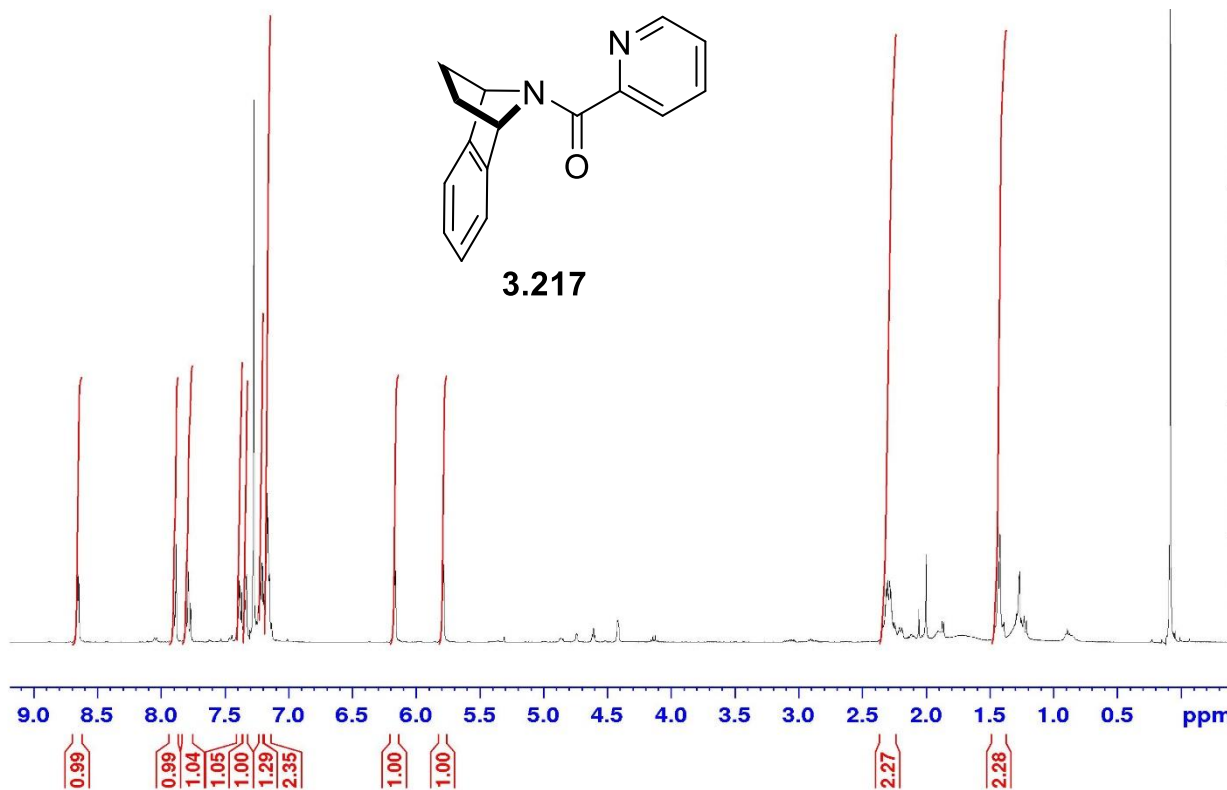
F2 - Acquisition Parameters
Date_ 20190426
Time 12.08
INSTRUM spect
PROBHD 5 mm Multinucl
PULPROG zg30
TD 65536
SOLVENT CDCl3
NS 16
DS 2
SWH 8278.146 Hz
FIDRES 0.126314 Hz
AQ 3.9583745 sec
RG 203.2
DW 60.400 usec
DE 6.00 usec
TE 300.0 K
D1 1.0000000 sec
TD0 1

===== CHANNEL f1 =====
NUC1 1H
P1 10.00 usec
PL1 3.80 dB
SFO1 400.1324710 MHz

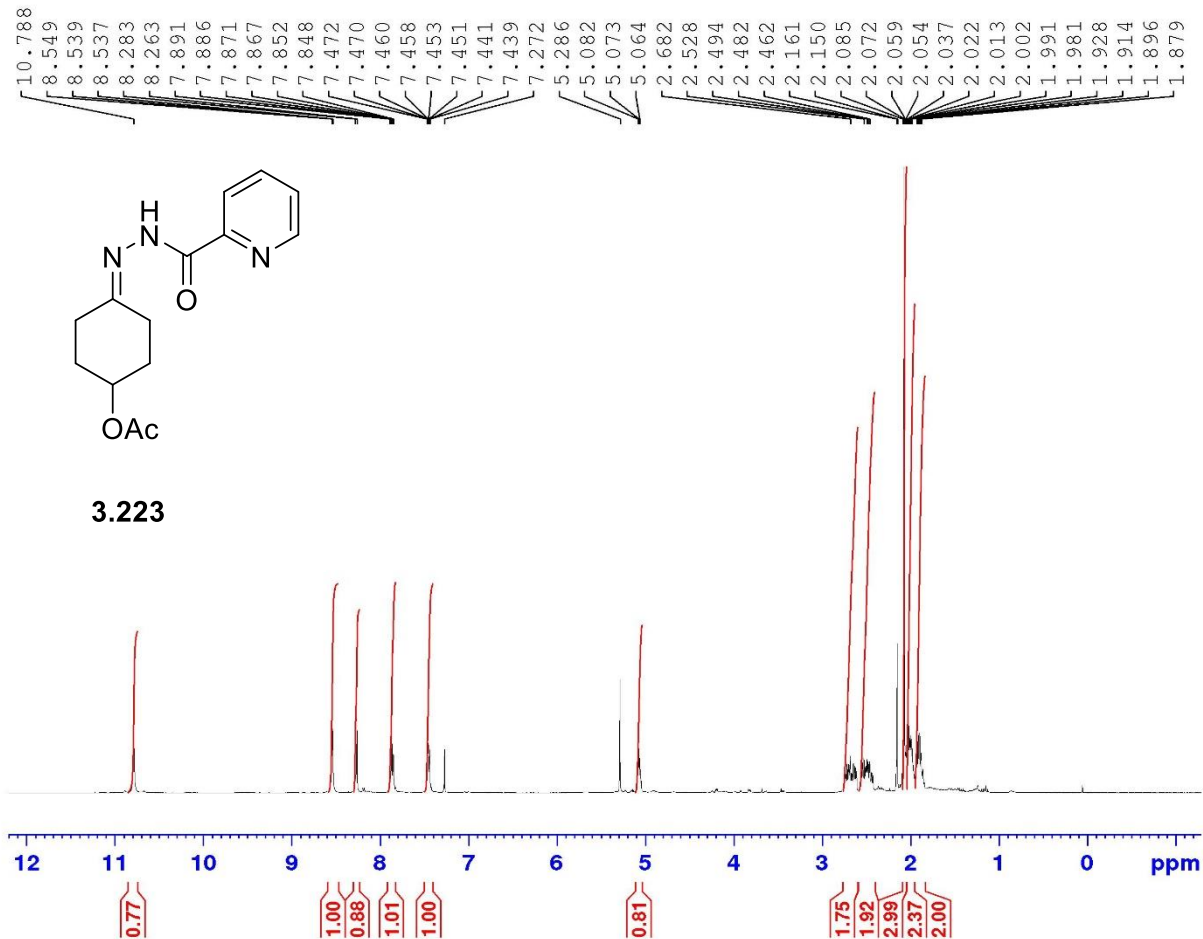
F2 - Processing parameters
SI 32768
SF 400.1300000 MHz
WDW EM
SSB 0
LB 0.30 Hz
GB 0
PC 1.00



3.217



Imine formation



Current Data Parameters
NAME V-Mn-68 i
EXPNO 1
PROCNO 1

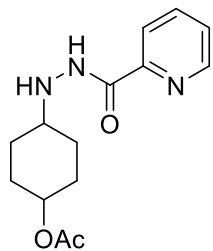
F2 - Acquisition Parameters
Date_ 20190301
Time 15.49
INSTRUM spect
PROBHD 5 mm Multinucl
PULPROG zg30
ID 65536
SOLVENT CDCl3
NS 16
DS 2
SWH 8278.146 Hz
FIDRES 0.126314 Hz
AQ 3.9583745 sec
RG 71.8
DW 60.400 usec
DE 6.00 usec
TE 300.0 K
D1 1.0000000 sec
TD0 1

===== CHANNEL f1 =====
NUC1 1H
P1 10.00 usec
PL1 3.80 dB
SFO1 400.1324710 MHz

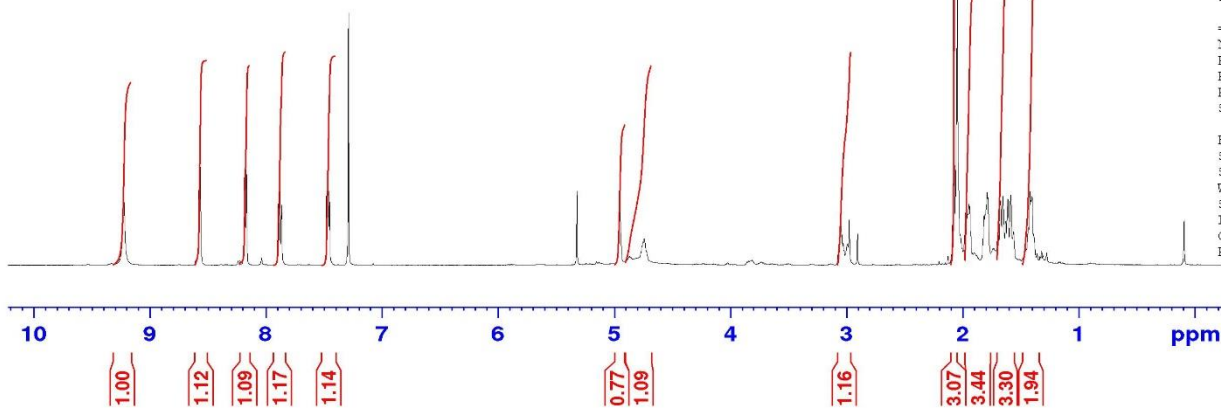
F2 - Processing parameters
SI 32768
SF 400.1300000 MHz
WDW EM
SSE 0
LB 0.30 Hz
GB 0
PC 1.00

Reduction of Imine : Diamide

9.223
8.574
8.566
8.184
8.168
7.895
7.879
7.864
7.476
7.464
7.451
7.289
7.286
5.320
5.318
4.951
3.045
3.037
2.974
2.901
2.075
2.072
2.044
2.041
1.971
1.964
1.953
1.944
1.937
1.813
1.803
1.787
1.779
1.695
1.689
1.671
1.649
1.626
1.608
1.582
1.559
1.428
1.415
1.399
1.385
0.090
0.087



3.224



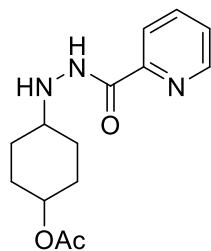
Current Data Parameters
NAME V-Mn-77 i
EXPNO 1
PROCNO 1

F2 - Acquisition Parameters
Date_ 20190311
Time 20.54
INSTRUM spect
PROBHD 5 mm PAQXI 1H/
PULPROG zg30
TD 65536
SOLVENT CDCl3
NS 16
DS 2
SWH 10330.578 Hz
FIDRES 0.157632 Hz
AQ 3.1719425 sec
RG 114
DW 48.400 usec
DE 6.50 usec
TE 298.4 K
D1 1.00000000 sec
TDO 1

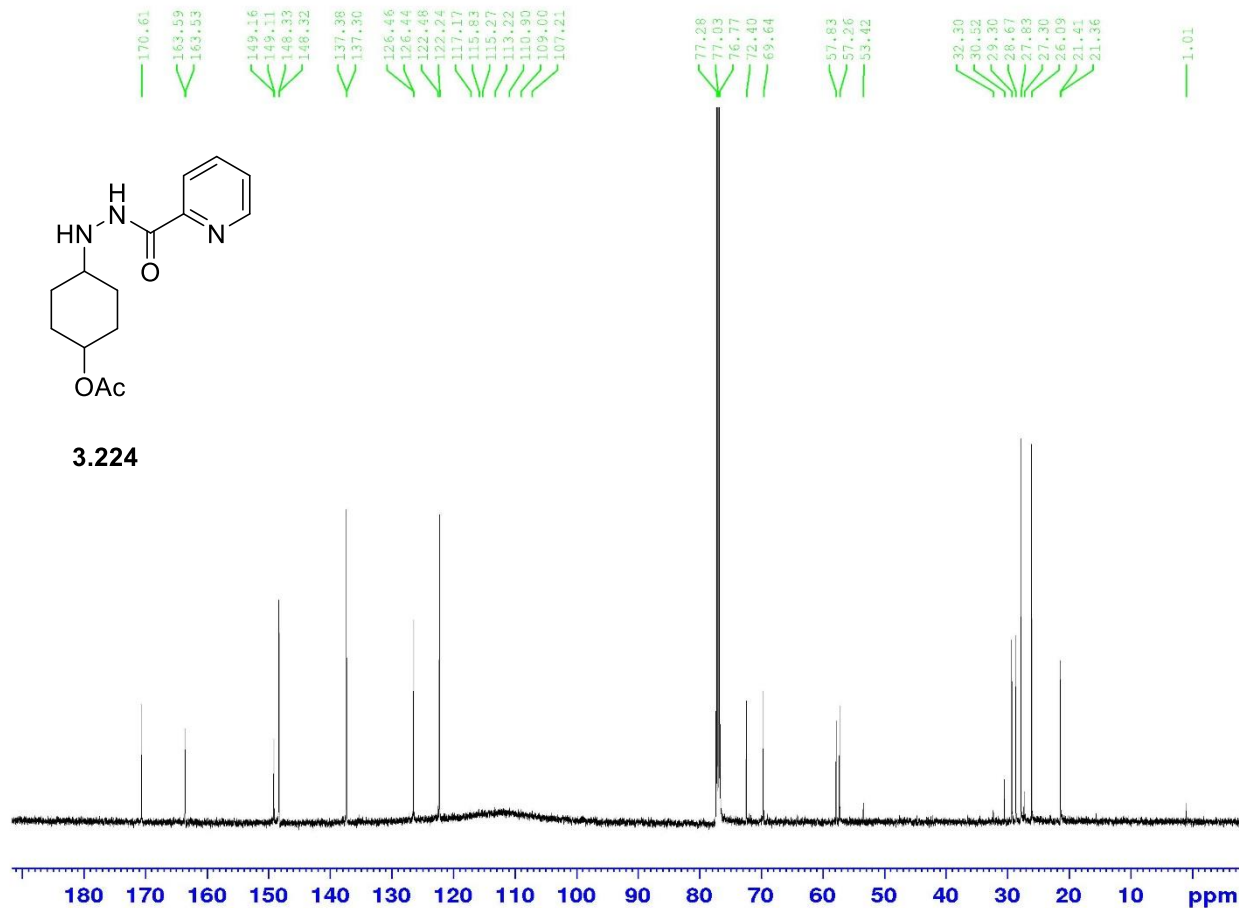
===== CHANNEL f1 =====
NUC1 1H
P1 9.50 usec
PL1 4.00 dB
PL1W 12.10000038 W
SFO1 500.1330885 MHz

F2 - Processing parameters
SI 32768
SF 500.1300000 MHz
WDW EM
SSB 0
LB 0.30 Hz
GB 0
PC 1.00

Reduction of Imine : Diamide



3.224



Current Data Parameters
 NAME V-Mn-77 i
 EXPNO 2
 PROCNO 1

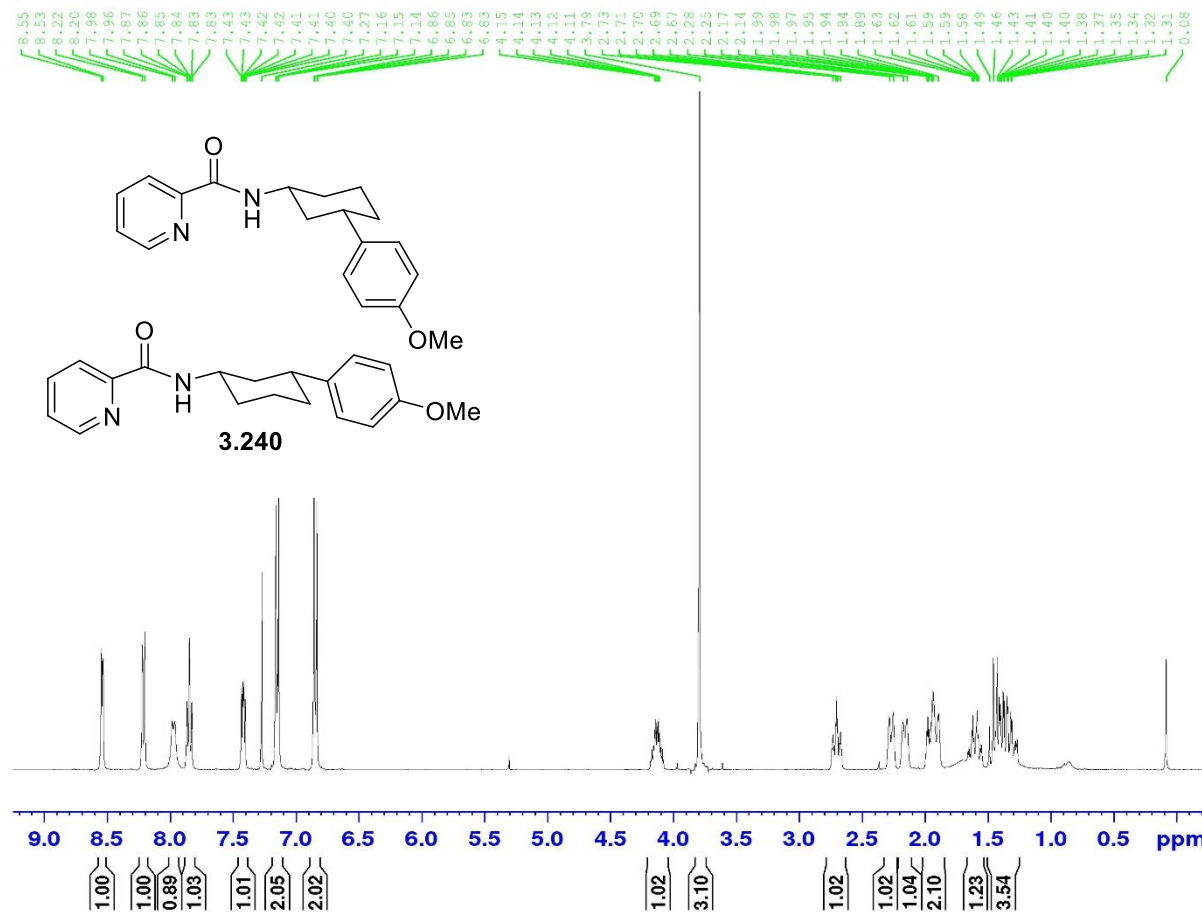
F2 - Acquisition Parameters
 Date_ 20190312
 Time 9.03
 INSTRUM spect
 PROBHD 5 mm PAQXI 1H/
 PULPROG zgpg30
 TD 65536
 SOLVENT cdcl3
 NS 13818
 DS 4
 SWH 30030.029 Hz
 FIDRES 0.458222 Hz
 AQ 1.0911744 sec
 RG 32768
 DW 16.650 usec
 DE 6.50 usec
 TE 298.9 K
 D1 2.0000000 sec
 D11 0.0300000 sec
 TD0 1

----- CHANNEL f1 -----
 NUC1 13C
 P1 12.00 usec
 PL1 -4.00 dB
 PL1W 172.88230896 W
 SFO1 125.7703643 MHz

----- CHANNEL f2 -----
 CPDPRG [2] waltz16
 NUC2 1H
 PCPD2 80.00 usec
 PL2 4.00 dB
 PL12 22.51 dB
 PL13 25.00 dB
 PL2W 12.10000038 W
 PL12W 0.17052394 W
 PL13W 0.09611372 W
 SFO2 500.1320005 MHz

F2 - Processing parameters
 SI 32768
 SF 125.7577890 MHz
 WDW EM
 SSB 0
 LB 1.00 Hz
 GB 0
 PC 1.40

Sp3-H



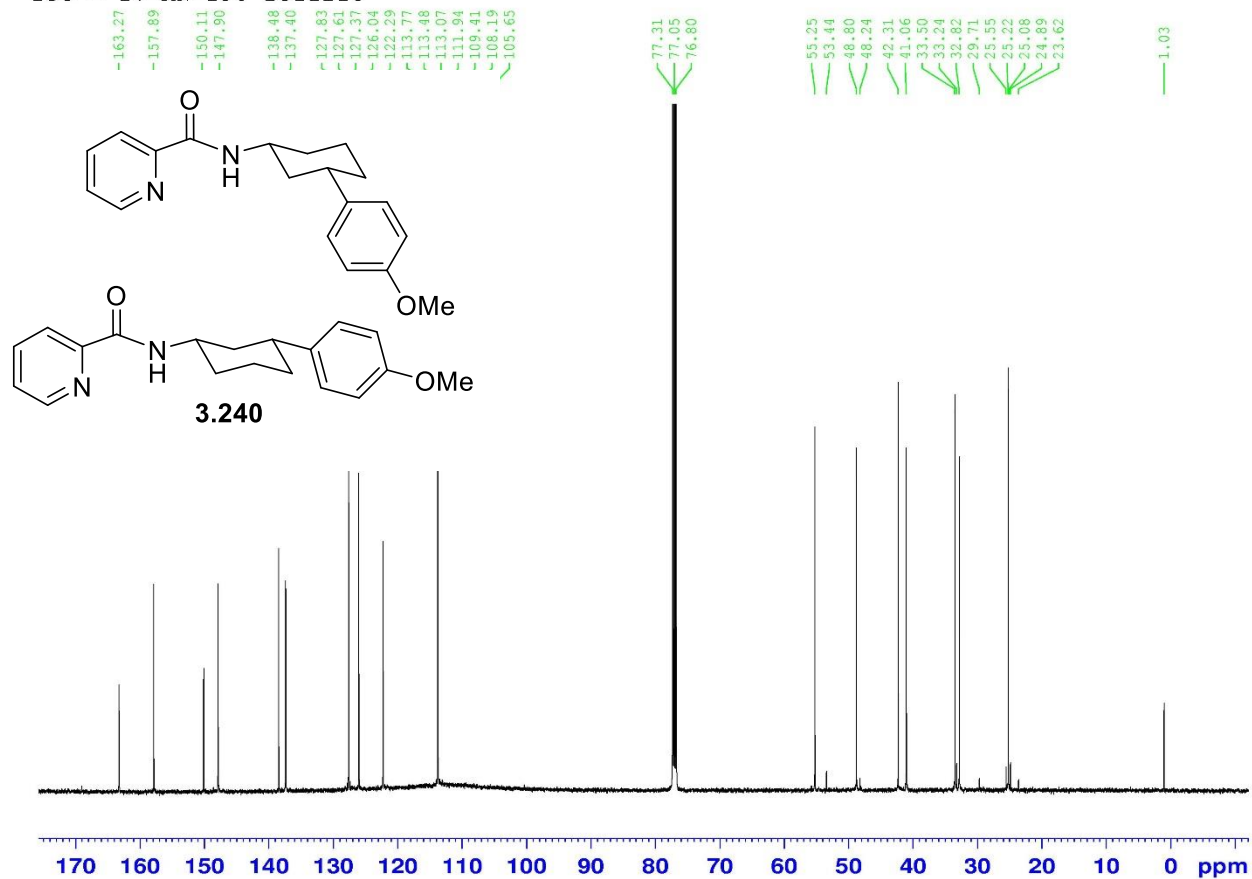
Current Data Parameters
NAME IV-Mn-192 pure
EXPNO 1
PROCNO 1

F2 - Acquisition Parameters
Date_ 20181121
Time 8.49
INSTRUM spect
PROBHD 5 mm Multinucl
PULPROG zg30
ID 65536
SOLVENT CDCl3
NS 16
DS 2
SWH 8278.146 Hz
FIDRES 0.126314 Hz
AQ 3.9583745 sec
RG 161.3
DW 60.400 usec
DE 6.00 usec
TE 300.0 K
D1 1.0000000 sec
TD0 1

===== CHANNEL f1 =====
NUC1 1H
P1 10.00 usec
PL1 3.80 dB
SF01 400.1324710 MHz

F2 - Processing parameters
SI 32768
SF 400.1300000 MHz
WDW EM
SSB 0
LB 0.30 Hz
GB 0
PC 1.00

13C - IV-MN-190 2511218



Current Data Parameters
NAME IV-MN-192 2511218
EXPNO 2
PROCNO 1

F2 - Acquisition Parameters
Date_ 20181126
Time 5.23
INSTRUM spect
PROBHD 5 mm PAQXI 1H/
PULPROG zgpg30
TD 65536
SOLVENT CDC13
NS 14384
DS 4
SWH 30030.029 Hz
FIDRES 0.458222 Hz
AQ 1.0911744 sec
RG 32768
DW 16.650 usec
DE 6.50 usec
TE 298.2 K
D1 2.00000000 sec
D11 0.03000000 sec
TD0 1

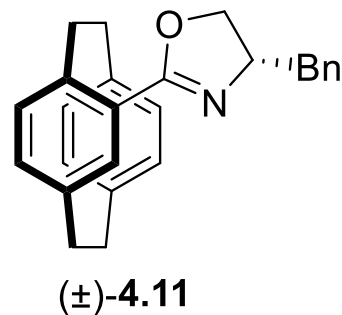
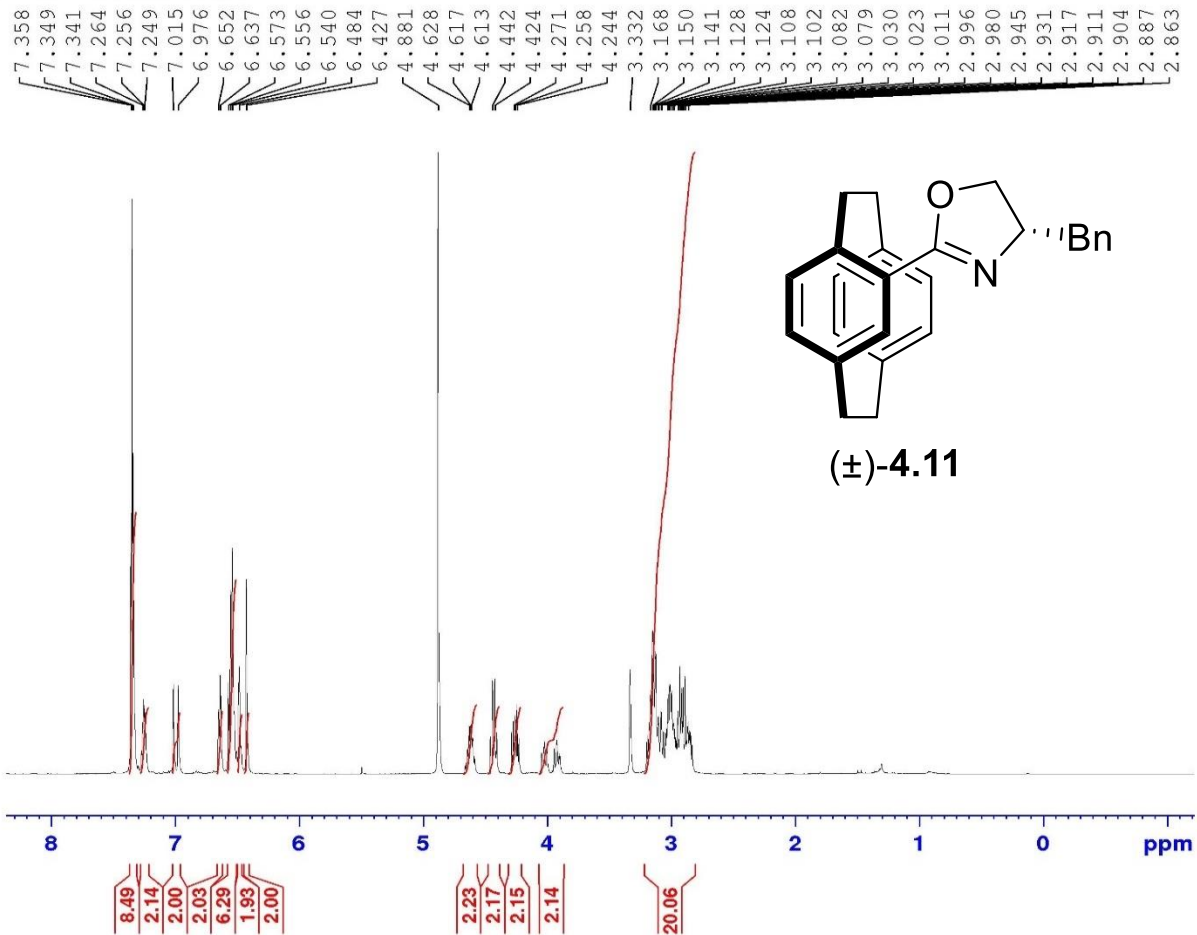
===== CHANNEL f1 =====
NUC1 13C
P1 12.00 usec
PL1 -4.00 dB
PL1W 172.88230896 W
SFO1 125.7703643 MHz

===== CHANNEL f2 =====
CPDPRG[2] waltz16
NUC2 1H
PCPD2 80.00 usec
PL2 4.00 dB
PL12 22.51 dB
PL13 25.00 dB
PL2W 12.10000038 W
PL12W 0.17052394 W
PL13W 0.09611372 W
SFO2 500.1320005 MHz

F2 - Processing parameters
SI 32768
SF 125.7577890 MHz
WDW EM
SSB 0
LB 1.00 Hz
GB 0
PC 1.40

Electronic Appendix for Chapter 4

PC and Bnoxazoline



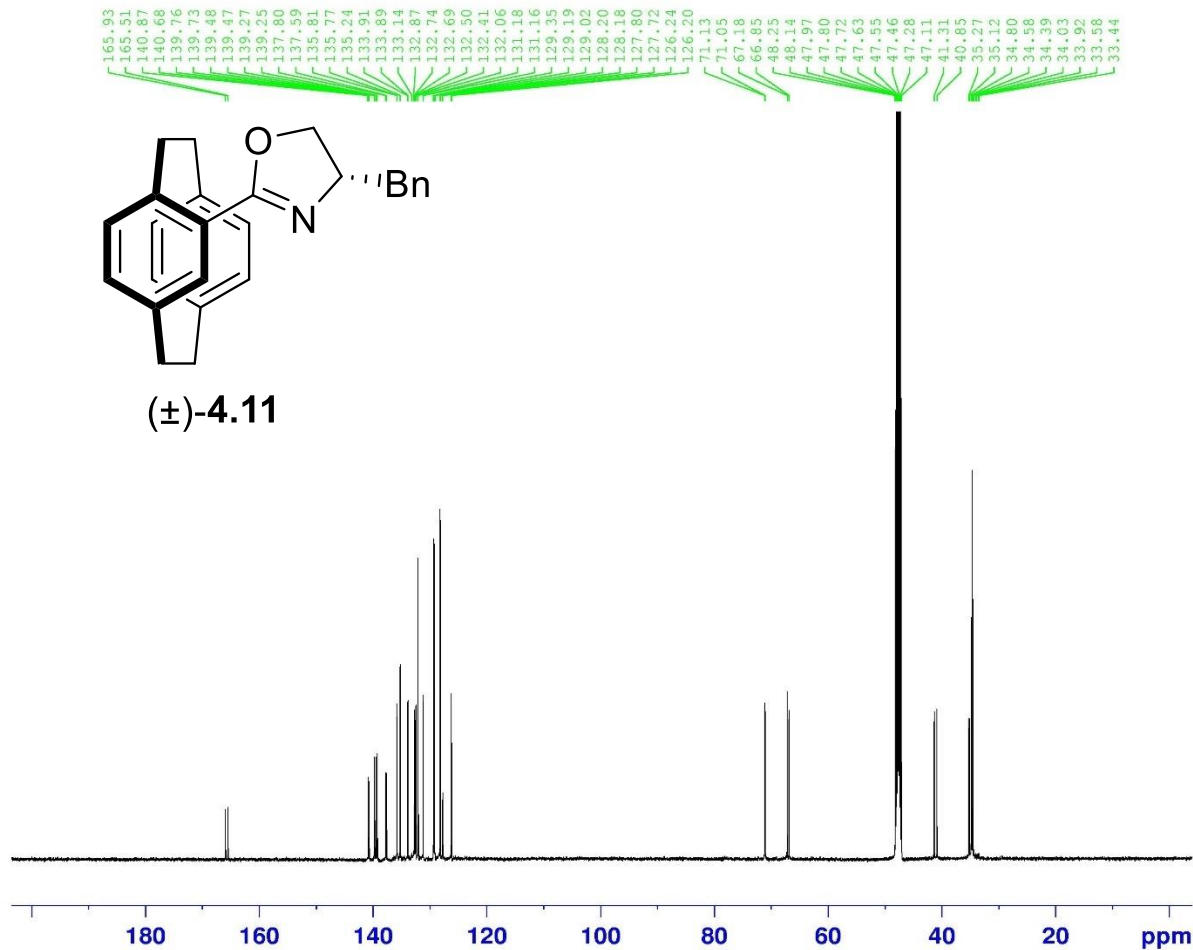
```
Current Data Parameters
NAME      V-Mn-160 i
EXPNO     1
PROCNO    1

F2 - Acquisition Parameters
Date_     20190615
Time      18.54
INSTRUM   spect
PROBHD    5 mm PAQXI 1H/
PULPROG   zg30
TD         65536
SOLVENT   MeOD
NS         16
DS         2
SWH        10330.578 Hz
FIDRES     0.157632 Hz
AQ         3.1719425 sec
RG         64
DW         48.400 usec
DE         6.50 usec
TE         298.2 K
D1         1.0000000 sec
TD0        1

===== CHANNEL f1 =====
NUC1       1H
P1         9.50 usec
PL1        4.00 dB
PL1W       12.1000038 W
SFO1       500.1330885 MHz

F2 - Processing parameters
SI         32768
SF         500.1300000 MHz
WDW        EM
SSB        0
LB         0.30 Hz
GB         0
SB         1.00
PC
```

13C : PC and Bnoxazoline



Current Data Parameters
 NAME V-Mn-160 1
 EXPNO 2
 PROCNO 1

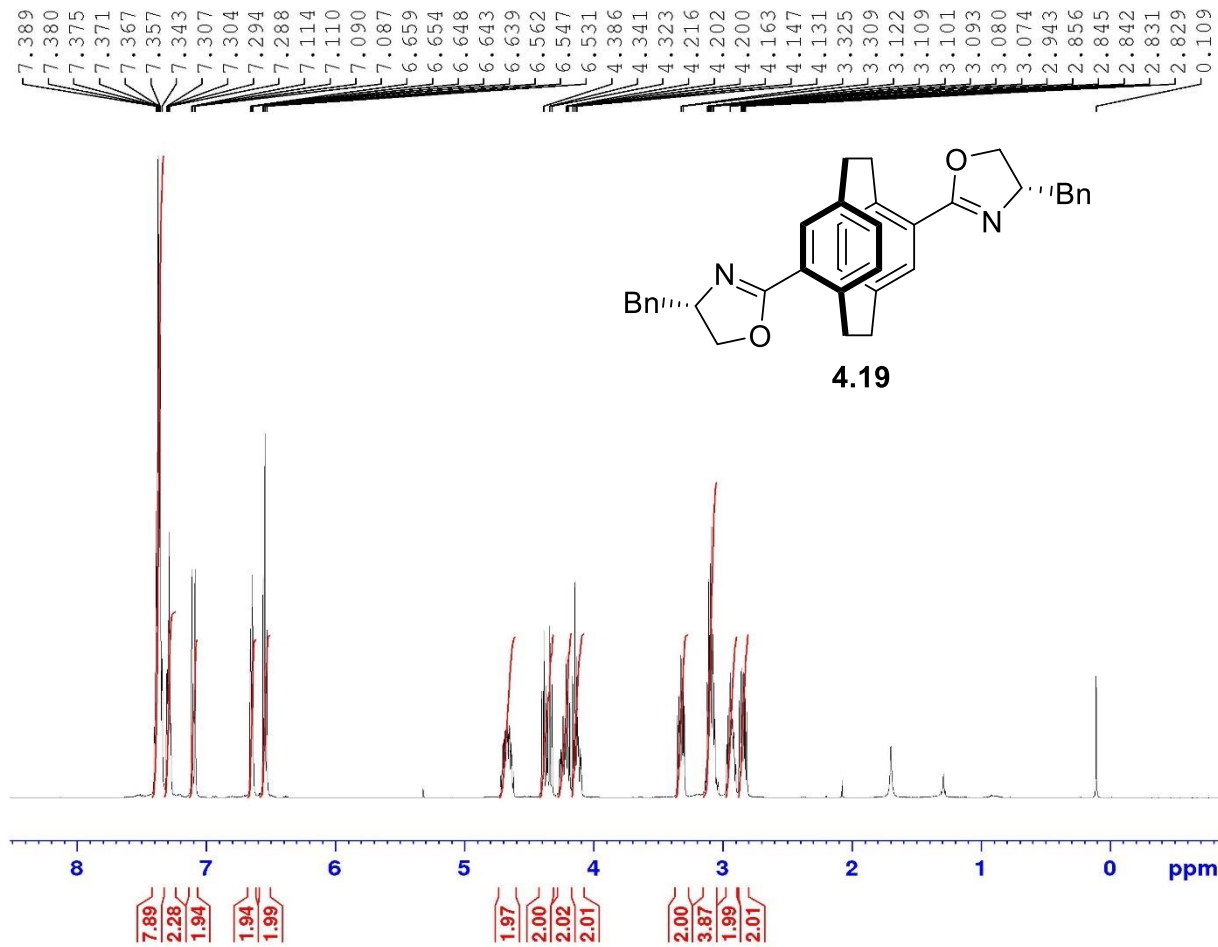
F2 - Acquisition Parameters
 Date_ 20190616
 Time 9.18
 INSTRUM spect
 PROBHD 5 mm PAQXI 1H/
 PULPROG zgpg30
 TD 65536
 SOLVENT MeOD
 NS 16384
 DS 4
 SWH 30030.029 Hz
 FIDRES 0.458222 Hz
 AQ 1.0911744 sec
 RG 32768
 DW 16.650 usec
 DE 6.50 usec
 TE 298.2 K
 D1 2.00000000 sec
 D11 0.03000000 sec
 TD0 1

===== CHANNEL f1 =====
 NUC1 13C
 P1 12.00 usec
 PL1 -4.00 dB
 PL1W 172.88230896 W
 SFO1 125.7703643 MHz

===== CHANNEL f2 =====
 CPDPRG[2] waltz16
 NUC2 1H
 PCPD2 80.00 usec
 PL2 4.00 dB
 PL12 22.51 dB
 PL13 25.00 dB
 PL2W 12.10000038 W
 PL12W 0.17052394 W
 PL13W 0.09611372 W
 SFO2 500.1320005 MHz

F2 - Processing parameters
 SI 32768
 SF 125.7577890 MHz
 WDW EM
 SSB 0
 LB 1.00 Hz
 GE 0
 PC 1.40

Pseudoparadirbromo PC & Bn Oxa (2.2eq.) Pd:L (10:20) LiOtBu : 5 eq.



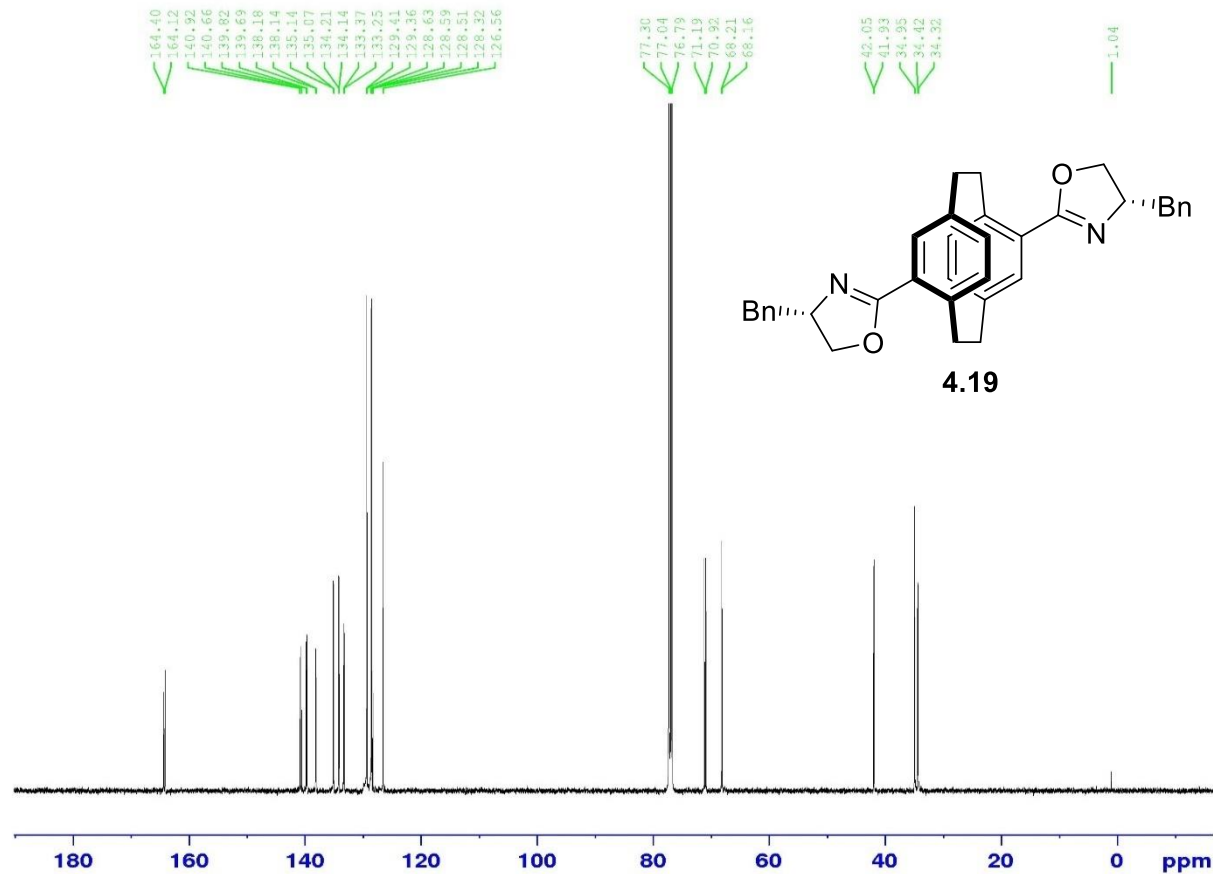
Current Data Parameters
NAME VI-Mn-55 ii
EXPNO 1
PROCNO 1

F2 - Acquisition Parameters
Date_ 20200208
Time 20.02
INSTRUM spect
PROBHD 5 mm PAQXI 1H/
PULPROG zg30
ID 65536
SOLVENT CDCl3
NS 16
DS 2
SWH 10330.578 Hz
FIDRES 0.157632 Hz
AQ 3.1719425 sec
RG 71.8
DW 48.400 usec
DE 6.50 usec
TE 298.2 K
D1 1.00000000 sec
TD0 1

===== CHANNEL f1 =====
NUC1 1H
P1 9.50 usec
PL1 4.00 dB
PL1W 12.10000038 W
SFO1 500.1330885 MHz

F2 - Processing parameters
SI 32768
SF 500.1300000 MHz
WDW EM
SSB 0
LB 0.30 Hz
GB 0
PC 1.00

13C : Pseudoparadirbromo PC & Bn Oxa (2.2eq.) Pd:L (10:20) LiOtBu : 5 eq.



Current Data Parameters
 NAME v1-Mn-55 i1
 EXPNO 2
 PROCNO 1

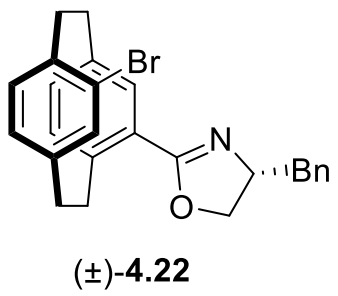
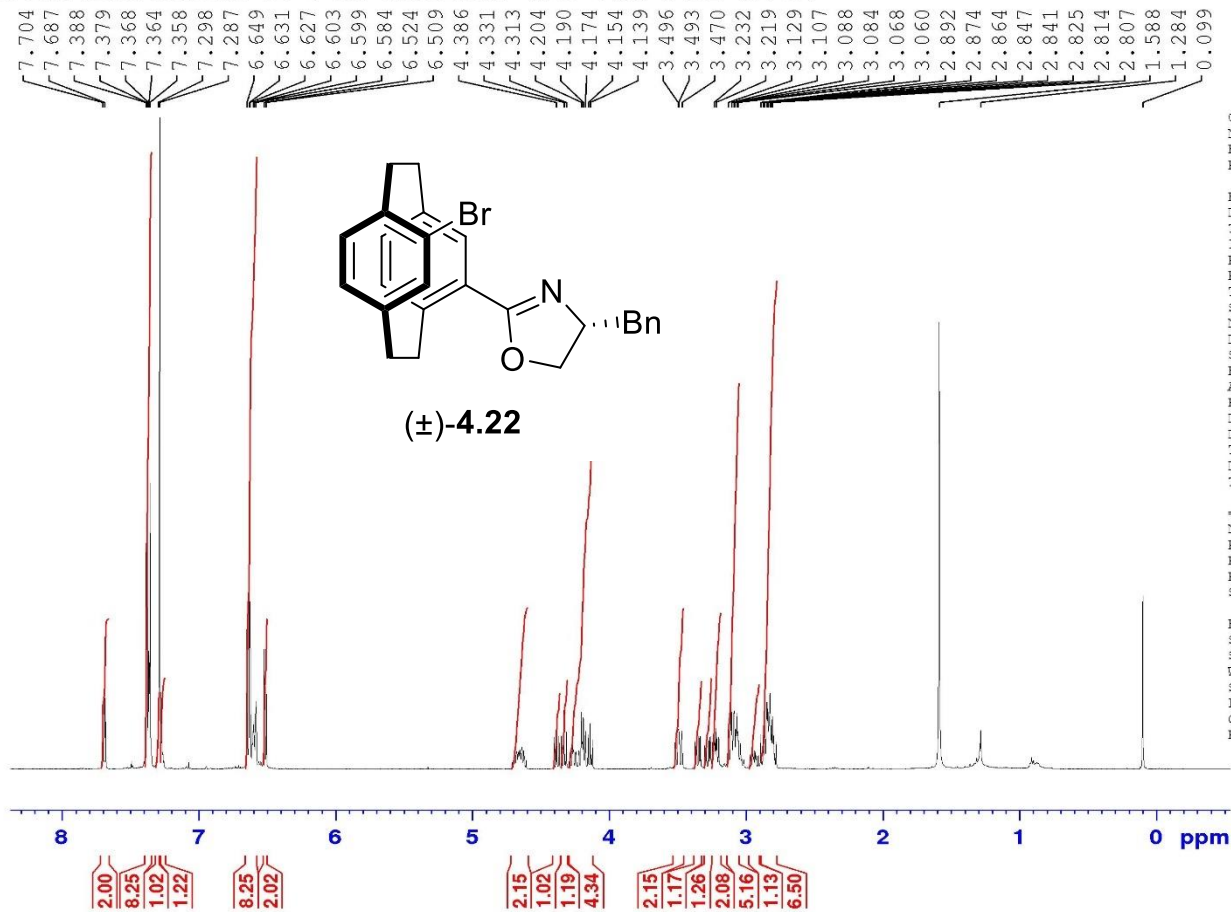
F2 - Acquisition Parameters
 Date_ 20200209
 Time 10.26
 INSTRUM spect
 PROBHD 5 mm PAQXI 1H/
 PULPROG zgpg30
 TD 65536
 SOLVENT cdcl3
 NS 16384
 DS 4
 SWH 30030.029 Hz
 FIDRES 0.458222 Hz
 AQ 1.0911744 sec
 RC 32768
 DW 16.650 usec
 DE 6.50 usec
 TE 298.2 K
 D1 2.00000000 sec
 D11 0.03000000 sec
 TD0 1

----- CHANNEL f1 -----
 NUC1 13C
 P1 12.00 usec
 PL1 -4.00 dB
 PL1W 172.88230896 W
 SFO1 125.7703643 MHz

----- CHANNEL F2 -----
 CPDPRG12 waltz16
 NUC2 1H
 PCPD2 80.00 usec
 PL2 4.00 dB
 PL12 22.51 dB
 PL13 25.00 dB
 PL2W 12.10000038 W
 PL12W 0.17052394 W
 PL13W 0.09611372 W
 SFO2 500.1320005 MHz

F2 - Processing parameters
 SI 32768
 SF 125.7577890 MHz
 WDW EM
 SSR 0
 LB 1.00 Hz
 GB 0
 PC 1.40

Pseudoorthodibromo PC & Bn oxazoline (1.1 eq.) Pd:L (5:10)



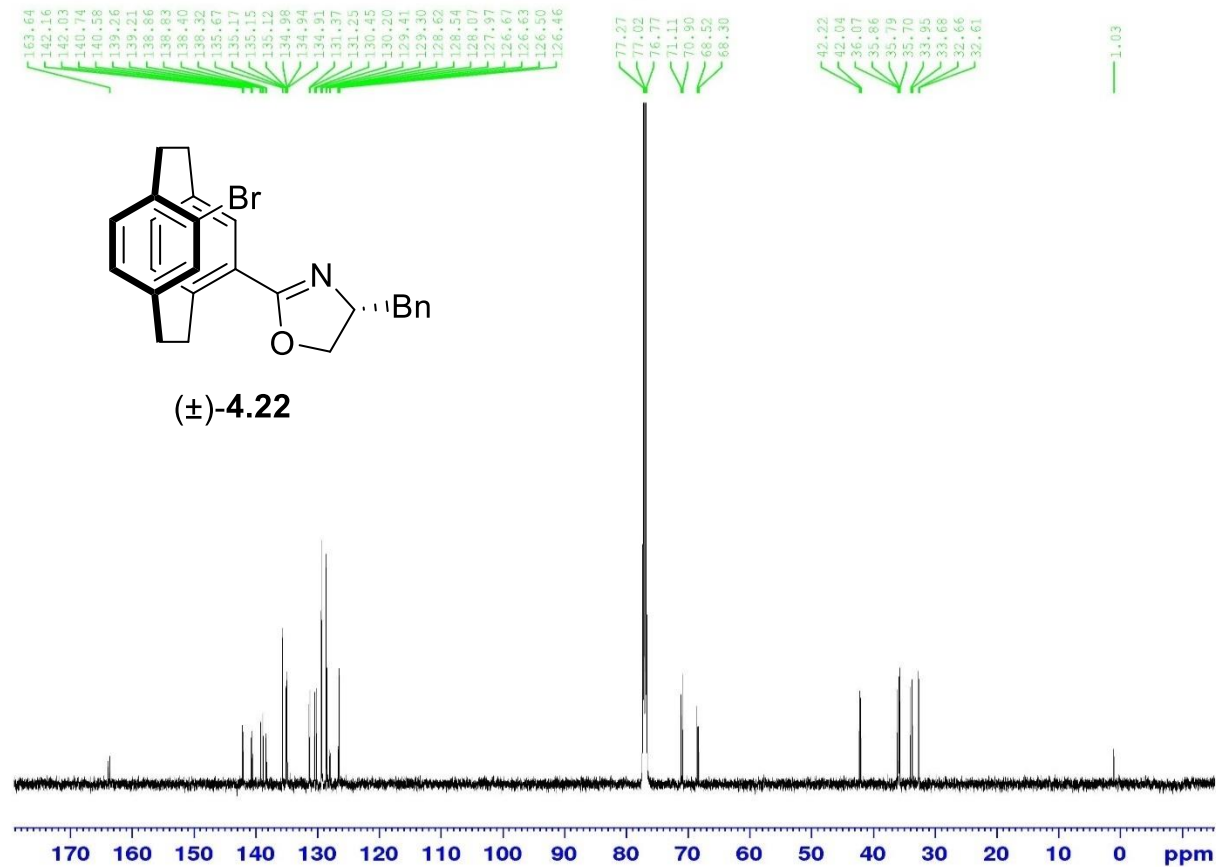
Current Data Parameters
 NAME VI-Mn-33 i
 EXFNO 1
 PROCNO 1

F2 - Acquisition Parameters
 Date_ 20200201
 Time_ 20.09
 INSTRUM spect
 PROBHD 5 mm PAQXI 1H/
 PULPROG zg30
 TD 65536
 SOLVENT CDCl3
 NS 16
 DS 2
 SWH 10330.578 Hz
 FIDRES 0.157632 Hz
 AQ 3.1719425 sec
 RG 256
 DW 48.400 usec
 DE 6.50 usec
 TE 298.2 K
 D1 1.0000000 sec
 TDC 1

----- CHANNEL f1 -----
 NUC1 1H
 P1 9.50 usec
 PL1 4.00 dB
 PL1W 12.10000038 W
 SFO1 500.1330885 MHz

F2 - Processing parameters
 SI 32768
 SF 500.1300000 MHz
 WDW EM
 SSB 0
 LB 0.30 Hz
 GB 0
 PC 1.00

Pseudoorthodibromo PC & Bn oxazoline (1.1 eq.) Pd:L (5:10)



Current Data Parameters
 NAME VI-Mn-53 i
 EXPNO 3
 PROCNO 1

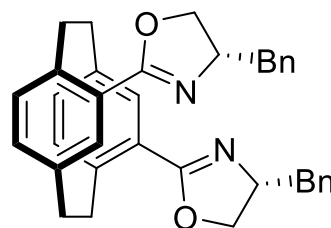
F2 - Acquisition Parameters
 Date_ 20200203
 Time 8.15
 INSTRUM spect
 PROBHD 5 mm PAQXI 1H/
 PULPROG zgpg30
 TD 65536
 SOLVENT CDCl3
 NS 16384
 DS 4
 SWH 30030.029 Hz
 FIDRES 0.458222 Hz
 AQ 1.0911744 sec
 RG 32768
 DW 16.650 usec
 DE 6.50 usec
 TE 298.2 K
 D1 2.00000000 sec
 D11 0.03000000 sec
 TDC 1

===== CHANNEL f1 =====
 NUC1 13C
 P1 12.00 usec
 PL1 -4.00 dB
 PL1W 172.88230896 W
 SFO1 125.7703643 MHz

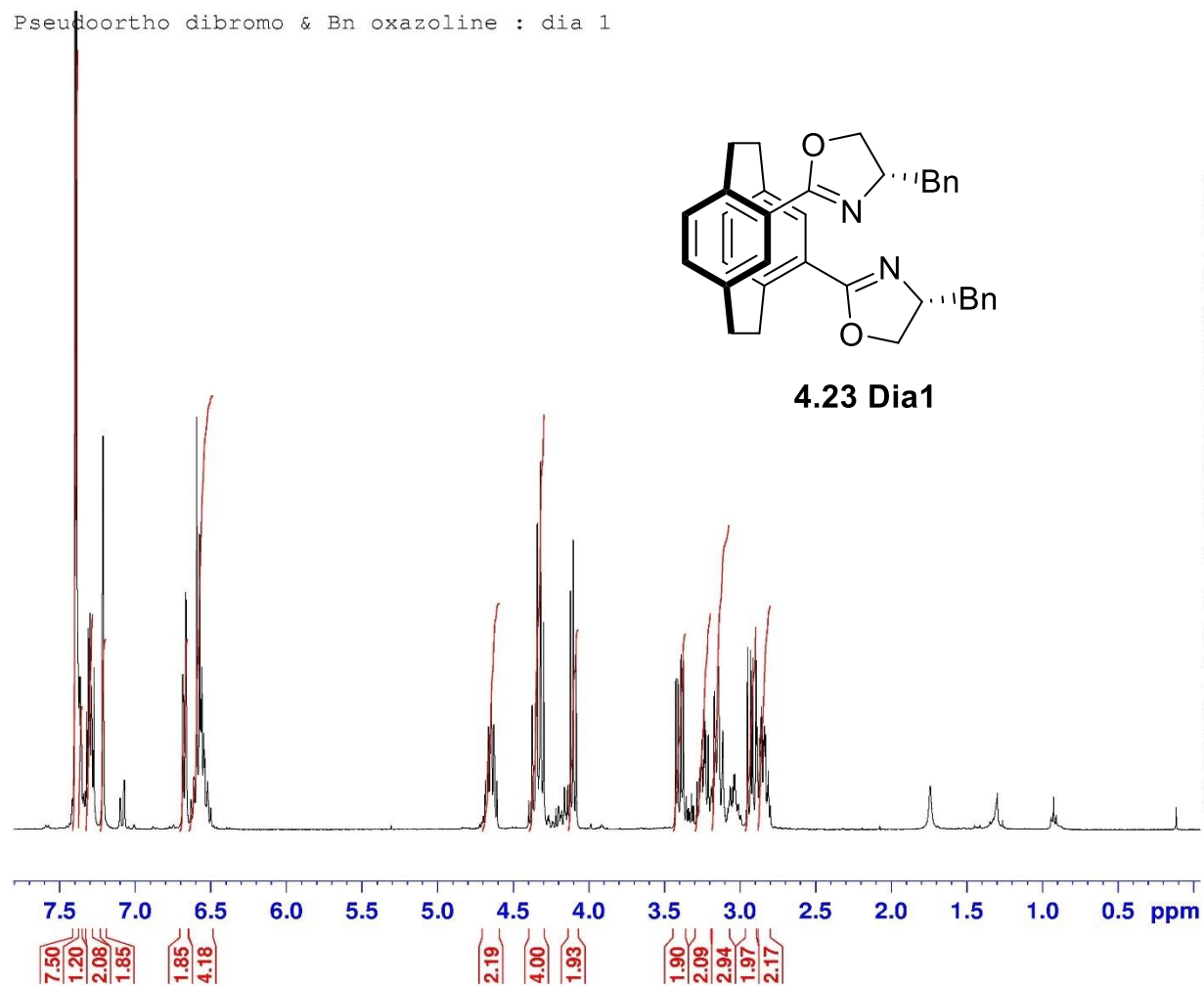
===== CHANNEL f2 =====
 CPDPRG[2] waltz16
 NUC2 1H
 PCPD2 80.00 usec
 PL2 4.00 dB
 PL12 22.51 dB
 PL13 25.00 dB
 PL2W 12.10000038 W
 PL12W 0.17052394 W
 PL13W 0.09611372 W
 SFO2 500.1320005 MHz

F2 - Processing parameters
 SI 32768
 SF 125.7577890 MHz
 WDW EM
 SSB 0
 LB 1.00 Hz
 GB 0
 PC 1.40

Pseudoortho dibromo & Bn oxazoline : dia 1



4.23 Dia1



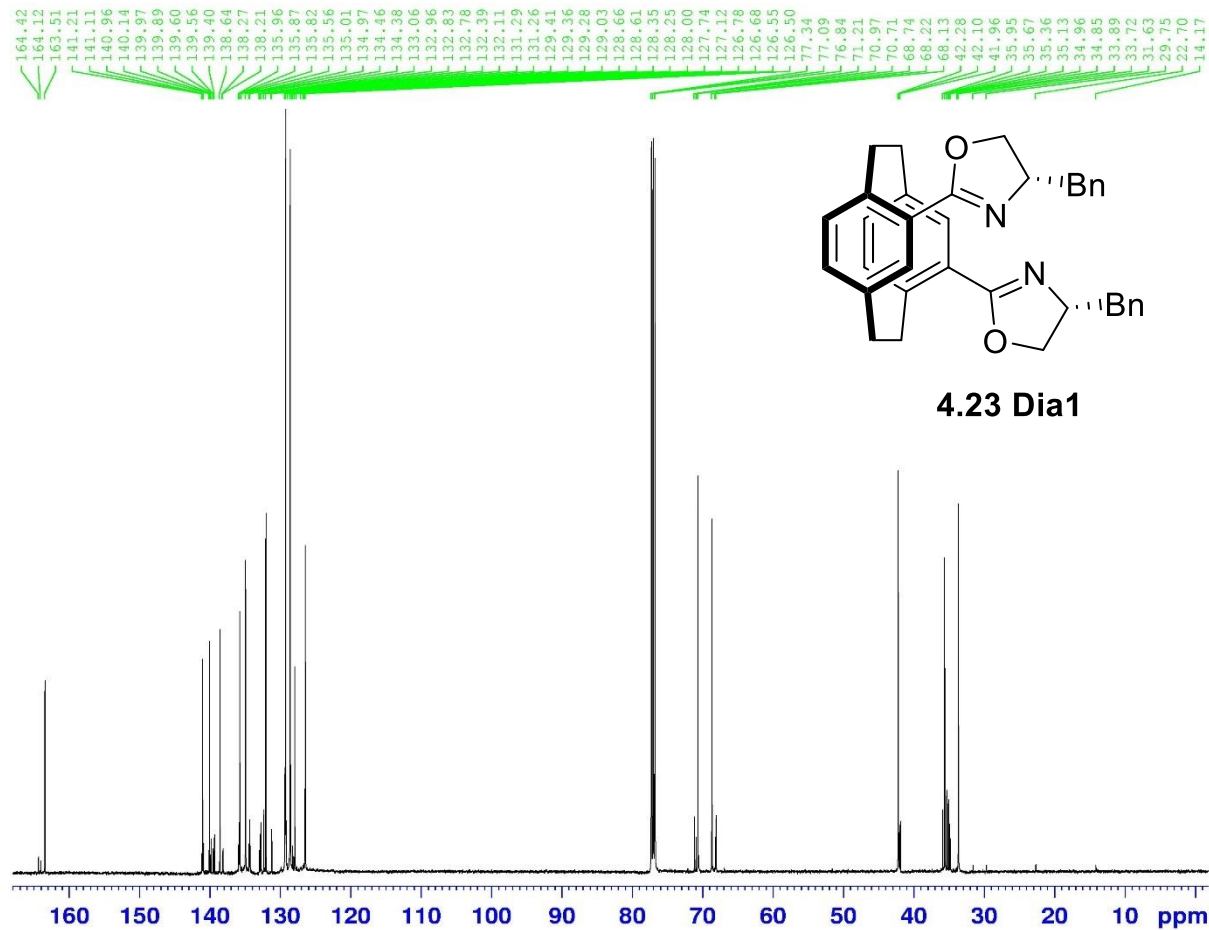
Current Data Parameters
NAME V-Mn-254 dia 1
EXPNO 1
PROCNO 1

F2 - Acquisition Parameters
Date_ 20191020
Time 21.19
INSTRUM spect
PROBHD 5 mm Multinucl
PULPROG zg30
TD 65536
SOLVENT CDC13
NS 16
DS 2
SWH 8278.146 Hz
FIDRES 0.126314 Hz
AQ 3.9583745 sec
RG 287.4
DW 60.400 usec
DE 6.00 usec
TE 300.0 K
D1 1.00000000 sec
TD0 1

===== CHANNEL f1 =====
NUC1 1H
P1 10.00 usec
PL1 3.10 dB
SFO1 400.1324710 MHz

F2 - Processing parameters
SI 32768
SF 400.1300000 MHz
WDW EM
SSB 0
LB 0.30 Hz
GB 0
PC 1.00

13C : PseudoorthoDiBr & Bn oxazoline : dial



Current Data Parameters
NAME V-Mn-254 Dial
EXPNO 2
PROCNO 1

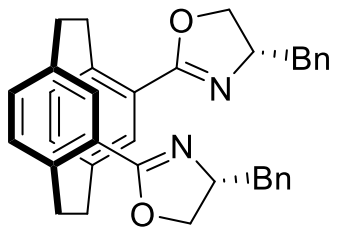
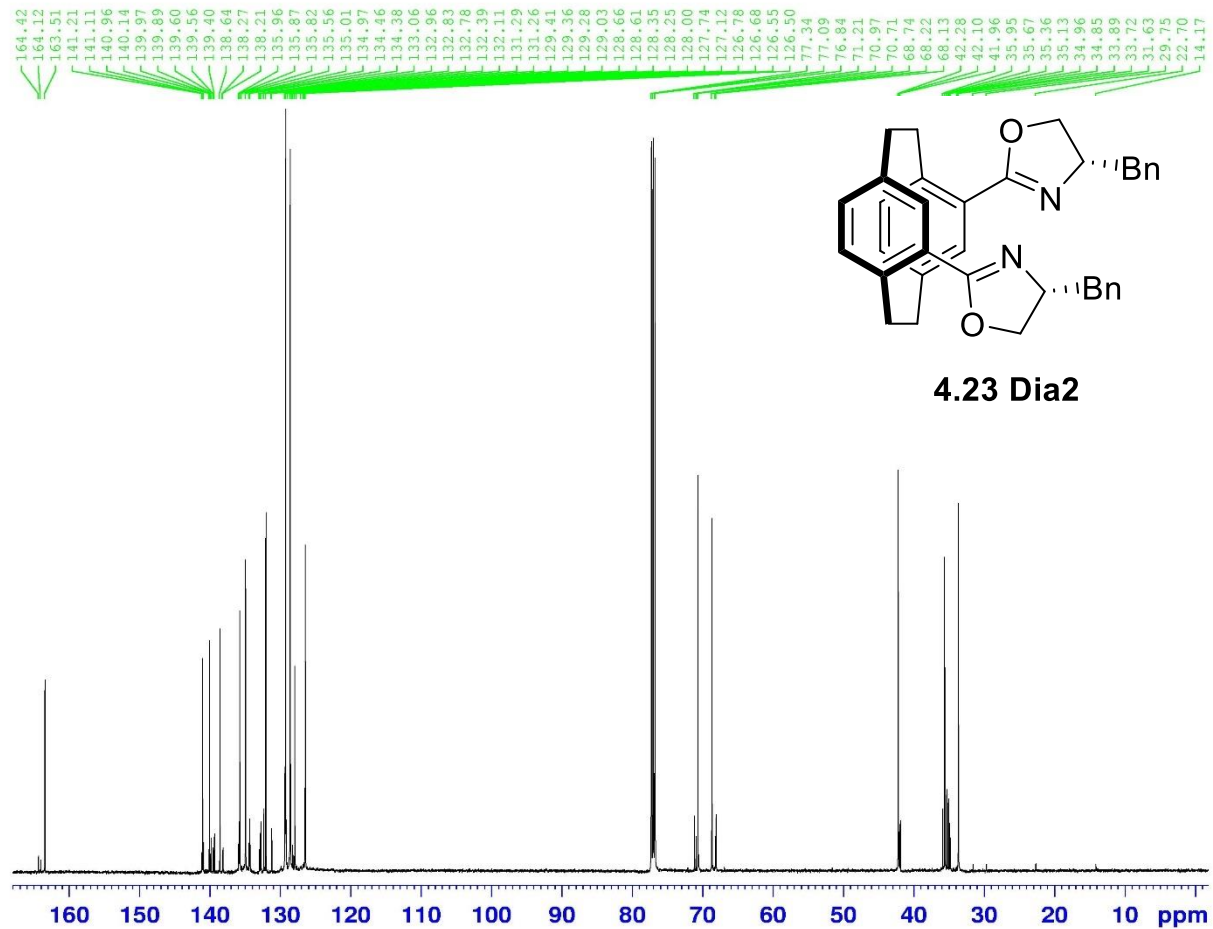
F2 - Acquisition Parameters
Date_ 20191104
Time 9.31
INSTRUM spect
PROBHD 5 mm PAQXI 1H/
PULPROG zgpg30
TD 65536
SOLVENT CDCl3
NS 16384
DS 4
SWH 30030.029 Hz
FIDRES 0.458222 Hz
AQ 1.0911744 sec
RG 32768
DW 16.650 usec
DE 6.50 usec
TE 296.0 K
D1 2.00000000 sec
D11 0.03000000 sec
TD0 1

----- CHANNEL f1 -----
NUC1 13C
P1 12.00 usec
PL1 -4.00 dB
PL1W 172.88230896 W
SFO1 125.7703643 MHz

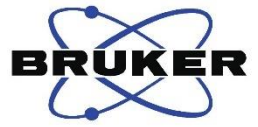
----- CHANNEL f2 -----
CPDPRG[2] waltz16
NUC2 1H
PCPD2 80.00 usec
PL2 4.00 dB
PL12 22.51 dB
PL13 25.00 dB
PL2W 12.10000038 W
PL12W 0.17052394 W
PL13W 0.09611372 W
SFO2 500.1320005 MHz

F2 - Processing parameters
SI 32768
SF 125.7577890 MHz
WDW EM
SSB 0
LB 1.00 Hz
GB 0
PC 1.40

13C : PseudoorthoDiBr & Bn oxazoline : dial



4.23 Dia2



Current Data Parameters
 NAME V-Mn-254 Dial
 EXPNO 2
 PROCNO 1

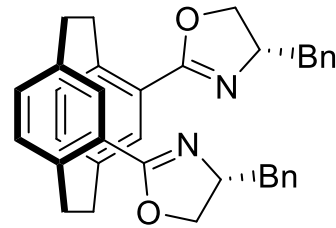
F2 - Acquisition Parameters
 Date_ 20191104
 Time 9.31
 INSTRUM spect
 PROBHD 5 mm PAQXI 1H/
 PULPROG zgpg30
 TD 65536
 SOLVENT CDC13
 NS 16384
 DS 4
 SWH 30030.029 Hz
 FIDRES 0.458222 Hz
 AQ 1.0911744 sec
 RG 32768
 DW 16.650 usec
 DE 6.50 usec
 TE 296.0 K
 D1 2.00000000 sec
 D11 0.03000000 sec
 TDO 1

----- CHANNEL f1 -----
 NUC1 13C
 P1 12.00 usec
 PL1 -4.00 dB
 PL1W 172.88230896 W
 SFO1 125.7703643 MHz

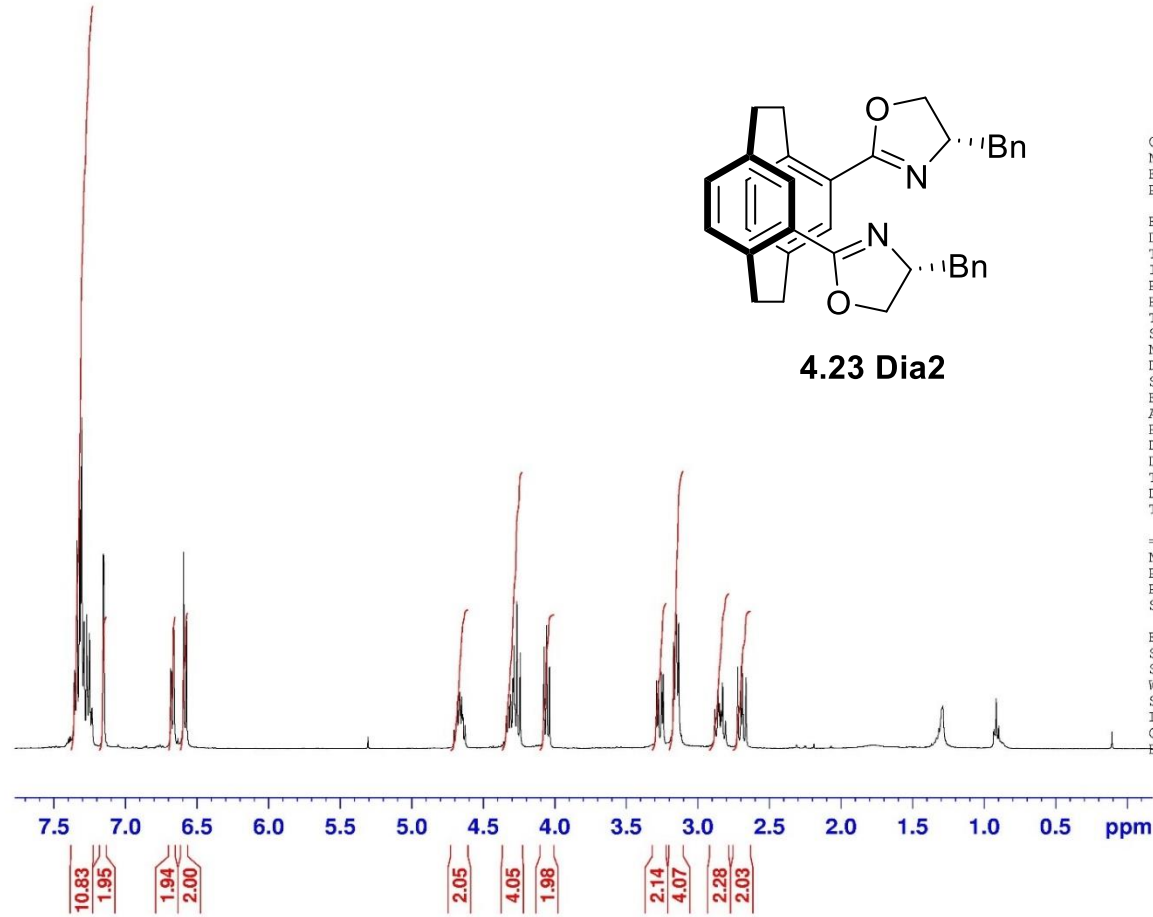
----- CHANNEL f2 -----
 CPDPRG2 waltz16
 NUC2 1H
 PCPD2 80.00 usec
 PL2 4.00 dB
 PL12 22.51 dB
 PL13 25.00 dB
 PL2W 12.10000038 W
 PL12W 0.17052394 W
 PL13W 0.09611372 W
 SFO2 500.1320005 MHz

F2 - Processing parameters
 SI 32768
 SF 125.7577890 MHz
 WDW EM
 SSB 0
 LB 1.00 Hz
 GB 0
 PC 1.40

Pseudoortho dibromo & Bn oxazoline : dia 2



4.23 Dia2



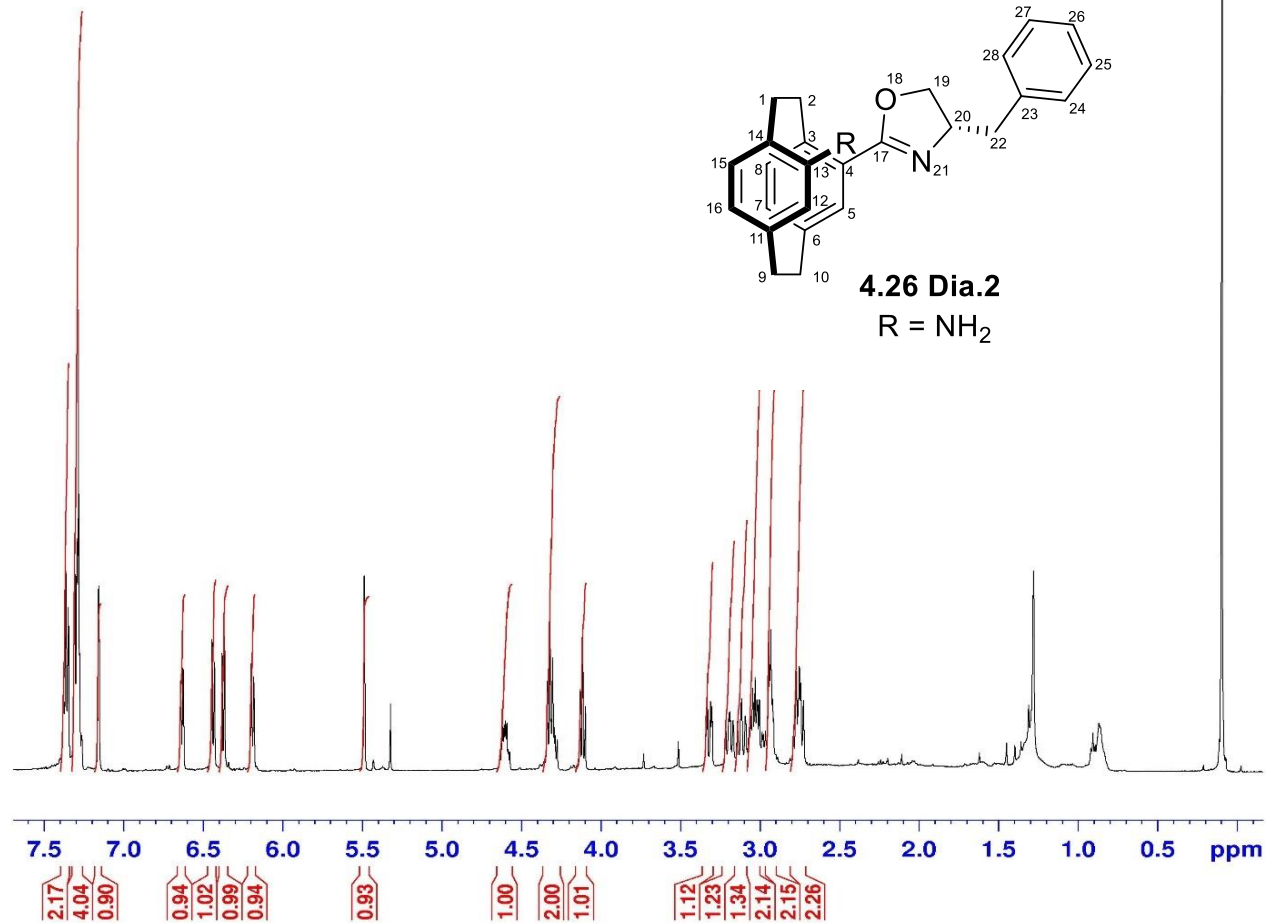
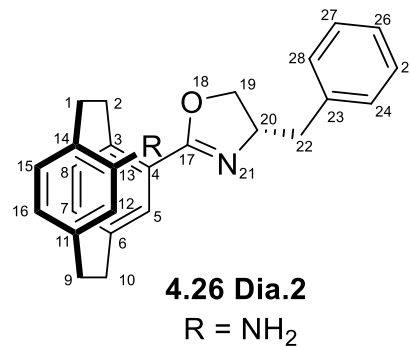
```
Current Data Parameters
NAME      V-Mn-254 dia 2
EXPNO     1
PROCNO    1

F2 - Acquisition Parameters
Date_     20191020
Time      21.33
INSTRUM   spect
PROBHD    5 mm Multinucl
PULPROG   zg30
TD         65536
SOLVENT   CDCl3
NS         16
DS         2
SWH        8278.146 Hz
FIDRES     0.126314 Hz
AQ         3.9583745 sec
RG         287.4
DW         60.400 usec
DE         6.00 usec
TE         300.0 K
D1         1.00000000 sec
TD0        1

===== CHANNEL f1 =====
NUC1       1H
P1         10.00 usec
PL1        3.10 dB
SFO1       400.1324710 MHz

F2 - Processing parameters
SI         32768
SF         400.1300000 MHz
WDW        EM
SSB        0
LB         0.30 Hz
GB         0
PC         1.00
```

Pseudo gem NH2 Br & Bn oxazoline



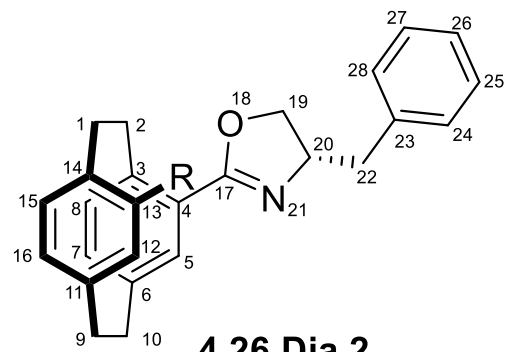
Current Data Parameters
NAME V-Mn-163 Dia 1
EXPNO 1
PROCNO 1

F2 - Acquisition Parameters
Date_ 20190707
Time 17.45
INSTRUM spect
PROBHD 5 mm PAQXI 1H/
PULPROG zg30
TD 65536
SOLVENT CDC13
NS 64
DS 2
SWH 10330.578 Hz
FIDRES 0.157632 Hz
AQ 3.1719425 sec
RG 512
DW 48.400 usec
DE 6.50 usec
TE 295.6 K
D1 1.00000000 sec
TD0 1

===== CHANNEL f1 =====
NUC1 1H
P1 9.50 usec
PL1 4.00 dB
PL1W 12.10000038 W
SFO1 500.1330885 MHz

F2 - Processing parameters
SI 32768
SF 500.1300000 MHz
WDW EM
SSB 0
LB 0.30 Hz
GB 0
PC 1.00

Pseudogem NH2 Br & Bn oxazoline : 2nd fraction



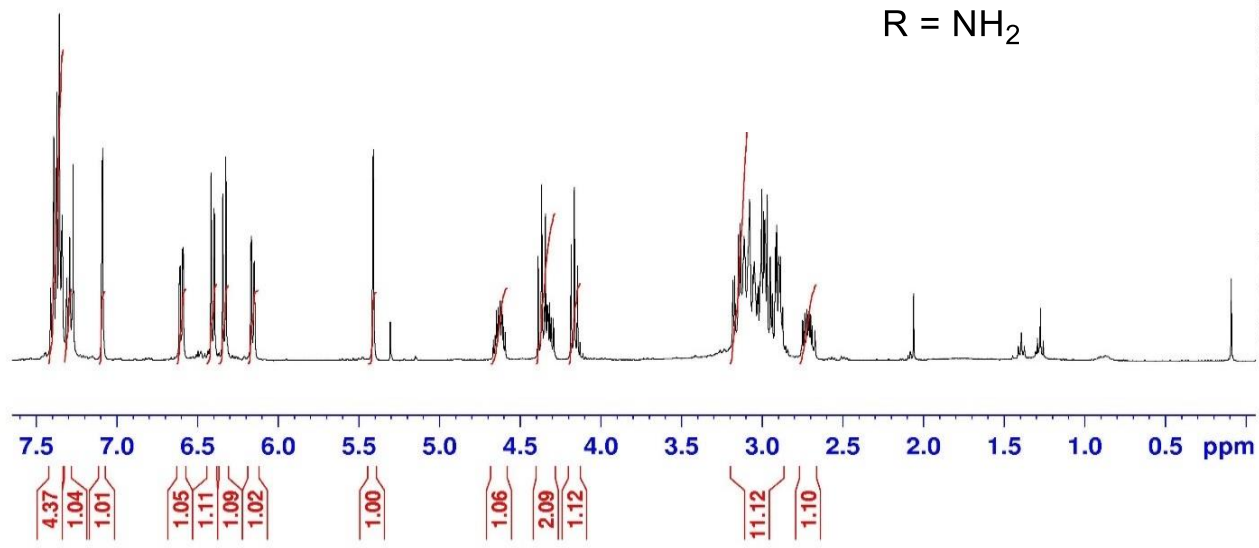
4.26 Dia.2
R = NH₂

```
Current Data Parameters
NAME      V-Mn-251 dia 2
EXPNO     2
PROCNO    1

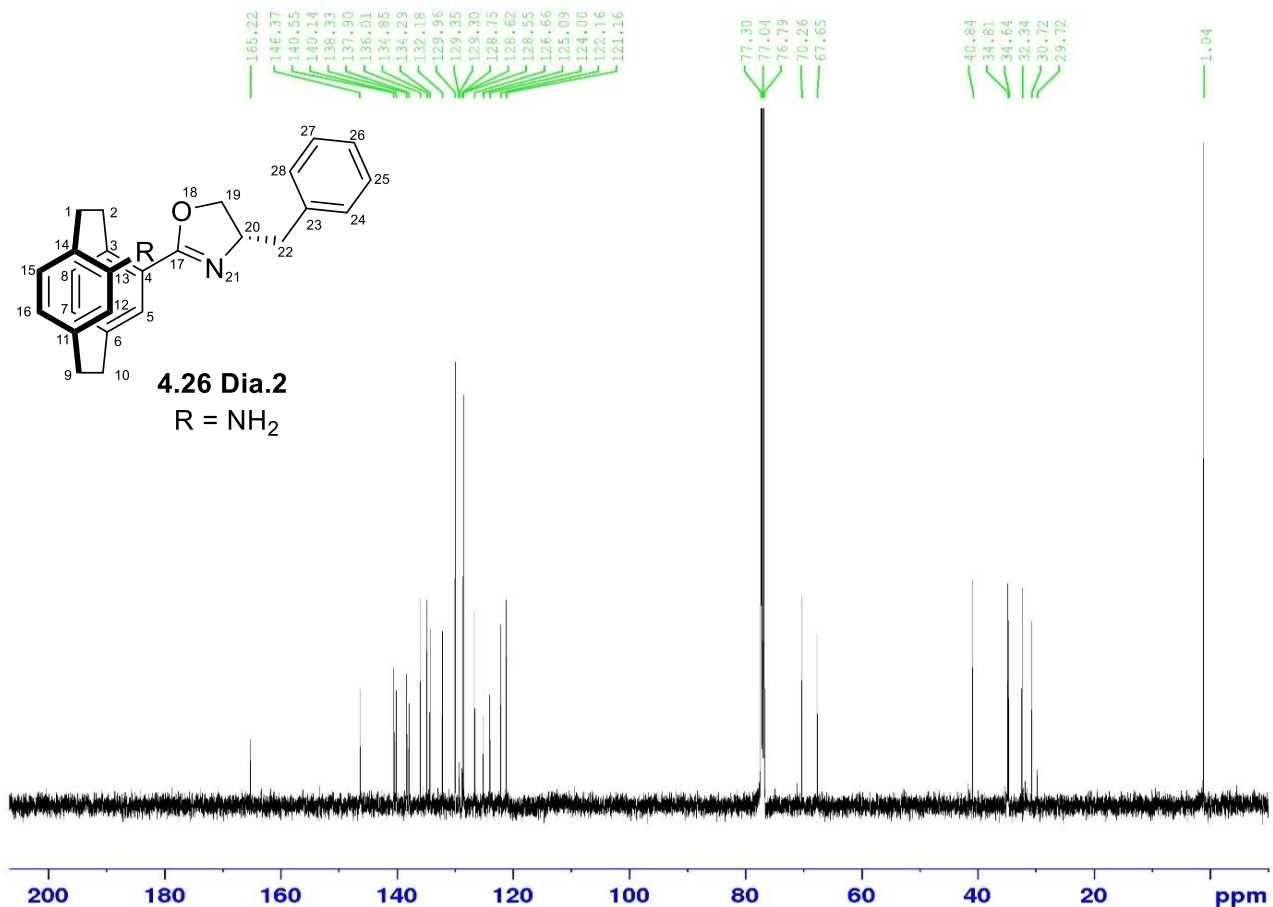
F2 - Acquisition Parameters
Date_     20191014
Time      8.38
INSTRUM   spect
PROBHD    5 mm Multinucl
PULPROG   zg30
TD         65536
SOLVENT   CDCl3
NS         16
DS         2
SWH        8278.146 Hz
FIDRES     0.126314 Hz
AQ         3.9583745 sec
RG         287.4
DW         60.400 usec
DE         6.00 usec
TE         300.0 K
D1         1.00000000 sec
TD0        1

===== CHANNEL f1 =====
NUC1       1H
P1         10.00 usec
PL1        3.10 dB
SFO1       400.1324710 MHz

F2 - Processing parameters
SI         32768
SF         400.1300000 MHz
WDW        EM
SSB        0
LB         0.30 Hz
GB         0
PC         1.00
```



13 C : Pseudo gem NH2 Br & Bn oxazoline



Current Data Parameters
 NAME V-Mn-163 Dia 2
 EXPNO 2
 PROCNO 1

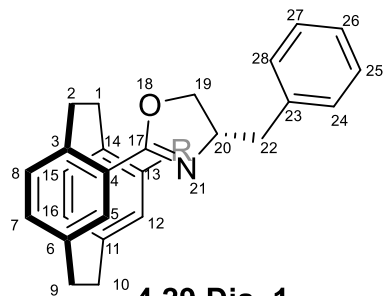
F2 - Acquisition Parameters
 Date_ 20190708
 Time 8.36
 INSTRUM spect
 PROBHD 5 mm PAQXI 1H/
 PULPROG zgpg30
 TD 65536
 SOLVENT CDCl3
 NS 16384
 DS 4
 SWH 30030.029 Hz
 FIDRES 0.458222 Hz
 AQ 1.0911744 sec
 RG 32768
 DW 16.650 usec
 DE 6.50 usec
 TE 296.0 K
 D1 2.0000000 sec
 D11 0.0300000 sec
 TDD 1

----- CHANNEL f1 -----
 NUC1 13C
 P1 12.00 usec
 PL1 4.00 dB
 PL1W 172.88230896 W
 SFO1 125.7703643 MHz

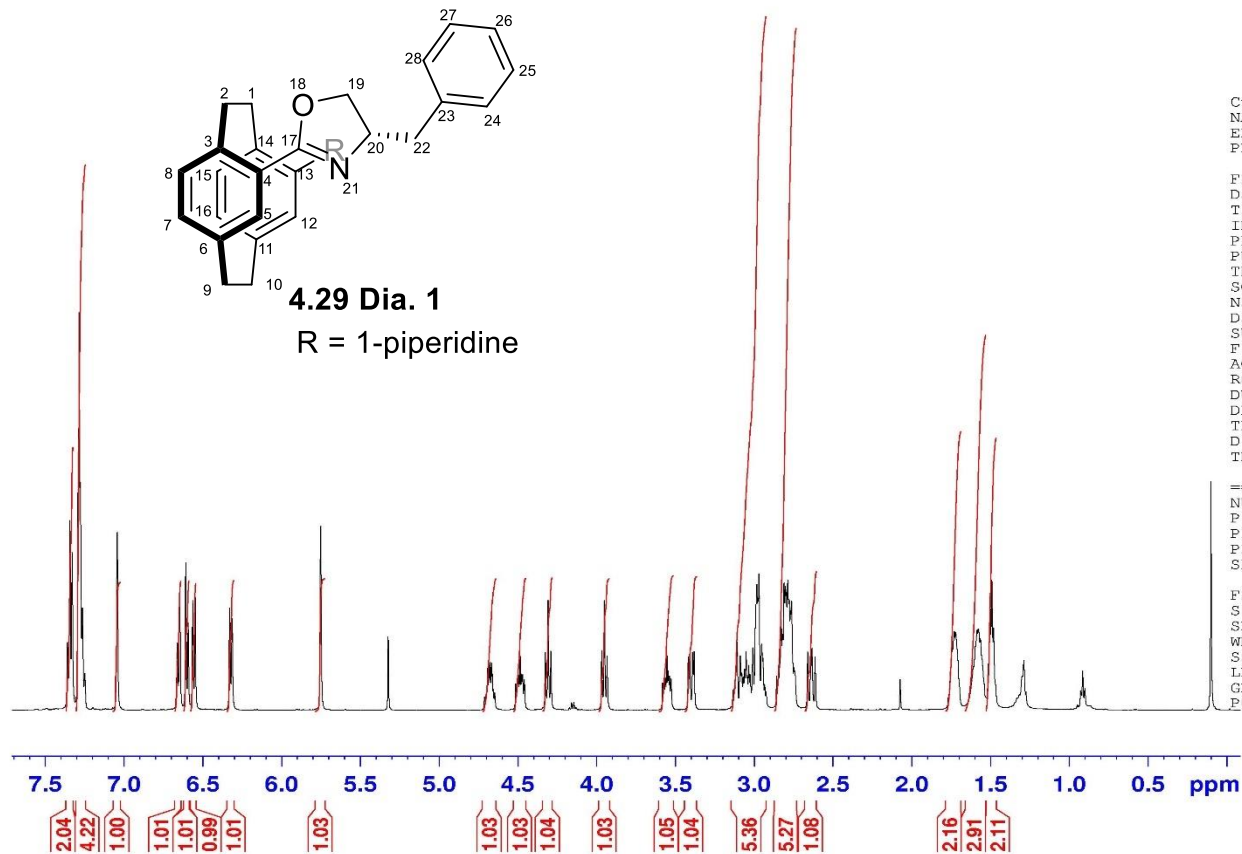
----- CHANNEL f2 -----
 CPDPRG12 waltz16
 NUC2 1H
 PCPD2 80.00 usec
 PL2 4.00 dB
 PL12 22.51 dB
 PL13 25.00 dB
 PL2W 12.10000038 W
 PL12W 0.17052394 W
 PL13W 0.09611372 W
 SFO2 500.1320005 MHz

F2 - Processing parameters
 SI 32768
 SF 125.7577890 MHz
 WDW EM
 SSB 0
 LB 1.00 Hz
 GB 0
 PC 1.40

V-Mn-164 i 1st diastereoisomer



4.29 Dia. 1
R = 1-piperidine



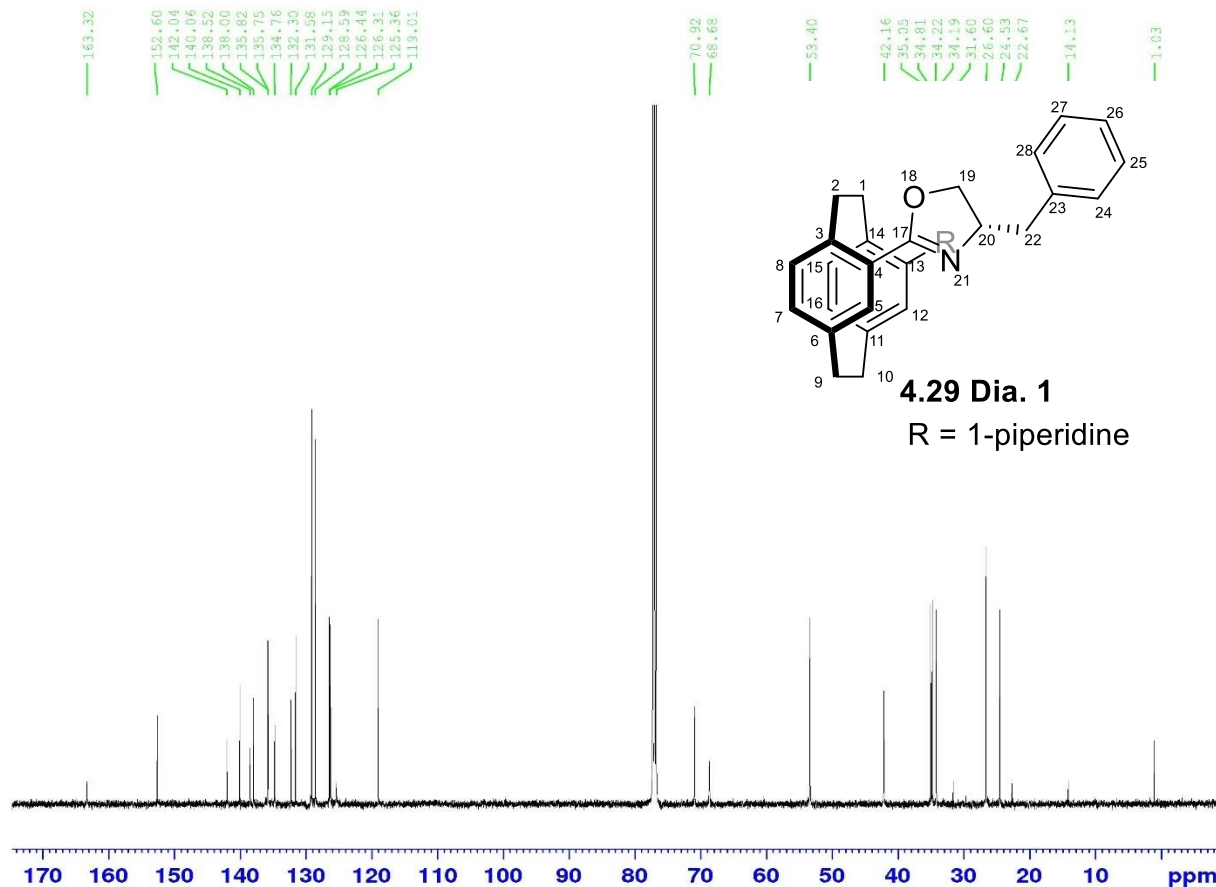
Current Data Parameters
NAME V-Mn-164 i
EXPNO 1
PROCNO 1

F2 - Acquisition Parameters
Date_ 20190627
Time 18.09
INSTRUM spect
PROBHD 5 mm PAQXI 1H/
PULPROG zg30
TD 65536
SOLVENT CDC13
NS 16
DS 2
SWH 10330.578 Hz
FIDRES 0.157632 Hz
AQ 3.1719425 sec
RG 90.5
DW 48.400 usec
DE 6.50 usec
TE 298.2 K
D1 1.0000000 sec
TD0 1

===== CHANNEL f1 =====
NUC1 1H
P1 9.50 usec
PL1 4.00 dB
PL1W 12.10000038 W
SFO1 500.1330885 MHz

F2 - Processing parameters
SI 32768
SF 500.1300000 MHz
WDW EM
SSB 0
LB 0.30 Hz
GB 0
PC 1.00

13C : V-Mn-164 i 1st diastereoisomer



Current Data Parameters
NAME V-Mn-164 i
EXPNO 3
PROCNO 1

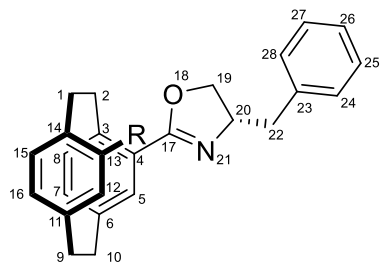
F2 - Acquisition Parameters
Date_ 20190701
Time 8.42
INSTRUM spect
PROBHD 5 mm PAQXI 1H/
PULPROG zgpg30
TD 65536
SOLVENT cdcl3
NS 15605
DS 4
SWH 30030.029 Hz
FIDRES 0.458222 Hz
AQ 1.0911744 sec
RG 32768
DW 16.650 usec
DE 6.50 usec
TE 298.2 K
D1 2.0000000 sec
D11 0.03000000 sec
TD0 1

----- CHANNEL f1 -----
NUC1 13C
P1 12.00 usec
PL1 -4.00 dB
PL1W 172.88230896 W
SFG1 125.7703643 MHz

----- CHANNEL f2 -----
CPDPRG2 wallz16
NUC2 1H
PCPD2 80.00 usec
PL2 4.00 dB
PL12 22.51 dB
PL13 25.00 dB
PL2W 12.10000038 W
PL12W 0.17052394 W
PL13W 0.09611372 W
SFG2 500.1320005 MHz

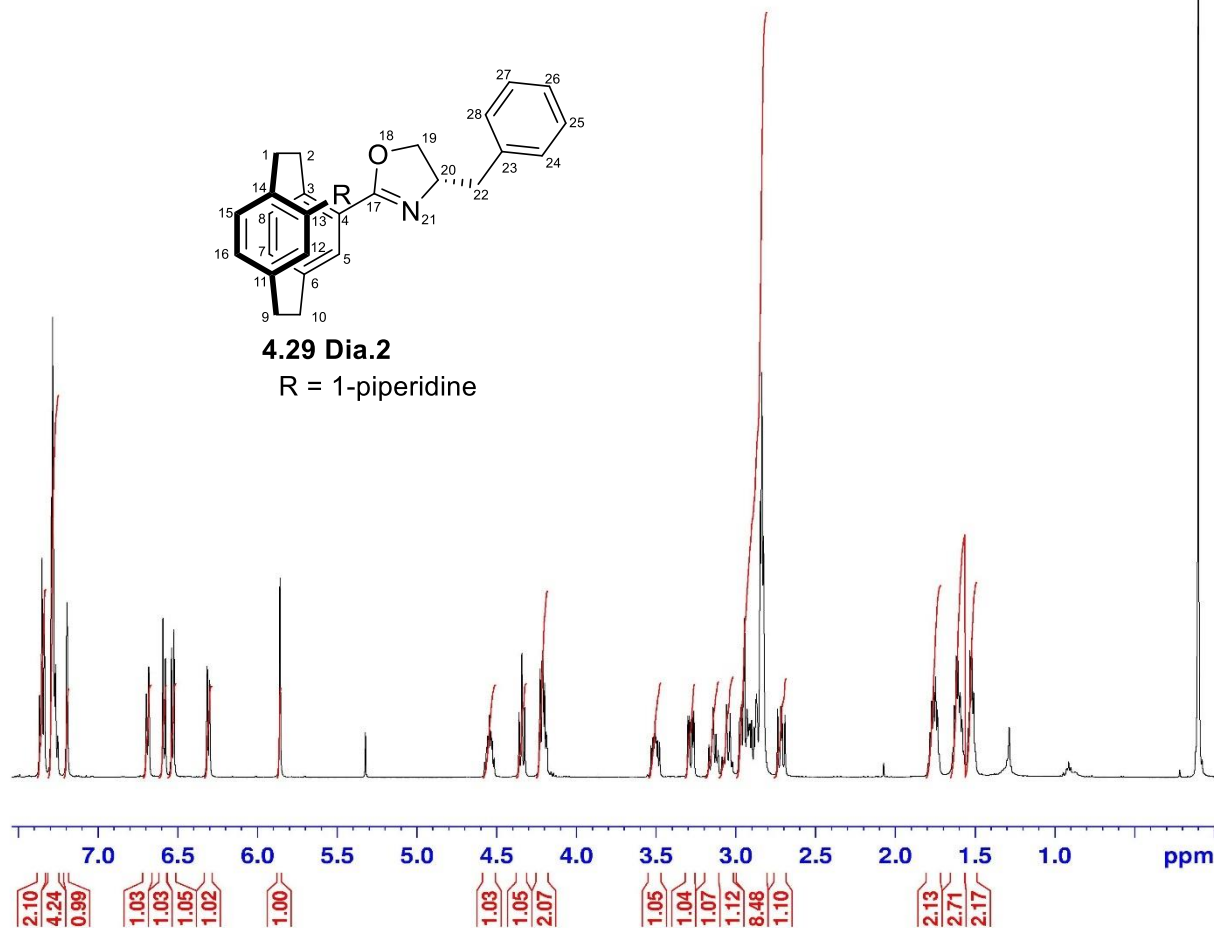
F2 - Processing parameters
SI 32768
SF 125.7577890 MHz
WDW EM
SSB 0
LB 1.00 Hz
CB 0
PC 1.40

V-Mn-164 i 2nd diastereoisomer



4.29 Dia.2

R = 1-piperidine



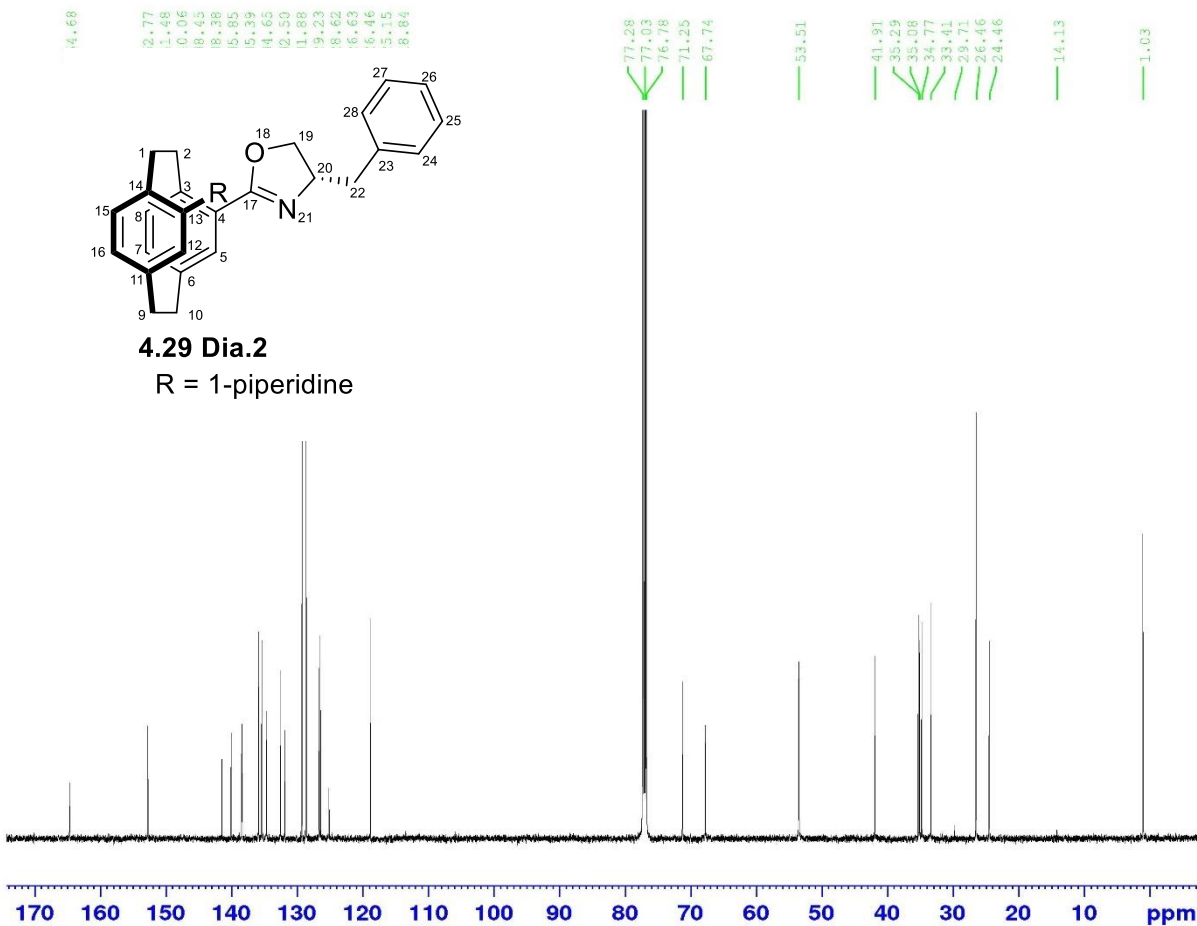
Current Data Parameters
NAME V-Mn-164 ii
EXPNO 1
PROCNO 1

F2 - Acquisition Parameters
Date_ 20190627
Time 18.41
INSTRUM spect
PROBHD 5 mm PAQXI 1H/
PULPROG zg30
TD 65536
SOLVENT CDCl3
NS 16
DS 2
SWH 10330.578 Hz
FIDRES 0.157632 Hz
AQ 3.1719425 sec
RG 90.5
DW 48.400 usec
DE 6.50 usec
TE 298.2 K
D1 1.00000000 sec
TD0 1

=====
CHANNEL f1
NUC1 1H
P1 9.50 usec
PL1 4.00 dB
PL1W 12.10000038 W
SFO1 500.1330885 MHz

F2 - Processing parameters
SI 32768
SF 500.1300000 MHz
WDW EM
SSB 0
LB 0.30 Hz
GB 0
PC 1.00

13C : V-Mn-164 i 2nd diastereoisomer



Current Data Parameters
NAME V-Mn-164 11
EXPNO 2
PROCNO 1

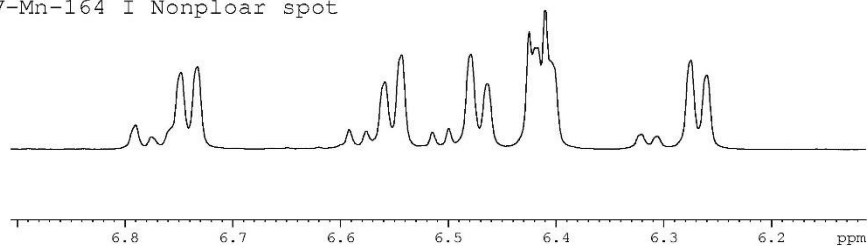
F2 - Acquisition Parameters
Date_ 20190628
Time 9.08
INSTRUM spect
PROBHD 5 mm PAQXI 1H/
PULPROG zgpg30
TD 65536
SOLVENT cdcl3
NS 16077
DS 4
SWH 30030.029 Hz
FIDRES 0.458222 Hz
AQ 1.091744 sec
RG 32768
DW 16.650 usec
DE 6.50 usec
TR 298.0 K
D1 2.00000000 sec
D11 0.03000000 sec
TD0 1

===== CHANNEL f1 =====
NUC1 13C
P1 12.00 usec
PL1 -4.00 dB
PL1W 172.88230896 W
SFO1 125.7703643 MHz

===== CHANNEL f2 =====
CPDPRG[2] waltz16
NUC2 1H
PCPD2 80.00 usec
PL2 4.00 dB
PL12 22.51 dB
PL13 25.00 dB
PL2W 12.10000038 W
PL12W 0.17052394 W
PL13W 0.09611372 W
SFO2 500.1320005 MHz

F2 - Processing parameters
ST 32768
SF 125.7577890 MHz
WDW FM
SSB 0
LB 1.00 Hz
GB 0
PC 1.40

V-Mn-164 I Nonpolar spot

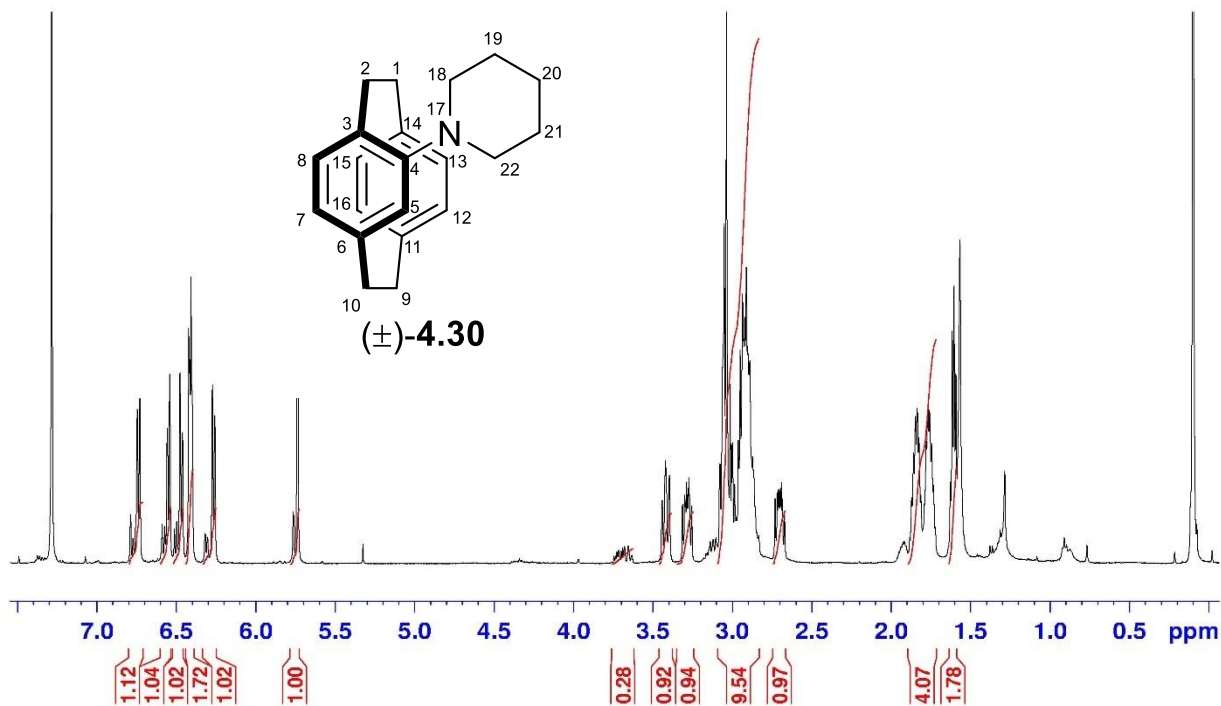


Current Data Parameters
NAME V-Mn-164 I Nonpolar
EXPNO 1
PROCNO 1

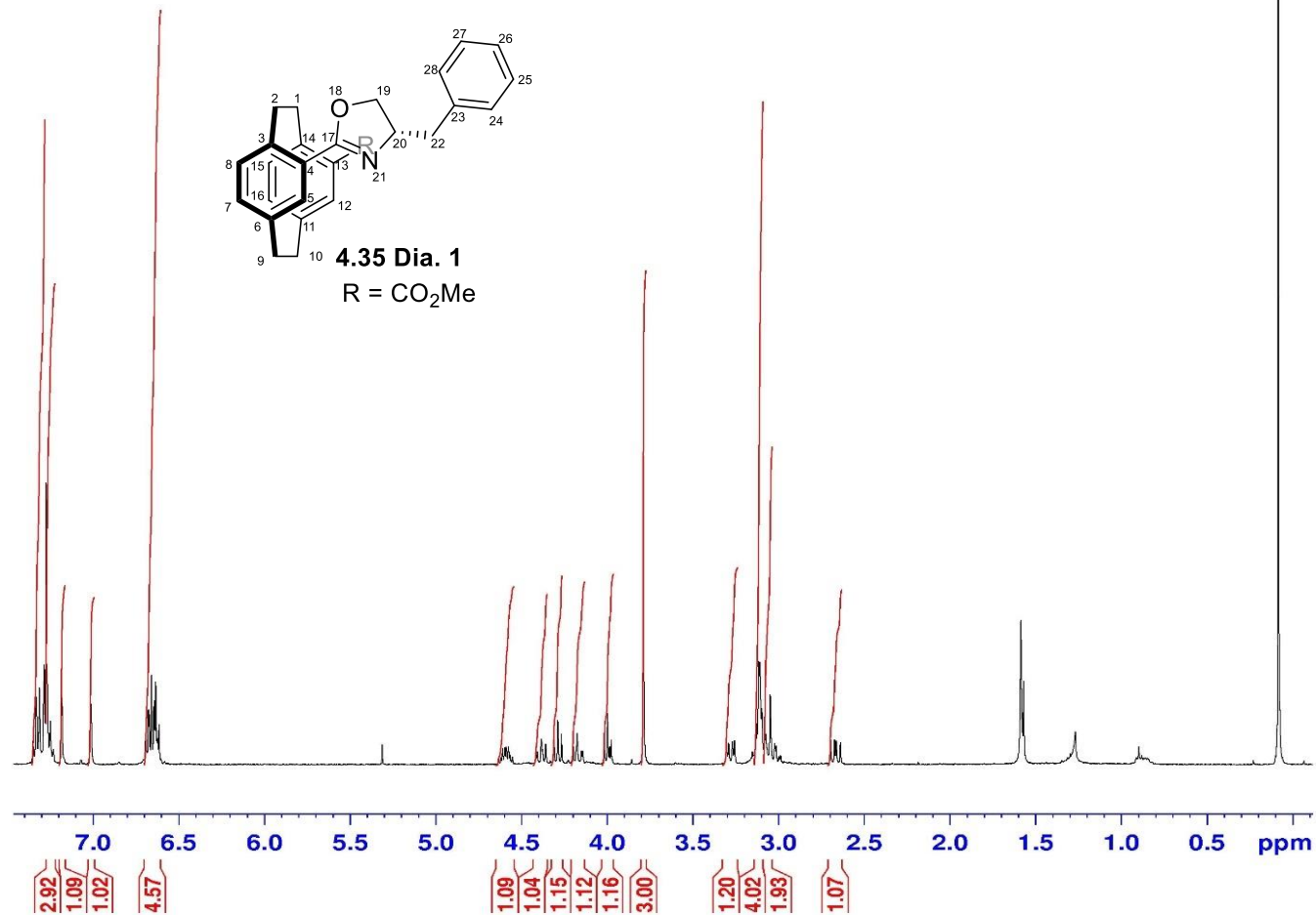
F2 - Acquisition Parameters
Date_ 20190627
Time 17.51
INSTRUM spect
PROBHD 5 mm PAQXI 1H/
PULPROG zg30
TD 65536
SOLVENT CDCl3
NS 16
DS 2
SWH 10330.578 Hz
FIDRES 0.157632 Hz
AQ 3.1719425 sec
RG 228.1
DW 48.400 usec
DE 6.50 usec
TE 298.2 K
D1 1.00000000 sec
TD0 1

==== CHANNEL f1 =====
NUC1 1H
P1 9.50 usec
PL1 4.00 dB
PL1W 12.10000038 W
SFO1 500.1330885 MHz

F2 - Processing parameters
SI 32768
SF 500.1300000 MHz
WDW EM
SSB 0
LB 0.30 Hz
GB 0
PC 1.00



Pseudogem CO2Me Br & Bnoxazoline : Dia 1



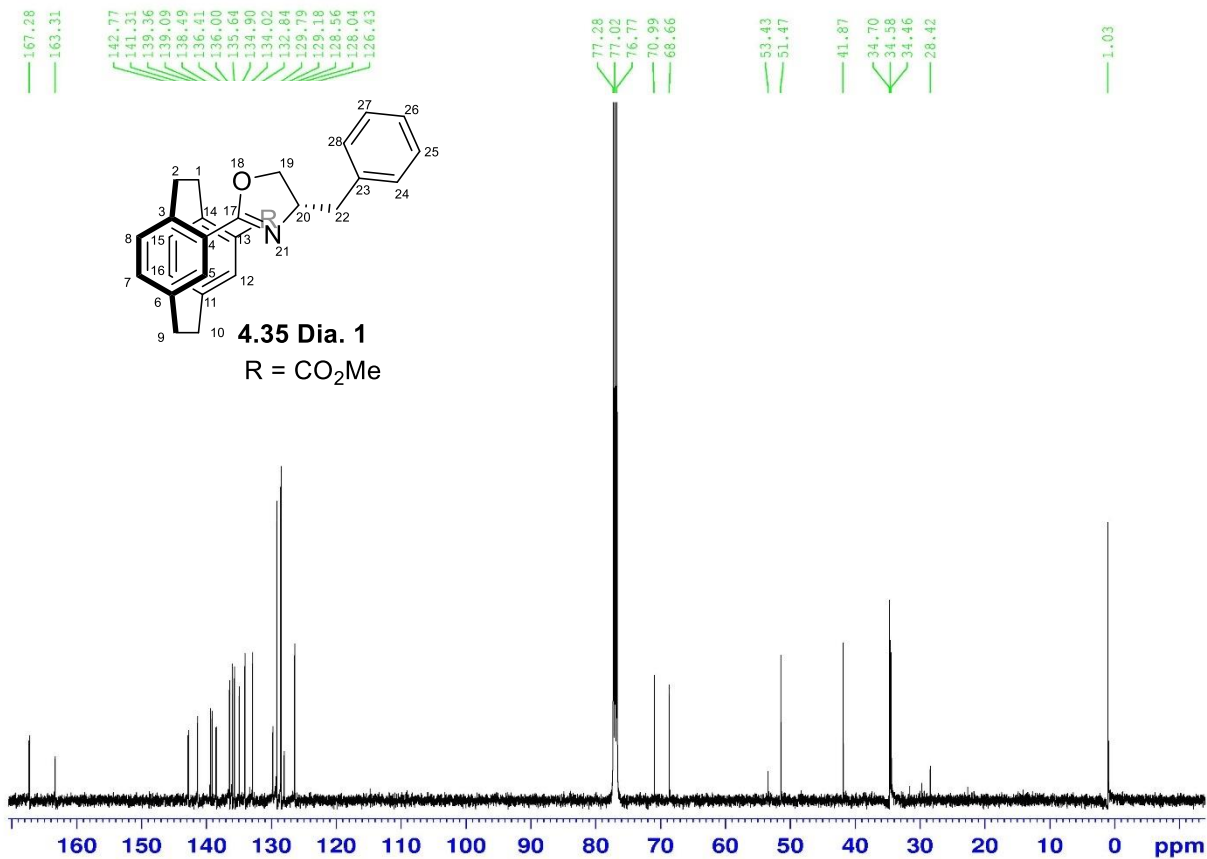
Current Data Parameters
NAME V-Mn-253 Dia 1
EXPNO 1
PROCNO 1

F2 - Acquisition Parameters
Date_ 20191020
Time 21.49
INSTRUM spect
PROBHD 5 mm Multinucl
PULPROG zg30
TD 65536
SOLVENT CDCl3
NS 16
DS 2
SWH 8278.146 Hz
FIDRES 0.126314 Hz
AQ 3.9583745 sec
RG 1625.5
DW 60.400 usec
DE 6.00 usec
TE 300.0 K
D1 1.00000000 sec
TDO 1

===== CHANNEL f1 =====
NUC1 1H
P1 10.00 usec
PL1 3.10 dB
SFO1 400.1324710 MHz

F2 - Processing parameters
SI 32768
SF 400.1300000 MHz
WDW EM
SSB 0
LB 0.30 Hz
GB 0
PC 1.00

Pseudogem CO2Me Br & Bn oxazoline : Dia 1 13C



```

Current Data Parameters
NAME      V-Mn-253 Dial
EXPNO    2
PROCNO   1

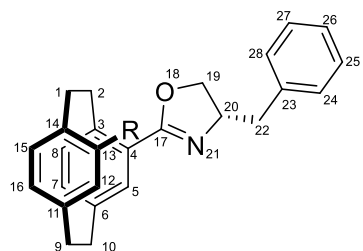
F2 - Acquisition Parameters
Date_    20191029
Time     8.19
INSTRUM  spect
PROBHD   5 mm PAQXI 1H/
PULPROG  zgpg30
TD       65536
SOLVENT  CDCl3
NS       16384
DS       4
SWH      30030.029 Hz
FIDRES   0.458222 Hz
AQ       1.0911744 sec
RG       32768
DW       16.650 usec
DE       6.50 usec
TE       296.3 K
D1       2.00000000 sec
D11      0.03000000 sec
TD0      1

===== CHANNEL f1 =====
NUC1     13C
P1       12.00 usec
PL1      -4.00 dB
PL1W     172.88230896 W
SFO1     125.7703643 MHz

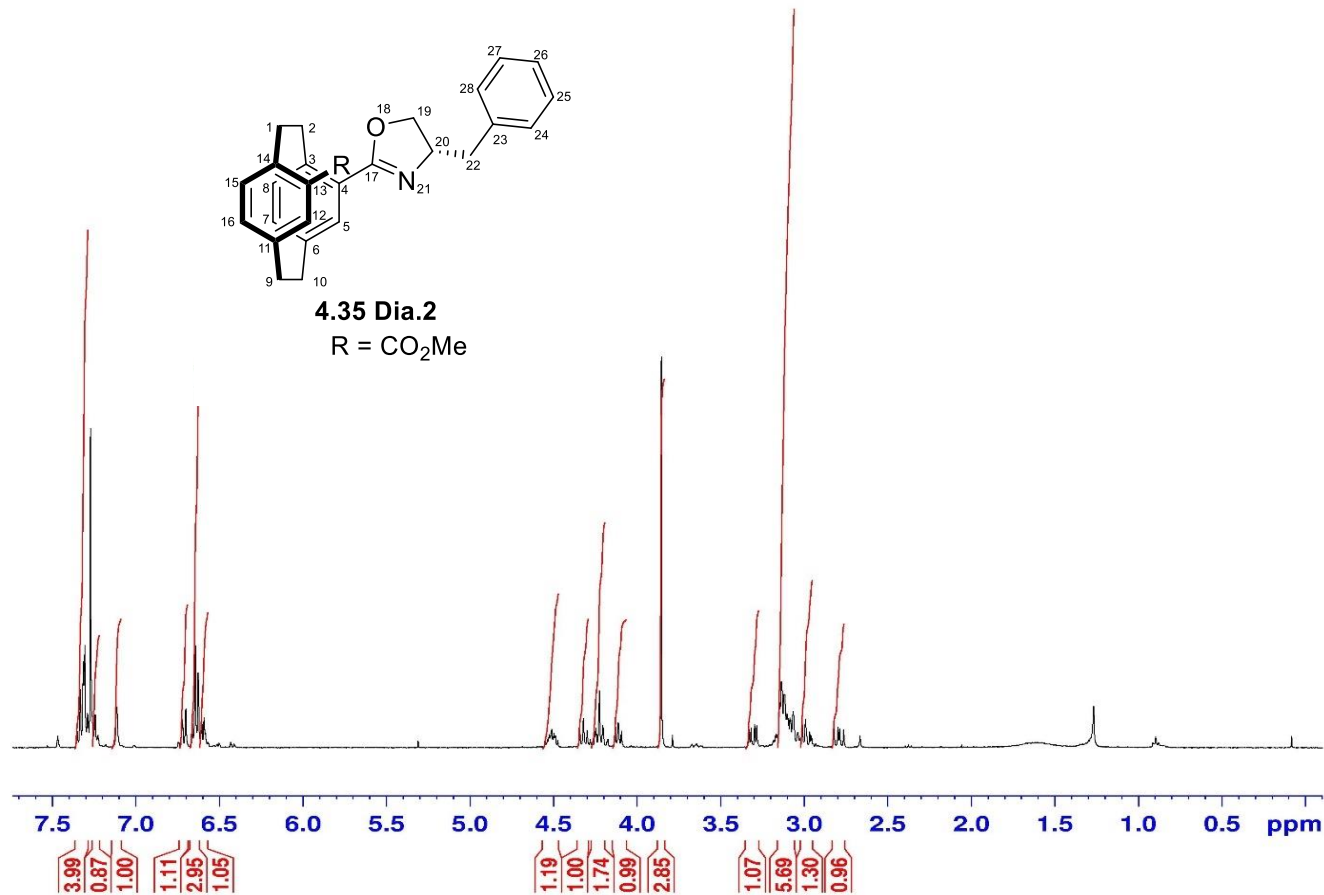
===== CHANNEL f2 =====
CPDPRG[2] waltz16
NUC2     1H
PCPD2    80.00 usec
PL2      4.00 dB
PL12     22.51 dB
PL13     25.00 dB
PL2W     12.10000038 W
PL12W    0.17052394 W
PL13W    0.09611372 W
SFO2     500.1320005 MHz

F2 - Processing parameters
SI       32768
SF       125.7577890 MHz
WDW      EM
SSB      0
LB       1.00 Hz
GB       0
PC       1.40
    
```

Pseudogem CO2Me Br & Bnoxazoline : Dia 2



4.35 Dia.2
R = CO₂Me



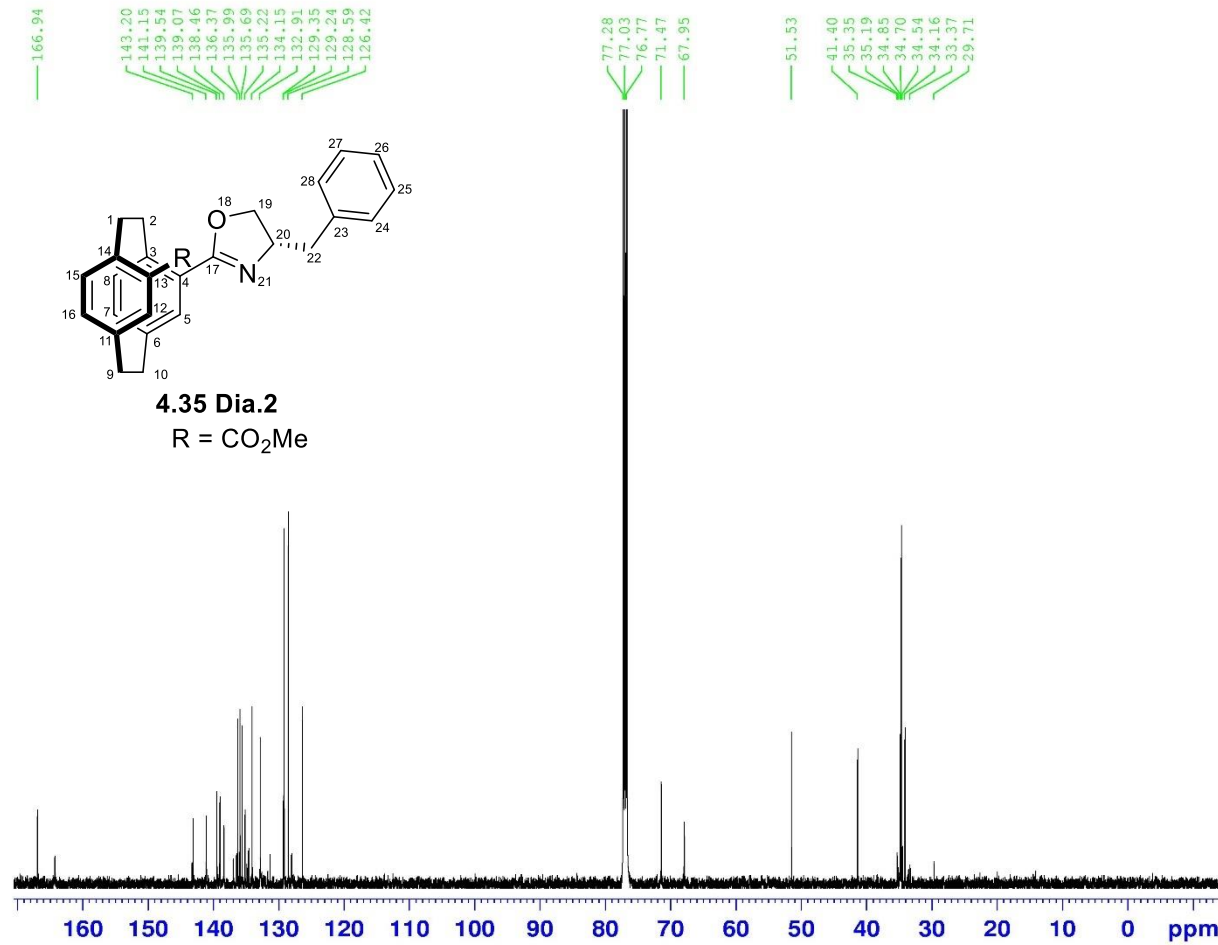
Current Data Parameters
NAME V-Mn-253 Dia 2
EXPNO 1
PROCNO 1

F2 - Acquisition Parameters
Date_ 20191020
Time 21.56
INSTRUM spect
PROBHD 5 mm Multinucl
PULPROG zg30
TD 65536
SOLVENT CDC13
NS 16
DS 2
SWH 8278.146 Hz
FIDRES 0.126314 Hz
AQ 3.9583745 sec
RG 1448.2
DW 60.400 usec
DE 6.00 usec
TE 300.0 K
D1 1.0000000 sec
TDO 1

===== CHANNEL f1 =====
NUC1 1H
P1 10.00 usec
PL1 3.10 dB
SFO1 400.1324710 MHz

F2 - Processing parameters
SI 32768
SF 400.1300000 MHz
WDW EM
SSB 0
LB 0.30 Hz
GB 0
PC 1.00

Pseudogen CO2Me Br & En oxazoline : dia2



```

Current Data Parameters
NAME      V-Mn-253 Dia2
EXPNO     2
PROCNO    1

F2 - Acquisition Parameters
Date_     20191101
Time      10.37
INSTRUM   spect
PROBHD    5 mm PAQXI 1H/
PULPROG   zgpg30
TD         65536
SOLVENT   CDCl3
NS         16384
DS         4
SWH        30030.029 Hz
FIDRES     0.458222 Hz
AQ         1.0911744 sec
RG         32768
DW         16.650 usec
DE         6.50 usec
TE         296.3 K
D1         2.00000000 sec
D11        0.03000000 sec
TD0        1

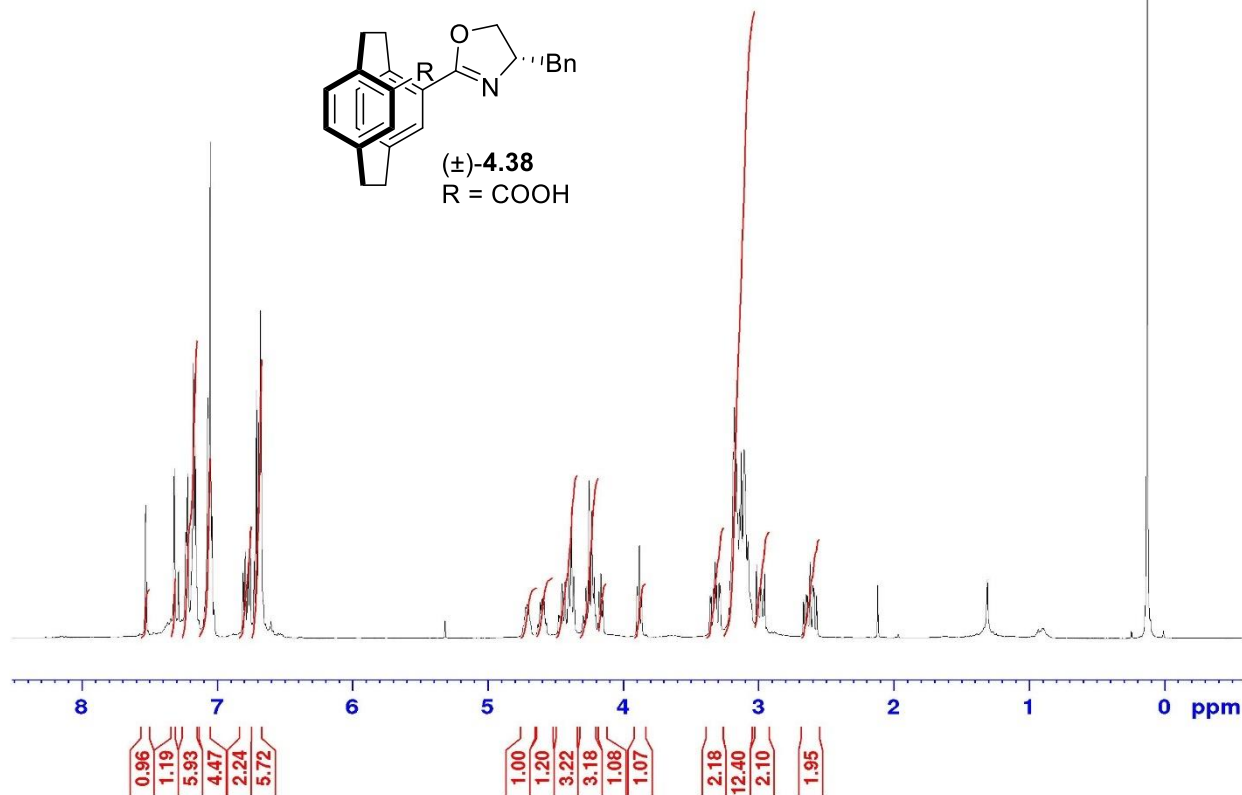
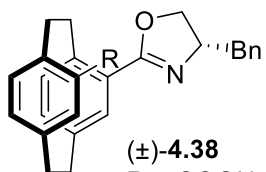
===== CHANNEL f1 =====
NUC1       13C
P1         12.00 usec
PL1        -4.00 dB
PL1W       172.88230896 W
SFO1       125.7703643 MHz

===== CHANNEL f2 =====
CPDPRG[2]  waltz16
NUC2       1H
PCPD2      80.00 usec
PL2        4.00 dB
PL12       22.51 dB
PL13       25.00 dB
PL2W       12.10000038 W
PL12W      0.17052394 W
PL13W      0.09611372 W
SFO2       500.1320005 MHz

F2 - Processing parameters
SI         32768
SF         125.7577890 MHz
WDW        EM
SSB        0
LB         1.00 Hz
GB         0
PC         1.40
    
```

Pseudogem Br COOH & Bn oxazoline

7.530
7.318
7.287
7.233
7.220
7.177
7.163
7.070
7.052
7.040
6.809
6.793
6.775
6.759
6.728
6.711
6.695
6.680
4.451
4.430
4.405
4.384
4.365
4.252
4.232
4.215
4.165
3.897
3.880
3.321
3.310
3.291
3.282
3.185
3.177
3.164
3.139
3.126
3.105
3.078
3.014
2.982
2.955
2.618
2.597
2.117
1.308
0.126



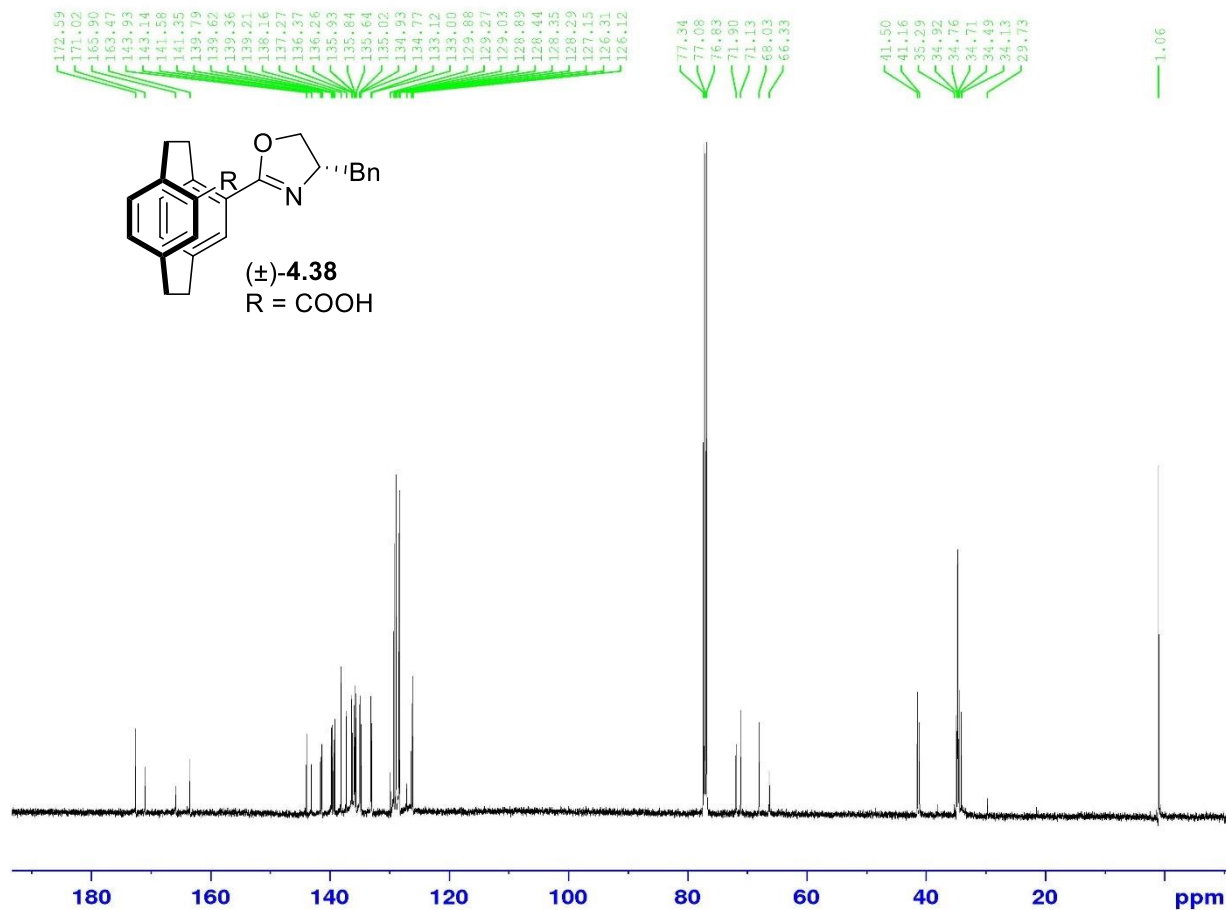
Current Data Parameters
NAME V-Mn-276 II
EXPNO 1
PROCNO 1

F2 - Acquisition Parameters
Date_ 20200815
Time 19.01
INSTRUM spect
PROBHD 5 mm PAQXI 1H/
PULPROG zg30
TD 65536
SOLVENT CDCl3
NS 16
DS 2
SWH 10330.578 Hz
FIDRES 0.157632 Hz
AQ 3.1719425 sec
RG 71.8
DW 48.400 usec
DE 6.50 usec
TE 298.2 K
D1 1.00000000 sec
TDO 1

===== CHANNEL f1 =====
NUC1 1H
P1 9.50 usec
PL1 4.00 dB
PL1W 12.10000038 W
SFO1 500.1330885 MHz

F2 - Processing parameters
SI 32768
SF 500.1300000 MHz
WDW EM
SSB 0
LB 0.30 Hz
GB 0
PC 1.00

13C : Pseudogem Br COOH & Bn oxazoline



```

Current Data Parameters
NAME      V-Mn-276  11
EXPNO    2
PROCNO   1

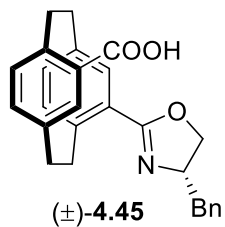
F2 - Acquisition Parameters
Date_    20200816
Time     9.25
INSTRUM  spect
PROBHD   5 mm PAQXI 1H/
PULPROG  zgpg30
TD       65536
SOLVENT  CDCl3
NS       16384
DS       4
SWH      30030.029 Hz
FIDRES   0.458222 Hz
AQ       1.0911744 sec
RG       32768
DW       16.650 usec
DE       6.50 usec
TE       298.2 K
D1       2.0000000 sec
D11      0.0300000 sec
TD0      1

===== CHANNEL f1 =====
NUC1     13C
P1       12.00 usec
PL1      -4.00 dB
PL1W     172.88230896 W
SFO1     125.7703643 MHz

===== CHANNEL f2 =====
CPDPRG2  waltz16
NUC2     1H
PCPD2    80.00 usec
PL2       4.00 dB
PL12     22.51 dB
PL13     25.00 dB
PL2W     12.10000038 W
PL12W    0.17052394 W
PL13W    0.09611372 W
SFO2     500.1320005 MHz

F2 - Processing parameters
SI       32768
SF       125.7577690 MHz
WDW      EM
SSB      0
LR       1.00 Hz
CB       0
PC       1.40
    
```

Pseudoortho Br COOH & Bn oxazoline

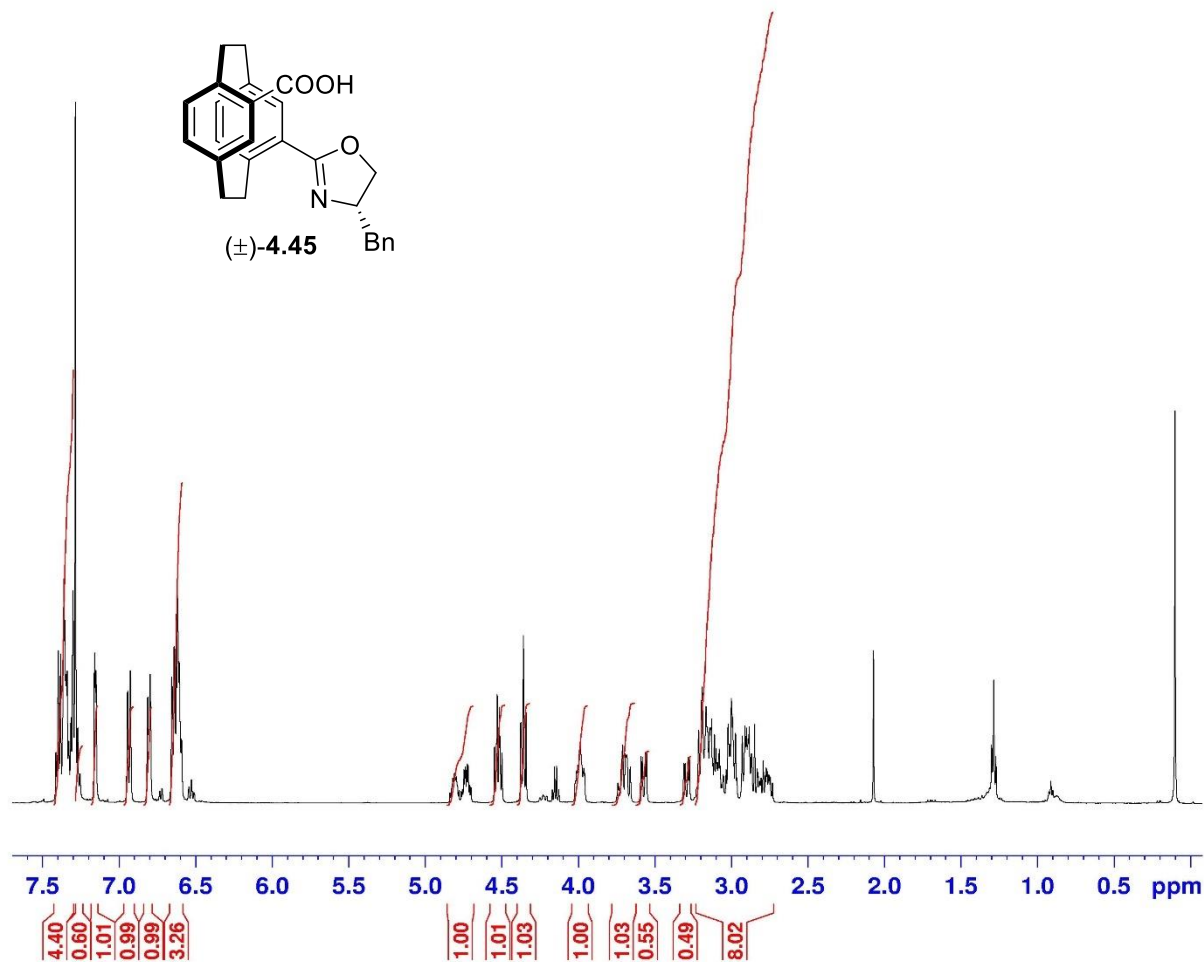


Current Data Parameters
NAME VI-Mn-56 ii
EXPNO 1
PROCNO 1

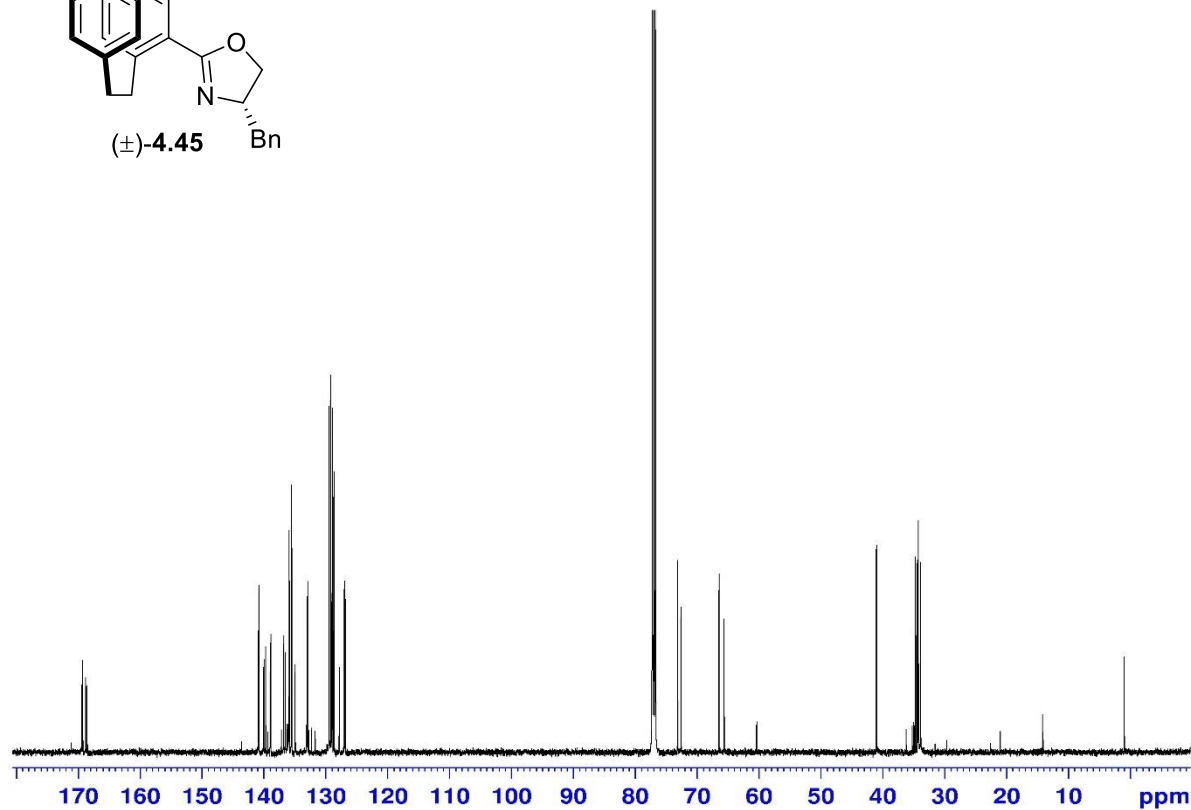
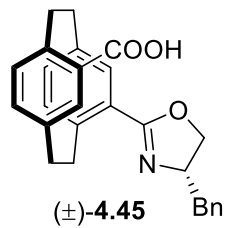
F2 - Acquisition Parameters
Date_ 20200206
Time 19.05
INSTRUM spect
PROBHD 5 mm PAQXI 1H/
PULPROG zg30
TD 65536
SOLVENT CDC13
NS 16
DS 2
SWH 10330.578 Hz
FIDRES 0.157632 Hz
AQ 3.1719425 sec
RG 71.8
DW 48.400 usec
DE 6.50 usec
TE 298.2 K
D1 1.00000000 sec
TD0 1

===== CHANNEL f1 =====
NUC1 1H
P1 9.50 usec
PL1 4.00 dB
PL1W 12.10000038 W
SFO1 500.1330885 MHz

F2 - Processing parameters
SI 32768
SF 500.1300000 MHz
WDW EM
SSB 0
LB 0.30 Hz
GB 0
PC 1.00



13C : Pseudoortho Br COOH & Bn oxazoline



```
Current Data Parameters
NAME      VI-Mn-56 ii
EXPNO     2
PROCNO    1

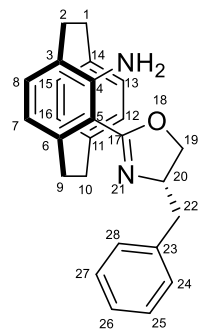
F2 - Acquisition Parameters
Date_     20200207
Time      9.30
INSTRUM   spect
PROBHD    5 mm PAQXI 1H/
PULPROG   zgpg30
TD         65536
SOLVENT   CDCl3
NS         16384
DS         4
SWH        30030.029 Hz
FIDRES     0.458222 Hz
AQ         1.0911744 sec
RG         32768
DW         16.650 usec
DE         6.50 usec
TE         298.2 K
D1         2.00000000 sec
D11        0.03000000 sec
TD0        1

===== CHANNEL f1 =====
NUC1       13C
P1         12.00 usec
PL1        -4.00 dB
PL1W       172.88230896 W
SFO1       125.7703643 MHz

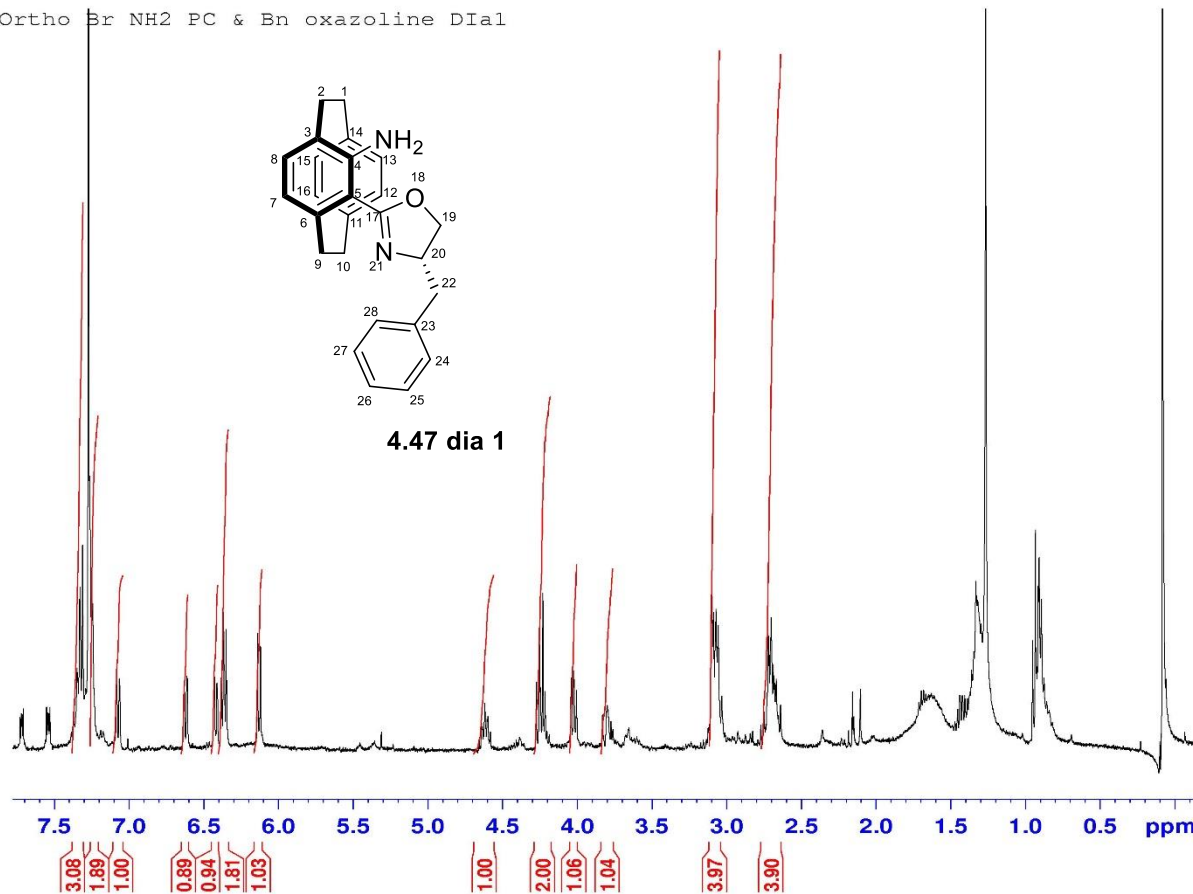
===== CHANNEL f2 =====
CPDPRG[2] waltz16
NUC2       1H
PCPD2      80.00 usec
PL2        4.00 dB
PL12       22.51 dB
PL13       25.00 dB
PL2W       12.10000038 W
PL12W      0.17052394 W
PL13W      0.09611372 W
SFO2       500.1320005 MHz

F2 - Processing parameters
SI         32768
SF         125.7577890 MHz
WDW        EM
SSB        0
LB         1.00 Hz
GB         0
PC         1.40
```

Ortho Br NH2 PC & Bn oxazoline Dial



4.47 dia 1



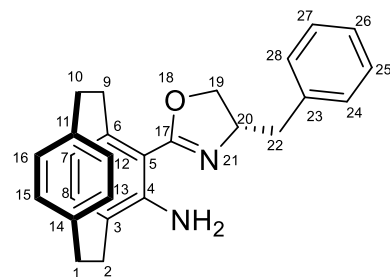
Current Data Parameters
NAME V-Mn-290 i
EXPNO 2
PROCNO 1

F2 - Acquisition Parameters
Date_ 20191130
Time 21.52
INSTRUM spect
PROBHD 5 mm Multinucl
PULPROG zg30
TD 65536
SOLVENT CDC13
NS 2048
DS 2
SWH 8278.146 Hz
FIDRES 0.126314 Hz
AQ 3.9583745 sec
RG 2580.3
DW 60.400 usec
DE 6.00 usec
TE 300.0 K
D1 1.00000000 sec
TD0 1

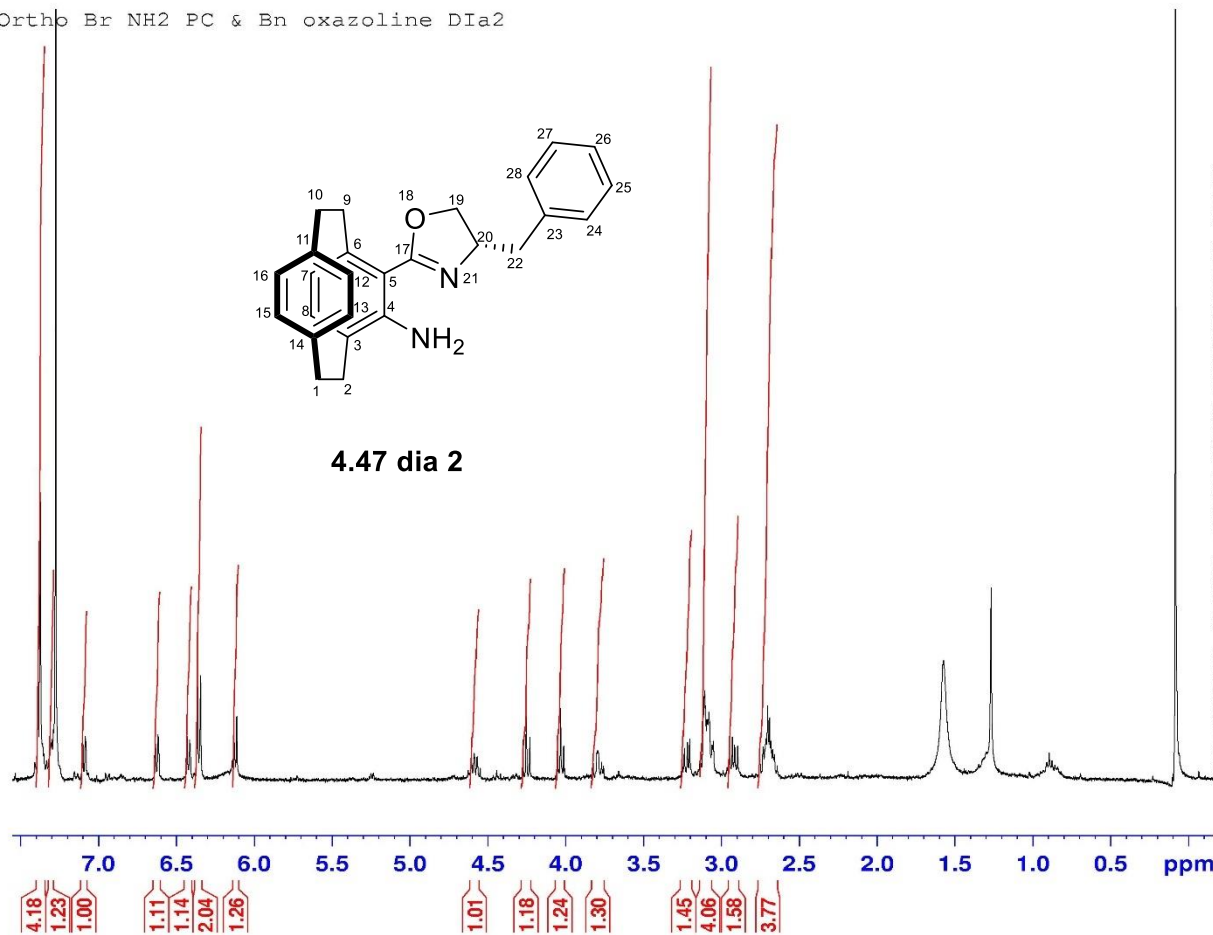
===== CHANNEL f1 =====
NUC1 1H
P1 10.00 usec
PL1 3.10 dB
SFO1 400.1324710 MHz

F2 - Processing parameters
SI 32768
SF 400.1300000 MHz
WDW EM
SSB 0
LB 0.30 Hz
GB 0
PC 1.00

Ortho Br NH2 PC & Bn oxazoline DIa2



4.47 dia 2

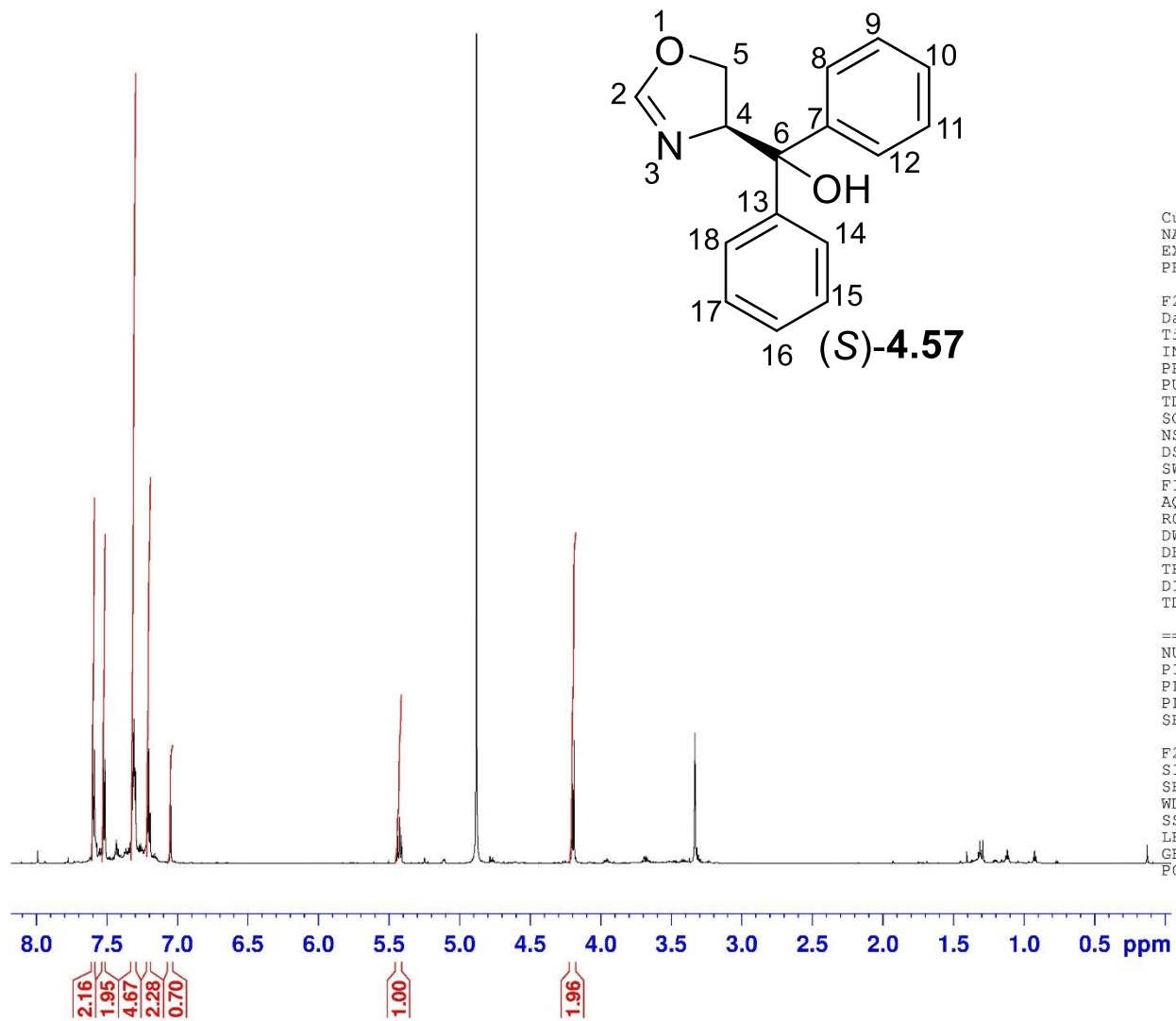


Current Data Parameters
NAME V-Mn-290 ii
EXPNO 2
PROCNO 1

F2 - Acquisition Parameters
Date_ 20191130
Time_ 18.20
INSTRUM spect
PROBHD 5 mm Multinucl
PULPROG zg30
TD 65536
SOLVENT CDCl3
NS 1024
DS 2
SWH 8278.146 Hz
FIDRES 0.126314 Hz
AQ 3.9583745 sec
RG 5160.6
DW 60.400 usec
DE 6.00 usec
TE 300.0 K
D1 1.00000000 sec
TD0 1

===== CHANNEL f1 =====
NUC1 1H
P1 10.00 usec
PL1 3.10 dB
SFO1 400.1324710 MHz

F2 - Processing parameters
SI 32768
SF 400.1300000 MHz
WDW EM
SSB 0
LB 0.30 Hz
GB 0
PC 1.00

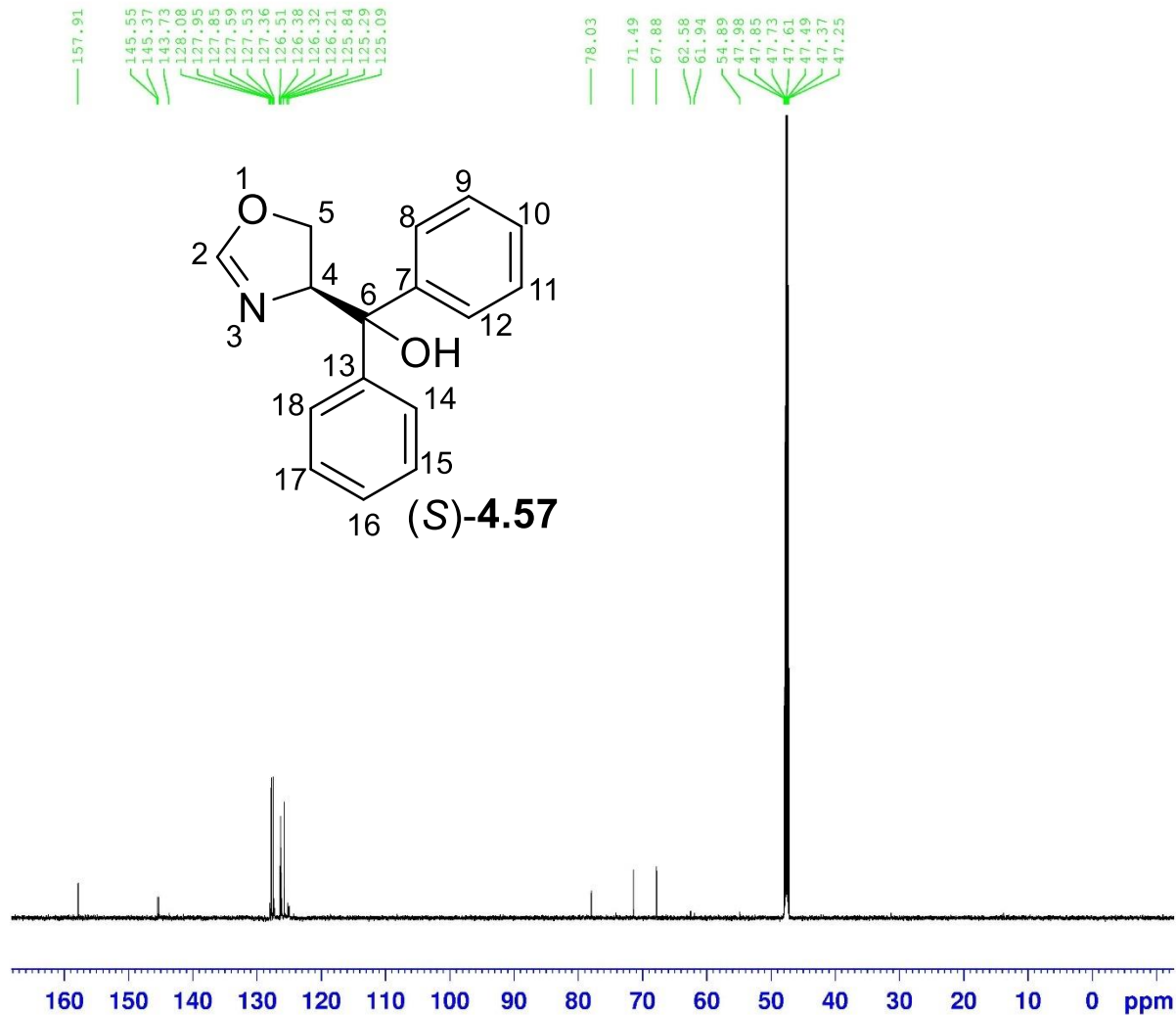


Current Data Parameters
 NAME maulik_V_mn_226
 EXPNO 1
 PROCNO 1

F2 - Acquisition Parameters
 Date_ 20191004
 Time 12.29
 INSTRUM spect
 PROBHD 5 mm CPTCI 1H-
 PULPROG zg30
 TD 65536
 SOLVENT MeOD
 NS 4
 DS 2
 SWH 14492.754 Hz
 FIDRES 0.221142 Hz
 AQ 2.2609921 sec
 RG 35.9
 DW 34.500 usec
 DE 6.50 usec
 TE 298.0 K
 D1 1.00000000 sec
 TD0 1

===== CHANNEL f1 =====
 NUC1 1H
 P1 10.00 usec
 PL1 6.90 dB
 PL1W 10.71880245 W
 SFO1 700.1343236 MHz

F2 - Processing parameters
 SI 32768
 SF 700.1300000 MHz
 WDW EM
 SSB 0
 LB 0.30 Hz
 GB 0
 PC 1.00



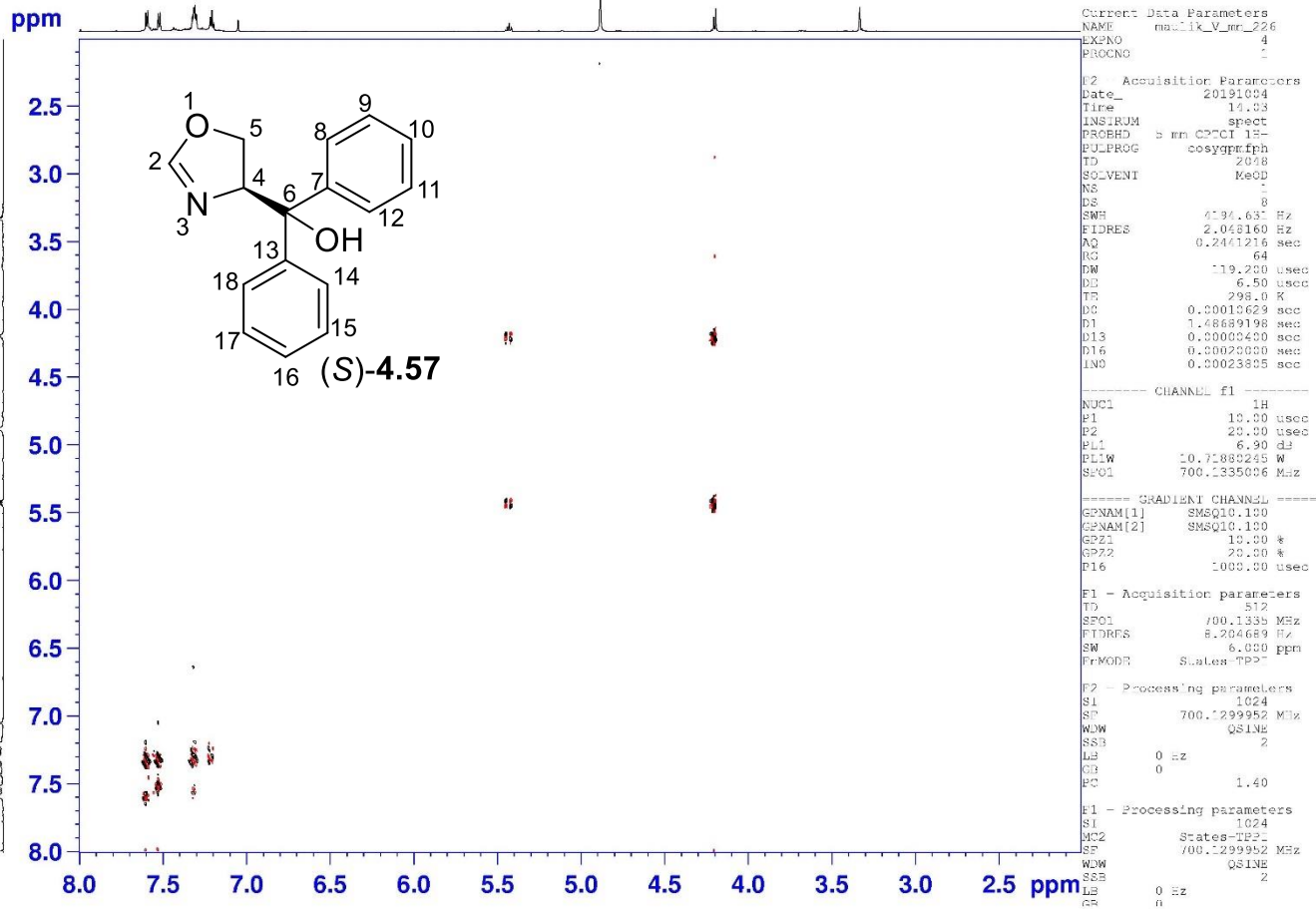
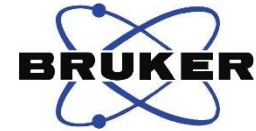
Current Data Parameters
NAME maulik_V_mn_226
EXPNO 2
PROCNO 1

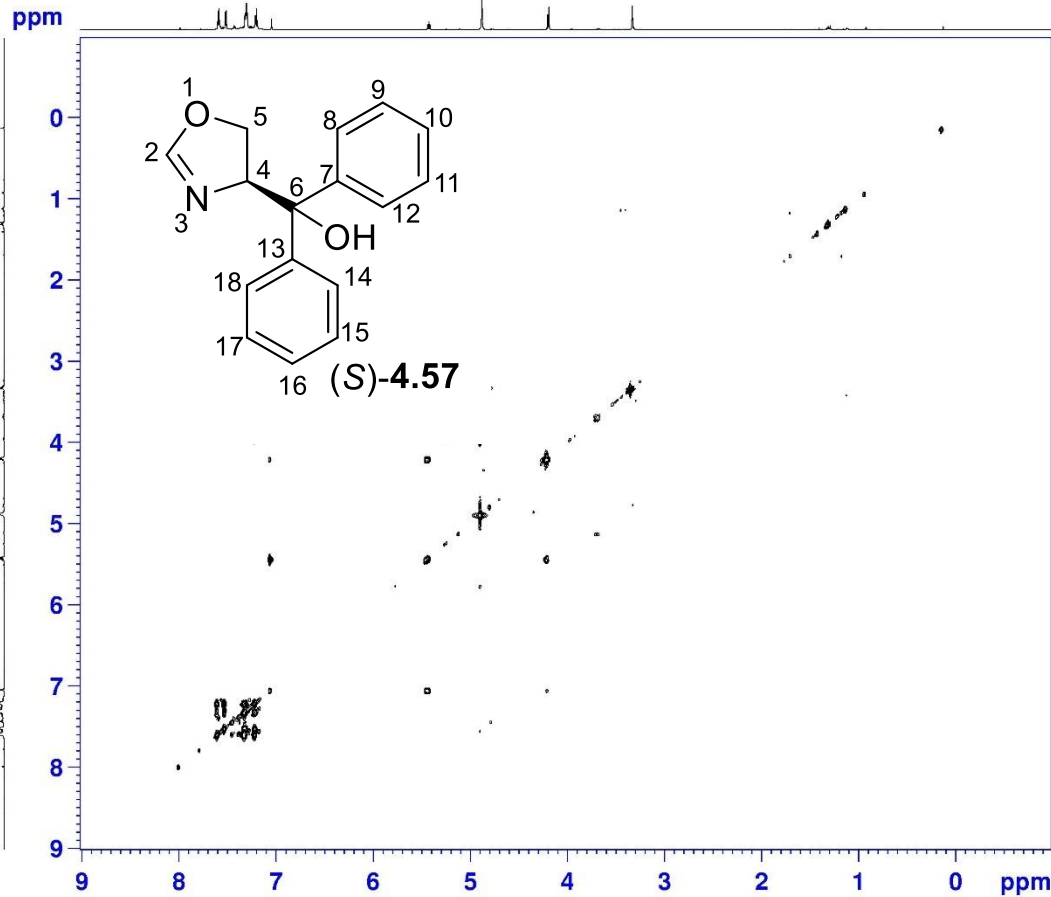
F2 - Acquisition Parameters
Date_ 20191004
Time 13.01
INSTRUM spect
PROBHD 5 mm CPTCI 1H-
PULPROG zgpg30
TD 65536
SOLVENT MeOD
NS 512
DS 4
SWH 42016.809 Hz
FIDRES 0.641126 Hz
AQ 0.7798784 sec
RG 32768
DW 11.900 usec
DE 6.50 usec
TE 298.1 K
D1 2.00000000 sec
D11 0.03000000 sec
TD0 1

===== CHANNEL f1 =====
NUC1 13C
P1 13.00 usec
PL1 -2.60 dB
PL1W 164.55174255 W
SFO1 176.0654333 MHz

===== CHANNEL f2 =====
CPDPRG[2] waltz16
NUC2 1H
PCPD2 80.00 usec
PL2 6.90 dB
PL12 24.96 dB
PL13 19.50 dB
PL2W 10.71880245 W
PL12W 0.16755076 W
PL13W 0.58904201 W
SFO2 700.1328005 MHz

F2 - Processing parameters
SI 32768
SF 176.0478290 MHz
WDW EM
SSB 0
LB 1.00 Hz
GB 0
PC 1.40





Current Data Parameters
NAME maulik_v_mn_226
EXPNO 3
PROCNO 1

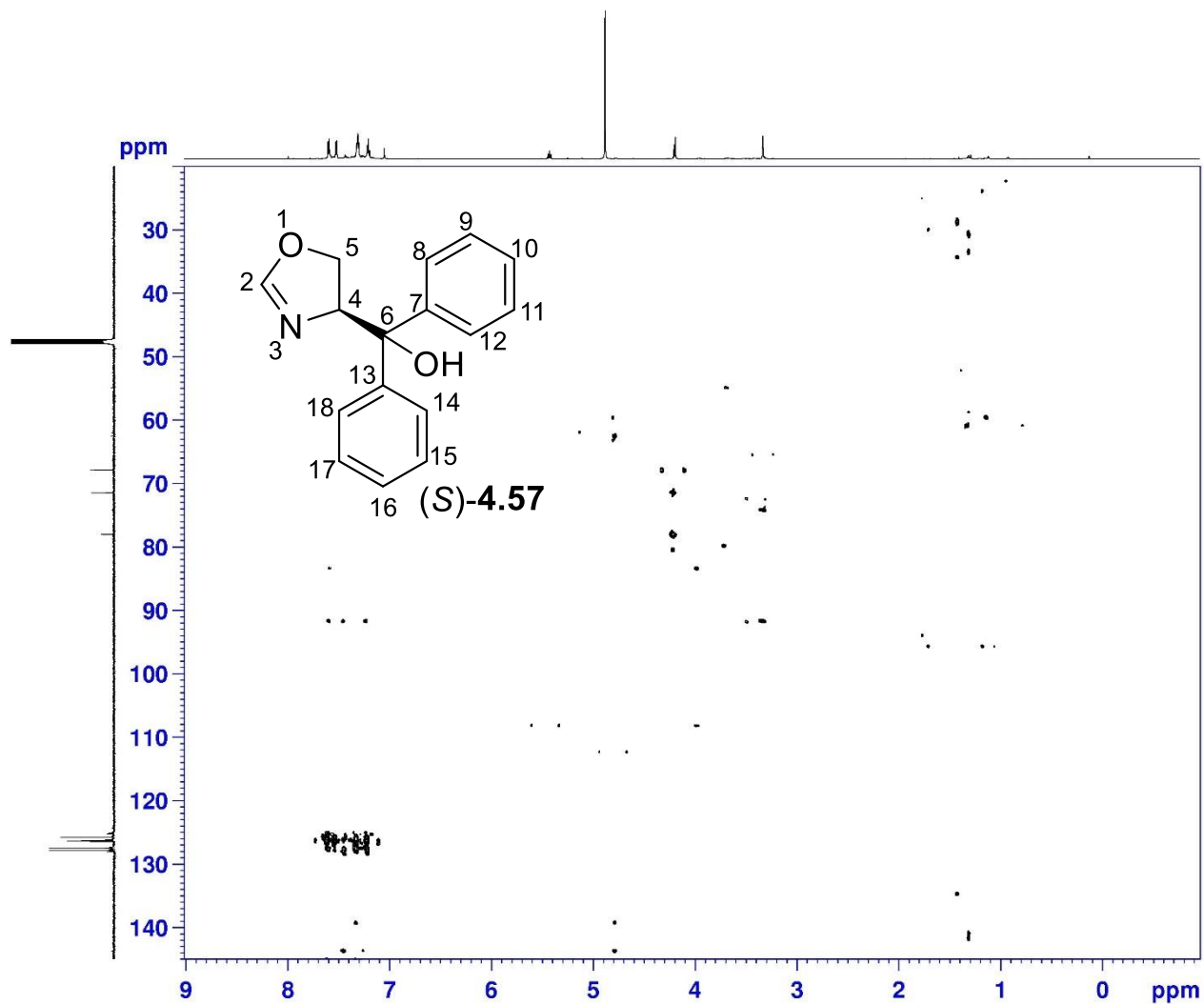
F2 - Acquisition Parameters
Date_ 20191004
Time 13.02
INSTRUM spect
PROBHD 5 mm CPTCI 1H-
PULPROG cosyldrqf
TD 2048
SOLVENT MeOD
NS 4
DS 16
SWH 7002.801 Hz
FIDRES 3.419337 Hz
AQ 0.1462272 sec
RG 512
DW 71.400 usec
DE 6.50 usec
TE 298.1 K
D0 0.0000300 sec
D1 1.5000000 sec
D6 0.2000000 sec
IN0 0.00014285 sec

==== CHANNEL f1 =====
NUC1 1H
P1 10.00 usec
PL1 6.90 dB
PL1W 10.71880245 W
SFO1 700.1328005 MHz

F1 - Acquisition parameters
TD 434
SFO1 700.1328 MHz
FIDRES 16.132092 Hz
SW 10.000 ppm
F1MODE QF

F2 - Processing parameters
SI 1024
SF 700.1299886 MHz
WDW SINE
SSB 0
LB 0 Hz
GB 0
PC 1.40

F1 - Processing parameters
SI 1024
MC2 QF
SF 700.1299886 MHz
WDW SINE
SSB 0
LB 0 Hz
GB 0



Current Data Parameters
NAME msulik_V_m_226
EXPNO 7
PROCNO 1

F2 - Acquisition Parameters
Date_ 201104
Time 21.12
INSTRUM spect
PROBHD 5 mm CPIC 1H-
PULPROG hmcgcp1p00g
TD 6536
SOLVENT MeOD
NS 16
DS 16
SWH 7002.801 Hz
FIDRES 1.703668 Hz
AQ 0.292054 sec
RG 236
RW 71.400 usec
CF 6.50 usec
TE 298.0 K
CNS12 145.000000
CNS13 8.000000
D0 0.0000300 sec
D1 1.5000000 sec
D2 0.30344828 sec
D6 0.0620000 sec
D16 0.0002000 sec
RG 0.50001775 sec

==== CHANNEL f1 =====
NUC1 1H
P1 10.00 usec
P2 20.00 usec
PL1 6.90 dB
PL12 10.71880745 W
SFO1 700.1326000 MHz

==== CHANNEL f2 =====
NUC2 13C
P3 13.00 usec
PL2 -2.60 dB
PL2W 166.95274250 W
SFO2 176.0643358 MHz

==== GRADIENT CHANNELS =====
GPNAM[1] SMSQ0.100
GPNAM[2] SMSQ0.100
GPNAM[3] SMSQ0.100
CP21 30.00 %
CP22 30.00 %
CP23 40.00 %
PL6 1000.00 usec

F1 - Acquisition parameters
ID S12
SFO1 176.0654 MHz
FIDRES 95.020547 Hz
SW 160.000 ppm
FREQCZ QF

F2 - Processing parameters
SI 2048
SF 700.1299889 MHz
WVW SINE
SFB C
LB C Hz
GB C
PC 1.40

F1 - Processing parameters
SI 1024
KQZ QF
SF 176.0478250 MHz
WVW SINE
SFB C
LB C Hz
CB C



Current Data Parameters
NAME: nraulik_v_mn_226
EXPNO: 6
PROCNO: 1

F2 - Acquisition Parameters
Date_: 20191004
Time: 16.15
INSTRUM: spect
PROBHD: 5 mm QNP1H-
PULPROG: noesygpph
TD: 2648
SOLVENT: MeOD
NS: 16
DS: 16
SWH: 7002.801 Hz
FIDRES: 3.419337 Hz
AQ: 0.1462272 sec
RG: 256
DW: 71.400 usec
DE: 6.50 usec
TE: 298.0 K
D0: 0.0005868 sec
D1: 1.5000000 sec
D8: 0.3000000 sec
D16: 0.0002000 sec
LNG: 0.00014285 sec

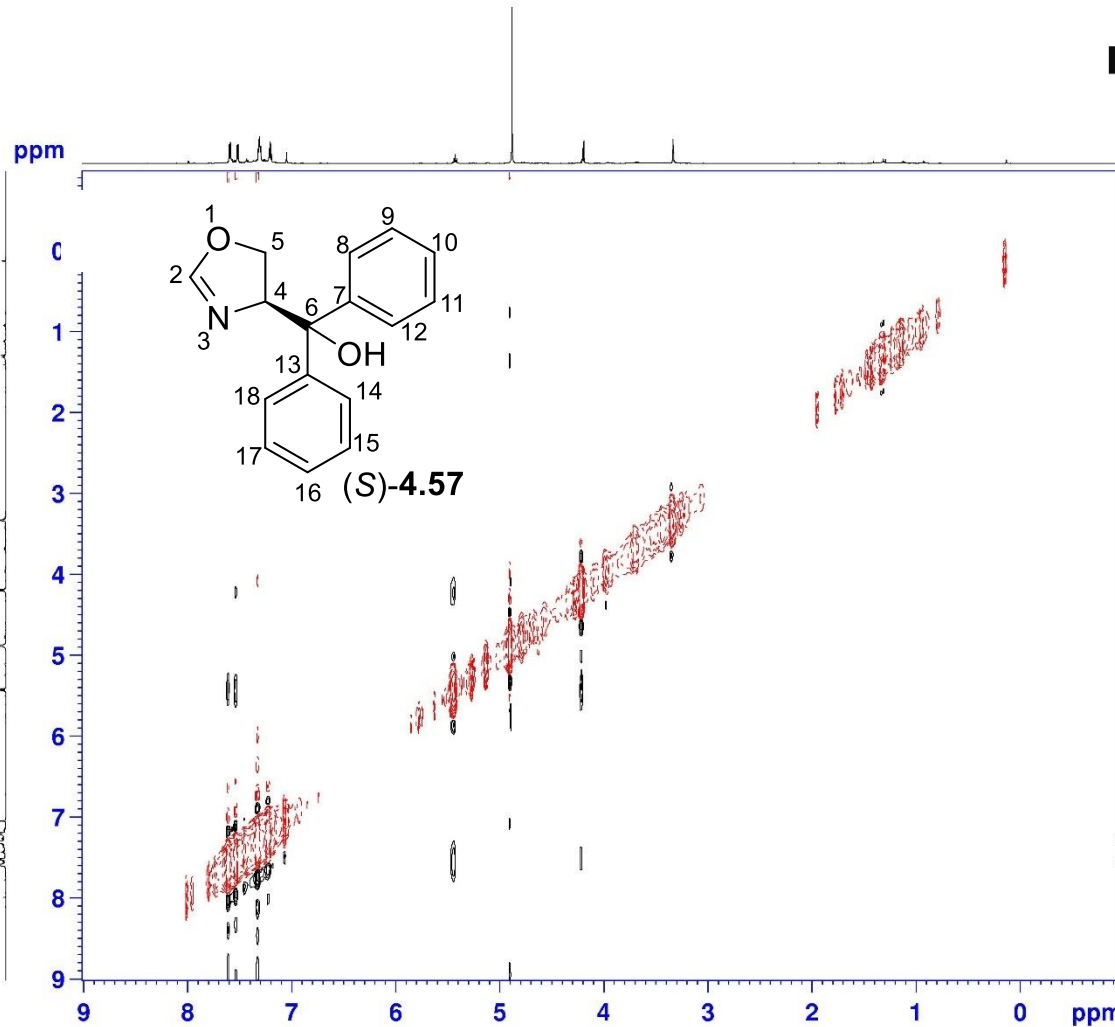
----- CHANNEL f1 -----
NUC1: 1H
P1: 10.00 usec
P2: 20.00 usec
PL1: 6.90 dB
PL1W: 10.71889245 W
SFO1: 700.1328005 MHz

----- GRADIENT CHANNEL -----
GPNAM[1]: SMSQ10.100
GP21: 40.00 %
P16: 1000.00 usec

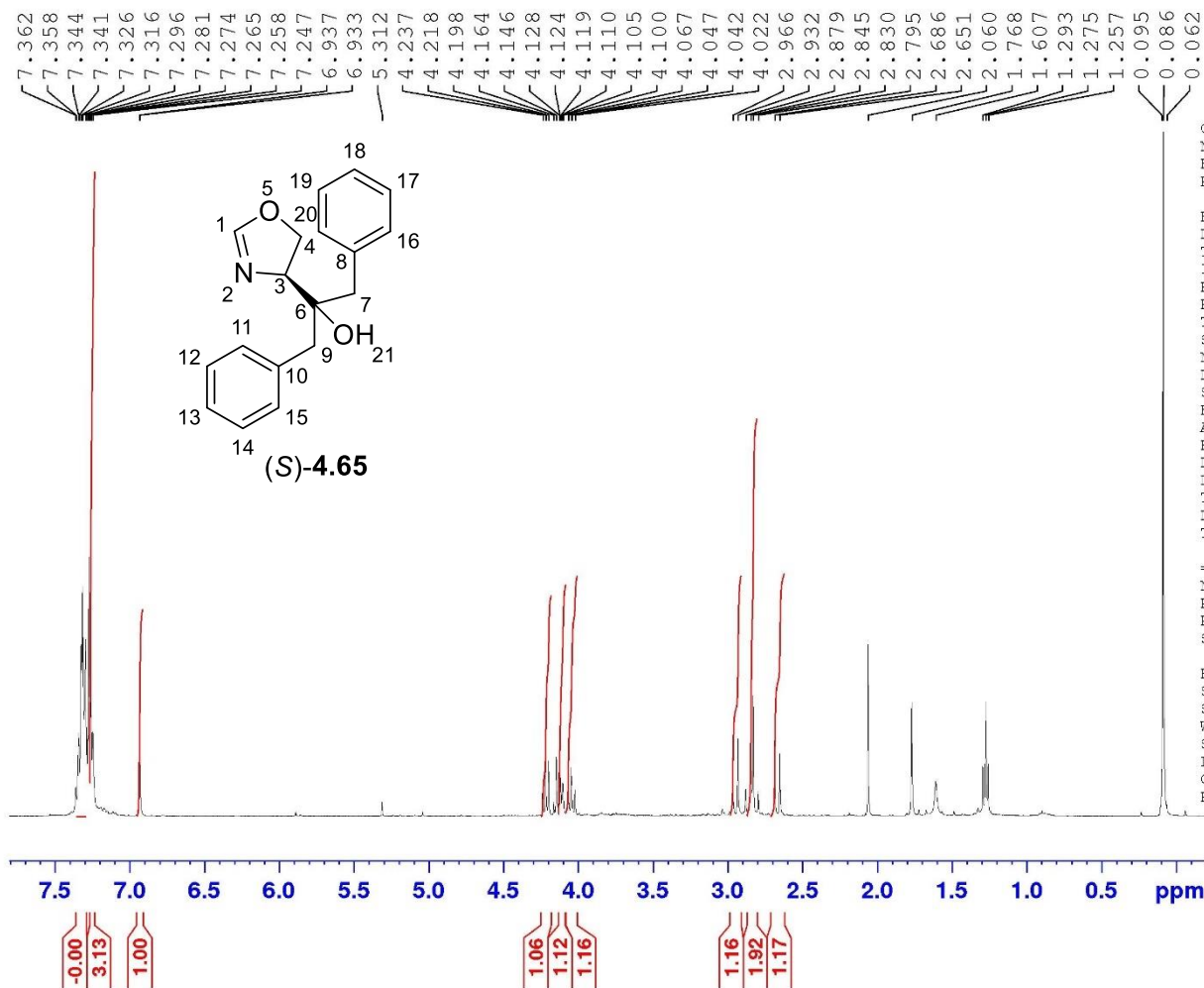
F1 - Acquisition parameters
TD: 312
SFO1: 700.1328 MHz
FIDRES: 13.674469 Hz
SW: 10.000 ppm
FRMODE: States-TPPI

F2 - Processing parameters
SI: 3274
SF: 700.1239886 MHz
WDW: QSINE
SSB: 2
LB: 0 Hz
GB: 0
PC: 1.40

F1 - Processing parameters
SI: 1024
MC2: States-TPPI
SF: 700.1239886 MHz
WDW: QSINE
SSB: 2
LB: 0 Hz
GB: 0



Grignard : Bn oxazoline : Pure aminoalcohol



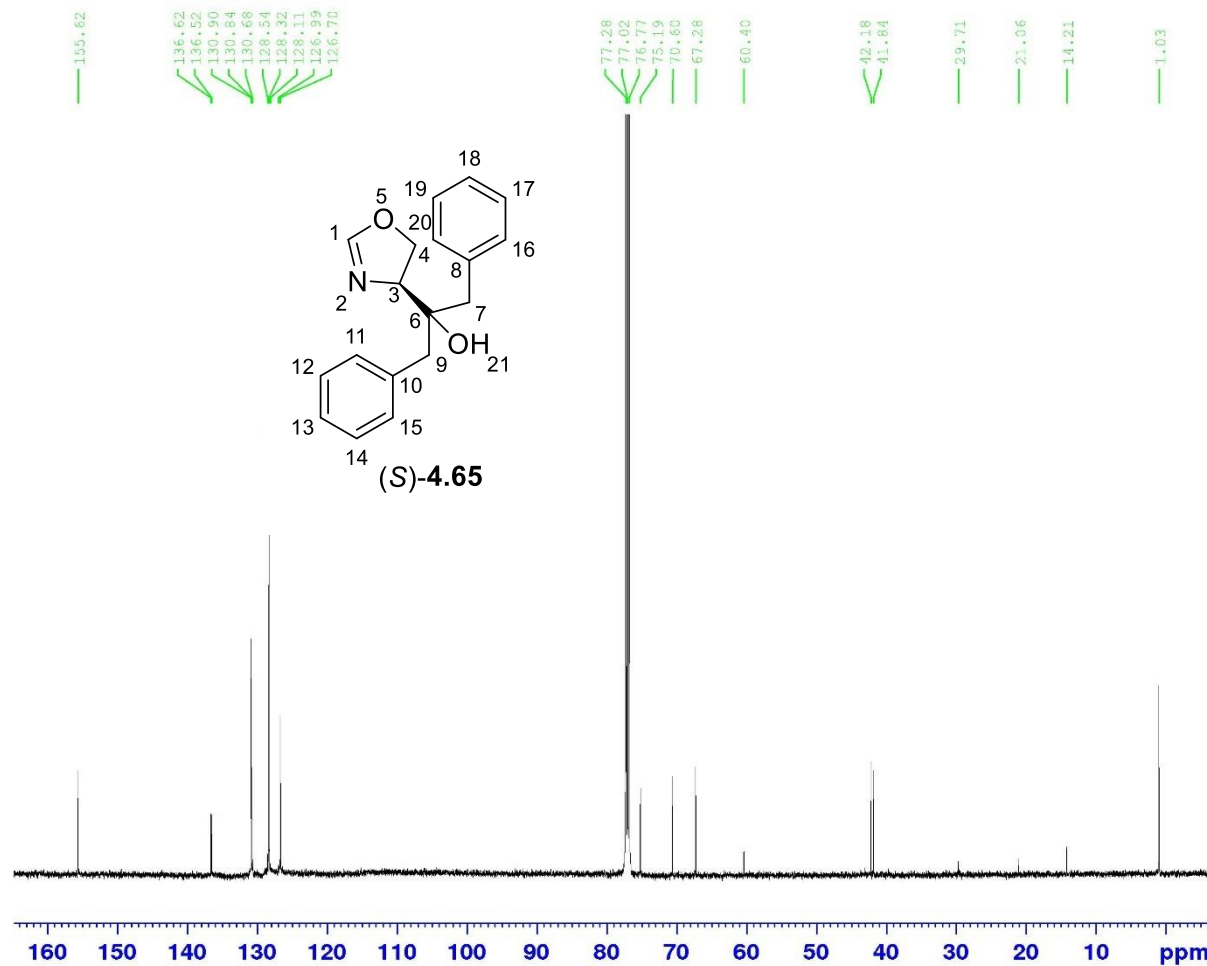
Current Data Parameters
 NAME V-Mn-293 i
 EXPNO 1
 PROCNO 1

F2 - Acquisition Parameters
 Date_ 20191129
 Time 13.29
 INSTRUM spect
 PROBHD 5 mm Multinuel
 PULPROG zg30
 TD 65536
 SOLVENT CDC13
 NS 16
 DS 2
 SWH 8278.146 Hz
 FIDRES 0.126314 Hz
 AQ 3.9583745 sec
 RG 203.2
 DW 60.400 usec
 DE 6.00 usec
 TE 300.0 K
 D1 1.00000000 sec
 TD0 1

===== CHANNEL f1 =====
 NUC1 1H
 P1 10.00 usec
 PL1 3.10 dB
 SF01 400.1324710 MHz

F2 - Processing parameters
 SI 32768
 SF 400.1300000 MHz
 WDW EM
 SSB 0
 LB 0.30 Hz
 GB 0
 PC 1.00

13C : Grignard: Bn oxazoline



Current Data Parameters
 NAME V-Mn-293 i
 EXPNO 2
 PROCNO 1

F2 - Acquisition Parameters
 Date_ 20191130
 Time 8.45
 INSTRUM spect
 PROBHD 5 mm PAQXI 1H/
 PULPROG zgpg30
 TD 65536
 SOLVENT CDCl3
 NS 16384
 DS 4
 SWH 30030.029 Hz
 FIDRES 0.458222 Hz
 AQ 1.0911744 sec
 RG 32768
 DW 16.650 usec
 DE 6.50 usec
 TE 297.4 K
 D1 2.00000000 sec
 D11 0.03000000 sec
 TD0 1

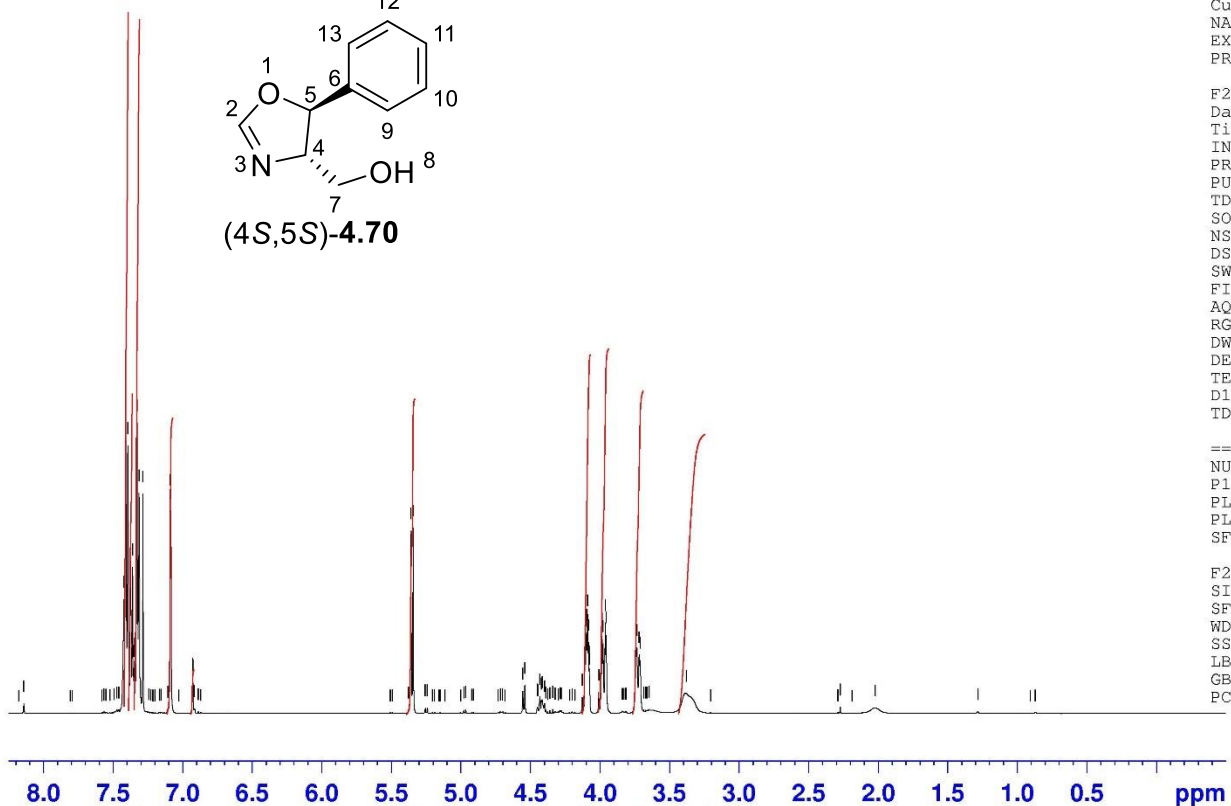
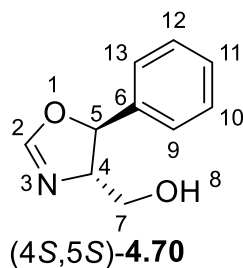
----- CHANNEL f1 -----
 NUC1 13C
 P1 12.00 usec
 PL1 4.00 dB
 PL1W 172.88230896 W
 SFO1 125.7703643 MHz

----- CHANNEL f2 -----
 CPDPRG[2] waltz16
 NUC2 1H
 PCPD2 80.00 usec
 PL2 4.00 dB
 PL12 22.51 dB
 PL13 25.00 dB
 PL2W 12.10000038 W
 PL12W 0.17052394 W
 PL13W 0.09611372 W
 SFO2 500.1320005 MHz

F2 - Processing parameters
 SI 32768
 SF 125.7577890 MHz
 WDW EM
 SSB 0
 LB 1.00 Hz
 GB 0
 PC 1.40

oxazoline : Phenyl CH2OH

7.424
7.420
7.410
7.395
7.376
7.366
7.361
7.355
7.350
7.347
7.331
7.329
7.315
7.287
7.089
7.085
6.930
6.927
5.359
5.344
4.555
4.540
4.432
4.421
4.417
4.127
4.109
4.105
4.101
4.097
4.093
4.090
4.086
4.082
4.078
4.074
4.010
4.010
3.992
3.986
3.979
3.962
3.955
3.742
3.735
3.719
3.712
3.379



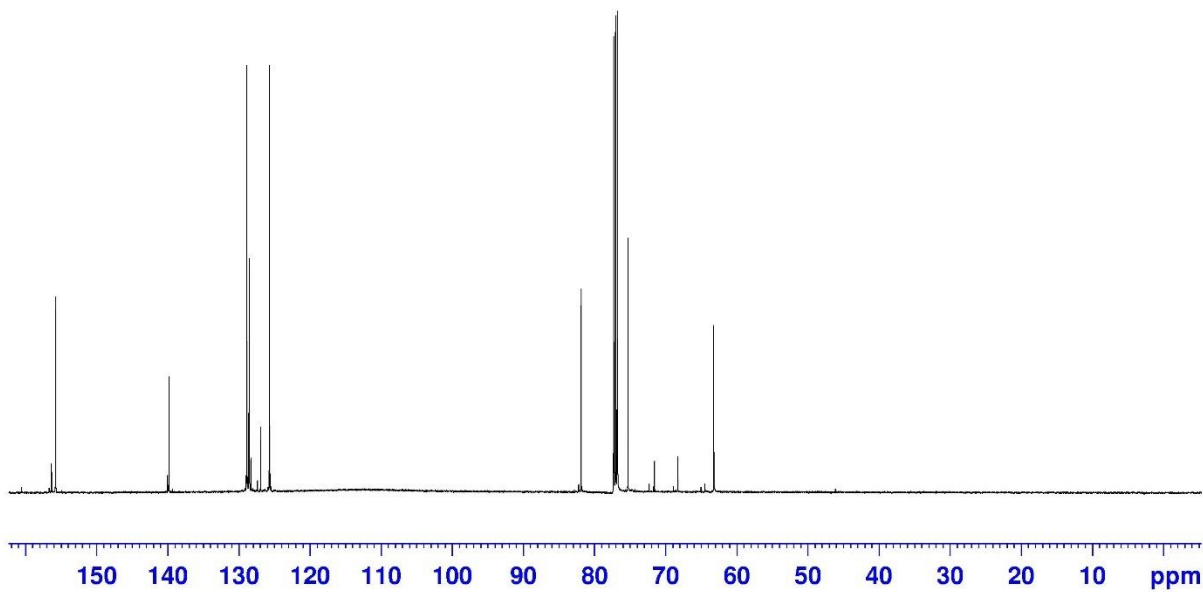
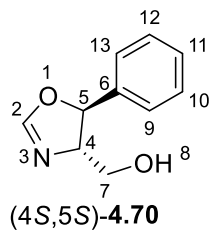
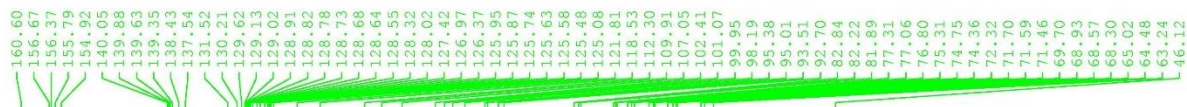
Current Data Parameters
 NAME VI-Mn-05 i
 EXPNO 1
 PROCNO 1

F2 - Acquisition Parameters
 Date_ 20191216
 Time 18.54
 INSTRUM spect
 PROBHD 5 mm PAQXI 1H/
 PULPROG zg30
 TD 65536
 SOLVENT CDCl3
 NS 16
 DS 2
 SWH 10330.578 Hz
 FIDRES 0.157632 Hz
 AQ 3.1719425 sec
 RG 71.8
 DW 48.400 usec
 DE 6.50 usec
 TE 298.3 K
 D1 1.00000000 sec
 TD0 1

===== CHANNEL f1 =====
 NUC1 1H
 P1 9.50 usec
 PL1 4.00 dB
 PL1W 12.10000038 W
 SFO1 500.1330885 MHz

F2 - Processing parameters
 SI 32768
 SF 500.1300000 MHz
 WDW EM
 SSB 0
 LB 0.30 Hz
 GB 0
 PC 1.00

13C : oxazoline : Phenyl CH2OH



Current Data Parameters
 NAME VI-Mn-05 i
 EXPNO 2
 PROCNO 1

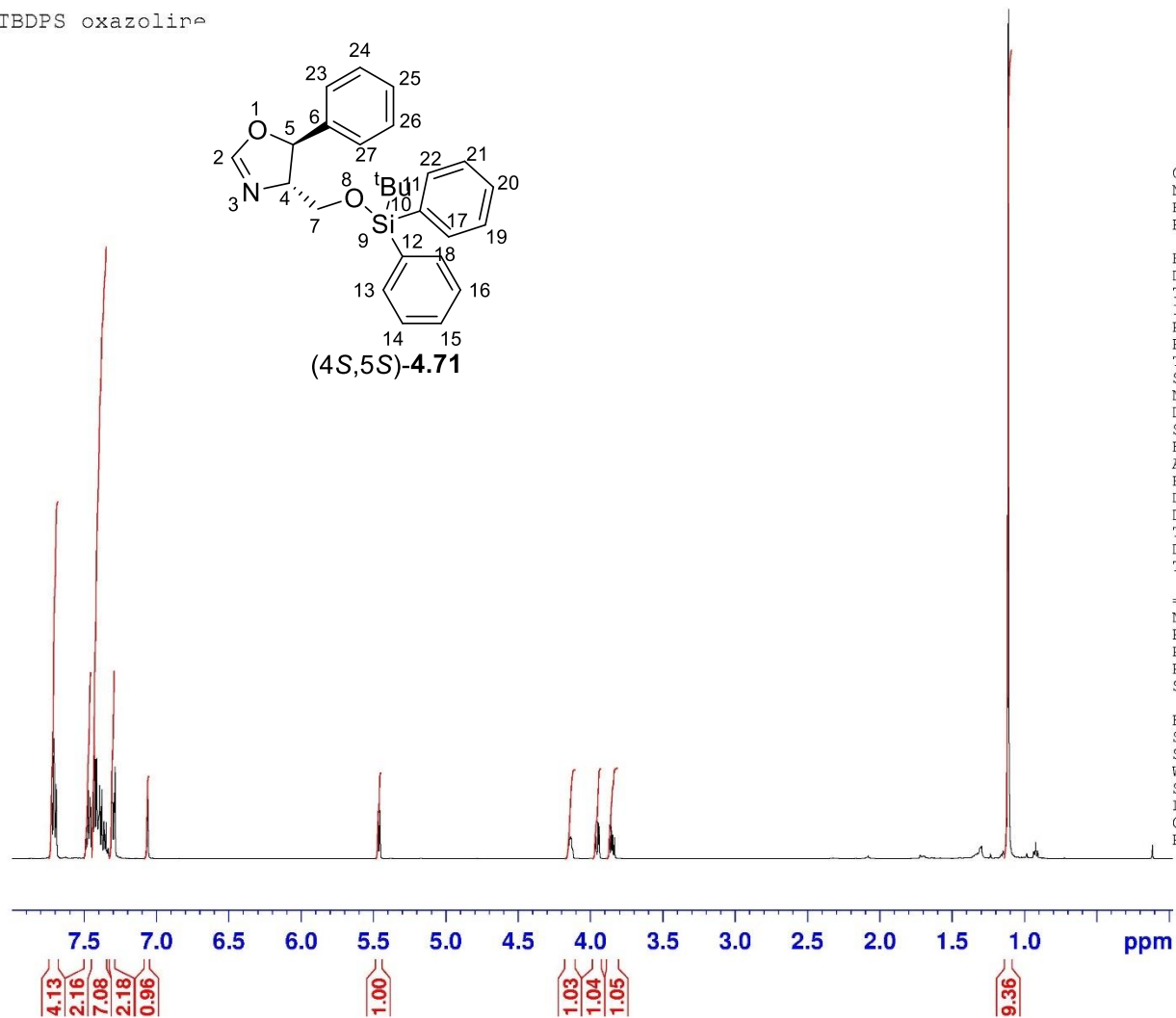
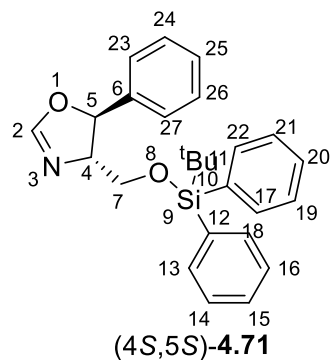
F2 - Acquisition Parameters
 Date_ 20191217
 Time 9.21
 INSTRUM spect
 PROBHD 5 mm PAQXI 1H/
 PULPROG zgpg30
 TD 65536
 SOLVENT CDCl3
 NS 16384
 DS 4
 SWH 30030.029 Hz
 FIDRES 0.458222 Hz
 AQ 1.0911744 sec
 RG 32768
 DW 16.650 usec
 DE 6.50 usec
 TE 298.2 K
 D1 2.0000000 sec
 D11 0.0300000 sec
 TD0 1

===== CHANNEL f1 =====
 NUC1 13C
 P1 12.00 usec
 PL1 -4.00 dB
 PL1W 172.88230896 W
 SFO1 125.7703643 MHz

===== CHANNEL f2 =====
 CPDPRG[2] waltz16
 NUC2 1H
 FCPD2 80.00 usec
 PL2 4.00 dB
 PL12 22.51 dB
 PL13 25.00 dB
 PL2W 12.10000038 W
 PL12W 0.17052394 W
 PL13W 0.09611372 W
 SFO2 500.1320005 MHz

F2 - Processing parameters
 SI 32768
 SF 125.7577890 MHz
 WDW EM
 SSB 0
 LB 1.00 Hz
 GB 0
 PC 1.40

TBDPS oxazoline



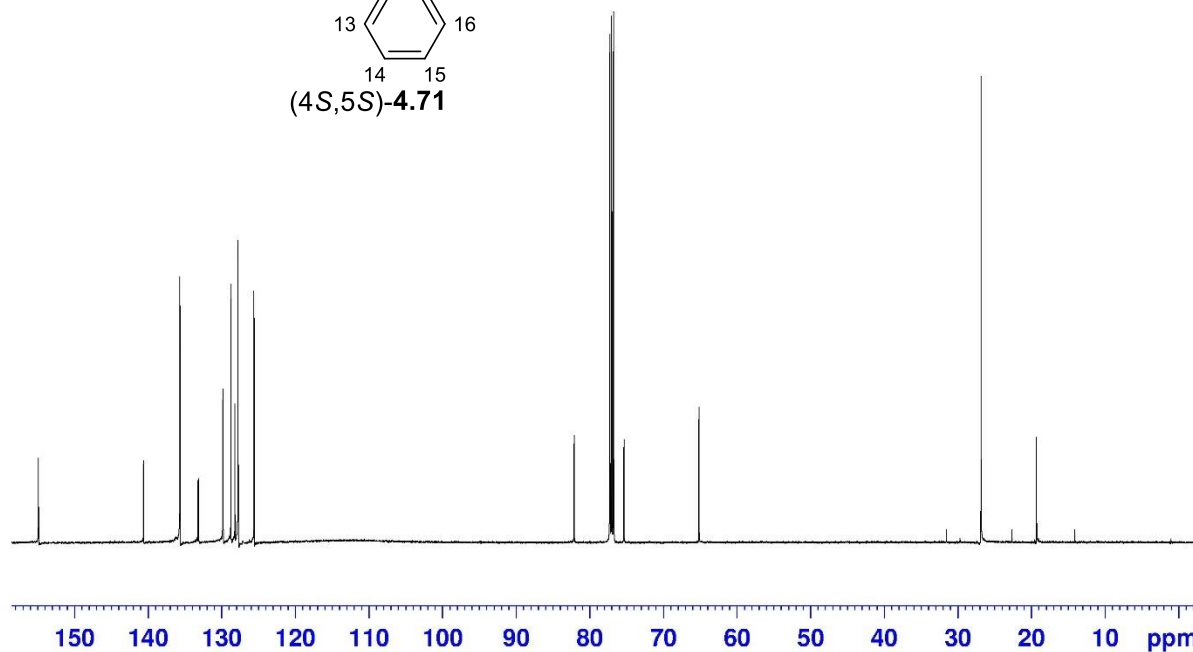
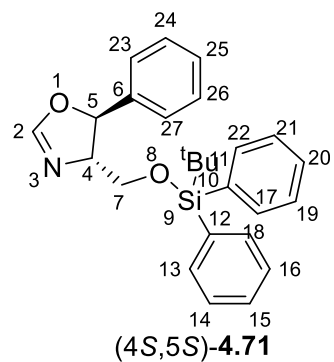
Current Data Parameters
NAME VI-Mn-01 i
EXPNO 1
PROCNO 1

F2 - Acquisition Parameters
Date_ 20191211
Time 18.35
INSTRUM spect
PROBHD 5 mm PAQXI 1H/
PULPROG zg30
TD 65536
SOLVENT CDCl3
NS 16
DS 2
SWH 10330.578 Hz
FIDRES 0.157632 Hz
AQ 3.1719425 sec
RG 57
DW 48.400 usec
DE 6.50 usec
TE 297.9 K
D1 1.0000000 sec
TD0 1

===== CHANNEL f1 =====
NUC1 1H
P1 9.50 usec
PL1 4.00 dB
PL1W 12.10000038 W
SFO1 500.1330885 MHz

F2 - Processing parameters
SI 32768
SF 500.1300000 MHz
WDW EM
SSB 0
LB 0.30 Hz
GB 0
PC 1.00

13C : TBDPS oxazoline



Current Data Parameters
NAME VI-Mn-01 i
EXPNO 2
PROCNO 1

F2 - Acquisition Parameters
Date_ 20191212
Time 8.58
INSTRUM spect
PROBHD 5 mm PAQXI 1H/
PULPROG zgpg30
TD 65536
SOLVENT CDCl3
NS 16384
DS 4
SWH 30030.029 Hz
FIDRES 0.458222 Hz
AQ 1.0911744 sec
RG 32768
DW 16.650 usec
DE 6.50 usec
TE 297.8 K
D1 2.00000000 sec
D11 0.03000000 sec
TD0 1

=====
CHANNEL f1
NUC1 13C
P1 12.00 usec
PL1 -4.00 dB
PL1W 172.88230896 W
SFO1 125.7703643 MHz

=====
CHANNEL f2
CPDPRG[2] waltz16
NUC2 1H
PCPD2 80.00 usec
PL2 4.00 dB
PL12 22.51 dB
PL13 25.00 dB
PL2W 12.10000038 W
PL12W 0.17052394 W
PL13W 0.09611372 W
SFO2 500.1320005 MHz

F2 - Processing parameters
SI 32768
SF 125.7577890 MHz
WDW EM
SSB 0
LB 1.00 Hz
GB 0
PC 1.40

4-Br PC & Ph oxazoline CH2OH

7.486
7.474
7.448
7.441
7.417
7.404
7.392
7.380
7.373
7.287
7.205
7.169
6.667
6.652
6.635
6.604
6.589
6.565
6.550
6.524
6.508
5.518
5.503
4.393
4.385
4.378
4.366
4.257
4.234
4.123
4.115
4.100
4.092
3.859
3.851
3.190
3.177
3.159
3.143
3.131
3.077
3.069
3.048
3.030
3.023
2.901
1.290
0.106

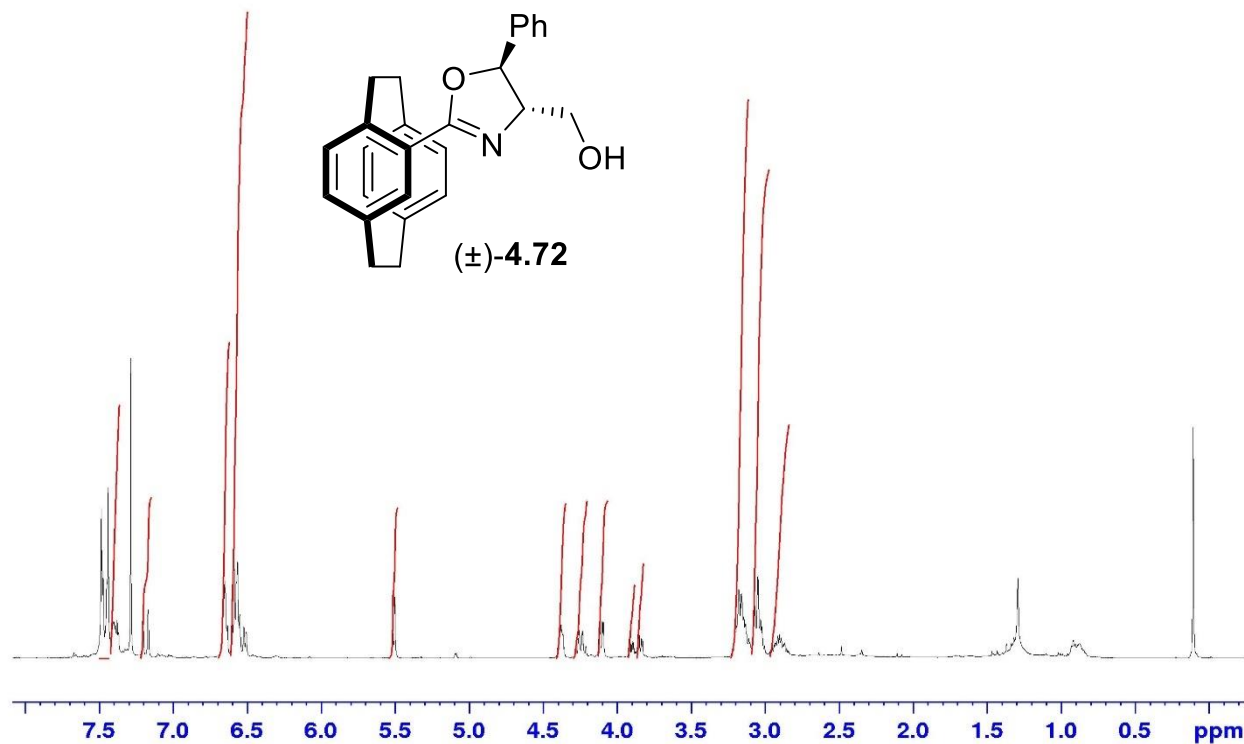
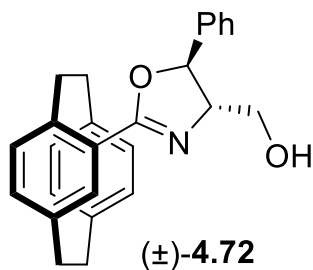


Current Data Parameters
NAME VI-Mn-08 ii
EXPNO 1
PROCNO 1

F2 - Acquisition Parameters
Date_ 20191222
Time 18.39
INSTRUM spect
PROBHD 5 mm PAQXI 1H/
PULPROG zg30
TD 65536
SOLVENT CDCl3
NS 16
DS 2
SWH 10330.578 Hz
FIDRES 0.157632 Hz
AQ 3.1719425 sec
RG 71.8
DW 48.400 usec
DE 6.50 usec
TE 297.8 K
D1 1.0000000 sec
TD0 1

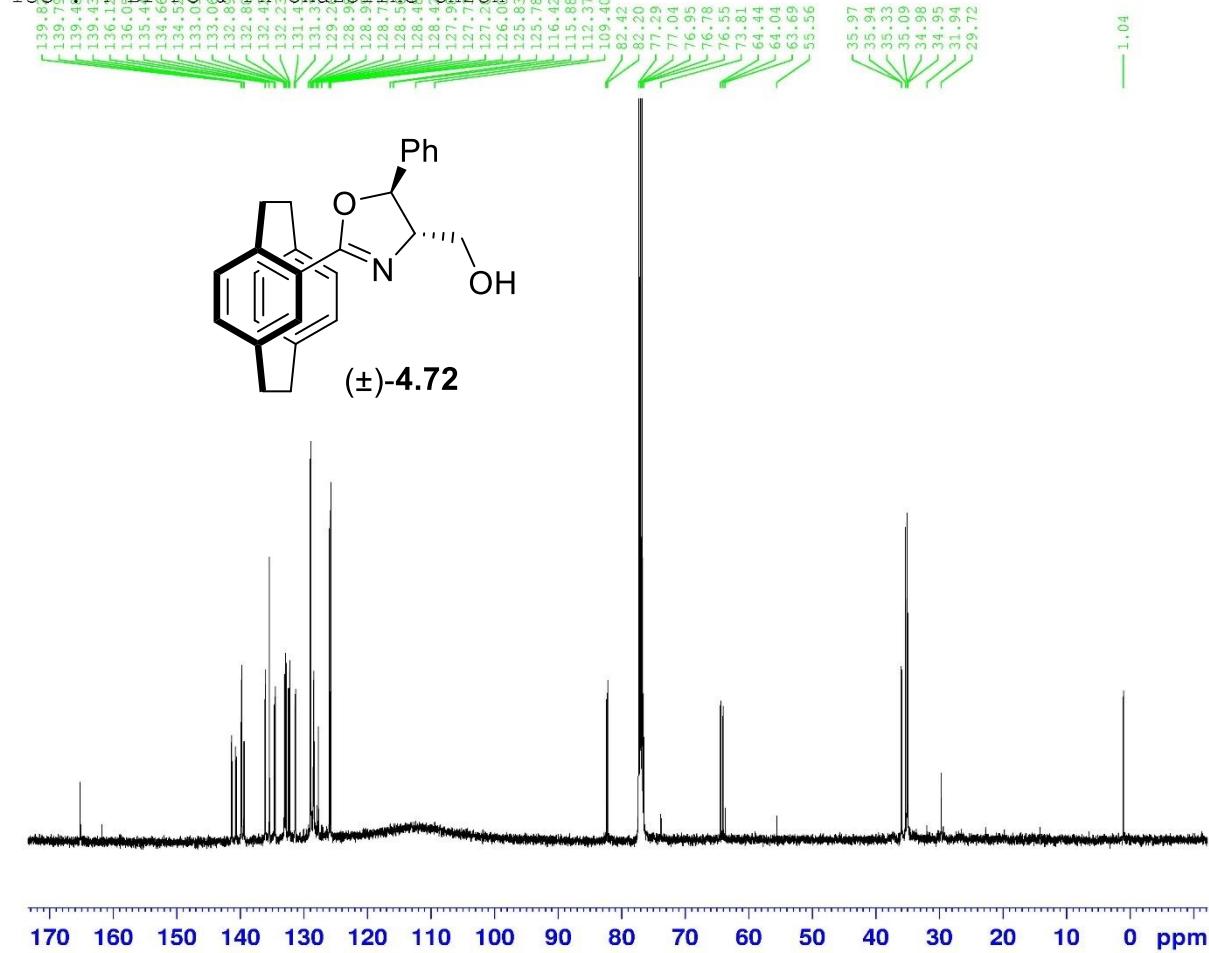
===== CHANNEL f1 =====
NUC1 1H
P1 9.50 usec
PL1 4.00 dB
PL1W 12.1000038 W
SFO1 500.1330885 MHz

F2 - Processing parameters
SI 32768
SF 500.1300000 MHz
WDW EM
SSB 0
LB 0.30 Hz
GB 0
PC 1.00



Integration values:
-0.00
3.16
2.00
3.94
8.04
1.88
1.92
1.98
1.96
0.92
1.21
7.02
6.08
2.92

¹³C: 4-Br PC & Ph oxazoline CH₂OH



Current Data Parameters
 NAME VI-Mn-08 ii
 EXPNO 2
 PROCNO 1

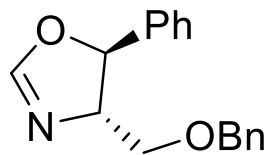
F2 - Acquisition Parameters
 Date_ 20191223
 Time 9.05
 INSTRUM spect
 PROBHD 5 mm PAQXI 1H/
 PULPROG zgpg30
 TD 65536
 SOLVENT CDCl₃
 NS 16384
 DS 4
 SWH 30030.029 Hz
 FIDRES 0.458222 Hz
 AQ 1.0911744 sec
 RG 32768
 DW 16.650 usec
 DE 6.50 usec
 TE 296.9 K
 D1 2.0000000 sec
 D11 0.0300000 sec
 TD0 1

===== CHANNEL f1 =====
 NUC1 13C
 P1 12.00 usec
 PL1 -4.00 dB
 PL1W 172.88230896 W
 SFO1 125.7703643 MHz

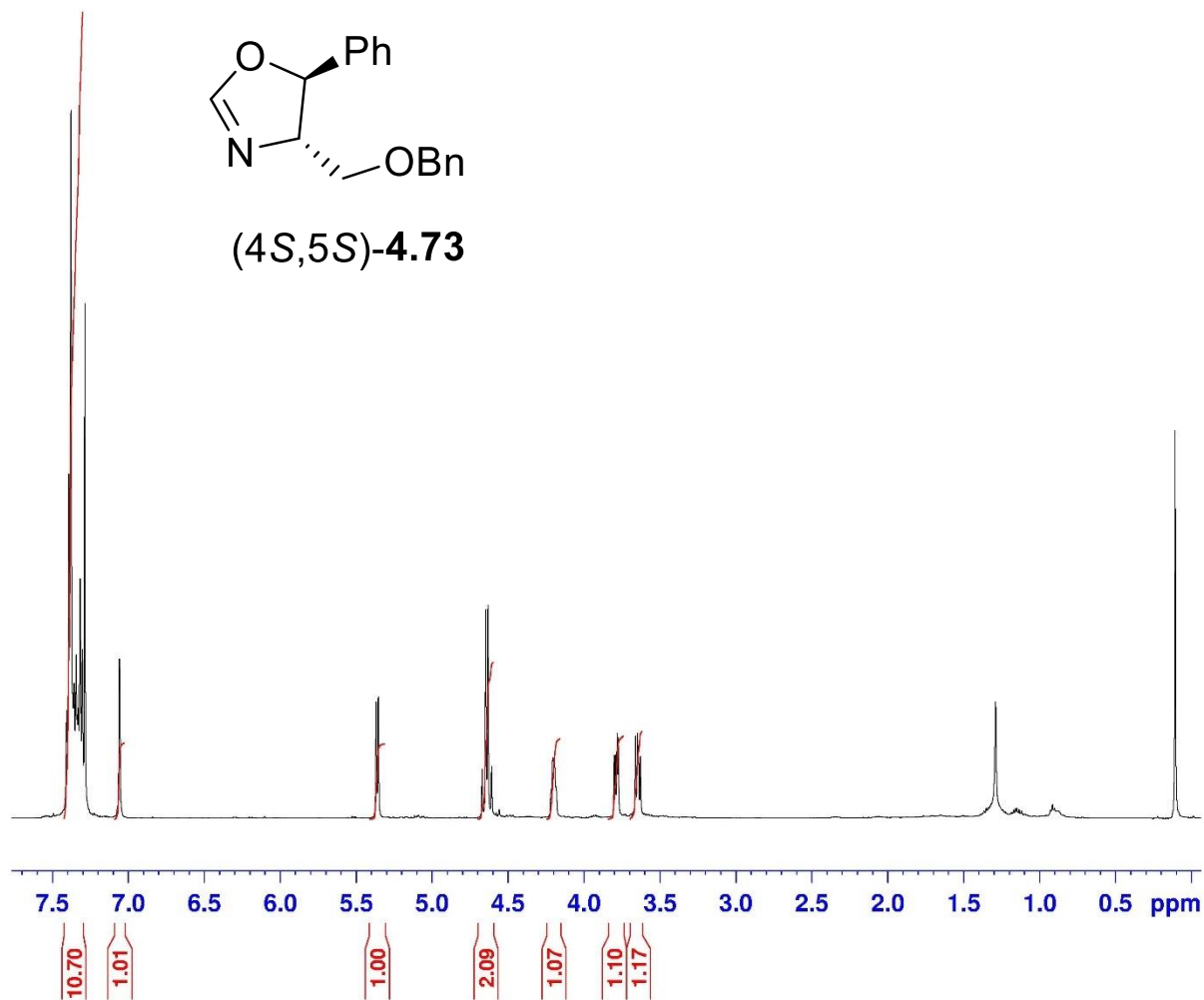
===== CHANNEL f2 =====
 CPDPRG2 waltz16
 NUC2 1H
 PCPD2 80.00 usec
 PL2 4.00 dB
 PL12 22.51 dB
 PL13 25.00 dB
 PL2W 12.10000038 W
 PL12W 0.17052394 W
 PL13W 0.09611372 W
 SFO2 500.1320005 MHz

F2 - Processing parameters
 SI 32768
 SF 125.7577890 MHz
 WDW EM
 SSB 0
 LB 1.00 Hz
 GB 0
 PC 1.40

Oxazoline Ph Bn



(4S,5S)-4.73



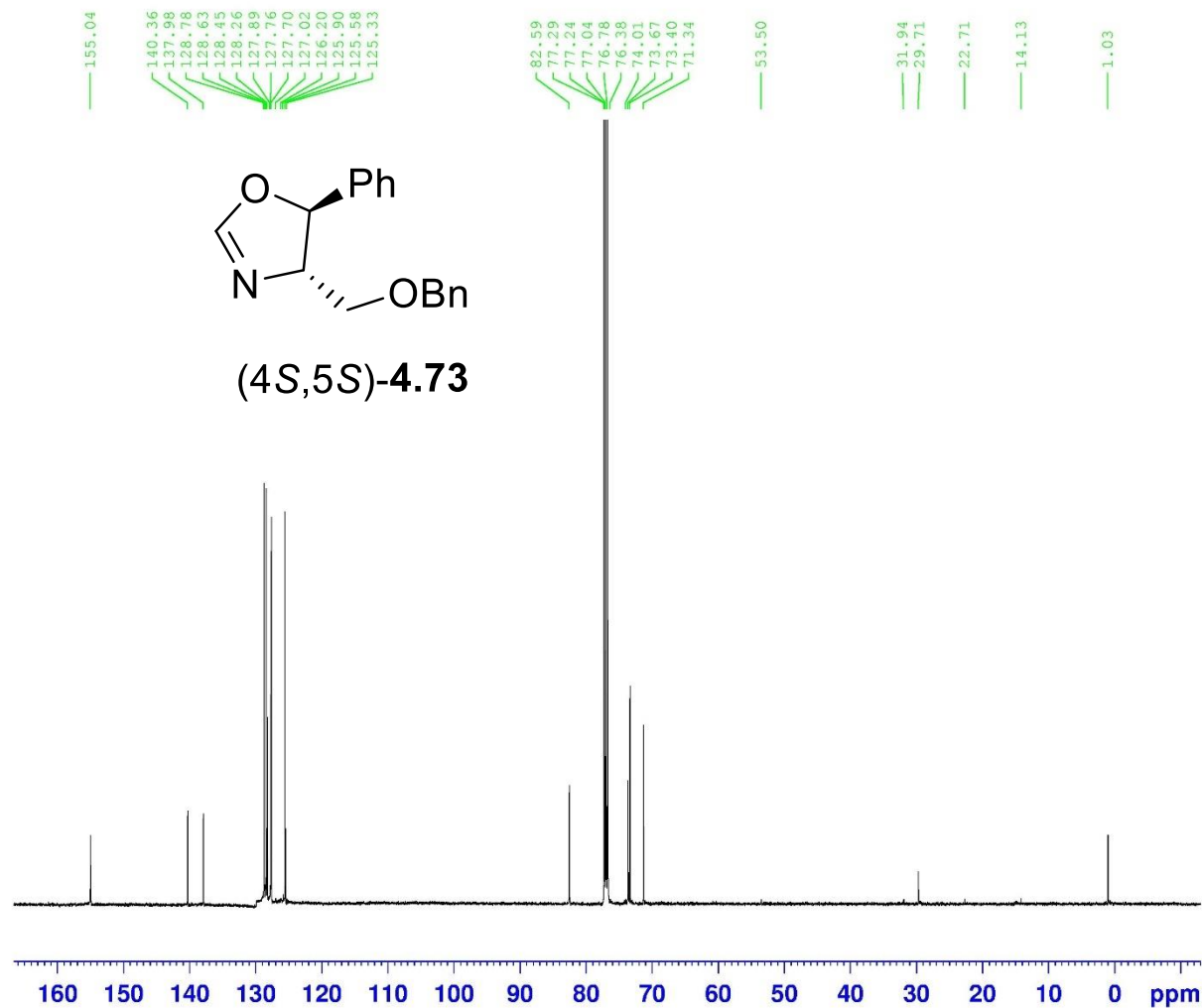
Current Data Parameters
NAME VI-Mn-27
EXPNO 1
PROCNO 1

F2 - Acquisition Parameters
Date_ 20200112
Time 13.18
INSTRUM spect
PROBHD 5 mm PAQXI 1H/
PULPROG zg30
TD 65536
SOLVENT CDCl3
NS 16
DS 2
SWH 10330.578 Hz
FIDRES 0.157632 Hz
AQ 3.1719425 sec
RG 71.8
DW 48.400 usec
DE 6.50 usec
TE 297.3 K
D1 1.00000000 sec
TD0 1

===== CHANNEL f1 =====
NUC1 1H
P1 9.50 usec
PL1 4.00 dB
PL1W 12.10000038 W
SFO1 500.1330885 MHz

F2 - Processing parameters
SI 32768
SF 500.1300000 MHz
WDW EM
SSB 0
LB 0.30 Hz
GB 0
PC 1.00

Oxazoline Ph Bn



Current Data Parameters
NAME VI-Mn-27
EXPNO 2
PROCNO 1

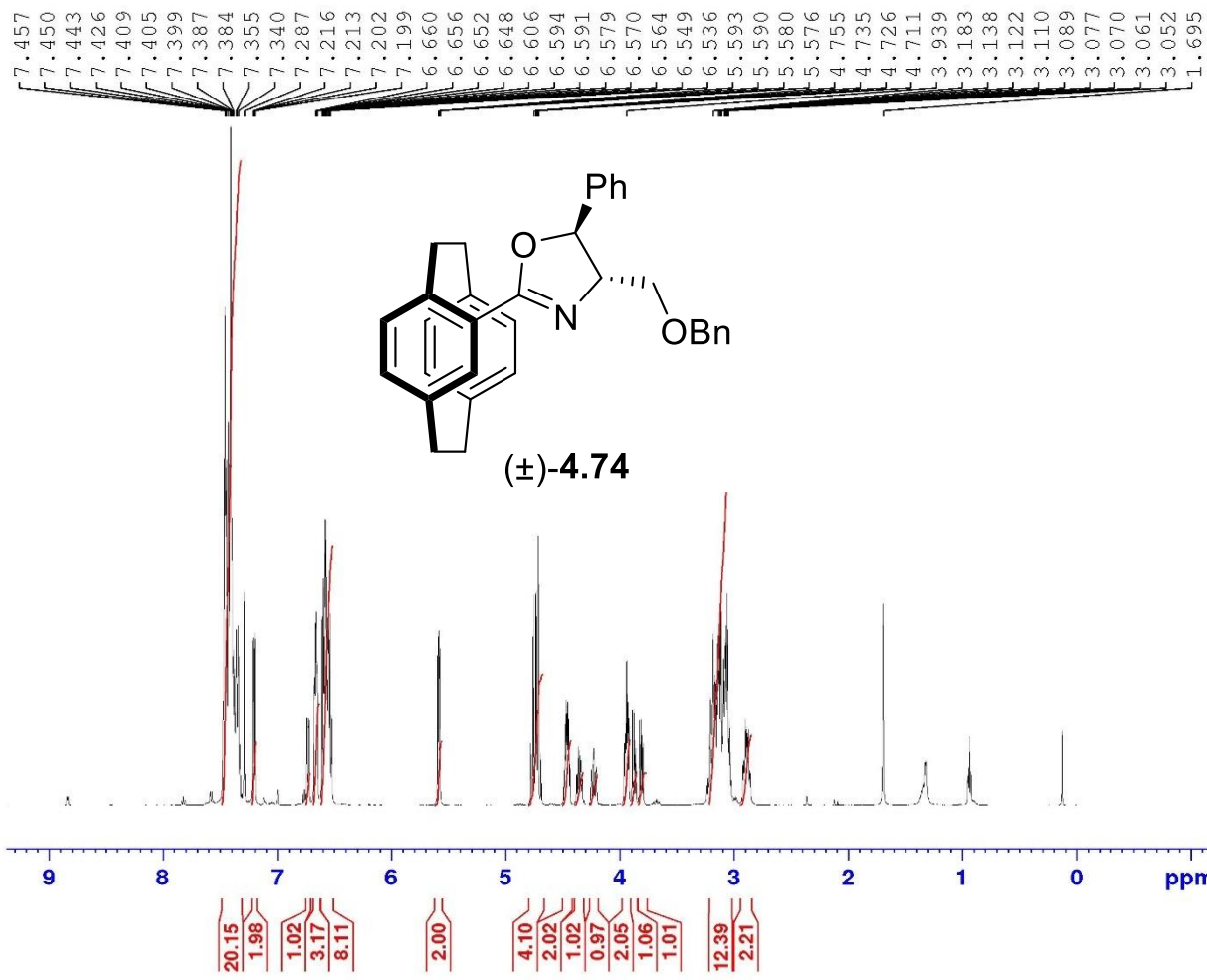
F2 - Acquisition Parameters
Date_ 20200113
Time 3.42
INSTRUM spect
PROBHD 5 mm PAQXI 1H/
PULPROG zgpg30
TD 65536
SOLVENT CDC13
NS 16384
DS 4
SWH 30030.029 Hz
FIDRES 0.458222 Hz
AQ 1.0911744 sec
RG 32768
DW 16.650 usec
DE 6.50 usec
TE 298.7 K
D1 2.0000000 sec
D11 0.0300000 sec
TD0 1

==== CHANNEL f1 =====
NUC1 13C
P1 12.00 usec
PL1 -4.00 dB
PL1W 172.88230896 W
SFO1 125.7703643 MHz

==== CHANNEL f2 =====
CPDPRG[2] waltz16
NUC2 1H
PCPD2 80.00 usec
PL2 4.00 dB
PL12 22.51 dB
PL13 25.00 dB
PL2W 12.10000038 W
PL12W 0.17052394 W
PL13W 0.09611372 W
SFO2 500.1320005 MHz

F2 - Processing parameters
SI 32768
SF 125.7577890 MHz
WDW EM
SSB 0
LB 1.00 Hz
GB 0
PC 1.40

4-Br PC & Ph Bn oxazoline



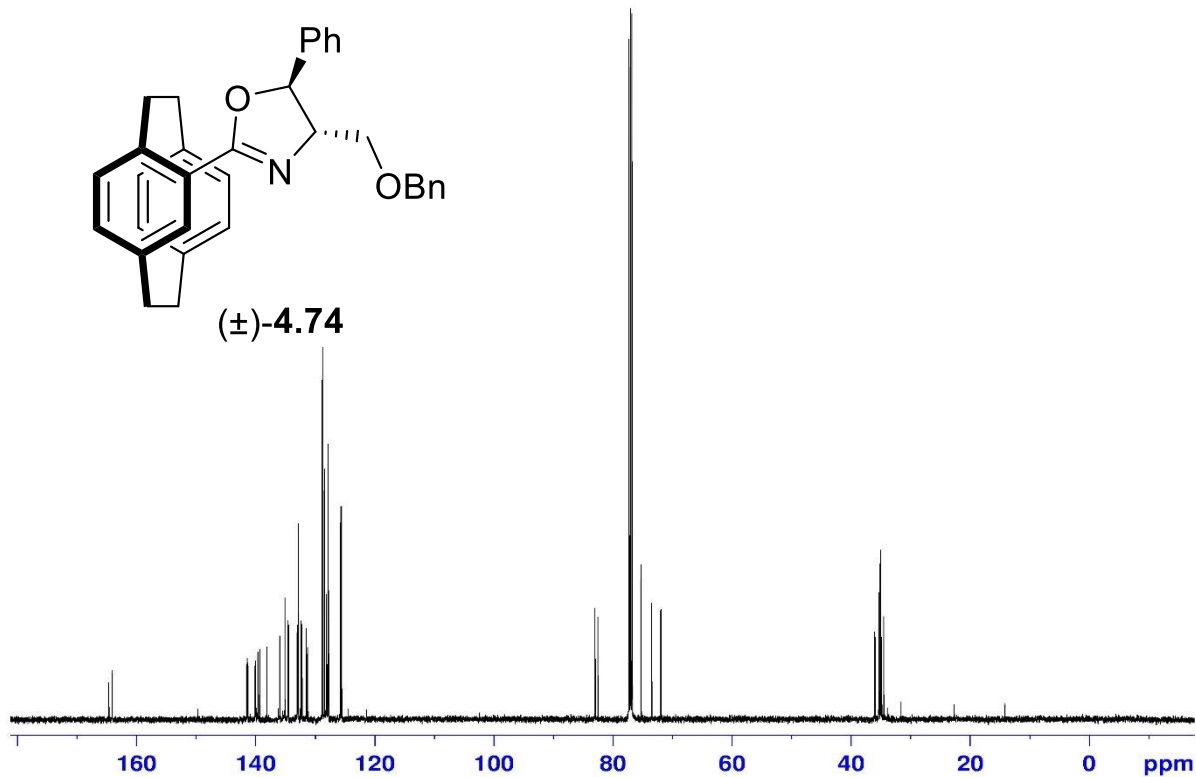
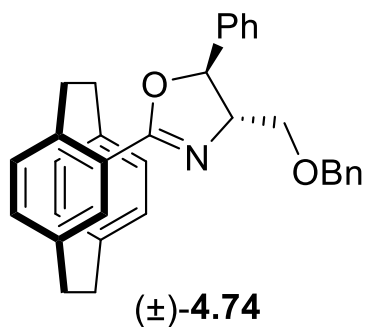
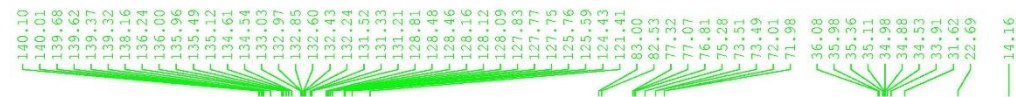
Current Data Parameters
 NAME VI-Mn-43 ii
 EXPNO 1
 PROCNO 1

F2 - Acquisition Parameters
 Date_ 20200121
 Time 11.00
 INSTRUM spect
 PROBHD 5 mm PAQXI 1H/
 PULPROG zg30
 ID 65536
 SOLVENT CDCl3
 NS 16
 DS 2
 SWH 10330.578 Hz
 FIDRES 0.157632 Hz
 AQ 3.1719425 sec
 RG 45.3
 DW 48.400 usec
 DE 6.50 usec
 TE 298.1 K
 D1 1.0000000 sec
 TD0 1

==== CHANNEL f1 =====
 NUC1 1H
 P1 9.50 usec
 PL1 4.00 dB
 PL1W 12.10000038 W
 SF01 500.1330885 MHz

F2 - Processing parameters
 SI 32768
 SF 500.1300000 MHz
 WDW EM
 SSB 0
 LB 0.30 Hz
 GB 0
 PC 1.00

4-Br PC & Ph Bn oxazoline



Current Data Parameters
NAME VI-Mn-43 ii
EXPNO 2
PROCNO 1

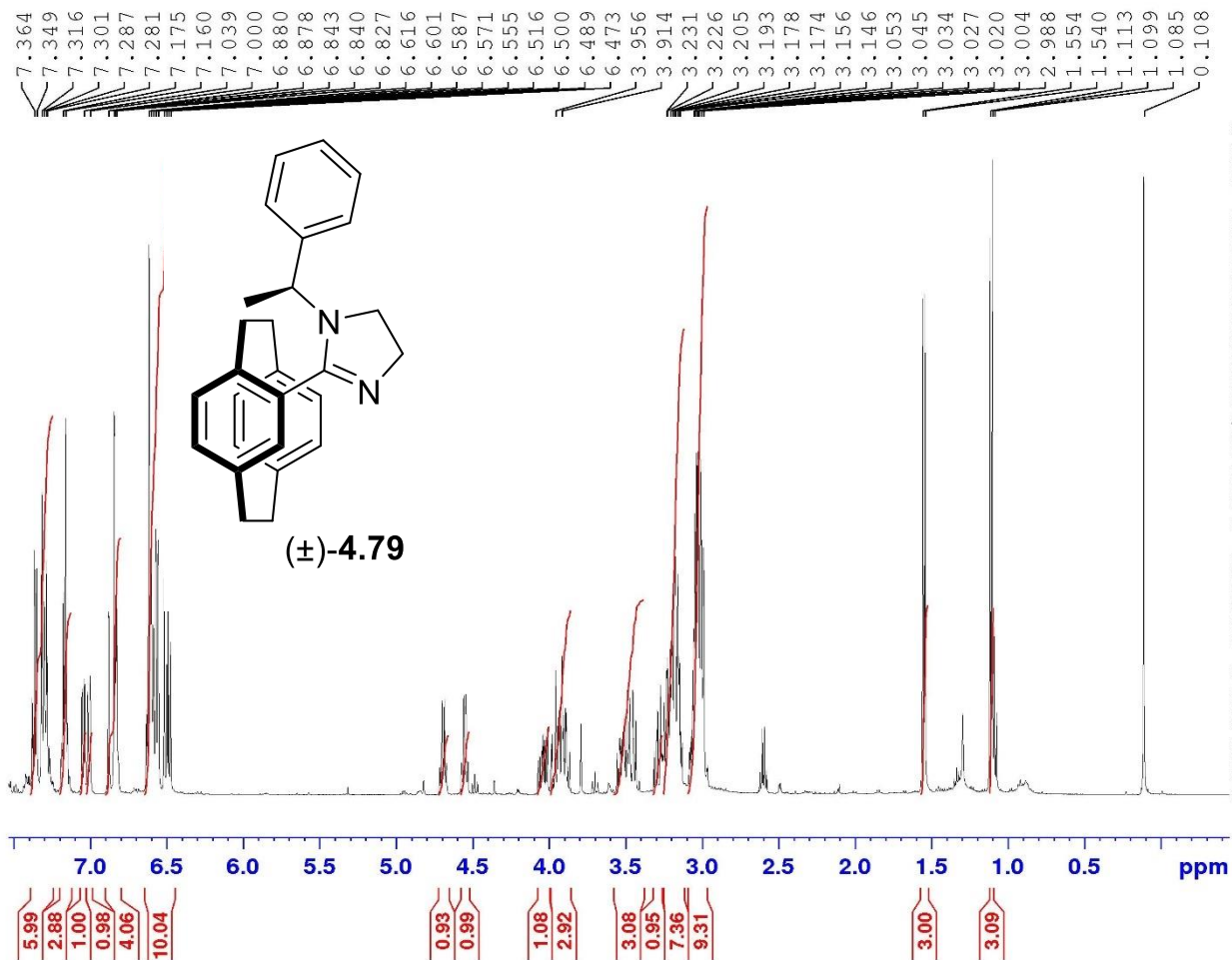
F2 - Acquisition Parameters
Date_ 20200121
Time 12.50
INSTRUM spect
PROBHD 5 mm PAQXI 1H/
PULPROG zgpg30
TD 65536
SOLVENT CDCl3
NS 2048
DS 4
SWH 30030.029 Hz
FIDRES 0.458222 Hz
AQ 1.0911744 sec
RG 32768
DW 16.650 usec
DE 6.50 usec
TE 298.3 K
D1 2.00000000 sec
D11 0.03000000 sec
TD0 1

===== CHANNEL f1 =====
NUC1 13C
P1 12.00 usec
PL1 -4.00 dB
PL1W 172.86230896 W
SFO1 125.7703643 MHz

===== CHANNEL f2 =====
CPDPRG2 waltz16
NUC2 1H
PCPD2 80.00 usec
PL2 4.00 dB
PL12 22.51 dB
PL13 25.00 dB
PL2W 12.10000038 W
PL12W 0.17052394 W
PL13W 0.09611372 W
SFO2 500.1320005 MHz

F2 - Processing parameters
SI 32768
SF 125.7577890 MHz
WDW EM
SSB 0
LB 1.00 Hz
GB 0
PC 1.40

4-Br PC & imidazolidine



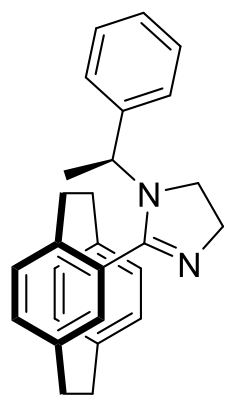
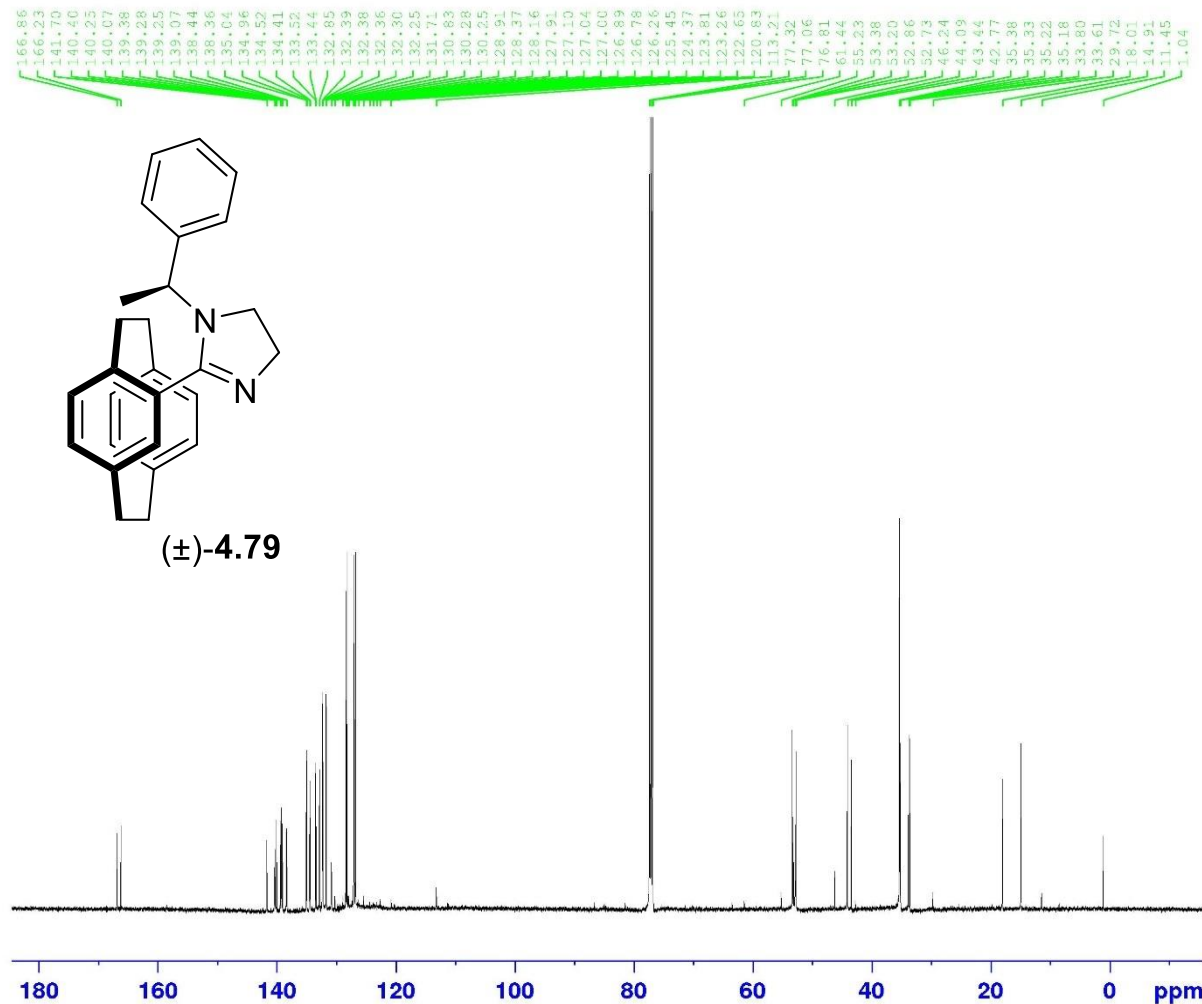
Current Data Parameters
 NAME V-Mn-196 ii
 EXPNO 1
 PROCNO 1

F2 - Acquisition Parameters
 Date_ 20190814
 Time 17.38
 INSTRUM spect
 PROBHD 5 mm PAQXI 1H/
 PULPROG zg30
 TD 65536
 SOLVENT CDCl3
 NS 16
 DS 2
 SWH 10330.578 Hz
 FIDRES 0.157632 Hz
 AQ 3.1719425 sec
 RG 57
 DW 48.400 usec
 DE 6.50 usec
 TE 298.2 K
 D1 1.0000000 sec
 TDC 1

----- CHANNEL f1 -----
 NUC1 1H
 P1 9.50 usec
 PL1 4.00 dB
 PL1W 12.10000038 W
 SF01 500.1330885 MHz

F2 - Processing parameters
 SI 32768
 SF 500.1300000 MHz
 WDW EM
 SSB 0
 LB 0.30 Hz
 GB 0
 PC 1.00

13C : 4-Br PC & imidazolidine



Current Data Parameters
 NAME V-Mn-196 ii
 EXPNO 2
 PROCNO 1

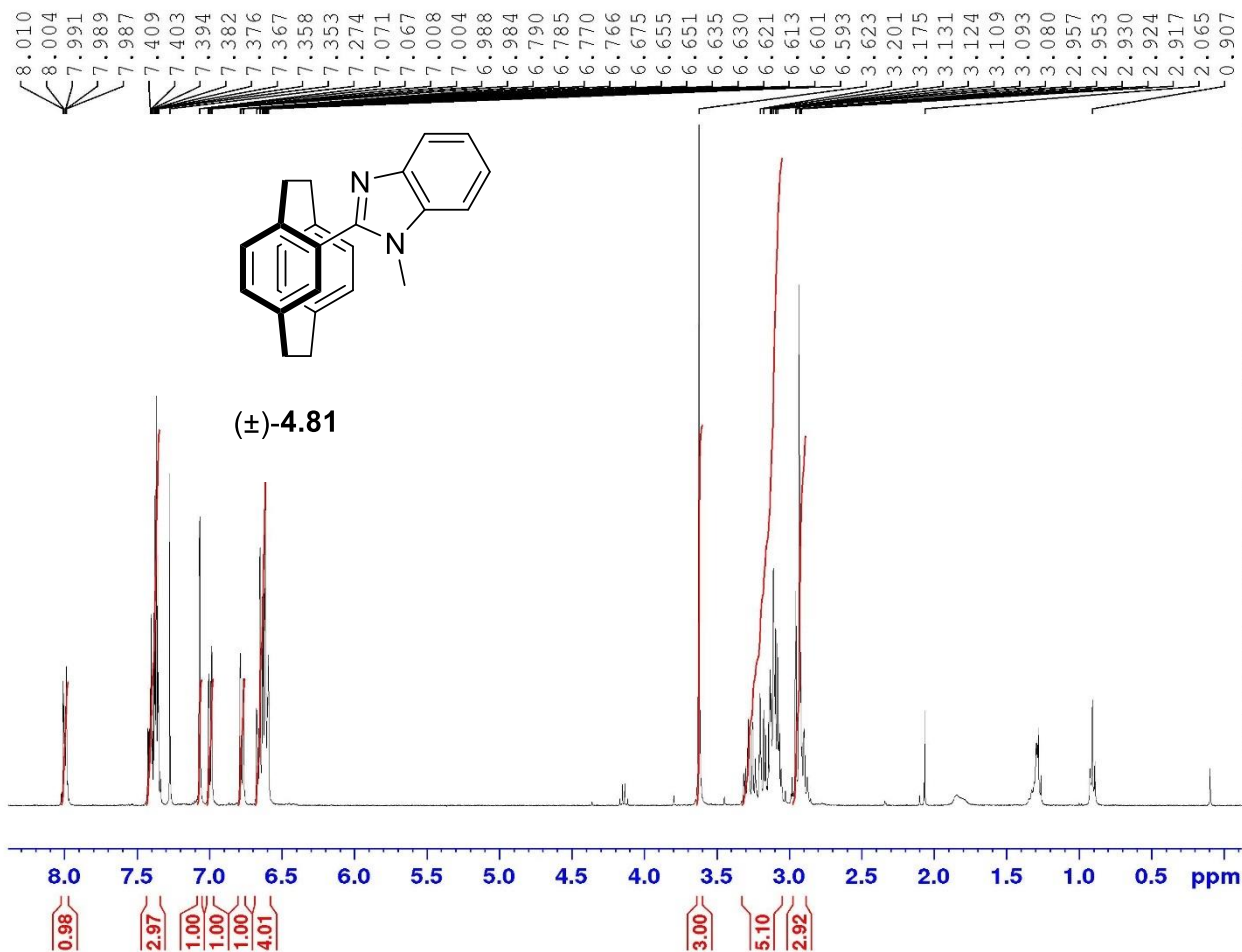
F2 - Acquisition Parameters
 Date_ 20190815
 Time 6.21
 INSTRUM spect
 PROBHD 5 mm PAQXI 1H/
 PULPROG zgpg30
 TD 65536
 SOLVENT CDC13
 NS 14386
 DS 4
 SWH 30030.029 Hz
 FIDRES 0.458222 Hz
 AQ 1.0911744 sec
 RG 32768
 DW 16.650 usec
 DE 6.50 usec
 TE 298.2 K
 D1 2.0000000 sec
 D11 0.0300000 sec
 TDO 1

----- CHANNEL f1 -----
 NUC1 13C
 P1 12.00 usec
 PL1 -4.00 dB
 PL1W 172.88230896 W
 SFO1 125.7703643 MHz

----- CHANNEL f2 -----
 CPDPRG[2] waltz16
 NUC2 1H
 PCPD2 80.00 usec
 PL2 4.00 dB
 PL12 22.51 dB
 PL13 25.00 dB
 PL2W 12.10000038 W
 PL12W 0.17052394 W
 PL13W 0.09611372 W
 SFO2 500.1320005 MHz

F2 - Processing parameters
 SI 32768
 SF 125.7577890 MHz
 WDW EM
 SSB 0
 LB 1.00 Hz
 GB 0
 PC 1.40

4-Br PC & N-Me Benzimidazole



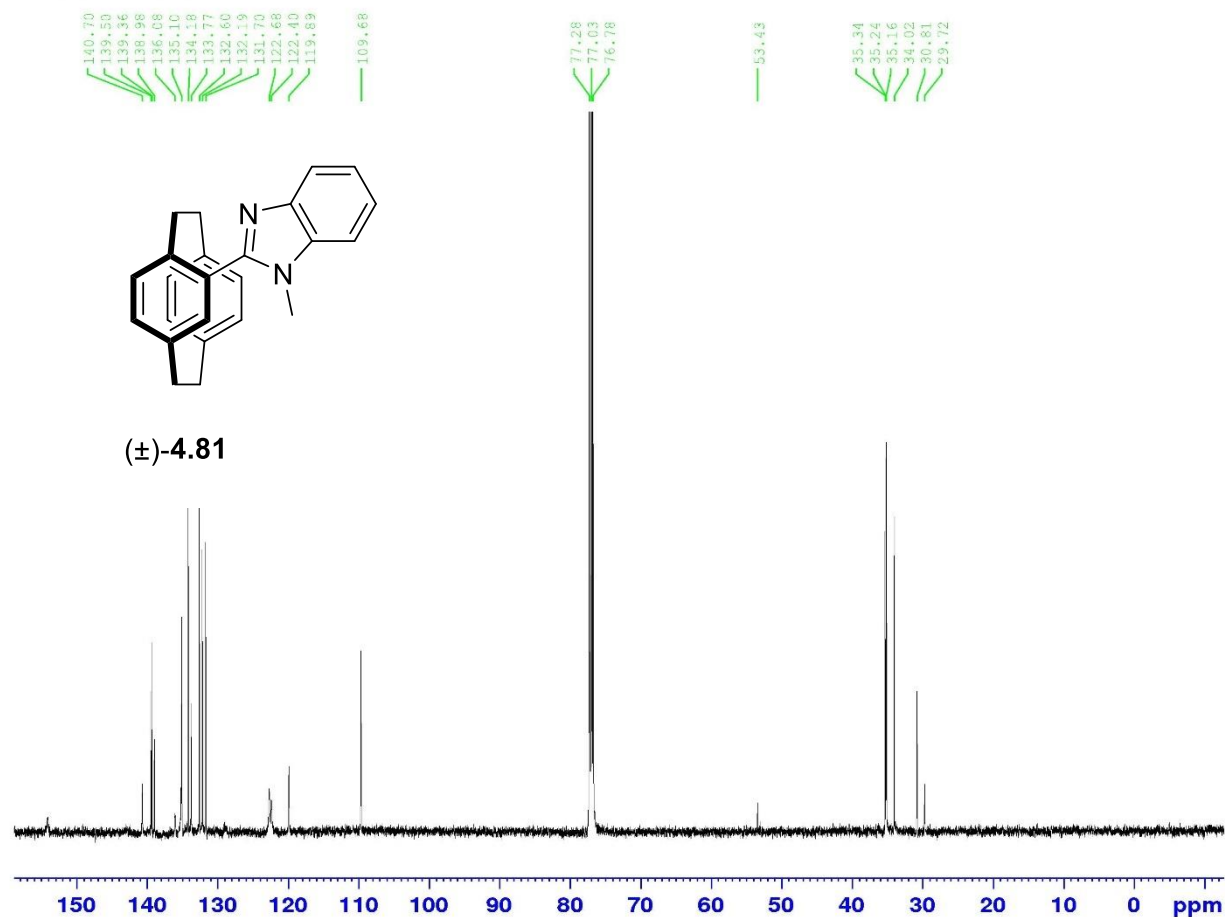
Current Data Parameters
 NAME V-Mn-256 mainspot
 EXPNO 1
 PROCNO 1

F2 - Acquisition Parameters
 Date_ 20191021
 Time 8.22
 INSTRUM spect
 PROBHD 5 mm Multinucl
 PULPROG zg30
 TD 65536
 SOLVENT CDCl3
 NS 16
 DS 2
 SWH 8278.146 Hz
 FIDRES 0.126314 Hz
 AQ 3.9583745 sec
 RG 512
 DW 60.400 usec
 DE 6.00 usec
 TE 300.0 K
 D1 1.00000000 sec
 TDO 1

----- CHANNEL f1 -----
 NUC1 1H
 P1 10.00 usec
 PL1 3.10 dB
 SFO1 400.1324710 MHz

F2 - Processing parameters
 SI 32768
 SF 400.1300000 MHz
 WDW EM
 SSB 0
 LB 0.30 Hz
 GB 0
 PC 1.00

13C : PC-Benimidazole



Current Data Parameters
 NAME V-Mn-256
 EXPNO 2
 PROCNO 1

F2 - Acquisition Parameters
 Date_ 20200617
 Time 6.45
 INSTRUM spect
 PROBHD 5 mm PAQXI 1H/
 PULPROG zgpg30
 TD 65536
 SOLVENT CDCl3
 NS 16384
 DS 4
 SWH 30030.029 Hz
 FIDRES 0.458222 Hz
 AQ 1.0911744 sec
 RG 32768
 DW 16.650 usec
 DE 6.50 usec
 TE 298.2 K
 D1 2.0000000 sec
 D11 0.0300000 sec
 TDC 1

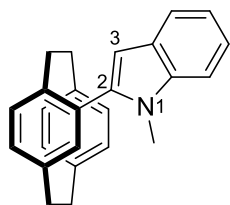
----- CHANNEL f1 -----
 NUC1 13C
 P1 12.00 usec
 PL1 -4.00 dB
 PL1W 172.88230896 W
 SFO1 125.7703643 MHz

----- CHANNEL f2 -----
 CPDPRG[2] waltz16
 NUC2 1H
 PCPD2 80.00 usec
 PL2 4.00 dB
 PL12 22.51 dB
 PL13 25.00 dB
 PL2W 12.10000038 W
 PL12W 0.17052394 W
 PL13W 0.09611372 W
 SFO2 500.1320005 MHz

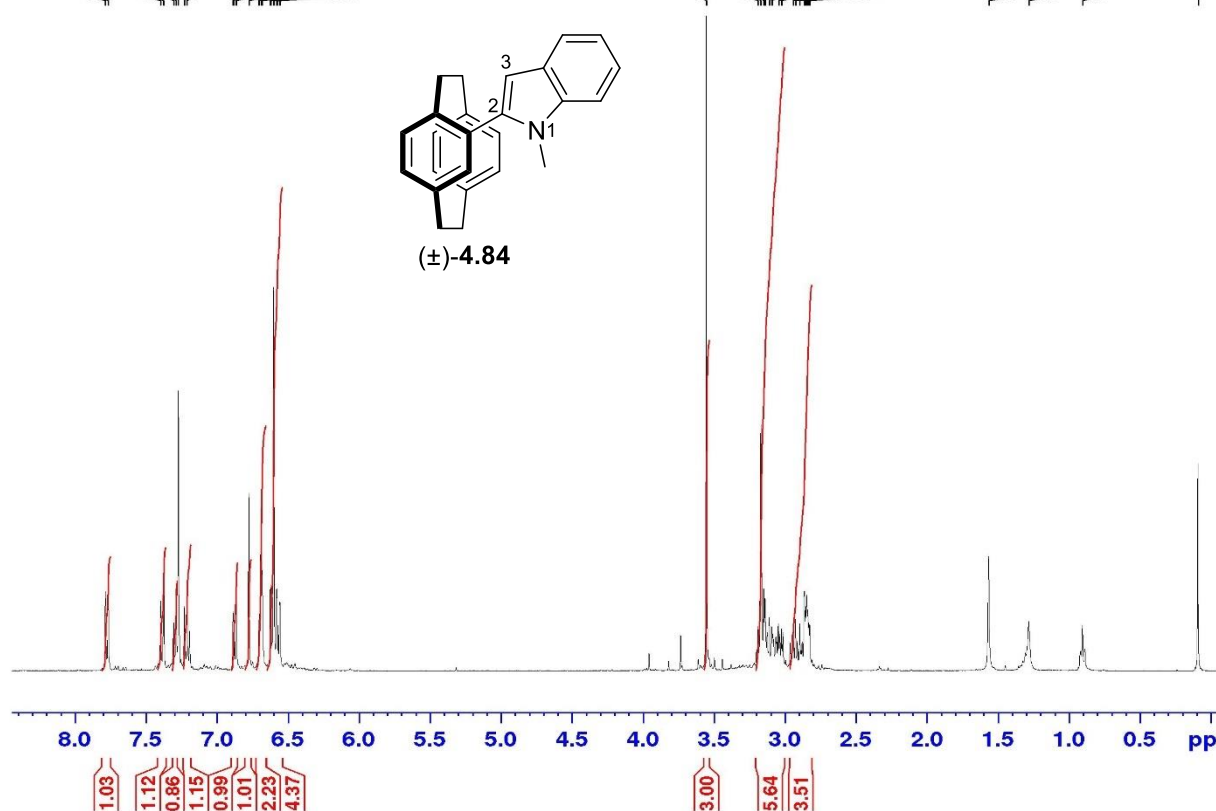
F2 - Processing parameters
 SI 32768
 SF 125.7577890 MHz
 WDW EM
 SSB 0
 LB 1.00 Hz
 GB 0
 PC 1.40

4-¹³Br PC & 1-Me Indole

7.787
7.768
7.397
7.377
7.307
7.289
7.273
7.231
7.212
6.888
6.884
6.868
6.865
6.777
6.706
6.702
6.691
6.683
6.625
6.621
6.602
6.581
6.578
6.561
6.558
3.554
3.190
3.169
3.150
3.140
3.110
3.092
3.046
3.024
2.941
2.926
2.896
2.863
2.854
2.846
2.840
2.833
2.825
1.565
1.283
0.904
0.091



(±)-4.84



```

Current Data Parameters
NAME          V-Mn-162  i
EXPNO        2
PROCNO       1

F2 - Acquisition Parameters
Date_        20190617
Time         11.23
INSTRUM      spect
PROBHD       5 mm Multinucl
PULPROG      zg30
TD           65536
SOLVENT      CDCl3
NS           16
DS           2
SWH          8278.146 Hz
FIDRES       0.126314 Hz
AQ           3.9583745 sec
RG           228.1
DW           60.400 usec
DE           6.00 usec
TE           300.0 K
D1           1.00000000 sec
TDC          1

----- CHANNEL f1 -----
NUC1         1H
P1           10.00 usec
PL1          3.80 dB
SFO1         400.1324710 MHz

F2 - Processing parameters
SI           32768
SF           400.1300000 MHz
WDW          EM
SSB          0
LB           0.30 Hz
GB           0
PC           1.00
    
```

4-Br PC & 1-Me Indole

7.660
7.640
7.416
7.395
7.314
7.295
7.273
7.251
7.188
7.168
7.150
6.771
6.751
6.689
6.673
6.670
6.622
6.603
6.595
6.591
6.580
6.559
6.527
6.508
3.955
3.550
3.384
3.165
3.154
3.144
3.132
3.081
3.066
3.046
3.040
2.947
2.846
2.838
2.822
1.577
1.458
1.300
1.278
0.915
0.899
0.882
0.085

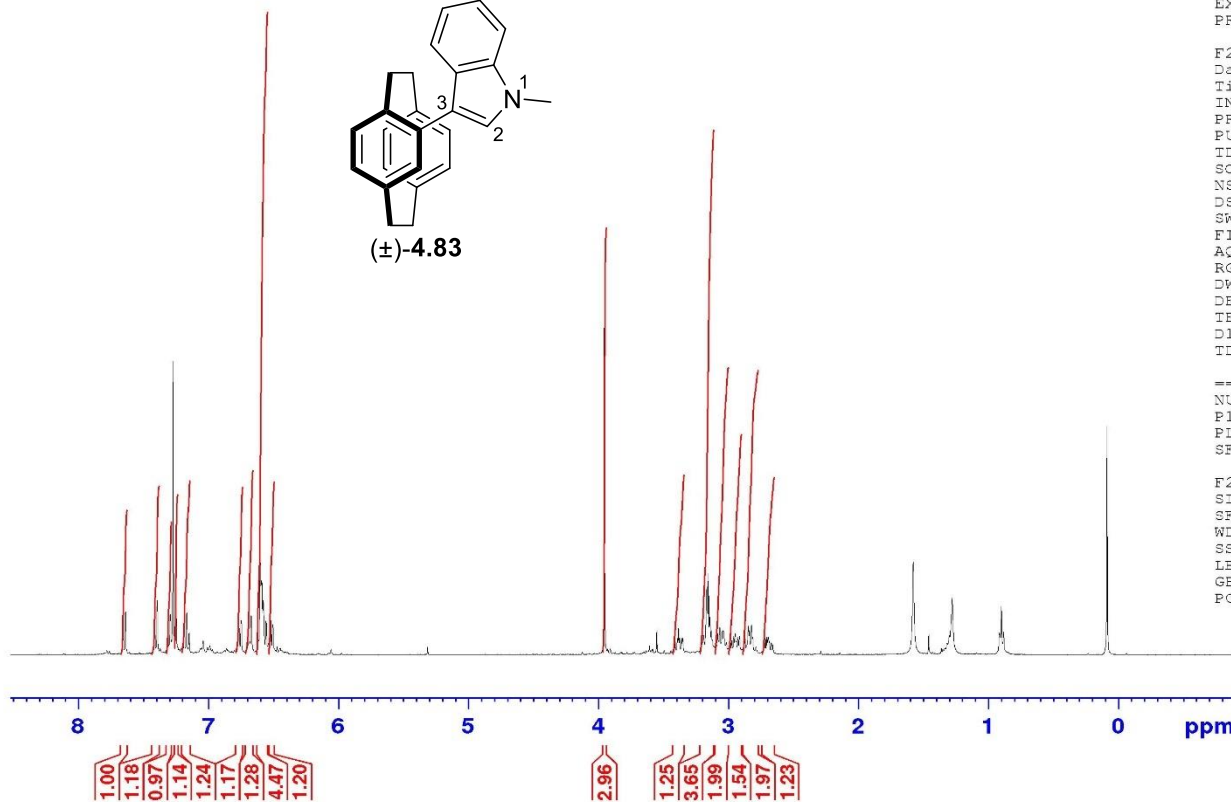
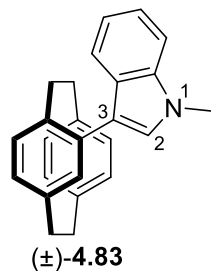


Current Data Parameters
NAME V-Mn-162 ii
EXPNO 3
PROCNO 1

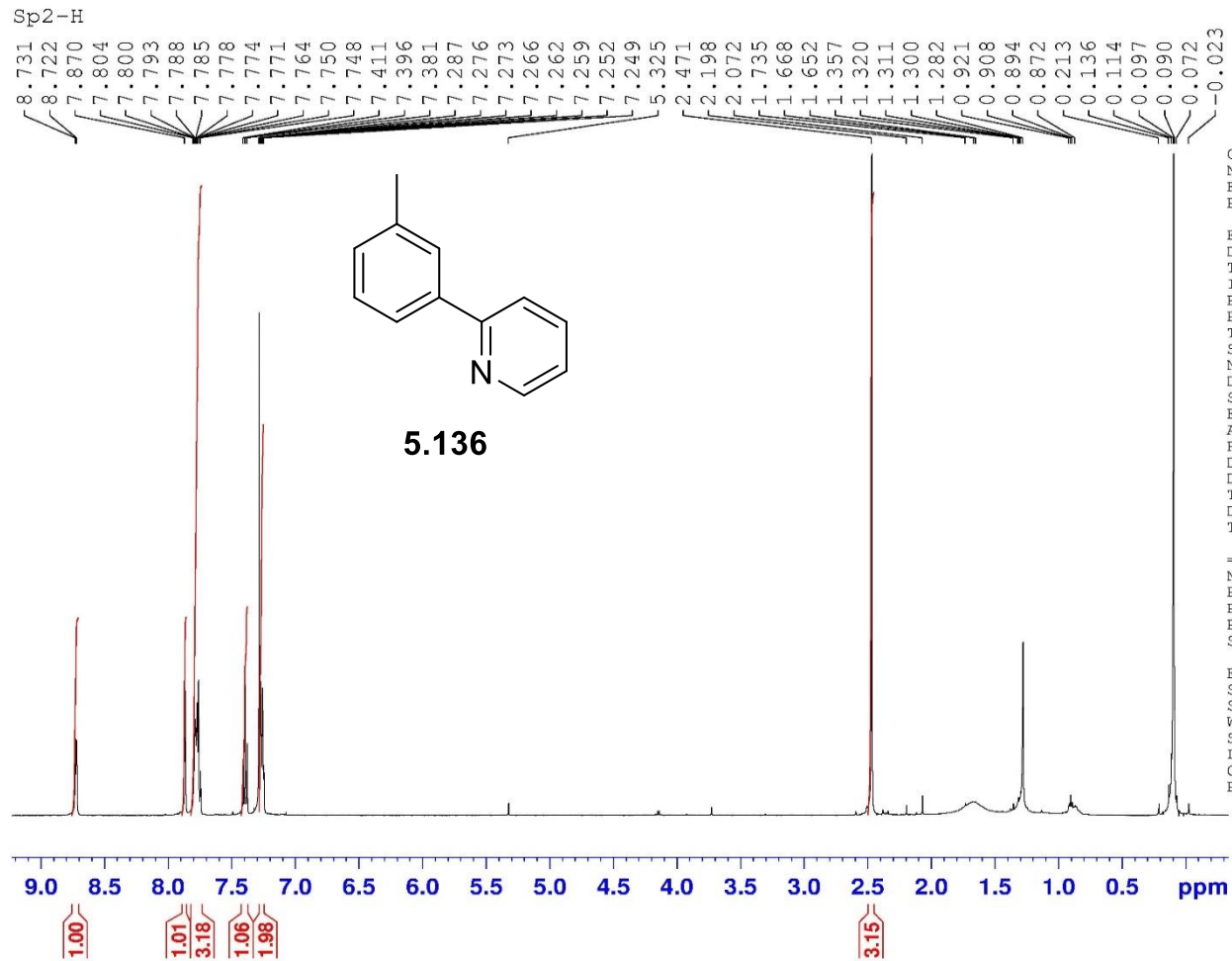
F2 - Acquisition Parameters
Date_ 20190617
Time 11.30
INSTRUM spect
PROBHD 5 mm Multinucl
PULPROG zg30
TD 65536
SOLVENT CDCl3
NS 16
DS 2
SWH 8278.146 Hz
FIDRES 0.126314 Hz
AQ 3.9583745 sec
RG 362
DW 60.400 usec
DE 6.00 usec
TE 300.0 K
D1 1.0000000 sec
TDC 1

===== CHANNEL f1 =====
NUC1 1H
P1 10.00 usec
PL1 3.80 dB
SFO1 400.1324710 MHz

F2 - Processing parameters
SI 32768
SF 400.1300000 MHz
WDW EM
SSB 0
LB 0.30 Hz
GB 0
PC 1.00



Electronic Appendix for Chapter 5 and Chapter 6



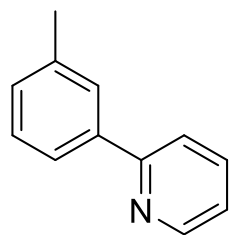
Current Data Parameters
 NAME IV-Mn-31 i
 EXPNO 1
 PROCNO 1

F2 - Acquisition Parameters
 Date_ 20180716
 Time 17.40
 INSTRUM spect
 PROBHD 5 mm PAQXI 1H/
 PULPROG zg30
 TD 65536
 SOLVENT CDCl3
 NS 16
 DS 2
 SWH 10330.578 Hz
 FIDRES 0.157632 Hz
 AQ 3.1719425 sec
 RG 362
 DW 48.400 usec
 DE 6.50 usec
 TE 298.2 K
 D1 1.00000000 sec
 TDO 1

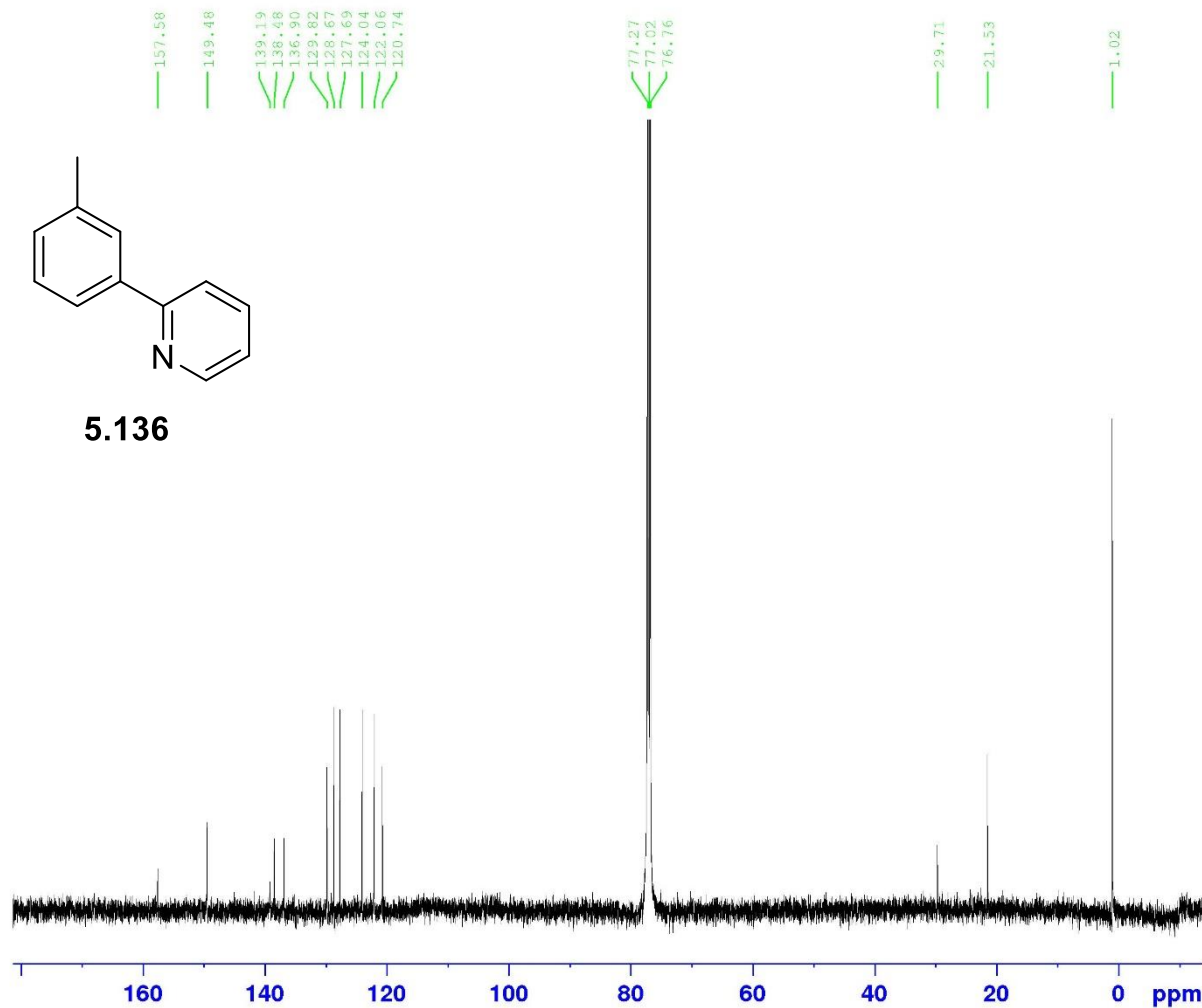
===== CHANNEL f1 =====
 NUC1 1H
 P1 9.50 usec
 PL1 4.00 dB
 PLLW 12.10000038 W
 SFO1 500.1330885 MHz

F2 - Processing parameters
 SI 32768
 SF 500.1300000 MHz
 WDW EM
 SSB 0
 LB 0.30 Hz
 GB 0
 PC 1.00

Sp2-H



5.136



Current Data Parameters
NAME IV-Mn-31 i
EXPNO 2
PROCNO 1

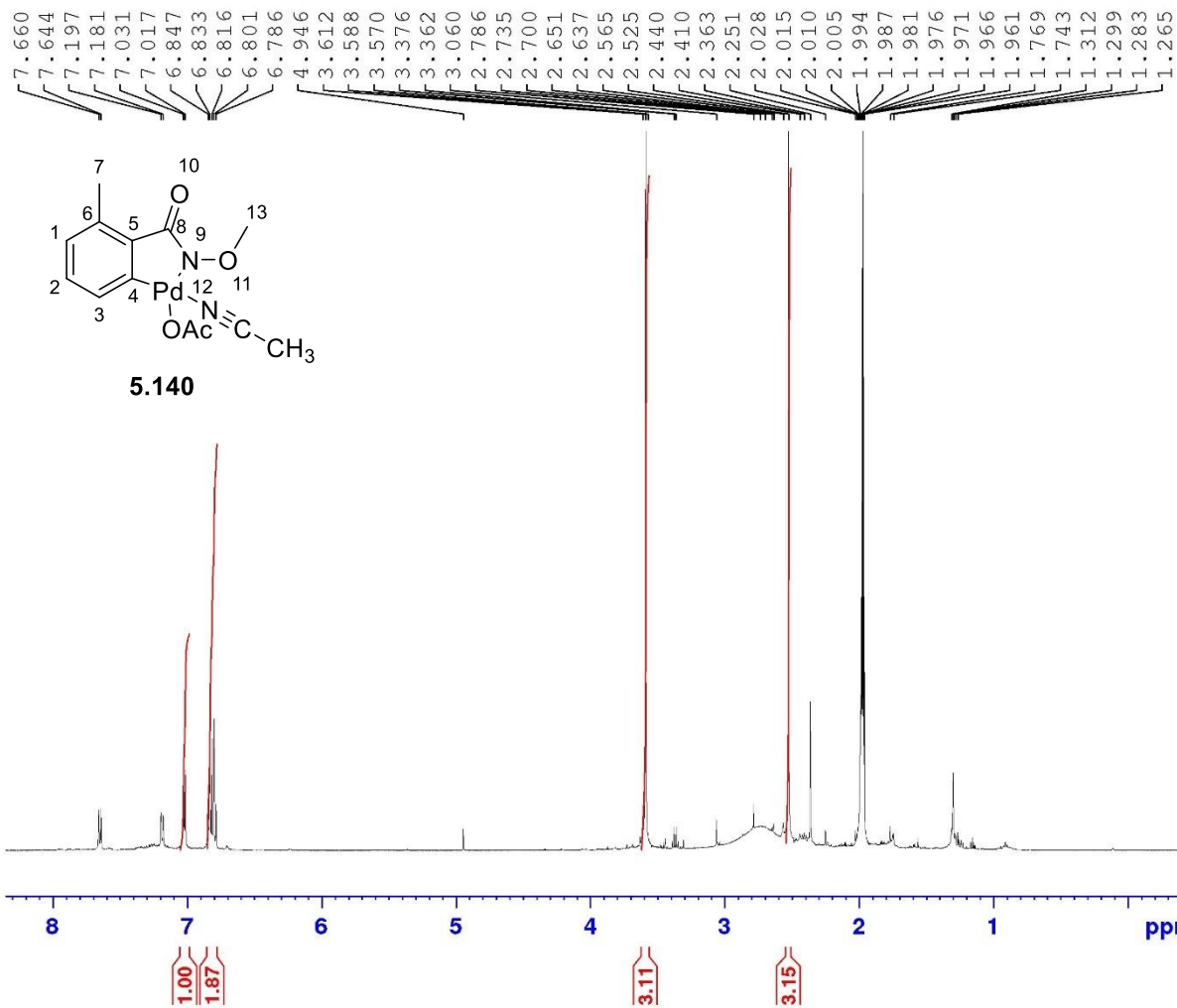
F2 - Acquisition Parameters
Date_ 20180717
Time 2.45
INSTRUM spect
PROBHD 5 mm PAQXI 1H/
PULPROG zgpg30
TD 65536
SOLVENT CDCl3
NS 10240
DS 4
SWH 30030.029 Hz
FIDRES 0.458222 Hz
AQ 1.0911744 sec
RG 32768
DM 16.650 usec
DE 6.50 usec
TE 298.2 K
D1 2.00000000 sec
D11 0.03000000 sec
TD0 1

===== CHANNEL f1 =====
NUC1 13C
P1 12.00 usec
PL1 -4.00 dB
PL1W 172.88230896 W
SFO1 125.7703643 MHz

===== CHANNEL f2 =====
CPDPRG2 waltz16
NUC2 1H
PCPD2 80.00 usec
PL2 4.00 dB
PL12 22.51 dB
PL13 25.00 dB
PL2W 12.10000038 W
PL12W 0.17052394 W
PL13W 0.09611372 W
SFO2 500.1320005 MHz

F2 - Processing parameters
SI 32768
SF 125.7577690 MHz
WDW EM
SSB 0
LB 1.00 Hz
GB 0
PC 1.40

Amide palladacycle



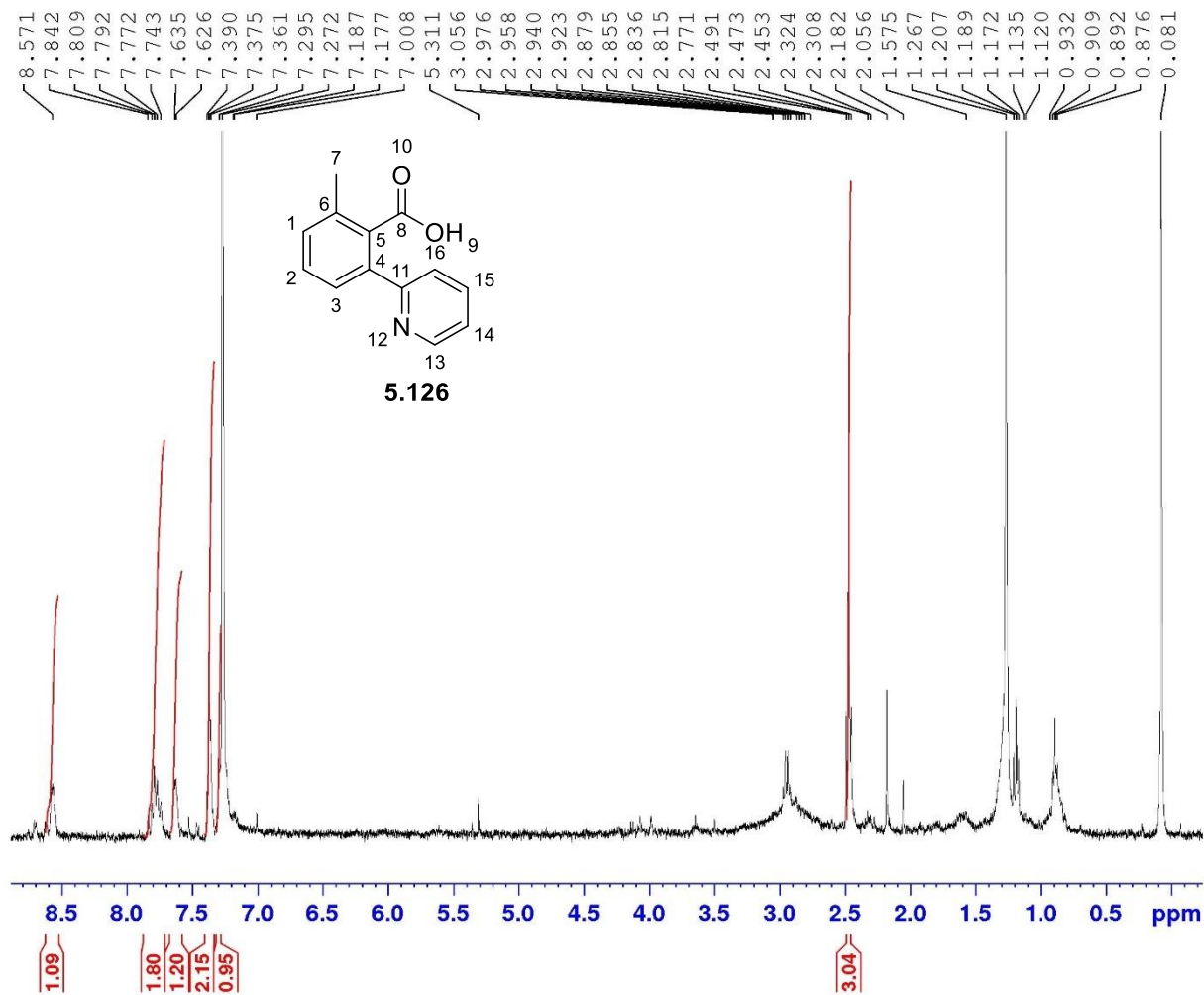
Current Data Parameters
 NAME IV-Mn-63
 EXPNO 1
 PROCNO 1

F2 - Acquisition Parameters
 Date_ 20180806
 Time 9.10
 INSTRUM spect
 PROBHD 5 mm PAQXI 1H/
 PULPROG zg30
 TD 65536
 SOLVENT CD3CN
 NS 16
 DS 2
 SWH 10330.578 Hz
 FIDRES 0.157632 Hz
 AQ 3.1719423 sec
 RG 181
 DW 48.400 usec
 DE 6.50 usec
 TE 298.2 K
 D1 1.00000000 sec
 TDC 1

----- CHANNEL f1 -----
 NUC1 1H
 P1 9.50 usec
 PL1 4.00 dB
 PLLW 12.10000038 W
 SFO1 500.1330885 MHz

F2 - Processing parameters
 SI 32768
 SF 500.1300000 MHz
 WDW EM
 SSB 0
 LB 0.30 Hz
 GB 0
 PC 1.00

Sp2-H : amide palladacycle



Current Data Parameters
NAME IV-Mn-73 i
EXPNO 3
PROCNO 1

F2 - Acquisition Parameters
Date_ 20180821
Time 21.00
INSTRUM spect
PROBHD 5 mm Multinucl
PULPROG zg30
TD 65536
SOLVENT CDCl3
NS 1024
DS 2
SWH 8278.146 Hz
FIDRES 0.126314 Hz
AQ 3.9583745 sec
RG 4096
DW 60.400 usec
DE 6.00 usec
TE 300.0 K
D1 1.00000000 sec
TD0 1

----- CHANNEL f1 -----
NUC1 1H
P1 10.00 usec
PL1 3.80 dB
SFO1 400.1324710 MHz

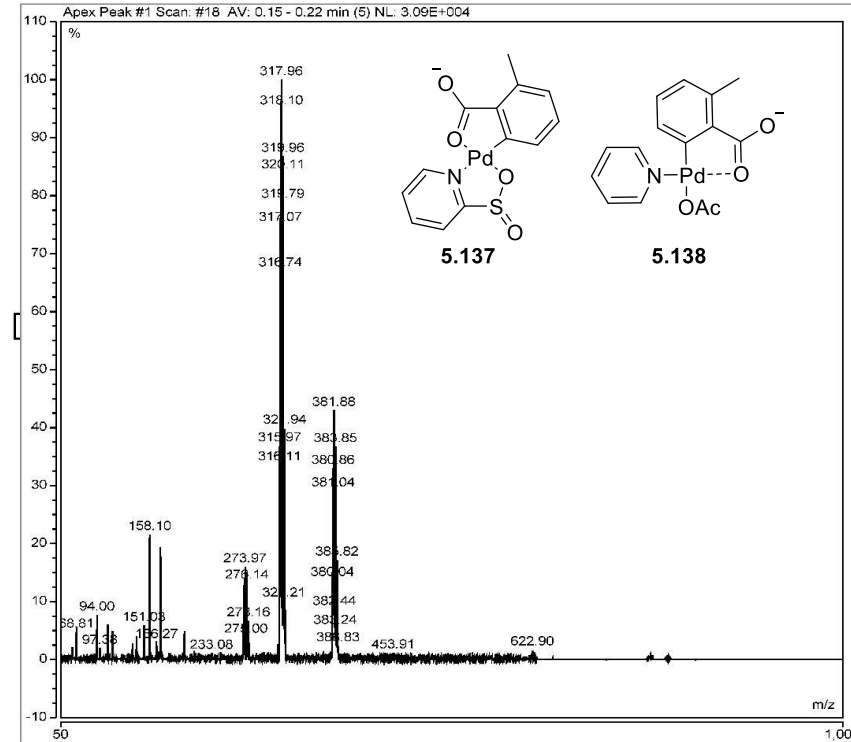
F2 - Processing parameters
SI 32768
SF 400.1300000 MHz
WDW EM
SSB 0
LB 0.30 Hz
GB 0
PC 1.00

Peak Analysis

Injection Details

Injection Name:	IV-Mn-561 & II 2ndspot (repuri)	Run Time (min):	1.49
Vial Number:	BD1	Injection Volume:	10.00
Injection Type:	Unknown		
Calibration Level:			
Instrument Method:	Bypass (Neg) CH3OH (50-1000)	Dilution Factor:	1.0000
Processing Method:	MS Quantitative	Sample Weight:	1.0000
Injection Date/Time:	01/Aug/18 09:16		

Mass Spectrum

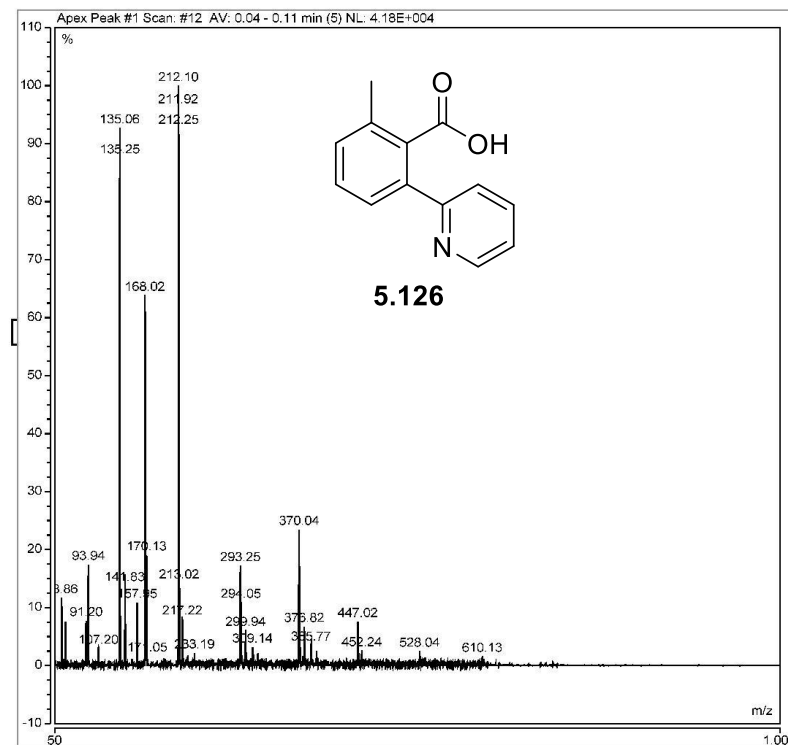


Peak Analysis

Injection Details

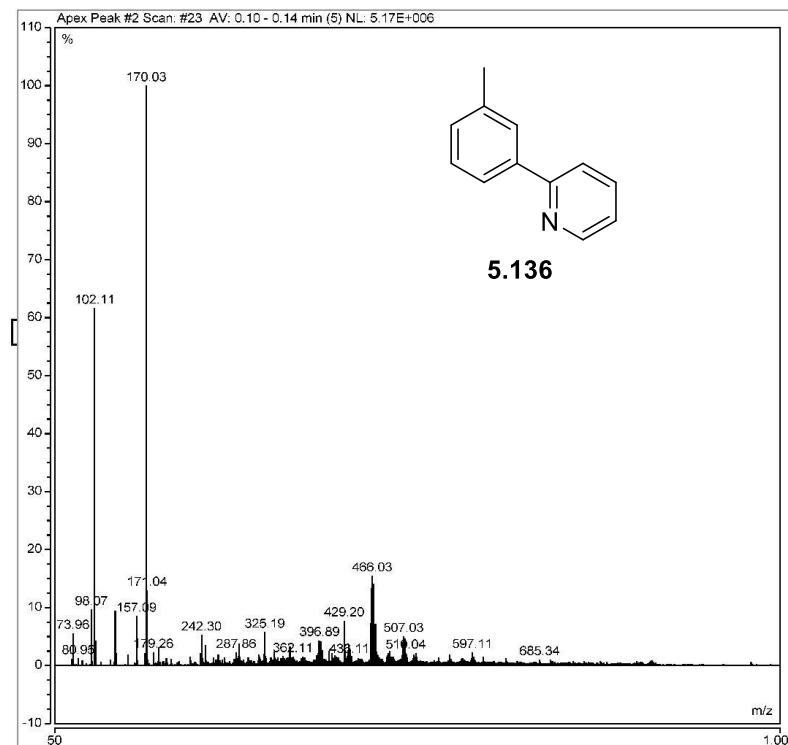
Injection Name:	IV-Mn-56 aft 8 hrs	Run Time (min):	1.49
Vial Number:	BD4	Injection Volume:	10.00
Injection Type:	Unknown		
Calibration Level:			
Instrument Method:	Bypass (Neg) CH3OH (50-1000)	Dilution Factor:	1.0000
Processing Method:	MS Quantitative	Sample Weight:	1.0000
Injection Date/Time:	30/Jul/18 10:10		

Mass Spectrum



Peak Analysis**Injection Details**

Injection Name:	IV-MN-03	Run Time (min):	1.50
Vial Number:	BD5	Injection Volume:	5.00
Injection Type:	Unknown		
Calibration Level:			
Instrument Method:	Bypass CH3OH (50-1000)		
Processing Method:	MS Quantitative	Dilution Factor:	1.0000
Injection Date/Time:	02/Jul/18 17:13	Sample Weight:	1.0000

Mass Spectrum

4-Br PC & 2-PyrSO2Na

8.800
8.790
7.820
7.817
7.805
7.803
7.790
7.787
7.556
7.540
7.287
7.281
7.270
7.266
7.256
6.867
6.653
6.639
6.624
6.614
6.611
6.605
6.594
6.579
5.322
3.724
3.719
3.229
3.211
3.199
3.176
3.133
3.126
3.113
3.104
3.087
3.077
3.004
2.994
2.979
2.965
2.703
2.692
2.684
2.669
1.293
0.109

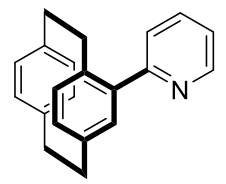


Current Data Parameters
NAME V-Mn-148 i
EXPNO 1
PROCNO 1

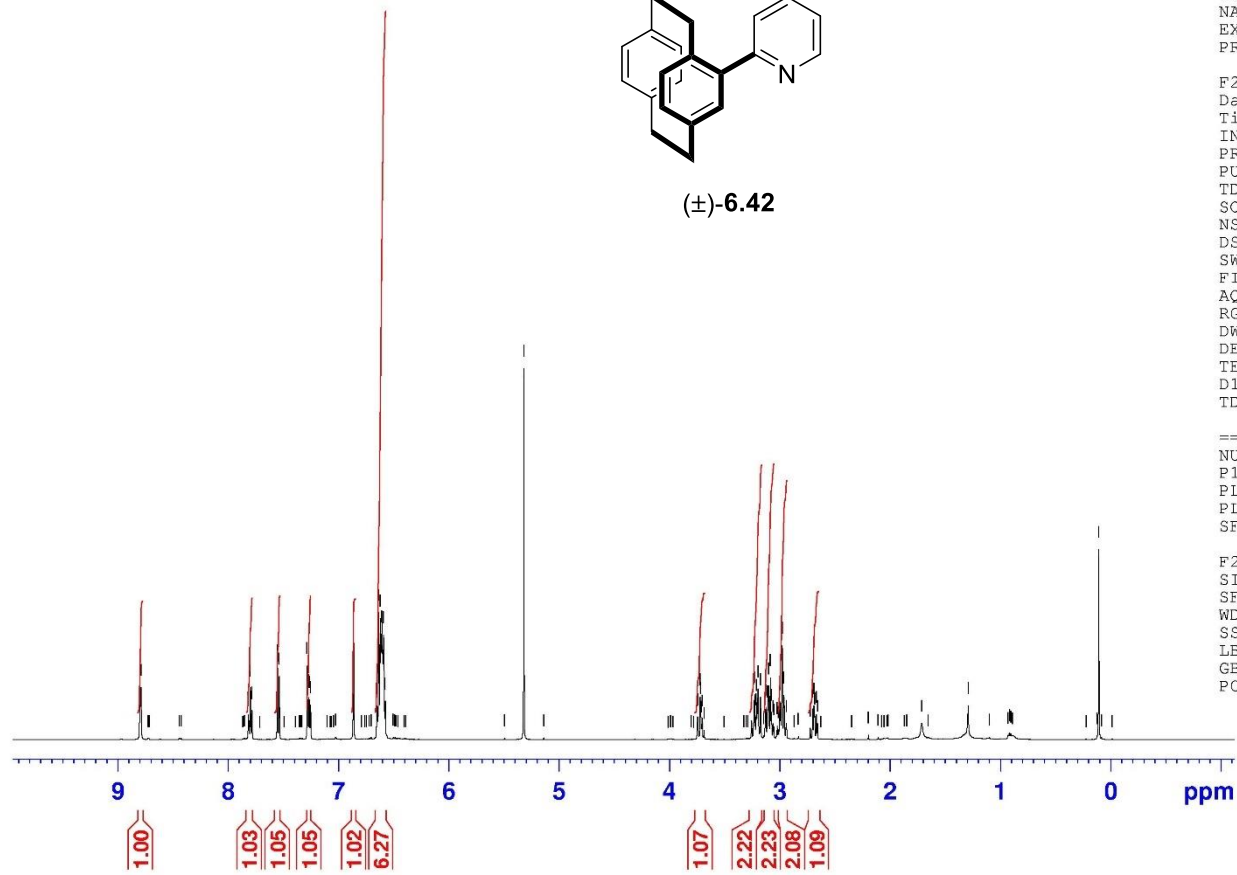
F2 - Acquisition Parameters
Date_ 20190620
Time 20.51
INSTRUM spect
PROBHD 5 mm PAQXI 1H/
PULPROG zg30
TD 65536
SOLVENT CDC13
NS 16
DS 2
SWH 10330.578 Hz
FIDRES 0.157632 Hz
AQ 3.1719425 sec
RG 71.8
DW 48.400 usec
DE 6.50 usec
TE 298.2 K
D1 1.00000000 sec
TD0 1

==== CHANNEL f1 =====
NUC1 1H
P1 9.50 usec
PL1 4.00 dB
PL1W 12.10000038 W
SFO1 500.1330885 MHz

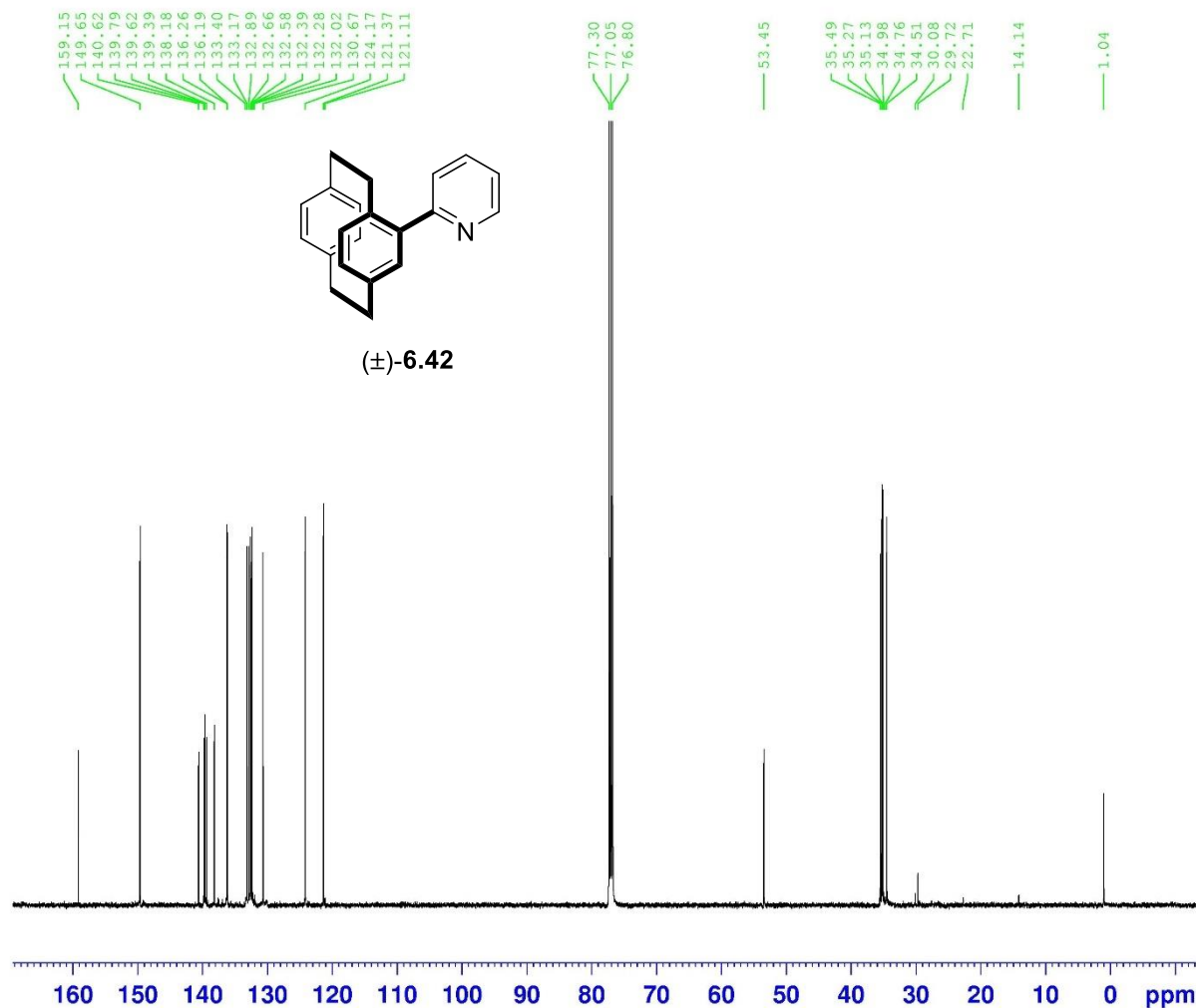
F2 - Processing parameters
SI 32768
SF 500.1300000 MHz
WDW EM
SSB 0
LB 0.30 Hz
GB 0
PC 1.00



(±)-6.42



4-Br PC & 2-PyrSO₂Na



Current Data Parameters
NAME V-Mn-148 1
EXPNO 2
PROCNO 1

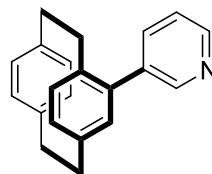
F2 - Acquisition Parameters
Date_ 20190621
Time 8.53
INSTRUM spect
PROBHD 5 mm PAQXI 1H/
PULPROG zgpg30
TD 65536
SOLVENT CDCl3
NS 13712
DS 4
SWH 30030.029 Hz
FIDRES 0.458222 Hz
AQ 1.0911744 sec
RG 32768
DW 16.650 usec
DE 6.50 usec
TE 298.2 K
D1 2.0000000 sec
D11 0.0300000 sec
TD0 1

===== CHANNEL f1 =====
NUC1 13C
P1 12.00 usec
PL1 -4.00 dB
PL1W 172.88230896 W
SFO1 125.7703643 MHz

===== CHANNEL f2 =====
CPDPRG[2] waltz16
NUC2 1H
PCPD2 80.00 usec
PL2 4.00 dB
PL12 22.51 dB
PL13 25.00 dB
PL2W 12.10000038 W
PL12W 0.17052394 W
PL13W 0.09611372 W
SFO2 500.1320005 MHz

F2 - Processing parameters
SI 32768
SF 125.7577890 MHz
WDW EM
SSB 0
LB 1.00 Hz
GB 0
PC 1.40

4-Br PC & 3-PyrSO2Na



(±)-6.52

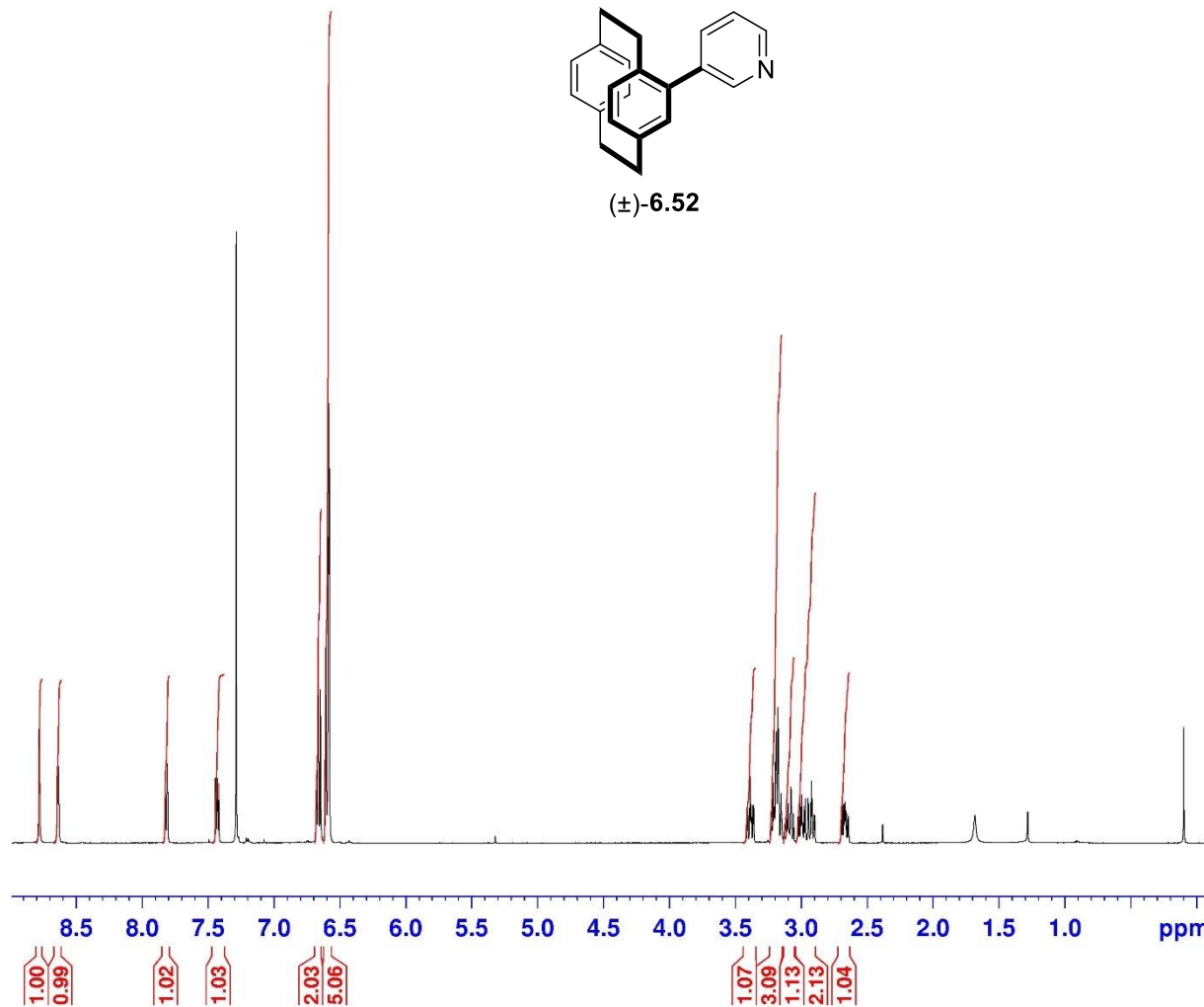


Current Data Parameters
NAME V-Mn-201 i
EXPNO 1
PROCNO 1

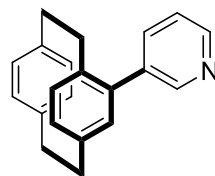
F2 - Acquisition Parameters
Date_ 20190825
Time 16.44
INSTRUM spect
PROBHD 5 mm PAQXI 1H/
PULPROG zg30
TD 65536
SOLVENT CDC13
NS 16
DS 2
SWH 10330.578 Hz
FIDRES 0.157632 Hz
AQ 3.1719425 sec
RG 128
DW 48.400 usec
DE 6.50 usec
TE 298.2 K
D1 1.00000000 sec
TD0 1

===== CHANNEL f1 =====
NUC1 1H
P1 9.50 usec
PL1 4.00 dB
PL1W 12.10000038 W
SFO1 500.1330885 MHz

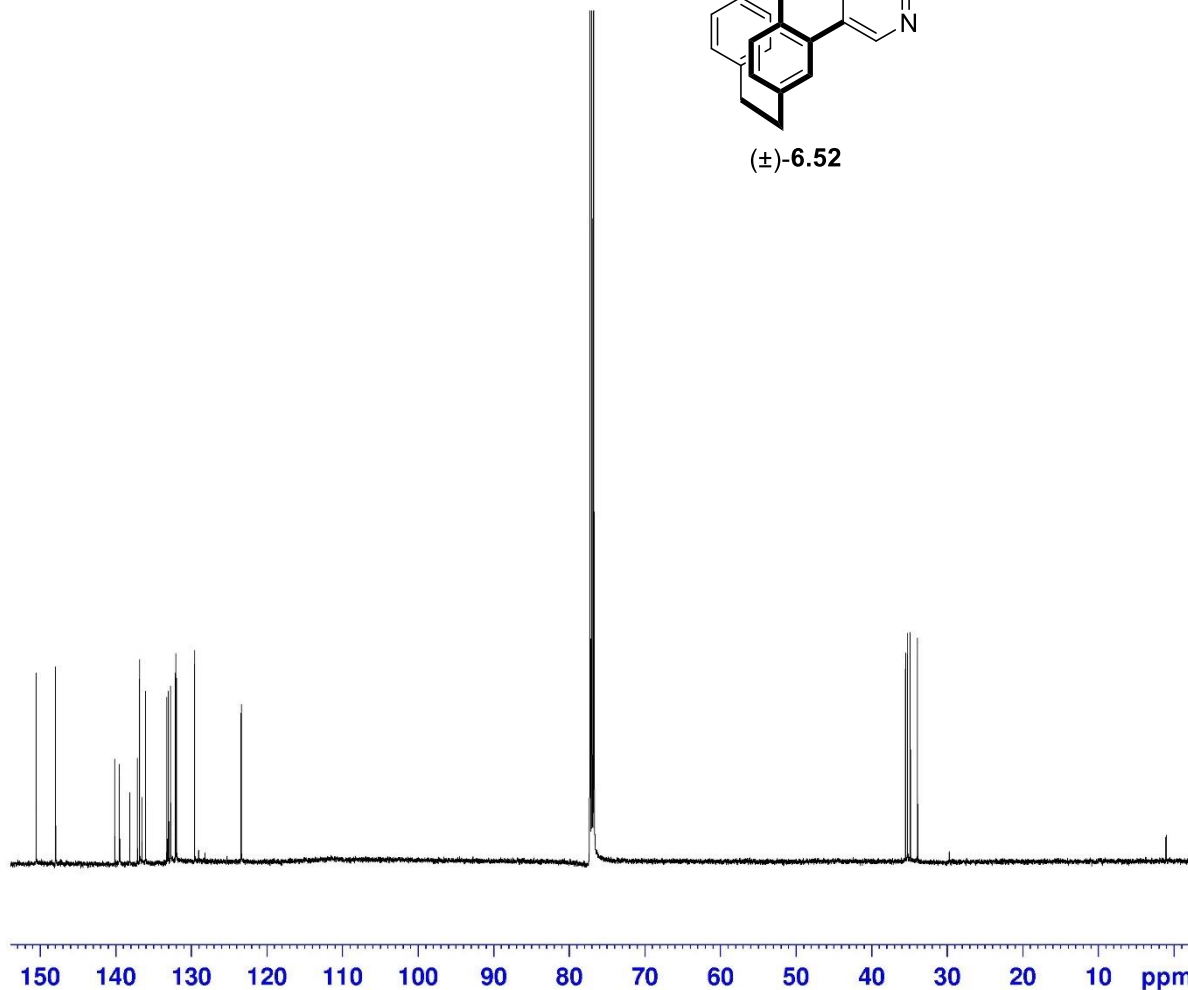
F2 - Processing parameters
SI 32768
SF 500.1300000 MHz
WDW EM
SSB 0
LB 0.30 Hz
GB 0
PC 1.00



¹³C : 4-Br PC & 3-PyrSO₂Na



(±)-6.52



Current Data Parameters
NAME V-Mn-201 i
EXPNO 2
PROCNO 1

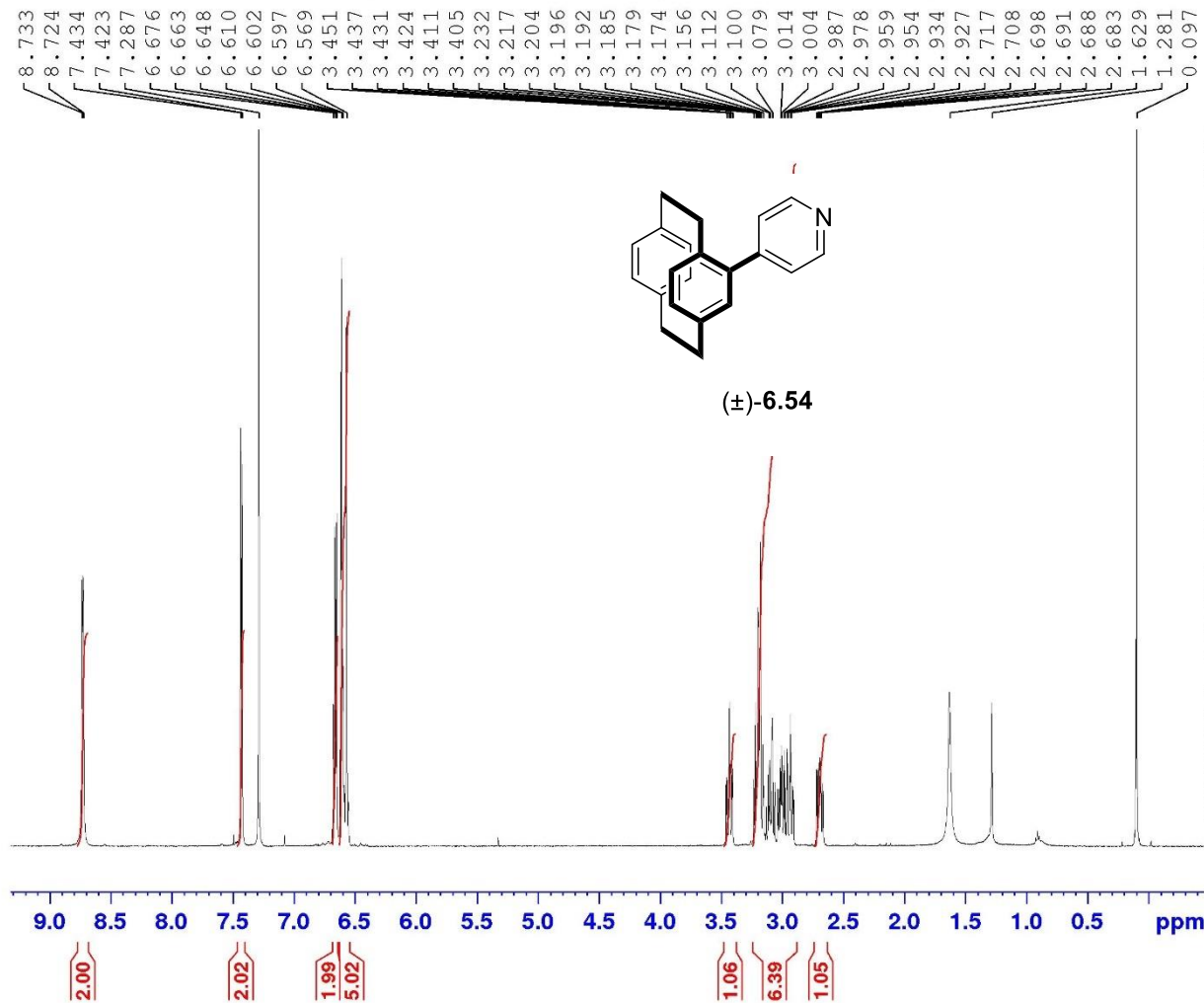
F2 - Acquisition Parameters
Date_ 20190826
Time 7.08
INSTRUM spect
PROBHD 5 mm PAQXI 1H/
PULPROG zgpg30
TD 65536
SOLVENT CDCl3
NS 16384
DS 4
SWH 30030.029 Hz
FIDRES 0.458222 Hz
AQ 1.0911744 sec
RG 32768
DW 16.650 usec
DE 6.50 usec
TE 298.2 K
D1 2.00000000 sec
D11 0.03000000 sec
TDO 1

=====
CHANNEL f1
NUC1 13C
P1 12.00 usec
PL1 -4.00 dB
PL1W 172.88230896 W
SFO1 125.7703643 MHz

=====
CHANNEL f2
CPDPRG[2] waltz16
NUC2 1H
PCPD2 80.00 usec
PL2 4.00 dB
PL12 22.51 dB
PL13 25.00 dB
PL2W 12.10000038 W
PL12W 0.17052394 W
PL13W 0.09611372 W
SFO2 500.1320005 MHz

F2 - Processing parameters
SI 32768
SF 125.7577890 MHz
WDW EM
SSB 0
LB 1.00 Hz
GB 0
PC 1.40

1H : 4-Br PC & 4-pyrSo2Na pd(OAc)2 20 mol%, Pcy3 80%, K2CO3 (3 eq)



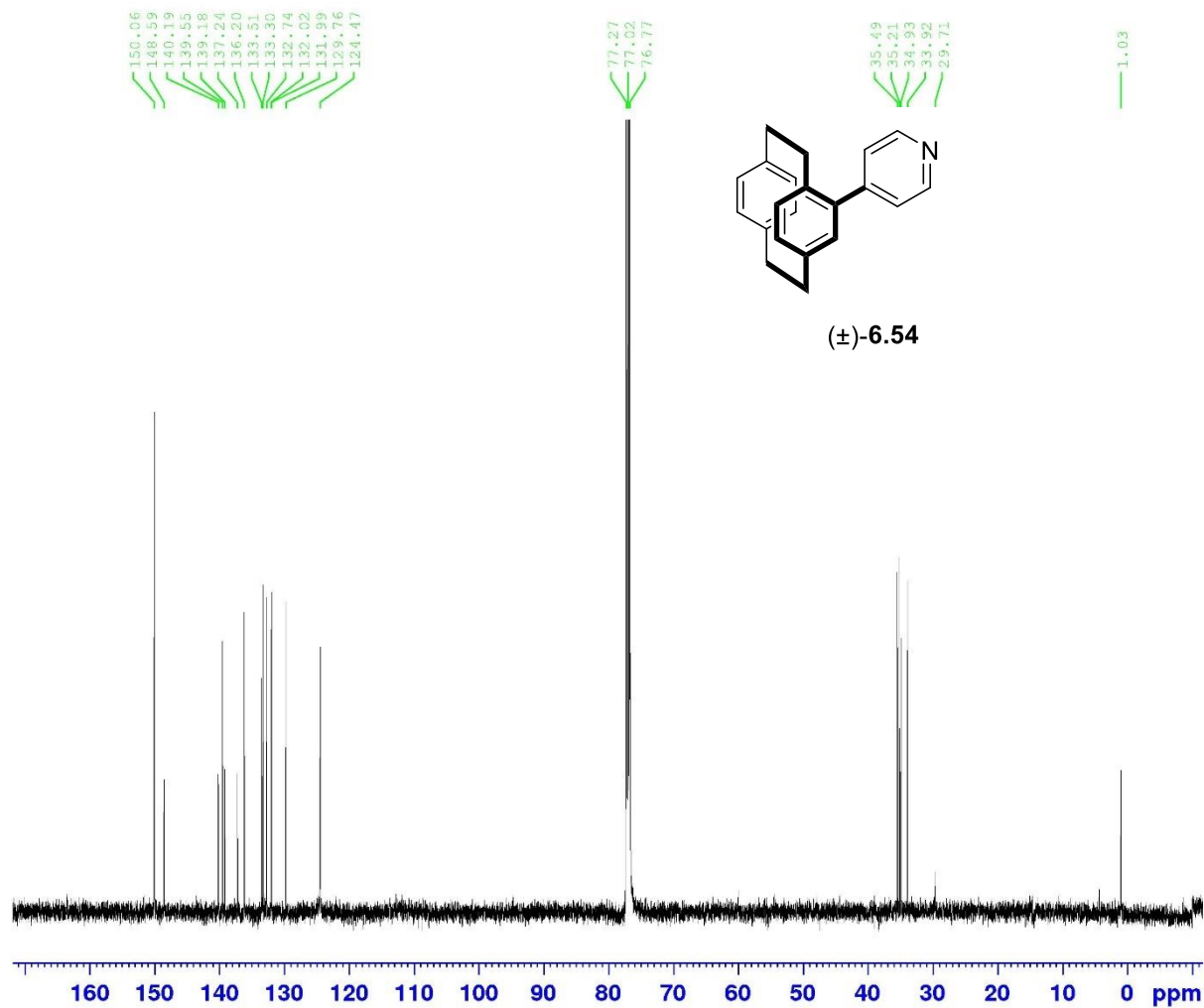
Current Data Parameters
NAME V-Mn-222 main
EXPNO 1
PROCNO 1

F2 - Acquisition Parameters
Date_ 20200305
Time 18.33
INSTRUM spect
PROBHD 5 mm PAQXI 1H/
PULPROG zg30
TD 65536
SOLVENT CDC13
NS 16
DS 2
SWH 10330.578 Hz
FIDRES 0.157632 Hz
AQ 3.1719425 sec
RG 362
DW 48.400 usec
DE 6.50 usec
TE 297.1 K
D1 1.00000000 sec
TD0 1

==== CHANNEL f1 =====
NUC1 1H
P1 9.50 usec
PL1 4.00 dB
PL1W 12.10000038 W
SF01 500.1330885 MHz

F2 - Processing parameters
SI 32768
SF 500.1300000 MHz
WDW EM
SSB 0
LB 0.30 Hz
GB 0
PC 1.00

¹³C: 4-Br PC & 4-pyrSo2Na pd(OAc)2 20 mol%, Pcy3 80%, K2CO3 (3 eq)



Current Data Parameters
 NAME V-Mn-222 main
 EXPNO 2
 PROCNO 1

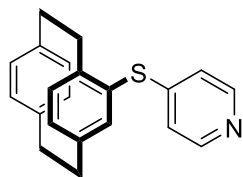
F2 - Acquisition Parameters
 Date_ 20200306
 Time_ 8.59
 INSTRUM spect
 PROBHD 5 mm PAQXI 1H/
 PULPROG zgpg30
 TD 65536
 SOLVENT CDC13
 NS 16384
 DS 4
 SWH 30030.029 Hz
 FIDRES 0.458222 Hz
 AQ 1.0911744 sec
 RG 32768
 DW 16.650 usec
 DE 6.50 usec
 TE 296.6 K
 D1 2.0000000 sec
 D11 0.0300000 sec
 TD0 1

===== CHANNEL f1 =====
 NUC1 13C
 P1 12.00 usec
 PL1 -4.00 dB
 PL1W 172.88230896 W
 SP01 125.7703643 MHz

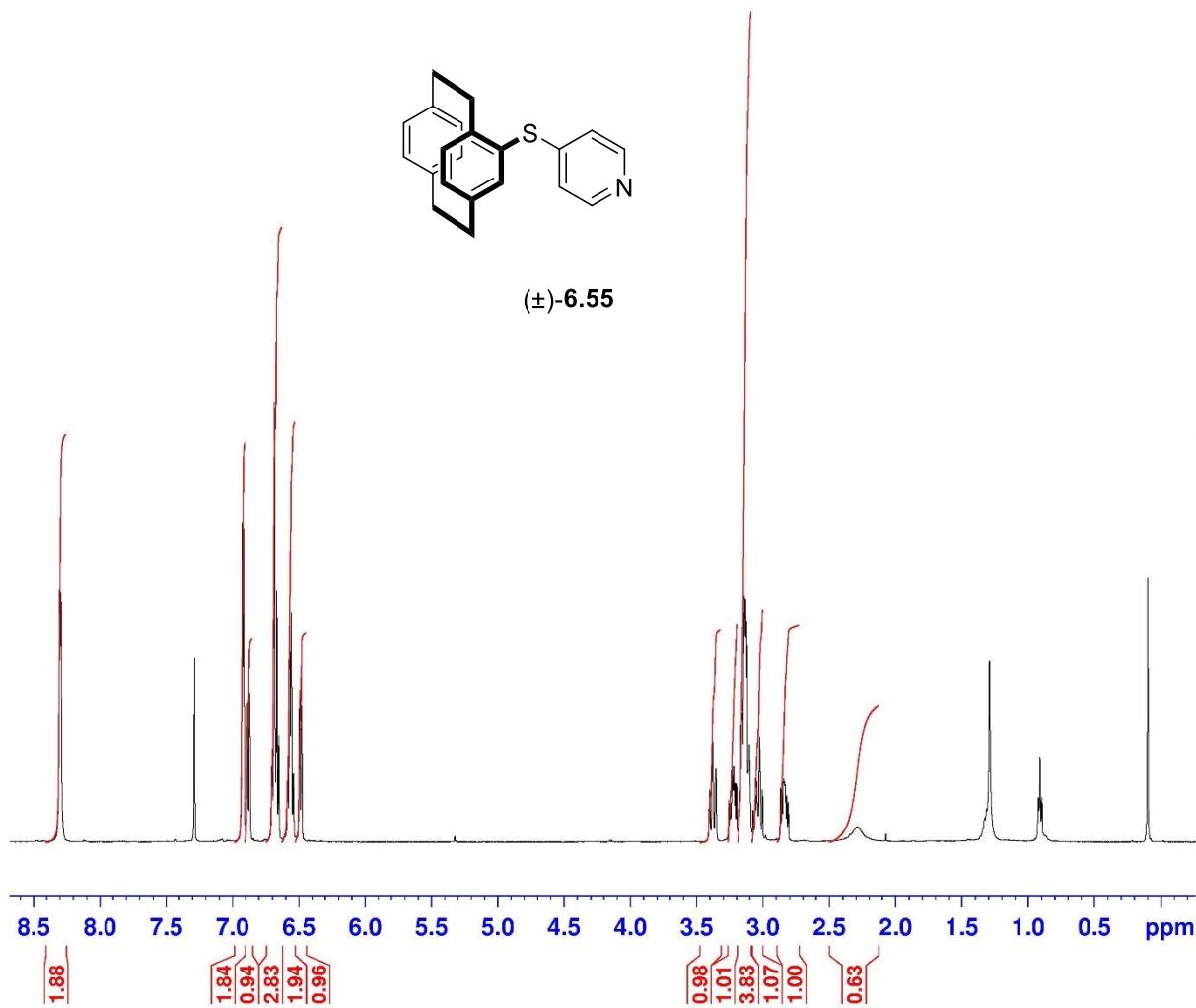
===== CHANNEL f2 =====
 CPDPRG[2] waltz16
 NUC2 1H
 PCPD2 80.00 usec
 PL2 4.00 dB
 PL12 22.51 dB
 PL13 25.00 dB
 PL2W 12.10000038 W
 PL12W 0.17052394 W
 PL13W 0.09611372 W
 SP02 500.1320005 MHz

F2 - Processing parameters
 SI 32768
 SF 125.7577890 MHz
 WDW EM
 SSB 0
 LB 1.00 Hz
 GB 0
 PC 1.40

4-Br [2.2]PC & 4-pyrSH



(±)-6.55



Current Data Parameters
NAME V-Mn-155 i
EXPNO 1
PROCNO 1

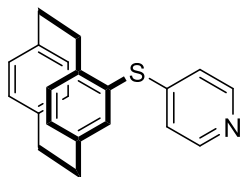
F2 - Acquisition Parameters
Date_ 20190619
Time 20.53
INSTRUM spect
PROBHD 5 mm PAQXI 1H/
PULPROG zg30
TD 65536
SOLVENT CDCl3
NS 16
DS 2
SWH 10330.578 Hz
FIDRES 0.157632 Hz
AQ 3.1719425 sec
RG 114
DW 48.400 usec
DE 6.50 usec
TE 298.2 K
D1 1.00000000 sec
TD0 1

===== CHANNEL f1 =====
NUC1 1H
P1 9.50 usec
PL1 4.00 dB
PL1W 12.10000038 W
SFO1 500.1330885 MHz

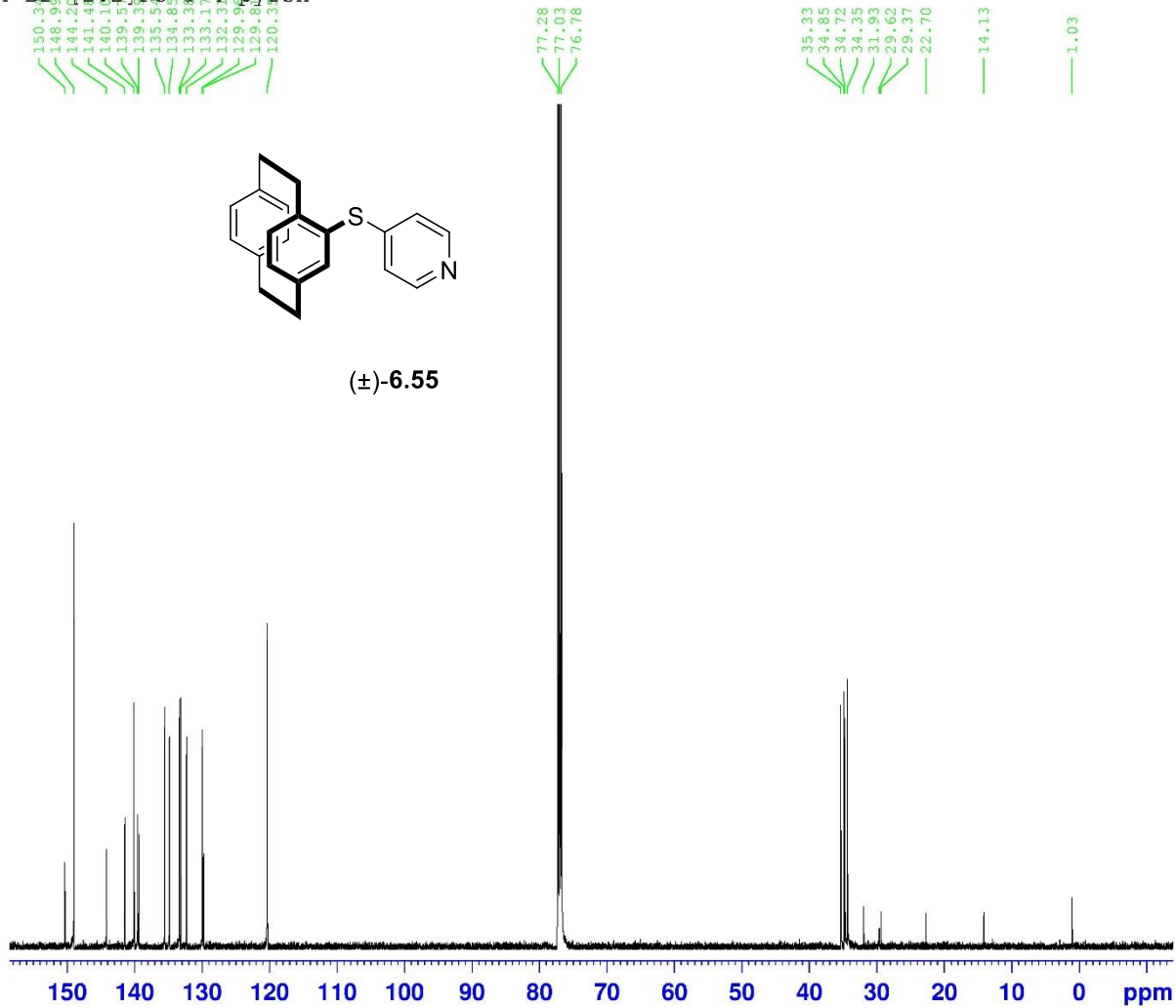
F2 - Processing parameters
SI 32768
SF 500.1300000 MHz
WDW EM
SSB 0
LB 0.30 Hz
GB 0
PC 1.00

4-Br-[2,2]PC & 4-pyrSH

150.31
148.97
144.24
141.44
140.11
139.55
139.34
135.51
134.85
133.38
133.17
132.31
129.96
129.84
120.31



(±)-6.55



Current Data Parameters
NAME V-Mn-155 i
EXPNO 2
PROCNO 1

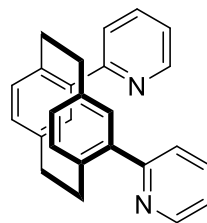
F2 - Acquisition Parameters
Date_ 20190620
Time 8.35
INSTRUM spect
PROBHD 5 mm PAQXI 1H/
PULPROG zgpg30
TD 65536
SOLVENT CDCl3
NS 13134
DS 4
SWH 30030.029 Hz
FIDRES 0.458222 Hz
AQ 1.0911744 sec
RG 32768
DW 16.650 usec
DE 6.50 usec
TE 298.2 K
D1 2.0000000 sec
D11 0.0300000 sec
TD0 1

===== CHANNEL f1 =====
NUC1 13C
P1 12.00 usec
PL1 -4.00 dB
PL1W 172.88230896 W
SFO1 125.7703643 MHz

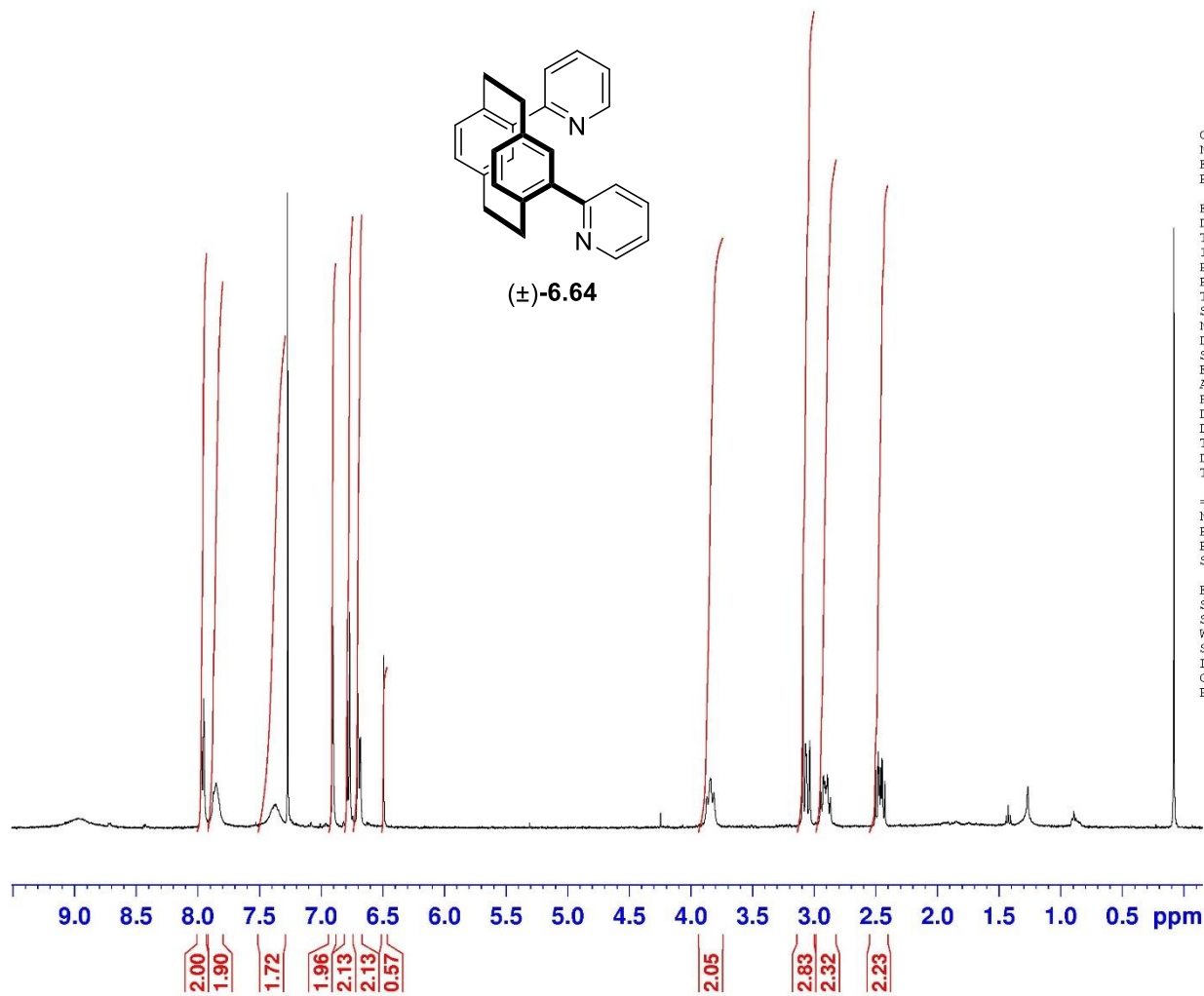
===== CHANNEL f2 =====
CPDPRG[2] waltz16
NUC2 1H
PCPD2 80.00 usec
PL2 4.00 dB
PL12 22.51 dB
PL13 25.00 dB
PL2W 12.10000038 W
PL12W 0.17052394 W
PL13W 0.09611372 W
SFO2 500.1320005 MHz

F2 - Processing parameters
SI 32768
SF 125.7577890 MHz
WDW EM
SSB 0
LB 1.00 Hz
GB 0
PC 1.40

Pseudoortho dibromo PC & 2-PyrSO₂Na (Pd:1) (20:80), K₂CO₃ (3 eq.)



(±)-6.64



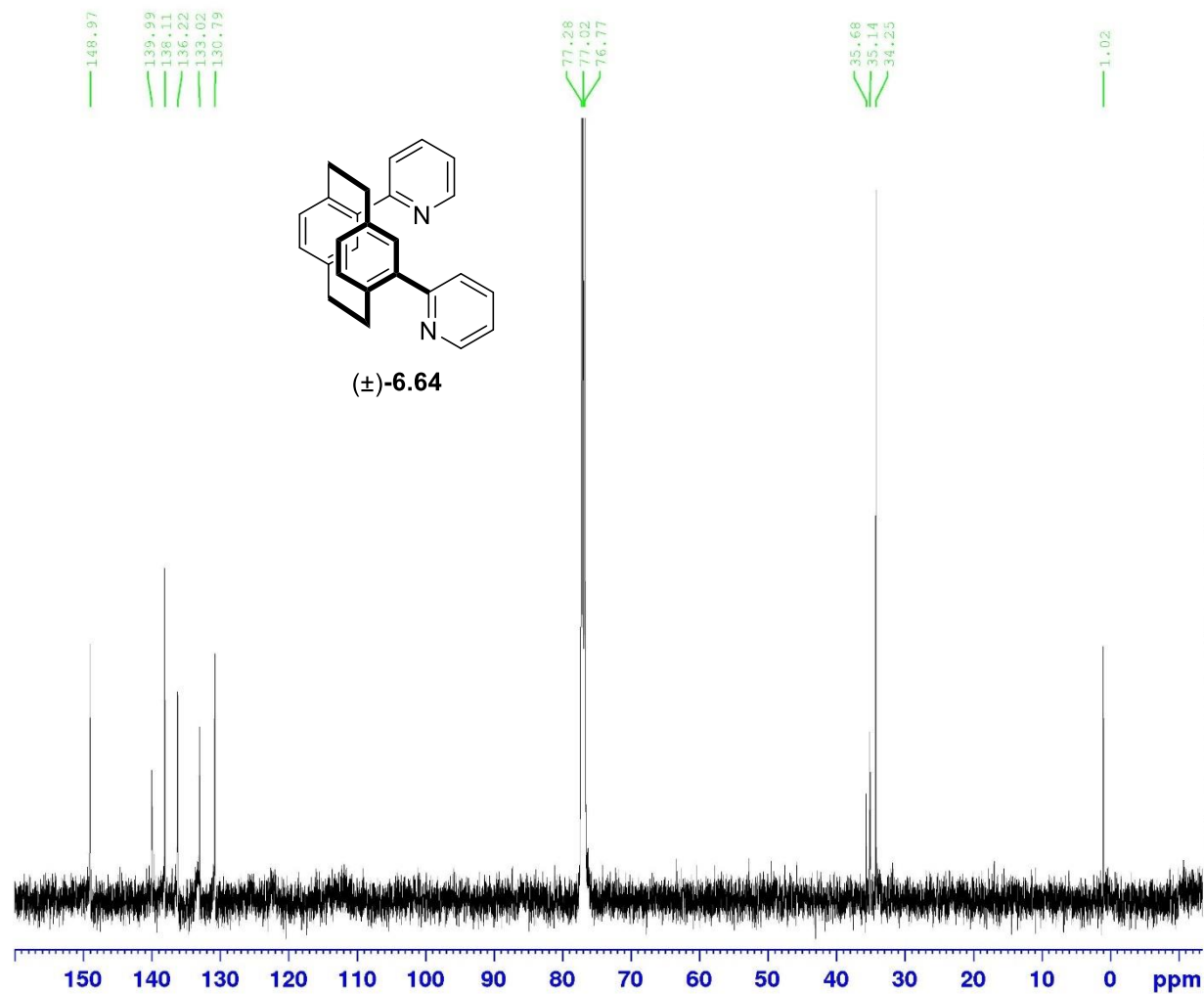
Current Data Parameters
NAME V-Mn-216III 2nd fraction
EXPI0 1
PROCNO 1

F2 - Acquisition Parameters
Date_ 20190906
Time 18.27
INSTRUM spect
PROBHD 5 mm Multinucl
PULPROG zg30
TD 65536
SOLVENT CDC13
NS 16
DS 2
SWH 8278.146 Hz
FIDRES 0.126314 Hz
AQ 3.9583745 sec
RG 1625.5
DW 60.400 usec
DE 6.00 usec
TE 300.0 K
D1 1.00000000 sec
TDO 1

===== CHANNEL f1 =====
NUC1 1H
P1 10.00 usec
PL1 3.80 dB
SFO1 400.1324710 MHz

F2 - Processing parameters
SI 32768
SF 400.1300000 MHz
WDW EM
SSB 0
LB 0.30 Hz
GB 0
PC 1.00

V-Mn-216 III 2nd fraction



Current Data Parameters
NAME V-Mn-216 III 2nd fraction
EXPNO 2
PROCNO 1

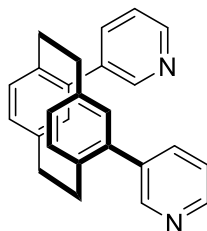
F2 - Acquisition Parameters
Date_ 20200320
Time 8.45
INSTRUM spect
PROBHD 5 mm PAQXI 1H/
PULPROG zgpg30
TD 65536
SOLVENT CDCL3
NS 16384
DS 4
SWH 30030.029 Hz
FIDRES 0.458222 Hz
AQ 1.091744 sec
RG 32768
DW 16.650 usec
DE 6.50 usec
TE 296.7 K
D1 2.0000000 sec
D11 0.0300000 sec
TD0 1

===== CHANNEL f1 =====
NUC1 13C
P1 12.00 usec
PL1 -4.00 dB
PL1W 172.88230896 W
SFO1 125.7703643 MHz

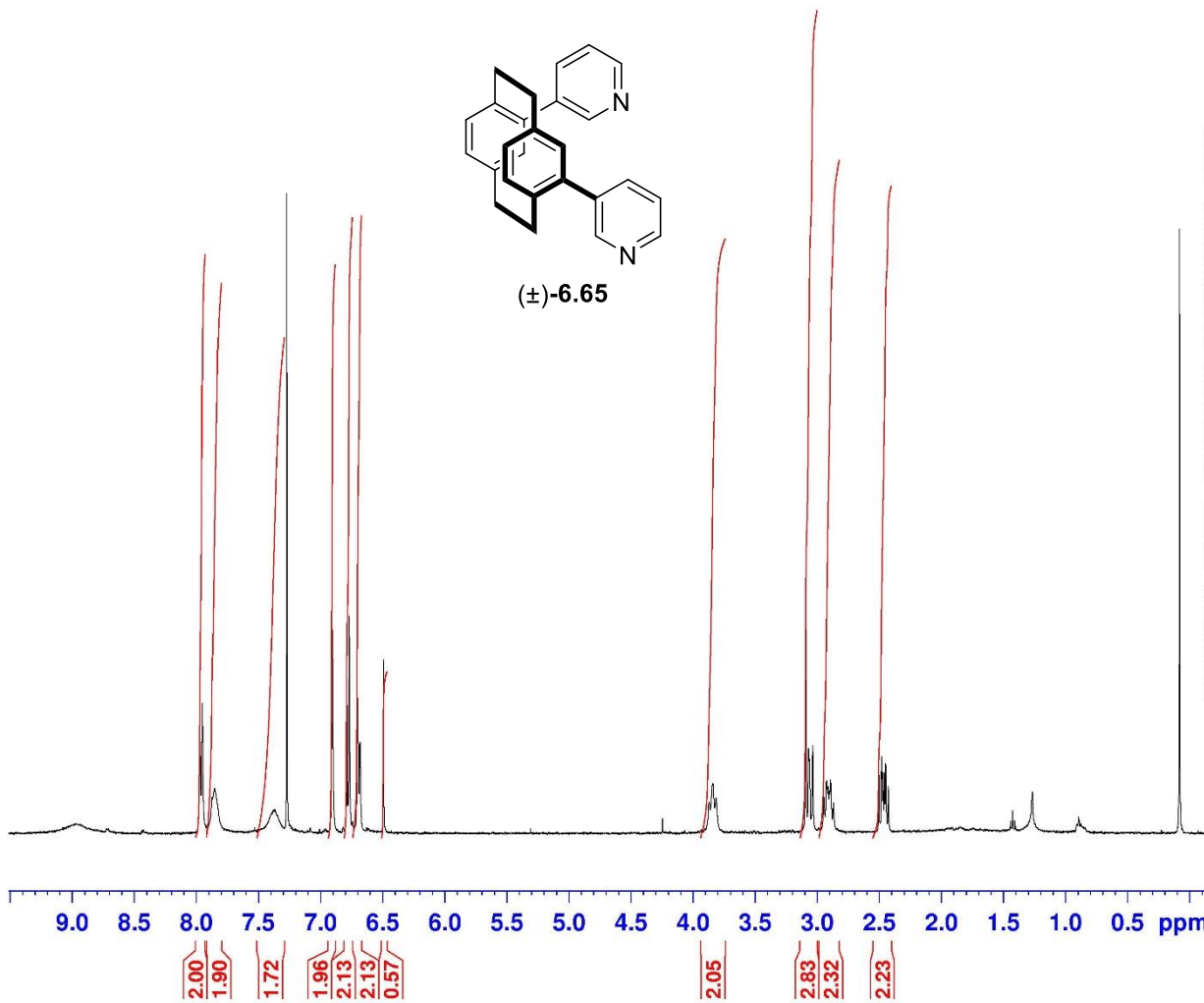
===== CHANNEL f2 =====
CPDPRG[2] waltz16
NUC2 1H
PCPD2 80.00 usec
PL2 4.00 dB
PL12 22.51 dB
PL13 25.00 dB
PL2W 12.10000038 W
PL12W 0.17052394 W
PL13W 0.09611372 W
SFO2 500.1320005 MHz

F2 - Processing parameters
SI 32768
SF 125.7577890 MHz
WDW EM
SSB 0
LB 1.00 Hz
GB 0
PC 1.40

Pseudoortho dibromo PC & 2-PyrSO₂Na (Pd:1) (20:80), K₂CO₃ (3 eq.)



(±)-6.65



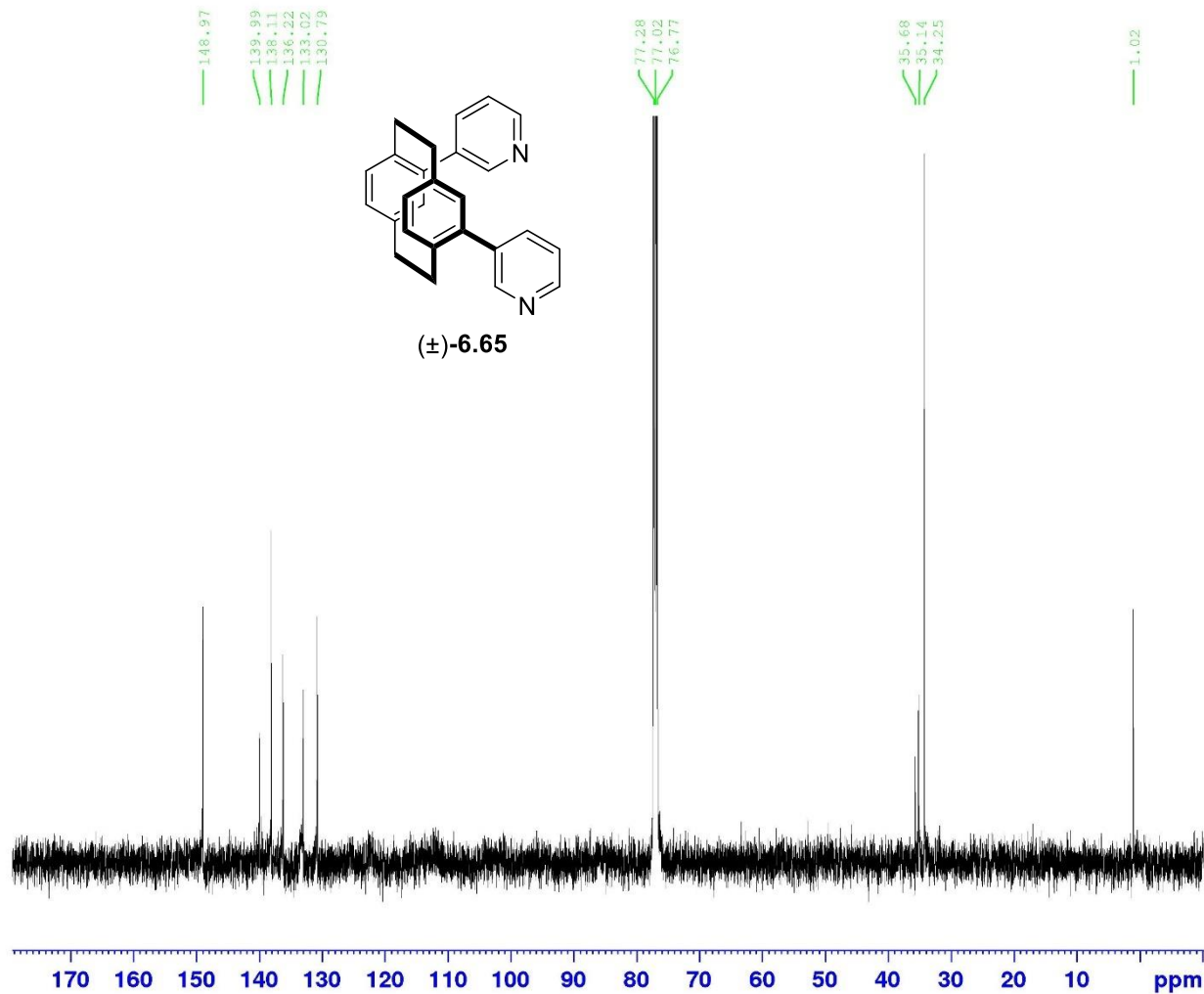
Current Data Parameters
NAME V-Mn-216III 2nd fraction
EXPIRO 1
PROCNO 1

F2 - Acquisition Parameters
Date_ 20190906
Time 18.27
INSTRUM spect
PROBHD 5 mm Multinucl
PULPROG zg30
TD 65536
SOLVENT CDC13
NS 16
DS 2
SWH 8278.146 Hz
FIDRES 0.126314 Hz
AQ 3.9583745 sec
RG 1625.5
DW 60.400 usec
DE 6.00 usec
TE 300.0 K
D1 1.00000000 sec
TDO 1

===== CHANNEL f1 =====
NUC1 1H
P1 10.00 usec
PL1 3.80 dB
SFO1 400.1324710 MHz

F2 - Processing parameters
SI 32768
SF 400.1300000 MHz
WDW EM
SSB 0
LB 0.30 Hz
GB 0
PC 1.00

V-Mn-216 III 2nd fraction



Current Data Parameters
NAME V-Mn-216 III 2nd fraction
EXPNO 2
PROCNO 1

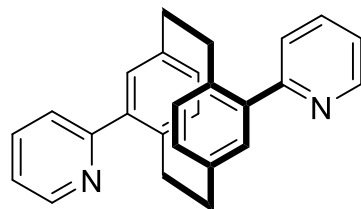
F2 - Acquisition Parameters
Date_ 20200320
Time 8.43
INSTRUM spect
PROBHD 5 mm PAQXI 1H/
PULPROG zgpg30
TD 65336
SOLVENT CDCl3
NS 16384
DS 4
SWH 30030.029 Hz
FIDRES 0.458222 Hz
AQ 1.0911744 sec
RG 32768
DW 16.650 usec
DE 6.50 usec
TE 296.7 K
D1 2.0000000 sec
D11 0.0300000 sec
TDC 1

----- CHANNEL f1 -----
NUC1 13C
P1 12.00 usec
PL1 -4.00 dB
PL1W 172.88230896 W
SFO1 125.7703643 MHz

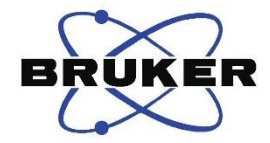
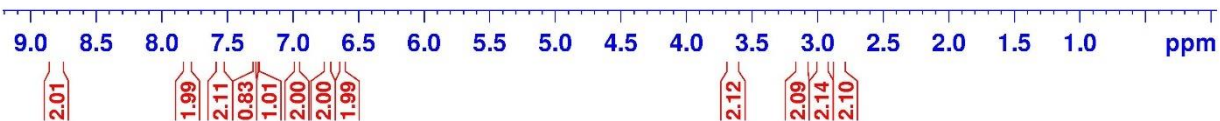
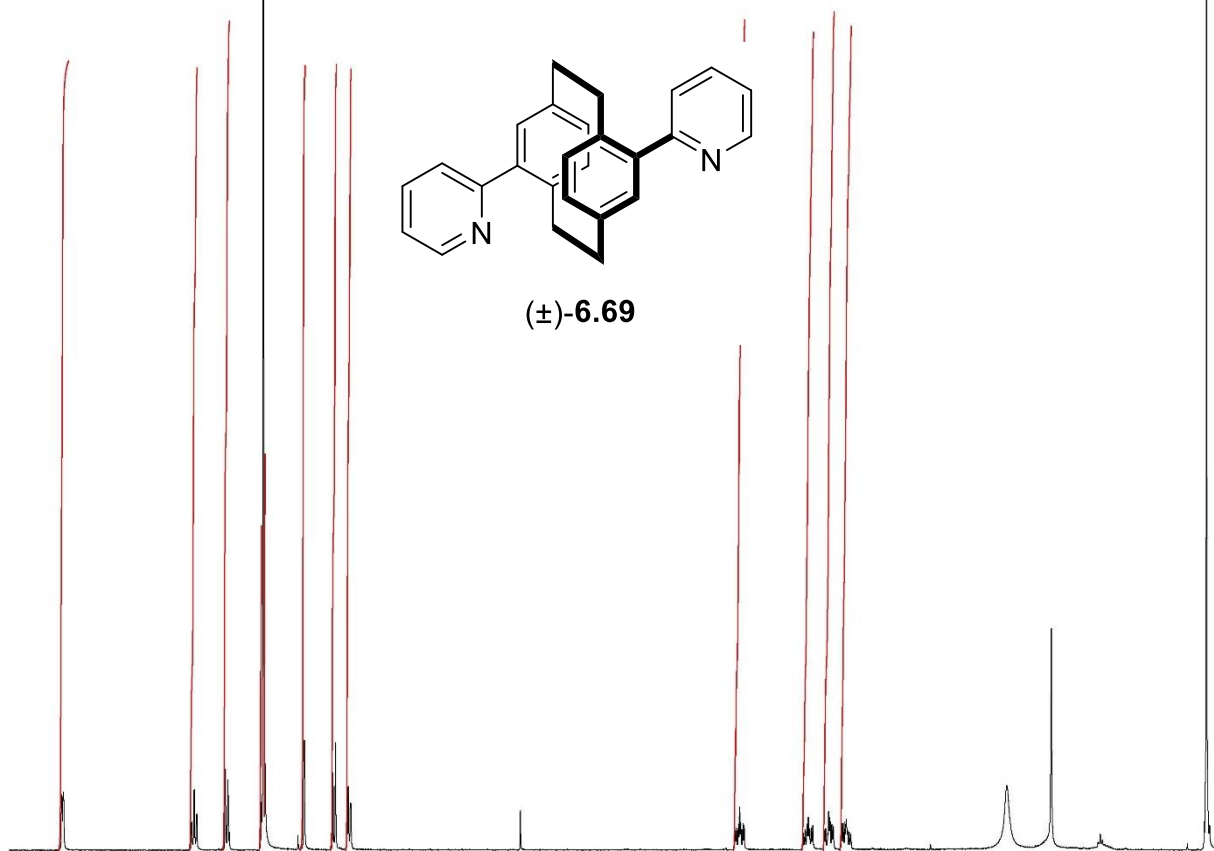
----- CHANNEL f2 -----
CPDPRG[2] waltz16
NUC2 1H
PCPD2 80.00 usec
PL2 4.00 dB
PL12 22.51 dB
PL13 25.00 dB
PL2W 12.10000038 W
PL12W 0.17052394 W
PL13W 0.09611372 W
SFO2 500.1320005 MHz

F2 - Processing parameters
SI 32768
SF 125.7577890 MHz
WDW EM
SSB 0
LB 1.00 Hz
GB 0
PC 1.40

pseudoparadibromo & 2-pyrSO2Na : purified again



(±)-6.69



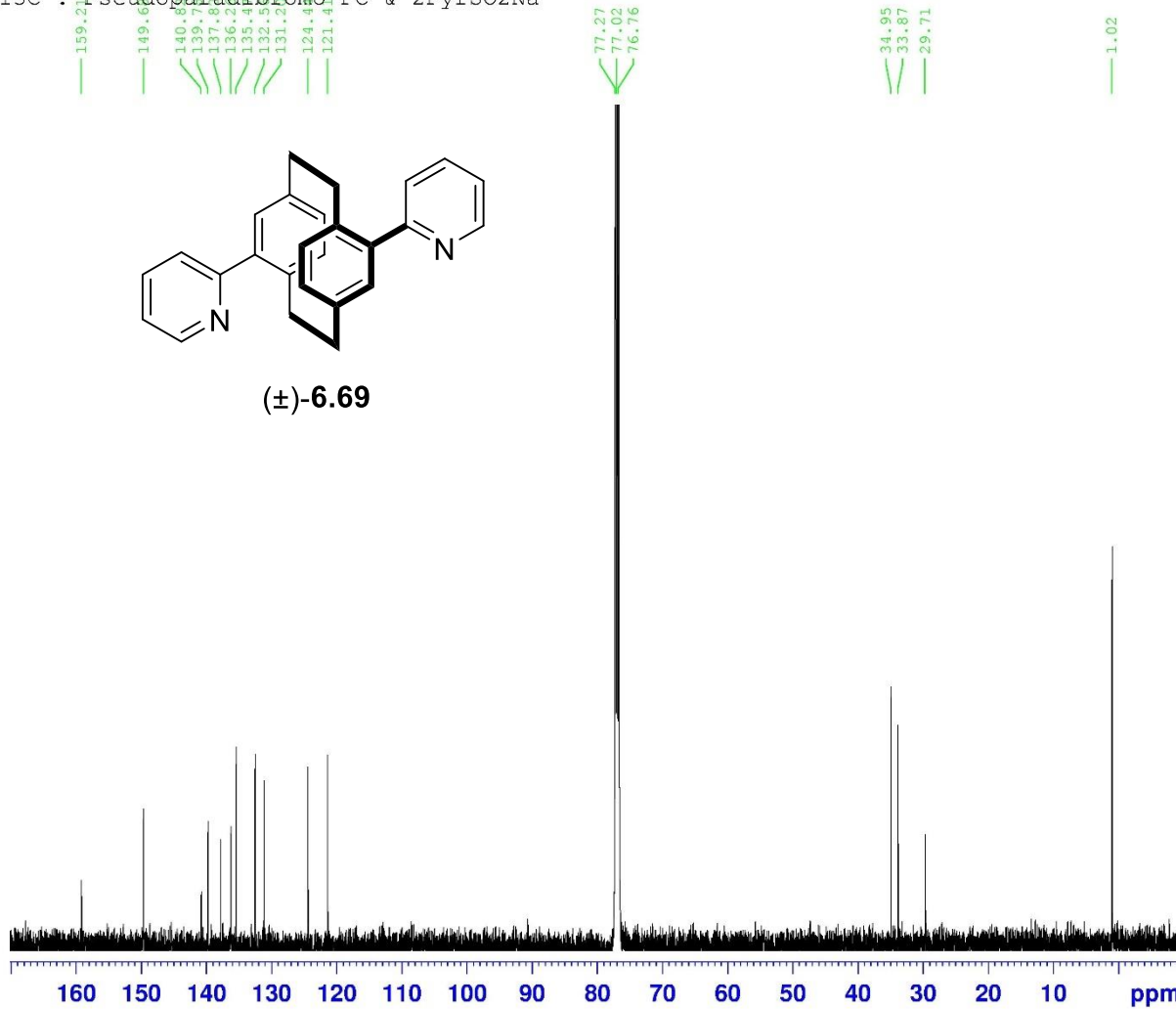
Current Data Parameters
NAME V-Mn-180 main spot
EXPNO 1
PROCNO 1

F2 - Acquisition Parameters
Date_ 20190811
Time 20.18
INSTRUM spect
PROBHD 5 mm Multinucl
PULPROG zg30
TD 65536
SOLVENT CDCl3
NS 16
DS 2
SWH 8278.146 Hz
FIDRES 0.126314 Hz
AQ 3.9583745 sec
RG 574.7
DW 60.400 usec
DE 6.00 usec
TE 300.0 K
D1 1.00000000 sec
TD0 1

===== CHANNEL f1 =====
NUC1 1H
P1 10.00 usec
PL1 3.80 dB
SFO1 400.1324710 MHz

F2 - Processing parameters
SI 32768
SF 400.1300000 MHz
WDW EM
SSB 0
LB 0.30 Hz
GB 0
PC 1.00

¹³C : Pseudoparadibromo PC & 2PyrSO₂Na



Current Data Parameters
NAME Desktop
EXPNO 2
PROCNO 1

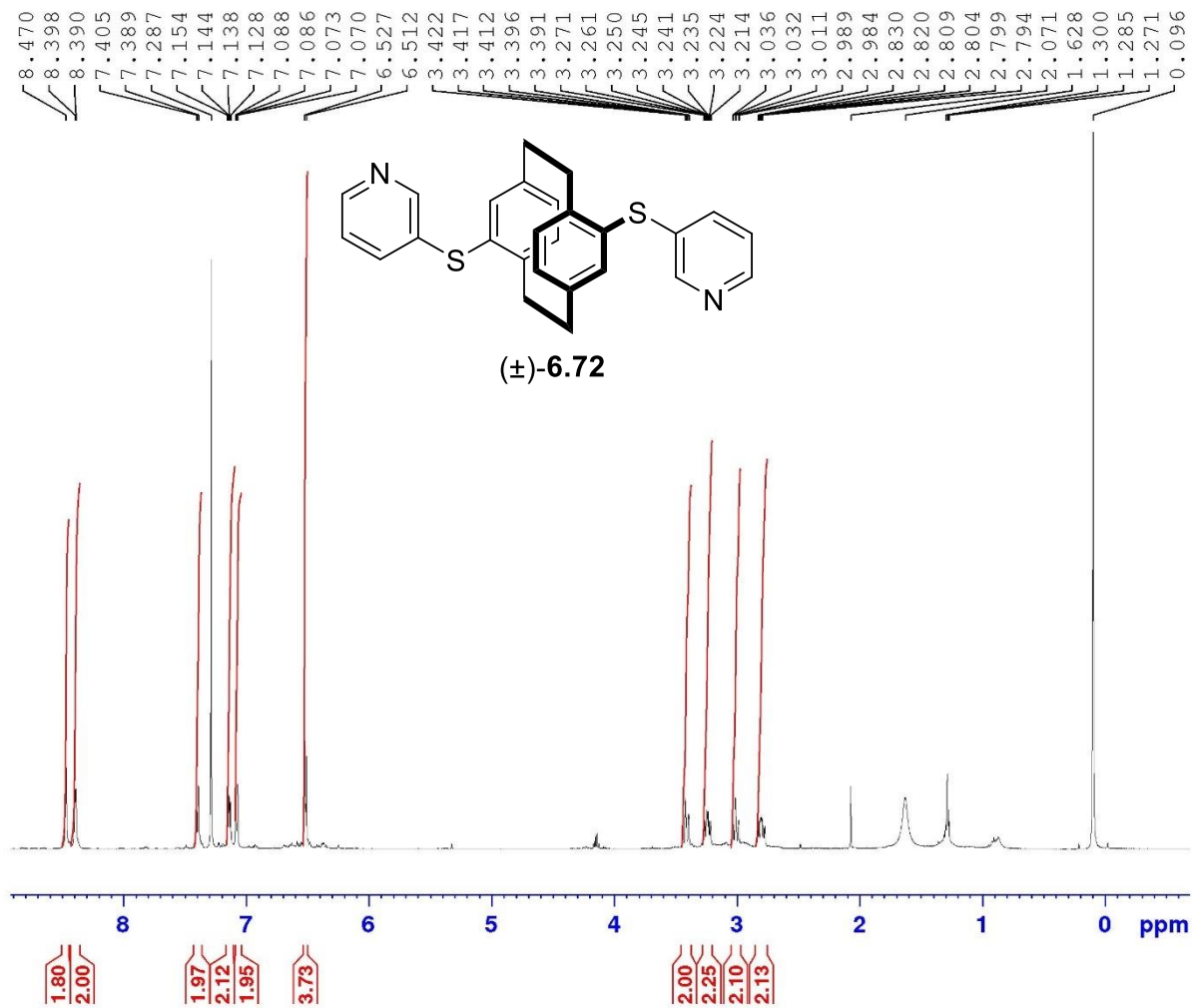
F2 - Acquisition Parameters
Date_ 20190919
Time 8.47
INSTRUM spect
PROBHD 5 mm PAQXI 1H/
PULPROG zgpg30
TD 65536
SOLVENT CDCl₃
NS 14990
DS 4
SWH 30030.029 Hz
FIDRES 0.458222 Hz
AQ 1.0911744 sec
RG 32768
DW 16.650 usec
DE 6.50 usec
TE 298.0 K
D1 2.0000000 sec
D11 0.0300000 sec
TD0 1

===== CHANNEL f1 =====
NUC1 13C
P1 12.00 usec
PL1 -4.00 dB
PL1W 172.88230896 W
SFO1 125.7703643 MHz

===== CHANNEL f2 =====
CPDPRG[2] waltz16
NUC2 1H
PCPD2 80.00 usec
PL2 4.00 dB
PL12 22.51 dB
PL13 25.00 dB
PL2W 12.10000038 W
PL12W 0.17052394 W
PL13W 0.09611372 W
SFO2 500.1320005 MHz

F2 - Processing parameters
SI 32768
SF 125.7577890 MHz
WDW EM
SSB 0
LB 1.00 Hz
GB 0
PC 1.40

Pseudoparadirbomo PC & 3-PyrSO₂Na (4 eq.) Pd:1 (2:8)



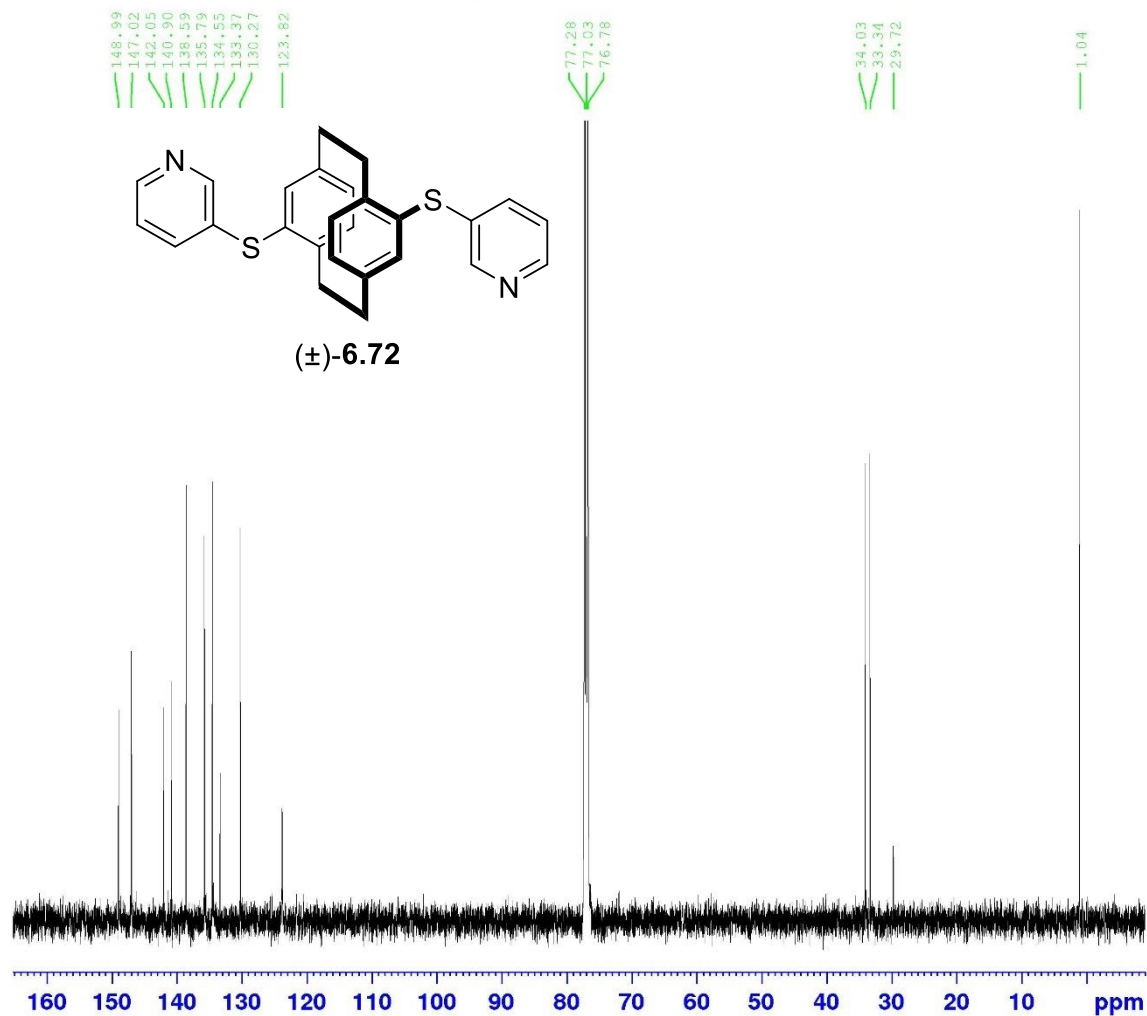
Current Data Parameters
NAME VI-Mn-44 ii
EXPNO 1
PROCNO 1

F2 - Acquisition Parameters
Date_ 20200127
Time 8.59
INSTRUM spect
PROBHD 5 mm PAQXI 1H/
PULPROG zg30
TD 65536
SOLVENT CDCl3
NS 16
DS 2
SWH 10330.578 Hz
FIDRES 0.157632 Hz
AQ 3.1719425 sec
RG 256
DW 48.400 usec
DE 6.50 usec
TE 298.2 K
D1 1.00000000 sec
TDO 1

----- CHANNEL f1 -----
NUC1 1H
P1 9.50 usec
PL1 4.00 dB
PL1W 12.10000038 W
SFO1 500.1330885 MHz

F2 - Processing parameters
SI 32768
SF 500.1300000 MHz
WDW EM
SSB 0
LB 0.30 Hz
GB 0
PC 1.00

¹³C : Pseudoparadirbomo PC & 3-PyrSO₂Na (4 eq.) Pd:1 (2:8)



Current Data Parameters
 NAME VI-Mn-44 ii
 EXPNO 3
 PROCNO 1

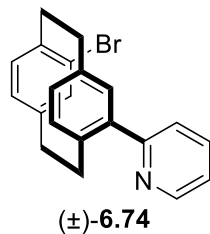
F2 - Acquisition Parameters
 Date_ 20200529
 Time 6.36
 INSTRUM spect
 PROBHD 5 mm PAQXI 1H/
 PULPROG zgpg30
 TD 65536
 SOLVENT CDCl3
 NS 16384
 DS 4
 SWH 30030.029 Hz
 FIDRES 0.458222 Hz
 AQ 1.0911744 sec
 RG 32768
 DW 16.650 usec
 DE 6.50 usec
 TE 293.9 K
 D1 2.0000000 sec
 D11 0.0300000 sec
 TD0 1

===== CHANNEL f1 =====
 NUC1 ¹³C
 P1 12.00 usec
 PL1 -4.00 dB
 PL1W 172.88230896 W
 SF01 125.7703643 MHz

===== CHANNEL f2 =====
 CPDPRG[2] waltz16
 NUC2 ¹H
 PCPD2 80.00 usec
 PL2 4.00 dB
 PL12 22.51 dB
 PL13 23.00 dB
 PL2W 12.10000038 W
 PL12W 0.17052394 W
 PL13W 0.09611372 W
 SF02 500.1320005 MHz

F2 - Processing parameters
 SI 32768
 SF 125.7577890 MHz
 WDW EM
 SSB 0
 LB 1.00 Hz
 GB 0
 PC 1.40

Pseudoorthodibromo & 2-Pyr Pd:L (1:4)

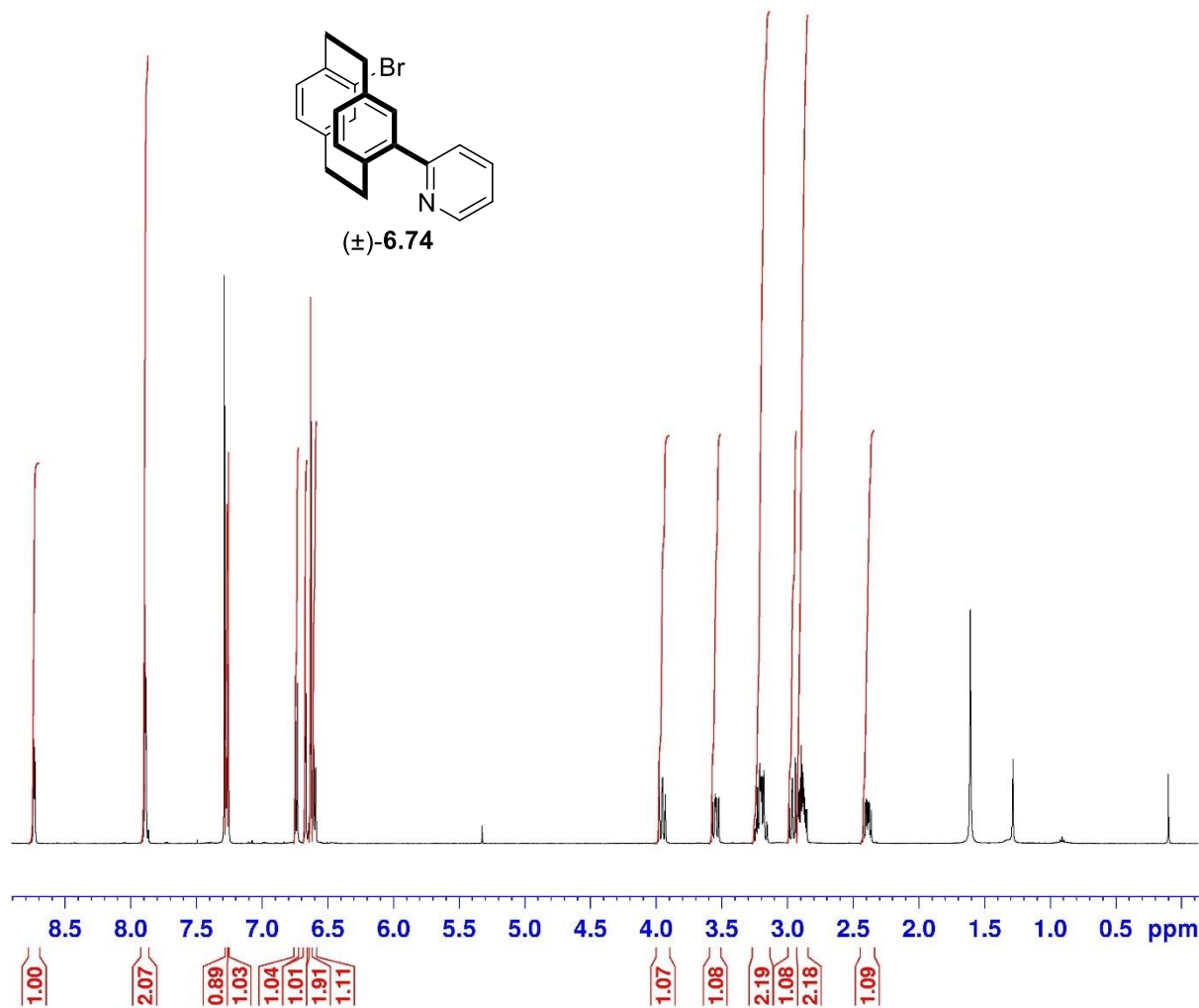


Current Data Parameters
NAME VI-Mn-30 i
EXPNO 1
PROCNO 1

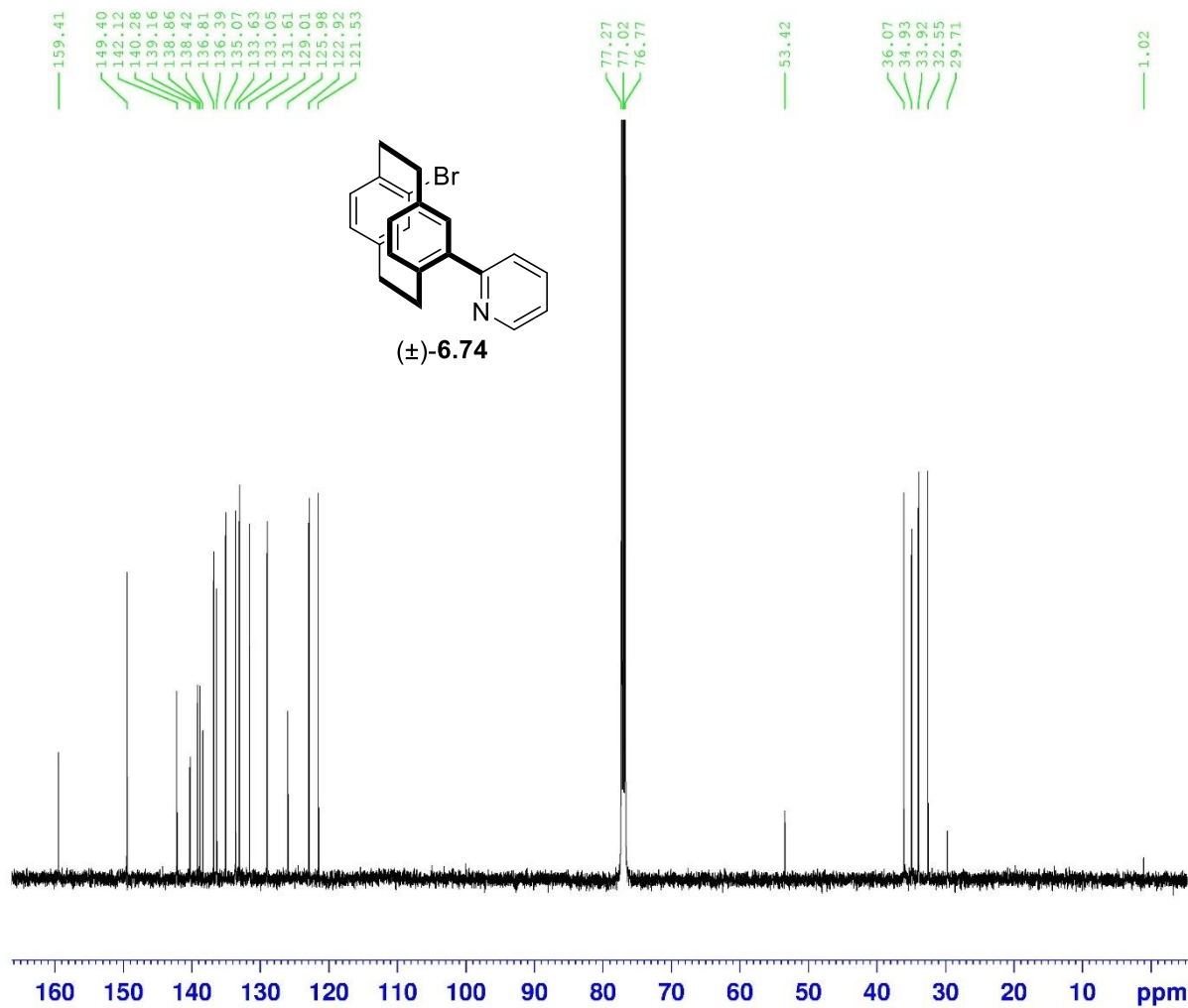
F2 - Acquisition Parameters
Date_ 20200123
Time 18.26
INSTRUM spect
PROBHD 5 mm PAQXI 1H/
PULPROG zg30
TD 65536
SOLVENT CDC13
NS 16
DS 2
SWH 10330.578 Hz
FIDRES 0.157632 Hz
AQ 3.1719425 sec
RG 256
DW 48.400 usec
DE 6.50 usec
TE 298.0 K
D1 1.00000000 sec
TD0 1

===== CHANNEL f1 =====
NUC1 1H
P1 9.50 usec
PL1 4.00 dB
PL1W 12.10000038 W
SF01 500.1330885 MHz

F2 - Processing parameters
SI 32768
SF 500.1300000 MHz
WDW EM
SSB 0
LB 0.30 Hz
GB 0
PC 1.00



13C : Pseudoorthodibromo & 2-Pyr Pd:L (1:4)



Current Data Parameters
 NAME VI-Mn-30 i
 EXPNO 2
 PROCNO 1

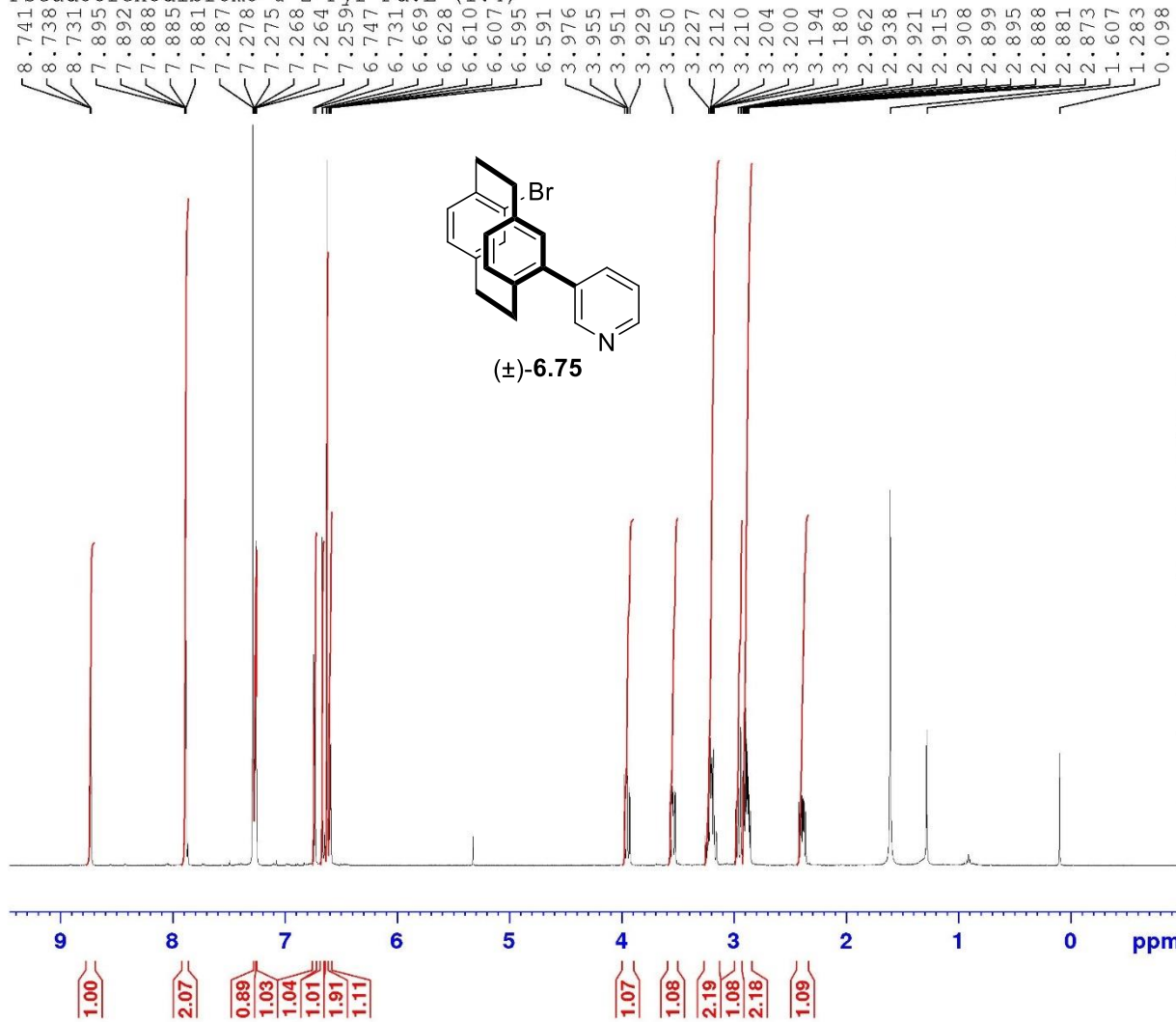
F2 - Acquisition Parameters
 Date_ 20200124
 Time 8.38
 INSTRUM spect
 PROBHD 5 mm PAQXI 1H/
 PULPROG zgpg30
 TD 65536
 SOLVENT CDCl3
 NS 16144
 DS 4
 SWH 30030.029 Hz
 FIDRES 0.458222 Hz
 AQ 1.0911744 sec
 RG 32768
 DW 16.650 usec
 DE 6.50 usec
 TE 298.5 K
 D1 2.00000000 sec
 D11 0.03000000 sec
 TD0 1

===== CHANNEL f1 =====
 NUC1 13C
 P1 12.00 usec
 PL1 -4.00 dB
 PL1W 172.88230896 W
 SFO1 125.7703643 MHz

===== CHANNEL f2 =====
 CPDPRG[2] waltz16
 NUC2 1H
 PCPD2 80.00 usec
 PL2 4.00 dB
 PL12 22.51 dB
 PL13 25.00 dB
 PL2W 12.10000038 W
 PL12W 0.17052394 W
 PL13W 0.09611372 W
 SFO2 500.1320005 MHz

F2 - Processing parameters
 SI 32768
 SF 125.7577890 MHz
 WDW EM
 SSB 0
 LB 1.00 Hz
 GB 0
 PC 1.40

Pseudoorthodibromo 2-Pyr Pd:L (1:4)



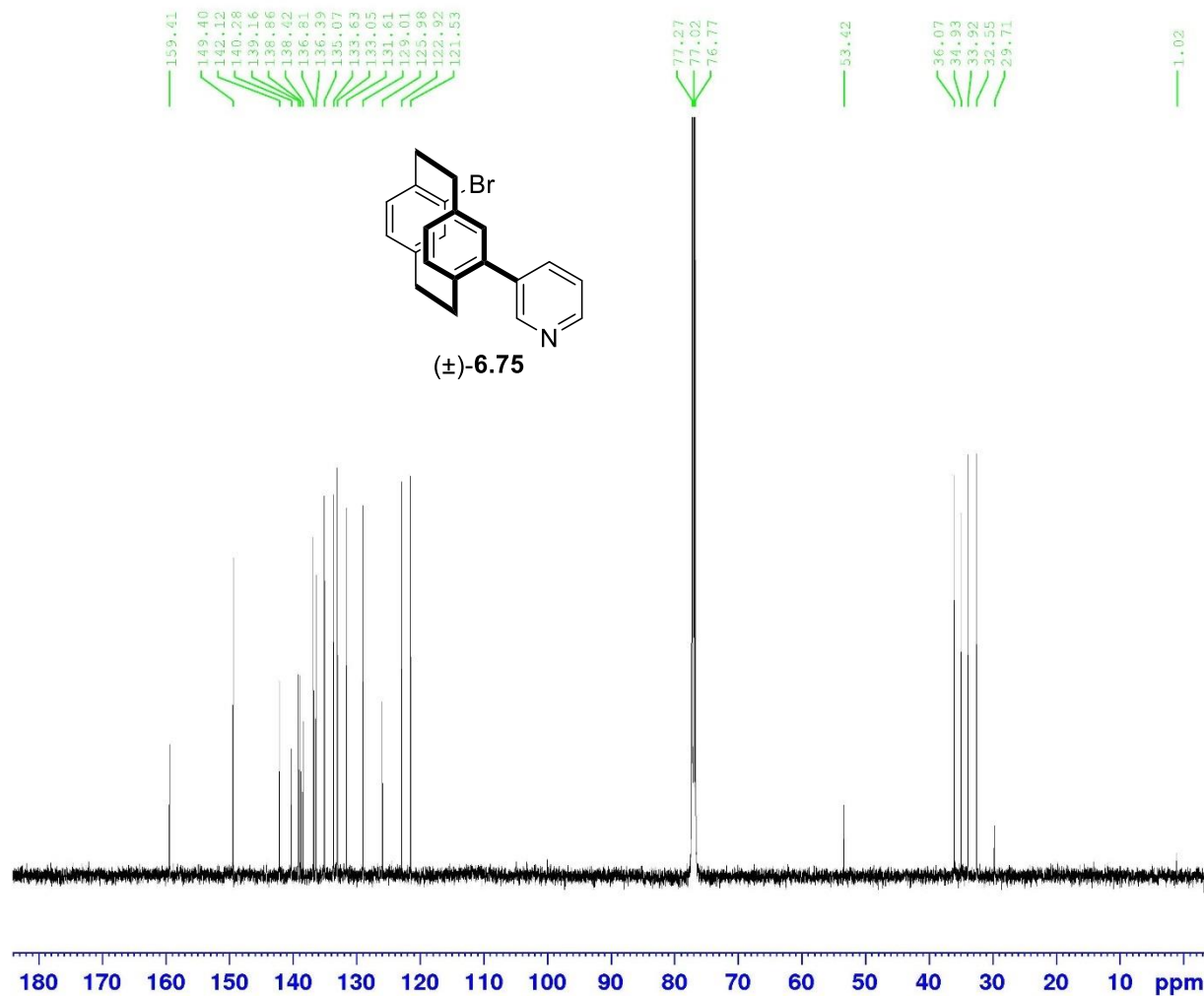
Current Data Parameters
 NAME VI-Mn-30 i
 EXPNO 1
 PROCNO 1

F2 - Acquisition Parameters
 Date_ 20200123
 Time 18.26
 INSTRUM spect
 PROBHD 5 mm PAQXI 1H/
 PULPROG zg30
 TD 65536
 SOLVENT CDCl3
 NS 16
 DS 2
 SWH 10330.578 Hz
 FIDRES 0.157632 Hz
 AQ 3.1719425 sec
 RG 256
 DW 48.400 usec
 DE 6.50 usec
 TE 298.0 K
 D1 1.00000000 sec
 TD0 1

==== CHANNEL f1 =====
 NUC1 1H
 P1 9.50 usec
 PL1 4.00 dB
 PL1W 12.10000038 W
 SFO1 500.1330885 MHz

F2 - Processing parameters
 SI 32768
 SF 500.1300000 MHz
 WDW EM
 SSB 0
 LB 0.30 Hz
 GB 0
 PC 1.00

¹³C : Pseudoorthodibromo & 2-Pyr Pd:L (1:4)



Current Data Parameters
 NAME VI-Mn-3C i
 EXPNO 2
 PROCNO 1

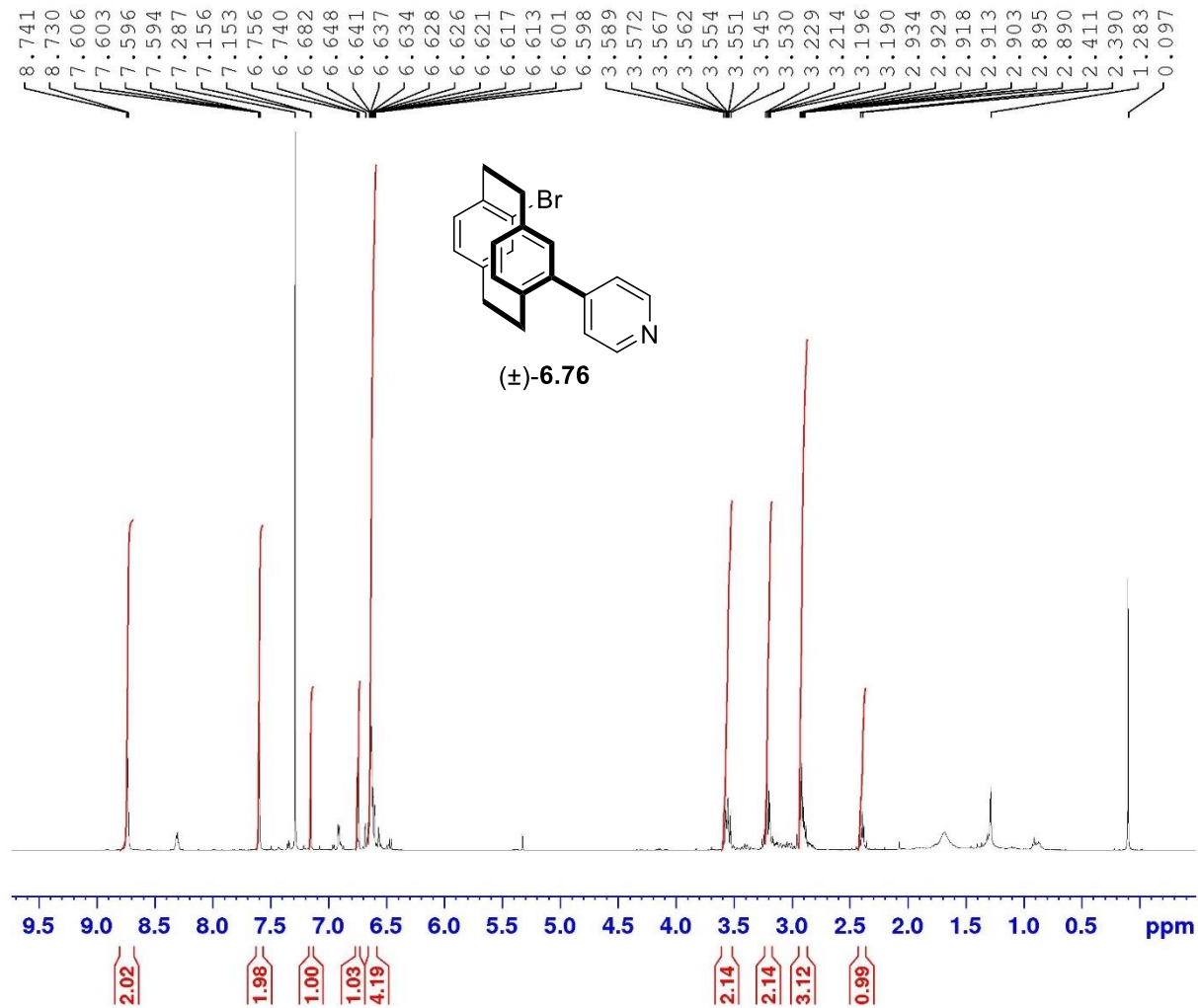
F2 - Acquisition Parameters
 Date_ 20200124
 Time 8.38
 INSTRUM spect
 PROBHD 5 mm PAQXI 1H/
 PULPROG zgpg30
 TD 65536
 SOLVENT CDCl3
 NS 16144
 DS 4
 SWH 30030.029 Hz
 FIDRES 0.458222 Hz
 AQ 1.0911744 sec
 RG 32768
 DW 16.650 usec
 DE 6.50 usec
 TE 298.5 K
 D1 2.0000000 sec
 D11 0.0300000 sec
 TD0 1

----- CHANNEL f1 -----
 NUC1 13C
 P1 12.00 usec
 PL1 -4.00 dB
 PL1W 172.88230896 W
 SFG1 125.7703643 MHz

----- CHANNEL f2 -----
 CPDPRG[2] waltz16
 NUC2 1H
 PCPD2 80.00 usec
 PL2 4.00 dB
 PL12 22.51 dB
 PL13 25.00 dB
 PL2W 12.10000038 W
 PL12W 0.17052394 W
 PL13W 0.09611372 W
 SFG2 500.1320005 MHz

F2 - Processing parameters
 SI 32768
 SF 125.7577890 MHz
 WDW EM
 SSB 0
 LB 1.00 Hz
 GB 0
 PC 1.40

Pseudoorthodibromo PC & 4-PyrSO₂Na (2 eq.) (1:4)



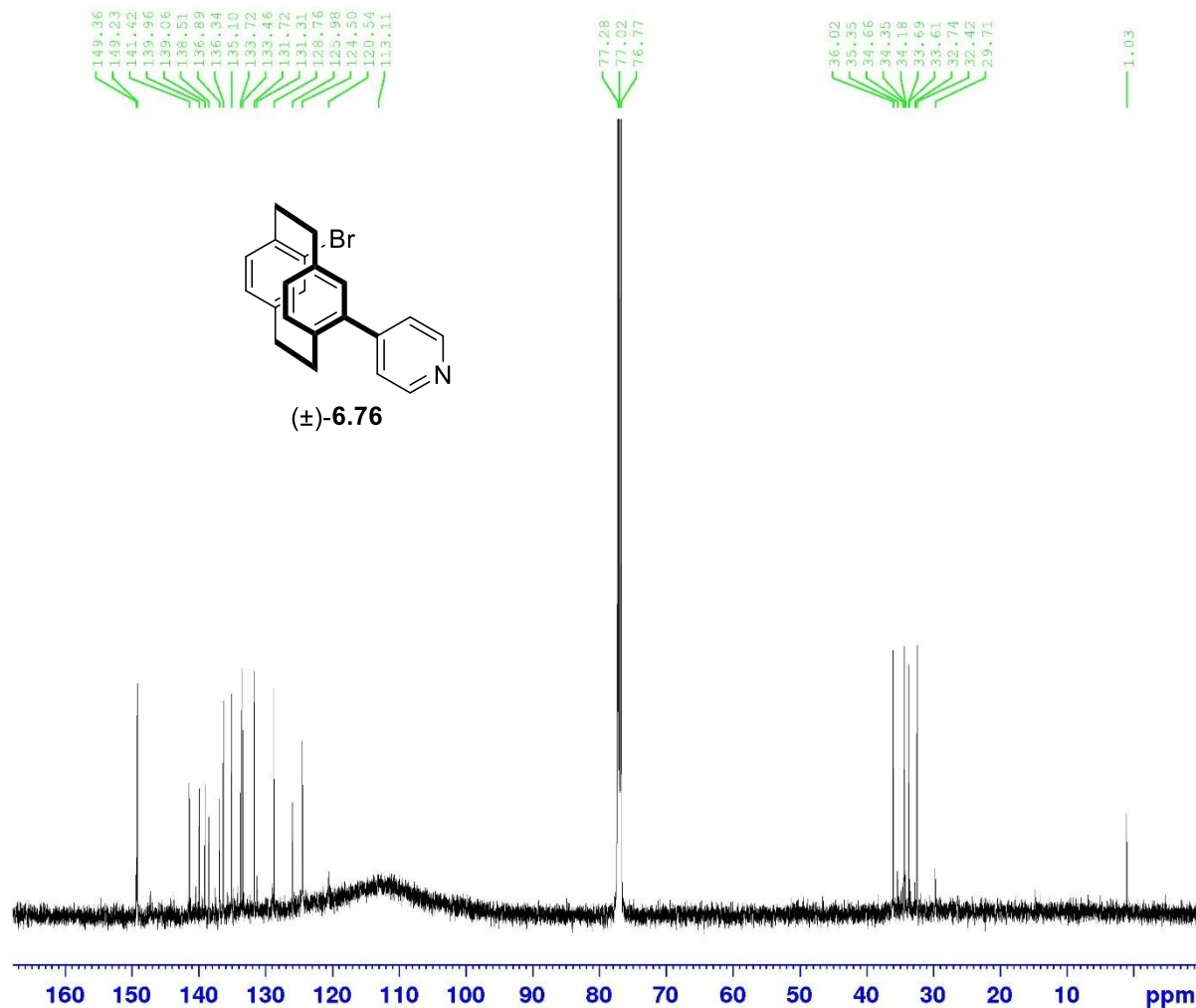
Current Data Parameters
 NAME VI-Mn-51 ii
 EXPNO 1
 PROCNO 1

F2 - Acquisition Parameters
 Date_ 20200202
 Time 17.34
 INSTRUM spect
 PROBHD 5 mm PAQXI 1H/
 PULPROG zg30
 TD 65536
 SOLVENT CDCl3
 NS 16
 DS 2
 SWH 10330.578 Hz
 FIDRES 0.157632 Hz
 AQ 3.1719425 sec
 RG 228.1
 DW 48.400 usec
 DE 6.50 usec
 TE 298.2 K
 D1 1.00000000 sec
 TD0 1

----- CHANNEL f1 -----
 NUC1 1H
 P1 9.50 usec
 PL1 4.00 dB
 PL1W 12.10000038 W
 SF01 500.1330885 MHz

F2 - Processing parameters
 SI 32768
 SF 500.1300000 MHz
 WDW EM
 SSB 0
 LB 0.30 Hz
 GB 0
 PC 1.00

¹³C : Pseudoorthodibromo PC & 4-PyrSO₂Na (2 eq.) (1:4)



Current Data Parameters
 NAME VI-Mn-51 11
 EXPNO 3
 PROCNO 1

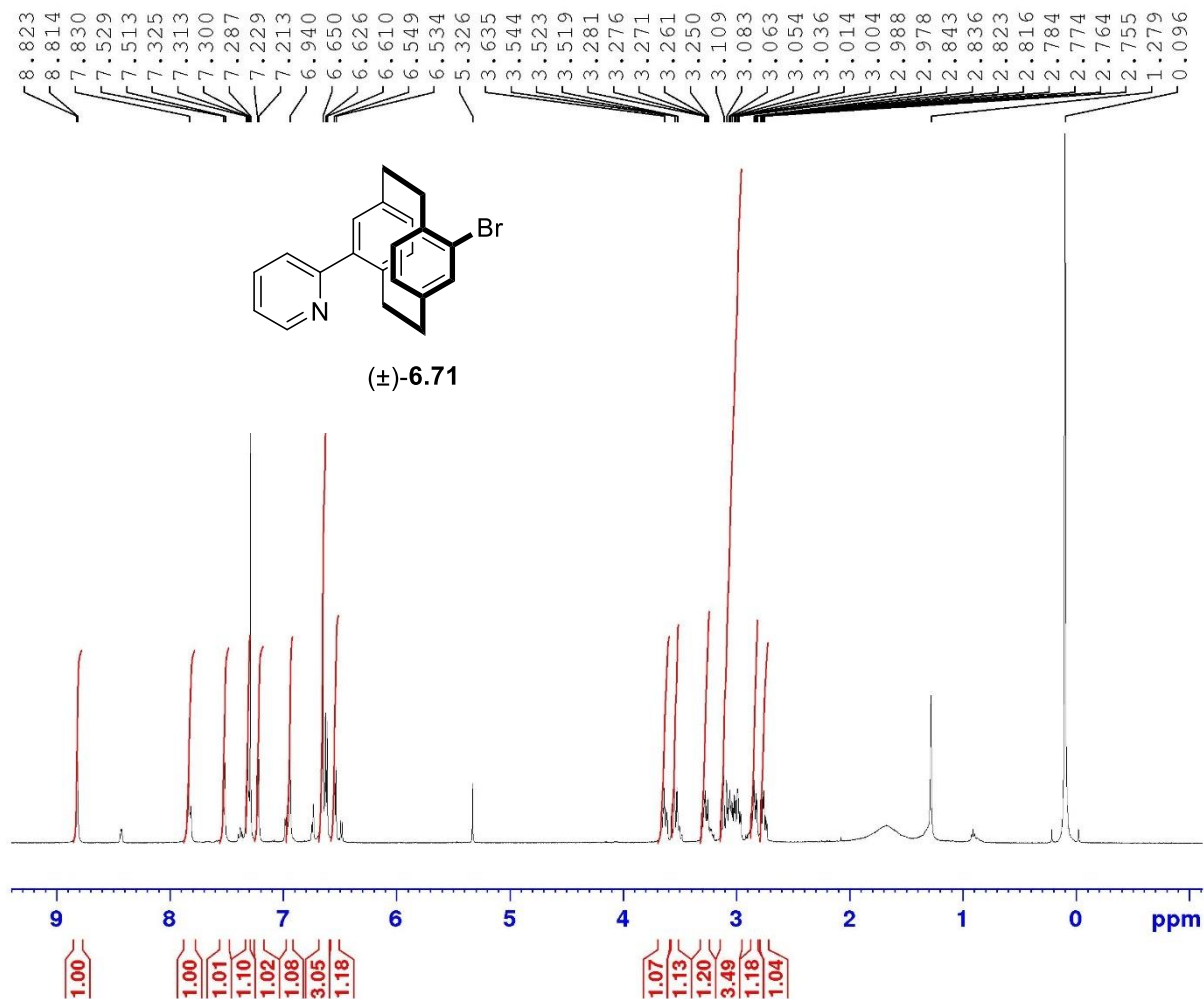
F2 - Acquisition Parameters
 Date_ 20200613
 Time 6.14
 INSTRUM spect
 PROBHD 5 mm PAQXI 1H/
 PULPROG zgpg30
 TD 65536
 SOLVENT cdcl3
 NS 16384
 DS 4
 SWH 30030.029 Hz
 FIDRES 0.458222 Hz
 AQ 1.0911744 sec
 RG 32768
 DW 16.650 usec
 DE 6.50 usec
 TE 298.2 K
 D1 2.0000000 sec
 D11 0.0300000 sec
 TDO 1

----- CHANNEL f1 -----
 NUC1 13C
 P1 12.00 usec
 PL1 -4.00 dB
 PL1W 172.88230896 W
 SFO1 125.7703643 MHz

----- CHANNEL f2 -----
 CPDPRG[2] waltz16
 NUC2 1H
 PCPD2 80.00 usec
 PL2 4.00 dB
 PL12 22.51 dB
 PL13 25.00 dB
 PL2W 12.10000038 W
 PL12W 0.17052394 W
 PL13W 0.09611372 W
 SFO2 500.1320003 MHz

F2 - Processing parameters
 SI 32768
 SF 125.7577890 MHz
 WDW EM
 SSB 0
 LB 1.00 Hz
 GB 0
 PC 1.40

PseudoparadibromoPC & 2-PyrSO₂Na (2 eq.), PD:L (1:4)) :purified again



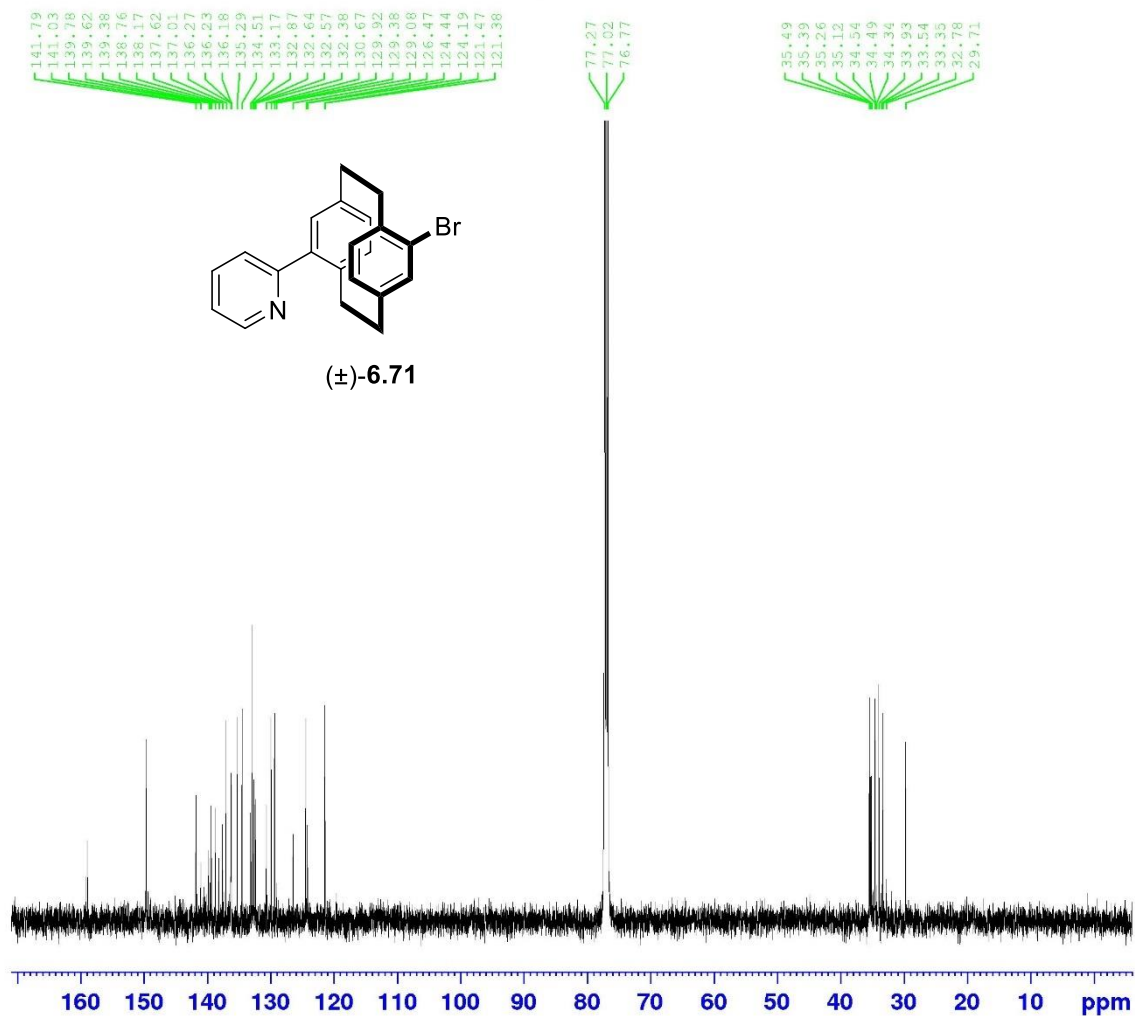
Current Data Parameters
 NAME VI-Mn-34 i
 EXPNO 3
 PROCNO 1

F2 - Acquisition Parameters
 Date_ 20200604
 Time 16.10
 INSTRUM spect
 PROBHD 5 mm PAQXI 1H/
 PULPROG zg30
 TD 65536
 SOLVENT CDCl3
 NS 64
 DS 2
 SWH 10330.578 Hz
 FIDRES 0.157632 Hz
 AQ 3.1719425 sec
 RG 512
 DW 48.400 usec
 DE 6.50 usec
 TE 294.2 K
 D1 1.00000000 sec
 TD0 1

===== CHANNEL f1 =====
 NUC1 1H
 P1 9.50 usec
 PL1 4.00 dB
 PLLW 12.1000038 W
 SFO1 500.1330885 MHz

F2 - Processing parameters
 SI 32768
 SF 500.130000 MHz
 WDW EM
 SSB 0
 LB 0.30 Hz
 GB 0
 PC 1.00

PseudoparadibromoPC & 2-PyrSO₂Na (2 eq.), PD:L (1:4)



Current Data Parameters
 NAME VI-Mn-34 i
 EXPNO 2
 PROCNO 1

F2 - Acquisition Parameters
 Date_ 20200227
 Time 9.32
 INSTRUM spect
 PROBHD 5 mm PAQXI 1H/
 PULPROG zgpg30
 TD 65536
 SOLVENT CDCl3
 NS 16384
 DS 4
 SWH 30030.029 Hz
 FIDRES 0.458222 Hz
 AQ 1.091744 sec
 RG 32768
 DW 16.653 usec
 DE 6.50 usec
 TE 298.2 K
 D1 2.0000000 sec
 D11 0.0300000 sec
 TD0 1

===== CHANNEL f1 =====
 NUC1 13C
 P1 12.00 usec
 PL1 -4.00 dB
 PL1W 172.88230896 W
 SFO1 125.7703643 MHz

===== CHANNEL f2 =====
 CPDPRG12 waltz16
 NUC2 1H
 PCPD2 80.00 usec
 P12 4.00 dB
 PL12 22.51 dB
 PL13 25.00 dB
 PL2W 12.10000038 W
 PL12W 0.17052394 W
 PL13W 0.09611372 W
 SFO2 500.1320005 MHz

F2 - Processing parameters
 SI 32768
 SF 125.7577893 MHz
 WDW EM
 SSB 0
 LB 1.00 Hz
 GB 0
 PC 1.40

Pseudopara dibromo & 3-PyrSO₂Na Pd:1 (1:4)

8.771
8.767
8.651
8.649
8.641
7.803
7.800
7.787
7.784
7.446
7.436
7.431
7.421
7.287
7.256
7.253
7.240
7.237
6.658
6.651
6.635
6.618
6.615
6.572
6.557
6.545
6.529
6.525
5.325
3.584
3.339
3.331
3.321
3.310
3.296
3.103
3.099
3.078
3.072
3.051
2.951
2.804
2.743
2.723
1.630
1.282
0.097

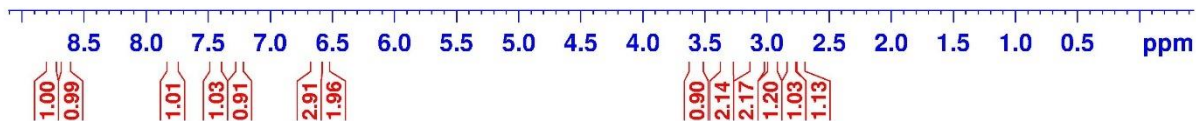
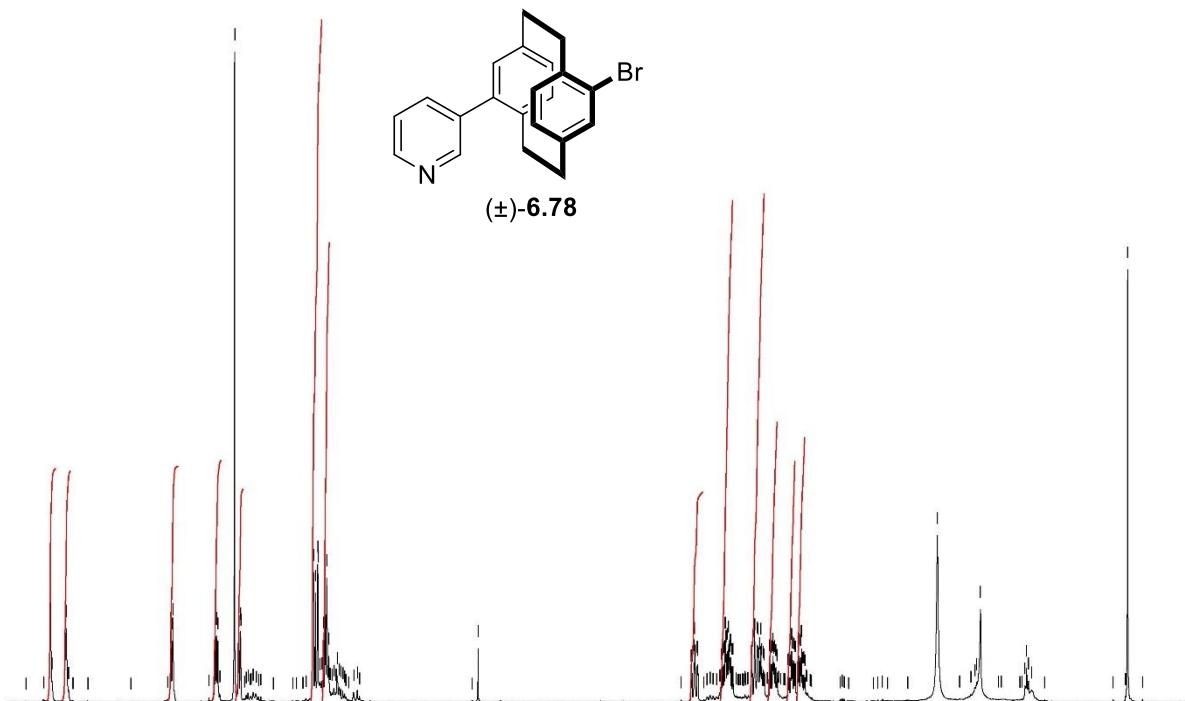
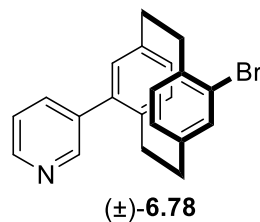


Current Data Parameters
NAME VI-Mn-35
EXPNO 1
PROCNO 1

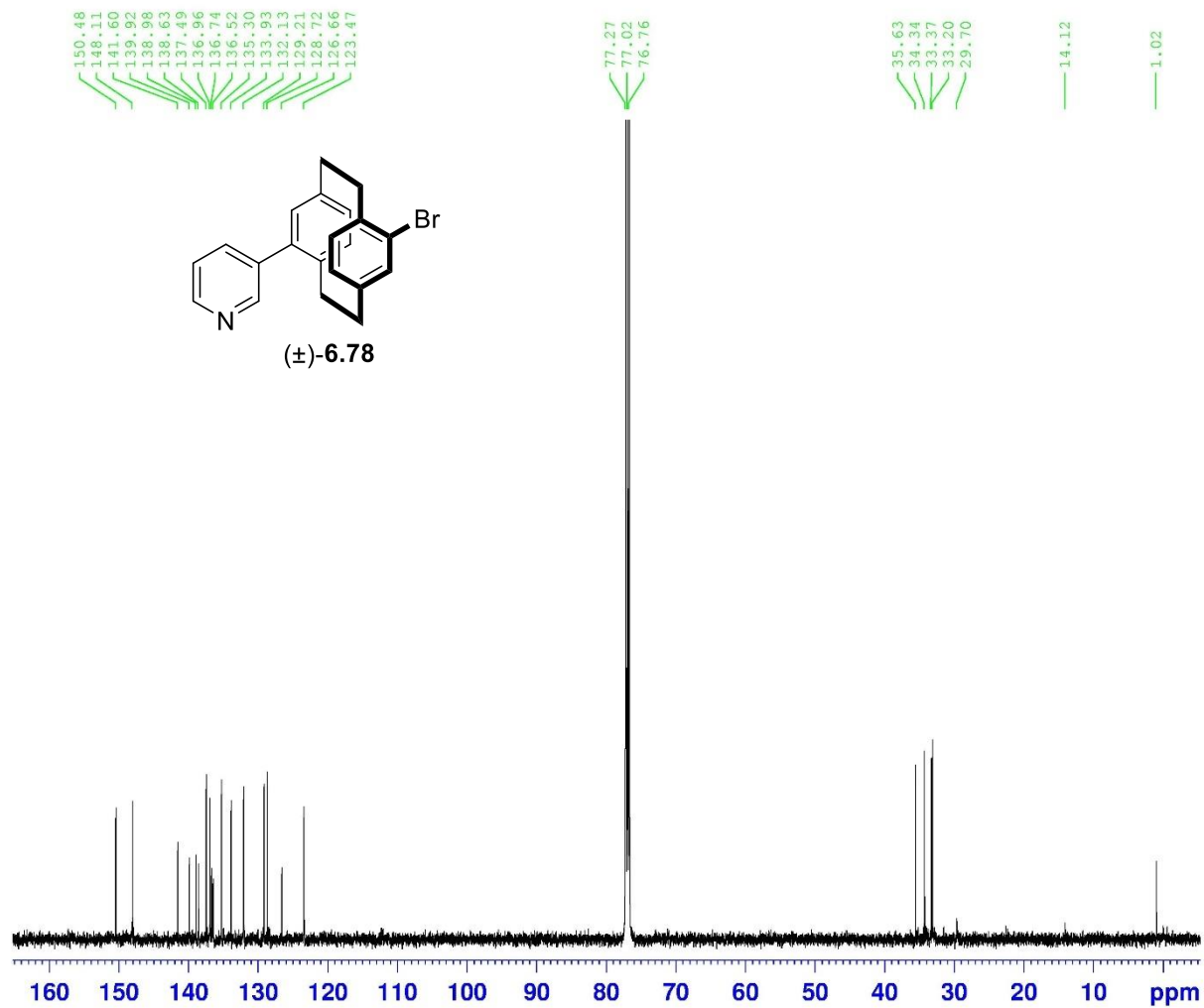
F2 - Acquisition Parameters
Date_ 2020122
Time 18.03
INSTRUM spect
PROBHD 5 mm PAQXI 1H/
PULPROG zg30
TD 65536
SOLVENT CDC13
NS 16
DS 2
SWH 10330.578 Hz
FIDRES 0.157632 Hz
AQ 3.1719425 sec
RG 181
DW 48.400 usec
DE 6.50 usec
TE 297.9 K
D1 1.00000000 sec
TD0 1

===== CHANNEL f1 =====
NUC1 1H
P1 9.50 usec
PL1 4.00 dB
PL1W 12.10000038 W
SFO1 500.1330885 MHz

F2 - Processing parameters
SI 32768
SF 500.1300000 MHz
WDW EM
SSB 0
LB 0.30 Hz
GB 0
PC 1.00



¹³C : Pseudopara dibromo & 3-PyrSO₂Na Pd:1 (1:4)



Current Data Parameters
 NAME VI-Mn-35
 EXPNO 2
 PROCNO 1

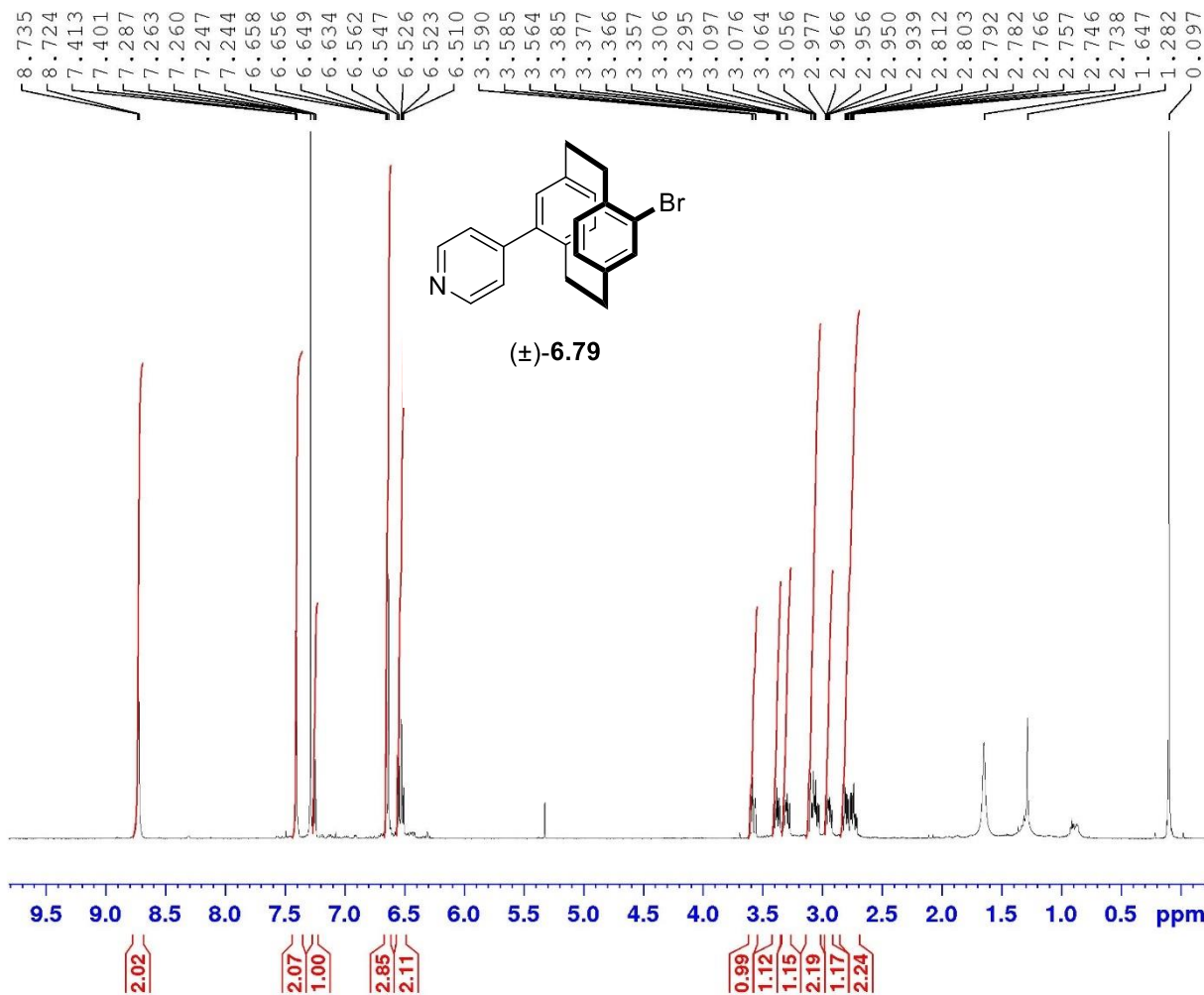
F2 - Acquisition Parameters
 Date_ 20200123
 Time 8.30
 INSTRUM spect
 PROBHD 5 mm PAQXI 1H/
 PULPROG zgpg30
 TD 65536
 SOLVENT CDCl3
 NS 16384
 DS 4
 SWH 30030.029 Hz
 FIDRES 0.458222 Hz
 AQ 1.0911744 sec
 RG 32768
 DW 16.650 usec
 DE 6.50 usec
 TE 297.8 K
 D1 2.00000000 sec
 D11 0.03000000 sec
 TD0 1

===== CHANNEL f1 =====
 NUC1 13C
 P1 12.00 usec
 PL1 -4.00 dB
 PL1W 172.88230896 W
 SFO1 125.7703643 MHz

===== CHANNEL f2 =====
 CPDPRG[2] waltz16
 NUC2 1H
 PCPD2 80.00 usec
 PL2 4.00 dB
 PL12 22.51 dB
 PL13 25.00 dB
 PL2W 12.10000038 W
 PL12W 0.17052394 W
 PL13W 0.09611372 W
 SFO2 500.1320005 MHz

F2 - Processing parameters
 SI 32768
 SF 125.7577890 MHz
 WDW EM
 SSB 0
 LB 1.00 Hz
 GB 0
 PC 1.40

Pseudoparadibromo PC & 4-PyrSO₂Na (2 eq.) (1:4)



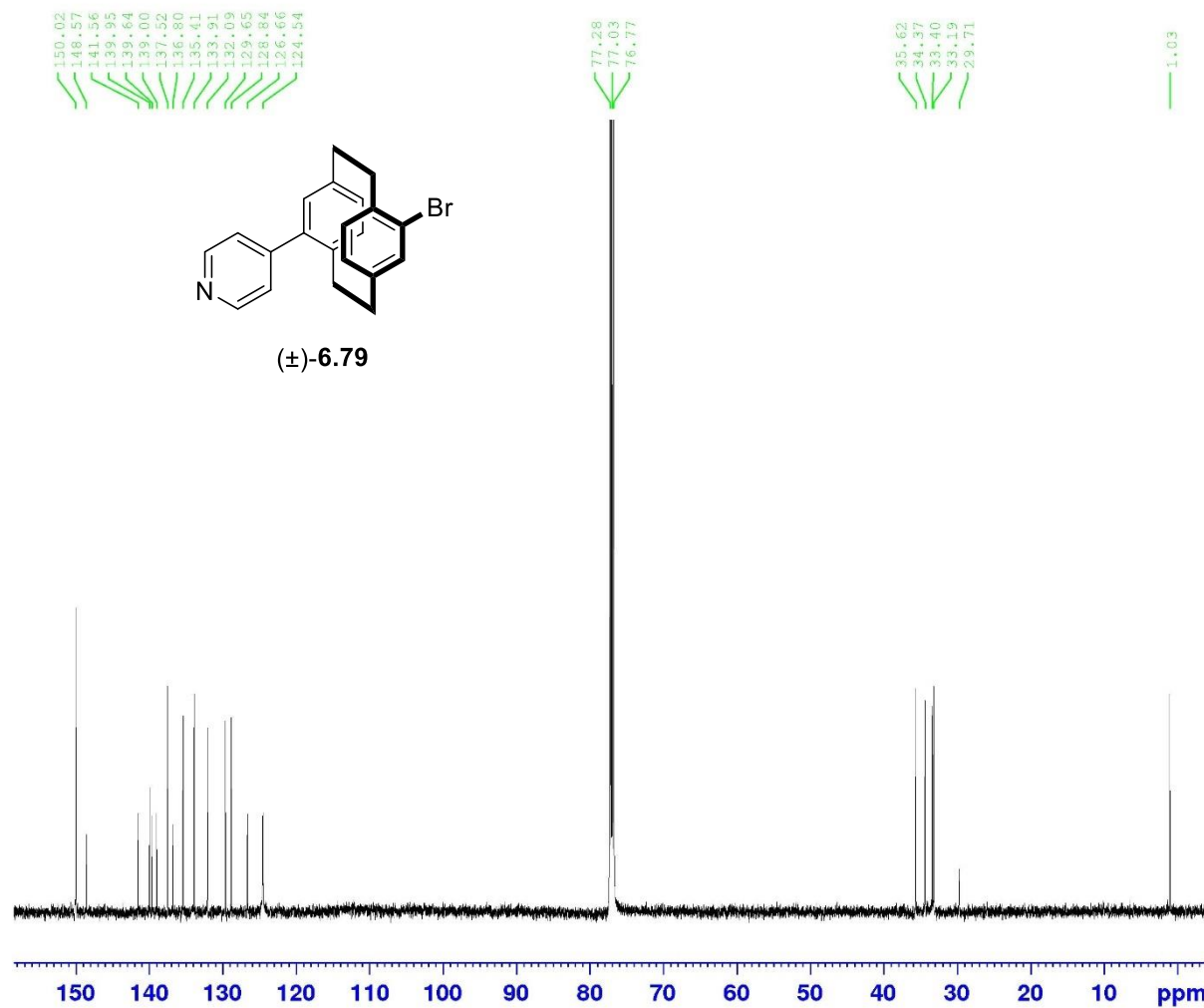
Current Data Parameters
 NAME VI-Mn-52 iii
 EXPNO 1
 PROCNO 1

F2 - Acquisition Parameters
 Date_ 20200201
 Time 15.19
 INSTRUM spect
 PROBHD 5 mm PAQXI 1H/
 PULPROG zg30
 TD 65536
 SOLVENT CDCl₃
 NS 16
 DS 2
 SWH 10330.578 Hz
 FIDRES 0.157632 Hz
 AQ 3.1719425 sec
 RG 256
 DW 48.400 usec
 DE 6.50 usec
 TE 298.2 K
 DI 1.00000000 sec
 TDO 1

===== CHANNEL f1 =====
 NUC1 1H
 P1 9.50 usec
 PL1 4.00 dB
 PL1W 12.10000038 W
 SFO1 500.1330885 MHz

F2 - Processing parameters
 SI 32768
 SF 500.1300000 MHz
 WDW EM
 SSB 0
 LB 0.30 Hz
 GB 0
 PC 1.00

¹³C : Pseudoparadibromo PC & 4-PyrSO₂Na (2 eq.) (1:4)



Current Data Parameters
 NAME VI-Mn-52 i11
 EXPNO 3
 PROCNO 1

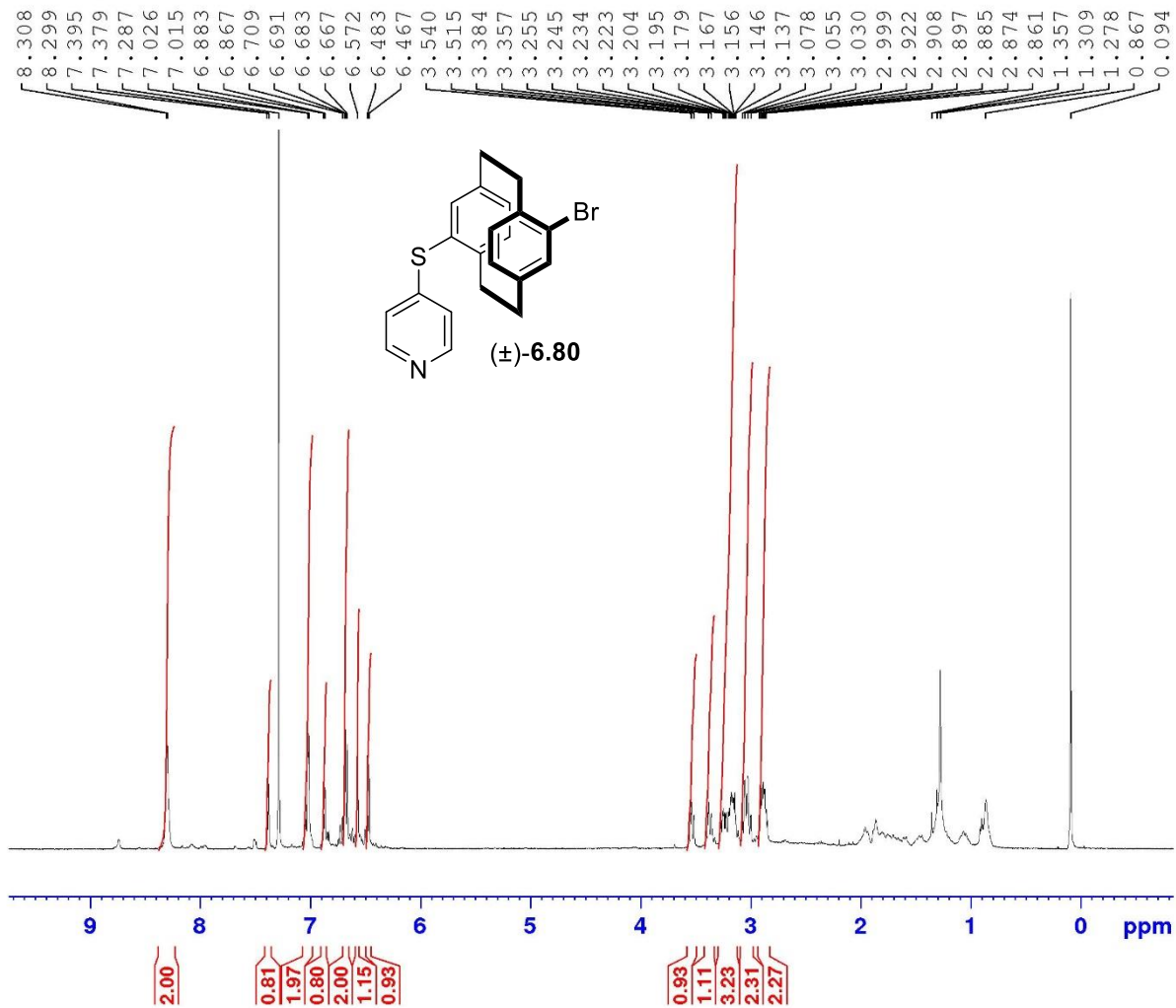
F2 - Acquisition Parameters
 Date_ 20200324
 Time 9.32
 INSTRUM spect
 PROBHD 5 mm PAQXI 1H/
 PULPROG zgpg30
 TD 65536
 SOLVENT CDCl3
 NS 16384
 DS 4
 SWE 30030.029 Hz
 FIDRES 0.458222 Hz
 AQ 1.0911744 sec
 RG 32768
 DW 16.650 usec
 DE 6.50 usec
 TE 295.9 K
 D1 2.0000000 sec
 D11 0.03000000 sec
 TD0 1

----- CHANNEL f1 -----
 NUC1 13C
 P1 12.00 usec
 PL1 -4.00 dB
 PL1W 172.88233896 W
 SFO1 125.7703643 MHz

----- CHANNEL f2 -----
 CPDPRG[2] waltz16
 NUC2 1H
 PCPD2 80.00 usec
 PL2 4.00 dB
 PL12 22.51 dB
 PL13 25.00 dB
 PL2W 12.1000038 W
 PL12W 0.17052394 W
 PL13W 0.09611372 W
 SFO2 500.1320005 MHz

F2 - Processing parameters
 SI 32768
 SF 125.7577890 MHz
 WDW EM
 SSB 0
 LB 1.00 Hz
 GB 0
 PC 1.40

Pseudoparadibromo PC & 4-PyrSO2Na (2 eq.) (1:4)



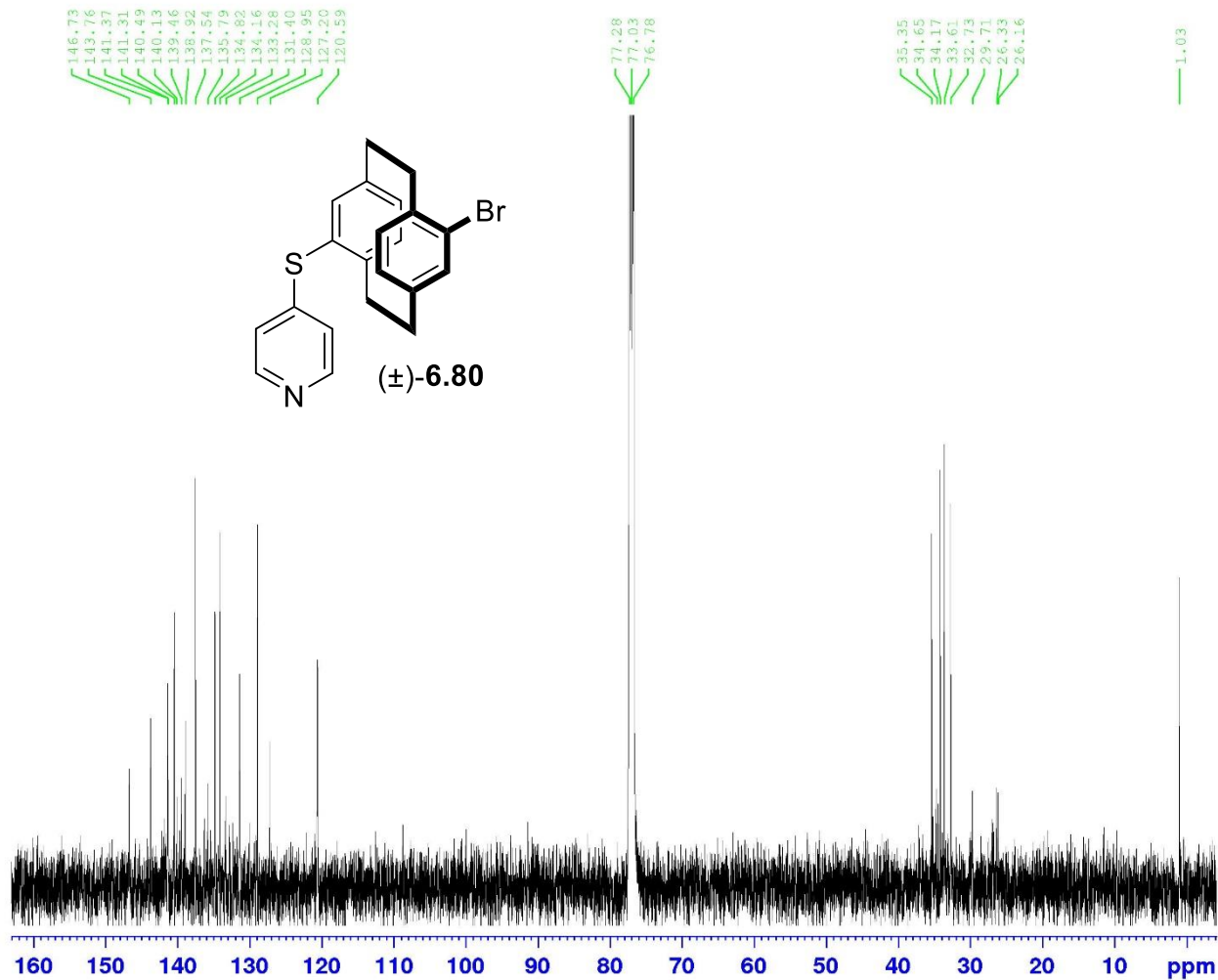
Current Data Parameters
 NAME VI-Mn-S2 ii
 EXPNO 2
 PROCNO 1

F2 - Acquisition Parameters
 Date_ 20200608
 Time 16.42
 INSTRUM spect
 PROBHD 5 mm PAQXI 1H/
 PULPROG zg30
 TD 65536
 SOLVENT CDCl3
 NS 16
 DS 2
 SWH 10330.578 Hz
 FIDRES 0.157632 Hz
 AQ 3.1719425 sec
 RG 362
 DW 48.400 usec
 DE 6.50 usec
 TE 294.5 K
 D1 1.00000000 sec
 TDO 1

===== CHANNEL f1 =====
 NUC1 1H
 P1 9.50 usec
 PL1 4.00 dB
 PL1W 12.10000038 W
 SFO1 500.1330885 MHz

F2 - Processing parameters
 SI 32768
 SF 500.1300000 MHz
 WDW EM
 SSB 0
 LB 0.30 Hz
 GB 0
 PC 1.00

13C : Pseudoparadibromo PC & 4-PyrSO2Na (2 eq.) (1:4)



C
NAME VI-Mn-52 ii
EXPNO 3
PROCNO 1

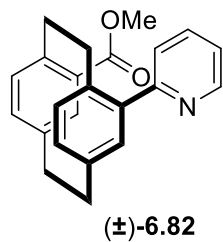
F2 - Acquisition Parameters
Date_ 20200609
Time 7.05
INSTRUM spect
PROBHD 5 mm PAQXI 1H/
PULPROG zgpg30
TD 65536
SOLVENT CDCl3
NS 16384
DS 4
SWH 30030.029 Hz
FIDRES 0.458222 Hz
AQ 1.0911744 sec
RG 32768
DW 16.650 usec
DE 6.50 usec
TE 294.5 K
D1 2.0000000 sec
D11 0.0300000 sec
TDC 1

===== CHANNEL f1 =====
NUC1 13C
P1 12.00 usec
PL1 -4.00 dB
PL1W 172.88230896 W
SFO1 125.7703643 MHz

===== CHANNEL f2 =====
CPDPRG[2] waltz16
NUC2 1H
PCPD2 80.00 usec
PL2 4.00 dB
PL12 22.51 dB
PL13 25.00 dB
PL2W 12.10000038 W
PL12W 0.17052394 W
PL13W 0.09611372 W
SFO2 500.1320005 MHz

F2 - Processing parameters
SI 32768
SF 125.7577890 MHz
WDW EM
SSB 0
LB 1.00 Hz
GB 0
PC 1.40

Pseudogem CO2Me Br & 2-Pyr

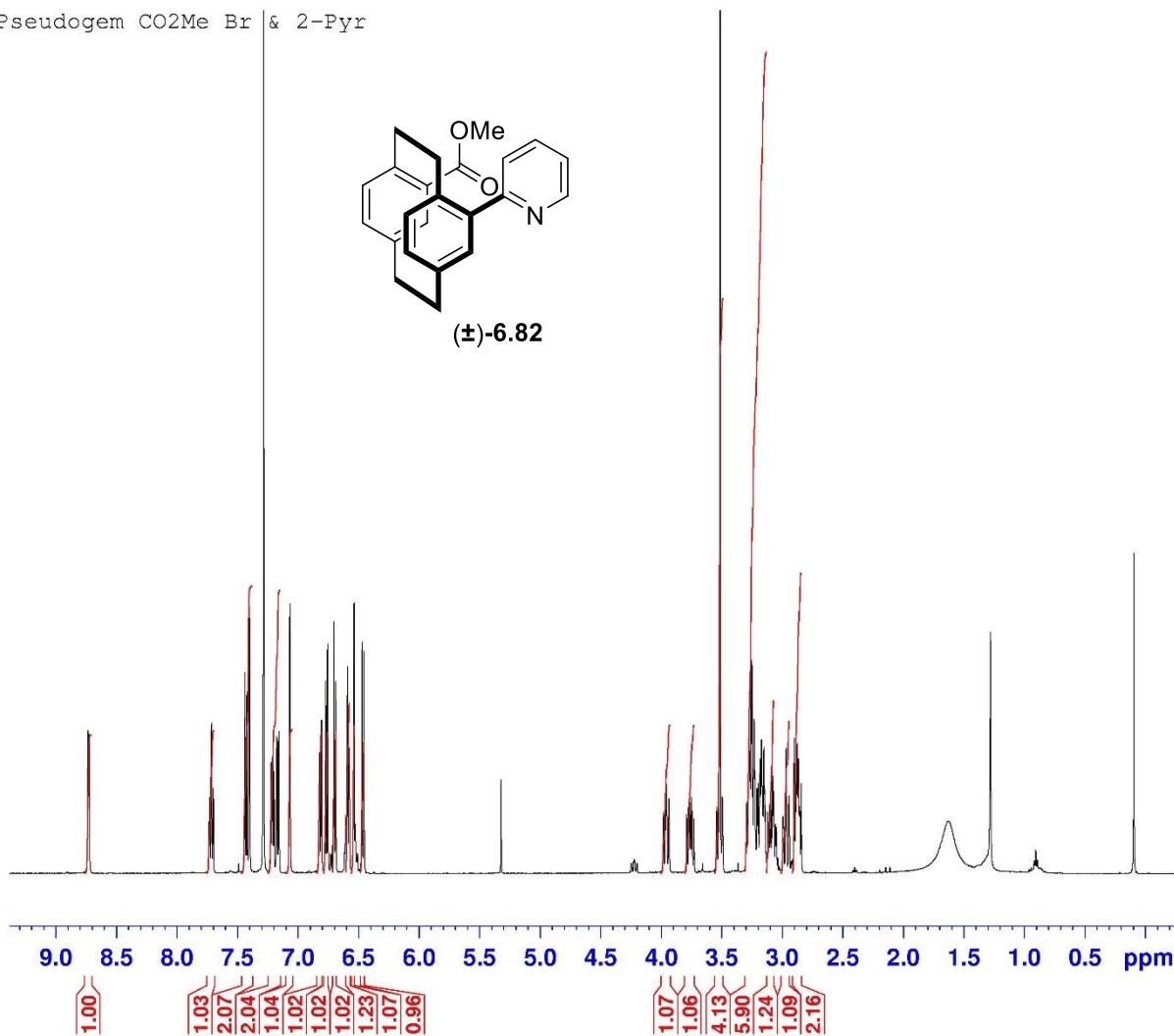


Current Data Parameters
NAME V-Mn-297 II
EXPNO 6
PROCNO 1

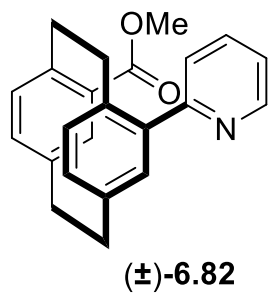
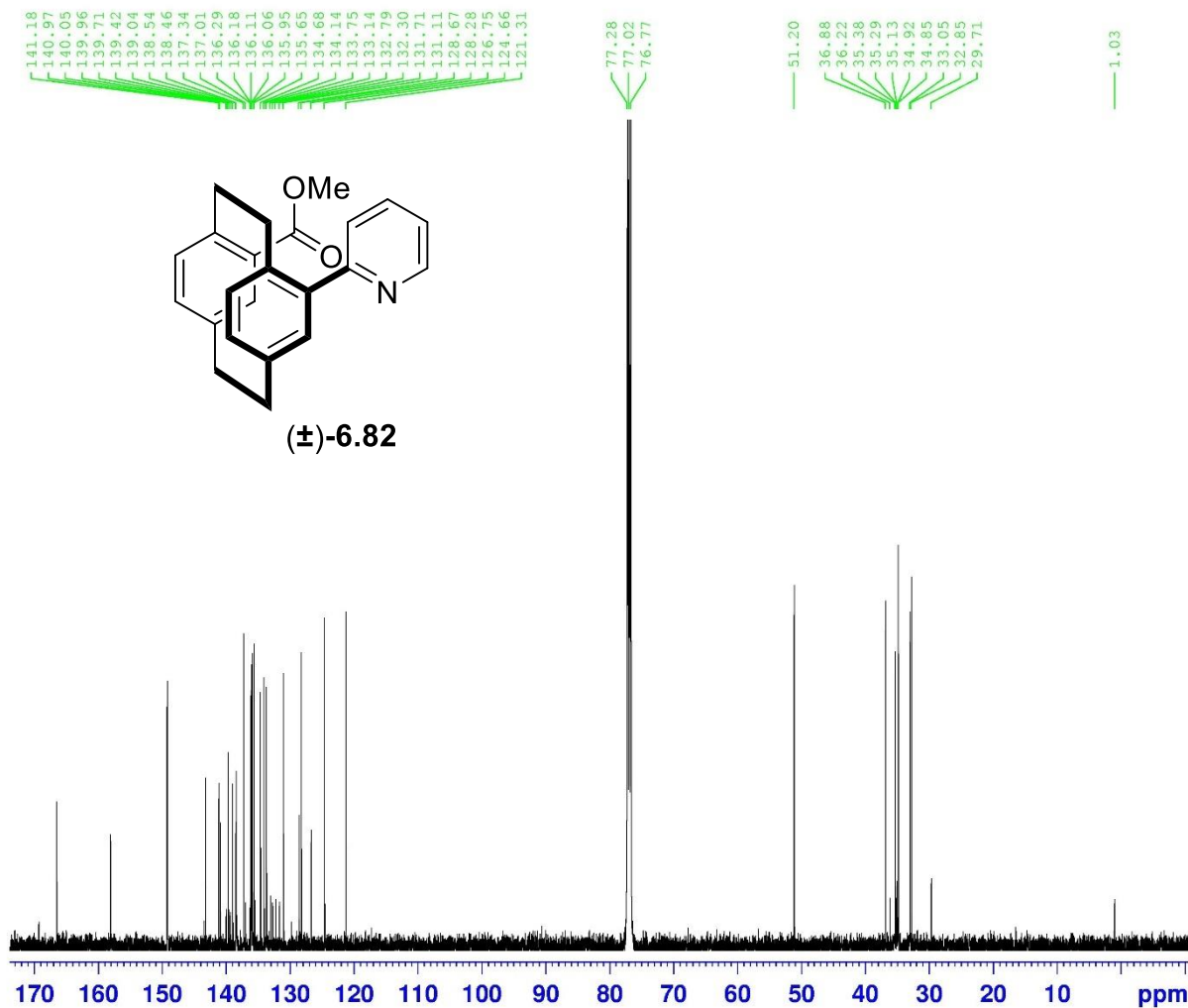
F2 - Acquisition Parameters
Date_ 20200201
Time 20.39
INSTRUM spect
PROBHD 5 mm PAQXI 1H/
PULPROG zg30
TD 65536
SOLVENT CDC13
NS 64
DS 2
SWH 10330.578 Hz
FIDRES 0.157632 Hz
AQ 3.1719425 sec
RG 256
DW 48.400 usec
DE 6.50 usec
TE 298.2 K
D1 1.00000000 sec
TD0 1

==== CHANNEL f1 =====
NUC1 1H
P1 9.50 usec
PL1 4.00 dB
PLIW 12.10000038 W
SFO1 500.1330885 MHz

F2 - Processing parameters
SI 32768
SF 500.1300000 MHz
WDW EM
SSB 0
LB 0.30 Hz
GB 0
PC 1.00



13C : Pseudogem CO2Me Br & 2-Pyr



Current Data Parameters
 NAME V-Mn-297 II
 EXPNO 7
 PROCNO 1

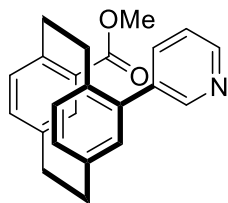
F2 - Acquisition Parameters
 Date_ 20200202
 Time 11.02
 INSTRUM spect
 PROBHD 5 mm PAQXI 1H/
 PULPROG zgpg30
 TD 65536
 SOLVENT CDCl3
 NS 16384
 DS 4
 SWH 30030.029 Hz
 FIDRES 0.458222 Hz
 AQ 1.0911744 sec
 RG 32768
 DW 16.650 usec
 DE 6.50 usec
 TE 298.2 K
 D1 2.00000000 sec
 D11 0.03000000 sec
 TD0 1

==== CHANNEL f1 =====
 NUC1 13C
 P1 12.00 usec
 PL1 -4.00 dB
 PL1W 172.88230896 W
 SFO1 125.7703643 MHz

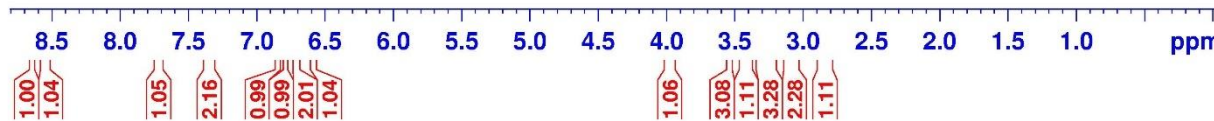
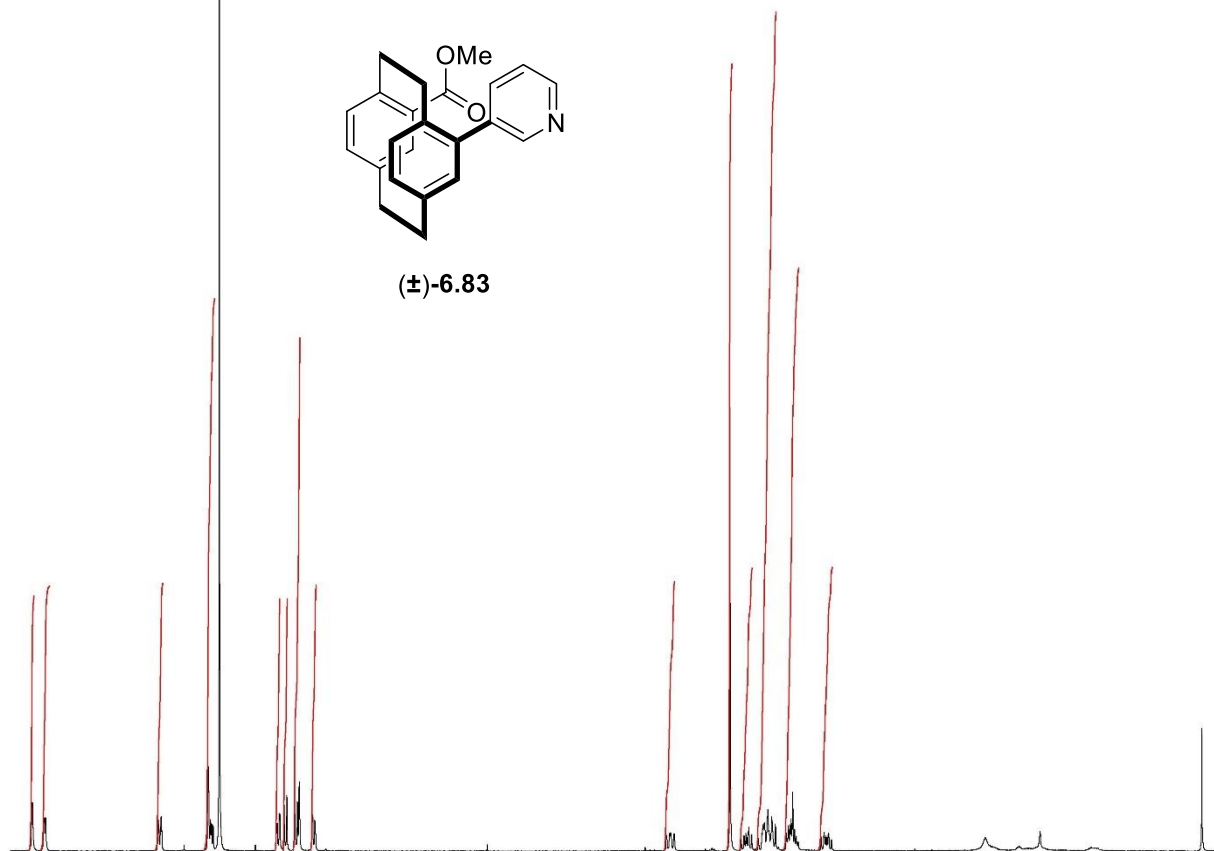
==== CHANNEL f2 =====
 CPDPRG[2] waltz16
 NUC2 1H
 PCPD2 80.00 usec
 PL2 4.00 dB
 PL12 22.51 dB
 PL13 25.00 dB
 PL2W 12.10000038 W
 PL12W 0.17052394 W
 PL13W 0.09611372 W
 SFO2 500.1320005 MHz

F2 - Processing parameters
 SI 32768
 SF 125.7577890 MHz
 WDW EM
 SSB 0
 LB 1.00 Hz
 GB 0
 PC 1.40

Pseudoortho Br CO2Me & 3-PyrSO2Na (Pd:1) (10:40), K2CO3 (1.5 eq.) 1,4-dioxane



(±)-6.83



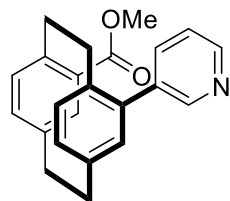
Current Data Parameters
NAME V-Mn-240 iii
EXPNO 1
PROCNO 1

F2 - Acquisition Parameters
Date_ 20191005
Time 20.22
INSTRUM spect
PROBHD 5 mm Multinucl
PULPROG zg30
TD 65536
SOLVENT CDCl3
NS 16
DS 2
SWH 8278.146 Hz
FIDRES 0.126314 Hz
AQ 3.9583745 sec
RG 574.7
DW 60.400 usec
DE 6.00 usec
TE 300.0 K
D1 1.00000000 sec
TD0 1

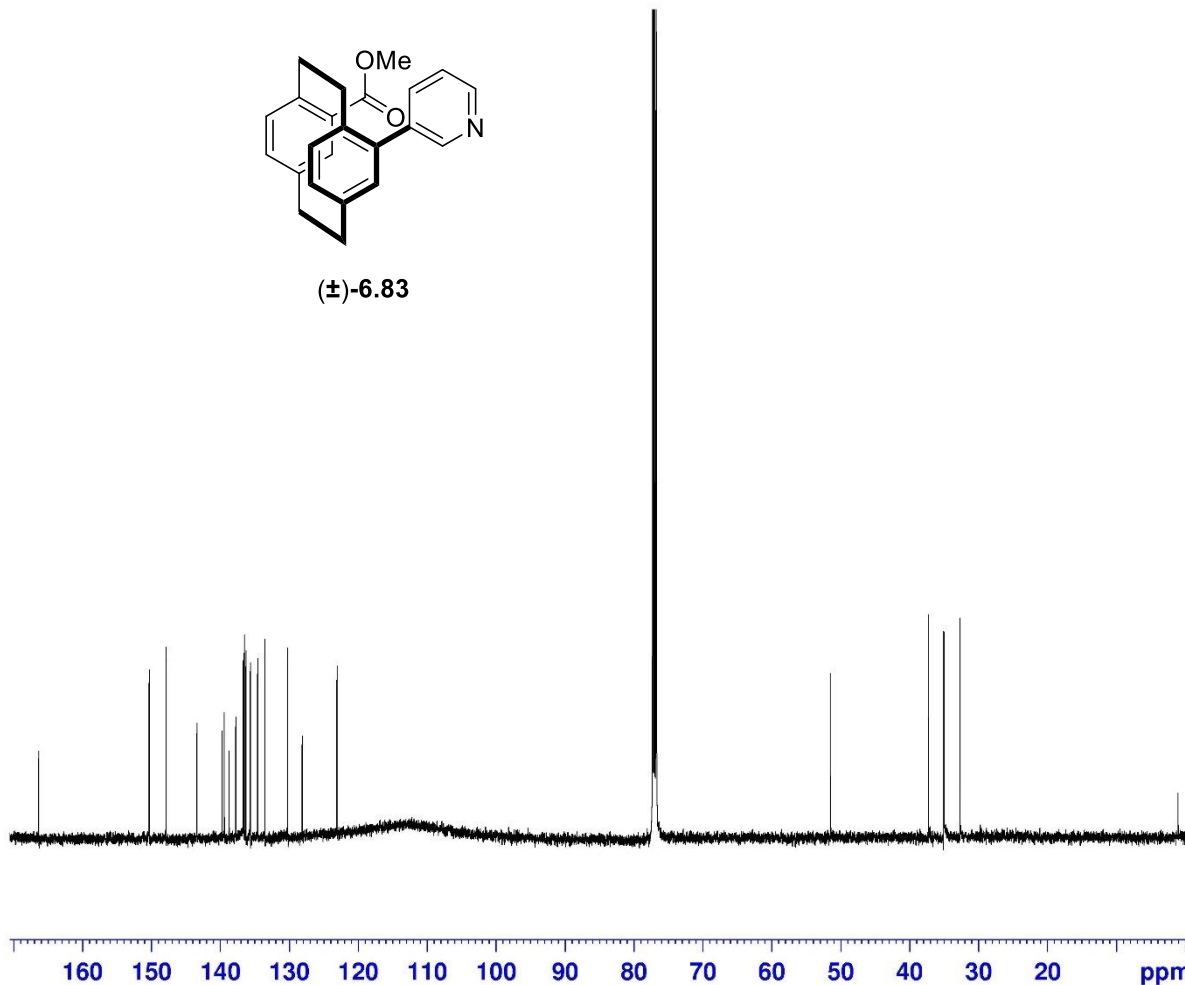
==== CHANNEL f1 =====
NUC1 1H
P1 10.00 usec
PL1 3.10 dB
SFO1 400.1324710 MHz

F2 - Processing parameters
SI 32768
SF 400.1300000 MHz
WDW EM
SSB 0
LB 0.30 Hz
GB 0
PC 1.00

¹³C :Pseudo gem CO2Me Br & 3-PyrSO2Na



(±)-6.83



Current Data Parameters
NAME V-Mn-240 iii
EXPNO 2
PROCNO 1

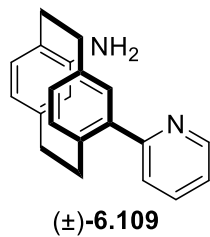
F2 - Acquisition Parameters
Date_ 20191007
Time 7.11
INSTRUM spect
PROBHD 5 mm PAQXI 1H/
PULPROG zgpg30
TD 65536
SOLVENT CDCl3
NS 16384
DS 4
SWH 30030.029 Hz
FIDRES 0.458222 Hz
AQ 1.0911744 sec
RG 32768
DW 16.650 usec
DE 6.50 usec
TE 298.0 K
D1 2.0000000 sec
D11 0.0300000 sec
TD0 1

=====
CHANNEL f1
NUC1 13C
P1 12.00 usec
PL1 -4.00 dB
PL1W 172.88230896 W
SFO1 125.7703643 MHz

=====
CHANNEL f2
CPDPRG[2] waltz16
NUC2 1H
PCPD2 80.00 usec
PL2 4.00 dB
PL12 22.51 dB
PL13 25.00 dB
PL2W 12.10000038 W
PL12W 0.17052394 W
PL13W 0.09611372 W
SFO2 500.1320005 MHz

F2 - Processing parameters
SI 32768
SF 125.7577890 MHz
WDW EM
SSB 0
LB 1.00 Hz
GB 0
PC 1.40

Pseudo ortho NH2 Br & 2-PyrSO2Na

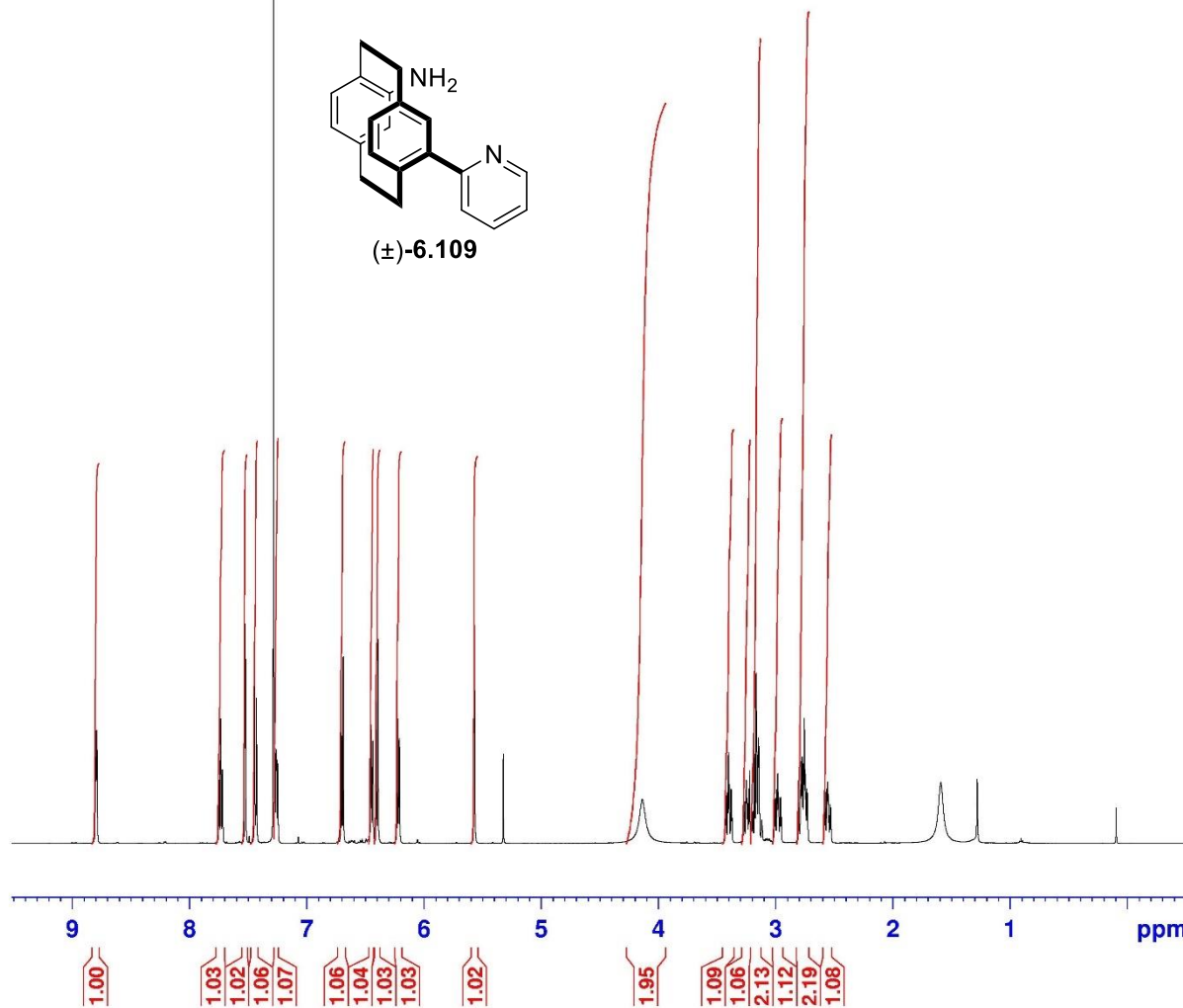


Current Data Parameters
NAME VI-Mn-48 ii
EXPNO 2
PROCNO 1

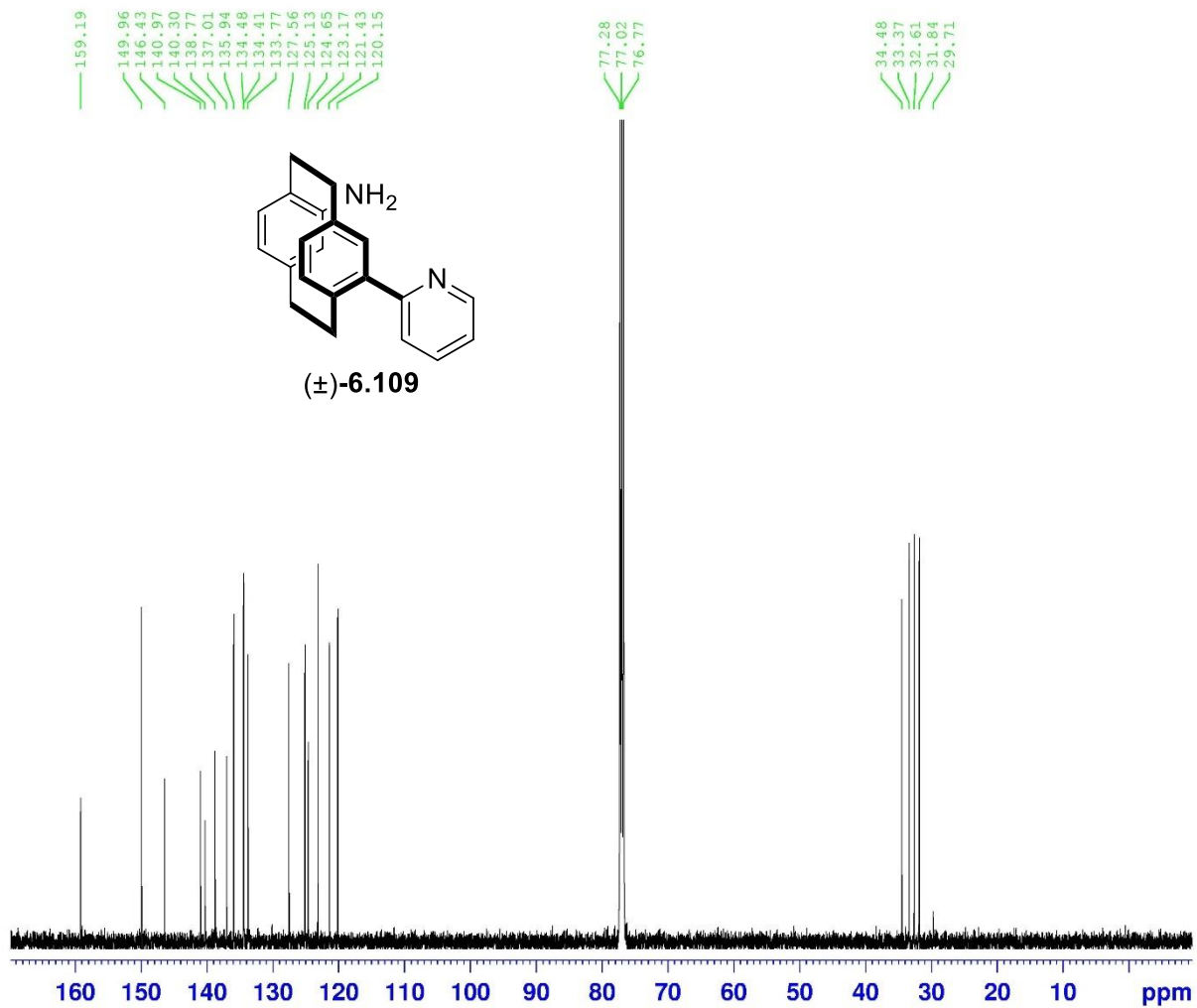
F2 - Acquisition Parameters
Date_ 20200128
Time 19.01
INSTRUM spect
PROBHD 5 mm PAQXI 1H/
PULPROG zg30
TD 65536
SOLVENT CDCl3
NS 64
DS 2
SWH 10330.578 Hz
FIDRES 0.157632 Hz
AQ 3.1719425 sec
RG 256
DW 48.400 usec
DE 6.50 usec
TE 298.2 K
D1 1.00000000 sec
TD0 1

==== CHANNEL f1 =====
NUC1 1H
P1 9.50 usec
PL1 4.00 dB
PL1W 12.10000038 W
SFO1 500.1330885 MHz

F2 - Processing parameters
SI 32768
SF 500.1300000 MHz
WDW EM
SSB 0
LB 0.30 Hz
GB 0
PC 1.00



¹³C : Pseudo ortho NH₂ Br & 2-PyrSO₂Na



Current Data Parameters
 NAME VI-Mn-48 ii
 EXPNO 3
 PROCNO 1

F2 - Acquisition Parameters
 Date_ 20200129
 Time 9.19
 INSTRUM spect
 PROBHD 5 mm PAQXI 1H/
 PULPROG zgpg30
 TD 65536
 SOLVENT CDCl₃
 NS 16288
 DS 4
 SWH 30030.029 Hz
 FIDRES 0.458222 Hz
 AQ 1.0911744 sec
 RG 32768
 DW 16.650 usec
 DE 6.50 usec
 TE 298.2 K
 D1 2.0000000 sec
 D11 0.0300000 sec
 TD0 1

===== CHANNEL f1 =====
 NUC1 13C
 P1 12.00 usec
 PL1 -4.00 dB
 PL1W 172.88230896 W
 SFO1 125.7703643 MHz

===== CHANNEL f2 =====
 CPDPRG[2] waltz16
 NUC2 1H
 PCPD2 80.00 usec
 PL2 4.00 dB
 PL12 22.51 dB
 PL13 25.00 dB
 PL2W 12.10000038 W
 PL12W 0.17052394 W
 PL13W 0.09611372 W
 SFO2 500.1320005 MHz

F2 - Processing parameters
 SI 32768
 SF 125.7577890 MHz
 WDW EM
 SSB 0
 LB 1.00 Hz
 GB 0
 PC 1.40

1H : Ortho Br CHO & 4-PyrSO2Na

9.514
8.813
8.780
8.728
7.287
7.150
6.855
6.840
6.776
6.760
6.677
6.661
6.645
6.562
6.547
6.481
6.465
3.961
3.948
3.937
3.929
3.921
3.913
3.340
3.333
3.324
3.312
3.068
3.044
3.024
3.011
2.977
2.961
2.952
2.943
2.935
2.918
2.904
2.883
2.872
2.852
2.841
2.827
2.818
1.277
0.095

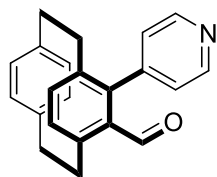


Current Data Parameters
NAME V-Mn-257 Main
EXPNO 1
PROCNO 1

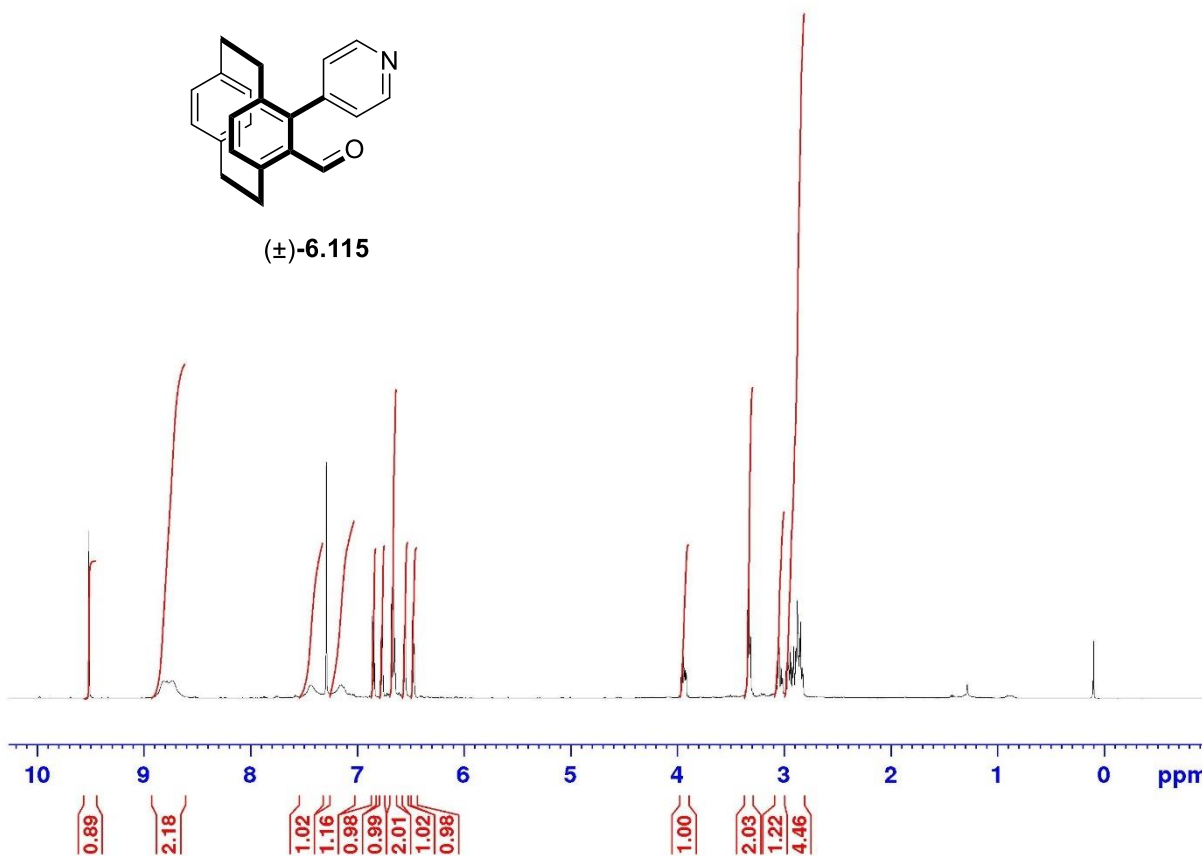
F2 - Acquisition Parameters
Date_ 20200602
Time 17.20
INSTRUM spect
PROBHD 5 mm PAQXI 1H/
PULPROG zg30
TD 65536
SOLVENT CDCl3
NS 16
DS 2
SWH 10330.578 Hz
FIDRES 0.157632 Hz
AQ 3.1719425 sec
RG 90.5
DW 48.400 usec
DE 6.50 usec
TE 294.6 K
D1 1.00000000 sec
TDO 1

===== CHANNEL f1 =====
NUC1 1H
P1 9.50 usec
PL1 4.00 dB
PL1W 12.10000038 W
SFO1 500.1330885 MHz

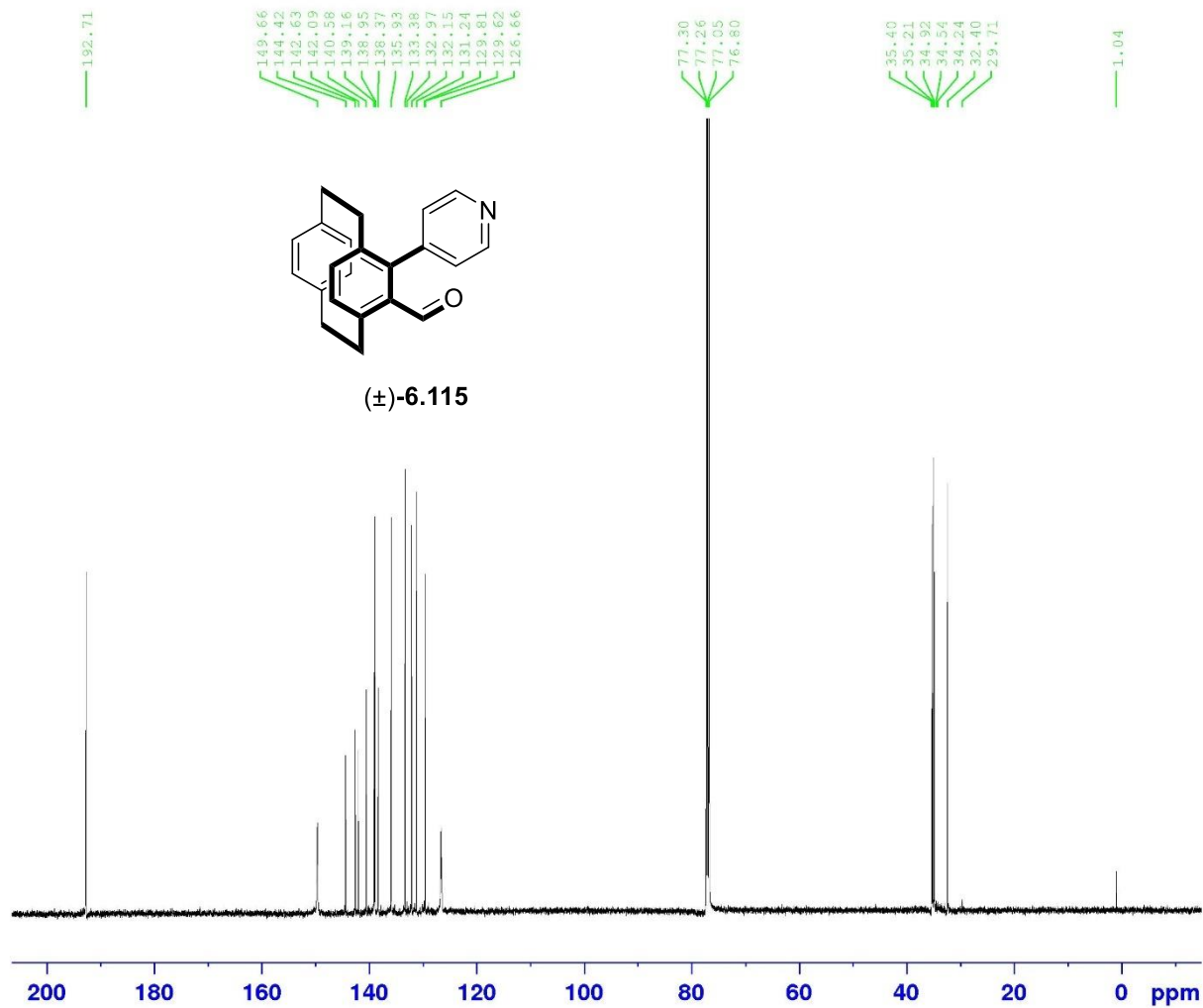
F2 - Processing parameters
SI 32768
SF 500.1300000 MHz
WDW EM
SSB 0
LB 0.30 Hz
GB 0
PC 1.00



(±)-6.115



¹³C : Ortho Br CHO & 4-PyrSO₂Na



Current Data Parameters
 NAME V-Mn-257 Main
 EXPNO 2
 PROCNO 1

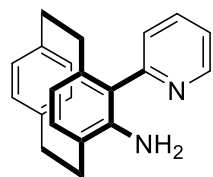
F2 - Acquisition Parameters
 Date_ 20200603
 Time 7.44
 INSTRUM spect
 PROBHD 5 mm PAQXI 1H/
 PUIPROG zgpg30
 TD 65536
 SOLVENT CDCl3
 NS 16384
 DS 4
 SWH 30030.029 Hz
 FIDRES 0.458222 Hz
 AQ 1.0911744 sec
 RG 32768
 DW 16.650 usec
 DE 6.50 usec
 TE 295.1 K
 D1 2.0000000 sec
 D11 0.0300000 sec
 TD0 1

----- CHANNEL f1 -----
 NUC1 13C
 P1 12.00 usec
 PL1 -4.00 dB
 PL1W 172.88230896 W
 SFO1 125.7703643 MHz

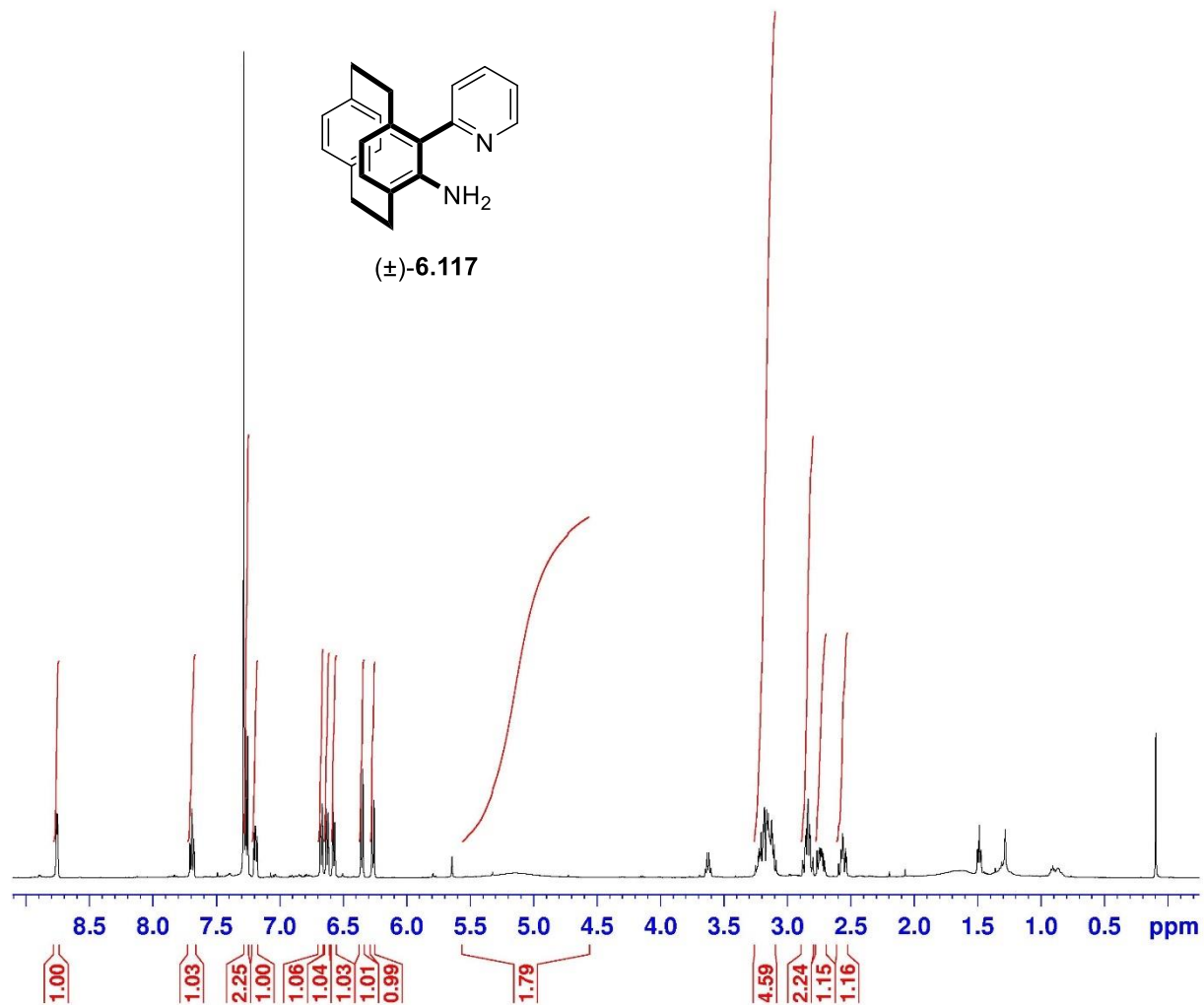
----- CHANNEL f2 -----
 CPDPRG[2] waltz16
 NUC2 1H
 PCPD2 80.00 usec
 PL2 4.00 dB
 PL12 22.51 dB
 PL13 25.00 dB
 PL2W 12.10000038 W
 PL12W 0.17052394 W
 PL13W 0.09611372 W
 SFO2 500.1320005 MHz

F2 - Processing parameters
 SI 32768
 SF 125.7577890 MHz
 WDW EM
 SSB 0
 LB 1.00 Hz
 GB 0
 PC 1.40

Ortho NH2 Br & 2-PyrSO2Na



(±)-6.117



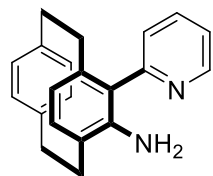
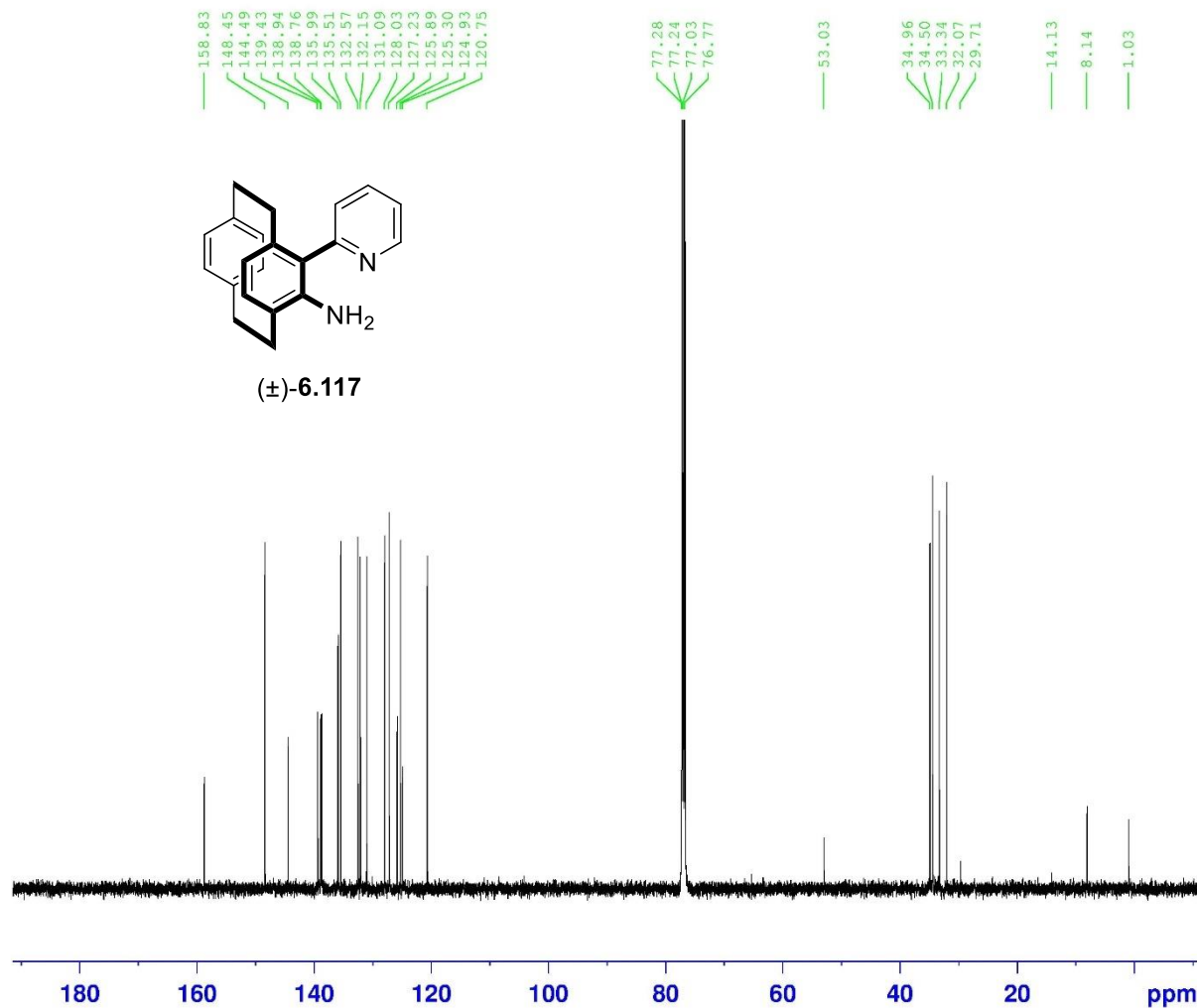
Current Data Parameters
NAME VI-Mn-15 iii
EXPNO 1
PROCNO 1

F2 - Acquisition Parameters
Date_ 20191231
Time 14.05
INSTRUM spect
PROBHD 5 mm PAQXI 1H/
PULPROG zg30
TD 65536
SOLVENT CDCl3
NS 64
DS 2
SWH 10330.578 Hz
FIDRES 0.157632 Hz
AQ 3.1719425 sec
RG 128
DW 48.400 usec
DE 6.50 usec
TE 297.1 K
D1 1.00000000 sec
TD0 1

==== CHANNEL f1 =====
NUC1 1H
P1 9.50 usec
PL1 4.00 dB
PL1W 12.10000038 W
SFO1 500.1330885 MHz

F2 - Processing parameters
SI 32768
SF 500.1300000 MHz
WDW EM
SSB 0
LB 0.30 Hz
GB 0
PC 1.00

¹³C : Ortho NH2 Br & 2-PyrSO2Na



Current Data Parameters
NAME VI-Mn-15 iii
EXPNO 2
PROCNO 1

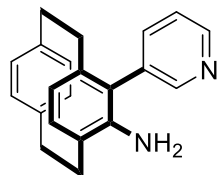
F2 - Acquisition Parameters
Date_ 20200101
Time 4.29
INSTRUM spect
PROBHD 5 mm PAQXI 1H/
PULPROG zgpg30
TD 65536
SOLVENT CDCl3
NS 16384
DS 4
SWH 30030.029 Hz
FIDRES 0.458222 Hz
AQ 1.0911744 sec
RG 32768
DW 16.650 usec
DE 6.50 usec
TE 298.3 K
D1 2.00000000 sec
D11 0.03000000 sec
TD0 1

----- CHANNEL f1 -----
NUC1 13C
P1 12.00 usec
PL1 -4.00 dB
PL1W 172.88230896 W
SFO1 125.7703643 MHz

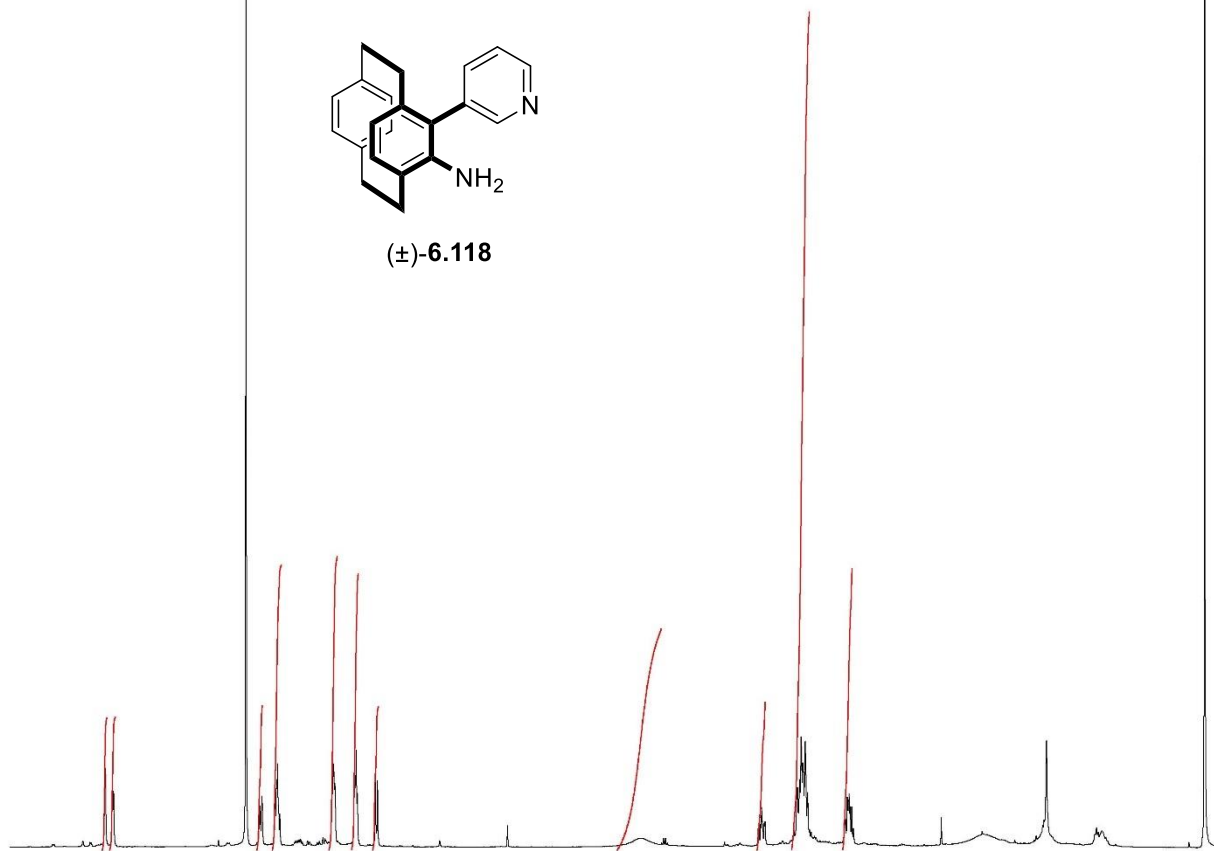
----- CHANNEL f2 -----
CPDPRG[2] waltz16
NUC2 1H
PCPD2 80.00 usec
PL2 4.00 dB
PL12 22.51 dB
PL13 25.00 dB
PL2W 12.10000038 W
PL12W 0.17052394 W
PL13W 0.09611372 W
SFO2 500.1320005 MHz

F2 - Processing parameters
SI 32768
SF 125.7577890 MHz
WDW EM
SSB 0
LB 1.00 Hz
GB 0
PC 1.40

Ortho NH2 Br & 3-PyrSO2Na



(±)-6.118

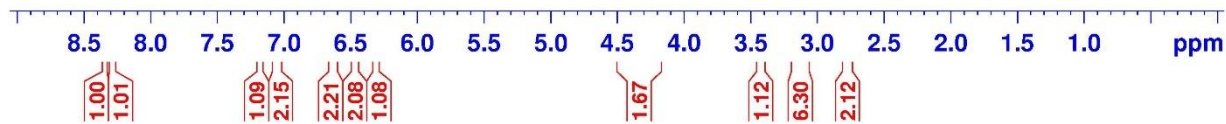


Current Data Parameters
NAME VI-Mn-16 ii
EXPNO 2
PROCNO 1

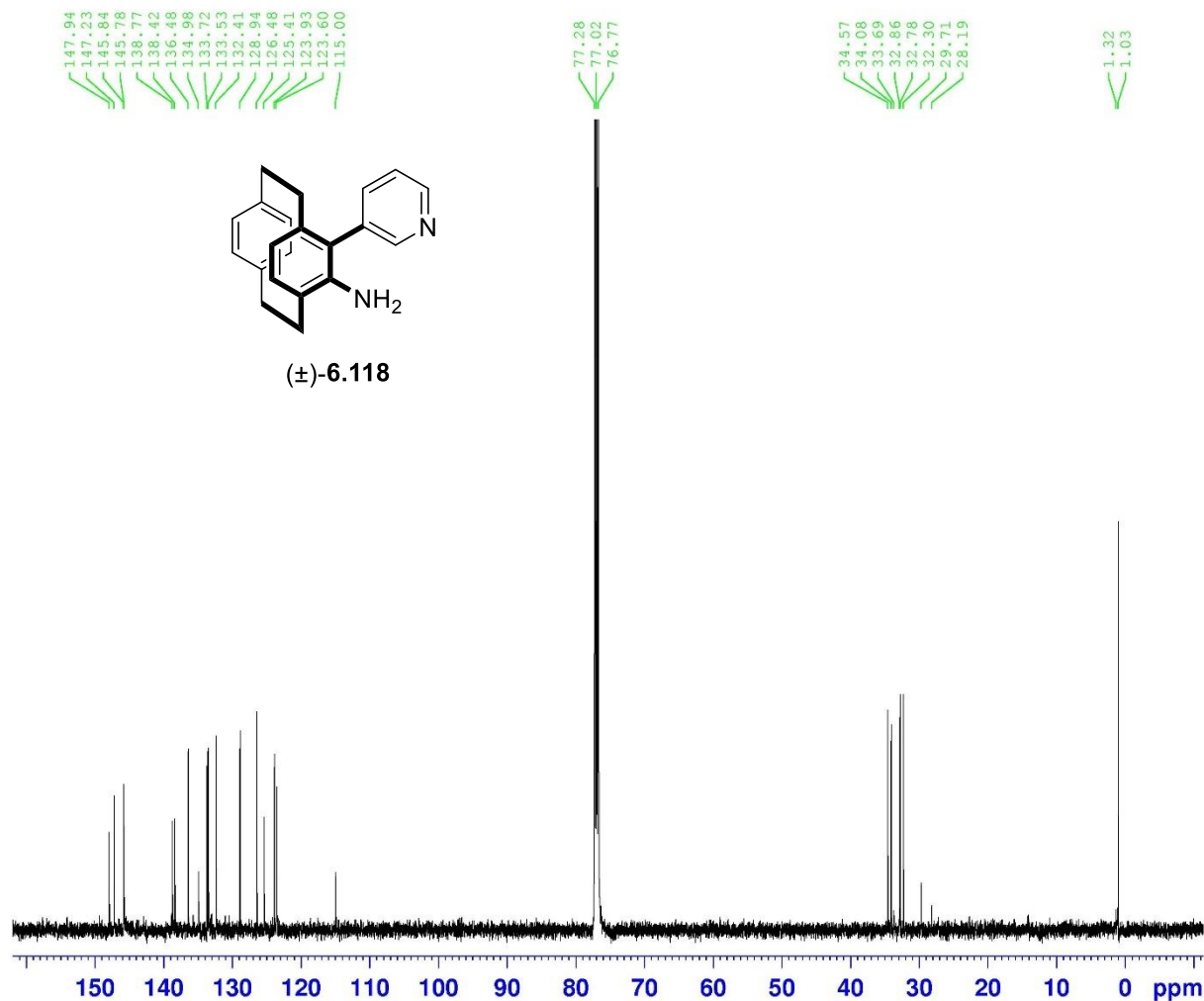
F2 - Acquisition Parameters
Date_ 20191230
Time 15.40
INSTRUM spect
PROBHD 5 mm PAQXI 1H/
PULPROG zg30
TD 65536
SOLVENT CDC13
NS 64
DS 2
SWH 10330.578 Hz
FIDRES 0.157632 Hz
AQ 3.1719425 sec
RG 128
DW 48.400 usec
DE 6.50 usec
TE 296.9 K
D1 1.00000000 sec
TDO 1

==== CHANNEL f1 =====
NUC1 1H
P1 9.50 usec
PL1 4.00 dB
PL1W 12.10000038 W
SFO1 500.1330885 MHz

F2 - Processing parameters
SI 32768
SF 500.1300000 MHz
WDW EM
SSB 0
LB 0.30 Hz
GB 0
PC 1.00



¹³C : Ortho NH2 Br & 3-PyrSO2Na



Current Data Parameters
NAME VI-Mn-16 ii
EXPNO 3
PROCNO 1

F2 - Acquisition Parameters
Date_ 20191231
Time 6.05
INSTRUM spect
PROBHD 5 mm PAQXI 1H/
PULPROG zgpg30
TD 65536
SOLVENT CDCl3
NS 16384
DS 4
SWH 30030.029 Hz
FIDRES 0.458222 Hz
AQ 1.0911744 sec
RG 32768
DW 16.650 usec
DE 6.50 usec
TE 296.8 K
D1 2.0000000 sec
D11 0.0300000 sec
TD0 1

===== CHANNEL f1 =====
NUC1 ¹³C
P1 12.00 usec
PL1 -4.00 dB
PL1W 172.88230896 W
SFO1 125.7703643 MHz

===== CHANNEL f2 =====
CPDPRG2 waltz16
NUC2 ¹H
PCPD2 80.00 usec
PL2 4.00 dB
PL12 22.51 dB
PL13 25.00 dB
PL2W 12.10000038 W
PL12W 0.17052394 W
PL13W 0.09611372 W
SFO2 500.1320005 MHz

F2 - Processing parameters
SI 32768
SF 125.7577890 MHz
WDW EM
SSB 0
LB 1.00 Hz
GB 0
PC 1.40